Scientific and Technical Aerospace Reports

STAR

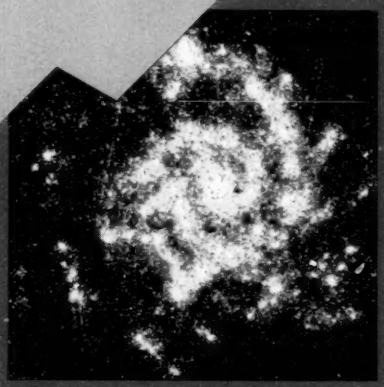

An Abstract Journal

NASA STI PROGRAM SCIENTIFIC & TECHNICAL INFORMATION

Volume 30, Number 17
September 8, 1992
N92-26171 to N92-27197

Scientific and Technical Aerospace Reports

Scientific and Technical Aerospace Reports (STAR) is an abstract journal that provides comprehensive coverage of worldwide aerospace-related reports. It is a major product of the International Aerospace Database managed by the NASA Scientific and Technical Information (STI) Program. The coverage includes reports on aeronautics, space, and supporting disciplines. *STAR* lists current, publicly available reports entered into the NASA STI Database during the 2-week period preceding publication. A typical citation and abstract appear on page viii. They explain how to read the items that are announced in this journal.

NASA sponsors a companion journal, *International Aerospace Abstracts (IAA)* (*NOVA* for internal NASA use) that lists abstracts of the open literature on aerospace subjects available worldwide. *IAA* is available for sale through the AIAA.

Entries found in *STAR* and *IAA* are available through NASA's online service, RECON, as the International Aerospace Database and through DIALOG as the Aerospace Database.

Information on aerospace and related subjects is gathered by the NASA STI Program through national and international agreements and exchanges and is made available to the NASA community as well as to the public in many forms through various outlets. The section on NASA STI Program Products and Services contains additional information.

For further information please contact:
NASA Center for AeroSpace Information (CASI)
P.O. Box 8757
Baltimore, Maryland 21240-0757
(301) 621-0390

US ISSN 0036-8741

Volume 30 Number 17 / September 8, 1992

TABLE OF CONTENTS

AERONAUTICS For related information see also *Astronautics.*

01 AERONAUTICS (GENERAL) ..... **N.A.**

02 AERODYNAMICS **2849**
Includes aerodynamics of bodies, combinations, wings, rotors, and control surfaces; and internal flow in ducts and turbomachinery. For related information see also *34 Fluid Mechanics and Heat Transfer.*

03 AIR TRANSPORTATION AND SAFETY **2850**
Includes passenger and cargo air transport operations; and aircraft accidents. For related information see also *16 Space Transportation* and *85 Urban Technology and Transportation.*

04 AIRCRAFT COMMUNICATIONS AND NAVIGATION **2850**
Includes digital and voice communication with aircraft; air navigation systems (satellite and ground based); and air traffic control. For related information see also *17 Space Communications, Spacecraft Communications, Command and Tracking* and *32 Communications and Radar.*

05 AIRCRAFT DESIGN, TESTING AND PERFORMANCE **2852**
Includes aircraft simulation technology. For related information see also *18 Spacecraft Design, Testing and Performance* and *39 Structural Mechanics.* For land transportation vehicles see *85 Urban Technology and Transportation.*

06 AIRCRAFT INSTRUMENTATION ..... **N.A.**
Includes cockpit and cabin display devices; and flight instruments. For related information see also *19 Space craft Instrumentation* and *35 Instrumentation and Photography.*

07 AIRCRAFT PROPULSION AND POWER **2853**
Includes prime propulsion systems and systems components, e.g., gas turbine engines and compressors; and onboard auxiliary power plants for aircraft. For related information see also *20 Spacecraft Propulsion and Power, 28 Propellants and Fuels,* and *44 Energy Production and Conversion.*

08 AIRCRAFT STABILITY AND CONTROL ..... **N.A.**
Includes aircraft handling qualities; piloting; flight controls; and autopilots. For related information see also *05 Aircraft Design, Testing and Performance.*

09 RESEARCH AND SUPPORT FACILITIES (AIR) **2856**
Includes airports, hangars and runways; aircraft repair and overhaul facilities; wind tunnels; shock tubes; and aircraft engine test stands. For related information see also *14 Ground Support Systems and Facilities (Space).*

ASTRONAUTICS For related information see also *Aeronautics.*

12 ASTRONAUTICS (GENERAL) **2856**
For extraterrestrial exploration see *91 Lunar and Planetary Exploration.*

13 ASTRODYNAMICS **2857**
Includes powered and free-flight trajectories; and orbital and launching dynamics.

14 GROUND SUPPORT SYSTEMS AND FACILITIES (SPACE) ..... **N.A.**
Includes launch complexes, research and production facilities; ground support equipment, e.g., mobile transporters; and simulators. For related information see also *09 Research and Support Facilities (Air).*

15 LAUNCH VEHICLES AND SPACE VEHICLES **2857**
Includes boosters; operating problems of launch/space vehicle systems; and reusable vehicles. For related information see also *20 Spacecraft Propulsion and Power.*

16 SPACE TRANSPORTATION **2858**
Includes passenger and cargo space transportation, e.g., shuttle operations; and space rescue techniques. For related information see also *03 Air Transportation and Safety* and *18 Spacecraft Design, Testing and Performance.* For space suits see *54 Man/System Technology and Life Support.*

17 SPACE COMMUNICATIONS, SPACECRAFT COMMUNICATIONS, COMMAND AND TRACKING . **2858**
Includes telemetry; space communications networks; astronavigation and guidance; and radio blackout. For related information see also *04 Aircraft Communications and Navigation* and *32 Communications and Radar.*

N.A.—no abstracts were assigned to this category for this issue.

18 SPACECRAFT DESIGN, TESTING AND PERFORMANCE **2858**
Includes satellites; space platforms; space stations; spacecraft systems and components such as thermal and environmental controls; and attitude controls. For life support systems see *54 Man/System Technology and Life Support.* For related information see also *05 Aircraft Design, Testing and Performance, 39 Structural Mechanics,* and *16 Space Transportation.*

19 SPACECRAFT INSTRUMENTATION ..... **N.A.**
For related information see also *06 Aircraft Instrumentation* and *35 Instrumentation and Photography.*

20 SPACECRAFT PROPULSION AND POWER **2860**
Includes main propulsion systems and components, e.g., rocket engines; and spacecraft auxiliary power sources. For related information see also *07 Aircraft Propulsion and Power, 28 Propellants and Fuels, 44 Energy Production and Conversion,* and *15 Launch Vehicles and Space Vehicles.*

CHEMISTRY AND MATERIALS

23 CHEMISTRY AND MATERIALS (GENERAL) ..... **N.A.**

24 COMPOSITE MATERIALS **2867**
Includes physical, chemical, and mechanical properties of laminates and other composite materials. For ceramic materials see *27 Nonmetallic Materials.*

25 INORGANIC AND PHYSICAL CHEMISTRY **2870**
Includes chemical analysis, e.g., chromatography; combustion theory; electrochemistry; and photochemistry. For related information see also *77 Thermodynamics and Statistical Physics.*

26 METALLIC MATERIALS **2876**
Includes physical, chemical, and mechanical properties of metals, e.g., corrosion; and metallurgy.

27 NONMETALLIC MATERIALS **2880**
Includes physical, chemical, and mechanical properties of plastics, elastomers, lubricants, polymers, textiles, adhesives, and ceramic materials. For composite materials see *24 Composite Materials.*

28 PROPELLANTS AND FUELS **2883**
Includes rocket propellants, igniters and oxidizers; their storage and handling procedures; and aircraft fuels. For related information see also *07 Aircraft Propulsion and Power, 20 Spacecraft Propulsion and Power,* and *44 Energy Production and Conversion.*

29 MATERIALS PROCESSING **2884**
Includes space-based development of products and processes for commercial application. For biological materials see *55 Space Biology.*

ENGINEERING For related information see also *Physics.*

31 ENGINEERING (GENERAL) **2886**
Includes vacuum technology; control engineering; display engineering; cryogenics; and fire prevention.

32 COMMUNICATIONS AND RADAR **2887**
Includes radar; land and global communications; communications theory; and optical communications. For related information see also *04 Aircraft Communications and Navigation* and *17 Space Communications, Spacecraft Communications, Command and Tracking.* For search and rescue see *03 Air Transportation and Safety,* and *16 Space Transportation.*

33 ELECTRONICS AND ELECTRICAL ENGINEERING **2891**
Includes test equipment and maintainability; components, e.g., tunnel diodes and transistors; microminiaturization; and integrated circuitry. For related information see also *60 Computer Operations and Hardware* and *76 Solid-State Physics.*

34 FLUID MECHANICS AND HEAT TRANSFER **2895**
Includes boundary layers; hydrodynamics; fluidics; mass transfer and ablation cooling. For related information see also *02 Aerodynamics* and *77 Thermodynamics and Statistical Physics.*

35 INSTRUMENTATION AND PHOTOGRAPHY **2906**
Includes remote sensors; measuring instruments and gauges; detectors; cameras and photographic supplies; and holography. For aerial photography see *43 Earth Resources and Remote Sensing.* For related information see also *06 Aircraft Instrumentation* and *19 Spacecraft Instrumentation.*

36 LASERS AND MASERS **2910**
Includes parametric amplifiers. For related information see also *76 Solid-State Physics.*

37 MECHANICAL ENGINEERING **2913**
Includes auxiliary systems (nonpower); machine elements and processes; and mechanical equipment.

38 QUALITY ASSURANCE AND RELIABILITY **2916**
Includes product sampling procedures and techniques; and quality control.

39 STRUCTURAL MECHANICS **2916**
Includes structural element design and weight analysis; fatigue; and thermal stress. For applications see *05 Aircraft Design, Testing and Performance* and *18 Spacecraft Design, Testing and Performance.*

GEOSCIENCES For related information see also *Space Sciences.*

42 GEOSCIENCES (GENERAL) **2921**

43 EARTH RESOURCES AND REMOTE SENSING **2921**
Includes remote sensing of earth resources by aircraft and spacecraft; photogrammetry; and aerial photography. For instrumentation see *35 Instrumentation and Photography.*

44 ENERGY PRODUCTION AND CONVERSION **2926**
Includes specific energy conversion systems, e.g., fuel cells; global sources of energy; geophysical conversion; and windpower. For related information see also *07 Aircraft Propulsion and Power, 20 Spacecraft Propulsion and Power,* and *28 Propellants and Fuels.*

45 ENVIRONMENT POLLUTION **2928**
Includes atmospheric, noise, thermal, and water pollution.

46 GEOPHYSICS **2934**
Includes aeronomy; upper and lower atmosphere studies; ionospheric and magnetospheric physics; and geomagnetism. For space radiation see *93 Space Radiation.*

47 METEOROLOGY AND CLIMATOLOGY **2944**
Includes weather forecasting and modification.

48 OCEANOGRAPHY **2948**
Includes biological, dynamic, and physical oceanography; and marine resources. For related information see also *43 Earth Resources and Remote Sensing.*

LIFE SCIENCES

51 LIFE SCIENCES (GENERAL) **2950**

52 AEROSPACE MEDICINE **2952**
Includes physiological factors; biological effects of radiation; and effects of weightlessness on man and animals.

53 BEHAVIORAL SCIENCES **2953**
Includes psychological factors; individual and group behavior; crew training and evaluation; and psychiatric research.

54 MAN/SYSTEM TECHNOLOGY AND LIFE SUPPORT **2954**
Includes human engineering; biotechnology; and space suits and protective clothing. For related information see also *16 Space Transportation.*

55 SPACE BIOLOGY ..... **N.A.**
Includes exobiology; planetary biology; and extraterrestrial life.

MATHEMATICAL AND COMPUTER SCIENCES

59 MATHEMATICAL AND COMPUTER SCIENCES (GENERAL) ..... **N.A.**

60 COMPUT4R OPERATIONS AND HARDWARE **2970**
Includes hardware for computer graphics, firmware, and data processing. For components see *33 Electronics and Electrical Engineering.*

61 COMPUTER PROGRAMMING AND SOFTWARE **2971**
Includes computer programs, routines, algorithms, and specific applications, e.g., CAD/CAM.

62 COMPUTER SYSTEMS **2978**
Includes computer networks and special application computer systems.

63 CYBERNETICS **2981**
Includes feedback and control theory, artificial intelligence, robotics and expert systems. For related information see also *54 Man/System Technology and Life Support.*

64 NUMERICAL ANALYSIS **2985**
Includes iteration, difference equations, and numerical approximation.

65 STATISTICS AND PROBABILITY **2989**
Includes data sampling and smoothing; Monte Carlo method; and stochastic processes.

66 SYSTEMS ANALYSIS **2990**
Includes mathematical modeling; network analysis; and operations research.

67 THEORETICAL MATHEMATICS **2990**
Includes topology and number theory.

PHYSICS For related information see also *Engineering.*

70 PHYSICS (GENERAL) **2990**
For precision time and time interval (PTTI) see *35 Instrumentation and Photography;* for geophysics, astrophysics or solar physics see *46 Geophysics, 90 Astrophysics,* or *92 Solar Physics.*

71 ACOUSTICS **2991**
Includes sound generation, transmission, and attenuation. For noise pollution see *45 Environment Pollution.*

72 ATOMIC AND MOLECULAR PHYSICS **2993**
Includes atomic structure, electron properties, and molecular spectra.

73 NUCLEAR AND HIGH-ENERGY PHYSICS **2995**
Includes elementary and nuclear particles; and reactor theory. For space radiation see *93 Space Radiation.*

74 OPTICS **2996**
Includes light phenomena and optical devices. For lasers see *36 Lasers and Masers.*

75 PLASMA PHYSICS **2999**
Includes magnetohydrodynamics and plasma fusion. For ionospheric plasmas see *46 Geophysics.* For space plasmas see *90 Astrophysics.*

76 SOLID-STATE PHYSICS **3001**
Includes superconductivity. For related information see also *33 Electronics and Electrical Engineering* and *36 Lasers and Masers.*

77 THERMODYNAMICS AND STATISTICAL PHYSICS **3007**
Includes quantum mechanics; theoretical physics; and Bose and Fermi statistics. For related information see also *25 Inorganic and Physical Chemistry* and *34 Fluid Mechanics and Heat Transfer.*

SOCIAL SCIENCES

80 SOCIAL SCIENCES (GENERAL) ..... **N.A.**
Includes educational matters.

81 ADMINISTRATION AND MANAGEMENT **3008**
Includes management planning and research.

82 DOCUMENTATION AND INFORMATION SCIENCE **3010**
Includes information management; information storage and retrieval technology; technical writing; graphic arts; and micrography. For computer documentation see *61 Computer Programming and Software.*

83 ECONOMICS AND COST ANALYSIS **3014**
Includes cost effectiveness studies.

84 LAW, POLITICAL SCIENCE AND SPACE POLICY **3014**
Includes NASA appropriation hearings; aviation law; space law and policy; international law; international cooperation; and patent policy.

85 URBAN TECHNOLOGY AND TRANSPORTATION **3015**
Includes applications of space technology to urban problems; technology transfer; technology assessment; and surface and mass transportation. For related information see *03 Air Transportation and Safety, 16 Space Transportation,* and *44 Energy Production and Conversion.*

SPACE SCIENCES For related information see also *Geosciences.*

88 SPACE SCIENCES (GENERAL) ..... **N.A.**

89 ASTRONOMY **3015**
Includes radio, gamma-ray, and infrared astronomy; and astrometry.

90 ASTROPHYSICS **3016**
Includes cosmology; celestial mechanics; space plasmas; and interstellar and interplanetary gases and dust. For related information see also *75 Plasma Physics.*

91 LUNAR AND PLANETARY EXPLORATION **3019**
Includes planetology; and manned and unmanned flights. For spacecraft design or space stations see *18 Spacecraft Design, Testing and Performance.*

92 SOLAR PHYSICS **3019**
Includes solar activity, solar flares, solar radiation and sunspots. For related information see *93 Space Radiation.*

93 SPACE RADIATION **3020**
Includes cosmic radiation; and inner and outer earth's radiation belts. For biological effects of radiation see *52 Aerospace Medicine.* For theory see *73 Nuclear and High-Energy Physics.*

GENERAL

Includes aeronautical, astronautical, and space science related histories, biographies, and pertinent reports too broad for categorization; histories or broad overviews of NASA programs.

99 GENERAL **3022**

SUBJECT INDEX **I-1**

PERSONAL AUTHOR INDEX **I-73**

CORPORATE SOURCE INDEX **I-81**

CONTRACT NUMBER INDEX **I-95**

REPORT NUMBER INDEX **I-97**

ACCESSION NUMBER INDEX **I-105**

APPENDIX **A-1**

TYPICAL CITATION AND ABSTRACT

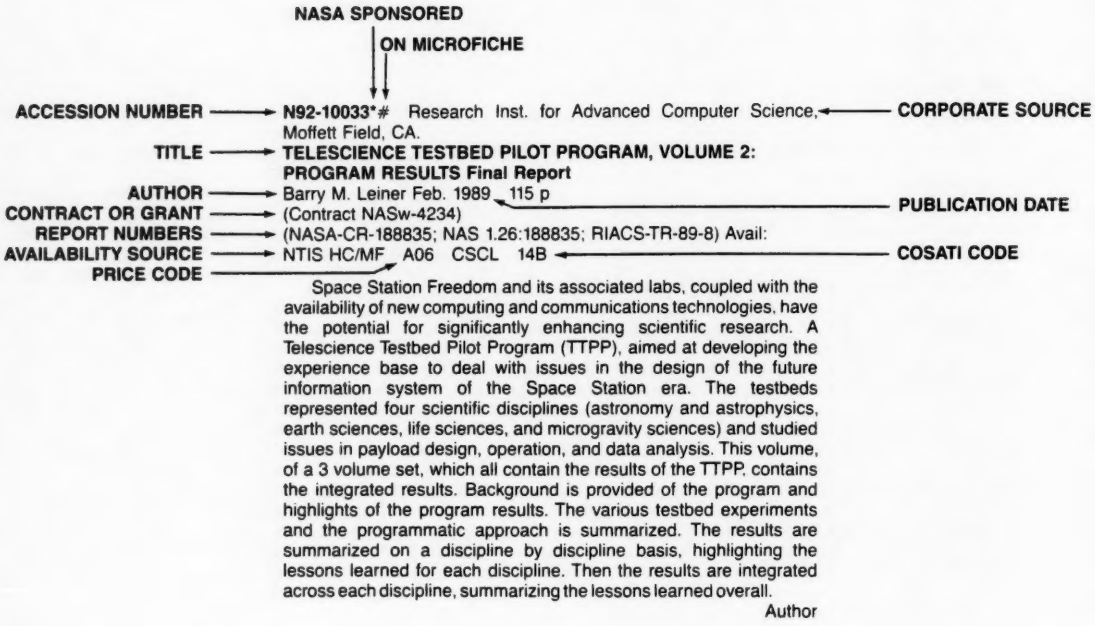
NASA SPONSORED
ON MICROFICHE
ACCESSION NUMBER
N92-10033*# Research Inst. for Advanced Computer Science, Moffett Field, CA.
CORPORATE SOURCE
TITLE
TELESCIENCE TESTBED PILOT PROGRAM, VOLUME 2: PROGRAM RESULTS Final Report
AUTHOR
Barry M. Leiner Feb. 1989 115 p
PUBLICATION DATE
CONTRACT OR GRANT
(Contract NASw-4234)
REPORT NUMBERS
(NASA-CR-188835; NAS 1.26:188835; RIACS-TR-89-8) Avail:
AVAILABILITY SOURCE
NTIS HC/MF A06 CSCL 14B
COSATI CODE
PRICE CODE
Space Station Freedom and its associated labs, coupled with the availability of new computing and communications technologies, have the potential for significantly enhancing scientific research. A Telescience Testbed Pilot Program (TTPP), aimed at developing the experience base to deal with issues in the design of the future information system of the Space Station era. The testbeds represented four scientific disciplines (astronomy and astrophysics, earth sciences, life sciences, and microgravity sciences) and studied issues in payload design, operation, and data analysis. This volume, of a 3 volume set, which all contain the results of the TTPP, contains the integrated results. Background is provided of the program and highlights of the program results. The various testbed experiments and the programmatic approach is summarized. The results are summarized on a discipline by discipline basis, highlighting the lessons learned for each discipline. Then the results are integrated across each discipline, summarizing the lessons learned overall.
Author

VOLUME 30 NUMBER 17 / SEPTEMBER 8, 1992

Scientific and Technical Aerospace Reports

A Semimonthly Publication of the National Aeronautics and Space Administration

01 AERONAUTICS (GENERAL)

No abstracts in this category.

02 AERODYNAMICS

Includes aerodynamics of bodies, combinations, wings, rotors, and control surfaces; and internal flow in ducts and turbomachinery.

For related information see also *34 Fluid Mechanics and Heat Transfer.*

N92-26585 Virginia Polytechnic Inst. and State Univ., Blacksburg.

THREE-DIMENSIONAL UPWIND SCHEME FOR SOLVING THE EULER EQUATIONS ON UNSTRUCTURED TETRAHEDRAL GRIDS Ph.D. Thesis

Neal Tilson Frink 1991 129 p

Avail: Univ. Microfilms Order No. DA9209606

A new upwind scheme is developed for solving the three-dimensional Euler equations on unstructured tetrahedral meshes. The method yields solution accuracy and efficiency comparable to that currently available from similar structured-grid codes. The key to achieving this result is a novel cell reconstruction process which is based on an analytical formulation for computing solution gradients within tetrahedral cells. Prior methodology requires the application of cumbersome numerical procedures to evaluate surface integrals around the cell volume. The result is that higher-order differences can now be constructed more efficiently to attain computational times per cell comparable to those of structured codes. The underlying philosophy employed in constructing the basic flow solver is to draw on proven structured-grid technology whenever possible in order to reduce risk. Thus, spatial discretization is accomplished by a cell-centered finite-volume formulation using flux-difference splitting. Solutions are advanced in time by a 3-stage Runge-Kutta time-stepping scheme with convergence accelerated to steady state by local time stepping and implicit residual smoothing. The flow solver operates at a speed of 34 microseconds per cell per cycle on a CRAY-2S supercomputer and requires 64 words of memory per cell. Dissert. Abstr.

N92-26612*# National Aeronautics and Space Administration. Lewis Research Center, Cleveland, OH.

HELIUM BUBBLE FLOW VISUALIZATION OF THE SPANWISE SEPARATION ON A NACA 0012 WITH SIMULATED GLAZE ICE

M. Kerho, M. Bragg (Illinois Univ., Urbana.), and J. Shin Jan. 1992 17 p Presented at the 30th Aerospace Sciences Meeting and Exhibit, Reno, NV, 6-9 Jan. 1992; sponsored by AIAA Previously announced in IAA as A92-28192

(RTOP 505-68-10)

(NASA-TM-105742; E-7147; NAS 1.15:105742; AIAA-92-0413)

Copyright Avail: NTIS HC/MF A03

Research was performed to experimentally visualize and document the flow separation due to simulated glaze ice accretion on a NACA 0012 semispan with 30 deg sweep using helium bubbles as flow tracers. Results are compared to Navier-Stokes computational simulations for different angles of attack. Prior to acquiring data for the semispan model, a two dimensional experiment was conducted to determine the accuracy of using the helium bubbles as flow tracers. Results from the three dimensional experiment compare well to the computational simulations. Author

N92-26616 Virginia Polytechnic Inst. and State Univ., Blacksburg.

OBSERVATION AND MEASUREMENTS OF FLOW STRUCTURES IN THE STAGNATION REGION OF A WING-BODY JUNCTION Ph.D. Thesis

Sangho Kim 1991 280 p

Avail: Univ. Microfilms Order No. DA9208424

The behavior of a junction vortex formed around an obstacle in a boundary layer flow was studied experimentally in a water tunnel for two low speed cases. A wing consisting of a 3:2 elliptical nose and an NACA 0020 tail was used to simulate the function vortex. A visual study using a hydrogen bubble technique was extensively conducted to investigate the flow structures in the stagnation region of the wing. It was observed that a multiple vortex system exists in this region and shows an acyclic flow pattern. LDV measurements were performed in the plane of symmetry upstream of the wing. The visual evidence of acyclic flow pattern was consistent with the LDV measurements, and revealed that aperiodic stretching of the junction vortex appears responsible for the bimodal structure in the velocity histograms. An attempt to measure the three dimensional instantaneous velocity field in this region was made. A stereo vision approach was implemented to capture two orthogonal views simultaneously for three dimensional motion analysis. Dissert. Abstr.

N92-26651*# Vigyan Research Associates, Inc., Hampton, VA.

HIGH-ALPHA VORTEX DECOUPLING INVESTIGATIONS ON A CHINE FOREBODY/DELTA WING CONFIGURATION AT TRANSONIC MACH NUMBERS

Dhanvada M. Rao and M. K. Bhat Jun. 1992 45 p

(Contract NAS1-18856; RTOP 505-68-30-03)

(NASA-CR-189642; NAS 1.26:189642) Avail: NTIS HC/MF A03

A test program conducted in the LaRC 8-foot Transonic Pressure Tunnel on a blended chine/delta wing model to verify the concept of controlled vortex decoupling via inboard leading-edge flaps for improved high-alpha lateral/directional characteristics is discussed. This test extended the Mach number range of a data base previously generated in a LaRC 7 ft. by 10 ft High Speed Tunnel investigation. Six-component force/moment, forebody surface pressures, and central and twin tall static and dynamic loads were measured at Mach numbers of 0.4 to 1.2; laser light-sheet visualizations were also performed. Selected data are analyzed and discussed, emphasizing lateral/directional improvements and tail environment enhanced attainable by leading-edge flaps in the maximum lift region. Author

N92-26652*# Vigyan Research Associates, Inc., Hampton, VA.

SUBSONIC INVESTIGATIONS OF VORTEX INTERACTION CONTROL FOR ENHANCED HIGH-ALPHA AERODYNAMICS OF A CHINE FOREBODY/DELTA WING CONFIGURATION

Dhanvada M. Rao and M. K. Bhat Jun. 1992 56 p
(Contract NAS1-18856; RTOP 505-68-30-03)
(NASA-CR-189641; NAS 1.26:189641) Avail: NTIS HC/MF A04

A proposed concept to alleviate high alpha asymmetry and lateral/directional instability by decoupling of forebody and wing vortices was studied on a generic chine forebody/ 60 deg. delta configuration in the NASA Langley 7 by 10 foot High Speed Tunnel. The decoupling technique involved inboard leading edge flaps of varying span and deflection angle. Six component force/moment characteristics, surface pressure distributions and vapor-screen flow visualizations were acquired, on the basic wing-body configuration and with both single and twin vertical tails at M sub infinity = 0.1 and 0.4, and in the range alpha = 0 to 50 deg and beta = -10 to +10 degs. Results are presented which highlight the potential of vortex decoupling via leading edge flaps for enhanced high alpha lateral/directional characteristics. Author

N92-26947# Aeronautical Research Labs., Melbourne (Australia).
F-111C FLIGHT DYNAMIC MODEL AERODYNAMIC DATA-BASE DEVELOPMENT AND VERIFICATION
R. W. Eustace, M. I. Cooper, and C. A. Martin Dec. 1991 32 p
(AD-A246356; ARL-FLIGHT-MECH-TM-437; DODA-AR-006-595)
Avail: NTIS HC/MF A03

A description is given of the process used to develop and verify the aerodynamic data-base of the F-111C flight dynamic computer model. The process uses stability and control derivatives obtained from flight trials performed at the RAAF's Aircraft Research and Development Unit (ARDU). Model response has been verified against aircraft time histories measured during the trials. The results presented compare the aircraft response in lateral maneuvers, at various wing sweeps. A very good degree of matching is possible, although further investigation should correct inaccuracies which can cause poor estimation of yaw rate. GRA

N92-27054 Pennsylvania State Univ., University Park.
TURBULENT MIXING IN SUPERSONIC JETS Ph.D. Thesis
Krishnamurthy Viswanathan 1991 326 p
Avail: Univ. Microfilms Order No. DA9204307

A clear understanding of supersonic shear layers and the physics of supersonic mixing are vital to the development of high-speed flight vehicles. This computational study examines the stability and mixing characteristics of high-speed jets, both in the presence and absence of confining walls. The unsteady motion of the shear layer is described using instability wave modeling. Two models are developed for turbulent mixing in axisymmetric jets, taking into account the importance of the large scale structures. The current models emphasize the time-dependent motion of the shear layer, and a notable feature of these models is the absence of any model constants. The instabilities of highly supersonic jets are examined and classified. The modifications of these instabilities by the presence of an external stream and an outer wall are studied in detail. The instability wave modes of supersonic jets of arbitrary cross sections confined in arbitrary-shaped ducts are analyzed by a boundary integral formulation of the inviscid, compressible perturbation equations. A numerical method, using the boundary element method, is developed to treat this problem. The results of this study indicate that the mixing and development of free shear layers are related closely to the spatial stability characteristics of the mean flow. The effects of compressibility are quite pronounced. Even small changes in the duct geometry have a significant impact on the instability modes of the confined jet. Dissert. Abstr.

N92-27172# Colorado Univ., Boulder. Dept. of Aerospace Engineering Sciences.
AERODYNAMIC INTERFERENCE BETWEEN STORES Final Report, 1 Feb. 1989 - 30 Jun. 1991
F. C. Dougherty 30 Jan. 1992 19 p
(Grant AF-AFOSR-0235-89)
(AD-A247207; AFOSR-92-0086TR) Avail: NTIS HC/MF A03

Five tasks were initiated to study the aerodynamic interference between stores and aircraft. Both viscous and inviscid calculations were made. Steady state interference calculations matched well with experimental results and with other computational results. Unsteady time-accurate inviscid results showed the feasibility of using the Chimera scheme to simulate store separation. Free-fall calculations were made, demonstrating the ability to compute the new position of the store from the aerodynamic forces and moments on the store after its release from the aircraft. GRA

N92-27191*# Vanderbilt Univ., Nashville, TN. Dept. of Mechanical Engineering.
RAREFIED-FLOW AERODYNAMICS Final Report, 1 Jan. 1989 - 31 May 1992
J. Leith Potter 31 May 1992 21 p
(Grant NAG1-921)
(NASA-CR-190452; NAS 1.26:190452) Avail: NTIS HC/MF A03

Means for relatively simple and quick procedures are examined for estimating aerodynamic coefficients of lifting reentry vehicles. The methods developed allow aerospace designers not only to evaluate the aerodynamics of specific shapes but also to optimize shapes under given constraints. The analysis was also studied of the effect of thermomolecular flow on pressures measured by an orifice near the nose of a Space Shuttle Orbiter at altitudes above 75 km. It was shown that pressures corrected for thermomolecular flow effect are in good agreement with values predicted by independent theoretical methods. An incidental product was the insight gained about the free molecular thermal accommodation coefficient applicable under 'real' conditions of high speed flow in the Earth's atmosphere. The results are presented as abstracts of referenced papers. One reference paper is presented in its entirety. Author

03 AIR TRANSPORTATION AND SAFETY

Includes passenger and cargo air transport operations; and aircraft accidents.

For related information see also *16 Space Transportation* and *85 Urban Technology and Transportation.*

N92-26349# Deutsche Forschungsanstalt fuer Luft- und Raumfahrt, Oberpfaffenhofen (Germany, F.R.). Inst. fuer Physik der Atmosphaere.
THE ICING OF THE WING UPPER SIDE AND BOTTOM SIDE OF THE ICING RESEARCH AIRCRAFT OF THE DLR [DIE VEREISUNG DER TRAGFLAECHENOBERSEITE UND -UNTERSEITE DES VEREISUNGSFORSCHUNGSFLUGZEUGS DER DLR]
Hans-Eberhard Hoffmann and Johann Demmel *In its* Contributions to Atmospheric Physics in Honor of Dr. Manfred Reinhardt on His 65th Birthday Sep. 1991 p 215-222 In GERMAN; ENGLISH summary (For primary document see N92-26329 17-46)
Avail: NTIS HC/MF A11; DLR, Wissenschaftliches, Berichtswesen, Postfach 90 60 58, Cologne, Fed.Republic of Germany, HC 60 Deutsche marks

04 AIRCRAFT COMMUNICATIONS AND NAVIGATION

Includes digital and voice communication with aircraft; air navigation systems (satellite and ground based); and air traffic control.

For related information see also *17 Space Communications, Spacecraft Communications, Command and Tracking* and *Communications and Radar.*

N92-26272# Institute for Defense Analyses, Alexandria, VA.
THE STATE OF MULTIPLE SENSOR, MULTIPLE TARGET TRACKING IN BALLISTIC MISSILE DEFENSE Final Report, Nov. 1990 - Sep. 1991
Barry E. Fridling Sep. 1991 105 p

(Contract MDA903-89-C-0003)
(AD-A245433; AD-E501470; IDA-P-2590; IDA/HQ-91-38012)
Avail: NTIS HC/MF A06

This report addresses the latest developments and some of the critical issues pertaining to tracking algorithm development for ballistic missile defense (BMD). For the last several years, tracking has been recognized as one of the most complex and challenging tasks in BMD. During this time tracking algorithm development has been pursued vigorously, with substantial results and continuing progress. Part 1 of this report has the character of a survey of the latest developments and describes the activities in different organizations and the results obtained in critical technical areas. It describes developments in two areas pertaining to algorithm development and to algorithm simulation and evaluation; Data Association; Cluster Tracking; Tracking Simulation; and the Surveillance Testbed (STB). Part 2 is essentially a technical analysis of issues, problems, and candidate approaches in selected key areas. Some remaining problems pertaining to the design, utilization, and evaluation of tracking algorithms are: Birth-to-Death Tracking; Booster Tracking and Template Matching; Midcourse Track Initiation, and Scoring Methods for Track Performance. GRA

N92-26291# Defence Research Establishment, Ottawa (Ontario).
AN EVALUATION OF SUPERRESOLUTION METHODS FOR TACTICAL RADIO DIRECTION FINDING
William J. Read Oct. 1991 123 p
(AD-A246316; DREO-1091) Avail: NTIS HC/MF A06

This report evaluates superresolution direction finding methods for land tactical narrowband very high frequency/ultrahigh frequency purposes. The DF methods are described and evaluated in depth using a common theoretical framework beginning with classical methods and ending with modern day eigenanalysis based methods. Based on this analysis, superresolution methods can be described in terms of a five step procedure where each step has a unique purpose in the estimation process. Different methods vary according to the operations performed at each step. This is useful in analyzing and comparing the theoretical performance of various DF methods under the same conditions. The results from simulations are also included to support the theoretical evaluations. GRA

N92-26415# Naval Postgraduate School, Monterey, CA.
CHARACTERIZATION OF THE CLOCK IN A NEW INEXPENSIVE GPS RECEIVER: THE MAGNAVOX MX 4200 M.S. Thesis
Manuel Pardo Sep. 1991 135 p
(AD-A246165; NPS-OC-91-004) Avail: NTIS HC/MF A07

A new generation of inexpensive GPS receivers is emerging, which utilize temperature compensated crystal oscillators (TCXO) as clocks. The MX4200 has been chosen as a representative sample of this emerging technology receiver. A detailed discussion on the receiver architecture and its implications in the measurement process is given. Experiments on the sensitivity of its clock to environmental effects, as well as the duration of the transient regime are described. One limitation to the use of these receivers in geodetic applications is the stability of its clock. The noise in the receiver clock has been characterized by the Allan variance for sampling intervals up to 4000 seconds. The implication of the noise levels for short time intervals on the applicability of the receiver to high precision work is examined. GRA

N92-26427# Carnegie-Mellon Univ., Pittsburgh, PA. Robotics Inst.
PERCEPTION FOR OUTDOOR NAVIGATION Annual Report No. 2
Charles Thorpe and Takeo Kanade Dec. 1991 95 p
(Contract DACA76-89-C-0014)
(AD-A245715; CMU-RI-TR-91-28) Avail: NTIS HC/MF A05

The contract made significant progress across a broad front on the problems of computer vision for outdoor mobile robots. New algorithms were built in neural networks, range data analysis, object recognition, and road finding. Perception modules were integrated into new systems (including on-road and off-road, notably on the new Navlab II vehicle); and there were notable programmatic events, ranging from generating two new thesis proposals to playing a major role in the 'Tiger Team', shaping the architecture for the new DARPA program in Unmanned Ground Vehicles. This report begins with a summary of the year's activities and accomplishments. Chapter 2, '3-D Landmark Recognition from Range Image', provides more detail on object recognition from multiple sensor locations. Chapter 3, 'Representation and Recovery of Road Geometry in YARF', discusses geometry issues in YARF, our symbolic road tracking system. The last two chapters discuss systems issues that are important in providing cues and constraints for an active vision approach to robot driving.' A Computational Model of Driving for Autonomous Vehicles', Chapter 4, introduces the complexities of reasoning for driving in traffic. The fifth and final chapter, 'Combining artificial neural networks and symbolic processing for autonomous robot guidance', shows how we combine neural nets with map data in a complete system. GRA

N92-26623 Stanford Univ., CA.
AN ADAPTIVE CORRECTION TECHNIQUE FOR DIFFERENTIAL GLOBAL POSITIONING SYSTEM Ph.D. Thesis
Hsing-Tung Chou 1991 155 p
Avail: Univ. Microfilms Order No. DA9205614

Accuracy and reliability are of the most important issues regarding the potential of the Global Positioning System (GPS) to become a sole means air navigation system. The purpose of this dissertation is to propose solutions to these problems. The Differential GPS (DGPS) is the most effective technique to improve the accuracy of the GPS. Many experiment results prove that the DGPS can make significant improvements. However, the current DGPS accuracy still cannot meet the ICAO category 2 approach/landing precision requirements. Thus, there is a need to explore the filtering technique to make further improvements. Low pass filters, the Hatch/Eschenbach filter, and the Kalman filter are investigated as candidate filters to improve the quality of the correction signals; the Hatch/Eschenbach filter and the Kalman filter are implemented as the user filter to smooth navigation solutions. Better accuracy can be achieved by the optimization of the DGPS filter configuration. Through static and dynamic tests, it is found that the most accurate and robust choice for DGPS is the Hatch/Eschenbach filter. It was used as both reference station correction signal filter and user's navigation filter. Using this Hatch/Eschenbach filter configuration, the accuracy under the elevation mask of 7.5 degrees is lateral-0.98 m (2 sigma); vertical-1.81 m (2 sigma); absolute positioning-2.50 m (2 sigma). One serious problem of DGPS is the latency effect, which is the accuracy degradation caused by the delay of the correction signals. It greatly reduces the DGPS system reliability. To alleviate the latency effect, an adaptive correction technique (ACT) is developed. This technique adaptively identifies the autoregressive model parameters and order of the correction signals by using a Recursive Least Squares Lattice Filter (RLSLF). Using these parameters, the delta-step predictor of the RLSLF can generate better correction signals than the existing RTCM SC-104 correction algorithm. The static test results prove that ACT is better than RTCM SC-104 when the latency is longer than 180 seconds. In addition, it is very effective to suppress the growth of positioning error for very long latency. Based on results of the current research and the GPS 21 primary satellite constellation, a DGPS-aided landing precision database is constructed. This database provides the landing precision information of various combinations of latitudes and mask angles. It is a projection of the landing precision of the DGPS implementation in this research under full operational GPS. Dissert. Abstr.

N92-26756# Naval Postgraduate School, Monterey, CA.
THE NAVIGATION DATA LOGGER FOR A SUITCASE NAVIGATION SYSTEM M.S. Thesis
Yu-Chi Chin Jun. 1991 66 p
(AD-A245997) Avail: NTIS HC/MF A04

This thesis presents the design, implementation, and description

of a Data Logger for the Suitcase Navigation System. All the programs and examples presented in this thesis were implemented in the Ada programming language, which has successfully incorporated the low level I/O ports communication with high level abstraction. The software is portable as desired and can be reused by LCCDS when needed. GRA

N92-26795# Naval Postgraduate School, Monterey, CA.
PRECISION OF THE LONG BASELINE ACOUSTIC NAVIGATION SYSTEM USED BY PEGASUS M.S. Thesis
Margaret F. Haskell Jun. 1991 109 p
(AD-A246598) Avail: NTIS HC/MF A06

A least squares algorithm is developed to solve for the trajectory and transponder array coordinates of the current velocity profiler, Pegasus. Measurement residuals and parameter precision are computed for data quality analysis. Travel times from a maximum of four seafloor transponders, pressure sensor depths, and transponder positions are input with their respective accuracy estimates. The algorithm is used to analyze a 2250 m profile from the Monterey Canyon with four transponders, one of which had not been positioned. This transponder's unknown position is found and problems in the other array coordinated identified. Transponder coordinate precision improves by factors of ten in the horizontal and five in depth, to about 13 m (DRMS) and 2 m (1 sigma) respectively. Trajectory precision is about 7 m (Drms) horizontal, with high correlation between points. Thus, the precision of horizontal velocity components, determined by time differencing points, is better than 11 cm/s (1 sigma). Depth precision is better than 3 m (1 sigma), except in the deeper portions where anomalous pressure residuals near the depth of the transponder array suggest systematic pressure errors needing further study. GRA

N92-26948# Surveillance Research Lab., Salisbury (Australia).
BUFFERED SERIAL DATA CARD
G. Fielke May 1991 35 p
(AD-A246435; SRL-0058-TM; DODA-AR-006-440) Avail: NTIS HC/MF A03

NAVSTAR Global Positioning System (GPS) User Equipments (UEs) send out navigation information in the form of blocks of serial data. The format and transmitting rate of the data varies between UEs. Several agencies within the Australian Department of Defense require the collection of GPS UE data. As a personal computer general purpose data logging card was not available commercially, it was decided to design and develop such a card to enable collection of data from any GPS UE. This card may be used to collect data from any source which transmits data at either RS232 or RS422 levels. This manual describes the operation of the Buffered Serial Data Card and the process of writing user software. GRA

05 AIRCRAFT DESIGN, TESTING AND PERFORMANCE

Includes aircraft simulation technology.

For related information see also *18 Spacecraft Design, Testing and Performance* and *39 Structural Mechanics*.For land transportation vehicles see *85 Urban Technology and Transportation*.

N92-26408# Army Missile Command, Redstone Arsenal, AL. Guidance and Control Directorate.
EFFECT OF GYRO NOISE ON ADKEM GYRO-ONLY MISSILE SYSTEM PERFORMANCE Interim Technical Report, Jan. - Mar. 1991
Vicki C. LeFevre Sep. 1991 25 p
(AD-A246150; AD-E951752; AMSMI/TR-RD-GC-91-6) Avail: NTIS HC/MF A03

This report presents results from a series of deterministic and Monte Carlo runs which indicate that the addition of three bits of noise to the sixteen bit A/D converter used with the gyros that will be mounted on the gyro-only demonstration ADKEM flight vehicles will not adversely affect system performance. These results are based on modeling the three bits of noise on the gyros and using Monte Carlo statistical analysis to quantify its effects on system performance. Author (GRA)

N92-26435*# Notre Dame Univ., IN.
GAMMA GROUP-THE PALE HORSE: A PROPOSAL IN RESPONSE TO A COMMERCIAL AIR TRANSPORTATION STUDY ORT STUDY Final Design Proposal
T. Ehler, J. Hawkins, J. Newell, M. OHara, Karl Schudt, G. Soha, and S. Vandenberg May 1991 80 p Sponsored in part by Boeing Commercial Airplane Co.
(Contract NASw-4435)
(NASA-CR-190019; NAS 1.26:190019) Avail: NTIS HC/MF A05

A conventional remotely piloted vehicle (RPV) was designed to operate in a fictional 'Aeroworld' as a 30 passenger aircraft. The topics addressed include: economic/cost analysis, aerodynamics, weight and structures, propulsion, stability and control, and performance. Author

N92-26655*# Massachusetts Inst. of Tech., Cambridge. Technology Lab. for Advanced Composites.
COMPOSITE FUSELAGE TECHNOLOGY (SUMMARY OF YEAR 2) Annual Report, 7 Apr. 1990 - 6 Apr. 1991
Michael J. Graves and Paul A. Lagace Dec. 1991 38 p
(Grant NAG1-991)
(NASA-CR-190434; NAS 1.26:190434; TELAC-91-17) Avail: NTIS HC/MF A03

The overall objective of this work is to identify and understand, via directed experimentation and analysis, the mechanisms which control the structural behavior of fuselages in their response to damage (resistance, tolerance, and arrest). A further objective is to develop straightforward design methodologies which can be employed by structural designers in preliminary design stages to make intelligent choices concerning the material, layup, and structural configuration so that a more efficient structure with structural integrity can be designed and built. Author

N92-26673# Rand Graduate Inst. for Policies Study, Santa Monica, CA.
THE LOCKHEED F-117A
Clayton K. S. Chun 1991 15 p
(RAND-P-7746-RGS) Avail: NTIS HC/MF A03

How the U.S. Air Force's F-117A tactical fighter embodies stealth technology is explored. First, a background on the aircraft is provided. Second, the F-117A's ability to avoid visual, radar, sound, and heat detection is examined. Finally, some possible policy implications for the Air Force's use of the F-117A today and in the future are investigated. Author

N92-26896# Naval Postgraduate School, Monterey, CA.
COMPUTER PROGRAM FOR CALCULATING IN-FLIGHT AIRCRAFT-STORE INTERFACE REACTION LOADS M.S. Thesis
Stephen A. Modzelewski Dec. 1991 112 p
(AD-A245782) Avail: NTIS HC/MF A06

This thesis utilizes Military Specification, Mil-A-8591H, to provide and document a new computer program for calculating store reaction forces, due to inertial loads and airloads, at the aircraft-store interface. Due to the fact that the store is a statically indeterminate structure with unknown flexibility characteristics, the analysis to calculate the reaction forces is a relatively complex problem. The program was written to incorporate new requirements and techniques for calculating reaction loads at the aircraft-store interface, in accordance with Mil-A-8591 revision H. This computer program was developed to be used on the VAX/MS Computer System. A detailed User's Manual which is included in Appendix A of this thesis was written to accompany the computer program. The computer program will enable graduate students in the Aircraft, Helicopter, and Missile Design courses to utilize current military specifications for preliminary design and weapon system integration. GRA

N92-26944# Eidgenoessisches Flugzeugwerk, Emmen (Switzerland). Abt. Aerodynamik und Flugmechanik.
SEPARATION OF EXTERNAL STORES: COMPARISON OF RESULTS
H. Affolter 12 Feb. 1991 53 p In GERMAN; ENGLISH summary
(F+W-TF-2058; ETN-92-90820) Avail: NTIS HC/MF A04

Different methods allowing prediction of the separation behavior of external stores from an aircraft are presented. The separation of two different external fuel tanks from a Mirage 3 aircraft is shown, and the results of the different methods are compared. The separation behavior predicted by wind tunnel tests and computer calculations is confirmed with good accuracy in flight tests. ESA

N92-27185# Department of the Navy, Washington, DC.
HIGH LIFT AIRCRAFT Patent
Edward E. Betts, inventor (to Navy) 10 Dec. 1991 16 p Filed 29 Nov. 1989
(AD-D015215; US-Patent-5,071,088; US-Patent-Appl-SN-453658; US-Patent-Class-244-12.1) Avail: US Patent and Trademark Office

A high lift vertical takeoff and landing aircraft has first and second fuselages connected by a central airfoil. Jet engines at the leading edge of the airfoil expel propulsive stream simultaneously over top and bottom surfaces of the foil. Extendable flaps are utilized at a trailing edge of the airfoil with a horizontal control blade being attached to the leading edge of the foil. The control blade is within the jet's propulsive stream to permit proportioning of the stream above and below the airfoil. An extendable augmenter wing is attached between the fuselages aft and above the main airfoil to permit airflow in this region to be directed downwardly, accelerating the flow and providing additional lift. The main airfoil is positioned so that the fuselage walls extend above and below the foil. Lateral flow of the main engine exhaust is restrained by these walls. Above the wing walls and airfoil create a venturi to speed airflow and decrease pressure. Below the wing the walls and extended flaps dam exhaust and ambient flow to create a high pressure region. Outboard wings provide secondary lift and reduce main wing loading. A canard is attached between the fuselages to provide pitch control. Both top and bottom canard surfaces are blown by forward mounted engines or exhaust ducts to add lift to the aircraft and to permit upward tilting of the aircraft during takeoff and landing. GRA

N92-27188 Department of the Navy, Washington, DC.
PNEUMATICALLY ACTUATED MULTIPLE STORE LAUNCHER Patent
Frank P. Marshall, inventor (to Navy) and Bruce W. Travor, inventor (to Navy) 10 Dec. 1991 6 p Filed 30 Oct. 1990
(AD-D015237; US-Patent-5,070,760; US-Patent-Appl-SN-605902; US-Patent-Class-89-1.51) Avail: US Patent and Trademark Office

The present invention discloses a pneumatically actuated, multi-store dispenser wherein a discharge of gas causes sequential launching of stores from their tandem position inside a launch container. In some environments, it is desirable to dispense multiple store, for instances sonobuoys, in dense patterns from a launch vehicle that carries an abundant supply of pneumatic gas. Due to physical limitations of space in the dispensing vehicle, an effort was made to miniaturize the active components inside the store and therefore reduce the overall outer dimensions thereof. Once the size of the store was reduced, in order to meet the demands of the denser patterns, the inside of the individual launch containers were modified to allow each to hold and dispense more than one store. This new type of launch container, in addition to maintaining the size requirement dictated by the transporting vehicle's pneumatic system. GRA

06 AIRCRAFT INSTRUMENTATION

Includes cockpit and cabin display devices; and flight instruments.

For related information see also *19 Spacecraft Instrumentation* and *35 Instrumentation and Photography.*

No abstracts in this category.

07 AIRCRAFT PROPULSION AND POWER

Includes prime propulsion systems and systems components, e.g., gas turbine engines and compressors; and onboard auxilliary power plants for aircraft.

For related information see also *20 Spacecraft Propulsion and Power, 28 Propellants and Fuels,* and *44 Energy Production and Conversion.*

N92-26405*# Georgia Tech Research Inst., Atlanta.
ACOUSTIC INTERACTIONS BETWEEN AN ALTITUDE TEST FACILITY AND JET ENGINE PLUMES: THEORY AND EXPERIMENTS Final Report, May 1990 - Oct. 1991
K. K. Ahuja, R. R. Jones, III, C. K. Tam (Florida State Univ., Tallahassee.), K. C. Massey, and A. J. Fleming Jan. 1992 162 p
(Contract NAS1-19061)
(NASA-CR-190423; NAS 1.26:190423; AD-A245463; GTRI-A8612-001; AEDC-TR-91-20) Avail: NTIS HC/MF A08

The overall objective of the described effort was to develop an understanding of the physical mechanisms involved in the flow/acoustic interactions experienced in full-scale altitude engine test facilities. This is done by conducting subscale experiments and through development of a theoretical model. Model cold jet experiments with an axisymmetric convergent nozzle are performed in a test setup that stimulates a supersonic jet exhausting into a cylindrical diffuser. The measured data consist of detailed flow visualization data and acoustic spectra for a free and a ducted plume. It is shown that duct resonance is most likely responsible by theoretical calculations. Theoretical calculations also indicate that the higher discrete tones observed in the measurements are related to the screech phenomena. Limited experiments on the sensitivity of a free 2-D, C-D nozzle to externally imposed sound are also presented. It is shown that a 2-D, C-D nozzle with a cutback is less excitable than a 2-D C-D nozzle with no cutback. At a pressure ratio of 1.5 unsteady separation from the diverging walls of the nozzle is noticed. This separation switches from one wall to the opposite wall thus providing an unsteady deflection of the plume. It is shown that this phenomenon is related to the venting provided by the cutback section. GRA

N92-26480 Purdue Univ., West Lafayette, IN.
PERFORMANCE PREDICTION AND DESIGN OF MAXIMUM THRUST PLANAR SUPERSONIC NOZZLES USING A FLUX-DIFFERENCE-SPLITTING TECHNIQUE Ph.D. Thesis
John Howard Doty 1991 292 p
Avail: Univ. Microfilms Order No. DA9201318

An analysis and computer program have been developed for the design of maximum thrust nozzles for hypersonic vehicles and applied to planar, inviscid, supersonic rotational flow of a thermally and calorically perfect gas. The flowfield analysis is accomplished by a flux-difference-splitting (FDS) technique. The nozzle wall thrust is maximized for parabolic nozzle contours using a direct search optimization procedure. Three different Riemann solvers were investigated as the basis for the FDS method. The exact Riemann solver is superior to either the approximate or the linearized-approximate Riemann solver when applied to a local Riemann problem. However, when used in the FDS method to solve an entire flowfield, numerical results with all three are comparable. The major advantage of the linearized-approximate

Riemann solver is the savings in computational time. First order accurate FDS solutions agree well with exact solutions. For the cases studied, the second order accurate FDS method was more accurate than the first order method. However, this should be weighed against the increased computation time and coding complexity. Dissert. Abstr.

N92-26553*# National Aeronautics and Space Administration. Lewis Research Center, Cleveland, OH.
A PARAMETRIC NUMERICAL STUDY OF MIXING IN A CYLINDRICAL DUCT
V. L. Oechsle, H. C. Mongia (General Motors Corp., Indianapolis, IN.), and J. D. Holdeman Jul. 1992 22 p Proposed for presentation at the 28th Joint Propulsion Conference and Exhibit, Nashville, TN, 6-8 Jul. 1992; sponsored by AIAA, SAE, ASME, and ASEE Original contains color illustrations
(RTOP 537-02-02)
(NASA-TM-105695; E-7083; NAS 1.15:105695) Copyright
Avail: NTIS HC/MF A03; 11 functional color pages

The interaction is described of some of the important parameters affecting the mixing process in a quick mixing region of a rich burn/quick mix/lean burn (RQL) combustor. The performance of the quick mixing region is significantly affected by the geometric designs of both the mixing domain and the jet inlet orifices. Several of the important geometric parameters and operating conditions affecting the mixing process were analytically studied. Parameters such as jet-to-mainstream momentum flux ratio (J), mass flow ratio (MR), orifice geometry, orifice orientation, and number of orifices/row (equally spaced) around the circumferential direction were analyzed. Three different sets of orifice shapes were studied: (1) square, (2) elongated slots, and (3) equilateral triangles. Based on the analytical results, the best mixing configuration depends significantly on the penetration depth of the jet to prevent the hot mainstream flow from being entrained behind the orifice. The structure in a circular mixing section is highly weighted toward the outer wall and any mixing structure affecting this area significantly affects the overall results. The increase in the number of orifices per row increases the mixing at higher J conditions. Higher slot slant angles and aspect ratios are generally the best mixing configurations at higher momentum flux ratio (J) conditions. However, the square and triangular shaped orifices were more effective mixing configurations at lower J conditions. Author

N92-26561*# National Aeronautics and Space Administration. Lewis Research Center, Cleveland, OH.
CFD MIXING ANALYSIS OF JETS INJECTED FROM STRAIGHT AND SLANTED SLOTS INTO CONFINED CROSSFLOW IN RECTANGULAR DUCTS
D. B. Bain, C. E. Smith (CFD Research Corp., Huntsville, AL.), and J. D. Holdeman Jul. 1992 24 p Proposed for presentation at the 28th Joint Propulsion Conference and Exhibit, Nashville, TN, 6-8 Jul. 1992; sponsored by AIAA, SAE, ASME, and ASEE Original contains color illustrations
(RTOP 537-02-20)
(NASA-TM-105699; E-7087; NAS 1.15:105699; AIAA-92-3087)
Copyright Avail: NTIS HC/MF A03; 5 functional color pages

A CFD study was performed to analyze the mixing potential of opposed rows of staggered jets injected into confined crossflow in a rectangular duct. Three jet configurations were numerically tested: (1) straight (0 deg) slots; (2) perpendicular slanted (45 deg) slots angled in opposite directions on top and bottom walls; and (3) parallel slanted (45 deg) slots angled in the same direction on top and bottom walls. All three configurations were tested at slot spacing-to-duct height ratios (S/H) of 0.5, 0.75, and 1.0; a jet-to-mainstream momentum flux ratio (J) of 100; and a jet-to-mainstream mass flow ratio of 0.383. Each configuration had its best mixing performance at S/H of 0.75. Asymmetric flow patterns were expected and predicted for all slanted slot configurations. The parallel slanted slot configuration was the best overall configuration at x/H of 1.0 for S/H of 0.75. Author

N92-26586 Rensselaer Polytechnic Inst., Troy, NY.
AN EXPERIMENTAL INVESTIGATION OF A 2-D SCRAMJET INLET AT FLOW MACH NUMBERS OF 8 TO 25 AND STAGNATION TEMPERATURES OF 800 TO 4,100 K Ph.D. Thesis
Marco Antonio SalaMinucci 1991 354 p
Avail: Univ. Microfilms Order No. DA9209274

The development of air-breathing hypersonic vehicles, such as the National Aerospace Plane (NASP) and NASP Derived Vehicles (NDV), requires the detail understanding of the physics of the hypersonic internal and external flowfields. The internal flow through the Supersonic Combustion Ramjet (scramjet) is particularly important for these vehicles since hypersonic velocities up to Mach 25 must be achieved by the use of this type of propulsion system. The limited available experimental data for the internal air flow in a scramjet inlet at high Mach numbers and stagnation temperatures motivated this study. A 0.25 m span variable geometry 2-D scramjet inlet was designed, constructed, and tested in the Rensselaer Polytechnic Institute 0.61 m diameter Hypersonic Shock Tunnel. For these tests, the flow Mach number in the test section was varied from 8 to 25 and the reservoir temperatures investigated were in the 800 - 4,100 K range. The free stream until Reynolds number varied from 1.3 x 10 exp 4 to 2.3 x 10 exp 6/m and the leading edge free stream Knudsen number was in the 0.1 - 31 range. The lower end of the reservoir temperature, 800 - 1,100 K, was generated by operating the shock tunnel in the reflected mode. On the other hand, the equilibrium interface mode of operation, with helium in the driver section, was required to produce the upper end of the stagnation temperature range of 4,100 K, with real gas effects.
Dissert. Abstr.

N92-26613*# National Aeronautics and Space Administration. Lewis Research Center, Cleveland, OH.
USE OF AN APPROXIMATE SIMILARITY PRINCIPLE FOR THE THERMAL SCALING OF A FULL-SCALE THRUST AUGMENTING EJECTOR
Wendy S. Barankiewicz, Gail P. Perusek, and Mounir B. Ibrahim (Cleveland State Univ., OH.) Jul. 1992 14 p Proposed for presentation at the 28th Joint Propulsion Conference, Nashville, TN, 6-8 Jul. 1992; sponsored by AIAA, ASME, SAE, and ASEE
(RTOP 505-62-71)
(NASA-TM-105724; E-7124; NAS 1.15:105724; AIAA-92-3792)
Avail: NTIS HC/MF A03

Full temperature ejector model simulations are expensive, and difficult to implement experimentally. If an approximate similarity principle could be established, properly chosen performance parameters should be similar for both hot and cold flow tests if the initial Mach number and total pressures of the flow field are held constant. Existing ejector data is used to explore the utility of one particular similarity principle; the Munk and Prim similarity principle for isentropic flows. Static performance test data for a full-scale thrust augmenting ejector are analyzed for primary flow temperatures up to 1560 R. At different primary temperatures, exit pressure contours are compared for similarity. A nondimensional flow parameter is then used to eliminate primary nozzle temperature dependence and verify similarity between the hot and cold flow experiments. Author

N92-26697# Oak Ridge National Lab., TN.
SIMULATION OF 3D NON-PLANAR FATIGUE CRACK GROWTH IN A TURBINE BLADE ROOT
D. O. Potyondy, A. R. Ingraffea (Cornell Univ., Ithaca, NY.), and L. J. Gray 1992 31 p Presented at the American Society of Mechanical Engineers Pressure Vessel and Piping Conference, New Orleans, LA, 21-25 Jun. 1992
(Contract DE-AC05-84OR-21400)
(DE92-006859; CONF-920631-7) Avail: NTIS HC/MF A03

A case study of fatigue life predictions for the root of a turbine blade containing an initial flaw is presented. A fracture simulation system is utilized to perform simulations of low cycle (startup/shutdown) fatigue crack growth in the root. The turbine blade has a complex structural geometry, and the cracks have

been observed to grow in a highly non-planar fashion. Simulation of these cracks requires the capability to model three dimensional geometry and to allow for arbitrary non-planar crack growth. A geometric model of the portion of the root near the crack is created. Boundary conditions for this substructure are obtained from a finite element model of the entire blade (without a crack), loaded by centrifugal forces. One approach of transferring these boundary conditions to the geometric model is described. A small initial crack is added to the geometric model, and a linear elastic boundary element analysis is performed in order to compute the stress intensity factor variation (modes 1, 2, and 3) along the crack front. The crack growth rate curve for the blade material is used along with the mode-1 stress intensity factor variation to predict the number of cycles, and new crack shape, for a user-specified increment of growth. The model is then locally remeshed for the next boundary element analysis. Comparisons with experimental fatigue tests of this same configuration are presented. DOE

N92-27037*# National Aeronautics and Space Administration. Lewis Research Center, Cleveland, OH.
INTERFACE OF AN UNCOUPLED BOUNDARY LAYER ALGORITHM WITH AN INVISCID CORE FLOW ALGORITHM FOR UNSTEADY SUPERSONIC ENGINE INLETS
Douglas Darling and Barbara Sakowski Jul. 1992 12 p Proposed for presentation at the 28th Joint Propulsion Conference and Exhibit, Nashville, TN, 6-8 Jul. 1992; sponsored by AIAA, SAE, ASME, and ASEE
(RTOP 505-62-20)
(NASA-TM-105684; E-7063; NAS 1.15:105684; AIAA-92-3083)
Avail: NTIS HC/MF A03

An uncoupled boundary layer algorithm was combined with an inviscid core flow algorithm to model flows within supersonic engine inlets. The inviscid flow algorithm that was used was the LArge Perturbation INlet Code (LAPIN). The boundary layer and inviscid core flow algorithms were formulated in different manners. The boundary layer algorithm was two dimensional and solved in nonconservation form, while the core flow algorithm was one dimensional and solved in conservation form. In order to interface the two codes, the following modifications were important. The coordinate system was set up to maintain the parabolic nature of the boundary layer algorithm while approaching the one dimensional core flow solution far from a wall. The pressure gradient used in the boundary layer equation was calculated using the core flow values and the boundary layer equations, so the boundary layer solution smoothly approached the core flow values far from the wall. Flaring was used for the advection terms perpendicular to the core flow to maintain the stability of the algorithm. With these modifications, the combined viscous/inviscid algorithm matched well with experimental observations of pressure distributions with a supersonic inlet. Author

N92-27039# Rolls-Royce Ltd., Bristol (England).
VSTOL ENGINE DESIGN EVOLUTION: GROWTH OF THE PEGASUS ENGINE FOR HARRIER
A. B. Street 1 Nov. 1990 12 p
(PNR-90805; ETN-92-90775) Copyright Avail: NTIS HC/MF A03

The Pegasus engine entered service in 1969 powering the Harrier aircraft and has been progressively developed. The operational background of the Harrier/AV8 family of aircraft was used to define a demonstrator program primarily aimed at improving performance. The XG15 demonstrator program for the Pegasus 11-61 was successfully completed in 1987 followed by durability demonstration in early 1988. The results formed the basis of the improved F402-RR-408 engine offering reduced life cycle costs at higher thrust according to prevailing operational requirements. The production engine validation test program commenced with an engine roll out in Jun. 1988, flight testing commencing at Bristol (United Kingdom) one year later with completion due in May 1990 at the same time as commencement of production engine delivery. A summary of the program and technical arisings is given. ESA

N92-27040# Rolls-Royce Ltd., Bristol (England).
ASTOVL ENGINE CONTROL
B. J. Quinn 1 Nov. 1990 7 p
(PNR-90808; ETN-92-90777) Copyright Avail: NTIS HC/MF A02

The future Advanced Short Take Off and Vertical Landing (ASTOVL) aircraft will probably require good supersonic capability and combine the attributes of the F16 aircraft with those of the Harrier, and the engine will undoubtedly be placed at the back of the aircraft. Thus the front lift nozzles mounted forward of the aircraft center of gravity, will require long ducts from the engine. To minimize hot gas injection effects and the weight of the ducting to the front lift nozzles, it is proposed that fan delivery air should be used directly. This introduces the need for a dual cycle engine configuration, unmixed for lift, mixed for propulsion, and thus for movable blocker doors to ensure that only lift or propulsive nozzles are selected. However, during mode change it is probable that fan running line control will be necessary to minimize potential surge or flutter problems. Further, the much larger separation between the front and back lift nozzles will generate potentially large pitching moments during engine modulation at various landing weights for which back lift nozzle area variation is a possible solution. Clearly control is thus becoming more sophisticated than on Harrier/Pegasus, and has certainly generated the need for extensive aircraft/engine integration studies. A possible control architecture is identified, and it is concluded that this approach is reasonable. ESA

N92-27041# Rolls-Royce Ltd., Derby (England).
ASTOVL PROPULSION SYSTEMS: CONFIGURATION AND CONCEPT CHOICE
N. A. Mitchell 1 Nov. 1990 11 p Sponsored in part by Ministry of Defence
(PNR-90809; ETN-92-90778) Copyright Avail: NTIS HC/MF A03

A wide variety of Advanced Short Takeoff and Vertical Landing (aircraft) (ASTOVL) propulsion concepts were studied against a number of different customer requirements including NST6464. These studies are reviewed with particular reference to those aspects which affect concept choice and the quality of the overall system. Once these studies were complete, a reexamination of the principal attributes of a STOVL aircraft was carried out by visiting Harrier operations on deployment both on land and at sea. This together with the results of the full scale landing simulations of an ASTOVL aircraft led to the evolution of a propulsion system for supersonic STOVL aircraft. The key elements of this propulsion system are that in the STOVL regime the propulsion system is unmixed and has the characteristics of the Pegasus (i.e., cool front jets and full nozzle vectoring) but is a mixed flow afterburning turbofan in the flight regime. The critical technologies for this propulsion system are identified and the programs required to underwrite them are outlined. The major characteristics of this propulsion system are compared with other systems and those elements which contribute to a low risk propulsion system are identified. ESA

N92-27042# Rolls-Royce Ltd., Bristol (England).
HOT-GAS REINGESTION ENGINE RESPONSE CONSIDERATIONS
D. D. Williams 1 Nov. 1990 14 p Sponsored by Ministry of Defence
(PNR-90810; ETN-92-90779) Copyright Avail: NTIS HC/MF A03

Some of the fundamentals of hot gas reingestion in the context of engine stability are reviewed. Generic time variant total temperature distortion descriptors are discussed against a background of external work and of small and full scale experience from simulated vertical landings of an augmented Pegasus/Harrier vectored thrust installation. Results are presented of compression system component and overall engine simulations intended to provide guidelines to engine total temperature distortion sensitivity and stability margin assessment. ESA

N92-27043# Rolls-Royce Ltd., Derby (England).
SIMULTANEOUS ENGINEERING IN AERO-GAS TURBINE DESIGN AND MANUFACTURE
T. Broughton 15 Nov. 1990 13 p
(PNR-90811; ETN-92-90780) Copyright Avail: NTIS HC/MF A03

The increasingly competitive world in which manufacturing companies now operate imposes rigorous requirements in bringing the right product at the right price to the market place. Aerogas turbines are an example of a product which is extremely complex in terms of design, manufacture and development and, hence, they provide an enormous challenge to the management of their engineering and manufacturing processes. Simultaneous engineering is seen as a means of managing engineering activities to achieve a competitive advantage. The manner in which simultaneous engineering has been implemented within the company is highlighted. ESA

N92-27062# Royal Aircraft Establishment, Farnborough (England).
THE CHANGING ROLE OF EXPERIMENTATION IN AEROENGINE R AND D: THE POINT OF VIEW OF THE RESEARCH WORKER
J. Dunham Nov. 1991 19 p
(AD-A246372; RAE-TM-P1216; DRIC-BR-307984) Avail: NTIS HC/MF A03

The pioneers of the gas turbine based their components designs on simple mathematical models which employed many empirical factors. They conducted two types of experiment: Trials of engines and components, to develop their mechanical integrity and endurance, and to improve their performance and stability (development tests), and Parametric experiments on simplified components or simulated component geometries, to evolve better models and to generate empirical correlations of component behavior (research tests). Fifty years later, the same need for development tests remains, but as design methods have evolved from simple empirical models to complex computational fluid dynamics (CFD) models, the nature of research tests has changed. There is still a need for experiments aimed at evolving better mathematical models, but the empiricism is at a more detailed level (such as transition prediction) and so are the experiments. But component testing has moved away from a parameter variation to tests aimed at the development and verification of better CFD models. Meanwhile, instrumentation techniques have also improved a great deal, enabling more accurate and detailed measurements. GRA

08 AIRCRAFT STABILITY AND CONTROL

Includes aircraft handling qualities; piloting; flight controls; and autopilots.

For related information see also *05 Aircraft Design, Testing and Performance.*

No abstracts in this category.

09 RESEARCH AND SUPPORT FACILITIES (AIR)

Includes airports, hangars and runways; aircraft repair and overhaul facilities; wind tunnels; shock tubes; and aircraft engine test stands.

For related information see also *14 Ground Support Systems and Facilities (Space).*

N92-26527# Aerospace Medical Research Labs., Brooks AFB, TX.
MICROCOMPUTER-BASED INSTRUMENT FLIGHT SIMULATION: UNDERGRADUATE PILOT TRAINING STUDENT ATTITUDE ASSESSMENT Final Report, Jan. - Feb. 1991
Brian K. Rogers Dec. 1991 23 p
(AF Proj. 1123)
(AD-A245449; AL-TR-1991-0039) Avail: NTIS HC/MF A03

The purpose of this investigation was to assess United States Air Force (USAF) Undergradate Pilot Training (UPT) student attitudes toward using a T-37 tailored personal computer (PC) or microcomputer-based simulation as an addition to the formal training syllabus. Eight student classes were surveyed in Phases 1 and 2 of the three phases of UPT. As hypothesized the UPT students were most receptive to using a microcomputer simulation for instrument training after having completed both instrument academics and the initial instrument simulator missions. Only 36 pct. of the students starting UPT were likely to use a microcomputer simulation to replace 75 pct. or more of their chair-flying, compared to 51.4 pct. of the students who had completed an instrument simulator sortie. On the average, UPT students having completed 12106 (two sorties prior to the instrument check ride) said they would use a microcomputer simulation on a daily basis to enhance their training. After attempting to learn the instrument procedures, students indicated they were eager to use a microcomputer simulation. It was demonstrated that, in general, UPT students are sensitive to their difficulties in learning instrument procedures and are willing to replace chair-flying with a microcomputer simulation. GRA

N92-26720# Los Alamos National Lab., NM.
AN EXPLOSIVELY DRIVEN, FAST SHOCK TUBE
T. H. Tan and S. Marsh 1992 9 p Presented at the 2nd International Symposium on Intense Dynamic Loading and Its Effects, Chengdu, China, 9-12 Jun. 1992
(Contract W-7405-eng-36)
(DE92-008437; LA-UR-92-356; CONF-920688-7) Avail: NTIS HC/MF A02

A simple, cylindrically configured fast shock tube (FST) has been employed as a tool to investigate the hydrodynamics of plate drive under a very high impulse loading condition. The shock tube has a high explosive outer shell and a low density foam core. The implosion produces a well defined Mach disk that is then subsequently used to drive a metallic plate. A thin stainless steel (SS) plate has been successfully launched to 9 km/s with this device. The experimental results from the study of material flow will be presented and compared with numerical calculation. Various interesting measurement techniques will also be discussed. DOE

12 ASTRONAUTICS (GENERAL)

For extraterrestrial exploration see *91 Lunar and Planetary Exploration.*

N92-26192# RAND Corp., Santa Monica, CA.
APOGEE, PERIGEE, AND RECOVERY: CHRONOLOGY OF ARMY EXPLOITATION OF SPACE
Eddie Mitchell 1991 178 p
(Contract MDA903-86-C-0059)
(RAND-N-3103-A) Avail: NTIS HC/MF A09

This study was conducted in RAND's Arroyo Center by an Army Fellow working within the Applied Technology program. The

research is associated with and contributes to a continuing series of products on the 'Army Exploitation of Space'. This Note should be of interest to military or civilian personnel seeking a systemic understanding of the ground service's development and application of space in the technology areas of long-range missiles, satellites, ground stations, and ballistic missile defense. Author

N92-26818# Brookhaven National Lab., Upton, NY.
HUMAN ROUND TRIP TO MARS: SIX MONTHS AND RADIATION SAFE
O. W. Lazareth, E. Schmidt, H. Ludewig, and J. R. Powell 1991 12 p Presented at the 9th Symposium on Space Nuclear Power Systems, Albuquerque, NM, 13-16 Jan. 1992
(Contract DE-AC02-76CH-00016)
(DE92-010160; BNL-46287-Rev; CONF-920104-6-Rev) Avail: NTIS HC/MF A03

We describe a different type of round trip to Mars, using a combination of spacecraft. Compared to typical proposals, this flight is relatively fast and relatively safe from biological radiation dosage. Our study is concerned with the trip from Earth orbit to Mars orbit. Four spacecraft are required for the round trip. The crew spends most of their time on board a comparatively large, well shielded spacecraft (LC) which is in free (non-powered) orbit about the sun. The crew travels from Earth orbit to the LC while on board a comparatively small, powered spacecraft (SC). At Mars, the procedure is reversed and the crew returns on a second LC. In addition, a cargo craft, with no crew, is sent to Mars prior to the crew leaving Earth orbit. The trip time is about six months and the radiation dose equivalent is within guidelines recommended by the National Commission on Radiation Protection and Measurements. DOE

N92-27008# Futuro S.R.L., Florence (Italy).
MULTI-CULTURAL COMPONENTS AND KEYS FOR EUROPEAN WORLDWIDE SPACE PROGRAMS
Roberto Pinotti *In* ESA, 4th European Symposium on Space Environmental Control Systems, Volume 2 Dec. 1991 p 1021-1023 (For primary document see N92-26950 17-54)
Avail: NTIS HC/MF A23; ESA, EPD, ESTEC, Noordwijk, Netherlands, HC 150 Dutch guilders (2 vols)

13 ASTRODYNAMICS

Includes powered and free-flight trajectories; and orbital and launching dynamics.

N92-26268*# National Aeronautics and Space Administration. Marshall Space Flight Center, Huntsville, AL.
REPORT FOR NEUTRAL BUOYANCY SIMULATIONS OF TRANSFER ORBIT STAGE CONTINGENCY EXTRAVEHICULAR ACTIVITIES
J. D. Sexton Jun. 1992 66 p
(NASA-TM-103583; NAS 1.15:103583) Avail: NTIS HC/MF A04

The transfer orbit stage (TOS) will propel the advanced communications technology satellite (ACTS) from the Space Shuttle to an Earth geosynchronous transfer orbit. Two neutral buoyancy test series were conducted at MSFC to validate the extravehicular activities (EVA) contingency operations for the ACTS/TOS/mission. The results of the neutral buoyancy tests are delineated and a brief history of the TOS EVA program is given. Author

14 GROUND SUPPORT SYSTEMS AND FACILITIES (SPACE)

Includes launch complexes, research and production facilities; ground support equipment, e.g., mobile transporters; and simulators.

For related information see also *09 Research and Support Facilities (Air).*

No abstracts in this category.

15 LAUNCH VEHICLES AND SPACE VEHICLES

Includes boosters; operating problems of launch/space vehicle systems; and reusable vehicles.

For related information see also *20 Spacecraft Propulsion and Power.*

N92-26402# Naval Postgraduate School, Monterey, CA.
A COMPARISON OF HEAVY LIFT LAUNCH VEHICLE OPTIONS FOR THE 1990S M.S. Thesis
Jonathan K. Schreiber Sep. 1991 76 p
(AD-A245617) Avail: NTIS HC/MF A05

This thesis compares attributes of the heavy lift launch vehicle options that are available for the United States to use in support of the Space Exploration Initiative. The systems compared are the Advanced Launch System, Shuttle-C, Saturn V/F-1 and Energia. The F-1 development history is presented along with the proposed development of the ALS and Shuttle-C. Advantages and disadvantages of each of the systems are presented and possible trade-offs between them are discussed. The thesis shows that the option that is most cost effective and can be used to support the deployment of Space Station Freedom is that of developing a booster with a core engine like the F-1. In conclusion, a recommendation is given as to what the best option, with regard to both short and long term mission requirements, is for a new heavy lift launch vehicle for the United States. GRA

N92-26515# Naval Postgraduate School, Monterey, CA.
A PROTOTYPE MULTI-MEDIA DATA BASE FOR TRACKING INTERFACE RELATIONSHIPS AND PERFORMING COST TRADEOFFS FOR THE SEA LAUNCH AND RECOVERY (SEALAR) SPACE LAUNCH SYSTEM M.S. Thesis
Joseph F. Mark Sep. 1991 101 p
(AD-A245481) Avail: NTIS HC/MF A06

This thesis develops a prototype multimedia database from which interface relationships and cost tradeoffs in the early stage and development of the Sea Launch and Recovery System (SEALAR) program can be rapidly and easily explored and evaluated. This prototype is developed employing HyperCard/Macintosh and demonstrates the feasibility of employing off the shelf technology to solve real world problems. The goal of attaining a cost effective system for access to space is thereby enhanced and brought one step closer to reality. Implementation issues are discussed and evaluated along with possible future enhancements to the model. Author (GRA)

N92-26693# Los Alamos National Lab., NM.
NUMERICAL SIMULATIONS OF GUN-LAUNCHED KINETIC ENERGY PROJECTILES SUBJECTED TO ASYMMETRIC PROJECTILE BASE PRESSURE
D. A. Rabern 1991 9 p Presented at the Symposium on Ballistics, Stockholm, Sweden, 1-3 Jun. 1992
(Contract W-7405-eng-36)
(DE92-005065; LA-UR-91-3988; CONF-920689-1) Avail: NTIS HC/MF A02

Three dimensional numerical simulations were performed to determine the effect of an asymmetric base pressure on kinetic

energy projectiles during launch. A matrix of simulations was performed in two separate launch environments. One launch environment represented a severe lateral load environment, while the other represented a nonsevere lateral load environment based on the gun tube straightness. The orientation of the asymmetric pressure field, its duration, the projectile's initial position, and the tube straightness were altered to determine the effects of each parameter. The pressure asymmetry translates down the launch tube to exit parameters and is washed out by tube profile. Results from the matrix of simulations are presented. DOE

N92-27013# European Space Agency. European Space Research and Technology Center, ESTEC, Noordwijk (Netherlands).
WINGED LAUNCHER THERMAL DESIGN ASPECTS
K. Keller *In its* 4th European Symposium on Space Environmental Control Systems, Volume 2 Dec. 1991 p 1051-1056 (For primary document see N92-26950 17-54)
Avail: NTIS HC/MF A23; ESA, EPD, ESTEC, Noordwijk, Netherlands, HC 150 Dutch guilders (2 vols)

16 SPACE TRANSPORTATION

Includes passenger and cargo space transportation, e.g., shuttle operations; and space rescue techniques.

For related information see also *03 Air Transportation and Safety* and *18 Spacecraft Design, Testing and Performance.* For space suits see *54 Man/System Technology and Life Support.*

N92-26884*# Sandia National Labs., Albuquerque, NM. Parachute Systems Div.
CRITICAL SOFT LANDING TECHNOLOGY ISSUES FOR FUTURE US SPACE MISSIONS Final Report
J. M. Macha, D. W. Johnson, and D. D. McBride Jan. 1992 26 p
(NASA Order T-9317R)
(NASA-CR-185673; NAS 1.26:185673) Avail: NTIS HC/MF A03

A programmatic need for research and development to support parachute-based landing systems has not existed since the end of the Apollo missions in the mid-1970s. Now, a number of planned space programs require advanced landing capabilities for which the experience and technology base does not currently exist. New requirements for landing on land with controllable, gliding decelerators and for more effective impact attenuation devices justify a renewal of the landing technology development effort that existed during the Mercury, Gemini, and Apollo programs. A study was performed to evaluate the current and projected national capability in landing systems and to identify critical deficiencies in the technology base required to support the Assured Crew Return Vehicle and the Two-Way Manned Transportation System. A technology development program covering eight landing system performance issues is recommended. Author

17 SPACE COMM., SPACECRAFT COMM., COMMAND & TRACKING

Includes telemetry; space communications networks; astronavigation and guidance; and radio blackout.

For related information see also *04 Aircraft Communications and Navigation* and *32 Communications and Radar.*

N92-26621# Naval Postgraduate School, Monterey, CA.
DEVELOPMENT AND TESTING OF AN UNMANNED AIR VEHICLE TELEMETRY SYSTEM M.S. Thesis
Kevin T. Wilhelm Sep. 1991 83 p
(AD-A246577) Avail: NTIS HC/MF A05

Unmanned air vehicles (UAV's) provide a low-cost, low-maintenance, and effective platform upon which experimentation can be performed to validate conceptual aerodynamic ideas. However, the UAV flight test data acquisition process is complex and requires a reliable recording system for post-flight data analysis. The thrust of this thesis was the development, construction, and validation of a viable telemetry system for data gathering and processing. Major areas of focus were: integration of the telemetry into a 1/8 scale model, radio controlled F-16A airplane; telemetry circuitry optimization; recording and display of instrumented parameters; and data reduction techniques necessary to obtain useful information. A flight test was flown and data was gathered using a steady-heading side-slip maneuver to demonstrate successful integration of all supporting elements. GRA

N92-26667*# National Aeronautics and Space Administration. Goddard Space Flight Center, Greenbelt, MD.
SMALL EXPLORER DATA SYSTEM MIL-STD-1773 FIBER OPTIC BUS
Mark Flanegan and Ken LaBel Jun. 1992 30 p
(NASA-TP-3227; NAS 1.60:3227; Rept-92B00041) Avail: NTIS HC/MF A03

The MIL-STD-1773 Fiber Optic Data Bus as implemented in the GSFC Small Explorer Data System (SEDS) for the Small Explorer Program is described. It provides an overview of the SEDS MIL-STD-1773 bus components system design considerations, reliability figures, acceptance and qualification testing requirements, radiation requirements and tests, error handling considerations, and component heritage. The first mission using the bus will be launched in June of 1992. Author

18 SPACECRAFT DESIGN, TESTING AND PERFORMANCE

Includes satellites; space platforms; space stations; spacecraft systems and components such as thermal and environmental controls; and attitude controls.

For life support systems see *54 Man/System Technology and Life Support.* For related information see also *05 Aircraft Design, Testing and Performance, 39 Structural Mechanics,* and *16 Space Transportation.*

N92-26605# Naval Postgraduate School, Monterey, CA.
INVESTIGATION OF DEEP DIELECTRIC CHARGING AND SUBSEQUENT CURRENTS ON GEOSYNCHRONOUS SPACECRAFT M.S. Thesis
Donald S. Smith Dec. 1991 94 p
(AD-A245764) Avail: NTIS HC/MF A05

Deep dielectric charging is the suspected mechanism for formation of potential barriers aboard the ISEE 1 spacecraft. Energetic electron distribution functions in the plasmasheet were examined for both surface and deep dielectric charging. Surface charging was found to be dependent on whether the satellite surfaces were in shadow. The surface potential is regulated by photoelectric emission, and is two orders of magnitude higher than other mechanisms. Deep dielectric charging deposits charge within dielectrics, and are independent of surface effects, such as photoemission and radiation-induced conductivity. Deposition of electrons into solar array cover cells begins at approximately 10 keV. GRA

N92-26610 Auburn Univ., AL.
OPTIMIZATION OF SPACE STRUCTURES TO MINIMIZE DYNAMIC RESPONSE Ph.D. Thesis
Dhaneshkumar Narasim Manikanahally 1991 176 p
Avail: Univ. Microfilms Order No. DA9201246

The scope for minimizing vibration response of space structures by optimization was examined. The space structures were modeled as hysteretically damped mass-loaded beam systems. Optimization consisted of optimizing the structure and in addition attaching optimized vibration absorbers. The vibration absorbers vibrating out phase with the structure minimize the vibration response of the structure. The investigation was both theoretical and experimental. The theoretical investigation consisted of modeling a large space structure as a mass-loaded beam. Optimization of

this simplified model and attaching optimized vibration absorbers resulted in a significantly lower response in comparison to a model designed without optimization and optimized vibration absorbers. The experimental investigation was conducted on a cantilever beam loaded with two masses. The focus of the investigation was to verify the natural frequencies of the beam system obtained from theory, to measure the hysteretic damping factor of the beam system and to design, fabricate and test the use of vibration absorbers. The experimental results were in good agreement with the theoretical prediction. The measured response of the beam system with vibration absorbers shows that absorbers can significantly reduce vibration response. Dissert. Abstr.

N92-27030# Naval Postgraduate School, Monterey, CA.
KALMAN SMOOTHER APPLIED TO LACE M.S. Thesis
Frank R. Thorngren Dec. 1991 58 p
(AD-A246439) Avail: NTIS HC/MF A04

The ability to determine the structural dynamics of space-based platforms from ground-based radar resolved Doppler measurements will aid in the study of control/structure interaction. The Naval Research Laboratory and Lincoln Laboratory conducted an experiment to determine the feasibility of this method. To accomplish this experiment the LACE satellite was equipped with retroreflectors and the ground-based Firepond laser radar facility was employed. Vibrational information is found from the difference between the reflected Doppler frequencies of the retroreflectors. The method of extracting the Doppler separation was to obtain the power spectrum of the heterodyne signal envelope. A pulse-by-pulse processing of the data yields the Doppler separation history over time. Due to a relatively large amount of clutter in the processed data, a filtering mechanism was employed. The histogram technique is the current filtering-based method employed to obtain a Doppler separation history. This thesis addresses the implementation of the Kalman filter algorithm in conjunction with the Rauch-Tung-Striebel fixed-interval optimal smoother algorithm to perform this filtering task. The Kalman smoother filtering based method of processing the data produced superior results when compared with the histogram filtering based method. GRA

N92-27074# Naval Postgraduate School, Monterey, CA.
ORBITAL MAINTENANCE OF ENDOATMOSPHERIC LOW EARTH-ORBITING SATELLITES M.S. Thesis
David D. Pauls Dec. 1991 63 p
(AD-A246381) Avail: NTIS HC/MF A04

The optimization of spacecraft trajectories in vacuum has received extensive consideration since the inception of space flight, yet, the effects of atmosphere have been largely neglected. The advent of low Earth-orbiting, large satellites and platforms necessitates that atmosphere be included in the optimization process. A practical means of studying this topic is as a problem in minimum-fuel orbital maintenance. Optimal control theory advances the notion that orbital maintenance is optimized through periodic thrusting as opposed to forcing Keplarian motion by nullifying the effects of drag with thrust. Further, this must be optimized by primer vectoring. This thesis examined the efficiency of a simple method of orbital maintenance using fixed-angle transverse thrusting. Results show that for the purpose of fuel-minimization, the width of the radial band in which the satellite is to be maintained, is dependent upon thruster size. In nearly all cases, a thrust-angle of 70 degs maximized the fuel saved. This thesis shows that fixed-angle transverse thrusting does not improve on forced Keplarian motion and hence thrust vectoring must be optimized. GRA

N92-26965# Teledyne Brown Engineering, Huntsville, AL.
DESIGN AND PERFORMANCE OF THE SPACELAB ASTRO-1 MISSION HEAT PIPE RADIATOR
Richard M. Hamner and Linda S. Hornsby *In* ESA, 4th European Symposium on Space Environmental Control Systems, Volume 2 Dec. 1991 p 721-728 (For primary document see N92-26950 17-54)
Avail: NTIS HC/MF A23; ESA, EPD, ESTEC, Noordwijk, Netherlands, HC 150 Dutch guilders (2 vols)

N92-26966# Centre National d'Etudes Spatiales, Toulouse (France).
SIGMA VCHP RADIATOR: IN-ORBIT PERFORMANCE
Joel Gayrard *In* ESA, 4th European Symposium on Space Environmental Control Systems, Volume 2 Dec. 1991 p 729-733 (For primary document see N92-26950 17-54)
Avail: NTIS HC/MF A23; ESA, EPD, ESTEC, Noordwijk, Netherlands, HC 150 Dutch guilders (2 vols)

N92-26967# Aerospatiale, Cannes (France).
DEVELOPMENT OF FLUID LOOP AND HYBRID RADIATORS: TEST RESULTS
M. Amidieu and T. Maciaszek *In* ESA, 4th European Symposium on Space Environmental Control Systems, Volume 2 Dec. 1991 p 735-740 Prepared in cooperation with Centre National d'Etudes Spatiales, Toulouse, France (For primary document see N92-26950 17-54)
Avail: NTIS HC/MF A23; ESA, EPD, ESTEC, Noordwijk, Netherlands, HC 150 Dutch guilders (2 vols)

N92-26968# Akademiya Nauk BSSR, Minsk. Heat and Mass Transfer Inst.
HEAT PIPE-BASED RADIATIVE PANEL
L. L. Vasiliev, L. E. Kanonchik, D. K. Khrustalev, and V. A. Babenko *In* ESA, 4th European Symposium on Space Environmental Control Systems, Volume 2 Dec. 1991 p 741-745 (For primary document see N92-26950 17-54)
Avail: NTIS HC/MF A23; ESA, EPD, ESTEC, Noordwijk, Netherlands, HC 150 Dutch guilders (2 vols)

N92-26970# Erno Raumfahrttechnik G.m.b.H. Bremen (Germany, F.R.).
BATTERY THERMAL CONTROL OF THE COLUMBUS FREE FLYER
B. Miedza, A. Lanteri, and P. Moeller (Dornier System G.m.b.H., Friedrichshafen, Germany, F.R.) *In* ESA, 4th European Symposium on Space Environmental Control Systems, Volume 2 Dec. 1991 p 755-759 (For primary document see N92-26950 17-54)
Avail: NTIS HC/MF A23; ESA, EPD, ESTEC, Noordwijk, Netherlands, HC 150 Dutch guilders (2 vols)

N92-26971# Erno Raumfahrttechnik G.m.b.H. Bremen (Germany, F.R.).
THERMAL ANALYSIS OF THE SPACELAB MISSION D2 UTILITY SUPPORT STRUCTURE AND ITS PAYLOADS
W. Wessels *In* ESA, 4th European Symposium on Space Environmental Control Systems, Volume 2 Dec. 1991 p 761-767 (For primary document see N92-26950 17-54)
Avail: NTIS HC/MF A23; ESA, EPD, ESTEC, Noordwijk, Netherlands, HC 150 Dutch guilders (2 vols)

N92-26996# Alenia Spazio S.p.A., Rome (Italy).
ITALSAT THERMAL CONTROL: THE IN-ORBIT PERFORMANCES
Marco Giommi, Stefano Liverani, and Enrico Sacchi *In* ESA, 4th European Symposium on Space Environmental Control Systems, Volume 2 Dec. 1991 p 931-937 (For primary document see N92-26950 17-54)
Avail: NTIS HC/MF A23; ESA, EPD, ESTEC, Noordwijk, Netherlands, HC 150 Dutch guilders (2 vols)

N92-26997# Dornier System G.m.b.H., Friedrichshafen (Germany, F.R.).
ROSAT: MEASURED TEMPERATURES VERSUS THERMAL ANALYSIS RESULTS
Albert Braig and Peter Pawlowski (Deutsche Agentur fuer Raumfahrtangelegenheiten G.m.b.H., Bonn, Germany, F.R.) *In* ESA, 4th European Symposium on Space Environmental Control Systems, Volume 2 Dec. 1991 p 939-944 (For primary document see N92-26950 17-54)
Avail: NTIS HC/MF A23; ESA, EPD, ESTEC, Noordwijk, Netherlands, HC 150 Dutch guilders (2 vols)

N92-26998# Centre National d'Etudes Spatiales, Toulouse (France).
SPOT MULTIMISSION PLATFORM THERMAL CONTROL: FIVE YEARS OF IN-FLIGHT RESULTS
Irenee Alet *In* ESA, 4th European Symposium on Space Environmental Control Systems, Volume 2 Dec. 1991 p 945-949 (For primary document see N92-26950 17-54)
Avail: NTIS HC/MF A23; ESA, EPD, ESTEC, Noordwijk, Netherlands, HC 150 Dutch guilders (2 vols)

N92-26999# Fokker Space and Systems, Amsterdam (Netherlands).
ULYSSES, ONE YEAR AFTER THE LAUNCH
H. Petersen *In* ESA, 4th European Symposium on Space Environmental Control Systems, Volume 2 Dec. 1991 p 951-956 (For primary document see N92-26950 17-54)
Avail: NTIS HC/MF A23; ESA, EPD, ESTEC, Noordwijk, Netherlands, HC 150 Dutch guilders (2 vols)

N92-27000# All-Union Research Inst. of Electromechanics, Moscow (USSR).
FLIGHT TEST RESULTS OF THE PASSIVE COOLING SYSTEM
A. I. Abrosimov, O. V. Baryshev, V. A. Khoronenko, and U. G. Furdak *In* ESA, 4th European Symposium on Space Environmental Control Systems, Volume 2 Dec. 1991 p 957-959 (For primary document see N92-26950 17-54)
Avail: NTIS HC/MF A23; ESA, EPD, ESTEC, Noordwijk, Netherlands, HC 150 Dutch guilders (2 vols)

N92-27014# European Space Agency. Centre Spatial de Toulouse (France).
WARM STRUCTURES AND THERMAL PROTECTION OF THE EUROPEAN SPACEPLANE HERMES [STRUCTURES CHAUDES ET PROTECTIONS THERMIQUES DE L'AVION SPATIAL EUROPEEN HERMES]
J. P. Vialaneix, E. Werling, and J. C. Verneuil (Centre Spatial Dassault, Blagnac, France) *In its* 4th European Symposium on Space Environmental Control Systems, Volume 2 Dec. 1991 p 1057-1064 In FRENCH (For primary document see N92-26950 17-54)
Avail: NTIS HC/MF A23; ESA, EPD, ESTEC, Noordwijk, Netherlands, HC 150 Dutch guilders (2 vols)

N92-27024# Progetto Area, Rome (Italy).
INFLUENCE OF ARCHITECTURE ON THE DEFINITION OF A SPACE STATION CONFIGURATION
Luca Bradini and Luca Galofaro (Rome Univ., Italy) *In* ESA, 4th European Symposium on Space Environmental Control Systems, Volume 2 Dec. 1991 p 1137-1140 (For primary document see N92-26950 17-54)
Avail: NTIS HC/MF A23; ESA, EPD, ESTEC, Noordwijk, Netherlands, HC 150 Dutch guilders (2 vols)

N92-27028# European Space Agency. European Space Research and Technology Center, ESTEC, Noordwijk (Netherlands).
HEATSHIELD CONCEPTS FOR THE ROSETTA AEROCAPSULE
M. Eiden, D. Desnoyer, C. Chiarelli (Alenia Spazio S.p.A., Rome, Italy), and A. Smith *In its* 4th European Symposium on Space Environmental Control Systems, Volume 2 Dec. 1991 p 1163-1173 (For primary document see N92-26950 17-54)
Avail: NTIS HC/MF A23; ESA, EPD, ESTEC, Noordwijk, Netherlands, HC 150 Dutch guilders (2 vols)

N92-27116*# National Aeronautics and Space Administration. Marshall Space Flight Center, Huntsville, AL.
THERMAL CONTROL SURFACES EXPERIMENT FLIGHT SYSTEM PERFORMANCE
Donald R. Wilkes, Leigh L. Hummer (AZ Technology, Huntsville, AL.), and James M. Zwiener *In* NASA. Langley Research Center, LDEF: 69 Months in Space. First Post-Retrieval Symposium, Part 3 Jan. 1992 p 1577-1591 (For primary document see N92-27083 17-99)
Avail: NTIS HC/MF A21; 1 functional color page

N92-27129*# American Space Technology, Inc., Santa Monica, CA.
RETRIEVABLE PAYLOAD CARRIER: NEXT GENERATION LONG DURATION EXPOSURE FACILITY
Arthur T. Perry *In* NASA. Langley Research Center, LDEF: 69 Months in Space. First Post-Retrieval Symposium, Part 3 Jan. 1992 p 1691-1700 (For primary document see N92-27083 17-99)
Avail: NTIS HC/MF A21; 1 functional color page

19 SPACECRAFT INSTRUMENTATION

For related information see also *06 Aircraft Instrumentation* and *35 Instrumentation and Photography.*

N92-26973# Alenia Spazio S.p.A., Turin (Italy).
THERMAL DESIGN FOR THE SPACE-EXPOSED INSTRUMENTS FOR THE SCIENTIFIC SATELLITE SAX
Gaetano Poidomani and Gianfranco Bonino *In* ESA, 4th European Symposium on Space Environmental Control Systems, Volume 2 Dec. 1991 p 775-778 (For primary document see N92-26950 17-54)
Avail: NTIS HC/MF A23; ESA, EPD, ESTEC, Noordwijk, Netherlands, HC 150 Dutch guilders (2 vols)

20 SPACECRAFT PROPULSION AND POWER

Includes main propulsion systems and components, e.g., rocket engines; and spacecraft auxilliary power sources.

For related information see also *07 Aircraft Propulsion and Power, 28 Propellants and Fuels, 44 Energy Production and Conversion,* and *15 Launch Vehicles and Space Vehicles.*

N92-26362# Naval Postgraduate School, Monterey, CA.
SOLID FUEL RAMJET INFRARED SIGNATURE M.S. Thesis
Russell P. Luehrsen Dec. 1991 76 p
(AD-A246299) Avail: NTIS HC/MF A05

The objective of the thesis was to determine the effects of equivalence ratio and fuel composition on the infrared signature of solid fueled ramjets (SFRJ). Solid fuels investigated were Plexiglas, HTPB, and HTPB with aluminum, silicon, boron carbide, and or magnesium. They were tested at chamber pressures of 80-170 psia and with equivalence ratios between 0.3 and 1.4. With the plume emissivity set to 1.0, plume irradiance was found to increase approximately with the second power of the actual combustor stagnation temperature. In addition to providing needed plume signature data for the SFRJ, this information can be used to validate numerical predictions from the SPF (Standardized Plume Flowfield) and SIRRM (Standardized Infrared Radiation Model) computer codes, which are used to predict the plume infrared signature. GRA

N92-26601 Case Western Reserve Univ., Cleveland, OH.
HEAT RECEIVERS FOR SOLAR DYNAMIC SPACE POWER SYSTEMS Ph.D. Thesis
Marla Esther Perez-Davis 1991 175 p
Avail: Univ. Microfilms Order No. DA9202231

A review of state-of-the-art technology is presented and discussed for phase change materials. Some of the advanced solar dynamic designs developed as part of the Advanced Heat Receiver Conceptual Design Study performed for LeRC are discussed. The heat receivers are analyzed and several recommendations are proposed, including two new concepts. The first concept evaluated the effect of tube geometries inside the heat receiver. It was found that a triangular configuration would provide better heat transfer to the working fluid, although not necessarily with a reduction in receiver size. A sensible heat receiver considered in this study uses vapor grown graphite fiber-carbon (VGCF/C) composite as the thermal storage media

and was designed for a 7 kW Brayton engine. The proposed heat receiver stores the required energy to power the system during eclipse in the VGCF/C composite. The heat receiver analysis was conducted through the Systems Improved Numerical Differencing Analyzer and Fluid Integrator (SINDA) software package. The proposed heat receiver compares well with other latent and advanced sensible heat receivers while avoiding the problems associated with latent heat storage salts and liquid metal heat pipes. The weight and size of the system can be optimized by changes in geometry and technology advances for this new material. In addition to the new concepts, the effect of atomic oxygen on several materials is reviewed. A test was conducted for atomic oxygen attack on boron nitride, which experienced a negligible mass loss when exposed to an atomic oxygen fluence of 5 x 10 exp 21 atoms/sq cm. This material could be used to substitute the graphite aperture plate of the heat receiver.
Dissert. Abstr.

N92-26654*# National Aeronautics and Space Administration. Lewis Research Center, Cleveland, OH.
HEAT TRANSFER IN OSCILLATING FLOWS WITH SUDDEN CHANGE IN CROSS SECTION
Mounir Ibrahim, Waqar Hashim (Cleveland State Univ., OH.), Roy C. Tew, and James E. Dudenhoefer 1992 8 p Proposed for presentation at the 27th Intersociety Energy Conversion Engineering Conference, San Diego, CA, 3-7 Aug. 1992; sponsored by SAE, ACS, AIAA, ASME, IEEE, AIChE, and ANS
(RTOP 590-13-11)
(NASA-TM-105692; E-7077; NAS 1.15:105692) Avail: NTIS HC/MF A02

Oscillating fluid flow (zero mean) with heat transfer, between two parallel plates with a sudden change in cross section, was examined computationally. The flow was assumed to be laminar and incompressible with inflow velocity uniform over the channel cross section but varying sinusoidally with time. Over 30 different cases were examined; these cases cover wide ranges of Re sub max (187.5 to 30000), Va (1 to 350), expansion ratio (1:2, 1:4, 1:8, and 1:12) and A sub r (0.68 to 4). Three different geometric cases were considered (asymmetric expansion and/or contraction, symmetric expansion/contraction, and symmetric blunt body). The heat transfer cases were based on constant wall temperature at higher (heating) or lower (cooling) value than the inflow fluid temperature. As a result of the oscillating flow, the fluid undergoes sudden expansion in one half of the cycle and sudden contraction in the other half. One heating case is examined in detail, and conclusions are drawn from all the cases (documented in detail elsewhere). Instantaneous friction factors and heat transfer coefficients, for some ranges of Re sub max and Va, deviated substantially from those predicted with steady state correlations.
Author

N92-26792*# National Aeronautics and Space Administration. Lewis Research Center, Cleveland, OH.
NASA/DOE/DOD NUCLEAR PROPULSION TECHNOLOGY PLANNING: SUMMARY OF FY 1991 INTERAGENCY PANEL RESULTS
John S. Clark, Timothy J. Wickenheiser, Michael P. Doherty, Albert Marshall, Samit K. Bhattacharryya, and John Warren (Department of Energy, Germantown, MD.) 1992 12 p Proposed for presentation at the Nuclear Technologies for Space Exploration, Jackson Hole, WY, 16-19 Aug. 1992
(RTOP 593-71-00)
(NASA-TM-105703; E-7092; NAS 1.15:105703) Avail: NTIS HC/MF A03

Interagency (NASA/DOE/DOD) technical panels worked in 1991 to evaluate critical nuclear propulsion issues, compare nuclear propulsion concepts for a manned Mars mission on a consistent basis, and to continue planning a technology development project for the Space Exploration Initiative (SEI). Panels were formed to address mission analysis, nuclear facilities, safety policy, nuclear fuels and materials, nuclear electric propulsion technology, and nuclear thermal propulsion technology. A summary of the results and recommendations of the panels is presented. Author

N92-27033*# National Aeronautics and Space Administration. Lewis Research Center, Cleveland, OH.
ROCKET ENGINE DIAGNOSTICS USING QUALITATIVE MODELING TECHNIQUES
Michael Binder, William Maul, Claudia Meyer (Sverdrup Technology, Inc., Brook Park, OH.), and Amy Sovie 1992 15 p Proposed for presentation at the 28th Joint Propulsion Conference, Nashville, TN, 6-8 Jul. 1992; sponsored by AIAA, SAE, ASME, and ASEE
(Contract NAS3-25266; RTOP 593-12-21)
(NASA-TM-105714; E-7108; NAS 1.15:105714; AIAA-92-3164)
Avail: NTIS HC/MF A03

Researchers at NASA Lewis Research Center are presently developing qualitative modeling techniques for automated rocket engine diagnostics. A qualitative model of a turbopump interpropellant seal system was created. The qualitative model describes the effects of seal failures on the system steady state behavior. This model is able to diagnose the failure of particular seals in the system based on anomalous temperature and pressure values. The anomalous values input to the qualitative model are generated using numerical simulations. Diagnostic test cases include both single and multiple seal failures. Author

N92-27034*# National Aeronautics and Space Administration. Lewis Research Center, Cleveland, OH.
OVERVIEW OF NASA SUPPORTED STIRLING THERMODYNAMIC LOSS RESEARCH
Roy C. Tew and Steven M. Geng 1992 8 p Proposed for presentation at the 27th Intersociety Energy Conversion Engineering Conference, San Diego, CA, 3-7 Aug. 1992; sponsored by SAE
(RTOP 590-13-11)
(NASA-TM-105690; E-7071; NAS 1.15:105690) Avail: NTIS HC/MF A02

NASA is funding research to characterize Stirling machine thermodynamic losses. NASA's primary goal is to improve Stirling design codes to support engine development for space and terrestrial power. However, much of the fundamental data is applicable to Stirling cooling and heat pump applications. The research results are reviewed. Much was learned about oscillating flow hydrodynamics, including laminar/turbulent transition, and tabulated data was documented for further analysis. Now, with a better understanding of the oscillating flow field, it is time to begin measuring the effects of oscillating flow and oscillating pressure level on heat transfer in heat exchanger flow passages and in cylinders.
Author

N92-27035*# National Aeronautics and Space Administration. Lewis Research Center, Cleveland, OH.
THE 3D ROCKET COMBUSTOR ACOUSTICS MODEL
Richard J. Priem (Priem Consultants, Inc., Cleveland, OH.) and Kevin J. Breisacher Jul. 1992 13 p Proposed for presentation at the 28th Joint Propulsion Conference and Exhibit, Nashville, TN, 6-8 Jul. 1992; sponsored by AIAA, SAE, ASME, and ASEE
(RTOP 590-21-21)
(NASA-TM-105734; E-7137; NAS 1.15:105734; AIAA-92-3228)
Avail: NTIS HC/MF A03

The theory and procedures for determining the characteristics of pressure oscillations in rocket engines with prescribed burning rate oscillations are presented. Analyses including radial and hub baffles and absorbers can be performed in one, two, and three dimensions. Pressure and velocity oscillations calculated using this procedure are presented for the SSME to show the influence of baffles and absorbers on the burning rate oscillations required to achieve neutral stability. Comparisons are made between the results obtained utilizing 1-D, 2-D, and 3-D assumptions with regards to capturing the physical phenomena of interest and computational requirements.
Author

N92-27036*# National Aeronautics and Space Administration. Lewis Research Center, Cleveland, OH.
EFFECT OF MODEL SELECTION ON COMBUSTOR PERFORMANCE AND STABILITY PREDICTIONS USING ROCCID

James E. Giuliani (Ohio Aerospace Inst., Brook Park.) and Mark D. Klem Jul. 1992 16 p Proposed for presentation at the 28th Joint Propulsion Conference and Exhibit, Nashville, TN, 6-8 Jul. 1992; sponsored by AIAA, SAE, ASME, and ASEE
(RTOP 590-21-21)
(NASA-TM-105750; E-7154; NAS 1.15:105750; AIAA-92-3226)
Avail: NTIS HC/MF A03

The ROCket Combustor Interactive Design (ROCCID) methodology is an interactive computer program that combines previously developed combustion analysis models to calculate the combustion performance and stability of liquid rocket engines. Test data from 213 kN (48,000 lbf) Liquid Oxygen (LOX)/RP-1 combustor with an O-F-O (oxidizer-fuel-oxidizer) triplet injector were used to characterize the predictive capabilities of the ROCCID analysis models for this injector/propellant configuration. Thirteen combustion performance and stability models were incorporated into ROCCID, and ten of them, which have options for triplet injectors, were examined. Calculations using different combinations of analysis models, with little or no anchoring, were carried out on a test matrix of operating combinations matching those of the test program. Results of the computer analyses were compared to test data, and the ability of the model combinations to correctly predict combustion stability or instability was determined. For the best model combination(s), sensitivity of the calculations to fuel drop size and mixing efficiency was examined. Error in the stability calculations due to uncertainty in the pressure interaction index (N) was examined. The recommended model combinations for this O-F-O triplet LOX/RP-1 configuration are proposed. Author

N92-27065# Naval Postgraduate School, Monterey, CA.
SUBSCALE SOLID ROCKET MOTOR INFRARED SIGNATURE AND PARTICLE BEHAVIOR M.S. Thesis
John A. Racine Dec. 1991 54 p
(AD-A246416) Avail: NTIS HC/MF A04

A combined optical and particle collection probe which used an in situ particle size distribution measurement method and an infrared camera were used to obtain data that could be used to validate solid propellant rocket motor plume signature prediction codes. The probe design was optimized and the required rates for window purge and ejector flows were determined which provided proper functioning of the probe when placed in the supersonic region of the plume. At the nozzle exit the particle size distribution was quadramodal with most particles smaller than 0.5 micron and the largest particles with diameters less than 25 microns. The larger particles at the nozzle exhaust were not present further aft in the plume. This behavior was believed to result from the breakup of the large Al2O3 particles in the plume Mach discs. However, further work is required to determine if the probe alters the particle size distribution. GRA

N92-27130*# National Aeronautics and Space Administration. Marshall Space Flight Center, Huntsville, AL.
THE 1990 NASA AEROSPACE BATTERY WORKSHOP
Lewis M. Kennedy, comp. Washington May 1991 888 p Workshop held in Huntsville, AL, 4-6 Dec. 1990
(NASA-CP-3119; M-661; NAS 1.55:3119) Avail: NTIS HC/MF A99

This document contains the proceedings of the 21st annual NASA Aerospace Battery Workshop, hosted by the Marshall Space Flight Center on December 4-6, 1990. The workshop was attended by scientists and engineers from various agencies of the U.S. Government, aerospace contractors, and battery manufacturers as well as participation in like kind from the European Space Agency member nations. The subjects covered included nickel-cadmium, nickel-hydrogen, silver-zinc, lithium based chemistries, and advanced technologies as they relate to high reliability operations in aerospace applications. For individual titles, see N92-27131 through N92-27168.

N92-27131*# National Aeronautics and Space Administration. Goddard Space Flight Center, Greenbelt, MD.
COBE BATTERY OVERVIEW: HISTORY, HANDLING, AND PERFORMANCE
Thomas Yi, Smith Tiller, and David Sullivan *In* NASA. Marshall Space Flight Center, The 1990 NASA Aerospace Battery Workshop May 1991 p 19-42 (For primary document see N92-27130 17-20)
Avail: NTIS HC/MF A99

The following topics are presented in viewgraph format: Cosmic Background Explorer (COBE) mission background; battery background and specifications; cell history; battery mechanical/structural design; battery test data; and flowcharts of the various battery approval procedures. H.A.

N92-27132*# National Aeronautics and Space Administration. Goddard Space Flight Center, Greenbelt, MD.
END-OF-LIFE EVALUATION OF THE SOLAR MAXIMUM MISSION BATTERIES
Doris Jallice and Thomas Yi *In* NASA. Marshall Space Flight Center, The 1990 NASA Aerospace Battery Workshop May 1991 p 43-69 (For primary document see N92-27130 17-20)
Avail: NTIS HC/MF A99

The following topics are covered in viewgraph format: Solar Maximum Mission (SSM) background; battery background and specifications; and battery rundown tests. H.A.

N92-27133*# Jet Propulsion Lab., California Inst. of Tech., Pasadena. Battery Systems Group.
MAGELLAN BATTERY OPERATIONS: AN OVERVIEW
Paul J. Timmerman and Peter R. Glueck *In* NASA. Marshall Space Flight Center, The 1990 NASA Aerospace Battery Workshop May 1991 p 71-93 (For primary document see N92-27130 17-20)
Avail: NTIS HC/MF A99

The Magellan Spacecraft's mission to map Venus's surface provides a unique application for Nickel-Cadmium batteries. An overview of the spacecraft, power subsystem, battery, and mission requirements are presented. The reliability and performance of the batteries were extensively studied with a comprehensive test and analysis program. Actual data for cruise and a limited number of mapping orbits is also presented. Author

N92-27134*# Ball Aerospace Systems Div., Boulder, CO.
THE EFFECT OF SWITCHED ARRAY BATTERY CHARGE CONTROL ON CRRES SPACECRAFT: 3 + MONTH DATA SUMMARY
Phil Olbert *In* NASA. Marshall Space Flight Center, The 1990 NASA Aerospace Battery Workshop May 1991 p 95-105 (For primary document see N92-27130 17-20)
Avail: NTIS HC/MF A99

The following topics are covered in viewgraph format: Combined Release and Radiation Effects Satellite (CRRES) orbit parameters; battery charge control; battery description; battery current and voltage output during one orbit; and battery reconditioning discharge profile. H.A.

N92-27135*# Eagle-Picher Industries, Inc., Colorado Springs, CO.
SUPER NiCd BATTERY PROGRAM: HISTORY AND PERFORMANCE
Jeff Hayden and Tim Edgar *In* NASA. Marshall Space Flight Center, The 1990 NASA Aerospace Battery Workshop May 1991 p 107-151 (For primary document see N92-27130 17-20)
Avail: NTIS HC/MF A99

The following topics are covered in viewgraph format: electrochemically deposited electrodes; electrode development and production; electrochemical characterization and electrode stress tests; sintering process; cell design and assembly; and separator qualification program. H.A.

N92-27136*# Hughes Aircraft Co., Torrance, CA. Industrial Electronics Group.
HUGHES ADVANCED NICKEL-CADMIUM BATTERIES: AN UPDATE
R. Sam Bogner *In* NASA. Marshall Space Flight Center, The

1990 NASA Aerospace Battery Workshop May 1991 p 153-180 (For primary document see N92-27130 17-20)
Avail: NTIS HC/MF A99

After delivering a significant data base on boilerplate and prototype advanced nickel cadmium (Ni/Cd) battery cells, Hughes decided to start using the Advanced Ni/Cd batteries on several of their flight programs. The advanced cell can been operated at 80 percent depth of discharge (DOD) for more than 10 years, and possibly 15 years, in geosynchronous earth orbit (GEO) applications. This cell offers an important weight saving over the standard Ni/Cd cell that is usually only operated at 50 to 60 percent DOD in GEO applications. The negative and positive electrodes are manufactured using electrochemical deposition methods which reduce the sinter corrosion problems encountered by the chemical deposition process used in the standard cells. The degradable nylon separators used in standard cells was replaced by polymer impregnated Zirconia separators. Author

N92-27137*# Societe des Accumulateurs Fixes et de Traction, Romainville (France). Aerospace Dept.
SAFT NICKEL-CADMIUM CELL PERFORMANCES FOR GEO AND LEO APPLICATIONS
Olivier Puig *In* NASA. Marshall Space Flight Center, The 1990 NASA Aerospace Battery Workshop May 1991 p 181-212 (For primary document see N92-27130 17-20)
Avail: NTIS HC/MF A99

The following topics are covered in viewgraph format: test matrix and cycling status; test results at 30 percent depth of discharge (DOD); test results at 40 percent DOD; capacity evolution; and dissipated power evolution. H.A.

N92-27138*# Aerospace Corp., El Segundo, CA. Chemistry and Physics Lab.
OXYGEN RECOMBINATION IN THE SEALED NICKEL-CADMIUM CELL
Al H. Zimmerman and Tom P. Barrera *In* NASA. Marshall Space Flight Center, The 1990 NASA Aerospace Battery Workshop May 1991 p 213-226 (For primary document see N92-27130 17-20)
Avail: NTIS HC/MF A99

The purpose of this study was to determine what parameters are most critical for controlling overcharge pressure in a sealed nickel cadmium cell. Topics covered in viewgraph format are: parameters examined; oxygen evolution and recombination; experimental test description; and effect of parameters on recombination rate. H.A.

N92-27139*# Jet Propulsion Lab., California Inst. of Tech., Pasadena. Battery Systems Group.
A CONSTANT CURRENT CHARGE TECHNIQUE FOR LOW EARTH ORBIT LIFE TESTING
Peter Glueck *In* NASA. Marshall Space Flight Center, The 1990 NASA Aerospace Battery Workshop May 1991 p 227-235 (For primary document see N92-27130 17-20)
Avail: NTIS HC/MF A99

A constant current charge technique for low earth orbit testing of nickel cadmium cells is presented. The method mimics the familiar taper charge of the constant potential technique while maintaining cell independence for statistical analysis. A detailed example application is provided and the advantages and disadvantages of this technique are discussed. Author

N92-27140*# Jet Propulsion Lab., California Inst. of Tech., Pasadena.
CHEMICAL EVALUATION OF NON-WOVEN NYLON SEPARATORS USED IN Ni/Cd CELLS
Edward F. Cuddihy *In* NASA. Marshall Space Flight Center, The 1990 NASA Aerospace Battery Workshop May 1991 p 237-262 (For primary document see N92-27130 17-20)
Avail: NTIS HC/MF A99

The goals of the chemical analysis was to identify Gates 2505 degradation mechanism, to determine if Eagle-Pitcher 2505 supply suitable for flight, and to assess the 2538 as a candidate replacement, based on chemical findings. Chemical testing strongly indicates that the Gates 2505 stored in Florida had undergone partial chemical deterioration, believed caused by exposure to high humidities and temperature. A suspected role of zinc chloride as a separator concern during storage was not verified in this study (the effect of ZnCl2 on cell/electrode performance was not addressed). No substantial chemical issues or concerns with using EP 2505 as Ni/Cd battery separator for Mars Observer and TOPEX could be found. No chemical issues or concerns with using 2538 as Ni/Cd battery separator were found, in fact, chemical evidence suggest that 2538 may be a better material, as compared to 2505. E.R.

N92-27141*# Aerospace Corp., Los Angeles, CA.
EXPLORING POSSIBLE RELATIONSHIPS BETWEEN PLATE PORE SIZE CHARACTER AND CELL PERFORMANCE
Lawrence H. Thaller, Melvin Hill, Lawrence A. Tinker, and R. Dan Dell (Gates Aerospace Batteries, Gainesville, FL.) *In* NASA. Marshall Space Flight Center, The 1990 NASA Aerospace Battery Workshop May 1991 p 263-273 (For primary document see N92-27130 17-20)
Avail: NTIS HC/MF A99

The pore size character and plate manufacturing information for selected samples of older plate material were reviewed. When compared to certain cell performance parameters, certain correlations were found between plate pore character and cell performance. This technique may be useful for screening out certain types of plate material prior to assembly into cells. Author

N92-27142*# National Aeronautics and Space Administration. Lyndon B. Johnson Space Center, Houston, TX.
NASA. JOHNSON SPACE CENTER PRIMARY BATTERY APPLICATIONS
Bob J. Bragg *In* NASA. Marshall Space Flight Center, The 1990 NASA Aerospace Battery Workshop May 1991 p 279-296 (For primary document see N92-27130 17-20)
Avail: NTIS HC/MF A99

The role of the Power Branch/EP5 of JSC in primary battery applications is to support those JSC organizations having direct application responsibility with trade studies, battery selection recommendations, and with development, qualification, and provisioning of primary batteries. Battery subsystem management is provided. Payload hazard report preparation is supported, as is the review and comment of such reports for the JSC Payload Safety Panel, who approves the flight safety for all Orbiter payloads. JSC battery users are provided with safety analysis and test support to achieve safety approval. Finally, it is the responsibility of the Power Branch to define and maintain battery safety requirement documentation for JSC. Author

N92-27143*# United Technologies Corp., Huntsville, AL.
STS LITHIUM/CF(x) BATTERY
Dee Gnacek *In* NASA. Marshall Space Flight Center, The 1990 NASA Aerospace Battery Workshop May 1991 p 297-314 (For primary document see N92-27130 17-20)
Avail: NTIS HC/MF A99

Lithium carbon fluoride batteries are used on Space Shuttle Rocket Boosters and external tanks. These batteries have been extremely successful in terms of mission reliability with the exception of cell yield variances. The function/system and battery descriptions are given. A description is given of the battery range safety system. Author

N92-27144*# Catalyst Research Corp., Sparks, MD.
NASA Li/CF(x) CELL PROBLEM ANALYSIS: SCANNING ELECTRON MICROSCOPY WITH ENERGY DISPERSIVE X RAY SPECTROMETRY
John Baker *In* NASA. Marshall Space Flight Center, The 1990 NASA Aerospace Battery Workshop May 1991 p 319-338 (For primary document see N92-27130 17-20)
Avail: NTIS HC/MF A99

An analysis was made of Lithium/carbon fluoride cell parts for possible chloride contamination induced by exposure to thionyl

chloride (SOCl2); various samples were submitted for analysis. Only a portion of the analysis which has been conducted is covered, herein, namely analysis by scanning electron microscopy with energy dispersive x ray spectrometry (SEM/EDS). A strip of nickel was exposed to SOCl2 vapors to observe variations in surface concentrations of sulfur and chlorine with time. By detecting chlorine one can not infer contamination by SOCl2 only that contamination is present. Six samples of stainless steel foil were analyzed for chlorine using EDS. Chlorine was not detected on background samples but was detected on the samples which had been handled including those which had been cleaned. Cell covers suspected of being contaminated while in storage and covers which were not exposed to the same storage conditions were analyzed for chlorine. Although no chlorine was found on the covers from cells, it was found on all stored covers. Results are presented with techniques shown for analysis and identification. Relevant photomicrographs are presented. Author

N92-27145*# Catalyst Research Corp., Sparks, MD.
NASA LI/CF(x) CELL PROBLEM ANALYSIS: ANION EXCHANGE CHROMATOGRAPHY ANALYSIS
Joseph Bytella *In* NASA. Marshall Space Flight Center, The 1990 NASA Aerospace Battery Workshop May 1991 p 339-367 (For primary document see N92-27130 17-20)
Avail: NTIS HC/MF A99

An analysis was made of wiper samples used to wipe down lithium/chlorine fluorine battery components and production equipment. These components and equipment were potentially exposed to thionyl chloride vapors. In the presence of moisture, thionyl chloride decomposes to sulfur dioxide and hydrogen chloride. The wiper samples were analyzed for soluble chlorides and fluorides by anion exchange chromatography. During the examination of the test chromatographs, fluoride contamination was discovered in wiper samples from the test equipment. An analytical method to determine fluoride was developed. The first 3 extracts from the potentially exposed and clean wiper samples were tested, and the total fluoride from both groups determined. A comparison of the results from both groups was made to determine the extent of fluoride contamination. Author

N92-27146*# National Aeronautics and Space Administration. Lyndon B. Johnson Space Center, Houston, TX.
CALORIMETRIC DETERMINATION OF THE THERMONEUTRAL POTENTIAL FOR Li/BrCl IN SOCl2 (BCX) CELLS
Eric C. Darcy, Eric E. Kalu, and Ralph E. White (Texas A&M Univ., College Station.) *In* NASA. Marshall Space Flight Center, The 1990 NASA Aerospace Battery Workshop May 1991 p 369-394 (For primary document see N92-27130 17-20)
Avail: NTIS HC/MF A99

Proliferation of lithium cells into large modular battery packs are projected for future space applications. Assuring battery design safety while maintaining high energy density requires accurate and precise knowledge of the thermal parameters of the battery cell. Specifically, the thermoneutral potential was determined using heat conduction calorimetry on Li/BrCl in SOCl2 (BCX) DD-cells and compared to measurements obtained on Li/SOCl2 D-cells. Over 20 to 60 C, the Li/BCX cells were found to have a thermoneutral potential significantly higher (near 4.0 volts) than that for the Li/SOCl2 cells tested. The higher heat generation measured during discharge reflects the higher electrochemical polarization observed with the BCX cells. Author

N92-27147*# Wilson Greatbatch Ltd., Clarence, NY.
LI/BCX, SVO, AND CSC CELLS: POWER SOURCES FOR AEROSPACE APPLICATIONS
William D. K. Clark *In* NASA. Marshall Space Flight Center, The 1990 NASA Aerospace Battery Workshop May 1991 p 395-440 (For primary document see N92-27130 17-20)
Avail: NTIS HC/MF A99

The operating characteristics and designs are given for some electrochemical cells. All of the electrochemistries have lithium compounds. Descriptions are given for each cell including open circuit voltage, room temperature discharge currents, operating temperature range, weight, safety fuse, energy density, and discharge currents. Author

N92-27148*# Societe des Accumulateurs Fixes et de Traction, Romainville (France). Advanced Battery Div.
PERFORMANCES OF 250 AMP-HR LITHIUM/THIONYL CHLORIDE CELLS
Jacques Goualard *In* NASA. Marshall Space Flight Center, The 1990 NASA Aerospace Battery Workshop May 1991 p 441-464 (For primary document see N92-27130 17-20)
Avail: NTIS HC/MF A99

A 250 Ah lithium thionyl chloride battery is being developed for a booster rocket engine. Extensive cell testing is running to evaluate functional and safety performances. Some results are presented. The lithium/thionyl chloride batteries were selected for their high energy density (low weight) as compared to other sources. The temperature of a lower weight item will be more sensitive to variations of internal and external heat fluxes than a heavier one. The use of high energy density L/TC batteries is subjected to stringent thermal environments to have benefit of energy density and to stay safe in any conditions. The battery thermal environment and discharge rate have to be adjusted to obtain the right temperature range at cell level, to have the maximum performances. Voltage and capacity are very sensitive to temperature. This temperature is the cell internal actual temperature during discharge. This temperature is directed by external thermal environment and by cell internal heat dissipation, i.e., cell actual voltage. Author

N92-27149*# Yardney Technical Products, Inc., Pawcatuck, CT.
DEVELOPMENT OF A 300 AMP-HR HIGH RATE LITHIUM THIONYL CHLORIDE CELL
Gerard H. Boyle *In* NASA. Marshall Space Flight Center, The 1990 NASA Aerospace Battery Workshop May 1991 p 465-469 Sponsored in part by JPL and AF (For primary document see N92-27130 17-20)
Avail: NTIS HC/MF A99

The development of a high-rate lithium thionyl chloride cylindrical cell with parallel plate electrodes is discussed. The development was divided into three phases: phase 1, a 150 Amp/hour low rate (1 mA/sq cm) design; phase 2, a 25 Amp/hour high rate (5 mA/sq cm) design; and phase 3, a 300 Amp/hour high rate (5 mA/sq cm) design. The basic design is the same for all three cells. The electrodes are perpendicular to the axis of the cylinder. Multiple electrodes are bussed up the side of the cylinder, 180 deg apart allowing excellent anode and cathode utilization. It is a lithium limited design with excess electrolyte. The cathode is Shawinigan or Gulf Acetylene black with no catalyst. The electrolyte is 1.8 Molar lithium tetrachloroaluminate (LiAlCl4) in thionyl chloride. All cell cases are 304L Stainless Steel with a BS&B burst disc. Author

N92-27150*# Catalyst Research Corp., Sparks, MD.
SAFETY TESTING OF LITHIUM CELLS
Nick Liberto *In* NASA. Marshall Space Flight Center, The 1990 NASA Aerospace Battery Workshop May 1991 p 471-474 (For primary document see N92-27130 17-20)
Avail: NTIS HC/MF A99

Safety testing is intended to simulate, under laboratory conditions and controls, situations that will subject a cell to externally induced stress. The stresses can occur at any time during the useful life of the cell, from the time of manufacture until it is expended during mission deployment. Abuse testing can be divided into three major categories: Electrical, Mechanical, and Thermal. Although electrical abuses are generally found to occur during handling or deployment, Mechanical and Thermal stresses can be induced during transportation and storage. Therefore, it would be prudent to include predicted environmental exposure as part of the test plan. In the selection of a test program. specific test requirements should be tailored to meet the predicted mission requirements. D.R.D.

N92-27151*# Tracor Battery Technology Center, Rockville, MD.
EXAMINATION OF THE DISCHARGE MECHANISM OF LI/CF(x) CELLS: COMPARISON OF THE ELECTROCHEMICAL REDUCTION MECHANISMS OF PTFE AND (CF(x))n BY LITHIUM
Carl C. Baxam and N. Margalit (Tracor Battery Technology Center, Burke, VA.) *In* NASA. Marshall Space Flight Center, The 1990 NASA Aerospace Battery Workshop May 1991 p 475-493 (For primary document see N92-27130 17-20)
Avail: NTIS HC/MF A99

Swelling of (CF(x))(sub n) electrodes in commercial Li/(CF(x))(sub n) cells presents a limiting factor in cell design optimization. Examination of cathodes from such cells, after discharge, reveals a relation between cell operating temperatures and cathode swelling. Attempts to explain the swelling using the prevailing model for the cathode reaction have failed. A more suitable reaction mechanism is proposed based on the observed behavior of (CF(x))(sub n) electrodes on discharge and a comparison of the reaction products of (CF(x))(sub n) and polytetra fluoroethylene (PTFE) with lithium amalgams. The proposed mechanism is in agreement with the experimental data found in the literature. Author

N92-27152*# National Aeronautics and Space Administration. Lyndon B. Johnson Space Center, Houston, TX.
ZINC-OXYGEN BATTERY DEVELOPMENT PROGRAM
Deborah S. Bourland *In* NASA. Marshall Space Flight Center, The 1990 NASA Aerospace Battery Workshop May 1991 p 495-506 (For primary document see N92-27130 17-20)
Avail: NTIS HC/MF A99

The purpose of this Zinc-Oxygen development program is to incorporate the improved air/oxygen cathode and zinc anode technology developed in recent years into relatively large cells (150-200 amp/hr, 25-100 hour rate) and smaller high rate cells (9-12 amp/hr, 3-12 hour rate). Existing commercial cells manufactured by Duracell and Rayovac are currently being utilized on the Space Shuttle Orbiter in a mini-oscilloscope, the crew radio, and other crew equipment. These applications provide a basis for other Orbiter systems that require portable, storable, electrical power as well as emergency power for the Space Station major payload systems power and for Space Station equipment applications. Author

N92-27153*# National Aeronautics and Space Administration. Marshall Space Flight Center, Huntsville, AL.
LIFE TESTING OF SECONDARY Ag-Zn CELLS
Jeffrey C. Brewer and Rajiv Doreswamy *In its* The 1990 NASA Aerospace Battery Workshop May 1991 p 507-529 (For primary document see N92-27130 17-20)
Avail: NTIS HC/MF A99

Testing on a variety of secondary silver-zinc (Ag-Zn) cells has continued at MSFC for the past six years. The latest test involves a 350 amp/hr cell design that was cycled for 12 months and has undergone approximately 5400 low-earth-orbit cycles as well as 12 deep discharges. This test is not only a life test of these cells, but it also addresses different methods of storing the cells between deep discharges. Also, impedance measurements are made on one of the packs during periodic deep discharges. It is hoped that this will give a good correlation between the health of a cell and its impedance. Author

N92-27154*# Jet Propulsion Lab., California Inst. of Tech., Pasadena. Battery Systems Group.
CYCLE LIFE CHARACTERISTICS OF LI-TIS2 CELLS
Frank Deligiannis, D. Shen, C. K. Huang, and S. Surampudi *In* NASA. Marshall Space Flight Center, The 1990 NASA Aerospace Battery Workshop May 1991 p 531-546 (For primary document see N92-27130 17-20)
Avail: NTIS HC/MF A99

The development of lithium ambient temperature rechargeable cells is discussed. During the development process, we hope to gain a greater understanding of the materials and the properties of the Li-TiS2 cell and its components. The design will meet the requirements of 100 Wh/Kg and 1000 cycles, at 50 percent depth-of-discharge, by 1995. Author

N92-27155*# Rockwell International Corp., Canoga Park, CA. Satellite and Space Electronics Div.
ACCELERATED CYCLE LIFE PERFORMANCE FOR OVONIC NICKEL-METAL HYDRIDE CELLS
Burton M. Otzinger *In* NASA. Marshall Space Flight Center, The 1990 NASA Aerospace Battery Workshop May 1991 p 547-557 (For primary document see N92-27130 17-20)
Avail: NTIS HC/MF A99

Nickel-Metal Hydride (Ni-MH) rechargeable batteries have emerged as the leading candidate for commercial replacement of nickel-cadmium (Ni-Cd) batteries. An important incentive is that the Ni-MH cell provides approximately twice the capacity of a Ni-Cd cell for a given size. A six-cell battery was committed to an accelerated cycle life test to determine the effect of separation type on performance. Results of the test may also show the Ni-MH battery to be a replacement candidate for the aerospace Ni-Cd battery. Author

N92-27156*# European Space Agency. European Space Research and Technology Center, ESTEC, Noordwijk (Netherlands).
EVALUATION OF SODIUM-NICKEL CHLORIDE CELLS FOR SPACE APPLICATIONS
B. Hendel and G. J. Dudley *In* NASA. Marshall Space Flight Center, The 1990 NASA Aerospace Battery Workshop May 1991 p 559-580 (For primary document see N92-27130 17-20)
Avail: NTIS HC/MF A99

The status of the European Space Agency (ESA) program on sodium nickel chloride batteries is outlined. Additionally, the results of initial tests of two prototype space cells are reported. After 2800 cycles typical of a low-earth orbit (LEO) application without failure, the recharge ratio remained at unity, the round trip energy efficiency remained high (87 percent), and the increase in internal cell resistance was modest. Initial tear-down analysis data show no degradation whatsoever of the beta-alumina electrolyte tubes. The low-rate capacity did, however drop by some 40 percent, which needs further investigation, but overall results are encouraging for future use of this couple in geosynchronous (GEO) and LEO spacecraft. Author

N92-27157*# Johnson Controls, Inc., Milwaukee, WI.
UTILIZATION OF A BIPOLAR LEAD ACID BATTERY FOR THE ADVANCED LAUNCH SYSTEM
William O. Gentry, Robin Vidas, Ronald Miles, and Steven Eckles (General Dynamics Corp., Saint Louis, MO.) *In* NASA. Marshall Space Flight Center, The 1990 NASA Aerospace Battery Workshop May 1991 p 581-597 (For primary document see N92-27130 17-20)
Avail: NTIS HC/MF A99

The development of a battery comprised of bipolar lead acid modules is discussed. The battery is designed to satisfy the requirements of the Advanced Launch System (ALS). The battery will have the following design features: (1) conventional lead acid chemistry; (2) thin electrode/active materials; (3) a thin separator; (4) sealed construction (gas recombinant); and (5) welded plastic frames for the external seal. Author

N92-27158*# University of the Pacific, Forest Grove, OR. Dept. of Chemistry.
RECENT DEVELOPMENTS IN NICKEL ELECTRODE ANALYSIS
Richard V. Whiteley, M. E. Daman, and E. Q. Kaiser (Space Systems/Loral, Palo Alto, CA.) *In* NASA. Marshall Space Flight Center, The 1990 NASA Aerospace Battery Workshop May 1991 p 599-615 (For primary document see N92-27130 17-20)
Avail: NTIS HC/MF A99

Three aspects of nickel electrode analysis for Nickel-Hydrogen and Nickel-Cadmium battery cell applications are addressed: (1)

the determination of active material; (2) charged state nickel (as NiOOH + CoOOH); and (3) potassium ion content in the electrode. Four deloading procedures are compared for completeness of active material removal, and deloading conditions for efficient active material analyses are established. Two methods for charged state nickel analysis are compared: the current NASA procedure and a new procedure based on the oxidation of sodium oxalate by the charged material. Finally, a method for determining potassium content in an electrode sample by flame photometry is presented along with analytical results illustrating differences in potassium levels from vendor to vendor and the effects of stress testing on potassium content in the electrode. The relevance of these analytical procedures to electrode performance is reviewed.
Author

N92-27159*# Eagle-Picher Industries, Inc., Joplin, MO. Electronics Div.
EUTELSAT 2: SAR-10009 NICKEL-HYDROGEN BATTERY
Lee Miller *In* NASA. Marshall Space Flight Center, The 1990 NASA Aerospace Battery Workshop May 1991 p 617-629 (For primary document see N92-27130 17-20)
Avail: NTIS HC/MF A99

The topics are presented in viewgraph form and include SAR-10009 design features, specific energy, analyses and testing, redundant structural insulation, electronics, corrosion protection, battery cell life cycle tests, and spacecraft launches. Author

N92-27160*# Eagle-Picher Industries, Inc., Joplin, MO. Nickel-Hydrogen Group.
LOW COST BATTERY DESIGNS FOR SMALL SATELLITE APPLICATIONS
Jack Brill *In* NASA. Marshall Space Flight Center, The 1990 NASA Aerospace Battery Workshop May 1991 p 631-652 (For primary document see N92-27130 17-20)
Avail: NTIS HC/MF A99

The topics are presented in viewgraph form and include the following: EPI nickel-hydrogen flight history; designs developed and tested; 3.5 inch diameter common pressure vessel (CPV); nickel-hydrogen system advantages; 2.5 inch diameter individual pressure vessel (IPV) and CPV; 5 AH CPV charge voltage/pressure; 5 AH CPV cell design; RNH-5-1 charge retention test; nickel-hydrogen cell specifications; sealed prismatic nickel metal hydride; nickel metal hydride life test; nickel-hydride cell specifications; and nickel metal hydride system advantages.
Author

N92-27161*# National Aeronautics and Space Administration. Lewis Research Center, Cleveland, OH.
THE EVALUATION OF LAYERED SEPARATORS FOR NICKEL-HYDROGEN CELLS
Randall F. Gahn *In* NASA. Marshall Space Flight Center, The 1990 NASA Aerospace Battery Workshop May 1991 p 653-676 (For primary document see N92-27130 17-20)
Avail: NTIS HC/MF A99

The concept of using layered separators to achieve the required electrolyte retention and bubble pressure fo nickel-hydrogen cells was evaluated in a boilerplate cell test. Zircar cloth, polyethylene paper and polypropylene felt were combined with a layer of radiation-grafted polyethylene film to achieve the required properties. Three cells of each layered separator were built and tested by characterization cycling and by low earth orbit cycling for 5000 cycles at 80 percent DOD. Three cells containing asbestos separators were used as the reference. Author

N92-27162*# Aerospace Corp., Los Angeles, CA.
UPDATE OF A NICKEL-HYDROGEN CYCLE LIFE MODEL
Lawrence H. Thaller *In* NASA. Marshall Space Flight Center, The 1990 NASA Aerospace Battery Workshop May 1991 p 677-689 (For primary document see N92-27130 17-20)
Avail: NTIS HC/MF A99

The topics are presented in viewgraph form and include the following: a cell capacity diagram, life predictions; compilation of Ni-H2 life test data; Fritts' electrode strain; Lim's electrode bending; Davolio's flexural Young's modulus; behavior of sintered nickel electrode; visualization of modified model; and nickel hydrogen technology status. Author

N92-27163*# Eagle-Picher Industries, Inc., Joplin, MO.
HUBBLE SPACE TELESCOPE BATTERY BACKGROUND
Dan Standlee *In* NASA. Marshall Space Flight Center, The 1990 NASA Aerospace Battery Workshop May 1991 p 691-713 (For primary document see N92-27130 17-20)
Avail: NTIS HC/MF A99

The following topics are presented in viewgraph form and include the following: the MSFC Hubble Space Telescope (HST) Nickel-Hydrogen Battery Contract; HST battery design requirements; HST nickel-hydrogen battery development; HST nickel-hydrogen battery module; HST NiH2 battery module hardware; pressure vessel design; HST NiH2 cell design; offset non-opposing vs. rabbit ear cell; HST NiH2 specified capacity; HST NiH2 battery design; and HST NiH2 module design. Author

N92-27164*# National Aeronautics and Space Administration. Marshall Space Flight Center, Huntsville, AL.
HUBBLE SPACE TELESCOPE NiH2 SIX BATTERY TEST
Thomas H. Whitt and J. Roy Lanier *In its* The 1990 NASA Aerospace Battery Workshop May 1991 p 715-741 (For primary document see N92-27130 17-20)
Avail: NTIS HC/MF A99

The primary objectives of the test are: (1) to get a better understanding of the operating characteristics of the NiH2 batteries in the Hubble Space Telescope (HST) Electric Power Subsystem (EPS) by simulating every aspect of the expected operating environment; (2) to determine the optimum charge level and charge scheme for the NiH2 batteries in the HST EPS; (3) to predict the performance of the actual HST EPS; (4) to observe the aging characteristics of the batteries; and (5) to test different EPS anomalies before experiencing the anomalies on the actual HST.
Author

N92-27165*# National Aeronautics and Space Administration. Marshall Space Flight Center, Huntsville, AL.
HUBBLE SPACE TELESCOPE NICKEL-HYDROGEN FLIGHT SPARE BATTERY TEST
Jeffrey C. Brewer and Thomas H. Whitt *In its* The 1990 NASA Aerospace Battery Workshop May 1991 p 743-758 (For primary document see N92-27130 17-20)
Avail: NTIS HC/MF A99

For several years, MSFC has been engaged in a series of battery tests in support of the Hubble Space Telescope (HST) Program. Now that the HST is in orbit, many of these tests will continue in order to give those responsible for the HST a reasonable prediction on the performance of the flight batteries. These tests will also be a source of needed low earth orbit (LEO) data for nickel hydrogen (Ni-H2) batteries and cells. One of the tests currently in progress at MSFC is a mission simulation test on a 22-cell Ni-H2 battery. This battery is composed of spare cells taken from the lot of cells out of which the Flight Spare Module was assembled. This module is one of two modules launched on the HST. This battery has been on test since Jun. 1989 and has completed nearly 8000 LEO cycles. A series of characterization tests were run prior to the start of the mission simulation and a launch scenario test was run in Feb. and Mar. 1990 to test the behavior of the cells through a simulated launch. The results from these tests as well as the overall performance of the battery as it continues to cycle are reported. Author

N92-27166*# Johnson Controls, Inc., Milwaukee, WI.
MULTIPLE CELL CPV NICKEL-HYDROGEN BATTERY
Ken R. Jones and Jeffrey P. Zagrodnik *In* NASA. Marshall Space Flight Center, The 1990 NASA Aerospace Battery Workshop May 1991 p 759-788 (For primary document see N92-27130 17-20)
Avail: NTIS HC/MF A99

Johnson Controls, Inc. has developed a multiple cell CPV nickel hydrogen battery that offers significant weight, volume, and cost

advantages for aerospace applications. The baseline design was successfully demonstrated through the testing of a 26-cell prototype, which completed over 7000 44 percent depth-of-discharge low earth orbit cycles. Prototype designs using both nominal 5 and 10 inch diameter vessels are currently being developed for a variety of customers and applications. Author

N92-27167*# National Aeronautics and Space Administration. Lewis Research Center, Cleveland, OH.
RESULTS OF A TECHNICAL ANALYSIS OF THE HUBBLE SPACE TELESCOPE NICKEL-CADMIUM AND NICKEL-HYDROGEN BATTERIES
Michelle A. Manzo et al *In* NASA. Marshall Space Flight Center, The 1990 NASA Aerospace Battery Workshop May 1991 p 789-860 (For primary document see N92-27130 17-20)
Avail: NTIS HC/MF A99

The Hubble Space Telescope (HST) Program Office requested the expertise of the NASA Aerospace Flight Battery Systems Steering Committee (NAFBSSC) in the conduct of an independent assessment of the HST's battery system to assist in their decision of whether to fly nickel-cadmium or nickel-hydrogen batteries on the telescope. In response, a subcommittee to the NAFBSSC was organized with membership comprised of experts with background in the nickel-cadmium/nickel-hydrogen secondary battery/power systems areas. The work and recommendations of that subcommittee are presented. Author

N92-27168*# National Aeronautics and Space Administration. Marshall Space Flight Center, Huntsville, AL.
NICKEL-HYDROGEN LEO CYCLING AT 20 PERCENT - 50 PERCENT DOD
John E. Lowery *In its* The 1990 NASA Aerospace Battery Workshop May 1991 p 861-897 (For primary document see N92-27130 17-20)
Avail: NTIS HC/MF A99

The test setup consists of four major elements: the programmable power supplies and load banks, the data acquisition and control system control computer, and the NiH2 specimen test cells. A simplified block diagram of the test setup is shown. The test setup provides complete battery isolation should a fault occur, and fusing as necessary to protect the battery cells and other equipment. Front panel switches provide for power supply configuration and battery isolation. Front panel meters provide continuous real-time visual monitoring of the voltage and current for each pack of cells. A strip chart recorder provides a hard copy of the voltage and current profiles for each of the packs. The test operates continuously with minimal human interface, except during special tests. The two power supplies are controlled by resistance programming. A bank of resistors and relays was built which can be switched by the control computer to provide control over the charge current to the batteries. The load banks are controlled by the 3497A. The 3497A is equipped with a 0.5 volt programmable power supply which is used to voltage program the load banks. A Hewlett-Packard Vectra 9000 running an HP Basic program is used as the control computer to remotely instruct the 3497A (data acquisition and control) to scan the data channels and retrieve test data. The program then reads, calculates, and stores the data. If an anomaly occurs, the program will disconnect the cells and shut down the test to avoid damage to the cells or equipment. Author

23 CHEMISTRY AND MATERIALS (GENERAL)

N92-27084*# National Aeronautics and Space Administration. Goddard Space Flight Center, Greenbelt, MD.
SYSTEMS SPECIAL INVESTIGATION GROUP OVERVIEW
James B. Mason, Harry Dursch, and Joel Edelman (Long Duration Exposure Facility Newsletter, Silver Spring, MD.) *In* NASA. Langley Research Center, LDEF: 69 Months in Space. First Post-Retrieval Symposium, Part 3 Jan. 1992 p 1217-1223 (For primary document see N92-27083 17-99)
Avail: NTIS HC/MF A21; 1 functional color page

N92-27117*# Centre National d'Etudes Spatiales, Toulouse (France).
FRENCH COOPERATIVE PASSIVE PAYLOAD (FRECOPA)
Christian Durin *In* NASA. Langley Research Center, LDEF: 69 Months in Space. First Post-Retrieval Symposium, Part 3 Jan. 1992 p 1593-1605 (For primary document see N92-27083 17-99)
Avail: NTIS HC/MF A21; 1 functional color page

N92-27128*# NASA Space Station Program Office, Reston, VA.
THE ROLE OF THE LONG DURATION EXPOSURE FACILITY IN THE DEVELOPMENT OF SPACE SYSTEMS
Sally A. Little *In* NASA. Langley Research Center, LDEF: 69 Months in Space. First Post-Retrieval Symposium, Part 3 Jan. 1992 p 1687-1690 (For primary document see N92-27083 17-99)
Avail: NTIS HC/MF A21; 1 functional color page

24 COMPOSITE MATERIALS

Includes physical, chemical, and mechanical properties of laminates and other composite materials.
For ceramic materials see *27 Nonmetallic Materials.*

N92-26380# Naval Academy, Annapolis, MD.
A METHOD TO IMPROVE POST IMPACT COMPRESSIVE STRENGTH IN GRAPHITE/EPOXY COMPOSITE MATERIALS AFTER LOW TEMPERATURE IMPACT Final Report, 1990-1991
Robert C. Dunn 13 May 1991 53 p
(AD-A245395; USNA-TSPR-179) Avail: NTIS HC/MF A04

A study was performed to investigate a method to improve the post impact compressive strength in graphite/epoxy composite materials due to low temperature impact. Aerospace quality 32 ply quasi-isotropic IM6/3501-6 test panels were utilized in the study. These panels were modified by adding FM300 interleafs, which have greater impact toughness, over the zero degree piles in four different locations in the symmetric layups. Ultrasonic C-scan inspections were used to characterize the quality of the panels, and provided a basis for comparison after the panels were impacted. The panels were impacted at -67 F by an instrumented impactor that produced load versus time and energy versus time curves. A compression after impact (CAI) test was performed to determine the post impact compressive strength of the panel. The results of the compression after impact test, post impact ultrasonic inspection, and optical microscopy were used to determine fracture-mode and effects of interleafs. GRA

N92-26383# Naval Postgraduate School, Monterey, CA.
COMPOSITE STRENGTH STATISTICS FROM FIBER STRENGTH STATISTICS M.S. Thesis
Eric P. Johnson Jun. 1991 112 p
(AD-A245616) Avail: NTIS HC/MF A06

Utilization of composites in critical design applications requires an extensive engineering experience data base which is generally lacking, especially for rapidly developing constituent fibers. As a supplement, an accurate reliability theory can be applied in design. This investigation is part of a research effort to develop a probabilistic model of composite reliability capable of using data produced in small laboratory test samples to predict the behavior of large structures with respect to their actual dimensions. This work included testing of composite strength which was then used in exploring the methodology of predicting composite reliability from the parent single filament fiber strength statistics. This required testing of a coordinate set of test samples which consisted of a composite and its parent fibers. Previously collected fiber strength statistics from two different production spools were used in conjunction with the current effort. This investigation established that, for a well made composite, the Local Load Sharing Model of

reliability prediction exhibited outstanding correlation with experimental data and was sufficiently sensitive to predict deficient composite strength due to a specific fiber spool with an abnormally weak lower tail. In addition, it provided an upper bound on the composite reliability. This investigation is unique in that is used a coordinate set of data with an unambiguous genesis of parent fiber and subsequent composite. GRA

N92-26386# Naval Postgraduate School, Monterey, CA.
EFFECT OF THERMAL RESIDUAL STRESSES ON THE STRESS-STRAIN BEHAVIOR OF METAL-MATRIX COMPOSITES M.S. Thesis
Daniel M. Seigenthaler Jun. 1991 91 p
(AD-A246136) Avail: NTIS HC/MF A05

A phenomenological and parametric study was conducted to assess the effect of thermal residual stresses on the stress-strain response of a discontinuous fiber-reinforced metal-matrix composite in tensile and compressive loading. The material chosen for this investigation was the silicon carbide whisker reinforced aluminum 6061. The difference between composite flow behavior in tension and compression, as well as the effects of volume fraction, fiber aspect ratio, and fiber spacing were analyzed within the framework of axisymmetric finite element models to determine the overall constitutive response of the composite and to solve for local field quantities in the fiber and the matrix. The composite was modeled as a periodic array of cylindrical fibers with perfect interfacial bonding and complete fiber alignment with the tensile/compressive axis. It was found that the presence of residual stresses affected the stress-strain behavior of the composite by influencing the load transfer characteristics between the matrix and the fiber as well as the initiation and growth of the plastic deformation in the matrix. The results of the study indicated that a significant strength differential exists between tensile and compressive loading and that this effect diminishes with increasing volume fraction. The results also indicated that composite stiffness, yield strength, and work-hardening rate increase with increasing volume fraction and fiber aspect ratio. GRA

N92-26525# Instituut TNO voor Bouwmaterialen en Bouwconstructies, Delft (Netherlands).
EXPERIMENTAL STUDY OF SHEAR FRACTURE AND AGGREGATE INTERLOCK IN CEMENTBASED COMPOSITES
J. G. M. vanMier, M. B. Nooru-Mohamed, and G. Timmers 1991 109 p Prepared in cooperation with Technische Hogeschool, Delft, Netherlands Sponsored in part by AF
(PB92-151521) Avail: NTIS HC/MF A06

The results of an exploratory study are presented from the recently developed biaxial tension/shear apparatus. The apparatus is unique in the sense that square double edge notched concrete plates up to a size of 200 x 200 mm can be loaded in any combination of tension and shear in displacement control. The two loading axes are completely independent of one another. Both results of experiments on plain concrete and on slurry infiltrated fiber concrete are presented. The experiments can be divided into two categories. In the first, aggregate interlock was studied for narrow cracks (between 10 and 400 microns) that can still transmit tensile loads normal to the crack plane. In the second category, specimens were sheared off without precracking them (mode 2), but in a few cases with simultaneous tensile loading (mixed mode 1 and 2). The shear tests on specimens containing narrow cracks revealed an abundance of secondary cracking. The exact boundary conditions were very important. Tests were carried out with either zero confinement or with a very small confinement of -1 kN perpendicular to the crack during shear. Author

N92-26532# Naval Academy, Annapolis, MD.
OPTICAL STRAIN MONITORING IN COMPOSITE MATERIALS Final Report, 1990 - 1991
Daniel B. Robinson 13 May 1991 65 p
(AD-A245474; USNA-TSPR-186) Avail: NTIS HC/MF A04

Composite materials are substances made up of at least two components. Typically, one phase is fibrous and the second phase is a resin. The fibers provide the strength while the resin supports and protects the fibers. Optical fibers embedded within a composite structure during its layup offer a means of monitoring the structure. This project studied two different types of monitoring. Both utilized the Mach-Zehnder interferometer configuration. The first provided a signal that was used to obtain a detailed calibration for the optical strain gauge as the composite beam was deflected in three point bending. The second provided a signal in the audio spectrum that was used to monitor a composite specimen under various driving forces. This signal was evaluated subjectively and also quantitatively through the use of a computer. GRA

N92-26559 Brown Univ., Providence, RI.
FAILURE STUDIES OF BIMATERIAL INTERFACES AND CONSTRAINED DUCTILE LAYERS Ph.D. Thesis
Andrew George Varias 1991 141 p
Avail: Univ. Microfilms Order No. DA9204975

The constrained plastic deformation of the ductile phase in ceramic-matrix composites elevates the stresses in the ductile phase and the neighboring regions of the surrounding elastic matrix. The stress elevation may trigger one of the several competing failure mechanisms. The competition among these mechanisms is examined in the simple case of a cracked metal foil, bonded between stiff ceramic blocks and subjected to mode 1, mode 2 and mixed mode loading, under small scale yielding conditions. The composite may fail at the crack-tip by void nucleation, growth and coalescence, which is driven by the high strains developed in that region. It may also fail away from the crack-tip by a mechanism which is triggered by the high stresses developed at a distance of the order of the layer thickness. There are three possible failure mechanisms, which may operate away from the crack tip: (1) interfacial de-adhesion; (2) high triaxiality cavitation; and (3) fracture of the ceramic. The first operates at a critical normal interfacial traction, the second at a critical mean stress in the ductile phase and the third at a critical tensile stress in the ceramic. The effect of mode mixity, material and micromechanical parameters on the competition of the failure mechanisms and consequently on the toughness of the composite is examined. The failure of bimaterial interfaces with periodic arrays of flows is also examined. An adhesive relation is prescribed for the interface which governs the normal and shear stress versus normal and shear displacement response. Based on this model, the effect of geometry and interfacial properties on the fields of propagating flaws as well as on the toughness, and failure modes of bimaterial interfaces is studied. Dissert. Abstr.

N92-26564 Delaware Univ., Newark.
ANALYSIS AND MODELING OF HIGH-TEMPERATURE PERFORMANCE OF ADVANCED FIBER COMPOSITES Ph.D. Thesis
Yuan Ruo Wang 1991 215 p
Avail: Univ. Microfilms Order No. DA9206305

The thermo-mechanical behavior of high-temperature composites was investigated. The three-dimensional transient interlaminar thermal stresses in cross- and angle-ply laminated composites due to sudden changes in the thermal boundary conditions have been studied by solving the heat conduction equation and by perturbation analysis of the equilibrium equations, respectively. The thermal shock resistance capability of laminated ceramic matrix composites has been predicted through the studies of transient thermal stresses and laminate failure mechanisms. Finally, the investigations of high temperature creep behavior of short and continuous fiber reinforced ceramic matrix composites has been performed. Numerical results for a four-layer laminate have shown that the interlaminar normal stress near the free edge is significantly higher than that in the interior region and it increases rapidly with the fiber volume fraction. The maximum allowable temperature change, Delta Tau(sub max), has been taken as a measure of the thermal shock resistance capability of composites. The effects of fiber orientation, volume fraction, thermal expansion coefficient, Young's modulus, and thermal conductivity on the thermal shock resistance capability of laminated ceramic matrix composites have been assessed. A unidirectional short fiber composite model under off-axis tension has been established and

analyzed using a multiaxial creep constitutive relation and an advanced shear-lag method to study the steady-state flow activated composite creep behavior. The stress distributions in the fiber and matrix, and the composite creep rate as functions of applied stress have been determined. Parametric studies have been performed for the effects of fiber volume fraction and fiber/matrix interface sliding factor on composite creep rate. For damage-induced creep of unidirectional ceramic matrix composite, the composite has been regarded as a transversely isotropic elastic continuum having a microstructure consisting of distributed damage entities which have been represented by tensorial internal state variables. Under an external sustained stress along the fiber direction, the internal damage field has been assumed to evolve in time resulting in the creep deformation. The creep strain rate has been derived for two damage configurations: matrix cracking and fiber/matrix interfacial debonding in conjunction with matrix cracking. Dissert. Abstr.

N92-26607 Washington Univ., Saint Louis, MO.
MESOMECHANICS OF VISCOPLASTIC METAL MATRIX COMPOSITES Ph.D. Thesis
David Leigh Buchanan 1991 247 p
Avail: Univ. Microfilms Order No. DA9209163

This dissertation describes the development of a method for investigating the inelastic behavior of continuous fiber reinforced metal matrix composite materials under general in-plane loading conditions. This methodology will be used in performing two types of analysis. A macroscopic analysis of the composite material will be performed in which the effects of the individual fiber and matrix constituents are detected as only apparent properties of the presumed homogeneous composite. A microscopic analysis of the heterogeneous composite material will also be performed in which the contribution of the individual fiber and matrix constituents are examined in detail. This methodology will be based on the construction of a finite element model using the geometric microstructure of a representative unit cell of the composite, and on the inelastic properties of the individual constituent materials. A coarse unit cell finite element model of the entire composite material will be used in performing the macroscopic analysis, while a refined unit cell finite element model will be used in performing the microscopic analysis. Dissert. Abstr.

N92-26650*# National Aeronautics and Space Administration. Goddard Space Flight Center, Greenbelt, MD.
ANALYSIS OF YTTRIUM-BARIUM-COPPER-OXIDE BY X RAY DIFFRACTION AND MECHANICAL CHARACTERIZATION
Petar Arsenovic Jun. 1992 25 p
(NASA-TM-104562; NAS 1.15:104562; Rept-92A01664) Avail: NTIS HC/MF A03

The efforts in developing high-temperature superconductor (HTSC) YBa2Cu3O7 electrical leads are to benefit future NASA missions that will carry payloads with sensitive instruments operating at cryogenic temperatures. Present-day leads made of copper or magnesium are responsible for as much as 50 percent of the parasitic heat load on cryogenic systems. A reduction of this load could be achieved by replacing the conventional materials with HTSC ceramic electrical leads. Superconductor quality has become a concern in the industry, as has the development of effective evaluation methods. The factors that need to be examined for these materials include material purity, mechanical properties, and superconducting ability below the critical temperature. We applied several methods to study these factors: thermogravimetric analysis, x-ray diffraction, tensile testing, and laser-generated ultrasound. Our objectives were to determine the average tensile strength and Young's modulus of the HTSC material and to compare them to those values for copper and manganin. Author

N92-26679# Argonne National Lab., IL.
APPLICATION OF NEUTRON DIFFRACTION TO MEASURE RESIDUAL STRAINS IN HIGH TEMPERATURE COMPOSITES
A. Saigal (Tufts Univ., Medford, MA.) and D. S. Kupperman 1991 20 p Presented at the 6th Japan-US Conference on Composite Materials, Orlando, FL, 22-25 Jun. 1992
(Contract W-31-109-eng-38)
(DE91-014021; ANL/CP-73280; CONF-920624-1) Avail: NTIS HC/MF A03

An experimental neutron diffraction technique was used to measure residual thermal strains developed in high temperature composites during postfabrication cooling. Silicon carbide fiber reinforced titanium aluminide (over the temperature range 20 to 950 C) and tungsten and saphikon fiber reinforced nickel aluminide composites (at room temperature) were investigated. As a result of thermal expansion mismatch, compressive residual strains and stresses were generated in the silicon carbide fibers during cooldown. The axial residual strains were tensile in the matrix and were lower in nickel aluminide matrix as compared to those in titanium aluminide matrix. The average transverse residual strains in the matrix were compressive. Liquid nitrogen dipping and thermal cycling tend to reduce the fabrication induced residual strains in silicon carbide fiber reinforced titanium aluminide matrix composite. However, matrix cracking can occur as a result of these processes. DOE

N92-26796# Army Cold Regions Research and Engineering Lab., Hanover, NH.
BUCKLING OF UNIDIRECTIONAL GRAPHITE/EPOXY COMPOSITE PLATES AT LOW TEMPERATURES
Piyush K. Dutta, David Hui, and Yvonne M. Traynham Nov. 1991 17 p
(DA Proj. 4A7-62784-AT-42)
(AD-A246602; CRREL-SR-91-20) Avail: NTIS HC/MF A03

A theoretical and experimental study of the buckling and postbuckling behavior of unidirectionally laminated graphite/epoxy plates was conducted under combined thermal cooling and compressive loading. The rectangular plates were simply supported at the loaded edges and free in the remaining edges. The plates were found to bend during cooling even without mechanical loads because of the negative thermal expansion coefficient of the material in the loading direction and the in-plane end constraints at the two-loaded edges. Such bending from thermal load was treated as an initial geometric imperfection, and the analysis was based on Koiter's theory of elastic stability. The experimental postbuckling curves agreed well with the theoretical values. GRA

N92-26827 Florida Univ., Gainesville.
FINITE ELEMENT MODELING OF STATIC INDENTATION DAMAGE IN LAMINATED COMPOSITES Ph.D. Thesis
Han Soo Jung 1991 147 p
Avail: Univ. Microfilms Order No. DA9209028

The objective of this research is to study progressive failure of circular laminated brittle matrix composite plates due to static indentation loading using finite elements. The plates are assumed to be simply supported along the edge and are indented by a rigid indenter with a hemispherical nose. A quasi-isotropic homogenization process is used to make the problem axisymmetric. Four noded, isoparametric, quadrilateral, axisymmetric solid elements are used to model the plate. A new algorithm is used to analyze the progressive contact between the indenter and the plate. Hashin's failure criteria are modified so that they can be applied to axisymmetric, transversely isotropic laminates. Stiffness matrices of failed elements are modified suitably. A new slip surface is introduced when delamination occurs. Very stiff springs are attached to nodes on delamination surfaces to prevent interpenetration of the nodes. The results from incremental damage analysis agree well with experimental results. This program can be applied to analyze impact problems involving large masses impacting at very low velocities. Dissert. Abstr.

N92-26861 California Univ., Berkeley.
PENETRATION OF LAMINATED COMPOSITES BY PROJECTILES Ph.D. Thesis
Guoqi Zhu 1990 193 p
Avail: Univ. Microfilms Order No. DA9126860

Penetration of laminated Kevlar/polyester composites by 12.7 mm diameter hard-steel cylindro-conical projectiles with a mass of

28.9 g was investigated by experimental, theoretical, and numerical methods. The specimens used in the penetration experiments were circular, and quasi-static perforation tests were performed to investigate the effects of thickness, global stiffness, delamination, size and angle of the indenters, and friction on the resistance of the specimens. The projectile loads and displacements were measured. In the dynamic tests, the initial and terminal velocities of the strikers were recorded. The ballistic limits of plates with different thicknesses and the terminal velocities obtained with 5 and 10 ply samples were experimentally determined. The effects of lay-up, delamination, and volume fraction on perforation were investigated. The global deflection, local deformation, and damage of the laminates were represented in a theoretical analysis. Whitney-Pagano's laminate theory was employed to approximate the global response. A three-stage penetration model, that separately examined the indentation, perforation, and exit phases, was proposed to simulate this process. Delamination and fiber failure were also analyzed. A finite difference program was developed to evaluate the proposed model. The displacement, velocity, and deceleration of the projectile during dynamic penetration were calculated using this program. The theoretical predictions of ballistic limits and terminal velocities of the projectiles were in good agreement with the experimental results.

Dissert. Abstr.

N92-26882# Advanced Technology Materials, Inc., Danbury, CT.

NOVEL MOLECULAR SOURCES FOR DISPERSING BORON IN CARBON-CARBON COMPOSITES Final Report, 1 Jun. - 30 Nov. 1991

Philip S. Chen and Ward C. Stevens 31 Dec. 1991 53 p

(Contract F49620-91-C-0046)

(AD-A246999) Avail: NTIS HC/MF A04

Improving the oxidation resistance of carbon-carbon composites is the key to expanding the use of this material system into higher temperature applications. While boron particles have been added to these materials to seal cracks in protective coatings, oxidation of the carbon matrix neighboring the boron particles seriously affects composite strength. This problem is exacerbate by a natural segregation of the boron particles to fiber rich areas of the composites. Carborane, a robust molecular source of boron, was used as the precursor for atomically dispersed boron in a phenolic derived carbon matrix. Modifications of the chemical structure of carborane were used to improve the solubility in phenolic. Additions of carboranes into the phenolic resins dramatically improved the oxidation resistance of the carbonized char. The char yield of the phenolic resin was also increased significantly. GRA

25 INORGANIC AND PHYSICAL CHEMISTRY

Includes chemical analysis, e.g., chromatography; combustion theory; electrochemistry; and photochemistry.

For related information see also *77 Thermodynamics and Statistical Physics.*.

N92-26201# Westinghouse Savannah River Co., Aiken, SC.

MATERIALS COMPATIBILITY AND WALL STRESSES IN HYDRIDE STORAGE BEDS

E. A. Clark, K. A. Dunn, S. T. McKillip, and C. E. Bannister 1991 15 p Presented at the 1991 Storage Science Meeting, Aiken, SC, 22-26 Apr. 1991

(Contract DE-AC09-89SR-18035)

(DE92-009432; WSRC-MS-91-142; CONF-9104246-2) Avail: NTIS HC/MF A03

Hydrogen isotope handling and storage will be accomplished using solid-state hydride compounds at the Savannah River Site in the new Replacement Tritium Facility (RTF). The hydride powder is contained in a horizontal cylindrical vessel, and the combination of hydride powder, vessel, and associated heating and cooling facilities are termed a hydride storage bed. The materials compatibility of the storage powder with the stainless steel vessel was examined, and the stresses developed in the vessel due to expansion of the powder by absorbing hydrogen were measured.

DOE

N92-26209# California Univ., Berkeley. Lawrence Berkeley Lab.

CONVERSION OF ETHANE AND OF PROPANE TO HIGHER OLEFIN HYDROCARBONS

H. Heinemann and G. A. Somorjai Oct. 1991 21 p

(Contract DE-AC03-76SF-00098)

(DE92-009487; LBL-31230) Avail: NTIS HC/MF A03

Purely thermal reactions for the conversion of ethane were carried out in an empty and in a quartz chip filled reactor over a temperature range of 300-800 C in the absence and presence of oxygen and oxygen plus water. Ethane alone shows no conversion below 600 C and some conversion to CH4 and very little C2H4 at 700 and 800 C. Ethane and oxygen produce CO2 as the major product above 400 C. The additional presence of water does not appreciably change this picture. Converting ethane with oxygen and water over a Ca3NiK(0.1) catalyst at very low space velocity gave increasing conversion with temperature, primarily CO2 production and a small amount of C(3+) hydrocarbons. The CO2 production was decreased and slightly more C3 hydrocarbons were produced when the potassium concentration of the catalyst was increased. Activation energies have been calculated for the various ethane conversion reactions. It appears that the CaNiK oxide catalyst is not suited for oxidative ethane coupling at the conditions, thus, far investigated. The indications are that much shorter contact times are required to prevent oxidation of intermediates. Blank runs with propane and oxygen in the absence of a catalyst have shown significant reaction at temperatures as low as 400 C.

DOE

N92-26212# California Univ., Berkeley. Lawrence Berkeley Lab.

GAS PHASE CHROMATOGRAPHY OF HALIDES OF ELEMENTS 104 AND 105

A. Tuerler, K. E. Gregorich, K. R. Czerwinski, N. J. Hannink, R. A. Henderson, D. C. Hoffman, C. D. Kacher, B. Kadkhodayan, S. A. Kreek, and D. M. Lee et al Apr. 1991 15 p Presented at the International Topical Conference on Methods and Applications of Radioanalytical Chemistry II (MARC-2), Kona, HI, 21-27 Apr. 1991

(Contract DE-AC03-76SF-00098)

(DE92-010284; LBL-31442; CONF-910422-9) Avail: NTIS HC/MF A03

On-line isothermal gas phase chromatography was used to study halides of (sup 261)104 (T sub 1/2 = 65 s) and (sup 262,263)105 (T sub 1/2) = 34 s and 27 s) produced an atom-at-a time via the reactions (248)Cm((O-18, 5n) and (249)Bk(O-18), 5n, 4n), respectively. Using HBr and HCl gas as halogenating agents, we were able to produce volatile bromides and chlorides of the above mentioned elements and study their behavior compared to their lighter homologs in Groups 4 or 5 of the periodic table. Element 104 formed more volatile bromides than its homolog Hf. In contrast, element 105 bromides were found to be less volatile than the bromides of the group 5 elements Nb and Ta. Both 104 and Hf chlorides were observed to be more volatile than their respective bromides. DOE

N92-26217# Westinghouse Savannah River Co., Aiken, SC.

AGING EFFECTS IN PALLADIUM AND LaNi(4.25)Al(0.75) TRITIDES

A. Nobile, J. R. Wermer, and R. T. Walters 1991 7 p Presented at the 4th Topical Meeting on Tritium Technology in Fission, Fusion, and Isotopic Applications, Albuquerque, NM, 30 Sep. - 4 Oct. 1991

(Contract DE-AC09-89SR-18035)

(DE92-009945; WSRC-MS-91-076; CONF-910920-19) Avail: NTIS HC/MF A02

Palladium and LaNi(5-x)Al(x) (x = 0.30, 0.75, 0.85), which form reversible hydrides, are used for tritium processing and storage in the Savannah River Site (SRS) tritium facilities. As part of a program to develop technology based on the use of reversible

metal hydrides for tritium processing and storage, the effects of aging on the thermodynamic behavior of palladium and LaNi(4.25)Al(0.75) tritides are under investigation. During aging, the (3)He tritium decay product remains in the tritide lattice and changes the thermodynamics of the tritium-metal tritide system. Aging effects in 755-day-aged palladium and 1423-day-aged LaNi(4.25)Al(0.75) tritides are reported. Changes in the thermodynamics were determined by measuring tritium desorption isotherms on aging samples. In palladium, aging decreases the desorption isotherm plateau pressure and changes the alpha-phase portion of the isotherm. Aging-induced changes in desorption isotherms are more drastic in LaNi(4.25)Al(0.75). Among the changes noted are: (1) decreased isotherm plateau pressure; (2) increased isotherm plateau slope; and (3) appearance of deep-trapped tritium, removable only by exchange with deuterium. DOE

N92-26220# California Univ., Berkeley. Lawrence Berkeley Lab.
ELECTROCATALYSTS FOR OXYGEN ELECTRODES
E. B. Yeager (Case Western Reserve Univ., Cleveland, OH.) Oct. 1991 43 p
(Contract DE-AC03-76SF-00098)
(DE92-009491; LBL-31278) Avail: NTIS HC/MF A03

The research was carried out in hopes of developing further understanding of the factors controlling O2 reduction and generation in various electrocatalysts, such as the transition metal macrocycles and oxides. This understanding will help to identify and develop much higher activity catalysts, both monofunction and bifunction. Finally, it was attempted to establish how catalytic activity for a given O2 electrocatalyst depends on catalyst-support interactions and to identify stable catalyst supports for bifunctional electrodes. DOE

N92-26236# Hampton Univ., VA. Dept. of Chemistry.
THE USE OF ION CHROMATOGRAPHY-DC PLASMA ATOMIC EMISSION SPECTROMETRY FOR THE SPECIATION OF TRACE METALS
I. T. Urasa 20 Sep. 1991 42 p
(Contract DE-FG05-86ER-13589)
(DE92-010317; DOE/ER-13589/4) Avail: NTIS HC/MF A03

The original objectives of this research program were: to interface d.c. plasma atomic emission spectrometer with an ion chromatograph; to characterize and optimize the combined systems for application in the speciation of metals in aqueous solutions; to use this system in the study of the solution chemistry of various metals; and to find ways in which the measurement sensitivity of the method can be enhanced, thereby, allowing the detection of metal species at low ppb concentration levels. This approach has been used to study the chemistry of and speciate several elements in solution including: arsenic, chromium, iron, manganese, nickel phosphorus, platinum, selenium, and vanadium. During the course of this research, we have found that the solution chemistry of the elements studied and the speciation data obtained can vary considerably depending on the solution, and the chromatographic conditions employed. The speciation of chromium, iron, and vanadium was found to be highly influenced by the acidity of the sample. The element selective nature of the d.c. plasma detector allows these changes to be monitored, thereby, providing quantitative information on the new moieties formed. New approaches are being developed including the use of chelating ligands as preconcentration agents for purposes of reducing further the detection limits of the elements of interest and to improve the overall element speciation scheme. New thrusts are being directed towards the employment of post-column derivatization method coupled with colorimetric measurements to detect and quantify metal species eluting from the chromatographic column. The influence of sample acidity on these investigations will be carefully evaluated. These new thrusts are described in the accompanying Project Renewal Proposal. DOE

N92-26257# Technische Univ., Delft (Netherlands).
THE INFLUENCE OF PRESSURE ON THE PHASE BEHAVIOUR OF WATER + OIL + SURFACTANT SYSTEMS Ph.D. Thesis
Cornelis Laurentius Sassen 1991 125 p Sponsored by Koninklijke/Shell Exploratie en Produktie Lab.
(ISBN-90-6275-732-4; ETN-92-91303) Copyright Avail: NTIS HC/MF A06

The experimental determination of the influence of pressure in the phase behavior of water + oil + surfactant systems and the development of a thermodynamic model that can describe this influence are addressed. Experimental data for various water + oil + C(sub i)E(sub j) systems is generated and a phenomenological model to explain the influence of pressure on the phase behavior is postulated. The influence of pressure and electrolyte in the phase behavior of the system water + heptane + sodium dodecyl sulphate + 1-butanol + NaCl is investigated. An attempt to model the influence of pressure on the phase behavior of the binary subsystems water + C(sub i)E(sub j) and oil + C(sub i)E(sub j) is made. Concepts and models to describe the phase behavior of water + oil + surfactant systems at atmospheric pressure are reviewed. ESA

N92-26261# Technische Univ., Delft (Netherlands).
ACTIVATION AND CHARACTERIZATION OF SOME MOLECULAR SIEVE CATALYSTS Ph.D. Thesis
Theodorus Ludovicus Maesen 1990 118 p
(ETN-92-91306) Avail: NTIS HC/MF A06

The exploration of new methods to activate molecular sieve catalysts is described. Conventional ammonium exchange of an as-synthesized sodium neutralized Fau-type zeolite (Na-Y), at temperatures well below, 373 K is studied by Na-23 magic-angle, spinning-nutation Nuclear Magnetic Resonance (NMR). Combination of kinetic and NMR data allows the ammonium exchange mechanism to be unraveled in three distinct steps and the sodium cations to be unambiguously located in fully hydrated (partially exchanged) Na-Y zeolite. These data are used in a study of the hydrothermal ammonium exchange of Na-Y at 433 K in order to attain 100 percent ammonium exchange. To explore whether a 100 percent ammonium exchanged Na-Y zeolite is worth attaining, 'deep bed' calcination of this product is compared with ultrastabilization of conventional, around 70 percent, ammonium exchanged Na-Y. 'Shallow bed' and plasma calcination of ammonium exchanged Na-Y and hydronium exchanged at near neutral pH are also employed to try to obtain a fully intact hydronium neutralized zeolite Y framework. Plasma calcination is compared with mild, shallow bed calcination of ammonium exchanged Fau and (platinum doped) ammonium exchanged MOR. Applicability of low temperature oxygen plasma calcination for the oxidative removal of organic templates from as-synthesized zeolites is explored. ESA

N92-26262# Department of Energy, Morgantown, WV.
A MODEL FOR AERODYNAMICALLY-VALVED PULSE COMBUSTION
G. A. Richards and L. L. Narayanaswami (Embry-Riddle Aeronautical Univ., Daytona Beach, FL.) 1992 7 p Presented at the Combustion Institute, Central States Spring Meeting on Combustion Fundamentals and Applications, Columbus, OH, 26-28 Apr. 1992
(DE92-009887; DOE/METC-C/92/7006; CONF-9204103-1)
Avail: NTIS HC/MF A02

This paper presents a simulation of aerovalve pulse combustion. Starting from the conservative laws, a simplified set of governing equations that identifies crucial parameters is obtained. The combustor is assumed to be well-stirred, and modified slug flow models are applied to the flows in the inlet and exit pipes. The simulation has been used to study the influence of geometry and operational parameters on the operation of the pulse combustor. DOE

N92-26274# Princeton Univ., NJ.
AROMATIC-RADICAL OXIDATION KINETICS

1992 50 p
(Contract DE-FG02-86ER-13554)
(DE92-010821; DOE/ER-13554/6) Avail: NTIS HC/MF A03

Research progress in three areas is described. Progress achieved in the extensive experimental investigation of the oxidation and pyrolysis of cyclopentadiene is summarized first. The mechanistic implications of the experimental work are also discussed. An overview is given of the successful research effort devoted to modeling flow reactor toluene and benzene oxidation data. As mentioned above, one of the ultimate goals of this research is to develop a comprehensive, detailed chemical kinetic model of aromatics oxidation. The success already achieved in this effort augurs well for reaching the broader goal. The toluene/benzene model, however, does have a number of shortcomings which suggest the need for further experiments. A description is given of attempts to predict the laminar flame speeds of toluene and benzene. The difficulties encountered and the solutions found highlight the need of an examination of certain chemical steps that impact most of the energy release of a burning aromatic fuel. DOE

N92-26281# Stanford Univ., CA. High Temperature Gasdynamics Lab.
SPECTROSCOPY AND KINETICS OF COMBUSTION GASES AT HIGH TEMPERATURES
R. K. Hanson and C. T. Bowman Dec. 1991 6 p
(Contract DE-FG03-88ER-13857)
(DE92-011216; DOE/ER-13857/T2) Avail: NTIS HC/MF A02

This program involves two complementary activities: (1) development and application of cw ring dye laser absorption methods for sensitive detection of radical species and measurement of fundamental spectroscopic parameters at high temperatures; and (2) shock tube studies of radical-molecule and radical-radical reactions relevant to combustion. Species currently under investigation in the spectroscopic portion of the research include NO and CH3; this has necessitated the development of a unique intracavity frequency-doubling system for our cw laser which operates at wavelengths in the range 210-230 nm. Shock tube studies of reaction kinetics currently are focused on reactions of CH3 radicals. Work during the current reporting period has been focused on the following activities: high resolution spectroscopy, and methyl diagnostics and kinetics. DOE

N92-26285# International Flame Research Foundation, Ijmuiden (Netherlands).
FUEL STAGING AND ITS IMPLEMENTATION IN A NOVEL INTERNALLY STAGED BURNER Ph.D. Thesis
Kevin James Knill 1990 211 p Sponsored by Netherlands Agency for Energy and Environment Prepared in cooperation with Technische Univ., Delft, Netherlands
(ETN-92-91307) Avail: NTIS HC/MF A10

A study to investigate the process parameters which influence coal reburning and to apply these principles in designing and testing a coal fired, fuel staged burner is presented. This burner was intended to be used on wall fired boilers with both coal and natural gas considered as reburn fuels. The study was conducted in three experimental parts: a reburn zone investigation into the influence of process parameters on NOx, HCN, and NH3 reduction in the reburn zone; a furnace investigation into the NOx emissions from a fuel staging furnace, operated with incomplete mixing of reburn fuel and primary combustion products; and an Internally Fuel Staged Burner (IFSB) based on the concept of injecting the coal or natural gas reburn fuel through the center of the burner and reducing primary NOx at the downstream end of the internal recirculation zone. It is believed that the IFSB merits further development. The NOx emissions from the IFSB were low compared to existing low NOx burners. Also, burner performance was not adversely affected by operating with low NOx emissions. The CO emission did not exceed 5 ppm and the flame was compact and stable for all tests. Additional tests are recommended to improve the design and to establish scaling criteria. ESA

N92-26351# Interfacial Sciences, Inc., Santa Clara, CA.
LOW TEMPERATURE ELECTROCHEMICAL ACTIVATION OF METHANE Annual Report, 1 May 1990 - 1 May 1991
K. W. Frese, F. Wang, and C. C. Chen 27 Dec. 1991 94 p
(Contract GRI-5090-260-1973)
(PB92-152917; GRI-91/0345) Avail: NTIS HC/MF A05

Methane is presently an abundant raw material supplied by the gas industry. It would be advantageous from an economic point of view if methane could be effectively converted to chemicals more suitable to uses other than combustion and without costly reforming. The report is the first annual covering the initial year of a new contract between Interfacial Sciences Inc. and GRI concerning the partial oxidation of methane. The partial oxidation of methane in O2 containing concentrated KOH and NaOH(1-2 M) with cathodic current flow was the main topic of the last annual. The present research is focussed on chemistry of reactions of methane and oxygen in aqueous media under different conditions such as open circuit and mildly elevated temperatures. Unlike most other partial oxidation work sponsored by GRI, the authors are investigating low reaction temperatures, from room temperature to 150 C. The authors believe that intermediates such as Methylhydroperoxide (MHP), formaldehyde, and methanol can be stabilized in this temperature range, indicating the extent that methane oxidation can be limited and CO2 can be avoided. GRA

N92-26404# Defence Research Establishment, Ottawa (Ontario).
DIFFERENTIAL SCANNING CALORIMETRY (DSC) FOR THE ANALYSIS OF ACTIVATED CARBON
S. H. Liang and L. E. Cameron Oct. 1991 55 p
(AD-A245899; DREO-1098) Avail: NTIS HC/MF A04

The technique of Differential Scanning Calorimetry (DSC) has been applied to the characterization and the analysis of several activated carbons. These activated carbons included BPL carbon (a base carbon), ASC carbon (a BPL carbon impregnated with copper, chromium and silver) and ASC/T carbon (an ASC carbon impregnated with triethylenediamine, TEDA). DSC has been shown to be capable of measuring enthalpic changes associated with transitions and/or reactions of the surface species on the activated carbon. Physical changes or chemical reactions occurring on the carbon surface and the surface impregnants are observed as endotherms or exotherms (enthalpic changes) on the DSC curves (thermograms). The data from this study have demonstrated that DSC can be used quantitatively in the determination of the amount of TEDA impregnant on the activated carbon surface. This is based on the linear relationship between the area under the DSC curve and the amount of TEDA present. Qualitatively, DSC is shown to be able to differentiate between carbons which have been impregnated with different organic and/or metal impregnants, because each impregnated carbon produces a DSC thermogram which is unique to the compounds on its surface. GRA

N92-26431# Colorado State Univ., Fort Collins. Dept. of Chemistry.
VIBRATIONAL DYNAMICS OF ANILINE (N2)1 CLUSTERS IN THEIR FIRST EXCITED SINGLET STATE
E. R. Bernstein, M. F. Hineman, S. K. Kim, and D. F. Kelley 4 Feb. 1992 24 p
(Contract N00014-89-J-1237)
(AD-A245812; TR-75) Avail: NTIS HC/MF A03

The vibrational dynamics of van der Waals (vdW) clusters have recently attracted considerable experimental and theoretical attention. The most extensively studied vdW clusters consist of a chromophore molecule and one or more solvent molecules. The cluster is excited by absorption of a photon to a chromophore vibronic state which can then relax by three different pathways: fluorescence or radiationless processes (intersystem crossing or internal conversion); intra cluster vibrational redistribution of the excess chromophore vibrational energy to the van der Waals modes (IVR); and vibrational predissociation (VP) if the chromophore vibrational energy is greater than the cluster binding energy. The first excited singlet state vibrational dynamics of aniline clusters

are studied and compared to previous results of aniline. Intramolecular vibrational energy redistribution (IVR) and vibrational predissociation (VP) rates fall between the two extremes of the CH4 (fast IVR, slow VP) and Ar (slow IVR, fast VP) cluster results as is predicted by a serial IVR/VP model using Fermi's golden rule to describe IVR processes and a restricted RRKM theory to describe unimolecular VP rates. GRA

N92-26454# Lawrence Livermore National Lab., CA.
HELIUM-3 MASS SPECTROMETRY FOR LOW-LEVEL TRITIUM ANALYSIS OF ENVIRONMENTAL SAMPLES
K. A. Surano, G. B. Hudson, R. A. Failor, J. M. Sims, R. C. Holland, S. C. MacLean, and J. C. Garrison Apr. 1991 16 p Presented at the International Topical Conference on Methods and Applications of Radioanalytical Chemistry II (MARC-2), Kona, HI, 21-27 Apr. 1991
(Contract W-7405-eng-48)
(DE92-008937; UCRL-JC-107042; CONF-910422-8) Avail: NTIS HC/MF A03

Helium-3 (He-3) mass spectrometry for the analysis of low level tritium (H-3) concentrations in environmental sample matrices was compared with conventional low level beta-decay counting methods. The mass spectrometry method compared favorably, equaling or surpassing conventional decay-counting methods with respect to most criteria. Additional research and method refinements may make He-3 mass spectrometry the method of choice for routine, low level to very-low-level H-3 measurements in a wide variety of environmental samples in the future. DOE

N92-26457# Pittsburgh Univ., PA. Dept. of Chemical and Petroleum Engineering.
LOW SEVERITY UPGRADING OF F-T WAXES WITH SOLID SUPERACIDS
I. Wender and J. W. Tierney 1991 7 p
(Contract DE-FG22-91PC-91304)
(DE92-009081; DOE/PC-91304/T1) Avail: NTIS HC/MF A02

We have discovered that the isomerization and hydrocracking of a long chain paraffin, n-hexadecane, with a solid superacid such as ZrO2/SO4 gives very high selectivities, (i.e., greater than 90 pct. to hydrocracked isoparaffins, C4-C13) in the presence of platinum and a low pressure of hydrogen. Undesirable light gases (methane and ethane) are not produced during these reactions. In addition, a high multi-branched to monobranched ratio of long chain hydrocarbons is produced. We have written the formula for this catalyst as Pt/ZrO2/SO4. Early attempts during this first quarter to reproduce this catalyst for the hydrocracking and isomerization of n-hexadecane gave results which were not reproducible, conversion varying from a few pct. to 70 pct. It was, therefore, of utmost importance to devise a procedure that could be depended upon to synthesize a reproducible catalyst would give high conversions and high selectivities to cracked and isomerized products of high fuel and lubricating oil values. The catalysts should be active under mild conditions, i.e., below 170 C and hydrogen pressures below 350 psi. Conventional heavy end cracking catalysts (modified zeolites) are active at 300 to 400 C. DOE

N92-26508# Colorado Univ., Boulder. Dept. of Chemical Engineering.
REACTION/SEPARATION PROCESS FOR ENHANCED METHANE CONVERSION Annual Report, Oct. 1990 - Sep. 1991
J. L. Falconer and R. D. Noble Dec. 1991 12 p
(Contract GRI-5090-260-2005)
(PB92-149657; GRI-92/0011) Avail: NTIS HC/MF A03

A summary of the progress made during the first year of work on the fundamental processes involved in catalytic membrane reactors for the partial oxidation of methane to methanol is presented. Reactor design was finalized, and a system for permeation measurements was built. The system was modified to withstand higher temperatures and pressures, to make runs easier to set up and reproduce, and to improve control of the feed flow rates. Initial permeation experiments provided evidence for the surface diffusion of methanol. A basic model incorporating component mass balances was formulated and checked against experimental results for the dehydrogenation of butane. The model predicted that a catalytic membrane reactor would give higher conversion than a conventional packed bed reactor, and the overall butane conversion was found to depend on the reactor's ratio of impermeable length to permeable length. A more physically realistic model for highly permeable membranes was then developed by including mechanical energy balance equations to account for the axial pressure drops. These simulations showed a reversal in the permeation direction for the gas entering the reactor on the low pressure side. GRA

N92-26516# Pennsylvania State Univ., University Park.
ENHANCE METHANE REACTIVITY Annual Report, Jan. - Dec. 1991
A. Sen Jan. 1992 25 p
(Contract GRI-5091-260-2184)
(PB92-154822; GRI-91/0383) Avail: NTIS HC/MF A03

Methods were sought for the selective, catalytic, activation, and oxidation of methane to useful organic molecules. Two basic strategies were used. The first involved the use of electrophilic metal species to effect the heterolytic cleavage of a carbon-hydrogen bone of methane to form the corresponding metal-methyl species. The metyl group was subsequently oxidized by the metal to give an oxidized organic product, such as methanol. The addition of a second oxidant that was capable of reoxidizing the metal made the system catalytic in the metal species. The overall reaction then became a metal catalyzed oxidation of methane by the cooxidant. By using this approach, it was possible to oxidize methane to methanol using the divalent palladium or platinum ion as catalyst and either hydrogen peroxide or oxygen as the oxidant. The second strategy involved the use of a powerful one electron oxidant that was capable of forming methyl radical from methane by H2 atoms abstraction. The methyl radical was subsequently converted to a functionalized organic molecule. Thus, by using the persulfate ion as the oxidant and CO as a trapping agent for the methyl radical, methane was converted to acetic acid. Author

N92-26521# Northern Research and Engineering Corp., Woburn, MA.
TURBOCHARGED PRESSURIZED COMBUSTION SYSTEM Final Report, Nov. 1987 - Jul. 1990
A. F. Carter Dec. 1991 91 p
(Contract GRI-5087-234-1608)
(PB92-142579; NREC-1656-1; GRI-91/0180) Avail: NTIS HC/MF A05

A laboratory unit was designed and tested to demonstrate a turbine-based approach to pressurized combustion systems for a variety of industrial process heat requirements. The natural gas burner is located between a centrifugal compressor and a radial inflow turbine and operates at pressure levels up to 5 psig. The turbine extracts a small percentage of the heat from combustion to drive both the compressor ahead of the combustor and a fan providing additional air. Two versions of the system were demonstrated: fan air was heated by the turbine exhaust in a downstream heat exchanger to provide uncontaminated heat air and mixed with the turbine exhaust gases in the second version. The approach eliminates the need for electrical motor drives for the air movers. The system's gas turbine-type burner has low NO(x) emission characteristics. By choice of cycle operating parameters, a wide range of delivery temperature can be provided at process input pressures up to 2 psig. The pressure could be used to either increase the operating pressure levels in the downstream process or to provide high velocity inputs to enhance process efficiencies and/or productivities by means of improved heat transfer rates. The report also contains summaries of results obtained from two subcontracted efforts with respect to an assessment of the market turbine-based approach and the commercialization potential for products based on the approach. GRA

N92-26526# Colorado State Univ., Fort Collins. Dept. of Chemistry.
TOLUENE-WATER CLUSTERS: ION FRAGMENTATION AND CHEMISTRY
Shijian Li and Elliot R. Bernstein 4 Feb. 1992 45 p
(Contract N00014-89-J-1237)
(AD-A245813; TR-76) Avail: NTIS HC/MF A03

In this report we explore the cluster ion chemistry of toluene/water clusters. The chemistry of toluene/ammonia cluster ions is dealt with in a separate report. The particular focus of this paper concerns four main themes: association of a given resolved spectrum with a specific cluster C6H5CH3(H20)(sub n); identification of particular cluster ion fragmentation patterns as a function of ionization energy; demonstration that the observation chemistry does indeed occur on the ground state ion potential surface and not the S(sub 0), S(sub 1) or T(sub n) surfaces; and association of (qualitative) cluster structure with the observed chemistry. GRA

N92-26541# Syracuse Univ., NY. Inst. for Energy Research.
NON-DESTRUCTIVE ANALYSIS FOR HYDROGEN CONCENTRATIONS IN MATERIALS Final Report, Aug. 1987 - Aug. 1991
Walter Meyer and William H. Miller 31 Oct. 1991 15 p
(Contract DAAL03-87-K-0105)
(AD-A246098; ARO-25199.3-MS) Avail: NTIS HC/MF A03

The objective of the proposed research is to conduct several preliminary experiments to verify calculations made by these investigators that show it to be possible to non-destructively and quantitatively determine hydrogen content in steel and possibly other host materials at the parts per million level (minimum level of from 100 to 1 ppm). The hydrogen analysis is based on the fact that 24 keV neutrons readily penetrate large thicknesses of materials composed mainly of iron with little scattering and the scattering that does occur, is nearly isotropic. However, the presence of a light material (small mass number) such as hydrogen will cause significant scattering of the neutrons in a preferred forward angle, which permits these hydrogen-scattered neutrons to be distinguished from other neutrons by their particular scattering angle and energy. The number of neutrons scattered at angles and energies peculiar to hydrogen will be directly proportional to the concentration of hydrogen in the host material. Thus, the measurement of the number of hydrogen scattered neutrons will permit the quantitative, nondestructive measurement of the hydrogen concentration in test articles or samples and/or whole prototypes. GRA

N92-26608# Colorado State Univ., Fort Collins. Dept. of Chemistry.
SOLVATION EFFECTS ON THE ELECTRONIC STRUCTURE OF 4-N,N-DIMETHYLAMINOBENZONITRILE: MIXING OF THE LOCAL pipi* AND CHARGE TRANSFER STATES
E. R. Bernstein and Q.-Y. Shang 4 Feb. 1992 34 p
(Contract N00014-89-J-1237)
(AD-A245814; TR-77) Avail: NTIS HC/MF A03

The effect of polar solvents acetonitrile and water on the electronic excited states of 4-N, N-dimethylaminobenzonitrile (DMABN), is studied through the optical spectroscopy of small clusters of DMABN/solvent. The clusters are created in a supersonic jet expansion. The results of mass resolved excitation spectroscopy (MRES), fluorescence excitation (FE), dispersed emission (DE), and photo-depletion studies demonstrate that the solvent molecule can bind to DMABN at two distinct sites for the 1:1 cluster. Both DMABN(H2O)1 clusters generate small blue shifts for the cluster transition and evidence low energy vibronic structure nearly identical to that found for the bare molecule. The DMABN(CH3CN)1 clusters behave quite differently. One cluster geometry induces a small blue shift of the electronic transition with little change in its vibronic structure and intensity pattern. We suggest this binding site involves the cyano end of the DMABN molecule. The second cluster geometry induces a large red shift (ca. 1000 per centimeter and significant broadening (greater than 1000 per centimeter) of the lowest energy transition. This red shifted transition is associated with a charge transfer transition within the DMABN molecule lowered in energy due to the acetonitrile coordination with the DMABN aromatic ring. GRA

N92-26615 Michigan Univ., Ann Arbor.
THEORETICAL AND NUMERICAL STUDY OF FLAME PROPAGATION AND TRANSITION TO DETONATION Ph.D. Thesis
Chong Oh Lee 1991 185 p
Avail: Univ. Microfilms Order No. DA9208590

The ability of accelerating, turbulent flames, which have been observed to reach velocities on the order of hundreds of meters per second, to generate precursor shock waves is of fundamental significance to the transition from deflagration to detonation (DDT) and in a variety of destructive explosions. For sufficiently high flame velocities, the precursor shock becomes strong enough to initiate an explosion in the region between the flame and the shock which can lead to transition to detonation. The numerical code validated for steady flames was also used to study the flowfields generated by accelerating flames for four different regimes of flame acceleration. It was found that due to the interaction between shock waves, flames, expansion waves, and contact surfaces which arises in the flowfields generated by accelerating flames, the overpressure generated by an accelerating flame may exceed that produced by a constant velocity flame propagating at the final or maximum velocity of the accelerating flame. Dissert. Abstr.

N92-26632# Westinghouse Savannah River Co., Aiken, SC.
GAMMA-RAY SPECTROMETRY OF LDEF SAMPLES
W. G. Winn 1991 62 p
(Contract DE-AC09-89SR-18035)
(DE92-009947; WSRC-RD-91-16) Avail: NTIS HC/MF A04

A total of 31 samples from the Long Duration Exposure Facility (LDEF), including materials of aluminum, vanadium, and steel trunnions were analyzed by ultra-low-level gamma spectroscopy. The study quantified particle induced activations of Na-22, Sc-46, Cr-51,Mn-54, Co-56, Co-57, Co-58, and Co-60. The samples of trunnion sections exhibited increasing activity toward the outer end of the trunnion and decreasing activity toward its radial center. The trunnion sections did not include end pieces, which have been reported to collect noticeable Be-7 on their leading surfaces. No significant Be-7 was detected in the samples analyzed. The Underground Counting Facility at Savannah River Laboratory (SRL) was used in this work. The facility is 50 ft. underground, constructed with low-background shielding materials, and operated as a clean room. The most sensitive analyses were performed with a 90 pct. efficient HPGe gamma ray detector, which is enclosed in a purged active/passive shield. Each sample was counted for one to six days in two orientations to yield more representative average activities for the sample. The non-standard geometries of the LDEF samples prompted the development of a novel calibration method, whereby the efficiency about the samples surfaces (measured with point sources) predicted the efficiency for the bulk sample. DOE

N92-26634# Westinghouse Savannah River Co., Aiken, SC.
GRAVIMETRIC GAS DETERMINATIONS FOR VOLUME CALIBRATIONS
P. W. Gibbs 1991 6 p Presented at the 32nd Inst. of Nuclear Materials Management Annual Meeting, New Orleans, LA, 28-31 Jul. 1991
(Contract DE-AC09-89SR-18035)
(DE92-010041; WSRC-MS-91-062; CONF-910774-102) Avail: NTIS HC/MF A02

Gravimetric measurement of gases is one of the methods available for calibrating gas volumes. By inputting a known quantity of gas and measuring the resulting pressure and temperature, the system volume can be calculated using gas law principles. Historically, this method has been less accurate due to the difficulty in the mass determination. This difficulty comes from several sources. Two examples are the large tare weight of the gas container relative to the weight of gas and the external volume of the gas container relative to the standards. The application of a

gravimetric gas determination to tank volume calibrations at the Savannah River Site is discussed. Mass determinations on a 25,000 gram gas container were such that a 1500 gram quantity of gas was routinely determined to within (+ or -)0.2 gram at the 99 pct. confidence level. The weighing design and the methods used to address the difficulties of the mass determination are detailed.
DOE

N92-26670*# National Aeronautics and Space Administration. Lewis Research Center, Cleveland, OH.
PROGRESS IN THE DEVELOPMENT OF LIGHTWEIGHT NICKEL ELECTRODE
Doris L. Britton Jun. 1992 8 p Proposed for presentation at the 35th International Power Sources Symposium, Cherry Hill, NJ, 22-25 Jun. 1992; sponsored by IEEE, Industry Application Society
(RTOP 506-41-21)
(NASA-TM-105638; E-6984; NAS 1.15:105638) Avail: NTIS HC/MF A02

The use of the lightweight nickel electrode, in place of the heavy-sintered state-of-the-art nickel electrode, will lead to improvements in specific energy and performance of the nickel-hydrogen cell. Preliminary testing indicates that a nickel fiber mat is a promising support candidate for the nickel hydroxide active material. Nickel electrodes made from fiber mats, with nickel and cobalt powder added to the fiber, were tested at LeRC. To date, over 8000 cycles have been accumulated, at 40 percent depth-of-discharge, using the lightweight fiber electrode, in a boiler plate nickel-hydrogen cell.
Author

N92-26687# Utah Univ., Salt Lake City. Dept. of Chemistry.
NEW THEORETICAL METHODS FOR ELECTRONIC STRUCTURE AND GAS-PHASE STATE SPECIFIC OXIDATION/REDUCTION STUDIES Final Report, 1 Jan. 1989 - 31 Dec. 1991
Jack Simons 29 Jan. 1992 6 p
(Contract N00014-89-J-1497)
(AD-A246127) Avail: NTIS HC/MF A02

The integrated impact of this grant is detailed in the twenty-four technical reports and their associated refereed publications. A very visible achievement was our successful solution of the world's largest matrix eigenvalue problem: a one billion by one billion configuration interaction eigenvalue problem technical report 7. Our work on finding transition states on potential energy surfaces has had substantial impact; these tools are now incorporated in many ab initio codes such as the GAUSSIAN and GAMESS programs. Work on so-called Double Rydberg Anions is now reaching maturity and is gaining a reasonable amount of recognition among experimental, physical, and inorganic chemists. Their importance in materials containing their parent cation cores is now believed to be very important. The work of this group on excited-state potential energy surfaces and reactivity of metal atoms and small main-group clusters will have considerable impact within the next five years. The mechanisms for chemical reaction and electronic-to-vibrational energy flow operative in such prototype species are now of interest to experimental chemist.
GRA

N92-26717# Westinghouse Savannah River Co., Aiken, SC.
METAL HYDRIDE BASED ISOTOPE SEPARATION: LARGE-SCALE OPERATIONS
A. S. Horen and Myung W. Lee 1991 6 p Presented at the 4th Topical Meeting on Tritium Technology in Fission, Fusion, and Isotopic Applications, Albuquerque, NM, 30 Sep. - 4 Oct. 1991
(Contract DE-AC09-89SR-18035)
(DE92-009830; WSRC-MS-91-016; CONF-910920-22) Avail: NTIS HC/MF A02

A program to develop a metal hydride based hydrogen isotope separation process began at the Savannah River Laboratory in 1980. This semi-continuous gas chromatographic separation process will be used in new tritium facilities at the Savannah River Site. A tritium production unit is scheduled to start operation in 1993. An experimental, large-scale unit is currently being tested using protium and deuterium. Operation of the large-scale unit has demonstrated separation of mixed hydrogen isotopes (55 percent protium and 45 percent deuterium), resulting in protium and deuterium product streams with purities better than 99.5 percent.
DOE

N92-26718# Westinghouse Savannah River Co., Aiken, SC.
A NEW PHASE IN PALLADIUM HYDRIDE TECHNOLOGY
R. T. Walters 1991 6 p Presented at the 4th Topical Meeting on Tritium Technology in Fission, Fusion, and Isotopic Applications, Albuquerque, NM, 30 Sep. - 4 Oct. 1991
(Contract DE-AC09-89SR-18035)
(DE92-009852; WSRC-MS-91-008; CONF-910920-25) Avail: NTIS HC/MF A02

Two plateaux are observed in both the absorption and desorption isotherms of palladium hydride. For the absorption isotherm, a change in plateau pressure is observed at a hydrogen to metal (H/M) ratio of about 0.35 for all temperatures studied. For the desorption isotherm, the change in plateau pressure appears to be a function of temperature, ranging from an H/M ratio of 0.18 at 80 C to 0.3 at 140 C. These data are interpreted as being experimentally observed boundaries to an equilibrium phase line located in the miscibility gap of the palladium/hydrogen phase diagram. This new phase does not appear to be a stoichiometric compound, but rather its composition seems to vary with temperature.
DOE

N92-26722# Sandia National Labs., Albuquerque, NM.
BURN-RATE STUDIES WITH IRON/POTASSIUM PERCHLORATE HEAT PELLETS
J. W. Reed, R. R. Walters (EG and G Mound Applied Technologies, Miamisburg, OH.), R. A. Guidotti, and A. K. Jacobson 1991 4 p Proposed for presentation at the 35th International Power Sources Symposium, Cherry Hill, NJ, 22-25 Jun. 1992
(Contract DE-AC04-76DP-00789)
(DE92-008524; SAND-91-2347C; CONF-920669-1) Avail: NTIS HC/MF A01

A detailed study was conducted on factors which could possibly influence the burn rate of Fe/KCl04 heat pellets. The burning process was monitored with a high speed (1000 frames per second) video analysis system. The substrate and pellet thickness had little effect upon the burn rate of heat pellets. The pellet density, composition, and Fe particle size, however, affected the burn rates significantly. By proper adjustment of these parameters, the burn rate of heat pellets can be affected. This, in turn, can be used to influence the rise times of thermal batteries that use this type of pyrotechnic heat source.
DOE

N92-26724# North Dakota Univ., Grand Forks. Energy and Environmental Research Center.
HIGH-YIELD HYDROGEN PRODUCTION BY CATALYTIC GASIFICATION OF COAL OR BIOMASS
W. B. Hauserman 1992 11 p Proposed for presentation at the 9th World Hydrogen Energy Conference, Paris, France, 22-25 Jun. 1992
(Contract DE-FC21-86MC-10637)
(DE92-008770; DOE/MC-10637/92/C0002; CONF-920643-2)
Avail: NTIS HC/MF A03

Gasification of coal or wood, catalyzed by soluble metallic cations to maximize reaction rates and hydrogen yields, offers a potential for large scale, economical hydrogen production with near commercial technology. With optimum reaction conditions and catalysts, product gas rich in both hydrogen and methane can be used in fuel cells to produce electricity at efficiencies nearly double those of a conventional power plant. If plantation silvaculture techniques can produce wood at a raw energy cost competitive with coal, further enhancement of product gas yields may be possible, with zero net contribution of CO2 to the atmosphere.
DOE

N92-26726# Oak Ridge National Lab., TN.
TECHNOLOGY TRANSFER AND APPLICATION OF SERS CONTINUOUS MONITOR FOR TRACE ORGANIC COMPOUNDS
D. W. Swindle, Jr., T. Vo-Dinh, and M. G. Yalcintas 1992 5 p Presented at the Mediterranean Conference on Environmental

Geotechnology, Cesme, Turkey, 25-27 May 1992
(Contract DE-AC05-84OR-21400)
(DE92-008900; CONF-9205121-2) Avail: NTIS HC/MF A01

An in situ-enhanced Raman Scattering (SERS) continuous monitoring system was developed for exciting and collecting SERS signals generated on silver-coated microparticles deposited on a continuously rotating filter-paper support. SERS measurements were successfully conducted for several organic compounds. An in situ SERS fiber-optic system was also developed for exciting and collecting SERS signals generated from a sensing tip having silver coated microparticles deposited on a glass plate support. These devices will be very useful in remote identification of unknown chemicals from hazardous waste sites. This patented technology has been licensed from Oak Ridge National Laboratory to an analytical instrumentation firm which is in the process of completing development and marketing these detectors. Advantages to using this technology range from increased safety and sensitivity for detecting hazardous compounds to better statistics and reliable results. During this presentation, efforts of the Environmental Restoration Program to evaluate and support development of this technology will be described. DOE

N92-26782# General Electric Co., Schenectady, NY.
ADVANCING NATURAL GAS COMBUSTION SCIENCE AND TECHNOLOGY-LOW NOx Annual Report, Jun. 1990 - Jun. 1991
S. M. Correa and R. V. Gemmer Jul. 1991 35 p
(Contract GRI-5089-260-1912)
(PB92-137652; GRI-91/0313) Avail: NTIS HC/MF A03

Preliminary results of bench-scale research on lean premixed combustion of methane at gas-turbine conditions are described. The goal is to develop understanding of the ultra-lean high pressure combustion regime, leading to sub-10 ppm NO(x) at greater than 50 percent thermodynamic efficiency in combined cycle gas turbines. Measurements of NO(x) and CO in a lean premixed 5 cm diameter perforated-plate burner in the range 3-10 atm, inlet temperature 300-615 K, and equivalence ratio 0.5-0.8. Good comparison is obtained with a stirred/plug flow reactor model. NO(x) is produced by the thermal sub-mechanism above 1850 K or so, and by the prompt and nitrous oxide submechanisms below 1750 K or so; at the latter conditions NO(x) formation is slow enough to decouple from the turbulence. NO(x) is also independent of pressure in lean enough flames. Analyses indicate that post-flame gas flow over cooled 1100 K combustor walls, turbulent mixing of post-flame gas with dilution jets at compressor discharge temperature, and interaction with pressure oscillations in post-flame gas, cannot in general quench CO. The Discrete Vortex Method for unsteady (shedding) flows was reformulated for lean premixed combustion in axisymmetric burners. A 15 cm burner facility was readied for the supporting experimental at very lean conditions approaching blowoff. GRA

N92-26783# AeroChem Research Labs., Inc., Princeton, NJ.
MICROWAVE BACKSCATTERING FUEL/AIR RATIO CONTROL AND FLAME MONITORING DEVICE Final Report, Aug. 1990 - May 1991
C. H. Berman, R. Orlando, and H. F. Calcote May 1991 26 p
(Contract GRI-5090-260-2014)
(PB92-141779; AeroChem-TP-497; GRI-91/0402) Avail: NTIS HC/MF A03

A microwave backscatter technique was developed to maintain fuel/air ratios in natural gas/air diffusion flames at values that achieve maximum burning efficiency and/or low emissions over the complete range of burner firing rates. In addition, reliable flame monitoring systems are needed to shut off the gas flow if a flame is extinguished. The technique is nonintrusive to the combustor process and provides nearly instantaneous information on the flame. Relatively inexpensive and small microwave transceivers were used and many prove to be adequate in practical burner systems. A procedure was developed for determining the percent excess air that involves analyzing: (1) the average value of the total reflected signal strength to determine the absolute air flow rate; and (2) a characteristic frequency to determine firing rate. The bluff-body stabilized burner that was tested was operated at a maximum firing rate of over 40 k Btu/h from slightly fuel rich to 50 percent excess air and a turndown ratio of 4:1. The microwave transceiver acted as a very accurate air flow meter when aimed at the flame. A final evaluation of accuracy should be made using the desired type of burner operating over its normal range of conditions. GRA

N92-26812# National Oceanic and Atmospheric Administration, Boulder, CO. Climate Monitoring and Diagnostics Lab.
RULE-BASED EXPERT SYSTEM FOR EVALUATING THE QUALITY OF LONG-TERM, IN-SITU, GAS CHROMATOGRAPHIC MEASUREMENTS OF ATMOSPHERIC METHANE
K. A. Masarie, L. P. Steele, and P. M. Lang Nov. 1991 43 p
(PB92-128560; NOAA-TM-ERL-CMDL-3) Avail: NTIS HC/MF A03

Methane is an important trace constituent of the earth's atmosphere because it is active both chemically and radiatively. The absorption of infrared radiation by atmospheric methane, and the rapid increase in the global atmospheric burden of methane over the past century combine to raise concerns that continued increases may contribute to global warming and climate change within the next century. The use of a rule-based expert system to assess the integrity of in situ gas chromatographic methane measurements made at the NOAA/CMDL Point Barrow, Alaska and Mauna Loa, Hawaii observatories is presented. The expert system flags ambient samples analyzed during chromatograph system instability and excludes them from further scientific analysis. The development and implementation of the expert system are described in detail. A comparison between data sets flagged by a human expert and by the expert system shows that the expert system can successfully reproduce the efforts of a human when evaluating gas chromatograph system stability. Advantages and limitations of the use of an expert system for the task are also discussed. GRA

N92-26867# Los Alamos National Lab., NM.
VIBRATIONAL SPECTROSCOPY IN SHOCK-COMPRESSED LIQUIDS
S. C. Schmidt and D. S. Moore 1992 9 p Presented at the 2nd International Symposium on Intense Dynamic Loading and its Effects, Chengdu, China, 9-12 Jun. 1992
(Contract W-7405-eng-36)
(DE92-007713; LA-UR-92-120; CONF-920688-3) Avail: NTIS HC/MF A02

Coherent anti-Stokes Raman spectroscopy is being used to study the structure and energy transfer in simple molecular liquids at the high pressures and temperatures characteristic of explosive detonation. Dense fluids at several thousand degrees temperature and several hundred kilobars pressure are obtained using the shock-compression technique. Vibrational frequencies, third-order susceptibility ratios, and linewidths were measured for N2, O2, CO, mixtures of N2, O2, and CO, and N2O. Frequencies are found to increase with pressure. The transition intensity and line-width data suggest that the thermal equilibrium of the vibrational levels is attained in less than a few nanoseconds at these high pressures and temperatures. Vibrational temperatures obtained are compared to those derived from equation-of-state calculations. DOE

26 METALLIC MATERIALS

Includes physical, chemical, and mechanical properties of metals, e.g., corrosion; and metallurgy.

N92-26172# GTE Sylvania, Inc., Towanda, PA. Chemical and Metallurgical Div.
RELATIONSHIP BETWEEN COMPOSITION, STRUCTURE, PROPERTIES, THERMO-MECHANICAL PROCESSING AND BALLISTIC PERFORMANCE OF TUNGSTEN HEAVY ALLOYS Final Report, Mar. 1986 - Jul. 1991

James R. Spencer and James A. Mullendore Nov. 1991 221 p
(Contract DAAL04-86-C-0023)
(AD-A245649; MTL-TR-91-44) Avail: NTIS HC/MF A10

Traditional tungsten heavy alloys are 'tungsten nickel iron' or 'tungsten nickel copper' alloys containing 88 to 98 pct. tungsten. Cobalt is also used in these alloys but to a lesser extent. These alloys are produced by blending the elemental powders, pressing billets from the blend and then liquid-phase sintering the billets. These alloys were first developed to provide high density materials that were easy to machine but were developed with little concern for mechanical properties. Initially W-Ni-Cu alloys were most common because the low melting point of copper made these alloys easier to sinter. As the demand for alloys with good mechanical properties increased, a shift occurred from the W-Ni-Cu alloys to the W-Ni-Fe alloys. Processing techniques to consistently produce high quality tungsten heavy alloys were developed. The purpose of this program was to do a thorough study of tungsten heavy alloys and the interrelationship between chemical composition, impurities, thermo-mechanical processing history, structure and ballistic properties. Ballistic testing was to include a wide range of types and sizes ranging from an in-house 20 mm range to full scale testing. GRA

N92-26213# California Univ., Berkeley. Lawrence Berkeley Lab.
WHY FIRST-PRINCIPLES CALCULATIONS FOR ALLOYS?
D. deFontaine Oct. 1991 9 p Presented at the North Atlantic Treaty Organization Advanced Research Workshop, Irsee, Germany, 23-29 Jun. 1991
(Contract DE-AC03-76SF-00098)
(DE92-010285; LBL-31512; CONF-9106275-6) Avail: NTIS HC/MF A02

A brief non-technical overview of first-principles calculations is presented, with emphasis on prediction of phase equilibria. Merits and drawbacks of various methods are briefly discussed. DOE

N92-26223# Lawrence Livermore National Lab., CA.
DYNAMIC RESTORATION MECHANISMS IN Al-5.8 AT. PERCENT Mg DEFORMED TO LARGE STRAINS IN THE SOLUTE DRAG REGIME
G. A. Henshall, M. E. Kassner, and H. J. McQueen (Concordia Univ., Montreal, Quebec) Dec. 1991 26 p
(Contract W-7405-eng-48)
(DE92-009529; UCRL-CR-107026) Avail: NTIS HC/MF A03

An Al-5.8 atomic percent Mg (5.2 weight percent Mg) alloy was deformed in torsion within the solute drag regime to various strains, up to the failure strain of 10.8. Optical and transmission electron microscopy were used to analyze the evolution of the microstructure and to determine the dynamic restoration mechanism. TEM revealed that the subgrain is sluggish but that subgrains eventually (bar-epsilon approximately 1) fill the grains. The steady-state subgrain size (lambda approximately 6 microns) and misorientation angle (Theta approximately 1.6 deg) are reached by bar-epsilon approximately 2. These observations confirm that subgrains eventually form during deformation in the solute drag regime, though they do not appear to significantly influence the strength. At low strains, nearly all of the boundaries form by dislocation reaction and are low angle (Theta is less than 10 deg). At a strain of 10.8, however, the boundary misorientation histogram is bimodal, with nearly 25 percent of the boundaries having high angles due to their ancestry in the original grain boundaries. This is consistent with optical microscopy observations of the elongation and thinning of the original grains as they spiral around the torsion axis. No evidence was found for discontinuous dynamic recrystallization, a repeating process in which strain-free nucleate, grow, deform, and give rise to new nuclei. It is concluded that dynamic recovery in the solute drag regime gives rise to geometric dynamic recrystallization in a manner very similar to that already established for pure aluminum, suggesting that geometric dynamic recrystallization may occur generally in materials with a high stacking-fault energy deformed to large strains. DOE

N92-26251# Pennsylvania Univ., Philadelphia. Dept. of Materials Science and Engineering.
ATOMISTIC STUDIES OF GRAIN BOUNDARIES IN ALLOYS AND COMPOUNDS
V. Vitek Feb. 1992 13 p
(Contract DE-FG02-87ER-45295)
(DE92-010792; DOE/ER-45295/2) Avail: NTIS HC/MF A03

In this research project we carry out theoretical computer modeling studies of the atomic structure of grain boundaries in binary alloys. Both ordered and disordered alloys are investigated. The goal is to analyze those structural, chemical, and electronic features that distinguish alloys from pure metals and are responsible for remarkably different intergranular fracture behavior of alloys when compared with pure metals. The most important phenomenon is, of course, segregation and related structural changes in the boundary region. When studying segregation phenomena copper-bismuth is a very suitable model system since bismuth segregation occurs readily, leads to boundary faceting and, thus, to remarkable changes in the boundary structure, as well as to a very strong embrittlement. Our recent research concentrated on the investigation of the structure of sigma = 3 (111)/(11(bar 1)) facets formed during segregation from boundaries which were originally curved. DOE

N92-26252# Philips Gloeilampenfabrieken N.V., Eindhoven (Netherlands).
MAGNETIC ANISOTROPY FROM FIRST PRINCIPLES Ph.D. Thesis
Gerardus Henricus Ot Daalderop 16 Dec. 1991 197 p Prepared in cooperation with Technische Univ., Delft, Netherlands
(ISBN-90-9004483-3; ETN-92-91288) Avail: NTIS HC/MF A09

The anisotropy energies of experimentally well characterized magnetic metals, Fe, Co, Ni, and several metallic multilayers, are considered. The following studies are detailed: first principles calculation of the magnetocrystalline anisotropy energy of Fe, Co, and Ni; first principles calculation of the magnetocrystalline anisotropy energy of Co(n)X(m) multilayers; prediction and experimental verification of perpendicular anisotropy in Co/Ni multilayers; analysis of the magnetic anisotropy of a Co monolayer and Co/X multilayers; magnetocrystalline anisotropy of YCo5 and related RCo5 compounds; and magnetocrystalline anisotropy and orbital moments in transition metal compounds. Trends in the magnetic anisotropy energy are shown to be predictable using first principles theory. ESA

N92-26520# Massachusetts Inst. of Tech., Cambridge.
FUNDAMENTAL MECHANISMS AFFECTING FRICTION WELDING UNDER VACUUM M.S. Thesis
Benedicta R. Jacoby Jun. 1991 70 p
(Contract N00123-89-G-0580)
(AD-A245685) Avail: NTIS HC/MF A04

Inertia welding of 2024-T3 aluminum alloy studs to 2024-T3 plate is investigated at atmospheric pressure and under vacuum to determine the effects of vacuum, surface contamination, material, weld force and weld speed on the integrity of the weld. The vacuum conditions are limited to 10 torr or less due to experimental apparatus. The fundamental parameters involved in inertia friction welding are investigated here to lead to the development of a mathematical model for their affects in on-orbit welding in the construction of a space station. A bend test is used to determine a sufficient weld. The special conditions required for on-orbit welding are discussed along with a survey of current welding methods and their feasibility and limitations for space station construction. Friction welding, as one of only a few joining techniques that is showing promise for all areas of concern for construction in space - minimal power consumption, ease of automation, minimal operator skill and lack of toxic by-products - is discussed in detail prior to the experimental presentation. GRA

N92-26542# Florida Univ., Gainesville. Dept. of Physics.
X RAY SCATTERING STUDIES OF NON-EQUILIBRIUM ORDERING PROCESSES

S. E. Nagler 1991 20 p
(Contract DE-FG05-86ER-45280)
(DE92-010311; DOE/ER-45280/T3) Avail: NTIS HC/MF A03

We report on the progress of the project entitled 'X ray Scattering Studies of Non-Equilibrium Ordering Processes.' The past year has seen continued progress in the study of kinetic effects in metallic binary alloys and polymers. In addition, work has begun on a low dimensional CDW system: blue bronze. A sample chamber has been constructed to perform small angle neutron scattering measurements on a model quantum system with phase separation: solid He3/He4. Work is continuing on magnetic systems. Planned future experiments include an investigation of crystallization in Rubidium. DOE

N92-26563# Brookhaven National Lab., Upton, NY.
APPLICATION OF IN SITU X RAY ABSORPTION AND FLUORESCENCE MEASUREMENTS TO ANALYZE SOLUTIONS IN A SIMULATED PIT
H. S. Isaacs, A. J. Davenport, J. H. Cho, M. L. Rivers, and S. R. Sutton 1991 10 p Presented at the 180th Meeting of the Electrochemical Society, Phoenix, AZ, 13-18 Oct. 1991
(Contract DE-AC02-76CH-00016)
(DE92-009159; BNL-47180; CONF-911047-20) Avail: NTIS HC/MF A02

X-ray energy dispersive spectroscopy has been used to study the compositions of metal ions in solutions developed during localized corrosion. An electrochemical cell was designed to simulate a corrosion pit, maintaining one dimensional diffusion and fulfilling the requirements for x-ray fluorescence measurements. The working electrode consisted of a dissolving thin foil of Type 304 stainless steel sealed between Mylar sheets through which the x-ray beam passed. Concentration gradients within the artificial pit were quantitatively determined. DOE

N92-26635# Westinghouse Savannah River Co., Aiken, SC.
RETENTION AND RELEASE OF TRITIUM IN ALUMINUM CLAD, Al-Li ALLOYS
M. R. Louthan, Jr. 1991 5 p Presented at the 4th Topical Meeting on Tritium Technology in Fission, Fusion, and Isotopic Applications, Albuquerque, NM, 30 Sep. - 4 Oct. 1991
(Contract DE-AC09-89SR-18035)
(DE92-009905; WSRC-MS-91-110; CONF-910920-27) Avail: NTIS HC/MF A01

Tritium retention in and release from aluminum clad, aluminum-lithium alloys is modeled from experimental and operational data developed during the thirty plus years of tritium production at the Savannah River Site. The model assumes that tritium atoms, formed by the Li-6(n, alpha)He-3 reaction, are produced in solid solution in the Al-Li alloy. Because of the low solubility of hydrogen isotopes in aluminum alloys, the irradiated Al-Li rapidly becomes supersaturated in tritium. Newly produced tritium atoms are trapped by lithium atoms to form a lithium tritide. The effective tritium pressure required for trap or tritide stability is the equilibrium decomposition pressure of tritium over a lithium tritide-aluminum mixture. The temperature dependence of tritium release is determined by the permeability of the cladding to tritium and the local equilibrium at the trap sites. This model is used to calculate tritium release from aluminum clad, aluminum-lithium alloys. DOE

N92-26642*# Old Dominion Univ., Norfolk, VA. Dept. of Mechanical Engineering and Mechanics.
NUMERICAL FORMULATION FOR THE PREDICTION OF SOLID/LIQUID CHANGE OF A BINARY ALLOY Final Report, 16 May 1989 - 31 Dec. 1989
G. E. Schneider and S. N. Tiwari Aug. 1990 41 p
(Contract NAS1-18584; RTOP 694-80-70-01)
(NASA-CR-188468; NAS 1.26:188468) Avail: NTIS HC/MF A03

A computational model is presented for the prediction of solid/liquid phase change energy transport including the influence of free convection fluid flow in the liquid phase region. The computational model considers the velocity components of all non-liquid phase change material control volumes to be zero but fully solves the coupled mass-momentum problem within the liquid region. The thermal energy model includes the entire domain and uses an enthalpy like model and a recently developed method for handling the phase change interface nonlinearity. Convergence studies are performed and comparisons made with experimental data for two different problem specifications. The convergence studies indicate that grid independence was achieved and the comparison with experimental data indicates excellent quantitative prediction of the melt fraction evolution. Qualitative data is also provided in the form of velocity vector diagrams and isotherm plots for selected times in the evolution of both problems. The computational costs incurred are quite low by comparison with previous efforts on solving these problems. Author

N92-26659# Naval Postgraduate School, Monterey, CA.
FACTORS INFLUENCING THE MICROSTRUCTURAL AND MECHANICAL PROPERTIES OF ULCB STEEL WELDMENTS M.S. Thesis
Paul F. McHale Dec. 1991 104 p
(AD-A245523) Avail: NTIS HC/MF A06

The U.S. Navy has maintained a continuous research, development and certification program in High Strength Low Alloy (HSLA) and Ultra Low Carbon Bainitic (ULCB) steels as a replacement for the HY steels used in ship construction. The major benefit of the HSLA and ULCB steels stems from the relative ease of weldability as compared with the HY steels which require large amounts of preheating to prevent weld metal crack formation. This study focused on ULCB steel weldment mechanical properties which were shown to be largely dependent on the heat input and to a lesser extent the base plate composition, cover gas and nonmetallic inclusion composition and content. The heat input rate and subsequent cooling rate for the ULCB/ULCB steel weldments determined the degree of constitutional supercooling indicating a high heat input (large constitutional supercooling) resulted in a tough, finely grained macrostructure while the lower heat input (small constitutional supercooling) generated a weak, columnar/dendritic macrostructure. The utilization of HY-130 base metal resulted in increased carbon pickup in the fusion zone and consequently poorer mechanical properties. The use of a reactive cover gas markedly increased the inclusion density and promoted the formation of carbides producing the poorest overall mechanical properties. The majority of the nonmetallic inclusions identified were spherical, complex aluminum silicates or manganese aluminum silicates. GRA

N92-26727# Ames Lab., IA.
EVALUATION OF PLASMA SPRAYED CRUCIBLE COATINGS FOR MELT PROCESSING COPPER-REFRACTORY METAL ALLOYS
1992 6 p Presented at the 1992 International Thermal Spray Conference, Orlando, FL, 1-5 Jun. 1992
(Contract W-7405-eng-82)
(DE92-008912; IS-M-698; CONF-9206135-1) Avail: NTIS HC/MF A02

A study was made to access the suitability of several plasma arc sprayed coatings applied to graphite for application as containment crucibles for melt processing copper refractory metal alloys. Coatings of Ta, TaC, TaB2 and ZrO2*8w/o Y2O3 were evaluated and compared to uncoated graphite. The ZrO2*8w/o Y2O3 coating was sprayed over a tungsten bond coat. Prealloyed samples of Cu-15v/o Cr and Cu-15v/o Nb were placed within the crucibles and heated inductively to 1800 C and 2100 C, respectively. Compatibility of the coating-alloy system was evaluated by optical and scanning electron microscopy, energy dispersive spectroscopy (EDS), x ray diffraction (XRD), and combustion chromatography. DOE

N92-26732# Lawrence Livermore National Lab., CA.
AN ELECTROPLATER'S VIEW OF PVD PROCESSING
J. W. Dini Jan. 1992 22 p Proposed for presentation at the 1992 American Electroplaters and Surface Finishers Society Conference, Atlanta, GA, 22-25 Jun. 1992

(Contract W-7405-eng-48)
(DE92-009052; UCRL-JC-109419; CONF-9206129-2) Avail: NTIS HC/MF A03

This paper provides a comparison of electroplating and physical vapor deposition (PVD) processing from the viewpoint of a person who has been involved with the electroplating industry for the past 42 years and PVD processing for the past 12 years. During this recent 12 year period he has served as a manager of groups involved with both electroplating and PVD operations so he has had the chance to closely observe both technologies. After a brief description of each of the coating processes, comparisons are provided with respect to coating choices, deposition rates, properties, adhesion, costs and waste minimization. In addition, examples are provided to demonstrate that by combining the deposition technologies synergism can often be obtained. The conclusion drawn from these comparisons is that both deposition technologies are viable processes and each has its own particular benefits/drawbacks. DOE

N92-26770 Georgia Inst. of Tech., Atlanta.
AN INVESTIGATION OF THE MECHANICAL PROPERTIES AND MICROSCOPIC STRUCTURE OF EXTRUDED POWDER ALUMINUM SUBJECTED TO BIAXIAL LOADINGS AT ELEVATED TEMPERATURE Ph.D. Thesis
Terry ORiska Woods 1991 131 p
Avail: Univ. Microfilms Order No. DA9206117

Nuclear fuel can be fabricated using powder metallurgy processes by compacting uranium oxide powder with aluminum powder to form a cermet and then extruding the cermet to form fuel tubes. This method of production allows greater control of uranium oxide particle size and distribution in the tube, and makes the production of fuel with greater concentrations of uranium oxide possible, thus decreasing the volume of radioactive waste remaining after the fuel is spent. As the concentration of uranium oxide increases, however, there is an increase in failures during extrusion. In order to begin to address the extrusion problem, it was felt that a necessary first step was to examine the response of extruded powder aluminum, a material with a structure similar to that of the cermet, to complex loadings of the type experienced by a material during extrusion. The goal here is to investigate the high temperature deformation behavior of extruded powder aluminum. Test fixtures were developed and software was written to control constant strain rate tension, compression, torsion, combined tension-torsion, and combined compression-torsion tests performed using a computer controlled biaxial testing machine. Extruded powder aluminum and 1100 aluminum specimens were tested at 427 C, the powder aluminum extrusion temperature, under those loading conditions. Each specimen was subjected to only one loading cycle, and data was recorded during loading only. Tested specimens were sectioned and examined microscopically. A model for the post yield behavior in extruded powder aluminum which includes information derived both from the macroscopic stress-strain behavior of 1100 aluminum and extruded powder aluminum and from the observed microscopic structure of the extruded powder aluminum was developed. The uniaxial (tension) model was developed first. It was then adapted to describe the post yield shear stress-shear strain behavior seen in the torsion and tension-torsion specimens. Software was written to determine the model parameters using a nonlinear least squares method. The model provides a good fit to the data, and the calculated model parameters are physically reasonable, indicating that the proposed model offers a reasonable explanation for the behavior of extruded powder aluminum at elevated temperature.
Dissert. Abstr.

N92-26787# Helsinki Univ. of Technology, Espoo (Finland). Lab. of Materials Processing and Powder Metallurgy.
SPHEROIDIZATION AND DENSIFICATION OF NICKEL POWDERS BY RF-INDUCTION PLASMA
Y. Yang, P. Taskinen, and J. Talja 14 Nov. 1991 37 p
(PB92-151893; TKK-V-B65; ISBN-951-22-0850-4) Avail: NTIS HC/MF A03

Spheroidization or densification of irregular or porous powders is one of the main applications of radio frequency (RF)-induction plasma. The experimental results were reported on the induction plasma spheroidization and densification of three types of irregular nickel powders produced by hydrogen reduction in an organic solution. All of those parameters were found to have significant effects on the efficiencies of powder spheroidization and densification. The experimental results were discussed in association with the thermal efficiency of the present plasma system. The enthalpy estimation of different gas mixtures calculated with the SOLGASMIX program and the mathematical modeling results from literatures were used in depicting the thermal behaviors of nickel powders in the torch. Due to the strong coupling phenomena in the plasma-particle system, fine adjustment of different operating parameters was important for sustaining a stable plasma and for achieving a better thermal efficiency of powder spheroidization and densification. GRA

N92-26813# Brookhaven National Lab., Upton, NY.
THE APPLICATION OF XPS TO THE STUDY OF MIC
J. R. Kearns, C. R. Clayton, G. P. Halada, J. B. Gillow, and A. J. Francis Jan. 1992 13 p Presented at the Corrosion 1992 Conference and Exhibition, Nashville, TN, 27 Apr. - 1 May 1992
(Contract DE-AC02-76CH-00016)
(DE92-010156; BNL-45092; CONF-920458-3) Avail: NTIS HC/MF A03

The biotic and abiotic factors that contribute to Microbiologically Influenced Corrosion (MIC) involve the transformation of chemical species at a metal surface. X-ray Photoelectron Spectroscopy (XPS) is utilized in conjunction with conventional microbiological and Quantitative Chemical Analytical techniques to better understand the effect of environmental conditions on microbial behavior as well as the ability of bacteria to alter local environmental conditions. Specifically, the interaction of Fe, Cr, Ni, Mo ions with Desulfovibrio sp. under anoxic conditions were studied. This is the first phase of a systematic study of microbial activity and the effects of alloy elements and thermo-mechanical treatments on the MIC resistance of stainless steels. DOE

N92-26848# Westinghouse Hanford Co., Richland, WA.
IMPROVING THE FRACTURE RESISTANCE OF IRRADIATED MARTENSITIC STEELS
F. H. Huang Jan. 1992 25 p Presented at the 16th Annual Symposium of American Society of Testing and Materials (ASTM), Denver, CO, 21-22 Jun. 1992
(Contract DE-AC06-87RL-10930)
(DE92-008387; WHC-SA-1432; CONF-920673-2) Avail: NTIS HC/MF A03

Martensitic steels are used in fast breeder reactors because of their resistance to radiation-induced swelling and creep. However, the fracture resistance of the material under neutron irradiation needs to be assessed. These steels undergo a change in the fracture mode from ductile dimple rupture to brittle cleavage as temperature decreases. Neutron exposure can raise the ductile-brittle transition temperature and produce a condition of low toughness during service. This study examines the effects of cold-work, heat treatment, and chromium content on the post-irradiation fracture behavior of selected steels to provide a better understanding of fracture resistance in hopes of improving it. Experimental materials included alloy HT9 containing 12 percent Cr, a vacuum remelt of HT9, modified HT9 containing 10 percent Cr, and 9Cr-1MO. The initiation fracture toughness of irradiated martensitic steels increased with increasing chromium content and tempering temperature. Remelting of HT9 slightly raised the fracture toughness of the irradiated materials. Cold work did not improve the fracture resistance of irradiated ferritic steels as it did for austenitic steels. DOE

N92-26939# Pennsylvania State Univ., University Park. Dept. of Materials Science and Engineering.
DEFORMATION BEHAVIOR OF AN AGE-HARDENABLE BETA+ALPHA-TWO TITANIUM ALLOY
L. S. Quattrocchi and D. A. Koss 28 Jan. 1992 17 p

(Contract N00014-91-J-1414)
(AD-A246362; TR-3) Avail: NTIS HC/MF A03

The beta Ti alloy Ti-23Nb-11Al (at. pct.) differs from other beta Ti alloys in that it is age-hardenable due to the formation of lath-like, alpha-two precipitates based on Ti3Al. This study reports the room temperature deformation and slip behavior of the Ti-23Nb-11Al alloy as a function of heat treatment. The results indicate that the formation of the alpha-two precipitates results in not only a large increase in yield stress but also can induce a change in slip mode from inhomogeneous to uniform slip. GRA

N92-26945# Forschungszentrum Juelich G.m.b.H. (Germany, F.R.). Inst. fuer Reaktorwerkstoffe.
DEVELOPMENT OF A MICROSTRUCTURAL-RELATED DESCRIPTION FOR THE HIGH TEMPERATURE STRESS-STRAIN BEHAVIOUR OF THE TURBINE BLADE MATERIAL IN 738 LC Ph.D. Thesis - Technische Hochschule
B. Londschien, H. J. Penkalla, F. Schubert, and H. Nickel Apr. 1991 131 p In GERMAN; ENGLISH summary
(JUEL-2466; ISSN-0366-0885; ETN-92-90823) Avail: NTIS HC/MF A07

The high temperature deformation behavior of the nickel phase alloy IN738LC was correlated with the morphology of the gamma prime precipitates. It was found that the deformation rate in short term creep experiments, for example up to a thousand hours, depended on the initial microstructure of the cast alloy. The microstructure could be characterized by gamma prime particle size and distribution in the matrix. Strain rate controlled tension torsion tests in hollow round samples showed that the multiaxial stress strain behavior could be calculated, using the invariant theory for isotropic materials with a comparative stress value from the uniaxial creep experiment, applying the von Myses theory. ESA

N92-27044# Rolls-Royce Ltd., Derby (England).
POWDER PROCESSING OF AERO-ENGINE COMPONENTS
D. Driver 15 Nov. 1990 20 p Presented at the PM 1990 World Conference on Powder Metallurgy, London, England, 3-6 Jul. 1990 Submitted for publication
(PNR-90813; ETN-92-90781) Copyright Avail: NTIS HC/MF A03

More powerful and efficient jet propulsion requires that individual components run faster and hotter; as operating temperatures approach the materials melting point then the manufacturing options and the 'process window' within which the material can be manipulated correspondingly decrease. Casting is available as a near net shape manufacturing route but can be accompanied by extensive segregation for the complex alloys used in aeroengine applications. Powder processing therefore provides a route whereby highly alloyed materials can be rapidly solidified to form a relatively segregation free microstructurally refined, powder product of controlled size and cleanliness which can be consolidated to yield a consistent material suitable either for direct use within the engine or, by predictable process modeling, can subsequently be forged and heat treated to generate specific microstructural property combinations within particular regions of a component. As the use of metallic aeroengine materials is replaced by intermetallics and ultimately ceramics, then the opportunities for powder processing will increase accordingly. ESA

N92-27067# Naval Postgraduate School, Monterey, CA.
ELEVATED TEMPERATURE PROPERTIES OF A DISPERSION STRENGTHENED Al-(Fe, V, Si) ALLOY M.S. Thesis
Matthew B. Cissel Dec. 1991 71 p
(AD-A246427) Avail: NTIS HC/MF A04

The mechanical properties at elevated temperatures of a new dispersion strengthened aluminum, iron, vanadium silicon alloy were evaluated. Constant extension rate (tension) tests were conducted on an Instron machine and strain rate sensitivity, yield stress and elongation changes with temperature were obtained. The mechanical behavior appeared to change at approx. 250 C, with intergranular fracture and necking occurring at low temperatures; and transgranular dimples with uniform plastic deformation at high temperatures. Creep tests in tension were conducted and the stress dependence n, of the steady state creep rate was obtained. A change in the n value was seen from 16 down to 4 at low stresses and temperatures. The activation energy for creep was calculated from the slope of steady state creep rate vs 1/temperature plot and from an iterative technique based on plotting all the data on one curve using an approximate value of activation energy for the temperature compensated strain rate plotted against the modulus compensated stress. GRA

N92-27192*# National Aeronautics and Space Administration. Lewis Research Center, Cleveland, OH.
POST-TEST EXAMINATION OF A POOL BOILER RECEIVER
Robert L. Dreshfield, Thomas J. Moore, and Paul A. Bartolotta Apr. 1992 15 p
(Contract DE-AI04-85AL-33408; RTOP 590-13-11)
(NASA-TM-105635; E-6978; DOE/NASA/33408-6; NAS 1.15:105635) Avail: NTIS HC/MF A03

A subscale pool boiler test apparatus to evaluate boiling stability developed a leak after being operated with boiling NaK for 791.4 hr at temperatures from 700 to 750 C. The boiler was constructed using Inconel 625 with a type 304L stainless steel wick for the boiler and type 316 stainless steel for the condenser. The boiler assembly was metallurgically evaluated to determine the cause of the leak and to assess the effects of the NaK on the materials. It was found that the leak was caused by insufficient (about 30 pct.) joint penetration in a butt joint. There was no general corrosion of the construction materials, but the room temperature ductility of the Inconel 625 was only about 6.5 pct. A crack in the heat affected zone of the Inconel 625 near the Inconel 625 to type 316 stainless steel butt joint was probably caused by excessive heat input. The crack was observed to have a zone depleted of iron at the crack surface and porosity below that zone. The mechanism of the iron depletion was not conclusively determined. Author

N92-27115*# Boeing Co., Seattle, WA. Defense and Space Group.
ON-ORBIT COLDWELDING: FACT OR FRICTION?
Harry Dursch and Steve Spear *In* NASA. Langley Research Center, LDEF: 69 Months in Space. First Post-Retrieval Symposium, Part 3 Jan. 1992 p 1565-1576 (For primary document see N92-27083 17-99)
(Contract NAS1-18224)
Avail: NTIS HC/MF A21; 1 functional color page

N92-27119*# Aerospatiale, Cannes (France). Space and Strategic Systems Div.
MICROWELDING (OR COLD-WELDING) OF VARIOUS METALLIC MATERIALS UNDER THE ULTRA-VACUUM LDEF EXPERIMENT AO 138-10
Jean-Pierre Assie and Eric Conde (Centre National d'Etudes Spatiales, Toulouse, France) *In* NASA. Langley Research Center, LDEF: 69 Months in Space. First Post-Retrieval Symposium, Part 3 Jan. 1992 p 1613-1623 (For primary document see N92-27083 17-99)
Avail: NTIS HC/MF A21; 1 functional color page

27 NONMETALLIC MATERIALS

Includes physical, chemical, and mechanical properties of plastics, elastomers, lubricants, polymers, textiles, adhesives, and ceramic materials.

For composite materials see *24 Composite Materials.*

N92-26275# Institute for Defense Analyses, Alexandria, VA.
ADVANCED MATERIALS ASPECTS OF CONCURRENT ENGINEERING Final Report, Aug. - Oct. 1991
George Mayer Oct. 1991 29 p
(Contract MDA903-89-C-0003)
(AD-A245437; AD-E501463; IDA-D-1033; IDA/HQ-91-40225)
Avail: NTIS HC/MF A03

Unique opportunities are offered for new devices and systems through the use of advanced materials, such as composites, ceramics, and intermetallics. Concurrent engineering approaches to the use of these materials are key to assuring successful applications. Generic steps in concurrent engineering with special reference to advanced materials are reviewed. Examples are provided of intelligent processing and net-shape processing, which provide routes to more reproducible materials. It is anticipated that a wide range of DARPA applications will be affected by the approaches described here, including the metal-matrix composites model factory, composite hulls and chassis for lightweight ground vehicles, and the polymer composite submarine hull. GRA

N92-26283# Army Materials Technology Lab., Watertown, MA.
SLIP CASTING AND GREEN BODY EVALUATION OF 6 PERCENT YTTRIA, 2 PERCENT ALUMINA SILICON NITRIDE Final Report
Janet Quinn Dec. 1991 22 p
(AD-A245817; MTL-TR-91-52) Avail: NTIS HC/MF A03

The superior high temperature properties of silicon nitride are well known. It has good strength, excellent high temperature strength, oxidation resistance, and is resistant to thermal shock. These properties make silicon nitride a good choice for many structural ceramics. Additionally, its high thermal conductivity and low dielectric constant make it a possible candidate for electronic substrates. Knowledge in the areas of characterization, machining, and proper firing parameters is growing and crucial to the production of modern ceramics. Such knowledge also makes it increasingly evident that a poor initial green body cannot result in a good final product. Many fabrication problems can be traced back to the processes such as casting and green body preparation and attention is being concentrated in these areas. GRA

N92-26451# California Inst. of Tech., Pasadena.
INFRARED SPECTROSCOPY AND HYDROGEN ISOTOPE GEOCHEMISTRY OF HYDROUS SILICATE GLASSES
S. Epstein and E. Stolper 1992 3 p
(Contract DE-FG03-85ER-13445)
(DE92-008398; DOE/ER-13445/T1) Avail: NTIS HC/MF A01

The focus of this project is the combined application of infrared spectroscopy and stable isotope geochemistry to the study of hydrogen bearing species dissolved in silicate melts and glasses. We are conducting laboratory experiments aimed at determining the fractionation of D and H between melt species (OH and H2O) and hydrous vapor and the diffusivities of these species in glasses and melts. Knowledge of these parameters is critical to understanding the behavior of hydrogen isotopes during igneous processes and hydrothermal processes. These results also could be valuable in application of glass technology to development of nuclear waste disposal strategies. DOE

N92-26455# General Electric Co., Schenectady, NY. Knolls Atomic Power Lab.
MICROSTRUCTURAL EVALUATION OF AS-SOLIDIFIED AND HEAT TREATED GAMMA-TiAl BASED POWDERS
G. E. Fuchs and S. Z. Hayden Oct. 1991 26 p Presented at the International Conference on High Temperature Aluminides and Intermetallics, San Diego, CA, 17-19 Sep. 1991
(Contract DE-AC12-76SN-00052)
(DE92-008956; KAPL-4730; CONF-910938-9) Avail: NTIS HC/MF A03

Powders with nominal compositions (in atomic pct.) Ti-48Al and Ti-48Al-2Nb-2Cr were prepared by the plasma rotating electrode process (PREP) and gas atomization (GA) techniques. As-solidified and heat treated (1000 C/3 hr) powder samples were examined by metallography, SEM, X ray diffraction, and TEM. The microstructures of the powders were characterized as a function of atomization technique, alloy content, powder particle size (solidification rate), and thermal history. All of the as-solidified powders were comprised of disordered, alpha, and ordered alpha sub 2-Ti3Al and gamma-TiAl. For both alloys, a larger volume fraction of alpha and alpha sub 2 was observed in the PREP powders relative to GA powders of comparable size. Additionally, for both alloys and both atomization techniques, the volume fraction of alpha sub 2 was observed to increase with decreasing powder particle size. In general, the PREP powders appeared to solidify more rapidly than the GA powders. Possible reasons for the differences in microstructures and solidification rates observed for the two atomization techniques will be discussed. Upon heat treatment, the microstructure of the powders was similar. The heat treated powders were comprised predominently of equiaxed gamma grains with limited amounts of lamellar alpha sub 2/gamma grains also present. The GA powders did exhibit a slightly higher volume fraction of alpha sub 2 than the PREP powders, possibly due to slight differences in the Al content of the alloys or the higher oxygen content of the GA alloys. DOE

N92-26492 Florida Univ., Gainesville.
COMPRESSIVE DAMAGE AND FRACTURE MODELING OF CERAMIC SUBJECTED TO HIGH-VELOCITY IMPACT Ph.D. Thesis
William Howard Cook 1991 188 p
Avail: Univ. Microfilms Order No. DA9208996

Ceramics are often used as protective measures against impact damage in applications such as spacecraft and military vehicles. The processes of impact and penetration of a high velocity projectile against ceramic are not well understood, and they have not been adequately modeled. Since ceramics are much weaker in tension than in compression, most failure work for ceramics deals with tensile crack growth. At high impact velocities, however, compressive failure occurs directly under the impact point and well ahead of the actual penetration path because of the extreme loading and the high sound speed of the ceramic. The objectives of this research program were to develop, implement, and demonstrate a failure model for aluminum oxide ceramic that considers compressive failure under impact loading. The necessary data for the development of such a model were not available, so a comprehensive test program for a single type of aluminum oxide (Coors AD-85) was conducted. Four types of experiments provided a basis for the development of the ceramic failure model. Quasi-static compressive tests and dynamic compressive tests on a split Hopkinson pressure bar were used to evaluate strain rate effects. Plate impact recovery tests were used to evaluate damage and fragment size versus loading magnitude and duration of load. Rod-on-rod impact tests were used to provide supplemental data on high strain rate strength, and a macroscopic view of the propagation speed of failure. A fifth type of experiment, metallic rod impacts against confined ceramic targets with preperforated front metal cover plates, was used to demonstrate an application of the model. The experimental program did not provide sufficient recovered compressively damaged ceramic data in a form suitable for a microstatistical failure model. Test data did support a fragment size correlation with loading rate. A model was developed incorporating these data implemented in a finite difference wave propagation continuum mechanics code. Comparisons of the results of this model to penetration tests were positive. Dissert. Abstr.

N92-26543# Stanford Univ., CA. Dept. of Materials Science and Engineering.
FUNDAMENTAL STUDIES OF THE CHEMICAL VAPOR DEPOSITION OF DIAMOND
D. A. Stevenson 1991 14 p
(Contract DE-FG05-88ER-45345)
(DE92-010327; DOE/ER-45345/T1) Avail: NTIS HC/MF A03

The plasma or thermally enhanced low pressure chemical vapor deposition of diamond films is an exciting development with many challenging fundamental problems. The early stages of nucleation is relevant to the initial growth rate and the perfection and morphology of the deposit. To isolate one of the factors that influence nucleation, we have studied the effect of surface topography on the nucleation process. Our earlier work has shown preferential nucleation on sharp convex features and we have proposed several possible reasons for this behavior, including dangling bonds at the convex features. In our recent work, we have extended our investigation to include a novel patterning of silicon substrates used to pattern silicon solar cells. The results

are consistent with our earlier observations that the majority of nucleation events occur on protruding surface features. In an effort to establish whether dangling bonds at the protruding surfaces may be responsible for the selective nucleation, we have evaluated the dangling bond concentration using electron spin resonance. We have carried out deposition under nominally identical surface topography, but with different concentrations of dangling bonds at or near the surface. The results of this study indicate that dangling bonds play a minor role in enhancing nucleation, in contrast to a substantial role played by special surface topographical features. In the course of the past year, we have submitted four manuscripts for publication and have made six presentations. DOE

N92-26609# Army Materials Technology Lab., Watertown, MA.
COMPARISON OF CERAMIC UNIAXIAL COMPRESSION SPECIMENS THROUGH DETAILED FINITE ELEMENT MODELLING Final Report
Paul V. Cavallaro Dec. 1991 50 p
(AD-A245816; MTL-TR-91-50) Avail: NTIS HC/MF A03

Mechanical properties of advanced structural materials are determined through physical testing. In the area of high strength ceramics, routine testing includes techniques for measuring compressive strength. Successful and efficient characterization of compressive strength and other properties allows the design engineer to exploit the maximum structural potential for these advanced materials. This report details comparisons made between two proposed dumbbell-shaped, uniaxial ceramic compression specimens. Comparisons were made for alumina (aluminum oxides) material through detailed finite element modeling. Differences in stress distributions resulting from both geometries were then applied to experimentally obtained strength values to determine if these values were representative of the same statistical population. GRA

N92-26751# Cambridge Univ. (England). Dept. of Physics.
STUDIES OF RAIN EROSION MECHANISMS IN A RANGE OF IR TRANSMITTING CERAMICS INCLUDING COATED SAMPLES Annual Report, 1 Sep. 1990 - 30 Oct. 1991
J. E. Field Nov. 1991 83 p
(Grant AF-AFOSR-0384-87)
(AD-A245299; EOARD-TR-92-01) Avail: NTIS HC/MF A05

This report contains recent results on zinc sulfides and other infrared transparent window systems. Section 1 describes an investigation into the stress corrosion characteristics of zinc sulfides using the double torsion geometry. The results suggest that zinc sulfides are susceptible to moisture enhanced slow crack growth but to a lesser extent than, for instance soda lime glasses. Section 2 discusses the correct experimental procedure for the Brazilian test and then uses this geometry to determine the variation of both zinc sulfides and germanium fracture stress as a function of temperature. The average fracture stress fluctuates (as does the associated error) but remain above the room temperature value within the temperature range -70 to 600 C. Section 3 contains results from the bursting disc test performed on large (125 mm diameter by 5.45 mm) zinc sulfides windows rather than small (25 or 50 mm diameter) test pieces. The agreement between the results for the small and large scale samples suggests that the small samples give a good representation of the strength of a full size window and that the surface finish achieved on the small discs can be reproduced in the larger discs. Some results from the Multiple Impact Jet Apparatus (MIJA) are given in Section 4, describing the derivation of the threshold velocity for a GeC coated zinc sulfides system. The improvement in threshold velocity over that of the uncoated substrate is marginal. GRA

N92-26775 Utah Univ., Salt Lake City.
FRACTURE OF STRUCTURAL CERAMICS IN COMBINED MODE 1 AND MODE 2 LOADING Ph.D. Thesis
Dileep Singh 1991 162 p
Avail: Univ. Microfilms Order No. DA9128105

Fracture toughness and subcritical crack growth behavior of structural ceramics were studied in combined mode 1 and mode 2 loading using precracked chevron-notched diametral compression disk specimens. Different stress states such as pure mode 1, combined mode 1 and mode 2 and pure mode 2 were achieved in precracked disk specimens by loading in diametral compression at selected angles with respect to the symmetric radial crack. Mixed-mode fracture toughness for soda-lime glass, alumina, ceria-partially stabilized zirconia (Ce-TZP) and silicon nitride were assessed. The resulting fracture envelopes showed significant deviation to higher fracture toughness in mode 2 relative to the predictions of linear elastic fracture mechanics theory. The deviation was smallest for soda-lime glass and largest for polycrystalline alumina. Deviations were attributed to the effect of the stress stake in disk specimens in the case of soda-lime glass. Influence of the nonsingular term in the series solution for crack tip stresses on the mixed-mode fracture criterion was investigated. Subcritical crack growth behavior in combined mode was studied in soda-lime glass. Crack growth rate was monitored by measuring the resistance changes in a microcircuit grid consisting of parallel, electrically conducting grid lines deposited on the surface of the specimen using a photolithography process. Subcritical crack growth rates in pure mode 1, pure mode 2 and combined mode 1 and mode 2 loading could be described by an exponential relationship between crack growth rate and an effective crack driving force derived from a mode 1-mode 2 fracture toughness envelope. The effective crack driving force was based on an empirical representation of the non-coplanar strain energy release rate. A generalized crack velocity equation can be interpreted in terms of the theoretical models that treat subcritical crack growth as a thermally activated bond-rupture process. Stress intensities for kinked cracks were assessed using the method of caustics and an initial decrease and a subsequent increase in the subcritical crack growth rates of kinked cracks were shown to correlate with the variation of the mode 1 and the mode 2 stress intensities.
Dissert. Abstr.

N92-26859 Michigan Univ., Ann Arbor.
CERAMIC COMPOSITES: EXPERIMENTAL AND ANALYTICAL STUDY OF SiC/Si3N4 COMPOSITES Ph.D. Thesis
Temel Kotil 1991 187 p
Avail: Univ. Microfilms Order No. DA9135626

The mechanical behavior of fiber-reinforced SiC/Si3N4 ceramic matrix composites was analytically and experimentally studied. Experimental approaches for the mechanical testing of ceramic composite materials are discussed. Approaches used for the gripping of single fibers were also investigated; this investigation included the influence of misalignment on fiber strength. Both aligned and misaligned single fiber testing was conducted. Also, the stiffness properties of the fiber was measured and the bending strength of the fiber was determined. It was shown that the bending strength of the fiber is extremely high compared to the tensile strength. From monotonic tensile testing of the SiC/Si3N4 composite, a discontinuous stress/strain behavior is discovered. The tensile fatigue testing which was conducted at 10 Hz cyclic loading showed a gradual failure of the composite. Also, the hysteresis and the ratcheting were observed. The hysteresis behavior which was observed during the cyclic loading of SiC/Si3N4 composites was analytically modeled. It was shown that the interfacial friction forces which are produced along a debonded fiber/matrix interface give rise to stress-strain hysterises. The influence of the axial and radial residual stresses to the interfacial on debonding was explored. A new model for interfacial failure in fiber-reinforced ceramic composites was developed. This model was used to analyze experimental approaches for determining interfacial shear, such as fiber pushout and pullout specimens produces a stress singularity in the fiber/matrix interface; under this residual loading, debonding can propagate along the interface. For a brittle material, the fiber/matrix interface can easily fail during the pullout test due to this stress singularity. It was shown that the debonded fiber may separate from the matrix under tensile loading, resulting in complete debonding. Dissert. Abstr.

N92-27060# Stanford Univ., CA. Dept. of Materials Science and Engineering.
INFLUENCE OF SUBSTRATE TOPOGRAPHY ON THE NUCLEATION OF DIAMOND THIN FILMS
P. A. Dennig and D. A. Stevenson 1991 6 p Presented at the 1991 Applied Diamond Conference, Auburn, AL, 20-22 Aug. 1991
(Contract DE-FG05-88ER-45345)
(DE92-010777; CONF-910854-3) Avail: NTIS HC/MF A02

Polycrystalline diamond films are of interest because of their unique materials properties. However, depositing films with the desired morphology is hindered by the difficulty in controlling the nucleation process. A popular method of enhancing the nucleation rate and density is to abrade the substrate with diamond powder before deposition. Although effective, this procedure is difficult to analyze since it may leave residual powder, may introduce damage, and may modify the surface topography. In order to separate these effects, we have studied the nucleation on chemically etched silicon substrates. Our results show that the majority of nucleation events occur on protruding surface features. DOE

N92-27187 Department of the Navy, Washington, DC.
SELECTIVE METALLIZATION OF CARBONYL-CONTAINING POLYMER FILMS Patent
Charles M. Roland, inventor (to Navy) and Mark F. Sonnenschein, inventor (to Navy) 5 Nov. 1991 4 p Filed 29 Mar. 1990
(AD-D015219; US-Patent-5,062,939; US-Patent-Appl-SN-500979; US-Patent-Class-204-192-19) Avail: US Patent and Trademark Office

Carbonyl-containing polymer films, such as PET, are selectively metallized by contacting the films with a layer or film of metal, such as aluminum, and then irradiating selected portions of the surface of the film with infrared radiation thereby heating those selected portions of the film. The metal on or opposite the irradiated portions of the surface adhere to the film. The remaining metal may be readily removed. The process provides surprisingly good spatial resolution. The present process is particularly useful in the production of microcontacts for circuit boards. GRA

N92-27194*# National Aeronautics and Space Administration. Langley Research Center, Hampton, VA.
EFFECT OF TEMPERATURE AND GAP OPENING RATE ON THE RESILIENCY OF CANDIDATE SOLID ROCKET BOOSTER O-RING MATERIALS
Cynthia L. Lach Jul. 1992 14 p
(RTOP 505-63-50-03)
(NASA-TP-3226; L-17023; NAS 1.60:3226) Avail: NTIS HC/MF A03

In the redesign of the Space Shuttle solid rocket motor following the Challenger accident, the field and nozzle-to-case joints were designed to minimize gap opening caused by internal motor pressurization during ignition. The O-ring seals and glands for these joints were designed both to accommodate structural deflections and to promote pressure assisted sealing. The resiliency behavior of several candidate O-ring materials was evaluated for the effects of temperature and gap opening rates. The performance of three of the elastomeric materials was tested under the specific redesign gap opening requirement. Dynamic flexure conditions unique to launch produce low frequency vibrations in the gap opening. The effect of these vibrations on the ability of the O-ring to maintain contact with the sealing surface was addressed. The resiliency of the O-ring materials was found to be extremely sensitive to variations in temperature and gap opening rate. The top three elastomeric materials tracked the simulated solid rocket booster (SRB) field joint deflection at 75 and 120 F. The external tank/SRB attach strut load vibrations had a negligible effect on the ability of the O-ring to track the simulated SRB field joint deflection. Author

N92-27015# Central Research Inst. of Tech. and Machine Building, Moscow (USSR).
THE IMPORTANCE OF CHEMICAL REACTIONS WITH ENVIRONMENT FOR ABLATION PROCESS OF THERMAL PROTECTION AND STRUCTURAL MATERIALS
N. A. Anfimov *In* ESA, 4th European Symposium on Space Environmental Control Systems, Volume 2 Dec. 1991 p 1065-1070 (For primary document see N92-26950 17-54)
Avail: NTIS HC/MF A23; ESA, EPD, ESTEC, Noordwijk, Netherlands, HC 150 Dutch guilders (2 vols)

N92-27016# Erno Raumfahrttechnik G.m.b.H. Bremen (Germany, F.R.).
LIGHTWEIGHT FIBER INSULATIONS PERFORMANCE AND APPLICATION
J. Antonenko, W.-D. Ebeling, B. Schwarz, and F. Menn *In* ESA, 4th European Symposium on Space Environmental Control Systems, Volume 2 Dec. 1991 p 1071-1077 (For primary document see N92-26950 17-54)
Avail: NTIS HC/MF A23; ESA, EPD, ESTEC, Noordwijk, Netherlands, HC 150 Dutch guilders (2 vols)

N92-27086*# Grumman Aerospace Corp., Bethpage, NY. Corporate Research Center.
EFFECTS OF THE SPACE ENVIRONMENT ON SPACE-BASED RADAR PHASED-ARRAY ANTENNA; STATUS AND PRELIMINARY OBSERVATIONS (LDEF EXPERIMENT A0133)
J. B. Whiteside, D. Giangano, R. L. Heuer, E. Kamykowski, M. Kesselman, W. D. Rooney, R. Schulte, and M. Stauber *In* NASA. Langley Research Center, LDEF: 69 Months in Space. First Post-Retrieval Symposium, Part 3 Jan. 1992 p 1227-1240 (For primary document see N92-27083 17-99)
Avail: NTIS HC/MF A21; 1 functional color page

N92-27100*# National Aeronautics and Space Administration. Lewis Research Center, Cleveland, OH.
DURABILITY EVALUATION OF PHOTOVOLTAIC BLANKET MATERIALS EXPOSED ON LDEF TRAY S1003
Sharon K. Rutledge and Raymond M. Olle (Cleveland State Univ., OH.) *In* NASA. Langley Research Center, LDEF: 69 Months in Space. First Post-Retrieval Symposium, Part 3 Jan. 1992 p 1379-1394 (For primary document see N92-27083 17-99)
Avail: NTIS HC/MF A21; 1 functional color page

N92-27102*# Messerschmitt-Boelkow G.m.b.H., Munich (Germany, F.R.).
EVALUATION OF LDEF EXPERIMENT S1002
Ludwig Preuss *In* NASA. Langley Research Center, LDEF: 69 Months in Space. 1st Post-Retrieval Symposium, Part 3 Jan. 1992 p 1405-1417 (For primary document see N92-27083 17-99)
Avail: NTIS HC/MF A21; 1 functional color page

28 PROPELLANTS AND FUELS

Includes rocket propellants, igniters, and oxidizers; their storage and handling procedures; and aircraft fuels.

For related information see also *07 Aircraft Propulsion and Power, 20 Spacecraft Propulsion and Power,* and *44 Energy Production and Conversion.*

N92-26178# Naval Postgraduate School, Monterey, CA. Dept. of Operations Research.
PYROTECHNIC DEVICE RELIABILITY
Lyn R. Whitaker and Michael P. Bailey Dec. 1991 25 p
(AD-A245818; NPSOR-92-005) Avail: NTIS HC/MF A03

This report looks at the problem of determining when to award bonuses for reliability improvement in pyrotechnic devices based on data gathered under a lot acceptance sampling plan. GRA

N92-26547# Pittsburgh Univ., PA. Dept. of Chemical and Petroleum Engineering.
A NOVEL PROCESS FOR METHANOL SYNTHESIS

J. W. Tierney and I. Wender 28 Jan. 1992 20 p
(Contract DE-FG22-89PC-89786)
(DE92-010465; DOE/PC-89786/T8) Avail: NTIS HC/MF A03

A bench-scale reactor is being used to conduct studies of the conversion of synthesis gas to methanol by a novel process. In previous reports, we provided evidence for a two step reaction in series: the carbonylation of methanol to methyl formate taking place in a non-equilibrium region in the vicinity of the copper chromite surface, and the hydrogenolysis of methyl formate to methanol taking place on the surface of the copper chromite. The synergism between the two catalysts enhances the rate of methanol formation. In this quarter, we tested several copper chromites (with different surface areas and stabilizing agents) on the rate of methanol synthesis. It seems likely that pore diffusion limitations control the hydrogenolysis reaction since the rate of methanol formation is proportional to the square root of the copper chromite surface area. Elemental analyses using Inductively Coupled Plasma analysis and pore size distribution analysis of copper chromite were carried out. DOE

N92-26548# Lehigh Univ., Bethlehem, PA.
HIGH OCTANE ETHERS FROM SYNTHESIS GAS-DERIVED ALCOHOLS
K. Klier, R. G. Herman, M. Johansson, and O. C. Feeley Jan. 1992 25 p
(Contract DE-AC22-90PC-90044)
(DE92-010480; DOE/PC-90044/5) Avail: NTIS HC/MF A03

The objective of the proposed research is to synthesize high octane ethers, primarily methyl isobutyl ether (MIBE) and methyl tertiary butyl ether (MTBE), directly from H2/CO/CO2 coal-derived synthesis gas via alcohol mixtures that are rich in methanol and 2-methyl-1-propanol (isobutanol). The overall scheme involves gasification of coal, purification and shifting of the synthesis gas, higher alcohol synthesis, and direct synthesis of ethers. DOE

N92-26589# London Univ. (England). Toxicology Unit.
STUDY OF HYDRAZINE METABOLISM AND TOXICITY Final Report, 15 Sep. 1990 - 14 Sep. 1991
J. A. Timbrell 10 Jan. 1992 27 p
(Grant AF-AFOSR-0313-88)
(AD-A245755; EOARD-TR-92-03) Avail: NTIS HC/MF A03

Hydrazine is an important chemical substance being used extensively in industry, as a rocket fuel and it is a metabolite of two widely used drugs. We have previously studied hydrazine toxicity and metabolism, recently using the technique of high resolution nuclear magnetic resonance (NMR). We have shown that hydrazine does not cause lipid peroxidation and causes depletion of ATP in the liver after hepatotoxic doses. The object of this project was to study the metabolism and disposition of hydrazine in vivo and in vitro in relation to the hepatotoxicity. GRA

N92-26839# Naval Postgraduate School, Monterey, CA.
MODIFICATION AND EXPERIMENTAL VALIDATION OF A COMBINED OPTICAL AND COLLECTION PROBE FOR SOLID PROPELLANT EXHAUST ANALYSIS M.S. Thesis
Lyle J. Kellman Mar. 1991 89 p
(AD-A245387) Avail: NTIS HC/MF A05

A combined optical and collection particle sizing probe was further developed and utilized for insitu measurements in the exhaust plumes of solid propellant rocket motors. Probe shock-swallowing capabilities were verified using schlieren observations under restricted motor operating conditions. Particle size number distributions obtained optically using a Malvern Mastersizer and from an automated data retrieval system for scanning electron microscope photographs of collected particles were in good agreement when referenced to common measurement limits. Most of the particles were smaller than 0.5 micron, but a significant number were present with diameters to 10 microns. A very few particles larger than 15 microns were also present, some as single particles and some as agglomerates. SEM results showed that many particles were smaller than 0.2 micron, outside the measurement range of the Malvern instrument. Suggestions are made for further improvements and validation procedures for the probe. GRA

N92-26880 Department of the Navy, Washington, DC.
HIGH MELTING AROMATIC NITRATE ESTERS Patent
Michael E. Sitzmann, inventor (to Navy) 14 Jan. 1992 6 p Filed 17 May 1991
(AD-D015190; US-Patent-5,081,255; US-Patent-Appl-SN-704561; US-Patent-Class-548-145) Avail: US Patent and Trademark Office

Accordingly, an object of this invention is to provide novel, high-melting nitrate esters. Another object of this invention is to provide nitrate esters that have short term stability in the vicinity of 150 C. A further object of this invention is to provide high-melting nitrate esters with a wide range of melting points and sensitivities for use as initiation train explosives and/or as booster explosives. These and other objects of this invention are accomplished by providing a nitrate ester which is 2,4,6-trinitro-1-(2-hydroxyethylamino)- 3-(2-hydroxy ethyliitramino)-benzenetrinitrate; 2,2',4,4',6,6'- hexanitro-3- (2-hydroxy ethylnitramino)-stilbeneitrate; 2,5-bis(3- (hydroxyethylaminonitrate)-ethylnitramino)-stilbeneitrate; 2,5-bis(3- (hydroxyethylaminonitrate)-2,4,6-trinitrophenyl-)-1,3,4-oxadiazole; or 2,5-bis(3-(hydroxy ethylaminonitrate)- 5-(hydroxyethyl nitraminonitrate)- 2,4,6-trinitrophenyl)- 1,3,4-oxadiazole. GRA

N92-27085*# Thiokol Corp., Brigham City, UT.
SPACE AGING OF SOLID ROCKET MATERIALS Abstract Only
Dean M. Lester, Leon L. Jones, R. B. Smalley, Jr., and R. Neil Ord *In* NASA. Langley Research Center, LDEF: 69 Months in Space. First Post-Retrieval Symposium, Part 3 Jan. 1992 p 1225 (For primary document see N92-27083 17-99)
Avail: NTIS HC/MF A21; 1 functional color page

29 MATERIALS PROCESSING

Includes space-based development of products and processes for commercial applications.

For biological materials see *55 Space Biology.*

N92-26440# National Space Development Agency, Tokyo (Japan).
PARABOLIC FLIGHT: REPORTS OF MICROGRAVITY EXPERIMENTS BY AIRCRAFT, VOLUME 1, NO. 2
21 Aug. 1991 86 p In JAPANESE
(EG-910045; JTN-92-80348) Avail: NTIS HC/MF A05

Microgravity experiments that were carried out in aircraft are reported. The following topics are discussed: parabolic flight, microgravity, low gravity manufacturing, space processing, plasma processing, plasma behavior, plasma diagnostics, gravitational effects, bubble migration, bubble movement, vapor/liquid reorientation, liquid-vapor interface, liquid stability in containers, biomedical data acquisition, biological effects, and containerless melts. For individual titles, see N92-26441 through N92-26447.

N92-26441# Diamond Air Service, Inc. (Japan). Flight Operations.
OUTLINES OF PARABOLIC FLIGHT [PARABORIKKU FURAITO NI TSUITE]
Tarou Kageyama *In* NASDA, Parabolic Flight: Reports of Microgravity Experiments by Aircraft, Vol. 1, No. 2, 21 Aug. 1991 p 1-9 In JAPANESE (For primary document see N92-26440 17-29)
Avail: NTIS HC/MF A05

Microgravity experiments that utilize the parabolic flight path of aircraft are outlined. Among the topics discussed are the following: the underlying principles, normal parabolic flight patterns, flight restrictions, the level of microgravity produced, and the flight duration. Two of the main advantages that microgravity flight experiments provide, are cost effectiveness and a wide range of available gravity levels. Author (NASDA)

N92-26442# National Space Development Agency, Tokyo (Japan).
PRELIMINARY EXPERIMENT OF GDEF (GAS DYNAMICS EXPERIMENT FACILITY)
Kiwao Shibukawa, Keiji Murakami, Shinichi Kamei, Masamichi Ishikawa, Nobuhiro Oota, Naoji Fujimori, Tadao Inuzuka, and Youichirou Satou (National Inst. for Research in Inorganic Materials, Ibaraki, Japan) *In its* Parabolic Flight: Reports of Microgravity Experiments by Aircraft, Vol. 1, No. 2, 21 Aug. 1991 p 10-19 In JAPANESE (For primary document see N92-26440 17-29)
Avail: NTIS HC/MF A05

An experimental study of gravitational effects on the convection and the behavior of plasma in the CVD (Chemical Vapor Deposition) process is performed using the MU-300 airplane. This experiment is conducted as a preliminary study for the SFU (Space Flyer Unit) GDEF (Gas Dynamics Experiment Facility) mission. The visualization of gas flow at low pressure shows that the thermal convection of He is eliminated in the microgravity condition. A temperature fluctuation in the gas is observed in microgravity. It is synchronized with the G-jitter. This effect can not be observed in 1- and 2-G conditions. The characteristic of plasma is somewhat different between micro- and 1-G conditions. It is not difficult to ignite the plasma in micro-G. An experiment using methane hydrogen mixed gas, which will be used in GDEF mission, is planned in the next year. Author (NASDA)

N92-26443# National Space Development Agency, Tokyo (Japan).
PARABOLIC FLIGHT EXPERIMENTS ON BUBBLE MIGRATION UNDER REDUCED GRAVITY
Susumu Yoshitomi, Minoru Naki, Hiroto Samejima, Masaru Ooyama, Seizou Ishikura, Masamichi Ishikawa, Shinya Ishii, Toshikazu Goshozono, and Hiroaki Matsumoto (Mitsubishi Heavy Industries Ltd., Tokyo, Japan) *In its* Parabolic Flight: Reports of Microgravity Experiments by Aircraft, Vol. 1, No. 2, 21 Aug. 1991 p 20-26 In JAPANESE; In JAPANESE; ENGLISH summary (For primary document see N92-26440 17-29)
Avail: NTIS HC/MF A05

Bubble migration in a rectangular fluid container was studied, while undergoing parabolic flight. The two mechanisms that cause bubble movement are considered: impulsive shaking of the fluid container and the acoustic radiation pressure gradient. Bubble movement toward the acoustic pressure node was observed in the latter case. The resulting translational velocity is approximately 2 mm/sec. In this experiment, the piezo-electric shaker, acoustic transducer, and the automatic bubble injection system functioned well. The bubble radii ranged in size from 0 to 1.5 mm due to a constant piston insertion. This is because of an excess pressure head during the entry phase of a micro-G flight and a capillary effect inside of the injection needle. These experimental results will be used to improve the equipment that will be employed in the upcoming TR-1A (Test Rocket-1A) sounding rocket missions experiments. Author (NASDA)

N92-26444# National Space Development Agency, Ibaraki (Japan).
MICRO-GRAVITY EXPERIMENT OF VAPOR/LIQUID REORIENTATION INDUCED BY CAPILLARY FORCE
Masao Furukawa, Yasuo Ishii, Yoshirou Miyazaki, Tooru Iida, Tsutomu Yamazaki, Keiji Murata, Minoru Komori, and Yoshio Kuriyama (Toshiba Corp., Tokyo, Japan) *In its* Parabolic Flight: Reports of Microgravity Experiments by Aircraft, Vol. 1, No. 2, 21 Aug. 1991 p 27-35 In JAPANESE (For primary document see N92-26440 17-29)
Avail: NTIS HC/MF A05

The purpose of this experiment is to establish the concept of liquid reorientation and transfer under micro-gravity conditions. This is important for component design in the development of the Two-Phase Fluid Loop Thermal Management System, especially in terms of the accumulator and the reservoir design. Although it is known that liquid reorientation is achieved via capillary force (surface tension), the design parameters such as capillary core structure, wall material, and treatment are not well understood. In order to support the design, a model for an aircraft test was prepared. This model is composed of a copper container, a polycarbonate window, a copper core, and it uses water. The copper surfaces are treated to improve their wettability. Due to this design, water flows to the core in the microgravity regime due to capillary force and/or surface tension. Six types of core shape (core plate) are tested to determine the following : (1) acceleration direction before micro-gravity condition; (2) the water quantity; and (3) the existence of non-condensable gases. It is confirmed that core shape is most dominant for liquid reorientation, i.e., it is observed that, as the core angle is made larger and as the average core separation (equivalent to capillary gap) is made smaller, the liquid reorients to the core more easily and the vapor reorients to the outside of the core. Author (NASDA)

N92-26445# National Space Development Agency, Tokyo (Japan).
LIQUID MOTION ANALYSIS WITH LATERAL IMPACTS UNDER LOW GRAVITY
Morio Shimizu, Shunji Nagaoka, Ron Usami, Tsuneo Okuyama, Muneo Takaoki, Kazuhide Kamimura, Yoshio Kobayashi, Masaru Ooyama, Masahiro Fukui, and Seizou Ishikura (Japan Space Utilization Promotion Center, Tokyo.) *In its* Parabolic Flight: Reports of Microgravity Experiments by Aircraft, Vol. 1, No. 2, 21 Aug. 1991 p 36-50 In JAPANESE (For primary document see N92-26440 17-29)
Avail: NTIS HC/MF A05

The stability of liquid in cylindrical containers was studied under low gravity induced by parabolic flight. An aim of this experiment is to evaluate handling methodology for biological solutions in microgravity. Glass or acrylic cylinders with 3.4 to 20 mm inner diameters were half filled with physiological saline or 70 percent ethanol solution. The in-flight measurements were made by observing the sloshing induced by lateral impacts in a range of 0.1 G to 1.0 G. This level is equivalent to the magnitude of acceleration caused by casual human handling. The liquid (water) surface remained stable, during the parabolic flight, in the tubes with diameters smaller than 7 mm. The tubes smaller than 5 mm in diameter remained stable during the impact even under the microgravity. The sloshing in microgravity, after the impact, was more remarkable in larger tubes. The surface tension appeared to be the major stabilizing force that kept the liquid contained. This experiment suggested that the handling of small amounts of aqueous solutions may be performed in microgravity with an apparatus similar to laboratory equipment such as pipettes and small test tubes. Author (NASDA)

N92-26446# National Space Development Agency, Tokyo (Japan). Space Experiment Group.
BIOMEDICAL DATA ACQUISITION AND PROCESSING TECHNOLOGY
Shunji Nagaoka, Akira Miyamoto, Morio Shimizu, Satoru Watanabe, Sayumi Kaneko, Keisuke Suzuki, Shirou Usui, Masaki Kamiyama, Yutaka Hirata (Toyohashi Univ. of Technology, Aichi, Japan), and Teiryou Kojima et al *In its* Parabolic Flight: Reports of Microgravity Experiments by Aircraft, Vol. 1, No. 2, 21 Aug. 1991 p 51-64 In JAPANESE; ENGLISH summary (For primary document see N92-26440 17-29)
Avail: NTIS HC/MF A05

A parabolic flight experiment that investigated biomedical data acquisition from a human subject was performed. Six flights consisting of 9 to 11 parabolas per flight were successively performed using two different flight protocols, normal (2.3 G) and reduced (1.3 G) accelerations. A wide variety of fundamental physiological signals, such as Electro-Cardiogram (ECG), Galvanic Skin Reflex (GSR), respirogram, digital volume pulse wave, Blood Pressure (BP), Electro-Oculo-Gram (EOG), cardiac output, body temperature, percutaneous partial pressures of oxygen, and carbon dioxide, were simultaneously acquired during the flights. The signals were recorded from a healthy male subject under controlled posture, respiration rate, and field darkness. Of the signals acquired, the GSR, cardiac parameters and respirogram were found to be sensitively correlated to the acceleration environment, especially

to the reduced gravity phase. The EOG also showed clear vertical nystagmus, after the gravity truncation, in an upright posture. All collected data was digitized and processed to be formatted to MS-DOS files (360 M Byte). All of the processed data was compiled in a small database system which enables one to search and manage such a large volume of data with ease. The use of sophisticated digital signal processing techniques is discussed in terms of the software environment for the analytical support of the user. Author (NASDA)

N92-26447# National Space Development Agency, Tokyo (Japan).
THE EXPERIMENT UNDER MICROGRAVITY BY AIRCRAFT: THE EXPERIMENT IN FLOATING BY GAS FLOW
Susumu Yoshitomi, Minoru Naki, Hiroto Samejima, Tsuneo Machida, Kiyoshi Tanaka, Shin Nakamura, Kazuko Ishikawa, and Junji Hayakawa (Government Industrial Research Inst., Osaka, Japan) *In its* Parabolic Flight: Reports of Microgravity Experiments by Aircraft, Vol. 1, No. 2, 21 Aug. 1991 p 65-74 In JAPANESE (For primary document see N92-26440 17-29)
Avail: NTIS HC/MF A05

When materials melt and then solidify in the furnace, they gain impurities from the touching surface. It is important that materials are melted and solidified without physical contact. Equipment that uses a constant supply of Helium gas to float sample materials was tested during the parabolic flight of an aircraft. The results indicate that the sample materials could be successfully suspended between the nozzles. Author (NASDA)

N92-26611*# National Aeronautics and Space Administration. Lewis Research Center, Cleveland, OH.
COLOR IMAGE PROCESSING AND OBJECT TRACKING WORKSTATION
Robert B. Klimek and Michael J. Paulick (Baldwin-Wallace Coll., Berea, OH.) Apr. 1992 23 p Original contains color illustrations
(Contract NCC3-206; RTOP 694-03-00)
(NASA-TM-105561; E-6885; NAS 1.15:105561) Avail: NTIS HC/MF A03; 3 functional color pages

A system is described for automatic and semiautomatic tracking of objects on film or video tape which was developed to meet the needs of the microgravity combustion and fluid science experiments at NASA Lewis. The system consists of individual hardware parts working under computer control to achieve a high degree of automation. The most important hardware parts include 16 mm film projector, a lens system, a video camera, an S-VHS tapedeck, a frame grabber, and some storage and output devices. Both the projector and tapedeck have a computer interface enabling remote control. Tracking software was developed to control the overall operation. In the automatic mode, the main tracking program controls the projector or the tapedeck frame incrementation, grabs a frame, processes it, locates the edge of the objects being tracked, and stores the coordinates in a file. This process is performed repeatedly until the last frame is reached. Three representative applications are described. These applications represent typical uses and include tracking the propagation of a flame front, tracking the movement of a liquid-gas interface with extremely poor visibility, and characterizing a diffusion flame according to color and shape. Author

N92-27197*# National Aeronautics and Space Administration. Lewis Research Center, Cleveland, OH.
MICROGRAVITY COMBUSTION SCIENCE: PROGRESS, PLANS, AND OPPORTUNITIES
Apr. 1992 49 p Original contains color illustrations
(RTOP 674-22-05)
(NASA-TM-105410; E-6816; NAS 1.15:105410) Avail: NTIS HC/MF A03; 11 functional color pages

An earlier overview is updated which introduced the promise of microgravity combustion research and provided a brief survey of results and then current research participants, the available set of reduced gravity facilities, and plans for experimental capabilities in the space station era. Since that time, several research studies have been completed in drop towers and aircraft, and the first space based combustion experiments since Skylab have been conducted on the Shuttle. The microgravity environment enables a new range of experiments to be performed since buoyancy induced flows are nearly eliminated, normally obscured forces and flows may be isolated, gravitational settling or sedimentation is nearly eliminated, and larger time or length scales in experiments are feasible. In addition to new examinations of classical problems, (e.g., droplet burning), current areas of interest include soot formation and weak turbulence, as influenced by gravity. Author

N92-26964# Centre National d'Etudes Spatiales, Toulouse (France).
FEASIBILITY STUDY OF AN EXPERT SYSTEM FOR THE DESIGN OF FUSION/SOLIDIFICATION EXPERIMENT BOARDING ON SPACE FURNACE
B. Desaunettes, T. Duffar, A. Kessaci, D. Valentian, and F. R. Valette (Centre d'Etudes et de Recherches, Toulouse, France) *In* ESA, 4th European Symposium on Space Environmental Control Systems, Volume 2 Dec. 1991 p 713-717 (For primary document see N92-26950 17-54)
Avail: NTIS HC/MF A23; ESA, EPD, ESTEC, Noordwijk, Netherlands, HC 150 Dutch guilders (2 vols)

31 ENGINEERING (GENERAL)

Includes vacuum technology; control engineering; display engineering; cryogenics; and fire prevention.

N92-26246# Messerschmitt-Boelkow-Blohm G.m.b.H., Schrobenhausen (Germany, F.R.).
SPINNING JETS FROM SHAPED CHARGES WITH FLOW TURNED LINERS
Manfred Held 1990 8 p Presented at the 12th International Symposium on Ballistics, San Antonio, TX, 30 Oct. - 1 Nov. 1990
(MBB-UA-1197-90-PUB; ETN-92-98819) Avail: NTIS HC/MF A02

The production of shear formed liners, the self spin effect of the jet, and the results of tests with shear formed liners are discussed. The spin effect of shaped charged particles is caused by the distortion of the crystalline structure during the shear formating or flow forming process. In the case of statistically fired shear formed liners, rotation speed of individual jet particles of several hundred thousand rps can be measured. With antirotation, the crystalline structure imposed by shear forming compensates in their collapse process, leading to high penetration performance, for shaped charges fired with rotation. Good spin compensation can be attained at the relatively low rotation speed of 10 to 20 rps. The performance of a shear formed liner, compared with other liners, is 15 percent higher for short standoffs, and 30 percent higher for long standoffs in rotating shaped charges. ESA

N92-26656*# Old Dominion Univ., Norfolk, VA. Dept. of Electrical and Computer Engineering.
RECOGNITION OF 3-D SYMMETRIC OBJECTS FROM RANGE IMAGES IN AUTOMATED ASSEMBLY TASKS Final Report, period ending 31 Dec. 1990
Nicolas Alvertos and Ivan DCunha Dec. 1990 19 p
(Contract NAS1-18584; RTOP 549-02-41-50)
(NASA-CR-187664; NAS 1.26:187664) Avail: NTIS HC/MF A03

A new technique is presented for the three dimensional recognition of symmetric objects from range images. Beginning from the implicit representation of quadrics, a set of ten coefficients is determined for symmetric objects like spheres, cones, cylinders, ellipsoids, and parallelepipeds. Instead of using these ten coefficients trying to fit them to smooth surfaces (patches) based on the traditional way of determining curvatures, a new approach based on two dimensional geometry is used. For each symmetric object, a unique set of two dimensional curves is obtained from the various angles at which the object is intersected with a plane. Using the same ten coefficients obtained earlier and based on the discriminant method, each of these curves is classified as a

parabola, circle, ellipse, or hyperbola. Each symmetric object is found to possess a unique set of these two dimensional curves whereby it can be differentiated from the others. It is shown that instead of using the three dimensional discriminant which involves evaluation of the rank of its matrix, it is sufficient to use the two dimensional discriminant which only requires three arithmetic operations. Author

N92-26752# Sheffield Univ. (England). Dept. of Control Engineering.
ADAPTIVE REGULATION OF THE BOILER-TURBINE UNIT OF A COMBINED HEAT AND POWER (CHP) SYSTEM
M. Karrari and H. Nicholson Nov. 1990 26 p
(RR-417; ETN-92-98850) Avail: NTIS HC/MF A03

A simplified nonlinear model of a Combined Heat and Power (CHP) system is used to investigate the steady state errors, hunting phenomena and high interactions produced in the linear regulators currently employed in industry. In order to improve the regulation of the boiler turbine unit of the CHP system the gains of regulators should be changed adaptively according to the steam flow and valve position ratios and identical and fast acting servomotors should be chosen for the inlet and pass out values. ESA

N92-26898# Naval Postgraduate School, Monterey, CA.
NUMERICAL FIELD MODEL SIMULATION OF FULL-SCALE FIRE TESTS IN A CLOSED SPHERICAL/CYLINDRICAL VESSEL USING ADVANCED COMPUTER GRAPHICS TECHNIQUES M.S. Thesis
Timothy G. McCarthy Sep. 1991 187 p
(AD-A245810) Avail: NTIS HC/MF A09

Personnel and equipment casualties, caused by shipboard fires, have adversely affected overall readiness of the U.S. Navy for centuries. Understanding the phenomena of fire in enclosed spaces, such as those found on surface ships and submarines, will greatly enhance the Navy's ability to combat or prevent them. This computer model was developed for use in conjunction with Fire-1, an experimental fire chamber test facility at the Naval Research Laboratory in Washington, D.C. It is a three dimensional finite difference model which includes the phenomena of conduction, turbulence, global pressure correction, surface radiation, and strong buoyancy flows. Given specific data on heat release, it predicts velocities, temperatures, pressures, densities, and viscosities throughout its geometry. It was validated by comparison with experiments in Fire-1. Advanced graphics techniques, such as color contouring and three-dimensional vector field plotting, were applied to make output data more informative. This model, if easily modified to more specific geometries, may become a useful tool for naval architects in the design of the fire safe ship. GRA

N92-26986# Karlsruhe Univ. (Germany, F.R.). Inst. fuer Technische Thermodynamik.
THE TRANSPIRATOR, AN EFFICIENT AND LIGHT EVAPORATIVE COOLER FOR SPACE TECHNOLOGY
M. Alf and G. Ernst *In* ESA, 4th European Symposium on Space Environmental Control Systems, Volume 2 Dec. 1991 p 855-861 (For primary document see N92-26950 17-54)
Avail: NTIS HC/MF A23; ESA, EPD, ESTEC, Noordwijk, Netherlands, HC 150 Dutch guilders (2 vols)

N92-26988# Erno Raumfahrttechnik G.m.b.H. Bremen (Germany, F.R.).
THERMO-HYDRAULIC INVESTIGATIONS ON HEAT EXCHANGERS FOR COLUMBUS HYBRID RADIATORS
W.-D. Ebeling, R. Meyer, and W. Fischer *In* ESA, 4th European Symposium on Space Environmental Control Systems, Volume 2 Dec. 1991 p 873-879 (For primary document see N92-26950 17-54)
Avail: NTIS HC/MF A23; ESA, EPD, ESTEC, Noordwijk, Netherlands, HC 150 Dutch guilders (2 vols)

32 COMMUNICATIONS AND RADAR

Includes radar; land and global communications; communications theory; and optical communications.

For related information see also *04 Aircraft Communications and Navigation* and *17 Space Communications, Spacecraft Communications, Command and Tracking.* For search and rescue see *03 Air Transportation and Safety,* and *16 Space Transportation.*

N92-26237# Oak Ridge National Lab., TN.
MAGNETOHYDRODYNAMIC ELECTROMAGNETIC PULSE (MHD-EMP) INTERACTION WITH POWER TRANSMISSION AND DISTRIBUTION SYSTEMS
F. M. Tesche, P. R. Barnes, and A. P. S. Meliopoulos Feb. 1992 111 p Prepared in cooperation with Georgia Inst. of Tech., Atlanta, GA
(Contract DE-AC05-84OR-21400)
(DE92-010365; ORNL/Sub-90-SG828/1) Avail: NTIS HC/MF A06

This report discusses the effects of the late-time high-altitude electromagnetic pulse (HEMP) on electrical transmission and distribution (T&D) systems. This environment, known as the magnetohydrodynamic electromagnetic pulse (MHD-EMP), is a very slowly varying electric field induced in the earth's surface, similar to the field induced by a geomagnetic storm. It can result in the flow of a quasi-dc current in grounded power lines and in the subsequent magnetic saturation of transformers. This saturation, in turn, causes 6-Hz harmonic distortion and an increase in the reactive power required by generation facilities. This report analyzes and discusses these phenomena. The MHD-EMP environment is briefly discussed, and a simplified form of the earth-induced electric field is developed for use in a parametric study of transmission line responses. Various field coupling models are described, and calculated results for the responses of both transmission- and distribution-class power lines are presented. These calculated responses are compared with measurements of transformer operation under dc excitation to infer the MHD-EMP response of these power system components. It is found that the MHD-EMP environment would have a marked effect on a power system by inducing up to several hundreds of amperes of quasi-dc current on power lines. These currents will cause transformers to saturate which could result in excessive harmonic generation, voltage swings, and voltage suppression. The design of critical facilities which are required to operate during and after MHD-EMP events will have to be modified in order to mitigate the effects of these abnormal power system conditions. DOE

N92-26254# Technische Univ., Delft (Netherlands). Lab. of Electromagnetic Research.
TRANSIENT DIFFUSIVE ELECTROMAGNETIC FIELDS IN LAYERED ANISOTROPIC MEDIA Ph.D. Thesis
Leendert Combee 1991 232 p Sponsored by Koninklije/Shell Exploratie en Produktie Lab.
(ISBN-90-6275-722-7; ETN-92-91290) Copyright Avail: NTIS HC/MF A11

The 'structural' problem of the diffusion of transient electromagnetic fields into a plane-layered, nonpolarizable, and nonsuperparamagnetic arbitrarily anisotropic earth is investigated. An analytical method based on the Cagniard-De Hoop method is developed to solve the equations governing the behavior of diffusive electromagnetic fields. Closed formed analytical expressions in the form of well behaved integrals are obtained for the time behavior of the transient electromagnetic field at any point of the configuration. ESA

N92-26267# Stanford Linear Accelerator Center, CA.
SCALABLE COHERENT INTERFACE: LINKS TO THE FUTURE
D. B. Gustavson and E. Kristiansen (Dolphin Server Technology A.S., Oslo, Norway) Nov. 1991 6 p Presented at the COMPCON 1992, San Francisco, CA, 24-28 Feb. 1992
(Contract DE-AC03-76SF-00515)
(DE92-010728; SLAC-PUB-5699; CONF-920237-2) Avail: NTIS HC/MF A02

The Scalable Coherent Interface (SCI) was developed to support closely coupled multiprocessors and their caches in a distributed shared-memory environment, but its scalability and the efficient generality of its architecture make it work very well over a wide range of applications. It can replace a local area network for connecting workstations on a campus. It can be a powerful I/O channel for a supercomputer. It can be the processor, cache-memory I/O connection in a highly parallel computer. It can gather data from enormous particle detectors and distribute it among thousands of processors. It can connect a desktop microprocessor to memory chips a few millimeters away, disk drivers a few meters away, and servers a few kilometers away. DOE

N92-26363# Naval Postgraduate School, Monterey, CA.
PERFORMANCE ENHANCEMENT OF THE NPS TRANSIENT ELECTROMAGNETIC SCATTERING LABORATORY M.S. Thesis
Aldo E. Bresani Sep. 1991 104 p
(AD-A246300) Avail: NTIS HC/MF A06

This thesis describes the performance enhancement of the NPS Transient Electromagnetic Scattering Laboratory (TESL) accomplished by replacing the old HP 8349A microwave preamplifier of the dual amplifier configuration with a new Avantek 13533-5-13 GHz amplifier and optimizing the delay line length for the 1-6 GHz amplifier. New Matlab software was developed to process the signals scattered from canonical and complex targets. This software includes a program to calculate the correct delay line length for either amplifier in future modifications. The updated TESL is shown to provide measurements yielding excellent agreement with theoretically predicted responses of canonical targets demonstrating a significant improvement of the signal to noise ratio as compared with the previous configuration. A target library was created to support research in radar target identification based on natural resonances. GRA

N92-26374# Washington State Univ., Pullman.
EXACT SOLUTIONS FOR A MODE OF THE ELECTROMAGNETIC FIELD IN A RESONATOR WITH TIME-DEPENDENT CHARACTERISTICS OF THE INTERNAL MEDIUM
V. V. Dodonov, T. F. George, O. V. Manko, C. I. Um, and K. H. Yeon Jan. 1992 18 p
(Contract N00014-90-J-1193)
(AD-A245700; WSU/DC/92/TR-77) Avail: NTIS HC/MF A03

The problem of quantization of the electromagnetic field inside a resonator filled with a dielectric medium with time-dependent characteristics in the presence of the external alternating current is studied. The exact propagator, coherent, and Fock's states are obtained for a separate quantized mode of the field represented by a quantum oscillator with time-dependent frequency linearly coupled via momentum with the external current. Delta-pulse excitation of the medium is considered as an example. GRA

N92-26381# Air Force Inst. of Tech., Wright-Patterson AFB, OH. School of Engineering.
APPLICATIONS OF WAVELETS TO SIGNAL PROCESSING HELD IN WRIGHT-PATTERSON AFB, OHIO ON 20-22 MARCH 1991. VOLUME 2: TUTORIAL NOTES Final Report, 3 Oct. 1990 - 30 Apr. 1991
G. Warhola, M. Oxley, S. Rogers, M. Kabrisky, and B. Suter 30 Apr. 1991 236 p
(AD-A245567; AFIT/EN-TM-91-1-Vol-2) Avail: NTIS HC/MF A11

The Air Force Institute of Technology (AFIT) hosted the Symposium on Applications of Wavelets to Signal Processing during 20-22 March 1991 at the AFIT Science and Research Center, Wright-Patterson AFB, OH. This was the first major academic meeting of its kind held at AFIT. The symposium was sponsored by the Air Force Office of Scientific Research (AFOSR), Bolling AFB, DC. It focused on applications of wavelets to problems in image and speech processing, communications, and graphics and opened with a one-day short course, a tutorial on wavelets. The symposium was attended by more than 220 researchers worldwide. They represented 15 foreign countries, 34 US universities, 20 private industrial firms, 15 DoD organizations, and six non-DoD US government organizations. Professor Alexander Grossmann was sponsored by the AFOSR Window on Science program. Volumes 1 and 2 contain, respectively, a synopsis of the symposium and the complete set of tutorial notes. GRA

N92-26388# Naval Postgraduate School, Monterey, CA.
FAST ENVELOPE CORRELATION FOR PASSIVE RANGING M.S. Thesis
Frank J. Mika Sep. 1991 112 p
(AD-A246333) Avail: NTIS HC/MF A06

Application of classic triangulation methods will allow the location of a radar to be determined by passive sensors. Through the use of modern digital signal processing techniques this estimate can be made in a simpler fashion using a conventional receiver. A technique is developed for time difference of arrival (TDOA) estimation using a frequency domain based correlation detector driven by an envelope detector. Time lag boundaries are defined on the output of the correlator. A fixed detection threshold is calculated to permit constant false alarm rate (CFAR) detection. The performance of the correlation detector is plotted as a receiver operating characteristic (ROC) curve as a function of signal to noise ratio (SNR). An interactive MATLAB software program is provided to perform either spectral domain or time domain based correlation. Spectral domain based correlation uses the Fast Fourier Transform (FFT). Implicit with the use of FFT are finite arithmetic internal processing errors which are modeled as independent uncorrelated noise sources. A method is presented to account for SNR degradation at the output of the FFT. GRA

N92-26399# Naval Postgraduate School, Monterey, CA.
AN ANTENNA DESIGN FOR PANSAT USING NEC M.S. Thesis
Daniel A. Ellrick Jun. 1991 107 p
(AD-A245482) Avail: NTIS HC/MF A06

In this thesis the Numerical Electromagnetics Code (NEC) is used to design an omnidirectional antenna for the Petite Amateur Navy Satellite (PANSAT). The completed antenna design uses a tangential turnstile antenna to achieve a circularly polarized radiation pattern with predicted worst nulls of approximately -3.0 dBi. The use of NEC-3, recently ported to 80386 personal computers, demonstrates the potential of personal computers for performing this type of design work. A simple antenna feed system was also designed. Performance predictions for the completed antenna system were made through the application of simple statistical functions to the NEC output. Author (GRA)

N92-26419# Defence Research Establishment, Ottawa (Ontario).
A REFINED MAXIMUM LIKELIHOOD METHOD FOR TRACKING LOW-ALTITUDE TARGETS OVER THE SEA: RESULTS OF SIMULATION AND EXPERIMENTS
Eloi Bosse, Ross M. Turner, and Daniel Brookes Dec. 1991 41 p
(AD-A246534; DREO-1103) Avail: NTIS HC/MF A03

Accurate radar tracking of targets flying at low altitudes above a smooth surface is difficult because of the surface reflection. We propose a solution based on deterministic physical modeling of the specular multipath and the maximum likelihood method. This paper describes the techniques and the results of the performance studies. We derive the Cramer-Rao bound and show the benefit of using the refined propagation model. Monte-Carlo simulations are employed to compare the performance with the Cramer-Rao bound and demonstrate threshold effects on target height estimation. Finally, we present the results obtained with two X-band radar experimental systems. GRA

N92-26424# Communications Research Centre, Ottawa (Ontario).
A COMPARISON OF DIRECTION FINDING RESULTS FROM AN FFT PEAK IDENTIFICATION TECHNIQUE WITH THOSE

FROM THE MUSIC ALGORITHM
L. E. Montbriand Jul. 1991 51 p
(AD-A245675; CRC-1438) Avail: NTIS HC/MF A04

A peak identification technique which uses the fast Fourier transform (FFT) algorithm is presented for unambiguously identifying up to three sources in signals received by the sampled aperture receiving array (SARA) of the Communications Research Center. The technique involves removing phase rotations resulting from the FFT and the data configuration and interpreting this result as the direction cosine distribution of the received signal. The locations and amplitudes of all peaks for one array arm are matched with those in a master list for a single source in order to identify actual sources. The identification of actual sources was found to be subject to the limitations of the FFT in that there was an inherent bias for the secondary and tertiary sources to appear at the side-lobe positions of the strongest source. There appears to be a limit in the ratio of the magnitude of a weaker source to that of the strongest source, below which it becomes too difficult to reliably identify true sources. For the SARA array this ratio is near-10 dB. Some of the data were also analyzed using the more complex MUSIC algorithm which yields a narrower directional peak for the sources than the FFT. For the SARA array, using ungroomed data, the largest side and grating lobes that the MUSIC algorithm produces are some 10 dB below the largest side and grating lobes that are produced using the FFT algorithm. Consequently the source-separation problem is less than that encountered using the FFT algorithm, but is not eliminated. GRA

N92-26511# Technische Univ., Delft (Netherlands).
ELECTROMAGNETIC SCATTERING BY A MOVING OBJECT: THEORY AND EXPERIMENT Ph.D. Thesis
M. H. Vogel 28 Oct. 1991 207 p
(PB92-150911) Avail: NTIS HC/MF A10

An approximate method was developed to calculate the electromagnetic scattering by a moving object and non-moving scattering object. Experiments showed that the method was successful for the purpose. Knowledge about the scattering properties of targets is not only useful for the evaluation of the performance of proximity fuzes, but it can also be used to design proximity fuzes that recognize their target and the geometry of the interception. This would lead to the optimization of the burst point and increase the effectiveness of the defense. Author

N92-26592# Defence Research Establishment, Ottawa (Ontario).
ANALYSIS OF EMP RESPONSE OF STRUCTURES USING FREQUENCY DOMAIN ELECTROMAGNETIC INTERACTION CODES
Marc Dion and Satish Kashyap May 1991 36 p
(AD-A245758; DREO-1078) Avail: NTIS HC/MF A03

This report concerns the use of frequency domain computer codes such as the Numerical Electromagnetic Code (NEC) for computing the time domain Electromagnetic Pulse (EMP) response of structures such as antennas, aircraft or communication shelters. The proper representation of the EMP excitation and the selection of a number of appropriate frequencies to obtain a correct time domain EMP response are studied. The effects of adapting the modelling of the problem for different frequency ranges is discussed. Guidelines are given for obtaining a correct time domain response with the efficient use of computer time. GRA

N92-26595# Naval Postgraduate School, Monterey, CA.
EFFECTS OF NON-UNIFORM WINDOWING ON THE PERFORMANCE OF A FAST FREQUENCY-HOPPED NONCOHERENT MFSK RECEIVER OVER RICIAN FADING CHANNELS WITH PARTIAL-BAND INTERFERENCE AND DOPPLER SHIFT M.S. Thesis
Thomas W. Vece Jun. 1991 63 p
(AD-A245762) Avail: NTIS HC/MF A04

An error probability analysis is done for a DFT based, M-ary frequency-shift keying (MFSK) communications system employing fast frequency-hopped spread spectrum signals. A linear combination procedure referred to as noise normalization is employed at the receiver to minimize the effects of partial band interference, which is modeled as additive Gaussian noise. The performance of the receiver is studied as a function of signal Doppler shift and type of windowing used in the DFT. The use of fast frequency-hopped spread spectrum is found to improve the performance of the DFT based receiver in all but the most severe cases of Doppler shift. The use of a non-uniform window (i.e., a Hamming window) to improve receiver performance is effective only in the presence of large Doppler shifts. The amount of Doppler shift necessary to warrant the use of a non-uniform window depends on the amount of jamming noise power at the receiver, but is relatively insensitive to the frequency hop rate used. GRA

N92-26604 Northwestern Univ., Evanston, IL.
OPTICAL COMMUNICATIONS WITH NUMBER STATES Ph.D. Thesis
Stephen Paul Cruze 1991 122 p
Avail: Univ. Microfilms Order No. DA9128972

Number states are photon eigenstates of the electromagnetic field that possess reduced fluctuations in the photon number compared to coherent states. This property of number states makes them well suited to optical communication systems that use direct detection of the electromagnetic field. This dissertation examines coded quantum-limited optical communication systems when the carrier field is in a number state. The cutoff rate is examined for the modulation scheme pulse position modulation (PPM). Analytical results are obtained for M-ary PPM. The narrowband results are derived first for coherent state sources and number state sources. The results are then extended to wideband, arbitrary bandwidth, sources with an average power constraint. Conditions under which the narrowband results are close to the wideband results are then determined. Lower and upper bounds are derived for the cutoff rate. An upper bound on the cutoff rate for direct detection Poisson channels is generalized to include loss in the channel, and then extended to the case when the source emits number states. This upper bound is compared to results obtained for M-ary PPM to determine how close PPM comes to this bound. An argument based on channel capacity is used to find the minimum required bandwidth expansion in terms of the signalling rate in nats per photon for coherent state sources, including loss in the channel. This result, which is an old result, is extended to number state sources. Dissert. Abstr.

N92-26619# Naval Postgraduate School, Monterey, CA.
RADAR TARGET IDENTIFICATION BY NATURAL RESONANCES: EVALUATION OF SIGNAL PROCESSING ALGORITHMS M.S. Thesis
Gregory A. Lazarakos Sep. 1991 109 p
(AD-A246566) Avail: NTIS HC/MF A06

When a radar pulse impinges upon a target, the resultant scattering process can be solved as a linear time-invariant (LTI) system problem. The system has a transfer function with poles and zeros. Previous work has shown that the poles are independent on the target's structure and geometry. This thesis evaluates the resonance estimation performance of two signal processing techniques: the Kumaresan-Tufts algorithm and the Cadzow-Solomon algorithm. Improvements are made to the Cadzow-Solomon algorithm. Both algorithms are programmed using MATLAB. Test data used to evaluate these algorithms includes synthetic and integral equation generated signals, with and without additive noise, in addition to new experimental scattering data from a thin wire, aluminum spheres, and scale model aircraft.
Author (GRA)

N92-26653*# National Aeronautics and Space Administration. Langley Research Center, Hampton, VA.
ANALYSIS OF SURFACE WAVE PROPAGATION IN A GROUNDED DIELECTRIC SLAB COVERED BY A RESISTIVE SHEET
David G. Shively Jun. 1992 20 p
(RTOP 505-64-20-54)
(NASA-TM-107583; NAS 1.15:107583) Avail: NTIS HC/MF A03

Both parallel and perpendicular polarized surface waves are

known to propagate on lossless and lossy grounded dielectric slabs. Surface wave propagation on a grounded dielectric slab covered with a resistive sheet is considered. Both parallel and perpendicular polarizations are examined. Transcendental equations are derived for each polarization and are solved using iterative techniques. Attenuation and phase velocity are shown for representative geometries. The results are applicable to both a grounded slab with a resistive sheet and an ungrounded slab covered on each side with a resistive sheet. Author

N92-26764# Columbia Univ., New York, NY. Dept. of Physics.
SPONTANEOUS AND INDUCED COHERENT RADIATION GENERATION IN ATOMIC VAPORS Final Report, 1 Jun. 1988 - 31 Oct. 1991
Sven R. Hartmann 31 Jan. 1992 6 p
(Contract N00014-88-K-0299)
(AD-A246078) Avail: NTIS HC/MF A02

The time delayed four wave mixing technique using very wide band 300 angstroms laser noise has been applied to study nile blue and relaxation times in the low femtosecond regime have been measured as well as quantum beats which reveal vibronic structure. Relaxation in multi level systems has been analyzed and applied to the results in nile blue. Attosecond beats in K vapor have been observed and analyzed. Interference effects have been observed in Na vapor which allowed the erasing of photon echo information. Linear and nonlinear effects of local field corrections have been analyzed and applied to third harmonic generation and selective reflectivity. The local field corrections are found to effect both the line shape and the response frequency. When the input fields are intense an analysis which goes beyond the slowly varying amplitude approximation reveals that the transverse profile of the input beam is modified. GRA

N92-26799# Instituto de Fisica Teorica, Sao Paulo (Brazil).
VACUUM POLARIZATION TENSOR IN 3-DIMENSIONAL QUANTUM ELECTRODYNAMICS
B. M. Pimentel, A. T. Suzuki, and J. L. Tomazelli Aug. 1991 15 p
(DE92-621141; IFT-P-028/91) Avail: NTIS HC/MF A03

We evaluate the one loop vacuum polarization tensor for three dimensional quantum electrodynamics (QED), using an analytic regularization technique, implemented in a gauge-invariant way. We show thus that a gauge boson mass is generated at this level of radiative correction to the photon propagator. We also point out in our conclusions that the generalization for the non-Abelian case is straightforward. DOE

N92-26809# National Oceanic and Atmospheric Administration, Boulder, CO. Wave Propagation Lab.
USER'S GUIDE TO WPL MICROWAVE RADIATIVE TRANSFER SOFTWARE
J. A. Schroeder and E. R. Westwater Oct. 1991 91 p
(PB92-129931; NOAA-TM-ERL-WPL-213) Avail: NTIS HC/MF A05

A computer program that the NOAA Wave Propagation Laboratory (WPL) developed to simulate the brightness temperatures (T sub b) observed by an upward-looking microwave radiometer system along a vertical or slant path is described. FORTRAN source code listings are included as an appendix. WPL uses the software to calibrate radiometers, to simulate hypothetical radiometer systems, and to develop retrieval techniques. The program computes clear-sky T sub b from radiosonde profiles of pressure, temperature, and humidity after extrapolating them to 0.1 mb and interpolating between levels where necessary to approximate a continuous atmosphere. Clear-sky attenuation is calculated from the Liebe and Layton water vapor and oxygen absorption model, which is valid for frequencies up to 1 THz. An optional cloud-modeling scheme permits simulations under a variety of cloud configurations. The Rayleigh approximation that underlies the cloud absorption algorithm restricts its validity to nonprecipitating clouds with particle radii less than about 100 micrometers; scattering is neglected. Hence, the cloudy T sub b simulations are valid only for frequencies less than 100 GHz. GRA

N92-26872 Physics and Electronics Lab. TNO, The Hague (Netherlands).
A HIGH REPETITION RATE LIDAR Final Report [EEN LIDAR MET EEN HOGE HERHALINGSFREQUENTIE]
G. J. Kunz Apr. 1991 43 p
(Contract A84KL122)
(AD-A245382; FEL-90-A352; TD90-4059; ETN-92-91212)
Copyright Avail: TNO Physics and Electronics Lab., P.O. Box 96864, 2509 JG The Hague, Netherlands

Using optical radar (lidar) techniques, properties of the atmosphere can be determined by remote sensing. Examples are the horizontal visibility or the extinction coefficient, the vertical extinction or visibility profile, and the cloud base altitude. Because the time scales in the atmosphere are much shorter than the maximum sample rate of the lidar available at the start of this project, a need existed for a system with a repetition rate of at least 10 pulses per second. With such a system it is possible to measure the dynamics of the atmosphere on a subsecond time scale and to map smoke and dust clouds. The properties of such a system are described. Some typical examples of results obtained with this system are presented. ESA

N92-26874 Physics and Electronics Lab. TNO, The Hague (Netherlands).
A MEASURING FACILITY FOR TESTING RADIO COMMUNICATION EQUIPMENT Interim Report [EEN MEETSYSTEEM VOOR HET TESTEN VAN RADIOCOMMUNICATIE-APPARATUUR]
P. Feenstra Aug. 1991 54 p In DUTCH; ENGLISH summary
(Contract A89KL641)
(AD-A245621; FEL-91-A171; TD91-2232; ETN-92-91217)
Copyright Avail: TNO Physics and Electronics Lab., P.O. Box 96864, 2509 JG The Hague, Netherlands

A test facility for measuring the behavior and quality of radio communication equipment in a simulated operational environment is described. The test bed allows the selection of simulated propagation characteristics, such as attenuation, fading, and the occurrence of multipath effects. It is possible to insert various hamming signals. The criterion for classifying radio equipment under test is the quality of the transferred information, i.e., the SINAD value (SIgnal Noise And Distortion) in an analog system and the BER (Bit Error Rate) for a digital system. The test setup is controlled by a PC and the use of windows makes the operation easy. The test facility can be employed for developing and for examining specifications of existing radio communication equipment. ESA

N92-26876 Physics and Electronics Lab. TNO, The Hague (Netherlands).
A REAL-TIME SYNTHETIC APERTURE RADAR PROCESSOR: INTRODUCTION AND PROJECT DESCRIPTION Final Report [EEN REAL-TIME SYNTHETIC APERTURE RADAR PROCESSOR: INTRODUCTIE EN PROJECT BESCHRIJVING]
L. H. J. Bierens Nov. 1991 42 p
(AD-A245370; FEL-91-B295; TD91-3276; ETN-92-91225)
Copyright Avail: TNO Physics and Electronics Lab., P.O. Box 96864, 2509 JG The Hague, Netherlands

A project description for the design and realization of a real time Synthetic Aperture Radar (SAR) processor is presented. The principles of SAR processing and the state of the art are described. Conventional SAR processing techniques depend largely on fast Fourier transformation techniques and devices. These offer limited possibilities to increase speed and performance of a SAR processor. Therefore the design of new algorithms rather than architectures for existing algorithms is suggested. New architectures dedicated to the new algorithms are designed. By exploring parallel structures of the algorithms and by using VLSI (Very Large Scale Integration) array processing, speed and performance can be increased significantly. ESA

N92-26902# Sandia National Labs., Albuquerque, NM.
FEATURE DISCOVERY VIA NEURAL NETWORKS FOR OBJECT RECOGNITION IN SAR IMAGERY
R. J. Fogler, M. W. Koch, M. M. Moya, L. D. Hostetler, and D. R. Hush (New Mexico Univ., Albuquerque.) 1992 6 p Presented at the International Joint Conference on Neural Networks, Baltimore, MD, 7-11 Jun. 1992
(Contract DE-AC04-76DP-00789)
(DE92-007046; SAND-92-0134C; CONF-9206102-1) Avail: NTIS HC/MF A02

A two-stage self-organizing neural network architecture was applied to object recognition in Synthetic Aperture Radar imagery. The first stage performs feature extraction and implements a two-layer Neocognitron. The resulting feature vectors are presented to the second stage, an ART 2-A classifier network, which clusters the features into multiple target categories. Training is performed off-line in two steps. First, the Neocognitron self-organizes in response to repeated presentations of an object to recognize. During this training process, discovered features and the mechanisms for their extraction are captured in the excitatory weight patterns. In the second step, Necognitron learning is inhibited and the ART 2-A classifier forms categories in response to the feature vectors generated by additional presentations of the object to recognize. Finally, all training is inhibited and the system tested against a variety of objects and background clutter. In this paper we report the results of our initial experiments. The architecture recognizes a simulated tank vehicle at arbitrary azimuthal orientations at a single depression angle while rejecting clutter and other object returns. The neural architecture has achieved excellent classification performance using 20 clusters. DOE

N92-26933# Naval Postgraduate School, Monterey, CA.
A COMPARISON OF THE UHF FOLLOW-ON AND MILSTAR SATELLITE COMMUNICATION SYSTEMS M.S. Thesis
Clifton E. Perkins, Jr. Sep. 1991 72 p
(AD-A245806) Avail: NTIS HC/MF A04

The author compares the UHF Follow-On and MILSTAR satellite communication systems. The comparison uses an analytical hierarchy process. Although the two systems have been tasked with different missions, a comparison of cost, capability, and orbit is conducted. UFO provides many of the same capabilities as MILSTAR, but on a smaller scale. Since UFO is also a new space system acquisition, it is used to compare dollars spent to field a viable communication system. A review of frequency bands, losses, and problems is conducted to establish the relationship. Cost data is provided to establish the major difference in the systems. While MILSTAR does possess more total capability than UFO, it is 10 times more costly. Additionally, UFO is a satellite that will evolve with new technology while MILSTAR is built to full capability immediately. In the author's opinion, the incremental performance of MILSTAR does not justify its incremental cost. GRA

N92-26941# Naval Postgraduate School, Monterey, CA.
SYSTEM EVALUATION OF A FREQUENCY HOPPING COMBAT NET RADIO M.S. Thesis
Syed A. Hussain Sep. 1991 89 p
(AD-A246365) Avail: NTIS HC/MF A05

The importance of survivable radio communications in contemporary Electronic Warfare (EW) threat environments cannot be overemphasized. At the tactical level, in fast and fluid conditions, the radio will remain the primary means of communication for command and control. Thus, it will be subjected to hostile EW efforts, e.g., jamming, direction finding, interception, etc. Therefore, the aim of this thesis is to carry out a comparative evaluation of several state of the art frequency hopping combat net radios in order to select the best available choice for fielding into the Pakistan Army. The methodology of evaluation is primarily based on the system specifications provided by respective vendors. Greater emphasis is laid on the anti-jamming performance and upgradability of the systems in the process of evaluation. GRA

N92-27189*# National Aeronautics and Space Administration. Langley Research Center, Hampton, VA.
MODELING 3-D OBJECTS WITH PLANAR SURFACES FOR PREDICTION OF ELECTROMAGNETIC SCATTERING
M. B. Koch, F. B. Beck, and C. R. Cockrell Apr. 1992 13 p
(RTOP 505-64-70-01)
(NASA-TM-107598; NAS 1.15:107598) Avail: NTIS HC/MF A03

Electromagnetic scattering analysis of objects at resonance is difficult because low frequency techniques are slow and computer intensive, and high frequency techniques may not be reliable. A new technique for predicting the electromagnetic backscatter from electrically conducting objects at resonance is studied. This technique is based on modeling three dimensional objects as a combination of flat plates where some of the plates are blocking the scattering from others. A cube is analyzed as a simple example. The preliminary results compare well with the Geometrical Theory of Diffraction and with measured data. Author

33 ELECTRONICS AND ELECTRICAL ENGINEERING

Includes test equipment and maintainability; components, e.g., tunnel diodes and transistors; microminiaturization; and integrated circuitry.

For related information see also *60 Computer Operations and Hardware* and *76 Solid-State Physics.*

N92-26202# Los Alamos National Lab., NM.
PHOTOCATHODE TRANSFER AND STORAGE TECHNIQUES USING ALKALI VAPOR FEEDBACK CONTROL
R. W. Springer and B. J. Cameron 20 Dec. 1991 19 p Presented at the 13th International Free-Electron Laser Conference, Santa Fe, NM, 25-30 Aug. 1991
(Contract W-7405-eng-36)
(DE92-008449; LA-UR-92-474; CONF-9108118-46) Avail: NTIS HC/MF A03

Photocathodes of quantum efficiency above 1 percent at the doubled YAG frequency of 532 nM are very sensitive to the local vacuum environment. These cathodes must have a band gap of less than 2.3 eV, and a work function that is also on the order of approximately 2 volts or less. As such, these surfaces are very reactive as they provide many surface states for the residual gases that have positive electron affinities such as oxygen and omnipotent water. Attendant to this problem is that the optimal operating point for some of these cesium based cathodes is unstable. Three of the cesium series were tried, the Cs-Ag-Bi-O, the Cs3Sb and the K2CsSb. The most stable material found is the K2CsSb. The vacuum conditions can be met by a variety of pumping schemes. The vacuum is achieved by using sputter ion diode pumps, and baking at 250 C or less for whatever time is required to reduce the pump currents to below 1 uA at room temperature. To obtain the required partial pressure of cesium, a simple very sensitive diagnostic gauge has been developed that can discriminate between free alkali and other gases present. This Pressure Alkali Monitor (PAM) can be used on cesium sources to provide a low partial pressure using standard feedback techniques. Photocathodes of arbitrary composition have been transferred to a separate vacuum system and preserved for over 10 days with less than a 25 percent loss to the QE at 543.5 nM. DOE

N92-26205# California Univ., Berkeley. Lawrence Berkeley Lab.
THIN-FILM HIGH TEMPERATURE SUPERCONDUCTING FLUX TRANSFORMERS COUPLED TO SQUIDS
F. C. Wellstood, A. H. Miklich, J. J. Kingston, M. J. Ferrari, J. Clarke, M. S. Colclough, K. Char, and G. Zaharchuk (Conductus, Inc., Sunnyvale, CA.) Aug. 1991 7 p Presented at the 1991 Superconducting Quantum Interference Devices Meeting, Berlin, Germany, 18-21 Jun. 1991
(Contract DE-AC03-76SF-00098)
(DE92-010260; LBL-31158; CONF-9106224-3) Avail: NTIS HC/MF A02

Using photolithographic patterning and laser deposition, we have constructed a sensitive thin-film SQUID magnetometer from YBa2Cu3O(7-x) (YBCO). The device consists of a flux transformer, deposited on one substrate, which is coupled to a thin-film YBCO SQUID, made with bi-epitaxial junctions, deposited on another substrate. At 77 K, the magnetometer has attained a sensitivity of 1.8 pTHz(exp -1/2) at 1 Hz, and has been used to measure the magnetic signal from the human heart. DOE

N92-26224# Lawrence Livermore National Lab., CA.
TRANSPORTABLE 5 MW POWER SUPPLY SYSTEM FOR GYROTRON OPERATION
M. C. Jackson, D. R. Garner, D. S. Ravenscroft, and W. C. Weiss Sep. 1991 7 p Presented at the 14th IEEE Symposium on Fusion Engineering, San Diego, CA, 30 Sep. - 3 Oct. 1991
(Contract W-7405-eng-48)
(DE92-009051; UCRL-JC-107249; CONF-910968-76) Avail: NTIS HC/MF A02

A transportable power supply system was designed to operate gyrotrons at varying locations. The system is designed to operate with an output of -100 kV at 50 A during CW operation (5 MW). The system employs various components previously used on other fusion-related experiments and some newly constructed components. The existing components that were modified for the higher power operation, as well as for transportability, are the raw dc power supply and the modulator/regulator. A newly designed capacitor bank, with a crowbar, was installed as an intermediate element between the power supply and the modulator/regulator, using existing capacitors. When the time comes for the system to be moved to a new location, the system breaks down into six large pieces that can be reassembled in a week. The entire system is controlled by a computer automated measurement and control (CAMAC)-based computer control system that can easily be tied into the rest of the gyrotron subsystems or can be used as a stand-alone system running the power supply system itself. DOE

N92-26238# Sandia National Labs., Albuquerque, NM.
GAS-PRESSURE STUDIES WITH LI(SI)/FeS2 THERMAL BATTERIES
R. A. Guidotti and F. W. Reinhardt 1991 5 p Proposed for presentation at the 35th International Power Sources Symposium, Cherry Hill, NJ, 22-25 Jun. 1992
(Contract DE-AC04-76DP-00789)
(DE92-010801; SAND-91-2348C; CONF-920669-3) Avail: NTIS HC/MF A01

The internal gas pressure of thermal batteries can serve as an indicator of proper functioning. In the case of overheated batteries, venting of the gases can occur. Little information is available, however, as to the magnitude of the internal gas pressure under normal operating conditions. A study was undertaken to monitor the internal gas pressure of Li(Si)/FeS2 thermal batteries during discharge via a pressure transducer attached to the battery case. Factors that could influence the pressure were examined and included: temperature, FeS2 particle size, catholyte composition (lithiated vs. unlithiated), catholyte processing (fused vs. unfused), anode composition (flooded vs. unflooded), discharge load, and the presence of Li2O in the separator. Representative gas examples were also taken during discharge for analysis by gas chromatography. The gas pressure was strongly influenced by the migration of electrolyte from the separator into the catholyte and anode during activation and discharge which impacted the gettering of gases by the anode. DOE

N92-26244# Defence Research Establishment, Ottawa (Ontario).
ON THE DESIGN OF VLSI CIRCUITS FOR THE WINOGRAD FOURIER TRANSFORM ALGORITHM
Pierre Lavoie and Serge Martineau Dec. 1991 83 p
(AD-A246317; DREO-1108) Avail: NTIS HC/MF A05

A VLSI architecture for computing the discrete Fourier transform (DFT) using the Winograd Fourier transform algorithm (WFTA) is presented. This architecture is an addressless, routed, bit-serial scheme that directly maps an N-point algorithm onto silicon. The architecture appears to be far less costly than systolic schemes for implementing the WFTA, and faster than current FFT devices for similar transform sizes. The nesting method of Winograd is used for partitioning larger transformations into several circuits. The advantage of this partitioning technique is that it allows using circuits that are all of the same type. However, the number of input/output pins of each circuit is higher than with some other approaches like, for example, the prime factor algorithm. The design of a 20-point DFT circuit with logic diagrams of its major cells is presented. The gate array circuit has been sent for fabrication in a 0.7 micron CMOS technology. Five circuits interconnected together will compute 60-point complex transforms at a rate of one transformation every 0.53 micron. GRA

N92-26249# Technische Univ., Delft (Netherlands).
REDUCED MODELS FOR THE BEHAVIOR OF VLSI CIRCUITS Ph.D. Thesis
Arie Johannes vanGenderen 1991 194 p
(Contracts EEC-991; IOP-IC-45-009)
(ISBN-90-6275-721-9; ETN-92-91285) Copyright Avail: NTIS HC/MF A09

Several aspects of the modeling of the behavior of integrated circuits are addressed for verification purposes. The modeling of interconnect resistance in integrated circuits is described. The distribution of the interconnect capacitances over the resistance network is important to characterize the transmission behavior of the interconnections. The modeling of three dimensional capacitive effects between the interconnections of integrated circuits is discussed. The three dimensional capacitive effects become more prominent as the horizontal dimensions of the circuit are scaled down, while the vertical dimensions are unchanged. In order to compute reliable capacitance values for the most critical parts of the circuit, an accurate yet numerical technique that directly computes the capacitance values from the layout description of the circuit is described. A simulation model for quickly simulating the logic and timing behavior of large digital MOS circuits is described. Although the simulation model presented is not as accurate as the simulation model employed by a circuit simulator like Spice, it provides useful information about resistance division effects, charge sharing effects, delay times, spikes, and races occurring in the circuit, and it can be used, unlike Spice, to simulate on a workstation, in a reasonable amount of time, circuits containing over 100,000 transistors. ESA

N92-26260# Technische Univ., Delft (Netherlands).
SYNCHRONOUS DETECTION IN MONOLITHICALLY INTEGRATED AM UPCONVERSION RECEIVERS Ph.D. Thesis
Jacob vanderPlas 1990 148 p Sponsored by Netherlands Foundation for Technical Research
(ETN-92-91305) Avail: NTIS HC/MF A07

The design of a synchronous detector for an integrated AM (Amplitude Modulated) upconversion receiver with a tuning range from 150 kHz to 30 MHz is addressed. The following are described: synchronous detector architecture; design of the synchronous detector HF circuits; design of the on-chip continuous time audio low pass filter; and design of the synchronous detector LF circuits. The results of the calculations combined with the results of the prototypes confirm the technical feasibility of a synchronous detector that guarantees at least 50 dB additional channel selectivity. However, the relatively large amount of overhead circuitry for the regeneration of the carrier makes the economic feasibility for the consumer market doubtful. ESA

N92-26280# Ohio State Univ., Columbus. Electroscience Lab.
JOINT SERVICES ELECTRONICS PROGRAM Final Report
Leon Peters, Jr. Jan. 1992 16 p
(Contract N00014-89-J-1007)
(AD-A245636; Rept-721563-4) Avail: NTIS HC/MF A03

The JSEP studies at the ElectroScience Laboratory continue to focus on ELectromagnetics and Electromagnetics related subjects. The emphasis of this program was highlighted during our Major Review when all JSEP schools with an Electromagnetic component also presented their own activities in this discipline.

Research this past three years has involved Diffraction Studies, Integral Equation Studies, Hybrid Studies and Adaptive Array Packet Radio. GRA

N92-26497# Helsinki Univ. of Technology, Espoo (Finland). Dept. of Technical Physics.
HIGH FREQUENCY RAMAN CURRENT DRIVE
S. J. Karttunen, T. J. H. Paetikangas, R. R. E. Salomaa, and S. K. Sipilae 14 Dec. 1990 42 p
(PB92-142223; TKK-F-A671; ISBN-951-22-0472-X) Avail: NTIS HC/MF A03

Current drive in reactor grade tokamak plasmas with a pulsed high power free electron laser (FEL) is investigated. A stimulated Raman process generates fast, longitudinal electron plasma waves, which accelerate electrons to relativistic energies. The fast electrons with v(parallel) much greater than v (perpendicular) are not trapped toroidally, and the resulting current decays slowly. The authors present a systematic study of different combinations of Raman forward and backward scattering and FEL polarization. The optimal FEL frequencies fall within the range 2.2 to 4.0 omega(p) (LCP case) and 3.8 to 7.0 omega(p) (RCP case) in a typical tokamak plasma with Omega(e) approx equals 1.5 omega(p). In a reactor grade plasma, the best current drive efficiency, 5 x 10 (exp 19) A/w (sq m), is obtained by using the stimulated Raman forward process and a left circularly polarized FEL beam. The FEL driven current can be localized to the plasma center and amplified by the bootstrap effect to further enhance the overall efficiency. The Raman current drive in high temperature reactor plasmas is quite different from small scale experiments with Te about 1 keV, where the Raman backward process dominates and the current drive efficiency remains rather low. Author

N92-26540# Florida Univ., Gainesville.
INVESTIGATION OF KINETICS OF MOCVD SYSTEMS Final Report
Timothy J. Anderson Dec. 1991 262 p
(Contract F19628-86-K-0012)
(AD-A246090; RL-TR-91-325) Avail: NTIS HC/MF A12

Several issues related to epitaxy of III-V semiconductors by hydride VPE and MOCVD were investigated. A complex chemical equilibrium analysis was performed in order to investigate the controllability of hydride VPE. The critical control parameters for the deposition of InGaAsP Lattice matched to InP are deposition temperature, system pressure, Group III Molar Ratio, Group V Molar Ratio. An experimental characterization of the Ga and In source reactors was accomplished. A MOCVD System was constructed for the deposition of AlGaAs. An investigation was performed to determine the controlling parameters of laser-enhanced deposition of GaAs and AlGaAs using an argon ion laser. Enhancement of deposition was observed when the system was operated in the reaction limited regime. The use of a Ga/In alloy source was studied for the deposition of GaInAs by the Hydride method. The system was used to produce state-of-the-art P-I-N photo-detectors. GRA

N92-26606# Naval Postgraduate School, Monterey, CA.
THE DEVELOPMENT OF A MODEL BUILDER FOR A MICROCIRCUIT SUBSTRATE M.S. Thesis
Patric K. Roesch 7 May 1991 100 p
(AD-A245765) Avail: NTIS HC/MF A05

The Naval Postgraduate School is currently in possession of software designed to perform a thermal analysis of electronic components. This software package incorporates a model builder whose primary function is to generate a thermal model. In its present configuration, the model builder requires an inordinate amount of time for data input and model verification. This thesis describes the development of a model builder designed specifically to reduce the time required to model the substrate, epoxy, and carrier layers of a microcircuit assembly. GRA

N92-26636# Oak Ridge National Lab., TN.
FABRICATION AND CHARACTERIZATION OF AMORPHOUS LITHIUM ELECTROLYTE THIN FILMS AND RECHARGEABLE THIN-FILM BATTERIES
J. B. Bates, N. J. Dudney, G. R. Gruzalski, R. A. Zuhr, A. Choudhury, C. F. Luck, and J. D. Robertson Feb. 1992 4 p Presented at the 6th International Meeting on Lithium Batteries, Muenster, Germany, 10-15 May 1992
(Contract DE-AC05-84OR-21400)
(DE92-010108; CONF-920581-1) Avail: NTIS HC/MF A01

Research on the deposition and characterization of amorphous lithium electrolyte and vanadium oxide thin films was undertaken with the goal of developing a thin film rechargeable lithium battery. Most of this effort has focused on the electrolyte film, with less but increasing attention given to the cathode. Recent studies on these films and rechargeable thin film lithium cells is reviewed. DOE

N92-26637# Oak Ridge National Lab., TN.
NEW AMORPHOUS THIN-FILM LITHIUM ELECTROLYTE AND RECHARGEABLE MICROBATTERY
J. B. Bates, G. R. Gruzalski, N. J. Dudney, and C. F. Luck Feb. 1992 4 p Proposed for presentation at the 35th International Power Sources Symposium, Cherry Hill, NJ, 22-25 Jun. 1992
(Contract DE-AC05-84OR-21400)
(DE92-010110; CONF-920669-2) Avail: NTIS HC/MF A01

Sputtering of Li3PO4 in pure N2 results in the formation of an amorphous lithium electrolyte that is stable in contact with lithium and has electrical properties that are suitable for application in a thin film cell. Thin film rechargeable lithium cells have been fabricated and characterized using this electrolyte between a lithium anode and an amorphous vanadium oxide cathode. The open circuit voltage of the cell is 3.6 to 3.7 V, and it has a capacity of 130 micro-Ah/sq cm when discharged to 1.5 V. The ac impedance of the cells measured at different stages of discharge indicate a significant decrease in internal resistance at about the midpoint of the discharge. DOE

N92-26741# Naval Research Lab., Washington, DC.
FIELD-EMISSION ARRAYS: A POTENTIALLY BRIGHT SOURCE
Cha-Mei Tang, Antonio C. Ting, and Thomas Swyden (FM Technologies, Inc., Fairfax, VA.) 18 Feb. 1992 17 p
(AD-A246561; NRL-MR-6910) Avail: NTIS HC/MF A03

Field-Emission arrays are potentially a compact and bright electron source. Unlike a laser photocathode, external laser systems are not required. It is possible to have spatial control of the cathode emission. Temporal modulation up to 10 GHz may be possible. We estimate the emittance and brightness based on a reasonable FEA design. Since the FEA's are at an early stage of development for accelerator applications, many technical problems need to be addressed before they can become useful cathodes. This laboratory developing the field-effect controlled (FEC) vacuum field-emission cathode, which is designed to improve the performance of field-emission arrays and to enable the success of envisioned applications of these vacuum field-emitters. GRA

N92-26771# Raytheon Co., Lexington, MA.
RF VACUUM MICROELECTRONICS Quarterly Progress Report No. 1, 1 Oct. - 31 Dec. 1991
Alan Palevsky 31 Dec. 1991 8 p
(Contract MDA972-91-C-0032; ARPA Order 8162)
(AD-A246579) Avail: NTIS HC/MF A02

Improvement in the tip fabrication process and the investigation of burn-in and test procedures have been the focus for the first three months of the contract. The process development and improvement was an extension of internally funded work for flat panel displays. The mask set used was from this work. Since the basic tip process is not the limit to high frequency operation, using this mask set let us start work immediately. A variety of problems have been overcome or alleviated. These include gate/cathode leakage, tip height relative to the gate metal, yield, and cracking at metalization crossovers. GRA

N92-26821# National Inst. of Standards and Technology, Gaithersburg, MD. Semiconductor Electronics Div.
NUMERICAL MODELING OF SILICON PHOTODIODES FOR HIGH-ACCURACY APPLICATIONS WITH PC-1D
J. Geist, D. Chandler-Horowitz, A. M. Robinson, C. R. James, and R. Kohler Jan. 1992 93 p Prepared in cooperation with Alberta Univ., Edmon ton; and Bureau International des Poids et Mesures, Sevres, France
(PB92-148279; NISTIR-4592) Avail: NTIS HC/MF A05

The source code is provided for two Turbo Pascal 5.5 programs and an MSDOS batch program, along with a description of the program and examples of their use. These three programs serve as a batch mode interface to support high accuracy photodiode modeling with Version 2 of the semiconductor device modeling program with PC-1D. These programs are useful because the interactive user interface of PC-1D is optimized for solar cell modeling, and it is somewhat difficult to access the highest accuracy available from PC-1D through the interface. Part 1 describes PC-1D from the point of view of high accuracy photodiode modeling and describes the programs that support its use in the application. Parts 2 and 3 present examples of the use of the programs described in part 1 to model two different types of experiments performed on silicon photodiodes in various high accuracy applications. Author

N92-26847# Sandia National Labs., Albuquerque, NM.
FUNDAMENTALS OF ELECTROKINETICS
M. W. Kozak 1991 11 p Presented at the National Electrokinetics Workshop, Atlanta, GA, 22-23 Jan. 1992
(Contract DE-AC04-76DP-00789)
(DE92-008326; SAND-91-2739C; CONF-920168-2) Avail: NTIS HC/MF A03

The study of electrokinetics is a very mature field. Experimental studies date from the early 1800s, and acceptable theoretical analyses have existed since the early 1900s. The use of electrokinetics in practical field problems is more recent, but it is still quite mature. Most developments in the fundamental understanding of electrokinetics are in the colloid science literature. A significant and increasing divergence between the theoretical understanding of electrokinetics found in the colloid science literature and the theoretical analyses used in interpreting applied experimental studies in soil science and waste remediation has developed. The soil science literature has to date restricted itself to the use of very early theories, with their associated limitations. The purpose of this contribution is to review fundamental aspects of electrokinetic phenomena from a colloid science viewpoint. It is hoped that a bridge can be built between the two branches of the literature, from which both will benefit. Attention is paid to special topics such as the effects of overlapping double layers, applications in unsaturated soils, the influence of dispersivity, and the differences between electrokinetic theory and conductivity theory. DOE

N92-26881 Department of the Navy, Washington, DC.
MAIN AND AUXILIARY TRANSFORMER RECTIFIER SYSTEM FOR MINIMIZING LINE HARMONICS Patent
Leopold J. Johnson, inventor (to Navy) and Russell E. Hammond, inventor (to Navy) 5 Nov. 1991 13 p Filed 22 Mar. 1990
(AD-D015209; US-Patent-5,063,487; US-Patent-Appl-SN-497387; US-Patent-Class-363-3) Avail: US Patent and Trademark Office

A polyphase transformer design is presented in which transformers output phasors are accurately constructed in both voltage magnitude and relative phase angle. The design incorporates both main and auxiliary transformers that are used in unison to produce the accurately constructed phasors. The main transformer permits rough phasor adjustment to be made with the auxiliary transform permitting phasor fine tuning. Such a design is particularly suitable in transformer approaches that require output phases that are of a number not evenly divisible by three.
Author (GRA)

N92-26897# Naval Postgraduate School, Monterey, CA. Dept. of Mechanical Engineering.
STRESSES IN SOLDER JOINTS OF ELECTRONIC PACKAGES Final Report, Jan. - Sep. 1991
David Salinas and Philip Y. Shin 31 Dec. 1991 26 p
(AD-A245799; NPS-ME-92-001) Avail: NTIS HC/MF A03

Electronic chip packages are comprised of several components with different material properties and geometries. One of the most basic electronic packages is the tri-assembly system consisting of a chip attached to a board by a solder connection. During the fabrication of this simple unit, the soldering process subjects the device to a thermal field. Since the three components of the device have different material properties, in particular their Young's modulii, Poissons ratios, and thermal coefficients of expansion, the mismatch in these properties results in thermoelastic stresses. In addition to the thermal field arising from fabrication, thermal fields and hence thermoelastic stresses, result from the operation of the device itself. An investigation of stresses was undertaken. Two types of solder joints, a leaded device and an unleaded device, were compared for effectiveness. Procedures are shown for the analyses of these two types of solder joints. The analyses showed that the thermoelastic stresses for the stiff unleaded connection are significantly greater, by a factor of 20 for the particular arrangement studied in this report, than the stresses in the more flexible leaded connection. GRA

N92-26942# Nebraska Univ., Lincoln.
LINEAR AND NON-LINEAR RESPONSE OF LIQUID AND SOLID PARTICLES TO ENERGETIC RADIATION Final Report
Dennis R. Alexander and John P. Barton 11 Mar. 1991 441 p
(Contract DAAL03-87-K-0138)
(AD-A246368) Avail: NTIS HC/MF A19

The principal purpose of the research is to investigate the linear and nonlinear laser interaction with small aerosols and solid particles. Experimental work is devoted to excimer laser beam interaction with small droplets of water, methanol, and fog oil at irradiances up to 200 GWatts/sq cm. Also of interest in this research is the interactions with solid particles including Al2O3, SiC, glass spheres, Al spheres, CaF2 and W particles at both atmospheric and reduced pressures. Special attention is given to understanding the dynamics of the interaction processes by using a fast streak camera and excimer laser imaging. Jointly with the experimental work is the problem of understanding the electromagnetic interaction of focused laser beams with matter. Emphasis is given to developing computer codes to calculate internal and near electromagnetic fields for plane/focused laser beams incident upon spheres. Another phase of this investigation is devoted to theoretical modeling of the laser imaging system used to obtain nanosecond time scale shadow images of exploding droplets. In addition, theoretical models for both polarized and unpolarized particle thermometry are developed. GRA

N92-27061# Naval Postgraduate School, Monterey, CA.
COMPLEMENTARY METAL OXIDE SILICON CYCLIC REDUNDANCY CHECK GENERATORS M.S. Thesis
Miao Chin Jun. 1991 71 p
(AD-A246140) Avail: NTIS HC/MF A04

This thesis introduces an economical way of implementing the test pattern generation for built-in test. A layout generator as well as a netlist generator are written and validated. In addition, we use the netlist generator to investigate the properties of nonprimitive polynomials. When a logic chip or board has been fabricated, testing is performed on the finished product to ensure that it is free of manufacturing defects. The device is mounted in the test socket of the tester which drives its input terminals with logic signals called test vectors. The responses to these input stimuli are then obtained at the output terminals of the device. The test patterns are generated either by a software algorithm or by hardware built into the test equipment or by hardware actually embedded in the device to be tested. Good responses are obtained by stimulation or by measurement of the output of a number of 'good' devices. Responses to the test patterns may be compressed

into a unique binary number which accumulates all the response data. GRA

N92-27079# Naval Postgraduate School, Monterey, CA.
THE ONSET OF BREAKDOWN IN A FAST PULSED VACUUM DIODE M.S. Thesis
Michael P. Hallal, Jr. Jun. 1991 128 p
(AD-A246395) Avail: NTIS HC/MF A07

The mechanism by which plasma forms in a fast pulsed vacuum diode is not yet well understood. The most popular model of the phenomenon is the explosive emission model. Current densities required by the explosive emission model are much larger than can be provided by space charge limited currents. This study presents experimental results to support a new model which takes into account the ion current density resulting from ionization processes in front of the cathode surface. It is shown that ion heating of the surface is several orders of magnitude more efficient than Joule heating in exploding a whisker. The treatment of the model for an ideal diode predicts the voltage at which plasma formation begins. It also predicts the time delay between the voltage onset and the onset of plasma formation. The voltage at which the onset of plasma formation occurs and the time delay between the voltage onset and the plasma onset have been experimentally determined in this work. The experimental results compare favorably to the new model. Author (GRA)

N92-27176# Naval Postgraduate School, Monterey, CA.
EXPERIMENTAL RESULTS FOR INDUCTIVE STRIPS IN INHOMOGENEOUS FINLINE M.S. Thesis
John Muir Sep. 1991 65 p
(AD-A247254) Avail: NTIS HC/MF A04

This thesis discusses some experimental results involving inductive strips in inhomogeneous finline. One resonator bandpass filters were constructed in inhomogeneous finline for w/b = 1.0, 0.5, 0.2, and 0.1 in an X band waveguide. The frequency response of these filters was plotted using a scalar analyzer and the resonant frequency and crossover bandwidth were measured. The results were compared to those obtained using spectral-domain programs and CAD models developed at the NPS. GRA

N92-26974# Ecole Nationale Superieure de Mecanique et d'Aerotechnique, Poitiers (France). Lab. de Thermique.
INTEGRATED HEAT PIPE CONCEPT FOR LI/SOCI2 CELLS COOLING
A. Suleiman, A. Alexandre, and J. L. Firmin (Societe des Accumulateurs Fixes et de Traction, Romainville, France) *In* ESA, 4th European Symposium on Space Environmental Control Systems, Volume 2 Dec. 1991 p 779-783 Sponsored by Societe des Accumulateurs Fixes et de Traction (For primary document see N92-26950 17-54)
Avail: NTIS HC/MF A23; ESA, EPD, ESTEC, Noordwijk, Netherlands, HC 150 Dutch guilders (2 vols)

N92-27103*# TRW Space Technology Labs., Redondo Beach, CA.
LDEF SP-HVDE (SPACE PLASMA-HIGH VOLTAGE DRAINAGE EXPERIMENT) POST-FLIGHT RESULTS: LEAKAGE CURRENT AND DISCHARGE
J. Y. Yaung, W. C. Wong, B. K. Blakkolb, L. E. Ryan, J. E. Chedotte, and W. W. L. Taylor *In* NASA. Langley Research Center, LDEF: 69 Months in Space. First Post-Retrieval Symposium, Part 3 Jan. 1992 p 1419-1429 (For primary document see N92-27083 17-99)
Avail: NTIS HC/MF A21; 1 functional color page

N92-27111*# Martin Marietta Labs., Baltimore, MD.
RADIATION SENSITIVITY OF QUARTZ CRYSTAL OSCILLATORS EXPERIMENT FOR THE LONG DURATION EXPOSURE FACILITY (LDEF)
J. S. Ahearn and J. D. Venables *In* NASA. Langley Research Center, LDEF: 69 Months in Space. First Post-Retrieval Symposium, Part 3 Jan. 1992 p 1523-1531 (For primary document see N92-27083 17-99)
Avail: NTIS HC/MF A21; 1 functional color page

N92-27112*# Boeing Co., Seattle, WA. Defense and Space Group.
LDEF ELECTRONIC SYSTEMS: SUCCESSES, FAILURES AND LESSONS
E. A. Miller, L. K. Brooks, C. J. Johnson, J. L. Levorsen, O. R. Mulkey, D. C. Porter, and D. W. Smith *In* NASA. Langley Research Center, LDEF: 69 Months in Space. First Post-Retrieval Symposium, Part 3 Jan. 1992 p 1533-1546 (For primary document see N92-27083 17-99)
(Contract NAS1-19224)
Avail: NTIS HC/MF A21; 1 functional color page

N92-27118*# Aerospatiale, Cannes (France). Space and Strategic Systems Div.
EFFECTS OF ULTRA-VACUUM AND SPACE ENVIRONMENT ON CONTACT OHMIC RESISTANCE: LDEF EXPERIMENT AO 138-11
Jean-Pierre Assie and Alfred Perotto *In* NASA. Langley Research Center, LDEF: 69 Months in Space. First Post-Retrieval Symposium, Part 3 Jan. 1992 p 1607-1611 (For primary document see N92-27083 17-99)
Avail: NTIS HC/MF A21; 1 functional color page

34 FLUID MECHANICS AND HEAT TRANSFER

Includes boundary layers; hydrodynamics; fluidics; mass transfer; and ablation cooling.

For related information see also *02 Aerodynamics* and *77 Thermodynamics and Statistical Physics.*

N92-26214# California Univ., Berkeley. Lawrence Berkeley Lab.
FRACTAL CHARACTERISTICS OF FRACTURE ROUGHNESS AND APERTURE DATA
S. Kumar, G. S. Bodvarsson, and J. Boernge (Bureau of Reclamation, Denver, CO.) May 1991 9 p Presented at the 2nd Annual American Nuclear Society International High Level Radioactive Waste Management Conference, Las Vegas, NV, 28 Apr. - 3 May 1991
(Contract DE-AC03-76SF-00098)
(DE92-010302; LBL-31101; CONF-910435-94) Avail: NTIS HC/MF A02

Mathematical expressions are developed for the characteristics of apertures between rough surfaces. It is shown that the correlation between the opposite surfaces influences the aperture properties and different models are presented for these different surface correlations. Fracture and aperture profiles measured from intact fractures are evaluated, and it is found that they qualitatively follow the mathematically predicted trends. DOE

N92-26258# Aeronautical Research Labs., Melbourne (Australia).
AN OUTLINE OF A NUMERICAL SCHEME FOR CALCULATING TWO-DIMENSIONAL TIME LINEARISED TRANSONIC FLOW USING THE GREEN'S FUNCTION METHOD
I. H. Grundy Aug. 1991 15 p
(AD-A246349; ARL-Struc-TM-527; DODA-AR-006-091) Avail: NTIS HC/MF A03

A numerical scheme is outlined for the calculation of 2-D time-linearized transonic flow about an aerofoil or collection of components, using the Green's function method. Computed results are presented for various configurations for the simpler subproblem of steady subsonic flow. GRA

N92-26290# Naval Postgraduate School, Monterey, CA.
STUDY OF THE TRANSITION TO TURBULENCE WITHIN A CURVED RECTANGULAR CHANNEL WITH 40 TO 1 ASPECT RATIO M.S. Thesis
Steven J. Fuqua Sep. 1991 178 p
(AD-A246314) Avail: NTIS HC/MF A09

Longitudinal turbulence intensity and streamwise mean velocity variations are studied from measurements using single-sensor hot-wire probes at Dean numbers from 50 to about 450 in a curved rectangular channel with 40 to 1 aspect ratio, mild curvature, and an inner to outer radius ratio of 0.979. Measured results show significant increases in the longitudinal turbulence intensity as the Dean number increases above 150. These increases are first apparent near the concave surface in upwash regions between individual vortices which make up each vortex pair. Such increases correspond closely with twisting vortex motions, which is important in regard to transition from laminar to turbulent flow because these variations provide evidence that twisting results in the first important increases in turbulence energy at a given location as the Dean number increases. GRA

N92-26379# Wright State Univ., Dayton, OH. Dept. of Mechanical and Materials Engineering.
ANALYSIS OF FROZEN STARTUP OF HIGH-TEMPERATURE HEAT PIPES AND THREE-DIMENSIONAL MODELING OF BLOCK-HEATED HEAT PIPES Final Report, Jan. 1990 - May 1991
Amir Faghri Nov. 1991 164 p
(Contract F33615-86-C-2720)
(AD-A245327; WSU-TR-88-001; WL-TR-91-2086) Avail: NTIS HC/MF A08

The use of high-temperature heat pipes has been proposed for cooling the leading edges and nose cones of re-entry vehicles, rail guns, and laser mirrors, as well as for the thermal management of future hypersonic vehicle structures. The startup behavior of high temperature heat pipes from the frozen state was investigated both numerically and experimentally for various heat loads and input locations. A high temperature sodium/stainless steel heat pipe with multiple heat sources and sinks was fabricated, processed, and tested. A numerical simulation of the transient heat pipe performance including the vapor region, wick structure, and the heat pipe wall is given. Furthermore, experimental and numerical analyses of several operating parameters of a low-temperature copper-water heat pipe under uniform circumferential heating and block heating has been performed. Finally, a numerical analysis of transient heat pipe performance including nonconventional heat pipes with nonuniform heat distributions is presented. Numerical calculations were then made for a leading edge heat pipe with localized high heat fluxes. GRA

N92-26412# Arizona State Univ., Tempe. Dept. of Mechanical and Aerospace Engineering.
DIAPYCNAL MIXING, GRAVITY-CURRENT PROPAGATION, AND SEDIMENT DISPERSION IN TURBULENT FLUIDS Final Report, 1 Jan. 1990 - 31 Dec. 1991
H. J. Fernando 31 Dec. 1991 11 p
(Contract N00014-90-J-1598)
(AD-A246160; ERC-92038) Avail: NTIS HC/MF A03

This report discloses a major accomplishment which was the completion of several laboratory and numerical studies on sediment dispersion in turbulent fluids. The report covers sediment laden gravity currents and estuarine benthic boundary layers. Some of the work started under the previous contract on turbulent mixing in stratified and rotating fluids was also completed. The work performed under these two categories are described below: research on gravity currents and sediment laden turbulent flows and research on turbulent mixing in stratified flows. GRA

N92-26456# Illinois Inst. of Tech., Chicago. Dept. of Chemical Engineering.
COMPUTATION OF HYDRODYNAMICS USING KINETIC THEORY
D. Gidaspow Dec. 1991 11 p
(Contract DE-FG22-89PC-89769)
(DE92-009079; DOE/PC-89769/T8) Avail: NTIS HC/MF A03

Rigorous methods of kinetic theory were used to derive particular phase viscosities and granular conductivities. This new kinetic theory predicted flow behavior and oscillations in a complete loop of a CFB. The results were compared to computations with imposed gas phase turbulence in the riser. The computations were repeated for production of synthesis gas from char. DOE

N92-26496# Helsinki Univ. of Technology, Espoo (Finland). Inst. of Mathematics.
NUMERICAL SOLUTION OF PLASTIC LIQUIDS SHAPE FACTOR
S. Granlund and V. Hara Jun. 1991 10 p Prepared in cooperation with Technical Research Centre of Finland, Espoo; and Nokia Research Center, Espoo, Finland
(PB92-133958; RR-A297; ISBN-951-22-0724-9) Avail: NTIS HC/MF A02

In the connection of industrial processes that deal win non-Newtonian fluids, there is a need to calculate the rate of flow as a function of pressure and dimensions of the pipe or duct. Plastic flow which obeys the so-called power law is considered. The problem of calculating power-law flow in a straight pipe can be reduced to the problem of solving the so-called p-Poisson equation in two dimensions. Actually, the solution of the p-Poisson equation represents the speed profile for the flow and the total flow is obtained by integration. Consideration is restricted to rectangular cross sections for the pipe. Analytical solution is possible in case of circular cross sections and infinite strips. For rectangular cross-sections, a relatively simple numerical solution based on the finite differences method is possible. In fact, the study uses a successive overrelaxation method. For the design of ducts and pipes, the so-called shape factor is practical. By using the shape factor, the flow can be calculated as a function of p and dimensions of the rectangular cross-section. GRA

N92-26506# Sydney Univ. (Australia). School of Civil and Mining Engineering.
TESTS ON VARIOUS ARRANGEMENTS OF LIQUID COLUMN VIBRATION ABSORBERS
R. D. Watkins May 1991 19 p
(PB92-152610; R-639) Avail: NTIS HC/MF A03

The study was aimed at extending knowledge on the performance of various arrangements of the Liquid Column Vibration Absorber (LCVA) for possible reduction of vibrations of buildings or other large structures which may be subject to excitation by wind or other causes. An earlier laboratory study indicated the potential efficacy of one arrangement of LCVA, and the present studies were made on a number of possible variations of the basic system. The first set of tests was made to see what difference in performance occurred with a tenifold difference in the mass ratio of absorber mass to main body mass. The second set was to observe the effects of adding orifice restrictors to a LCVA. The third set of tests was to compare the performances of a long absorber and of a short absorber where both had the same mass. GRA

N92-26507# Helsinki Univ. of Technology, Espoo (Finland). Low Temperature Lab.
MUTUAL FRICTION IN SUPERFLUID He-3: EFFECTS OF BOUND STATES IN THE VORTEX CORE
N. B. Kopnin and M. M. Salomaa 1991 29 p Sponsored in part by Suomen Akatemja, Helsinki; and Akademiya Nauk SSSR, Moscow (USSR)
(PB92-142231; TKK-F-A673) Avail: NTIS HC/MF A03

The motion of singular quantized vortex lines in superfluid He-3 is considered for the A and B phases. Mutual friction is calculated within a microscopic quantum-mechanical Green's function formalism, valid for dynamical processes. This enables one to include all the different physical phenomena in a unified approach. The authors consider axisymmetric vortices for temperatures considerably lower than T(c). In the regime, the main contribution

to the force exerted on a moving vortex line originates from the localized Fermi excitations occupying quantized energy eigenstates in the vortex core. These He-3 quasiparticle states are similar to the quantized motion of charge in a magnetic field. Thus, vortex motion in He-3 resembles the Hall phenomena in metals. The authors also discuss vortex oscillations and predict that strong dissipation should be observed at a resonant frequency of about 10 kHz, owing to transitions between the bound-state energy levels. The effect should be used for detecting and measuring the quantization of the quasiparticle bound-state spectrum in the vortex-core matter for superfluid He-3. Author

N92-26556 Old Dominion Univ., Norfolk, VA.
ON SHOCK CAPTURING FOR LIQUID AND GAS MEDIA Ph.D. Thesis
Tze Jang Chen 1991 129 p
Avail: Univ. Microfilms Order No. DA9204155

The numerical investigation of shock phenomena in gas or liquid media where a specifying relation for internal energy is absent poses special problems. Classically, for gas dynamics the usual procedure is to employ a splitting scheme to remove the source terms from the Euler equations, then upwind-biased shock capturing algorithms are built around the Riemann problem for the system which remains. However, in the case where the Euler equations are formulated in the term of total enthalpy, a technical difficulty associated with equation splitting forces a pressure time derivative to be treated as a source term. This makes it necessary to pose the central Riemann problem for a system where one equation is not a conservation law. In the present research, it is established that successful upwind-biased shock capturing schemes can be applied to the pseudo-conservative system. A shock capturing method developed for this purpose is applied to solving the Riemann problem for pure water with a general (UNESCO 8) equation of state. A second objective of this research is the development of front tracking methods which possess sub-grid resolution capability. One envisions here continuous tracking of the front, as opposed to discrete (one grid point to the next) tracking, such as is provided by the random choice method. A front tracking scheme employing near-front cells which continuously evolve with time is developed. This scheme is applied to the problem of tracking a material interface in the underwater explosion problem. The Riemann problem for water and for a gas-water interface is analyzed, as a vehicle for applying the Godunov method to shock phenomena in liquid media. A by-product of this study is a mapping theorem which establishes a certain correspondence between solutions of the Riemann problem(s) for the ideal gas and the ideal water (modified-Tait equation of state). As a result, present codes which solve the Riemann problem for gases can readily be adapted for use with water. Dissert. Abstr.

N92-26591# California Univ., Berkeley. Coll. of Engineering.
WAVE VISCOSITY INTERACTION IN NONLINEAR ROLL MOTION Final Technical Letter
27 Dec. 1991 12 p
(Contract N00014-88-K-0629)
(AD-A245756) Avail: NTIS HC/MF A03

The objective of the our research program is to develop rationally-based hydrodynamic models for describing and analyzing viscous flows about ship sections, particularly, in the context of nonlinear roll motion of ships, where viscous damping is known to be important. Topics covered include: (1) grid generation mathematics for free surface flow; (2) hydrodynamic resonance in a closed domain and towing tanks; (3) time harmonic oscillating body in a viscous fluid; and (4) highly separated flows about blunt bodies. GRA

N92-26599 Oxford Univ. (England).
CELL VERTEX METHODS FOR COMPRESSIBLE GAS FLOWS Ph.D. Thesis
Michael A. Rudgyard 1990 181 p
Avail: Univ. Microfilms Order No. BRD-94193

The application of cell vertex, finite volume methods to the steady Euler equations is addressed. We consider simple test problems in both one and two dimensions, in order to develop our understanding of the scheme. We present numerical results for the Euler equations for subsonic, transonic, and hypersonic flows. In chapter 1, a background survey of the Euler equations is presented. Chapter 2 contains a review of relevant numerical techniques. In particular, we consider the class of finite volume methods. In chapter 3, we consider the cell vertex method applied to inhomogeneous equations in a single space dimension. We also examine a Lax-Wendroff time-stepping method and deduce a simple modification to this. In chapter 4, we discuss the application of the cell vertex scheme to 2-D problems. We analyze the basic discretization using Fourier techniques, for both hyperbolic and elliptic problems. Iterative methods based on a Lax-Wendroff time-stepping scheme are developed and these are combined with multigrid acceleration. In chapter 5, we develop shock recovery techniques which may be used in combination with Lax-Wendroff time-stepping. This technique is generalized to systems of equations in higher dimensions. The use of upwind iteration methods and the cell vertex scheme is examined in chapter 6. Other iterative methods are considered, including an efficient sweeping technique. In chapter 7, we attempt to generalize the upwind scheme to two dimensions, for both scalar, and vector unknowns. We examine basic properties of the cell vertex scheme, as well as the iterative techniques that are used to solve it.
Dissert. Abstr.

N92-26600 Case Western Reserve Univ., Cleveland, OH.
AN EXPERIMENTAL STUDY OF NATURAL AND FORCED MODES IN AN AXISYMMETRIC JET Ph.D. Thesis
Ganesh Ganapathi Raman 1991 207 p
Avail: Univ. Microfilms Order No. DA9202239

The present experimental investigation consists of two parts. The first part describes an effort to study naturally occurring instability modes in the axisymmetric shear layer of a high Reynolds number turbulent jet. Untripped (transitional) and tripped (turbulent) nozzle exit conditions, both with 0.1 percent core turbulence, were studied. For the turbulent nozzle exit boundary layer case, the core turbulence was varied systematically from 0.1 to 5 percent of the jet exit velocity using various grids located upstream of the nozzle exit. In the second part of this work, an effort to control the axisymmetric shear layer by artificially exciting target modes is described. Under optimum conditions, two-frequency excitation is indeed more effective than single frequency plane wave excitation. It was found that at high amplitudes of fundamental and subharmonic forcing, the subharmonic augmentation and the axial location of the peak are independent of the initial phase difference. However, two-frequency excitation also has its limitations, since axisymmetric waves are damped beyond the potential core. This work concludes with an effort to describe techniques to control an extended region of the jet by forcing combinations of both axisymmetric and helical modes. Higher spreading rates are obtained when multi-modal forcing is applied.
Dissert. Abstr.

N92-26644# Sandia National Labs., Albuquerque, NM.
A BOUNDARY INTEGRAL METHOD FOR STEADY UNSATURATED FLOW IN NONHOMOGENEOUS MEDIA
M. J. Martinez 1991 13 p Presented at the 7th International Conference on Boundary Element Technology, Albuquerque, NM, 3-5 Jun. 1992
(Contract DE-AC04-76DP-00789)
(DE92-009066; SAND-91-2555C; CONF-920664-1) Avail: NTIS HC/MF A03

A boundary integral equation method for steady unsaturated flow in nonhomogeneous porous media is presented. Steady unsaturated flow in porous media is described by the steady form of the so-called Richards equation, a highly nonlinear Fokker-Planck equation. By applying a Kirchhoff transformation and employing an exponential model for the relation between capillary pressure and hydraulic conductivity, the flow equation is rendered linear in each subdomain of a piece-wise homogeneous material. Unfortunately, the transformation results in nonlinear conditions along material interfaces, giving rise to a jump in the potential

along these boundaries. An algorithm developed to solve the nonhomogeneous flow problem is described and verified by comparison to analytical and numerical solutions. The code is applied to examine the moisture distribution in a layered porous medium due to infiltration from a strip source, a model for infiltration from shallow ponds and washes in arid regions. DOE

N92-26645# Lawrence Livermore National Lab., CA.
APPLICATION OF FLUORESCENT-PARTICLE IMAGING TO MEASURING FLOW IN COMPLEX MEDIA
M. A. Northrup, T. J. Kulp, and S. M. Angel Aug. 1991 26 p Presented at the 4th International Symposium on Quatitative Luminescence Spectrometry in Biomedical Sciences, Ghent, Belgium, 27-31 May 1991
(Contract W-7405-eng-48)
(DE92-009121; UCRL-JC-107359; CONF-9105317-1) Avail: NTIS HC/MF A03

In this paper, we report on the development of fluorescence-based experimental techniques that can be used to obtain quantitative information about the flow of fluids through porous media. Flow information is obtained by illuminating a 2-D slice of a 'refractive index matched' model of a porous medium with a planar laser beam. The flowing liquid phase is seeded with 10 micron diameter fluorescent particles, and time-sequenced photographs of the illuminated plane provide quantitative information about the velocity of the flowing liquid. The method provides simultaneous measurements of point-level and spatially averaged velocity vectors within the interstitial spaces of the medium. Porosity and preliminary tracer-concentration measurements were made in a similar manner with the use of a fluorescent dye. The use of fluorescence, spectral filtering, and 'refractive index matching' permits a unique application of particle and tracer imaging to the study of flow in porous systems. The results from this technique compare favorably with the expected macroscopically derived results; the significance of these results and methodology is that they provide experimental verification of fundamental multiphase transport equations. The application of this technique might be extended to experimental studies of flow in optically transparent models of biological, chemical, and physical systems. DOE

N92-26649*# Institute for Computer Applications in Science and Engineering, Hampton, VA.
SYSTEMATIC STUDY OF REYNOLDS STRESS CLOSURE MODELS IN THE COMPUTATIONS OF PLANE CHANNEL FLOWS Final Report
A. O. Demuren (Old Dominion Univ., Norfolk, VA.) and S. Sarkar Apr. 1992 30 p Submitted for publication
(Contract NAS1-18605; RTOP 505-90-52-01)
(NASA-CR-189646; NAS 1.26:189646; ICASE-92-19) Avail: NTIS HC/MF A03

The roles of pressure-strain and turbulent diffusion models in the numerical calculation of turbulent plane channel flows with second-moment closure models are investigated. Three turbulent diffusion and five pressure-strain models are utilized in the computations. The main characteristics of the mean flow and the turbulent fields are compared against experimental data. All the features of the mean flow are correctly predicted by all but one of the Reynolds stress closure models. The Reynolds stress anisotropies in the log layer are predicted to varying degrees of accuracy (good to fair) by the models. None of the models could predict correctly the extent of relaxation towards isotropy in the wake region near the center of the channel. Results from the directional numerical simulation are used to further clarify this behavior of the models. Author

N92-26680*# High Technology Corp., Hampton, VA.
DISTRIBUTED ACOUSTIC RECEPTIVITY IN LAMINAR FLOW CONTROL CONFIGURATIONS Final Report
Meelan Choudhari Washington NASA May 1992 47 p
(Contract NAS1-18240; RTOP 537-03-23-03)
(NASA-CR-4438; NAS 1.26:4438) Avail: NTIS HC/MF A03

A model problem related to distributed receptivity to free-stream acoustic waves in laminar flow control (LFC) configurations is studied, within the Orr-Sommerfield framework, by a suitable extension of the Goldstein-Ruban theory for receptivity due to localized disturbances on the airfoil surface. The results, thus, complement the earlier work on the receptivity produced by local variations in the surface suction and/or surface admittance. In particular, we show that the cumulative effect of the distributed receptivity can be substantially larger than that of a single, isolated suction strip or slot. Furthermore, even if the receptivity is spread out over very large distances, the most effective contributions come from a relatively short region in vicinity of the lower branch of the neutral stability curve. The length scale of this region is intermediate to that of the mean of these two length scales. Finally, it is found that the receptivity is effectively dominated by a narrow band of Fourier components from the wall-suction and admittance distributions, roughly corresponding to a detuning of less than ten percent with respect to the neutral instability wavenumber at the frequency under consideration. The results suggest that the drop-off in receptivity magnitudes away from the resonant wavenumber is nearly independent of the frequency parameter. Author

N92-26681*# High Technology Corp., Hampton, VA.
BOUNDARY-LAYER RECEPTIVITY DUE TO DISTRIBUTED SURFACE IMPERFECTIONS OF A DETERMINISTIC OR RANDOM NATURE Final Report
Meelan Choudhari Washington NASA May 1992 21 p
(Contract NAS1-18240; RTOP 537-03-23-03)
(NASA-CR-4439; NAS 1.26:4439) Avail: NTIS HC/MF A03

Acoustic receptivity of a Blasius boundary layer in the presence of distributed surface irregularities is investigated analytically. It is shown that, out of the entire spatial spectrum of the surface irregularities, only a small band of Fourier components can lead to an efficient conversion of the acoustic input at any given frequency to an unstable eigenmode of the boundary layer flow. The location, and width, of this most receptive band of wavenumbers corresponds to a relative detuning of O(R sub l.b.(exp -3/8)) with respect to the lower-neutral instability wavenumber at the frequency under consideration, R sub l.b. being the Reynolds number based on a typical boundary-layer thickness at the lower branch of the neutral stability curve. Surface imperfections in the form of discrete mode waviness in this range of wavenumbers lead to initial instability amplitudes which are O(R sub l.b.(exp 3/8)) larger than those caused by a single, isolated roughness element. In contrast, irregularities with a continuous spatial spectrum produce much smaller instability amplitudes, even compared to the isolated case, since the increase due to the resonant nature of the response is more than that compensated for by the asymptotically small band-width of the receptivity process. Analytical expressions for the maximum possible instability amplitudes, as well as their expectation for an ensemble of statistically irregular surfaces with random phase distributions, are also presented. Author

N92-26690*# National Aeronautics and Space Administration. Lewis Research Center, Cleveland, OH.
PROGRESS TOWARDS UNDERSTANDING AND PREDICTING CONVECTION HEAT TRANSFER IN THE TURBINE GAS PATH
Robert J. Simoneau and Frederick F. Simon 1992 32 p Proposed for presentation at the International Symposium on Heat Transfer in Turbomachinery, Athens, Greece, 24-28 Aug. 1992; sponsored by the International Centre for Heat and Mass Transfer
(RTOP 505-62-52)
(NASA-TM-105674; E-7043; NAS 1.15:105674) Avail: NTIS HC/MF A03

A new era is drawing in the ability to predict convection heat transfer in the turbine gas path. We feel that the technical community now has the capability to mount a major assault on this problem, which has eluded significant progress for a long time. We hope to make a case for this bold statement by reviewing the state of the art in three major heat transfer, configuration-specific experiments, whose data have provided the big picture and guided both the fundamental modeling research

and the code development. Following that, we review progress and directions in the development of computer codes to predict turbine gas path heat transfer. Finally, we cite examples and make observations on the more recent efforts to do all this work in a simultaneous, interactive, and more synergistic manner. We conclude with an assessment of progress, suggestions for how to use the current state of the art, and recommendations for the future. Author

N92-26698# Sandia National Labs., Albuquerque, NM.
REYNOLDS NUMBER DEPENDENCE OF THE DRAG COEFFICIENT FOR LAMINAR FLOW THROUGH FINE-SCALE SCREENS
T. J. OHern and J. R. Torczynski 1991 21 p Presented at the AIAA/ASME National Fluid Dynamics Congress, Los Angeles, CA, 15-18 Jun. 1991
(Contract DE-AC04-76DP-00789)
(DE92-002930; SAND-91-1429C; CONF-920605-2) Avail: NTIS HC/MF A03

The laminar flow downstream of fine mesh screens is studied experimentally and numerically. Two different screen types are examined experimentally, both with open areas greater than 50 percent and wire dimensions less than 100 micro-m. Such screens produce flow disturbances of much smaller scale than those examined in most previous studies of flow conditioning screens and grid generated turbulence. Instead of using standard woven wire screens, high uniformity screens are used which are fabricated by photo-etching holes into 50.8 micro-m thick Inconel sheets. The holes thus produced are square with rounded corners, arranged to form a square array, with a minimum wire thickness (located halfway between wire crossings) of D = 50.8 micro-m. A flow facility has been constructed for experiments with these screens. Air at 85 kPa and 295 K is passed through each screen at upstream velocities of 1 to 12 m/s, yielding Reynolds numbers Re(sub D) = (rho)UD/mu in the range 2 less than or equal to Re(sub D) less than or equal to 35. Pressure drops across the screens are measured at these conditions using pressure transducers and manometers. From these data, the Reynolds number dependence of the drag coefficient c(sub D) is determined. Three dimensional flow simulations are performed using the spectral element code NEKTON. The geometry of the photo-etched screens is simulated by a similar geometry with the same open area and minimum wire thickness. The drag coefficients are determined from the computed pressure differences across the screens and are in reasonable agreement with the experimental values, although the agreement degrades slightly with increasing Reynolds number. Such correlations are applicable for the present screens so long as the correct choices for screen open area fraction O and minimum wire thickness D are used in correlation. DOE

N92-26699# Massachusetts Inst. of Tech., Cambridge.
PASSIVE WATER HAMMER IN PIPES DUE TO FLASHING
A. R. Wolf, E. Sweeney, and P. Griffith Aug. 1991 17 p Presented at the ASME Pressure Vessel and Piping Conference, New Orleans, LA, 21-25 Jun. 1992
(Contract DE-FG07-88ER-12822)
(DE92-004180; CONF-920631-2) Avail: NTIS HC/MF A03

Peak water hammer pressures arising from flashing flows passing through flow restrictions have been measured in a variety of experiments. Water hammer pressures up to 60 psig have been measured. A homogeneous, equilibrium theory has been developed and shown to be conservative by a factor three or more in predicting the peak pressures. The most likely reasons for the poor prediction of the peak pressure are: (1) the pressure wave velocity (velocity of sound) is reduced due to small amounts of steam in the pipe probably due to flashing during the starting transient; and (2) thermal non-equilibrium in the flow restriction during flashing. DOE

N92-26700# Massachusetts Inst. of Tech., Cambridge.
WATER HAMMER DUE TO THE SUDDEN STOPPING OF A FLASHING FLOW
E. J. Sweeney and P. Griffith Aug. 1991 21 p Presented at the ASME Pressure Vessel and Piping Conference, New Orleans, LA, 21-25 Jun. 1992
(Contract DE-FG07-88ER-12822)
(DE92-004181; CONF-920631-4) Avail: NTIS HC/MF A03

Measurements of the peak pressure occurring when a valve at the end of a pipe passing a flashing flow is slammed shut have been made. Scatter is considerable. The pressure trace indicates that condensing of the vapor occurs at essentially constant pressure after which a single phase liquid water hammer occurs. A simplified hand calculation and a more elaborate computer calculation are both shown to bound the data. For designing pipe supports, the peak pressure can be conservatively estimated assuming the flow is pure liquid. Before the spike is experienced, however, a delay, while the pipe is being filled, ensues. What constitutes a rapid valve closure in this problem, compared to single phase liquid rapid valve closure, is quite different. To avoid the water hammer, a much slower stroking of the valve is needed. DOE

N92-26716# Sandia National Labs., Albuquerque, NM.
AN EXPERIMENTAL INVESTIGATION OF HIGH-SPEED WATER ENTRY FOR FULL SIZE AND SCALE-MODEL POINTED NOSE VEHICLE
J. K. Cole, C. E. Hailey, W. T. Gutierrez, and M. T. Ferrario 1991 17 p Presented at the Cavitation and Multiphase Flow Forum, Los Angeles, CA, 22-25 Jun. 1992
(Contract DE-AC04-76DP-00789)
(DE92-004363; SAND-91-2803C; CONF-920685-1) Avail: NTIS HC/MF A03

High speed water entry is a very complex, dynamic process. Numerical modelling of the process is being developed at Sandia National Laboratories for predicting the steady cavitating flow conditions about a vehicle traveling submerged at high speeds and for approximating the conditions of the cavity running phase of water entry. Now, numerical modelling is being developed to predict the unsteady flow about a vehicle entering or exiting the water and the dynamics of the gas/water interfaces. To assist this effort, tests were planned to measure the base pressure and axial accelerations of vehicles experiencing water entry. Previously most of the water entry results, both theoretical and experimental, have dealt with the forces at water impact and the shape and size of the cavity formed around the body. Only a few attempts have been made to measure cavity pressure during water entry and very limited results are available for high speed entry of pointed nose vehicles at oblique angles throughout the cavity running phase. Full scale water entry tests were conducted. The vehicles were instrumented to measure cavity pressure and three axis accelerations. Because full scale tests are expensive and take considerable time to assemble and conduct, it was decided to complement testing with scaled, instrumented models. A major concern was whether adequate instrumentation and data recording capability could be housed within models that were small enough to test in existing hydroballistic facilities. A special self contained, miniature data recorder and instrumentation package was designed and developed so that pressure and acceleration data could be acquired at high speed from vehicles unimpeded by trailing instrumentation cables. This paper describes the results of a full scale test and 1/10 scale tests which were conducted with self contained data recording/instrumentation packages at water entry velocities up to 319 m/s. DOE

N92-26740 Michigan Univ., Ann Arbor.
FINE SCALE STRUCTURE OF CONSERVED SCALAR MIXING IN TURBULENT SHEAR FLOWS: Sc MUCH GREATER THAN 1 AND Sc APPROXIMATELY EQUAL TO 1 Ph.D. Thesis
Kenneth Alvan Buch, Jr. 1991 245 p
Avail: Univ. Microfilms Order No. DA9208498

This work deals with an experimental investigation of the fine scale structure of conserved scalar mixing in turbulent flows, and presents three dimensional spatio-temporal (x-y-t) measurements of the conserved scalar field zeta(x,t) on the inner scales of the turbulent flow. The measurement resolution reaches down to the local strain limited molecular diffusion scale of the flow, so that,

together with the signal quality achieved, the resulting scalar field measurements are directly differentiable to allow determination of the scalar energy dissipation rate field, (ReSc)(exp -1)(del operator)zeta x (del operator)zeta(x,t), giving the molecular mixing rate field in the flow. Experiments were conducted at two different values of the Schmidt number, with Reynolds numbers from 2100 to 14,000. Results show that the canonical structural element of the mixing rate field is the same for Sc much greater than 1 and Sc approximately 1 turbulent mixing, and consists of strained laminar diffusion layers whose internal structure is well described by the classical solution of Burgers and Townsend for diffusion in the presence of a spatially uniform and locally planar strain rate field. Dissert. Abstr.

N92-26785 Michigan Univ., Ann Arbor.
THE INTERACTION OF A VORTEX RING WITH A CONTAMINATED FREE SURFACE Ph.D. Thesis
Nicholas James Kachman 1991 228 p
Avail: Univ. Microfilms Order No. DA9208573

The intersection between a vortex ring and a contaminated free surface is investigated experimentally using flow visualization and Particle Image Velocimetry (PIV). The surface tension was measured directly on the contaminated surfaces. A nondimensional contamination number, W, is introduced to characterize the effect of surface contamination. In the inclined incidence case, for low contamination numbers, W less than 5 the flow evolution was similar to that of the clean free surface. At W = 9, the flow evolution changed compared to the clean surface. In the bottom vortex core interaction, the vortex no longer reconnected to the surface. It is shown that this was due to the generation of secondary vorticity by the surface active agents at the surface. For all levels of contamination investigated, the top core interaction remained the same as for the clean case, with the vortex core reconnecting to the surface. For the normal incidence case, behavior similar to the inclined incidence case was observed. PIV measurements are described for the primary and secondary vorticity. The secondary vortex circulation was approximately 25 percent of the primary vortex. PIV measurements of the surface showed that the surface velocity decreased for increasing contamination number, but for the highest levels measured (W greater than 360), the surface was never immobilized. Dissert. Abstr.

N92-26836# Technische Univ., Delft (Netherlands).
TWO-PHASE FLOW OF NEWTONIAN AND NON-NEWTONIAN FLUIDS IN A POROUS MEDIUM APPLIED TO WATER CONING Ph.D. Thesis
F. J. T. Floris 25 Nov. 1991 159 p
(PB92-151109; ISBN-90-9004419-1) Avail: NTIS HC/MF A08

In the thesis, the two-phase flow of incompressible and immiscible fluids in a porous medium is considered. The attention is focused on the process of coning bottom water in oil reservoirs. Chapter 1 gives an introduction to the physical phenomena which occur and the basic laws used to model these phenomena. Chapter 2 discusses the instability of a sharp interface between two non-Newtonian fluids in a displacement process. In Chapter 3 a transition zone is included between the fluids and the influence of the non-Newtonian fluid rheology on the capillary diffusion zone is investigated. In Chapter 4 the exact proofs of theorems which have been given in their applied formulation in Chapter 3 are given. In Chapter 5 a full two-dimensional model for the simulation of water coning in heterogeneous reservoirs is given. After the main chapters, two appendices were added. The first appendix reports on a comparison study made between the simulator developed in Chapter 5 and two commercially available simulators. The second appendix shows some work done on raising the accuracy of the approximation of the saturation equation by using a higher order Godunov method. Author

N92-26849 Virginia Polytechnic Inst. and State Univ., Blacksburg.
A PARAMETRIC STUDY OF THE HYDRODYNAMIC STABILITY THEORY OF 3-D COMPRESSIBLE FREE SHEAR FLOWS Ph.D. Thesis
Peter Samuel King 1991 164 p
Avail: Univ. Microfilms Order No. DA9209608

A new and efficient numerical algorithm is developed to solve both the 2-D and 3-D compressible hydrodynamic stability problem. A parametric study of free shear flows with two or more supersonic streams is performed. Flows examined included shear layers, jets/wakes, and various geometrical combinations of these flows. The effect of Mach number on the stability characteristics of the flow is studied and found to confirm the work of other researchers who found that increasing the relative (or convective) Mach number increases the stability of the flow. For 2-D mean flows, the most amplified disturbance is shown to be axial for M less than 1.2 and fully 3-D for M less than 1.2. Disturbances for 3-D mean flows are found here to be axial in the presence of side walls. The variation of the eigenfunctions and flowfield disturbances as a function of Mach number and the flow geometry was also studied. Comparisons of the stability code results are also made to several turbulent mixing experiments. The stability code correctly predicts which parameters will accelerate mixing. New correlations of the effects of some important parameters on stability are developed. Dissert. Abstr.

N92-26853# Sandia National Labs., Albuquerque, NM.
EULERIAN COMPUTATIONAL METHODS
M. McGlaun 1991 14 p Presented at the 2nd International Symposium on Intense Dynamic Loading and its Effects, Chengdu, China, 9-12 Jun. 1992
(Contract DE-AC04-76DP-00789)
(DE92-008017; SAND-91-2865C; CONF-920688-5) Avail: NTIS HC/MF A03

Continuum dynamics codes are categorized as Lagrangian or Eulerian according to the motion of the mesh. A Lagrangian code's mesh moves with the material, so no mass flows between cells. An Eulerian code's mesh is stationary, so mass flows between the cells. Eulerian codes have improved to the point where they are routinely used to solve a broad variety of large deformation solid and fluid dynamics problems ranging from air flow over an airplane wing to meteor impact on space structures. This presentation will concentrate on multi-fluid Eulerian codes capable of modeling transient wave propagation in solids. These codes use a two-step process to integrate the physics across a time step. The first step, referred to as the Lagrangian step, integrates the physics on a Lagrangian mesh across the time step. The field values are then at the new time, but they are on the distorted Lagrangian mesh. The second step, referred to as the remap step, remaps the data on the distorted Lagrangian mesh back to the original Eulerian mesh thus completing one time step. The algorithms used in the first step are similar to those used in modern Lagrangian codes but they must be extended to handle multi-material cells. The algorithms used in the second step are complex and must be very carefully chosen to minimize errors. These algorithms include second-order, monotone advection equations to calculate the quantities flowing between cells. They also require algorithms that construct material interfaces inside multi-material cells. The strength and limitations of currently used numerical techniques will be discussed. New code development activities that combine the best features of both Lagrangian and Elurian codes will also be discussed. These new codes will employ the strengths of both technologies to address problems that cannot be adequately solved at this time. DOE

N92-26855# Los Alamos National Lab., NM.
WAVE STRUCTURE IN ONE AND TWO DIMENSIONAL FLUID FLOW
R. Menikoff 1992 5 p Presented at the 2nd International Symposium on Intense Dynamic Loading and Its Effects, Chengdu, China, 9-12 Jun. 1992
(Contract W-7405-eng-36)
(DE92-007421; LA-UR-92-49; CONF-920688-2) Avail: NTIS HC/MF A01

An equation of state characterizes the material properties needed to describe compressible fluid flow. Thermodynamic

consistency of the equation of state is too general to guarantee physically reasonable flows. Additional constraints may be obtained by analyzing wave structure of the solution to the fluid flow equations. Simple conditions on the equation of state can be derived from the requirements of existence, uniqueness and stability of the solution to the one dimensional Riemann problem. A geometric construction based on the concept of a wave curve is used to solve the Riemann problem. The necessary conditions are related to the monotonicity and asymptotic properties of the wave curve. The two dimensional (2-D) analog of the wave curve is called a shock polar. It can be used to solve a restricted class of 2-D Riemann problems corresponding to the steady state wave patterns that arise from the interaction of one shock wave with another shock wave or a contact. Well known problems such as the transition from regular to Mach reflection are related to the shock polar being neither monotonic nor unbounded. Additional boundary conditions and the bifurcation of 2-D wave patterns are discussed along with open questions that still need to be resolved. DOE

N92-26856# Los Alamos National Lab., NM.
NUMERICAL SIMULATION OF TWO-DIMENSIONAL SINGLE- AND MULTIPLE-MATERIAL FLOW FIELDS
A. R. Lopez, R. S. Baty (Sandia Labs., Albuquerque, NM.), and B. A. Kashiwa 1992 7 p Presented at the Cavitation and Multiphase Flow Forum, Los Angeles, CA, 22-25 Jun. 1992
(Contracts W-7405-eng-36; DE-AC04-76DP-00789)
(DE92-007428; LA-UR-92-3; CONF-920685-2; SAND-91-2788C)
Avail: NTIS HC/MF A02

Over the last several years, Sandia National Laboratories has had an interest in developing capabilities to predict the flow fields around vehicles entering or exiting the water at a wide range of speeds. Such prediction schemes have numerous engineering applications in the design of weapon systems. For example, such a scheme could be used to predict the forces and moments experienced by an air launched antisubmarine weapon on water entry. Furthermore, a water exit prediction capability could be used to model the complicated surface closure jet resulting from a missile being shot out of the water. The CCICE (Cell-Centered Implicit Continuous-fluid Eulerian) code developed at Los Alamos National Laboratory (LANL) was chosen to provide the fluid dynamics solver for high speed water entry and water exit problems. This implicit time marching, two dimensional, conservative, finite volume code solves the multi-material, compressible, inviscid fluid dynamics equations. The incompressible version of the CCICE code, CCMAC (Cell-Centered Marker and Cell), was chosen for low speed water entry and water exit problems in order to reduce the computational expense. These codes were chosen to take advantage of certain advances in numerical methods for computational fluid dynamics (CFD) that have taken place at LANL. Notable among these advances is the ability to perform implicit, multi-material, compressible flow simulations, with a fully cell-centered data structure. This means that a single set of control volumes are used, on which a discrete form of the conservation laws is satisfied. This is in control to the more classical staggered mesh methods, in which separate control volumes are defined for mass and momentum. DOE

N92-26871 Arizona Univ., Tucson.
LARGE-SCALE STRUCTURES AND THE SPATIAL EVOLUTION OF WAKES BEHIND AXISYMMETRIC BLUFF BODIES Ph.D. Thesis
Steven Cary Cannon 1991 143 p
Avail: Univ. Microfilms Order No. DA9208047

The wakes behind a variety of axisymmetric bodies were investigated with flow visualization and hot-wire measurements. The main objective of this study was to correlate changes in the time averaged features of the wake with changes in the characteristics of the coherent large scale structure resulting from changing the solidity of the wake generator or by introducing periodic disturbances to force the wake. The use of an axisymmetric probe holder permitted instantaneous decomposition of the axial-velocity field into temporal and azimuthal Fourier modes. Increases in the body solidity resulted in nearly proportional increases in the size of the mean wake boundary. For the non-shedding (low body solidity) wakes, flow visualization shows that the amplitude of discernible large scale structure is small in comparison to the wake diameter, and there is no evidence of a recirculation region. For the shedding wakes, flow visualization reveals large scale structure with amplitude that is comparable in size to the wake diameter, and a recirculation region is observed that oscillates in axial extent. Fourier analysis of velocity measurements discloses that the temporal scale of the coherent large scale structure for a non-shedding wake decreases in value with downstream distance while the corresponding scale for a shedding wake is constant. Dissert. Abstr.

N92-26883*# Institute for Computer Applications in Science and Engineering, Hampton, VA.
ON TESTING MODELS FOR THE PRESSURE-STRAIN CORRELATION OF TURBULENCE USING DIRECT SIMULATIONS Final Report
C. G. Speziale, T. B. Gatski (National Aeronautics and Space Administration. Langley Research Center, Hampton, VA.), and S. Sarkar Apr. 1992 43 p Submitted for publication
(Contract NAS1-18605; RTOP 505-90-52-01)
(NASA-CR-189638; ICASE-92-16; NAS 1.26:189638) Avail: NTIS HC/MF A03

Direct simulations of homogeneous turbulence have, in recent years, come into wide-spread use for the evaluation of models for the pressure-strain correlation of turbulence. While work in this area is beneficial, the increasingly common practice of testing the slow and rapid parts of these models separately in uniformly strained turbulent flows is shown in this paper to be unsound. For such flows, the decomposition of models, for the pressure-strain correlation, into slow and rapid parts is ambiguous. Consequently, when tested in this manner, misleading conclusions can be drawn about the performance of pressure-strain models. This point is amplified by illustrative calculations of homogeneous shear flow where other pitfalls in the evaluation of models are also uncovered. More meaningful measures for testing the performance of pressure-strain models in uniformly strained turbulent flows are proposed and the implications for turbulence modeling are discussed. Author

N92-26906# National Aerospace Lab., Tokyo (Japan).
PROCEEDINGS OF THE 5TH AND 6TH SEMINARS ON INVESTIGATION AND CONTROL OF BOUNDARY-LAYER TRANSITION [KYOKAISO SENI NO KAIMEI TO SEIGYO KENKYUKAI KOEN RONBUNSHU, DAI 5 KAI TO DAI 6 KAI]
Oct. 1990 55 p In JAPANESE Seminars held in Tokyo, Japan, 28-30 Jun. 1989 and 17-19 Jan. 1990 Original contains color illustrations
(NAL-SP-12; ISSN-0289-260X; JTN-92-80307) Avail: NTIS HC/MF A04

The following topics were discussed: research activities using CFD (Computational Fluid Dynamics); evolution and analysis of three dimensional boundary layer transition; computerized simulation; analysis of air flows around cylindrical bodies; the bullet trains; and an isolated surface roughness. For individual titles, see N92-26907 through N92-26922.

N92-26907# Institute of Flow Research (Japan).
PATTERN SEARCH IN TURBULENT FIELD
Hiroshi Sato and Toshio Otaguro *In* NAL, Proceedings of the 5th and 6th Seminars on Investigation and Control of Boundary-Layer Transition Oct. 1990 p 1-2 In JAPANESE
(For primary document see N92-26906 17-34)
Avail: NTIS HC/MF A04

In order to separate out an orderly moving flow from a turbulent flow, the application of wavelet analysis methods were presented. The wavelet method is an objective mathematical model, which is capable to extract a pattern from 'turbulent' conditions in natural and social phenomena without losing time dependent scale of disturbance distribution in the signal. In practice a wavelet function which has localized data in time axis is generated and an

interrelation between this function and a given function is calculated. The time constant of the wavelet function is varied in order to interrelate with different time scales. In this report the velocity variance signals in the well developed turbulent boundary layer was analyzed by the wavelet analysis, and the calculated results were presented in the diagrams. These diagrams clearly exhibited diverse scale variations of the turbulent flow and time dependence of the variations, and this is the advantage of the wavelet method. Author (NASDA)

N92-26908# Ship Research Inst., Tokyo (Japan).
RESEARCH ACTIVITIES ON CFD AT THE SHIP RESEARCH INSTITUTE [SENPAKU GIJUTSU KENKYUSHO NI OKERU CFD KENKYU NO DOKO]
Yoshiaki Kodama *In* NAL, Proceedings of the 5th and 6th Seminars on Investigation and Control of Boundary-Layer Transition Oct. 1990 p 3-4 In JAPANESE (For primary document see N92-26906 17-34)
Avail: NTIS HC/MF A04

The CFD (Computational Fluid Dynamics) method is used for the analysis of flow pattern in the area of ship fluid flow analysis. Research activities of the following themes utilizing the CFD method at the Ship Research Inst. were briefly described: viscous flow around the ship body, waves generated in free surface, the flow pattern around propellers, and interference between propellers and ship stern by the accompanying flow. The CFD can be utilized with advantages for the numerical simulation under hypothetical flow patterns. As one example of CFD application, control of water flow around the ship body by magnetohydrodynamics was simulated. The Lorentz force is developed in the sea water, when electric current is applied under high magnetic field. This Lorentz force can be useful for the control of fluid field. Author (NASDA)

N92-26909# Tohoku Univ., Sendai (Japan). Faculty of Engineering.
THREE DIMENSIONAL BOUNDARY LAYER TRANSITION ON A YAWED CYLINDER [NANAME ENCHU NO SANJIGEN KYOKAISO SENI]
Yasuaki Kohama *In* NAL, Proceedings of the 5th and 6th Seminars on Investigation and Control of Boundary-Layer Transition Oct. 1990 p 5-9 In JAPANESE Original contains color illustrations (For primary document see N92-26906 17-34)
Avail: NTIS HC/MF A04

The crossflow instability in three dimensional flow is influenced by sweepback angles of main wings and pressure distribution on wing surface. This crossflow instability is treated in two zones of pressure distribution on wing surface, one as a highly pressure decreasing zone at the front edge of wing and the other as a mildly pressure decreasing zone at other wing zone. In this paper, the criteria of crossflow instability generation and the turbulent flow transition process were analyzed using cylindrical model for the qualitative estimation of the strong pressure gradient of the crossflow instability. As for the aerodynamic heating process, the effects of transition zone on the heat conduction to the wall was investigated using heat sensitive liquid crystal. As the results of the investigation, in the transition zone where only primary instability emerged, the turbulent intensity was found not to increase and the heat conductivity to somewhat increase. Author (NASDA)

N92-26910# Osaka Univ. (Japan). Coll. of Engineering.
AN EVOLUTIONAL PROCESS OF THREE DIMENSIONAL DISTURBANCES IN LAMINAR BOUNDARY LAYERS [SANJIGEN KAKURAN NO HITOTSU NO HASSEI KATEI]
Masahito Asai *In* NAL, Proceedings of the 5th and 6th Seminars on Investigation and Control of Boundary-Layer Transition Oct. 1990 p 11-13 In JAPANESE (For primary document see N92-26906 17-34)
Avail: NTIS HC/MF A04

As for the turbulent flow transition of boundary layer starting from the growth of a T-S (Tollmien-Schlichting) wave, the three dimensional wave configuration caused from the development of peak valley structure is one of the most important models. The turbulent flow transition of planar Poiseuille flow were investigated. As the results of experiments, the most probable cause of three dimensional wave formation were concluded to come from the distortion of main flow in the span direction. The synchronous three dimensional wave (a pair of oblique waves) is generated from the nonlinear interference of a two dimensional T-S wave with the three dimensional distortion part of the main flow. As the amplitude of the T-S wave increased over the threshold value of one percent, a synchronous three dimensional wave is predicted to develop from the two dimensional instability model. Experimental results were as follows: (1) the two dimensional T-S wave and three dimensional distortion of mean flow were given as the initial disturbance to Poiseuille flow and the timely development of the disturbance was numerically simulated using the Fourier Chebyshev spectrum method; and (2) as the amplitude of the T-S wave increased over the threshold value of one percent, the amplified three dimensional wave emerged. The amplification of the peak valley wave was confirmed to be caused from distortion of the main flow. Author (NASDA)

N92-26911# Railway Technical Research Inst., Tokyo (Japan).
AERODYNAMIC DRAG ON THE BULLET TRAINS [SHINKANSEN DENSHA NO KUKI TEIKO]
Tatsuo Maeda *In* NAL, Proceedings of the 5th and 6th Seminars on Investigation and Control of Boundary-Layer Transition Oct. 1990 p 15-17 In JAPANESE (For primary document see N92-26906 17-34)
Avail: NTIS HC/MF A04

The running resistance of electric trains can be divided into two resistances, one is the air resistance and the other is the mechanical resistance. The reduction of air resistance of high speed electric trains is especially important, as air resistance of trains increases faster than mechanical resistance in high speed. The air resistance of a long electric train like the 'Shinkansen' (Bullet Train) is evaluated as the combination of the pressure resistance which is exerted at the head and tail parts of the train and of the friction resistance which is exerted along side surfaces of the train and is proportional to the train length. The air resistance is measured from the difference of air resistance between long and short trains by the wind tunnel tests. The air friction resistance is measured from the pressure increase on the side surface of the train, when the train enters a tunnel. The combined resistance (air resistance and mechanical resistance) of the electric trains moving in the tunnel was measured and the resistance difference in and out of the tunnels were assumed to be the air resistance of the train. With this experiment, accuracies of measurement methods were analyzed. Author (NASDA)

N92-26912# National Aerospace Lab., Tokyo (Japan).
CONING MOTION AND FLAT SPINNING OF SLENDER BODIES AT HIGH ANGLES OF ATTACK [HOSONAGA BUTTAI NO DAIGYOKAKU KONINGU TO FURATTO SUPIN NI TSUITE]
Takashi Yoshinaga and Atsushi Tate *In its* Proceedings of the 5th and 6th Seminars on Investigation and Control of Boundary-Layer Transition Oct. 1990 p 19-21 In JAPANESE (For primary document see N92-26906 17-34)
Avail: NTIS HC/MF A04

Slender bars with circular and rectangular cross sections often self-rotate in air flow. When an axisymmetrical bar is dropped in air, three different types of rotation are observed. In the beginning, the bar rotates about the axis perpendicular to the air flow and this rotation is call 'tumbling'. Next, the bar nutates about the axis parallel to the air flow and this nutation is called 'coning'. Finally, the bar rotates in the plane perpendicular to the air flow and this rotation is called 'flat spinning'. The 'flat spinning' phenomena in the critical Reynolds number range is discussed and applied to research for the analysis of flying bodies. The 'flat spinning' of a flying body is postulated as 'coning' in the high angle of attack and the cylindrical body of an aircraft is concluded to have a disadvantage for stability, as this body causes 'coning' motion in the high angle of attack. As for a rounded rectangular body, 'coning' motion is reduced in the range over the critical Reynolds number, but in the range under the critical Reynolds number range, the flying body becomes dynamically unstable as the effect of 'coning'

motion. In the wind tunnel, the behavior of a slender cylinder with angles was investigated for its 'flat spinning' motions in the Reynolds number range of 3 to 6 x 10 (exp 5), and 'coning' motions were observed. Author (NASDA)

N92-26913# Nihon Univ., Tokyo (Japan). Coll. of Science and Engineering.

FLOW AROUND AN ISOLATED SURFACE ROUGHNESS IN THE LAMINAR BOUNDARY LAYER [KORITSU SODO MAWARI NO NAGARE NI TSUITE]

Tatsuo Motohashi *In* NAL, Proceedings of the 5th and 6th Seminars on Investigation and Control of Boundary-Layer Transition Oct. 1990 p 23-24 In JAPANESE (For primary document see N92-26906 17-34)
Avail: NTIS HC/MF A04

The roughness of aircraft wings is an important factor for the air resistance of an aircraft. In order to reduce the air resistance, a method to keep boundary layers as laminar flow is often adapted. With this method, emergence of turbulent flow due to the roughness is not well understood. Especially when the roughness is somewhat large, strong disturbances are caused by the roughness, and turbulent flow occurs suddenly: the mechanism is not well understood. Experimental results in the air flow about isolated roughness (small stubs embedded on the boundary layer) were reported. The air about the isolated roughness were classified as three types according to the roughness Reynolds number of about under 200, 200 to 500, and over 500. In the range of Reynolds number from 200 to 500, the air flow becomes unstable due to the interference of eddy flow and boundary layer and finally becomes turbulent flow. Diagrams on the air flow about roughness, equal turbulence lines, and equal shear strain line in the down flow of roughness (stubs) were shown. Author (NASDA)

N92-26914# Gifu Univ. (Japan).

EXPERIMENTAL STUDIES ON THE FLAT PLATE BOUNDARY LAYER TRANSITION USING HYDROGEN BUBBLE METHOD [HEIBAN KYOKAISO SENI NO SUISO KIHOHO NI YORU JIKKENTEKI KENKYU]

Tatsuya Matsui, Muneshige Okude, and Noriyasu Ishida *In* NAL, Proceedings of the 5th and 6th Seminars on Investigation and Control of Boundary-Layer Transition Oct. 1990 p 25-27 In JAPANESE (For primary document see N92-26906 17-34)
Avail: NTIS HC/MF A04

The transition from laminar flow to turbulent flow in the flat plate boundary layer was studied. The flow pattern was visualized using the hydrogen bubble method and the velocity variable waveforms were measured using a heated wire flowmeter. Using the test results of the visualized flow pattern and velocity variable waveforms, the following three phenomena were analyzed: (1) the Tollmien-Schlichting (T-S) wave; (2) formation of high shear layer due to the development of lambda eddies and ejection and sweep; and (3) spikes developed in the velocity variable waveforms. In the first case, it was observed that the T-S wave can be represented by the visualized flow pattern. In the second case, the development of lambda eddy was continuously photographed with about four shots per second and the velocity variable waveforms perpendicular to the flat plate surface were shown. As the test results show, the large shear layers were observed between two legs of lambda eddies. In the third case, the air flow in the symmetrical plane of hairpin eddies was visualized by platinum wire perpendicular to the flat plate. At the same time, the continuous photographs and waveforms when a heated wire is placed in the upper and lower level with hairpin eddies were shown. The low velocity indicated downward and upward spike were observed. From test results, the interrelation between spike and hairpin eddies was clarified. Author (NASDA)

N92-26915# National Research Lab. of Metrology, Tokyo (Japan).

APPLICATION OF RIBLET SURFACE TO PIPE FLOW [TEIKO GENSHO GIJUTSU NO KANNAIRYU HENO OYO NI TSUITE]

Shinichi Nakao *In* NAL, Proceedings of the 5th and 6th Seminars on Investigation and Control of Boundary-Layer Transition Oct. 1990 p 29-30 In JAPANESE (For primary document see N92-26906 17-34)
Avail: NTIS HC/MF A04

The reduction of turbulent friction resistance to save energy consumption is important not only for aircrafts and ships but especially for pipelines' transportation of fluids. The following two turbulent friction resistance reduction technologies were applied for fluid flow in pipes: with flexible wall, and riblet. The experimental results and analysis are shown. In the experiment, a Teflon tube of 51 mm diameter and 0.05 mm thickness was used. The following three measurements were performed: (1) static axial pressure distribution in the pipe; (2) flow variables measurement by X type heated wire anemometer in the radial direction; and (3) vibration frequency and displacement in the pipe measurement by an eddy current displacement meter. The flow resistance increased at the Reynolds number of 10,000. The reason was attributed to the distortion of pipe wall due to the circumferential stress unequality when the tube was set. The resistance decreased about two percent at the Reynolds number of 30,000. This was due to a 0.25 mm increase in tube diameter. The test results were as follows: (1) the flow resistance was decreased about eight to ten percent; (2) the forms of grooves were V type or U type; and (3) the h+ of grooves was in the range of eight to 12 and s+ of grooves was ten to 20. (h is the height of grooves and s is the distance between grooves.) The riblet method is effective in reducing the surface friction resistance by etching longitudinal grooves on the wall surface. Author (NASDA)

N92-26916# Nihon Univ., Tokyo (Japan). Coll. of Science and Engineering.

NUMERICAL STUDIES ON LAMINAR TURBULENT TRANSITION AT THE STUTTGART UNIVERSITY, GERMANY [STUTTGART DAIGAKU NI OKERU SENI NO SUCHI KEISAN]

Tatsuo Motohashi *In* NAL, Proceedings of the 5th and 6th Seminars on Investigation and Control of Boundary-Layer Transition Oct. 1990 p 31-32 In JAPANESE (For primary document see N92-26906 17-34)
Avail: NTIS HC/MF A04

The stability calculations of boundary layer on the flat plate are introduced. The stability calculations of boundary layer postulated the parallel flow without regard to the development of boundary layer. In order to exclude this postulate, the addition of disturbance to fundamental equation of flow was considered best, and the meanings of this method were summarized as follows: from the chart of Reynolds number and the dimensionless number of disturbance frequency, it was estimated that disturbances decreased in the stable zone and increased in the unstable zone. On the chart which showed the development of disturbance in the direction of flow at the dimensionless frequency of 1.316 for four time series, the disturbances were calculated to: decrease until it crossed a neutral curve, increase in the unstable zone, and decrease in the stable zone. Presently, the following research themes are studied: stability of two dimensional Poiseuille flow against finite disturbance, stability of exfoliate bubble flow, three dimensional analysis of a Tollmien-Schlichting (T-S) wave, flow pattern in grooves, etc. Author (NASDA)

N92-26917# Tohoku Univ., Sendai (Japan). Faculty of Engineering.

INVESTIGATION ON THE BOUNDARY LAYER TRANSITION OF ALTERNATELY OSCILLATING FLOW IN DECELERATION PHASE [KOBAN SHINDORYU GENSOKU ISO NI OKERU KYOKAISO SENI NO JIKKEN]

Yu Fukunishi *In* NAL, Proceedings of the 5th and 6th Seminars on Investigation and Control of Boundary-Layer Transition Oct. 1990 p 33-34 In JAPANESE (For primary document see N92-26906 17-34)
Avail: NTIS HC/MF A04

The alternately oscillating flow in a duct transits to turbulent flow in the decreasing speed phase. This turbulent flow transition was studied experimentally using a heated wire flowmeter, and the results are reported. The oscillating flow develops a reverse pressure gradient in the decreasing speed phase and generates

disturbance near the wall due to small exfoliation of laminar flow. It was observed that a three dimensional eddy structure forms locally disturbed zones and this eddy structure resembles the organizational structures which are found on the conditional extraction from the turbulent flow boundary layer of the flat plate. The experiment to observe the difference of the average configuration of the organizational vortex structure formed in the early phase and in the late phase were found to be caused by the deformation due to the time difference. The results of the experiment show that the structure configurations which exist in the early phase were either to disappear or to develop as it flows downward, and no general rule was concluded. In this experiment, the distinction between structures formed in the upper region and lower region was found to be difficult. In order to extract the characteristic of each structure, the wavelet analysis was applied to speed variation signal. Author (NASDA)

N92-26918# Meijo Univ., Nagoya (Japan). Faculty of Science and Technology.
VORTEX STRUCTURE IN WAKE OF A CIRCULAR CYLINDER [ENCHU HANRYUNAI NO UZURETSU NO KOZO]
Muneshige Okude, Kunihisa Wada, and Tatsuya Matsui *In* NAL, Proceedings of the 5th and 6th Seminars on Investigation and Control of Boundary-Layer Transition Oct. 1990 p 35-37 In JAPANESE (For primary document see N92-26906 17-34)
Avail: NTIS HC/MF A04

When the boundary layers of the flat plate, transition of shear flows like adjunct flow phenomena from laminar flow to turbulent flow and well-developed turbulent flow are visualized, the flow patterns with large and small eddies can be observed. In these visualizations of flow patterns, the existence of eddies are described but usually the functions of eddy flows are seldom explained. One of the reasons is that the vortex structure in the flow are not well analyzed and often the vortex structure is so complex. As the vortex structure always exist in the transition process of flow, detailed analyses of vortex structure are desired. In this paper, the eddies in the vortex structure flows in the cylindrical adjunct flow at a Reynolds number of 140 was studied. The study covered the interrelation between vortex structure and velocity distribution in the cross sections of the adjunct flow obtained from heated wire anemometer and velocity variation and vortex structure distribution. Author (NASDA)

N92-26919# Osaka Univ. (Japan). Coll. of Engineering.
CONTROL OF TURBULENT MIXING IN HYPERSONIC FLOW [CHOONSOKU RANRYU KONGO NO SEIGYO]
Michio Nishioka *In* NAL, Proceedings of the 5th and 6th Seminars on Investigation and Control of Boundary-Layer Transition Oct. 1990 p 39-42 In JAPANESE (For primary document see N92-26906 17-34)
Avail: NTIS HC/MF A04

The conventional engines for present supersonic aircrafts have a drawback in the subsonic flights: they generate strong shock waves, increase total pressure losses, dissociate gases due to increased temperature, and substantially decrease fuel burning efficiencies. When the gases are burned in the supersonic flow, duration times of gases in the combustion chamber become too short. The development of a new technology is required to mix rapidly fuel (hydrogen) and oxygen in the supersonic flow and burn them in time. Flow instability of the initial turbulent flow structure in the hypersonic shear layer is simulated as fuel injection, and the after flow (Mach number of 2.5) is analyzed using the linear stability theory and is studied on the amplified disturbances. The growth of this supersonic disturbance is observed using the Schlieren method. The method for additional mixing of gases is studied to accelerate disturbances. Author (NASDA)

N92-26920# National Aerospace Lab., Tokyo (Japan).
NUMERICAL SIMULATION OF THE LAMINAR TURBULENT TRANSITION IN A STRATIFIED FLOW [SEISORYU SENI NO SUCHI SHIMYURESHON]
Kiyoshi Yamamoto *In its* Proceedings of the 5th and 6th Seminars on Investigation and Control of Boundary-Layer Transition Oct. 1990 p 43-45 In JAPANESE (For primary document see N92-26906 17-34)
Avail: NTIS HC/MF A04

The transition mechanism of heated laminar shear flow becomes more complex in comparison with no heating. For laminar shear flow, in addition to Reynolds number, Prandtl number and Rayleigh number (or Grashof number) are required to describe the flow conditions, or the boundary conditions of the flow have to be given as speed distribution and temperature distribution. Accordingly, the flow pattern changes irregularly with small differences of boundary conditions. The laminate effects of heating on the transition of laminar shear flow in the channel and in the rectangular duct were studied using numerical simulation. The results are given as follows. For the numerical simulation, the initial values problems of Navier-Stokes equations and energy equations are calculated using spectral method. The calculated results described the characteristics of the flow well. The numerical simulation was concluded to be useful for this type of analysis as the shear flow transition involves many parameters.
Author (NASDA)

N92-26921# Osaka Univ. (Japan). Coll. of Engineering.
RESPONSES OF BOUNDARY LAYERS TO STRONG EXTERNAL DISTURBANCES [TSUYOI GAIRAN NI TAISURU KYOKAISO NO OTO]
Masahito Asai *In* NAL, Proceedings of the 5th and 6th Seminars on Investigation and Control of Boundary-Layer Transition Oct. 1990 p 47-48 In JAPANESE (For primary document see N92-26906 17-34)
Avail: NTIS HC/MF A04

The transition from laminar flow to turbulent flow of the boundary layer is an important phenomenon for various problems in astronautical engineering. When the turbulence in the flow is weak, the boundary layer transition starts from the spatial amplification of a viscous T-S (Tollmien Schlichting) wave. The initial wave starts as a two dimensional wave and grows rapidly to a three dimensional wave with amplification. Finally, it corrupts to small scale hairpin eddies. The transitions starting from these wave amplifications are studied, and instability mechanisms are analyzed. In order to analyze the mechanism, the strength of turbulence (eddies) in the air flow that develops a transitional structure in the boundary layer and leads to a turbulent flow transition is analyzed. The responses of the boundary layers to the strong external disturbances are studied experimentally by introducing sonic wave which simulates hairpin eddies in the lower part of the front edge of a flat plate. Author (NASDA)

N92-26922# National Aerospace Lab., Tokyo (Japan).
CROSS-FLOW INSTABILITIES AND PRESSURE GRADIENTS IN BOUNDARY LAYERS [YOKONAGARE FUANTEI TO ATSURYOKU KOBAI]
Nobutake Ito *In its* Proceedings of the 5th and 6th Seminars on Investigation and Control of Boundary-Layer Transition Oct. 1990 p 49-51 In JAPANESE (For primary document see N92-26906 17-34)
Avail: NTIS HC/MF A04

A three dimensional boundary layer is characterized by the velocity component normal to the external nonviscous flow, that is, by the existence of the transverse flow. One of the causes is the combination of the sweptback angle of the wings and the pressure gradient in the direction of a chord and the other is the pressure gradient in the direction of a wing width. Generally, these two phenomena coexist in the three dimensional boundary layer of the sweptback wings. The transverse flow velocity is represented as the sum of velocity components of the two transverse flows. The simple example of this general three dimensional boundary layer occurs when a wedge type body is placed with a yaw against uniform flow and the pressure gradient is applied to the direction of front edge of the body. The accurate solution for this type of three dimensional boundary layer equation and the linear stability calculation using the Orr-Sommerfeld equation are studied. The calculated results contain many unknown facts. It is shown that, if the pressure gradient in the direction of wing width is not

considered, only a part of stability in the three dimensional boundary layer is observed and the most important characteristics are negiected. Author (NASDA)

N92-26934# Colorado State Univ., Fort Collins. Dept. of Atmospheric Science.
A SECOND-ORDER BULK BOUNDARY LAYER MODEL, REVISION
David A. Randall, Qingqiu Shao, and Chin-Hoh Moeng 6 Jan. 1992 63 p
(Contract N00014-89-J-1364)
(AD-A245828) Avail: NTIS HC/MF A04

Bulk mass flux models represent the large eddies that are primarily responsible for the turbulent fluxes in the planetary boundary layer as convective circulations, with an associated convective mass flux. In order for such models to be useful, it is necessary to determine the fractional area covered by rising motion in the convective circulations. This fraction can be used as an estimate of the cloud amount, under certain conditions. We have developed matching conditions that relate the convective mass flux to the ventilation and entrainment mass fluxes. These are based on conservation equations for the scalar means and variances in the entrainment and ventilation layer. Methods are presented to determine both the fractional area covered by rising motion and the convective mass flux. We also show how the requirement of variance balance can be used to relax the well mixed assumption. The vertical structures of the mean state and the turbulent fluxes are determined analytically. Several aspects of our model's formulation are evaluated usng results from large-eddy simulations. GRA

N92-27032*# Institute for Computer Applications in Science and Engineering, Hampton, VA.
SHOCK-TURBULENCE INTERACTIONS IN A REACTING FLOW Final Report
T. L. Jackson, M. Y. Hussaini, and H. S. Ribner (Toronto Univ., Downsview, Ontario) Apr. 1992 19 p Submitted for publication
(Contract NAS1-18605; AF-AFOSR-0180-91; RTOP 505-90-52-01)
(NASA-CR-189647; NAS 1.26:189647; ICASE-92-20) Avail: NTIS HC/MF A03

A specific reactive flow configuration, the interaction of a detonation wave with convected homogeneous isotropic weak turbulence (which can be constructed by a Fourier synthesis of small amplitude shear waves) is addressed. The effect of chemical heat release on the rms fluctuations downstream of the detonation is presented as a function of Mach number. In addition, for the particular case of the von Karman spectrum, the one dimensional power spectra of these flow quantities is given. Author

N92-27045# Eidgenoessisches Flugzeugwerk, Emmen (Switzerland). Abt. Aerodynamik und Flugmechanik.
THEORETICAL PRINCIPLES OF A EULER METHOD FOR THE CALCULATION OF THREE DIMENSIONAL FLOWS [THEORETISCHE GRUNDLAGEN EINER EULER-METHODE ZUR BERECHNUNG VON 3-DIMENSIONALEN STROEMUNGEN]
Marcel Schleicher 14 Nov. 1989 25 p In GERMAN
(F+W-TF-2012; ETN-92-90819) Avail: NTIS HC/MF A03

The theoretical background of an explicit upwind scheme for solving Euler equations in structured meshes is presented. The scheme produces shape resolution. The volume is decomposed in a number of individual units. Each unit is the carrier of constant functional values. Flow functions are defined at unit walls. They allow dating of functional values in the individual units. The direction of the characteristics are considered for the calculation of the flow functions. They carry only physically significant information from the interior of the unit to the unit wall. ESA

N92-27193*# National Aeronautics and Space Administration. Langley Research Center, Hampton, VA.
COMPUTATIONAL METHOD TO PREDICT THERMODYNAMIC, TRANSPORT, AND FLOW PROPERTIES FOR THE MODIFIED LANGLEY 8-FOOT HIGH-TEMPERATURE TUNNEL
S. Venkateswaran, L. Roane Hunt, and Ramadas K. Prabhu (Lockheed Engineering and Sciences Co., Hampton, VA.) Jul. 1992 36 p
(RTOP 506-43-31-05)
(NASA-TM-4374; L-17013; NAS 1.15:4374) Avail: NTIS HC/MF A03

The Langley 8 foot high temperature tunnel (8 ft HTT) is used to test components of hypersonic vehicles for aerothermal loads definition and structural component verification. The test medium of the 8 ft HTT is obtained by burning a mixture of methane and air under high pressure; the combustion products are expanded through an axisymmetric conical contoured nozzle to simulate atmospheric flight at Mach 7. This facility was modified to raise the oxygen content of the test medium to match that of air and to include Mach 4 and Mach 5 capabilities. These modifications will facilitate the testing of hypersonic air breathing propulsion systems for a wide range of flight conditions. A computational method to predict the thermodynamic, transport, and flow properties of the equilibrium chemically reacting oxygen enriched methane-air combustion products was implemented in a computer code. This code calculates the fuel, air, and oxygen mass flow rates and test section flow properties for Mach 7, 5, and 4 nozzle configurations for given combustor and mixer conditions. Salient features of the 8 ft HTT are described, and some of the predicted tunnel operational characteristics are presented in the carpet plots to assist users in preparing test plans. Author

N92-26962# Tsukuba Space Center, Ibaragi (Japan).
UNIFIED COMPUTATIONAL METHOD FOR DESIGN OF FLUID LOOP SYSTEMS
Masao Furukawa *In* ESA, 4th European Symposium on Space Environmental Control Systems, Volume 2 Dec. 1991 p 693-703 (For primary document see N92-26950 17-54)
Avail: NTIS HC/MF A23; ESA, EPD, ESTEC, Noordwijk, Netherlands, HC 150 Dutch guilders (2 vols)

N92-26969# European Space Agency. European Space Research and Technology Center, ESTEC, Noordwijk (Netherlands). Thermal Control and Life Support Div.
THE LIQUID DROPLET RADIATOR: STATUS OF DEVELOPMENT
J. Persson *In its* 4th European Symposium on Space Environmental Control Systems, Volume 2 Dec. 1991 p 747-752 (For primary document see N92-26950 17-54)
Avail: NTIS HC/MF A23; ESA, EPD, ESTEC, Noordwijk, Netherlands, HC 150 Dutch guilders (2 vols)

N92-26972# Kiev Polytechnic (USSR).
PASSIVE THERMOSTATE SYSTEM WITH APPLICATION OF GAS-FILLED HEAT PIPES AND THERMAL ENERGY OF SOLAR RADIATION
V. M. Baturkin, N. K. Gretchina, O. P. Moskalenko, and K. N. Shkoda *In* ESA, 4th European Symposium on Space Environmental Control Systems, Volume 2 Dec. 1991 p 769-774 (For primary document see N92-26950 17-54)
Avail: NTIS HC/MF A23; ESA, EPD, ESTEC, Noordwijk, Netherlands, HC 150 Dutch guilders (2 vols)

N92-27027# Erno Raumfahrttechnik G.m.b.H. Bremen (Germany, F.R.).
CONJUGATING BINARY SYSTEMS: ADVANCED COOLING LIQUIDS FOR USE IN SPACECRAFT ATCS
P. L. Mueller-Remmers, H. Papenberg, W.-D. Ebeling, M. Huerth, D. Woermann, J. Gmehling, and W. Supper (European Space Agency. European Space Research and Technology Center, ESTEC, Noordwijk, Netherlands) *In* ESA, 4th European Symposium on Space Environmental Control Systems, Volume 2 Dec. 1991 p 1157-1162 (For primary document see N92-26950

17-54)
(Contract ESTEC-8757/90/NL/PP(SC))
Avail: NTIS HC/MF A23; ESA, EPD, ESTEC, Noordwijk, Netherlands, HC 150 Dutch guilders (2 vols)

N92-27104*# National Aeronautics and Space Administration. Goddard Space Flight Center, Greenbelt, MD.
LONG DURATION EXPOSURE FACILITY (LDEF) LOW TEMPERATURE HEAT PIPE EXPERIMENT PACKAGE (HEPP) FLIGHT RESULTS
Roy McIntosh, Craig McCreight, and Patrick J. Brennan (OAO Corp., Greenbelt, MD.) *In* NASA. Langley Research Center, LDEF: 69 Months in Space. First Post-Retrieval Symposium, Part 3 Jan. 1992 p 1431-1439 (For primary document see N92-27083 17-99)
Avail: NTIS HC/MF A21; 1 functional color page

N92-27105*# National Aeronautics and Space Administration. Goddard Space Flight Center, Greenbelt, MD.
LONG DURATION EXPOSURE FACILITY (LDEF) LOW-TEMPERATURE HEAT PIPE EXPERIMENT PACKAGE POWER SYSTEM RESULTS
Smith E. Tiller and David Sullivan *In* NASA. Langley Research Center, LDEF: 69 Months in Space. First Post-Retrieval Symposium, Part 3 Jan. 1992 p 1441-1454 (For primary document see N92-27083 17-99)
Avail: NTIS HC/MF A21; 1 functional color page

N92-27106*# McDonnell-Douglas Electronics Co., Saint Louis, MO. Laser and Electronics Systems Div.
RESULTS FROM THE LDEF/A0076 CASCADED VARIABLE CONDUCTANCE HEATPIPE EXPERIMENT
Michael G. Grote *In* NASA. Langley Research Center, LDEF: 69 Months in Space. First Post-Retrieval Symposium, Part 3 Jan. 1992 p 1455-1466 (For primary document see N92-27083 17-99)
Avail: NTIS HC/MF A21; 1 functional color page

N92-27107*# National Aeronautics and Space Administration. Marshall Space Flight Center, Huntsville, AL.
TRANSVERSE FLAT PLATE HEAT PIPE EXPERIMENT
David Shular *In* NASA. Langley Research Center, LDEF: 69 Months in Space. First Post-Retrieval Symposium, Part 3 Jan. 1992 p 1467-1475 (For primary document see N92-27083 17-99)
Avail: NTIS HC/MF A21; 1 functional color page

35 INSTRUMENTATION AND PHOTOGRAPHY

Includes remote sensors; measuring instruments and gages; detectors; cameras and photographic supplies; and holography.

For aerial photography see *43 Earth Resources and Remote Sensing.* For related information see also *06 Aircraft Instrumentation,* and *19 Spacecraft Instrumentation.*

N92-26230# California Univ., Berkeley.
DIAGNOSTIC UPGRADES ON MTX
D. Nilson, T. Casper, J. Foote, C. Lasnier, P. Lopez, B. Rice, R. Stever, K. Hoshino, K. Odajima, and T. Oda Sep. 1991 5 p Presented at the 14th IEEE Symposium on Fusion Engineering, San Diego, CA, 30 Sep. - 3 Oct. 1991
(Contract W-7405-eng-48)
(DE92-009695; UCRL-JC-107241; CONF-910968-77) Avail: NTIS HC/MF A01

The MTX experiment diagnostic capabilities have been recently upgraded with the addition of five new diagnostics. A second beamline was added on the existing Michelson ECE waveguide to accommodate the new polychromator. This provides four orders of magnitude higher time resolution (1-2 microsec) than the Michelson with an improved spectral resolution (5 GHz) using up to nine separate channels. A new four-channel ECE microwave receiver system using both an inside and outside horn placed on the inner tokamak wall allows us to measure the hot electron emission generated from gyrotron and FEL heating. A 15-channel interferometer on MTX has recently been upgraded with the addition of polarimetry to provide measurements of the poloidal magnetic field. This upgrade uses a new technique that determines the Faraday rotation by measuring the phase of a rapidly rotating polarization ellipse. The novel high-speed rotating optics (greater than 60 K rpm) used to produce this state of polarization is reviewed. A new two-channel O-mode reflectometer spanning 75-105 GHz is being added to measure the movements of the cutoff layer. By varying the frequency of this diagnostic, we are able to measure fluctuations deep within the plasma. Finally, a new particle probe diagnostic currently under construction will measure the FEL electric field strength inside the tokamak plasma. Here, we will inject a helium neutral beam into the center of the plasma and excite it with a high power excimer laser, thus, producing a Stark effect emission that is dependent on the FEL electric field strength. DOE

N92-26377# Lawrence Livermore National Lab., CA.
INSTALLATION AND OPERATION OF THE 400 kW 140 GHz GYROTRON ON THE MTX EXPERIMENT
S. W. Ferguson, B. Felker, M. C. Jackson, D. E. Petersen, N. R. Sewall, and R. D. Stever Sep. 1991 9 p Presented at the 14th IEEE Symposium on Fusion Engineering, San Diego, CA, 30 Sep. - 3 Oct. 1991
(Contract W-7405-eng-48)
(DE92-009053; UCRL-JC-107251; CONF-910968-73) Avail: NTIS HC/MF A02

This paper describes the installation and operation of the 400 kW 140 GHz gyrotron used for plasma heating on the Microwave Tokamak Experiment (MTX) at Lawrence Livermore National Laboratory (LLNL). The Varian VGT-8140 gyrotron has operated at a power level of 400 kW for 100 ms in conjunction with MTX plasma shots. The gyrotron system is comprised of a high voltage (-80 kV) modulated power supply, a multistation CAMAC computer control, a 5-tesla superconducting magnet, a series of conventional copper magnets, a circulating fluorinert (FC75) window cooling system, a circulating oil cooling system, a water cooling system, and microwave frequency and power diagnostics. Additionally, a Vlasov launcher is used to convert the gyrotron TE 15,2 mode to a Gaussian beam. Two versions of the Vlasov launcher have been used on the gyrotron, one version designed by LLNL and one version designed by the Japan Atomic Energy Research Institute (JAERI). The Gaussian beam from the Vlasov launcher is transported to the MTX tokamak by a series of 5 mirrors in a 35-meter-long, high-efficiency, quasioptical beam transport system. A twist polarizer is built into one of the mirrors to adjust for horizontal polarization in the tokamak. No windows are used between the Vlasov reflector and the MTX tokamak. A laser alignment system is used to perform the initial system alignment. A summary of the design and operating characteristics of each of these systems is included. Also included is a summary of the system operation and performance. DOE

N92-26391 Max-Planck-Inst. fuer Physik und Astrophysik, Garching (Germany, F.R.). Werner-Heisenberg-Inst. fuer Physik.
CRYOGENIC DETECTOR DEVELOPMENT
S. Cooper, D. Dummer, M. Frank, P. Freund, H.-J. Gebauer, J. Igalson (Polish Academy of Sciences, Warsaw.), F. Proebst, A. Rulofs, W. Seidel, and L. Stodolsky et al Nov. 1991 54 p
(MPI-PhE/91-07; ETN-92-91736) Copyright Avail: Max-Planck-Inst. fuer Physik und Astrophysik, Foehringer Ring 6, D-8000 Munich, Fed. Republic of Germany

Seven papers concerned with the development of cryogenic detectors are presented. These detectors are used for the detection of small energies, for example, deposited energy from the elastic scattering of Wave Interacting Massive Particles (WIMPs), neutrinos, or the absorption of X-rays. The papers are entitled: cryogenic calorimeters for dark matter and neutrinos; calorimetric particle detectors with superconducting absorber materials; recent

progress in colorimeters with transition edge thermometers; signal to noise ratio expected for a calorimeter with transition edge thermometer; superconducting tunnel junctions; electron phonon decoupling and superconducting grains; and silicon drift chambers with integrated amplifiers as low energy detectors. For individual titles, see N92-26392 through N92-26398.

N92-26392 Max-Planck-Inst. fuer Physik und Astrophysik, Munich (Germany, F.R.).

CRYOGENIC CALORIMETERS FOR DARK MATTER AND NEUTRINOS

Susan Cooper *In its* Cryogenic Detector Development Nov. 1991 2 p Presented at the Joint International Lepton-Photon Symposium and Europhysics Conference on High Energy Physics, Geneva, Switzerland, 15 Jul. - 1 Aug. 1991 (For primary document see N92-26391 17-35)

Copyright Avail: Max-Planck-Inst. fuer Physik und Astrophysik, Foehringer Ring 6, D-8000 Munich, Fed. Republic of Germany

The development of massive cryogenic calorimeters for the detection of scattering events with small deposited energies (less than 1 keV) is considered. Tests of a 19 g silicon crystal with an iridium thermometer operated near 225 mK and irradiated with 5 MeV alpha particles are reported. The detected temperature pulse has two parts: a fast component with a decay time of 0.5 ms, and a slow one of 250 ms. The amplitude of the slow component agrees well with a decay time value. The fast one is a factor of 10 to 20 larger; the origin of this component is not yet understood. The energy resolution (FWHM) is 1 when the full pulse height is used, and 4 percent using only the amplitude of the slow component, which is believed to be the true thermal pulse. ESA

N92-26393 Technische Univ., Munich (Germany, F.R.). Dept. of Physics.

CALORIMETRIC PARTICLE DETECTORS WITH SUPERCONDUCTING ABSORBER MATERIALS

G. Forster, P. Ferger, F. v.Feilitzsch, R. L. Moessbauer, F. Azgui, and J. Igalson (Max-Planck-Inst. fuer Physik und Astrophysik, Munich, Germany, F.R.) *In* Max-Planck-Inst. fuer Physik und Astrophysik, Cryogenic Detector Development Nov. 1991 9 p Presented at the 4th International Workshop on Low Temperature Particle Detectors, Oxford, England, 4-7 Sep. 1991 (For primary document see N92-26391 17-35)

Copyright Avail: Max-Planck-Inst. fuer Physik und Astrophysik, Foehringer Ring 6, D-8000 Munich, Fed. Republic of Germany

Massive superconducting absorbers of molybdenum and vanadium are used as low temperature calorimeter particle detectors. The high temperature resolution of the thermometry system, consisting of a superconducting phase transition thermometer monitored with a DC Squid, enables the detection of alpha particles with large single crystals. With a 35 g molybdenum single crystal, an energy resolution of 10 percent Full Width Half Maximum (FWHM) on 5.8 MeV alpha particles is obtained. The observed temperature rise of 1.2 mK is a factor of eight less than expected from the calculated heat capacity. Using a 15g vanadium single crystal, the energy resolution in 5.8 MeV alpha particles is 1.2 percent FWHM. In this case, the pulse height is a factor of five smaller than expected from the calculated heat capacity. A possible reason for the large deviations from the expected heat capacity is the presence of hydrogen dissolved in these transition metals, another reason might be the presence of surface impurities or defects. ESA

N92-26394 Max-Planck-Inst. fuer Physik und Astrophysik, Munich (Germany, F.R.).

RECENT PROGRESS IN CALORIMETERS WITH TRANSITION EDGE THERMOMETERS

F. Proebst, Susan Cooper, D. Dummer, M. Frank, and W. Seidel *In its* Cryogenic Detector Development Nov. 1991 10 p Presented at the 4th International Workshop on Low Temperature Particle Detectors, Oxford, England, 4-7 Sep. 1991 (For primary document see N92-26391 17-35)

Copyright Avail: Max-Planck-Inst. fuer Physik und Astrophysik, Foehringer Ring 6, D-8000 Munich, Fed. Republic of Germany

Tests of two calorimeters, each composed of a 19 g silicon crystal and a superconducting phase transition thermometer monitored with a squid are discussed. The first calorimeter has an iridium thermometer and is operated near 225 mK. The relaxation of alpha particle signals is characterized by two time constants of approximately 1.4 ms and 280 ms. The amplitude corresponding to the fast relaxation time when interpreted as a temperature rise, is much larger than expected, whereas the amplitude of the slow component agrees to within 15 percent with the temperature rise expected from the Debye model heat capacity of the silicon crystal. The second calorimeter uses a gold iridium proximity thermometer with a very wide transition curve (approximately 100 mK), which allows the detector response in a wide temperature range to be studied. The height of signals induced by 122 keV photons, measured from 17 to 60 mK, does not agree with the expectations from the heat capacity. The signals are larger than expected for T greater than or equal to 50 mK and smaller for T less than or equal to 25 mK. An energy resolution of 1.2 keV Full Width Half Maximum (FWHM) was obtained for 60 keV photons detected at an operating temperature of 17 mK. ESA

N92-26395 Max-Planck-Inst. fuer Physik und Astrophysik, Munich (Germany, F.R.).

SIGNAL-TO-NOISE RATIO EXPECTED FOR A CALORIMETER WITH TRANSITION EDGE THERMOMETER

W. Seidel, D. Dummer, and F. Proebst *In its* Cryogenic Detector Development Nov. 1991 6 p Presented at the 4th International Workshop on Low Temperature Particle Detectors, Oxford, England, 4-7 Sep. 1991 (For primary document see N92-26391 17-35)

Copyright Avail: Max-Planck-Inst. fuer Physik und Astrophysik, Foehringer Ring 6, D-8000 Munich, Fed. Republic of Germany

A simple model of a calorimeter with dielectric absorber, superconducting transition edge thermometer, and squid readout is discussed. The effect of this method of temperature measurement on the pulse shape and on the spectral densities of the various noise contributions is considered. An expression for the signal to noise ratio that can be obtained with such a system using optimal pulse shaping is presented. ESA

N92-26396 Technische Univ., Munich (Germany, F.R.). Dept. of Physics.

SUPERCONDUCTING TUNNEL JUNCTIONS **c76**

H. Kraus, J. Jochum, B. Kemmather, M. Gutsche, F. v.Feilitzsch, and R. L. Moessbauer *In* Max-Planck-Inst. fuer Physik und Astrophysik, Cryogenic Detector Development Nov. 1991 9 p Presented at the 4th International Workshop on Low Temperature Particle Detectors, Oxford, England, 4-7 Sep. 1991 (For primary document see N92-26391 17-35)

Copyright Avail: Max-Planck-Inst. fuer Physik und Astrophysik, Foehringer Ring 6, D-8000 Munich, Fed. Republic of Germany

The development of superconducting detectors well suited for X-ray spectroscopy in the energy range below 10 keV is considered. Detectors equipped with superconducting thin film absorbers, which are well suited for X-ray spectroscopy in this range, are investigated. Superconducting tunnel junctions are discussed in general and the results along with superconducting X-ray detectors, exploiting quasi particle trapping, are presented. The relative charge output of superconducting tunnel junctions is considered. The epitaxial growth of vanadium absorbers, necessary to obtain detectors of long term stability is also considered. ESA

N92-26397 Max-Planck-Inst. fuer Physik und Astrophysik, Munich (Germany, F.R.).

ELECTRON-PHONON DECOUPLING AND SUPERCONDUCTING GRAINS **c76**

P. Freund, H.-J. Gebauer, and L. Stodolsky *In its* Cryogenic Detector Development Nov. 1991 11 p Presented at the 4th International Workshop on Low Temperature Particle Detectors, Oxford, England, 4-7 Sep. 1991 (For primary document see N92-26391 17-35)

Copyright Avail: Max-Planck-Inst. fuer Physik und Astrophysik, Foehringer Ring 6, D-8000 Munich, Fed. Republic of Germany

Well below Tc (critical temperature) the electronic heat capacity of a superconductor gets dramatically small, following the BCS factor exp (-(const.)Tc/T). If it were possible to use this small heat capacity for calorimetry one would have a system of very great sensitivity. The difficulty is that in a real superconductor there is also the phonon contribution to the specific heat, which will become dominant once the electronic part gets small. However, at low temperature the coupling between electrons and phonons gets progressively weaker, so that if there is an energy deposit on the electrons in the superconductor, as from a charged particle or a photon, the isolation of the electron and phonon systems from each other may lead to a large jump in the electron temperature. The time scale for the start of a flip in a metastable superconducting grain is very small. Thus the 'electron-phonon decoupling' should hold, even for a rather short time, noticeable effects in the 'flip field' would be expected as observed with the 'sweep-irradiation method'. Calculations on the effect and the results of a test with indium and 6 and 60 keV photons are presented. However, the results are more in agreement with a nondecoupling calculation where both phonon and electron heat capacities enter. A possible explanation is that the energy deposit is too large. ESA

N92-26398 Max-Planck-Inst. fuer Physik und Astrophysik, Munich (Germany, F.R.).
SILICON DRIFT CHAMBERS WITH INTEGRATED AMPLIFIERS AS LOW ENERGY DETECTORS
H.-J. Gebauer *In its* Cryogenic Detector Development Nov. 1991 5 p Presented at the 4th International Workshop on Low Temperature Particle Detectors, Oxford, England, 4-7 Sep. 1991 (For primary document see N92-26391 17-35)
Copyright Avail: Max-Planck-Inst. fuer Physik und Astrophysik, Foehringer Ring 6, D-8000 Munich, Fed. Republic of Germany

A detector which combines the two ideas of the silicon drift chamber and the planar Si detector to get the advantages of both is proposed. The detector consists of a silicon disk with concentric ring electrodes on both sides. An integrated resistor chain divides the applied voltage in a graded potential, guiding the ionization electrons to a point like readout electrode (anode) in the center. An on-chip transistor close to the anode acts as a front end amplifier. The diameter and thickness of the silicon wafer should be as large as possible to give a maximum mass per electronic channel. Limits are set by the bulk leakage current, which increases the noise, and by charge losses, which decrease the signal. ESA

N92-26401# Naval Postgraduate School, Monterey, CA.
DEVELOPMENT AND TESTING OF A PROTOTYPE ELECTRO-OPTICAL PHASE ENCODED POSITION TRANSDUCER M.S. Thesis
Gary R. Parriott Dec. 1991 61 p
(AD-A245486) Avail: NTIS HC/MF A04

A proof-of-concept experimental validation of a proposed idea for a prototype electro-optical phase encoded position transducer was conducted. The intensity of two IR LED beams were modulated sinusoidally at frequency omega, with a 90 degree temporal phase difference. They were further modulated by a pair of sinusoidal optical encoding masks with 90 degree spatial phase difference. The mask pair was mounted on a mechanical stage and translated perpendicular to the beam axis. The sum of the two signals produced by this electro-optical configuration constituted another sinusoid at temporal frequency omega, whose phase was proportional to mask position. Although small deviations from ideal behavior were observed, the validity of the technique has been established incontestably. GRA

N92-26459# Naval Postgraduate School, Monterey, CA.
FIBER-OPTIC FLEXURAL DISK ACCELEROMETER M.S. Thesis
Joanne E. Olcott Sep. 1991 99 p
(AD-A246203) Avail: NTIS HC/MF A05

The fabrication and calibration of a fiber-optic flexural disk accelerometer is discussed in this thesis. The accelerometer is comprised of a cylindrical body with thin, flexible end plates (or disks) and an interior spindle coupling the disks together ensuring proper phasing. The sensing mechanism is comprised of single mode optical fiber wound into flat coils and epoxied on to the inside faces of the disks, forming the legs of a Michelson interferometer. The use of both legs of this fiber-optic interferometer as sensing elements provides a push-pull enhancement and effectively doubles the accelerometer's response while providing common-mode rejection of pressure and temperature variations. GRA

N92-26517# Physics and Electronics Lab. TNO, The Hague (Netherlands).
DESCRIPTION OF THE MULTISPECTRAL CCD-CAMERA Final Report
R. A. Kemp Aug. 1991 38 p In DUTCH; ENGLISH summary
(AD-A245681; FEL-91-B234; TDCK-TD91-2901) Avail: NTIS HC/MF A03

The multispectral CCD camera system (MS-CCD) has been developed for the 'Background clutter project' (1990-1993), which is being carried out by the Infrared Group (Div. 4.2) in cooperation with the Technology Development Division (Div. 5) of TNO Physics and Electronics Laboratory in contract for the Dutch Royal Army. The Background clutter project aims to improve range predictions for detection and recognition of army vehicles in natural backgrounds. Digital imagery, which has been obtained using visible and IR imaging sensors is used to optimize range predictions. During the course of this project a need was felt for a system acquiring imagery of backgrounds in 12 different wavelength bands between 350 nm and 1100 nm. GRA

N92-26536*# Alabama Univ., Huntsville. Dept. of Chemical and Materials Engineering.
HIGH TEMPERATURE FURNACE MODELING AND PERFORMANCE VERIFICATIONS Final Technical Report, period ending 30 Sept. 1991
James E. Smith, Jr. Jun. 1992 163 p
(Grant NAG8-708)
(NASA-CR-190403; NAS 1.26:190403) Avail: NTIS HC/MF A08

Analytical, numerical, and experimental studies were performed on two classes of high temperature materials processing sources for their potential use as directional solidification furnaces. The research concentrated on a commercially available high temperature furnace using a zirconia ceramic tube as the heating element and an Arc Furnace based on a tube welder. The first objective was to assemble the zirconia furnace and construct parts needed to successfully perform experiments. The 2nd objective was to evaluate the zirconia furnace performance as a directional solidification furnace element. The 3rd objective was to establish a data base on materials used in the furnace construction, with particular emphasis on emissivities, transmissivities, and absorptivities as functions of wavelength and temperature. A 1-D and 2-D spectral radiation heat transfer model was developed for comparison with standard modeling techniques, and were used to predict wall and crucible temperatures. The 4th objective addressed the development of a SINDA model for the Arc Furnace and was used to design sample holders and to estimate cooling media temperatures for the steady state operation of the furnace. And, the 5th objective addressed the initial performance evaluation of the Arc Furnace and associated equipment for directional solidification. Results of these objectives are presented. Author

N92-26569# Oak Ridge National Lab., TN.
TUNED-CIRCUIT DUAL-MODE JOHNSON NOISE THERMOMETERS
R. L. Shepard, R. M. Carroll, D. D. Falter, T. V. Blalock, and M. J. Roberts (Tennessee Univ., Martin.) 1992 11 p Presented at the 7th International Symposium on Temperature: Its Measurement and Control in Science and Industry, Toronto, Ontario, 28 Apr. - 1 May 1992
(Contract DE-AC05-84OR-21400)
(DE92-010121; CONF-920423-2) Avail: NTIS HC/MF A03

Dual-mode Johnson noise and direct current (DC) resistance thermometers can be used in control systems where prompt

indications of temperature changes and long-term accuracy are needed. Such a thermometer is being developed for the SP-100 space nuclear electric power system that requires temperature measurement at 1400 K in space for 10 years, of which 7 are expected to be at full reactor power. Several direct coupled and transformer coupled, tuned resistance inductance capacitance (RLC) circuits that produce a single, continuous voltage signal were evaluated for noise temperature measurement. The simple direct coupled RLC circuit selected provides a mean squared noise voltage that depends only on the capacitance used and the temperature of the sensor, and it is independent of the value of or changes in the sensor resistance. These circuits provide a noise signal with long term accuracy but require integrating noise signals for a finite length of time. The four wire resistor for the noise temperature sensor allows simultaneous DC resistance measurements to be made that provide a prompt, continuous temperature indication signal. The DC current mode is employed continuously, and a noise voltage measurement is made periodically to correct the temperature indication. The differential noise voltage preamplifier used substantially reduces electromagnetic interference (EMI) in the system. A sensor has been tested that should provide good performance (+/- 1 percent accuracy) and long-term (10 year) reliability in space environments. Accurate noise temperature measurements were made at temperatures above 1300 K, where significant insulator shunting occurs, even though shunting does affect the dc resistance measurements and makes the system more susceptible to EMI. DOE

N92-26572# Brookhaven National Lab., Upton, NY.
DESIGN OF A HIGH-PRECISION TUNABLE DOUBLE CRYSTAL MONOCHROMATOR
M. Shleifer, S. Sharma, E. Rotela, and C. Brite Feb. 1992 6 p
(Contract DE-AC02-76CH-00016)
(DE92-010137; BNL-47194) Avail: NTIS HC/MF A02

The design of a high precision tunable double crystal monochromator is described. Each crystal of the monochromator can be aligned independently by a double-axis gimbal mechanism providing rotations about two perpendicular axes. Two orthogonal linear actuators operate the gimbal mechanism via a connecting bar. The exit beam height is controlled by separate linear actuators that change the distance between the crystals along the beam axis. Vertical separation between the crystals may also be adjusted. Thermal deformations are minimized in this compact ultrahigh vacuum (UHV) compatible design by water cooling of the first crystal. DOE

N92-26738 Michigan Univ., Ann Arbor.
AN INSTRUMENT FOR ENGINE TORQUE ESTIMATION AND MISFIRE DETECTION Ph.D. Thesis
Yibing Dong 1991 143 p
Avail: Univ. Microfilms Order No. DA9208528

The design of an instrument for the estimation of indicated torque and the detection of misfires in spark ignition internal combustion engines are addressed. The relationship between crankshaft angle of rotation and time is exploited to derive models describing engine torque production and the engine rotating dynamics in the angular position domain. Based on these models, an algorithm is developed to estimate engine indicated torque and a method is introduced to detect engine misfire. The implementation of the algorithm is also considered and leads to the design of an instrument for the estimation of engine indicated torque and the detection of engine misfire. The instrument is composed of two parts: (1) the engine angular speed variation (EASV) signal demodulator, which uses an engine angular speed driven tracking filter to realize engine crankshaft angle domain data processing; and (2) a special purpose microprocessor to implement the algorithm and detect engine misfire. A discrete implementation of the EASV demodulator was built and used successfully at the Vehicular Electronics Laboratory at the University of Michigan. A version of the very large scale integration (VLSI) implementation and layout for the demodulator is also introduced. The special purpose microprocessor has its own hardware multiplier and hardware DFT unit for real time on-board misfire detection. Dissert. Abstr.

N92-26786# Helsinki Univ. of Technology, Espoo (Finland). Radio Lab.
MEASUREMENT ELECTRONICS OF INDUSTRIAL MICROWAVE RESONATOR SENSORS
P. V. Vainikainen 17 Dec. 1991 110 p
(PB92-152750; ISBN-951-22-0722-2; S-194) Avail: NTIS HC/MF A06

The measurement methods of the properties of high-frequency electromagnetic resonators used as industrial sensors are described. The work contains: (1) a short overview of the utilization of microwaves in industrial measurements; (2) a theoretical analysis of the aspects affecting the performance of the measurement methods; and (3) the description of several practical realizations of the measurement electronics of different types of resonator sensors. In the overview, the different types of industrial microwave sensors are briefly presented. The specific features of the resonator sensors are their suitability to the measurement of the properties of small objects or small changes, flexibility, and high level of specification. In the application section, measurement electronics for the resonator sensors of five different industrial measurement problems are presented. The frequencies of the resonators reach from 150 MHz to 9.5 GHz and the quality factors from 100 to 2000. In all presented applications, discrete point measurement of the power response of the resonator is used. In two of the applications, both the resonant frequency and the quality factor of the resonator are needed, and in three applications, only the measurement of the resonant frequency is necessary. For many sensors, additional temperature measurement is also needed. GRA

N92-26794# Naval Postgraduate School, Monterey, CA.
INVESTIGATIONS OF A SINGLE POINT TEMPERATURE PROBE FOR MEASUREMENT OF ATMOSPHERIC TURBULENCE M.S. Thesis
Cloyes R. Hoover Dec. 1991 72 p
(AD-A246563) Avail: NTIS HC/MF A04

Gradients in the index of refraction caused by temperature fluctuations create optical turbulence. This optical turbulence greatly degrades the performance of imaging and laser systems operating in the atmosphere. There are several methods of measuring optical turbulence in the atmosphere, but few give a high resolution profile of the turbulence at all levels displaying the 'layers' of turbulence that exist. This thesis is an investigation of the use of a high speed temperature probe coupled with a VIZ 900 meteorological system to measure the optical turbulence in the atmosphere from a ground base to approximately 25 km. The processing of the data is done by a program developed as part of this research. GRA

N92-26879 Department of the Navy, Washington, DC.
LIQUID LEVEL AND VOLUME MEASUREMENT DEVICE Patent
Gair D. Brown, inventor (to Navy) 17 Dec. 1991 8 p Filed 30 Jul. 1990
(AD-D015189; US-Patent-5,073,720; US-Patent-Appl-SN-561413; US-Patent-Class-250-577) Avail: US Patent and Trademark Office

The presented liquid level measurement device is an electro-optical device which uses a light source (typically a light emitting diode (LED) or laser diode) and an optical detector to measure the level of a liquid in a container. The light beam is passed through the liquid and received by the optical detector. The detector output is processed to determine the liquid level or the liquid volume. A special feature is the ability to measure a continuum of fluid levels or volumes. GRA

N92-26930# Environmental Protection Agency, Research Triangle Park, NC. Atmospheric Research and Exposure Assessment Lab.
EVALUATION OF THE FOURIER TRANSFORM INFRARED SPECTROMETER FOR PARTICLE-ASSOCIATED AMMONIUM SULFATE DETERMINATION Final Report
K. J. Krost Mar. 1992 69 p
(PB92-160084; EPA/600/R-92/050) Avail: NTIS HC/MF A04

A commercial Fourier transform infrared (FTIR) spectrometer, modified for automated analysis of particulate-associated sulfate, was used to obtain transmission spectra of samples of particulate matter collected from the ambient air onto Teflon filters. An evaluation of the instrumentation was undertaken to determine its applicability for measuring sulfate and the correlation of results with those of ion chromatography and x-ray fluorescence. Particle samples from six geographical areas were analyzed in the study. Results from different filter sets, using individual filter blanks, show values of the coefficient of determination of 0.90 or higher for any two techniques with one notable exception. The exception is due to displacement of sulfate absorption from the wavelength interval used for analysis, and apparently indicates the effect of co-collected compounds in chemically shifting the spectra. The detection limit is 1.2 microgram/sq cm which corresponds to 0.4 microgram/cu m sampled over 24 hours at 13.3 L/min for ammonium sulfate. Author

N92-27181# Naval Postgraduate School, Monterey, CA.
PASSIVE DETERMINATION OF TEMPERATURE AND RANGE USING SPECTRAL BAND MEASUREMENTS OF PHOTON EMITTANCE M.S. Thesis
Shinji Hirakawa Sep. 1991 87 p
(AD-A247147) Avail: NTIS HC/MF A05

The established concept of temperature determination from dual spectral band radiometric measurement is analyzed for the case that the measurement device is sensitive to total photon emittance rather than radiant emittance. A temperature dependent ratio of measurements is calculated for two distinct spectral bands using a black body distribution. It is shown that, if the bands are not self-contained, then there exists a one-to-one correspondence between temperature and ratio. A prototype algorithm is proposed and tested which demonstrates the feasibility of extracting both the temperature and range by using three distinct spectral band measurements. The model assumes nonhomogeneous, wavelength-dependent atmospheric attenuation. The target and sensor systems each have an arbitrary location in a vertical plane relative to the earth. In the computer simulations, LOWTRAN data was used. GRA

N92-27092*# Instruments Service Aerodynamique, Longjumeau (France).
RULED AND HOLOGRAPHIC DIFFRACTION GRATINGS EXPERIMENT (AO 138-5)
Francis Bonnemason *In* NASA. Langley Research Center, LDEF: 69 Months in Space. First Post-Retrieval Symposium, Part 3 Jan. 1992 p 1301-1314 (For primary document see N92-27083 17-99)
Avail: NTIS HC/MF A21; 1 functional color page

N92-27109*# Eppley Lab., Inc., Newport, RI.
PASSIVE EXPOSURE OF EARTH RADIATION BUDGET EXPERIMENT COMPONENTS. LDEF EXPERIMENT AO-147: POST-FLIGHT EXAMINATIONS AND TESTS
John R. Hickey *In* NASA. Langley Research Center, LDEF: 69 Months in Space. First Post-Retrieval Symposium, Part 3 Jan. 1992 p 1493-1509 (For primary document see N92-27083 17-99)
(Contracts NAS1-15350; NAS3-25958)
Avail: NTIS HC/MF A21; 1 functional color page

N92-27113*# National Aeronautics and Space Administration. Langley Research Center, Hampton, VA.
EFFECT OF SPACE EXPOSURE OF PYROELECTRIC INFRARED DETECTORS
James B. Robertson *In its* LDEF: 69 Months in Space. First Post-Retrieval Symposium, Part 3 Jan. 1992 p 1547-1548 (For primary document see N92-27083 17-99)
Avail: NTIS HC/MF A21; 1 functional color page

36 LASERS AND MASERS

Includes parametric amplifiers.
For related information see also *76 Solid-State Physics.*

N92-26269# Sandia National Labs., Albuquerque, NM.
COMPARISON OF LASER AND CONVENTIONAL HEATING IN TLD DOSEMAPPING
S. C. Jones, J. A. Sweet (International Sensor Technology, Santa Ana, CA.), D. L. Fehl, B. R. Sujka, D. W. Vehar, and R. L. Westfall 1992 16 p Presented at the 9th Topical Conference on High-Temperature Plasma Diagnostics, Santa Fe, NM, 15-19 Mar. 1992
(Contract DE-AC04-76DP-00789)
(DE92-010773; SAND-92-0089C; CONF-920362-7) Avail: NTIS HC/MF A03

A new, laser-based system has been developed for rapid evaluation of monolithic thermoluminescence dosimetry (TLD) arrays. A precision controlled CO2 laser is used to sequentially heat 1.5 mm diameter, approximately 0.04 mm thick TLD's deposited on a .125 mm thick polymer substrate in a 3 mm x 3 mm grid. Array areas up to 30 cm x 30 cm are used (greater than 10,000 TLD elements), with evaluation times of 45-90 minutes. Isodose contours and various analysis functions are available on the system-operating PC. This system allows for greatly expanded dosimetry compared to standard TLD's, simultaneously decreasing effort and record keeping. We compared the dosimetric characteristics of this system with standard techniques, using near Si-equivalent CaF2:Mn TLD elements, in a test with 19 MeV end-point X radiation. The results show the laser system performs as well as the standard system. DOE

N92-26271# Physics and Electronics Lab. TNO, The Hague (Netherlands).
CONSTRUCTION AND FUNCTION OF A MULTIFUNCTION CO2-LASER SYSTEM Final Report
R. J. Lerou and P. H. Bentvelsen Sep. 1991 62 p In DUTCH; ENGLISH summary
(AD-A245425; FEL-91-A161; TDCK-TD-91-2909) Avail: NTIS HC/MF A04

A description is given of a multifunction laser system designed for applications such as range and velocity measurements, vibration detection and active imaging. The system is based on a wave guide CO2 laser operating in a continuous mode. The received radiation is detected by an optical heterodyne detection technique. Examples of the results of range, velocity, and vibration measurements with the laser system are shown and discussed. The laser beam is modulated with an Mullard 100A acousto-optical modulation in a frequency band of 90 to 110 MHz. The properties of this modulator has been determined. A digital integrator, designed and built for periodic and synchronous signals is described. It is designed to integrate a large number of periods and is capable of sampling at a frequency of 42 MHz, with digital conversion to 8 bit. The increase of the Signal to Noise Ratio with the number of integrations is described. The specially designed electronic transmitter/receiver unit of the system and a waveform recorder, including control software, is briefly discussed. GRA

N92-26287# Instituto de Pesquisas Energeticas e Nucleares, Sao Paulo (Brazil).
OPTIMIZATION OF A COLOR CENTER Q-SWITCHED Nd:YLF LASER
W. Rossi, N. D. VieiraJunior, F. E. Costa, S. L. Baldochi, and S. P. Morato 1992 4 p
(DE92-621612; INIS-BR-2897) Avail: NTIS HC/MF A01

Nd:YLF lasers, passive Q-switched and mode-locked, were

optimized by the control of the optical and physical parameters of a LiF crystal with F sub 2 sup (-) color center. , DOE

N92-26293# McDonnell Aircraft Co., Saint Louis, MO.
EARLY RISK REDUCTION PHASE 1 FLIR/LASER DESIGNATOR WINDOW Final Report
Robert J. Lord and Alfred Rosenfeld 31 Dec. 1991 174 p Revised
(Contract N00019-88-C-0051)
(AD-A246352; MDC-86PR0869-Rev) Avail: NTIS HC/MF A08

This program evaluated and tested materials and coatings for use as a common aperture for a laser target designator (LTD) and a Forward Looking Infrared (FLIR) designator. Desired characteristics include: transmission at 1.06 microns for laser and 8 to 11.5 microns for FLIR, radar frequency attenuation for low observability, and durability in tactical aircraft environments. The designs were a zinc sulfide/zinc selenide design and zinc selenide and gallium arsenide designs. All three designs had some degree of success in meeting optical transmission and RF attenuation goals, but all were damaged by sand and rain erosion. A large performance variability of the gallium arsenide used in this program indicated immaturity in the substrate manufacturing expertise. Our evaluation showed that substrate cost is high and the industrial base for the production of large window panels is small. Production cost ranges from $190 per cubic inch for zinc selenide to $500 per cubic inch for gallium arsenide. Multi-paned windows for large field of regard operation could cost as much as $500,000. GRA

N92-26462# Naval Postgraduate School, Monterey, CA.
ENERGY THRESHOLD FOR LASER INDUCED BREAKDOWN ON A METAL SURFACE UNDER HIGH AND ULTRA HIGH VACUUM CONDITIONS M.S. Thesis
Abdullah Gedik Jun. 1991 38 p
(AD-A246212) Avail: NTIS HC/MF A03

Unipolar arcing is the primary breakdown process when a powerful laser pulse interacts with a target surface. The unipolar arc model assumes that the initial ionization occurs in desorbed gas layers. To check this experimentally, a metal surface was illuminated under different vacuum conditions. The experiments were conducted at 10-4, 10-6, and 10-8 torr vacuum. A neodymium:glass laser of wavelength 1.06 microns in the Q-switched mode was utilized. Type 304, polished, stainless steel plates were used as targets. Results confirmed that higher laser energy was needed to trigger the laser induced breakdown at lower pressures. GRA

N92-26504# Lawrence Livermore National Lab., CA.
DIODE PUMPED 275 WATT AVERAGE POWER Nd:YAG SLAB LASER
B. Comaskey, R. Beach, G. Albrecht, B. Benett, B. Freitas, C. Petty, D. VanLue, D. Mundinger, and R. Solarz 16 Dec. 1991 12 p Presented at the Society of Photo-Optical Instrumentation Engineers' International Symposium on Laser Spectroscopy As Part of SPIE's Symposium on Optics, Electro-Optics and Laser Applications in Science and Engrg., Los Angeles, CA, 19-25 Jan. 1992
(Contract W-7405-eng-48)
(DE92-008604; UCRL-JC-109185; CONF-920124-14) Avail: NTIS HC/MF A03

We have developed and tested stackable microchannel cooled laser bar diode pump packages suitable for direct face pumping of slab lasers at high duty factor. A stack of 41 diode packages gives a pump array of 13.5 cm(exp 2) and produces a peak power of 3750 watts and an average power of 1000 watts, for an average irradiance of 75 watts/cm(exp 2). A high average power, total internal reflection face pumped Nd:YAG laser using 80 diode packages has been constructed. Average power of 275 watts is obtained at 2.5 kHz pulse repetition rates and 100 microsecond current pulse widths. DOE

N92-26505# Lawrence Livermore National Lab., CA.
FAIL SAFE SYSTEM FOR SUPPRESSING STIMULATED BRILLOUIN SCATTERING IN LARGE OPTICS ON THE NOVA LASER
C. E. Thompson, D. F. Browning, E. H. Padilla, T. L. Weiland, and J. D. Wintemute Jan. 1992 8 p Presented at the Society of Photo-Optical Instrumentation Engineers' International Symposium on Laser Spectroscopy as part of SPIE's Symposium on Optics, Electro-Optics and Laser Applications in Science and Engrg., Los Angeles, CA, 19-25 Jan. 1992
(Contract W-7405-eng-48)
(DE92-008608; UCRL-JC-107974; CONF-920124-13) Avail: NTIS HC/MF A02

We have designed and are testing a 'fail safe' system on Nova to suppress stimulated Brillouin scattering (SBS) in large optics at the output of the laser. The system increases the laser bandwidth to prevent SBS and prevents pulses with insufficient bandwidth from being injected into the amplifier chain. It is thus fail safe. The system design and experimental measurements will be presented. DOE

N92-26571 Southampton Univ. (England).
POLARISATION EFFECTS IN FIBRE LASERS Ph.D. Thesis
Jin-Tong Lin 1990 249 p
Avail: Univ. Microfilms Order No. BRDX92833

Single-mode fiber lasers are a new class of active fiber device, which play a remarkable role in optical fiber communications and sensors. They also exhibit a number of new phenomena, one of the most important being polarization effects. New unexpected fundamental polarization effects in fiber lasers was discovered. The phenomena are fluorescence depolarization, the existence of orthogonal polarization eigenmodes, and the dependence of the output polarizationon the pump polarization state. A unified theoretical model, incorporating the electric dipole model for rare-earth ions in a glass matrix, is formulated. The concept of effective pump power is introduced and can be applied to existing laser theory; thus, laser performance characteristics such as thresholds, slope efficiencies and the polarization state of the output can be predicted accurately. The good agreement between theory and experiment enables the derivation of the polarized cross-section ratio. This was done for Nd(3+) and Er(3+) ions in silica fibers. From the theoretical analysis, the optimum condition for single polarization operation is deduced. An effective technique for making single-polarization single-mode (SPSM) fiber lasers was developed using an integral fiber polarizer. The advantages of this technique are low insertion loss, high polarization extinction ratio and compatibility with existing single-mode fiber components. Laser-diode-pumped SPSM fibers of high performance, both in continuous-wave and Q-switched operations, were achieved.
Dissert. Abstr.

N92-26573# Los Alamos National Lab., NM.
MULTIQUANTA PHOTODETACHMENT FROM THE H(-) ION Ph.D. Thesis
Chen-Yau Tang Mar. 1992 175 p
(Contract W-7405-eng-36)
(DE92-010306; LA-12254T) Avail: NTIS HC/MF A08

Multiphoton detachment (MPD) of an electron from the loosely bound H(sup -) system (binding energy = 0.7542 eV) has been studied at various photon energies and laser intensities. In the center of mass of 800-MeV H(sup -) ions the CO2 laser photon energy, 0.117 eV, was Doppler tuned over a wide range, from 0.15 to 0.39 eV. The peak laser intensity in the lab frame was varied from 2 to 12 GW/cm(exp 2). The general behavior of MPD versus photon energy and the ac-Stark/ponderomotive effects are of special interest in the study. Characteristic threshold structures by absorption of 2, 3, 4, and 5 photons were observed, as evidenced by rapid changes in the signal amplitudes. These thresholds provide a straightforward picture of channel opening in MPD as the photon energy is increased. A fit of two-photon detachment data to the Wigner threshold law showed a good match with a small intensity induced shift in the threshold energy. A study of laser intensity effects demonstrated departures from

the simple power law predicted by lowest order perturbation theory, which is possibly another indication of pondermotive shifts in the threshold. The absolute MPD rates have been estimated and found to be in fairly good agreement with the results of Floquet theory.
DOE

N92-26603 Northwestern Univ., Evanston, IL.
SQUEEZED LIGHT AND TWIN BEAMS GENERATION WITH A Q-SWITCHED LASER Ph.D. Thesis
Orhan B. Aytur 1991 120 p
Avail: Univ. Microfilms Order No. DA9128945

Quantum noise reduction experiments with a Q-switched laser are described. These experiments involve the generation of squeezed light and quantum correlated twin beams using a traveling-wave optical parametric amplifier. The parametric amplifier is pumped by a Q-switched and mode-locked laser. As a result, the peak parametric gain can be very high, yielding large quantum noise reductions. We generate pulsed twin beams of light exhibiting fluctuations that are correlated by more than 15 dB, and achieving noise performance below the quantum limit by more than 6 dB. The absence of interaction enhancing cavities and the simplicity of direct detection make our approach to twin beams generation particularly attractive for measurements beyond the quantum limit. We also generate pulsed squeezed light, and demonstrate that the spatial and temporal profile of the local oscillator is generated using a second optical parametric amplifier, resulting in a 30 percent increase in detection efficiency. We also demonstrate that a temporally coherent pump source is not necessary to observe quantum optic effects. Quantum noise reduction can still be achieved when the longitudinal modes of the laser are not locked, in which case the resulting squeezed light or twin beams are temporally incoherent. Dissert. Abstr.

N92-26626 Dartmouth Coll., Hanover, NH.
OPERATION OF A SMITH-PURCELL FREE-ELECTRON LASER AT SUBMILLIMETER WAVELENGTHS Ph.D. Thesis
Edwin James Price 1991 154 p
Avail: Univ. Microfilms Order No. DA9130836

Experimental results demonstrating Planar Orotron operation in the submillimeter wavelength regime of 1 cm to 400 microns are presented. This device belongs to the class of Smith-Purcell free-electron lasers that utilize periodic metal grating structures to support electromagnetic waves with phase velocities slower than the speed of light. The J(vector) * E(vector) interaction between this slow wave and a mildly relativistic electron beam (15-130 keV) produces coherent radiation. Dispersion, electronic tuning, single particle gain, and start oscillation current expressions are developed for unique grating geometries that are seen to possess superior high frequency and tuning capabilities. Experimental data taken over a wide spectral range is extensively compared to the theoretical developments and excellent agreement is seen. Comparing the experimentally measured power of the device to a generic power model has resulted in valuable insights into designing device parameters that will optimize short wavelength operation. The experimental observation of multiple modes of laser operation has led to the development of several new models of how the device works, including one that links the TM dispersion formalism with the viewpoint of Smith and Purcell. This viewpoint is significant in that it allows for a statement on the ultimate short wavelength limits of the device to be made. Dissert. Abstr.

N92-26646# Lawrence Livermore National Lab., CA.
APPLICATION OF DECENTRALIZED CONTROL TO A LASER ALIGNMENT SYSTEM
T. W. Long and E. S. Bliss 15 Aug. 1991 16 p Proposed for presentation at the American Control Conference, Chicago, IL, 24-26 Jun. 1992
(Contract W-7405-eng-48)
(DE92-009692; UCRL-JC-108317; CONF-9206137-1) Avail: NTIS HC/MF A03

Light propagating through a large laser system is subject to numerous perturbations which can cause deviations from the desired path. Closed loop alignment controls are typically located at key points to compensate for such errors. We have tested a decentralized approach to the alignment control of such a laser. The decentralized control system has a modular structure in which the control command for each subsystem is a function of only two errors, the error detected by that subsystem's own sensor and the error detected by the sensor in the preceding subsystem. Therefore, although the controller uses local information, the whole alignment system can operate in a coordinated fashion. On the other hand, any design change of a subsystem will cause redesign of only one additional controller, the one for the subsystem immediately downstream. The rest of the system remains unchanged, as we verified in the laboratory by disabling one control loop to simulate a change in the subsystem. The control accuracy of the whole system remained the same after the controller downstream of the disabled loop was modified. This modular approach increases design flexibility and facilitates future expansion of the system. DOE

N92-26663# Interspec, Inc., Ambler, PA.
LARGE COHERENT ARRAYS FOR LASER RADARS, PHASE 1 Final Report
E. H. Attia Nov. 1991 63 p
(Contract N00014-91-C-0150)
(AD-A245528) Avail: NTIS HC/MF A04

A bistatic laser radar with a large-sparse, phased array, receive aperture has been previously proposed for various critical strategic defense applications such as discrimination, target tracking, pointing, and fire control. The same concept could also be applied to the difficult problem of theater missile defense (TMD) using an airborne platform (above any cloud cover). The basic problem is to ensure that the outputs of the receive subapertures are coherently combined in order to obtain the desired phased array performance. The general approach previously taken relaxes the tolerances on the locations of array elements and tries to compensate for the resulting phase errors adaptively, by phase conjugating returns from a 'phase-up' source of opportunity found within the target area. We recognized this procedure as the simplest among the class of 'self-cohering' techniques that Interspec has developed in the past decade for the purpose of obtaining diffraction-limited performance from distorted apertures for radar applications. In this effort, we adapted and applied a powerful self cohering technique to this problem. GRA

N92-26691# Sandia National Labs., Albuquerque, NM.
TRANSIENT GAS MOTION IN NUCLEAR-REACTOR-PUMPED LASERS: COMPUTATIONAL AND EXPERIMENTAL RESULTS
J. R. Torczynski and D. R. Neal 1991 26 p Presented at the American Institute of Astronautics and Aeronautics/American Society of Mechanical Engineers (AIAA/ASME) National Fluid Dynamics Congress, Los Angeles, CA, 15-18 Jun. 1992
(Contract DE-AC04-76DP-00789)
(DE92-002357; SAND-91-1441C; CONF-920605-1) Avail: NTIS HC/MF A03

In some types of nuclear reactor pumped lasers, the fission fragments that are used to excite gaseous lasing species heat the gas in a spatially nonuniform manner. This heating nonuniformity induces transient gas motion, which results in density and refractive index gradients that affect the laser's optical behavior. A model of the transient gas motion is developed using the acoustic filtering methodology, which neglects the spatial variation of the pressure. This model incorporates the effect of spatially varying gas density on fission fragment heating. Gas motion out of the laser cell into small, rapidly cooled regions is treated as a volumetric mass loss distributed over the laser cell. Although these regions have a relatively small fraction of the total volume, a large amount of gas can flow into them during the heating because of the rapid cooling therein. This gas removal from the cell during pumping, neglected in previous analyses, is important because fission fragment heating is strongly dependent on local gas density. To quantify the laser's optical behavior, experiments are performed in which a probe laser beam is passed through the laser cell. This probe beam acquires a wavefront distortion from the refractive index gradients and is imaged onto a wavefront slope sensor, which yields temporally

and spatially resolved measurements of the angular deflection (wavefront slope) of the probe laser beam. Experimental and model results for this quantity exhibit reasonably good agreement over a wide range of pressures and heating amplitudes. DOE

N92-26870*# Old Dominion Univ., Norfolk, VA. Dept. of Mathematics.
COMPARISON OF LASER MODELS Final Report, period ending 15 May 1992
John H. Heinbockel May 1992 47 p
(Grant NAG1-757)
(NASA-CR-190302; NAS 1.26:190302) Avail: NTIS HC/MF A03

The final phase of modeling solar pumped lasers considers the photodissociation of the perfloralkyl molecules n - C3F7I ,t - C4F9I, and i - C3F7I. Computer modeling was compared to laboratory data and good agreement between theory and experiment was achieved. The following is a summary of the modeling of solar pumped lasers. A perfloride gas enters a tube at a point z = 0 and travels a distance L at a velocity, W, and then exits at the point z = L. During the flow, the gas is solar pumped over the initial distance 0 less than or = z less than or = z sub 0, where z sub 0 is less than or equal to L. The perfloride gas interacts chemically with light and a chain of chemical reactions occur. Author

N92-27050# Air Force Systems Command, Wright-Patterson AFB, OH. Foreign Technology Div.
LASER GLITTERING IN THE RELATIVELY STABLE PROPAGATION LAYER NEAR THE SEA SURFACE
Shixiao Le 19 Nov. 1991 7 p Transl. into ENGLISH from Jiguang (China), v. 9, no. 5, 1982 p 107
(AD-A246374; FTD-ID(RS)T-0688-91) Avail: NTIS HC/MF A02

Communication transmission experiments were conducted on the optical path (some points were besides the wharves) and more than 95 pct. of the complete optical path was above water by using 10.6 micron collimated light beams for the experiments for distances of 4, 5, 7.8, 10, and 21 km at heights of 8, 10, 16, 53, and 70 m above the water. It was discovered that laser glittering near the water surface has a relatively weak property; however, the glittering at heights of 53 and 70 m did not exhibit this property. This conclusion puts to rest the doubt that the range of heights lower than 40 m from the sea surface is a forbidden zone for laser transmission, by proving that it is not a forbidden zone. This conclusion is helpful to progress in laser transmission between islands, thus lowering the capital costs, since higher investments are required for constructing communication points on mountain tops or high buildings. Author

N92-27173# Stanford Univ., CA. Dept. of Physics.
LASER COOLING AND TRAPPING OF ATOMS AND PARTICLES Final Report, 1 Sep. 1988 - 31 Aug. 1991
Steven Chu 16 Jan. 1992 7 p
(Grant AF-AFOSR-0349-88)
(AD-A247208; AFOSR-92-0093TR) Avail: NTIS HC/MF A02

The program was to explore the use of light to manipulate atoms and other particles. Particularly, the cooling and trapping of atoms, the manipulation of biological molecules, and the creations of new devices based on these techniques. GRA

N92-27178# Northeast Semiconductor, Inc., Ithaca, NY.
INNOVATIVE TECHNIQUES FOR THE PRODUCTION OF LOW COST 2D LASER DIODE ARRAYS Monthly Report No. 3, 1-29 Feb. 1992
Michael J. Cook 29 Feb. 1992 9 p
(Contract N00014-91-C-0222)
(AD-A247282) Avail: NTIS HC/MF A02

The primary objective of this program is to develop a low cost, high yielding methodology for processing, packaging, and characterization of MBE grown two dimensional high power laser diode arrays. Projected increases in overall yield of aluminum gallium arsenide diode lasers would reduce manufacturing cost from the current $10 to $20 per peak watt to below $3 per peak watt. Emphasis is placed on innovative packaging techniques that will utilize recent advances in diamond heat sinking technology. GRA

37 MECHANICAL ENGINEERING

Includes auxiliary systems (nonpower); machine elements and processes; and mechanical equipment.

N92-26219# Oak Ridge National Lab., TN.
TIME OPTIMAL TRAJECTORIES FOR MOBILE ROBOTS WITH TWO INDEPENDENTLY DRIVEN WHEELS
D. B. Reister and F. G. Pin Mar. 1992 47 p
(Contract DE-AC05-84OR-21400)
(DE92-010002; ORNL/TM-12070; CESAR-92/09) Avail: NTIS HC/MF A03

This paper addresses the problem of time-optional motions for a mobile platform in a planar environment. The platform has two non-steerable independently driven wheels. The overall mission of the robot is expressed in terms of a sequence of via points at which the platform must be at rest in a given configuration (position and orientation). The objective is to plan time-optimal trajectories between these configurations assuming an unobstructed environment. Using Pontryagin's maximum principle (PMP), we formally demonstrate that all time optimal motions of the platform for this problem occur for bang-bang controls on the wheels (at each instant, the acceleration on each wheel is either at its upper or lower limit). The PMP, however, only provides necessary conditions for time optimality. To find the time optimal robot trajectories, we first parameterize the bang-bang trajectories using the switch times on the wheels (the times at which the wheel accelerations change sign). With this parameterization, we can fully search the robot trajectory space and find the switch times that will produce particular paths to a desired final configuration of the platform. We show numerically that robot trajectories with three switch times (two on one wheel, one on the other) can reach any position, while trajectories with four switch times can reach any configuration. By numerical comparison with other trajectories involving similar or greater numbers of switch times, we then identify the sets of time-optimal trajectories. These are uniquely defined using ranges of the parameters, and consist of subsets of trajectories with three switch times for the problem when the final orientation of the robot is not specified, and four switch times when a full final configuration is specified. We conclude with a description of the use of the method for trajectory planning for one of our robots. DOE

N92-26234# Oak Ridge National Lab., TN.
ASSESSMENT OF DIAGNOSTIC METHODS FOR SOLENOID-OPERATED VALVES
R. C. Kryter and W. S. Farmer (Nuclear Regulatory Commission, Washington, DC.) 1992 24 p Presented at the Aging Research Information Conference, Rockville, MD, 24-27 Mar. 1992
(Contract DE-AC05-84OR-21400)
(DE92-009379; CONF-920375-3) Avail: NTIS HC/MF A03

Solenoid-operated valves (SOV's) were studied at Oak Ridge National Laboratory as part of the USNRC Nuclear Plant Aging Research (NPAR) Program. The primary objective of the study was to identify, evaluate, and recommend methods for inspection, surveillance, monitoring, and maintenance of SOV's that can help ensure their operational readiness - that is, their ability to perform required safety functions under all anticipated operating conditions, since failure of one of these small and relatively inexpensive devices could have serious consequences under certain circumstances. Intrusive techniques requiring the addition of magnetic or acoustic sensors or the application of special test signals were investigated briefly, but major emphasis was placed on the examination of condition-indicating techniques that can be applied with minimal cost and impact on plant operation. These include monitoring coil mean temperature remotely by means of coil dc resistance or ac impedance, determining valve plunger position by means of coil ac impedance, verifying unrestricted SOV plunger movement by

measuring current and voltage at their critical bistable (pull-in and drop-out) values, and detecting the presence of shorted turns or insulation breakdown within the solenoid coil using interrupted-current test methods. Experimental results are presented that demonstrate the technical feasibility and practicality of the monitoring techniques assessed in the study, and recommendations for further work are provided. DOE

N92-26284# Polish Academy of Sciences, Warsaw. Inst. Podstawowych Problemow Techniki.

ON CERTAIN METHODS OF DETERMINING THE ELLIPSES AN D ELLIPSOIDS OF THE POSITIONING ACCURACY OF ROBOT MANIPULATORS

Wojciech Szczepinski and Zbigniew Wesolowski May 1992 25 p Sponsored by the Polish Committee of Scientific Research (ISSN-0208-5658) Avail: NTIS HC/MF A03

It is important to know the size of the random deviations of the hand, end effector, from the desired position when you analyze the positioning accuracy of robot manipulators. We propose two methods of determining the ellipses and ellipsoids of the probability concentration. One method consists of determining the polygon or polyhedron of the positioning accuracy, and then finding the ellipse or ellipsoid of the principal axes and the second order moments that coincide with those of the polygon or polyhedron respectively. In the second method, a computer generates random Gaussian deviations from the desired joint positions. The calculated positioning errors form elliptical or ellipsoidal patterns that demonstrate good agreement with the theoretically obtained ellipses or ellipsoids of the probability concentration. Author

N92-26366# National Inst. of Standards and Technology, Gaithersburg, MD. Ceramics Div.

CERAMIC BEARING TECHNOLOGY: PROCEEDINGS OF THE NIST/DARPA WORKSHOP Final Report

S. Jahanmir Nov. 1991 222 p

(PB92-137553; NIST/SP-824) Avail: NTIS HC/MF A10; also available SOD $12.00 as 003-003-03131-3

The objectives of the workshop were to assess the status of ceramic bearing technology, and identify the key research topics needed to expand the range of applications for ceramic bearings. A total of eleven invited presentations were given at the workshop which was attended by 75 representatives from industry, government, and universities. The presentations and subsequent discussions covered present and potential future applications of ceramic bearings, and topics related to processing, machining, quality control design, testing, and performance evaluation. The report includes short abstracts and the viewgraphs used in the presentations, summary of the discussions, and a list of future recommendations for research. GRA

N92-26371# Princeton Univ., NJ. Dept. of Mechanical and Aerospace Engineering.

THROTTLELESS OTTO-CYCLE NATURAL GAS ENGINES Final Report, 1 Jun. 1988 - 31 Jan. 1991

M. Shoda, P. D. Ronney, and E. J. Durbin Jan. 1992 113 p

(Contract GRI-5088-260-1671)

(PB92-164482; GRI-90/0246) Avail: NTIS HC/MF A06

The results are presented of exploratory research on establishing the feasibility of using preheated intake air for power and torque control in place of conventional throttling. The Throttleless Otto Cycle Natural Gas Engine (TONE) concept was proposed as a way to make vehicular use of natural gas fueled engines more competitive. It was shown that it is possible to increase operating efficiency, and therefore fuel efficiency and range using the TONE concept. In addition, and perhaps more importantly, TONE operation is accompanied by a substantial reduction in NOx emissions. This result was not predicted, and makes the TONE concept attractive beyond the potential for increased operating efficiency. Author

N92-26389# Mississippi Univ., University. Physical Acoustics Research Lab.

THEORETICAL AND EXPERIMENTAL STUDY OF THERMOACOUSTIC ENGINES Annual Report, 1 Jan. - 31 Dec. 1991

Richard Rapset, Henry E. Bass, and W. P. Arnott 31 Dec. 1991 65 p

(Contract N00014-89-J-3087)

(AD-A246334; PARGUM-91-08) Avail: NTIS HC/MF A04

Thermoacoustic engines can be used to pump heat using a sound wave (refrigerator or heat pump) or pump a sound wave using a temperature gradient (prime mover). The basic arrangement is a gas-filled acoustic resonator with appropriately positioned thermoacoustic elements. Two types of thermoacoustic elements are used in these engines. The first type are heat exchanges which are used to communicate heat between the gas and external heat reservoirs. The second type is the thermoacoustic engine (TAE), also known as a stack. The TAE's are sections of porous media that support the temperature gradient, the transport heat on the acoustic wave between the exchangers, and that produces or absorbs acoustic power. Previous theoretical results in thermoacoustics have been developed for TAE's with circular or parallel slit pore geometries. We have developed a general linear formulation for gas-filled TAE's having pores of arbitrary cross-sectional geometry. This analysis, which is very helpful in designing optimal engines, indicates the parallel slit pore geometry optimizes heat and work flow. GRA

N92-26475 Illinois Univ., Chicago.

ADAPTIVE CONTROL OF ROBOTIC MANIPULATORS WITH STRUCTURAL FLEXIBILITY Ph.D. Thesis

Sijun Wu 1991 140 p

Avail: Univ. Microfilms Order No. DA9132318

The control problem of mechanically flexible systems was an important issue for the past decade due mainly to the growing needs for fast, precise manipulators in industry and space applications. In this thesis, stable, high precision, and high-bandwidth closed-loop tip position control of a one-link flexible robot was investigated. Two adaptive control methods are developed and studied. A non-dimensionalized dynamic model for the flexible robot arm is developed. Payload mass and moment of inertia are also considered in the modeling. It can be shown that with a set of strain gauge measurements, the payload mass and moment of inertia could be estimated. This provides a convenient tool to detect the variations of the payload, which is crucial for precision control. The lattice filter used in the tip position control of a flexible arm proves to be a good parameter identifier in the on-line identification of the robot due to its high convergence rate and noise rejection capability. Although the lattice filter is usualy designed for auto-regressive or moving-average processes, its applications are extended to include auto-regressive and moving-average processes. The proposed model reference adaptive inverse controller is in the form of a series type of model reference system. It differs from other model reference controller in that the forward controller is the identified systems inverse. Moreover, an additional control signal is applied which comes from a signal synthesis block to compensate the output tracking and parameter identification errors. Compared with other control techniques such as stable factorization and linear quadratic Gaussian, the predictive adaptive controller could provide faster control with reasonably low input energy level. Dissert. Abstr.

N92-26518# Federal Railroad Administration, Washington, DC.

NATIONAL MAGLEV INITIATIVE. MOVING AMERICA: NEW DIRECTIONS, NEW OPPORTUNITIES Annual Report, Nov. 1991

1991 44 p Prepared in cooperation with Corps of Engineers, Washington, DC; and DOE, Washington, DC

(PB92-163237) Avail: NTIS HC/MF A03

Activities carried out since the National Maglev Initiative (NMI) inception are summarized. The NMI is a cooperative effort of the Federal Railroad Administration (FRA) of the U.S. Dept. of Transportation, the U.S. Army Corps of Engineers (USACE), and

the Dept. of Energy (DOE), with support from other Federal agencies. This interagency partnership is conducting studies to evaluate the potential for magnetically levitated high speed ground transportation (maglev) systems in the U.S., to complement existing transportation systems and help meet transportation demand with an environmentally sound alternative, independent of petroleum based fuels. A major purpose of these studies is to address the opportunities for the U.S. to be a supplier of maglev rather than simply a customer of internationally developed maglev systems.
Author

N92-26555*# National Aeronautics and Space Administration. Lewis Research Center, Cleveland, OH.
GEAR TOOTH STRESS MEASUREMENTS OF TWO HELICOPTER PLANETARY STAGES
Timothy L. Krantz 1992 10 p Proposed for presentation at the Sixth International Power Transmission and Gearing Conference, Phoeniz, AZ, 13-16 Sep. 1992; sponsored by ASME
(RTOP 505-63-36; DA Proj. 1L1-62211-A-47-A)
(NASA-TM-105651; E-7015; NAS 1.15:105651;
AVSCOM-TR-91-C-038) Avail: NTIS HC/MF A02

Two versions of the planetary reduction stages from U.S. Army OH-58 helicopter main rotor transmissions were tested at NASA Lewis. One sequential and one nonsequential planetary were tested. Sun gear and ring gear teeth strains were measured, and stresses were calculated from the strains. The alternating stress at the fillet of both the loaded and unloaded sides of the teeth and at the root of the sun gear teeth are reported. Typical stress variations as the gear tooth moves through mesh are illustrated. At the tooth root location of the thin rimmed sun gear, a significant stress was produced by a phenomenon other than the passing of a planet gear. The load variation among the planets was studied. Each planet produced its own distinctive load distribution on the ring and sun gears. The load variation was less for a three planet, nonsequential design as compared to that of a four planet, sequential design. The reported results enhance the data base for gear stress levels and provide data for the validation of analytical methods.
Author

N92-26560*# National Aeronautics and Space Administration. Lewis Research Center, Cleveland, OH.
FULL-SCALE TRANSMISSION TESTING TO EVALUATE ADVANCED LUBRICANTS
David G. Lewicki, Harry J. Decker, and John T. Shimski (Naval Air Propulsion Test Center, Trenton, NJ.) 1992 9 p Proposed for presentation at the Sixth International Power Transmission and Gearing Conference, Phoenix, AZ, 13-16 Sep. 1992; sponsored by ASME
(RTOP 505-63-36; DA Proj. 1L1-62211-A-47-A)
(NASA-TM-105668; E-7032; NAS 1.15:105668;
AVSCOM-TR-91-C-035) Avail: NTIS HC/MF A02

Experimental tests were performed on the OH-58A helicopter main rotor transmission in the NASA Lewis 500 hp helicopter transmission test stand. The testing was part of a lubrication program. The objectives are to develop and show a separate lubricant for gearboxes with improved performance in life and load carrying capacity. The goal was to develop a testing procedure to fail certain transmission components using a MIL-L-23699 based reference oil and then to run identical tests with improved lubricants and show improved performance. The tests were directed at parts that failed due to marginal lubrication from Navy field experience. These failures included mast shaft bearing micropitting, sun gear and planet bearing fatigue, and spiral bevel gear scoring. A variety of tests were performed and over 900 hrs of total run time accumulated for these tests. Some success was achieved in developing a testing procedure to produce sun gear and planet bearing fatigue failures. Only marginal success was achieved in producing mast shaft bearing micropitting and spiral bevel gear scoring.
Author

N92-26731 Stanford Univ., CA.
EXPERIMENTS IN MODELLING AND END-POINT CONTROL OF TWO-LINK FLEXIBLE MANIPULATORS Ph.D. Thesis
Celia Marie Oakley 1991 366 p
Avail: Univ. Microfilms Order No. DA9205695

Current space manipulators employ control schemes that are severely limited by structural rigidity requirements. As a result, tasks are executed slowly and tediously. The goal of this research is to increase the performance of flexible manipulators by developing modeling techniques and control strategies that overcome these limitations. Toward this goal, nonlinear equations of motion for two-link structurally-flexible manipulators were developed using the assumed-modes method. A novel approach for representing the link deflections, called the System Modes Representation, was developed, to fully realize the advantages of the assumed-modes method. It produced an accurate, low-order model. Accuracy gained with this modeling technique improved controller performance. The manipulator model was used to design a variety of controllers - two are fully contrasted. The baseline controller is a conventional proportional-plus integral-plus derivative (PID) joint controller based on joint angle and joint rate measurements. The performance of this type of control is severely limited because the sensors are located coincident with the actuators. Direct measurement of the manipulator end point can be used to overcome the limitations of joint control. End-point measurements were integrated into a controller design based on linear-quadratic Gaussian (LQG) theory. The end-point controller improved, in some cases by an order of magnitude, the trajectory tracking and disturbance rejection capabilities of the baseline controller. An experimental two-link flexible manipulator, supported by air cushions on a smooth horizontal surface, was designed and constructed to verify and refine the modeling and control strategies.
Dissert. Abstr.

N92-26750# Oak Ridge National Lab., TN.
USING MIN-MAX OF TORQUE TO RESOLVE REDUNDANCY FOR A MOBILE MANIPULATOR
D. B. Reister 1991 32 p Presented at the IEEE International Conference on Robotics and Automation, Nice, France, 10-15 May 1992
(Contract DE-AC05-84OR-21400)
(DE92-000070; CONF-920540-5) Avail: NTIS HC/MF A03

We have considered the problem of determining the time trajectories of the joint variables of a mobile manipulator with many redundant degrees of freedom that will minimize the maximum value of the torque during a large scale motion by the manipulator. Conventional search techniques slowly solve min-max problems. Based on well known results from the Tchebycheff approximation of functions, we conjecture that at the min-max the magnitude of the normalized torques will be equal at all of the joints. It is an easier problem to find the values of the joint variables that equalize the torques than to perform a large set of slow searches. Furthermore, paths that equate the torques are likely to be continuous in joint space. We have explored paths that equalize the magnitude of the normalized torques for a three link planar manipulator on a platform and for the seven degree of freedom CESARm on a three degree of freedom platform. For the planar arm, we find many analytical solutions that minimize the torque in various regions of the workspace. For the CESARm, the most attractive solution covers a wide range of the workspace and has only one discontinuity in a joint variable. We have found paths that can bridge the discontinuity at a small penalty of increased torque. Paths that equate the torques are attractive candidates for large scale motion by a mobile manipulator.
DOE

N92-26816# John Deere Technologies International, Inc., Wood-Ridge, NJ. Rotary Engine Div.
DEVELOPMENT OF NATURAL GAS ROTARY ENGINES Final Report, Jun. 1986 - Jun. 1991
J. R. Mack Aug. 1991 50 p
(Contract GRI-5086-233-1262)
(PB92-149665; GRI-91/0290) Avail: NTIS HC/MF A03

Development of natural gas-fueled rotary engines was pursued on the parallel paths of converted Mazda automotive engines and of establishing technology and demonstration of a test model of

a larger John Deer Technologies Incorporated (JDTI) rotary engine with power capability of 250 HP per power section for future production of multi-rotor engines with power ratings 250, 500, and 1000 HP and upward. Mazda engines were converted to natural gas and were characterized by a laboratory which was followed by nearly 12,000 hours of testing in three different field installations. To develop technology for the larger JDTI engine, laboratory and engine materials testing was accomplished. Extensive combustion analysis computer codes were modified, verified, and utilized to predict engine performance, to guide parameters for actual engine design, and to identify further improvements. A single rotor test engine of 5.8 liter displacement was designed for natural gas operation based on the JDTI 580 engine series. This engine was built and tested. It ran well and essentially achieved predicted performance. Lean combustion and low NOW emission were demonstrated. Author

N92-26987# European Space Agency. European Space Research and Technology Center, ESTEC, Noordwijk (Netherlands).
CPA: A CONTROLLED PUMP ASSEMBLY FOR TWO-PHASE LOOPS APPLICATIONS
M. N. DeParolis and Peter Reusser (Reusser, Peter U. A.G., Zurich, Switzerland) *In its* 4th European Symposium on Space Environmental Control Systems, Volume 2 Dec. 1991 p 863-871 (For primary document see N92-26950 17-54)
Avail: NTIS HC/MF A23; ESA, EPD, ESTEC, Noordwijk, Netherlands, HC 150 Dutch guilders (2 vols)

N92-27114*# Boeing Co., Seattle, WA. Defense and Space Group.
LDEF MECHANICAL SYSTEMS
W. Steve Spear and Harry W. Dursch *In* NASA. Langley Research Center, LDEF: 69 Months in Space. First Post-Retrieval Symposium, Part 3 Jan. 1992 p 1549-1564 (For primary document see N92-27083 17-99)
(Contract NAS1-18224)
Avail: NTIS HC/MF A21; 1 functional color page

38 QUALITY ASSURANCE AND RELIABILITY

Includes product sampling procedures and techniques; and quality control.

N92-26602 Arizona Univ., Tucson.
MIXED WEIBULL DISTRIBUTIONS IN RELIABILITY ENGINEERING: STATISTICAL MODELS FOR THE LIFETIME OF UNITS WITH MULTIPLE MODES OF FAILURE Ph.D. Thesis
Siyuan Jiang 1991 234 p
Avail: Univ. Microfilms Order No. DA9125459

The finite mixed Weibull distribution is an appropriate distribution in modeling the lifetime of the units having more than one possible failure cause. Through a change of variable, 5 parameters in a two Weibull mixture can be reduced to 3. A parameter vector (P sub 1, eta, beta) defines a family of two-Weibull mixtures which have common characteristics. Numerous probability plots are investigated on Weibull probability paper (WPP). For a given P sub 1, the eta-beta plane is partitioned into seven regions which are labeled by A through F and S. The region S represents the two Weibull mixtures whose cumulative distribution functions (CDF) curves are very close to a straight line. The regions A through F represent six typical shapes of the CDF curves on WPP, respectively. The two-Weibull mixtures in one region have similar characteristics. Three important features of the two-Weibull mixture with well separated subpopulations are proved. Two existing methods for the graphical estimation of the parameters are discussed. The expectation-maximization (EM) algorithm is successfully applied to solve the maximum likelihood estimation (MLE) for mixed Weibull distributions when m, the number of subpopulations in a mixture is known. Extensive Monte Carlo simulations are performed. The distributions of the MLE of the parameters and of the reliability of a two Weibull mixture are studied. The MLE's of the parameters are sensitive to the degree of separation of the two subpopulation probability density functions (PDF's), but the MLE of the reliability is not. The generalized likelihood ratio (GLR) test is used to determine m. A FORTRAN computer program is developed to conduct simulation of the GLR test for less than or = m sub 0 less than m sub 1 less than or = 5. Dissert. Abstr.

N92-27038# Rolls-Royce Ltd., Derby (England). Control Systems Dept.
USE OF MARKOV METHODS IN ANALYSIS OF FAULT-TOLERANT SYSTEMS WITH FLEXIBLE REPAIR POLICIES
Paul White 1 Jun. 1990 5 p
(PNR-90801; ETN-92-90774) Copyright Avail: NTIS HC/MF A01

Some of the problems that have arisen in the application of traditional reliability methods to fault tolerant systems, particularly with the widely used fault tree approach are considered. The application of the Markov state flow equation to reliability analysis is considered and it is shown how many of the aforementioned problems disappear with this approach and how the basic equation can be manipulated to include repair policies, discrete events, and to calculate system reliability. Then the issues are taken on to the next step by considering how to set up a reliability model from system design information in such a way as to ensure the Markov states and transitions are correct and so as to ensure that the reliability analysis gives an upper bound for system failure. The concept of formulation of design information and automatic generation of a reliability model for any given system is explained and an example analysis given based on a typical jet engine control system. The advantages of the Markov method are examined, and the problems that still remain are considered together with how they are overcome with the Reliability Model Generation (RMG) method. ESA

39 STRUCTURAL MECHANICS

Includes structural element design and weight analysis; fatigue; and thermal stress.

For applications see *05 Aircraft Design, Testing and Performance* and *18 Spacecraft Design, Testing and Performance.*

N92-26259# Technische Univ., Delft (Netherlands).
COMPUTATIONAL MODELLING OF RUBBERLIKE MATERIALS Ph.D. Thesis
Petrus Antonius Joha vandenBogert 1991 158 p Sponsored by Rijkswaterstaat
(ETN-92-91304) Avail: NTIS HC/MF A08

The simulation of rubberlike material behavior on a finite element environment is studied with the focus on validation with respect to shear and compression shear experiments. Essential kinematic and static relations from continuum mechanics are adapted to account for large strains, and displacements are summarized. Strain-energy formulations for hyperelastic and rubberlike materials are categorized. The finite element implementation of nearly incompressible hyperelastic material descriptions is addressed. The necessity of comparing the strain-energy formulation with the experimental evidence on the solid rubber specimen is put forward. Experimental findings of solid rubber specimen loaded in nonhomogeneous shear and compression are presented. Examples that demonstrate the applicability of the numerical tools to analyze components made of rubberlike materials are given. ESA

N92-26282# Army Armament Research, Development and Engineering Center, Watervliet, NY.
CRACK ARREST AND STATIC FRACTURE TOUGHNESS TESTS OF A SHIP PLATE STEEL Final Report
J. H. Underwood, I. A. Burch, and J. C. Ritter Dec. 1991 32 p
(AD-A245641; ARCCB-TR-91035) Avail: NTIS HC/MF A03

The recently standardized ASTM crack arrest fracture toughness test method was modified for use with an Australian low alloy, 700 MPa strength, quenched and tempered steel used for ship plate. Specimens 50-mm thick in longitudinal and transverse orientations were tested at -60 C with various depths of side groove. Specimen configurations somewhat outside the range of the ASTM method were found to be useful for this steel and were suggested as modifications to the standard method. A different solution and expression for the stress intensity factor was used to evaluate the tests and to develop a method for predicting the crack length at which a running crack will arrest. Good agreement was obtained between the observed and predicted crack lengths at arrest. The wedge-loading arrangement of the crack arrest test procedure was used for static fracture toughness tests. Procedures for static wedge-loading fracture toughness were proposed for use, particularly for comparisons with crack arrest toughness test results obtained under similar test conditions. The static fracture toughness was more than twice the value of crack arrest toughness. GRA

N92-26537*# National Aeronautics and Space Administration. Langley Research Center, Hampton, VA.
IDENTIFICATION OF LINEAR SYSTEMS BY AN ASYMPTOTICALLY STABLE OBSERVER
Minh Q. Phan, Lucas G. Horta, Jer-Nan Juang, and Richard W. Longman (Columbia Univ., New York, NY.) Jun. 1992 69 p
(RTOP 590-14-61-01)
(NASA-TP-3164; L-16940; NAS 1.60:3164) Avail: NTIS HC/MF A04

A formulation is presented for the identification of a linear multivariable system from single or multiple sets of input-output data. The system input-output relationship is expressed in terms of an observer, which is made asymptotically stable by an embedded eigenvalue assignment procedure. The prescribed eigenvalues for the observer may be real, complex, mixed real and complex, or zero. In this formulation, the Markov parameters of the observer are identified from input-output data. The Markov parameters of the actual system are then recovered from those of the observer and used to obtain a state space model of the system by standard realization techniques. The basic mathematical formulation is derived, and extensive numerical examples using simulated noise-free data are presented to illustrate the proposed method. Author

N92-26557 Notre Dame Univ., IN.
ON THE STOCHASTIC FATIGUE CRACK GROWTH PROBLEM Ph.D. Thesis
Thomas Joseph Enneking 1991 142 p
Avail: Univ. Microfilms Order No. DA9206061

The research focuses on continuous and discrete stochastic models for fatigue crack growth which are based on Markov process theory. These models account for the random nature of fatigue crack growth which is not adequately explained by a deterministic approach. A hybrid finite element/finite difference solution methodology is developed and shown to be highly effective in determining the solution of the backward Kolmogorov equation and the Pontryagin-Vitt equation yielding the probabilistic description of the time to reach a critical crack size as a function of the initial crack size. Excellent comparisons are shown between this method, previous analytical studies, and experimental results. A significant reduction in computer processing time and storage is achieved with this approach. Alternatively, the forward Fokker-Planck-Kolmogorov equation is formulated, and a two-dimensional initial boundary value problem developed, to determine the distribution of crack sizes as a function of time. A two-dimensional finite element solution approach is used for problem solution. A major advantage of this problem formulation is that the entire probability density function is obtained as a function of cycle number. Studies of discrete Markov process models are also considered for the characterization of fatigue crack growth. A cell-to-cell mapping approach, which has been effectively utilized for other two-state problems in stochastic dynamics, is developed for the stochastic fatigue crack growth problem. In this approach the transitional probability matrix for crack transition from cell i to any other cell is determined using simulation with a two-state lognormal random process model. Repeated matrix multiplication is then used to determine the distribution of crack lengths at other times for a given initial flow size distribution. The effect of varying the initial fatigue quality may be evaluated without repeating the simulation of the probability transition matrix. Modifications are considered for improved solution performance. Lastly, a random load model for stochastic fatigue crack growth is presented and a boundary value problem formulated for the determination of the random time for a crack to grow to a critical length. Dissert. Abstr.

N92-26593# Naval Postgraduate School, Monterey, CA.
DIMENSIONAL ANALYSIS OF STRUCTURAL STEEL BEAM DESIGN M.S. Thesis
Michael A. Elizondo Mar. 1991 56 p
(AD-A245759) Avail: NTIS HC/MF A04

This thesis examines the representation of dimensional units as prime numbers to perform dimensional analysis within a computer-based model management system. A computer program applies this concept to simple span structural steel beam design, an engineering stress and strain problem. Most common applications of computers manipulate only the numeric value of the measure of physical objects. The user manually ensures that data is processed according to the meaning of its units. Prime-encoding of dimensional units in this application provides a numeric method of validating dimensional consistency in mathematical expressions for use on a computer. This study is implemented in TEFA, a computer-based modeling system with an embedded Prolog programming language. The beam design application demonstrates that model representation using prime-encoding of dimensional units simplifies the overhead required in data manipulation, and helps maintain meaningful results in the numerical processing of data. GRA

N92-26594 Minnesota Univ., Minneapolis.
COMPUTATIONAL ASPECTS OF AN IMPLICIT FINITE ELEMENT PROCEDURE FOR ELASTO-VISCOPLASTIC LARGE DEFORMATION PROBLEMS Ph.D. Thesis
Abul Fazal Muhammad Arif 1991 138 p
Avail: Univ. Microfilms Order No. DA9202795

The details of formulation, numerical implementation, and evaluation of an implicit finite element procedure for nonlinear problems involving large deformation and/or large rotations is presented. A two parameter family of incrementally objective integration schemes is proposed for the analysis of a hypoelastic model with a broad range of unified rate-dependent viscoplastic constitutive models in large deformation problems. These algorithms are a generalization of the mid-point integration rule. An important step in the solution of nonlinear deformation problems using a Newton-Raphson type of iterative scheme is the calculation of a tangent operator (the so-called Jacobian) by linearizing the involved field equations. Full linearization of the virtual work equation is performed in an updated Lagrangian framework together with a calculation of the consistent linearized material moduli. In general, the reference configuration is updated after each iteration to coincide instantaneously with the present guess of the unknown equilibrium configuration. Another approach is to use the previous equilibrium state as the reference configuration until the new equilibrium configuration at the end of the time step is found. The performance of the family of incrementally objective integration schemes and the two different Jacobians is explored with emphasis on their accuracy and convergence characteristics when large incremental steps are used. Some details of the finite element implementation are given for plane strain and axisymmetric problems and results for several numerical test and practical examples are presented and discussed. Finally, the above computational procedure is extended to problems where the theory of exact kinematics is considered and the hyperelastic approximation is used. Dissert. Abstr.

N92-26598 Virginia Polytechnic Inst. and State Univ., Blacksburg.
RELIABILITY AND FAILURE ANALYSES OF COMPOSITE BEAMS AND PLATES CONTAINING STRESS CONCENTRATIONS Ph.D. Thesis
Incheol Yeo 1991 229 p
Avail: Univ. Microfilms Order No. DA9204654

Size effects in brittle composite structures such as beams and plates with and without stress raisers are investigated experimentally and analytically. For stress analysis of isotropic beams under four-point bending and composite plates under in-plane loading, a finite element analysis program F2DELAST based on 2-D elasticity theory was developed and verified. For composite beams under four-point bending, ABAQUS is used. For stress and failure analysis of laminated composite plates under transverse loading, a nonlinear finite element analysis program FNCOMPLT which accounts for the geometrical nonlinearity in von Karman sense and transverse shear deformation was developed. Both the finite element programs written by the author and the ABAQUS were used for stress analysis. For post-processing purposes, PATRAN and I-DEAS are used. Linear and nonlinear stress analyses were performed for the case of composite plates under transverse loading. A methodology for reliability analysis is developed for composite beams and plates with and without stress concentration under various loading conditions and various finite element reliability analysis programs were written. The materials used for the analysis are mainly carbon-carbon composites, however graphite-epoxy composites are also used. The Weibull model was extended to account for the 3-D stress field including interlaminar stresses. The effect of interlaminar stresses on the total reliability is investigated. Various failure theories for composite materials are reviewed.
Dissert. Abstr.

N92-26669*# National Aeronautics and Space Administration. Marshall Space Flight Center, Huntsville, AL.
EFFECT OF TYPE OF LOAD ON STRESS ANALYSIS OF THIN-WALLED DUCTS
J. B. Min and P. K. Aggarwal Jun. 1992 18 p
(NASA-TP-3248; M-688; NAS 1.60:3248) Avail: NTIS HC/MF A03

The standard procedure for qualifying the design of duct (pipe) systems in the Space Shuttle Main Engine (SSME) has been fairly well defined. However, since pipe elbows are quite common and important in the SSME duct systems, a clear understanding of the detailed stress profile of the components is necessary for accurate structural and life assessments. This study was initiated to predict the stress profile at/near the tangent point along the cross section of the duct under various types of loads. Also, this study was further extended to understand the stiffening effect on stresses due to pressure at the tangent point. The intention of this study was to identify the importance of selecting proper locations for mounting strain gauges and to utilize the obtained results to anchor dynamic models for accurate structural and life assessments of the SSME ducts under a dynamic environment. The finite element method was utilized in this study. Author

N92-26694# Westinghouse Hanford Co., Richland, WA.
AN INVESTIGATION OF THE BEHAVIOR OF THE CLAMP-INDUCED BENDING STRESSES
S. N. Huang Dec. 1991 23 p Presented at the American Society of Mechanical Engineers Pressure Vessel and Piping Conference, New Orleans, LA, 21-25 Jun. 1992
(Contract DE-AC06-87RL-10930)
(DE92-006504; WHC-SA-1375; CONF-920631-6) Avail: NTIS HC/MF A03

The Fast Flux Test Facility is a demonstration and test facility for the sodium cooled fast breeder reactor. Insulated pipe clamps are used in the heat transport and safety related systems. This investigation determines whether the clamp induced pipe stresses should be classified as primary or secondary stresses. Three finite element models were developed using the ANSYS computer program. Inelastic analyses were performed to investigate the behavior of meridional bending stress and hoop bending stress. The double exponential creep law of 316 stainless steel was used in the creep analysis. Results indicate that pipe bending stresses do not completely relax with time. Therefore, a portion of the meridional bending stress and the hoop bending stress should be classified as primary stress. DOE

N92-26739 Wisconsin Univ., Madison.
ASYMPTOTIC ANALYSIS OF THE VIBRATIONS OF VARIABLE LENGTH CANTILEVER BEAMS Ph.D. Thesis
Mahmoud Aly Younis 1991 147 p
Avail: Univ. Microfilms Order No. DA9134351

We investigate the behavior of a uniform cantilever beam with a small mass at its tip. The beam can move out of a rigid body; thus, its span varies with time. The body can have no motion or can be spinning; both simulations are considered. The reasons for such investigations are: (1) it is the subject of current interest in connection with the recent developments in the space and robotics fields; and (2) to study the behavior analytically because very few analytical solutions are available. The interest here is in the linear vibratory motions of the beam with the objective of developing approximate asymptotic expressions for the beam displacements. A formulation of the problem is made which accounts for the time mass. Two ways to eject the beam out of the system are considered: root force ejection and time dependent acceleration field ejection. The assumed modes method is adopted to derive the corresponding modal equations that describe the in-plane lateral deflections of the beam. The case when there is no tip mass is also included. Approximate asymptotic expressions for the beam displacement are presented for three types of length variations: uniform, exponential, and a linear variation of the square of the length. In the course of the analysis, the system is allowed to spin about an axis normal to the ejection direction, and modal equations governing vibrations in and out of the plane of rotation are derived. Approximate expressions for the beam displacement are presented in the absence of the tip mass for the three length variations mentioned previously. An approximate solution for the beam loaded by a tip mass is presented only for uniform length variations. The results from the investigation are discussed.
Dissert. Abstr.

N92-26759# Naval Postgraduate School, Monterey, CA.
WEIGHT OPTIMUM ARCH STRUCTURES M.S. Thesis
Margaret A. Menzies Dec. 1991 195 p
(AD-A246001) Avail: NTIS HC/MF A09

This investigation is concerned with the optimization of arch structures. The DOT optimization code is used to minimize the volume of arch structures which are constrained by limits on stress, design geometry, and section dimensions. Modeling the arch structure by a series of barbeam elements, the finite element method is used to compute element stresses. The DOT optimization code selects section dimensions to prevent failure due to element stresses exceeding the material yield stress. Specifically, through coordinate transformations between local element coordinates and global system coordinates, the element stiffness matrices transform into the global stiffness matrix. The resulting system matrix equations are then solved for the system degrees of freedom, that is, displacements and slopes. The system degrees of freedom, in turn, are transformed back to the element level to compute the internal forces and moments and hence, the stresses. Results are presented for a number of cases with regard to optimization scheme and stress analysis. GRA

N92-26784# Oak Ridge National Lab., TN.
STUDY AND ANALYSIS OF THE STRESS STATE IN A CERAMIC, BUTTON-HEAD, TENSILE SPECIMEN
M. G. Jenkins, M. K. Ferber, R. L. Martin, V. T. Jenkins, and V. J. Tennery Sep. 1991 97 p
(Contract DE-AC05-84OR-21400)
(DE92-007794; ORNL/TM-11767) Avail: NTIS HC/MF A05

The final results are reported for a study to identify and correct the causes of nongage-section failures (notably button-head failures) in ceramic tensile specimens observed in several

laboratories. Numerical modeling of several candidate specimen gripping systems has shown inherent stress concentrations near the specimen button head at which the maximum stress may approach 75 to 100 percent of the gage-section stress for certain grip conditions. Empirical comparisons of both tapered- and straight-collet gripping systems revealed compromises in both systems. The straight-collet system, with deformable collets, is simpler to use but produces statistically significant greater average percent bending for all tests than those produced for the tapered-collet system, which is slightly more difficult to use. Empirical tensile tests of approximately 50 aluminum oxide and approximately 50 silicon nitride specimens were conducted to evaluate the loading capability of both gripping systems, the percent bending in each system, and the potential of consistently producing successful test results. These tests revealed that, due to variations in individuals specimens or the individual specimen/grip interfaces, neither of the gripping systems can consistently produce bending of less than 3 to 4 percent at failure although occasional values of approximately 0.5 percent bending were attained. Refinements of grinding procedures and dimensional measurement techniques have shown critical details in both the practices and consistency of machining necessary for achieving the dimensional tolerances while minimizing subsurface damage. Numerical integration techniques indicate that up to a consistent 5.0 percent bending during fast-fracture tests can be tolerated before large influences are detected in the determination of the Weibull modulus and the Weibull characteristic strength. DOE

N92-26829 Virginia Polytechnic Inst. and State Univ., Blacksburg.
MODELING CYCLE AND TIME-DEPENDENT CREEP/RELAXATION EFFECTS ON FATIGUE LIVES OF NOTCHED MEMBERS Ph.D. Thesis
DeRome Osmond Dunn 1991 257 p
Avail: Univ. Microfilms Order No. DA9208419

Mechanical cyclic variations in mean stress and strain amplitude is a well-known occurrence for metals even at room temperature. Many fatigue analysis procedures ignore these variations. Fatigue analysis which included both time and cycle dependent mechanical material behavior for metals at room temperature had not been previously studied except for the case of creep. An investigation studying transient mechanical effects on Ti-6Al-4V titanium and 7475-T651 Al alloys was done to determine how great an effect transients at room temperature would have on fatigue life under cyclic conditions. The mechanical material response was modeled using viscoplasticity constitutive laws and Neuber's rule eliminating the need for finite element modeling of uniaxially loaded notched members. However, the Neuber's modeling may be used with any material constitutive law. The procedures for fatigue damage used cycle counting to compute strain amplitude and mean stress. Since a large amount of fatigue data is reported as strain-life curves, the fatigue analysis was developed using this fatigue data although it did not include transients. If favorable results are obtained, development of modeling and testing to include transients in strain-life fatigue data could be avoided, and the existing fatigue data base utilized. Experimental work was undertaken and nonlinear optimization techniques used to compute model constants for the two alloys. However, small amounts of rate dependence were found for cyclic strain control testing. The viscoplasticity models became stiff when rate dependence was low causing numerical problems, and model constants for the viscoplastic constitutive law could not be determined since convergence was not achieved. Also, only small amounts of transient static stress relaxation was observed for extended hold periods. Dissert. Abstr.

N92-26845# Oak Ridge National Lab., TN.
PREDICTABILITY OF LONG-TERM CREEP AND RUPTURE IN A NOZZLE-TO-SPHERE VESSEL MODEL
J. M. Corum and R. L. Battiste 1992 23 p Presented at the American Society of Mechanical Engineers Pressure Vessel and Piping Conference, New Orleans, LA, 21-25 Jun. 1992
(Contract DE-AC05-84OR-21400)
(DE92-008099; CONF-920631-8) Avail: NTIS HC/MF A03

The results of a long-term, high-temperature, failure test of a pressurized nozzle-to-spherical-shell model made of a well-characterized heat of type 304 stainless steel are presented and compared with inelastic deformation and failure predictions. The model, which was tested at 593 C (1100 F), was instrumented with capacitive strain gages in key locations. In addition to recording strains, the surface of the model in the junction region was periodically examined throughout the test for the formation and progression of the creep cracking that ultimately led to a leakage failure. The inelastic analysis predictions were based on guidelines developed and used for design of elevated-temperature nuclear components. Likewise, the failure model used was that upon which the ASME elevated-temperature Code Case N-47 for nuclear components is based. Thus, the reasonable agreement observed between experimental results and predictions adds confidence in the overall design methodology for elevated-temperature components. DOE

N92-26846# Sandia National Labs., Albuquerque, NM.
ROLE OF SHOCK COMPRESSION TECHNIQUE FOR SCIENTIFIC AND ENGINEERING STUDIES
J. R. Asay and L. C. Chhabildas 1991 9 p Presented at the 2nd International Symposium on Intense Dynamic Loading and its Effects, Chengdu, China, 9-12 Jun. 1992
(Contract DE-AC04-76DP-00789)
(DE92-008324; SAND-91-2817C; CONF-920688-6) Avail: NTIS HC/MF A02

Shock compression techniques have been used for several decades to study the dynamic states of matter in temperature and pressure regimes inaccessible by other methods. Several experimental loading methods were developed for these studies, including the use of high explosives, high-velocity launchers, and energy deposition. Most recently the development of laboratory techniques for launching flat-plate impactors to velocities of 12 km/s has greatly expanded our ability to study equation-of-state (EOS) and dynamic mechanical properties in regimes previously inaccessible. This paper presents a brief review of the status of high-velocity launchers developed for the purpose of studying dynamic material response. Also included in this paper, a discussion of the launcher capabilities for probing the high-pressure EOS and mechanical response of materials. The range of material property information available from these studies is briefly reviewed and several applications are illustrated. The following methods are discussed: (1) measurements of the shock Hugoniot equation of state and unloading adiabats from the shocked state; (2) techniques for measuring mechanical strength to Mbar pressures under shock and isentropic loading; (3) measurement of tensile failure and the fragmentation of materials; (4) measurement of shock-induced vaporization; and (5) direct measurements of shear properties under shock loading. Shock compression techniques were useful in a variety of current applications, such as debris shield design for spacecraft, analysis of ground shock propagation in geological materials, and shock synthesis of materials. DOE

N92-26852# Sandia National Labs., Albuquerque, NM.
RECENT ADVANCES IN SHOCK AND QUASI-ISENTROPIC COMPRESSION TECHNIQUES FOR DYNAMIC MATERIAL PROPERTY STUDIES
L. C. Chhabildas and J. R. Asay 1991 6 p Presented at the 2nd International Symposium on Intense Dynamic Loading and its Effects, Chengdu, China, 9-12 Jun. 1992
(Contract DE-AC04-76DP-00789)
(DE92-007988; SAND-91-2815C; CONF-920688-4) Avail: NTIS HC/MF A02

In this paper, measurements of the quasi-isentropic compression of tungsten to stress levels of 250 GPa are reported. Results of these experiments were compared to those obtained under shock loading conditions to comparable stresses. These experiments have allowed tlfe determination of temperature, pressure, and loading rate effects on the dynamic yield strength of tungsten up to 250 GPa. These results show that the dynamic yield strength of tungsten is dependent on the loading rate with the strength being higher for the relatively slower rates of loading along the quasi-isentropic.

The pressure dependence of the yield strength of tungsten is determined nearly independent of temperature effects from quasi-isentropic loading experiments to 250 GPa, because the temperature rise in an quasi-loading experiment is much lower than those associated with shock loading experiments. DOE

N92-26860 Texas A&M Univ., College Station.
A FINITE ELEMENT METHOD INCLUDING TRANSVERSE STRESSES FOR THICK LAMINATED PLATES AND SHELLS Ph.D. Thesis
Joseph Patrick Fuehne 1990 166 p
Avail: Univ. Microfilms Order No. DA9118225

The work attempts to compute transverse shear and normal stresses in thick laminated composite plates and shells by using shear-deformable finite element formulations. Quasi-3D finite element formulations are conventional displacement formulations which relax the Kirchhoff hypothesis by independently prescribing three displacements and three rotations at each node. Interpolation functions are chosen to obtain the desired spatial variation in the transverse (interlaminar) stresses. A fully 3D solid finite element formulation containing three displacements per node with shear-deformable capability is also developed. It is the objective to extend the described formulations to include thick geometries by layering plate elements through the thickness and integrating the equilibrium equations through the sets of interfacing elements to obtain the transverse normal and shear stresses. Integrating the equilibrium equations to compute interlaminar stresses is performed through several layers of elements by modifying the procedure to account for the continuity between elements provided by the penalty functions. Interlaminar stress results for thick laminates subjected to sinusoidal and cylindrical bending shows the extended plate formulation to be an effective and accurate method for computing interlaminar stresses. Similarly, the integration of the equilibrium equations within the solid formulation improves the interlaminar stresses in thick laminates and near debonds. Dissert. Abstr.

N92-26869 Texas Univ., Austin.
DEGRADATION AND BUCKLING OF METAL TUBES UNDER CYCLIC BENDING AND EXTERNAL PRESSURE Ph.D. Thesis
Edmundo Corona 1991 270 p
Avail: Univ. Microfilms Order No. DA9128200

The response and stability of long tubular components under bending and external pressure were investigated. The behavior of the structure under monotonic as well as cyclic bending was examined through combined experimental and analytical efforts. The experiments involved metal seamless tubes with diameter-to-thickness ratios in the range of 17 to 35. Long specimens were tested under combined bending and pressure in a specially developed test facility. Bending-pressure interaction collapse envelopes were first generated for monotonically increasing loading histories. The two loads were found to interact strongly through the ovalization of the cross section and the collapse envelopes to depend on the loading history followed. Cyclic bending under various curvature controlled and moment controlled histories was considered. The factors influencing the rate of accumulation of ovalization and the resulting instabilities were studied parametrically. Buckling under cyclic loads occurred when the ovalization of the tubes reached a critical value approximately equal to the critical value developed under the corresponding monotonically applied loads. The problem was analyzed numerically using kinematics which capture the ovalization of the cross section. The predicted response was found to be very sensitive to the elastic-plastic constitutive models used. This sensitivity was carefully analyzed using state-of-the-art models. In the case of cyclic loading histories, the hardening rules used in such models were found to play a pivotal role in the accuracy of the predictions. The reasons for this sensitivity were studied through a parallel investigation of the behavior of the material under cyclic loads. Author

N92-26892* North Carolina State Univ., Raleigh. Center for Research in Scientific Computation.
HOMOGENIZATION MODELS FOR 2-D GRID STRUCTURES Abstract Only
H. T. Banks, D. Cioranescu, and D. A. Rebnord (Syracuse Univ., NY.) 22 Apr. 1992 2 p
(Grants NAG1-1116; AF-AFOSR-0091-90; NSF DMS-88-18530)
(NASA-CR-190321; NAS 1.26:190321) Avail: Issuing Activity

In the past several years, we have pursued efforts related to the development of accurate models for the dynamics of flexible structures made of composite materials. Rather than viewing periodicity and sparseness as obstacles to be overcome, we exploit them to our advantage. We consider a variational problem on a domain that has large, periodically distributed holes. Using homogenization techniques we show that the solution to this problem is in some topology 'close' to the solution of a similar problem that holds on a much simpler domain. We study the behavior of the solution of the variational problem as the holes increase in number, but decrease in size in such a way that the total amount of material remains constant. The result is an equation that is in general more complex, but with a domain that is simply connected rather than perforated. We study the limit of the solution as the amount of material goes to zero. This second limit will, in most cases, retrieve much of the simplicity that was lost in the first limit without sacrificing the simplicity of the domain. Finally, we show that these results can be applied to the case of a vibrating Love-Kirchhoff plate with Kelvin-Voigt damping. We rely heavily on earlier results of (Du), (CS) for the static, undamped Love-Kirchhoff equation. Our efforts here result in a modification of those results to include both time dependence and Kelvin-Voigt damping. Author

N92-26903*# National Aeronautics and Space Administration. Langley Research Center, Hampton, VA.
STRUCTURAL DYNAMIC INTERACTION WITH SOLAR TRACKING CONTROL FOR EVOLUTIONARY SPACE STATION CONCEPTS
Tae W. Lim, Paul A. Cooper, and J. Kirk Ayers (Lockheed Engineering and Sciences Co., Hampton, VA.) May 1992 12 p Presented at the 33rd Structures, Structural Dynamics and Materials Conference, Dallas, TX, 13-15 Mar. 1992 Previously announced in IAA as A92-34491
(RTOP 590-14-31-01)
(NASA-TM-107629; NAS 1.15:107629) Avail: NTIS HC/MF A03

The sun tracking control system design of the Solar Alpha Rotary Joint (SARJ) and the interaction of the control system with the flexible structure of Space Station Freedom (SSF) evolutionary concepts are addressed. The significant components of the space station pertaining to the SARJ control are described and the tracking control system design is presented. Finite element models representing two evolutionary concepts, enhanced operations capability (EOC) and extended operations capability (XOC), are employed to evaluate the influence of low frequency flexible structure on the control system design and performance. The design variables of the control system are synthesized using a constrained optimization technique to meet design requirements, to provide a given level of control system stability margin, and to achieve the most responsive tracking performance. The resulting SARJ control system design and performance of the EOC and XOC configurations are presented and compared to those of the SSF configuration. Performance limitations caused by the low frequency of the dominant flexible mode are discussed. Author

N92-26932# Naval Postgraduate School, Monterey, CA.
DYNAMIC RESPONSE OF CYLINDRICAL SHELLS TO UNDERWATER END-ON EXPLOSION M.S. Thesis
Luis A. Boticario Dec. 1991 84 p
(AD-A245804) Avail: NTIS HC/MF A05

Both numerical and experimental analyses were performed to investigate underwater shock propagation and the induced nonlinear response of cylindrical shells with end caps. The cylinders were subjected to shocks from explosive charges at 12 inches (near-field) and 28 feet (far-field) from the cylinder. An underwater

shock test was also performed with the far-field explosion. The numerical results were compared with the experimental data. Stresses and strains occurring in the structure as well as the pressure in the water were studied. The far-field explosion caused the largest circumferential deformations close to both end plates and an accordion-like oscillatory motion in the cylindrical shell. The near-field explosion caused severe plastic deformation in the neighborhood of the closest end plate to the charge. The stiffeners had, as expected, a larger effect on the circumferential stresses than on the longitudinal stresses. The measured and calculated strains agreed well qualitatively near the remote end plate from the charge. GRA

N92-27066# Naval Postgraduate School, Monterey, CA.
SENSITIVITY OF SENSORS FOR CHARACTERIZING CHAOS M.S. Thesis
Robert G. Vaughan Dec. 1991 68 p
(AD-A246423) Avail: NTIS HC/MF A04

Chaos describes a class of motions of a deterministic system whose time history is sensitive to initial conditions. Because of the sensitivity of initial conditions, the response of a dynamical system may result in instabilities. Hence, a study of nonlinear response of structures under the expected frequencies of excitation becomes important. Chaotic behavior, for example, may be found in the vibration response of large flexible space structures including trusses, booms, and radio antennas. Methods of quantifying chaos have been applied to flexible beams both analytically and experimentally. This research effort investigates the effects of sensors, strain gages and accelerometers, in studying chaotic motions. A long flexible beam is used to model the chaotic behavior, which is also mathematically modeled as Duffing's Equation. Time histories are recorded and analyzed using pseudo-phase space, Fourier spectrums, Poincare sections, Lyapunov exponents and fractal correlation dimensions. Comparison of the two sensors is also performed. Author (GRA)

42 GEOSCIENCES (GENERAL)

N92-26905*# National Aeronautics and Space Administration. Marshall Space Flight Center, Huntsville, AL.
FUNCTIONAL REQUIREMENTS DOCUMENT FOR NASA/MSFC EARTH SCIENCE AND APPLICATIONS DIVISION: DATA AND INFORMATION SYSTEM (ESAD-DIS). INTEROPERABILITY, 1992
J. Briscoe Stephens and Gary W. Grider (Nichols Research Corp., Huntsville, AL.) Jun. 1992 18 p
(NASA-TM-4388; M-690; NAS 1.15:4388) Avail: NTIS HC/MF A03

These Earth Science and Applications Division-Data and Information System (ESAD-DIS) interoperability requirements are designed to quantify the Earth Science and Application Division's hardware and software requirements in terms of communications between personal and visualization workstation, and mainframe computers. The electronic mail requirements and local area network (LAN) requirements are addressed. These interoperability requirements are top-level requirements framed around defining the existing ESAD-DIS interoperability and projecting known near-term requirements for both operational support and for management planning. Detailed requirements will be submitted on a case-by-case basis. This document is also intended as an overview of ESAD-DIs interoperability for new-comers and management not familiar with these activities. It is intended as background documentation to support requests for resources and support requirements. Author

43 EARTH RESOURCES AND REMOTE SENSING

Includes remote sensing of earth resources by aircraft and spacecraft; photogrammetry; and aerial photography.

For instrumentation see *35 Instrumentation and Photography.*

N92-26206# California Univ., Berkeley. Lawrence Berkeley Lab.
SPATIALLY VARIANT TOMOGRAPHIC IMAGING: ESTIMATION, IDENTIFICATION, AND OPTIMIZATION Ph.D. Thesis
J. R. Baker Nov. 1991 126 p
(Contract DE-AC03-76SF-00098)
(DE92-010262; LBL-31561) Avail: NTIS HC/MF A07

This thesis is an investigation of methods for processing multidimensional signals acquired using modern tomography systems that have an anisotropic or spatially variant response function. The main result of this research is the discovery of a new method to obtain better estimators of an unknown spatial intensity distribution by incorporating detailed knowledge about the tomograph system response function and statistical properties of the acquired signal into a mathematical model. DOE

N92-26478 Indiana Univ., Bloomington.
THE CARBON ISOTOPIC COMPOSITIONS OF INDIVIDUAL COMPOUNDS FROM ANCIENT AND MODERN DEPOSITIONAL ENVIRONMENTS Ph.D. Thesis
Katherine Haines Freeman 1991 161 p
Avail: Univ. Microfilms Order No. DA9203435

Pathways of carbon flow in depositional environments were identified using compound-specific isotope analyses in conjunction with biomarker identities and distributions. This work examines factors influencing the isotopic compositions of individual compounds and, consequently, that of preserved sedimentary organic matter. Specifically, isotope effects associated with reactions resulting in the production and degradation of organic matter in the water column and reactions affecting preservation during diagenesis are considered in three projects. Isotopic compositions of structurally-related polycyclic aromatic hydrocarbons (PAH) from the Messel Shale (Eocene) show little variation with increased unsaturation. Lack of isotopic fractionation related to aromatization indicates either that isotope effects associated with these reactions are small or that the reactions are essentially quantitative within a given sediment volume. The influence of environmental conditions on the isotopic composition of sedimentary organic carbon is documented by a comparison of the delta(C-13) of hydrocarbons in the marine Julia Creek Oil Shale (Toolebuc Formation, Cretaceous) and the lacustrine Condor Oil Shale (Tertiary). A model is proposed for identifying relative degrees of oxygenation and productivity within a paleoenvironment based on the observed C-13 contents of biomarkers. Effects of processes proposed in the environmental model are documented by an examination of hydrocarbons from the waters and sediments of the Black Sea and of the Cariaco Trench. Sources of individual compounds are identified by comparison of their C-13 content with that predicted for autotrophic biomass calculated from the concentration and C-13 content of CO2(aq) in the surface waters. Dissert. Abstr.

N92-26513# Research Inst. of National Defence, Linkoeping (Sweden). Huvudavdelning foer Informationsteknologi.
GENERATION OF MULTI-RESOLUTION MAPS [GENERERING AV KARTOR I VARIERANDE UPPLOESNINGAR]
J. Persson and E. Jungert Sep. 1991 68 p
(PB92-152206; FOA-C-30609-3.4) Avail: NTIS HC/MF A04

A motivation for maps hierarchically organized in different resolutions is due to the fact that low resolution maps in most applications require less heavy computations than maps represented in higher resolutions. Hierarchical spatial data structures that permit generation of maps in lower resolutions in a hierarchical fashion already exist, e.g., quadtrees and resolution

pyramids. Many other spatial data structures that are nonhierarchical do not permit the generation of resolution hierarchies like the two above. One such structure is the run length code (RLC), which has many powerful advantages that make the structure feasible in a geographic information system (GIS). For that reason, a method for generation of resolution hierarchies based on RLC is clearly needed. In the work, an approach to the problem of generating a resolution hierarchy from RLC is described and discussed. A generalization method based on recursive polygon approximation is described in detail. GRA

N92-26534# Fermi National Accelerator Lab., Batavia, IL.
ARCHITECTURE FLOW DIAGRAMS UNDER TEAMWORK
T. Nicinski Feb. 1992 10 p Presented at the Symposium on Assessments of Quality Software Development Tools, New Orleans, LA, 27-29 May 1992
(Contract DE-AC02-76CH-03000)
(DE92-010482; FNAL/C-92/58; CONF-9205128-1) Avail: NTIS HC/MF A02

The Teamwork CASE tool allows Data Flow Diagrams (DFDs) to be maintained for structured analysis. Fermilab has extended teamwork under UNIX (trademark) to permit Hatley and Pirbhai Architecture Flow Diagrams (AFDs) to be associated with DFDs and subsequently maintained. This extension, called TWKAFD, allows a user to open an AFD, graphically edit it, and replace it into a TWKAFD maintained library. Other aspects of Hatley and Pirbhai's methodology are supported. This paper presents a quick tutorial on Architecture Diagrams. It then describes the user's view of TWKAFD, the experience incorporating it into teamwork, and the successes with using the Architecture Diagram methodology along with the shortcomings of using the teamwork/TWKAFD tool. DOE

N92-26625 Nottingham Univ. (England).
AN ASSESSMENT OF SATELLITE REMOTE SENSING FOR LAND COVER CLASSIFICATION Ph.D. Thesis
Christopher J. Blazye 1989 389 p
Avail: Univ. Microfilms Order No. BRD-93170

The rate of countryside change in Britain has increased dramatically during the twentieth century as a result of urban and agricultural development. Therefore, a need has arisen for land cover information on a national basis. However, the information provided by current monitoring systems has proved inadequate for a number of reasons. The first part of this study assesses the extent to which remote sensing techniques may be used to provide an input to an existing monitoring system to improve the efficiency of land cover data collection. Although the study indicates that it is not feasible to incorporate remote sensing into an existing monitoring procedure, it identifies a need for more accurate land cover classification algorithms. The second part of the study tests a land cover classification procedure which uses the information provided by an existing monitoring system as a source of ancillary data to improve cover type identification. Although an improvement in classification accuracy is achieved over conventional techniques, the mean accuracy of the procedure remains low. Investigations suggest that further improvements in cover type identification could be achieved through the incorporation of carefully selected terrain variables into the classification procedure. The production of an effective land cover monitoring system is dependent upon a coordinated approach between the system developers and environmental organizations to ensure that the information produced is relevant to current needs. Dissert. Abstr.

N92-26661# Naval Postgraduate School, Monterey, CA.
MODELING OF EXPLORATIVE PROCEDURES FOR REMOTE OBJECT IDENTIFICATION M.S. Thesis
Juan C. Acosta Sep. 1991 140 p
(AD-A245525) Avail: NTIS HC/MF A07

This work addresses the issue of how humans manually explore remote objects using a telemanipulator. An understanding of how conceptual models are constructed is necessary since it will ultimately determine the efficiency of ROV's using telepresence. The representation of human search models is achieved by using the proprioceptive component of the haptic sensory system and the simulated foveal components of the visual system. Eventually it will allow multiple applications in remote sensing and superposition of sensory channels. The use of a force reflecting telemanipulator and computer simulated visual foveal component are the tools which offer the possibility of reconstructing these search patterns observed in different subjects under controlled laboratory conditions. The correlation between the two search strategies is explored and represented in code circles and strings which demonstrates the sequential nature of the two types of probing, as opposed of saccadic response in full vision.
Author (GRA)

N92-26674# Army Cold Regions Research and Engineering Lab., Hanover, NH.
A ONE-DIMENSIONAL TEMPERATURE MODEL FOR A SNOW COVER: TECHNICAL DOCUMENTATION FOR SNTHERM.89
Rachel Jordan Oct. 1991 61 p
(DA Proj. 4A1-61102-AT-24)
(AD-A245493; CRREL-SR-91-16) Avail: NTIS HC/MF A04

This report provides technical documentation for the computer code SNTHERM.89, which is one-dimensional mass and energy balance model of snow and frozen soil. The model is structured using a simplified mixture theory and addresses coupled mass and heat flow, phase change and snow metamorphism. The underlying theory and numerical equations are presented. Included are detailed descriptions of the computation of the energy fluxes at the air/snow interface and of optional routines for estimating short- and long-wave radiation on horizontal and sloped surfaces. GRA

N92-26701# National Space Development Agency, Tokyo (Japan).
INTERNATIONAL CONFERENCE ON JAPANESE EARTH OBSERVATION PROGRAMS: TRMM WORKSHOP
1 Nov. 1990 198 p Conference held in Ibaraki, Japan, 1 Nov. 1990
(JTN-92-80345) Avail: NTIS HC/MF A09

The following topics were discussed: outline of TRMM (Tropical Rainfall Measuring Mission), TRMM mission, mission team of TRMM Project, application of TRMM data, rain radar, active array radar, rainfall retrieval algorithms, precipitation observation, rainfall pattern observation, research plan, numerical model of precipitation, and hydrological cycle. All of the report is presented in viewgraph format. For individual titles, see N92-26702 through N92-26715.

N92-26702*# National Aeronautics and Space Administration. Goddard Space Flight Center, Greenbelt, MD.
THE TROPICAL RAINFALL MEASURING MISSION (TRMM) PROGRAM AT THE GODDARD SPACE FLIGHT CENTER (GSFC)
John Hrastar *In* NASDA, International Conference on Japanese Earth Observation Programs: TRMM Workshop 1 Nov. 1990 p 1-14 (For primary document see N92-26701 17-43)
(TW-1) Avail: NTIS HC/MF A09

Presented in viewgraph format, the status of Tropical Rainfall Measuring Mission (TRMM) Project at NASA Goddard Space Flight Center (GSFC) are outlined. Topics addressed include: TRMM Project organization; TRMM Project/Science interfaces; U.S./Japan responsibilities; TRMM spacecraft summary; TRMM instruments; implementation plan; status of activities; and schedule of project.
Author (NASDA)

N92-26703# Ministry of Posts and Telecommunications, Tokyo (Japan). Communications Research Lab.
STATUS OF TRMM PROJECT: RAIN RADAR IN THE TROPICAL RAINFALL MEASURING MISSION
Kenichi Okamote *In* NASDA, International Conference on Japanese Earth Observation Programs: TRMM Workshop 1 Nov. 1990 p 15-35 (For primary document see N92-26701 17-43)
(TW-2) Avail: NTIS HC/MF A09

Presented in viewgraph format, the rain radar development for TRMM (Tropical Rainfall Measuring Mission) satellite conducted

by Communications Research Laboratory (CRL) are outlined. Topics addressed include: schedule of TRMM Project; U.S./Japan responsibilities for project; mission requirement of radar; outline of active array radar RF (Radio Frequency) section; main system parameters of TRMM rain radar; status of TRMM rain radar development; radiation pattern of array antenna; and performance of manufactured phase shifter, high power amplifier, and low noise amplifier. Author (NASDA)

N92-26704# National Space Development Agency, Tokyo (Japan). Earth Observation Program Office.
STATUS OF TRMM (NASDA)
Shizuo Yamamoto *In its* International Conference on Japanese Earth Observation Programs: TRMM Workshop 1 Nov. 1990 p 37-51 (For primary document see N92-26701 17-43)
(TW-3) Avail: NTIS HC/MF A09

Presented in viewgraph format, status of Tropical Rainfall Measuring Mission (TRMM) Project in National Space Development Agency of Japan (NASDA) are outlined. Topics addressed include: NASDA's role and organization related to TRMM Project; cooperation and responsibility with other organizations; altitude profile of TRMM orbit; mission analysis; status of H-2 launch vehicle, new launch site, and launching schedule; technical interface between H-2 launch vehicle and TRMM, and TRMM S/C (Spacecraft) and rain radar; new phase budget proposal; and schedule of TRMM Project in NASDA. Author (NASDA)

N92-26705# National Space Development Agency, Tokyo (Japan). Earth Observation Program Office.
TRMM MISSION TEAM
Shizuo Yamamoto *In its* International Conferene on Japanese Earth Observation Programs: TRMM Workshop 1 Nov. 1990 p 53-61 (For primary document see N92-26701 17-43)
(TW-4) Avail: NTIS HC/MF A09

Presented in viewgraph format, activity of Tropical Rainfall Measuring Mission (TRMM) Mission Team supported by the National Space Development Agency (NASDA) of Japan are outlined. Topics addressed include: background of TRMM Mission Team; members of the team; objectives of the team;and present and future activities. Author (NASDA)

N92-26706*# National Aeronautics and Space Administration, Washington, DC.
TROPICAL RAINFALL MEASURING MISSION (TRMM) SCIENCE REPORT
Eastwood Im and John Theon *In* NASDA, International Conference on Japanese Earth Observation Programs: TRMM Workshop 1 Nov. 1990 p 63-73 (For primary document see N92-26701 17-43)
(TW-5) Avail: NTIS HC/MF A09

Presented in viewgraph format, a review of scientific researches utilizing the Tropical Rainfall Measuring Mission (TRMM) satellite data are described. Topics addressed include: global precipitation; TRMM orbit; satellite calibration; international cooperation; outline of TRMM research progress; status of TRMM science NRA; and the progress of the project for the last ten years and view of the project for the next ten years. Author (NASDA)

N92-26707# Ministry of Posts and Telecommunications, Tokyo (Japan). Communications Research Lab.
STORM MODEL AND BEAM FILLING PROBLEM FOR RAIN RETRIEVALS
Kenji Nakamura *In* NASDA, International Conference on Japanese Earth Observation Programs: TRMM Workshop 1 Nov. 1990 p 75-88 (For primary document see N92-26701 17-43)
(TW-6) Avail: NTIS HC/MF A09

Presented in viewgraph format, investigation of the beam filling problem using a model of rain statistics and/or real data are described. Topics addressed include: bias error; relationship between brightness temperature and rainfall rate; beam footprint of rain radar; field of view; rain cell model; convective rain; and Tropical Rainfall Measuring Mission (TRMM) satellite rain radar. Author (NASDA)

N92-26708# Ministry of Posts and Telecommunications, Tokyo (Japan). Communications Research Lab.
DEVELOPMENT OF TRMM RADAR RAINFALL RETRIEVAL ALGORITHMS
Toshiaki Kozu *In* NASDA, International Conference on Japanese Earth Observation Programs: TRMM Workshop 1 Nov. 1990 p 89-106 (For primary document see N92-26701 17-43)
(TW-7) Avail: NTIS HC/MF A09

Presented in viewgraph format, status of rainfall retrieval algorithms development for the Tropical Rainfall Measuring Mission (TRMM) rain radar are described. Topics addressed include: importance of radar measurement; requirements for TRMM rain radar resolution; processing flow of the radar data; rainfall parameters to be estimated such as rain rate, liquid water content (LWC), storm height, storm type, Z-R relation, and raindrop size distribution (RSD) ; merits and demerits of estimation method such as Z-R Method, Surface Reference (SRT) Method, Range Profiling Methods; outline of aircraft rainfall observation experiment conducted by NASA and the CommunicationsResearch Laboratory (CRL) of Japan; and issues, procedures, and plans for TRMM radar algorithm development. Author (NASDA)

N92-26709# Tokyo Univ. (Japan).
VALIDATION OF NUMERICAL MODELS BY TRMM AND VALIDATION OF TRMM BY NUMERICAL MODELS
Akiyoshi Sumi *In* NASDA, International Conference on Japanese Earth Observation Programs: TRMM Workshop 1 Nov. 1990 p 107-132 (For primary document see N92-26701 17-43)
(TW-8) Avail: NTIS HC/MF A09

Presented in viewgraph format, a method for validating Tropical Rainfall Measuring Mission (TRMM) radar data and for estimating performance of hydrological circulation model are described. Topics addressed include: comparison between observed data and calculated data of precipitation amount; buoy utilization; water circulation model; estimated precipitation and evaporation amount; and measurements of air temperature, Intraseasonal Variation (IVS); surface wind fields and Sea Surface Temperature (SST). Author (NASDA)

N92-26710# Nagoya Univ. (Japan). Water Research Inst.
WATER CYCLES AROUND THE SUBTROPICAL FRONTAL ZONE IN EAST ASIA
Kuranoshin Kato and Takao Takeda *In* NASDA, International Conference on Japanese Earth Observation Programs: TRMM Workshop 1 Nov. 1990 p 133-152 (For primary document see N92-26701 17-43)
(TW-9) Avail: NTIS HC/MF A09

Presented in viewgraph format, observations of subtropical frontal zone rainfall amount, meso-scale cloud cluster climatology, and relationships between the structure of subtropical high and rainfall amount in its surrounding areas using Tropical Rainfall Measuring Mission (TRMM) satellite data are explained. Topics addressed include: objectives of TRMM observation; distribution of precipitation amount; location of rain front in east Asia region; and subtropical high. Author (NASDA)

N92-26711# Nagoya Univ. (Japan).
RAINFALL PATTERN OVER THE TROPICAL RAIN FOREST
Hiroshi Tanaka *In* NASDA, International Conference on Japanese Earth Observation Programs: TRMM Workshop 1 Nov. 1990 p 153-166 (For primary document see N92-26701 17-43)
(TW-10) Avail: NTIS HC/MF A09

Presented in viewgraph format, reviews of water cycle associated with tropical rain forest are given. Topics addressed include: water cycle model over the tropical rain forest; Rutter Model; Manta Model; Global Climate Model (GCM); relation of rainfall to throughfall; comparison of calculated water on canopy with observed rainfall data; calculated throughfall and evaporation; accumulated difference between observed and calculated throughfall; simulated runoff losses; comparison of observed and predicted interception loss; and simulated monthly variation of precipitation. Author (NASDA)

N92-26712# Japan Meteorological Agency, Tokyo. Meteorological Coll.
UTILIZATION OF TROPICAL CONVECTION DATA FOR METEOROLOGICAL OPERATION
Tsuyoshi Nitta *In* NASDA, International Conference on Japanese Earth Observation Programs: TRMM Workshop 1 Nov. 1990 p 167-177 In ENGLISH and JAPANESE (For primary document see N92-26701 17-43)
(TW-11) Avail: NTIS HC/MF A09

Presented in viewgraph format, application of the Tropical Rainfall Measuring Mission (TRMM) tropical convection monitoring data to long-range forecasts are discussed. Topics addressed include: numerical forecast model; typhoon forecast; Intraseasonal Variation (ISV) of convection; Intraannual Variation (IAV) of convection; and relations of sea surface temperature around the tropical region and atmospheric temperature. Author (NASDA)

N92-26713# Meteorological Research Inst., Tsukuba (Japan).
TRMM AND ASIAN MONSOON
Masato Murakami *In* NASDA, International Conference on Japanese Earth Observation Programs: TRMM Workshop 1 Nov. 1990 p 179-189 (For primary document see N92-26701 17-43)
(TW-12) Avail: NTIS HC/MF A09

Presented in viewgraph format, application of Tropical Rainfall Measuring Mission (TRMM) data to the Asian monsoon investigation are explained. Topics addressed include: TRMM orbits; TRMM coverage area; precipitation in monsoon Asia; Intraseasonal Variation (ISV) of convection; rainfall intensity on small and large islands; and distribution of the Western Pacific upperair station. Author (NASDA)

N92-26714# Meteorological Research Inst., Tsukuba (Japan).
RESEARCH PLAN FOR UTILIZING TRMM DATA IN MRI
Tetsuo Nakazawa *In* NASDA, International Conference on Japanese Earth Observation Programs: TRMM Workshop 1 Nov. 1990 p 191-204 (For primary document see N92-26701 17-43)
(TW-13) Avail: NTIS HC/MF A09

Presented in viewgraph format, progress and plans of meteorological researches such as estimation of rainfall and sea surface conditions, analysis of rain-producing disturbances over the tropics, climate, modeling study utilizing Tropical Rainfall Measuring Mission (TRMM) data in Meteorological Research Institute (MRI) are outlined. Topics addressed include: Split Window Technique; cloud type classification; total column water vapor; sea surface wind speed; wide-range variations of tropical convections; Intraseasonal Variation (ISV); super cluster; cloud cluster; cumulus; interactions with multi-scale convective systems; importance of latent heat release; three dimensional heating profile; model climate by long term integration; cumulus parameterization; total precipitation; and air-sea interaction process by air-sea coupled model. Author (NASDA)

N92-26715# National Research Inst. for Earth Science and Disaster Prevention, Ibaraki (Japan).
RESEARCH PROGRAM ON HYDROLOGY
Takeo Kinoshita *In* NASDA, International Conference on Japanese Earth Observation Programs: TRMM Workshop 1 Nov. 1990 p 205-210 In ENGLISH and JAPANESE (For primary document see N92-26701 17-43)
(TW-14) Avail: NTIS HC/MF A09

Presented in viewgraph format, application of Tropical Rainfall Measuring Mission (TRMM) rainfall data to hydrological cycle investigation are discussed. Topics addressed include: hydrological cycle; hydrological forecasting; flood; drought; snow hazard; natural disaster reduction; atmospheric moisture; surface water; ground water; and runoff model. Author (NASDA)

N92-26728 Ohio State Univ., Columbus.
ESTIMATION OF GEOPOTENTIAL DIFFERENCES OVER INTERCONTINENTAL LOCATIONS USING SATELLITE AND TERRESTRIAL MEASUREMENTS Ph.D. Thesis
Nikolaos Konstantino Pavlis 1991 163 p
Avail: Univ. Microfilms Order No. DA9130537

An error analysis study was conducted in order to assess the currently achievable accuracies and the future anticipated improvements in the estimation of geopotential differences over intercontinental locations. Extending the ideas put forward by Colombo (1980), an observation/estimation scheme was proposed and studied, whereby gravity disturbance measurements on the Earth's surface, in caps surrounding the estimation points, are combined with corresponding data in caps directly over these points at the altitude of a low orbiting satellite, for the estimation of the geopotential difference between the terrestrial stations. The gravity disturbance data at altitude are inferred from GPS measurements made from the low orbiter to the high-altitude GPS satellites, in a multiple-high-single-low Satellite-to-Satellite Tracking (SST) configuration. The mathematical modeling required to relate the primary observables to the parameters to be estimated, was studied both for the terrestrial data and the data at altitude. Recurrence relations for the altitude generalized truncation coefficients implied by Hotine's kernel, and for the degree variances implied by a first-order Gauss-Markov covariance model were originally developed here. The error estimation for the geopotential differences was performed using both truncation theory and least-squares collocation with ring-averages, in case observations on the Earth's surface only are used. The error analysis indicated that with the currently available global geopotential model OSU89B and with gravity disturbance data in 2 degrees caps surrounding the estimation points, the error of the geopotential difference arising from errors in the reference model and the cap data is about 23 kgal cm, for 30 degree station separation. This error is expected to reduce to about 12 kgal cm, when the lower-degree harmonics of the reference model are improved by the incorporation of the global GPS-tracking data on Gravity Probe-B. Dissert. Abstr.

N92-26742# National Space Development Agency, Tokyo (Japan).
INTERNATIONAL CONFERENCE ON JAPANESE EARTH OBSERVATION PROGRAMS: PLENARY SESSION
29 Oct. 1990 110 p Conference held in Ibaraki, Japan, 29 Oct. 1990
(JTN-92-80342) Avail: NTIS HC/MF A06

Current status and future plans about earth observation programs of NASA, ESA, NASDA (National Space Development Agency of Japan), CNES (Centre National d'Etudes Spatiales), CCRS (Canadian Centre for Remote Sensing), and NRCT (National Research Council of Thailand) were outlined. Topics addressed include: earth observation satellites, remote sensing, satellite sounding, remote sensors, ground stations, data systems, data distribution, and land management. All of the reports are presented in viewgraph format. For individual titles, see N92-26743 through N92-26749.

N92-26743# National Space Development Agency, Tokyo (Japan).
JAPANESE EARTH OBSERVATION PROGRAM
Yukio Haruyama *In its* International Conference on Japanese Earth Observation Programs: Plenary Session 29 Oct. 1990 p 1-30 (For primary document see N92-26742 17-43)
Avail: NTIS HC/MF A06

Presented in viewgraph format, NASDA's (National Space Development Agency of Japan) earth observation program was outlined. Objectives, current status, characteristics, and operation schedules of Japanese satellites such as GMS (Geostationary Meteorological Satellite), MOS-1 (Marine Observation Satellite-1), MOS-1b, JERS-1 (Japan Earth Resources Satellite-1), ADEOS (Advanced Earth Observing Satellite), TRMM (Tropical Rainfall Measuring Mission) satellite, and JPOP (Japanese Polar Orbiting Platform) were presented. Author (NASDA)

N92-26744*# National Aeronautics and Space Administration, Washington, DC.
DISTRIBUTION OF PROPOSED EARTH PROBES AND OTHER RELATED MISSIONS
George F. Esenwein *In* NASDA, International Conference on Japanese Earth Observation Programs: Plenary Session 29 Oct. 1990 p 31-37 Sponsored by NASA (For primary document see N92-26742 17-43)
Avail: NTIS HC/MF A06

Presented in viewgraph format, missions and current status of NASA's earth observation program, and development and operations plans of satellites were outlined. Topics addressed include: ozone monitoring; outlines of TOMS (Total Ozone Mapping Spectrometer), NSCAT (NASA Scatterometer), and SeaWiFS (Sea-Viewing Wide Field Sensor); TRMM (Tropical Rainfall Measuring Mission) satellite; EOS (Earth Observing System) satellites; SSF (Space Station Freedom); Free Flyers; and NOAA satellites. Author (NASDA)

N92-26745# European Space Agency, Paris (France).
EUROPEAN EARTH OBSERVATION PROGRAM
V. Beruti *In* NASDA, International Conference on Japanese Earth Observation Programs: Plenary Session 29 Oct. 1990 p 39-64 (For primary document see N92-26742 17-43)
Avail: NTIS HC/MF A06

Presented in viewgraph format, objectives, missions, and current status of ESA's earth observation program and EARTHNET activities were outlined. Topics addressed include: EARTHNET network; environmental monitoring; ERS-1 satellite; ERS-2 satellite; ARISTOTELES satellite; COLUMBUS polar platform; METEOSAT satellite; POEM-1 (First Polar Orbit Earth Observation Mission); MOP-2 (METEOSAT Operational Program-2) satellite; MOP-3 satellite; ocean observation; ice observation; land observation; meteorological survey; solid earth mission; POEM (Polar Orbit Earth Observation Mission); and ground stations. Author (NASDA)

N92-26746# Centre National d'Etudes Spatiales, Paris (France).
FRENCH SPACE PROGRAMMES RELATED TO GLOBAL CHANGE
A. Ratier and J. L. Fellous *In* NASDA, International Conference on Japanese Earth Observation Programs: Plenary Session 29 Oct. 1990 p 65-78 (For primary document see N92-26742 17-43)
Avail: NTIS HC/MF A06

Presented in viewgraph format, current status and future plans of French national earth observation programs were outlined. Topics addressed include: outlines of CNES (Centre National d'Etudes Spatiales) Science Prospective Seminars; DORIS Tracking System; TOPEX/POSEIDON satellite; SPOT satellites; BEST (Tropical System Energy Budget) satellite; GLOBSAT satellite; ScaRaB; Balloon-borne instruments; and data systems.
Author (NASDA)

N92-26747# Canada Centre for Remote Sensing, Ottawa (Ontario). Data Acquisition Div.
CANADIAN EARTH OBSERVATION PROGRAM
Leon Bronstein *In* NASDA, International Conference on Japanese Earth Observation Programs: Plenary Session 29 Oct. 1990 p 79-89 (For primary document see N92-26742 17-43)
Avail: NTIS HC/MF A06

Presented in viewgraph format, current status and future plans of the Canadian earth observation program were outlined. Topics addressed include: characteristics of RADARSAT, earth resources satellite, and polar platform; outline of radar data observation system, Canadian ground system, and data system; major activities and fundamental research issues of CCRS (Canada Centre for Remote Sensing); priorities of activities; and radar data development program. Author (NASDA)

N92-26748# Canada Centre for Remote Sensing, Ottawa (Ontario).
ENVIRONMENTAL PROJECTS AT THE CANADA CENTRE FOR REMOTE SENSING
R. ONeil *In* NASDA, International Conference on Japanese Earth Observation Programs: Plenary Session 29 Oct. 1990 p 91-97 (For primary document see N92-26742 17-43)
Avail: NTIS HC/MF A06

Presented in viewgraph format, current status and future plans of environmental projects at the CCRS (Canada Centre for Remote Sensing) were outlined. Topics addressed include: land cover change project; global change encyclopedia; boreal forest experiment (BORIAS); Northern Biosphere Observation and Modelling Experiment (NBIOME); Cryospheric Systems (CRYSYS); GC (Global-Change) NET; ISY (International Space Year) project; Joint Global Oceans Flux Study (JGOFS); World Ocean Circulation Experiment (WOCE); Global Energy and Water Experiment (GEWEX); and Northern Wetlands Project. Author (NASDA)

N92-26749# National Research Council, Bangkok (Thailand).
MOS-1 ACTIVITY REPORT
P. Chanchai *In* NASDA, International Conference on Japanese Earth Observation Programs: Plenary Session 29 Oct. 1990 p 99-111 (For primary document see N92-26742 17-43)
Avail: NTIS HC/MF A06

Presented in viewgraph format, current status of Thailand earth observation program was outlined. Topics addressed include: activity of National Research Council of Thailand (NRCT); policy and plans of National Remote Sensing Coordinating Committee; ground stations; data systems; data reception from MOS-1 (Marine Observation Satellite-1), SPOT, LANDSAT and ERS-1; and outlines of ongoing joint research projects. Author (NASDA)

N92-26777 Nottingham Univ. (England).
THE GEOID, GPS, AND LEVELLING Ph.D. Thesis
Sara Margaret Elizab Gerrard 1990 273 p
Avail: Univ. Microfilms Order No. BRD-93582

The Global Positioning System (GPS) will be a feasible alternative to costly spirit leveling, if the derived ellipsoidal heights can be converted to orthometric heights above the geoid, with no significant loss of accuracy. Then the system can be used in engineering and topographic surveying and for the maintenance of the Ordnance Survey Leveling Network. A nationwide geoid database has been created with over 70,000 points. It is confidently concluded that, in most areas, the application of this database will facilitate the use of GPS leveling for many requirements, with a comparable quality to conventional techniques. Dissert. Abstr.

N92-26781 Colorado Univ., Boulder.
THE EFFECT OF GLOBAL CHANGE AND LONG PERIOD TIDES ON THE EARTH'S ROTATION AND GRAVITATIONAL POTENTIAL Ph.D. Thesis
Andrew Seth Trupin 1991 224 p
Avail: Univ. Microfilms Order No. DA9132625

The effects of a possible global warming, in particular the rising sea level and melting glaciers, has been a topic of great interest. The attempt here is to quantify the effect these changes and long period ocean tides have on the Earth's rotation and gravity. Global averages of tide gauge data, after correcting for the effects of post glacial rebound on individual station records, reveal an increase in sea level for the years 1900-1979, of between 1.5 and 2.0 mm/yr. The global response of sea level to atmospheric pressure is found to be inverted barometer at periods greater than two months. Tide gauge data are fitted to numerically generated tidal data to show that the 18.6 year lunar nodal tide and 14.3 month pole tide have amplitudes and phases that are consistent with a global equilibrium response. The large coherence at 437 days between pressure and sea level in the North Sea, Baltic Sea and the Gulf of Bothnia may be due to meteorological forcing. The effects on the Earth's rotation and gravitational potential due to changes in annual mass balance for 85 glaciers in 13 mountain glacier systems for the years 1965-1984 are generally at or below detectable limits, but the contribution to sea level rise for these glaciers is 0.14 mm/year. Gridded accumulation data for the Antarctic ice sheet and for the Greenland ice sheet are used along with estimates of the rate of discharge from the ice sheets to estimate the contributions these two regions make

to the Earth's gravity and rotation. The Antarctic contribution to the gravitational signal and to the displacement of the solid earth are found to be within the limits of detection by satellites. The secular trends in the X and Y-components of observed polar motion excitation agree well with the Antarctic contributions, for a model where the interior portions of the ice sheet undergo thinning and the coastal regions thicken. Changes in polar or glacial ice do not agree well with observed changes in the length of day during the last 80 years. Dissert. Abstr.

N92-26864 Washington Univ., Saint Louis, MO.
ANALYSIS OF THERMAL INFRARED DATA ACQUIRED OVER PLAYAS: SILVER LAKE AND DEEP SPRINGS LAKE, CALIFORNIA AND LUNAR LAKE, NEVADA Ph.D. Thesis
Shelley Bougan Petroy 1991 374 p
Avail: Univ. Microfilms Order No. DA9209189

In this study, airborne Thermal Infrared Multispectral Scanner (TIMS) data are used in conjunction with field observations and field and laboratory thermal infrared spectra to identify and map compositional and textural variations across fine-grained playa surfaces and saline ephemeral lakes. For dry, hard-packed playas such as Silver Lake, CA, the distribution of quartz sand, clay, and carbonate is readily determined using a ratio of TIMS channels 2 and 3. This ratio tracks the changes in absorption feature intensities as a function of the relative amounts of each component exposed at the surface (quartz, clay, or carbonate). It was also found that water chemistry during sediment deposition is critical; alkaline waters which contain some carbonates will facilitate slow settling which results in a low porosity surface. Such surfaces exhibited greater spectral contrast within major absorption features; as such, compositionally distinct components are easier to identify. In contrast, high porosity surfaces, such as an artificially disturbed surface at Lunar Lake, exhibit reduced spectral contrast which can often lead to ambiguities when attempting to determine the composition of the surface using only remotely acquired data. Dissert. Abstr.

N92-27070# Naval Oceanographic and Atmospheric Research Lab., Monterey, CA.
AVHRR SATELLITE DATA: USERS GUIDE FOR ACCESSING NOARL ARCHIVES Final Report
Arunas P. Kuciauskas Aug. 1991 78 p
(NR Proj. RM3-5-G-87)
(AD-A246142; AD-E040172; NOARL-TN-164) Avail: NTIS HC/MF A05

The Naval Oceanographic and Atmospheric Research Laboratory (NOARL) Atmospheric Directorate in Monterey, CA (NOARL West) houses nine-track magnetic tapes of Advanced Very High Resolution Radiometer (AVHRR) satellite data covering 3182 individual scenes in a time range between 15 July 1988 and 9 November 1989. A database has been assembled and a catalog developed to aid researchers wishing to access these data. This technical note describes the database and provides the entire catalog listing. GRA

N92-27195*# Jet Propulsion Lab., California Inst. of Tech., Pasadena.
A FEASIBILITY STUDY: CALIFORNIA DEPARTMENT OF FORESTRY AND FIRE PROTECTION UTILIZATION OF INFRARED TECHNOLOGIES FOR WILDLAND FIRE SUPPRESSION AND MANAGEMENT Final Report
J. D. Nichols, R. A. Britten, G. S. Parks, and J. M. Voss 15 Aug. 1990 70 p
(Contract NAS7-918)
(NASA-CR-190458; NAS 1.26:190458; JPL-Publ-90-33) Avail: NTIS HC/MF A04

NASA's JPL has completed a feasibility study using infrared technologies for wildland fire suppression and management. The study surveyed user needs, examined available technologies, matched the user needs with technologies, and defined an integrated infrared wildland fire mapping concept system configuration. System component trade-offs were presented for evaluation in the concept system configuration. The economic benefits of using infrared technologies in fire suppression and management were examined. Follow-on concept system configuration development and implementation were proposed. Author

N92-26337# Hamburg Univ. (Germany, F.R.). Inst. fuer Meteorologie.
INVESTIGATION OF CONVECTION OVER SEA BY AIRCRAFT OBSERVATIONS [FLUGZEUGMESSUNGEN ZUR KONVEKTION UEBER SEE]
Hans Hinzpeter *In* DLR, Contributions to Atmospheric Physics in Honor of Dr. Manfred Reinhardt on His 65th Birthday Sep. 1991 p 71-86 In GERMAN; ENGLISH summary (For primary document see N92-26329 17-46)
Avail: NTIS HC/MF A11; DLR, Wissenschaftliches, Berichtswesen, Postfach 90 60 58, Cologne, Fed.Republic of Germany, HC 60 Deutsche marks

44 ENERGY PRODUCTION AND CONVERSION

Includes specific energy conversion systems, e.g., fuel cells; global sources of energy; geophysical conversion; and windpower.

For related information see also *07 Aircraft Propulsion and Power, 20 Spacecraft Propulsion and Power,* and *28 Propellants and Fuels.*

N92-26190# Midwest Research Inst., Golden, CO.
PHOTOVOLTAIC MANUFACTURING TECHNOLOGY, PHASE 1
M. Izu (Energy Conversion Devices, Inc., Troy, MI.) Mar. 1992 86 p
(Contract DE-AC02-83CH-10093)
(DE92-001199; NREL/TP-214-4579-Phase-1) Avail: NTIS HC/MF A05

This report examines manufacturing multiple-band-gap, multiple-junction solar cells and photovoltaic modules. Amorphous silicon alloy material is deposited (using microwave plasma-assisted chemical vapor deposition) on a stainless-steel substrate using a roll-to-roll process that is continuous and automated. Rapid thermal equilibration of the metal substrate allows rapid throughput of large-area devices in smaller production machines. Potential improvements in the design, deposition, and module fabrication process are described. Problems are also discussed that could impede using these potential improvements. Manufacturing modules for less than $1.00 per peak watt and stable module efficiencies of greater than 10 percent are proposed goals. DOE

N92-26372# Iowa Univ., Iowa City. Dept. of Chemistry.
SYNTHESIS OF NOVEL FLUORINATED PHOSPHONIC ACID ELECTROLYTES FOR PHOSPHORIC ACID FUEL CELLS Final Report, 1 Jan. 1989 - 30 Jun. 1991
D. J. Burton Jan. 1992 28 p
(Contract GRI-5084-260-1081)
(PB92-164300; GRI-92/0066) Avail: NTIS HC/MF A03

A practical synthesis of fluorine containing phosphonic acids of the type, (HO)2P(O)(CF2)nP(O)(OH)2 (n = 1,2,3,4,6) was developed from commercially available precursors. Preliminary electrochemical evaluation of (HO)2P(O)CF2CF2P(O)(OH)2 demonstrated the enhanced oxygen solubility of this acid, and the performance of this acid exceeded H3PO4 in short term fuel cell experiments. Methodology for the preparation of (HO)2P(O)CF2SO3H and F2C = CF(CF)2nP(O)(OH)2 (OH)2 (n = 0,1) was also developed. Author

N92-26581 Arizona Univ., Tucson.
AIRCRAFT PHOTOVOLTAIC POWER-GENERATING SYSTEM Ph.D. Thesis
Oscar Leonard Doellner 1991 190 p
Avail: Univ. Microfilms Order No. DA9210289

Photovoltaic cells, appropriately cooled and operating in the combustion-created high radiant-intensity environment of

gas-turbine and jet engines, may replace the conventional (gearbox-driven) electrical power generators aboard jet aircraft. This study projects significant improvements not only in aircraft electrical power-generating-system performance, but also in overall aircraft performance. Jet-engine design modifications incorporating this concept not only save weight (and thus fuel), but are - in themselves - favorable to jet-engine performance. The dissertation concentrates on operational, constructional, structural, thermal, optical, radiometrical, thin-film, and solid-state theoretical aspects of the overall project. Dissert. Abstr.

N92-26683# Midwest Research Inst., Golden, CO.
SOLTECH 1992 PROCEEDINGS: SOLAR PROCESS HEAT PROGRAM, VOLUME 1
Mar. 1992 298 p Symposium held in Albuquerque, NM, 17-20 Feb. 1992 Prepared in cooperation with DOE, Washington, DC and SNL, Albuquerque, NM
(Contracts DE-AC02-83CH-10093; DE-AC04-76DP-00789)
(DE92-001238; NREL/TP-432-4804-Vol-1; CONF-920290-Vol-1)
Avail: NTIS HC/MF A13

This document is a limited Proceedings, documenting the presentations given at the symposia conducted by the U.S. Department of Energy's (DOE) Solar Industrial Program and Solar Thermal Electrical Program at SOLTECH92. The SOLTECH92 national solar energy conference was held in Albuquerque, New Mexico during the period February 17-20, 1992. The National Renewable Energy Laboratory manages the Solar Industrial Program; Sandia National Laboratories (Albuquerque) manages the Solar Thermal Electric Program. The symposia sessions were as follows: (1) Solar Industrial Program and Solar Thermal Electric Program Overviews, (2) Solar Process Heat Applications, (3) Solar Decontamination of Water and Soil, (4) Solar Building Technologies, (5) Solar Thermal Electric Systems, and (6) Photovoltaic (PV) Applications and Technologies. For each presentation given in these symposia, these Proceedings provide a one- to two-page abstract and copies of the viewgraphs and/or 35 mm slides utilized by the speaker. Some speakers provided additional materials in the interest of completeness. The materials presented in this document were not subjected to a peer review process. DOE

N92-26686# Midwest Research Inst., Golden, CO.
THE EFFECT OF SANDSTORMS ON PV ARRAYS AND COMPONENTS
J. P. Thornton Mar. 1992 7 p Presented at the National Solar Energy Conference, Cocoa Beach, FL, 13-18 Jun. 1992
(Contract DE-AC02-83CH-10093)
(DE92-001240; NREL/TP-411-4787; CONF-920678-1) Avail: NTIS HC/MF A02

Photovoltaic (PV) systems deployed in desert areas are exposed to wind blown particles during most of their lifetimes. Here I describe the characteristics of wind blown particles and their effect on exposed surfaces. I provide insights for use in array design to minimize the effects of exposure and keep system costs as low as possible. Finally, I present some data describing the exposure of polymer encapsulated arrays to both field and laboratory wind blown sand environments, and I present evidence that an encapsulated or 'soft' array has a higher abrasion resistance and, therefore, a much higher probability of surviving a severe sand environment. DOE

N92-26719# Westinghouse Electric Corp., Pittsburgh, PA.
ZIRCONIA-BASED FUEL CELLS FOR POWER GENERATION
S. C. Singhal 1992 11 p Presented at the International Forum on Fine Ceramics 1992, Nagoya, Japan, 9-11 Mar. 1992
(Contract DE-FC21-91MC-28055)
(DE92-009886; DOE/MC-28055/92/C0001; CONF-9203102-1)
Avail: NTIS HC/MF A03

This paper reviews the design and operation of the high temperature solid oxide fuel cells based on yttria stabilized zirconia electrolyte. The functional requirements of the various cell components are presented; and the materials and fabrication processes used for different cell components are described. Finally, the recent progress made toward commercialization of these cells for clean and efficient power generation is discussed. DOE

N92-26858# Arizona Univ., Tucson. Dept. of Biochemistry.
PHOTOCHEMICAL ENERGY CONVERSION BY MEMBRANE-BOUND PHOTOREDOX SYSTEMS
G. Tollin 1 Mar. 1992 14 p
(Contract DE-FG02-86ER-13631)
(DE92-008709; DOE/ER-13631/18) Avail: NTIS HC/MF A03

Most of our effort during the past grant period has been directed towards investigating electron transfer processes involving redox proteins at lipid bilayer/aqueous interfaces. This theme, as was noted in our previous three year renewal proposal, is consistent with our goal of developing biomimetic solar energy conversion systems which utilize the unique properties of biological electron transfer molecules. Thus, small redox proteins such as cytochrome c, plastocyanin and ferredoxin function in biological photosynthesis as mediators of electron flow between the photochemical systems localized in the membrane, and more complex soluble or membrane bound redox proteins which are designed to carry out specific biological tasks such as transbilayer proton gradient formation, dinitrogen fixation, ATP synthesis, dihydrogen synthesis, generation of strong reductants, etc. In these studies, we have utilized two principal experimental techniques, laser flash photolysis and cyclic voltammetry, both of which permit direct measurements of electron transfer processes. DOE

N92-26895*# Lockheed Missiles and Space Co., Sunnyvale, CA.
MILSTAR'S FLEXIBLE SUBSTRATE SOLAR ARRAY: LESSONS LEARNED, ADDENDUM
John Gibb [1990] 17 p Presented at the 26th Aerospace Mechanisms Symposium
(NASA-CP-3147-Add; NAS 1.55:3147-Add) Avail: NTIS HC/MF A03

MILSTAR's Flexible Substrate Solar Array (FSSA) is an evolutionary development of the lightweight, flexible substrate design pioneered at Lockheed during the seventies. Many of the features of the design are related to the Solar Array Flight Experiment (SAFE), flown on STS-41D in 1984. FSSA development has created a substantial technology base for future flexible substrate solar arrays such as the array for the Space Station Freedom. Lessons learned during the development of the FSSA can and should be applied to the Freedom array and other future flexible substrate designs. Author

N92-27087*# National Aeronautics and Space Administration. Marshall Space Flight Center, Huntsville, AL.
AN OVERVIEW OF THE FIRST RESULTS ON THE SOLAR ARRAY MATERIALS PASSIVE LDEF EXPERIMENT (SAMPLE), A0171
Ann F. Whitaker and Leighton E. Young *In* NASA. Langley Research Center, LDEF: 69 Months in Space. First Post-Retrieval Symposium, Part 3 Jan. 1992 p 1241-1254 (For primary document see N92-27083 17-99)
Avail: NTIS HC/MF A21; 1 functional color page

N92-27088*# Wright Lab., Wright-Patterson AFB, OH. Aerospace Power Div.
EXPERIMENT M0003-4: ADVANCED SOLAR CELL AND COVERGLASS ANALYSIS, AN OVERVIEW
Terry M. Trumble *In* NASA. Langley Research Center, LDEF: 69 Months in Space. First Post-Retrieval Symposium, Part 3 Jan. 1992 p 1255-1256 (For primary document see N92-27083 17-99)
Avail: NTIS HC/MF A21; 1 functional color page

N92-27101*# National Aeronautics and Space Administration. Lewis Research Center, Cleveland, OH.
ADVANCED PHOTOVOLTAIC EXPERIMENT, S0014: PRELIMINARY FLIGHT RESULTS AND POST-FLIGHT FINDINGS
David J. Brinker, John R. Hickey (Eppley Lab., Inc., Newport, RI.),

and David A. Scheiman *In* NASA. Langley Research Center, LDEF: 69 Months in Space. First Post-Retrieval Symposium, Part 3 Jan. 1992 p 1395-1404 (For primary document see N92-27083 17-99)
Avail: NTIS HC/MF A21; 1 functional color page

45 ENVIRONMENT POLLUTION

Includes atmospheric, noise, thermal, and water pollution.

N92-26231# Lamont-Doherty Geological Inst., Palisades, NY.
INVESTIGATION OF CARBON DIOXIDE IN THE SOUTH ATLANTIC AND NORTHERN WEDDELL SEA AREAS (WOCE SECTIONS A-12 AND A-21) DURING THE METEOR EXPEDITION 11/5, JANUARY - MARCH 1990
D. W. Chipman, Taro Takahashi, D. Breger, and S. C. Sutherland Dec. 1991 113 p
(Contract DE-FG02-90ER-60943)
(DE92-010027; DOE/ER-60943/1) Avail: NTIS HC/MF A06

This report summarizes the results of the investigation of the oceanographic expedition aboard the F/S METEOR in South Atlantic Ocean including the Drake Passage, the northern Weddell Sea, and the eastern South Atlantic during the austral summer of January through March 1990. The total CO2 concentration in about 1300 seawater samples and CO2 partial pressure (pCO2) in about 870 seawater samples collected at 77 stations were determined aboard the ship using a coulometer and equilibrator/gas chromatograph system. The temperature, salinity, dissolved oxygen, and nutrient salt data presented in this report were determined by other participants of the expedition including the members of the Oceanographic Data Facility of the Scripps Institution of Oceanography, Argentine Hydrographic Office, and German institutions. DOE

N92-26352# National Center for Atmospheric Research, Boulder, CO. Climate and Global Dynamics Div.
DESCRIPTION OF A GLOBAL SHALLOW WATER MODEL BASED ON THE SPECTRAL TRANSFORM METHOD
James J. Hack and Ruediger Jakob Feb. 1992 45 p Sponsored by NSF
(PB92-155258; NCAR/TN-343+STR) Avail: NTIS HC/MF A03

The most common formulation of the equations of motion for simulating large scale atmospheric flow, otherwise known as the meteorological primitive equations, includes the vertical dependence of the atmospheric state variables. Many of the mathematical and computational properties of these equations, however, are embodied in a simpler two dimensional system of equations that govern the behavior of a rotating, homogeneous, incompressible, and hydrostatic fluid with a finite free surface height. The purpose of the technical note is to document a global shallow water equation model based on the spectral transform method. The technical note includes a derivation of the governing system along with a detailed discussion of the spectral transform algorithm as applied to the shallow water system in spherical geometry, including the use of semi-implicit time differencing. Finally, a complete application code, including graphics and post analysis packages, is briefly described. GRA

N92-26354# Environmental Protection Agency, Cincinnati, OH. Risk Reduction Engineering Lab.
GAC ADSORPTION OF A MIXTURE OF NATURAL ORGANIC MATTER AND VOCs IN THE PRESENCE AND ABSENCE OF MOLECULAR OXYGEN
R. D. Vidic, G. A. Sorial, S. P. Papadimas, T. F. Speth, and M. T. Suidan 1991 21 p Presented at the American Water Works Association Annual Conference, Philadelphia, PA, 23-28 Jun. 1991 Prepared in cooperation with Cincinnati Univ., OH
(PB92-153782; EPA/600/A-92/052) Avail: NTIS HC/MF A03

In an attempt to determine the effect of molecular oxygen on activated carbon adsorption modeling, isotherms, microcolumns, and pilot columns are completed in the presence and absence of molecular oxygen. The results show that in oxic conditions, natural organic matter has a higher adsorption capacity than in anoxic conditions. Molecular oxygen does not affect the adsorption capacity of target compounds in distilled water, however in the presence of natural organic matter, the adsorption capacity of the target compounds decrease in oxic conditions due to an increased competitive effect from the natural organic matter. The results also show that the constant diffusivity scale-up approach is more accurate under these conditions than the linear diffusivity scale-up approach. GRA

N92-26373# Midwest Research Inst., Cary, NC.
SUMMARY OF NOx CONTROL TECHNOLOGIES AND THEIR AVAILABILITY AND EXTENT OF APPLICATION
Feb. 1992 105 p
(Contract EPA-68-D1-0115)
(PB92-158260) Avail: NTIS HC/MF A06

A summary is presented of previous documents dealing with NOx control technologies. A brief description is provided of existing NOx control technologies. The availability and extent of applications is discussed of these technologies for several industrial categories that are the main stationary sources of NOx emissions. Where available, achievable controlled NOx emission levels and percent reduction for each control technology are presented. Author

N92-26390# EG and G Rocky Flats, Inc., Golden, CO.
PLUME TRAJECTORY VALIDATION STUDY: BROWN CLOUD SUPPORT PROJECT OVERVIEW
M. A. Brown-Strattan, ed. 30 Sep. 1991 8 p
(Contract DE-AC34-90DP-62349)
(DE92-006911; RFP-4533) Avail: NTIS HC/MF A02

The brown cloud is an air pollution phenomenon of great concern to the Denver metropolitan area. Regulatory agencies, academia, and research organizations are involved in characterizing the development and transport of the brown cloud and identifying mitigation approaches. In support of this effort, NOAA conducted releases of small (one cubic meter) constant density balloons from sites in Denver and along the South Platte Valley. These balloons, called 'tetroons' because of their tetrahedral shape, carried five-ounce transponders and were tracked by radar as they rose to predetermined altitudes and followed airflow patterns at those altitudes. The data gathered from these releases included the geographic position and altitude of each tetroon over time. These data will aid efforts to understand brown cloud development, structure, and transport. DOE

N92-26473 Oxford Univ. (England).
TRACER TRANSPORT IN THE MIDDLE ATMOSPHERE Ph.D. Thesis
Neil F. Arnold 1990 231 p
Avail: Univ. Microfilms Order No. BRD-94131

The discovery of the ozone hole over Antarctica has stimulated a great deal of interest in the interaction between dynamics, radiation, and chemistry in the middle atmosphere. A hierarchy of tracer transport models was adopted to help to understand the results of satellite observations and detailed computer simulations. Zonally averaged models have met with some success in simulating the atmosphere because it is close to radiative/chemical equilibrium in the summer. A zonally averaged circulation derived from satellite observations of temperature and ozone was used to test various advection schemes and to reproduce the zonal mean seasonal cycle of long-lived tropospheric source gases. Three dimensional models impose more severe demands and so a number of finite difference schemes were reviewed and tested under idealized atmospheric conditions. To reduce the computational effort, winds were generated by the Meteorological Office Stratosphere Mesosphere Model (SMM) and passed to a transport model. The best transport scheme was the one which most closely resembled that used for heat and momentum transport. Time averaging of the winds was necessary to produce representative fields in the mesosphere. When the transport scheme was incorporated into the SMM, agreement between the dynamically derived potential temperature and potential vorticity and the tracer equivalents were

very good. During a major warming, the discrepancy between the vortex maximum between the model potential vorticity and the equivalent material tracer fields was 12 percent in the middle stratosphere and 50 percent in the upper stratosphere after twenty days. Most of this difference was due to the sensitivity of the potential vorticity to diabatic heating. Extensions of the work to include chemistry and more sophisticated satellite-derived circulations were suggested. Dissert. Abstr.

N92-26482# Technical Research Centre of Finland, Espoo. Nuclear Engineering Lab.

MODEL STUDIES OF THE TRANSFER OF RADIONUCLIDES IN THE FINNISH ENVIRONMENT Ph.D. Thesis - Helsinki Univ. of Technology

Riitta Korhonen Sep. 1991 118 p
(VTT-Publ-81; ISBN-951-38-4060-3; ISSN-0358-5069;
ETN-92-91263) Copyright Avail: NTIS HC/MF A06

Environmental modeling of the effects of radionuclide releases is reported. A computer model DETRA (Doses via Environmental Transfer of Radionuclides) was developed for evaluation of radionuclide transfer. A study was made of local, regional, and global scale scenarios, in which releases from repositories were assumed. Drinking of tainted water and eating of contaminated fish were the most important dose pathways. The transfer of Cs-137 to the Kamijoki watercourse was evaluated. One of the most important factors in the modeling proved to be the assumptions concerning the transfer to radionuclide sinks; in particular, transfer to sediment sinks was a significant term. Model validation was also performed within international projects, in particular by participating in the BIOMOVS (Biospheric Model Variation Study) project. For individual titles, see N92-26483 through N92-26488.

N92-26483# Technical Research Centre of Finland, Espoo. Nuclear Engineering Lab.

A COMPARATIVE ASSESSMENT OF RADIOLOGICAL IMPACT DUE TO NUCLEAR WASTE DISPOSAL IN HARD CRYSTALLINE BEDROCK, APPENDIX 1 Ph.D. Thesis

Riitta Korhonen, E. K. Peltonen, I. Savolainen (Technical Research Centre of Finland, Helsinki.), O. J. Heinonen, A. Muurinen, and M. Valkiainen *In its* Model Studies of the Transfer of Radionuclides in the Finnish Environment Sep. 1991 18 p Repr. from IAEA (Vienna, Austria), v. 4, 1983 p 257-274 Presented at IAEA Conference on Radioactive Waste Management, Seattle, WA, 16-20 May 1983 (For primary document see N92-26482 17-45)
(IAEA-CN-43/449) Copyright Avail: NTIS HC/MF A06

Analysis of spent fuel and low- and medium-level wastes from Boiling Water Reactor (BWR) plant operation and decommissioning is presented. The repositories are assumed to be situated in hard bedrock on the Baltic Sea coast. The repository lies at a depth of 500 m in the case of spent fuel and at a depth of about 100 m in the case of low- and medium-level wastes. The safety analyses are based on system models consisting of modules for radionuclide release from the repository, groundwater flow, radionuclide migration in bedrock and in the biosphere, and dose assessment. The most significant nuclide in the maximum individual dose rate was found to be Np-237 of the 4N + 1 actinide chain. In the basic scenarios both the low- and medium-level wastes and the spent fuel are assessed to cause equal dose rates in individuals on the local sea/lake scale. Preliminary results show that in certain cases the standard leaching methods may lead to nonconservative results. ESA

N92-26484# Technical Research Centre of Finland, Helsinki. Nuclear Engineering Lab.

ASSESSMENT OF BIOSPHERIC BEHAVIOUR OF RELEASES FROM NUCLEAR WASTE REPOSITORIES, APPENDIX 2

Riitta Korhonen and I. Savolainen *In its* Model Studies of the Transfer of Radionuclides in the Finnish Environment Sep. 1991 15 p Repr. from CEC (Luxemburg), v. 2, 1983 p 555-569 Presented at IAEA/CEC Seminar on the Environmental Transfer to Man of Radionuclides Released from Nuclear Installations, Brussels, Belgium, 17-21 Oct. 1983 (For primary document see N92-26482 17-45)
Copyright Avail: NTIS HC/MF A06

Methodology for estimation of radionuclide concentrations and radiation doses due to releases in the biosphere from nuclear waste repositories is presented. Preliminary results of applications to the releases in the biosphere from spent fuel and low- and medium-level waste repositories are also shown. Transport of long lived radionuclides through the compartment system is demonstrated using model calculations for the nuclides U-238 and Th-229. Calculated radionuclide concentrations are compared to measured concentrations of natural and fallout radionuclides. The dose rate to the individual can exceed the dose rate, due to the natural background, in the case of low- and medium-level wastes, mainly due to Sr-90, if a well is drilled to the contaminated groundwater within about one hundred years after the emplacement of the waste. In the case of spent fuel the dose rate to the individual is well below the dose rate due to the natural radiation; the most important nuclides are Np-237 and Ra-226. In the case of spent fuel the global scale dominates in the accumulation of long term collective doses via nuclides of U-238 decay chain. ESA

N92-26485# Technical Research Centre of Finland, Helsinki. Nuclear Engineering Lab.

ASSESSMENT OF RADIATION DOSES DUE TO RELEASES TO THE BIOSPHERE FROM NUCLEAR WASTE REPOSITORIES, APPENDIX 3 Ph.D. Thesis

Riitta Korhonen and I. Savolainen *In its* Model Studies of the Transfer of Radionuclides in the Finnish Environment Sep. 1991 4 p Repr. from Fachverband fuer Strahlenschutz (Juelic), v. 3, 1983 p 1358-1361 Presented at 6th International Radiation Protection Association International Congress, Berlin, Federal Rep. of Germany, 7-12 May 1983 (For primary document see N92-26482 17-45)
Copyright Avail: NTIS HC/MF A06

Estimation of radiation doses due to releases from nuclear waste repositories consists of three areas: a phase covering the nearfield, (that is, the behavior of radioactive waste products, canisters, buffer materials, and rock groundwater close to the repository), radionuclide migration in the geosphere, and migration in the biosphere and accumulation of radiation doses. Some details of the last phase from a full chain analysis are discussed. The biospheric model is described and the calculational behavior of two important radionuclides, Ra-226 and U-238, is shown. The total results for the basic spent fuel scenario are presented as an example of the type of information obtained from analyses. The waste type analyzed is the spent fuel of two Boiling Water Reactor (BWR) plants. The waste is placed in copper canisters and the repository is assumed to be located on the coast of the Baltic Sea at a depth of 500 m in hard crystalline bedrock. ESA

N92-26486# Technical Research Centre of Finland, Helsinki. Nuclear Engineering Lab.

SENSITIVITY ANALYSIS OF BIOSPHERIC BEHAVIOUR OF RADIONUCLIDES RELEASED FROM NUCLEAR WASTE REPOSITORIES, APPENDIX 4

Riitta Korhonen, I. Savolainen, and V. Suolanen *In its* Model Studies of the Transfer of Radionuclides in the Finnish Environment Sep. 1991 2 p Repr. from BNES, London, England, 1984 p 295-296 Presented at the Conference on Radioactive Waste Management, London, England, 27-29 Nov. 1984 (For primary document see N92-26482 17-45)
Copyright Avail: NTIS HC/MF A06

Sensitivity studies of the biospheric behavior of radionuclides released from a planned spent nuclear fuel repository are performed. The sensitivity of radionuclide concentrations in the biosphere to the sedimentation rate and to intercompartmental water exchange are studied. Solubility has a pronounced effect on sedimentation on the local scale and, in general, sediment sinks were found to be of major importance in the biospheric behavior of radionuclides. ESA

N92-26487# Technical Research Centre of Finland, Helsinki. Nuclear Engineering Lab.

BIOSPHERE MODEL VALIDATION BY INTERCOMPARISON TO OBSERVED BEHAVIOUR OF FALLOUT RADIONUCLIDES IN THE AQUATIC ENVIRONMENT, APPENDIX 5 Ph.D. Thesis

Riitta Korhonen and Seppo Vuori *In its* Model Studies of the Transfer of Radionuclides in the Finnish Environment Sep. 1991 8 p Repr. from Elsevier Applied Science Publishers, London, England, 1987 p 201-208 Presented at CEC Workshop on Methods for Assessing the Reliability of Environmental Transfer Model Predictions, Athens, Greece, 5-9 Oct. 1987 (For primary document see N92-26482 17-45)

Copyright Avail: NTIS HC/MF A06

To improve the reliability of environmental transport models, an extensive validation effort is necessary. The deposition brought about by the Chernobyl accident gave new insights and possibilities for model validation. A dynamic compartment model DETRA (Doses via Environmental Transfer of Radionuclides) is employed for the consideration of radionuclide transport in a large watercourse taking into account both direct reposition and runoff from the terrestrial environment. The results are compared with the experimental observations, but a comprehensive quantitative analysis can be performed only after the careful evaluation of extensive raw data has been completed. ESA

N92-26488# Technical Research Centre of Finland, Helsinki. Nuclear Engineering Lab.

MODELING TRANSFER OF Cs-137 FALLOUT IN A LARGE FINNISH WATERCOURSE, APPENDIX 6 Ph.D. Thesis

Riitta Korhonen *In its* Model Studies of the Transfer of Radionuclides in the Finnish Environment Sep. 1991 12 p Repr. from Health Physics, v. 59, no. 4, 1990 p 443-454 (For primary document see N92-26482 17-45)

Copyright Avail: NTIS HC/MF A06

A large watercourse in Finland was modeled using the dynamic compartment model DETRA. The model includes a fish model for roach, nonpredatory and predatory perches, and pike. Transfer of Cs-137 fallout onto the Kymijoki drainage area after the Chernobyl accident was calculated using the model. In the model, fallout was compared with measured concentrations. Lake Paijanne, the largest lake of the watercourse, was studied most extensively. Calculated concentrations in fish were lower than measured concentrations. To test the model by using additional experimental data, transfer of nuclear weapons testing fallout was also calculated. The process that caused the rather rapid removal of Cs-137 from lake water needs to be studied further using more detailed data. In the long term, runoff and resuspension of sedimentary material were considered to be important in causing concentrations in lake water. ESA

N92-26495# Environmental Protection Agency, Cincinnati, OH. Risk Reduction Engineering Lab.

RUNNING A CONFERENCE AS A CLEAN PRODUCT. INTERNATIONAL CONFERENCE ON POLLUTION PREVENTION: CLEAN TECHNOLOGIES AND CLEAN PRODUCTS

Kenneth R. Stone and Mary E. Bourassa (Science Applications International Corp., Falls Church, VA.) Jun. 1991 40 p Conference held in Washington, DC, 10-13 Jun. 1990

(Contract EPA-68-C8-0062)

(PB92-109099; EPA/600/2-91/026) Avail: NTIS HC/MF A03

More than 1000 attended the International Conference on Pollution Prevention: Clean Technologies and Clean Products, held in Washington, DC, June 10-13, 1990. With support from the Department of Defense, the Department of Energy, and the International Association for Clean Technology, this conference was sponsored by the EPA's Risk Reduction Engineering Laboratory in Cincinnati, Ohio. Featuring 52 sessions and more than 250 speakers, the conference explored the innovative technologies and socio-economic issues arising in the field of pollution prevention. With an agenda of presenting successful examples of clean technologies and clean products, the conference became the perfect opportunity to examine how a large meeting might itself be run as a clean product. Several pollution prevention options were identified and implemented, with varying degress of success. The development of the conference as a clean product, the options identified, how they were implemented and the level of success achieved are discussed. The common sense value of adopting clean practices at every level of their professional activities is demonstrated. Author

N92-26509# ManTech Environmental Technology, Inc., Corvallis, OR.

EQUILIBRIUM-ANALYSIS OF PROJECTED CLIMATE CHANGE EFFECTS ON THE GLOBAL SOIL ORGANIC MATTER POOL

D. P. Turner and R. Leemans 1992 14 p Presented at the Carbon Cycling in Boreal Forest and Subarctic Ecosystems Workshop, Corvallis, OR, 9-12 Sep. 1991 Submitted for publication

(Contracts EPA-68-C8-0006)

(PB92-153022; EPA/600/A-92/039) Avail: NTIS HC/MF A03

Increased rates of soil organic matter decomposition may represent a significant positive feedback to global warming. As a step towards assessing the potential magnitude of this response, an equilibrium analysis was performed in which representative carbon pools were associated with each vegetation type and the Holdridge vegetation/climate correlation system was used to compare distributions of the vegetation types under the current climate and doubled-CO2 climate scenarios from four general circulation models (GCMs). Two of the GCMs predicted a net loss of below ground carbon (55-101 Pg) because of large decreases in the areal extent of tundra and boreal ecosystems with high levels of below ground carbon storage. Vegetation redistribution projected under the other two GCMs would result in the accumulation of carbon (5-41 Pg) in the biosphere. However, this accumulation was driven primarily by an increase in the areal extent of tropical rain forests, which is unlikely given the constraints imposed by anthropogenic factors. Other considerations not treated by the equilibrium approach also support the likelihood of a transient pulse of carbon from the soil to the atmosphere. Author

N92-26510# Corvallis Environmental Research Lab., OR.

GLOBAL ASSESSMENT OF PROMISING FOREST MANAGEMENT PRACTICES FOR SEQUESTRATION OF CARBON

J. K. Winjum, R. K. Dixon, and P. E. Schroeder 17 Jan. 1992 20 p Presented at the US/Canada Symposium on Implications of Climate Change for Pacific NW Forest Management, Seattle, WA, Oct. 1991 Submitted for publication

(PB92-153006; EPA/600/A-92/037) Avail: NTIS HC/MF A03

The assessment produced productivity and cost data for forest and agroforestry management practices in 94 nations. That is, out of a total of 140 nations in the world with forest resources, about two thirds are represented in the database at present. The total forest and woodland area of the 94 nations is about 3.8 billion ha or approximately 94 percent of the world's total. In terms of mean carbon storage (MCS in t/ha) by categories of promising forest practices across latitudinal zones, several trends are seen. As expected, due to longer growing seasons towards the tropics, carbon sequestration in living biomass generally increases from the boreal, to the temperate, to the tropical latitudes. Silviculture has the lowest median values in tC/ha for all three latitudinal zones; boreal, 10; temperate, 26; and tropical, 34. While enhancing productivity in existing forest strands and plantations, silviculture does not directly contribute to increasing forest land area, an important attribute for significant contributions toward increasing global forest carbon sequestration. Author

N92-26519# Environmental Protection Agency, Research Triangle Park, NC. Atmospheric Research and Exposure Assessment Lab.

ROLE OF CLIMATE IN FOREST MONITORING AND ASSESSMENT: A NEW ENGLAND EXAMPLE

E. J. Cooter, S. K. LeDuc, L. Truppi, and D. R. Block Nov. 1991 121 p

(PB92-132885; EPA/600/3-91/074) Avail: NTIS HC/MF A06

The development of climatological information products to support ecological data collection and analysis is described. The scope of research is narrowed to issues of direct interest to the joint US Environmental Protection Agency Environmental Monitoring and Assessment Program and US Department of Agriculture Forest Service New England Forest Health Monitoring Program. Characteristics of climatological persistence and recurrence that are especially critical to New England forest health and productivity are identified. These include physical disturbance events (tornadoes, high winds, and wet snowfall), drought, growing degree days, and late spring freezes. Climatological data are assembled and presentations are developed based on the analysis issue to be addressed: backgrounds (status and persistence); most recent decade (short-term trends, modeling, and prediction); and near-term impacts (most recent sampling year). A Geographic Information System is used for presentation, data management, and analysis. Major research findings focus on the application of climate data and products to operational ecological monitoring and analysis situations. Possible future activities are identified in the areas of new climatologies, program design, database acquisition or development and applied research. All these efforts would result in significant contributions to the development of a more coherent theory of natural disturbance and ecosystem response. GRA

N92-26580# Oak Ridge National Lab., TN.
ORGANIC CARBON IN SOIL AND THE GLOBAL CARBON CYCLE
W. M. Post, III 1991 25 p Presented at the 2nd Ciocco Global Cycle Meeting, Ciocco, Italy, 8-20 Sep. 1991
(Contract DE-AC05-84OR-21400)
(DE92-010289; CONF-9109340-3) Avail: NTIS HC/MF A03

Soil organic matter is, simultaneously, the most inert carbon cycle component of terrestrial ecosystems, and the most dynamic component of terrestrail geologic systems placing it in a pivotal position in the biogeochemistry of carbon. The large size and potentially long residence time of the soil organic matter pool make it an important component of the global carbon cycle. Net terrestrial primary production of about 60 Pg C x yr(-1) is, over a several year period of time, balanced by an equivalent flux of litter production and subsequent decomposition of detritus and soil organic matter. However, the input rates and decomposition rates for different terrestrial ecosystems vary over several orders of magnitude resulting in widely different amounts and turnover rates of soil organic matter. The amounts of carbon stored in soils and the rates of exchange of soil carbon with the atmosphere depend on many factors related to the chemistry, biology, and physics of soil and soil organic matter. This report discusses work on organic carbon in soil and aspects of the carbon cycle. DOE

N92-26590 Delaware Univ., Newark.
THE IMPACT OF CLIMATE UPON VARIATION IN AIR POLLUTION USING A SYNOPTIC CLIMATOLOGICAL APPROACH Ph.D. Thesis
Jane Feng Powley 1991 192 p
Avail: Univ. Microfilms Order No. DA9206345

The Environmental Protection Agency (EPA) has set national ambient air quality standards for six different pollutants: sulfur dioxide, nitrogen dioxide, ozone, total suspended particulates, nitrogen oxides, and oxidants. The goal of this study was to apply an automatic air mass-based synoptic methodology to surface weather data in order to evaluate the impact of climate on the above pollutant concentrations in Philadelphia, PA; Dallas, TX; and St. Louis, MO. A group of synoptic categories depicting the summer and winter weather in each city was developed using principal components analysis and average linkage clustering. The concentrations of the six air pollutants were then related to the synoptic weather categories. The synoptic categories and associated weather conditions exhibiting particularly high pollution concentrations were analyzed in detail. Ultimately, the procedure was validated for prediction of future pollutant levels. The results support the conclusion that there is a close link between synoptic-air mass combinations and various pollutant concentrations. The climate-pollutant relationship seems to change from summer to winter in the three cities. It appears that climate thresholds could be found for high levels of various air pollutants. Similar synoptic conditions appear to lead to high accumulations of all six pollutants, although the transportation-related pollutants showed more dependency on the level of solar radiation. These pollutants seem to be more significant in the southern city of Dallas. The synoptic methodology proved to be of assistance in developing a weather/pollution watch-warning system; such a system would be designed to signal impending synoptic conditions which could significantly raise pollutant concentrations.
Dissert. Abstr.

N92-26633# Pacific Northwest Lab., Richland, WA.
USE OF THE EDMONDS-REILLY MODEL TO MODEL ENERGY-RELATED GREENHOUSE GAS EMISSIONS
D. W. Barns, J. A. Edmonds, and J. M. Reillyn Jan. 1992 43 p
(Contract DE-AC06-76RL-01830)
(DE92-010035; PNL-SA-20478) Avail: NTIS HC/MF A03

The purpose of this paper is to document the results of our application of the Edmonds-Reilly Model (ERM) using several scenarios provided for an Organization for Economic Cooperation and Development (OECD) project comparing global models. Because the output of this exercise is data-rich, most of this exposition is in graphical form, with the narrative serving mainly as a roadmap for moving from one highlight to the next. The first two sections of the paper briefly describe the model and some of the special modifications made for this effort. The case-by-case discussion is contained in Section 4, followed by a summary of the potential pitfalls involved in attempting to assess the cost of emissions reduction from the model data. DOE

N92-26793# Systems Applications International, San Rafael, CA.
IMPROVED PROCEDURES FOR QUANTIFYING KEY METEOROLOGICAL EFFECTS ON AMBIENT OZONE DATA Final Report
T. E. Stoeckenius, C. Daly, A. B. Hudischewskyj, and A. M. Noda Jun. 1991 201 p
(Contract ARB-A832-134)
(PB92-163278; ARB-R-92-478) Avail: NTIS HC/MF A10

An analysis of meteorological conditions and relative ozone concentration patterns has succeeded in identifying at least four groups of days that represent distinct sets of source history characteristics. Each source history categories is associated with a distinct spatial distribution of both relative and absolute ozone concentrations and with distinct meteorological features. It was concluded that the mechanisms leading to the afternoon ozone peak in each subregion (emission contributions, mixing, transport, and chemical transformation) are basically the same for days within the same category. Only details influenced by temperature variations, vary from day to day. Days within each of the four distinct categories are representative of one another with respect to the response of ozone concentrations on these days to a given set of emission control measures. Author

N92-26802# Systems Applications, Inc., San Rafael, CA.
ASSESSMENT OF COMPUTER MODELS FOR ESTIMATING VEHICLE EMISSION FACTORS. VOLUME 1: EXECUTIVE SUMMARY Final Report
19 Jul. 1991 18 p Sponsored in part by Coordinating Research Council, Inc., Atlanta, GA
(PB92-113059; SYSAPP-91/091A) Avail: NTIS HC/MF A03; also available in set of 3 reports HC/MF E99 as PB92-113042

Since the passage of the Clean Air Act of 1970, significant progress has been made toward improving air quality in the United States. Currently vehicles are the largest source of emissions in many U.S. cities. Because of this, particular attention has been focused on vehicle emissions, and numerous computer models have been developed to calculate vehicle emission rates for the major classes of on-road motor vehicles. A number of recent studies, such as the Southern California Air Quality Study (SCAQS) Tunnel Study conducted by Southwest Research Institute, have

revealed possible discrepancies between measured emissions and those predicted by the computer models used by the Environmental Protection Agency and the California Air Resources Board (MOBILE4 and EMFAC7E respectively). The two models are used to estimate emission factors by vehicle class for specific calendar years. Under the sponsorship of the Coordinating Research Council, Systems Applications International conducted an assessment of the MOBILE4 and EMFAC7E models. The summary highlights major findings and conclusions regarding fleet characterization, calculation of exhaust and evaporative emission rates, and correction factors for operating mode, speed, temperature, and fuel volatility in MOBILE4 and EMFAC7E. Author

N92-26803# Systems Applications, Inc., San Rafael, CA.
ASSESSMENT OF COMPUTER MODELS FOR ESTIMATING VEHICLE EMISSION FACTORS. VOLUME 2: DESCRIPTION AND COMPARISON OF THE MOBILE4 AND EMFAC7E MODELS Final Report
19 Jul. 1991 285 p Prepared in cooperation with Energy and Environmental Analysis, Inc., Arlington, VA Sponsored in part by Coordinating Research Council, Inc., Atlanta, GA
(PB92-113067; SYSAPP-91/091B) Avail: NTIS HC/MF A13; also available in set of 3 reports HC/MF E99 as PB92-113042

The estimation of emissions from motor vehicles is both complex and challenging. The U.S. Environmental Protection Agency (EPA) and the California Air Resources Board (ARB) have developed computer models to assist in these estimations. In May of this year the Air Pollution Research Advisory Committee (APRAC) of the Coordinating Research Council (CRC) retained Systems Applications International (SAI) to conduct an assessment of the methodologies used in MOBILE4 and EMFAC7 to estimate hydrocarbon (HC), carbon monoxide (CO), and oxides of nitrogen (NOx) emission factors. The assessment, as defined by the CRC, consisted of two parts; a thorough study of the structure and operation of the MOBILE4 and EMFAC7 computer models, and analysis of the sensitivity of MOBILE4 and EMFAC7 to determine which model data components most strongly influence the calculated emission factors. The volume of the report describes in detail the work completed in the structural evaluation of MOBILE4 and EMFAC7E. As a starting point, a brief description of MOBILE4 and EMFAC7 is presented to acquaint the reader with the basic structure of these models. Following this, an in-depth review of the major components of both MOBILE4 and EMFAC7 is presented. Author

N92-26810# Midwest Research Inst., Golden, CO.
ENVIRONMENTAL IMPLICATIONS OF INCREASED BIOMASS ENERGY USE
T. R. Miles, Sr. and T. R. Miles, Jr. Mar. 1992 47 p
(Contract DE-AC02-83CH-10093)
(DE92-001219; NREL/TP-230-4633) Avail: NTIS HC/MF A03

This study reviews the environmental implications of continued and increased use of biomass for energy to determine what concerns have been and need to be addressed and to establish some guidelines for developing future resources and technologies. Although renewable biomass energy is perceived as environmentally desirable compared with fossil fuels, the environmental impact of increased biomass use needs to be identified and recognized. Industries and utilities evaluating the potential to convert biomass to heat, electricity, and transportation fuels must consider whether the resource is reliable and abundant, and whether biomass production and conversion is environmentally preferred. A broad range of studies and events in the United States were reviewed to assess the inventory of forest, agricultural, and urban biomass fuels; characterize biomass fuel types, their occurrence, and their suitability; describe regulatory and environmental effects on the availability and use of biomass for energy; and identify areas for further study. The following sections address resource, environmental, and policy needs. Several specific actions are recommended for utilities, nonutility power generators, and public agencies. DOE

N92-26823# Radian Corp., Research Triangle Park, NC.
VOLATILE ORGANIC COMPOUND (VOC) AND PARTICULATE MATTER (PM) SPECIATION DATA SYSTEM USER'S MANUAL, VERSION 1.4
Susan K. Lynch Oct. 1991 65 p
(Contract EPA-68-DO-0125)
(PB92-105527; EPA/450/4-91/027; EPA/SW/DK-92/016A)
Avail: NTIS HC/MF A04

The U.S. Environmental Protection Agency (EPA) has several activities that require speciated volatile organic compound (VOC) or particle matter (PM) profiles from several source categories. To support these activities, EPA has produced the two volume Air Emissions Species Manual (EPA-450/2-90-001 a & b). Because of the large size of the Air Emissions Species Manual, over 1500 pages, EPA has decided to discontinue making it available in hard copy format. The document contains the documentation and users guide for the data system that replaces the Air Emissions Species Manual. The document must be accompanied by the 5 1/4 inch diskette which contains the VOC and PM data bases. In addition to all of the speciation profiles contained in the Manual, 43 new particulate matter profiles have been added to update the data system. GRA

N92-26825# Brookhaven National Lab., Upton, NY.
EVALUATION OF CARBON DIOXIDE EMISSION CONTROL STRATEGIES IN NEW YORK STATE
S. C. Morris, J. Lee, G. Goldstein, and D. Hill Jan. 1992 112 p
(Contract DE-AC02-76CH-00016)
(DE92-010162; BNL-47110) Avail: NTIS HC/MF A06

A MARKAL model was developed for the State of New York. It represents the state's energy system as a set of typical technologies for generating, converting, and using energy as it evolves over a 45 year period. NYMARKAL was applied here in demonstration analyses to explore strategies to reduce CO2 emissions. NYMARKAL was installed at the State Energy Office and in the Offices of the New York Power Pool. Staff members from both organizations and other state agencies were trained in its use. Example scenarios showed that it is more difficult and more expensive to reduce carbon emissions in New York State than in the United States as a whole. If a common carbon tax was instituted, it would have less effect in New York and most carbon emissions reduction would take place elsewhere in the country where it is more cost effective. Alternatively, were all states required to reduce CO2 emission an equal percentage (say by 20 percent), the cost per unit emissions reduction to New York would be much greater than in the rest of the country. DOE

N92-26873 Physics and Electronics Lab. TNO, The Hague (Netherlands).
INFRARED CLUTTER MEASUREMENTS OF MARINE BACKGROUNDS Interim Report [INFRAROOD CLUTTER METINGEN VAN MARITIEME ACHTERGRONDEN]
P. B. W. Schwering Apr. 1991 29 p Presented at the International Symposium and Exhibition on Optical Engineering and Photonics: Characterization, Propagation and Simulation of Sources and Backgrounds, Orlando, FL, 2-3 Apr. 1991
(Contract A88KM637)
(AD-A245422; FEL-91-A073; TD91-0993; ETN-92-91213)
Copyright Avail: TNO Physics and Electronics Lab., P.O. Box 96864, 2509 JG The Hague, Netherlands

Observations in the infrared wavelength band, 8-12 micrometers, of sea backgrounds were recorded with a Consultative Committee for International Radio (CCIR) compatible imager for a large number of sea states. Recordings took place in coastal areas as well as on open seas. The behavior of clutter in the infrared data was analyzed in space and in time. Clutter values are analyzed to give estimates for the physical appearance of the sea, such as wave structure. Elevation profiles are evaluated for sea state characteristics and show that the variation of the rms (root mean square) with elevation decreases with increasing sea state number. Infrared sequences are used to derive periods in the rms clutter values and to derive time constants of about 1 s for the images in the sequence to become uncorrelated. A constant

azimuthal wave velocity is found from the radiance images. Sunglint images were recorded with a MultiPath Transmissometer Radiometer (MPTR) simultaneously in six wavelength bands at 0.6, 0.8, 1.3, 2.1, 4.0 and 10.0 micrometers in coastal areas. The elevation averaged profiles are well fitted by a Gaussian pattern. Characteristic hotspot duration times were estimated to be 0.15 to 0.20 s. The spectral correlation is investigated and found to be present only on a global scale. ESA

N92-26878*# National Center for Atmospheric Research, Boulder, CO. Climate and Global Dynamics Div.

MONTHLY MEAN GLOBAL SATELLITE DATA SETS AVAILABLE IN CCM HISTORY TAPE FORMAT

James W. Hurrell and G. Garrett Campbell Apr. 1992 105 p Original contains color illustrations

(Contract NASw-17214; RTOP 578-41-29-03)

(NASA-CR-190344; NAS 1.26:190344; NCAR/TN-371+STR)

Avail: NTIS HC/MF A06; 1 functional color page

Satellite data for climate monitoring have become increasingly important over the past decade, especially with increasing concern for inadvertent antropogenic climate change. Although most satellite based data are of short record, satellites can provide the global coverage that traditional meteorological observations network lack. In addition, satellite data are invaluable for the validation of climate models, and they are useful for many diagnostic studies. Herein, several satellite data sets were processed and transposed into 'history tape' format for use with the Community Climate Model (CCM) modular processor. Only a few of the most widely used and best documented data sets were selected at this point, although future work will expand the number of data sets examined as well as update the archived data sets. An attempt was made to include data of longer record and only monthly averaged data were processed. For studies using satellite data over an extended period, it is important to recognize the impact of changes in instrumentation, drift in instrument calibration, errors introduced by retrieval algorithms and other sources of errors such as those resulting from insufficient space and/or time sampling. Author

N92-26889# Environmental Protection Agency, Cincinnati, OH. Risk Reduction Engineering Lab.

WASTE MINIMIZATION FOR NON-AGRICULTURAL PESTICIDE APPLICATORS: EPA'S POLLUTION PREVENTION GUIDE

T. M. Harten 1992 10 p Presented at the International Workshop on Research and Pesticide Treatment, Disposal, and Waste Minimization, Cincinnati, OH, 26-27 Feb. 1991 Submitted for publication

(PB92-153774; EPA/600/A-92/051) Avail: NTIS HC/MF A02

The U.S. EPA's Office of Research and Development is preparing a guide to be published later this year for non-agricultural pesticide applicators which will provide specific information about waste minimization for pesticide users in industries such as commercial lawn care, structural pest control, greenhouse operations, and forestry. The paper summarizes the major recommendations to be included in the upcoming manual for waste source reduction and recycling within the operational activities of the industry. Examples include implementation of an integrated pest management program, inventory control and storage, product substitution, containers and packaging changes, and improved mixing and application technology. The guide is one in a series of industry-specific pollution prevention guides that the EPA is publishing in cooperation with the California Department of Health Services. The first guide in the series, published in 1990, described waste reduction opportunities in the pesticide formulating industry. GRA

N92-26890# Environmental Protection Agency, Washington, DC. Office of Radiation Programs.

ENVIRONMENTAL RADIATION DATA Quarterly Report No. 63, Jul. - Sep. 1990

Mar. 1991 44 p

(PB92-164706; EPA/520/5-91/025) Avail: NTIS HC/MF A03

Environmental Radiation Data (ERD) contains data from the Environmental Radiation Ambients Monitoring System (ERAMS). Data from similar networks operated by contributing States, Canada, Mexico, and the Pan American Health Organization are reported in the ERD when available. The ERAMS is comprised of nationwide sampling stations that provide air, surface and drinking water, and milk samples from which environmental radiation levels are derived. Sampling locations are selected to provide optimal population coverage while functioning to monitor fallout from nuclear devices and other forms of radioactive contamination of the environment. The radiation analyses performed on the samples include gross alpha and gross beta levels, gamma analyses for fission products, and specific analyses for uranium, plutonium, strontium, iodine, radium, krypton, and tritium. GRA

N92-26928# Environmental Protection Agency, Cincinnati, OH. Risk Reduction Engineering Lab.

ENVIRONMENTAL PROTECTION AGENCY'S MUNICIPAL SOLID WASTE LANDFILL LINER DESIGN CRITERIA

R. E. Landreth 1992 10 p Presented at the 28th Technical Sessions of GRCDA's Annual International Solid Waste Exposition, Vancouver, British Columbia, 20-24 Aug. 1990 Submitted for publication

(PB92-153766; EPA/600/A-92/050) Avail: NTIS HC/MF A02

The soon to be published non-hazardous land disposal regulation, RCRA sub title D (40 CFR Parts 257 and 258) must achieve three objectives. The first is to be protective of human health and the environment, second to be flexible so as not to stifle innovative designs, and third to allow individual states the latitude to develop state specific regulations. The containment systems (liners) currently under consideration will achieve these three goals. The paper will briefly discuss the approach to the liner design. Additional information will be forth coming as final decisions are made. GRA

N92-26929# Environmental Protection Agency, Research Triangle Park, NC. Air and Energy Engineering Research Lab.

TECHNOLOGY FOR REDUCTION OF CO2 EMISSIONS FROM THE TRANSPORTATION SECTOR Report, Mar. 1991 - Jan. 1992

R. H. Borgwardt 1992 12 p Presented at the 1st International Conference on Carbon Dioxide Removal, Amsterdam, Netherlands, 3-6 Mar. 1992

(PB92-153733; EPA/600/A-92/047) Avail: NTIS HC/MF A03

The paper gives results of a preliminary assessment of the Hydrocarb process which indicates that substantially more fuel energy can be produced at a lower cost than with other current options for mitigating carbon dioxide (CO2) from mobile sources. The incremental cost of eliminating net CO2 emissions is estimated at $0.05 per gallon (3.78 liters) of gasoline displaced by methanol. About 80 percent reduction should be achievable at no incremental cost. It is concluded that, by sequestering byproduct carbon and replacing petroleum fuels with biomass-derived methanol, the Hydrocarb process can nullify the net effect of CO2 emissions from motor vehicles. Author

N92-26931# Geological Survey, Reston, VA. Water Resources Div.

COMPUTER PROGRAM ESTIMATE TREND (ESTREND): A SYSTEM FOR THE DETECTION OF TRENDS IN WATER-QUALITY DATA

T. L. Schertz, R. B. Alexander, and D. J. Ohe 1991 71 p

(PB92-147727; USGS/WRI-91-4040) Avail: NTIS HC/MF A04

A software system for the analysis of time trends in water-quality data is documented. The system, Estimate TREND (ESTREND), was initially developed to assist in the national and S inves-level USGS investigations of trends in stream water quality. Certain statistical and operational issues such as (1) the choice of a statistical test for trend, (2) methods of adjusting for flow and seasonal variations, (3) the choice of a minimum number of observations for trend testing, and (4) the selection of water-quality stations are discussed. Decisions related to these issues are based on methods investigations cited in the background section and

experience from national and state-level trend investigations.
Author

N92-26935# Lawrence Livermore National Lab., CA.
A FINITE ELEMENT/FINITE DIFFERENCE APPROACH FOR MODELING THREE-DIMENSIONAL FLOW AND POLLUTANT DISPERSION AROUND STRUCTURES
R. L. Lee 28 Oct. 1991 18 p Presented at the American Institute of Astronautics and Aeronautics/American Society of Mechanical Engineers (AIAA/ASME) National Fluid Dynamics Congress, Los Angeles, CA, 15-18 Jun. 1992
(Contract W-7405-eng-48)
(DE92-007322; UCRL-JC-107758; CONF-920605-4) Avail: NTIS HC/MF A03

We are developing state-of-the-art numerical tools that can be used to provide reliable estimates of potential emissions at industrial sites. In particular we have focused our efforts in generating models that can simulate the wind flow and dispersion of airborne pollutants around surface-mounted structures such as buildings or building complexes. The calculational procedure that was chosen consists of two sequential steps, namely: (1) prediction of the mean flow via a turbulent flow model; and (2) employment of the calculated flow field to drive a particle-in-cell transport and diffusion model. A benchmark simulation is performed in which numerical results from the flow model are compared with other numerical models and with experimental data for flow over a backward-facing step. We also present results from three-dimensional simulations of flow and dispersion over a two-building complex. DOE

N92-26936# Lawrence Livermore National Lab., CA.
ENSURING MASS CONVERSION IN A HEAVY-GAS DISPERSION MODEL USING THE GENERALIZED ANELASTIC EQUATIONS
S. T. Chan and P. M. Gresho 31 Oct. 1991 16 p Presented at the American Institute of Astronautics and Aeronautics/American Society of Mechanical Engineers (AIAA/ASME) National Fluid Dynamics Congress, Los Angeles, CA, 15-18 Jun. 1992
(Contract W-7405-eng-48)
(DE92-007323; UCRL-JC-107535; CONF-920605-3) Avail: NTIS HC/MF A03

To help understand the atmospheric dispersion of heavy-gas clouds, we developed a three dimensional model called FEM3A (and its predecessor-FEM3). The model is based on solving the time-dependent, generalized anelastic equations of mass, momentum, energy, and concentration of species. The model is useful for simulating a relatively wide range of heavy-gas dispersion problems, including those with variable terrain and obstructions. However, certain recent applications revealed that, for problems involving large density variations, the model was deficient in conserving both species and total mass. To extend the applicability of FEM3/FEM3A for such problems, a new and cost-effective algorithm, based on solving a slightly modified set of equations, was recently developed. In this paper, the algorithm is described and numerical results are presented to demonstrate the improvements obtained. DOE

N92-27082 International Council of Scientific Unions, Stockholm (Sweden).
PAGES. PAST GLOBAL CHANGES PROJECT: PROPOSED IMPLEMENTATION PLANS FOR RESEARCH ACTIVITIES
John A. Eddy, ed. 1992 108 p Sponsored in part by ICSU; IGBP; UNEP; Unesco; Commission of the European Communities; Swedish Council for Planning and Coordination of Research, NSF, Shell Netherlands, Dutch Electricity Generating Board; Canon Sweden; and Hewlett Packard Sweden
(IGBP-Rept-19-Attach-10; ISSN-0284-8015) Copyright Avail: Issuing Activity

The Past Global Changes (PAGES) project is directed at securing a better understanding of the natural and human induced variations of the Earth system in the past, through the organization of coordinated national and international endeavors to obtain and interpret a variety of natural and written records. To understand global changes of the past, or to predict the changes expected in the future, one needs to know a detailed history of environmental changes throughout the past, for every region of the globe. Among the research themes considered are: solar and orbital forcing and response; fundamental Earth system processes; rapid and abrupt global changes; multi-proxy mapping; palaeoclimate and environment modeling; and management of palaeodata. H.A.

N92-26332# Deutsche Forschungsanstalt fuer Luft- und Raumfahrt, Oberpfaffenhofen (Germany, F.R.). Inst. fuer Physik der Atmosphaere.
NOXIOUS MATTER TRANSPORTATION IN THE ALPINE REGIONS [SCHADSTOFFTRANSPORTE IN DIE ALPENREGION]
Jutta Graf and Dieter Heimann *In its* Contributions to Atmospheric Physics in Honor of Dr. Manfred Reinhardt on His 65th Birthday Sep. 1991 p 21-26 In GERMAN; ENGLISH summary Original contains color illustrations (For primary document see N92-26329 17-46)
Avail: NTIS HC/MF A11; DLR, Wissenschaftliches, Berichtswesen, Postfach 90 60 58, Cologne, Fed.Republic of Germany, HC 60 Deutsche marks

N92-26334# Deutsche Forschungsanstalt fuer Luft- und Raumfahrt, Oberpfaffenhofen (Germany, F.R.). Inst. fuer Physik der Atmosphaere.
A SIMPLE MODEL FOR THE CONVECTIVE BOUNDARY LAYER OVER WAVY TERRAIN WITH VARIABLE HEAT FLUX
Ulrich Schumann *In its* Contributions to Atmospheric Physics in Honor of Dr. Manfred Reinhardt on His 65th Birthday Sep. 1991 p 41-50 (For primary document see N92-26329 17-46)
Avail: NTIS HC/MF A11; DLR, Wissenschaftliches, Berichtswesen, Postfach 90 60 58, Cologne, Fed.Republic of Germany, HC 60 Deutsche marks

N92-26345# Meteorologisches Observatorium, Hohenpeissenberg (Germany, F.R.).
OZONE TRENDS [UEBER OZONTRENDS]
Klaus Wege and Winfried Vandersee *In* DLR, Contributions to Atmospheric Physics in Honor of Dr. Manfred Reinhardt on His 65th Birthday Sep. 1991 p 167-177 In GERMAN; ENGLISH summary Sponsored by Bundesministerium fuer Forschung und Technologie (For primary document see N92-26329 17-46)
Avail: NTIS HC/MF A11; DLR, Wissenschaftliches, Berichtswesen, Postfach 90 60 58, Cologne, Fed.Republic of Germany, HC 60 Deutsche marks

46 GEOPHYSICS

Includes aeronomy; upper and lower atmosphere studies; ionospheric and magnetospheric physics; and geomagnetism.

For space radiation see *93 Space Radiation.*

N92-26208# California Univ., Berkeley. Lawrence Berkeley Lab.
IMAGING EARTH'S INTERIOR: TOMOGRAPHIC INVERSIONS FOR MANTLE P-WAVE VELOCITY STRUCTURE Ph.D. Thesis
R. J. Pulliam Jul. 1991 268 p
(Contract DE-AC03-76SF-00098)
(DE92-010271; LBL-31377) Avail: NTIS HC/MF A12

A formalism is developed for the tomographic inversion of seismic travel time residuals. The travel time equations are solved both simultaneously, for velocity model terms and corrections to the source locations, and progressively, for each set of terms in succession. The methods differ primarily in their treatment of source mislocation terms. Additionally, the system of equations is solved directly, neglecting source terms. The efficacy of the algorithms is explored with synthetic data as we perform simulations of the general procedure used to produce tomographic images of Earth's mantle from global earthquake data. The patterns of seismic heterogeneity in the mantle that would be returned reliably by a tomographic inversion are investigated. We construct synthetic data

sets based on real ray sampling of the mantle by introducing spherical harmonic patterns of velocity heterogeneity and perform inversions of the synthetic data. DOE

N92-26239# California Univ., Berkeley. Lawrence Berkeley Lab.
FAULT ZONE STRUCTURE DETERMINED THROUGH THE ANALYSIS OF EARTHQUAKE ARRIVAL TIMES Ph.D. Thesis
A. Michelini Oct. 1991 202 p
(Contract DE-AC03-76SF-00098)
(DE92-010322; LBL-31534) Avail: NTIS HC/MF A10

This thesis develops and applies a technique for the simultaneous determination of P and S wave velocity models and hypocenters from a set of arrival times. The velocity models are parameterized in terms of cubic B-splines basis functions which permit the retrieval of smooth models that can be used directly for generation of synthetic seismograms using the ray method. In addition, this type of smoothing limits the rise of instabilities related to the poor resolving power of the data. V(sub P)/V(sub S) ratios calculated from P and S models generally display instabilities related to the different ray-coverages of compressional and shear waves. However, V(sub P)/V(sub S) ratios are important for correct identification of rock types and this study introduces a new methodology based on adding some coupling (i.e., proportionality) between P and S models which stabilizes the V(sub P)/V(sub S) models around some average preset value determined from the data. Tests of the technique with synthetic data show that this additional coupling regularizes effectively the resulting models. DOE

N92-26294# European Space Agency, Paris (France).
CLUSTER DAYSIDE POLAR CUSP
C. I. Barron, ed. Dec. 1991 200 p International workshop held in Longyearbyen, Norway, 16-19 Sep. 1991
(ESA-SP-330; ISBN-92-9092-162-5; ETN-92-91714) Copyright Avail: NTIS HC/MF A09; ESA, EPD, ESTEC, Noordwijk, Netherlands, HC 50 Dutch guilders

Papers on the planning and coordination of measurements from the Cluster mission, ground stations, balloons and rockets, in the dayside polar cusp region are presented. Research programs on Svalbard (Arctic) and other programs for cusps studies are reported. Other sessions report on: satellite projects; radar studies; polar cusp problems; needs and requirements; present status of observation techniques; need for balloon and rocket campaigns; data systems, future meetings and outlook. For individual titles, see N92-26295 through N92-26319.

N92-26295# Oslo Univ. (Norway). Dept. of Physics.
THE NORWEGIAN UPPER ATMOSPHERE PROGRAMME IN SVALBARD (NORWAY)
J. A. Holtet and A. Brekke (Auroral Observatory, Tromso, Norway) *In* ESA, Cluster Dayside Polar Cusp Dec. 1991 p 5-9 (For primary document see N92-26294 17-46)
Copyright Avail: NTIS HC/MF A09; ESA, EPD, ESTEC, Noordwijk, Netherlands, HC 50 Dutch guilders

Observations from Svalbard, the Arctic archipelago between 10 and 35 deg east and 74 and 81 deg north are reported. The geomagnetic latitude spans from approx. 71 and 77 deg north. The high geographic latitude at a geomagnetic latitude of 75 deg, makes Svalbard an ideal place for studies of dayside aurora and processes in the magnetospheric boundary regions. Conjugacy to stations in Antarctica makes Svalbard even more attractive. The observatories at Ny-Alesund and Longyearbyen are the master stations in a network which also includes field stations at Hopen, Hornsund, Bjornoya and Jan Mayen. The core instruments are photometers, optical imagers, magnetometers and riometers. Instruments such as spectrometers and ULF/ELF/VLF receivers add to the data sets. The observations form the basis for various studies of solar wind/magnetosphere coupling, electrodynamics, transient events and other magnetospheric and boundary layer phenomena. International cooperation is essential in the program. ESA

N92-26296# Alaska Univ., Fairbanks. Inst. of Geophysics.
U.S. GROUND-BASED SPACE RESEARCH PROGRAMS IN SVALBARD (NORWAY)
C. Deehr and R. W. Smith *In* ESA, Cluster Dayside Polar Cusp Dec. 1991 p 11-14 (For primary document see N92-26294 17-46)
Copyright Avail: NTIS HC/MF A09; ESA, EPD, ESTEC, Noordwijk, Netherlands, HC 50 Dutch guilders

U.S. participation on ground based space research programs in Svalbard, mainly carried out in cooperation with Norwegian groups, is reported. Coordination of instruments, personnel, and observing time and place has proceeded on an informal, but effective basis. Most studies are tied to the CEDAR (Coupling, Energetics, and Dynamics of Atmospheric regions), GEM (Geospace Environment Modeling), and STEP (Solar Terrestrial Energy Program) programs and involve optical observations of the aurora and airglow which takes advantage of the 24 hours darkness, but there are other polar cap studies as well. The auroral station at Longyearbyenius is central to the American effort and would provide a unique base for ground based observations associated with the Cluster mission. ESA

N92-26297# Nagoya Univ., Toyokawa (Japan). STE Lab.
RESEARCH PROGRAMMES AT SVALBARD (NORWAY)
Takasi Oguti *In* ESA, Cluster Dayside Polar Cusp Dec. 1991 p 15-18 (For primary document see N92-26294 17-46)
Copyright Avail: NTIS HC/MF A09; ESA, EPD, ESTEC, Noordwijk, Netherlands, HC 50 Dutch guilders

Research programs of aurorae, ionospheric absorption, electric and magnetic fields at Svalbard for the study of polar cusp dynamics, in connection with boundary layer processes, are described. The necessity for networks of low light level television cameras, imaging riometers and magnetic stations is emphasized in conjunction with an incoherent scatter radar. The networks would provide data of fine space time resolution and serve as a reference frame for satellite measurements. Significant conjugate studies could then be made between polar ionospheric and magnetospheric phenomena. ESA

N92-26298# Academy of Sciences (USSR), Apatity. Inst. of Polar Geophysics.
THE POLAR GEOPHYSICAL INSTITUTE PROGRAM OF THE THEORETICAL AND EXPERIMENTAL INVESTIGATION ON CUSP
V. G. Pivovarov *In* ESA, Cluster Dayside Polar Cusp Dec. 1991 p 19-22 (For primary document see N92-26294 17-46)
Copyright Avail: NTIS HC/MF A09; ESA, EPD, ESTEC, Noordwijk, Netherlands, HC 50 Dutch guilders

A theoretical and experimental program for studies of electrodynamical structure of cusp, part of a general program generation of electrical fields and currents in the ionosphere and magnetosphere, is discussed. Some tasks are discussed step by step within the framework of the program, including those on calculation of the magnetic barrier near the magnetopause, geomagnetic field inside of the magnetosphere, electrical field and fluxes in the near Earth space and others. Results of the research can be used during study of the cusp problem. ESA

N92-26299# Danish Meteorological Inst., Copenhagen.
CUSP AND CLEFT STUDIES IN GREENLAND
E. Friis-Christensen *In* ESA, Cluster Dayside Polar Cusp Dec. 1991 p 27-29 (For primary document see N92-26294 17-46)
Copyright Avail: NTIS HC/MF A09; ESA, EPD, ESTEC, Noordwijk, Netherlands, HC 50 Dutch guilders

The Danish Meterological Institute (DMI) plans for the coming years are outlined with special emphasis on SPEP (Solar Terrestrial Energy Program) and Cluster Related activities. The permanent observatory at Godhavn was established on 1926 as the first permanent observatory poleward of the auroral zone. DMI has also traditionally taken an active part in international observational programs in the Arctic regions. Today the Institute is the only Danish institution carrying on ground based upper atmosphere and magnetosphere studies on a permanent basis. This is done by an

extensive network of geophysical observatories and stations on the west and east coast of Greenland. The network forms the basis for a number of cooperative studies with foreign research institutions. ESA

N92-26300# Academy of Sciences (USSR), Leningrad. Arctic and Antarctic Research Inst.
POLAR CAP BOUNDARY AND STRUCTURE OF DAYSIDE CUSP AS DETERMINED BY ION PRECIPITATION
O. A. Troshichev *In* ESA, Cluster Dayside Polar Cusp Dec. 1991 p 31-34 (For primary document see N92-26294 17-46)
Copyright Avail: NTIS HC/MF A09; ESA, EPD, ESTEC, Noordwijk, Netherlands, HC 50 Dutch guilders

The results of particle measurements on board DMSP (Defense Meteorological Satellite Program) F6 and F7 spacecraft show that the ion precipitation features in the auroral oval and in the polar cap are systematically diverse: the ion precipitation in the oval is of a smoothed character, whereas that in the polar cap is of a patchy type. The boundary between these two types of ion precipitation can usually be detected by a quick fall in the ion total number flux below some definite level. The polar cap identified in such a way has a shape of a roughly Sun aligned ellipse when IMF (Interplanetary Magnetic Field) is northward. Under the influence of the azimuthal IMF the northern polar cap is shifted toward the dusk (dawn) when B sub y is greater than 0 (B sub y is less than 0). In the southern polar cap the effect is opposite. The following structural zones in the dayside oval can be separated using the ion data: cusp, cusp core (near the noon meridian), poleward edge of the cusp, equatorward edge of the cusp. ESA

N92-26301# British Antarctic Survey, Cambridge (England).
ANTARCTIC STUDIES OF THE CUSP
A. S. Rodger *In* ESA, Cluster Dayside Polar Cusp Dec. 1991 p 35-41 (For primary document see N92-26294 17-46)
Copyright Avail: NTIS HC/MF A09; ESA, EPD, ESTEC, Noordwijk, Netherlands, HC 50 Dutch guilders

Results from Antarctic studies are summarized. The advantages of these results from the very large displacement of the geographic and geomagnetic poles, there being a land mass upon which to deploy experiments, and a pollution free environment in which to make observations, are considered. In recent years, important results concerning the coupling of solar wind processes through the magnetosphere and into the ionosphere were determined using Antarctic datasets. The present and planned observing programs that are likely to be in place during the Cluster mission are also described. ESA

N92-26302# European Space Agency. European Space Research and Technology Center, ESTEC, Noordwijk (Netherlands). Space Science Dept.
LESSON LEARNED FROM GEOS AND ISEE
Arne Pedersen *In its* Cluster Dayside Polar Cusp Dec. 1991 p 47-51 (For primary document see N92-26294 17-46)
Copyright Avail: NTIS HC/MF A09; ESA, EPD, ESTEC, Noordwijk, Netherlands, HC 50 Dutch guilders

The GEOS and ISEE (International Sun Earth Explorers) 1 and 2 spacecraft were central spacecraft in the International Magnetospheric Study (IMS) initiated in 1976. These missions are reviewed with the aim of improvements for the Cluster mission. These spacecrafts had new instruments based on the experience of the first years in magnetospheric research, and the IMS aimed at comparing data from many instruments on spacecraft and between many different spacecraft and ground observations. Valuable science was produced on the basis of the data from these missions. However some of the more ambitious aims were not reached, partly because the technical means (computers, networks and storage media) were not sufficiently developed to deal with such a tremendous task. Certain organizational aspects could also have been improved. ESA

N92-26303# Rutherford High Energy Lab., Chilton (England).
INCOHERENT SCATTER RADAR MEASUREMENTS OF THE CUSP
Mike Lockwood *In* ESA, Cluster Dayside Polar Cusp Dec. 1991 p 57-65 (For primary document see N92-26294 17-46)
Copyright Avail: NTIS HC/MF A09; ESA, EPD, ESTEC, Noordwijk, Netherlands, HC 50 Dutch guilders

The effects of cusp particle precipitation have not been conclusively identified in data from Incoherent Scatter (IS) radars. For radars on the American continent, cusp effects have tended to be masked by the antiSunward transport of plasma which has been enhanced by photoionization on the dayside and by the high ion temperatures which are regularly, but not always, found in the cusp. The cusp is usually defined by the particle precipitation spectrum, and the relationships of all three magnetosheath like precipitations (cusp, cleft and mantle) to magnetospheric field topology are discussed. Combined satellite/IS observations have demonstrated that for southward IMF (Interplanetary Magnetic Field), the cusp lies on newly opened field lines which are moved east or west by magnetic tension, depending upon, polarity of the IMF B sub y component. This gives a powerful method by which the southward IMF cups can be identified on IS data, particularly when combined with optical observations of the dayside aurora, as can be made from Svalbard (Arctic). ESA

N92-26304# Johns Hopkins Univ., Laurel, MD. Applied Physics Lab.
CUSP STUDIES WITH HF RADARS
R. A. Greenwald, K. B. Baker, J. M. Ruohoniemi, J. R. Dudeney, and M. Pinnock (British Antarctic Survey, Cambridge, England) *In* ESA, Cluster Dayside Polar Cusp Dec. 1991 p 67-75 (For primary document see N92-26294 17-46)
Copyright Avail: NTIS HC/MF A09; ESA, EPD, ESTEC, Noordwijk, Netherlands, HC 50 Dutch guilders

Several years of significant contributions by HF coherent radars to the understanding of the physical characteristics of the ionospheric footprint of the magnetospheric cusp are discussed. It has been found to be a region of high velocity turbulence in which there is an abundance of irregularity structure. Simultaneous conjugate observations of ionospheric convection near the cusp have revealed flow patterns consistent with statistical and empirical patterns that have been derived by other workers. Changes in these patterns occur on time scales of a few minutes. There is evidence that current surges in the high latitude cusp and cleft may excite atmospheric gravity waves which propagate to lower latitudes. ESA

N92-26305# EISCAT Scientific Association, Kiruna (Sweden).
PLANS FOR THE EISCAT SVALBARD (NORWAY) RADAR
J. Roettger *In* ESA, Cluster Dayside Polar Cusp Dec. 1991 p 77-80 (For primary document see N92-26294 17-46)
Copyright Avail: NTIS HC/MF A09; ESA, EPD, ESTEC, Noordwijk, Netherlands, HC 50 Dutch guilders

The EISCAT Scientific Association operates incoherent scatter radars in northern Europe for studies of the auroral ionosphere and upper atmosphere. The plan for a extension of the EISCAT facilities to investigate phenomena on the cusp/cleft region and the polar cap by constructing an additional radar on Svalbard is addressed. The scientific rationale behind these plans is described and an outline of the possible instrumental configuration is given. ESA

N92-26306# Swedish Inst. of Space Physics, Kiruna.
THE PRESENT UNDERSTANDING OF THE CUSP
R. Lundin, J. Woch, and M. Yamauchi *In* ESA, Cluster Dayside Polar Cusp Dec. 1991 p 83-95 Sponsored by Swedish Board for Space Activities (For primary document see N92-26294 17-46)
Copyright Avail: NTIS HC/MF A09; ESA, EPD, ESTEC, Noordwijk, Netherlands, HC 50 Dutch guilders

Knowledge learnt on the dynamics and topology of the polar cusp from in situ plasma measurements primarily on board low and medium altitude satellite is reviewed. The polar cusp, first identified from low altitude orbiting satellites, is the only region in the topside terrestrial ionosphere that maintains continuous contact with plasma. The continuous inflow of plasma through the cusp

leads to a direct transfer of solar wind energy and momentum to the ionosphere and atmosphere. Thus, the cusp represents a particular 'hot spot' in the solar terrestrial relationship. New improved magnetic field mapping models have helped elucidating the connection of the low altitude cusp to the magnetospheric boundary region. ESA

N92-26307# Danish Meteorological Inst., Copenhagen.
SOLAR WIND-MAGNETOSPHERE COUPLING PROCESSES OBSERVED NEAR THE DAYSIDE CUSP/CLEFT
E. Friis-Christensen and K. H. Glassmeier (Cologne Univ., Germany, F.R.) *In* ESA, Cluster Dayside Polar Cusp Dec. 1991 p 97-103 (For primary document see N92-26294 17-46)
Copyright Avail: NTIS HC/MF A09; ESA, EPD, ESTEC, Noordwijk, Netherlands, HC 50 Dutch guilders

The physical processes involved on solar wind magnetosphere coupling are rather complex and not possible to describe adequately by means of single point measurements. Even in the case of multiple spacecraft mission: like Cluster, future investigations will have to rely on the full spectrum of available observations, including found based measurements in the cusp and cleft region. Some of the unsolved problems on solar wind magnetosphere coupling are identified and the capabilities of using modern dedicated ground based research facilities to obtain 'maps' of highly dynamic ionospheric signatures of magnetosphere boundary layer processes are demonstrated. These 'maps' may provide crucial information about the distribution and motion of the sources of the processes. ESA

N92-26308# National Aeronautics and Space Administration. Goddard Space Flight Center, Greenbelt, MD.
THE IONOSPHERIC SIGNATURE OF FLUX TRANSFER EVENTS
S. W. H. Cowley, M. P. Freeman, Mike Lockwood (Rutherford High Energy Lab., Chilton, England), and M. F. Smith *In* ESA, Cluster Dayside Polar Cusp Dec. 1991 p 105-112 (For primary document see N92-26294 17-46)
Copyright Avail: NTIS HC/MF A09; ESA, EPD, ESTEC, Noordwijk, Netherlands, HC 50 Dutch guilders

The effects at ionospheric heights which take place when transient reconnection events (i.e., Flux Tranfer Events (FTEs)) occur at the dayside magnetopause are considered. The nature of the FTE related ionospheric flows, the associated current systems, and the plasma precipitation, are discussed. In particular, the nature of the time dependent cusp precipitation which occurs on this case is outlined and expectations are compared with those based on steady magnetopause reconnection. ESA

N92-26309# Swedish Inst. of Space Physics, Uppsala.
MAPPING OF THE AURORAL OVAL TO THE TAIL
Georg Gustafsson *In* ESA, Cluster Dayside Polar Cusp Dec. 1991 p 113-117 (For primary document see N92-26294 17-46)
Copyright Avail: NTIS HC/MF A09; ESA, EPD, ESTEC, Noordwijk, Netherlands, HC 50 Dutch guilders

Three different cases of mapping between the ionosphere and the magnetotail are discussed. It has become possible to use multisatellite measurements to study auroral substorms. Global satellite images of the auroral can be combined with simultaneous particle and field measurements at geosynchronous altitude and in the magnetotail. The main tool to relate observations on different regions of the magnetosphere is a magnetic field model and it is, therefore, of crucial importance in studies of substorm phenomena. These studies indicate the development of and the need for further improvements for the auroral source regions in the tail. ESA

N92-26310# Swedish Inst. of Space Physics, Kiruna.
THE NEED OF COORDINATED OBSERVATIONS IN SPACE AND FROM GROUND
Bengt Hultqvist *In* ESA, Cluster Dayside Polar Cusp Dec. 1991 p 123-127 (For primary document see N92-26294 17-46)
Copyright Avail: NTIS HC/MF A09; ESA, EPD, ESTEC, Noordwijk, Netherlands, HC 50 Dutch guilders

The different role of ground based and spacecraft measurements are reviewed. The importance of the ground based measurements for the satellite projects is discussed. The ground based global observatory networks provide necessary reference systems for the 'front line' measurements on board satellites. Investigations of dynamic phenomena on a global scale depend primarily on the ground based networks, which provide continuity in space and time, but satellites contribute local observations of great importance for the progress of the research. The need of coordination of many kinds of measurements characterizes the solar terrestrial physics field. The main international coordinated program in the 90s is STEP (Solar Terrestrial Energy Program). ESA

N92-26311# National Center for Atmospheric Research, Boulder, CO. High Altitude Observatory.
GROUND-BASED STUDIES OF SENSING MAGNETOSPHERE/IONOSPHERE INTERACTIONS: CONVECTION AND SUBSTORMS
Y. Kamide (Kyoto Sangyo Univ., Japan) and A. D. Richmond *In* ESA, Cluster Dayside Polar Cusp Dec. 1991 p 129-137 (For primary document see N92-26294 17-46)
(Contract NASw-17384)
Copyright Avail: NTIS HC/MF A09; ESA, EPD, ESTEC, Noordwijk, Netherlands, HC 50 Dutch guilders

The importance of coordinated satellite and ground based observations in studies of 'ionosphere magnetosphere interactions' is stressed by showing examples of ionspheric electrodynamic parameters. Satellite and radar measurements of the ionospheric drift velocity, along with ground based magnetometer observations for 25 Oct. 1981, were combined to estimate instantaneous patterns of electric fields and currents in the high latitude ionosphere, using an updated version of the AMIE (Assimilative Mapping of Ionospheric Electrodynamics) technique. The period under study was characterized by a relatively stable southward IMF (Interplanetary Magnetic Field), so that the obtained electric field patterns reflect, in general, the state of sustained and enhanced plasma convection on the magnetosphere. During one of the satellite passes, an intense westward electrojet caused by a substorm intruded into the satellite and radar field of view on the premidnight sector, providing a unique opportunity to differentiate the enhanced convection and substorm expansion fields. The calculated potential distributions for the expansion phase of the substorm are indeed of general two cell patterns, but the night-morning cell has two positive peaks, one on the midnight sector and the other in the late morning hours, corresponding to the substorm expansion and the convection enhancement, respectively. ESA

N92-26312# Leningrad State Univ. (USSR). Inst. of Physics.
A MODEL OF THE DAYSIDE MAGNETOSPHERE AND BREAKUPS IN THE CUSP REGION
M. I. Pudovkin *In* ESA, Cluster Dayside Polar Cusp Dec. 1991 p 139-144 (For primary document see N92-26294 17-46)
Copyright Avail: NTIS HC/MF A09; ESA, EPD, ESTEC, Noordwijk, Netherlands, HC 50 Dutch guilders

A model of geomagnetic field in the dayside magnetosphere is discussed. The model is based on the supposition of the partial penetration of the magnetosheath's magnetic field into the magnetosphere in the vicinity of the reconnection line at the magnetopause. Configurations of the plasma in the vicinity of that line is analyzed, and electric field equipotentials are projected onto the polar ionosphere along the field lines of the model geomagnetic field. Effects of the potential and vortex components of the magnetopause electric field on the dynamics of the aurorae in the cusp region are discussed. On the basis of the model proposed, an interpretation of the auroral dynamics in the cusp region is given. ESA

N92-26313# Finnish Meteorological Inst., Helsinki.
OPTICAL GROUND-BASED NETWORK

R. Pellinen and K. Kaila (Oulu Univ., Finland) *In* ESA, Cluster Dayside Polar Cusp Dec. 1991 p 147-158 (For primary document see N92-26294 17-46)
Copyright Avail: NTIS HC/MF A09; ESA, EPD, ESTEC, Noordwijk, Netherlands, HC 50 Dutch guilders

The development of ground based optical observations of aurora is summarized. Existing optical networks in the Northern Hemisphere are described emphasizing the Scandinavia/Svalbard (Arctic) sector. Different observational techniques covering all sky photography, television cameras, photometers, spectrometers, and interferometers, are described. The physical limits and usefulness of the different techniques are critically reviewed. Some data examples are presented to demonstrate the capabilities of the different methods. Need for improvement and extension of the present networks is discussed. The specific problem of ground based optical support to the forthcoming Cluster and EISCAT Svalbard radar programs is detailed. ESA

N92-26314# Cologne Univ. (Germany, F.R.). Inst. fuer Geophysik und Meteorologie.
IMAGING THE EARTH'S MAGNETOSPHERE USING GROUND MAGNETOMETER ARRAYS
K. H. Glassmeier and E. Friis-Christensen (Danish Meteorological Inst., Copenhagen.) *In* ESA, Cluster Dayside Polar Cusp Dec. 1991 p 159-166 (For primary document see N92-26294 17-46)
Copyright Avail: NTIS HC/MF A09; ESA, EPD, ESTEC, Noordwijk, Netherlands, HC 50 Dutch guilders

A magnetometer array may be regarded as a telescope allowing imaging of magnetospheric dynamics in the ulta low frequency, near DC range of the electromagnetic spectrum. The field of view of such an array lies in the range of several thousand km depending on the array's size. The resolution is typically of the order of 50 to 100 km in the ionosphere, i.e., 1500 to 300 km in the magnetosphere. Highly sophisticated image processing tools were developed which make magnetometer arrays a very important tool to complement in situ measurements such as planned for the Cluster project. One of the aims of this project is the study of small scale plasma processes in, for example, the dayside polar cusp region. As the archipelago of Svalbard (Arctic) lies within the region of the northern polar cusp the installation of an international magnetometer array on Spitsbergen is strongly suggested. ESA

N92-26315# Academy of Sciences, Graz (Austria). Inst. of Space Research.
BALLOONS FOR CONJUGATE CUSP STUDIES IN THE 1990'S
W. Riedler, Iver B. Iversen (SPW, Birkerod, Denmark), and K. M. Torkar *In* ESA, Cluster Dayside Polar Cusp Dec. 1991 p 171-178 (For primary document see N92-26294 17-46)
Copyright Avail: NTIS HC/MF A09; ESA, EPD, ESTEC, Noordwijk, Netherlands, HC 50 Dutch guilders

The advantages of balloonborne measurements for magnetospheric studies is reviewed and a scenario of possible balloon, campaigns during the Cluster mission, with emphasis on the dayside polar cap region, is proposed. The proposal is preceded by a description of earlier and similar campaigns carried out in northen Europe and the Svalbard Islands (Arctic). ESA

N92-26316# European Space Agency. European Space Research and Technology Center, ESTEC, Noordwijk (Netherlands).
THE REQUIREMENTS FOR DATA EXCHANGE BETWEEN CLUSTER AND GROUND-BASED OBSERVATORIES, USING EISCAT AS AN ILLUSTRATIVE EXAMPLE
E. Dunford (Rutherford High Energy Lab., Chilton, England), R. Schmidt, and D. M. Willis *In its* Cluster Dayside Polar Cusp Dec. 1991 p 183-190 (For primary document see N92-26294 17-46)
Copyright Avail: NTIS HC/MF A09; ESA, EPD, ESTEC, Noordwijk, Netherlands, HC 50 Dutch guilders

The Cluster data system is described using EISCAT as an illustrative example for coordinated measurement campaigns. The formation of dedicated working group to coordinate observations by Cluster and ground based observatories implies the need for a ground data system that enables fast and reliable access to data bases. These data bases will not only hold science data derived from Cluster and ground observations, but also datasets required for the planning of joint measurement campaigns. These could include Cluster orbital information, schedules of ground observatories, access to plasma and field models, etc. There is a clear requirement that all participants follow standardized procedures when generating these data sets, in order to permit an efficient intercomparison of plasma quantities measured in space, in the ionosphere, and on the ground. ESA

N92-26317# Centre de Recherches en Physique de l'Environnement, Issy-les-Moulineaux (France).
RELATIONSHIPS BETWEEN IONOSPHERIC AND TAIL PHENOMENA
S. Perraut and J. A. Sauvaud (Centre d'Etude Spatiale des Rayonnements, Toulouse, France) *In* ESA, Cluster Dayside Polar Cusp Dec. 1991 p 191-201 Sponsored by CNRS, and CNES (For primary document see N92-26294 17-46)
Copyright Avail: NTIS HC/MF A09; ESA, EPD, ESTEC, Noordwijk, Netherlands, HC 50 Dutch guilders

Large scale processes taking place in the magnetotail and their consequences upon the ionosphere are addressed. The topics were selected in the light of the new information that can be expected from the Cluster mission and from the associated ground based measurements. Plasma convection is discussed, in particular, an attempt is made to establish the link between the classical picture of the convection at the ionospheric level and its magnetospheric projection. It is shown that Cluster can help to determine the location and the shape of the Harang discontinuity in the magnetosphere provided that the spacecraft are close enough to the Earth. The existence of the steady state convection is questioned in light of recent models. The relation between convection and magnetic activity is discussed. The mapping between auroral arcs and the various magnetospheric boundaries is investigated. Plasma dynamics in the midtail and in the inner plasma sheet is described with particular emphasis on some of the models proposed for substorms. Suggestions are made about complementary measurements to be performed by Cluster and ground based instruments to understand plasma circulation in the magnetosphere and its relation to substorms. ESA

N92-26318# Rutherford High Energy Lab., Chilton (England).
REQUIREMENTS FOR COORDINATED CLUSTER AND GROUND-BASED OBSERVATIONS OF THE CUSP
Mike Lockwood *In* ESA, Cluster Dayside Polar Cusp Dec. 1991 p 203-207 (For primary document see N92-26294 17-46)
Copyright Avail: NTIS HC/MF A09; ESA, EPD, ESTEC, Noordwijk, Netherlands, HC 50 Dutch guilders

The spatial and temporal resolutions and the fields of view required of ground based observations of the cusp are discussed by considering a typical example of a dayside auroral transient and plasma flow burst. Systems meeting such specifications would also be ideal for studying traveling convection vortices and would undoubtly reveal new spatial structure and temporal behavior of the cusp region. The implications of the Cluster orbit characteristics for coordinated cusp observations with ground based instruments are discussed. ESA

N92-26319# Academy of Sciences (USSR), Novosibirsk. Computer Center.
MATHEMATICAL MODEL OF PHYSICAL PROCESSES RESPONSIBLE FOR GENERATION OF MAGNETOSPHERIC ELECTRIC FIELDS AND THEIR PENETRATION INTO THE EARTH'S MAGNETOSPHERE
V. V. Denisenko, N. V. Erkaev, S. S. Zamay, A. V. Kitaev, A. V. Mezentsev, I. T. Matveenkov, and V. G. Pivovarov (Academy of Sciences, USSR, Apatity) *In* ESA, Cluster Dayside Polar Cusp Dec. 1991 p 211-216 (For primary document see N92-26294

17-46)
Copyright Avail: NTIS HC/MF A09; ESA, EPD, ESTEC, Noordwijk, Netherlands, HC 50 Dutch guilders

A program for the theoretical studies of generation of electric fields and currents in the ionosphere and magnetosphere connected with the interaction of the solar wind and the Earth's magnetic field is presented. Because of the problem complexity, it is divided into subsequent steps. The starting point of the program is a problem of formation of a magnetic barrier near the magnetopause which is the key for the whole magnetospheric physics. The important step of the program is generation of electric field in the magnetosphere due to viscous interaction and a process of reconnection. The proposed program can serve as a theoretical basis for planned global satellite and ground project. ESA

N92-26329# Deutsche Forschungsanstalt fuer Luft- und Raumfahrt, Oberpfaffenhofen (Germany, F.R.). Inst. fuer Physik der Atmosphaere.
CONTRIBUTIONS TO ATMOSPHERIC PHYSICS IN HONOR OF DR. MANFRED REINHARDT ON HIS 65TH BIRTHDAY [BEITRAEGE ZUR PHYSIK DER ATMOSPHAERE, GEWIDMET DR. MANFRED REINHARDT ZUM 65 GEBURTSTAG]
Ulrich Schumann, ed. and Klaus-Peter Hoinka, ed. Sep. 1991 229 p In ENGLISH and GERMAN Original contains color illustrations
(DLR-FB-91-30; ISSN-0939-2963; ETN-92-91389) Avail: NTIS HC/MF A11; DLR, Wissenschaftliches, Berichtswesen, Postfach 90 60 58, Cologne, Fed.Republic of Germany, HC 60 Deutsche marks

Theoretical, analytical and numerical work on the tropospheric process are discussed. The Eady model is reformulated. Vortex interaction and potential vorticity inversion are examined. Transport paths of air pollutions are investigated. Frontogenetical structures are compared. A simple model is derived for the convective boundary layer. The stability of barotropic vortices is studied. Aircraft observatories of a small scale solitary wave are reported. Climatic observations are presented. The existence of a capital similarity is assessed: ozone trends are given. Measuring systems are described. Results of field experiments are reported. For individual titles, see N92-26330 through N92-26350.

N92-26330# Eidgenoessische Technische Hochschule, Zurich (Switzerland). Atmospheric Physics.
A REFORMULATION OF THE EADY MODEL
Huw C. Davies *In* DLR, Contributions to Atmospheric Physics in Honor of Dr. Manfred Reinhardt on His 65th Birthday Sep. 1991 p 3-9 (For primary document see N92-26329 17-46)
Avail: NTIS HC/MF A11; DLR, Wissenschaftliches, Berichtswesen, Postfach 90 60 58, Cologne, Fed.Republic of Germany, HC 60 Deutsche marks

The perturbations of the classical Eady model are cast in the form of two coupled edge waves. This reformulation provides a compact and quantitative example of the wave coupling interpretation of quasi-geostrophic instabilities. This approach illustrates the twin effects of amplitude coupling and phase speed modulation, indicates the necessary conditions for synchronized growth and phase locking of the two waves, and highlights the difference between initial value and normal mode flow development. ESA

N92-26331# Technische Univ., Munich (Germany, F.R.). Inst. fuer Meteorologie.
UPPER/LOWER VORTEX INTERACTION AND POTENTIAL VORTICITY INVERSION
Joseph Egger *In* DLR, Contributions to Atmospheric Physics in Honor of Dr. Manfred Reinhardt on His 65th Birthday Sep. 1991 p 11-20 (For primary document see N92-26329 17-46)
Avail: NTIS HC/MF A11; DLR, Wissenschaftliches, Berichtswesen, Postfach 90 60 58, Cologne, Fed.Republic of Germany, HC 60 Deutsche marks

Upper/lower vortex interaction is studied using balance models where all flow variables are derived through an inversion of the potential vorticity distribution. The motion of vortices in shear flow so that an upper level vortex may move over a low level vortex is considered. Such models are found to help in understanding the interaction process. In particular, the inversion procedure predicts the pronounced deepening of the upper level trough if the upper vortex is located above the lower vortex. ESA

N92-26332# Deutsche Forschungsanstalt fuer Luft- und Raumfahrt, Oberpfaffenhofen (Germany, F.R.). Inst. fuer Physik der Atmosphaere.
NOXIOUS MATTER TRANSPORTATION IN THE ALPINE REGIONS [SCHADSTOFFTRANSPORTE IN DIE ALPENREGION] **c45**
Jutta Graf and Dieter Heimann *In its* Contributions to Atmospheric Physics in Honor of Dr. Manfred Reinhardt on His 65th Birthday Sep. 1991 p 21-26 In GERMAN; ENGLISH summary Original contains color illustrations (For primary document see N92-26329 17-46)
Avail: NTIS HC/MF A11; DLR, Wissenschaftliches, Berichtswesen, Postfach 90 60 58, Cologne, Fed.Republic of Germany, HC 60 Deutsche marks

Transport paths of air pollutions originating from major emission sources around the Alps are investigated using a mesoscale model. Eight numerical experiments of a daily cycle with varying direction of the prescribed large scale air flow yield typical mesoscale flow patterns modified by the Alpine orography. The simulations show that air pollutants are carried into the Alpine area only for three distinct large scale flow directions, but are transported around the Alps or remain in Alpine forelands for other directions. ESA

N92-26333# Bonn Univ. (Germany, F.R.). Inst. fuer Meteorologie.
COMPARISON OF FRONTOGENETICAL STRUCTURES FOR DIFFERENT CASES OF FRONTAL DEVELOPMENT **c47**
Helmut Kraus *In* DLR, Contributions to Atmospheric Physics in Honor of Dr. Manfred Reinhardt on His 65th Birthday Sep. 1991 p 27-40 (For primary document see N92-26329 17-46)
Avail: NTIS HC/MF A11; DLR, Wissenschaftliches, Berichtswesen, Postfach 90 60 58, Cologne, Fed.Republic of Germany, HC 60 Deutsche marks

The frontogenetical structures for five cases of meso and synoptic scale fronts are presented, demonstrating that the knowledge of the frontogenetical terms can serve for understanding the manifold phenomena in a frontal region. The following case studies are presented: a mesoscale sea breeze front; a synoptic scale quasi-geostrophic cold front; a synoptic model simulated cold front. The differences of the frontogenesis terms and of the forcing mechanisms for the cross frontal circulations become evident. ESA

N92-26334# Deutsche Forschungsanstalt fuer Luft- und Raumfahrt, Oberpfaffenhofen (Germany, F.R.). Inst. fuer Physik der Atmosphaere.
A SIMPLE MODEL FOR THE CONVECTIVE BOUNDARY LAYER OVER WAVY TERRAIN WITH VARIABLE HEAT FLUX **c45**
Ulrich Schumann *In its* Contributions to Atmospheric Physics in Honor of Dr. Manfred Reinhardt on His 65th Birthday Sep. 1991 p 41-50 (For primary document see N92-26329 17-46)
Avail: NTIS HC/MF A11; DLR, Wissenschaftliches, Berichtswesen, Postfach 90 60 58, Cologne, Fed.Republic of Germany, HC 60 Deutsche marks

A simple analytical model for the convective boundary layer over a wavy surface with variable surface heat flux and for zero mean wind is derived. The flow domain is approximated by four control volumina. Results from large eddy simulations and observations from motorgliders support the model up to a factor of two, but also show that small scale thermals which are not resolved by the presented model may be important. The model shows that scales smaller than the depth of the boundary layer should be of small relevance for climate modeling. ESA

N92-26335# Technische Univ., Munich (Germany, F.R.). Inst. fuer Meteorologie.

THE STABILITY OF BAROTROPIC VORTICES: IMPLICATIONS FOR TROPICAL CYCLONE MOTION **c47**

Harry C. Weber and Roger K. Smith *In* DLR, Contributions to Atmospheric Physics in Honor of Dr. Manfred Reinhardt on His 65th Birthday Sep. 1991 p 51-63 (For primary document see N92-26329 17-46)

(Contract N00014-90-J-1487)

Avail: NTIS HC/MF A11; DLR, Wissenschaftliches, Berichtswesen, Postfach 90 60 58, Cologne, Fed.Republic of Germany, HC 60 Deutsche marks

The existence of normal mode perturbations to barotropic vortices defined by tangential velocity profiles used in studies of tropical cyclone motion is investigated. For this purpose, a method to search systemically for the eigensolutions is developed. No unstable modes were found for relatively broad vortices, but a single neutral mode with zero frequency exists. One relatively narrow profile was found to have an unstable wavenumber two mode. The implications concerning vortex motion in nondivergent, barotropic models relevant to tropical cyclones are discussed. ESA

N92-26336# Deutsche Forschungsanstalt fuer Luft- und Raumfahrt, Oberpfaffenhofen (Germany, F.R.). Inst. fuer Physik der Atmosphaere.

AIRCRAFT OBSERVATION OF A SMALL-SCALE SOLITARY WAVE NEAR THE TROPOPAUSE

Thomas Hauf *In its* Contributions to Atmospheric Physics in Honor of Dr. Manfred Reinhardt on His 65th Birthday Sep. 1991 p 65-70 (For primary document see N92-26329 17-46)

Avail: NTIS HC/MF A11; DLR, Wissenschaftliches, Berichtswesen, Postfach 90 60 58, Cologne, Fed.Republic of Germany, HC 60 Deutsche marks

Aircraft observations at 10,100 m height provide evidence for a small scale solitary wave with 130 m half amplitude width. The instant snapshot taken with the aircraft is consistent with what is known from solitary waves. The measurements are discussed and the structures of the solitary wave are analyzed. ESA

N92-26337# Hamburg Univ. (Germany, F.R.). Inst. fuer Meteorologie.

INVESTIGATION OF CONVECTION OVER SEA BY AIRCRAFT OBSERVATIONS [FLUGZEUGMESSUNGEN ZUR KONVEKTION UEBER SEE] **c43**

Hans Hinzpeter *In* DLR, Contributions to Atmospheric Physics in Honor of Dr. Manfred Reinhardt on His 65th Birthday Sep. 1991 p 71-86 In GERMAN; ENGLISH summary (For primary document see N92-26329 17-46)

Avail: NTIS HC/MF A11; DLR, Wissenschaftliches, Berichtswesen, Postfach 90 60 58, Cologne, Fed.Republic of Germany, HC 60 Deutsche marks

Results of aircraft observations over the North Sea and the Greenland Sea are given. Their interpretation by different numerical models is discussed. It is shown that the model results depend on the parameterization of the vertical exchange, and that the development of open cells is still not understood. ESA

N92-26338# Deutsche Forschungsanstalt fuer Luft- und Raumfahrt, Oberpfaffenhofen (Germany, F.R.). Inst. fuer Physik der Atmosphaere.

MESOSCALE OBSERVATIONS OF A COLD FRONT ASSOCIATED WITH A PREFRONTAL HAILSTORM **c47**

Klaus P. Hoinka *In its* Contributions to Atmospheric Physics in Honor of Dr. Manfred Reinhardt on His 65th Birthday Sep. 1991 p 87-97 Original contains color illustrations (For primary document see N92-26329 17-46)

Avail: NTIS HC/MF A11; DLR, Wissenschaftliches, Berichtswesen, Postfach 90 60 58, Cologne, Fed.Republic of Germany, HC 60 Deutsche marks

The analyses of data taken during the passage of a cold front are discussed. The change in temperature and pressure related to the front suggests that there was an intensification of the cold front as it moved towards the east. These changes decrease apparantly towards the north, away from the Alps. Cross frontal structures are similar to those observed in Australian cold fronts: prefrontal low level jet and postfrontal flow towards the leading edge of the cold air. ESA

N92-26339# Consejo Superior de Investigaciones Cientificas, Madrid (Spain). Inst. de Estructura de la Materia.

UNDULATORY AIRFLOW OVER THE SPANISH SOUTHERN CENTRAL HIGHPLAIN WITH NORTHERN WINDS

Jaime Julve *In* DLR, Contributions to Atmospheric Physics in Honor of Dr. Manfred Reinhardt on His 65th Birthday Sep. 1991 p 99-106 (For primary document see N92-26329 17-46)

Avail: NTIS HC/MF A11; DLR, Wissenschaftliches, Berichtswesen, Postfach 90 60 58, Cologne, Fed.Republic of Germany, HC 60 Deutsche marks

The occurrence of soarable undulatory airflow in the southern lee of the Sistema Central (Spain) with northern winds in the period Jan. 1979 to Mar. 1984 is studied. Weather charts, soundings and pilot reports are used. An average of eleven cases per year is found, mainly concentrated in fall, winter and spring. ESA

N92-26340# Deutsche Forschungsanstalt fuer Luft- und Raumfahrt, Oberpfaffenhofen (Germany, F.R.). Inst. fuer Physik der Atmosphaere.

CIRRUS CLOUDS AND CONDENSATION TRAIL ON 18 OCT. 1989 OVER THE NORTH SEA (ICE '89). DETERMINATION OF HEIGHT AND OPTICAL DEPTH USING ALEX, AVHRR AND HIRS [CIRREN UND KONDENSSTREIFEN AM 18-10-89 UEBER DER NORDSEE (ICE '89): EMITTLUNG VON HOEHE UND OPTISCHER DICKE MIT ALEX, AVHRR UND HIRS]

Martina Kaestner, Karl-Theodor Kriebel, Ralf Meerkoetter, Wolfgang Renger, Gerhard Ruppersberg, and Peter Wendling *In its* Contributions to Atmospheric Physics in Honor of Dr. Manfred Reinhardt on His 65th Birthday Sep. 1991 p 107-123 In GERMAN Original contains color illustrations (For primary document see N92-26329 17-46)

Avail: NTIS HC/MF A11; DLR, Wissenschaftliches, Berichtswesen, Postfach 90 60 58, Cologne, Fed.Republic of Germany, HC 60 Deutsche marks

Data from International Cloud Experiment (ICE) on the height and optical depth of cirrus clouds obtained either by the Aircraftborne Aerosol Experiment (ALEX), or by satellite observations, Advanced Very High Resolution Radiometer (AVHRR) and High resolution Infrared Radiation Sounder (HIRS), are compared. It is shown that a 30 percent agreement is to be expected with regard to error estimation. The comparison between satellite data and aircraft observations of derived cloud parameters, shows that satellite data can give quantitative information on the physical properties of clouds. ESA

N92-26341*# National Center for Atmospheric Research, Boulder, CO.

CONVECTION WAVE STUDIES OVER LAND AND SEA

Joachim Kuettner and Robert Grossmann (Colorado Univ., Boulder.) *In* DLR, Contributions to Atmospheric Physics in Honor of Dr. Manfred Reinhardt on His 65th Birthday Sep. 1991 p 125-140 Original contains color illustrations (For primary document see N92-26329 17-46)

(Grants NAG1-115; NSF ATM-89-18879)

Avail: NTIS HC/MF A11; DLR, Wissenschaftliches, Berichtswesen, Postfach 90 60 58, Cologne, Fed.Republic of Germany, HC 60 Deutsche marks

Preliminary results of recent case studies conducted over land and sea are given. Two dimensional convection (roll vortex/cloudstreet) and three dimensional convection in the underlying boundary layer are dealt with. Vertical momentum flux profiles and time series of important parameters and vertical soundings taken in the experiment area are shown. The three cases described show that convection waves occur over land and over ocean, over three dimensional convection and over two dimensional convection. ESA

N92-26342# Deutsche Forschungsanstalt fuer Luft- und Raumfahrt, Oberpfaffenhofen (Germany, F.R.). Inst. fuer Physik der Atmosphaere.

PRECIPITATION FORMATION PROCESSES IN CONVECTIVE AND STRATIFORM CLOUDS AS DEDUCED BY COORDINATED POLARIMETRIC RADAR AND AIRCRAFT MEASUREMENTS **c47**

Peter Meischner, Martin Hagen, and Hartmut Hoeller *In its* Contributions to Atmospheric Physics in Honor of Dr. Manfred Reinhardt on His 65th Birthay Sep. 1991 p 141-149 Original contains color illustrations (For primary document see N92-26329 17-46)

Avail: NTIS HC/MF A11; DLR, Wissenschaftliches, Berichtswesen, Postfach 90 60 58, Cologne, Fed.Republic of Germany, HC 60 Deutsche marks

For two different case studies, an upslope situation and a multicell hailstorm, the processes of precipitation formation were analyzed using radar, Doppler, polarimetric and coordinated aircraft measurements. In the upslope situation, low density pristine dendrites were formed. Subsequent riming of these particles during their fallout resulted in irregular shapes and a tumbling fall behavior. The hail formation in the thunderstorm studied was connected with recirculations of graupels and raindrops into the main updraft of the storm. ESA

N92-26343# Innsbruck Univ. (Austria). Inst. fuer Meteorologie und Geophysik.

THE OBJECTIVE DETERMINATION OF FRONT LINES [ZUR OBJEKTIVEN BESTIMMUNG VON FRONTLINIEN] **c47**

Reinhold Steinacker *In* DLR, Contributions to Atmospheric Physics in Honor of Dr. Manfred Reinhardt on His 65th Birthday Sep. 1991 p 151-159 In GERMAN (For primary document see N92-26329 17-46)

Avail: NTIS HC/MF A11; DLR, Wissenschaftliches, Berichtswesen, Postfach 90 60 58, Cologne, Fed.Republic of Germany, HC 60 Deutsche marks

A method for the objective determination of front lines is presented. Possible climatologic frontal definitions are given. Any atmospheric scalar variable can be used. The application is discussed in the light of a case examined during the German 1987 front experiment. It is shown that single lines no longer coincide in the mesoscale. ESA

N92-26344# Deutsche Forschungsanstalt fuer Luft- und Raumfahrt, Oberpfaffenhofen (Germany, F.R.). Inst. fuer Physik der Atmosphaere.

ON THE EXISTENCE OF A CAPITAL SIMILARITY

Hans Volkert *In its* Contributions to Atmospheric Physics in Honor of Dr. Manfred Reinhardt on His 65th Birthday Sep. 1991 p 161-166 (For primary document see N92-26329 17-46)

Avail: NTIS HC/MF A11; DLR, Wissenschaftliches, Berichtswesen, Postfach 90 60 58, Cologne, Fed.Republic of Germany, HC 60 Deutsche marks

The historical backgrounds of working with analogies and similarities, which constitute an essential part in the abstracting process for scientific reasoning, is reviewed. Some similarities commonly used in the field of geophysical fluid dynamics are considered. A so far overlooked similarity, capital similarity is postulated. ESA

N92-26345# Meteorologisches Observatorium, Hohenpeissenberg (Germany, F.R.).

OZONE TRENDS [UEBER OZONTRENDS] **c45**

Klaus Wege and Winfried Vandersee *In* DLR, Contributions to Atmospheric Physics in Honor of Dr. Manfred Reinhardt on His 65th Birthday Sep. 1991 p 167-177 In GERMAN; ENGLISH summary Sponsored by Bundesministerium fuer Forschung und Technologie (For primary document see N92-26329 17-46)

Avail: NTIS HC/MF A11; DLR, Wissenschaftliches, Berichtswesen, Postfach 90 60 58, Cologne, Fed.Republic of Germany, HC 60 Deutsche marks

Trends in the ozone, observed by ozone soundings and measurements of total ozone since 1967 and measurements of ozone near the surface since 1971 are investigated. A statistically significant ozone decrease of 0.5 percent per year near the ozone maximum, and a 2 percent increase in the troposphere are found. An ozone decline is found to have occurred at altitudes around 30 km since 1977. The ozone trend is positive near the surface, amounting to about 1 percent per year. ESA

N92-26346# Flinders Univ., Adelaide (Australia). Inst. for Atmospheric and Marine Sciences.

THE COMPOSITE STRUCTURE OF THERMALS AS DERIVED FROM AIRCRAFT OBSERVATIONS

Alastair G. Williams and Joerg M. Hacker *In* DLR, Contributions to Atmospheric Physics in Honor of Dr. Manfred Reinhardt on His 65th Birthday Sep. 1991 p 179-198 Sponsored by Don Schultz of Glen Osmond, South Australia; Australian Research Council; and Commonwealth Postgraduate Research Award (For primary document see N92-26329 17-46)

Avail: NTIS HC/MF A11; DLR, Wissenschaftliches, Berichtswesen, Postfach 90 60 58, Cologne, Fed.Republic of Germany, HC 60 Deutsche marks

A compositing structure is used to construct average intersections through structures from aircraft runs of given heights and directions. Groups of composites are combined to form horizontal and vertical cross sections through the average structure. The internal flow patterns and distribution of physical variables associated with 'typical' coherent structures and their environment are presented in three dimensions. In addition to the well known along wind features of surface layer plumes, a strong consistent lateral inflow pattern is evident. It is shown that mixed layer thermal towers have a relatively simple form consisting primarily of large columns of warm upward moving turbulent air, which may occasionally be in a state of slow clockwise rotation. ESA

N92-26347# Deutsche Forschungsanstalt fuer Luft- und Raumfahrt, Oberpfaffenhofen (Germany, F.R.). Inst. fuer Physik der Atmosphaere.

REMOTE SENSING OF ATMOSPHERE WITH AIRCRAFT BORNE LIDAR SYSTEMS [FERNERKUNDUNG DER ATMOSPHAERE MIT FLUGZEUGGETRAGENEN LIDARSYSTEMEN]

Gerhard Ehret, Wolfgang Renger, Uwe Roesler, Christian Kiemle, Georg Simmet, and Gerhard Ruppersberg *In its* Contributions to Atmospheric Physics in Honor of Dr. Manfred Reinhardt on His 65th Birthday Sep. 1991 p 199-205 In GERMAN; ENGLISH summary Original contains color illustrations (For primary document see N92-26329 17-46)

Avail: NTIS HC/MF A11; DLR, Wissenschaftliches, Berichtswesen, Postfach 90 60 58, Cologne, Fed.Republic of Germany, HC 60 Deutsche marks

Spatial and temporal distribution of clouds and aerosols are measured by lidar. Their optical properties are evaluated using additional assumptions. Wind velocities are mapped by backscatter Doppler lidar systems. Raman lidars are to be used for the supervision of factory emissions. It is shown that Differential Absorptions Lidar (DIAL) systems offer considerable physical advantages in measuring atmospheric constituents; experiences with an airborne device are described. ESA

N92-26348# Deutsche Forschungsanstalt fuer Luft- und Raumfahrt, Oberpfaffenhofen (Germany, F.R.). Inst. fuer Physik der Atmosphaere.

THE DLR METEOROLOGICAL RESEARCH AIRCRAFT FALCON **c47**

Hans P. Fimpel *In its* Contributions to Atmospheric Physics in Honor of Dr. Manfred Reinhardt on His 65th Birthday Sep. 1991 p 207-213 (For primary document see N92-26329 17-46)

Avail: NTIS HC/MF A11; DLR, Wissenschaftliches, Berichtswesen, Postfach 90 60 58, Cologne, Fed.Republic of Germany, HC 60 Deutsche marks

The Dassault Falcon 20E, used as a platform for atmospheric research, is described. The meteorological instrumentation is presented. Indications, obtained by intercomparion flights, on the high quality of the data are given. ESA

N92-26349# Deutsche Forschungsanstalt fuer Luft- und Raumfahrt, Oberpfaffenhofen (Germany, F.R.). Inst. fuer Physik der Atmosphaere.
THE ICING OF THE WING UPPER SIDE AND BOTTOM SIDE OF THE ICING RESEARCH AIRCRAFT OF THE DLR [DIE VEREISUNG DER TRAGFLAECHENOBERSEITE UND -UNTERSEITE DES VEREISUNGSFORSCHUNGSFLUGZEUGS DER DLR] c03
Hans-Eberhard Hoffmann and Johann Demmel *In its* Contributions to Atmospheric Physics in Honor of Dr. Manfred Reinhardt on His 65th Birthday Sep. 1991 p 215-222 In GERMAN; ENGLISH summary (For primary document see N92-26329 17-46)
Avail: NTIS HC/MF A11; DLR, Wissenschaftliches, Berichtswesen, Postfach 90 60 58, Cologne, Fed.Republic of Germany, HC 60 Deutsche marks

It is shown by photographs, that when the wing bottom side is strongly iced, the upper side also attains large values: extension 40 cm, roughness 6 mm. This occurred when the total water was between 0.05 and 0.13 g/m(exp 3), the temperature between -2.1 and 3.4 C, and the median volume diameter between 115 and 236 micrometers. ESA

N92-26350# Deutsche Forschungsanstalt fuer Luft- und Raumfahrt, Oberpfaffenhofen (Germany, F.R.). Inst. fuer Physik der Atmosphaere.
MEASUREMENTS IN THE INHOMOGENEOUS CONVECTIVE BOUNDARY LAYER USING THREE POWERED GLIDERS
Anne M. Jochum, Anja Klebelsberg, Hermann Willeke, and Norbert Entstrasser *In its* Contributions to Atmospheric Physics in Honor of Dr. Manfred Reinhardt on His 65th Birthday Sep. 1991 p 223-228 (For primary document see N92-26329 17-46)
Avail: NTIS HC/MF A11; DLR, Wissenschaftliches, Berichtswesen, Postfach 90 60 58, Cologne, Fed.Republic of Germany, HC 60 Deutsche marks

Three instrumented powered gliders were built and used for turbulence measurements in the atmospheric boundary layer. The present status of the system is summarized. Results from a recent field experiment which demonstrate the horizontal variability of near surface evaporation fluxes on scales of the order of several km are presented. ESA

N92-26406*# Naval Oceanographic Office, Bay Saint Louis, MS.
THE JOINT US/UK 1990 EPOCH WORLD MAGNETIC MODEL Technical Report, 1990 - 1995
John M. Quinn, Rachel J. Coleman, Michael R. Peck, and Stephen E. Lauber Oct. 1991 216 p Sponsored by NASA Prepared in cooperation with Natural Environmental Research Council, London, England
(NASA-CR-190424; NAS 1.26:190424; AD-A245860; NOO-TR-304) Avail: NTIS HC/MF A10

A detailed summary of the data used, analyses performed, modeling techniques employed, and results obtained in the course of the 1990 Epoch World Magnetic Modeling effort are given. Also, use and limitations of the GEOMAG algorithm are presented. Charts and tables related to the 1990 World Magnetic Model (WMM-90) for the Earth's main field and secular variation in Mercator and polar stereographic projections are presented along with useful tables of several magnetic field components and their secular variation on a 5-degree worldwide grid. GRA

N92-26432# Colorado State Univ., Fort Collins. Dept. of Atmospheric Science.
THEORETICAL AND MODELING STUDIES OF THE MARINE PLANETARY BOUNDARY LAYER Final Report, 15 Dec. 1989 - 31 Dec. 1991
David A. Randall 31 Dec. 1991 13 p
(Contract N00014-89-J-1364)
(AD-A245903) Avail: NTIS HC/MF A03

We do not currently understand what determines the fractional cloudiness in partly cloudy boundary layers, how it is influenced by cloud-top entrainment instability, or what controls the transition from stratocumulus to cumulus conditions. These questions have a direct bearing on the radiation budget at both the top of the atmosphere and at the sea surface, and also on the entrainment rate. The importance of boundary layer clouds stems, to a large extent, from their powerful influence on the net radiation at the sea surface. They block incident solar radiation (with albedoes up to about 50 percent) and at the same time emit downward strongly in the infrared. Their net effect on the surface energy budget is believed to be a strong reduction in the energy absorbed by the ocean. Despite the obvious importance of this effect for the thermal structure of the upper ocean, very little is known about the coupling between the ocean mixed layer with boundary layer clouds. The coupling can work in both directions; the sea surface temperature strongly influences the type and amount of boundary-layer cloud, while large cloud amounts are favored where the sea surface temperature is low. GRA

N92-26489 North Carolina State Univ., Raleigh.
MEAN AND TURBULENT STRUCTURE OF THE MARINE ATMOSPHERIC BOUNDARY LAYER DURING COLD AIR OUTBREAKS OF DIFFERENT INTENSITIES: OBSERVATIONAL AND MODELLING ANALYSES Ph.D. Thesis
Robert James Wayland 1991 413 p
Avail: Univ. Microfilms Order No. DA9207691

Aircraft, surface, upper air and satellite measurements have been used to observe the evolution and growth of the convective Marine Atmospheric Boundary Layer offshore of North Carolina in close proximity to the Gulf Stream, during the intense cold air outbreak of 28 January 1986 and the moderate event of 12 February 1986, as part of the Genesis of Atlantic Lows Experiment (GALE). Air mass modification processes, driven primarily by the ocean-atmosphere exchanges of surface turbulent sensible and latent heat fluxes, caused the overlying air mass to warm and moisten as it advected over the warmer waters of the eastern United States continental shelf. Maximum observed near-surface total heat fluxes (W center dot m (exp -2)) were 1045 and 811 over the core of the Gulf Stream, for 28 January and 12 February 1986, respectively. The observed changes in the overlying air mass occur almost instantaneously as the ambient flow traverses different underlying sea surface temperature (SST) conditions. The turbulent structure showed a buoyancy dominated MABL below approximately 0.8 z/h. However, shear was also observed to be an important production term above 0.8 z/h below 0.1 z/h for the 28 January 1986 event. Dissipation of turbulent kinetic energy was the dominant destruction term in the budgets, but vertical transport of energy was a strong contributor below 0.5 z/h, above which this term became a source of turbulent energy. Additionally, the normalized standard deviations of the horizontal velocity components showed a near-equal contribution to the turbulence, while the vertical velocity components displayed the characteristic mid-layer maximum profile observed for a convective, well-mixed boundary layer. Dissert. Abstr.

N92-26490 Wisconsin Univ., Madison.
WATER VAPOR INFORMATION CONTENT OF ABSORPTION LINES OBSERVED IN THE SUN'S INFRARED RADIANCE Ph.D. Thesis
Arlindo Jose Claudin Arriaga 1991 193 p
Avail: Univ. Microfilms Order No. DA9134305

The water vapor information content of absorption lines is evaluated through a covariance analysis of the spectrum of the atmospheric transmittance, for different spectral resolutions and noise. The structure of the atmosphere is sampled with 120 real temperature and water vapor mixing ratio profiles. The transmittance of the atmosphere is simulated with a line-by-line radiative transfer model, possessing less than 6 percent rms error. Dissert. Abstr.

N92-26583 Michigan Univ., Ann Arbor.
COMPUTATIONS OF NONLINEAR GRAVITY WAVES BY A DESINGULARIZED BOUNDARY INTEGRAL METHOD Ph.D. Thesis
Yusong Cao 1991 184 p
Avail: Univ. Microfilms Order No. DA9208503

A desingularized boundary integral equation method combined with a Eulerian-Lagrangian time-stepping technique is developed for nonlinear gravity wave problems. The desingularization distance between the boundary and the sources is related to the local mesh size to ensure convergence. Tests for some simple problems show that desingularization significantly reduces the computer time required to compute the influence matrix of the resulting algebraic system. The algebraic system is still adequately well-conditioned to allow fast iterative solutions. Accurate solutions can be obtained for a large range of desingularization distances on the order of the mesh size. Dissert. Abstr.

N92-26622 California Univ., Los Angeles.
THE DYNAMIC RESPONSE OF THE WESTWARD AURORAL ELECTROJET AND POLAR CAP CURRENTS TO SOLAR WIND-MAGNETOSPHERE COUPLING Ph.D. Thesis
Lee Frost Bargatze 1991 321 p
Avail: Univ. Microfilms Order No. DA9128827

We present results of studies using high-time resolution data to determine the response of magnetospheric currents to coupling with the solar wind. In the first study, we apply the concept of dimensional analysis to the problem of solar wind-magnetosphere coupling in order to find the dependence of the coupling rate on solar wind variables. We find that energy input to the magnetosphere and as represented by the AE indices occurs at a rate proportional to p 1/6 EG(theta) where p is the solar wind dynamic pressure, E is the solar wind motional electric field and G(theta) is a 'leaky' gating function which expresses coupling rate dependence on the interplanetary magnetic field (IMF) orientation. In the second study, we determine the temporal relationship between the solar wind motional electric field (VB sub s) and the westward auroral electrojet index, AL, by using the linear prediction technique. We find that the VB sub s-AL response filters are composed of two response pulses. We hypothesize that the two response pulses each correspond to a different mode of the magnetosphere. We suggest that one response pulse corresponds to AL index activity driven directly by solar wind-magnetosphere interaction while the other corresponds to activity driven by energy loading and unloading from the magnetotail. In the third chapter, we attempt to test the bimodal model for magnetospheric response by means of a simple computer analogue that is designed to mimic the behavior of the magnetosphere. Using linear prediction tests, we find that the model system is a reasonable representation of the actual magnetosphere. In the fourth study, we examine the AE indices to determine the accuracy of the index. The chapter focuses on known problems with the indices and attempts to address them by modifying the index generation scheme. We find that the index accuracy can be improved especially during quiet times and at substorm onset. In the fifth chapter, we extend our analysis by studying the PC index which measures Hall current flow across the polar cap. We find that the PC index response filter closely resembles the AL index filter, a result which suggests that both PC and AL are accurately quantifying the response of the magnetosphere. The differences between the PC and AL response filters suggest that the PC index responds primarily to dayside reconnection whereas the AL index responds more than PC to nightside reconnection. These results are mainly consistent with the bimodal response model of the magnetosphere. Dissert. Abstr.

N92-26675# Boston Univ., MA. Center for Space Physics.
THE EFFECTS OF MAGNETIC STORM PHASES ON F-LAYER IRREGULARITIES FROM AURORAL TO EQUATORIAL LATITUDES Quarterly Report, 1 Oct. - 31 Dec. 1991
Jules Aarons and Michael Mendillo 31 Dec. 1991 3 p
(Contract N00014-89-J-1754)
(AD-A245495) Avail: NTIS HC/MF A01

Several periods of interest in the low sunspot years of 1985 and 1986 have been identified when data were available from Kiruna, Sweden and from Goose Bay, Labrador as well as from equatorial sites. A contouring program was developed to handle the Transit data and in fact have received data from several sample periods of very low magnetic activity over a period of several days. Just begun is this study of determining the pattern of F-layer irregularities during years of low solar flux. The evaluation of data sets has included new analysis (for Manila, for example) as well as evaluating older data, much of it at this date unused for scientific purposes. While F-region irregularities are frequently spoken of occurring in the auroral region, the behavior of the irregularities as a function of sunspot number is significantly different from the behavior of the auroral region. Auroral data, primarily of the E layer green line, show no significant changes as a function of sunspot number in the latitude of the occurrence of this phenomenon; F-region irregularities show a great movement towards the polar region with a low sunspot number. In order to predict the occurrence and level of the effects on trans-ionospheric propagation, the relationship to sunspot number must be ascertained. We feel the comparison of high latitude data from Sweden and Canada will allow us to state that a polar movement of the region during low sunspot years is a global phenomenon. GRA

N92-26753# Naval Postgraduate School, Monterey, CA.
AN ANALYSIS OF MIDDLE ULTRAVIOLET EMISSIONS OF MOLECULAR NITROGEN AND NITRIC OXIDE AND VACUUM CALIBRATION OF AN ULTRAVIOLET SPECTROGRAPH M.S. Thesis
Bryan D. Mack Jun. 1991 95 p
(AD-A245984) Avail: NTIS HC/MF A05

Ultraviolet emissions from the earth's ionosphere in the wavelength range 1850 to 2070 A are analyzed. Specifically, thirteen Lyman-Birge-Hopfield (LBH) band emissions from molecular nitrogen (N2) and the gamma, delta, and epsilon bands of nitric oxide (NO) are modeled with synthetic spectra to determine the atmospheric density of NO. Corrections to the Franck-Condon factors for the LBH emissions and the NO emissions are derived. Column emission rates are determined for N2 and compared with computer models. Vacuum calibration of the MUSTANG ultraviolet spectrograph is presented. GRA

N92-26820# Institut des Hautes Etudes Scientifiques, Bures-sur-Yvette (France).
TENSOR-MULTI-SCALAR THEORIES OF GRAVITATION
T. Damour and G. Esposito-Farese Dec. 1991 98 p Prepared in cooperation with Observatoire de Paris, France; and Centre National de la Recherche Scientifique, Marseilles, France
(PB92-152305; IHES/P/91/93) Avail: NTIS HC/MF A05

A generic class of theories where gravity is mediated by one tensor field together with an arbitrary number of scalar fields is considered. The predictions of these theories are worked out in four different observationally relevant regions: (1) quasi-stationary weak fields (solar system conditions); (2) rapidly-varying weak fields (gravitational wave experiments); (3) quasi-stationary strong fields (motion of systems of compact bodies, i.e., neutron stars or black holes); and (4) the mixing of strong and radiative field effects in the gravitational radiation of N-compact-body systems. Moreover, several significant relations between the theoretical quantities entering these predictions are derived. They show how strong-field-gravity effects in the motion and gravitational radiation of N-compact-body systems can be parametrized by a set of theory parameters that generalize the usual post-Newtonian parameters (gamma, beta,...) introduced in the context of quasi-stationary weak gravitational fields. These new parameters (beta(2), beta(prime), beta(3), beta(double prime),...) provide a chart for the yet essentially unexplored domain of strong-gravitational-field effects, and thereby suggest new directions for testing relativistic gravity. This is illustrated by studying in detail a specific two-parameter tensor-bi-scalar theory T(beta(prime), beta(double prime)) which has the same post-Newtonian limit as general relativity but leads to new, non-Einsteinian predictions for the various observables that can be extracted from binary pulsar data. Author

N92-26838# Environmental Protection Agency, Washington, DC. Office of Toxic Substances.
DETERMINATION OF RATES OF REACTION IN THE GAS PHASE IN THE TROPOSPHERE. THEORY AND PRACTICE. PART 3: RATE OF INDIRECT PHOTOREACTION
A. Leifer 20 Feb. 1992 238 p
(PB92-150374; EPA/700/R-92/002) Avail: NTIS HC/MF A11

The report describes the development of structure/reactivity (S/R) relationships for the estimation of the 2nd-order rate constant k(OH) for the reaction of OH radicals with organic chemicals in the troposphere. These S/R relationships were used to estimate k(OH) at 298 K of 405 chemicals covering a variety of classes and compares them with the experimental values (percent error). Of the 405 chemicals, 20 had a percent error greater than +100 and were omitted in the analyses. For the 385 remaining chemicals, the average percent ranged from +21 to -19. One hundred fifty-four chemicals were not used to derive the parameters in the S/R relationships and, therefore, were good candidates to test the validity of the S/R relationships. The average percent error of the 154 chemicals ranged from +24 to -20, thereby confirming the S/R relationships. A discussion is given on the estimation of the half-life of a chemical in the troposphere from k(OH) and the average OH concentration. The report represents the technical support document for a test guideline which can be used under section 4 of the Toxic Substances Control Act. Author

N92-26865 Alaska Univ., Fairbanks.
PLASMA DYNAMICS OF THE EARTH MAGNETOPAUSE-BOUNDARY LAYER AND ITS COUPLING TO THE POLAR IONOSPHERE Ph.D. Thesis
Chang-Quan Wei 1991 163 p
Avail: Univ. Microfilms Order No. DA9209706

In this thesis, the plasma dynamics of the Earth magnetopause-boundary layer and its coupling to the polar ionosphere are studied by using computer simulations. First, the plasma dynamics and structure of the magnetopause-boundary layer are studied by a two-dimensional incompressible magnetohydrodynamic simulation code. It is found that the Kelvin-Helmholtz instability with driven boundary conditions at the magnetopause can lead to the formation of plasma vortices observed in the magnetopause-boundary layer. In the later stage of development, a density plateau is formed in the central part of the boundary layer. Second, the coupling of plasma vortices formed in the boundary layer to the polar ionosphere is studied based on a magnetosphere-ionosphere coupling model. The finite ionospheric conductivity provides a dragging force to the plasma flow and leads to the decay of plasma vortices in the boundary layer. In the model, the ionospheric conductivity is allowed to be enhanced due to accelerated electrons precipitating in upward field-aligned current regions. The competing effect of the formation and decay of vortices leads to the formation of strong vortices only in limited regions. Several enhanced conductivity regions are formed along the post-noon auroral oval, which may account for the observed auroral bright spots. Dissert. Abstr.

N92-26866 Alaska Univ., Fairbanks.
STUDIES OF INERTIO-GRAVITY WAVES INDUCED BY GEOSTROPHIC ADJUSTMENT OF THE ATMOSPHERIC JET STREAM Ph.D. Thesis
Zhangai Luo 1991 115 p
Avail: Univ. Microfilms Order No. DA9209701

Motivated by observations that revealed very low frequency gravity waves throughout the lower and middle atmosphere, this thesis investigates inertio-gravity waves (IGWs) radiating from an ageostrophic jet stream assuming geostrophic adjustment to be the source mechanism. Fourier integral and Green's function techniques are employed to solve this problem. The ageostrophic components of the motion field are described by an initially unbalanced Gaussian velocity field which was chosen to have infinite and localized zonal extents corresponding to two-dimensional (2-D) and three-dimensional (3-D) cases. The adjustment process permits the radiation of IGWs and the attainment of an induced geostrophically balanced mean circulation. Dissert. Abstr.

N92-26877 Physics and Electronics Lab. TNO, The Hague (Netherlands).
DESCRIPTION OF THE RAYFLUX RAY TRACING PROGRAM AND COMPARISON WITH OTHER MODELS AND MEASUREMENTS Final Report [BESCHRIJVING VAN HET RAYFLUX RAY TRACING PROGRAMMA EN VERGELIJKING MET ANDERE MODELLEN EN METINGEN]
A. C. vanKoersel Nov. 1991 50 p In DUTCH; ENGLISH summary
(Contract A89KL661)
(AD-A245413; FEL-91-B335; TD91-3980; ETN-92-91227)
Copyright Avail: TNO Physics and Electronics Lab., P.O. Box 96864, 2509 JG The Hague, Netherlands

The FORTRAN 4 ray tracing program for the calculation of the acoustic transfer function in the atmosphere and its tests are described. The program can be used for the calculation of the acoustic transfer function in the atmosphere in a large number of weather and soil conditions. Results of the Rayflux program were compared with those of a wave field extrapolation model, a different ray tracing model and measurements. It can be concluded that Rayflux gives good results for not too high ranges. ESA

N92-26937# Colorado State Univ., Fort Collins. Dept. of Atmospheric Science.
DEVELOPMENT OF AN ADVANCED FINITE-DIFFERENCE ATMOSPHERIC GENERAL CIRCULATION MODEL
D. A. Randall Mar. 1992 5 p
(Contract DE-FG02-91ER-61218)
(DE92-010923; DOE/ER-61218/1) Avail: NTIS HC/MF A01

An advanced finite-difference climate model is developed for use in CHAMMP. The model includes advanced parameterizations of cumulus convection, boundary-layer processes, cloud formation, and land-surface vegetation. Additionally, the model contains parameterizations of radiative transfer and gravity wave drag. Postprocessing codes and a user's guide are provided. The following research tasks are being carried out in support of CHAMMP: (1) a base-line finite-difference model and postprocessing codes; (2) improved model physics to be developed in the course of the research project; (3) improved computational methods for use in the model; and (4) investigations of current and to-be-developed physical parameterizations and computational methods at very high resolution. DOE

47 METEOROLOGY AND CLIMATOLOGY

Includes weather forecasting and modification.

N92-26185*# Florida State Univ., Tallahassee. Dept. of Meteorology.
SURFACE ENERGY BUDGET AND EVAPOTRANSPIRATION MEASUREMENT SUPPORT Final Report
Eric A. Smith Jun. 1992 11 p
(Grant NAG8-881)
(NASA-CR-190059; NAS 1.26:190059) Avail: NTIS HC/MF A03

One of the primary aims of the Convection and Precipitation/Electrification (CaPE) experiment held at NASA Kennedy during 1991 was to correlate the sensible and latent heat flux from the vegetation canopy on Merritt Island with satellite imagery of the development and maturation of the thunderstorms which grow over Kennedy. The sensing systems which were used to collect surface observations of radiation, sensible heat flux, latent heat flux, and soil heat flux at two locations on Merritt Island. The observing systems which were built are called Surface Radiation and Energy Budget Systems (SREBS) and are integrated observing platforms comprised of five subsystems: the Bowen ratio subsystem; the radiation subsystem; the soil subsystem; the meteorological subsystem; and the electronics subsystem. Using both of the SREBS assembled, a complete picture was obtained

of the distribution and partitioning of the various components in the surface energy budget at two sites during CaPE. Author

N92-26288*# National Aeronautics and Space Administration. Marshall Space Flight Center, Huntsville, AL.
ATMOSPHERIC ENVIRONMENT FOR SPACE SHUTTLE COLUMBIA (STS-40) LAUNCH
G. L. Jasper and G. W. Batts (New Technology, Inc., Huntsville, AL.) Jun. 1992 46 p
(NASA-TM-103585; NAS 1.15:103585) Avail: NTIS HC/MF A03

A summary of selected atmospheric conditions observed near the Space Shuttle Columbia (STS-40) launch time on 5 Jun. 1991, at KSC is presented. Values of ambient pressure, temperature, moisture, ground winds, visual observation (cloud), and winds aloft are included. The sequence of prelaunch Jimsphere-measured vertical wind profiles is given. The final atmospheric tape, which consists of wind and thermodynamic parameters versus altitude, for STS-40 vehicle ascent was constructed. The STS-40 ascent atmospheric data tape was constructed by MSFC's Earth Science and Applications Division to provide an internally consistent data set for use in postflight performance assessments and represents the best estimate of the launch environment to the 400,000-ft altitude that was traversed by the STS-40 vehicle. Author

N92-26364# Naval Postgraduate School, Monterey, CA.
CHARACTERISTICS OF UPPER-LEVEL AND BOUNDARY LAYER FORCING IN WESTERN PACIFIC CYCLONES M.S. Thesis
Adam A. Kippes Sep. 1991 72 p
(AD-A246301) Avail: NTIS HC/MF A04

A study of the characteristics of upper-level and boundary layer forcing in Western Pacific cyclones is conducted. Data for this study consists of twenty seven cyclones identified during the months of February and March 1986 and 1987. The cyclones were stratified into three separate classes of weak, moderate, and intense cyclones based on observed deepening rates. Each class of cyclone was examined to determine general characteristics of the upper-level and boundary layer forcing. A representative cyclone from each class was chosen and a detailed examination of the upper-level and boundary layer forcing was conducted. Results indicate that during rapid deepening coupling between the upper-level forcing and forcing in boundary layer occurred only in the moderate and intense cases and was the result of strong baroclinic forcing aloft in these cyclones. GRA

N92-26409# Army Missile Command, Redstone Arsenal, AL. Weapons Science Directorate.
COMPARISON OF WIND PROFILES IN CLOSE PROXIMITY TO EACH OTHER Final Technical Report, Oct. 1990 - May 1991
Larry J. Levitt and Dorathy A. Stewart 22 Oct. 1991 70 p
(AD-A246152; AD-E951742; AMSMI/TR-RD-WS-91-9) Avail: NTIS HC/MF A04

Simultaneous wind profiles from the surface to 8 km at four pairs of German stations were examined. Three pairs are in the northern lowlands and one pair is in the central European highlands. Magnitudes of vector differences between stations in close proximity to each other are generally larger in winter than in summer. Wind differences in spring and fall are usually intermediate between those in summer and winter. Smallest mean differences are at the surface, and there is a relative minimum near 2.5 km. Largest differences are at the highest levels. Standard deviations show similar variations with season and altitude, and so do the individual wind components. The data set was not adequate to produce definitive results concerning diurnal variation.
Author (GRA)

N92-26474* Oklahoma Univ., Norman. Cooperative Inst. of Mesoscale Meteorological Studies.
PARAMETERIZATION OF WATER-SOLUBLE COMPONENT OF AEROSOL PARTICLES IN NUMERICAL CLOUD MODELS Abstract Only
Yefim L. Kogan and Seong Soo Yum 1992 2 p
(Grant NAG5-1528)
(NASA-CR-190225; NAS 1.26:190225) Avail: Issuing Activity

Explicit consideration of cloud droplet condensational growth in multidimensional cloud models is significantly complicated by the need to account for a two dimensional distribution function that depends on both the cloud droplet radius and the mass of the water soluble component of the cloud condensation nuclei. The large number of variables that need to be considered puts a very heavy load on the available computer resources and makes the problem impractical. In order to obtain a parameterization of the solubility factor valid for the case of stratocumulus clouds, an extensive set of numerical experiments were performed using a microphysical model with a very fine resolution of the droplet spectra. This resulted in a very accurate representation of the droplet condensational growth process. In the experiments the updraft velocity varied in the range from 0.05 to 2 m/s, and cloud condensation nuclei spectra typical for continental as well as maritime conditions were both tested. The time evolution was analyzed of the salt content over the whole range of the droplet spectra and its dependence on ambient conditions and integral parameters of the evolving droplet spectra. Author

N92-26514# National Weather Service, Fort Worth, TX. Scientific Services Div.
INTEGRATING WIND PROFILER DATA INTO FORECAST AND WARNING OPERATIONS AT NWS FIELD OFFICES
Stephen T. Rich (National Weather Service, Jackson, MS.) Mar. 1992 40 p
(PB92-146075; NOAA-TM-NWS-SR-141) Avail: NTIS HC/MF A03

A network of 29 wind profilers (Wind Profiler Demonstration Network, WPDN) in the central U.S. provides tropospheric wind data to National Weather Service field offices. The data are characterized by better horizontal resolution than that provided by the existing rawinsonde network and provide much better vertical and temporal resolution. The goal of the WPDN is to provide the NWS an opportunity to assess the utility of wind profiler data in an operational setting. The results of that assessment may help determine whether the WPDN will be followed by a national network. Four training manuals and associated videotapes were developed by the WPDN. The first manual deals with principles of wind profiler operation, while the second discusses quality control of profiler data. The third deals with warm season applications of profiler data to analysis and forecasting, and the fourth discusses cool season applications. Important information is combined from the training manuals, the AFOS profiler applications software, and some of the relatively few research papers dealing with profilers, and guidelines are established for NWS field offices to integrate wind profiler data into local forecast operations. Author

N92-26535*# Hamilton Standard, Windsor Locks, CT.
CONCEPTUAL DESIGN STUDY FOR THE USE OF COBE ROCKET ENGINES ON THE TROPICAL RAINFALL MEASURING MISSION Final Report, 10 Jan. - 16 Jun. 1992
15 Jun. 1992 243 p
(Contract NAS5-31889)
(NASA-CR-190383; NAS 1.26:190383; TRMM-SER-705; SVHSER-14841) Avail: NTIS HC/MF A11

The objective of this conceptual design study is to verify that the Cosmic Background Explorer (COBE) Hydrazine Propulsion Subsystem (HPS) Rocket Engine Assembly (REA) will satisfy the Tropical Rainfall Measuring Mission (TRMM) requirements and to develop a preliminary thruster module design using the existing REAs. The performance of the COBE HPS 5 lbf thrusters meet the TRMM mission requirements. The preliminary design consists of a single 5 lbf REA REM which is isolation mounted to a spacecraft interface angle bracket (5 or 10 deg angle). The REM incorporates a catalyst bed heater and sensor assembly, and propellant thermal control is achieved by thermostatically controlled heaters on the thruster valves. A ROM cost of approx. $950 K has been estimated for the phase 2 program to finalize the design, fabricate, and test the hardware using mechanical thermostats for thermal control. In the event that solid state thermostats are used,

the cost is estimated to be $160 K higher. A ROM cost is approx. $145 K is estimated to study the effects of using Japanese manufactured hydrazine for the TRMM mission. Author

N92-26562# Naval Postgraduate School, Monterey, CA.
ESTIMATING MESOSCALE, OROGRAPHICALLY ENHANCED PRECIPITATION USING SYNOPTIC SCALE DATA M.S. Thesis
Michael D. Angoev Dec. 1991 84 p LIMITED REPRODUCIBILITY: Availability: Document partially illegible
(AD-A245749) Avail: NTIS HC/MF A05

A method for resolving the mesoscale distribution of precipitation over mountainous regions is developed using synoptic scale analyses and a 40 km resolution of topography. The method consists of calculating the saturated moisture flux at a level assumed to be the cloud base and correlating this quantity with observed precipitation. General correlation coefficients ranged from -0.2 under conditions poorly represented by the synoptic surface analysis to -0.55 when these analyses are more representative of actual forcing. When applied regionally, correlation improved dramatically, suggesting potential incorporation into precipitation forecasts over mountainous areas. Over wider regions of less defined topography correlation is weaker, but is still an improvement over the current synoptic scale precipitation forecast products. GRA

N92-26735* Oklahoma Univ., Norman. Cooperative Inst. for Mesoscale Meteorological Studies.
STUDY OF ENTRAINMENT MECHANISMS IN CONVECTIVE CLOUDS Abstract Only
Yefim L. Kogan 1991 1 p
(Grant NAG5-1528)
(NASA-CR-190223; NAS 1.26:190223) Avail: Issuing Activity

Trajectory analysis based on a simulation data from a 3-D model with explicit formulation of microphysical processes has been utilized to study the entrainment mechanisms in convective clouds. It is shown that at the growing stage of cloud development there are three types of cloud entrainment mechanisms that significantly differ in the thermodynamic properties of the air masses feeding the cloud. Air masses at lower levels of the cloud and in central core of the updraft at all levels originate from the surface layers. These air parcels are high in moisture and concentration of cloud condensation nuclei (CCN). Upper levels of the growing cloud are formed, in part, by the air masses with negative buoyancy which are driven upward and to the sides of the cloud by the pressure gradient force. These air masses reach saturation after having been lifted along dry adiabats for, in some cases, as much as 1-2 km. This indicates that the cloud can grow not only from below but also from above. It is also remarkable that these air masses, relatively low in moisture and CCN, are very close to the central core of the updraft where they can mix and significantly dilute the air masses originating from the levels near the cloud base and which, therefore, are high in moisture and CCN content. The third mechanism of cloud entrainment is the lateral entrainment of air parcels originating from the upper levels near the cloud top and driven to the middle and lower levels by the compensating downdrafts. This cloud feeding mechanism plays an ever increasing role at the mature and decay stages of cloud evolution. It is estimated from the simulation data, that air masses brought into the cloud by this mechanism may contribute up to 40-50 percent of the total cloud mass. Author

N92-26736* Oklahoma Univ., Norman. Cooperative Inst. of Mesoscale Meteorological Studies.
ANALYSIS OF MIXING MECHANISMS IN NUMERICALLY SIMULATED CONVECTIVE CLOUDS Abstract Only
Yefim L. Kogan 1991 1 p
(Grant NAG5-1528)
(NASA-CR-190222; NAS 1.26:190222) Avail: Issuing Activity

In a set of numerical experiments more than 400 air parcel trajectories have been analyzed in one- and multicell cloud simulations. It is shown that at the growing stage of cloud development there are three types of cloud entrainment mechanisms that significantly differ in the thermodynamic properties of the air masses feeding the cloud. Air masses at lower levels of the cloud and in the central core of the updraft at all levels originate from the surface layers. These air parcels are high in moisture and concentration of cloud condensation nuclei (CCN). Middle levels of the growing cloud are formed, in part, by the negatively-buoyant air which is driven upward and to the sides of the cloud by the strong perturbation pressure gradient forces. These air masses are diluted during their ascent by turbulent mixing and reach saturation after having been lifted along dry adiabats for, in some cases, as much as 1-2 km. It is remarkable that these air masses, relatively low both in moisture and CCN, are very close to the central core of the updraft where they can mix and significantly dilute air masses that originate from the levels near the cloud base and, therefore, are high in moisture and CCN content. The third mechanism of cloud entrainment is the lateral entrainment of air parcels originating from the upper levels near the cloud top and driven to the middle and lower levels by the compensating downdrafts. This cloud feeding mechanism plays an ever increasing role at the mature and decay stages of cloud evolution. It is estimated from the simulation data, that air masses brought into the cloud by this mechanism may contribute up to 40-50 percent of the total cloud mass. The effect of different entrainment mechanisms on rain formation is also discussed. Author

N92-26822# National Meteorological Center, Washington, DC. Climate Analysis Center.
CLIMATE RESEARCH AT REGIONAL CLIMATE CENTERS IN 1991
Oct. 1991 101 p Presented at the 1991 Conferences of the American Meteorological Society on Applied Climatology, Agricultural and Forest Meteorology, and Biometeorology and Aerobiology, Salt Lake City, UT, 10-13 Sep. 1991
(PB92-160399) Avail: NTIS HC/MF A06

The climate service mission of the National Oceanic and Atmospheric Administration (NOAA) is to supply high quality climate data and information to a diverse user community through a program of data acquisition, monitoring, and product development. The mission also includes determining the impacts of climate on the environment, commerce, and the economy of the U.S. To meet these goals of a nation wide system of climate services on the regional and local scale, NOAA sponsors a group of six Regional Climate Centers (RCCs) located throughout the contiguous U.S. The primary purpose of the assemblage of papers is to provide a resource for applied research performed either by personnel at RCCs or by scientists who have received support from the RCCs, and to furnish an example of the climate services rendered by the centers. The 14 papers presented on applied research can be grouped into four general categories. Six of the papers deal with information that can be used in design applications, three address climate change or impacts, three deal with climate records, and two address soil moisture related subjects. In addition, three papers on RCC operations and climate services are presented. GRA

N92-26899# Army Lab. Command, White Sands Missile Range, NM. Atmospheric Sciences Lab.
ON THE SUBJECT OF GEOMETRIC SPACING OF METEOROLOGICAL SENSORS Final Report
Henry Rachele and Arnold Tunick Nov. 1991 25 p
(AD-A245824; ASL-TMR-0011) Avail: NTIS HC/MF A03

To estimate turbulence characteristics such as the friction velocity, temperature scaling length, and the Obukhov length from discretely measured data, it is desirable and efficient, but not necessary, to have the sensors spaced geometrically with height. The mathematical argument for geometric spacing was not developed or presented. Furthermore, we could not find a reference for it. Even so, we considered the traditional geometric spacing equations and compared results from them with our more general formulations based on the mean value theorem for a few examples and found that for practical applications the differences were not significant. For most turbulence studies in the boundary layer, one desires single values of the turbulence characteristics through a

layer of perhaps 20, 30, or 100 m; that is, one typically assumes that the characteristic lengths are constant with height. A procedure for determining the total layer values is to compute the values in the geometrically spaced sublayers and then average the sublayer values. In this study we consider the case where the sensors are geometrically spaced. We then present our mathematical development requiring geometric spacing for a single sublayer based on the mean value theorem and assume that the values for the total layer (summation of sublayers) can be determined by averaging the sublayer values. GRA

N92-26901# Colorado State Univ., Fort Collins. Dept. of Atmospheric Science.
PHYSICAL PROCESSES WITHIN THE NOCTURNAL STRATUS-TOPPED BOUNDARY LAYER, REVISION
Chin-Hoh Moeng, Shaohua Shen, and David A. Randall Jan. 1992 36 p
(Contract N00014-89-J-1364)
(AD-A245829) Avail: NTIS HC/MF A03

There are many physical processes involved in the stratus-topped boundary layer: longwave radiation cooling, entrainment, latent heating, surface heating, solar heating, and drizzling, for example. The manner in which the processes combine to maintain the turbulence within the stratus-topped boundary layer remains an unsolved problem. The large eddy simulation technique is used to examine the first four physical processes mentioned above. First, the contribution of each physical process to the thermodynamic differences between the updraft and downdraft branches of turbulent circulations is examined through a conditional sampling. Second, these mean thermodynamic differences are shown to express well the vertical distributions of heat and moisture fluxes within stratus-topped boundary layers. These provide a method to validate the process partitioning technique. (This technique assumes that the net flux profile can be partitioned into different component-flux profiles according to physical processes, and that each partitioned component flux is linear in height.) In this paper, the heat and moisture fluxes are process partitioned, and each component-flux is found to contribute to the net flux in a way that is consistent with its corresponding process contribution to the mean thermodynamic differences between updrafts and downdrafts. Also, the net flux obtained by summing all component-fluxes agrees very well with that obtained directly from the large-eddy simulations. GRA

N92-26923# World Meteorological Organization, Geneva (Switzerland). World Climate Data and Monitoring Program.
REPORT OF THE CC1 WORKING GROUP ON CLIMATE CHANGE DETECTION
Oct. 1991 73 p First Session held in Geneva, Switzerland, 21-25 Oct. 1991
(WCDMP-14; WMO-TD-466) Avail: NTIS MF A04; print copy available at WMO, Geneva, Switzerland

A number of topics were discussed, including the problem of detection of the greenhouse effect, climate normals datasets, the importance of the interdisciplinary approach to the detection problem, the sources of uncertainties in the climate record, the status of climate sets for climate change detection, the Climate Change Detection Project (CCDP), and working group recommendations. Author

N92-26924# World Meteorological Organization, Geneva (Switzerland). World Climate Data and Monitoring Program.
CC1 EXPERTS MEETING ON CLIMAT CODE ADAPTATION
Nov. 1991 28 p Meeting held in Geneva, Switzerland, 5-6 Nov. 1991
(WCDMP-15; WMO-TD-468) Avail: NTIS MF A03; print copy available at WMO, Geneva, Switzerland

The participants discussed the history of the CLIMAT code and agreed that a knowledge of how the code developed and its current usefulness were important in the determination of the nature and extent of adaptation. CLIMAT is the meteorological coded report of monthly means and totals for a land surface station. The experts strongly recommended retaining all of the information in the present codes, adding monthly mean maximum and mean minimum temperatures, and adding group identifiers. The experts provisionally endorsed changes that would result in the addition of daily maximum, minimum, and mean temperatures, and the addition of additional departure and occurrence statistics (e.g. the number of days with snow cover greater than 1 centimeter, or with the occurrence of hail or thunderstorms). Author

N92-26925# World Meteorological Organization, Geneva (Switzerland). World Climate Data and Monitoring Program.
REPORT OF THE CC1 EXPERTS MEETING ON TRACKING AND TRANSMISSION OF CLIMATE SYSTEM MONITORING INFORMATION
Nov. 1991 64 p Meeting held in Geneva, Switzerland, 7-8 Nov. 1991
(WCDMP-16; WMO-TD-465) Avail: NTIS MF A04; print copy available at WMO, Geneva, Switzerland

A number of topics related to the tracking and transmission of climate system monitoring information were discussed. Topics discussed included climate message monitoring, the World Meteorological Organization (WMO) Ozone Bulletin, the Meteorological Data Distribution (MDD)/OWSE Africa experiment, station information, and world weather records. Author

N92-27075# Naval Postgraduate School, Monterey, CA.
HIGH FREQUENCY ANALYSES OF COASTAL METEOROLOGICAL PHENOMENA AFFECTING REFRACTIVITY M.S. Thesis
Anthony A. Martinez Dec. 1991 90 p
(AD-A246383) Avail: NTIS HC/MF A05

An eastern Pacific Ocean survey was conducted 7-10 May 1991 along the California coast to determine temporal and spatial variability in refractive conditions. Refractive profiles obtained from high frequency radiosonde measurements at shore sites and a ship, plus continuous shipboard surface measurements, found a high degree of refractive variability to be associated with frontal passage. Local and synoptic scale conditions were found to have a major impact on the degree of refractive variability. The variability was in the occurrence of elevated layers and the evaporation duct height. With passage of the cold front, the evaporation duct height increased from values that would not affect shipboard sensors to those that would. Survey soundings and refractive profiles were also compared with subjective refractive analyses and forecast profiles from the Navy Atmospheric Boundary Layer model. In situ measurements revealed significant variability in refractive profiles that were not revealed in the model forecasts. GRA

N92-26333# Bonn Univ. (Germany, F.R.). Inst. fuer Meteorologie.
COMPARISON OF FRONTOGENETICAL STRUCTURES FOR DIFFERENT CASES OF FRONTAL DEVELOPMENT
Helmut Kraus *In* DLR, Contributions to Atmospheric Physics in Honor of Dr. Manfred Reinhardt on His 65th Birthday Sep. 1991 p 27-40 (For primary document see N92-26329 17-46)
Avail: NTIS HC/MF A11; DLR, Wissenschaftliches, Berichtswesen, Postfach 90 60 58, Cologne, Fed.Republic of Germany, HC 60 Deutsche marks

N92-26335# Technische Univ., Munich (Germany, F.R.). Inst. fuer Meteorologie.
THE STABILITY OF BAROTROPIC VORTICES: IMPLICATIONS FOR TROPICAL CYCLONE MOTION
Harry C. Weber and Roger K. Smith *In* DLR, Contributions to Atmospheric Physics in Honor of Dr. Manfred Reinhardt on His 65th Birthday Sep. 1991 p 51-63 (For primary document see N92-26329 17-46)
(Contract N00014-90-J-1487)
Avail: NTIS HC/MF A11; DLR, Wissenschaftliches, Berichtswesen, Postfach 90 60 58, Cologne, Fed.Republic of Germany, HC 60 Deutsche marks

N92-26338# Deutsche Forschungsanstalt fuer Luft- und Raumfahrt, Oberpfaffenhofen (Germany, F.R.). Inst. fuer Physik der Atmosphaere.
MESOSCALE OBSERVATIONS OF A COLD FRONT ASSOCIATED WITH A PREFRONTAL HAILSTORM
Klaus P. Hoinka *In its* Contributions to Atmospheric Physics in Honor of Dr. Manfred Reinhardt on His 65th Birthday Sep. 1991 p 87-97 Original contains color illustrations (For primary document see N92-26329 17-46)
Avail: NTIS HC/MF A11; DLR, Wissenschaftliches, Berichtswesen, Postfach 90 60 58, Cologne, Fed.Republic of Germany, HC 60 Deutsche marks

N92-26342# Deutsche Forschungsanstalt fuer Luft- und Raumfahrt, Oberpfaffenhofen (Germany, F.R.). Inst. fuer Physik der Atmosphaere.
PRECIPITATION FORMATION PROCESSES IN CONVECTIVE AND STRATIFORM CLOUDS AS DEDUCED BY COORDINATED POLARIMETRIC RADAR AND AIRCRAFT MEASUREMENTS
Peter Meischner, Martin Hagen, and Hartmut Hoeller *In its* Contributions to Atmospheric Physics in Honor of Dr. Manfred Reinhardt on His 65th Birthay Sep. 1991 p 141-149 Original contains color illustrations (For primary document see N92-26329 17-46)
Avail: NTIS HC/MF A11; DLR, Wissenschaftliches, Berichtswesen, Postfach 90 60 58, Cologne, Fed.Republic of Germany, HC 60 Deutsche marks

N92-26343# Innsbruck Univ. (Austria). Inst. fuer Meteorologie und Geophysik.
THE OBJECTIVE DETERMINATION OF FRONT LINES [ZUR OBJEKTIVEN BESTIMMUNG VON FRONTLINIEN]
Reinhold Steinacker *In* DLR, Contributions to Atmospheric Physics in Honor of Dr. Manfred Reinhardt on His 65th Birthday Sep. 1991 p 151-159 In GERMAN (For primary document see N92-26329 17-46)
Avail: NTIS HC/MF A11; DLR, Wissenschaftliches, Berichtswesen, Postfach 90 60 58, Cologne, Fed.Republic of Germany, HC 60 Deutsche marks

N92-26348# Deutsche Forschungsanstalt fuer Luft- und Raumfahrt, Oberpfaffenhofen (Germany, F.R.). Inst. fuer Physik der Atmosphaere.
THE DLR METEOROLOGICAL RESEARCH AIRCRAFT FALCON
Hans P. Fimpel *In its* Contributions to Atmospheric Physics in Honor of Dr. Manfred Reinhardt on His 65th Birthday Sep. 1991 p 207-213 (For primary document see N92-26329 17-46)
Avail: NTIS HC/MF A11; DLR, Wissenschaftliches, Berichtswesen, Postfach 90 60 58, Cologne, Fed.Republic of Germany, HC 60 Deutsche marks

48 OCEANOGRAPHY

Includes biological, dynamic, and physical oceanography; and marine resources.

For related information see also *43 Earth Resources and Remote Sensing.*

N92-26173# Hawaii Univ., Honolulu. School of Ocean and Earth Science and Technology.
PROCEEDINGS OF 6TH HAWAIIAN WINTER WORKSHOP ON DYNAMICS OF OCEANIC INTERNAL GRAVITY WAVES Report, 1 Jul. 1990 - 31 Dec. 1991
Peter Mueller and Diane Henderson Nov. 1991 504 p Workshop held in Manoa, HI, 15-18 Jan. 1991
(Contract N00014-90-J-4010)
(AD-A245650) Avail: NTIS HC/MF A22

The proceedings of the conference are presented. Some areas of discussion are as follow: Internal Wave Shear and Dissipation; Internal Wave Dissipation in a Non-Garrett-Munk Ocean; Testing the Critical Reflection Hypothesis; Observations of Near-Inertial Internal Waves and Mixing in the Seasonal Thermocline; On the Statistics of Fine Scale Strain in the Thermocline; Spatial Structure of Thermocline and Abyssal Internal Waves; Estimates of Small-Scale Horizontal Divergence and Relative Vorticity in the Ocean; Measurements of Ertel Vorticity Fine structure in the Eastern North Atlantic; Symmetry Preserving Mode Truncations of Inviscid Geophysical Fluid Dynamical Equations; Weak Wave and Vortex Interactions, Internal Wave-Wave Resonance Theory: Fundamentals and Limitations; Choosing Variables for internal Wave Dynamics; Is Scattering or Reflection More Effective in Causing Boundary Mixing; On the Exchange of Energy Between Surface and Internal Wave Fields; The Saturation of Middle-Atmosphere Gravity Waves; Diagnosing Diapycnal Mixing; Energy Transfers Across an Internal Wave/Vortical Mode Spectrum; Large-Eddy Simulation of Internal Wave Motions; Numerical Modeling of the Large-Scale Dynamics of Internal Waves; Parameterizing Mixing in Inverse Models; Oceanic Model Testing; and Acoustic Implications of a New Model. GRA

N92-26245# Scripps Institution of Oceanography, La Jolla, CA.
MERIDIONAL ZONATION OF THE BARENTS SEA ECOSYSTEM INFERRED FROM SATELLITE REMOTE SENSING AND IN SITU BIO-OPTICAL OBSERVATIONS
B. G. Mitchell, Eric A. Brody, Eueng-Nan Yeh, Charles McClain, and Josefina Comiso 1991 32 p
(Contract N00014-89-J-1639)
(AD-A246323) Avail: NTIS HC/MF A03

The Barents Sea is a productive, shallow, high latitude marine ecosystem with complex hydrographic conditions. Zonal hydrographic bands defined by a coastal current, North Atlantic water, the polar front, and the seasonally variable marginal ice edge zone create a meridional zonation of the ecosystem during the spring-summer transition. The features reveal themselves in satellite imagery and by high resolution (vertical and horizontal) physical optical biological sampling. Surprisingly, the long-term (7 year) mean of Coastal Zone Color Scanner (CZCS) imagery reveals the Barents Sea as an anomalous 'blue water' regime at high latitudes that are otherwise dominated by satellite observed surface blooms. A combination of satellite imagery and in situ bio-optical analyses indicate that this pattern is caused by strong stratification in summer with surface nutrient depletion. GRA

N92-26270# Lawrence Livermore National Lab., CA.
GEOCHEMICAL CONSTRAINTS ON OCEAN GENERAL CIRCULATION MODELS
W. S. Broecker Feb. 1992 14 p
(Contract W-7405-eng-48)
(DE92-010805; UCRL-CR-109689) Avail: NTIS HC/MF A03

This progress report discusses aspects of geochemical constraints on ocean general circulation models. During the past year, we have concentrated on four research topics: (1) the study of dynamic constraints on the extent of CO2 uptake by an iron fertilized Antarctic Ocean; (2) the mixing dynamics of Antarctic Ocean; (3) interhemispheric transport of CO2 through the ocean; and (4) the role of marine biology in fossil fuel CO2 uptake by sea. DOE

N92-26360# Naval Postgraduate School, Monterey, CA.
OCEAN BOTTOM MODELING FOR RAY ACOUSTICS M.S. Thesis
Trevor N. Jones Dec. 1991 141 p
(AD-A246287) Avail: NTIS HC/MF A07

Akima cubic spline and spatial Fourier series (SFS) techniques for modeling ocean bottom contours from bathymetric data were comparatively analyzed. SFS methods encountered difficulty in ocean bottom reconstruction despite several enhancements to the fundamental technique. Both Akima cubic spline and SFS approaches proved unsatisfactory in reproducing first and second-order derivatives for several arbitrarily shaped ocean bottom contours. A simple reflection angle algorithm for arbitrary one-dimensional bottom models was examined and found to be accurate. A graphical demonstration of acoustic ray interaction

with the ocean bottom using a variety of mathematical ocean bottom models and the reflection angle algorithm was conducted. GRA

N92-26387# Coastal Engineering Research Center, Vicksburg, MS.
HINDCAST WAVE INFORMATION FOR THE GREAT LAKES: LAKE HURON. WAVE INFORMATION STUDIES OF US COASTLINES
Dec. 1991 420 p
(AD-A246326; CERC-WIS-26) Avail: NTIS HC/MF A18

The primary purpose of this study is to provide an accurate and comprehensive database of information descriptive of the long-term wave climate for the Great Lakes. The goal is to accurately represent mean values of wave parameters such as height, period, and direction. At any station, the hindcast values may at times differ from measured values, but this difference will generally be small and, in the mean, approach zero. It is also expected that the extreme values at any station will accurately represent actual conditions and provide reliable design wave information. This report describes the selection of a grid and hindcast sites, methods used to process and prepare input wind fields, numerical model calibration and verification, and production of a 32-year (1956-1987) hindcast. Information of this nature is essential to the efforts currently being undertaken by both US and Canadian interest in developing workable shoreline management guidelines and navigational aids. Projects benefiting from such information include dredging and dredge disposal, beach nourishment and erosion studies, and the design of coastal structures, beach nourishment and erosion studies, and the design of coastal structures such as jetties, harbors, revetments, and breakwaters, as well as local projects for improving recreation safety. GRA

N92-26411# California Univ., Santa Barbara. Marine Science Inst.
QUANTITATIVE ASSESSMENT OF THE SLOPE RESOLUTION OF SEAFLOOR MAPPING SYSTEMS Final Report
Ken C. Macdonald 4 Feb. 1992 14 p
(Contract N00014-90-J-1737)
(AD-A246158) Avail: NTIS HC/MF A03

The depth to the seafloor and the sediment thickness were observed with the SIO-MPL Deep Tow system from an altitude of 100 m on the western flank of the Mid-Atlantic Ridge near the FAMOUS area, 37 N, providing what is probably the most appropriate high resolution data set available at this time for roughness studies of the abyssal hill terrain of the Western North Atlantic. We have re-analyzed the original Deep Tow sonar record at a 3-m horizontal sample spacing. Along the MAR Deep Tow profile, individual sediment ponds of thickness up to 15 m are detected, although approximately half the profile has less than 1 m of sediment cover. A histogram of the original data shows that 77 percent of all slopes are less than 22 degrees, but 3 percent are greater then 71 degrees. The fall-off of the power spectrum is consistent with a fractal dimension D = 1.0 over the wavelengths 8 km to 10 m. GRA

N92-26423# Naval Postgraduate School, Monterey, CA.
OCEAN BOTTOM SIMULATION USING FRACTAL GEOMETRY M.S. Thesis
Candace J. Robertson Sep. 1991 80 p
(AD-A245477) Avail: NTIS HC/MF A05

Fractal geometry can simulate natural topography, creating data that can be used in sonar models as realistic ocean bottom features. An algorithm using recursive subdivision, or midpoint replacement, is used to create the fractals. The appearance, statistics, and dimension of the fractal can be controlled through the use of variables. The variables control the initial corner values and the amount that each subdivision can vary from the average of its two initial points. The choice of a random number distribution also affects the final fractal. The statistics, fractal dimension, and appearance of data generated by the fractal algorithm are comparable to real data. GRA

N92-26463# Institute for Naval Oceanography, Bay Saint Louis, MS.
THE UTILITY OF ACOUSTIC TRAVEL TIMES IN LOCATING THE NORTH WALL OF THE GULF STREAM
Michael S. Foster Oct. 1991 29 p
(AD-A246219; AD-E040177; INO-TM-5) Avail: NTIS HC/MF A03

Eighty-seven days of travel time data for ocean acoustic transmissions across the north wall of the Gulf Stream were examined. The data collected from 7 Jul. to 1 Oct. 1990 during the 1990 Applied Tomography Experiment (ATE90), sponsored by the Chief of Naval Research. The acoustic ray paths were, generally, perpendicular to the north wall. The analysis indicates that acoustic ray travel times can be useful in locating ocean frontal features and in reliably augmenting subjective techniques based on infrared (IR) satellite imagery and bathythermograph (BT) data. This document presents the procedures employed during the study and discusses the results. GRA

N92-26533# Naval Postgraduate School, Monterey, CA.
SYMBOLIC SOLUTION OF A MULTILAYER OCEAN WAVEGUIDE PROBLEM WITH ARBITRARY DEPTH DEPENDENT AMBIENT DENSITY AND SOUND SPEED PROFILES M.S. Thesis
Charles J. Young, Jr. Dec. 1991 232 p
(AD-A245476) Avail: NTIS HC/MF A11

The main purpose of this thesis was to obtain the symbolic solution of a multilayer (four fluid media) ocean waveguide problem. The waveguide was assumed to have depth-dependent ambient density and sound speed profiles in all fluid media, and arbitrarily shaped boundaries between all fluid media. A system of 28 equations in 17 unknowns was generated by satisfying all of the boundary conditions (including the boundary condition at the source) in cylindrical coordinates. The problem was set up as a weighted least squares problem symbolic solution by the computer program Mathematical. Due to software and hardware constraints, a symbolic solution for the most general case was not obtained. However, by making all of the boundaries plane, parallel boundaries, two cases were successfully programmed, yielding symbolic solutions which were verified by comparison to previously known results. GRA

N92-26568 Dartmouth Coll., Hanover, NH.
NUMERICAL INVESTIGATION OF THE CIRCULATION OF AN ICE-COVERED ARCTIC OCEAN Ph.D. Thesis
Peter Henry Ranelli 1991 172 p
Avail: Univ. Microfilms Order No. DA9130840

A high resolution (80 km) prognostic version of the Hibler-Bryan ice-ocean model is used to simulate the circulation of the ice-ocean system in the Arctic, Greenland and Norwegian Seas. The ocean model is changed to Cartesian coordinates to correct an imbalance between the ice mass balance and the salt flux into the ocean. The ice model is modified to determine ice velocities every ten years and uses specified velocities otherwise. A monthly varying precipitation and river runoff are used to specify the freshwater flux into the ocean and maintain the salt balance. The inflow of an annual average of 7.5 Sv of North Atlantic water through the Faro-Shetland Passage is found to be a substantial factor in the circulation of the GIN Sea and the Central Arctic Ocean. A two gyre system, consisting of a cyclonic gyre in the Eurasian Basin and an anti-cyclonic gyre in the Canadian Basin, develops in this case while the gyre in the Canadian Basin grows to dominate the Arctic Ocean if the transport is freely simulated by the model. A long term simulation to equilibrium is used to study different processes on the circulation of the Polar oceans. These simulations show the ice interaction force is a necessary component of the stress acting on the ocean by changing the direction and hence the curl of the stress. The overall circulation is greatly improved and includes a cyclonic gyre in the Eurasian Basin and improved inflow of Atlantic water at intermediate depths. The meridional heat transport through the Faro-Shetland Passage is found to be consistent with observations when an annual average transport of 7.5 Sv is forced through the model's southern boundary. The

heat budget is found to be unbalanced due to an increase in the heat content in the layer of Atlantic water and the deep water in the Arctic Ocean. The salt content in the model is found to be balanced. This is particularly important since changes in the density and the baroclinic velocity fields are dominated by the salinity.
Dissert. Abstr.

N92-27029# Naval Postgraduate School, Monterey, CA.
OBSERVATIONS OF WIND FORCED CIRCULATION ON THE CONTINENTAL SHELF OFF POINT SUR, CALIFORNIA FROM A SELF-CONTAINED ACOUSTIC DOPPLER CURRENT PROFILER M.S. Thesis
Christopher L. Abbott Dec. 1991 105 p
(AD-A246437) Avail: NTIS HC/MF A06

To study the current structure of the California Current as it manifests itself on the continental shelf a subsurface mooring, P1, was anchored 5 km west of Point Sur at 36 17' N, 121 59' W from 28 February through 11 May 1990. The P1 Mooring, placed on the 84 m isobath, consisted of a Self-Contained Acoustic Doppler Current Profiler (SC-ADCP) housed in a syntactic foam sphere and secured to an anchor. The mooring geometry placed the transducer heads at 80 m depth. The instrument operated at 307 kHz with each beam inclined 30 from the vertical. An ensemble average of 170 one-second pings were recorded every 15 minutes for 70 days. Good velocity data to within 17 m of the surface were obtained at 4 m intervals throughout the record. Low-pass filtered data indicated high coherence between the observed currents and the local wind forcing measured at the Monterey Bay NOAA buoy located 53 km to the northwest. During equatorward wind events the current response was vertically sheared and time-lagged at depth with near surface speeds up to 35 cm s. During wind relaxations (periods of no wind) and poleward winds a pressure induced barotropic poleward flow, on the order of 10 cm s, developed throughout the water column. These poleward currents became more frequent and better developed later in the record. Analysis of adjusted sea level (ASL) differences between stations located to the north and south of mooring P1 suggest an increasing poleward pressure gradient during the span of the record. Alongshore differences in the alongshore wind stress component contributed to the increasing difference in ASL. GRA

N92-27069# Naval Postgraduate School, Monterey, CA.
HYDROGRAPHIC DATA FROM THE COASTAL TRANSITION ZONE (CTZ) PROGRAM, 5-19 JULY 1988 Technical Report, Oct. 1987 - Sep. 1988
Paul F. Jessen and Steven R. Ramp 31 Dec. 1991 348 p
(Contract N00014-87-WR-24018; NR Proj. RR0-3103)
(AD-A245517; NPS-OC-92-002) Avail: NTIS HC/MF A15

This is a data report which presents hydrographic (CTD) data from a cruise off Point Arena, CA during 5-19 July 1988. The study area was between 37 deg 2 min N to 39 deg 21 min N and 123 deg 20 min W to 126 deg 20 min W. The sampling plan consisted of a grid of six alongshore transects 40 km apart, with 5 to 9 stations approx. 25 km apart along each transect. The sampling grid was occupied twice during the cruise, starting each time at the southeast corner of the study area. A total of 114 CTD to 500 m and 16 XBT drops to 450 m were made. The data are presented as individual vertical profiles, vertical sections, and property distributions on horizontal surfaces. The data were collected as part of the ONR Coastal Transition Program to study cold filaments in the region. GRA

N92-27071# Naval Oceanographic and Atmospheric Research Lab., Bay Saint Louis, MS.
A COMPENDIUM OF ENVIRONMENTAL DATA COLLECTED DURING THE SOUTHWEST FLORIDA SHALLOW-WATER ACOUSTIC SEA TEST Final Report
B. R. Gomes, P. J. Bucca, and J. M. Null Dec. 1991 75 p
(AD-A246143; AD-E040175; NOARL-TN-208) Avail: NTIS HC/MF A04

During 14-20 June 1991, an active acoustics exercise was conducted under the auspices of the Program Executive Officer of the Air, ASW, Assault and Special Mission Programs office. This exercise was located on the continental shelf, slope and in the basin between the Florida Keys and St. Petersburg, Florida. The objective of this mission is to make noise, reverberation and transmission loss measurements using fully calibrated sources, receivers, and recording devices. This data set is intended to support the validation of candidate shallow-water transmission loss and reverberation models for use in the development of next generation airborne ASW sensor systems. To adequately interpret the exercise results and to support the modeling effort, a robust suite of supporting environmental measurements were made aboard the research vessel NADC-38, owned by the Naval Air Development Center (NADC). These measurements include a depiction of the sound speed structure, bathymetry, meteorological conditions, and navigation along 11 projector tow tracks and at 3 drifting ambient noise and 4 reverberation sites. This technical note provides a brief description of the oceanographic and geological structure in the exercise area followed by a compendium of the collected data. GRA

51 LIFE SCIENCES (GENERAL)

N92-26203# California Univ., Berkeley. Lawrence Berkeley Lab.
LIFE SCIENCES AND ENVIRONMENTAL SCIENCES
Feb. 1992 111 p
(Contract DE-AC03-76SF-00098)
(DE92-010254; LBL-PUB-696) Avail: NTIS HC/MF A06

The DOE laboratories play a unique role in bringing multidisciplinary talents -- in biology, physics, chemistry, computer sciences, and engineering -- to bear on major problems in the life and environmental sciences. Specifically, the laboratories utilize these talents to fulfill OHER's mission of exploring and mitigating the health and environmental effects of energy use, and of developing health and medical applications of nuclear energy-related phenomena. At Lawrence Berkeley Laboratory (LBL) support of this mission is evident across the spectrum of OHER-sponsored research, especially in the broad areas of genomics; structural biology; basic cell and molecular biology; carcinogenesis; energy and environment; applications to biotechnology; and molecular, nuclear, and radiation medicine. These research areas are briefly described. DOE

N92-26266*# National Aeronautics and Space Administration, Washington, DC.
SPACE LIFE SCIENCES STRATEGIC PLAN, 1991
1992 58 p
(NASA-TM-107856; NAS 1.15:107856) Avail: NTIS HC/MF A04

Over the last three decades the life sciences program has significantly contributed to NASA's manned and unmanned exploration of space, while acquiring new knowledge in the fields of space biology and medicine. The national and international events which have led to the development and revision of NASA strategy will significantly affect the future of life sciences programs both in scope and pace. This document serves as the basis for synthesizing the option to be pursued during the next decade, based on the decisions, evolution, and guiding principles of the National Space Policy. Author

N92-26289# Naval Academy, Annapolis, MD.
A FRACTAL COMPUTER MODEL OF MACROMOLECULE-CELL SURFACE INTERACTIONS Final Report, 1990-1991
Jeffrey S. Dodge 13 May 1991 83 p
(AD-A245394; USNA-TSPR-178) Avail: NTIS HC/MF A05

Macromolecules involved in binding to cell surface receptors are important in many biological systems. The cross-linking and clustering of receptors that an antigen can cause is a vital event in the activation of the B-lymphocyte cell and the subsequent initiation of the immune response. This project set out to create a computer model of the interactions between a large molecule with several binding sites, and receptors on the cell surface. In order

to have some correlation with a real system, a multivalent antigen and a B-cell were used for physical parameters. The model was designed to provide insight into the behavior of the system, and information on the configurations of bound macromolecules. Analysis of the results from the computer model took two forms: interpretations of the visual output; and numerical analysis of the bound receptor clusters. Fractal geometry was used to characterize the shapes of the cross-linked cell receptors. GRA

N92-26493# California Univ., Los Angeles. Dept. of Chemistry and Biochemistry.

TIME-RESOLVED LASER STUDIES ON THE PROTON PUMP MECHANISM OF BACTERIORHODOPSIN

M. A. El-Sayed 1991 10 p

(Contract DE-FG03-88ER-13828)

(DE92-003218; DOE/ER-13828/4) Avail: NTIS HC/MF A02

Investigations were carried out in four major areas: (1) on the nature of the binding site of Eu(3+) in which a fluorescence technique was used to determine the binding equilibrium constant from the concentration of the free Eu(3+) in equilibrium with the bound ions; (2) on the mechanism of the slow deprotonation process of bacteriorhodopsin during its photocycle from the observed temperature and pH dependence of its kinetics; (3) using the circular dichroism spectrum of rB and its perturbed forms to examine the nature of the primary process as well as the origin of the non-exponential kinetic behavior of its photocycle; (4) on bacteriorhodopsin mutants to identify the important amino acids that are part of the reaction coordinate of the deprotonation process as well as to assign the species that are important in giving rise to UV transient absorption whose origin was controversial. Further details of each of these areas are presented. DOE

N92-26721# Instituto de Pesquisas Espaciais, Sao Jose dos Campos (Brazil).

DIFFERENTIATION ON GENUS OF AQUATIC MACROPHYTES THROUGH REMOTE SENSING IN THE TUCURUI RESERVOIR, PARA STATE, BRAZIL

Myrian deMoura Abdon and Marion Meyer (Fundacao de Ciencia, Aplicacoes e Technologia Espaciais, Sao Jose dos Campos, Brazil) Aug. 1991 14 p Presented at the 24th International Symposium on Remote Sensing of Environment, Rio de Janeiro, Brazil, 27-31 May 1991; and at the 5th Simposio Latino Americano de Percepcion Remota, Cusco, Peru, 28 Oct. - 1 Nov. 1991

(INPE-5315-PRE/1712) Avail: NTIS HC/MF A03

The purpose of this research is to evaluate the potential of digital data of LANDSAT-TM satellite spectral bands for detecting areas covered by several genus of aquatic macrophytes in the Tucurui Reservoir. Remote sensing is an adequate technique for studies developed in the Amazonian region, where the Tucurui Reservoir is very large, its aquatic plants communities occupy extensive areas and are of difficult access. Thus, the management of this environment becomes possible, as for instance, monitoring hosts of endemic diseases, which live between the roots of aquatic vegetation. For this reason, it used an image of July 16th, 1989, and simultaneous observations were done in field work to verify the occurrence and localization of floating aquatic plants in the Tucurui Reservoir. Histograms acquired from spectral attributes in bands 2, 3, 4, 5 and 7 were analyzed. A vegetation index was done in areas of the reservoir which were occupied by different aquatic macrophytes. Spectral attributes in bands 2 and 7 were selected as those ones that offered better separability between areas occupied by genus Salvinia sp, Scirpus sp, Pistia sp and by several genus of acquatic plants. A supervised classification of the area was done. The spectral attribute in band 5 was added to the supervised classification in order to reduce the confusion between the targets nondense terrestrial vegetation and floating vegetation. Band 5 better separates flooded from nonflooded areas, contributing additionally to distinguishing areas with Scirpus sp from areas with Salvinia sp. The results of the supervised classification are presented on a mpa on the scale of 1:250.000. Author

N92-26850# Federal Coordinating Council for Science, Engineering and Technology, Washington, DC. Committee on Life Sciences and Health.

BIOTECHNOLOGY FOR THE 21ST CENTURY, FY 1993

Feb. 1992 125 p

(DE92-007757; DOE-92007757) Avail: NTIS HC/MF A06

This report outlines the Federal role in biotechnology research and describes the foundation for a coordinated national initiative that will, over the coming years, maximize the effectiveness of the Federal investment in biotechnology research. Specifically, this report discusses the following topics: (1) the baseline of programmatic activity and Federal funding in biotechnology research; (2) ongoing agency programs and new initiatives; (3) national strategic objectives for biotechnology research; (4) the first interagency Federal biotechnology research budget; and (5) suggests directions for future efforts. The following Biotechnology Research Areas are discussed: Agriculture, Energy, Environment, Health, Manufacturing/Bioprocessing, General Foundations, Genome Projects, Marine Biotechnology, Structural Biology, Social Impact Research, and Infrastructure. DOE

N92-26938# Wisconsin Univ., Madison.

CARBON MONOXIDE METABOLISM BY THE PHOTOSYNTHETIC BACTERIUM RHODOSPIRILLUM RUBRUM

P. W. Ludden and G. P. Roberts 1991 5 p

(Contract DE-FG02-87ER-13691)

(DE92-010953; DOE/ER-13691/T2) Avail: NTIS HC/MF A01

Carbon monoxide metabolism in the Rhodospirillum rubrum is investigated. In the past year, progress was made in four areas: (1) the identification and isolation of the physiological electron carrier from monoxide dehydrogenase (CODH) to hydrogenase in R. rubrum; (2) the isolation, sequencing, and mutagenesis of the genes encoding the components of the CO oxidation system in R. rubrum; (3) the purification and characterization of the CO-induced hydrogenase activity of R. rubrum; and (4) the spectroscopic investigation of the cobalt-substituted form of the enzyme. DOE

N92-26977# Centre d'Etude de l'Energie Nucleaire, Mol (Belgium). Lab. of Genetics and Biotechnology.

THIOCAPSA ROSEOPERSICINA, A BACTERIUM FOR SULFUR-RECYCLING IN MICROBIAL ECOSYSTEMS DESIGNED FOR CELSS AND SPACE PURPOSES

P. Jansen and M. Mergeay *In* ESA, 4th European Symposium on Space Environmental Control Systems, Volume 2 Dec. 1991 p 799-803 Sponsored by Institut pour l'Encouragement de la Recherche Scientifique dans l'Industrie et l'Agriculture and ESA/ESTEC (For primary document see N92-26950 17-54)

Avail: NTIS HC/MF A23; ESA, EPD, ESTEC, Noordwijk, Netherlands, HC 150 Dutch guilders (2 vols)

N92-26978# European Space Agency. European Space Research and Technology Center, ESTEC, Noordwijk (Netherlands). Thermal Control and Life Support Div.

HIGHER PLANT GROWTH IN CLOSED ENVIRONMENT: PRELIMINARY EXPERIMENTS IN LIFE SUPPORT FACILITY AT ESA-ESTEC

Christian Tamponnet, Roger Binot, and Daniel deChambure *In its* 4th European Symposium on Space Environmental Control Systems, Volume 2 Dec. 1991 p 805-810 (For primary document see N92-26950 17-54)

Avail: NTIS HC/MF A23; ESA, EPD, ESTEC, Noordwijk, Netherlands, HC 150 Dutch guilders (2 vols)

N92-26979# Academy of Sciences (USSR), Krasnoyarsk. Inst. of Biophysics.

CHEMOLITHOTROPIC HYDROGEN-OXIDIZING BACTERIA AND THEIR POSSIBLE FUNCTIONS IN CLOSED ECOLOGICAL LIFE-SUPPORT SYSTEMS

T. G. Volova, J. G. Gitelson, F. Y. Sidko, and I. N. Trubachev *In* ESA, 4th European Symposium on Space Environmental Control Systems, Volume 2 Dec. 1991 p 811-815 (For primary

document see N92-26950 17-54)
Avail: NTIS HC/MF A23; ESA, EPD, ESTEC, Noordwijk, Netherlands, HC 150 Dutch guilders (2 vols)

N92-26982# MATRA Espace, Paris-Velizy (France). Applications de la Microgravite.
MODELLING LIGHT TRANSFER INSIDE PHOTOBIOFERMENTORS: APPLICATIONS TO THE PHOTOSYNTHETIC COMPARTMENTS OF CELSS
J. F. Cornet, C. G. Dussap, G. Dubertret, and J. B. Gros (Clermont-Ferrand Univ., France) *In* ESA, 4th European Symposium on Space Environmental Control Systems, Volume 2 Dec. 1991 p 831-836 (For primary document see N92-26950 17-54)
Avail: NTIS HC/MF A23; ESA, EPD, ESTEC, Noordwijk, Netherlands, HC 150 Dutch guilders (2 vols)

N92-27120*# Park (George W.) Seed Co., Inc., Greenwood, SC.
SEEDS IN SPACE EXPERIMENT
Jim A. Alston *In* NASA. Langley Research Center, LDEF: 69 Months in Space. First Post-Retrieval Symposium, Part 3 Jan. 1992 p 1625-1634 (For primary document see N92-27083 17-99)
Avail: NTIS HC/MF A21; 1 functional color page

N92-27121*# Oklahoma State Univ., Stillwater.
SPACE EXPOSED EXPERIMENT DEVELOPED FOR STUDENTS (SEEDS) (P0004-2)
Doris K. Grigsby and Nelson J. Ehrlich *In* NASA. Langley Research Center, LDEF: 69 Months in Space. First Post-Retrieval Symposium, Part 3 Jan. 1992 p 1635-1636 (For primary document see N92-27083 17-99)
Avail: NTIS HC/MF A21; 1 functional color page

N92-27122*# The Research Inst. of the Gulf of Maine, South Portland.
SURVIVAL OF EPIPHYTIC BACTERIA FROM SEED STORED ON THE LONG DURATION EXPOSURE FACILITY (LDEF) Abstract Only
Andrew C. Schuerger, Bret L. Norman, and Joseph A. Angelo, Jr. (Science Applications International Corp., Melbourne, FL.) *In* NASA. Langley Research Center, LDEF: 69 Months in Space. First Post-Retrieval Symposium, Part 3 Jan. 1992 p 1637 (For primary document see N92-27083 17-99)
Avail: NTIS HC/MF A21; 1 functional color page

N92-27123*# Deutsche Forschungsanstalt fuer Luft- und Raumfahrt, Cologne (Germany, F.R.). Inst. for Aerospace Medicine.
PRELIMINARY TOTAL DOSE MEASUREMENTS ON LDEF
G. Reitz *In* NASA. Langley Research Center, LDEF: 69 months in Space. First Post-Retrieval Symposium, Part 3 p1643-1649 (SEE N92-27083 17-99) Jan. 1992 (For primary document see N92-27083 17-99)
Avail: NTIS HC/MF A21; 1 functional color page

N92-27124*# Johann-Wolfgang-Goethe-Univ., Frankfurt am Main (Germany, F.R.). Botanical Inst.
TOTAL DOSE EFFECTS (TDE) OF HEAVY IONIZING RADIATION IN FUNGUS SPORES AND PLANT SEEDS: PRELIMINARY INVESTIGATIONS
A. R. Kranz, M. W. Zimmermann, R. Stadler, K. E. Gartenbach, and M. Pickert *In* NASA. Langley Research Center, LDEF: 69 Months in Space. First Post-Retrieval Symposium, Part 3 Jan. 1992 p 1651-1660 (For primary document see N92-27083 17-99)
Avail: NTIS HC/MF A21; 1 functional color page

N92-27125*# Marburg Univ. (Germany, F.R.). Dept. of Environmental Sciences and Space Medicine.
PRELIMINARY RESULTS OF THE ARTEMIA SALINA EXPERIMENTS IN BIOSTACK ON LDEF
E. H. Graul, W. Ruether, and C. O. Hiendl *In* NASA. Langley Research Center, LDEF: 69 Months in Space. First Post-Retrieval Symposium, Part 3 Jan. 1992 p 1661-1665 (For primary document see N92-27083 17-99)
Avail: NTIS HC/MF A21; 1 functional color page

N92-27126*# Deutsche Forschungsanstalt fuer Luft- und Raumfahrt, Cologne (Germany, F.R.). Inst. of Aerospace Medicine.
LONG-TERM EXPOSURE OF BACTERIAL SPORES TO SPACE
G. Horneck, H. Buecker, and G. Reitz *In* NASA. Langley Research Center, LDEF: 69 Months in Space. First Post-Retrieval Symposium, Part 3 Jan. 1992 p 1667-1673 (For primary document see N92-27083 17-99)
Avail: NTIS HC/MF A21; 1 functional color page

52 AEROSPACE MEDICINE

Includes physiological factors; biological effects of radiation; and effects of weightlessness on man and animals.

N92-26263*# Pennsylvania Univ., Philadelphia. Inst. for Environmental Medicine.
BIOCHEMICAL, ENDOCRINE, AND HEMATOLOGICAL FACTORS IN HUMAN OXYGEN TOLERANCE EXTENSION: PREDICTIVE STUDIES 6 Final Report
C. J. Lambertsen and J. M. Clark 31 Mar. 1992 112 p
(Grant NAG9-342)
(NASA-CR-190341; NAS 1.26:190341) Avail: NTIS HC/MF A06
The Predictive Studies VI (Biochemical, endocrine, and hematological factors in human oxygen tolerance extension) Program consisted of two related areas of research activity, integrated in design and performance, that were each based on an ongoing analysis of human organ oxygen tolerance data obtained for the continuous oxygen exposures of the prior Predictive Studies V Program. The two research areas effectively blended broad investigation of systematically varied intermittent exposure patterns in animals with very selective evaluation of specific exposure patterns in man. D.R.D.

N92-26470# Navy Clothing and Textile Research Facility, Natick, MA.
EFFECTIVENESS OF A SELECTED MICROCLIMATE COOLING SYSTEM IN INCREASING TOLERANCE TIME TO WORK IN THE HEAT. APPLICATION TO NAVY PHYSIOLOGICAL HEAT EXPOSURE LIMITS (PHEL) CURVE 5 Final Report, Jun. 1988 - Mar. 1989
Nancy A. Pimental and Barbara A. Avellini Jan. 1992 36 p
(AD-A246529; NCTRF-181) Avail: NTIS HC/MF A03
The effectiveness of a passive cooling ice vest in reducing heat strain was evaluated. The SteeleVest is a canvas vest with pockets which hold frozen gel packs against the torso (total weight 5.1 kg). Eight test volunteers attempted 10, 4-hour heat exposures (five environments, with and without the vest) in hot-humid and hot-dry environments having wet bulb globe temperatures (WBGT) of 36-39 C. Dry bulb temperatures ranged from 38-49 C, with 25-80 percent relative humidity. Subjects wore the Navy utility uniform and exercised at 272 W. This corresponded to a work rate equivalent to the Navy PHEL Curve 5. In all environments, the SteeleVest significantly reduced thermal strain, as evidenced by reduced rectal and skin temperatures, heart rate, and sweat rate. Use of the SteeleVest approximately doubled tolerance times compared with tests without the vest. The gel packs lasted approximately 2 hours before they required replacement. When the hot-humid and hot-dry environments having equivalent WGBT's were compared, thermal strain was higher in the more humid environments. In addition to its effectiveness in reducing heat strain, the SteeleVest is relatively lightweight, has a low profile, requires little maintenance, and is not susceptible to mechanical problems. These characteristics make it potentially feasible for shipboard use. GRA

N92-26512# Johns Hopkins Univ., Baltimore, MD. Dept. of Epidemiology.
ADVERSE REPRODUCTIVE EVENTS AND ELECTROMAGNETIC RADIATION
W. Stewart and R. Ouellet-Hellstrom 31 Jul. 1991 44 p Sponsored by NIOSH, Cincinnati, OH
(Grant NIOSH-R01-OH-02373)
(PB92-145796) Avail: NTIS HC/MF A03

In 1989, approximately 42,000 questionnaires were mailed to female physical therapists to assess the risk of adverse reproductive effects among those exposed to electromagnetic radiation at radio frequencies. From the resulting data, the risk of early recognized fetal loss was assessed using a nested case-control design. The cases (1753 miscarriages) were matched to controls (1753 other pregnancies except ectopics) on mother's age at conception and the number of years elapsed between conception and interview. The results of the study indicate that female physical therapists who work with microwave diathermy 6 months prior to the pregnancy and/or during the first trimester were at increased risk of experiencing a recognized early fetal loss, but female physical therapists who work with shortwave diathermy were not at an increased risk. This association was shown to hold even when the mother's age at conception, the number of years elapsed between conception and interview, the number of prior early fetal losses, mother's conditions ever diagnosed, and use of other modalities were controlled. The data also suggest a possible association between exposure to transcutaneous electrical nerve stimulation with an elevated risk of early recognized fetal loss. GRA

N92-27063# Weizmann Inst. of Science, Rehovoth (Israel).
LOW POWER LASER IRRADIATION EFFECT WITH EMPHASIS ON INJURED NEURAL TISSUES Midterm Report, 1 Mar. 1990 - 31 Mar. 1991
Michael Schwartz and Michael Belkin 1 Apr. 1991 26 p
(Contract DAMD17-90-Z-0008; DA Proj. 3M1-62787-A-878)
(AD-A246410) Avail: NTIS HC/MF A03

A few years ago, the use was initiated of lower power helium neon (He-Ne) laser (632.8 nm) for the treatment of injured nerves of the central nervous system (CNS) and of the peripheral nervous system. In those early studies it was shown that the low energy He-Ne laser treatment, if started immediately after injury, delays the posttraumatic degeneration but does not prevent it. We have suggested that the use of such treatment might be beneficial in cases of marginally injured axons which do not degenerate as a result of the primary lesion, but will degenerate as a second event and cases of severe injuries, in combination with a treatment modality which induces or facilitates growth. It was shown that the most successful growth of injured adult rabbit optic nerve (a nonregenerative system) into their own degenerative environment, which is hostile to growth when treatment is omitted. A daily irradiation for 10-14 consecutive days combined with application at the time of the injury of soluble substances, shown to facilitate growth, resulted in abundant growth of axons from the retinal ganglion cells of the injured fibers of optic nerves, as well as from the cut tips of the the injured fibers. GRA

N92-27068* National Aeronautics and Space Administration, Washington, DC.
AEROSPACE MEDICINE AND BIOLOGY: A CONTINUING BIBLIOGRAPHY WITH INDEXES (SUPPLEMENT 362)
May 1992 118 p
(NASA-SP-7011(362); NAS 1.21:7011(362)) Avail: NTIS HC A06: NTIS standing order as PB92-912300, A03

This bibliography lists 357 reports, articles and other documents introduced into the NASA Scientific and Technical Information System during May 1992. Subject coverage includes: aerospace medicine and physiology, life support systems and man/system technology, protective clothing, exobiology and extraterrestrial life, planetary biology, and flight crew behavior and performance. Author

N92-27011# Design Models, Inc., Los Angeles, CA. Space Projects Group.
ARCHITECTURAL STUDIES RELATING TO HUMAN BODY MOTION MORPHOLOGY IN MICROGRAVITY
Regis Fauquet and Jun Okushi *In* ESA, 4th European Symposium on Space Environmental Control Systems, Volume 2 Dec. 1991 p 1037-1043 (For primary document see N92-26950 17-54)
Avail: NTIS HC/MF A23; ESA, EPD, ESTEC, Noordwijk, Netherlands, HC 150 Dutch guilders (2 vols)

N92-27012# Deutsche Forschungsanstalt fuer Luft- und Raumfahrt, Cologne (Germany, F.R.). Inst. of Aerospace Medicine.
LBNP AS COUNTERMEASURE: AN AUTOMATED SCENARIO
Friedhelm Baisch, Luis Beck, Frank Kirchner, and Diego Loyola *In* ESA, 4th European Symposium on Space Environmental Control Systems, Volume 2 Dec. 1991 p 1045-1048 (For primary document see N92-26950 17-54)
Avail: NTIS HC/MF A23; ESA, EPD, ESTEC, Noordwijk, Netherlands, HC 150 Dutch guilders (2 vols)

53 BEHAVIORAL SCIENCES

Includes psychological factors; individual and group behavior; crew training and evaluation; and psychiatric research.

N92-27047 Institute for Perception RVO-TNO, Soesterberg (Netherlands). Traffic Behavior Group.
SELECTIVE SEARCH FOR THE TARGET PROPERTIES COLOR AND FORM Final Report [SELECTIEF ZOEKEN NAAR KLEUR EN VORM]
J. Theeuwes 4 Sep. 1991 24 p Sponsored by TNO Defence Research
(IZF-1991-B-13; TD91-3298; ETN-92-91236) Copyright Avail: TNO Inst. for Perception, Kampweg 5, P.O. Box 23, 3769 ZG Soesterberg, Netherlands

Three search experiments are used to test whether the preattentive parallel stage of visual processing can selectively guide the attentive stage to a particular known-to-be-relevant-target feature. Subjects search multielement displays for a salient green circle which has a unique form when surrounded by green nontarget squares and a unique color when surrounded by red nontarget circles. In the distractor conditions, a salient item on the other dimension is also presented. As an extension of earlier findings the results shown that topdown selectivity towards a particular feature is not possible, even after extended and consistent practice. The results reveal that selectivity depends on the relative discriminability of the form and color dimension. In an additional analysis the effect of the distance between target and distractor is examined. ESA

N92-26992# Compagnia Italiana Servizi Tecnici, Rome. Space Div.
CBT: ROLE AND FUTURE APPLICATION FOR CREW TRAINING
A. Guerrazzi, S. Masullo, S. Randisi, and E. Sala *In* ESA, 4th European Symposium on Space Environmental Control Systems, Volume 2 Dec. 1991 p 905-909 (For primary document see N92-26950 17-54)
Avail: NTIS HC/MF A23; ESA, EPD, ESTEC, Noordwijk, Netherlands, HC 150 Dutch guilders (2 vols)

54 MAN/SYSTEM TECHNOLOGY AND LIFE SUPPORT

Includes human engineering; biotechnology; and space suits and protective clothing.

For related information see also *16 Space Transportation.*

N92-26179# North Carolina Univ., Chapel Hill. Dept. of Computer Science.

ADVANCED TECHNOLOGY FOR PORTABLE PERSONAL VISUALIZATION Research Progress Report, Sep. 1990 - Mar. 1991

Frederick P. Brooks, Jr. and Henry Fuchs Mar. 1991 67 p (Contract DAEA18-90-C-0044)

(AD-A245819) Avail: NTIS HC/MF A04

The user of a Head-Mounted Display is immersed in a computer-simulated or remotely-sensed three-dimensional world. Despite an avalanche of publicity for virtual reality in the popular press, many difficult technical problems remain unsolved for this technology, and no application of it has yet been demonstrated to be commercially viable. We believe that the hardware and software required to create high bandwidth, multi-sensory virtual worlds will in a decade be as cheap and ubiquitous, and that virtual worlds systems will be used in a variety of applications. We are therefore working on three fronts: improving the crucial hardware components required, developing a software base, and demonstrating the usefulness of this technology to solve selected real-world problems. GRA

N92-26186# Atomic Energy Research Inst., Daeduk (Republic of Korea).

APPLICATION OF IRRADIATION TECHNIQUES TO FOOD AND FOODSTUFFS

Joong Ho Kwon, Myung Woo Byun, Suc Won Kim, Jae Seung Yang, and Han Ok Cho Feb. 1991 97 p In KOREAN; ENGLISH summary

(DE92-614952; KAERI/RR-976/90) Avail: NTIS HC/MF A05

A preservation study of dried fish, anchovies, has been conducted to determine the effect of gamma irradiation and laminated (nylon/polyethylene) film packaging on microbiological, physicochemical, and organoleptic qualities of stored samples under room, refrigeration, and freezing temperatures. Irradiation at less than 5 kGy and NY/PE-laminated film packaging are anticipated to be significantly effective for over 10 months in terms of improving the hygienic quality and extending the storage life of boiled-dried anchovies. In a survey of 700 participating consumers, respondents preferred irradiated food to chemically-treated one. However, the majority of respondents (55.7 percent) was ignorant of the fact that the Korean government and the international organizations concerned have approved the wholesomeness of irradiated food. Insufficiency of public information and understanding of irradiated food was indicated as a major cause for the retardation of the commercial utilization of food irradiation technology. In a response concerning the perception and acceptance toward irradiated food, there was a significant difference between the radiation worker and the general public. DOE

N92-26193*# RAND Corp., Santa Monica, CA.

HUMAN SUPPORT ISSUES AND SYSTEMS FOR THE SPACE EXPLORATION INITIATIVE: RESULTS FROM PROJECT OUTREACH

J. Aroesty, R. Zimmerman, and J. Logan 1991 131 p Sponsored by NASA, Washington (Contract F49620-86-C-0008)

(NASA-CR-190320; NAS 1.26:190320; RAND-N-3287-AF/NASA) Avail: NTIS HC/MF A07

The analyses and evaluations of the Human Support panel are discussed. The Human Support panel is one of eight panels created by RAND to screen and analyze submissions to the Space Exploration Initiative (SEI) Outreach Program. Submissions to the Human Support panel were in the following areas: radiation protection; microgravity; life support systems; medical care; and human factors (behavior and performance). Author

N92-26242# Army Natick Labs., MA.

MAINTENANCE MANUAL FOR NATICK'S FOOTWEAR DATABASE Final Report, Nov. 1990 - Dec. 1991

Paula M. Poole, Carolyn K. Bensel, and Richard M. Rosenstein Jan. 1992 15 p

(AD-A246273; Natick/TR-92/015) Avail: NTIS HC/MF A03

Natick's Footwear Database is a computerized system for the management of literature regarding lower extremity health and comfort as they relate to footwear. Six major topics define the focus and the contents of the database. These are: (1) anatomy; (2) biomechanics; (3) environment; (4) footwear; (5) injury; and (6) physiology. System capabilities include: text and keyword searches of the literature in the database; presentation on the computer screen of the results of searches; and generation of printed reports of the results of searches. An entry in the database contains the complete reference, the keywords assigned, and an overall summary of the contents. In the case of a paper dealing with an experiment, summaries of the methods employed and the results of the work are also presented. This report contains detailed information regarding the operation of the maintenance version of the footwear database. Included are instructions for installing the database, adding keywords, and updating the database contents by entering new literature or modifying existing entries. GRA

N92-26243# Army Natick Labs., MA.

USER MANUAL FOR NATICK'S FOOTWEAR DATABASE Final Report, Nov. 1990 - Dec. 1991

Paula M. Poole, Carolyn K. Bensel, and Richard M. Rosenstein Jan. 1992 77 p

(AD-A246275; Natick/TR-92/016) Avail: NTIS HC/MF A05

Natick's Footwear Database is a computerized system for the management of literature regarding lower extremity health and comfort as they relate to footwear. Six major topics define the focus and the contents of the database. These are: (1) anatomy; (2) biomechanics; (3) environment; (4) footwear; (5) injury; and (6) physiology. System capabilities include: text and keyword searches of the literature in the database; presentation on the computer screen of the results of searches; and generation of printed reports of the results of searches. An entry in the database contains the complete reference, the keywords assigned, and an overall summary of the contents. In the case of a paper dealing with an experiment, summaries of the methods employed and the results of the work are also presented. This report contains detailed information regarding the operation of the user version of the footwear database. Included are instructions for installing the database, conducting text and keyword searches, and obtaining outputs from the searches. GRA

N92-26255# Technische Univ., Delft (Netherlands). Faculty of Mechanical Engineering and Marine Technology.

MAN-MACHINE ASPECTS OF REMOTELY CONTROLLED SPACE MANIPULATORS Ph.D. Thesis

Jan Frans Tonnis Bos 1991 190 p Sponsored by Netherlands Technology Foundation

(ISBN-90-370-0056-8; ETN-92-91291) Avail: NTIS HC/MF A09

The design of a man-machine interface for a space manipulator using the specifications for HERA (Hermes Robot Arm) is addressed. The research deals with the manual control situation. Three problems were investigated: the lack of direct vision; the control of up to six Degrees Of Freedom (DOF); and the influence of the nonlinear and slow dynamics. Results from the investigation of the use of graphical displays showed that the presence of reference enhanced the three dimensional perception, resulting in safer task execution. The use of a target frame as the reference frame for controlling the six DOF mode instead of the end effector frame was investigated. A two DOF mode was judged to be easier. Predictive displays of the stopping configuration and a trajectory are evaluated for a rough positioning task in the presence of obstacles. A preliminary investigation of the most effective length

of the time-horizon was carried out. Results indicate that predictive control theory can serve as a means to describe human controller behavior. ESA

N92-26355# Logicon, Inc., Dayton, OH.
MAN-MACHINE INTERFACE ANALYSES FOR BOMBER FLIGHT MANAGEMENT SYSTEM Final Report, Jul. - Dec. 1990
Karen J. Peio, Robyn L. Crawford, and Gilbert G. Kuperman May 1991 174 p
(Contract F33615-89-C-0532)
(AD-A245707; AL-TR-1991-0018) Avail: NTIS HC/MF A08

The research reported in this document represents a concept definition study directed to exploring the MMI issues inherent in the development and integration of an FM avionic subsystem into a manned, penetrating bomber weapons system. The report addresses four specific FM/MMI objectives: (1) develop and document 'optimum' FM/MMI conceptual display formats; (2) integrate a laboratory (i.e., non-flyable) software development/demonstration FM processor into DET 1 AL's Strategic Avionics Battle-Management Evaluation and Research (SABER) advanced conceptual bomber crew system simulator; (3) conduct a laboratory, part-mission demonstration of FM avionics concept in the SABER facility; and (4) provide consultative support to government and industry for review and critique of FM/MMI conceptual display formats. This report documents the initial (Concept Definition) phase of the design of 'optimum' flight management display formats. The intent is to lay the foundation for an information requirements analysis for an FM system and subsequent design of a conceptual MMI. GRA

N92-26375# Oak Ridge National Lab., TN.
LIFE SUPPORT RESEARCH AND DEVELOPMENT, A DEPARTMENT OF ENERGY PROGRAM FOR THE SPACE EXPLORATION INITIATIVE
C. D. Scott, T. C. Scott, L. J. Johnson, W. W. Schertz, and J. A. Wise (Pacific Northwest Lab., Richland, WA.) 1992 9 p Presented at the International Conference on Life Support and Biospherics, Huntsville, AL, 19-20 Feb. 1992
(Contract DE-AC05-84OR-21400)
(DE92-007681; CONF-920263-1) Avail: NTIS HC/MF A02

The materials needed to sustain life in space operations can either be brought from Earth or created in place from wastes or in situ resources. Long-term missions of the future will require an approach in which most of the waste materials are processed and recycled and/or local resources are utilized. The concept of a Controlled Ecological Life Support System (CELSS) is under consideration for this task. Although a great amount of information exists in this area, a technical data base does not yet exist for the design of such systems. Such CELSS systems can really be considered as highly integrated physical/chemical/biological processing systems that must have very high reliability. Department of Energy (DOE) national laboratories have established a significant competence in the treatment of waste materials, especially with bioprocessing systems. Similar approaches will be used in life support R&D within the Space Exploration Initiative of the DOE. Initial research will concentrate on the processing and recycle of waste materials using microbial, enzymatic, or thermochemical processing. Other research areas will also be considered. The resulting innovative technology developed for space applications could also be the basis for important new approaches to the solution of terrestrial problems, particularly for the processing and recycle of waste materials. DOE

N92-26472# Defence Research Establishment, Ottawa (Ontario).
EFFECT OF TEXTILE TEST SAMPLE SIZE ON ASSESSMENT OF PROTECTION TO SKIN FROM THERMAL RADIATION
George A. Grant, Brian H. Harrison, and L. A. Main Oct. 1991 23 p
(AD-A246535; DREO-1096) Avail: NTIS HC/MF A03

Test samples of textile materials of 2.5, 7.6, 15.2, or 30.5 cm diameter were exposed to thermal radiation sources at Central Receiver Test Facility and the Thermal Radiation Source at Kirtland Air Force Base, New Mexico. The materials were exposed to fluences of 5, 10, 15, and 30 cal/sq. cm. in 1 or 3 seconds. The thermal pulse was square or approximately that of 1 KT weapon. Generally, damage to materials increased with an increase in the test sample (30.5 cm) ignited prior to 2.5 cm diameter samples. It was evident that testing with small samples of material would over-estimate the protection afforded. Comparison of test results of materials exposed to simulated and non-simulated nuclear weapons support the conclusion that protection is over-estimated by assessment of damage on exposed small test samples. GRA

N92-26494# Oak Ridge National Lab., TN.
LIFE SUPPORT RESEARCH AND DEVELOPMENT FOR THE DEPARTMENT OF ENERGY SPACE EXPLORATION INITIATIVE
Charles D. Scott, LaMar J. Johnson, William W. Schertz, James A. Wise (Pacific Northwest Lab., Richland, WA.), and Charles E. Wyman 1992 6 p
(Contracts DE-AC05-84OR-21400; W-31-109-eng-38; DE-AC02-83CH-10093; DE-AC07-76ID-01570)
(DE92-007239; CONF-920473-1) Avail: NTIS HC/MF A02

Long-term, manned space missions of the future will require an approach to life support systems in which most of the waste materials must be processed and recycled and/or local resources are utilized. The requirement for a reliable life support system has been recognized as an important component of the Space Exploration Initiative, and the Department of Energy (DOE), in conjunction with the National Aeronautics and Space Agency, is organizing a program in support of the development of this type of technology. It is quite likely that bioprocesses will be important components of the integrated system, and this will be the primary area of R&D within the DOE national laboratories. Initial research will include investigation of microbial, enzymatic, and thermochemical processing of wastes. Other research areas of interest include water and air purification by plants, microbial detection systems, biophotochemical CO2 recycle, tissue cultures for food, single-cell protein, bioadsorbents for pollutant removal, and several others. The resulting innovative technology developed for space exploration could also be the basis for new approaches for the processing and recycle of waste materials on Earth. DOE

N92-26528# Aerospace Medical Research Labs., Brooks AFB, TX.
THE ELECTRONIC EVALUATION OF THE ADVANCED DYNAMIC ANTHROPOMORPHIC MANIKIN (ADAM) IN HIGH TEMPERATURE ENVIRONMENTS Final Report, Apr. 1990 - Mar. 1991
Eric K. Spittle, Roy R. Rasmussen, and Ints Kaleps Mar. 1991 9 p
(AF Proj. 7231)
(AD-A245459; AL-TR-1991-0079) Avail: NTIS HC/MF A02

From the results of the 987 tests, it is concluded that the ADAM may have difficulty operating in high ambient temperatures above 160 F. The tests described in this report were used to determine probable causes of manikin shutdown at temperatures above this range. The safe viscera operational temperature threshold was determined to be 180 F. This correlates to a safe ambient operations temperature threshold of 130 F with a worst case manikin set up. To determine when the ADAM shut down above this temperature, manikin internal load cells, potentiometers, and accelerometers were excited and monitored external to the manikin. Additionally, circuit board voltages were externally monitored to determine when and which circuit boards shut down during a test. Finally, data were collected from the ADAM periodically to monitor the operational status of the manikin and any effect the temperatures were having on the sensors and data acquisition system of the manikin. The temperature profiles selected were representative of the operational temperatures the ADAM will experience in the F-16 cockpit mockup on the Multi-Axis Seat Ejection (MASE) sled, where the ADAM will be used for ejection tests in the near future. GRA

N92-26538*# National Aeronautics and Space Administration. Lyndon B. Johnson Space Center, Houston, TX.
THE VALIDATION OF A HUMAN FORCE MODEL TO PREDICT DYNAMIC FORCES RESULTING FROM MULTI-JOINT MOTIONS
Abhilash K. Pandya, James C. Maida, Ann M. Aldridge, Scott M. Hasson (Texas Womens Univ. Research Inst., Denton.), and Barbara J. Woolford Jun. 1992 33 p
(Contract NAS9-17900)
(NASA-TP-3206; S-670; NAS 1.60:3206) Avail: NTIS HC/MF A03

The development and validation is examined of a dynamic strength model for humans. This model is based on empirical data. The shoulder, elbow, and wrist joints were characterized in terms of maximum isolated torque, or position and velocity, in all rotational planes. This data was reduced by a least squares regression technique into a table of single variable second degree polynomial equations determining torque as a function of position and velocity. The isolated joint torque equations were then used to compute forces resulting from a composite motion, in this case, a ratchet wrench push and pull operation. A comparison of the predicted results of the model with the actual measured values for the composite motion indicates that forces derived from a composite motion of joints (ratcheting) can be predicted from isolated joint measures. Calculated T values comparing model versus measured values for 14 subjects were well within the statistically acceptable limits and regression analysis revealed coefficient of variation between actual and measured to be within 0.72 and 0.80. Author

N92-26665# Naval Medical Research Inst., Bethesda, MD.
PHYSIOLOGICAL DESIGN GOALS AND PROPOSED THERMAL LIMITS FOR US NAVY THERMAL GARMENTS: PROCEEDINGS OF 2 CONFERENCES SPONSORED BY THE NAVAL MEDICAL RESEARCH AND DEVELOPMENT COMMAND Technical Report, Jul. 1976 - Sep. 1980
Paul W. Webb, E. L. Beckman, Philip Sexton, and W. S. Vaughn Nov. 1991 51 p Conference No. 1 on Proposed Thermal Limits for Divers: A Guide for the Designers of Thermally Protective Equipment held July 1976; Conference No. 2 on Physiological Design Goals for Thermal Protection of Divers held Sep. 1980
(Contracts N00014-72-C-0057; N00014-80-C-0193)
(AD-A245543; NMRI-91-85) Avail: NTIS HC/MF A04

The proceedings of two conferences that were held to develop physiological limits and design goals for passive thermal garments are presented. These proceedings have not been achieved in the literature, but were in the form of reports submitted to the Office of Naval Research and Naval Medical Research and Development Command. This technical report has been published solely to archive these proceedings, which are of historic value. The first proceeding is entitled 'Proposed Thermal Limits for Divers: A Guide for Designers of Thermally Protective Equipment', held in July 1976. This proceedings sets the physiologic limits for both cold and heat exposure within which protective gear must maintain individuals. Total body and respiratory heat loss, core temperature, skin temperature, and hand and foot limits are discussed. A section on performance factors is also given. GRA

N92-26682*# National Aeronautics and Space Administration. Lyndon B. Johnson Space Center, Houston, TX.
CORRELATION AND PREDICTION OF DYNAMIC HUMAN ISOLATED JOINT STRENGTH FROM LEAN BODY MASS
Abhilash K. Pandya, Scott M. Hasson, Ann M. Aldridge (Lockheed Engineering and Sciences Co., Houston, TX.), James C. Maida, and Barbara J. Woolford Jun. 1992 64 p
(Contract NAS9-17900)
(NASA-TP-3207; S-671; NAS 1.60:3207) Avail: NTIS HC/MF A04

A relationship between a person's lean body mass and the amount of maximum torque that can be produced with each isolated joint of the upper extremity was investigated. The maximum dynamic isolated joint torque (upper extremity) on 14 subjects was collected using a dynamometer multi-joint testing unit. These data were reduced to a table of coefficients of second degree polynomials, computed using a least squares regression method. All the coefficients were then organized into look-up tables, a compact and convenient storage/retrieval mechanism for the data set. Data from each joint, direction and velocity, were normalized with respect to that joint's average and merged into files (one for each curve for a particular joint). Regression was performed on each one of these files to derive a table of normalized population curve coefficients for each joint axis, direction, and velocity. In addition, a regression table which included all upper extremity joints was built which related average torque to lean body mass for an individual. These two tables are the basis of the regression model which allows the prediction of dynamic isolated joint torques from an individual's lean body mass. Author

N92-26891# Institute of Sound and Vibration Research, Southampton (England).
DESIGN GUIDE FOR SADDLE SEATING ON SMALL HIGH-SPEED CRAFT
A. J. Messenger and M. J. Griffin Feb. 1992 19 p Sponsored in part by Inst. of Naval Medicine, Ministry of Defence (Navy), Alverstoke, England
(ISVR-TR-205) Avail: NTIS HC/MF A03

This design guide gives recommendations for the design of saddle-type seating fitted in small high-speed craft. Recommendations are made for the dimensions, angles, contouring and padding of the seat pan and backrest. Body depth and lateral space clearances are also considered, as are the positioning and dimensions of toe-straps and hand-holds. The recommendations are based on the principle of matching seat dimensions to the relevant dimensions of the user population so as to minimize passenger discomfort and reduce fatigue caused by inappropriate sitting postures. The dimensions suggested are appropriate for British males aged between 19 and 45 years. The anthropometric dimensions and population percentile values used in recommending each dimension are also specified so that the given values can be replaced by those appropriate to a different user population. The rationale behind the suggested dimensions and the consequences of deviating from the recommended values are specified. Author

N92-26950# European Space Agency, Paris (France).
FOURTH EUROPEAN SYMPOSIUM ON SPACE ENVIRONMENT CONTROL SYSTEMS, VOLUME 2
T.-Duc Guyenne, ed. and James J. Hunt, ed. Dec. 1991 526 p In ENGLISH and FRENCH Symposium held in Florence, Italy, 21-24 Oct. 1991
(ESA-SP-324-Vol-2; ISBN-92-9092-138-2; ISSN-0379-6566; ETN-92-91356) Avail: NTIS HC/MF A23; ESA, EPD, ESTEC, Noordwijk, Netherlands, HC 150 Dutch guilders (2 vols)

Papers of the fourth European symposium on space environmental control systems covering activities on space thermal control life support and habitability are presented. The subjects covered, range from cryogenic cooling to reentry thermal protection systems, from atmosphere management to water and waste management, and from internal architecture to astronaut food selection. In volume 2, the following topics are addressed: water management, computational environment, heat rejection, instrument and equipment thermal control, Controlled Ecological Life Support Systems (CELSS), cooling loop components, habitability, in orbit thermal performance, extravehicular activity, thermal protection streams, architecture, and interior design. For individual titles, see N92-26951 through N92-27028.

N92-26951# Nauchno-Proizvodstvennoe Obedinenie Niichimmash, Moscow (USSR).
WATER RECOVERY FROM CONDENSATE OF CREW RESPIRATION PRODUCTS ABOARD THE SPACE STATION
N. M. Samsonov, N. S. Farafonov, V. M. Novikov, L. S. Bobe, V. M. Gordeyev, G. K. Abramov, N. N. Protasov, J. E. Sinjak, I. V. Lavrov (Nauchno-Proizvodstvennoe Obedinenie Energija, Kaliningrad, USSR), and P. I. Glushenko et al *In* ESA, 4th European Symposium on Space Environmental Control Systems,

Volume 2 Dec. 1991 p 625-627 (For primary document see N92-26950 17-54)
Avail: NTIS HC/MF A23; ESA, EPD, ESTEC, Noordwijk, Netherlands, HC 150 Dutch guilders (2 vols)

The process and equipment for water recovery from condensate derived from atmosphere thermal/moisture control facilities of the long endurance Mir manned Space Station are considered. The recovery process includes the reception and separation of liquid from the gas/liquid stream, water purification from contaminants, purified water saturation with food salts, and preservation to prevent the growth of microflora. Low energy processes and equipment for the system in zero gravity space flight are discussed. The recovery system is currently in operation aboard the orbital space station Mir. The energy requirements for recovered water (without water preheating on ingestion) and the specific weight of equipment are 4 W hr and 0.2 kg per kg of recovered water with about 100 percent of water recovery from condensate feed, and the quality conforming to the relevant standard. With the minor modification, the system may be used for future orbital space stations of new generation, Mars spaceships, and lunar bases. ESA

N92-26952# Nauchno-Proizvodstvennoe Obedinenie Niichimmash, Moscow (USSR).
WATER RECLAMATION FROM URINE ABOARD THE SPACE STATION
N. M. Samsonov, V. M. Novikov, L. S. Bobe, B. J. Pinski, V. A. Leonov, N. N. Protasov, V. V. Komolov, V. B. Filonenko (Nauchno-Proizvodstvennoe Obedinenie Vniigidromash, Moscow, USSR), and S. S. Bocharov *In* ESA, 4th European Symposium on Space Environmental Control Systems, Volume 2 Dec. 1991 p 629-631 (For primary document see N92-26950 17-54)
Avail: NTIS HC/MF A23; ESA, EPD, ESTEC, Noordwijk, Netherlands, HC 150 Dutch guilders (2 vols)

A system designed for water reclamation from urine by atmospheric distillation with condensate sorption post treatment is considered. A schematic process diagram and a system operation sequence are described. Some research and engineering problems relating to the development of equipment for the orbital Space Station are outlined. A process for water evaporation from solution into a vapor/gas fluid at the surface restricted by a capillary/porous hydrophilic selective membrane which ensures the process performance at zero gravity is analyzed. Some results of the operation of the system aboard the Soviet orbital Space Station Mir are discussed. The effectiveness and promise for water reclamation systems aboard the current and future Space Stations are shown. For long endurance orbital Space Stations, the most effective method is to reclaim water from urine. The reclaimed water is used as potable water and for food preparation (after additional conditioning) or for producing electrolyzed O2. The latter can fully provide the crew with simulated atmosphere for breathing. ESA

N92-26953*# Boeing Co., Houston, TX. Defense and Space Group.
SPACE STATION FREEDOM REGENERATIVE WATER RECOVERY SYSTEM CONFIGURATION SELECTION
R. Reysa and J. Edwards *In* ESA, 4th European Symposium on Space Environmental Control Systems, Volume 2 Dec. 1991 p 633-642 (For primary document see N92-26950 17-54)
(Contract NAS8-50000)
Avail: NTIS HC/MF A23; ESA, EPD, ESTEC, Noordwijk, Netherlands, HC 150 Dutch guilders (2 vols)

The Space Station Freedom (SSF) must recover water from various waste water sources to reduce 90 day water resupply demands for a four/eight person crew. The water recovery system options considered are summarized together with system configuration merits and demerits, resource advantages and disadvantages, and water quality considerations used to select the SSF water recovery system. ESA

N92-26954# Niigata Univ. (Japan). Faculty of Engineering.
CATALYTIC WET-OXIDATION OF HUMAN WASTE PRODUCED IN A SPACE HABITAT: PURIFICATION OF THE OXIDIZED LIQUOR FOR HUMAN DRINKING
Y. Takahashi, N. Takeda, T. Aoyagi, and K. Tanaka *In* ESA, 4th European Symposium on Space Environmental Control Systems, Volume 2 Dec. 1991 p 643-647 (For primary document see N92-26950 17-54)
Avail: NTIS HC/MF A23; ESA, EPD, ESTEC, Noordwijk, Netherlands, HC 150 Dutch guilders (2 vols)

In order to elucidate the reproducibility and durability of the Ru-Rh catalyst developed formerly for wet oxidation, the filtrate of noncatalytically wet oxidized sewage sludge was wet oxidized again at 300 C using the catalyst. This test was carried out as a batch one and repeated 32 times using only one catalyst. Almost complete oxidation and denitrification occurred regardless of the repetition number. The reproducibility and durability of the catalyst was ensured. In order to reuse the product of the catalytic wet oxidation for hygiene and/or potable water, it was treated by granulated activated carbon and ion exchange resin. Organic matter, conductivity, and color was removed effectively to the levels of potable water. The catalytically wet oxidized liquor can be reused at least for hygiene water. The reuse of potable water is also promising. ESA

N92-26955# Nauchno-Proizvodstvennoe Obedinenie Niichimmash, Moscow (USSR).
HYGIENE WATER RECOVERY ABOARD THE SPACE STATION
N. M. Samsonov, N. S. Farafonov, L. K. Abramov, S. S. Bocharov, N. N. Protasov, V. V. Komolov, V. B. Filonenko, and A. A. Berlin (Institute of Biomedical Problems, Moscow, USSR) *In* ESA, 4th European Symposium on Space Environmental Control Systems, Volume 2 Dec. 1991 p 649-651 (For primary document see N92-26950 17-54)
Avail: NTIS HC/MF A23; ESA, EPD, ESTEC, Noordwijk, Netherlands, HC 150 Dutch guilders (2 vols)

The system for hygiene water recovery, which is currently in operation aboard the orbital Space Station Mir, is considered. The system receives untreated hygiene water as a water/air mixture from the handwash and shower facilities, separates the mixture phases, stores untreated water, purifies water from mechanical and dissolved impurities, decontaminates and stores purified water, and preheats and feeds purified water to the handwash and shower facilities. A schematic of the system is presented. The operations of the system, the method of water recovery, and design of main blocks are described. The ways of system updating are illustrated. The energy/mass characteristics of the system supporting the evidence of effectiveness of the system aboard the long term orbital space stations are listed. ESA

N92-26956# Kiev Polytechnic (USSR).
THE CENTRIFUGAL MASS EXCHANGE APPARATUS IN AIR-CONDITIONING SYSTEM OF ISOLATED, INHABITED OBJECT AND ITS WORK CONTROL
P. A. Barabash, V. G. Rifert, L. S. Bobe, N. N. Goliyad, and V. B. Filonenko (Nauchno-Proizvodstvennoe Obedinenie Vniigidromash, Moscow, USSR) *In* ESA, 4th European Symposium on Space Environmental Control Systems, Volume 2 Dec. 1991 p 653-658 (For primary document see N92-26950 17-54)
Avail: NTIS HC/MF A23; ESA, EPD, ESTEC, Noordwijk, Netherlands, HC 150 Dutch guilders (2 vols)

The results of the research conducted in the hydrodynamic and heat and mass transfer processes taking place in separators-distillers are obtained, and recommendations for the design and manufacture of the equipment are given. A tradeoff analysis of several known methods of measuring the small concentrations of gas inclusions in liquids and aerosols is conducted, and, on the basis of this analysis, the integral method of light dispersion is chosen for implementation. ESA

N92-26957# National Space Development Agency, Tokyo (Japan).
DESIGN OF JEM TEMPERATURE AND HUMIDITY CONTROL SYSTEM
Tadashi Suzuki, Syozo Shibutani, Akira Hattori, Saburou Miwa, and Masaharu Takagishi (Kawasaki Heavy Industries Ltd., Gifu, Japan) *In* ESA, 4th European Symposium on Space Environmental Control Systems, Volume 2 Dec. 1991 p 659-664 (For primary document see N92-26950 17-54)
Avail: NTIS HC/MF A23; ESA, EPD, ESTEC, Noordwijk, Netherlands, HC 150 Dutch guilders (2 vols)

The design of the Japanese Experiment Module (JEM) to be attached to the Columbus Space Station is addressed. Environmental requirements for two crew members in the module are outlined. The design status of JEM Temperature and Humidity Control (THC) subsystem is described. Design requirements derived from the whole JEM system design are introduced. The THC subsystem and the THC assembly design are presented. Some test results in cabin ventilation testing and component testing are outlined. ESA

N92-26958# Fokker Space and Systems, Amsterdam (Netherlands).
FIESTA: AN INTEGRATED APPROACH TO THERMAL MODEL PROCESSING **c61**
J. P. A. deKoning and H. deWolf *In* ESA, 4th European Symposium on Space Environmental Control Systems, Volume 2 Dec. 1991 p 667-673 Sponsored by Netherlands Agency for Aerospace Programs (For primary document see N92-26950 17-54)
Avail: NTIS HC/MF A23; ESA, EPD, ESTEC, Noordwijk, Netherlands, HC 150 Dutch guilders (2 vols)

FIESTA (Fokker's Integrated Engineering System for Thermal Analysis), a set of integrated software tools to assist the thermal engineer in processing thermal mathematical models and preparation/evaluation of thermal tests, is considered. FIESTA supports the main thermal control analysis tools ESATAN (ESA Thermal Analysis Network), SINDA (for thermal network analysis: computation of temperatures and powers in thermal mathematical models), and THERMICA or VWHEAT (for computation of radiative couplings and external fluxes in geometric models). The tools enable and encourage a 'structural modeling' approach to thermal mathematical modeling, using the ideas of software engineering methods. FIESTA is coded in standard FORTRAN 77 plus some operating system dependent code isolated in library procedures. The system currenty runs under VAX/VMS. ESA

N92-26959# Bertin et Cie., Plaisir (France).
INTEGRATED COMMUNICATION ENVIRONMENT FOR THERMAL ANALYSIS SOFTWARE **c61**
P. Lecuyer, D. Neveu, G. Chenut, and C. Stroom (European Space Agency. European Space Research and Technology Center, ESTEC, Noordwijk, Netherlands) *In* ESA, 4th European Symposium on Space Environmental Control Systems, Volume 2 Dec. 1991 p 675-679 (For primary document see N92-26950 17-54)
Avail: NTIS HC/MF A23; ESA, EPD, ESTEC, Noordwijk, Netherlands, HC 150 Dutch guilders (2 vols)

ICETAS (Integrated Communication Environment for Thermal Analysis Software), which aims to provide the European space community with a software environment enforcing data and tools exchangeability, is considered. The current ICETAS project established the user requirements for the architectural design of ICETAS software and resulted in the production of a baseline product in order to assess ICETAS concept validity and feasibility. The project bakground and objectives are discussed and the ICETAS system is described. The ICETAS baseline, hardware, and software environment are also considered. ESA

N92-26960# Centre National d'Etudes Spatiales, Toulouse (France).
DEFINITION OF THE COMMON STRUCTURE OF DATA TO PROMOTE THE COMMUNICATION BETWEEN DIFFERENT THERMAL SOFTWARE TOOLS **c61**
Bruno Desaunettes and Christian Viguier *In* ESA, 4th European Symposium on Space Environmental Control Systems, Volume 2 Dec. 1991 p 681-686 (For primary document see N92-26950 17-54)
Avail: NTIS HC/MF A23; ESA, EPD, ESTEC, Noordwijk, Netherlands, HC 150 Dutch guilders (2 vols)

To perform thermal analysis, space industry engineers use different software tools to carry out geometric modelization and numerical simulation. The transfer of data between these software tools is not easy because most of the data is internal and specific to each software tool. Therefore, each company is obliged to define several interfaces that will change the format of the data. It is obvious that a common structure of data would improve this type of communication. To make this possible, the data should be formatted independently from the tools which use it. Initiatives concerning this topic and work done in order to define completely the needs and to propose a well adapted solution are presented. ESA

N92-26961# VEGA Space Systems Engineering Ltd., Harpenden (England).
GRABE: A SIMPLE GRAPHICAL BACK-END FOR THERMAL SIMULATION PACKAGES **c61**
A. N. Pidgeon, L. Dawson, R. A. D. Melvin, and C. Stroom (European Space Agency. European Space Research and Technology Center, ESTEC, Noordwijk, Netherlands) *In* ESA, 4th European Symposium on Space Environmental Control Systems, Volume 2 Dec. 1991 p 687-691 (For primary document see N92-26950 17-54)
Avail: NTIS HC/MF A23; ESA, EPD, ESTEC, Noordwijk, Netherlands, HC 150 Dutch guilders (2 vols)

The analysis of the results of thermal simulations often requires the data to be displayed in a graphical form. Most users of ESATAN (ESA Thermal Analysis Network) and other thermal simulation packages have developed in-house tools to enable plots of various parameters against time. In complex systems it is often useful to view the dynamics of the system as it evolves. GRABE (Graphical Back End), which allows output from a simulation package to be displayed as graphical plots and to drive dynamic diagrams of the system being simulated, is considered. GRABE is an interactive drawing package which allows the user to create a dynamic representation of the system being modeled. Time stepped data from a simulation package can be read in and displayed in the dynamic drawing using graphs and/or graphical objects whose color or shape changes dynamically with the data. ESA

N92-26962# Tsukuba Space Center, Ibaragi (Japan).
UNIFIED COMPUTATIONAL METHOD FOR DESIGN OF FLUID LOOP SYSTEMS **c34**
Masao Furukawa *In* ESA, 4th European Symposium on Space Environmental Control Systems, Volume 2 Dec. 1991 p 693-703 (For primary document see N92-26950 17-54)
Avail: NTIS HC/MF A23; ESA, EPD, ESTEC, Noordwijk, Netherlands, HC 150 Dutch guilders (2 vols)

Various kinds of empirical formulas of Nusselt numbers, fanning friction factors, and pressure loss coefficients were collected and reviewed with the object of constructing a common basis of design calculations of pumped fluid loop systems. The practical expressions obtained after numerical modifications are listed in tables with identification numbers corresponding to configurations of the flow passages. Design procedure of a cold plate and of a space radiator are clearly shown in a series of mathematical relations coupled with a number of detailed expressions which are put in the tables in order of numerical computations. Weight estimate models and several pump characteristics are given in the tables as a result of data regression. A unified computational method based upon the above procedure is presented for preliminary design analyses of a fluid loop system consisting of cold plates, plane radiators, mechanical pumps, valves, and so on. ESA

N92-26963# Erno Raumfahrttechnik G.m.b.H. Bremen (Germany, F.R.).
A PROCESSING ENVIRONMENT FOR TEST AND SIMULATION DATA OF THERMODYNAMIC SYSTEMS **c61**
R. Mueller and G. Kleinert-Alvarado *In* ESA, 4th European Symposium on Space Environmental Control Systems, Volume 2 Dec. 1991 p 705-711 (For primary document see N92-26950 17-54)
Avail: NTIS HC/MF A23; ESA, EPD, ESTEC, Noordwijk, Netherlands, HC 150 Dutch guilders (2 vols)

The characteristics of a data processing environment which was established to support the development of advanced, fast responding systems and components are described. The environment consists of a data acquisition system, a mainframe data processing computer, data transfer networks, and several programs. It is ideally suited for the development of fast heat exchangers and was used within the first development phases of the Hermes water evaporator assembly and ammonia boiler assembly. A description of the data acquisition system, the interconnection of the elements, and the data processing after testing is given. Requirements, boundary conditions, and further activities are outlined. ESA

N92-26964# Centre National d'Etudes Spatiales, Toulouse (France).
FEASIBILITY STUDY OF AN EXPERT SYSTEM FOR THE DESIGN OF FUSION/SOLIDIFICATION EXPERIMENT BOARDING ON SPACE FURNACE **c29**
B. Desaunettes, T. Duffar, A. Kessaci, D. Valentian, and F. R. Valette (Centre d'Etudes et de Recherches, Toulouse, France) *In* ESA, 4th European Symposium on Space Environmental Control Systems, Volume 2 Dec. 1991 p 713-717 (For primary document see N92-26950 17-54)
Avail: NTIS HC/MF A23; ESA, EPD, ESTEC, Noordwijk, Netherlands, HC 150 Dutch guilders (2 vols)

The use of an expert system for the definition of a fusion/solidification experiment taking place in a space furnace on board a space shuttle is addressed. A feasibility study which identified and collected a part of the expert knowledge and established a methodology for the design of a cartridge is reported. Currently, all the knowledge required for study is ready for representation through a formalism offered by an expert system generator. ESA

N92-26965# Teledyne Brown Engineering, Huntsville, AL.
DESIGN AND PERFORMANCE OF THE SPACELAB ASTRO-1 MISSION HEAT PIPE RADIATOR **c18**
Richard M. Hamner and Linda S. Hornsby *In* ESA, 4th European Symposium on Space Environmental Control Systems, Volume 2 Dec. 1991 p 721-728 (For primary document see N92-26950 17-54)
Avail: NTIS HC/MF A23; ESA, EPD, ESTEC, Noordwijk, Netherlands, HC 150 Dutch guilders (2 vols)

The US Space Shuttle mission STS-35 carried a payload of ultraviolet telescopes into low Earth orbit which used a passive radiator affixed with heat pipes for thermal control. The radiator system was designed to maintain the temperature of certain supporting electronic packages within the range -10 to +35 C, regardless of payload orientation or orbiter orientation in space. The design and performance of the radiator system during its analysis and preflight testing as well as during its flight of 2-10 Dec. 1990 is reported. The flight performance proved to be within limits for the orbit conditions flown. ESA

N92-26966# Centre National d'Etudes Spatiales, Toulouse (France).
SIGMA VCHP RADIATOR: IN-ORBIT PERFORMANCE **c18**
Joel Gayrard *In* ESA, 4th European Symposium on Space Environmental Control Systems, Volume 2 Dec. 1991 p 729-733 (For primary document see N92-26950 17-54)
Avail: NTIS HC/MF A23; ESA, EPD, ESTEC, Noordwijk, Netherlands, HC 150 Dutch guilders (2 vols)

SIGMA, a gamma imaging telescope, is the main experiment (1000 kg, D = 1.2 m, H = 3.5 m) of the GRANAT Soviet vehicle dedicated to gamma experiments. The SIGMA thermal control heat rejection device is a Variable Conductance Heat Pipe (VCHP) radiator (0.9 by 0.9 m). For SIGMA, six heat pipes are used with a L geometry, a total length of 2.3 m and a 140 cu cm reservoir. The design and ground thermal test of SIGMA VCHP radiator are presented, and the inflight performance since the beginning of SIGMA's operational life is detailed. ESA

N92-26967# Aerospatiale, Cannes (France).
DEVELOPMENT OF FLUID LOOP AND HYBRID RADIATORS: TEST RESULTS **c18**
M. Amidieu and T. Maciaszek *In* ESA, 4th European Symposium on Space Environmental Control Systems, Volume 2 Dec. 1991 p 735-740 Prepared in cooperation with Centre National d'Etudes Spatiales, Toulouse, France (For primary document see N92-26950 17-54)
Avail: NTIS HC/MF A23; ESA, EPD, ESTEC, Noordwijk, Netherlands, HC 150 Dutch guilders (2 vols)

Activities in the field of active thermal control led to the development of fluid loop and hybrid radiators. Results of thermal and hydraulical tests performed on specific models are presented. Concerning the fluid loop radiator, the definition of the model was performed in accordance with the Hermes program specifications which require large panels with a low mass and a low manufacturing cost. With regard to the hybrid radiator, the study was oriented with respect to the heat exchanger. The development was engaged with the view of a possible application in the Columbus Program. ESA

N92-26968# Akademiya Nauk BSSR, Minsk. Heat and Mass Transfer Inst.
HEAT PIPE-BASED RADIATIVE PANEL **c18**
L. L. Vasiliev, L. E. Kanonchik, D. K. Khrustalev, and V. A. Babenko *In* ESA, 4th European Symposium on Space Environmental Control Systems, Volume 2 Dec. 1991 p 741-745 (For primary document see N92-26950 17-54)
Avail: NTIS HC/MF A23; ESA, EPD, ESTEC, Noordwijk, Netherlands, HC 150 Dutch guilders (2 vols)

The Heat Pipe based Radiative Panel (HPRP) as a heat sink at 300 K for space applications is proposed. The HPRP operation under stationary and nonstationary conditions is studied. The experimental data obtained for the aluminum HPRP show its high efficiency and operability after defreezing. A HPRP mathematical model was developed using the solution of a two dimensional heat conduction problem describing gas channel wall to heat pipe evaporator heat transfer. A good agreement between theoretical and experimental data was found. The effect of process and design parameters in radiator characteristics is discussed. ESA

N92-26969# European Space Agency. European Space Research and Technology Center, ESTEC, Noordwijk (Netherlands). Thermal Control and Life Support Div.
THE LIQUID DROPLET RADIATOR: STATUS OF DEVELOPMENT **c34**
J. Persson *In its* 4th European Symposium on Space Environmental Control Systems, Volume 2 Dec. 1991 p 747-752 (For primary document see N92-26950 17-54)
Avail: NTIS HC/MF A23; ESA, EPD, ESTEC, Noordwijk, Netherlands, HC 150 Dutch guilders (2 vols)

The ever greater amounts of power to be dissipated onboard future spacecraft, together with their limited external dimensions, will make it increasingly difficult to use conventional radiator technology without imposing a severe mass penalty. Hunting for lightweight alternatives to current heat rejection systems has become a matter of growing urgency, which explains the great interest that the Liquid Droplet Radiator (LDR) has attracted. Tradeoff analyses indicate that an LDR may be as much as an order of magnitude lighter than a comparable conventional radiator. A literature study examining the progress of the LDR research and some of its possible applications is reviewed. An investigation of the LDR heat rejection capability is presented. ESA

N92-26970# Erno Raumfahrttechnik G.m.b.H. Bremen (Germany, F.R.).

BATTERY THERMAL CONTROL OF THE COLUMBUS FREE FLYER **c18**

B. Miedza, A. Lanteri, and P. Moeller (Dornier System G.m.b.H., Friedrichshafen, Germany, F.R.) *In* ESA, 4th European Symposium on Space Environmental Control Systems, Volume 2 Dec. 1991 p 755-759 (For primary document see N92-26950 17-54)

Avail: NTIS HC/MF A23; ESA, EPD, ESTEC, Noordwijk, Netherlands, HC 150 Dutch guilders (2 vols)

The thermal control concept of the Columbus Free Flyer batteries is described. The Columbus Free Flyer energy storage assembly consists of six nickel hydrogen battery packages designed for five years in orbit lifetime at 31 percent depth of discharge. In particular, the lifetime requirement imposes the need for extensive effort on the electrical and thermal control design of the batteries. The battery thermal control concept is mainly driven by 0 +/- 10 C, by the extreme external environmental load variations and by the battery charge and discharge cycles. ESA

N92-26971# Erno Raumfahrttechnik G.m.b.H. Bremen (Germany, F.R.).

THERMAL ANALYSIS OF THE SPACELAB MISSION D2 UTILITY SUPPORT STRUCTURE AND ITS PAYLOADS **c18**

W. Wessels *In* ESA, 4th European Symposium on Space Environmental Control Systems, Volume 2 Dec. 1991 p 761-767 (For primary document see N92-26950 17-54)

Avail: NTIS HC/MF A23; ESA, EPD, ESTEC, Noordwijk, Netherlands, HC 150 Dutch guilders (2 vols)

The Utility Support Structure (USS) with its mounted payloads will be located in the Space Transportation System (STS) cargo bay behind the Spacelab module during the 2nd German Spacelab Mission (D2), currently foreseen for STS flight 55 in January 1993. The most critical USS payloads from the thermal point of view are two optical experiments, Galactical Ultrawide Angle Schmidt System (GAUSS) camera and Modular Optical Multispectral Scanner (MOMS-O2). The interaction between USS and payload thermal analyses and the definition of effective passive thermal control concepts are described. ESA

N92-26972# Kiev Polytechnic (USSR).

PASSIVE THERMOSTATE SYSTEM WITH APPLICATION OF GAS-FILLED HEAT PIPES AND THERMAL ENERGY OF SOLAR RADIATION **c34**

V. M. Baturkin, N. K. Gretchina, O. P. Moskalenko, and K. N. Shkoda *In* ESA, 4th European Symposium on Space Environmental Control Systems, Volume 2 Dec. 1991 p 769-774 (For primary document see N92-26950 17-54)

Avail: NTIS HC/MF A23; ESA, EPD, ESTEC, Noordwijk, Netherlands, HC 150 Dutch guilders (2 vols)

An approach to creating passive or half passive thermocontrol systems, using heat energy of solar radiation for functioning and variable conductance heat pipes as temperature control elements, is analyzed with conditions of considerably altering (more than 2 times) solar constant conditions. Results of calculation of control system specimens with two parallel metal fibrous methanol heat pipes are presented for the typical instrument unsealed module with conditions: range of solar constant values 500 to 1400 W/cu m; variations of the temperature on mount places 253 to 323 K; and device temperature level 280 to 300 K. ESA

N92-26973# Alenia Spazio S.p.A., Turin (Italy).

THERMAL DESIGN FOR THE SPACE-EXPOSED INSTRUMENTS FOR THE SCIENTIFIC SATELLITE SAX **c19**

Gaetano Poidomani and Gianfranco Bonino *In* ESA, 4th European Symposium on Space Environmental Control Systems, Volume 2 Dec. 1991 p 775-778 (For primary document see N92-26950 17-54)

Avail: NTIS HC/MF A23; ESA, EPD, ESTEC, Noordwijk, Netherlands, HC 150 Dutch guilders (2 vols)

The objective of the Italian-Dutch scientific satellite SAX (Satellite for X-ray Astronomy) is the observation of celestial X-ray sources over a large energy range 0.1 to 300 keV. Eight Scientific Instruments (SI) are carried on SAX. Four of these SI's are the concentrators (covering the 0.1 + 10 keV energy range), they consist of a detector and a mirror unit which are directly exposed to the space cooling effect. A dedicated thermal design was studied to guarantee the temperature requirement of these instruments and a development test was carried out to evaluate its performance. ESA

N92-26974# Ecole Nationale Superieure de Mecanique et d'Aerotechnique, Poitiers (France). Lab. de Thermique.

INTEGRATED HEAT PIPE CONCEPT FOR LI/SOCI2 CELLS COOLING **c33**

A. Suleiman, A. Alexandre, and J. L. Firmin (Societe des Accumulateurs Fixes et de Traction, Romainville, France) *In* ESA, 4th European Symposium on Space Environmental Control Systems, Volume 2 Dec. 1991 p 779-783 Sponsored by Societe des Accumulateurs Fixes et de Traction (For primary document see N92-26950 17-54)

Avail: NTIS HC/MF A23; ESA, EPD, ESTEC, Noordwijk, Netherlands, HC 150 Dutch guilders (2 vols)

A new thermal control system based on heat pipe to support the development of a primary lithium/thionyl chloride (Li/SOCI2) battery designed for future space applications is shown. Performances of the used heat pipe are considered and range performances of a traditional cell cooling concept based on the use of an aluminum pipe put around the cell and fixed to a coldplate is shown. A mock up was carried out and compared to thermal model of the whole system using ESACAP software. This model includes about 120 nodes to present the cell and the aluminum pipe. These results are compared to those of the proposed new cooling concept based on a grooved nickel/F11 heat pipe integrated in the cell. In this case, a mock up was performed and a corresponding nodal model was built. The experimental and modeling results show that the new concept decreases thermal gradient and weight and increases the available current discharge rate compared with the traditional cooling concept. ESA

N92-26975# Max-Planck-Inst. fuer Aeronomie, Katlenburg-Lindau (Germany, F.R.).

DEVELOPMENT OF A THERMAL CONTROL CONCEPT FOR THE OPTICAL SYSTEM OF THE SUMER EXPERIMENT ON SOHO **c74**

W. Curdt and H. Rathjen *In* ESA, 4th European Symposium on Space Environmental Control Systems, Volume 2 Dec. 1991 p 785-790 Prepared in cooperation with Erno Raumfahrttechnik G.m.b.H. Bremen, Fed. Republic of Germany (For primary document see N92-26950 17-54)

Avail: NTIS HC/MF A23; ESA, EPD, ESTEC, Noordwijk, Netherlands, HC 150 Dutch guilders (2 vols)

The experiment, Solar Ultraviolet Measurements of Emitted Radiation (SUMER), will observe the solar atmosphere on board the SOHO spaceprobe. The telescope/spectrometer operates in the far UV spectral range with excellent spatial and spectral resolution. The thermal control of SUMER is a delicate task due to extreme thermal requirements and unfavorable boundary conditions. The optical fidelity requires extremely stable mechanical conditions free from dilatation or distortion. Consequently, the operational temperature range is very small and gradients within the structure can not be tolerated. This task is complicated by limitations of heater power and cleanliness requirements dictating the material selection. Internal heat sources (dissipation, absorbed solar flux, and heater power) are small compared to the large surface area. Thus, the long term stability of multilayer insulation performance is an important factor of the thermal design. A detailed thermal mathematical model was established and an exhaustive thermal analysis was performed in several iterations to identify critical areas and to define a reliable thermal design by reducing the uncertainties. ESA

N92-26976# Dornier System G.m.b.H., Friedrichshafen (Germany, F.R.).
THERMAL CONTROL OF TELESCOPE APERTURES BY OPTIMIZED BAFFLE HEATING **c89**
R. Gessner, K. Eckert, and F. Zilly *In* ESA, 4th European Symposium on Space Environmental Control Systems, Volume 2 Dec. 1991 p 791-796 (For primary document see N92-26950 17-54)
Avail: NTIS HC/MF A23; ESA, EPD, ESTEC, Noordwijk, Netherlands, HC 150 Dutch guilders (2 vols)

Observational instruments in space put hard requirements on temperature stability and thermal gradients due to their sensitive detector equipment. The thermal subsystem has to take into account that direct heating of the optical instruments is not often possible due to geometrical or technical reasons. An indirect heating concept including an optimization approach to design heated thermal baffles in front of telescope apertures is described. The optimization is formulated for arbitrary geometrical configurations, and verification aspects are discussed together with an alternative optimization approach. An application to practical problems is given in terms of tradeoff studies for the configurational design of the X-ray Multi Mirror Mission (XMM) thermal baffle. ESA

N92-26977# Centre d'Etude de l'Energie Nucleaire, Mol (Belgium). Lab. of Genetics and Biotechnology.
THIOCAPSA ROSEOPERSICINA, A BACTERIUM FOR SULFUR-RECYCLING IN MICROBIAL ECOSYSTEMS DESIGNED FOR CELSS AND SPACE PURPOSES **c51**
P. Jansen and M. Mergeay *In* ESA, 4th European Symposium on Space Environmental Control Systems, Volume 2 Dec. 1991 p 799-803 Sponsored by Institut pour l'Encouragement de la Recherche Scientifique dans l'Industrie et l'Agriculture and ESA/ESTEC (For primary document see N92-26950 17-54)
Avail: NTIS HC/MF A23; ESA, EPD, ESTEC, Noordwijk, Netherlands, HC 150 Dutch guilders (2 vols)

Thiocapsa roseopersicina, an anoxygenic phototrophic bacterium, is used to oxidize/recycle reduced sulfur compounds and to consume degradation products, which are produced in the Microbial Ecological Life Support System Alternative (MELISSA) model (waste recycling and biomass production model). MELISSA is an early, simplified model of a Controlled Ecological Life Support System (CELSS). The tests, which were performed at laboratory scale in batch processes, investigate the different growth conditions and degradation efficiencies of the microorganism for acids and reduced sulfur compounds. The obtained results show the versatility of T. roseopersicina and its interesting potential for use in space projects. The bacterium is able to grow in the dark, in the light, under microaerophilic and anaerobic conditions, under autotrophy and is able to use sulfide, acetate, lactate, ethanol and urea. The results were found by measuring chemical parameters and by evaluating the optical density (660 nm) of the culture in the medium. ESA

N92-26978# European Space Agency. European Space Research and Technology Center, ESTEC, Noordwijk (Netherlands). Thermal Control and Life Support Div.
HIGHER PLANT GROWTH IN CLOSED ENVIRONMENT: PRELIMINARY EXPERIMENTS IN LIFE SUPPORT FACILITY AT ESA-ESTEC **c51**
Christian Tamponnet, Roger Binot, and Daniel deChambure *In its* 4th European Symposium on Space Environmental Control Systems, Volume 2 Dec. 1991 p 805-810 (For primary document see N92-26950 17-54)
Avail: NTIS HC/MF A23; ESA, EPD, ESTEC, Noordwijk, Netherlands, HC 150 Dutch guilders (2 vols)

The air loop bench of the Environmental Control and Life Support (ECLS) unit of the mechanical systems laboratory at ESTEC was adapted to the culture of plants. CO2 consumption, O2 production, water and air contaminants release were measured and/or controlled during the growth cycle of the chosen plant: Raphanus sativus L. After 28 days of continuous growth under low light intensity (15 W/sq m) 2.191 g of fresh biomass were obtained (yield of 2.98 kg /sq m) comprising 368 g of radishes (roots), i.e., a harvest ratio of 0.168 if the roots are considered as the only edible part. The main gaseous contaminant was nitrous oxide (N2O, up to 170 ppm) and was mainly produced by the plant itself. Transpiration water was considered hygienic but not potable because of its higher than maximum allowable concentration total organic carbon content. These results validated the adapted air loop as a potential tool to study the higher plant compartment of CELSS (Controlled Ecological Life Support Systems). ESA

N92-26979# Academy of Sciences (USSR), Krasnoyarsk. Inst. of Biophysics.
CHEMOLITHOTROPIC HYDROGEN-OXIDIZING BACTERIA AND THEIR POSSIBLE FUNCTIONS IN CLOSED ECOLOGICAL LIFE-SUPPORT SYSTEMS **c51**
T. G. Volova, J. G. Gitelson, F. Y. Sidko, and I. N. Trubachev *In* ESA, 4th European Symposium on Space Environmental Control Systems, Volume 2 Dec. 1991 p 811-815 (For primary document see N92-26950 17-54)
Avail: NTIS HC/MF A23; ESA, EPD, ESTEC, Noordwijk, Netherlands, HC 150 Dutch guilders (2 vols)

Results of experimental studies of chemolithotrophic hydrogen oxidizing bacteria (hydrogen bacteria and carboxidotrophic bacteria) are surveyed. The data on growth and nutrition physiology of these microorganisms and physiological characteristics, correlated with the growth conditions, are given. Prospects to apply chemolythotrophs as producers of biosynthesis target products and as a feasible link in a closed human life support system are discussed. The prospects of applying the culture of Alkaligenes eutrophus hydrogen bacteria to perform a number of basic functions of a regeneration component in a closed life support system are analyzed. These functions include: the utilization of the carbonic acid exhaled by man; the reclamation of water and utilization of human exometabolites; and the reclamation of the nutrient substances, mainly the protein component of the diet. ESA

N92-26980*# National Aeronautics and Space Administration. Ames Research Center, Moffett Field, CA.
IMPACT OF DIET ON THE DESIGN OF WASTE PROCESSORS IN CELSS
Ahmad Waleh, Valery Kanevsky, Thoi K. Nguyen, Ravi Upadhye (Lawrence Livermore National Lab., CA.), and Theodore Wydeven *In* ESA, 4th European Symposium on Space Environmental Control Systems, Volume 2 Dec. 1991 p 817-821 (For primary document see N92-26950 17-54)
(Contract NAS2-13260)
Avail: NTIS HC/MF A23; ESA, EPD, ESTEC, Noordwijk, Netherlands, HC 150 Dutch guilders (2 vols)

The preliminary results of a design analysis for a waste processor which employs existing technologies and takes into account the constraints of human diet are presented. The impact of diet is determined by using a model and an algorithm developed for the control and management of diet in a Controlled Ecological Life Support System (CELSS). A material and energy balance model for thermal oxidation of waste is developed which is consistent with both physical/chemical methods of incineration and supercritical water oxidation. The two models yield quantitative analysis of the diet and waste streams and the specific design parameters for waste processors, respectively. The results demonstrate that existing technologies can meet the demands of waste processing, but the choice and design of the processors or processing methods will be sensitive to the constraints of diet. The numerical examples are chosen to display the nature and extent of the gap in the available experiment information about CELSS requirements. ESA

N92-26981# European Space Agency. European Space Research and Technology Center, ESTEC, Noordwijk (Netherlands).
MELISSA: PHYSICAL LINKS OF COMPARTMENTS NITROBACTER/SPIRULINA
C. Lasseur, R. A. Binot (MATRA Espace, Paris-Velizy, France),

C. Tamponnet, and J. F. Cornet *In its* 4th European Symposium on Space Environmental Control Systems, Volume 2 Dec. 1991 p 823-829 (For primary document see N92-26950 17-54)
Avail: NTIS HC/MF A23; ESA, EPD, ESTEC, Noordwijk, Netherlands, HC 150 Dutch guilders (2 vols)

The MELISSA (Micro Ecological Life Support System Alternative) project, conceived as a microorganism based ecosystem, is preparing an early, simplified, model of a future biological life support system for planned space missions. The preparation of the physical linkage of the nitrification and photosynthetic compartments is presented. These two compartments are representative at the control level (cascade between two compartments and feed back on the gas phase) and at the technological level (low and high biomass production, immobilization, culture medium recycling, gas transfer, etc.). The general requirements applicable to all the compartments of the loop are presented and the specific requirements of the above two are described. The first technologies selected and first results obtained are presented. Advantages and weaknesses of the actual design and the development planned for the future is presented. ESA

N92-26982# MATRA Espace, Paris-Velizy (France). Applications de la Microgravite.
MODELLING LIGHT TRANSFER INSIDE PHOTOBIOFERMENTORS: APPLICATIONS TO THE PHOTOSYNTHETIC COMPARTMENTS OF CELSS **c51**
J. F. Cornet, C. G. Dussap, G. Dubertret, and J. B. Gros (Clermont-Ferrand Univ., France) *In* ESA, 4th European Symposium on Space Environmental Control Systems, Volume 2 Dec. 1991 p 831-836 (For primary document see N92-26950 17-54)
Avail: NTIS HC/MF A23; ESA, EPD, ESTEC, Noordwijk, Netherlands, HC 150 Dutch guilders (2 vols)

The application of light transfer modeling to the photosynthetic compartments of Closed Ecological Life Support System (CELSS) is addressed. The study of interactions between physical limitation by light and biological limitations in photobioreactors leads to very complex partial differential equations. Modeling of radiant energy absorbed in photoreactors requires an equation including two parameters for light absorption and scattering in the culture medium. A simple model based on the simplified, monodimensional equation of Schuster for radiative transfer is discussed. This approach provides a simple way to determine a working illuminated volume in which growth occurs. The analysis is extended to more complex geometries such as cylindrical reactors. ESA

N92-26983# Bioclear Environmental Biotechnology, Groningen (Netherlands).
BIODEGRADATION STUDIES WITH SPACE CABIN CONTAMINANTS TO DETERMINE THE FEASIBILITY OF BIOLOGICAL AIR FILTRATION (BAF) IN SPACE CABINS
S. Keuning, D. Jager, P. G. Paul, and R. A. Binot (European Space Agency. European Space Research and Technology Center, ESTEC, Noordwijk, Netherlands) *In* ESA, 4th European Symposium on Space Environmental Control Systems, Volume 2 Dec. 1991 p 837-841 (For primary document see N92-26950 17-54)
Avail: NTIS HC/MF A23; ESA, EPD, ESTEC, Noordwijk, Netherlands, HC 150 Dutch guilders (2 vols)

The development of a Biological Air Filter (BAF), a biologically based and self regenerable device for trace contaminant removal in space cabins, is considered. The efficient operation of a BAF is largely dependent on the kinetic properties of the microbial community of 'biocatalyst' in the biofilter device. In a biological air filter a variety of chemical compounds have to be degraded by a mixed population of microorganisms with different degradation capacities. Such a system is rather complex with many interaction effects. To investigate these effects and determine kinetic properties biodegradation experiments were performed with pure and mixed bacterial cultures in which the number of contaminants and of bacterial strains with specific degradation capabilities were gradually increased. A significant positive influence of cultivating on mixed substrated was observed. A complex culture composed of up to six different strains efficiently degraded a mixture of six different organic compounds and remained stable over a long period. The results of the biodegradation studies obtained so far show good prospectives for the applicability of biological air filtration during manned space missions. ESA

N92-26984# Erno Raumfahrttechnik G.m.b.H. Bremen (Germany, F.R.).
PROGRESS IN THE DEVELOPMENT OF THE HERMES EVAPORATORS
C. Goehre, R. Bohlen, B. J. G. Leidinger, R. Mueller, P. Mueller-Remmers, and R. Rohr *In* ESA, 4th European Symposium on Space Environmental Control Systems, Volume 2 Dec. 1991 p 845-850 (For primary document see N92-26950 17-54)
Avail: NTIS HC/MF A23; ESA, EPD, ESTEC, Noordwijk, Netherlands, HC 150 Dutch guilders (2 vols)

The results of the first development approaches of the three evaporators for the Hermes Spaceplane, used for rejecting waste heat, are presented: the Water Evaporator Assembly (WEA), the Ammonia Boiler Assembly (ABA) and the Hydraulic Thermal Control Assembly (HTCA). Some important development activities, in particular tests of the technology demonstration models for WEA and ABA, are summarized. Tests with these first evaporator prototypes of WEA and ABA showed that the requirements for the flight unit can be met and certain problems have to be solved. On HTA, sample tests are envisaged up to now. ESA

N92-26985# Japan Systems Corp., Kawasaki.
THERMAL ANALYSIS OF EVAPORATIVE COOLERS **c77**
Masatoshi Ohuchi, Masao Furukawa (National Space Development Agency, Ibaraki, Japan), and Koichi Oshima *In* ESA, 4th European Symposium on Space Environmental Control Systems, Volume 2 Dec. 1991 p 851-854 (For primary document see N92-26950 17-54)
Avail: NTIS HC/MF A23; ESA, EPD, ESTEC, Noordwijk, Netherlands, HC 150 Dutch guilders (2 vols)

In order to develop the conceptual design of the Thermal Control System (TCS) of HOPE (Japanese orbiting plane planned to be launched by H2 rocket), the thermal model of the evaporative cooling system of the U.S. Space Shuttle was analyzed. This consists of Flash Evaporator Subsystem (FES) at high altitude and Ammonia Boiler Subsystem (ABS) at low altitude, both of which are for cooling of the freon loops, and Water Spray Boiler Subsystem (WSB), for cooling of the oil loops. Simplified thermal models of these devices were constructed based in the reported data such as the geometries and the design requirements. The simulated results based on these thermal models were compared with the Shuttle postflight data. Integration of these subsystem models into the total TCS model is underway. ESA

N92-26986# Karlsruhe Univ. (Germany, F.R.). Inst. fuer Technische Thermodynamik.
THE TRANSPIRATOR, AN EFFICIENT AND LIGHT EVAPORATIVE COOLER FOR SPACE TECHNOLOGY **c31**
M. Alf and G. Ernst *In* ESA, 4th European Symposium on Space Environmental Control Systems, Volume 2 Dec. 1991 p 855-861 (For primary document see N92-26950 17-54)
Avail: NTIS HC/MF A23; ESA, EPD, ESTEC, Noordwijk, Netherlands, HC 150 Dutch guilders (2 vols)

The optimization of transpirators, light and efficient evaporative coolers, is considered. A program for computation of the maximum cooling capacity under given conditions, based on, test results is being developed. Advantages of the transpirators are: no loss of evaporating coolant in liquid or solid state; low weight and low volume; good adaptability to heat rejection at different temperature levels; numerous possibilities of configuration and subdivision. The mode of operation and design of the transpirators are described. Test results are presented. The influence of various components on the cooling capacity is shown. ESA

N92-26987# European Space Agency. European Space Research and Technology Center, ESTEC, Noordwijk (Netherlands).

CPA: A CONTROLLED PUMP ASSEMBLY FOR TWO-PHASE LOOPS APPLICATIONS **c37**

M. N. DeParolis and Peter Reusser (Reusser, Peter U. A.G., Zurich, Switzerland) *In its* 4th European Symposium on Space Environmental Control Systems, Volume 2 Dec. 1991 p 863-871 (For primary document see N92-26950 17-54)

Avail: NTIS HC/MF A23; ESA, EPD, ESTEC, Noordwijk, Netherlands, HC 150 Dutch guilders (2 vols)

A technology development program to design, manufacture and test an engineering model of a controlled pump assembly to be used primarily in two phase loops is considered. The requirements and the main problems expected for the assembly design and manufacturing are reviewed and the activities performed during phase 1 and part of phase 2 are described. The activities included an important series of tests in prototype pumps, the results of which are presented together with their impact on the subsequent design process. The critical areas and the need for futher work are identified and the solutions, when available, given. ESA

N92-26988# Erno Raumfahrttechnik G.m.b.H. Bremen (Germany, F.R.).

THERMO-HYDRAULIC INVESTIGATIONS ON HEAT EXCHANGERS FOR COLUMBUS HYBRID RADIATORS **c31**

W.-D. Ebeling, R. Meyer, and W. Fischer *In* ESA, 4th European Symposium on Space Environmental Control Systems, Volume 2 Dec. 1991 p 873-879 (For primary document see N92-26950 17-54)

Avail: NTIS HC/MF A23; ESA, EPD, ESTEC, Noordwijk, Netherlands, HC 150 Dutch guilders (2 vols)

The development of the heat exchanger and the heat pipes for the hybrid radiators of the pressurized module of the Columbus Man Tended Free Flyer (MTFF) is considered. The present heat exchanger concept, which uses plane and offset strip fins as load carrying items in order to minimize the mass, is described. The evaluation of thermohydraulic component tests is outlined. Resulting heat transfer rates and pressure drops of the investigated offset strip fin configuration are compared with predictions using different empirical correlations and analytical models. ESA

N92-26989# Aerospatiale, Les Mureaux (France). Strategic and Space System Div.

HUMAN FACTORS IN THE CONCEPTION OF THE HERMES SPACE VEHICLE

F. Winisdoerffer *In* ESA, 4th European Symposium on Space Environmental Control Systems, Volume 2 Dec. 1991 p 883-892 (For primary document see N92-26950 17-54)

Avail: NTIS HC/MF A23; ESA, EPD, ESTEC, Noordwijk, Netherlands, HC 150 Dutch guilders (2 vols)

The status of the habitability studies performed during the course of the development of the Hermes space vehicle in terms of functions to be fulfilled is presented. Based on crew role definition and scenario, usage analysis was performed through computer simulations and full sale testing in 1 g and neutral buoyancy conditions, to specify and to verify the adequacy of the configuration with respect to its utilization by the crew. Some results of these usage analyses are presented in terms of human factors engineering, design rules and requirements that will enable the system and subsystem designers to efficiently take into account the presence of man on board at an early stage of the definition. This process is aimed at enhancing the 'vehicle/man fit' that will greatly contribute to the overall mission success. ESA

N92-26990# Compagnia Italiana Servizi Tecnici, Rome. Space Div.

LOGISTICS IN SPACE: TOOLS TO SUPPORT ASTRONAUTS **c81**

G. F. DeLuca, S. Masullo, and A. Schisano *In* ESA, 4th European Symposium on Space Environmental Control Systems, Volume 2 Dec. 1991 p 893-898 (For primary document see N92-26950 17-54)

Avail: NTIS HC/MF A23; ESA, EPD, ESTEC, Noordwijk, Netherlands, HC 150 Dutch guilders (2 vols)

The importance, in a space manned environment, of the separation of tasks of item onboard management from the human intervention, in order to achieve more crew time devoted to payload tasks and a more accurate stowage of onboard items, is shown. The major objectives of a tool able to take over the following tasks are analyzed: identification of the features of needed items, help crew find items, and minimization of flight and ground intervention. The available technologies are evaluated for their possible integration in such a logistic tool, taking into account the specific constraints the space environment levies on it. The important aspect of the related man machine interface such a tool must be equipped with is illustrated. Possible architectural configurations are addressed for use in a pressurized space laboratory, in compliance with the related interfaces of the other space subsystems. Recommendations for possible implementation of various options are made for the future space environments, where astronauts have to live and work. ESA

N92-26991# Alenia Spazio S.p.A., Turin (Italy).

CAD SYSTEM FOR HFE ANALYSES: ZERO-g POSTURE IN OPTIMISATION OF COLUMBUS APM CREW WORKSTATIONS

Fabiana Bobba, Pier Luigi Giorgi, and Enrico Gaia *In* ESA, 4th European Symposium on Space Environmental Control Systems, Volume 2 Dec. 1991 p 899-904 (For primary document see N92-26950 17-54)

Avail: NTIS HC/MF A23; ESA, EPD, ESTEC, Noordwijk, Netherlands, HC 150 Dutch guilders (2 vols)

A comparison between the required and the preferred (neutral) workstation posture of the human body in microgravity is made. This analysis is supported by tridimensional modelization via Computer Aided Design (CAD). The software simulation tool is capable of faithfully reproducing the internal Attached Pressurized Module (APM) environment and human models. From this comparison a validation of the considered workstation configuration follow, together with suggestions useful when design modifications are required in order to meet the Human Factors Engineering (HFE) requirements and to allow the performance of crew tasks with high efficiency and comfort. Two humans models were created for the analysis via the CAD system on the basis of the anthropometric data established by referring to a 95th percentile American male and a 5th percentile Japanese female. The most representative working areas are analyzed: module control station, viewport, airlock, and standoff portions. ESA

N92-26992# Compagnia Italiana Servizi Tecnici, Rome. Space Div.

CBT: ROLE AND FUTURE APPLICATION FOR CREW TRAINING **c53**

A. Guerrazzi, S. Masullo, S. Randisi, and E. Sala *In* ESA, 4th European Symposium on Space Environmental Control Systems, Volume 2 Dec. 1991 p 905-909 (For primary document see N92-26950 17-54)

Avail: NTIS HC/MF A23; ESA, EPD, ESTEC, Noordwijk, Netherlands, HC 150 Dutch guilders (2 vols)

A set of Computer Based Training (CBT) tools for crew training are considered. These tools are seen and described as a complementary means with the other training facilities needed to conduct an efficient training program for this flight crew. Their current capabilities are explored and explained in order to show how their use can improve training achievements within time and budget constraints. The basic features are analyzed for comparison with the other tools usually used: ease in learning; response analysis; courseware update and upgrade; multimedial techniques (audio, video, text, graphics, etc.). Their possible architecture for the specific application of crew training is addressed, taking into account the necessity of having a coherence of the various coursewares in a possible European scenario. Requirements in terms of hardware and software are consequently derived for minimal and optimal configurations with the related benefits and

drawbacks. Recommendations for implementation in the future crew training environments are addressed. ESA

N92-26993# Alenia Spazio S.p.A., Turin (Italy).
CREW SUPPORT EQUIPMENT: IDENTIFICATION AND DEFINITION OF ADDITIONAL HARDWARE FOR COLUMBUS APM LABORATORY HABITABILITY
Simona Ferraris, Giorgio Musso, and Enrico Gaia *In* ESA, 4th European Symposium on Space Environmental Control Systems, Volume 2 Dec. 1991 p 911-916 (For primary document see N92-26950 17-54)
Avail: NTIS HC/MF A23; ESA, EPD, ESTEC, Noordwijk, Netherlands, HC 150 Dutch guilders (2 vols)

Habitability problems for the design of the Columbus APM (Attached Pressurized Module) are addressed. All equipment required to support the crew is identified from analysis of the following: crew and equipment stability/mobility aids; interior design; activity aids. A design definition concept is proposed for each item according to criteria of efficiency, reliability, easy usability, minimization of weights and volumes, and where possible, standardization. ESA

N92-26994# European Space Agency. European Space Research and Technology Center, ESTEC, Noordwijk (Netherlands).
MICROGRAVITY SIMULATION
K. Verge-Depre *In its* 4th European Symposium on Space Environmental Control Systems, Volume 2 Dec. 1991 p 917-921 (For primary document see N92-26950 17-54)
Avail: NTIS HC/MF A23; ESA, EPD, ESTEC, Noordwijk, Netherlands, HC 150 Dutch guilders (2 vols)

Microgravity simulation facilities such as 'parabolic flights and neutral buoyancy facility' developed to perform microgravity studies were analyzed. The analysis of constraints related to microgravity simulation facilities emphasized the strong and weak points of each environment in terms of microgravity effects on task reliability, result validity, etc. The microgravity simulation facilities are described and the type of information which could be extracted is defined. ESA

N92-26995# European Space Agency. European Space Research and Technology Center, ESTEC, Noordwijk (Netherlands). Columbus Crew Activities and On-Board Payload Operations.
ENGINEERING OF A NEW OVERALL SYSTEM TO IMPROVE THE INTERACTION BETWEEN THE CREW AND THE GROUND-BASED SCIENTISTS AND PERSONNEL
Carlo Viberti *In its* 4th European Symposium on Space Environmental Control Systems, Volume 2 Dec. 1991 p 923-928 (For primary document see N92-26950 17-54)
Avail: NTIS HC/MF A23; ESA, EPD, ESTEC, Noordwijk, Netherlands, HC 150 Dutch guilders (2 vols)

A system to optimize efficiency and flexibility of onboard crew tasks is described. The basic idea consists of moving all the payload related and some payload to system related control functions from what is normally a fixed control station to a portable computer and a portable terminal, thus allowing interaction with various experimental equipment without being constrained by strict system software requirements. An overview of the technological features of such a system concept is given. ESA

N92-26996# Alenia Spazio S.p.A., Rome (Italy).
ITALSAT THERMAL CONTROL: THE IN-ORBIT PERFORMANCES **c18**
Marco Giommi, Stefano Liverani, and Enrico Sacchi *In* ESA, 4th European Symposium on Space Environmental Control Systems, Volume 2 Dec. 1991 p 931-937 (For primary document see N92-26950 17-54)
Avail: NTIS HC/MF A23; ESA, EPD, ESTEC, Noordwijk, Netherlands, HC 150 Dutch guilders (2 vols)

Italsat F1 is a three axes stabilized communication satellite. The Italsat system consists of a global beam and a multibeam package (20/30 GHz) for domestic communication services and an experimental propagation package at 40/50 GHz with European coverage. The spacecraft thermal control design was experimentally qualified by means of a solar simulation test performed on a dedicated structural and thermal model. Correlation analysis with test temperatures was performed in order to verify the thermal mathematical models. The flight unit was submitted to a thermal vacuum test in order to prove the system performances. Dedicated thermal balance phases allowed verification of the final spacecraft thermal design. Italsat F was successfully launched by Ariane 4 on Jan. 15 1991. It is presently on station on the nominal operating configuration. Flight temperatures to date show excellent performance of the spacecraft thermal control. Spacecraft thermal design and test verification methods are provided. In orbit thermal performance as well as analysis correlation with test and flight temperatures are presented and discussed. ESA

N92-26997# Dornier System G.m.b.H., Friedrichshafen (Germany, F.R.).
ROSAT: MEASURED TEMPERATURES VERSUS THERMAL ANALYSIS RESULTS **c18**
Albert Braig and Peter Pawlowski (Deutsche Agentur fuer Raumfahrtangelegenheiten G.m.b.H., Bonn, Germany, F.R.) *In* ESA, 4th European Symposium on Space Environmental Control Systems, Volume 2 Dec. 1991 p 939-944 (For primary document see N92-26950 17-54)
Avail: NTIS HC/MF A23; ESA, EPD, ESTEC, Noordwijk, Netherlands, HC 150 Dutch guilders (2 vols)

The German X-ray satellite Rosat belongs to a new concept of large astrophysics facilities. Because of the specific Earth orbit parameters, it experienced a number of full Sun orbit phases passing over to eclipse orbits with up to 36 minutes. Up to now, all measured temperatures were within their limits showing an excellent performance of the thermal control subsystem. The thermal behavior of the spacecraft as predicted by the thermal mathematical models is compared with the flight performance. Particular attention is given to the thermal design load cases. ESA

N92-26998# Centre National d'Etudes Spatiales, Toulouse (France).
SPOT MULTIMISSION PLATFORM THERMAL CONTROL: FIVE YEARS OF IN-FLIGHT RESULTS **c18**
Irenee Alet *In* ESA, 4th European Symposium on Space Environmental Control Systems, Volume 2 Dec. 1991 p 945-949 (For primary document see N92-26950 17-54)
Avail: NTIS HC/MF A23; ESA, EPD, ESTEC, Noordwijk, Netherlands, HC 150 Dutch guilders (2 vols)

The SPOT platform is a multimission platform designed for Earth observation missions in the sunsynchronous orbits from 9 to 15 solar hours (ascending or descending node). A family of present satellites and in the near future will use this platform: SPOT 1, 2, 3, 4, Helios, ERS, etc. The thermal control system of SPOT multimission platform is described and inflight temperature measurements of SPOT 1 and 2 are given. An attempt is made to explain why the evolution of the temperatures is slightly different from the expected one. The 'Therme' experiment, flying in SPOT 2, 3 and 4 satellites, which is dedicated to the study of the thermal control coatings aging under space environment, especially in heliosynchronous orbits with solar UV and atomic oxygen, is presented. ESA

N92-26999# Fokker Space and Systems, Amsterdam (Netherlands).
ULYSSES, ONE YEAR AFTER THE LAUNCH **c18**
H. Petersen *In* ESA, 4th European Symposium on Space Environmental Control Systems, Volume 2 Dec. 1991 p 951-956 (For primary document see N92-26950 17-54)
Avail: NTIS HC/MF A23; ESA, EPD, ESTEC, Noordwijk, Netherlands, HC 150 Dutch guilders (2 vols)

Ulysses is currently one year underway in a huge heliocentric orbit. A late change in some of the blankets' external material was required to prevent electrical charging due to contamination

by nozzle outgassing products. Test results are shown, governing various ranges of plasma parameters and sample temperatures. Even clean materials show a few volts charging due to imperfections in the conductive film. Thermal environment in the Shuttle cargo bay proved to be slightly different from prelaunch predictions: less warm with doors closed, and less cold with doors opened. Temperatures experienced in orbit are nominal. A problem was caused by a complex interaction of a Sun induced thermal gradient in a sensitive boom on the dynamic stability of the spacecraft. A user interface program was an invaluable tool to ease computations with the mathematical models, eliminate error risk and provide configuration control. ESA

N92-27000# All-Union Research Inst. of Electromechanics, Moscow (USSR).

FLIGHT TEST RESULTS OF THE PASSIVE COOLING SYSTEM **c18**

A. I. Abrosimov, O. V. Baryshev, V. A. Khoronenko, and U. G. Furdak *In* ESA, 4th European Symposium on Space Environmental Control Systems, Volume 2 Dec. 1991 p 957-959 (For primary document see N92-26950 17-54)

Avail: NTIS HC/MF A23; ESA, EPD, ESTEC, Noordwijk, Netherlands, HC 150 Dutch guilders (2 vols)

An onboard power cooler model is described. The flight test results for three years are given. It is shown that during the radiator exposure, of the cooler external stage to Sun, for about 15 minutesat each orbit, and at the maximum angle of the Sunascension, less than 30 degrees, the radiator temperature of the radiator detector is 105 K. ESA

N92-27001# European Space Agency. European Space Research and Technology Center, ESTEC, Noordwijk (Netherlands). Thermal Control and Life Support Div.

THERMAL IMPLICATIONS FROM THE HUBBLE SPACE TELESCOPE SOLAR ARRAY BI-STEM BOOM IN-ORBIT DISTURBANCE **c89**

P. Poinas and G. I. M. Beere *In its* 4th European Symposium on Space Environmental Control Systems, Volume 2 Dec. 1991 p 961-967 (For primary document see N92-26950 17-54)

Avail: NTIS HC/MF A23; ESA, EPD, ESTEC, Noordwijk, Netherlands, HC 150 Dutch guilders (2 vols)

The Hubble Space Telescope, launched on Apr. 24 1990, has two solar array wings. After the deployment of the arrays in orbit, attitude control disturbances were apparent, affecting the telescope, and which are believed to be due to the solar arrays. The main disturbances occur at two significant periods, namely the night/day and day/night transitions. As part of an investigative program to understand the phenomena, an especially detailed mechanical/thermal analysis was performed in the array bi-stems. An ESATAN (ESA Thermal Analysis Network) thermal mathematical model was created and the emphasis was on the transient thermal response at the penumbra passage. In particular, this shows the rate of change of the temperature gradients and their possible significance in relation to the transition periods. The thermal analysis was then extended to support the solution suggested by the previous work and considered to reduce/alleviate the problem. This solution could be implemented on the second pair of solar arrays, already in manufacture for the planned in orbit replacement. The effects of introducing a thermal shield in the form of a bellows is presented and the consequential improvement discussed. ESA

N92-27002# Dornier System G.m.b.H., Friedrichshafen (Germany, F.R.).

EVA LIFE SUPPORT DESIGN AND TECHNOLOGY DEVELOPMENTS

R. Vaeth and A. I. Skoog *In* ESA, 4th European Symposium on Space Environmental Control Systems, Volume 2 Dec. 1991 p 971-983 Sponsored by ESA (For primary document see N92-26950 17-54)

Avail: NTIS HC/MF A23; ESA, EPD, ESTEC, Noordwijk, Netherlands, HC 150 Dutch guilders (2 vols)

The technology development activities for the Extra Vehicular Activity (EVA) life support system within the framework of the ESA initiated EVA space suit system development program was completed as part of the predevelopment Phase C1. The achieved results and the progressing of the system design work resulted in an enhanced life support system design concept for the start of Phase C/D. While working towards an improved concept with respect to the main design drivers mass and cost, the technical concept was improved with respect to functional safety and ease of handling. The design concept status for Phase C/D and the results of the predevelopment of critical technologies for the EVA life support system are provided. The results of the investigations on breadboard model level and the design implications are analyzed. ESA

N92-27003# Avions Marcel Dassault-Breguet Aviation, Saint-Cloud (France).

GENESIS AND EVALUATION OF AN ERGONOMIC ARCHITECTURE FOR THE ESA EVA SUIT

Y. Ollivier, C. Mandin, and M. Diener (Dornier System G.m.b.H., Friedrichshafen, Germany, F.R.) *In* ESA, 4th European Symposium on Space Environmental Control Systems, Volume 2 Dec. 1991 p 985-990 (For primary document see N92-26950 17-54)

Avail: NTIS HC/MF A23; ESA, EPD, ESTEC, Noordwijk, Netherlands, HC 150 Dutch guilders (2 vols)

Few complex systems are closed to the human body and so constrained by human factors than the Extra Vehicular Activity (EVA) spacesuit. At the beginning of development analysis/test/development methods are necessary in order to insure the required human performances. Such methods are illustrated by the EVA phase 1/subphase C1 suit demonstrator development and tests, the purpose of which is to perform key technological assessments at subsystem level before starting the design of a fully representative development model. The main steps of this ergonomic oriented approach consist basically of parametric studies, computer aided design ergonomic simulations, 'man in the loop' evaluations; they are the following: from actional analysis to suit sections ergonomic performances; theoretical determination of the suit ergonomic architecture; mock up evaluations and suit ergonomic architecture refinement ergonomic test of the suit demonstrator. The purpose and the definition of these steps are described and the main results obtained for the suit enclosure during the C1 phase are provided. ESA

N92-27004# Alenia Spazio S.p.A., Turin (Italy).

EVA SPACE SUIT THERMAL CONTROL AND MICROMETEOROID PROTECTION

Maria Cristina Tosi, Gianluigi Gera, and Antonio Moscatelli *In* ESA, 4th European Symposium on Space Environmental Control Systems, Volume 2 Dec. 1991 p 991-998 (For primary document see N92-26950 17-54)

Avail: NTIS HC/MF A23; ESA, EPD, ESTEC, Noordwijk, Netherlands, HC 150 Dutch guilders (2 vols)

The Extra Vehicular Activity (EVA) space suit item necessary to guarantee the thermal control and micrometeroid protection functions is the Thermal and Micrometeroid Protection (TMP), covering the whole body of the crewmember and the EVA suit back pack. A comprehensive analysis of the materials, configuration research and screening is presented, showing the compliance with the requirements. The preferred baseline design solution to be applied to the manufacturing of the breadboard TMP arm is also described. The dedicated technology program, including a thermal vacuum test developed to demonstrate the thermal capability of the EVA space suit breadboard TMP arm, is also discussed. ESA

N92-27005# Zodiac Espanola S.A., Figueras (Spain).

DEVELOPMENT OF THE SUIT ENCLOSURE SOFT JOINTS OF THE EUROPEAN EVA SPACE SUIT

V. Menendez and Y. Ollivier (Avions Marcel Dassault-Breguet Aviation, Saint-Cloud, France) *In* ESA, 4th European Symposium on Space Environmental Control Systems, Volume 2 Dec. 1991

p 999-1004 (For primary document see N92-26950 17-54)
Avail: NTIS HC/MF A23; ESA, EPD, ESTEC, Noordwijk, Netherlands, HC 150 Dutch guilders (2 vols)

Results of efforts carried out for the definition, design, development, manufacturing and testing of an Extra Vehicular Activity (EVA) space suit soft joint breadboard operating at 500 hPa are described. The Suit Enclosure Subsystem (SES) will be able to provide the astronaut with the test protection against the environment while providing him with the best mobility. The driving parameter of this optimization is the suit internal pressure established at 500 hPa as the goal value for the suit design. The elbow was chosen as the SES soft joint representative to assess, though a breadboard evaluation, the feasibility and performance. The elbow joint was evaluated but also the adjustment devices and the representative interface to validate the related selected concepts. In addition to the elbow joint breadboard, a test bench allowing a complete evaluation of the breadboard was designed and manufactured. A description of the breadboard and the test bench is given and the main results of the evaluation are presented. ESA

N92-27006# Technofan, Blagnac (France). Labinal Group.
FAN/PUMP/SEPARATOR TECHNOLOGY DEVELOPMENT FOR EVA
J. M. Lassus, V. Boitel, B. Merchie, J. Witt, S. Klingele, and H. Funke (Dornier System G.m.b.H., Friedrichshafen, Germany, F.R.) *In* ESA, 4th European Symposium on Space Environmental Control Systems, Volume 2 Dec. 1991 p 1005-1010 Sponsored by ESA (For primary document see N92-26950 17-54)
Avail: NTIS HC/MF A23; ESA, EPD, ESTEC, Noordwijk, Netherlands, HC 150 Dutch guilders (2 vols)

Concept tradeoffs and design definitions have confirmed the gain in power, mass and volume achieved by integrating all three functions into a single unit, driven by one common brushless DC motor at 8150 rpm. The performance requirements for the three basic functions (oxygen and coolant water circulation and water separation) were derived from the layout of the life support system for the European Extra Vehicular Activity (EVA) space suit system. The functional units were studied and developed separately before final assembly of the integrated breadboard, which was successfully tested. The development approach, the concept selection, the design and tests results are described. A special water pump design with an integrated 'degassing device' was proposed. Corresponding investigations are presented. ESA

N92-27007# Nuevas Tecnologias Espaciales S.A., Llissa d'Amunt (Spain).
STUDY ON THE REQUIREMENTS FOR THE INSTALLATION OF A CES AND HABITABILITY CENTRE
A. Tomas, G. Monserrat, and M. Pastor *In* ESA, 4th European Symposium on Space Environmental Control Systems, Volume 2 Dec. 1991 p 1013-1019 Sponsored by ESA and Spanish Space Delegation (For primary document see N92-26950 17-54)
Avail: NTIS HC/MF A23; ESA, EPD, ESTEC, Noordwijk, Netherlands, HC 150 Dutch guilders (2 vols)

The need for a center carrying out research activities and technological developments in Closed Ecological Systems (CES) and habitability, as interrelated disciplines when studying life support systems, is pointed out by presenting a list of problems to be solved in space and terrestrial applications. A summary of present developments in the discipline is given and a tentative description for a center is presented, identifying the different functional areas and giving figures of surface and power for these areas. Requirements for the center placement are also suggested. Elements for establishing a schedule for center construction and operations are presented by analyzing the planned space programs and expected terrestrial spin offs. ESA

N92-27008# Futuro S.R.L., Florence (Italy).
MULTI-CULTURAL COMPONENTS AND KEYS FOR EUROPEAN WORLDWIDE SPACE PROGRAMS **c12**
Roberto Pinotti *In* ESA, 4th European Symposium on Space Environmental Control Systems, Volume 2 Dec. 1991 p 1021-1023 (For primary document see N92-26950 17-54)
Avail: NTIS HC/MF A23; ESA, EPD, ESTEC, Noordwijk, Netherlands, HC 150 Dutch guilders (2 vols)

The role of different cultures in space missions is considered with regard to NASA and ESA astronauts and Russian cosmonauts. The identification of all the psychological and socio-anthropological components in the behavior of human groups in space is extremely important to understand and solve different problems and obtain the mission's success. In this light, the creation of a multicultural atmosphere aboard is considered a positive aspect for future space programs, and the synthesis of European cultural elements is a definite key to develop morale and productivity. ESA

N92-27009# Texas Southern Univ., Houston.
AN EVALUATIVE STUDY OF THE SENSORY QUALITIES OF SELECTED EUROPEAN AND ASIAN FOODS FOR INTERNATIONAL SPACE MISSIONS (A FRENCH FOOD STUDY)
S. Ahmed and P. V. Cornish *In* ESA, 4th European Symposium on Space Environmental Control Systems, Volume 2 Dec. 1991 p 1025-1030 (For primary document see N92-26950 17-54)
Avail: NTIS HC/MF A23; ESA, EPD, ESTEC, Noordwijk, Netherlands, HC 150 Dutch guilders (2 vols)

European and Asian foods for international space missions were investigated by evaluating sensory qualities. Selected Russian, French, Japanese foods were prepared and evaluated by a taste panel for acceptability. Entrees, soups, desserts, vegetables, salads, beverages and snacks were evaluated on the basis of appearance, odor, favor and texture. Food samples were scored on a nine point hedonic scale. The result for the food samples comparatively studied showed significant differences between quality characteristics, foodtypes and compared groups (trained panelist and ethnic panelists) for the Russian and French food samples. The Japanese food samples indicated a significant difference between quality characteristics only at the 0.10 confidence level. Japanese foodtypes and compared groups were significantly different at the 0.05 confidence level. As a result of this study, forty three Russian, thirty five French, and thirty seven Japanese foods were identified as possible candidates for international space missions. ESA

N92-27010# CJB Developments Ltd., Portsmouth (England).
CRITICAL TECHNOLOGIES: SPACECRAFT HABITABILITY, AN UPDATE
R. A. J. Dams *In* ESA, 4th European Symposium on Space Environmental Control Systems, Volume 2 Dec. 1991 p 1031-1036 (For primary document see N92-26950 17-54)
Avail: NTIS HC/MF A23; ESA, EPD, ESTEC, Noordwijk, Netherlands, HC 150 Dutch guilders (2 vols)

A study to identify critical technologies relating to spacecraft habitability was performed. Five technologies were identified which were worthy of continuous study because of their magnitude or because it was considered continuous updating of latest terrestrial developments was required. These 'ongoing' technologies were: new methods of food processing and new kinds of space food; space motion sickness, identifying prevention; radiation, acceptable life time limits; provision of artificial gravity; habitation mockup. Latest developments in these technologies, both in space and on Earth are reviewed. ESA

N92-27011# Design Models, Inc., Los Angeles, CA. Space Projects Group.
ARCHITECTURAL STUDIES RELATING TO HUMAN BODY MOTION MORPHOLOGY IN MICROGRAVITY **c52**
Regis Fauquet and Jun Okushi *In* ESA, 4th European Symposium on Space Environmental Control Systems, Volume 2 Dec. 1991 p 1037-1043 (For primary document see N92-26950 17-54)
Avail: NTIS HC/MF A23; ESA, EPD, ESTEC, Noordwijk, Netherlands, HC 150 Dutch guilders (2 vols)

In microgravity the human body experiences dramatic postural physiological and perceptual changes. These transformations make a human being in weightlessness a different person with different

needs. Mobility becomes a central issue of human life in orbit where the absence of gravity constitutes a handicap. The architectural layout of the hardware in a space habitat must not only be engineered properly, but also be tailored to the mobility needs of the human body in microgravity. Thus, the interface between human movements and the environment must be observed to understand the morphology of body motion and to assess what types of environmental conditions have the greatest potential to support adequately human mobility in weightlessness. From these observations a tentative elementary taxonomy of movements was formulated to serve as a design reference tool. The current definition of body envelope was expanded to take on consideration the kinetic characteristics of human motion that revealed geometries with intriguing implications for the design of future space habitats. ESA

N92-27012# Deutsche Forschungsanstalt fuer Luft- und Raumfahrt, Cologne (Germany, F.R.). Inst. of Aerospace Medicine.

LBNP AS COUNTERMEASURE: AN AUTOMATED SCENARIO **c52**

Friedhelm Baisch, Luis Beck, Frank Kirchner, and Diego Loyola *In* ESA, 4th European Symposium on Space Environmental Control Systems, Volume 2 Dec. 1991 p 1045-1048 (For primary document see N92-26950 17-54)

Avail: NTIS HC/MF A23; ESA, EPD, ESTEC, Noordwijk, Netherlands, HC 150 Dutch guilders (2 vols)

Restitution of body fluids to Earth based standards is desirable for astronauts preparing their return to Earth after a prolonged space mission. Repeated Lower Body Negative Pressure (LBNP) application can assist in reaching this objective. However, use of rigorous LBNP profile includes the risk of syncope. A system that allows controlled LBNP application to minimize risks is described. The system enables the user to define an LBNP exposure profile. While a given profile runs, the system records and analyzes different physiological signals and provides online monitoring capability for critical parameters. Systolic, diastolic, and mean blood pressure derived by a 'Port a pres' (trademark) device, heart rate for electrocardiogram and a stroke volume correlate can be displayed on a beat by beat basis. The LBNP session can be both terminated by the system itself according to the predefined exposure profile or by an independent observer. It is planned to increase the system's capabilities by including intelligent features such as recognition of critical hemodynamic patterns. This would trigger automatic interruption of LBNP application. A system of such characteristics could enable routine LBNP application on a space station without increasing operational burden and increase LBNP's efficiency as a countermeasure. ESA

N92-27013# European Space Agency. European Space Research and Technology Center, ESTEC, Noordwijk (Netherlands).

WINGED LAUNCHER THERMAL DESIGN ASPECTS **c15**

K. Keller *In its* 4th European Symposium on Space Environmental Control Systems, Volume 2 Dec. 1991 p 1051-1056 (For primary document see N92-26950 17-54)

Avail: NTIS HC/MF A23; ESA, EPD, ESTEC, Noordwijk, Netherlands, HC 150 Dutch guilders (2 vols)

The need for significant reduction in launch cost favors the consideration of reusable space transportation systems which are assisted by aerodynamic lift. The thermomechanical and thermochemical environments and the basic design requirements of two airbreathing vehicle classes are put in relation to vehiles like Shuttle and Hermes. Similarities as well as essential differences between the various vehicles are highlighted. State of the art thermal protection concepts and materials are analyzed with respect to winged launcher concepts. Future development trends for design and materials with potential application are identified. The need for improved thermostructural analysis and optimization techniques is outlined. ESA

N92-27014# European Space Agency. Centre Spatial de Toulouse (France).

WARM STRUCTURES AND THERMAL PROTECTION OF THE EUROPEAN SPACEPLANE HERMES [STRUCTURES CHAUDES ET PROTECTIONS THERMIQUES DE L'AVION SPATIAL EUROPEEN HERMES] **c18**

J. P. Vialaneix, E. Werling, and J. C. Verneuil (Centre Spatial Dassault, Blagnac, France) *In its* 4th European Symposium on Space Environmental Control Systems, Volume 2 Dec. 1991 p 1057-1064 In FRENCH (For primary document see N92-26950 17-54)

Avail: NTIS HC/MF A23; ESA, EPD, ESTEC, Noordwijk, Netherlands, HC 150 Dutch guilders (2 vols)

The estimated surface temperature of the Hermes spaceplane being more than 1600 C locally in nominal flight conditions requires the development of new materials and new technologies for the thermal protection of the vehicle. General functional requirements applicable to thermal protection are given and the thermal environment to which the plane is exposed during different parts of its mission is described. Means of protection materials and technologies are presented. The dimensioning analysis and testing of the thermal insulation is illustrated through work carried out on the 'tile system'. ESA

N92-27015# Central Research Inst. of Tech. and Machine Building, Moscow (USSR).

THE IMPORTANCE OF CHEMICAL REACTIONS WITH ENVIRONMENT FOR ABLATION PROCESS OF THERMAL PROTECTION AND STRUCTURAL MATERIALS **c27**

N. A. Anfimov *In* ESA, 4th European Symposium on Space Environmental Control Systems, Volume 2 Dec. 1991 p 1065-1070 (For primary document see N92-26950 17-54)

Avail: NTIS HC/MF A23; ESA, EPD, ESTEC, Noordwijk, Netherlands, HC 150 Dutch guilders (2 vols)

Contribution of chemical reactions to the ablation process is examined. The important factor is presence of oxygen in the air or oxygenating potential of other environments, where thermal protection coatings can be used. The principal heat and mass transfer relations for different kinds of ablation processes are dealt with. The consideration is conducted for simple materials (metals, graphite). Theoretical results are compared with experimental data. In conclusion some possible methods of counteracting a chemical interaction of thermal protection materials with environment are discussed. ESA

N92-27016# Erno Raumfahrttechnik G.m.b.H. Bremen (Germany, F.R.).

LIGHTWEIGHT FIBER INSULATIONS PERFORMANCE AND APPLICATION **c27**

J. Antonenko, W.-D. Ebeling, B. Schwarz, and F. Menn *In* ESA, 4th European Symposium on Space Environmental Control Systems, Volume 2 Dec. 1991 p 1071-1077 (For primary document see N92-26950 17-54)

Avail: NTIS HC/MF A23; ESA, EPD, ESTEC, Noordwijk, Netherlands, HC 150 Dutch guilders (2 vols)

Lightweight microfiber insulations are realized in Europe for the first time for the Hermes Flexible External Insulation (FEI). FEI is an assembly of quilted blankets, composed of a silica microfiber insulation core, embedded in silica fiber and glass fiber fabrics and held together by sewing with silica and glass threads. The thermal performance is adjustable by variation of blanket thickness, core density and number of reflective layers. By use of ABS (Alumina and Silica with minor additions of e.g., baron oxide) fabrics, threads and microfibers, the application temperature can be expanded as far as 1300 C. The structural strength can be designed by proper choice of threads and fabrics. Several applications are presented, including the present developments for Hermes FEI and Ariane 5 electrical power system heat shield and the proposed solutions for the insulation of the Express reentry capsule's rear, the Huygens probe's rear and the Ariane 4 payload assembly level. ESA

N92-27017# European Space Agency. European Space Research and Technology Center, ESTEC, Noordwijk (Netherlands).

DETERMINATION OF VENTILATION REQUIREMENTS FOR A SPACE SUIT HELMET

J. Witt and R. Seurig *In its* 4th European Symposium on Space Environmental Control Systems, Volume 2 Dec. 1991 p 1081-1085 (For primary document see N92-26950 17-54)
Avail: NTIS HC/MF A23; ESA, EPD, ESTEC, Noordwijk, Netherlands, HC 150 Dutch guilders (2 vols)

Tests were carried out to study the ventilation in a space suit helmet representative of the European space suit system. Visor fogging and CO2 exposure were determined at different ventilation flow rates, inlet conditions and metabolic rates. Different configurations at the inlet duct for the ventilation of the helmet were tested. A mockup of the hard upper torso and a breathing manikin able to simulate the CO2 and humidity production of an astronaut performing extravehicular activity were designed and built. Test results are presented and discussed. ESA

N92-27018# Nord-Micro Elektronic Feinmechanik G.m.b.H., Frankfort (Germany, F.R.).

DEVELOPMENT OF EUROPEAN SUBLIMATOR TECHNOLOGY FOR EVA

Christine Planert, Peter Kremer, Volker General, and Johannes Witt (European Space Agency. European Space Research and Technology Center, ESTEC, Noordwijk, Netherlands) *In* ESA, 4th European Symposium on Space Environmental Control Systems, Volume 2 Dec. 1991 p 1087-1091 Sponsored by Dornier G.m.b.H. (For primary document see N92-26950 17-54)
Avail: NTIS HC/MF A23; ESA, EPD, ESTEC, Noordwijk, Netherlands, HC 150 Dutch guilders (2 vols)

Temperature and humidity control are important functions for the astronaut's comfort and safety in an Extra Vehicular Activity (EVA) space suit. Several sources within the suit are permanently producing heat and humidity; both have to be removed to prevent visor fogging and overheating of the astronaut. In the European space suit heat will be removed by using the transformation of ice into vapor in vacuum (sublimation process). In the sublimator this process will take place in a porous plate, which is mounted onto a liquid gas heat exchanger. A breadboad unit was manufactured from stainless steel and a new porous plate was developed. Performance tests demonstrated the technical feasibility of the design concept. Results obtained during manufacturing and testing of the European sublimator breadboard are presented. ESA

N92-27019# Draegerwerk A.G., Luebeck (Germany, F.R.).

INVESTIGATION ON A PARTIAL PRESSURE CARBON DIOXIDE SENSOR

K. Ammann and J. Witt (European Space Agency. European Space Research and Technology Center, ESTEC, Noordwijk, Netherlands) *In* ESA, 4th European Symposium on Space Environmental Control Systems, Volume 2 Dec. 1991 p 1093-1098 Sponsored by ESA/ESTEC (For primary document see N92-26950 17-54)
Avail: NTIS HC/MF A23; ESA, EPD, ESTEC, Noordwijk, Netherlands, HC 150 Dutch guilders (2 vols)

A summary of a technology research program aimed at the development of a CO2 partial pressure sensor suitable for monitoring the ppCO2 inside the oxygen ventilation loop of the extravehicular activity life support module is given. Tradeoffs of candidate sensor concepts are presented. As result, the infrared optical sensor concept was selected. A breadboard model of the ppCO2 sensor together with a test set up was established. The sensor was subjected to a test program and main results are given. The findings are discussed in the light of the development of future flight hardware. ESA

N92-27020# AiResearch Mfg. Co., Torrance, CA.

HEAT REJECTION SYSTEM FOR AN ADVANCED EXTRAVEHICULAR MOBILITY UNIT PORTABLE LIFE SUPPORT SYSTEM

Hal J. Strumpf and A. A. Vuigner *In* ESA, 4th European Symposium on Space Environmental Control Systems, Volume 2 Dec. 1991 p 1099-1106 (For primary document see N92-26950 17-54)
Avail: NTIS HC/MF A23; ESA, EPD, ESTEC, Noordwijk, Netherlands, HC 150 Dutch guilders (2 vols)

A study is being conducted on the design, development, fabrication, integration, and testing of subsystems for an advanced extravehicular mobility unit Portable Life Support System (PLSS). A subsystem, the Heat Rejection System (HRS), is discussed. The function of the HRS is to remove metabolic and equipment heat loads and provide a comfortable thermal environment for a crew person during extravehicular activity. Two versions of the HRS were studied. The first version is discussed. It comprises a Regenerable Nonventing Thermal Sink (RNTS). The RNTS consists of cold plate heat exchangers, a radiator to reject a fraction of the generated heat load, and a regenerable thermal storage unit to absorb the remaining heat load. The second version of the HRS, not discussed, comprises a radiator (with no thermal storage) and a vented water evaporator. ESA

N92-27021*# AiResearch Mfg. Co., Torrance, CA.

METAL OXIDE ABSORBENTS FOR REGENERATIVE CARBON DIOXIDE AND WATER VAPOR REMOVAL FOR ADVANCED PORTABLE LIFE SUPPORT SYSTEMS

Joan M. Hart, Joseph B. Borghese, Craig H. Chang, and Greg T. Stonesifer (Lockheed Engineering and Sciences Co., Moffett Field, CA.) *In* ESA, 4th European Symposium on Space Environmental Control Systems, Volume 2 Dec. 1991 p 1107-1111 (For primary document see N92-26950 17-54)
(Contract NAS9-17900)
Avail: NTIS HC/MF A23; ESA, EPD, ESTEC, Noordwijk, Netherlands, HC 150 Dutch guilders (2 vols)

Recent studies of Allied Signal metal oxide based absorbents demonstrated that these absorbents offer a unique capability to regeneratively remove both metabolic carbon dioxide and water vapor from breathing air; previously, metal oxides were considered only for the removal of CO2. The concurrent removal of CO2 and H2O vapor can simplify the astronaut Portable Life Support System (PLSS) by combining the CO2 and humidity control functions into one regenerative component. The use of metal oxide absorbents for removal of both CO2 ad H2O vapor in the PLSS is the focus of an ongoing program. The full scale Metal Oxide Carbon dioxide and Humidity Remover (MOCHR) and regeneration unit is described. ESA

N92-27022# Alenia Spazio S.p.A., Turin (Italy).

NEW PERSPECTIVES OF LIVING IN SPACE: HABITABILITY GUIDELINES FOR FUTURE MANNED SPACE SYSTEMS

Maria Stella Lavitola, Carlo Tomatis, and Roberto Pinotti (Futuro S.R.L., Florence, Italy) *In* ESA, 4th European Symposium on Space Environmental Control Systems, Volume 2 Dec. 1991 p 1115-1120 (For primary document see N92-26950 17-54)
Avail: NTIS HC/MF A23; ESA, EPD, ESTEC, Noordwijk, Netherlands, HC 150 Dutch guilders (2 vols)

Key aspects to be considered when designing inhabited space vehicles and structures are discussed. These include: mission duration, number of crew, level of gravity, level of radiation, and distance from Earth. Information gathered from previous space missions and from terrestrial analogs which can be used for deriving architectural guidelines for future manned space systems is considered. The following are discussed: ergonomy, internal volume distribution, environment quality, acoustic isolation, food management, rest and recreation health maintenance, hygiene, sleeping, physical exercise. Two possible habitat configurations for a Moon base are presented; an inflatable spherical structure able to house a large community (12 to 13 people) and a module structure conceived for an initial limited community, with the capability to be extended further for up to 12 astronauts. ESA

N92-27023# Nelson Space Services Ltd., London (England).
CONCEPT FOR A EUROPEAN SPACE STATION: HABITABILITY, LIFE SUPPORT, AND LABORATORY FACILITIES
R. C. Huttenbach, S. D. Oram, D. A. Nixon, Nick Larter, and M. Colasson (Colasson, M., Paris, France) *In* ESA, 4th European Symposium on Space Environmental Control Systems, Volume 2 Dec. 1991 p 1121-1135 (For primary document see N92-26950 17-54)
Avail: NTIS HC/MF A23; ESA, EPD, ESTEC, Noordwijk, Netherlands, HC 150 Dutch guilders (2 vols)

A concept for a European space station is described and details of its habitability, life support, safety, power supply, control and laboratory facilities are outlined. There are many opportunities to improve the design of crew accommodation, environmental control, life support systems and laboratory facilities beyond those planned for Space Station Freedom. Using an advanced configuration of the Station, the following are described: approaches to the design of crew habitability facilities; the outfitting of equipment; environmental control and life support; crew safety and survivability; power supply; data and communications; and the design of laboratory facilities. Driving these proposals is the need to provide a stimulating and sustaining environment that will accommodate crew safety and in a manner that will optimize their efficiency and productivity during all stages of the Station's build up. ESA

N92-27024# Progetto Area, Rome (Italy).
INFLUENCE OF ARCHITECTURE ON THE DEFINITION OF A SPACE STATION CONFIGURATION c18
Luca Bradini and Luca Galofaro (Rome Univ., Italy) *In* ESA, 4th European Symposium on Space Environmental Control Systems, Volume 2 Dec. 1991 p 1137-1140 (For primary document see N92-26950 17-54)
Avail: NTIS HC/MF A23; ESA, EPD, ESTEC, Noordwijk, Netherlands, HC 150 Dutch guilders (2 vols)

The connection between architecture, locus, and human is considered with regard to definition of space station configuration. The use of geometry as message and not as aggregative final result is considered to suggest interesting possibilities in the realization of the external shapes. The choice of a cube arises from the need of marking a place through a purely artificial sign. Architecture is supposed to become, according to its instruments of realization, the connecting link between a physical condition: gravity and the absence of gravity. The functional zoning and the arrangement of spaces become a figurative language capable of helping the human. ESA

N92-27025# European Space Agency. European Space Research and Technology Center, ESTEC, Noordwijk (Netherlands). Columbus Crew Activities and On-Board Payload Operations.
CREW-FRIENDLY SUPPORT SYSTEMS FOR INTERNAL VEHICULAR ACTIVITIES IN ZERO GRAVITY, EXPERIMENTED UNDERWATER FOR THE COLUMBUS PROGRAMME
Carlo Viberti *In its* 4th European Symposium on Space Environmental Control Systems, Volume 2 Dec. 1991 p 1141-1146 (For primary document see N92-26950 17-54)
Avail: NTIS HC/MF A23; ESA, EPD, ESTEC, Noordwijk, Netherlands, HC 150 Dutch guilders (2 vols)

With respect to the past manned enterprises, the new European challenge in space, the Columbus program, is characterized by a completely new operational scenario; this calls for comprehensive tests in representative zero gravity environments not only of external vehicular activities, but also of internal operations to verify design solutions and evaluate both operational aspects and crew procedures inside the Columbus modules, especially as far as crew support systems such as mobility and stability aids are concerned. The first results attained in parabolic flights and underwater testing are highlighted. ESA

N92-27026# Alenia Spazio S.p.A., Turin (Italy).
MOON BASE HABITABILITY ASPECTS
Maria Antonietta Perino *In* ESA, 4th European Symposium on Space Environmental Control Systems, Volume 2 Dec. 1991 p 1147-1154 (For primary document see N92-26950 17-54)
Avail: NTIS HC/MF A23; ESA, EPD, ESTEC, Noordwijk, Netherlands, HC 150 Dutch guilders (2 vols)

The main habitat requirements for a Moon base are identified and analyzed. Various issues and technologies related to the local environment in which human beings will operate must be considered so as to choose from among different scenarios and to identify possible design solutions. Moreover, the mission characteristics play an important role in the basic sizing of the habitat, that depend heavily on the crew size and length of stay according to the different phases of the enterprise. Considerations about the influence of human aspects on the habitat design are also drawn, and the requirements to ensure maximum crew safety are outlined. The main habitat features are described, according to a multistep Moon base design approach. The Environment Control and Life Support System (ECLSS) is also regarded as an essential subsystem for any manned space system, and it will require a growing level of self sufficiency with the development of the Moon base's needs. A modular design of the ECLSS is proposed to adapt it for either variable capacities or different evolutionary stages. ESA

N92-27027# Erno Raumfahrttechnik G.m.b.H. Bremen (Germany, F.R.).
CONJUGATING BINARY SYSTEMS: ADVANCED COOLING LIQUIDS FOR USE IN SPACECRAFT ATCS c34
P. L. Mueller-Remmers, H. Papenberg, W.-D. Ebeling, M. Huerth, D. Woermann, J. Gmehling, and W. Supper (European Space Agency. European Space Research and Technology Center, ESTEC, Noordwijk, Netherlands) *In* ESA, 4th European Symposium on Space Environmental Control Systems, Volume 2 Dec. 1991 p 1157-1162 (For primary document see N92-26950 17-54)
(Contract ESTEC-8757/90/NL/PP(SC))
Avail: NTIS HC/MF A23; ESA, EPD, ESTEC, Noordwijk, Netherlands, HC 150 Dutch guilders (2 vols)

The drastic increase of the specific heat of Conjugating Binary Systems (CBS) very near to the critical temperature resulting in an enhanced heat transport capability is of interest with respect to the heat transport capabilities of standard spacecraft cooling liquids, R114 and water, and hence for use in spacecraft ACTS (Active Thermal Control Subsystem). An almost complete list of CBS (status end 1990) with suitable chemical properties and suitable values of the critical temperature was selected from a database of thermodynamic data. A simple procedure was developed to determine the temperature dependence of the specific heat and the excess specific heat of CBS around the critical temperature. The CBS finally analyzed show maximum specific heat data in the range of water or freezing points in the range of water freezing points in the range of R114 or dynamic properties (density, dynamic viscosity and thermal conductivity) better or equal than those of the reference systems. Future investigations are proposed. ESA

N92-27028# European Space Agency. European Space Research and Technology Center, ESTEC, Noordwijk (Netherlands).
HEATSHIELD CONCEPTS FOR THE ROSETTA AEROCAPSULE c18
M. Eiden, D. Desnoyer, C. Chiarelli (Alenia Spazio S.p.A., Rome, Italy), and A. Smith *In its* 4th European Symposium on Space Environmental Control Systems, Volume 2 Dec. 1991 p 1163-1173 (For primary document see N92-26950 17-54)
Avail: NTIS HC/MF A23; ESA, EPD, ESTEC, Noordwijk, Netherlands, HC 150 Dutch guilders (2 vols)

The goal of Rosetta mission is to increase the human knowledge about the comet nucleus properties. The mission will consist, after a space flyby, in a landing on a comet nucleus, a collection of samples and a return to Earth with the samples stowed in a capsule performing a direct reentry. After recovery of the capsule, the samples will be analyzed in scientific laboratories. The history

of the capsule thermal protection study is explained from original concepts to the new thermal protection concept. Tradeoffs and justifications are presented. ESA

N92-27179# North Atlantic Treaty Organization, Brussels (Belgium).
THE STUDY ON A DIRECTORY OF HUMAN PERFORMANCE MODELS FOR SYSTEM DESIGN (DEFENCE RESEARCH GROUP PANEL 8 ON THE DEFENCE APPLICATIONS OF HUMAN AND BIO-MEDICAL SCIENCES)
1992 310 p
(AD-A247346; AC/243(PANEL 8)TR/1) Avail: NTIS HC/MF A14

This report catalogues over fifty human performance models and model development tools which are applicable to system design. It provides potential model users with brief reviews of each model, presented in a standard format. It is meant to be a practical source book, and does not address mathematical or theoretical issues to any great extent. Each chapter is aimed at a specific problem area in the system design/development cycle. Chapter topics include task allocation and workload prediction, single task models, multi-task models, multi-operator models, biomechanics and work space design, training and skill retention models, and network Modeling tools. Author (GRA)

55 SPACE BIOLOGY

Includes exobiology; planetary biology; and extraterrestrial life.

No abstracts in this category.

59 MATHEMATICAL AND COMPUTER SCIENCES (GENERAL)

No abstracts in this category.

60 COMPUTER OPERATIONS AND HARDWARE

Includes hardware for computer graphics, firmware, and data processing.

For components see *33 Electronics and Electrical Engineering.*

N92-26382# Naval Postgraduate School, Monterey, CA.
RECONFIGURATION IN ROBUST DISTRIBUTED REAL-TIME SYSTEMS BASED ON GLOBAL CHECKPOINTS M.S. Thesis
Ronnie D. Puett Dec. 1991 94 p
(AD-A245615) Avail: NTIS HC/MF A05

Fast, ultra-reliable, real-time computing is fundamental in today's weapons system. Increased system throughput and reliability can be achieved by utilizing distributed systems in which a single application program executes on multiple processors, connected to a network. The distributed nature of such systems make it possible to tolerate failures and react to overloads without the application level performance degrading unacceptably. Fault tolerance in these systems typically involves fault detection and recovery. Repair following failure involves smooth integration of the repaired processor and subsequent reconfiguration. These actions must take place transparently, that is without the application program noticing it. Therefore, sufficient information must be maintained through the use of checkpointing to describe the state of the system at any time and ensure correct operation after failure/repair. This thesis investigates a possible framework for achieving a fault-tolerant real time distributed system which provides transparent function-to-function message passing, status monitoring using periodic health messages and maintains a globally consistent system state by carrying out independent checkpointing procedures. The proposed scheme is simulated using concurrent Ada processing for a four mode, twelve function distributed system. GRA

N92-26439 Politecnico di Milano (Italy). Dipartimento di Elettronica.
HARDWARE SYNTHESIS USING HIGH-LEVEL PETRI NETS
Kim Portman 1991 33 p Sponsored in part by Finnish Academy
(Rept-91-071; ETN-92-91358) Avail: Politecnico di Milano, Piazza Leonardo da Vinci 32, 20133 Milan, Italy

The use of high level Petri nets in hardware synthesis is discussed. A new time Petri net formalism, called Environment/Relationship is presented. Its use for specifying and realizing hardware systems is described. Hardware synthesis is implemented by translating the Petri net specification into a program in hardware description language, like VHDL or Hardware-C. This translation is done with a rule based Petri net code generator, which is part of the design environment CABERNET. The generated hardware program can further be processed by other synthesis tools, like circuit simulators and hardware compilers. The circuit can be specified with Petri nets, and turned into silicon with automatic tool support. ESA

N92-26551# California Univ., Berkeley. Lawrence Berkeley Lab.
THE SIXTEEN CHANNEL CAMAC CONSTANT FRACTION DISCRIMINATOR FOR APEX
M. R. Maier, M. Robertson, F. L. H. Wolfs, and P. A. A. Perera (Rochester Univ., NY.) Nov. 1991 6 p Presented at the IEEE Nuclear Science Symposium, Santa Fe, NM, 5-9 Nov. 1991
(Contract DE-AC03-76SF-00098)
(DE92-010550; LBL-31450; CONF-911106-90) Avail: NTIS HC/MF A02

We report on the construction and the performance of a sixteen channel constant fraction discriminator (CFD) for the Atlas Positron Experiment (APEX). We have used an integrated circuit (IC), recently introduced commercially, which contains all the electronic building blocks needed to construct a CFD. We have placed 16 channels of CFD into a CAMAC module. An important feature is the time to charge converter (TQC) that we have included for every CFD channel. Its calibration constant is controlled via CAMAC. The TQC allows the use charge sensitive analog to digital converters (QDC) for timing measurements. Results for CFD walk, resolution and crosstalk as well as for TQC linearity will be presented. DOE

N92-26773# Naval Postgraduate School, Monterey, CA.
AN OBJECT-ORIENTED APPROACH TO COMPUTER ARCHITECTURE SIMULATION M.S. Thesis
Kevin A. Fontes Sep. 1991 208 p
(AD-A246597) Avail: NTIS HC/MF A10

An object-oriented approach to modeling and simulating computer architectures is presented. This approach yields a 'generic' class hierarchy that supports the simulation of basic computer microarchitecture components found in most computers. This is accomplished by concentrating on the more generic concepts of processors, memories, register, etc., rather than concentrating on a specific system. This 'generic' class hierarchy is tested by developing microarchitecture simulators for two different microarchitecture designs. GRA

61 COMPUTER PROGRAMMING AND SOFTWARE

Includes computer programs, routines, alogorithms, and specific applications, e.g., CAD/CAM.

N92-26181*# Research Inst. for Computing and Information Systems, Houston, TX.
ADVANCED SOFTWARE DEVELOPMENT WORKSTATION. ENGINEERING SCRIPTING LANGUAGE GRAPHICAL EDITOR: DRAFT DESIGN DOCUMENT Interim Report
9 Jul. 1991 56 p Prepared in cooperation with Inference Corp., El Segundo, CA
(Contract NCC9-16; RICIS Proj. SE-41)
(NASA-CR-190393; NAS 1.26:190393) Avail: NTIS HC/MF A04

The Engineering Scripting Language (ESL) is a language designed to allow nonprogramming users to write Higher Order Language (HOL) programs by drawing directed graphs to represent the program and having the system generate the corresponding program in HOL. The ESL system supports user generation of HOL programs through the manipulation of directed graphs. The components of this graphs (nodes, ports, and connectors) are objects each of which has its own properties and property values. The purpose of the ESL graphical editor is to allow the user to create or edit graph objects which represent programs. Author

N92-26182*# Research Inst. for Computing and Information Systems, Houston, TX.
ADVANCED SOFTWARE DEVELOPMENT WORKSTATION. ENGINEERING SCRIPTING LANGUAGE GRAPHICAL EDITOR: DRAFT CODE DOCUMENTATION Interim Report
30 Aug. 1991 90 p Prepared in cooperation with Inference Corp., El Segundo, CA
(Contract NCC9-16; RICIS Proj. SE-41)
(NASA-CR-190389; NAS 1.26:190389) Avail: NTIS HC/MF A05

The computer program for the Advanced Software Development Workstation is presented. Author

N92-26183*# Research Inst. for Computing and Information Systems, Houston, TX.
ADVANCED SOFTWARE DEVELOPMENT WORKSTATION PROJECT: ENGINEERING SCRIPTING LANGUAGE. GRAPHICAL EDITOR
14 Feb. 1992 43 p
(Contract NCC9-16; RICIS Proj. SE-41)
(NASA-CR-190391; NAS 1.26:190391) Avail: NTIS HC/MF A03

Software development is widely considered to be a bottleneck in the development of complex systems, both in terms of development and in terms of maintenance of deployed systems. Cost of software development and maintenance can also be very high. One approach to reducing costs and relieving this bottleneck is increasing the reuse of software designs and software components. A method for achieving such reuse is a software parts composition system. Such a system consists of a language for modeling software parts and their interfaces, a catalog of existing parts, an editor for combining parts, and a code generator that takes a specification and generates code for that application in the target language. The Advanced Software Development Workstation is intended to be an expert system shell designed to provide the capabilities of a software part composition system. Author

N92-26188# Westinghouse Savannah River Co., Aiken, SC.
DISTRIBUTED VISUALIZATION
T. R. Arnold 1991 9 p Presented at the Visions of Supercomputing Conference, Santa Fe, NM, 23-27 Sep. 1991
(Contract DE-AC09-89SR-18035)
(DE92-009405; WSRC-MS-91-305; CONF-9109276-9) Avail: NTIS HC/MF A02

Within the last half decade or so, two technological evolutions have culminated in mature products of potentially great utility to computer simulation. One is the emergence of low-cost workstations with versatile graphics and substantial local CPU power. The other is the adoption of UNIX as a de facto 'standard' operating system on at least some machines offered by virtually all vendors. It is now possible to perform transient simulations in which the number-crunching capability of a supercomputer is harnessed to allow both process control and graphical visualization on a workstation. Such a distributed computer system is described as it now exists: a large FORTRAN application on a CRAY communicates with the balance of the simulation on a SUN-3 or SUN-4 via remote procedure call (RPC) protocol. The hooks to the application and the graphics are very flexible. Piping of output from the CRAY to the SUN is nonselective, allowing the user to summon data and draw or plot at will. The ensemble of control, application, data handling, and graphics modules is loosely coupled, which further generalizes the utility of the software design. DOE

N92-26189# New Mexico Inst. of Mining and Technology, Socorro. Dept. of Geoscience.
DESCRIPTION OF AND USERS MANUAL FOR TUBA: A COMPUTER CODE FOR GENERATING TWO-DIMENSIONAL RANDOM FIELDS VIA THE TURNING BANDS METHOD
D. A. Zimmerman and J. L. Wilson Jan. 1992 150 p
(Contract DE-AC22-85BC-10850)
(DE92-001020; DOE/BC-10850/19) Avail: NTIS HC/MF A07

TUBA is a computer code for the generation of synthetic two-dimensional random fields via the Turning Bands Method. It is primarily used to generate synthetic permeability fields for hydrologic and petroleum engineering applications, but it has applications wherever synthetic random fields are employed. This is version 2.0 of TUBA, a completely redesigned and rewritten code. It generates stationary or non-stationary, isotropic and anisotropic, and point or areal average random fields. Five functional covariance models are available in the code. These are Gaussian, Bessel, Telis, and Generalized Covariance models. The user can supply other forms. The random fields can be generated onto a gridded system (e.g., at the nodes of a point centered finite difference model, or the blocks of a block centered model), or at arbitrary locations in space (e.g., at the Gauss points of a finite element grid). TUBA can be used to generate the field values in local areas at much greater resolution than the original simulated field. The fields can be generated with a normal or a lognormal distribution. The size of the simulation is limited only by the virtual memory capabilities of the computer on which it is run. Random fields with over a million nodes have been generated with TUBA on a 386PC running Xenix. The code has been run on 286 and 386 PC's running DOS, on Sun 3's and 4's using Unix, and on Dec VAX's running VMS. DOE

N92-26195# Naval Postgraduate School, Monterey, CA.
USING SOLID MODELING TECHNIQUES TO CONSTRUCT THREE-DIMENSIONAL ICONS FOR A VISUAL SIMULATOR M.S. Thesis
Jane S. Polcrack Sep. 1991 64 p
(AD-A245784) Avail: NTIS HC/MF A04

Realistic three dimensional (3D) models are an essential part of any battle simulator. They contribute greatly to the quality of the scenarios and the decision making training the system can provide. Commercial programs are available to build and modify these models, also known as icons, but they tend to be very expensive and complicated. They also tend to be very specific as to the file format used to store icons. The developers of the Naval Postgraduate School's battle simulator, NPSNET, need a simple, easy to use, and inexpensive system which allows them to quickly build and modify icons stored in Object File Format (OFF). We present the program NPSICON to meet this need and also discuss some of the issues involved in building 3D icons. NPSICON runs on commercially available Silicon Graphics, Inc. IRIS workstations. GRA

N92-26196# Air Force Academy, CO.
TESTBANK (1.0) USER'S MANUAL Final Report
Steven M. Hadfield Jun. 1991 33 p
(AD-A245895; USAFA-TR-91-18) Avail: NTIS HC/MF A03

This document describes the Testbank program, which is designed to enhance the reliability and efficiency of test development. Testbank accomplishes this goal by maintaining a data base of test items together with reference data for each time the item has been used. A test developer can then query the test database for items that satisfy any number of query parameters. A full range of test editing functions are available to modify and revise the test. Upon completion of a test, the Testbank software will create a ChiWriter document of the test. In order to enhance the reliability of the produced test, the Testbank software will use the reference data from the included items to predict the mean and standard deviation for the produced test. GRA

N92-26197*# Research Inst. for Computing and Information Systems, Houston, TX.
EXTRACTING FUZZY RULES UNDER UNCERTAINTY AND MEASURING DEFINABILITY USING ROUGH SETS Technical Report
Donald E. Culas (Houston Univ., Clear Lake, TX.) 9 Dec. 1991 66 p
(Contract NCC9-16; RICIS Proj. SR-01)
(NASA-CR-190396; NAS 1.26:190396) Avail: NTIS HC/MF A04

Although computers have come a long way since their invention, they are basically able to handle only crisp values at the hardware level. Unfortunately, the world we live in consists of problems which fail to fall into this category, i.e., uncertainty is all too common. A problem is looked at which involves uncertainty. To be specific, attributes are dealt with which are fuzzy sets. Under this condition, knowledge is acquired by looking at examples. In each example, a condition as well as a decision is made available. Based on the examples given, two sets of rules are extracted, certain and possible. Furthermore, measures are constructed of how much these rules are believed in, and finally, the decisions are defined as a function of the terms used in the conditions. Author

N92-26198*# Research Inst. for Computing and Information Systems, Houston, TX.
MEASURING UNCERTAINTY BY EXTRACTING FUZZY RULES USING ROUGH SETS Technical Report
Jeffrey A. Worm (Houston Univ., Clear Lake, TX.) 9 Dec. 1991 76 p
(Contract NCC9-16; RICIS Proj. SR-01)
(NASA-CR-190395; NAS 1.26:190395) Avail: NTIS HC/MF A05

Despite the advancements in the computer industry in the past 30 years, there is still one major deficiency. Computers are not designed to handle terms where uncertainty is present. To deal with uncertainty, techniques other than classical logic must be developed. The methods are examined of statistical analysis, the Dempster-Shafer theory, rough set theory, and fuzzy set theory to solve this problem. The fundamentals of these theories are combined to possibly provide the optimal solution. By incorporating principles from these theories, a decision making process may be simulated by extracting two sets of fuzzy rules: certain rules and possible rules. From these rules a corresponding measure of how much these rules is believed is constructed. From this, the idea of how much a fuzzy diagnosis is definable in terms of a set of fuzzy attributes is studied. Author

N92-26233# Lawrence Livermore National Lab., CA.
IMPLEMENTING ERROR VALUES IN APPLICATIVE LANGUAGES
P. J. Miller Mar. 1991 15 p Presented at the Conference on Functional Programming Languages and Computer Architecture, Cambridge, MA, 28-30 Aug. 1991
(Contract W-7405-eng-48)
(DE92-008927; UCRL-JC-106539; CONF-9108202-1) Avail: NTIS HC/MF A03

Not unlike procedural languages, functional and applicative languages must address exception and error handling issues. Since functional languages do not have global state, other means are needed to identify erroneous and exceptional information. Some functional and applicative languages, like FP, VAL, and SISAL signal errors through the use of error values that propagate through a computation. Tracking the errors is very important if a result is to be meaningful. Writing large, useful programs that will never produce error values is very difficult. Unfortunately, the richer the error semantics of a language, the more time consuming its implementation becomes. This time is consumed by physically checking an operation's input data for error values and from other, secondary effects on the architecture. One solution to this problem is to divide an execution into two states. In the first state, it can be asserted that no errors have been produced and so operations do not need to check for errors. In the second, SHADOW state, an error is possible, and operations must check inputs for error values. A computation's inputs are pre-checked for error values to validate the first assertion. After an operation produces an error (from error free input), the computation must transition to the SHADOW state where subsequent operations check for input errors. If errors are rare, a computation will spend most of its time in the faster initial state. This allows a programmer to take advantage of a language's error semantics without paying any penalty. DOE

N92-26248# Naval Postgraduate School, Monterey, CA.
VHDL BEHAVIORAL DESCRIPTION OF DISCRETE COSINE TRANSFORM IN IMAGE COMPRESSION M.S. Thesis
An-Te Deng Sep. 1991 139 p
(AD-A245389) Avail: NTIS HC/MF A07

This thesis describes a VHSIC Hardware Description Language (VHDL) simulation of hardware 8 x 8 Discrete Cosine Transform (DCT) which can be applied to image compression. A top-down design approach is taken in the study, a discussion of DCT theory is presented, along with a description of the 1-D DCT circuit architecture and its simulation in VHDL. Results of the 2-D DCT simulation are included for two simple test patterns and verified by hand calculation, demonstrating the validity of the simulation. Shortcomings found in the simulation are described, together with suggestions for correcting them. In the future, the VHDL description of the 8 x 8 image block 2-D DCT can be further developed into structural and gate-level description, after which hardware circuit implementation can occur. GRA

N92-26273# Institute for Defense Analyses, Alexandria, VA.
ASSESSMENTS OF SELECTED REAL-TIME COMPUTING TECHNOLOGIES Final Report
Karen D. Gordon and Kevin J. Rappoport Jul. 1991 112 p
(Contract MDA903-89-C-0003)
(AD-A245434; AD-E501456; IDA-P-2422; IDA/HQ-90-035650)
Avail: NTIS HC/MF A06

Developing dependable software for large, complex, real time systems is one of the major challenges now facing the software industry. The software R and D community is responding to this challenge; numerous efforts have been initiated on various aspects of real time software development. In this paper, we review and evaluate ongoing R and D efforts in light of the needs of strategic defense systems. We identify and discuss four recent developments that hold promise for facilitating the design and implementation of real time software for strategic defense systems: (1) rate monotonic scheduling theory; (2) real time extensions to the IEEE Portable Operating System Interface for Computer Environments (POSIX); (3) several distributed real time operating system prototypes; and (4) various methods for enhancing real time system robustness by trading precision of results for timeliness of results. We also point out an area of major concern to real time software developers and, in particular, to the SDIO: the lack of analytical methods for evaluating the performance of complex real time systems. A series of recommendations are made on how the SDIO should follow up on the real time R&D topics covered. GRA

N92-26276# Institute for Defense Analyses, Alexandria, VA.
SOFTWARE MATURITY MODEL APPLIED TO SDI Final Report
Beth Springsteen Sep. 1991 69 p
(Contract MDA903-89-C-0003)
(AD-A245439; AD-E501471; IDA-D-1042; IDA/HQ-91-40280)
Avail: NTIS HC/MF A04

The Strategic Defense Initiative Organization (SDIO) is undertaking initiatives to mitigate software risks and to stimulate the DoD contractor community to improve its software practices. To that end, IDA assessed the Software Engineering Institute's (SEI) software process maturity model and developed an implementation plan for its use within the SDI program. Under this plan, SDI element programs will use the SEI method to select software contractors with mature practices and to monitor contracts after they have been awarded. This document describes the SEI maturity model and the experience of contractors and government agencies. It also explains SDIO's plans to implement the model program-wide and the benefits and lessons learned from using the model on two contracts. GRA

N92-26292# Communications Research Centre, Ottawa (Ontario).
AN ADAPTIVE, PACKET-SWITCHED HF DATA TERMINAL: FUNCTIONAL OVERVIEW AND INITIAL PERFORMANCE
Gerard R. Nourry Jul. 1991 47 p
(AD-A246318; CRC-TR-1423) Avail: NTIS HC/MF A03

This report describes the first-prototype version of an automatic, adaptive HF data terminal developed from 1983-1986. The terminal's main forms of adaptivity include a real-time channel evaluation and channel selection mechanism, an adaptive link protocol for channel optimization, and a fully distributed and adaptive routing algorithm for the selection of routes in an HF network. The terminal design is characterized by a suite of robust, low-overhead, adaptive protocols that work in low-bandwidth, error-prone, and time-variant environments. The terminal's performance is illustrated with results from tests over short and long HF links carried out in fall of 1984 and winter of 1985-86. GRA

N92-26370# National Inst. of Standards and Technology, Gaithersburg, MD.
REFERENCE MODEL FOR FRAMEWORKS OF SOFTWARE ENGINEERING ENVIRONMENTS
Dec. 1991 108 p
(PB92-158328; NIST/SP-500/201; ECMA-TR/55-ed-2) Avail: NTIS HC/MF A06

The document describes a Reference Model (RM) for Software Engineering Environment (SEE) Frameworks. A SEE deals with information about: (1) the software under development (e.g., specifications, design data, source code, test data, project plans); and (2) project resources (e.g., costs, computer resources, and policy, standards and guidelines on the production of software). A SEE frameworks reference model is a conceptual basis for describing existing SEEs using the common reference terms and structures provided by the RM and to provide a basis for determining interfaces between environment components in order to create consistent interface standards. GRA

N92-26384# Carnegie-Mellon Univ., Pittsburgh, PA. Robotics Inst.
SHAPE FROM PERIODIC TEXTURE USING THE SPECTROGRAM
John Krumm and Steven A. Shafer Nov. 1991 26 p
(Contract F33615-90-C-1465)
(AD-A245855; CMU-RI-TR-91-29) Avail: NTIS HC/MF A03

Texture has long been recognized in computer vision as an important monocular shape cue, with texture gradients yielding information on surface orientation. A more recent trend is the analysis of images in terms of local spatial frequencies, where each pixel has associated with its own spatial frequency distribution. This has proven to be a successful method of reasoning about and exploiting many imaging phenomena. Thinking about both shape from texture and local spatial frequency, it seems that texture gradients would cause systematic changes in local frequency, and that these changes could be analyzed to extract shape information. However, there does not yet exist a theory that connects texture, shape, and the detailed behavior of local spatial frequency. We show how local spatial frequency is related to the surface normal of a textured surface. We find that the Fourier power spectra of any two similarly textured patches on a plane are approximately related to each other by an affine transformation. The transformation parameters are a function of the plane's surface normal. We use this relationship as the basis of a new algorithm for finding surface normals of textured shapes using the spectrogram, which is one type of local spatial frequency representation. We validate the relationship by testing the algorithm on real textures. GRA

N92-26400# Naval Postgraduate School, Monterey, CA.
INVESTIGATING THE UTILITY OF COUPLING COCOMO WITH A SYSTEM DYNAMICS SIMULATION OF SOFTWARE DEVELOPMENT M.S. Thesis
Richard W. Smith Sep. 1991 174 p
(AD-A245484) Avail: NTIS HC/MF A08

Cost estimation of software, in this era of budgetary constraints, is vitally important to the success or failure of a software project. Although there are many cost estimation models available, cost overruns and late deliveries still persist. Coupling the Constructive Cost Model (COCOMO) and the System Dynamics Model of Software Project Management can provide a tool to study project management over the life of a project, to use sensitivity analysis to enhance COCOMO's cost driver set, and to utilize an automated optimization system for software cost estimation in a single or multi-project environment. This new type of model creates a means to study the multi-project environment and determine what the advantages and disadvantages are to sharing resources between different software projects. Several 'C' programs were developed, that when interfaced and coupled with the system dynamic model, provide a tool to optimize cost estimates in a two project environment. It also creates an environment to perform extensive sensitivity analysis for the enhancement of COCOMO's cost driver set in the single and two project environment. GRA

N92-26418# Naval Postgraduate School, Monterey, CA.
A FREQUENCY DOMAIN BASED APPROACH TO ON-LINE SYSTEM IDENTIFICATION M.S. Thesis
Chi-Shun Chao Jun. 1991 74 p
(AD-A246193) Avail: NTIS HC/MF A04

This thesis addresses the problem of identifying the dynamics of a linear system in the frequency domain. An algorithm operating on the Fast Fourier Transform (FFT) of blocks of signals is developed and its performance evaluated through computer simulation. Several properties are tested, in particular, its convergence and its capabilities of identifying the frequency response of the unknown system. GRA

N92-26421 Politecnico di Milano (Italy). Dipartimento di Elettronica.
THE SOL OBJECT-ORIENTED DATABASE LANGUAGE
R. Zicari, F. Cacace, C. Capelli, A. Galipo, A. Pirovano, A. Romboli, and G. Lamperti (TXT Ingegneria Informatica S.p.A., Milan, Italy) Nov. 1991 30 p Sponsored by Commission of the European Communities
(Rept-91-053; ETN-92-91250) Avail: Politecnico di Milano, Piazza Leonardo da Vinci 32, 20133 Milan, Italy

SOL (Stretch Object oriented data base Language), a language for databases with tuples, sets, lists, object identity, and multiple inheritance, is presented. Other features of SOL are: the existence of a generic type which allows the definition of the schema by stepwise refinements, and the use of null values to express incomplete information in objects. A uniform way of coding both methods and programs is provided through an algebra for objects. The algebra is used both for querying and updating a SOL database. ESA

N92-26448 Politecnico di Milano (Italy). Dipartimento di Elettronica.
PROVING PROPERTIES OF REAL-TIME SYSTEMS THROUGH LOGICAL SPECIFICATIONS AND PETRI NET MODELS
Miguel Felder, Dino Mandrioli, and Angelo Morzenti 1991 71 p Sponsored in part by CNR and Commission of the European

Communities
(Rept-91-072; ETN-92-91359) Avail: Politecnico di Milano, Piazza Leonardo da Vinci 32, 20133 Milan, Italy

The formal analysis of the properties of real-time systems is discussed. A method that allows specification of system properties in the TRIO language and modeling of the system as a timed Petri net is proposed. Such an approach is more general than analyzing program properties. The proof method is based on an axiomatization of timed Petri nets in terms of TRIO so that their properties can be derived as suitable theorems in much the same spirit as classical Hoare's method allows proving of properties of programs coded in a Pascal-like language. The method is exemplified through an elevator system and the dining philosophers problem. A review of the related literature and a comparison thereof with the new method is also provided. Possible alternative methods, theoretical extensions, and practical applications are considered. ESA

N92-26449 Politecnico di Milano (Italy). Dipartimento di Elettronica.
A RANDOM POLYNOMIAL ALGORITHM FOR THE MATROID PARITY BASE PROBLEM
Luca Breveglieri 10 Dec. 1991 21 p
(Rept-91-079; ETN-92-91360) Avail: Politecnico di Milano, Piazza Leonardo da Vinci 32, 20133 Milan, Italy

A random algorithm with a polynomial complexity for the computation of the base of a linearly represented matroid of maximal rank with parity constraints is presented. This algorithm is a modification of the random NC algorithm for the computation of the perfect matching of a graph that admits one, and of the deterministic polynomial algorithm for the linear matroid parity problem. It is shown that the base of the matroid is computable with a polynomially bounded number of processors and in a polynomially bounded time. It yields a polynomial time computational complexity if the algorithm is to be run serially on a single processor. The case of linear weighted matroids with parity constraints is analyzed and solved. ESA

N92-26450 National Physical Lab., Teddington (England). Div. of Information Technology and Computing.
IMPROVING CMM SOFTWARE QUALITY
M. G. Cox Jan. 1992 13 p
(NPL-DITC-194/92; ISSN-0262-5369; ETN-92-91372) Copyright Avail: National Physical Lab., Teddington, Middlesex, TW11 0LW, England

Methodologies for CMM (Coordinated Measuring Machines) software conformance testing are enumerated and one in particular, the use of reference data sets, or soft gauges, is addressed. The advantages of such an evaluation mechanism are identified and discussed. Progress on a draft standard concerned with the use of reference data sets for conformance testing of CMM software and preliminary work on a method of operation of a third parity CMM software conformance testing service are described. Related activity which includes work on reference software for CMMs, European CMM software intercomparisons and further relevant standardization, is reported. The importance of software traceability is emphasized. ESA

N92-26458# Naval Postgraduate School, Monterey, CA.
NAVAL POSTGRADUATE SCHOOL AIRCRAFT SYNTHESIS PROGRAM (USER'S MANUAL) M.S. Thesis
John T. Parker Sep. 1991 301 p
(AD-A246198) Avail: NTIS HC/MF A14

A menu driven computer program has been developed to serve as a user's interface with ACSYNT, the NASA-AMES program for aircraft synthesis. The interface program, CREATE, drastically reduces the amount of time required to learn how to use ACSYNT, thus, allowing the power of ACSYNT to be used more effectively by the aircraft design curriculum at the Naval Postgraduate School. CREATE has been developed to reduce the required number of inputs to ACSYNT and is ideal for use with the early phases of the Aeronautical Engineering Curriculum. It can provide rapid feedback when examining the effects that different aircraft parameters have on the overall aircraft performance, thus, enhancing the students understanding of the relationships between the numerous variables of aircraft studies. Included in the thesis are four examples that demonstrate some of the capabilities of ACSYNT and the use of CREATE. GRA

N92-26461# Naval Postgraduate School, Monterey, CA.
AN EMPIRICAL APPROACH TO ANALYSIS OF SIMILARITIES BETWEEN SOFTWARE FAILURE REGIONS M.S. Thesis
Lelon L. Ginn Sep. 1991 154 p
(AD-A246208) Avail: NTIS HC/MF A08

Previous authors have postulated that faults are related to each other and testers have tried to exploit the effect. However, the evidence and applications have been largely anecdotal. This thesis uses an analytical derivation of software failure regions to develop a quantitative metric of the relationship of one fault to another. This metric is then applied in an empirical study of a population of failure regions derived from faults used in a previous experiment. The failure regions were analyzed for clustering behavior using graph theory techniques. The goal of this study is to be able to use information about known faults in a program as a means of finding other faults in the same program. This study provides strong evidence that failure regions have a tendency to form clusters. Further, two specific characteristics of failure regions that lead to cluster formation are identified: shared bounding conditions (the identical dimension) and shared variables that appear in different contexts (the coincidental dimension). The nature of the clusters formed by these two dimensions are markedly different. The identical dimension clusters are small, isolated, and strongly connected. The coincidental dimension clusters are larger and more loosely connected. Software testing implications of failure region clustering behavior are discussed. GRA

N92-26464# Institute for Naval Oceanography, Bay Saint Louis, MS.
SOFTWARE REQUIREMENTS DOCUMENT FOR THE NETCDF INTERFACE WITHIN ECMOP, VERSION 1.0
Louise Perkins and Wen Qian Oct. 1991 71 p
(NR Proj. R10-300)
(AD-A246220; AD-E040179; INO-TM-3) Avail: NTIS HC/MF A04

This document presents the software requirements for the Network Common Data Format (netCDF) interfaces that are being used to modularize the Experimental Center for Mesoscale Ocean Prediction (ECMOP) being built at the Institute for Naval Oceanography (INO). ECMOP is currently under development. It has been designed to be a bread-board test bed for ocean model evaluation and comparisons. GRA

N92-26468# Naval Postgraduate School, Monterey, CA.
PERFORMANCE ANALYSIS OF IMAGE MOTION ANALYSIS ALGORITHMS M.S. Thesis
Ibrahim Aksu Jun. 1991 81 p
(AD-A246522) Avail: NTIS HC/MF A05

Computer simulation studies of image motion analysis algorithms are presented. The algorithms are the extended Kalman filter algorithm, linear feature-based algorithms (perspective and orthogonal), and the accumulative differencing algorithm. The simulation studies both using computer generated and real images are conducted to determine the performance of the algorithms on low signal to noise ratio images. Using the results of simulation studies, a comparison of the performance of image motion analysis algorithms is performed. GRA

N92-26479 California Univ., San Francisco.
INTEGRATING REVERSE ENGINEERING INTO COMPUTER-AIDED SOFTWARE ENGINEERING (CASE) Ph.D. Thesis
Thaddeus W. Usowicz 1991 214 p
Avail: Univ. Microfilms Order No. DA9202461

A framework for the integration of reverse engineering of software systems into computer aided software engineering (CASE) tools was developed and applied to C source code. The process

of coding a system conceals design information useful for system and code change and upgrading as the system evolves during the operation and maintenance phase of its life cycle. The design recovery framework emphasizes the identification of: module dependencies; visibility of information exchanged between modules, specifically, what data is exchanged and in which direction; visibility of information among modules through the global data area; and appropriate module assignments to subhierarchies in a structure chart. A software tool for reverse engineering code to structure charts (RESC) is developed to show the framework. The RESC system uses heuristic rules to ensure repeatability, consistency, and correctness. The RESC system requirements are specified for several steps. A final program is specified to take the detailed files provided and create a structure chart description file which can be imported directly into an existing CASE tool which has graphic display, editing, and analyses capabilities. Dissert. Abstr.

N92-26500# Helsinki Univ. of Technology, Espoo (Finland). Digital Systems Lab.
AUTOMATED INTERPRETATION OF S-INVARIANTS OF PREDICATE/TRANSITION NETS: AN APPLICATION OF NON-CLASSICAL LOGICS
A. Moslemie Oct. 1991 37 p
(PB92-143544; ISBN-951-22-0814-8; SER-A-15) Avail: NTIS HC/MF A03

As an application of nonclassical logics, the interpretation of S-invariants of predicate/transition nets is automated. The intention is to provide system designers with facilities for interpreting these invariants automatically. The idea is to prove compound logical consequences of two finite sets of premises derived from a given predicate/transition net model: a set of global premises consisting of formulae constructed from the S-invariants of the net and axioms of an equality theory associated with the net, and a set of local premises consisting of formulae representing the initial marking of the net. Construction of these premises is performed in three main steps. In the first step, two algorithms for performing the transformations from two disjoint classes of S-invariants of the net into the formulae of first order modal logic are given. A finite axiomatization of a suitable equality theory associated with the net and, a set of literals representing the initial marking of the net are given in the second and third steps, respectively. A simplified proof method obtained by performing a number of simplifications to a more general already existing method is given. It is employed for proving compound logical consequences of these two sets of premises within an adequate calculus of first order modal logic. A theorem stating the unprovability of formulae expressing progress properties and two representative examples illustrating the discussion for both classes of S-invariants are presented. GRA

N92-26524# Massachusetts Inst. of Tech., Cambridge.
ALGORITHMS FOR BLENDING SURFACE GENERATION M.S. Thesis
Peter C. Filkins Jun. 1991 126 p
(Contract N00123-89-G-0580)
(AD-A245686) Avail: NTIS HC/MF A07

This thesis presents a general algorithm for the representation and approximation of blending surfaces between two non-uniform rational B-spline (NURBS) surfaces using surfaces of the same class. The algorithm permits the approximation of blending surfaces with up to curvature continuous boundary conditions along the intersection of the blending surface with the primary surfaces to be joined. These intersections are called the linkage curves. The blending surfaces are approximated by low degree Beta-spline surfaces, created using a lofting method. Isoparameter curves of the approximating blending surface are constructed based on differential geometry properties of the underlying surfaces. First derivative properties are required to satisfy tangent plane continuity boundary conditions. To satisfy curvature continuity conditions, the cross-link curves are constructed to match the curvature of a normal section of the underlying surface at the end point of the cross-link curves on the linkage curves. An adaptive sampling procedure is used to improve the approximation. Finally, the algorithm is applied to the practical problem of designing a fillet for the intersection of a marine propeller blade with a hub. An adaptation of the method which creates a standard marine propeller fillet automatically is also presented. GRA

N92-26529# Naval Research Lab., Washington, DC.
A COMPUTER PROGRAM FOR THE CALCULATION OF DAUBECHIES WAVELETS Report, May - Oct. 1990
David M. Drumheller 22 Jan. 1992 25 p
(AD-A245461; NRL-MR-6923) Avail: NTIS HC/MF A03

Recently, it has been found that the set of all square summable functions can be represented as a countable sum of time local functions called wavelets. A particular class of functions, Daubechies wavelets, are truly time local. They have compact support on the real line. This report presents and documents a FORTRAN program that calculates Daubechies wavelets. GRA

N92-26530# Naval Surface Warfare Center, Dahlgren, VA.
STATLIB/PC USERS GUIDE Final Report
Gary Johnson Nov. 1991 34 p
(AD-A245462; NAVSWC-TR-91-549) Avail: NTIS HC/MF A03

STATLIB/PC Users Guide is an addendum to STATLIB:NSWC Library of Statistical Programs and Subroutines (NSWC TR 89-97). STATLIB/PC is composed of 34 programs for statistical data analysis and probability evaluation and 24 subroutines for random number generation. This document is intended to aid Center scientists and engineers in applying STATLIB software on the IBM PC. GRA

N92-26587*# Texas A&M Univ., College Station. Dept. of Industrial Engineering.
[RESEARCH ACCOMPLISHED AT THE KNOWLEDGE BASED SYSTEMS LAB: IDEF3, VERSION 1.0]
Richard J. Mayer, Christopher P. Menzel, and Paula S. D. Mayer Jan. 1991 56 p Sponsored by NASA
(NASA-CR-190279; NAS 1.26:190279) Avail: NTIS HC/MF A04

An overview is presented of the foundations and content of the evolving IDEF3 process flow and object state description capture method. This method is currently in beta test. Ongoing efforts in the formulation of formal semantics models for descriptions captured in the outlined form and in the actual application of this method can be expected to cause an evolution in the method language. A language is described for the representation of process and object state centered system description. IDEF3 is a scenario driven process flow modeling methodology created specifically for these types of descriptive activities. Author

N92-26647# Lawrence Livermore National Lab., CA.
SCIENTIFIC DOCUMENTARY ANIMATION: HOW MUCH ACCURACY IS ENOUGH?
N. L. Max Feb. 1992 17 p Proposed for presentation at the Computer Graphics International 1992, Tokyo, Japan, 22-26 Jun. 1992
(Contract W-7405-eng-48)
(DE92-009698; UCRL-JC-109767; CONF-9206136-1) Avail: NTIS HC/MF A03

Scientific documentary animation presents final results, and thus has a somewhat different purpose than the scientific visualization used in their discovery. For an audience of non-specialists, production quality in the graphics, pacing, narration, music, and story-telling are important. However, the animation need only be qualitatively correct in order to communicate the desired information. When physical simulations are used to produce animated movement, the laws of motion can be adjusted to give a nicer appearance, to allow for easier programming, to compensate for incompatible time or size scales, or to artifically push things in a desired direction. Graphic tricks may even be used to disguise inadequacies in the simulation. Biological structures which are not yet completely understood may be given an arbitrary or approximate form in order to show their function. But in illustrating mathematics, it is often easy to be completely accurate. DOE

N92-26658# Naval Postgraduate School, Monterey, CA.
ITERATIVE SYSTEM MODELING USING MULTIGRID TECHNIQUES M.S. Thesis
Dean A. Richter Dec. 1991 134 p
(AD-A245522) Avail: NTIS HC/MF A07

One and two-dimensional system identification and modeling algorithms utilizing multigrid techniques are presented. Finite impulse response (FIR), autoregressive (AR), infinite impulse response (IIR), and 2-D block matrix iterative system modeling algorithms are enhanced and made more efficient using the multigrid methods. The convergence performance of these algorithms is improved with the multigrid techniques. The reduction in the number of iterations required to converge to a solution is realized by forcing the low frequency error components to appear to be at a higher frequency by transferring to a coarser sampling period. Performance comparisons are presented for FIR, AR, IIR, and 2-D block matrix modeling simulations with and without the multigrid-techniques employed. GRA

N92-26685# Massachusetts Univ., Amherst. Dept. of Computer and Information Science.
THE 8TH IEEE WORKSHOP ON REAL-TIME OPERATING SYSTEMS Final Report, 1 Nov. 1990 - 30 Jan. 1991
Krithi Ramamritham Jan. 1992 209 p Workshop held in Atlanta, GA, 15-17 May 1991
(Contract N00014-91-J-1369)
(AD-A246126) Avail: NTIS HC/MF A10

This workshop was held May 15-17, 1991 in Atlanta, Georgia. It was the eighth in a continuing series of workshops on real-time operating systems and software and was held in conjunction with the 17th IFAC/IFIP Workshop on Realtime Programming. The workshop was co-sponsored by the IEEE Computer Society Technical Committee on Real-Time Systems and the Office of Naval Research and its goals were: to investigate advances in real-time operating systems, software, and programming languages; to promote interaction among researchers and practitioners; to evaluate the maturity and evolutionary directions of realtime programming theories and approaches. This report contains the proceedings of the workshop as well as the Final Report to IEEE, the IFAC/IFIP Final Report, and additional budgetary information provided to the Office of Naval Research. GRA

N92-26696# Sandia National Labs., Albuquerque, NM.
EXPERIENCES IN USING C++ TO DEVELOP A NEXT GENERATION STRONG SHOCK WAVE PHYSICS CODE
J. S. Peery and K. G. Budge 1992 8 p Presented at the American Society of Civil Engineers (ASCE) Conference, Dallas, TX, 7-9 Jun. 1992
(Contract DE-AC04-76DP-00789)
(DE92-006675; SAND-92-0033C; CONF-9206101-1) Avail: NTIS HC/MF A02

The goals and time constraints of developing the next generation shock code, RHALE++, for the Computational Dynamics and Adaptive Structures Department at Sandia National Laboratories have forced the development team to closely examine their program development environment. After a thorough investigation of possible programming languages, the development team has switched from a FORTRAN programming environment to C++. This decision is based on the flexibility, strong type checking, and object oriented features of the C++ programming language. RHALE++ is a three dimensional, multi-material, arbitrary Lagrangian Eulerian hydrocode. Currently, RHALE++ is being developed for von Neumann, vector, and MIMD/SIMD computer architectures. Using the object oriented features of C++ facilitates development on these different computer architectures since architecture dependences such as inter processor communication, can be hidden in base classes. However, the object oriented features of the language can create significant losses in efficiency and memory utilization. Techniques, such as reference counting, have been developed to address efficiency problems that are inherent in the language. Presently, there has been very little efficiency loss realized on SUN scalar and nCUBE massively parallel computers; however, although some vectorization has been accomplished on CRAY systems, significant efficiency losses exist. This paper presents the current status of using C++ as the development language for RHALE++ and the efficiency that has been realized on SUN, CRAY, and nCUBE systems. DOE

N92-26758# Naval Postgraduate School, Monterey, CA.
IMPLEMENTATION OF MULTI-FREQUENCY MODULATION WITH TRELLIS ENCODING AND VITERBI DECODING USING A DIGITAL SIGNAL PROCESSING BOARD M.S. Thesis
John W. Wisniewski Jun. 1991 95 p
(AD-A245998) Avail: NTIS HC/MF A05

Multi-Frequency Modulation has been the topic of several papers at NPS. In past systems the majority of time required for the generation of the MFM signal was due to the software routine used to implement the FFT. In this report a Digital Signal Processor was used to reduce the time needed to generate the FFT. The use of Trellis coding and Viterbi decoding on a Digital Signal Processor was also investigated. Assembly language programs for three encoder/decoder systems were developed. The first uses a 16 QAM signal, the second uses a 2/3 rate convolutional encoder and Viterbi decoder, and the third uses the V.32 convolutional encoder and a Viterbi decoder. GRA

N92-26766# Naval Research Lab., Washington, DC.
EVALUATION CRITERIA FOR REAL-TIME SPECIFICATION LANGUAGES Final Report
Paul C. Clements, Carolyn E. Gasarch, and Ralph D. Jeffords (Locus, Inc., Alexandria, VA.) 11 Feb. 1992 27 p Prepared in cooperation with Texas Univ., Austin
(AD-A246612; NRL-MR-6935) Avail: NTIS HC/MF A03

We develop a set of general evaluation criteria for (formal and informal) real-time specification languages. These criteria cover important properties of a specification (applicability to real-time systems, completeness, etc.) as well as techniques for analyzing those properties (verification traceability, etc.). These general criteria are intended as a guide to development of more specific criteria during actual evaluations of languages. GRA

N92-26797# Lawrence Livermore National Lab., CA.
FORGING A PATH WITH TOOL AND DATA ATTRIBUTES Ph.D. Thesis
T. A. Longstaff Jun. 1991 129 p
(Contract W-7405-eng-48)
(DE92-009800; UCRL-LR-108508) Avail: NTIS HC/MF A07

This thesis describes the path forger model and implementation, designed to organize a variety of reformatting and filter tools into a directed graph of possibilities (the tool grid), which is used to generate sequences of operations named tool paths. When numerous tool paths are available to perform a single task, the model uses attributes of the defined data and tools to select the path most likely to satisfy the user's restriction on the possible values of these attributes. Unlike many constraint-based systems, the use of attribute restrictions will not modify the instantiated or propagated attribute values, but uses inconsistencies between the attribute values, and restrictions placed on these values are used to determine if a tool path will satisfy the needs of the user expressed in terms of restrictions placed on the possible values of the desired attributes. The model uses an object-oriented paradigm for the definition of each data and tool object described herein. As an example of the usefulness of the model, it is applied to two application domains: simulation post-processing and audit-log analysis. Included is a detailed description of the path forger model and the issues and limitations involved in an implementation of the model. DOE

N92-26835# Gosudarstvennyi Komitet po Ispolzovaniyu Atomnoi Energii, Serpukhov (USSR). Inst. Fiziki Vysokikh Ehnergij.
ON INCREASING THE CAPABILITIES OF THE SMART ADAPTIVE RANDOM NUMBER GENERATOR
V. A. Anikeeva and G. G. Takhtamyshev 1991 6 p In RUSSIAN; ENGLISH summary
(DE92-621106; IFVE-OMVT-91-12) Avail: NTIS HC/MF A02

The algorithm is proposed to achieve accelerated convergence

when calculating multiple integrals by the Monte Carlo method for the case of strong correlation. The algorithm is based on nonlinear coordinate system transformation similar to the rotation but the domain is left to be unitary hypercube. The examples show that the number of points to achieve the given precision becomes smaller by the factor of ten. DOE

N92-26840# Naval Postgraduate School, Monterey, CA.
THE FIDELITY ENHANCEMENT PROCESS M.S. Thesis
Charles A. Chase, VII Sep. 1991 82 p
(AD-A245388) Avail: NTIS HC/MF A05

This study addresses the issues concerning the upgrade and reuse of computer simulation models and presents a comprehensive methodology 'The Fidelity Enhancement Process' for conducting a model upgrade. Recent advances in software technology, specifically object-oriented programming and open architecture system development, have made this process feasible and provide unprecedented opportunities for model reuse. The Fidelity Enhancement Process was developed and applied to the Marine Corps Communication Architecture Analysis Model (MCCAAM) during its upgrade. MCCAAM simulates Marine Air Ground Task Force (MAGTF) single-channel communications architectures. MCCAAM was modified to evaluate architecture performance under different allocations of next-generation radios to units in the MAGTF, where the performance of an allocation was tactically driven. GRA

N92-26868* Georgia Univ., Athens. Computer Software Management and Information Center.
COSMIC SOFTWARE CATALOG, 1992 EDITION
1992 480 p
(NASA-CR-188973; NAS 1.26:188973) Avail: COSMIC, Athens, GA, 30602 $25.00

This publication contains descriptions of the software supplied by NASA's Computer Software Management and Information Center. Abstracts for over 1200 NASA sponsored computer programs are included. Author

N92-26904*# National Aeronautics and Space Administration. Goddard Space Flight Center, Greenbelt, MD.
SOFTWARE ARCHITECTURE FOR A DISTRIBUTED REAL-TIME SYSTEM IN Ada, WITH APPLICATION TO TELEROBOTICS
Douglas R. Olsen, Steve Messiora (Fairchild Space Co., Germantown, MD.), and Stephen Leake Jun. 1992 36 p
(NASA-TM-4367; Rept-92B00063; NAS 1.15:4367) Avail: NTIS HC/MF A03

The architecture structure and software design methodology presented is described in the context of telerobotic application in Ada, specifically the Engineering Test Bed (ETB), which was developed to support the Flight Telerobotic Servicer (FTS) Program at GSFC. However, the nature of the architecture is such that it has applications to any multiprocessor distributed real-time system. The ETB architecture, which is a derivation of the NASA/NBS Standard Reference Model (NASREM), defines a hierarchy for representing a telerobot system. Within this hierarchy, a module is a logical entity consisting of the software associated with a set of related hardware components in the robot system. A module is comprised of submodules, which are cyclically executing processes that each perform a specific set of functions. The submodules in a module can run on separate processors. The submodules in the system communicate via command/status (C/S) interface channels, which are used to send commands down and relay status back up the system hierarchy. Submodules also communicate via setpoint data links, which are used to transfer control data from one submodule to another. A submodule invokes submodule algorithms (SMA's) to perform algorithmic operations. Data that describe or models a physical component of the system are stored as objects in the World Model (WM). The WM is a system-wide distributed database that is accessible to submodules in all modules of the system for creating, reading, and writing objects. Author

N92-26949# Naval Postgraduate School, Monterey, CA. Dept. of Operations Research.
PROXIMAL MINIMIZATION ALGORITHMS WITH CUTTING PLANES
Siriphong Lawphongpanich Dec. 1991 44 p
(AD-A246436; NPS-OR-92-011) Avail: NTIS HC/MF A03

This paper examines a class of proximal minimization algorithms in which the objective function of the underlying convex program is approximated by cutting planes. This class includes algorithms such as cutting plane, cutting plane with line search and bundle methods. Among these algorithms, the bundle methods can be viewed as a quadratic counterpart of the cutting plane algorithm with line search, for they both attempt to decrease the true objective function at every iteration. On the other hand, the cutting plane algorithm does not explicitly and/or directly attempt to decrease the true objective function. However, it relies on the monotonicity of the approximating function to guarantee convergence to an optimal solution. This prompts the question of whether there exists a quadratic counterpart for the cutting plane algorithm. To provide an affirmative answer, this paper constructs a new convergent algorithm which resembles, but is different from, the bundle methods. Also, to make the relationship between bundle methods and proximal minimization more concrete, this paper also supplies a convergence proof for a variant of the bundle methods which utilizes analysis common to proximal minimization. GRA

N92-27052# Naval Postgraduate School, Monterey, CA.
AN Ada OBJECT ORIENTED MISSILE FLIGHT SIMULATION M.S. Thesis
John V. Waite Sep. 1991 194 p
(AD-A246378) Avail: NTIS HC/MF A09

This thesis uses the Ada programming language in the design and development of an air-tc-air missile flight simulation with object oriented techniques and sound software engineering principles. The simulation is designed to be more understandable, modifiable, efficient and reliable than earlier FORTRAN simulations. The principles of abstraction, information hiding, modularity, high cohesion and low coupling are used to achieve these goals. The resulting simulation is an accurate mapping of the problem space into software. The simulation is a three Degree-of-Freedom (3-DOF) model of RF-IR guided air-to-air missile. Two targets are also modeled. The simulation is primarily intended to study missile kinematics. GRA

N92-27053 Cornell Univ., Ithaca, NY.
ALGORITHMS FOR CAPACITY COMPUTATIONS AND ALGEBRAIC CASCADE CODING WITH APPLICATIONS TO DATA STORAGE Ph.D. Thesis
Rajeev Krishnamoorthy 1991 101 p
Avail: Univ. Microfilms Order No. DA9203948

The capacity of several types of peak and power-constrained channels, such as multilevel storage memory cells, runlength limited channels, and constrained photon detection channels, is achieved using a discrete input distribution. We consider the problem of multilevel storage cells, which we model as additive Gaussian channels with amplitude constrained inputs, and present an algorithm to compute to capacity of these channels, as well as the optimal input distribution which achieves the capacity. A simple modification of this algorithm allows the computation of the capacity of peak and power-constrained Gaussian channels. This method can be used as a general technique to determine the capacity of channels which have input signal sets with similar constraints. We consider the noisy run-length channel, one that is frequently used in magnetic recording, and extend the algorithm to determine the bounds to the capacity of this channel. As in the multilevel storage channel, we characterize the optimal (capacity achieving) input distribution and prove that the presented algorithm computes sequences of distributions that iteratively converge to the optimal result. Finally, we consider the problem of cascade codes which are constructed by using Reed-Solomon codes as both component and inner codes. These codes have large blocklengths, good distance/rate tradeoffs, and are easily encoded. We use spectral techniques to derive the constraint structure of cascaded

Reed-Solomon codes. A decoding algorithm is presented, and we describe the manner in which the decoding capability of this algorithm may be verified for specific codes. Dissert. Abstr.

N92-27073# Naval Postgraduate School, Monterey, CA.
NPSNET: HIERARCHICAL DATA STRUCTURES FOR REAL-TIME THREE-DIMENSIONAL VISUAL SIMULATION M.S. Thesis
Randall L. Mackey Sep. 1991 91 p
(AD-A246380) Avail: NTIS HC/MF A05

NPSNET is a low-cost visual simulation system designed and constructed at the Naval Postgraduate School. NPSNET uses digital terrain data and renders scenes involving vehicles, aircraft, cultural features, and natural features in real-time. The implementation of a terrain paging algorithm in NPSNET is discussed. Terrain paging expands the terrain area available for simulation and overcomes the limits of main memory size. Hierarchical data structures commonly used in visual simulation systems are surveyed. The generation of a multi-resolution terrain dataset and the implementation of a hierarchical data structure are explained. The multi-resolution dataset is created by generating lower resolution descriptions of polygons from the original data. The hierarchical data structure used in NPSNET, based on quadtrees, provides a means to attenuate the resolution of terrain over distance and cull those portions of terrain outside of the user's field of view. GRA

N92-27177# Unisys Corp., Reston, VA. Tactical Systems Div.
UT40 - ASSET LIBRARY OPEN ARCHITECTURE FRAMEWORK (ALOAF) Informal Technical Data
22 Nov. 1991 88 p
(Contract F19628-88-D-0031)
(AD-A247268; GR-7670-1317(NP); STARS-TC-04041/001/00)
Avail: NTIS HC/MF A05

The STARS (Software Technology for Adaptive, Reliable Systems) Asset Library Open Architecture Framework (ALOAF) addresses the exchange of reusable assets among diverse libraries, and the definition of an asset library platform upon which portable reuse tools may be constructed. Asset interchange and asset service interfaces are critical elements in achieving a broader objective-asset libraries which interoperate to such an extent that the boundaries between individual libraries become invisible to the end user. In general terms, this is the STARS vision of seamless library interoperation. As the STARS vision of seamless interoperation matures, the ALOAF will be updated and expanded to address additional, more advanced requirements. GRA

N92-26958# Fokker Space and Systems, Amsterdam (Netherlands).
FIESTA: AN INTEGRATED APPROACH TO THERMAL MODEL PROCESSING
J. P. A. deKoning and H. deWolf *In* ESA, 4th European Symposium on Space Environmental Control Systems, Volume 2 Dec. 1991 p 667-673 Sponsored by Netherlands Agency for Aerospace Programs (For primary document see N92-26950 17-54)
Avail: NTIS HC/MF A23; ESA, EPD, ESTEC, Noordwijk, Netherlands, HC 150 Dutch guilders (2 vols)

N92-26959# Bertin et Cie., Plaisir (France).
INTEGRATED COMMUNICATION ENVIRONMENT FOR THERMAL ANALYSIS SOFTWARE
P. Lecuyer, D. Neveu, G. Chenut, and C. Stroom (European Space Agency. European Space Research and Technology Center, ESTEC, Noordwijk, Netherlands) *In* ESA, 4th European Symposium on Space Environmental Control Systems, Volume 2 Dec. 1991 p 675-679 (For primary document see N92-26950 17-54)
Avail: NTIS HC/MF A23; ESA, EPD, ESTEC, Noordwijk, Netherlands, HC 150 Dutch guilders (2 vols)

N92-26960# Centre National d'Etudes Spatiales, Toulouse (France).
DEFINITION OF THE COMMON STRUCTURE OF DATA TO PROMOTE THE COMMUNICATION BETWEEN DIFFERENT THERMAL SOFTWARE TOOLS
Bruno Desaunettes and Christian Viguier *In* ESA, 4th European Symposium on Space Environmental Control Systems, Volume 2 Dec. 1991 p 681-686 (For primary document see N92-26950 17-54)
Avail: NTIS HC/MF A23; ESA, EPD, ESTEC, Noordwijk, Netherlands, HC 150 Dutch guilders (2 vols)

N92-26961# VEGA Space Systems Engineering Ltd., Harpenden (England).
GRABE: A SIMPLE GRAPHICAL BACK-END FOR THERMAL SIMULATION PACKAGES
A. N. Pidgeon, L. Dawson, R. A. D. Melvin, and C. Stroom (European Space Agency. European Space Research and Technology Center, ESTEC, Noordwijk, Netherlands) *In* ESA, 4th European Symposium on Space Environmental Control Systems, Volume 2 Dec. 1991 p 687-691 (For primary document see N92-26950 17-54)
Avail: NTIS HC/MF A23; ESA, EPD, ESTEC, Noordwijk, Netherlands, HC 150 Dutch guilders (2 vols)

N92-26963# Erno Raumfahrttechnik G.m.b.H. Bremen (Germany, F.R.).
A PROCESSING ENVIRONMENT FOR TEST AND SIMULATION DATA OF THERMODYNAMIC SYSTEMS
R. Mueller and G. Kleinert-Alvarado *In* ESA, 4th European Symposium on Space Environmental Control Systems, Volume 2 Dec. 1991 p 705-711 (For primary document see N92-26950 17-54)
Avail: NTIS HC/MF A23; ESA, EPD, ESTEC, Noordwijk, Netherlands, HC 150 Dutch guilders (2 vols)

62 COMPUTER SYSTEMS

Includes computer networks and special application computer systems.

N92-26199*# Research Inst. for Computing and Information Systems, Houston, TX.
DISTRIBUTED AND PARALLEL Ada AND THE Ada 9X RECOMMENDATIONS
Richard A. Volz, Stephen J. Goldsack, R. Theriault, Raymond S. Waldrop, and A. A. Holzbacher-Valero (Imperial Coll. of Science and Technology, London, England) Apr. 1992 28 p
(Contract NCC9-16; RICIS Proj. SE-35)
(NASA-CR-190392; NAS 1.26:190392) Avail: NTIS HC/MF A03

Recently, the DoD has sponsored work towards a new version of Ada, intended to support the construction of distributed systems. The revised version, often called Ada9x, will become the new standard sometimes in the 1990s. It is intended that Ada9x should provide language features giving limited support for distributed system construction. The requirements for such features are given. Many of the most advanced computer applications involve embedded systems that are comprised of parallel processors or networks of distributed computers. If Ada is to become the widely adopted language envisioned by many, it is essential that suitable compilers and tools be available to facilitate the creation of distributed and parallel Ada programs for these applications. The major languages issues impacting distributed and parallel programming are reviewed, and some principles upon which distributed/parallel language systems should be built are suggested. Based upon these, alternative language concepts for distributed/parallel programming are analyzed. Author

N92-26227# Naval Postgraduate School, Monterey, CA.
REQUIREMENTS ANALYSIS AND DESIGN FOR IMPLEMENTATION OF A SATELLITE LINK FOR A LOCAL

AREA COMPUTER NETWORK M.S. Thesis
Richard B. Lorentzen Sep. 1991 84 p
(AD-A245610) Avail: NTIS HC/MF A05

The purpose is to provide naval computer students with a basic knowledge on very small aperture terminal (VSAT) satellite technology and to define the hardware and software requirements at the interface between a VSAT and a local area network (LAN). By restricting a computer network to terrestrial links, a vast amount of knowledge is not accessed because either the terrestrial links can't access the information or the information service are only available via satellite. Existing satellite networks could fill this void. It is important for naval officers to understand the VSAT alternative to terrestrial networking. For the purpose of demonstration, a functional design will be presented for the VSAT linkage to an existing Naval Postgraduate School (NPS) Administrative Sciences (AS) Department Token-Ring LAN. This study will include a technological overview of a VSAT network, requirements analysis for establishing a VSAT link to a LAN, and the functional design of a VSAT link to the NPS AS Department Token-Ring LAN. GRA

N92-26277# Pacific Northwest Lab., Richland, WA.
MODELING NODE BANDWIDTH LIMITS AND THEIR EFFECTS ON VECTOR COMBINING ALGORITHMS
R. J. Littlefield 13 Jan. 1992 14 p
(Contract DE-AC06-76RL-01830)
(DE92-010829; PNL-SA-20425) Avail: NTIS HC/MF A03

Each node in a message-passing multicomputer typically has several communication links. However, the maximum aggregate communication speed of a node is often less than the sum of its individual link speeds. Such computers are called node bandwidth limited (NBL). The NBL constraint is important when choosing algorithms because it can change the relative performance of different algorithms that accomplish the same task. This paper introduces a model of communication performance for NBL computers and uses the model to analyze the overall performance of three algorithms for vector combining (global sum) on the Intel Touchstone DELTA computer. Each of the three algorithms is found to be at least 33 percent faster than the other two for some combinations of machine size and vector length. The NBL constraint is shown to significantly affect the conditions under which each algorithm is fastest. DOE

N92-26278# Cornell Univ., Ithaca, NY. Dept. of Computer Science.
PARALEX: AN ENVIRONMENT FOR PARALLEL PROGRAMMING IN DISTRIBUTED SYSTEMS Interim Report
Ozalp Babaoglu, Lorenzo Alvisi, Alessandro Amoroso, Renzo Davoli, and Luigi A. Giachini 7 Dec. 1991 21 p
(AD-A245445; TR-91-1250) Avail: NTIS HC/MF A03

Modern distributed systems consisting of powerful workstations and high speed interconnection networks are an economical alternative to special purpose super computers. The technical issues that need to be addressed in exploiting the parallelism inherent in a distributed system include heterogeneity, high latency communication, fault tolerance and dynamic load balancing. Current software systems for parallel programming provide little or no automatic support towards these issues and require users to be experts in fault tolerant distributed computing. The Paralex system is aimed at exploring the extent to which the parallel application programmer can be liberated from the complexities of distributed systems. Paralex is a complete programming environment and makes extensive use of graphics to define, edit, execute and debug parallel scientific applications. All of the necessary code for distributing the computation across a network and replicating it to achieve fault tolerance and dynamic load balancing is automatically generated by the system. In this paper we give an overview of Paralex and present our experiences with a prototype implementation. GRA

N92-26279# Cornell Univ., Ithaca, NY. Dept. of Computer Science.
RUN-TIME SUPPORT FOR DYNAMIC LOAD BALANCING AND DEBUGGING IN PARALEX Interim Report
Ozalp Babaoglu, Lorenzo Alvisi, Alessandro Amoroso, Renzo Davoli, and Luigi A. Giachini 7 Dec. 1991 14 p
(Contract N00014-91-J-1219)
(AD-A245446; TR-91-1251) Avail: NTIS HC/MF A03

Paralex is a programming environment for developing and executing parallel applications in distributed systems. The user is spared complexities of distributed programming including remote execution, data representation, communication, synchronization and fault tolerance as they are handled automatically by the system. Once an application starts execution in a distributed system it may be interacted with at two levels: by Paralex itself to achieve automatic fault tolerance and dynamic load balancing; or by the user in association with performance tuning and debugging. In this paper, we describe the set of monitors and control mechanisms that constitute the Paralex run-time system and their use for implementing dynamic load balancing and debugging. GRA

N92-26359# Washington Univ., Seattle. Lab. for Integrated Systems.
MESH AND TORUS CHAOTIC ROUTING (UPDATED VERSION)
Kevin Bolding and Lawrence Snyder 16 Jan. 1992 22 p
(Contract N00014-91-J-4041)
(AD-A246284; TR-91-04-04) Avail: NTIS HC/MF A03

The chaos router is an adaptive nonminimal message router for multicomputers that is simple enough to compete with the fast, oblivious routes now in use in commercial machines. It improves on previous adaptive routers by using randomization, which eliminates the need for complex livelock protection and speeds the router. The two-dimensional chaos router is shown to be theoretically sound and physically realizable. Extensive simulation studies compare chaos routing with oblivious and deflection routing in mesh and torus networks. Chaos routing is shown to be competitive for mesh networks and superior for torus networks. This high performance is perhaps unexpected for the mesh since there is no finite bound on the delivery time of any message. GRA

N92-26361# Naval Postgraduate School, Monterey, CA.
SELECTION AND SPECIFICATION OF A DATA LINK PROTOCOL FOR VSAT BASED INTER-LAN COMMUNICATIONS M.S. Thesis
Eugene S. Benvenutti, Jr. Sep. 1991 78 p
(AD-A246289) Avail: NTIS HC/MF A05

This thesis proposes an architecture for the development of inter-local area network communication across a VSAT network. The architecture of a VSAT node consists of the entities node, bridge, buffer, transmitter, receiver, and frame assembler/disassembler. Each of these entities contains a finite state machine, predicate/action tables, and local variables. A selective repeat, sliding window data link protocol for the very small aperture terminal architecture, the transmitter, and receiver is formally specified using the systems of communicating machines model. A partial analysis of the specified protocol is performed using reachability diagrams. GRA

N92-26417# Naval Postgraduate School, Monterey, CA.
DESIGN AND IMPLEMENTATION OF A TOOLBOX OF MODULARIZED C PROGRAMS TO CONSTRUCT, ANALYZE, AND TEST NETWORK OPTIMIZATION ALGORITHMS M.S. Thesis
Homero Fernandes Oliveira Sep. 1991 80 p
(AD-A246191) Avail: NTIS HC/MF A05

A portable computer system to construct, test, and analyze algorithms for large-scale network and graph problems was designed and partially implemented. The system provides an analyst with high-level easy-to-use constructs to specify network and graph algorithms. It produces efficient computer implementations of the algorithms, and constructs large scale unstructured and structured random network problems to test and

analyze the algorithms. The system is written in the computer language C and has been tested on personal computers and workstations. The present implementation includes algorithms for graph coloring, minimum spanning tree, and shortest path problems and some tools to analyze the results. GRA

N92-26430# Michigan State Univ., East Lansing. Dept. of Electrical Engineering and Systems Science.
THEORETICAL ISSUES IN ADAPTIVE SET-MEMBERSHIP-BASED SIGNAL PROCESSING. Progress Report, 1991
John R. Deller and Majid Nayeri 20 Jan. 1992 209 p
(Contract N00014-91-J-1329)
(AD-A245721) Avail: NTIS HC/MF A10

The general purpose of this research is the development and exploration of new set membership-based algorithms for adaptive identification of parametric signal and system models. We are pleased to report progress in several important aspects, both theoretical and applied, of this general scope. The report consists of several preprints of papers in review by respected journals, published and preprinted conference papers, and some other supporting material. A clear understanding of our progress is inherent in the discussion of each item in the following. These discussions are meant to illuminate the directions, rationale, and achievements of our research, with the technical details left to the papers. The items appearing in the following are grouped into papers written for journals, followed by conference papers, descriptions of dissertations in preparation, then documents showing further evidence of research progress. Within each group, the items appear in chronological order. GRA

N92-26501# National Inst. of Standards and Technology, Gaithersburg, MD. Technology Administration.
MASSIVELY PARALLEL IMPLEMENTATION OF CHARACTER RECOGNITION SYSTEMS
M. D. Garris, C. L. Wilson, J. L. Blue, G. T. Candela, and P. Grother Jan. 1992 16 p Presented at SPIE's Conference on Machine Vision Applications in Character Recognition and Industrial Inspection, San Jose, CA, 1992
(PB92-149863; NISTIR-4750) Avail: NTIS HC/MF A03

A massively parallel character recognition system was implemented. The system is designed to study the feasibility of the recognition of handprinted text in a loosely constrained environment. The system consists of eight functional components. The loading of the image into the system and storing the recognition results from the system are Input/Output components. In between are components responsible for image processing and recognition. The image processing necessary to load and isolate 34 fields on a scientific workstation takes 900 seconds. The same processing takes only 11 seconds using a massively parallel array processor. The image processing components, including the time to load the image data, use 94 percent of the system time. The segmentation time is 15 ms/character and segmentation accuracy is 89 percent for handprinted digits and alphas. Character recognition accuracy for medium quality machine print is 99.8 percent. On the handprinted digits, the recognition accuracy is 96 percent and recognition speeds of 10,100 character/second can be realized. The limiting factor in the recognition portion of the system is feature extraction, which occurs at 806 characters/second. Through the use of a massively parallel machine and neural recognition algorithms, significant improvements in both accuracy and speed were achieved. GRA

N92-26531# Naval Ocean Systems Center, San Diego, CA.
MATCHED FIELD PROCESSING ON THE CONNECTION MACHINE Final Report, Dec. 1988 - Jul. 1991
T. A. Adams Jul. 1991 40 p
(AD-A245469; NOSC-TR-1440) Avail: NTIS HC/MF A03

Matched field processing was implemented on the Thinking Machine Corporation's Connection Machine (model CM-2), which employs thousands of bit-serial processors. The potential of the CM-2 was not realized in this initial implementation because the programming style and language features used led to a large interprocessor communications burden. In subsequent efforts at developing signal processing on parallel processors, there should be additional emphasis on decomposing the overall processing into a relatively small set of building blocks that are of higher level than elementary arithmetic operations on scalars. GRA

N92-26596# Naval Postgraduate School, Monterey, CA.
THE MINIMIZATION OF MULTIPLE VALUED LOGIC EXPRESSIONS USING PARALLEL PROCESSORS M.S. Thesis
Sabri O. Oral Sep. 1991 125 p
(AD-A245763) Avail: NTIS HC/MF A06

The process of finding an exact minimization for a multiple-valued logic (MVL) expression requires an extensive search and enormous computation time. One of the heuristics to reduce this computation time is the Neighborhood Decoupling (ND) Algorithm by Yang and Wang. This algorithm finds near-optimal solutions for the given MVL expressions. The ND algorithm is an extension of Heuristic Analyzer for Multiple-valued Logic Expressions (HAMLET). The primary goal of this thesis is to reduce the computation time of the ND algorithm by using parallel processors. We developed a parallel version of the ND algorithm and tested it on an Intel Parallel Supercomputer (iPSC/2). The parallel version of the ND Algorithm actually executes in parallel a portion of the ND algorithm known as the clustering factor calculation. The number of nodes needed to run the programs is twice the number of input variables of the expression. The results indicate that the parallel version of ND algorithm halves the computation time compared to the sequential version. A secondary goal of this thesis is to initiate the parallelization of HAMLET and the study of parallel computers, i.e., iPSC/2. The experiences we obtained with iPSC/2 suggest an alternative algorithm. The ND algorithm searches the first branch of the search tree assuming that the optimum solution will be on that branch. We developed a Multi-branch Concurrent ND (MCMD) algorithm which concurrently searches multiple branches, hence increasing the probability of reaching the optimum. GRA

N92-26677# Cornell Univ., Ithaca, NY. Dept. of Computer Science.
TOOLS AND TECHNIQUES FOR ADDING FAULT TOLERANCE TO DISTRIBUTED AND PARALLEL PROGRAMS Interim Report
Ozalp Babaoglu 7 Dec. 1991 15 p
(AD-A245510; TR-91-1249) Avail: NTIS HC/MF A03

The scale of parallel computing systems is rapidly approaching dimensions where fault tolerance can no longer be ignored. No matter how reliable the individual components may be, the complexity of these systems results in a significant probability of failure during lengthy computations. In the case of distributed memory multiprocessors, fault tolerance techniques developed for distributed operating systems and applications can be applied also to parallel computations. In the paper we survey some of the principal paradigms for fault-tolerant distributed computing and discuss their relevance to parallel processing. One particular technique (passive replication) is explored in detail as it forms the basis for fault tolerance in the Paralex parallel programming environment. GRA

N92-26801# Washington Univ., Seattle.
THE ORCA PROJECT: RESEARCH ON HIGH PERFORMANCE PARALLEL COMPUTER PROGRAMMING ENVIRONMENTS Final Report, 1 Apr. - 31 Mar. 1990
Lawrence Snyder, David Notkin, and Loyce Adams 31 Mar. 1990 11 p LIMITED REPRODUCIBILITY: Availability: Document partially illegible
(Grant AF-AFOSR-0282-89; AF Proj. 2304)
(AD-A234648; AFOSR-91-0263TR) Avail: NTIS HC/MF A03

Research was performed on programming massively parallel computers. Previous work on the 'Ensamble' concept of programming was extended and a study into nonshared memory models of parallel computation was undertaken. Previous work on the 'Ensamble' concept defined a set of programming abstractions and was used to organize the programming task into three distinct

levels; Composition of machine instruction, composition of processes, and composition of phrases. It was applied to shared memory models of computations. During the present research period, these concepts were extended to nonshared memory models. GRA

N92-26854# Los Alamos National Lab., NM.
SOLUTION OF THE FIRST-ORDER FORM OF THE 3-D DISCRETE ORDINATES EQUATIONS ON A MASSIVELY PARALLEL MACHINE
K. R. Koch, R. S. Baker, and R. E. Alcouffe 1991 6 p Presented at the ANS Annual Meeting, Boston, MA, 7-12 Jun. 1992
(Contract W-7405-eng-36)
(DE92-004575; LA-UR-91-4157; CONF-920606-2) Avail: NTIS HC/MF A02

A common approach used today to solve the neutron transport equation is to apply the discrete ordinates method, with source iteration, to the first order form of the transport equation. Although the use of synthetic acceleration greatly reduces the number of source iterations required for convergence, we have found that the time spent in inverting the transport operator still forms a large part of the overall computational effort. In today's production codes, this inversion is performed directly through the use of a transport sweep. Although a transport sweep is inherently a sequential operation, sweep algorithms which successfully vectorize (i.e., diagonal line sweeps) have been developed and implemented for vector machines such as the CRAY. However, with the advent of massively parallel SIMD architectures, it has been the accepted belief that an efficient algorithm for direct inversion of the transport operator could not be successfully adapted to machines such as the CM-2. Instead, interest has focused on alternative approaches to solving the transport equation, such as the second order (even parity) form, or response matrix methods, which require an iterative inversion of the transport operator. The purpose of this paper is to show that an efficient algorithm for the solution of the standard, first order form of the transport equation does exist for massively parallel architectures, and that the direct inversion of the transport operator can indeed be successfully parallelized. DOE

N92-27183*# Dartmouth Coll., Hanover, NH. Dept. of Mathematics and Computer Science.
A SECURITY ANALYSIS OF VERSION 2 OF THE NETWORK TIME PROTOCOL (NTP): A REPORT TO THE PRIVACY AND SECURITY RESEARCH GROUP
Matt Bishop 1991 24 p
(Grant NAG2-628)
(NASA-CR-190428; NAS 1.26:190428; PCS-TR91-154) Avail: NTIS HC/MF A03

The Network Time Protocol is being used throughout the Internet to provide an accurate time service. The security requirements are examined of such a service, version 2 of the NTP protocol is analyzed to determine how well it meets these requirements, and improvements are suggested where appropriate. Author

63 CYBERNETICS

Includes feedback and control theory, artificial intelligence, robotics and expert systems.

For related information see also *54 Man/System Technology and Life Support.*

N92-26356# Carnegie-Mellon Univ., Pittsburgh, PA. Robotics Inst.
DYNAMIC CONTROL OF A SPACE ROBOT SYSTEM WITH NO THRUST JETS CONTROLLED BASE
Yangsheng Xu and Heung-Yeung Shum Aug. 1991 27 p
(AD-A245711; CMU-RI-TR-91-33) Avail: NTIS HC/MF A03

In this paper we discuss dynamic control of a free-flying space robot system where the base attitude is not controlled by thrust jets. Without external forces and moments, the system is governed by linear and angular momentum conservation laws. We first derive the system dynamic formulations in joint space and in inertia space, based on Lagrangian dynamics. Then we discuss the fact that dynamics of a space robot system can not be linearly parameterized, as opposed to the case of a fixed-based robot. Revealing this property is significant since the linearity of parameterization is used as a prerequisite for various adaptive and nonlinear control schemes currently used in the robot control. Based on the dynamic model of the space robot system, a simple linear control scheme is presented for the normal regulation problem for tasks in space, such as holding lights for illuminating objects or handing an astronaut tools in extra-vehicular activity. A globally stable dynamic control scheme is proposed for trajectory tracking applications, such as catching moving objects or structure inspection for the Space Station. The dynamic control algorithm exhibits a fast and accurate motion response even when the mass/inertia ratio of the base with respect to the robot is low. The effectiveness of the proposed algorithms are demonstrated by simulation studies. GRA

N92-26357# Carnegie-Mellon Univ., Pittsburgh, PA. Robotics Inst.
A FRAMEWORK FOR RECOGNIZING GRASPS
Sing B. Kang and Katsushi Ikeuchi Nov. 1991 40 p
(Contract F33615-90-C-1465; ARPA Order 7597)
(AD-A245712; CMU-RI-TR-91-24) Avail: NTIS HC/MF A03

Many of the tasks that are potential candidates for automation involve grasping. We are interested in the programming of robots to perform grasping tasks. To do this, we propose the notion of perceptual programming, where the key idea is to enable a system to observe a human performing a task, understand it, and perform the task with minimal human intervention. This allows the programmer to easily choose the grasp strategy. A grasping task is composed of three phases: pre-grasp phase, static grasp phase, and manipulation phase. The first step in recognizing a grasping task is identifying the grasp itself (within the static grasp phase). We propose to identify the grasp by mapping the low-level hand configuration to increasingly more abstract grasp descriptions. To this end, we introduce a grasp representation called the contact web which is composed of a pattern of effective contact points between the hand and the object. We also propose a grasp taxonomy based on the contact web to systematically identify a grasp. Results from grasping experiments show that it is possible to distinguish between various types of grasps. GRA

N92-26410# Massachusetts Inst. of Tech., Cambridge. Artificial Intelligence Lab.
A COMPUTATIONAL ANALYSIS OF PROPERTIES AND LIMITATIONS OF NEURAL NETWORKS: TOWARD NEW PARALLEL ARCHITECTURES FOR LEARNING Final Report
T. A. Poggio and R. Rivest 1992 12 p
(AD-A246156) Avail: NTIS HC/MF A03

The goal of our work has been to develop a solid theoretical framework for the problem of learning from examples, in order to evaluate neural network architecture and develop new powerful parallel techniques and algorithms. Our approach was based on the formulation of the problem of learning from examples as a problem of approximation of multivariate functions from sparse data, in such a way as to take advantage of the existing large body of results in function approximation theory and regularization. Our work has been successful beyond our original expectations that we had at the time we wrote the proposal. We have developed a sizable body of theoretical results and applications. Several projects, many outside our own group, are now pursuing different aspects of the theory, and are developing algorithms and applying the technique to practical domains. GRA

N92-26428# Carnegie-Mellon Univ., Pittsburgh, PA. Robotics Inst.
HYBRID EFFICIENT CONTROL ALGORITHMS FOR ROBOT MANIPULATORS
Ju-Jang Lee Nov. 1991 28 p
(AD-A245716; CMU-RI-TR-91-30) Avail: NTIS HC/MF A03

In this report, we discuss accurate and robust sliding mode tracking control for highly nonlinear robot manipulators using a

disturbance observer. We attempt to eliminate the chattering problem that existed in conventional Sliding Mode Control (SMC) approach, which is caused by modeling errors and uncertainties. The efficient compensation of the disturbance observer was introduced. The proposed sliding mode control is presented in two theorems. The bounded stability of the proposed control method is proven and the efficiency of the control algorithms is demonstrated by simulations of position tracking control of a two-link robot subject to parameter and payload uncertainties.
GRA

N92-26429*# Carnegie-Mellon Univ., Pittsburgh, PA. Robotics Inst.
DEAD RECKONING NAVIGATION FOR WALKING ROBOTS
Gerald P. Roston and Eric P. Krotkov Nov. 1991 23 p
(Grant NAGw-1175)
(NASA-CR-190296; NAS 1.26:190296; AD-A245717; CMU-RI-TR-91-27) Avail: NTIS HC/MF A03

Autonomous and teleoperated mobile robots require an accurate knowledge of their spatial location in order to accomplish many tasks. Many mobile robots make use of dead reckoning navigation because of its simplicity, low cost, and robustness. Although dead reckoning navigation was used for centuries on ships and wheeled vehicles, the application to a walking machine is novel. Since walking machines differ greatly from ships and wheeled vehicles, a new approach to dead reckoning was developed to solve this problem. This paper discusses the problem, a solution, preliminary test results, and future goals for dead reckoning navigation. Experiments were done with the CMU Ambler, an autonomous, six-legged walking robot, but the results are general and apply to any statically stable walking robot. The current results show a systematic bias of two percent of body advance in the direction of travel. Although the cause of this bias is unknown, it is corrected in the position estimation routines.
GRA

N92-26434# Sandia National Labs., Albuquerque, NM.
CONSTRAINED NEURAL NETWORK ARCHITECTURES FOR TARGET RECOGNITION
D. R. Hush, Shang-Ying Clark, and M. M. Moya 1992 10 p Presented at the International Society for Photo Optical Engineering Conference, Orlando, FL, 20-24 Apr. 1992
(Contract DE-AC04-76DP-00789)
(DE92-011159; SAND-92-0648C; CONF-920471-3) Avail: NTIS HC/MF A02

This paper describes several different types of constraints that can be placed on multilayered feedforward neural networks which are used for automatic target recognition (ATR). We show how unconstrained networks are likely to give poor generalization on the ATR problem. We also show how the ATR problem requires a special type of classifier called a one-class classifier. The network constraints come in two forms: architectural constraints and learning constraints. Some of the constraints are used to improve generalization, while others are incorporated so that the network will be forced to perform one-class classification.
DOE

N92-26597 Virginia Polytechnic Inst. and State Univ., Blacksburg.
PARAMETER ROBUST REDUCED-ORDER CONTROL OF FLEXIBLE STRUCTURES Ph.D. Thesis
Stephen H. Jones 1991 128 p
Avail: Univ. Microfilms Order no. DA9204642

The concept of internal feedback loop modeling, due to Tahk and Speyer, to arrive at two new linear quadratic Gaussian LQG-based methods of parameter robust control is generalized. One component of the robustness procedure, common to both methods, is the application of an auxiliary cost functional penalty to desensitize the system to variations in selected parameters of the state-space model. The other component consists of the formulation of a fictitious noise model to accommodate the effect of these parameter variations. The frequency-domain method utilizes knowledge of the system dynamics to create a frequency-shaped noise model with a power spectrum that approximates the frequency content of unknown error signals in the system due to parametric uncertainties. This design method requires augmentation of additional dynamics to the plant, which results in higher-dimensional full-order controllers. However, the controller design computations are identical to those of a standard LQG problem. The time-domain method emulates the same error signals by means of a multiplicative white noise model which reflects the time-domain behavior of those signals. The resulting robust controller is of the same order as the standard LQG controller, although the design involves a more complex computational algorithm. The application of multiplicative white noise to the system model requires the solution of a system of four coupled equations: two modified Riccati equations and two modified Lyapunov equations. In addition, the optimal projection equations are applied to both robustness methods to reduce the controller order with minimal loss in performance. Comparisons are drawn between these and related robust control methods, and it is shown that the relative effectiveness of such methods is problem dependent. Parameter sensitivity analysis is carried out on a simply supported plate model subject to external disturbances. The appropriate robust controller is selected, and it is found to stabilize the plate with little sacrifice in performance.
Dissert. Abstr.

N92-26627*# National Aeronautics and Space Administration. Ames Research Center, Moffett Field, CA.
A DESIGN RATIONALE FOR NASA TILEWORLD
Andrew B. Philips, Keith J. Swanson, Mark E. Drummond, and John L. Bresina (Sterling Federal Systems, Inc., Moffett Field, CA.) Apr. 1991 10 p Prepared in cooperation with Rutgers-The State Univ., New Brunswick, NJ
(NASA-TM-107882; FIA-91-04; NAS 1.15:107882) Avail: NTIS HC/MF A02

Automated systems that can operate in unrestricted real-world domains are still well beyond current computational capabilities. This paper argues that isolating essential problem characteristics found in real-world domains allows for a careful study of how particular control systems operate. By isolating essential problem characteristics and studying their impact on autonomous system performance, we should be able to more quickly deliver systems for practical real-world problems. For our research on planning, scheduling, and control, we have selected three particular domain attributes to study: exogenous events, uncertain action outcome, and metric time. We are not suggesting that studies of these attributes in isolation are sufficient to guarantee the obvious goals of good methodology, brilliant architectures, or first-class results; however, we are suggesting that such isolation facilitates the achievement of these goals. To study these attributes, we have developed the NASA TileWorld. We describe the NASA TileWorld simulator in general terms, present an example NASA TileWorld problem, and discuss some of our motivations and concerns for NASA TileWorld.
Author

N92-26628*# National Aeronautics and Space Administration. Ames Research Center, Moffett Field, CA.
PRINCIPAL INVESTIGATOR IN A BOX: VERSION 1.2 DOCUMENTATION
Jurine Adolph, Rajiv Bhatnagar, Silvano P. Colombano, Michael Compton, Richard Frainer, Nicolas Groleau, Kritina Holden, Sen-Hao Lai, Chih-Chao Lam, and Meera Manahan (Lockheed Engineering and Sciences Co., Houston, TX.) et al Nov. 1990 47 p
(NASA-TM-107886; FIA-90-11-05-1; NAS 1.15:107886) Avail: NTIS HC/MF A03

Principal Investigator (PI) in a box is a computer system designed to help optimize the scientific results of experiments that are performed in space. The system will assist the astronaut experimenters in the collection and analysis of experimental data, recognition and pursuit of 'interesting' results, optimal use of the time allocated to the experiment, and troubleshooting of the experiment apparatus. This document discusses the problems that motivate development of 'PI-in-a-box', and presents a high- level system overview and a detailed description of each of the modules that comprise the current version of the system.
Author

N92-26629*# National Aeronautics and Space Administration. Ames Research Center, Moffett Field, CA.
INTRODUCTION IN IND AND RECURSIVE PARTITIONING
Wray Buntine and Rich Caruana (San Jose State Univ., Moffett Field, CA.) 23 Sep. 1991 100 p
(NASA-TM-107879; FIA-91-28; NAS 1.15:107879) Avail: NTIS HC/MF A05

This manual describes the IND package for learning tree classifiers from data. The package is an integrated C and C shell re-implementation of tree learning routines such as CART, C4, and various MDL and Bayesian variations. The package includes routines for experiment control, interactive operation, and analysis of tree building. The manual introduces the system and its many options, gives a basic review of tree learning, contains a guide to the literature and a glossary, and lists the manual pages for the routines and instructions on installation. Author

N92-26630*# National Aeronautics and Space Administration. Ames Research Center, Moffett Field, CA.
COMPUTER MODELING OF HUMAN DECISION MAKING
William B. Gevarter Dec. 1991 45 p
(NASA-TM-107868; FIA-91-32; NAS 1.15:107868) Avail: NTIS HC/MF A03

Models of human decision making are reviewed. Models which treat just the cognitive aspects of human behavior are included as well as models which include motivation. Both models which have associated computer programs, and those that do not, are considered. Since flow diagrams, that assist in constructing computer simulation of such models, were not generally available, such diagrams were constructed and are presented. The result provides a rich source of information, which can aid in construction of more realistic future simulations of human decision making. Author

N92-26631*# National Aeronautics and Space Administration. Ames Research Center, Moffett Field, CA.
TWO PAPERS ON FEED-FORWARD NETWORKS
Wray L. Buntine and Andreas S. Weigend (Stanford Univ., CA.) 5 Jul. 1991 46 p
(NASA-TM-107840; FIA-91-22; NAS 1.15:107840) Avail: NTIS HC/MF A03

Connectionist feed-forward networks, trained with back-propagation, can be used both for nonlinear regression and for (discrete one-of-C) classification, depending on the form of training. This report contains two papers on feed-forward networks. The papers can be read independently. They are intended for the theoretically-aware practitioner or algorithm-designer; however, they also contain a review and comparison of several learning theories so they provide a perspective for the theoretician. The first paper works through Bayesian methods to complement back-propagation in the training of feed-forward networks. The second paper addresses a problem raised by the first: how to efficiently calculate second derivatives on feed-forward networks. Author

N92-26643*# National Aeronautics and Space Administration. Ames Research Center, Moffett Field, CA.
AN ANALYSIS OF COMMITMENT STRATEGIES IN PLANNING: THE DETAILS
Steven Minton, John Bresina, Mark Drummond, and Andrew B. Philips (Sterling Federal Systems, Inc., Moffett Field, CA.) 30 Dec. 1991 31 p
(NASA-TM-107881; FIA-91-08; NAS 1.15:107881) Avail: NTIS HC/MF A03

We compare the utility of different commitment strategies in planning. Under a 'least commitment strategy', plans are represented as partial orders and operators are ordered only when interactions are detected. We investigate claims of the inherent advantages of planning with partial orders, as compared to planning with total orders. By focusing our analysis on the issue of operator ordering commitment, we are able to carry out a rigorous comparative analysis of two planners. We show that partial-order planning can be more efficient than total-order planning, but we also show that this is not necessarily so. Author

N92-26657# Oak Ridge National Lab., TN.
A BAYES-MAXIMUM ENTROPY METHOD FOR MULTI-SENSOR DATA FUSION
M. Beckerman 1991 14 p Presented at the IEEE International Conference on Robotics and Automation, Nice, France, 10-15 May 1992
(Contract DE-AC05-84OR-21400)
(DE92-000680; CONF-920540-13) Avail: NTIS HC/MF A03

In this paper we introduce a Bayes-Maximum Entropy formalism for multi-sensor data fusion, and present an application of this methodology to the fusion of ultrasound and visual sensor data as acquired by a mobile robot. In our approach the principle of maximum entropy is applied to the construction of priors and likelihoods from the data. Distances between ultrasound and visual points of interest in a dual representation are used to define Gibbs likelihood distributions. Both one- and two-dimensional likelihoods are presented, and cast into a form which makes explicit their dependence upon the mean. The Bayesian posterior distributions are used to test a null hypothesis, and Maximum Entropy Maps used for navigation are updated using the resulting information from the dual representation. DOE

N92-26734 Rensselaer Polytechnic Inst., Troy, NY.
A SUPERVISORY CONTROL STRATEGY FOR NAVIGATION OF MOBILE ROBOTS IN DYNAMIC ENVIRONMENTS Ph.D. Thesis
Kanstantinos J. Kyriakopoulos 1991 142 p
Avail: Univ. Microfilms Order No. DA9202186

Collision avoidance for a mobile robot in an environment of moving obstacles is examined. The proposed scheme, in addition to collision avoidance, is concerned with performance in terms of time consistency with a nominal plan. A nominal plan, that guarantees collision avoidance with the static environment, is assumed to be available from off-line computation. In order to be able to apply the proposed scheme in real time, the information from the nominal plan is utilized and sensing information relevant only to the unpredictable moving objects is processed. The shape of both the mobile robot and the moving obstacles is modeled as convex polyhedron. The dynamic model of the mobile robot and the constraints are derived and formally define the problem. The considered problem is decomposed into two parts: collision prediction and collision avoidance. Within this framework, and trying to achieve time consistency with the nominal plan, three strategies were developed: (1) optimal control strategy (OCS); (2) minimum interference strategy (MIS); and (3) potential fields strategy (PFS). The three algorithms are compared in terms of: (1) optimality of solution; (2) computational complexity; and (3) robustness and recomputability. The comprehensive study clearly shows that MIS is generally the most applicable. Dissert. Abstr.

N92-26789*# National Aeronautics and Space Administration. Ames Research Center, Moffett Field, CA.
EXPLANATION-BASED GENERALIZATION OF PARTIALLY ORDERED PLANS
Subbarao Kambhampati and Smadar Kedar (Sterling Federal Systems, Inc., Moffett Field, CA.) May 1991 10 p Submitted for publication
(NASA-TM-107869; FIA-91-15; NAS 1.15:107869) Avail: NTIS HC/MF A02

Most previous work in analytic generalization of plans dealt with totally ordered plans. These methods cannot be directly applied to generalizing partially ordered plans, since they do not capture all interactions among plan operators for all total orders of such plans. We introduce a new method for generalizing partially ordered plans. This method is based on providing explanation-based generalization (EBG) with explanations which systematically capture the interactions among plan operators for all the total orders of a partially-ordered plan. The explanations are based on the Modal Truth Criterion which states the necessary and sufficient conditions for ensuring the truth of a proposition at any point in a plan, for a class of partially ordered plans. The generalizations obtained by this method guarantee successful and interaction-free execution of any total order of the generalized plan. In addition, the systematic

derivation of the generalization algorithms from the Modal Truth Criterion obviates the need for carrying out a separate formal proof of correctness of the EBG algorithms. Author

N92-26791*# National Aeronautics and Space Administration. Ames Research Center, Moffett Field, CA.
DISCRETE SEQUENCE PREDICTION AND ITS APPLICATIONS
Philip Laird Jan. 1992 9 p
(Grant NSF INT-90-08726)
(NASA-TM-107865; FIA-92-01; NAS 1.15:107865) Avail: NTIS HC/MF A02

Learning from experience to predict sequences of discrete symbols is a fundamental problem in machine learning with many applications. We apply sequence prediction using a simple and practical sequence-prediction algorithm, called TDAG. The TDAG algorithm is first tested by comparing its performance with some common data compression algorithms. Then it is adapted to the detailed requirements of dynamic program optimization, with excellent results. Author

N92-26814# National Inst. of Standards and Technology, Gaithersburg, MD. Robot Systems Div.
REPRESENTATIONS IN VISUAL MOTION
D. Raviv and J. S. Albus Jan. 1992 28 p Prepared in cooperation with Florida Atlantic Univ., Boca Raton
(PB92-148287; NISTIR-4747) Avail: NTIS HC/MF A03

Discussed here are motion based image transformations that lead to new representations of 3-D objects for a rectilinear motion of the observer. In the new representations, a stationary environment is kept invariant or 'frozen', in spite of the fact that the images on the retina are continuously changing. Since the 3-D stationary environment is also represented as stationary environment, moving objects can be easily detected and a good estimation of the scene from a long sequence of noisy images can be obtained. Three basic observations which are related to translational motion of an observer led to the new representations. One is that the radial distance of a point in 3-D space from the camera translational path is kept constant at any instant of time. The second observation is that the relative depth along the translational path between two points is the same at any point in time. The third observation is that points in the image plane move away from the Focus of Expansion (FOE) and towards the Focus of Contraction (FOC). The new representations are simple. All measurements for these representations are taking place in camera coordinates. Only one camera is necessary, and the magnitude of the camera velocity vector needs not be known. The mathematics involved are simple, and thus it may be suitable for real time applications. Author

N92-26885*# National Aeronautics and Space Administration. Ames Research Center, Moffett Field, CA.
APPLYING KNOWLEDGE COMPILATION TECHNIQUES TO MODEL-BASED REASONING
Richard M. Keller (Sterling Federal Systems, Inc., Moffett Field, CA.) Jan. 1991 14 p Submitted for publication
(Contracts NAS2-13210; NCC2-537)
(NASA-TM-107876; FIA-91-01; NAS 1.15:107876) Avail: NTIS HC/MF A03

Researchers in the area of knowledge compilation are developing general purpose techniques for improving the efficiency of knowledge-based systems. In this article, an attempt is made to define knowledge compilation, to characterize several classes of knowledge compilation techniques, and to illustrate how some of these techniques can be applied to improve the performance of model-based reasoning systems. Author

N92-26887*# National Aeronautics and Space Administration. Ames Research Center, Moffett Field, CA.
THE 1990 PROGRESS REPORT AND FUTURE PLANS
Peter Friedland, Monte Zweben, and Michael Compton Apr. 1990 67 p
(NASA-TM-107911; RIA-90-4-27-1; NAS 1.15:107911) Avail: NTIS HC/MF A04

This document describes the progress and plans of the Artificial Intelligence Research Branch (RIA) at ARC in 1990. Activities span a range from basic scientific research to engineering development and to fielded NASA applications, particularly those applications that are enabled by basic research carried out at RIA. Work is conducted in-house and through collaborative partners in academia and industry. Our major focus is on a limited number of research themes with a dual commitment to technical excellence and proven applicability to NASA short, medium, and long-term problems. RIA acts as the Agency's lead organization for research aspects of artificial intelligence, working closely with a second research laboratory at JPL and AI applications groups at all NASA centers. Author

N92-26888*# National Aeronautics and Space Administration. Ames Research Center, Moffett Field, CA.
MoCog1: A COMPUTER SIMULATION OF RECOGNITION-PRIMED HUMAN DECISION MAKING
William B. Gevarter Aug. 1991 31 p
(NASA-TM-107872; FIA-91-23; NAS 1.15:107872) Avail: NTIS HC/MF A03

This report describes the successful results of the first stage of a research effort to develop a 'sophisticated' computer model of human cognitive behavior. Most human decision-making is of the experience-based, relatively straight-forward, largely automatic, type of response to internal goals and drives, utilizing cues and opportunities perceived from the current environment. This report describes the development of the architecture and computer program associated with such 'recognition-primed' decision-making. The resultant computer program was successfully utilized as a vehicle to simulate findings that relate how an individual's implicit theories orient them toward particular goals, with resultant cognitions, affects, and behavior in response to their environment. The present work is an expanded version and is based on research reported while the author was an employee of NASA ARC. Author

N92-26893*# National Aeronautics and Space Administration. Ames Research Center, Moffett Field, CA.
MODELLING DEFAULT AND LIKELIHOOD REASONING AS PROBABILISTIC
Wray Buntine 11 Sep. 1990 38 p Prepared in cooperation with University of Technology, Sydney, Australia; and Turing Inst., Glasgow, Scotland
(NASA-TM-107889; FIA-90-09-11-01; NAS 1.15:107889) Avail: NTIS HC/MF A03

A probabilistic analysis of plausible reasoning about defaults and about likelihood is presented. 'Likely' and 'by default' are in fact treated as duals in the same sense as 'possibility' and 'necessity'. To model these four forms probabilistically, a logic QDP and its quantitative counterpart DP are derived that allow qualitative and corresponding quantitative reasoning. Consistency and consequence results for subsets of the logics are given that require at most a quadratic number of satisfiability tests in the underlying propositional logic. The quantitative logic shows how to track the propagation error inherent in these reasoning forms. The methodology and sound framework of the system highlights their approximate nature, the dualities, and the need for complementary reasoning about relevance. Author

N92-27055*# National Aeronautics and Space Administration. Ames Research Center, Moffett Field, CA.
THE APT/ERE PLANNING AND SCHEDULING MANIFESTO
Mark Drummond, John Bresina, Keith Swanson, Andy Philips, and Rich Levinson Aug. 1991 16 p
(NASA-TM-107906; FIA-91-24; NAS 1.15:107906) Avail: NTIS HC/MF A03

The Entropy Reduction Engine, ERE project, is focusing on the construction of integrated planning and scheduling systems. Specifically, the project is studying the problem of integrating planning and scheduling in the context of the closed loop plan use. The results of this research are particularly relevant when there is some element of dynamism in the environment, and thus

some chance that a previously formed plan will fail. After a preliminary study of the APT management and control problem, it was felt that it presents an excellent opportunity to show some of the ERE Project's technical results. Of course, the alignment between technology and problem is not perfect, so planning and scheduling for APTs presents some new and difficult challenges as well. Author

N92-27056*# National Aeronautics and Space Administration. Ames Research Center, Moffett Field, CA.
THE STRUCTURE AND FORMATION OF NATURAL CATEGORIES
Douglas Fisher (Vanderbilt Univ., Nashville, TN.) and Pat Langley 20 Feb. 1990 40 p Submitted for publication
(NASA-TM-107896; RIA-90-02-15-1; NAS 1.15:107896) Avail: NTIS HC/MF A03

Categorization and concept formation are critical activities of intelligence. These processes and the conceptual structures that support them raise important issues at the interface of cognitive psychology and artificial intelligence. The work presumes that advances in these and other areas are best facilitated by research methodologies that reward interdisciplinary interaction. In particular, a computational model is described of concept formation and categorization that exploits a rational analysis of basic level effects by Gluck and Corter. Their work provides a clean prescription of human category preferences that is adapted to the task of concept learning. Also, their analysis was extended to account for typicality and fan effects, and speculate on how the concept formation strategies might be extended to other facets of intelligence, such as problem solving. Author

N92-27057*# National Aeronautics and Space Administration. Ames Research Center, Moffett Field, CA.
MODEL COMPILATION: AN APPROACH TO AUTOMATED MODEL DERIVATION
Richard M. Keller, Catherine Baudin, Yumi Iwasaki, Pandurang Nayak, and Kazuo Tanaka (Stanford Univ., CA.) Apr. 1990 15 p
(Contracts NAS2-11555; NAS2-12952)
(NASA-TM-107895; FIA-90-04-06-01; NAS 1.15:107895) Avail: NTIS HC/MF A03

An approach is introduced to automated model derivation for knowledge based systems. The approach, model compilation, involves procedurally generating the set of domain models used by a knowledge based system. With an implemented example, how this approach can be used to derive models of different precision and abstraction is illustrated, and models are tailored to different tasks, from a given set of base domain models. In particular, two implemented model compilers are described, each of which takes as input a base model that describes the structure and behavior of a simple electromechanical device, the Reaction Wheel Assembly of NASA's Hubble Space Telescope. The compilers transform this relatively general base model into simple task specific models for troubleshooting and redesign, respectively, by applying a sequence of model transformations. Each transformation in this sequence produces an increasingly more specialized model. The compilation approach lessens the burden of updating and maintaining consistency among models by enabling their automatic regeneration. Author

N92-27072# Naval Oceanographic and Atmospheric Research Lab., Bay Saint Louis, MS.
DOCUMENTATION FOR THE SEMI-AUTOMATED MESOSCALE ANALYSIS SYSTEM 1.1 Final Report
Nov. 1991 89 p
(AD-A246144; AD-E040167; NOARL-TN-193) Avail: NTIS HC/MF A05

Several software modules have been developed for or by the Naval Oceanographic and Atmospheric Research Laboratory to automate the analysis and interpretation of satellite infrared imagery in the Gulf Stream region of the Northwest Atlantic Ocean. The modules have been integrated to form the Semi-Automated Mesoscale Analysis System Version 1.1 (SAMAS). This document provides the information required for an analyst to use SAMAS 1.1. This document provides descriptions of how the modules of SAMAS 1.1 work and the user inputs and outputs are described. This document also provides information on the location of source code and special data files required for SAMAS 1.1. GRA

N92-27169# Texas Univ., Austin. Dept. of Electrical and Computer Engineering.
ADAPTIVE CONTROL OF NONLINEAR AND STOCHASTIC SYSTEMS Final Report, 15 Nov. 1990 - 14 Nov. 1991
Steven I. Marcus and Aristotle Arapostathis 10 Jan. 1992 11 p
(Grant AF-AFOSR-0033-91)
(AD-A247204; AFOSR-92-0118TR) Avail: NTIS HC/MF A03

Significant progress was made in a number of aspects of nonlinear and stochastic systems. An important problem in the adaptive control of a finite state Markov chain was solved, and significant progress was made along more general directions. A controlled switching diffusion model was developed to study the hierarchical control of flexible manufacturing systems and significant results were obtained. In the area of deterministic nonlinear systems the work continued on nonlinear observers and linearizable dynamics. Finally, some important problems in the area of discrete event systems were solved. GRA

64 NUMERICAL ANALYSIS

Includes iteration, difference equations, and numerical approximation.

N92-26229# Washington Univ., Seattle. Dept. of Statistics.
BIAS ROBUST ESTIMATION OF SCALE
R. D. Martin and Ruben H. Zamar Aug. 1991 34 p
(Contract N00014-91-J-1074)
(AD-A245698) Avail: NTIS HC/MF A03

We consider the problem of robust estimation of the scale of the location residuals when the underlying distribution of the data belongs to a contamination neighborhood of a parametric location-scale family. We define the class of M-estimates of scale with general location, and show that under certain regularity assumptions, these scale estimates converge to their asymptotic functionals uniformly with respect to the underlying distribution, and with respect to the M-estimate defining score function x. We establish expressions for the maximum asymptotic bias of M-estimates of scale over the contamination neighborhood as a function of the fraction of contamination. Using these expressions, we construct asymptotically min-max bias robust estimates of scale. In particular, we show that a scaled version of the Madm (median of absolute residuals about the median) is approximately min-max bias-robust within the class of Huber's proposal 2 joint estimates of location and scale. We also consider the larger class of M-estimates of scale with general location, and show that a scaled version of the Shorth (the shortest half of the data) is approximately min-max bias robust in this class. Finally, we present the results of a Monte Carlo study showing that the Shorth has attractive finite sample size mean squared error properties for contaminated Gaussian data. GRA

N92-26232# California Univ., Berkeley. Lawrence Berkeley Lab.
HAMILTONIAN LATTICE FIELD THEORY: COMPUTER CALCULATIONS USING VARIATIONAL METHODS Ph.D. Thesis
R. L. Zako 3 Dec. 1991 60 p
(Contract DE-AC03-76SF-00098)
(DE92-010479; LBL-31589; UCB-PTH-91/69) Avail: NTIS HC/MF A04

I develop a variational method for systematic numerical computation of physical quantities -- bound state energies and scattering amplitudes -- in quantum field theory. An infinite-volume, continuum theory is approximated by a theory on a finite spatial lattice, which is amenable to numerical computation. I present an

algorithm for computing approximate energy eigenvalues and eigenstates in the lattice theory and for bounding the resulting errors. I also show how to select basis states and choose variational parameters in order to minimize errors. The algorithm is based on the Rayleigh-Ritz principle and Kato's generalizations of Temple's formula. The algorithm could be adapted to systems such as atoms and molecules. I show how to compute Green's functions from energy eigenvalues and eigenstates in the lattice theory, and relate these to physical (renormalized) coupling constants, bound state energies, and Green's functions. Thus, one can compute approximate physical quantities in a lattice theory that approximates a quantum field theory with specified physical coupling constants. I discuss the errors in both approximations. In principle, the errors can be made arbitrarily small by increasing the size of the lattice, decreasing the lattice spacing and computing sufficiently long. Unfortunately, I do not understand the infinite-volume and continuum limits well enough to quantify errors due to the lattice approximation. Thus, the method is currently incomplete. I apply the method to real scalar field theories using a Fock basis of free particle states. All needed quantities can be calculated efficiently with this basis. The generalization to more complicated theories is straightforward. I describe a computer implementation of the method and present numerical results for simple quantum mechanical systems. DOE

N92-26358# Naval Postgraduate School, Monterey, CA.
ESTIMATION OF MOTION PARAMETERS FROM IMAGE SEQUENCES M.S. Thesis
Fatih Ildiz Jun. 1991 94 p
(AD-A246135) Avail: NTIS HC/MF A05

The image motion analysis algorithms that generate the two dimensional velocity of objects in a sequence of images are developed. The algorithms considered consist of: the parallel extended Kalman filter method; the spatiotemporal gradient methods; the spatiotemporal frequency methods; and the one-dimensional FFT methods. These algorithms are designed to perform on low signal to noise ratio images. Each of these algorithms is applied to a sequence of computer generated images with varying signal to noise ratios. Simulations are used to evaluate the performance of each algorithm. Author (GRA)

N92-26367# Vrije Univ., Amsterdam (Netherlands). Subfaculteit Wiskunde en Informatica.
HYPERSPACES OF INFINITE-DIMENSIONAL COMPACTA
H. Gladdines and J. vanMill Jul. 1991 14 p
(PB92-149335; WS-382) Avail: NTIS HC/MF A03

If X is an infinite product of nondegenerate Peano continua, then the set dim(sub infinity)(X) = (A epsilon)2(exp x):dim A = infinity) is an F(sub sigma, delta)-absorber in 2(exp X). As a consequence, there is a homeomorphism f:2(exp X) yields Q(sup infinity) such that f(dim(infinity)(X)) = B(sup infinity), where B denotes the pseudo-boundary of the Hilbert cube Q. There is a locally infinite-dimensional Peano continuum X such that for every n, dim(infinity)(X(sup n)) is not homeomorphic to B(sup infinity). GRA

N92-26407*# National Aeronautics and Space Administration. Lyndon B. Johnson Space Center, Houston, TX.
NEURAL NETWORK ERROR CORRECTION FOR SOLVING COUPLED ORDINARY DIFFERENTIAL EQUATIONS
R. O. Shelton, J. A. Darsey, B. G. Sumpter, and D. W. Noid (Oak Ridge National Lab., TN.) 1992 6 p Presented at the International Joint Conference on Neural Networks, Baltimore, MD, 7-11 Jun. 1992
(Contract DE-AC05-84OR-21400)
(NASA-TM-101796; NAS 1.15:101796; DE92-007241; CONF-9206102-2) Avail: NTIS HC/MF A02

A neural network is demonstrated to learn errors generated by a numerical algorithm for solving coupled nonlinear differential equations. Comparisons are made for training the neural network using backpropagation and a new method which is found to converge with fewer iterations. DOE

N92-26414# Colorado Univ., Boulder.
NONLINEAR WAVES AND INVERSE SCATTERING Final Report, 1 Jan. 1990 - 31 Dec. 1991
Mark J. Ablowitz 29 Jan. 1992 9 p
(Contract N00014-90-J-1218)
(AD-A246164; Rept-153425) Avail: NTIS HC/MF A02

Research in nonlinear waves and inverse scattering is continuing with many new and interesting results obtained. A summary of the key areas of research is given and a list of research publications and preprints has been compiled. The main areas of interest include: multidimensional nonlinear wave equations of physical significance, multidimensional inverse scattering, numerically induced instabilities and chaos, and forced nonlinear wave problems. GRA

N92-26420 Politecnico di Milano (Italy). Dipartimento di Elettronica.
FINDING A BEST SUBTREE OF A TREE
Francesco Maffioli 1991 12 p Sponsored in part by Italian Ministry of University and Scientific and Technological Research
(Grant NATO-RG-85-0240)
(Rept-91-041; ETN-92-91249) Avail: Politecnico di Milano, Piazza Leonardo da Vinci 32, 20133 Milan, Italy

The k cardinality tree problem asks for an optimum (minimum or maximum weight) tree containing exactly k arcs in a given graph G: the problem is NP hard. A polynomial algorithm for solving the problem when G is itself a tree is presented. ESA

N92-26502# Helsinki Univ. of Technology, Espoo (Finland). Inst. of Mathematics.
NONEXPANSIVE PROLONGATIONS AND DIFFERENCE SCHEMES FOR THE ADVECTION EQUATION
R. Jeltsch and O. Nevanlinna May 1991 16 p Prepared in cooperation with Eidgenoessische Technische Hochschule, Zurich, Switzerland
(PB92-141530; RR-A295; ISBN-951-22-0670-6) Avail: NTIS HC/MF A03

Picard-like iteration for solving large systems of ordinary differential equations on parallel computers can be accelerated by using a rough mesh early in the iterations. When the mesh is refined, nonexpansive accurate prolongations are needed to interpolate data from the old grid points onto the new grid points. It is shown that finding such prolongations is strongly related to finding stable finite difference schemes for the linear advection equation and to the stable complex approximation of z(sup mu), mu epsilon (0,1) close to z = 1. The results known for these approximations are used to give high order nonexpansive prolongations and barriers to the accuracy of such prolongations. Author

N92-26503# Technische Univ., Twente (Netherlands). Faculty of Applied Mathematics.
DEVELOPMENTS OF SOLUTIONS OF SOME SPECIAL ELLIPTIC EQUATIONS AT A CORNER
G. J. Still Sep. 1991 27 p
(PB92-148741; MEMO-996) Avail: NTIS HC/MF A03

The report discusses developments of solutions of elliptic boundary-value problems at a corner of the region. Under some analyticity conditions, general asymptotic developments were derived. The authors are interested in more explicit expansions and consider the question in what case can they expect a 'true' expansion, i.e., an expansion with positive radius of convergence, or only an asymptotic expansion. In the case of a corner formed by straight segments for some equations which allow a certain form of separation in polar coordinates the authors obtain such explicit expansions in an elementary way by only using classical Fourier theory. A closer inspection of the coefficients in these developments shows, that already in this simple situation the existence of a 'true' expansion depends on number-theoretic properties of the opening angle omega = pi/alpha at the corner. It follows that the expansions are 'true' if alpha is an algebraic number. However, for transcendental numbers alpha the radius of convergence of the developments could be zero. Author

N92-26545# Oak Ridge National Lab., TN.
N-LEARNERS PROBLEM: LEARNING BOOLEAN COMBINATIONS OF HALFSPACES
N. S. V. Rao, E. M. Oblow, and C. W. Glover Mar. 1992 15 p
(Contract DE-AC05-84OR-21400)
(DE92-010390; ORNL/TM-11905; CESAR-91/24) Avail: NTIS HC/MF A03

Given two subsets S sub 1 and S sub 2 (not necessarily finite) of Re sup d separable by a Boolean combination of N halfspaces, we consider the problem of learning the separation function from a finite set of examples, i.e., we produce with high probability a function close to the actual separating function. Our solution consists of a system of N perceptrons and a single consolidator which combines the outputs of the individual perceptrons. We show that an off-line version of this problem, where the examples are given in a batch, can be solved in time polynomial in the number of examples. We also provide an on-line learning algorithm that incrementally solves the problem by suitably training a system of N perceptrons much in the spirit of the classical perceptron learning algorithm. This solution constitutes an example of a composite system of N learners capable of accomplishing a task that is not achievable by a single learner, for a single perceptron is incapable of separating sets that are not linearly separable.
DOE

N92-26620# Naval Postgraduate School, Monterey, CA.
A MODELING STRATEGY FOR LARGE-SCALE OPTIMIZATION BASED ON ANALYSIS AND VISUALIZATION PRINCIPLES M.S. Thesis
Cheryl A. Bither and Julie A. Dougherty Sep. 1991 100 p
(AD-A246570) Avail: NTIS HC/MF A05

A modeling strategy for the validation and analysis of large-scale optimization models is defined and demonstrated. The strategy is based on nine principles of analysis and eight principles of visualization that are applied in a user controlled hierarchical structure which is customized to a particular optimization problem. For each model a set of analytic tools, such as spreadsheets and graphs, is structured to validate and verify data and analyze the model and its results. These tools can be quickly recreated with data from subsequent runs of the model and from the sensitivity analysis and comparisons. As a demonstration, the strategy is applied to PHOENIX, a large-scale U.S. Army helicopter force planning model. The strategy incorporates available technology using commercially prepared software and a computer workstation. The application of techniques such as hypertext, data access, and backward compatibility enhance the ease of use and effectiveness of this approach. GRA

N92-26624 Colorado Univ., Boulder.
APPLICATION OF PARAMETRIZED VARIATIONAL PRINCIPLES IN THE FINITE ELEMENT METHOD Ph.D. Thesis
Carmelo Militello 1991 246 p
Avail: Univ. Microfilms Order No. DA9206622

High-performance (HP) elements are simple finite elements constructed to deliver engineering accuracy with coarse arbitrary mesh grids. The effective construction of HP elements relies on devices, sometimes called tricks or variational crimes, that do not fit a priori in the classical variational framework. Many devices were tried: reduced and selective integration, incompatible modes, mixed and hybrid formulations, stress and strain projections, free formulation (FF), and assumed natural strains (ANS). How several high performance element construction methods can be embedded within an extended variational framework that uses parameterized hybrid functionals is studied. The plan of attack involved parameterization of the conventional elasticity functionals and treatment of element interfaces through generalization of the hybrid approach. The present treatment decriminalizes kinematic constraint tricks by adjoining Lagrange multipliers, hence placing the ensemble in a proper variational setting. Satisfaction of the individual element test (IET) provides further constraints that should be satisfied in order to guarantee stability and convergence in the realm of Iron's Patch-Test. As a result of this treatment, the general structure of the stiffness matrices and forcing vectors of HP elements are obtained. Three new elements are developed within this framework, one triangular Kirchhoff plate and two triangular Hellinger-Reissner plates. The Kirchhoff plate is transformed in a shell element through the addition of a membrane stiffness. The FF and ANS method for constructing HP finite elements are presented within this variational setting and some combined forms emerge naturally from it. In addition, we have also explored 3-D adaptive mesh refinement by node relocation, introducing a new kind of local error indicator based on the above mentioned variational principle. Shell problems are studied to check the performance of the error indicator. Dissert. Abstr.

N92-26668*# Institute for Computer Applications in Science and Engineering, Hampton, VA.
THE MODELING AND CONTROL OF ACOUSTIC/STRUCTURE INTERACTION PROBLEMS VIA PIEZOCERAMIC ACTUATORS: 2-D NUMERICAL EXAMPLES Final Report
H. T. Banks, R. J. Silcox (National Aeronautics and Space Administration. Langley Research Center, Hampton, VA.), and R. C. Smith Apr. 1992 31 p Submitted for publication
(Contracts NAS1-18605; NAS1-18107; NAG1-1116; AF-AFOSR-0091-90; RTOP 505-90-52-01)
(NASA-CR-189639; NAS 1.26:189639; ICASE-92-17) Avail: NTIS HC/MF A03

The modeling and active control of acoustic pressure in a 2-D cavity with a flexible boundary (a beam) is considered. Control is implemented in the model via piezoceramic patches on the beam which are excited in a manner so as to produce pure bending moments. The incorporation of the feedback control in this manner leads to a system with an unbounded input term. Approximation techniques are discussed and by writing the resulting system as an abstract Cauchy equation, the problem of reducing interior pressure fluctuations can be posed in the context of a linear quadratic regulator (LQR) time domain state space formulation. Examples illustrating the dynamic behavior of the coupled system as well as demonstrating the viability of the control method on a variety of problems with periodic forcing functions are presented.
Author

N92-26737# Technische Univ., Twente (Netherlands). Faculty of Applied Mathematics.
SUBGRAPHS, CLOSURES AND HAMILTONICITY
H. J. Broersma and I. Schiermeyer Sep. 1991 12 p Prepared in cooperation with Technische Hochschule, Aachen, Fed. Republic of Germany
(PB92-148766; MEMO-998) Avail: NTIS HC/MF A03

Closure theorems in hamiltonian graph theory are of the following type: Let G be a 2-connected graph and let (u,v) be two distinct nonadjacent vertices of G. If the condition c(u,v) holds, then G is hamiltonian if and only if G = uv is hamiltonian. The authors discuss several results of this type in which u and v are vertices of a subgraph H of G on 4 vertices and c(u,v) is a condition on the neighborhoods of the vertices of H (in G). The authors also discuss corresponding sufficient conditions for hamiltonicity of G.
Author

N92-26755# Naval Postgraduate School, Monterey, CA.
STURM-LIOUVILLE EIGENFUNCTIONS EXPRESSED IN DETERMINANT FORM M.S. Thesis
Michael D. Phillips Jun. 1991 60 p
(AD-A245991) Avail: NTIS HC/MF A04

The purpose of this thesis is to investigate and establish Sturm-Liouville properties for special eigenfunctions which are expressed in determinant form. In particular, a special case is presented where the elements of the determinant are Legendre polynomials. This type of determinant has a probability background dealing in birth and death processes. The method of analysis used in this thesis is a new approach to solving this specific example. This investigation involves systems of differential equations and Prufer's analysis in the phase plane. The following are new results obtained in addition to solving the special case mentioned above. Special determinants of hypergeometric functions also possess Sturm-Liouville properties. As a special

case, a different proof of Turan's Inequality is provided. Finally, several theorems are presented for Sturm-Liouville systems of differential equations with polynomial coefficients. GRA

N92-26788# Institut des Hautes Etudes Scientifiques, Bures-sur-Yvette (France).
DVORETZKY'S THEOREM: 30 YEARS LATER
V. Milman Jan. 1992 29 p Presented at the Conference on Banach Spaces, Jerusalem, Israel, Jun. 1991 Prepared in cooperation with Ohio State Univ., Columbus; and Tel-Aviv Univ. (Israel)
(PB92-153212; IHES/M/92/1) Avail: NTIS HC/MF A03

About thirty years ago A. Dvoretzky solved a conjecture of Grothendieck who, in his turn, was inspired by analyzing the Dvoretzky-Rogers lemma. It quickly became clear that it was an outstanding breakthrough in Geometrical Functional Analysis. It is believed that it would be useful and timely to go through the story of development of a new high dimensional intuition which began at Dvoretzky's theorem. The influence of Dvoretzky's theorem will be followed on the change in ones understanding of high dimensional spaces and convex sets rather than its influence on technical development and achievements, although this was also crucial and even more striking. From this point of view, the work is not a presentation of the achievements of Local Theory (the theory of finite dimensional normed spaces). Probability connections are not discussed, nor is type-cotype theory, technical applications to Local Theory and to constructions of infinite dimensional spaces with special properties. A more 'technically directed' survey on Dvoretzky's theorem was written by Lindenstrauss. Author

N92-26817# Technische Univ., Twente (Netherlands). Faculty of Applied Mathematics.
DECOMPOSITION OF BIPARTITE GRAPHS UNDER DEGREE CONSTRAINTS
H. J. Broersma, J. vandenHeuvel, R. J. Faudree, and H. J. Veldman Jul. 1991 13 p Prepared in cooperation with Memphis State Univ., TN
(PB92-148626; MEMO-984) Avail: NTIS HC/MF A03

Let G = (A,B;E) be a bipartite graph. Let e(sub1),e(sub 2) be nonnegative integers and f(sub 1),f(sub 2) nonnegative integer-valued functions on V(G) such that e(sub i) is equal to or less than (absolute value of E) equal to or less than e(sub 1) + e(sub 2) and f(sub i)(v) equal to or less than d(v) equal to or less than f(sub 1)(v) + f(sub 2)(v) for all v epsilon V(G) (i = 1,2). Necessary and sufficient conditions are obtained for G to admit a decomposition in spanning subgraphs G(sub 1) = (A,B;E(sub 1)) and G(sub 2) = (A,B;E(sub 2)) such that (absolute value of E(sub 1) is equal to or less than e(sub i) and d(sub G(sub i))(v) equal to or less than fi(v) for all v epsilon V(G) (i = 1,2). The result generalizes a known characterization of bipartite graphs with a k-factor. Its proof uses flow theory and is a refinement of the proof of an analogous result. By applying corresponding flow algorithms, the described decomposition can be found in polynomial time if it exists. As an application, as assignment problem is solved. Author

N92-26831# Laboratorio de Computacao Cientifica, Rio de Janeiro (Brazil).
LYAPUNOV EQUATION FOR INFINITE-DIMENSIONAL DISCRETE BILINEAR SYSTEMS
O. L. V. Costa and C. S. Kubrusly Mar. 1991 12 p
(DE92-621066; LNCC-004/91) Avail: NTIS HC/MF A03

Mean square stability for discrete systems requires that uniform convergence is preserved between input and state correlation sequences. Such a convergence preserving property holds for an infinite dimensional bilinear system if and only if the associate Lyapunov equation has a unique strictly positive solution. DOE

N92-26834# Academy of Pedagogical Sciences of the USSR, Moscow. Nauchno-Issledovatelskij Inst. Yadernoj Fiziki.
UNIVERSAL R-MATRIX FOR QUANTIZED (SUPER)ALGEBRAS
S. M. Khoroshkin and V. N. Tolstoj 1991 28 p In RUSSIAN; ENGLISH summary
(DE92-621067; NIIYAF-MGV-91-13-217) Avail: NTIS HC/MF A03

For quantum deformations of finite dimensional contragredient Lie (super)algebras an explicit formula for the universal R-matrix is given. This formula generalizes the analogous formulae for quantized semisimple Lie algebras obtained by M. Rosso, A.N. Kirillov and N. Reshetikhin, Ya.S. Soibelman and S.Z. Levendorskii. Approach is based on careful analysis of quantized rank 1 and 2 (super)algebras, a combinatorial structure of the root systems and algebraic properties of q-exponential functions. Quantum Weyl group is not used. DOE

N92-26837# Instituto de Fisica Teorica, Sao Paulo (Brazil).
ON THE EVALUATION OF THE U(3) CONTENT OF THE MATRIX ELEMENTS OF 1- AND 2-BODY OPERATORS
V. Vanagas (Academy of Sciences of the Lithuanian SSR, Vilnius.) and J. A. C. Alcaras Sep. 1991 43 p
(DE92-621113; IFT-P-031/91) Avail: NTIS HC/MF A03

An expression for the U(3) content of the matrix elements of one- and two-body operators in Elliott's basis is obtained. Three alternative ways of evaluating this content with increasing performance in computing time are presented. All of them allow an exact representation of that content in terms of integers, avoiding rounding errors in the computer codes. The role of dual bases in dealing with non-orthogonal bases is also clarified. DOE

N92-26894*# National Aeronautics and Space Administration. Ames Research Center, Moffett Field, CA.
BAYESIAN CLASSIFICATION THEORY
Robin Hanson, John Stutz, and Peter Cheeseman (Research Inst. for Advanced Computer Science, Moffett Field, CA.) May 1991 11 p
(NASA-TM-107885; FIA-90-12-7-01; NAS 1.15:107885) Avail: NTIS HC/MF A03

The task of inferring a set of classes and class descriptions most likely to explain a given data set can be placed on a firm theoretical foundation using Bayesian statistics. Within this framework and using various mathematical and algorithmic approximations, the AutoClass system searches for the most probable classifications, automatically choosing the number of classes and complexity of class descriptions. A simpler version of AutoClass has been applied to many large real data sets, has discovered new independently-verified phenomena, and has been released as a robust software package. Recent extensions allow attributes to be selectively correlated within particular classes, and allow classes to inherit or share model parameters though a class hierarchy. We summarize the mathematical foundations of AutoClass. Author

N92-26900# Naval Postgraduate School, Monterey, CA.
DOWNDATING OF SZEGO POLYNOMIALS AND DATA FITTING APPLICATIONS Technical Report, Jan. - Jun. 1991
William Gragg, Greg Ammar, and Lother Reichel 2 Jan. 1992 23 p LIMITED REPRODUCIBILITY: Availability: Document partially illegible
(AD-A245825; NPS-MA-92-002) Avail: NTIS HC/MF A03

Many algorithms for polynomial least squares approximation of a real-valued function on a real interval determine polynomials that are orthogonal with respect to a suitable inner product defined on this interval. Analogously, it is convenient to computer Szego polynomials (polynomials that are orthogonal with respect to an inner product on the unit circle) when approximating a complex-valued function on the unit circle in the least squares sense. It may also be appropriate to determine Szego polynomials in algorithms for least squares approximation of real-valued periodic functions by trigonometric polynomials. This paper is concerned with Szego polynomials that are defined by a discrete inner product on the unit circle. We present a scheme for downdating the Szego polynomials and the given least squares approximant when a node is deleted from the inner product. Our scheme uses the QR algorithm for unitary upper Ilessenberg matrices. We describe a

data-fitting application that illustrates how our scheme can be combined with the fast Fourier transform algorithm when the given nodes are not equidistant. Application to sliding windows is discussed. GRA

N92-27180# Naval Postgraduate School, Monterey, CA.
VLSI IMPLEMENTATION OF FUZZY LOGIC OPERATOR UNIT M.S. Thesis
Ismail B. Dewa Jun. 1991 55 p
(AD-A247146) Avail: NTIS HC/MF A04

Fuzzy logic is widely used in many applications that deal with uncertainty and approximate reasoning in decision making. Decisions can be made based on fuzzy inferences. Because of the ease with which Very Large Scale Integration (VLSI) circuits can be made, hardware implementation of fuzzy logic is seen to be an appropriate step to be taken to fully realize its potential. Fuzzy operations are based on three basic operators - the maximum, minimum, and inverse functions. This thesis investigates its implementation in VLSI circuits, specifically for digital systems. Design structures such as bit-cascade, bit-slice, block-cascade, and block-slice were implemented. Comparisons between these designs are provided. GRA

N92-27196*# National Aeronautics and Space Administration. Lewis Research Center, Cleveland, OH.
INSTITUTE FOR COMPUTATIONAL MECHANICS IN PROPULSION (ICOMP) Annual Report No. 6, 1991
Charles E. Feiler, ed. May 1992 50 p
(Contract NCC3-233; RTOP 505-62-21)
(NASA-TM-105612; ICOMP-92-01; E-6950; NAS 1.15:105612)
Avail: NTIS HC/MF A03

The Institute for Computational Mechanics in Propulsion (ICOMP) is a combined activity of Case Western Reserve University, Ohio Aerospace Institute (OAI) and NASA Lewis. The purpose of ICOMP is to develop techniques to improve problem solving capabilities in all aspects of computational mechanics related to propulsion. The activities at ICOMP during 1991 are described. Author

65 STATISTICS AND PROBABILITY

Includes data sampling and smoothing; Monte Carlo method; and stochastic processes.

N92-26177# Naval Postgraduate School, Monterey, CA. Dept. of Operations Research.
LOWER CONFIDENCE LIMIT EXPRESSIONS FOR P(X GREATER THAN y) AND P(X GREATER THAN Y) UNDER NORMALITY
W. M. Woods Dec. 1991 18 p
(Contract NPSOR-92-010)
(AD-A245787) Avail: NTIS HC/MF A03

Lower confidence limit expressions for P(X greater than y) and P(X.Y) are provided when both X and Y have normal probability distributions with unknown means and variances. The cases of equal variances and unequal variances are treated separately. The expressions are approximate but highly accurate as shown in the report. GRA

N92-26180# Texas Univ., Austin. Applied Research Lab.
CHARACTERIZATION OF DISCRETE-TIME LINEAR PERIODICALLY TIME-VARYING SYSTEMS
Kevin W. Baugh 26 Jul. 1991 119 p
(AD-A245822; ARL-TR-91-20) Avail: NTIS HC/MF A06

Techniques for empirically characterizing linear time-invariant systems are well established in the technical literature. Classic techniques rely on both the linearity of the underlying system and on the time invariance of the system parameters. Methods for analytically characterizing linear time-varying systems are also well-established in the literature. Typically, these methods rely on the time-varying impulse response or on the system response function. The focus of these methods is on the analytical evaluation of systems with known parameters, not on the empirical characterization of systems. The following paper presents techniques for empirically characterizing discrete-time linear time-varying systems whose system parameters may be only partially specified. GRA

N92-26467# Naval Postgraduate School, Monterey, CA.
EFFECTS OF VIDEO BANDWIDTH ON THE PERFORMANCE OF A SQUARE LAW DETECTOR WITH GAUSSIAN IF AND VIDEO FILTERS M.S. Thesis
Wee L. Chang Sep. 1991 69 p
(AD-A246506) Avail: NTIS HC/MF A04

The effects of Gaussian-shaped IF and video filters on the performance of a square-law detector employing post-detection integration are analyzed. The number of additional noise-only samples that are integrated due to a finite video bandwidth is determined. Emerson's method is used to obtain an expression for the cumulants of the output probability density function. These cumulants are used in Edgeworth's asymptotic series expansion of the density functions. By integrating these density functions, the receiver operating characteristics are determined for various ratios of IF bandwidth to video bandwidth. A collapsing ratio which takes into account the Gaussian shape of the filters is formulated and compared against Barton's approximate formula for the collapsing ratio. For typical video bandwidths, Barton's approximate formula is found to overestimate the collapsing loss by an amount less than 0.5 db. Author (GRA)

N92-27174# Washington Univ., Seattle. Dept. of Statistics.
STOCHASTIC VERSIONS OF THE EM ALGORITHM
Jean-Claude Biscarat, Gilles Celeux, and Jean Diebolt Jan. 1992 21 p
(Contract N00014-91-J-1074)
(AD-A246929; TR-227) Avail: NTIS HC/MF A03

We compare three different stochastic versions of the EM algorithm - the SEM algorithm, the SAEM algorithm and the MCEM algorithm. We suggest that the most relevant contribution of the MCEM methodology is what we call the simulated annealing MCEM algorithm, which turns out to be very close to SAEM. We focus particularly on the mixture of distributions problem. In this context, we review the available theoretical results on the convergence of these algorithms and on the behavior of SEM as the sample size tends to infinity. Finally, we illustrated these results with some Monte Carlo numerical simulation. GRA

N92-27175# Wisconsin Univ., Madison. Center for Mathematical Sciences.
ON THE CONSTRUCTION OF MULTIVARIATE (PRE)WAVELETS
Carl deBoor, Ronald A. DeVore (South Carolina Univ., Columbia.), and Amos Ron Feb. 1992 43 p
(Contract DAAL03-90-G-0090; NSF DMS-90-00053)
(AD-A247105; CMS-TSR-92-09) Avail: NTIS HC/MF A03

A new approach for the construction of wavelets and prewavelets on IR sup d from multiresolution is presented. The method uses only properties of shift-invariant spaces and orthogonal projectors from L2(IR sup d) onto these spaces, and requires neither decay nor stability of the scaling function. Furthermore, this approach allows a simple derivation of previous, as well as new, constructions of wavelets, and leads to a complete resolution of questions concerning the nature of the intersection and the union of a scale of spaces to be used in a multiresolution. GRA

66 SYSTEMS ANALYSIS

Includes mathematical modeling; network analysis; and operations research.

N92-26194# RAND Corp., Santa Monica, CA.
THE ROLE OF THE B-2 IN THE NEW US DEFENSE STRATEGY
George L. Donohue 1991 21 p
(RAND-P-7744) Avail: NTIS HC/MF A03

A summation of senate testimony is presented. The testimony discusses the research undertaken in a two-year Project AIR FORCE study entitled, 'Future Strategic Aerodynamic Forces: Roles, Missions, and Force Mixes'. This project focussed on the future of the B-2 bomber. Author

67 THEORETICAL MATHEMATICS

Includes topology and number theory.

N92-26466# Naval Postgraduate School, Monterey, CA.
FRACTALS AND CHAOS M.S. Thesis
Philip F. Beaver Jun. 1991 179 p
(AD-A246502) Avail: NTIS HC/MF A09

The study of fractal geometry and chaotic dynamical systems has received considerable attention in the past decade. Motivated by the interesting computer graphics produced by these fields, mathematicians have attempted to formalize the theoretical structure of the results, physicists have attempted to apply the theory to real world phenomena, and laymen have enjoyed much of the popular literature and television programs that the field has fostered. Unfortunately, the mathematics associated with these subjects has made them inaccessible to most undergraduates, even if they have a strong background in mathematics. This thesis presents the basic ideas of fractal geometry and chaotic dynamical systems in a setting that can be understood by undergraduate students who have had a course in advanced calculus. We hope it will allow them to gain an appreciation of the fields and motivate them to pursue further study. GRA

N92-26798# Academy of Sciences of the Ukrainian SSR, Kiev. Inst. Teoreticheskoj Fiziki.
SPECTRAL BOUNDARY CONDITIONS AND INDEX THEOREM FOR 2-DIMENSIONAL COMPACT MANIFOLD WITH BOUNDARY
A. V. Mishchenko and Yu. A. Sitenko 1991 40 p
(DE92-621115; ITP-91-16) Avail: NTIS HC/MF A03

A set of nonlocal conditions influencing the index problem for a compact surface with boundary in an external magnetic field is considered. These conditions being relevant for the case of a nonflat boundary are shown to make the index value to be dependent on the second fundamental form of the boundary. The Atiyah-Patodi-Singer boundary condition is modified in order to get the condition which is equivalent to the square integrability of zero modes on a noncompact surface. DOE

70 PHYSICS (GENERAL)

For precision time and time interval (PTTI) see *35 Instrumentation and Photography;* for geophysics, astrophysics or solar physics see *46 Geophysics, 90 Astrophysics,* or *92 Solar Physics.*

N92-26460# Naval Postgraduate School, Monterey, CA.
PROPOSED MODEL OF THERMIONICALLY ASSISTED BREAKDOWN AND IMPLEMENTATION ON ELECTROSTATIC THRUSTERS M.S. Thesis
Walter J. Bell Dec. 1991 63 p
(AD-A246207) Avail: NTIS HC/MF A04

A model for thermionically assisted breakdown is proposed which predicts the voltage reduction experienced in low voltage discharges. This reduction in breakdown voltage has been beneficial to numerous engineering applications of arcs and is explored specifically for electrostatic thrusters. Full advantage in employing thermionically assisted breakdown is attained by establishing a continuum of electron emission across the primary discharge gap. These electrons must be independent of the discharge itself, being established prior to ignition. The electron emission is therefore achieved by auxiliary emitters across the gap. Electrons amass in a space charge in the vicinity of the assisting device. The particular processes which induce charge multiplication are proposed to be multistep ionization and neutralization of the space charge by ions. Breakdown criteria and a means of estimating the reduction in breakdown voltage requirement are derived. One proposal for the thermionically assisting emission device is the coiled-coil filament, and a scheme for installing such filaments in ionization chambers for electrostatic thrusters is described. Thermionically assisted breakdown implementation should also pertain to arc applications for various primary electrode geometries as well as certain gases. GRA

N92-26471# Defence Research Establishment, Ottawa (Ontario).
STATIC ELECTRICITY: A LITERATURE REVIEW
Rita M. Crow Nov. 1991 22 p
(AD-A246533; DREO-TN-91-28) Avail: NTIS HC/MF A03

The major concern with static electricity is its discharging in a flammable atmosphere which can explode and cause a fire. Textile materials can have their electrical resistivity decreased by the addition of antistatic finishes, imbedding conductive particles into the fibres or by adding metal fibers to the yarns. The test methods used in the studies of static electricity include measuring the static properties of materials, of clothed persons, and of the ignition energy of flammable gases. Surveys have shown that there is sparse evidence for fires definitively being caused by static electricity. However, the 'worst-case' philosophy has been adopted and a static electricity safety code is described, including correct grounding procedures and the wearing of anti-static clothing and footwear. GRA

N92-26671*# National Aeronautics and Space Administration. Lewis Research Center, Cleveland, OH.
COMPUTATIONAL TECHNIQUES IN TRIBOLOGY AND MATERIAL SCIENCE AT THE ATOMIC LEVEL
J. Ferrante and G. H. Bozzolo (Analex Corp., Brook Park, OH.) 1992 30 p Presented at the NATO Research Inst. Workshop on Fundamentals of Friction, Braunlage, Germany, 5-19 Aug. 1991; sponsored by the North Atlantic Treaty Organization
(RTOP 505-90-53)
(NASA-TM-105573; E-6777; NAS 1.15:105573) Avail: NTIS HC/MF A03

Computations in tribology and material science at the atomic level present considerable difficulties. Computational techniques ranging from first-principles to semi-empirical and their limitations are discussed. Example calculations of metallic surface energies using semi-empirical techniques are presented. Finally, application of the methods to calculation of adhesion and friction are presented. Author

N92-26768# Naval Research Lab., Washington, DC.
THEORY OF ELECTROMAGNETIC INSTABILITY OF AN INTENSE BEAM IN A QUADRUPOLE FOCUSING SYSTEM Interim Report
Cha-Mei Tang, J. Krall, and T. Swyden (FM Technologies, Inc., Fairfax, VA.) 18 Feb. 1992 31 p
(AD-A246560; NRL-MR-6914) Avail: NTIS HC/MF A03

Discrete quadrupole focusing system are subject to an electromagnetic instability wherein the growing transverse motion of the beam interacts with the quadrupole field and the TE sub 11 waveguide mode. The dispersion relation is derived, which is a matrix equation of infinite dimension. We show that an appropriately truncated matrix equation is able to give exact growth rates. Furthermore, analytical growth rates are obtained and instability boundaries are established. Numerical solutions of the dispersion

relation show that the overall stability properties are not favorable for long pulse, high-current electron beams. The stability properties of ion beams are also discussed. GRA

N92-26769# Naval Research Lab., Washington, DC.
REFLECTION OF X RAYS FROM REPEATED MULTILAYER STRUCTURES
Herbert B. Rosenstock (SFA, Inc., Landover, MD.) and Dennis B. Brown 11 Feb. 1992 26 p
(AD-A246562; NRL-MR-6942) Avail: NTIS HC/MF A03

A calculation for obtaining the expected reflectivity of soft x rays from repeated multilayers is described. The calculation is a 'classical' or 'optical' one in the sense that the incoming radiation is described as a plane wave (rather than a collection of photons), and each layer is assumed to be described by a complex index of refraction (not by discrete atoms). A guide to a computer program incorporating this calculation is provided. GRA

N92-26772# Texas Univ., Austin. Applied Research Lab.
NONSTATIONARY HIGHER ORDER SPECTRAL ANALYSIS
Gary R. Wilson and Keith R. Hardwicke 23 Apr. 1991 77 p
(Contract N00014-89-J-1967)
(AD-A246580; ARL-TR-91-8) Avail: NTIS HC/MF A05

This report discusses the detection performance of a variety of higher order spectra for a variety of signals. Of particular significance is the introduction of a new type of higher order spectra called nonstationary higher order spectra. Nonstationary higher order spectra are not the stationary higher order spectral representations of nonstationary process, but are in fact different spectra which contain the stationary higher order spectra as a subset of their domain. It is shown quantitatively through theoretical predictions and simulations that these type of spectra perform better at detecting nonstationary signals than do the traditional stationary spectra. For the first time, small sample statistics have been derived and applied to the detection performance rather than asymptotic statistics, resulting in a more accurate performance prediction for typical sample sizes for nonstationary signals. GRA

N92-26940# Utah Univ., Salt Lake City. Dept. of Chemistry.
STATIC, MICROWAVE, INFRARED, AND VISIBLE PERMITTIVITY RELATED TO CHEMICAL STRUCTURE: N-METHYLACETAMIDE, N-DIMETHYLACETAMIDE AND THEIR MIXTURES IN CCl4 AT 32 C
Paul Firman, Edward M. Eyring, Meizhen Xu, Andrea Marchetti, and Sergio Petrucci 26 Jun. 1991 32 p
(Contract DAAL03-89-K-0148)
(AD-A246364; ARO-26636.2-CH) Avail: NTIS HC/MF A03

Static dielectric permittivities, E sub 0, and visible refractive indices, n sub d (at the sodium doublet wavelength = 589.3 nm) are reported for N-methylacetamide (NMA), N-dimethylacetamide (DMA), their mixtures with CCl4 over a broad concentration range and for NMA-DMA mixtures over a broad range of concentrations at 32 C. UHF and microwave complex permittivities from 0.3 to 90 GHz and far infrared refractive indices at frequency = 130 and frequency = 380/cm for NMA and their mixtures with CCl4 and at frequency = 130/cm for DMA-CCl4 mixtures up to 1 M DMA at 32 C are also reported. Dramatic differences between NMA and DMA in both the static permittivities and relaxation times (for both pure liquids and their mixtures in CCl4) are attributed to chain formation through H-bonding for the monosubstituted amides. DMA acts as a kind of chain-terminator when added to NMA. The difference in behavior between the two liquids disappears in the case of infrared permittivities and visible (n sub d)sq values. GRA

N92-27078# Naval Postgraduate School, Monterey, CA.
MODELING FOR IMPROVED MINIMUM RESOLVABLE TEMPERATURE DIFFERENCE MEASUREMENTS M.S. Thesis
Alejandro R. Ugarte Sep. 1991 105 p
(AD-A246389) Avail: NTIS HC/MF A06

The minimum resolvable temperature difference (MRTD) is widely accepted as the parameter that best describes the field performance of a thermal imaging system (TIS). Mathematical modeling that accurately predicts the MRTD has been of major interest to the infrared community over the last 30 years. This work reviews the currently accepted models for predicting the MRTD. Simplifying assumptions used by these models which deal with the target spectrum are discussed and tested using specifications taken from a standard forward looking infrared (FLIR) system. In addition new models are proposed and tested. Two of these models are a direct extension of the recently proposed Vortman-Bar-Lev adaptive matched filter. A third model is based on the novel concept that the MRTD curve is predictable from a threshold condition on the visibility rather than the signal-to-noise ratio, of the system-degraded bar pattern. GRA

N92-27182# Naval Postgraduate School, Monterey, CA.
HIGHER ORDER PARAMETRIC X RAYS M.S. Thesis
Michael J. Osborne Dec. 1991 103 p
(AD-A247148) Avail: NTIS HC/MF A06

Parametric x-radiation (PXR) may be described as the Bragg scattering of virtual photons to produce real x-rays which satisfy the Bragg condition dsin theta = n(lambda), where theta is the angle between the electron beam direction and a crystal axis. Enhanced higher order parametric x-radiation from the (002) plane of a mosaic graphite crystal has been observed. Production of PXR of the order n = 2 exceed that from the first order, and x-rays of order up to n = 6 are readily seen. The production of higher order x-radiation is obtained by using a thick crystal where the formation and attenuation lengths are exploited to enhance higher energy x-ray formation relative to the lower energy first order x-radiation. Photons of energy 5 to 30 KeV have been measured. The experiment was conducted with a 90 MeV electron beam from the Naval Postgraduate School electron linear accelerator. A three axis target position program, Easy-Mover, was developed to allow for precision orientation of the crystal axis with respect to the electron beam. GRA

71 ACOUSTICS

Includes sound generation, transmission and attenuation. For noise pollution see *45 Environmental Pollution.*

N92-26175# Colorado School of Mines, Golden. Dept. of Mathematics and Computer Sciences.
COMPARISON OF ONE-WAY WAVE PROPAGATION ALGORITHMS IN UNDERWATER ACOUSTICS-ERROR ESTIMATES AND SENSITIVITY Final Report, 1 Oct. 1989 - 30 Sep. 1991
Louis Fishman 6 Jan. 1992 15 p
(Contract N00014-90-J-1023)
(AD-A245660) Avail: NTIS HC/MF A03

The long-range objective is to develop and apply microscopic phase space methods and global path integral constructions to gain a deeper theoretical and computational understanding of acoustic, electromagnetic, and seismic direct and inverse wave propagation problems. This seems to be an appropriate approach for ocean seismo-acoustic modeling, which is characterized by rapidly changing, multidimensional environments extending over many wavelengths. Much of the mathematical development can indeed be motivated by the well-known parabolic (paraxial) approximation. Combining wave field splitting, invariant imbedding, and phase space (pseudo-differential and Fourier integral operator) methods has led to the development of both one- and two-way direct Helmholtz solvers, in addition to providing the framework for multidimensional profile reconstruction algorithms based on exact solution methods. GRA

N92-26228# Naval Postgraduate School, Monterey, CA.
RECURSIVE RAY ACOUSTICS FOR THREE-DIMENSIONAL SOUND-SPEED PROFILES M.S. Thesis
F. W. Polnicky Sep. 1991 111 p
(AD-A245613) Avail: NTIS HC/MF A06

A comparison of simple recursive ray acoustics algorithm versus

a ray acoustics algorithm based on solving a system of first-order ordinary differential equations was conducted. The recursive ray acoustics (RRA) algorithm was found to be accurate and relatively fast. The RRA algorithm is capable of handling sound speed as a function of all three spatial coordinates, and this capability was demonstrated. Two separate methods of representing a sound-speed profile (SSP) based on data points were examined: Akima cubic spline and spatial Fourier series (SFS). The SFS representation encountered difficulties in accurately modeling SSP's. Various techniques were applied to improve the SFS sound speed representation. While accurate sound-speed fits were eventually achieved, difficulties remained in the SFS modeling of first and second-order derivatives of the sound-speed data. The RRA algorithm was tested using the SFS sound-speed representation and found to be significantly inaccurate. A demonstration was conducted of the ability of the SFS sound-speed representation to incorporate randomness in the SSP. GRA

N92-26413# Colorado Univ., Boulder.
OPTICAL HIDDEN LAYER NETWORK Final Report, Sep. 1987 - Mar. 1991
Dana Z. Anderson 1 Jul. 1991 10 p
(Contract DAAL03-87-K-0140)
(AD-A246162; ARO-25273.6-PH) Avail: NTIS HC/MF A02

An optical implementation of what is known as a 'supervised learning' algorithm was implemented with volume photorefractive holographic medium and a spatial light modulator. We investigated how one could apply neural network principles to temporal information using photorefractive media. For this purpose, the transfer function and impulse response of photorefractive two-beam coupling amplifiers was derived and experimentally verified. As part of the investigation on temporal processing of information, we built and demonstrated a fiber optic acoustic transducer for audio sound processing. The sound spectra generated by the transducer were stored in a volume holographic medium. The stored sounds were used to recognize identical or similar sounds in real time. GRA

N92-26558 Stanford Univ., CA.
COMPUTATIONAL METHODS FOR PROBLEMS OF ACOUSTICS WITH PARTICULAR REFERENCE TO EXTERIOR DOMAINS Ph.D. Thesis
Isaac Harari 1991 235 p
Avail: Unsiv. Microfilms Order No. DA9205643

Finite element methods are constructed for the reduced wave equation with special attention to unbounded domains. Exterior boundary conditions for a computational problem are derived from an exact relation between the solution and its derivatives on an artificial boundary by the DtN method, precluding singular behavior in finite element models. The DtN formulation is shown to give rise to exact (and thereby unique) solutions. We prove that a local approximation of the boundary conditions restores uniqueness for all wave numbers, and derive its three-dimensional version. Galerkin, Galerkin/least-squares and Galerkin/gradient least-squares finite element methods are presented. Model problems of radiation with inhomogeneous Neumann boundary conditions in plane and spherical configurations are employed to design and evaluate the numerical methods in the entire range of propagation and decay. General convergence results for fixed computational domains guarantee the good performance of Galerkin/least-squares methods on all configurations of practical interest. Numerical tests validate these conclusions. The cost of obtaining solutions to problems governed by the Helmholtz equation by means of boundary element and finite element methods is studied and compared. The main emphasis is on the computational effort required to solve the systems of equations emanating from the two methods. Both direct and iterative solution techniques are examined. For interior problems, finite element methods are more economical on most practical configurations. Finite elements also appear to possess a certain computational advantage on the exterior problems examined, and, in general, are definitely competitive with boundary element methods. The cost-effectiveness of the two solution strategies is examined. Some issues of equation formation are addressed as well.
Dissert. Abstr.

N92-26618# William Beaumont Army Hospital, El Paso, TX. Dept. of Clinical Investigation.
CLINICAL INVESTIGATION PROGRAM, FISCAL YEAR 1991 Annual Report, 1 Oct. 1990 - 30 Sep. 1991
Manuel Schydlower 3 Feb. 1992 211 p
(AD-A246558) Avail: NTIS HC/MF A10

Subject report identifies the research activities conducted at William Beaumont Army Medical Center by investigators who had protocols approved by the Clinical Investigation Committee, the Institutional Review Board, and the Animal Use Committee. This report includes all protocols registered with the Department of Clinical Investigation during FY 1991. All known presentations and publications are also included. The research protocols described were conducted under the provisions of AR 40-38 (Clinical Investigation Program); AR 40-7 (Use of Investigational Drugs in Humans and the Use of Schedule 1 Controlled Substances); AR 70-25 (Usle of Volunteers as Subjects of Research); HSC 40-32 (Management of Clinical Investigation Protocols and Reports); and AR 70-18 (The Use of Animals in DOS programs). GRA

N92-26678# Naval Postgraduate School, Monterey, CA.
SOURCE LOCATION IN THIN PLATES USING CROSSCORRELATION Ph.D. Thesis
Steven M. Ziola Dec. 1991 115 p
(AD-A245521) Avail: NTIS HC/MF A06

Alternative methods to first threshold crossing techniques for acoustic emission (AE) source location in dispersive media are presented. The accuracy of source location in dispersive media can be improved by locating frequency components in the transducer outputs to determine the difference in arrival times. Two methods were developed in this study for the arrival time determination. The first involved crosscorrelating the transducer outputs with a cosine wave modulated by a Gaussian pulse to locate a single frequency in the outputs. The second method narrowband filtered the transducer outputs and then crosscorrelated the filtered signals to determine the difference in arrival times. The techniques were experimentally verified by performing lead breaks on the surface of aluminum and graphite/epoxy plates. The results indicate that accurate source location can be attained in dispersive media by taking the wave propagation into account. GRA

N92-26688# Naval Postgraduate School, Monterey, CA.
EVALUATION OF THE COMPUTATIONAL VALIDITY OF THE IMAGE MODEL IN PREDICTING THE SOUND FIELD IN A WEDGE-SHAPED LAYER USING ACOUSTICAL RECIPROCITY M.S. Thesis
Kyung T. Lee Dec. 1991 56 p
(AD-A246548) Avail: NTIS HC/MF A04

Computer models based on the method of image were used to investigate and calculate the pressure amplitude distribution in wedge-shaped (tapered) water layer overlying a fast, absorbing bottom. The pressure amplitude of the field was generated and compared at reciprocal positions of source and receiver. The results showed that the ratio of pressure was larger when the position of source receiver was closer to the bottom and nearer the apex.
GRA

N92-27031# Naval Postgraduate School, Monterey, CA.
APPARATUS FOR MEASURING THE ABSORPTION OF SOUND BY NOISE IN ONE DIMENSION M.S. Thesis
Stephen J. Dorff Dec. 1991 40 p
(AD-A246442) Avail: NTIS HC/MF A03

A travelling wave tube for the study of high intensity acoustics has been constructed. The tube has inner diameter two inches and length 70 feet, and consists of seven 10 foot long sections smoothly joined by collars and flanges. Attached to one end is a housing that contains two JBL horn drivers connected to the tube by a Y adapter. An anechoic end termination spans the length of

the last section. The termination is made of steel wool of tapered density distribution. Pulse reflection measurements yielded an absorption of 40 dB or greater for frequencies of 500 Hz and higher. Reflected signals of the junctions were typically 40 dB down. Linear attenuation measurements indicated no appreciable acoustic losses at the junctions. Sum, difference and second harmonic generation measurements revealed that interactions were occurring in the medium of interest (air) and were not the result of the drivers or intermodulations of the two drivers. The performance under these preliminary tests indicates that the apparatus is suitable for nonlinear acoustics investigations. GRA

N92-27076# Naval Postgraduate School, Monterey, CA.
ACOUSTICALLY PROBED TAYLOR-COUETTE FLOW APPARATUS M.S. Thesis
Kevin M. Blum Dec. 1991 32 p
(AD-A246385) Avail: NTIS HC/MF A03

A Taylor Couette cell for the investigation of geometrical phase in acoustics has been constructed. The inner and outer cylinders are made of acrylic. The cell has an inner cylinder radius of 9.477 cm, radius ratio of 0.902, and cavity aspect ratio of 49.2. Two high performance d.c. motors can independently rotate the cylinders. The angular speed of the cylinders is monitored by a photo-interrupter. A piezoelectric polymer (PVDF) transducer mounted on the inner cylinder drives the acoustic field in the cavity and a 6.02 mm diameter electret microphone embedded in the wall of the inner cylinder acts as a receiver. Static measurements of the acoustic modes in the annular cavity show good agreement with theory, though measurements at different angular locations of the transducer reveal 2 pct. nonuniformities. The effects of nonuniformities could be overcome by rotating the cylinders at high speeds. The performance under these preliminary tests indicate that an apparatus of this design is suitable for investigations of acoustics in rotating flows. GRA

N92-27184 Department of the Navy, Washington, DC.
BINAURAL ULTRASOUND DETECTOR AND IMAGER Patent
Thomas I. Kirkpatrick, inventor (to Navy) 26 Nov. 1991 12 p Filed 15 Feb. 1990
(AD-D015214; US-Patent-5,068,832; US-Patent-Appl-SN-481421; US-Patent-Class-G015-15.00) Avail: US Patent and Trademark Office

This patent discloses a frequency translator which converts inaudible sounds into audible sounds while preserving the phase relationship of the sounds. The translator mixes a local reference frequency with an inaudible receive signal to translate the receive signal to an audible frequency. If the receive signal exceeds a predetermined value, the reference frequency gets shifted in phase to correspond to the phase of the receive signal at that moment. The resulting translated signal is thus in phase with the receive signal at the moment of shift, so that the time-of-arrival of the receive signal is not lost. When used individually in conjunction with left and right listening channels, the translator enables a listener to hear as well as sense the time-of-arrival of otherwise inaudible signals. GRA

72 ATOMIC AND MOLECULAR PHYSICS

Includes atomic structure, electron properties, and molecular spectra.

N92-26171# Naval Academy, Annapolis, MD.
ACQUIRED POLARIZATION IN FUNDAMENTAL SYMMETRY EXPERIMENTS Final Report, 1990 - 1991
Paul A. Larson 13 May 1991 46 p
(AD-A245646; USNA-TSPR-183) Avail: NTIS HC/MF A03

One interesting class of fundamental symmetry violation tests involves the measurement of low energy neutron transmission through a thick target as projectile/target spin orientations are changed. As the neutron beam propagates through a target, certain components are preferentially absorbed by nuclear resonances. This induces regenerative effects in thick targets, known as the acquired polarization effect, which complicate the interpretation of transmission measurements. We focus on the role that nuclear resonance spectroscopy plays in beam modification. We determine three basic results. First, with known resonance parameters for spin 1/2 targets Fe-57, Rh-102, Cd-111, Cd-113, Sn-117, and Tl-203, and spin 7/2 target La-139, the relative sizes of the various terms are determined, including the values of the cross sections, transmission percentages, the size of the transmission effect, and the percentage of the transmission effect caused by acquired polarization. Second, the effect of imperfect target polarization reversal on the value of the transmission effect is determined in the case of Cd-113. It is found that target orientation inefficiencies as small as 3 pct. will mimic a parity violation. Third, the effect of the depolarization term on the relative size of the acquired polarization is explored. GRA

N92-26200*# Science Applications International Corp., Prospect, TN.
GEOMETRY AND MASS MODEL OF IONIZING RADIATION EXPERIMENTS ON THE LDEF SATELLITE Final Report
B. L. Colborn and T. W. Armstrong Apr. 1992 45 p
(Contract NAS8-39121)
(NASA-CR-184325; NAS 1.26:184325; SAIC-TN-9202) Avail: NTIS HC/MF A03

Extensive measurements related to ionizing radiation environments and effects were made on the LDEF satellite during its mission lifetime of almost 6 years. These data, together with the opportunity they provide for evaluating predictive models and analysis methods, should allow more accurate assessments of the space radiation environment and related effects for future missions in low Earth orbit. The LDEF radiation dosimetry data is influenced to varying degrees by material shielding effects due to the dosimeter itself, nearby components and experiments, and the spacecraft structure. A geometry and mass model is generated of LDEF, incorporating sufficient detail that it can be applied in determining the influence of material shielding on ionizing radiation measurements and predictions. This model can be used as an aid in data interpretation by unfolding shielding effects from the LDEF radiation dosimeter responses. Use of the LDEF geometry/mass model, in conjunction with predictions and comparisons with LDEF dosimetry data currently underway, will also allow more definitive evaluations of current radiation models for future mission applications. Author

N92-26207# California Univ., Berkeley. Lawrence Berkeley Lab.
GENERATION OF NONEQUILIBRIUM OPTICAL PHONONS IN GaAs/AlAs QUANTUM WELLS BY INTRASUBBAND AND INTERSUBBAND SCATTERINGS
K. R. Wald, Dai-sik Kim, and P. Y. Yu Nov. 1991 11 p Presented at the Recent Advances in the Uses of Light in Physics, Chemistry and Medicine, New York, NY, 19-21 Jun. 1991
(Contract DE-AC03-76SF-00098)
(DE92-010264; LBL-31481; CONF-9106105-1) Avail: NTIS HC/MF A03

The generation of a nonequilibrium population of optical phonons by photoexcited hot electrons in semiconductor quantum wells is investigated theoretically. The microscopic model of electron-phonon interaction proposed by Huang and Zhu has been used to compute the distributions of confined longitudinal optical phonons and interface modes in GaAs/AlAs quantum wells as a function of well width. Experimental tests of the calculated distributions by Raman scattering are discussed. DOE

N92-26225# Sandia National Labs., Albuquerque, NM.
CALIBRATION OF CR-39 FOR DETECTING FUSION NEUTRONS
M. T. Collopy, P. Carpenter, C. D. Harmon, J. Vandenberg, G. W. Cooper (New Mexico Univ., Albuquerque.), C. L. Ruiz, P. Reyes, W. A. Stygar, and A. Schmidlapp 1992 13 p Presented at the 9th Topical Conference on High-Temperature Plasma Diagnostics, Santa Fe, NM, 15-19 Mar. 1992

(Contract DE-AC04-76DP-00789)
(DE92-009063; SAND-92-0063C; CONF-920362-2) Avail: NTIS HC/MF A03

We have measured the efficiency (tracks per incident neutron) of pure CR-39 for detecting deuterium-deuterium (DD) and deuterium-tritium (DT) neutrons. Neutrons having average energies of 2.9 MeV (DD) and 14.8 MeV (DT) were produced by a 200 keV electrostatic accelerator and the neutron yields were measured using the associated particle counting technique. All CR-39 samples irradiated by DD or DT neutrons were etched for two hours in a 70 degree, 6.25 (und N) NaOH bath. For bare CR-39, the efficiencies for detecting 2.9-MeV and 14.8-MeV neutrons were found to be (1.3 +/- 0.4) x 10(exp -4) and (5.0 +/- 1.8) x 10(exp -5), respectively. We also investigated using CR-39 and polyimide as proton radiators. For detecting 2.9-MeV neutrons, the radiators had no significant effect on efficiency, but for detecting 14.8 MeV neutrons, the polyimide radiator increased the efficiency to (7.8 +/- 2.8) x 10(exp -5). DOE

N92-26235# California Univ., Berkeley. Lawrence Berkeley Lab.
BIS (PENTAMETHYLCYCLOPENTADIENYL) YTTERBIUM: ELECTRON-TRANSFER REACTIONS WITH ORGANOTRANSITION METAL COMPLEXES Ph.D. Thesis
P. T. Matsunaga Nov. 1991 213 p
(Contract DE-AC03-76SF-00098)
(DE92-010300; LBL-31491) Avail: NTIS HC/MF A10

The divalent lanthanide complex, (Me5C5)2Yb, reacts with methylcopper to produce the base-free, ytterbium-methyl complex, (Me5C5)2YbMe. This product forms an asymmetric, methyl-bridged dimer in the solid state. The bulky alkyl complex, (Me5C5)2YbCH(SiMe3)2, displays similar chemistry to (Me5C5)2YbMe, but at a reduced reaction rate due to the limited accessibility of the metal in (Me5C5)2YbCH(SiMe3)2. Copper and silver halide salts react with (Me5C5)2V to produce the trivalent halide derivatives, (Me5C5)2VX (X = F, Cl, Br, I). The chloride complex, (Me5C5)2VCl, reacts with lithium reagents to form the phenyl and borohydride species. Nitrous oxide transfers an oxygen atom to (Me5C5)2V producing the vanadium-oxo complex, (Me5Ce5)2VO. The trivalent titanium species, (Me5C5)2TiX (X = Cl, Br, Me, BH4), form bimetallic coordination complexes with (Me5C5)2Yb. The magnetic behavior of the products indicates that electron transfer has not occurred. The solid state structures of the chloride and bromide complexes show unusual bend angles for the halide bridges between ytterbium and titanium. A model based on frontier orbital theory has been proposed to account for the bending behavior in these species. The bimetallic methyl complex contains a linear methyl bridge between ytterbium and titanium. DOE

N92-26240# Michigan Univ., Ann Arbor. Dept. of Atmospheric, Oceanic and Space Science.
ENERGY TRANSFER PROPERTIES AND MECHANISMS
J. R. Barker 30 Jan. 1992 4 p
(Contract DE-FG02-85ER-13442)
(DE92-011215; DOE/ER-13442/6) Avail: NTIS HC/MF A01

The overall objective of the research carried out under this program is to determine the principles of collisional energy transfer and use them in predictive models and theories. In order to accomplish this goal, energy transfer properties must be determined and then analyzed to discern the underlying principles involved. In this laboratory, the experimental determination of energy transfer parameters is based on techniques that use physical properties to monitor the amount of energy in excited molecules. These techniques differ from chemical methods, based on unimolecular reaction studies, which are susceptible to interferences from complex chemical mechanisms and other complications. The physical methods have their own weaknesses and limitations, however, and much of our effort has been directed toward gaining a better understanding of these deficiencies. Two physical techniques have been proved to be particularly useful: time-resolved infrared fluorescence and time-dependent thermal lensing. As described later, we will shortly begin work using resonance enhanced multiphoton ionization techniques to investigate energy transfer in bulbs and 'half collisions' in free jets. We also have been completing some calculational efforts to model formation of polycyclic aromatic hydrocarbons in stellar atmospheres. DOE

N92-26365# International Centre for Theoretical Physics, Trieste (Italy).
Li-6,d REACTION ON sd-, fp- AND g-SHELL NUCLEI IN ZR- AND FR-DWBA FORMALISMS
M. A. Rahman, M. Mecking, and U. Strohbusch (Hamburg Univ., Germany, F.R.) Jun. 1991 10 p
(DE92-614353; IC-91/130) Avail: NTIS HC/MF A02

(Li-6,d) reaction angular distributions on target nuclei A between 16 and 90 were analyzed using both ZR- and FR-DWBA formalisms. The most prevalent method of analysis of alpha-transfer reactions such as (Li-6,d) and its reverse (d, Li-6) (where the wave function at zero distance in the p-state of relative cluster motion in the A = 6 nuclei will not have node) is the ZR-DWBA calculations due to the relatively short time of computation. It is of particular interest to verify whether FR-DWBA calculations result in similar S(sub alpha) values to those of ZR-DWBA or not. It is found that to derive similar S(sub alpha)-values as in FR-DWBA calculations, one requires relatively large real well depth in ZR-DWBA calculations. Qualitative discussions have been made in this direction. DOE

N92-26539*# National Aeronautics and Space Administration. Ames Research Center, Moffett Field, CA.
THE COMPUTATION OF C-C AND N-N BOND DISSOCIATION ENERGIES FOR SINGLY, DOUBLY, AND TRIPLY BONDED SYSTEMS
Stephen R. Langhoff, Charles W. Bauschlicher, Jr., and Peter R. Taylor (Eloret Corp., Palo Alto, CA.) 1989 14 p Previously announced as A91-54398
(Contract NCC2-371)
(NASA-CR-190254; NAS 1.26:190254) Avail: NTIS HC/MF A03

The bond dissociation energies (D sub e) of C2H2, C2H4, C2H6, N2, N2H2, and N2H4 are studied at various levels of correlation treatment. The convergence of D sub e with respect to the one particle basis is studied at the single reference modified coupled-pair functional (MCPF) level. At all levels of correlation treatment, the errors in the bond dissociation energies increase with the degree of multiple bond character. The multireference configuration interaction (MRCI) D sub e values, corrected for an estimate of higher excitations, are in excellent agreement with those determined using the size extensive averaged coupled pair functional (ACPF) method. It was found that the full valence complete active space self consistent field (CASSCF)/MRCI calculations are reproduced very well by MRCI calculations based on a CASSCF calculation that includes in the active space only those electrons involved in the C-C or N-N bonds. To achieve chemical accuracy (1 kcal/mole) for the D sub e values of the doubly bonded species C2H4 and N2H2 requires one particle basis sets including up through h angular momentum functions (l = 5) and a multireference treatment of electron correlation: still higher levels of calculation are required to achieve chemical accuracy for the triply bonded species C2H2 and N2. Author

N92-26570# Vanderbilt Univ., Nashville, TN. Dept. of Physics and Astronomy.
NEW APPROACHES TO STUDIES OF EXOTIC NUCLEI
J. H. Hamilton 1991 34 p Presented at the International School of Nuclear Physics on 4Pi High Resolution Gamma-ray, Erice, Italy, 20-28 Sep. 1991
(Contracts DE-AC05-84OR-21400; DE-AC05-76OR-00033; DE-FG05-88ER-40407)
(DE92-010127; CONF-9109332-4) Avail: NTIS HC/MF A03

New generations of 4pi gamma ray detectors, recoil mass spectrometers (RMS), and radioactive beam accelerators will open up many new areas of research, including present inaccessible in-beam and radioactive decay studies of exotic nuclei still farther off stability. The new generation RMS and radioactive beam

developments at the Holifield Heavy Ion Research Facility are presented. Current research and further prospects to probe the N-Z line up to Sn-100 are described. Superdeformation in A-70 to 190 nuclei is described in terms of its underlying physics of reinforcing proton and neutron shell gaps which lead to new superdeformed, doubly-magic nuclei. Recent results provide new insights into the coexistence of multiple nuclear shapes near the ground states. DOE

N92-26574# Toledo Univ., OH. Dept. of Physics and Astronomy.
MEASUREMENTS OF SCATTERING PROCESSES IN NEGATIVE ION-ATOM COLLISIONS
T. J. Kvale 1992 12 p
(Contract DE-FG05-88ER-13971)
(DE92-010319; DOE/ER-13971/13) Avail: NTIS HC/MF A03

This Technical Progress Report describes the progress made on the research objectives during the past twelve months. This research project is designed to provide measurements of various scattering processes which occur in H(sup -) collisions with atomic (specifically, noble gas and atomic hydrogen) targets at intermediate energies. These processes include: elastic scattering, single and double-electron detachment, and target excitation/ionization. For the elastic and target inelastic processes where H(sup -) is scattered intact, the experimental technique of Ion Energy-Loss Spectroscopy (IELS) will be employed to identify the final target state(s). In most of the above processes, cross sections are unknown both experimentally and theoretically. The measurements in progress will provide either experimentally determined cross sections or set upper limits to those cross sections. In either case, these measurements will be stringent tests of our understanding in energetic negative ion-atom collisions. This series of experiments required the construction of a new facility and the initial ion beam was accelerated through the apparatus in April 1991. DOE

N92-26588# California Univ., Berkeley. Dept. of Chemistry.
QUANTUM DYNAMICS OF HELIUM CLUSTERS Final Report
K. B. Whaley 1992 5 p
(Contract N00014-89-J-1755)
(AD-A245752) Avail: NTIS HC/MF A01

Our study of helium clusters was motivated by the desire to understand the scaling of the unusual properties of bulk He-4, a quantum liquid, in finite size systems as one goes from the macroscopic regime to the regime of molecular dimensions. This is fully in the spirit of general cluster research, namely to develop our understanding of how the transition from molecular to bulk systems (or vice versa) is reflected in the internal structure and dynamics of finite size aggregates. The unique feature of helium is its dominant quantum behavior, resulting from a low mass and weak interatomic binding energy. Clusters of helium are therefore very weakly bound van der Waals species, whose properties are expected to be dominated by zero point delocalization effects. During this grant period, we devoted our attention exclusively to clusters of He-4, which are Bose systems. These are more strongly bound than the fermionic species He-3(sub N), and are also easier and cheaper to study experimentally. Furthermore, analogy with the bulk behavior suggests that any superfluid effects, if present, will occur at considerably higher and therefore more experimentally accessible temperatures for He-4(sub N). GRA

N92-26800# Gosudarstvennyi Komitet po Ispolzovaniyu Atomnoi Energii, Serpukhov (USSR). Inst. Fiziki Vysokikh Ehnergij.
NEW DESCRIPTION OF MULTIPLICITY DISTRIBUTION IN INELASTIC MESON-PROTON INTERACTIONS
O. G. Chikilev and P. V. Shlyapnikov 1991 10 p In RUSSIAN; ENGLISH summary
(DE92-621167; IFVE-ONF-91-34) Avail: NTIS HC/MF A02

It is shown that the two-parameter function P(sub N)(epsilon,b), describes well experimental data on negatively charged particle multiplicity distributions in inelastic meson-proton interactions. The parameter b rises with energy square root of s as ln(square root of s), whereas the second parameter epsilon has a strong energy dependence only at low square root of s. DOE

N92-26844# Instituto Politecnico Nacional, Mexico City. Escuela Superior de Fisica y Matematicas.
NUMERICAL SOLUTION OF THE EQUATION OF NEUTRONS TRANSPORT ON PLANE GEOMETRY BY ANALYTICAL SCHEMES USING ACCELERATION BY SYNTHETIC DIFFUSION Ph.D. Thesis [SOLUCION NUMERICA DE LA ECUACION DE TRANSPORTE DE NEUTRONES EN GEOMETRIA PLANA MEDIANTE ESQUEMAS ANALITICOS EMPLEANDO ACELERACION POR DIFUSION SINTETICA]
G. Alonso-Vargas 1991 136 p In SPANISH
(DE92-621426; INIS-mf-13134) Avail: NTIS HC/MF A07

A computer program has been developed which uses a technique of synthetic acceleration by diffusion by analytical schemes. Both in the diffusion equation as in that of transport, analytical schemes were used which allowed a substantial time saving in the number of iterations required by source iteration method to obtain the K(sub e)ff. The program developed ASD (Synthetic Diffusion Acceleration) by diffusion was written in FORTRAN and can be executed on a personal computer with a hard disc and mathematical O-processor. The program is unlimited as to the number of regions and energy groups. The results obtained by the ASD program for K(sub e)ff is nearly completely concordant with those obtained by utilizing the ANISN-PC code for different analytical type problems in this work. The ASD program allowed obtention of an approximate solution of the neutron transport equation with a relatively low number of internal reiterations with good precision. One of its applications would be in the direct determinations of axial distribution neutronic flow in a fuel assembly as well as in the obtention of the effective multiplication factor. DOE

73 NUCLEAR AND HIGH-ENERGY PHYSICS

Includes elementary and nuclear particles; and reactor theory.

For space radiation see *93 Space Radiation.*

N92-26692# Los Alamos National Lab., NM.
ASSESSMENT OF A HOT HYDROGEN NUCLEAR PROPULSION FUEL TEST FACILITY
H. H. Watanabe, S. D. Howe, and P. J. Wantuck 1991 10 p Presented at the 9th World Hydrogen Energy Conference, Paris, France, 22-25 Jun. 1992
(Contract W-7405-eng-36)
(DE92-004571; LA-UR-91-4177; CONF-920643-1) Avail: NTIS HC/MF A02

Subsequent to the announcement of the Space Exploration Initiative (SEI), several studies and review groups have identified nuclear thermal propulsion as a high priority technology for development. To achieve the goals of SEI to place man on Mars, a nuclear rocket will operate at near 2700 K and in a hydrogen environment at near 60 atmospheres. Under these conditions, the operational lifetime of the rocket will be limited by the corrosion rate at the hydrogen/fuel interface. Consequently, the Los Alamos National Laboratory has been evaluating requirements and design issues for a test facility. The facility will be able to directly heat fuel samples by electrical resistance, microwave deposition, or radio frequency induction heating to temperatures near 3000 K. Hydrogen gas at variable pressure and temperatures will flow through the samples. The thermal gradients, power density, and operating times envisioned for nuclear rockets will be duplicated as close as reasonable. The post sample flow stream will then be scrubbed and cooled before reprocessing. The baseline design and timetable for the facility will be discussed. DOE

N92-26815# Brookhaven National Lab., Upton, NY.
OPEN PROBLEMS AND FUTURE PROSPECTS FOR HYPERNUCLEAR PHYSICS

C. B. Dover Jan. 1992 18 p Presented at the International Symposium on Hypernuclear and Strange Particle Physics, Shimoda, Japan, 9-12 Dec. 1991
(Contract DE-AC02-76CH-00016)
(DE92-010158; BNL-47115; CONF-911208-7) Avail: NTIS HC/MF A03

We appraise the current status of our knowledge of hypernuclear structure physics, and emphasize the unsolved problems. The prospects for significant advances in high resolution hypernuclear spectroscopy with CW electron beams at CEBAF or intense pion beams at the proposed PILAC facility at LPF are discussed. These facilities could greatly extend our understanding of strangeness S = -1 hypernuclear systems. For S = -2 systems, new events have been seen in a (K(sup -),K(sup +)) hybrid counter emulsion experiment at KEK in Japan. We give a theoretical interpretation of one of these events, as well as some further possibilities for the exploration of (Lambda)(Lambda) hypernuclear spectroscopy via Xi(sup -)-atoms. We mention some possible enhancements of (K(sup -),K(sup +)) or (K(sup -),K(sup 0)) cross sections to discrete states, due to Xi(N)-(Lambda)(Lambda) configuration mixing in a shell model description of S = -2 hypernuclei. Finally, we explore the possibilities for producing multi-strange nuclei or droplets of strange quark matter ('strangelets') in relativistic heavy ion collisions. DOE

N92-26832*# National Aeronautics and Space Administration. Langley Research Center, Hampton, VA.
QUASI-ELASTIC NUCLEAR SCATTERING AT HIGH ENERGIES
Francis A. Cucinotta, Lawrence W. Townsend, and John W. Wilson May 1992 23 p
(RTOP 593-42-21-01)
(NASA-TM-4362; L-17036; NAS 1.15:4362) Avail: NTIS HC/MF A03

The quasi-elastic scattering of two nuclei is considered in the high-energy optical model. Energy loss and momentum transfer spectra for projectile ions are evaluated in terms of an inelastic multiple-scattering series corresponding to multiple knockout of target nucleons. The leading-order correction to the coherent projectile approximation is evaluated. Calculations are compared with experiments. Author

N92-26841# Argonne National Lab., IL.
EVALUATION OF INTEGRAL MEASUREMENTS FOR THE SP-100 SPACE REACTOR
P. J. Collins, G. L. Grasseschi, and S. E. Aumeier (Michigan Univ., Ann Arbor.) 1992 32 p Presented at the Advances in Reactor Physics, Charleston, SC, 8-11 Mar. 1992
(Contract W-31-109-eng-38)
(DE92-009717; ANL/CP-73148; CONF-920308-16) Avail: NTIS HC/MF A03

Experiments in support of the SP-100 space reactor were done in the Zero Power Physics Reactor-20 (ZPPR-20). Biases in calculations were found for criticality predictions and control worths. Although the biases were on the conservative side for SP-100, the more general question of the reasons for the calculational errors is important for design optimization and for other fast space reactor designs. A data sensitivity analysis was made for the ZPPR-20 results using the GMADJ code. Results for ZPPR-20 are used in comparison with a wide database of fast reactor parameters. It is shown that calculations of criticality for the reference core, for a core simulating water immersion, and for the control rod worths are consistent with all other benchmark data and that differences in prediction are within uncertainties in nuclear data. The results from ZPPR-20 can be used with confidence for prediction of calculational bias factors and uncertainties in SP-100 and related designs. The most effective use of the ZPPR-20 data would be to create a sensitivity file for SP-100 and use the GMADJ system to produce biases and uncertainties. DOE

74 OPTICS

Includes light phenomena; and optical devices.
For lasers see *36 Lasers and Masers.*

N92-26187# California Univ., Berkeley. Lawrence Berkeley Lab.
SPECTROSCOPIC IMAGING, DIFFRACTION, AND HOLOGRAPHY WITH X RAY PHOTOEMISSION
Feb. 1992 322 p Presented at the Spectroscopic Imaging, Diffraction, and Holography With X-ray Photo Emission, Berkeley, CA, 14-16 Aug. 1991
(Contract DE-AC03-76SF-00098)
(DE92-009142; LBL-31853; CONF-9108191) Avail: NTIS HC/MF A14

X-ray probes are capable of determining the spatial structure of an atom in a specific chemical state, over length scales from about a micron all the way down to atomic resolution. Examples of these probes include photoemission microscopy, energy-dependent photoemission diffraction, photoelectron holography, and X-ray absorption microspectroscopy. Although the method of image formation, chemical-state sensitivity, and length scales can be very different, these X-ray techniques share a common goal of combining a capability for structure determination with chemical-state specificity. This workshop will address recent advances in holographic, diffraction, and direct imaging techniques using X-ray photoemission on both theoretical and experimental fronts. A particular emphasis will be on novel structure determinations with atomic resolution using photoelectrons. DOE

N92-26241# Naval Postgraduate School, Monterey, CA.
CLUSTER MODEL OF POLARIZATION REFLECTION FROM METALLIC SURFACES M.S. Thesis
Craig W. Baldwin Dec. 1991 68 p
(AD-A245781) Avail: NTIS HC/MF A04

Polarization of light is at best only partially explained by current models. A new model is proposed to account for this phenomenon involving 'native clusters'. These clusters are assumed to be an integral part of some bulk surfaces and to manifest their dielectric properties in the visible region. An index of refraction may be computed based on a pseudo-Brewster angle, that angle of incidence where the minimum perpendicular reflectance occurs. Next, the model identifies the cluster-to-bulk surface area ratio of the material and formulates the contribution of reflection from these areas by utilizing the Fresnel equations. Reflectance from the remainder, the bulk surface area, is computed by applying conventional metallic reflection techniques. By combining the two contributions of reflectance for angles of incidence from 0 to 90 degrees, reflectance curves are generated for gold, silver, nickel, and aluminum. These calculations assume a wide-band radiating source of light. Although the magnitude of reflectance for the model showed some variance over the range of angles of incidence (within 10 percent), the curves are similar in shape. GRA

N92-26376# Oak Ridge National Lab., TN.
RESULTS OF A PORTABLE FIBER-OPTIC WEIGH-IN-MOTION SYSTEM
J. D. Muhs, J. K. Jordan, M. B. Scudiere, and K. W. Tobin, Jr. 1991 14 p Presented at the SPIE Meeting, Boston, MA, 3-6 Sep. 1991
(Contract DE-AC05-84OR-21400)
(DE92-009011; CONF-9109230-11) Avail: NTIS HC/MF A03

Experimental results on a portable, low-speed, fiber-optic weigh-in motion system are described that demonstrate the applicability of fiber-optic-based sensors in transportation, defense, and law enforcement applications where accurate weight determination of moving vehicles is necessary. Results are given on the systems' dynamic range (0.1-30 metric tons), velocity range (up to 5 km/h), accuracy error (0.5-3.0 percent), and repeatability. Also included in the paper is a discussion of the sources of error associated with low-speed weigh-in-motion systems and methods of minimizing these errors for practical deployment. DOE

N92-26425# Carnegie-Mellon Univ., Pittsburgh, PA. Robotics Inst.
DYNAMIC LENS COMPENSATION FOR ACTIVE COLOR IMAGING AND CONSTANT MAGNIFICATION FOCUSING
Reg G. Willson and Steven A. Shafer Nov. 1991 52 p
(Contract F33615-90-C-1465; ARPA Order 7597)
(AD-A245713; CMU-RI-TR-91-26) Avail: NTIS HC/MF A04

Vision researchers base their work on assumptions that lenses behave ideally. In practice, the image formation process is complex and camera lenses have many non-ideal behaviors that can cause problems in simple vision tasks like color image analysis and range from focus. For example, unlike the ideal lens, the refractive power of a real lens is actually a function of wavelength. This means that images of a scene taken under different wavelengths will have slightly different focus and magnification. The resulting misregistration between the images when they are superimposed to form a composite color image can cause significant problems in color image analysis. Another property of real lenses is that focusing the lens also changes its magnification. In range from focus, these changes in image magnification can bias the position of a sharpness criterion function's peak leading to errors in the range estimates. By precisely controlling the lens during imaging, it is possible to make lenses behave more ideally. We have developed a procedure we call Active Color Imaging in which lens magnification and focus are precisely compensated to produce color images that are over ten times better registered than uncompensated color images. We have also developed a procedure we call Constant Magnification Focusing which allows a user to focus a lens without changing the image magnification, eliminating focus magnification induced errors in range from focus tasks.
GRA

N92-26452# Sandia National Labs., Albuquerque, NM.
THE DEVELOPMENT OF AN OPTICAL FIBER ACCELEROMETER
S. A. Casalnuovo, G. E. Sleefe, and C. E. James (Ktech Corp., Albuquerque, NM.) 1992 11 p Presented at the Department of Defense Fiber Optics Conference, McLean, VA, 25 Mar. 1992
(Contract DE-AC04-76DP-00789)
(DE92-008680; SAND-91-2751C; CONF-920367-6) Avail: NTIS HC/MF A03

We describe the design and operation of an optical fiber accelerometer intended for environments inhospitable to electronic components. An overview of the device is presented along with descriptions of the optical, electronic, and mechanical components. The performance of the current prototype is equivalent to state of the art piezoelectric accelerometers. Improvements to the current design are discussed.
DOE

N92-26565# Argonne National Lab., IL.
MAGNETO-OPTICAL MULTILAYERS
S. D. Bader Feb. 1992 12 p Presented at the SPIE Technical Conference and Exhibition on Electronic Imaging, San Jose, CA, 9-14 Feb. 1992
(Contract W-31-109-eng-38)
(DE92-009726; ANL/CP-75618; CONF-920212-2) Avail: NTIS HC/MF A03

Magneto-optical multilayers are of interest to the optical data storage community as a possible second-generation medium of the future. The important Co/Pt-superlattice system is introduced in this respect, and an extensive reference listing is provided to previous research. Magneto-optical modeling studies of Co/Pt are presented, and it is concluded that the interfacial Pt is magnetized and is magneto-optically active at the short wavelengths of interest (approximately 4 eV) for applications. Magneto-optics in the ultrathin limit are discussed, and an additivity law is presented and verified experimentally utilizing data for epitaxial Fe/Ag(111) superlattices. Finally, the surface magnetic anisotropy that provides the vertical easy axes of magnetization in candidate superlattice systems is discussed and illustrated experimentally using ultrathin epitaxial films of Fe grown on a variety of substrates. It is concluded that magneto-optic multilayers will provide many stimulating basic and applied challenges in the years ahead.
DOE

N92-26662# Naval Postgraduate School, Monterey, CA.
REAL TIME IMAGING AND INFRARED BACKGROUND SCENE ANALYSIS USING THE NAVAL POSTGRADUATE SCHOOL INFRARED SEARCH AND TARGET DESIGNATION (NPS-IRSTD) SYSTEM M.S. Thesis
Jean D. Bernier Sep. 1991 105 p
(AD-A245527) Avail: NTIS HC/MF A06

The imaging in real time of infrared background scenes with the Naval Postgraduate School Infrared Search and Target Designation (NPS-IRSTD) System was achieved through extensive software developments in protected mode assembly language on an Intel 80386 33 MHz computer. The new software processes the 512 by 480 pixel images directly in the extended memory area of the computer where the DT-2861 frame grabber memory buffers are mapped. Direct interfacing, through a JDR-PR10 prototype card, between the frame grabber and the host computer AT bus enables each load of the frame grabber memory buffers to be effected under software control. The protected mode assembly language program can refresh the display of a six degree pseudo-color sector in the scanner rotation within the two second period of the scanner. A study of the imaging properties of the NPS-IRSTD is presented with preliminary work on image analysis and contrast enhancement of infrared background scenes.
Author (GRA)

N92-26676# Martin Marietta Corp., Orlando, FL. Electronics Information and Missiles Group.
CONQUEST OF DARKNESS BY MANAGEMENT OF THE STARS
Robert S. Wiseman 1991 33 p
(AD-A245496) Avail: NTIS HC/MF A03

This text was presented as the Thomas B. Dowd Memorial Lecture for 1991 national Infrared Information Symposium (IRIS). The history of Army Night Vision from World War II to 1972 proves how the right organization with talented people and proper support can succeed. This presentation not only illustrates the growth of image intensifier technology and families of equipment, but the key events and stars that made it all happen. Described are the management techniques used and how to organize for effective research, development, engineering, and production programs; the evolution of the Far Infrared Common Module program is described; and how the Night Vision Laboratory was unique.
GRA

N92-26754# Naval Postgraduate School, Monterey, CA.
FOCUSING X RAY TRANSITION RADIATION WITH CYLINDRICAL AND ELLIPTICAL OPTICS M.S. Thesis
Paul M. Votruba Dec. 1991 99 p
(AD-A245987) Avail: NTIS HC/MF A05

We have demonstrated the ability of a nickel elliptical tube to focus the conically diverging pattern of x ray transition radiation. The x ray TR was produced by passing moderate-energy (60 to 100 MeV) electron beams through targets consisting of thin (1 micron) multiple foils of aluminum and titanium. The foils were placed in a vacuum chamber; perpendicular to the Naval Postgraduate School's linac primary beamline. An elliptical nickel tube, with a length of 30.5 cm, was placed concentric to the axis of the conical photon beam (as defined by the axis of the electron beam) with an entrance and exit of 1.4 and 1.7 m, respectively, from the source of the TR at the end of the foil stack. The intensity profile was subsequently measured with a linear image detector placed 3.0 m from the exit of the foil stack. Through a series of experiments, taking into account the effects of surface roughness, the nickel elliptical tube demonstrated the ability to collect 3 to 5 times more energy than a cylindrical quartz tube.
GRA

N92-26862# Department of the Navy, Washington, DC.
OPTICAL FLOW SENSOR Patent Application
Thomas G. Giallorenzi, inventor (to Navy) 30 Sep. 1991 15 p
(AD-D015200; US-Patent-Appl-SN-767189; Navy-Case-70938)
Avail: NTIS HC/MF A03

A thermal dilation type optical flow sensor includes an optical heating source for heating a flowing fluid and a sensor disposed

in a downstream direction from a said heating source wherein the sensor includes a probe for varying a reflected light according to the temperature of the probe, a Michelson type interferometer for measuring the temperature of the probe according to the phase of the reflected light, and a calculating device for determining the flow rate based on the temperature of the probe, the distance between the heating source and the probe, and the amount of heat produced by the heating source. In an alternative embodiment, a thermal dilation type optical flow sensor includes a reflecting probe disposed in the flowing fluid for reflecting an incident light with a phase varied according to the probe temperature, an optical heater for heating the probe with a predetermined heat, and a calculating device for calculating a flow rate based on the predetermined heat and the phase of the reflected light. GRA

N92-26943# Arizona Univ., Tucson. Optical Sciences Center.
HIGH-SPEED PULSE DETECTION ROOM-TEMPERATURE OPTICAL NONLINEARITIES FOR GaInAs/A1InAs AND GaA1InAs/A1InAs MULTIPLE QUANTUM WELLS AND INTEGRATED MIRROR ETALON AT 1.3 MICROMETERS Final Report, Dec. 1989 - Jul. 1991
N. Peyghambarian, Steven T. Johns, Mark F. Krol, John L. Stacy, and Raymond K. Boncek Dec. 1991 35 p
(Contract F30602-88-D-0026)
(AD-A246369; RL-TR-91-341) Avail: NTIS HC/MF A03

As a result of the advances in optical fiber communication technology, the dream of a high bit-rate telecommunication system now becomes possible. However, the performance of optical fiber communication systems is limited due to the lack of a high speed signal processor to process the information. At present, the processing speed of an optical fiber communications system is determined by the speed of an electronic logic gate. Currently, the switching times of an electronic transistor is usually in 0.1 to 1 ns range and this switching speed is already approaching some of its fundamental limits. On the other hand, optical switching devices have exhibited sub-picosecond switching speeds, so photonic processing is an alternative technology of processing signals in optical fiber communications systems. Photonic processing also has the potential to avoid the optical-electronic conversion which is used now in the telecommunication system. The optical time-division multiplexing technique is an extension of the well-known electronic multiplexing technique. In an optical time-division multiplexing system, a high bit-rate data stream is constructed directly by time-multiplexing several lower bit-rate signals. Similarly, at the receiver end of the system, the very high bit-rate optical signal is demultiplexed to several lower bit-rate optical signals before detection and conversion to the electronic domain. GRA

N92-27186 Department of the Navy, Washington, DC.
DIFFERENTIAL POLARIMETRIC FIBER OPTIC SENSOR Patent
Alan D. Kersey, inventor (to Navy) 8 Oct. 1991 8 p Filed 16 Jan. 1990
(AD-D015218; US-Patent-5,054,922; US-Patent-Appl-SN-465677; US-Patent-Class-356-345) Avail: US Patent and Trademark Office

A differential polarimetric fiber optic sensor is disclosed in which a local compensating fiber section is spatially separated from a remote sensing fiber section by input and output polarization-maintaining fibers in order to permit the remote passive interrogation of the remote sensing fiber section by the direct polarization analysis of the light at the output of the local compensating fiber section. GRA

N92-26975# Max-Planck-Inst. fuer Aeronomie, Katlenburg-Lindau (Germany, F.R.).
DEVELOPMENT OF A THERMAL CONTROL CONCEPT FOR THE OPTICAL SYSTEM OF THE SUMER EXPERIMENT ON SOHO
W. Curdt and H. Rathjen *In* ESA, 4th European Symposium on Space Environmental Control Systems, Volume 2 Dec. 1991 p 785-790 Prepared in cooperation with Erno Raumfahrttechnik G.m.b.H. Bremen, Fed. Republic of Germany (For primary document see N92-26950 17-54)
Avail: NTIS HC/MF A23; ESA, EPD, ESTEC, Noordwijk, Netherlands, HC 150 Dutch guilders (2 vols)

N92-27089*# Phillips Lab., Kirkland AFB, NM. Optoelectronics Section.
PRELIMINARY ANALYSES OF WL EXPERIMENT NO. 701, SPACE ENVIRONMENT EFFECTS ON OPERATING FIBER OPTIC SYSTEMS
E. W. Taylor, J. N. Berry, A. D. Sanchez, R. J. Padden, and S. P. Chapman *In* NASA. Langley Research Center, LDEF: 69 Months in Space. First Post-Retrieval Symposium, Part 3 Jan. 1992 p 1257-1282 (For primary document see N92-27083 17-99)
Avail: NTIS HC/MF A21; 1 functional color page

N92-27090*# Jet Propulsion Lab., California Inst. of Tech., Pasadena.
LDEF FIBER OPTIC EXPOSURE EXPERIMENT NO. S-0109
A. R. Johnston, L. A. Bergman, and R. Hartmayer *In* NASA. Langley Research Center, LDEF: 69 Months in Space. First Post-Retrieval Symposium, Part 3 Jan. 1992 p 1283-1298 (For primary document see N92-27083 17-99)
Avail: NTIS HC/MF A21; 1 functional color page

N92-27091*# Optical Coating Lab., Inc., Santa Rosa, CA.
OPTICAL PERFORMANCE OF EXPOSED SOLAR CELL COVERS Abstract Only
Thomas H. Allen, Bryant P. Hichwa, Steven R. Selee, Jerry Dodds, and Greg S. Long *In* NASA. Langley Research Center, LDEF: 69 Months in Space. First Post-Retrieval Symposium, Part 3 Jan. 1992 p 1299 (For primary document see N92-27083 17-99)
Avail: NTIS HC/MF A21; 1 functional color page

N92-27093*# McDonnell-Douglas Electronics Co., Saint Louis, MO.
POST-FLIGHT CHARACTERIZATION OF OPTICAL SYSTEM SAMPLES, THERMAL CONTROL SAMPLES, AND DETECTORS FROM LDEF EXPERIMENT M0003, SUB-EXPERIMENTS 6 AND 13 Abstract Only
Randall R. Hodgson, James N. Holsen, and Robert A. Drerup, Jr. (Wright Lab., Wright-Patterson AFB, OH.) *In* NASA. Langley Research Center, LDEF: 69 Months in Space. First Post-Retrieval Symposium, Part 3 Jan. 1992 p 1315 (For primary document see N92-27083 17-99)
Avail: NTIS HC/MF A21; 1 functional color page

N92-27094*# Georgia Inst. of Tech., Atlanta.
LDEF ACTIVE OPTICAL SYSTEM COMPONENTS EXPERIMENT
M. D. Blue *In* NASA. Langley Research Center, LDEF: 69 Months in Space. First Post-Retrieval Symposium, Part 3 Jan. 1992 p 1317-1326 (For primary document see N92-27083 17-99)
Avail: NTIS HC/MF A21; 1 functional color page

N92-27095*# National Aeronautics and Space Administration. Langley Research Center, Hampton, VA.
EFFECTS OF LONG-DURATION EXPOSURE ON OPTICAL SYSTEM COMPONENTS
Gale A. Harvey *In its* LDEF: 69 Months in Space. First Post-Retrieval Symposium, Part 3 Jan. 1992 p 1327-1340 (For primary document see N92-27083 17-99)
Avail: NTIS HC/MF A21; 1 functional color page

N92-27096*# Eastman Kodak Co., Rochester, NY.
EFFECTS OF LONG TERM EXPOSURE ON OPTICAL SUBSTRATES AND COATINGS (SOO50-2)
John Vallimont and Keith Havey *In* NASA. Langley Research Center, LDEF: 69 Months in Space. First Post-Retrieval Symposium, Part 3 Jan. 1992 p 1341-1342 (For primary document see N92-27083 17-99)
Avail: NTIS HC/MF A21; 1 functional color page

N92-27097*# MATRA Service Aerodynamique, Velizy-Villacoublay (France).
VACUUM DEPOSITED OPTICAL COATINGS EXPERIMENT
Jean Charlier *In* NASA. Langley Research Center, LDEF: 69 Months in Space. First Post-Retrieval Symposium, Part 3 Jan. 1992 p 1343-1360 (For primary document see N92-27083 17-99)
Avail: NTIS HC/MF A21; 1 functional color page

N92-27098*# Naval Weapons Center, China Lake, CA.
SPACE ENVIRONMENTAL EFFECTS ON COATED OPTICS
T. M. Donovan, J. M. Bennett, R. Z. Dalbey, D. K. Burge, and S. Gyetvay (Aerospace Corp., Los Angeles, CA.) *In* NASA. Langley Research Center, LDEF: 69 Months in Space. First Post-Retrieval Symposium, Part 3 Jan. 1992 p 1361-1375 (For primary document see N92-27083 17-99)
(DARPA Order 3154)
Avail: NTIS HC/MF A21; 1 functional color page

N92-27099*# National Aeronautics and Space Administration. Marshall Space Flight Center, Huntsville, AL.
CONTAMINATION OF OPTICAL SURFACES IN EARTH ORBIT Abstract Only
Donald L. Kinser, Robert A. Weller, M. H. Mendenhall, D. E. Wiedlocher (Vanderbilt Univ., Nashville, TN.), R. Nichols, D. Tucker, and A. Whitaker *In* NASA. Langley Research Center, LDEF: 69 Months in Space. First Post-Retrieval Symposium, Part 3 Jan. 1992 p 1377 (For primary document see N92-27083 17-99)
Avail: NTIS HC/MF A21; 1 functional color page

N92-27108*# Reading Univ. (England). Infrared Multilayer Lab.
EXPOSURE TO SPACE RADIATION OF HIGH-PERFORMANCE INFRARED MULTILAYER FILTERS AND MATERIALS TECHNOLOGY EXPERIMENT (A0056)
Gary J. Hawkins, John S. Seeley, and Roger Hunneman *In* NASA. Langley Research Center, LDEF: 69 Months in Space. First Post-Retrieval Symposium, Part 3 Jan. 1992 p 1477-1491 (For primary document see N92-27083 17-99)
Avail: NTIS HC/MF A21; 1 functional color page

N92-27110*# Barr Associates, Inc., Westford, MA.
TRANSMITTANCE MEASUREMENTS OF ULTRAVIOLET AND VISIBLE WAVELENGTH FILTERS FLOWN ABOARD LDEF
Thomas A. Mooney and Ali Smajkiewicz *In* NASA. Langley Research Center, LDEF: 69 Months in Space. First Post-Retrieval Symposium, Part 3 Jan. 1992 p 1511-1521 (For primary document see N92-27083 17-99)
Avail: NTIS HC/MF A21; 1 functional color page

75 PLASMA PHYSICS

Includes magnetohydrodynamics and plasma fusion.

For ionospheric plasmas see *46 Geophysics*. For space plasmas see *90 Astrophysics*.

N92-26256# Texas Univ., Austin. Inst. for Fusion Studies.
MODE STRUCTURE AND CONTINUUM DAMPING OF HIGH-N TOROIDAL ALFVEN EIGENMODES
M. N. Rosenbluth, H. L. Berk, J. W. VanDam, and D. M. Lindberg Feb. 1992 46 p
(Contracts DE-FG05-80ET-53088; DE-FG03-88ER-53275)
(DE92-010547; DOE/ET-53088/537; IFSR-537) Avail: NTIS HC/MF A03

An asymptotic theory is described for calculating the mode structure and continuum damping of short wave-length toroidal Alfven eigenmodes (TAE). The formalism somewhat resembles the treatment used for describing low-frequency toroidal modes with singular structure at a rational surface, where an inner solution, which for the TAE mode has toroidal coupling, is matched to an outer toroidally uncoupled solution. A three-term recursion relation among coupled poloidal harmonic amplitudes is obtained, whose solution gives the structure of the global wavefunction and the complex eigenfrequency, including continuum damping. Both analytic and numerical solutions are presented. The magnitude of the damping is essential for determining the thresholds for instability driven by the spatial gradients of energetic particles (e.g., neutral beam-injected ions or fusion-product alpha particles) contained in a tokamak plasma. DOE

N92-26286# Canadian Fusion Fuels Technology Project, Toronto (Ontario).
FUSION ENERGY AND CANADA'S ROLE
T. S. Drolet 1992 18 p
(DE92-621553; INIS-MF-13116) Avail: NTIS HC/MF A03

Fusion is the process of releasing energy from matter which occurs in our sun. Canada is contributing to the development of technology which will permit this process to be harnessed and made available on earth. The international effort has increased from a modest beginning in the 1950s to a level of approximately two billion dollars annually in the 1980s. The purpose of this booklet is to introduce the concept of fusion energy as a technology which should make an important addition to the mix of energy sources for our future. Through a co-ordinated approach, Canada has established several projects which will contribute significantly to the development of technologies in specific areas leading to opportunities now for Canadian industry in the international effort. DOE

N92-26416# Naval Postgraduate School, Monterey, CA.
PLASMA INTERACTIONS IN A PLASMA EROSION OPENING SWITCH M.S. Thesis
Christopher B. Thomas Dec. 1991 85 p
(AD-A246179) Avail: NTIS HC/MF A05

Plasma Erosion Opening Switches (PEOS) are important elements in pulsed power equipment. The conduction and opening properties of these switches are highly dependent on the near cathode electric and magnetic fields, and plasma surface interactions. The cathode interaction is highly nonuniform and micron sized cathode spots form within nanoseconds. The mechanism for the formation of these spots and their contribution to the conduction and opening phases of the switch is not yet well understood. The existing model of explosive electron emission does not adequately explain the performance of the switch during operation. The proposed new model for the near cathode effects accounts for time delays in the onset of conduction in the switch which have been seen experimentally. This is the first experiment in a series to verify this model, and to model a possible mechanism for cessation of conduction. GRA

N92-26546# Texas Univ., Austin. Inst. for Fusion Studies.
KINETIC THEORY OF TOROIDICITY-INDUCED ALFVEN EIGENMODE
R. R. Mett and S. M. Mahajan Mar. 1992 29 p
(Contract DE-FG05-80ET-53088)
(DE92-010424; DOE/ET-53088/543; IFSR-543) Avail: NTIS HC/MF A03

An analytic kinetic description of the toroidicity-induced Alfven eigenmode (TAE) is presented. The theory includes electron parallel dynamics non-perturbatively, an effect which is found to strongly influence the character and damping of the TAE; contrary to previous theoretical predictions. We use a parallel conductivity model that includes collisionless (Landau) damping on the passing electrons and collisional damping on both trapped and passing electrons. Together, these mechanisms damp the TAE more strongly than previously expected. This is because the TAE couples (or merges) with the kinetic Alfven wave (KAW) if the gap is sufficiently thin and/or the magnitude of the conductivity is sufficiently small. The high damping could be relevant to recent experimental measurements of the TAE damping coefficient. In addition, the theory predicts a 'kinetic' TAE, whose eigenfrequency lies just above the gap, whose existence depends on finite conductivity, and which is formed by the coupling of two KAWs. DOE

N92-26549# Texas Univ., Austin. Inst. for Fusion Studies.
EFFECTS OF ORBIT SQUEEZING ON ION TRANSPORT IN THE BANANA REGIME IN TOKAMAKS
K. C. Shaing (Oak Ridge National Lab., TN.) and R. D. Hazeltine Feb. 1992 15 p
(Contracts DE-FG05-80ET-53088; DE-AC05-84OR-21400)
(DE92-010548; DOE/ET-53088/539; IFSR-539) Avail: NTIS HC/MF A03

It is shown that ion transport in the banana regime in tokamaks is reduced in the presence of a strong shear in the radial electric field, E sub r, as is often observed in the edge region. For simplicity, the ordering with rho sub pi (d ln E sub r/dr) (much greater than) 1 but c(E sub r)/B sub p upsilon sub ti) less than 1 is adopted. Here, rho sub pi is the ion poloidal gyroradius, B sub p is the poloidal magnetic field strength, upsilon sub ti is the ion thermal speed, and c is the speed of light. A kinetic transport theory similar to those for bumpy tori and stellarators is developed to show that the ion thermal conductivity Chi sub i is reduced by a factor of roughly S sup -3/2, where S = 1 - (rho sub pi d ln E sub r/dr)(cE sub r/B sub rho upsilon sub ti). The result reflects more than simple orbit squeezing: the fraction of trapped ions is also modified by S. DOE

N92-26550# Texas Univ., Austin. Inst. for Fusion Studies.
SCENARIOS FOR THE NONLINEAR EVOLUTION OF ALPHA PARTICLE INDUCED ALFVEN WAVE INSTABILITY
H. L. Berk, B. N. Breizman, and Huanchun Ye Mar. 1992 14 p
(Contract DE-FG05-80ET-53088)
(DE92-010549; DOE/ET-53088/542; IFSR-542) Avail: NTIS HC/MF A03

Various nonlinear scenarios are given for the evolution of energetic particles that are slowing down in a background plasma and simultaneously causing instability of the background plasma waves. If the background damping is sufficiently weak, a steady-state wave is established as described by Berk and Breizman. For larger background damping rate pulsations develop. Saturation occurs when the wave amplitude rises to where the wave trapping frequency equals the growth rate. The wave then damps due to the small background dissipation present and a relatively long quiet interval exists between bursts while the free energy of the distribution is refilled by classical transport. In this scenario the anomalous energy loss of energetic particles due to diffusion is small compared to the classical collisional energy exchange with the background plasma. However, if at the trapping frequency, the wave amplitude is large enough to cause orbit stochasticity, a phase space 'explosion' occurs where the wave amplitudes rise to higher levels which leads to rapid loss of energetic particles. DOE

N92-26577# Oak Ridge National Lab., TN.
A FORTRAN 90 CODE FOR MAGNETOHYDRODYNAMICS
D. W. Walker Mar. 1992 27 p
(Contract DE-AC05-84OR-21400)
(DE92-010362; ORNL/TM-12032) Avail: NTIS HC/MF A03

This report describes progress in developing a FORTRAN 90 version of the KITE code for studying plasma instabilities in Tokamaks. In particular, the evaluation of convolution terms appearing in the numerical solution is discussed, and timing results are presented for runs performed on an 8k processor Connection Machine (CM-2). Estimates of the performance on a full-size 64k CM-2 are given, and range between 100 and 200 Mflops. The advantages of having a Fortran 90 version of the KITE code are stressed, and the future use of such a code on the newly announced CM5 and Paragon computers is considered. DOE

N92-26666# Sandia National Labs., Albuquerque, NM.
EROSION OF A RELATIVISTIC ELECTRON BEAM PROPAGATING IN A PLASMA CHANNEL
P. W. Werner (Department of the Navy, Washington, DC.), E. Schamiloglu, and J. R. Smith 1992 8 p Proposed for presentation at the Charged Particle Beam Conference, Beltsville, MD, 25-27 Jun. 1992
(Contract DE-AC04-76DP-00789)
(DE92-009059; SAND-92-7070C; CONF-9206134-1) Avail: NTIS HC/MF A02

A relativistic electron beam has propagated 91 m in a laser-ionized plasma channel across applied magnetic fields much larger than the geomagnetic field. Beam currents ranged from 0.3 to 1.0 kA and transverse magnetic fields from 0.1 to 4.0 G. Beam degradation in the form of a shortening of the current pulse (erosion) was observed. The two erosion processes were inductive and magnetic erosion. Observed total erosion rates are in agreement with the theoretical inductive and magnetic erosion rates when they are summed. Magnetic erosion was enhanced when the beam radius was larger than the channel. DOE

N92-26695# Sandia National Labs., Albuquerque, NM.
ADVANCES IN THE ENGINEERING OF HIGH FIELD APPLIED-B ION DIODES FOR INERTIAL CONFINEMENT FUSION
D. C. Rovang 1992 20 p Presented at the 10th Topical Meeting on Technology of Fusion Energy, Boston, MA, 7-12 Jun. 1992
(Contract DE-AC04-76DP-00789)
(DE92-006528; SAND-92-0103C; CONF-920607-1) Avail: NTIS HC/MF A03

Pulsed high field magnet coils are an integral part of the applied-B ion diode used in the light ion Inertial Confinement Fusion program at Sandia National Laboratories. Several factors have contributed in recent years to the need for higher magnetic fields of these applied-B ion diodes. These increased magnetic field requirements have precipitated the development of better engineering tools and techniques for use in the design of applied-B ion diodes. This paper describes the status of the applied-B ion diode engineering at Sandia. The design process and considerations are discussed. A systematic approach for maximizing the field achievable from a particular coil system consisting of the capacitor bank, the feeds, and the coil is presented. A coupled electromechanical finite element analysis is also described. DOE

N92-26729# Lawrence Livermore National Lab., CA.
INERTIAL FUSION ENERGY POWER PLANT DESIGN USING THE COMPACT TORUS ACCELERATOR: HYLIFE-CT
R. W. Moir, J. H. Hammer, C. W. Hartman, R. L. Leber, B. G. Logan, R. W. Petzoldt, M. Tabak, M. T. Tobin, and R. L. Bieri Mar. 1992 9 p Presented at the 10th Topical Meeting on Technology of Fusion Energy, Boston, MA, 7-12 Jun. 1992
(Contract W-7405-eng-48)
(DE92-008941; UCRL-JC-109680; CONF-920607-2) Avail: NTIS HC/MF A02

The Compact Torus Accelerator (CTA), under development at Lawrence Livermore National Laboratory, offers the promise of a low cost, high efficiency, high energy, high power density driver for ICF and MICF (Magnetically Insulated ICF) type fusion systems. A CTA with 100 MJ driver capacitor bank energy is predicted to deliver approximately 30 MJ Compact Torus (CT) kinetic energy to a 1 cm(exp 2) target in several nanoseconds for a power density of approximately 10(exp 16) watts/cm(exp 2). The estimated cost of delivered energy is approximately 3$/Joule, or $100 million for 30 MJ. This driver appears to be cost effective and, in this regard, is virtually alone among IFE drivers. We discuss indirect drive ICF with a DT fusion energy gain Q = 70 for a total yield of 2 GJ. The CT can be guided to the target inside a several meter long disposable cone made of frozen Li2BeF4, the same material as the coolant. We have designed a power plant including CT injection, target emplacement, containment, energy recovery, and tritium breeding. The cost of electricity is predicted to be 4.8 (cents)/kWh, which is competitive with future coal and nuclear costs. DOE

N92-26806# Academy of Sciences of the Ukrainian SSR, Kiev. Inst. Teoreticheskoj Fiziki.
DYNAMIC PROPERTIES OF QUASI-TWO-DIMENSIONAL ONE COMPONENT PLASMAS

J. Ortner and I. M. Tkachenko 1991 20 p In RUSSIAN; ENGLISH summary
(DE92-621523; ITF-91-14) Avail: NTIS HC/MF A03

A short review of properties of electronic states on the surface of liquid helium as an example of a quasi-two-dimensional plasma is given. The collective excitations in quasi-dimensional plasmas are discussed. The classic method of moments is applied for the determination of the dispersion law of the quasi-two-dimensional Coulomb system soft collective mode. An interpolation formula is found for the longitudinal dielectric permeability, satisfying all known exact relations and sum rules. The sum rules (the inverse dielectric permeability imaginary part frequency moments) are calculated taking into account the magnetic interaction between the electrons. DOE

N92-26807# Academy of Sciences of the Ukrainian SSR, Kiev. Inst. Teoreticheskoj Fiziki.
DIELECTRIC TENSOR OF STRONGLY COUPLED PLASMAS
V. M. Rylyuk and I. M. Tkachenko 1991 36 p
(DE92-621524; ITP-91-19) Avail: NTIS HC/MF A03

Complex conductivity and dielectric permeability tensors of strongly coupled plasmas are studied and constructed on the basis of exact relations and sum rules. Both Coulomb and magnetic correlation are taken into account. The electromagnetic mode dispersion law is studied. The magnetostatic properties of a system of charged particles are investigated in detail. DOE

N92-26808# Academy of Sciences of the Ukrainian SSR, Kiev. Inst. Teoreticheskoj Fiziki.
SHORT-WAVE LOW-FREQUENCY SPECTRA IN A CURRENT-CARRYING PLASMA
M. O. Vakulenko 1991 12 p In RUSSIAN; ENGLISH summary
(DE92-621529; ITF-91-11) Avail: NTIS HC/MF A03

The finite low frequency, short wave electromagnetic fluctuations in a current carrying plasma, are investigated. The linear stationary electrostatic, cross and magnetostatic spectra are obtained. In strongly nonlinear regime, within the scope of the renormalized statistical approach, the suprathermal stationary electrostatic and effective magnetic potential fluctuations spectra are calculated, together with their renormalized widths and the relevant anomalous electron heat conductivity coefficient. The Kolmogorov spectra are found, also. DOE

76 SOLID-STATE PHYSICS

Includes superconductivity.

For related information, see also *33 Electronics and Electrical Engineering* and *36 Lasers and Masers.*

N92-26204# California Univ., Berkeley. Lawrence Berkeley Lab.
STUDIES OF DEEP LEVEL TRANSIENT SPECTROSCOPY OF DX CENTERS IN GaAlAs: Te UNDER UNIAXIAL STRESS
Ming-Fu Li and Y. P. Yu Nov. 1991 6 p Presented at the 16th International Conference on Defects in Semiconductors, Bethlehem, PA, 22-26 Jul. 1991
(Contract DE-AC03-76SF-00098)
(DE92-010258; LBL-31480; CONF-9107146-4) Avail: NTIS HC/MF A02

DX centers in Al(0.38)Ga(0.62)As doped with Te have been studied by Deep Level Transient Spectroscopy (DLTS) as a function of uniaxial stress. No splitting nor broadening of the DLTS peaks were observed. However, the peak positions and heights depend on the stress and its directions. The results have been analyzed by comparison with existing models and hydrostatic pressure measurements. DOE

N92-26210# Argonne National Lab., IL.
RECENT RESULTS IN CHARACTERIZATION OF MELT-GROWN AND QUENCH-MELT-GROWN YBCO SUPERCONDUCTORS
U. Balachandran, R. B. Poeppel, and A. K. Gangopadhyay Feb. 1992 8 p Presented at the High T(sub C)SUH Workshop on High Temperature Superconductivity Materials, Bulk Processing and Bulk Applications, Houston, TX, 27-28 Feb. 1992
(Contract W-31-109-eng-38)
(DE92-010281; ANL/CP-75188; CONF-920240-2) Avail: NTIS HC/MF A02

From the standpoint of applications, melt-grown (MG) and quench-melt-grown (QMG) bulk YBCO superconductors are of considerable interest. We studied the intragranular critical current density (J(sub c)), the apparent pinning potential (U(sub o)), and the irreversibility temperature (T(sub irr)) of MG and QMG samples and compared the results to those for conventionally sintered YBCO. A systematic increase in U(sub o) and a slower drop in J(sub c) with temperature indicate a systematic improvement in flux-pinning properties in progressing from the sintered YBCO to QMG and MG samples. Weaker pinning is observed in the QMG YBCO than in the MG samples. DOE

N92-26222# California Univ., Berkeley. Lawrence Berkeley Lab. Accelerator and Fusion Research Div.
DIFFRACTION PHENOMENA IN SPONTANEOUS AND STIMULATED RADIATION BY RELATIVISTIC PARTICLES IN CRYSTALS (REVIEW)
V. G. Baryshevsky and I. Ya. Dubovskaya Dec. 1991 120 p
(Contract DE-AC03-76SF-00098)
(DE92-009501; LBL-31695) Avail: NTIS HC/MF A06

The dispersion characteristics of parametric x-ray radiation (PXR) and diffraction radiation of oscillators is discussed. Additionally, cooperative effects in x-ray radiation by charged particles in crystals and diffraction x-ray radiation by relativistic oscillator are presented. DOE

N92-26226# Syracuse Univ., NY.
CADMIUM TELLURIDE THIN FILMS ON SILICON SUBSTRATES Final Technical Report
T. C. Kuo, Y. T. Chi, P. G. Kornreich, and P. K. Ghosh Oct. 1991 13 p
(Contract F30602-88-D-0027)
(AD-A245309; RL-TR-91-266) Avail: NTIS HC/MF A03

This report discusses the epitaxial growth of CdTe films on silicon substrates by the use of a closed hot wall epitaxy (CHWE) system. Deposition parameters were varied in order to determine the growth condition for obtaining good quality CdTe films. The characteristics of the films were investigated by scanning electron microscopy, x-ray diffraction, and Auger electron spectroscopy. Experimental data show that no film grows when the source temperature is below 450 C. The film growth changes linearly with source temperature at a rate of 0.0252 Angstrom/sec/deg. C, and the best film was grown at a source temperature of 475 C. It was found that the lattice constant of the CdTe films was 6.487 + or - 0.004A. GRA

N92-26265*# Eloret Corp., Sunnyvale, CA.
SIMULATION STUDIES FOR SURFACES AND MATERIALS STRENGTH Semiannual Progress Report, 1 Nov. 1991 - 30 Apr. 1992
Timur Halicioglu 30 Apr. 1992 98 p
(Contract NCC2-297)
(NASA-CR-190340; NAS 1.26:190340) Avail: NTIS HC/MF A05

Investigations were carried out in two major areas during the last reporting period. Energy- and structure-related properties of small gold clusters deposited on the GaAs(110) surface were investigated using a molecular dynamics procedure. Additionally, a comparative study of the many-body potentials of silicon systems was performed. Author

N92-26320# Technical Research Centre of Finland, Espoo. Reactor Lab.
DEVELOPMENT AND APPLICATIONS OF THE REVERSE NEUTRON TIME-OF-FLIGHT METHOD WITH FOURIER-TYPE BEAM CHOPPER Ph.D. Thesis - Helsinki Univ. of Technology

Olli K. Antson Sep. 1991 149 p In ENGLISH and RUSSIAN (VTT-Publ-82; ISBN-951-38-3956-7; ISSN-0357-5069; ETN-92-91264) Copyright Avail: NTIS HC/MF A07

The neutron powder diffraction method was applied to the crystal structure analysis of high temperature superconductors, optically active yttriumformate, and beta phase of deuterated acetonitrile, CD3CN. The structural information, containing symmetry, positional and thermal parameters, occupation factors and the order parameter, was obtained by measuring the coherent elastic scattering cross section. The Rietveld profile refinement method was used for the extraction of structural parameters from experimental data. The diffraction spectra were obtained by measuring the time of flight distribution of neutrons with a Fourier type beam chopper. The neutron diffraction spectrum is created by the online synthesis of the cross correlation function between the beam modulation function and the detector intensity. Such an operational mode, called the reverse time of flight method, has many unique properties. For individual titles, see N92-26321 through N92-26328.

N92-26321# Technical Research Centre of Finland, Espoo. Reactor Lab.

ESTIMATION OF PEAK INTENSITIES FROM FREQUENCY FILTERED TOTAL SCATTERING DATA OF NEUTRONS OBTAINED BY THE REVERSE FOURIER METHOD

P. Hiismaeki and Olli K. Antson *In its* Development and Applications of the Reverse Neutron Time-of-Flight Method with Fourier-Type Beam Chopper Sep. 1991 13 p Repr. from Nuclear Instruments and Methods, v. 219, 1984 p 356-368 (For primary document see N92-26320 17-76)

Copyright Avail: NTIS HC/MF A07

A formalism for obtaining the minimum variance estimates and covariances of the diffraction peak intensities from the total scattering data synthetized with continuous frequency filter by the reverse Fourier method is presented. With properly chosen bandpass filter several advantages are shown over the low pass filters exclusively applied up to now: elimination of the background contributions, improvement in the resolving power almost by factor three reduced sensitivity to possible nonidealities of the frequency filter and the possibility of eliminating the higher harmonic contributions. ESA

N92-26322# Leningrad Nuclear Physics Inst. (USSR).

THE HIGH RESOLUTION DIFFRACTOMETER MINI-SFINKS

V. A. Trunov, V. A. Kudryashev, V. A. Ulyanov, A. P. Bulkin, V. G. Muratov, T. K. Korotkova, A. F. Shchebetov, P. Hiismaeki, H. Poeyry, and A. Tiitta (Technical Research Centre of Finland, Espoo.) et al *In* Technical Research Centre of Finland, Development and Applications of the Reverse Neutron Time-of-Flight Method with Fourier-Type Beam Chopper 60 p(SEE N92-26320 17-76) Sep. 1991 Repr. from Leningrad Nuclear Physics Inst., no. 1277 (Leningrad, USSR), 1987 60 p In RUSSIAN; ENGLISH summary (For primary document see N92-26320 17-76)

Copyright Avail: NTIS HC/MF A07

The theoretical principles of the reverse time of flight method, the main concepts of the calculation and optimization of the neutron guides and information about the time focusing conditions in the time of flight method are reported. The description of the time of flight high resolution diffractometer 'Mini-SFINKS' and some experimental results are presented. ESA

N92-26323# Technical Research Centre of Finland, Espoo. Reactor Lab.

HIGH-RESOLUTION FOURIER TOF POWDER DIFFRACTION. 1: PERFORMANCE OF THE MINI-SFINKS FACILITY

Olli K. Antson, A. P. Bulkin, P. E. Hiismaeki, T. K. Korotkova, V. A. Kudryashev, H. S. Kukkonen, V. G. Muratov, H. O. Poeyry, A. F. Shchebetov (Leningrad Nuclear Physics Inst., USSR), and A. T. Tiitta et al *In its* Development and Applications of the Reverse Neutron Time-of-Flight Method with Fourier-Type Beam Chopper Sep. 1991 4 p Repr. from Physica B, v. 156 - v. 157, 1989 p 567-570 (For primary document see N92-26320 17-76)

Copyright Avail: NTIS HC/MF A07

A description of the Finnish-Soviet Fourier TOF (Time Of Flight) neutron powder diffractrometer Mini-SFINKS is given. The facility has been used in its present configuration for a growing number of experiments since 1986. Some examples of these, including studies of high temperature superconductors, are given to illustrate the performance of the machine. ESA

N92-26324# Technical Research Centre of Finland, Espoo. Reactor Lab.

NEUTRON POWDER DIFFRACTION STUDY OF DEUTERATED BETA-ACETONITRILE

Olli K. Antson, K. J. Tilli, and N. H. Andersen (Risoe National Lab., Roskilde, Denmark) *In its* Development and Applications of the Reverse Neutron Time-of-Flight Method with Fourier-Type Beam Chopper Sep. 1991 6 p Repr. from Acta Crystallographica B43, 1987 p 296-301 (For primary document see N92-26320 17-76)

Copyright Avail: NTIS HC/MF A07

The structure of the low temperature beta phase of deuterated acetonitrile, CD3CN, was determined by neutron powder diffraction. Experiments were performed using both a triple axis spectrometer in the elastic mode and a time of flight diffractometer with a Fourier chopper. The diffraction patterns obtained were analyzed by Rietveld refinements in which the molecules were constrained to C(sub 3v) symmetry. A final R(sub wp) factor of 7.7 percent was obtained for an orthorhombic model; space group Cmc2(sub 1), cell parameters at 100 K: a = 6.05(4), b = 5.24(4), c = 7.79(6) A, Z = 4. The acetonitrile molecules were found to lie in the mirror planes. The phase transformation alpha to beta is accompanied by changes in the orientation of permanent dipoles of the molecules, which lead to a structure with a macroscopic polarization in the c direction. ESA

N92-26325# Leningrad Nuclear Physics Inst. (USSR).

DETERMINATION OF THE STRUCTURE OF Y(HCOO)3 BY THE NEUTRON TIME-OF-FLIGHT DIFFRACTION METHOD

V. A. Trunov, V. A. Kudryashev, A. P. Bulkin, V. A. Ulyanov, A. A. Loshmanov, N. G. Furmanova, Olli K. Antson, P. Hiismaeki, H. Mutka, and H. Poeyry (Technical Research Centre of Finland, Espoo.) et al *In* Technical Research Centre of Finland, Development and Applications of the Reverse Neutron Time-of-Flight Method with Fourier-Type Beam Chopper Sep. 1991 3 p Repr. from Solid State Communications, v. 59, 1987 p 95-97 Sponsored by Academy of Sciences and Academy of Finland (For primary document see N92-26320 17-76)

Copyright Avail: NTIS HC/MF A07

Optical measurements have shown that the two types of Y(HCOO)3, that is, the powder type and the recrystallized type, have notable differences in second harmonic properties as measured with a Nd:YAG laser. A neutron time of flight measurement on the powder type was performed in order to explain the optical behavior by structural differences. The results show that the position parameters of the heavy atoms of the powder type as the same as those given by a single crystal X-ray study for the recrystallization type. The position parameters of the hydrogen atoms were determined for the first time. The effect of contamination determined by neutron activation analysis is summarized. ESA

N92-26326# Technical Research Centre of Finland, Espoo. Reactor Lab.

A HIGH-RESOLUTION NEUTRON POWDER DIFFRACTION STUDY IN HIGH-T(SUB c) SUPERCONDUCTOR YBa2Cu3O7

Olli K. Antson, P. E. Hiismaeki, H. O. Poeyry, A. T. Tiitta, K. M. Ullakko, V. A. Trunov, and V. A. Ulyanov (Leningrad Nuclear Physics Inst., USSR) *In its* Development and Applications of the Reverse Neutron Time-of-Flight Method with Fourier-Type Beam Chopper Sep. 1991 4 p Repr. from Solid State Communications, v. 64, no. 5, 1987 p 757-760 (For primary document see N92-26320 17-76)

Copyright Avail: NTIS HC/MF A07

A high resolution neutron time of flight diffraction measurement of superconductive Y-Ba-Cu-O (T(sub co) = 91 K) was performed

both at room temperature and at 77 K. Profile refinements of the measured data resulted in a unit cell of stoichiometry YBa2Cu3O7. The positions of the oxygen deficiencies were also determined. Refinement of the anisotropic thermal parameters for the oxygen atoms seem to indicate some changes in the form of the thermal ellipsoids of these atoms when cooled below T(sub c). ESA

N92-26327# Leningrad Nuclear Physics Inst. (USSR).
ANOMALOUS STRUCTURAL BEHAVIOUR OF THE HIGH-TEMPERATURE SUPERCONDUCTING COMPOUND La(1.8)Sr(0.2)CuO(4-y)
R. L. Bolotovskii, A. P. Bulkin, G. A. Krutov, V. A. Kudryashev, S. V. Maleyev, A. L. Malyshev, B. P. Toperverg, V. A. Trunov, V. A. Ulyanov, and S. B. Vakhrushev (Academy of Sciences, USSR, Leningrad) et al *In* Technical Research Centre of Finland, Development and Applications of the Reverse Neutron Time-of-Flight Method With Fourier-Type Beam Chopper Sep. 1991 4 p Repr. from Solid State Communications, v. 65, no. 10, 1988 p 1167-1170 (For primary document see N92-26320 17-76)
Copyright Avail: NTIS HC/MF A07

High resolution neutron and X-ray results are considered with special emphasis laid on some anomalous features connected with the tetragonal to orthorhombic phase transition. A theoretical model based on random fields of lattice strains is given in order to explain the enhancement of T(sub c). ESA

N92-26328# Technical Research Centre of Finland, Espoo. Reactor Lab.
NEUTRON POWDER DIFFRACTION STUDY ON Eu-SUBSTITUTED Bi2Sr2CaCu2O(8+y) HIGH TEMPERATURE SUPERCONDUCTOR
Olli K. Antson, T. T. Karlemo, M. J. Karppinen, and K. M. Ullakko (Helsinki Univ. of Technology, Espoo, Finland) *In its* Development and Applications of the Reverse Neutron Time-of-Flight Method with Fourier-Type Beam Chopper Sep. 1991 10 p Repr. from Physica C, v. 173, 1991 p 65-74 (For primary document see N92-26320 17-76)
(Grant AF-4732/4014/89)
Copyright Avail: NTIS HC/MF A07

A neutron powder diffraction method was used to study the structural changes in the Bi2Sr2Ca(1-x)Eu(x)Cu2O(8+y) compound caused by the artificial substitution of Ca by Eu. Besides the systematic variation of the parameters of the orthorhombic 5.4 by 5.4 by 30.7 A subcell, atomic rearrangment in the BiO layer and modifications in the square pyramidal coordination polyhedra of the Cu ion were observed. The onset temperature as determined by the AC susceptibility method has a broad maximum at x = 0.3, and no superconductivity is observed at x = 0.6 in the temperature range T greater than 4.2 K. The reasons for the broadening of the transition range and the decrease of the Meissner fraction concomitant to the increase of the Eu concentration are discussed. ESA

N92-26433# Department of the Navy, Washington, DC.
METHOD FOR IMPLANTING IMPURITIES IN SEMICONDUCTORS AND SEMICONDUCTOR IMPLANTED WITH IMPURITIES Patent Application
Frederick G. Moore, inventor (to Navy) and Harry B. Dietrich, inventor (to Navy) 26 Aug. 1991 25 p
(AD-D015196; US-Patent-Appl-SN-749825; Navy-Case-72812)
Avail: NTIS HC/MF A03

The inventors herein have discovered that the percentage of electrical activation of high concentrations of dopants in semiconductors is enhanced by controlling the dose rates of the ion-implantation of the dopants. In particular, silicon and sulphur ions implanted into GaAs at controlled implantation dose rates which accumulate to high dopant concentrations exhibit high electrical activation percentages when annealed. The method described herein comprises implanting a dopant species in a semiconductor material at a predetermined rate, said predetermined rate being based on a rate determined so that a maximum in a characteristic graph of percentage activation as a function of dopant species implantation rate is the predetermined rate. It will be appreciated that different dopant species, implantation parameters (e.g., implantation energy) and different semiconductor materials will give rise to different characteristic graphs which relate percentage electrical activation to dopant species implantation rates. The optimal dose rate can be determined from a characteristic experimentally determined graph of activation versus ion dose rate. GRA

N92-26579# Oak Ridge National Lab., TN.
A COMPREHENSIVE REVIEW OF THE XRD DATA OF THE PRIMARY AND SECONDARY PHASES PRESENT IN THE BSCCO SUPERCONDUCTOR SYSTEM
B. J. Reardon and C. R. Hubbard Feb. 1992 64 p
(Contract DE-AC05-84OR-21400)
(DE92-010363; ORNL/TM-11949) Avail: NTIS HC/MF A04

X-ray powder patterns for the phases in the CaO-SrO-PbO ternary system, along with the corresponding crystal structures, were obtained from the literature and from the Powder Diffraction File (PDF). Available X-ray diffraction (XRD) patterns were compared with each other and, when possible, with a calculated pattern for each phase, yielding a recommended reference pattern. The simulated powder patterns presented here deal with the phases found within the (Ca,Sr)2PbO4 solid solution series and are recommended for the PDF. DOE

N92-26582# California Univ., Berkeley. Lawrence Berkeley Lab.
MAGNETIC FLUX NOISE IN COPPER OXIDE SUPERCONDUCTORS Ph.D. Thesis
M. J. Ferrari Nov. 1991 172 p
(Contract DE-AC03-76SF-00098)
(DE92-010299; LBL-31553) Avail: NTIS HC/MF A08

Magnetic flux noise and flux creep in thin films and single crystals of YBa2Cu3O(7-x), Bi2Sr2CaCu2O(8+x), Tl2Ca2Ba2Cu3O(x), and TlCa2Ba2Cu3O(x) are measured with a superconducting quantum interference device (SQUID). The noise power spectrum generally scales as 1/f (f is frequency) from 1 Hz to 1 kHz, increases with temperature, and decreases in higher quality films. It is proportional to the magnetic field B in which the sample is cooled, at least in the range B between 0.1 mT and 3 mT. A model of thermally activated vortex motion is developed which explains the dependence of the noise on frequency, temperature, current, and applied magnetic field. The pinning potential is idealized as an ensemble of double wells, each with a different activation energy separating the two states. From the noise measurements, this model yields the distribution of pinning energies in the samples, the vortex hopping distance, the number density of mobile vortices, and the restoring force on a vortex at a typical pinning site. The distribution of pinning energies in YBa2Cu3O(7-x) shows a broad peak below 0.1 eV. The small ambient magnetic field, and the detection of noise even in the absence of a driving force, insure that the measured pinning energies are characteristic of isolated vortices near thermal equilibrium. The observed vortex density in fields much less than 0.1 mT is too large to be explained by the ambient field, suggesting a mechanism intrinsic to the sample which produces trapped vortices. DOE

N92-26584# California Univ., Berkeley. Lawrence Berkeley Lab.
THE DEBYE TEMPERATURE OF YBa2Cu3O(7-(DELTA)) AND ITS DEPENDENCE ON THE VOLUME FRACTION OF SUPERCONDUCTIVITY
R. A. Fisher, N. E. Phillips, and J. E. Gordon Dec. 1991 8 p Presented at the Lattice Effects in High (Tc) Superconductors, Santa Fe, NM, 13-15 Jan. 1992
(Contract DE-AC03-76SF-00098)
(DE92-010305; LBL-31663; CONF-920141-6) Avail: NTIS HC/MF A02

Specific heat measurements, on polycrystalline samples of YBa2Cu3O(7-(delta)), YBCO, have shown sample-to-sample variations in the volume fraction of superconductivity, f sub s,

which is correlated with the concentration of Cu(2+) magnetic moments in the YBCO lattice. At low temperatures the lattice specific heat also varies with f sub s, but these variations do not persist above approx. 20 K. The low-temperature data show that Theta sub 0(-3) varies linearly with f sub 3, and give values of 520 and 390 K for Theta sub o for fully superconducting and 'fully normal' YBCO, respectively. These results suggest that the long wavelength phonon modes are altered when Cu(2+) magnetic moments are present in the lattice. The fact that different samples have the same lattice specific heat at approx. 20 K and above T sub c indicates that the higher energy phonon modes are insensitive to these Cu(2+) moments. DOE

N92-26638# Oak Ridge National Lab., TN.
MOBILITY OF ELECTRONS AND HOLES IN SEMICONDUCTORS
G. D. Mahan, B. A. Sanborn, and P. B. Allen Mar. 1992 11 p Presented at the Symposium on Advances in Semiconductors and Superconductors: Physics Toward Device Applications, Somerset, NJ, 23-27 Mar. 1992
(Contract DE-AC05-84OR-21400)
(DE92-010125; CONF-920309-1) Avail: NTIS HC/MF A03

The mobility of electrons and holes is calculated in silicon as a function of temperature and the concentration of impurities. Calculations are done for both majority and minority carriers. Special care has been taken in the calculation of the contribution from impurity scattering. Both the dielectric function, and the local field corrections, have been calculated as a function of temperature and impurity concentration. The results agree with the data at low temperature, and at high doping at room temperature. DOE

N92-26639# Princeton Univ., NJ. Dept. of Chemistry.
PHOTOINDUCED CHARGE SEPARATION IN SOLID-STATE AND MOLECULAR SYSTEMS Yearly Progress Report No. 3
A. B. Bocarsly 1991 12 p
(Contract DE-FG02-85ER-13438)
(DE92-010130; DOE/ER-13438/3) Avail: NTIS HC/MF A03

Our goal is to understand the role of intrinsic cyanometalate overlayers in modulating interfacial photoinduced charge transfer processes occurring at the cadmium chalconide/aqueous ferri-ferrocyanide interface. To accomplish this goal, detailed structural and charge transfer studies of (CdFe(CN)6)(2-/1-) overlayers generated either intrinsically via photoelectrochemistry at the illuminated CdX/(Fe(CN)6)(4-/32) (X=S or Se) interface, or synthesized as chemical modification layers on inert metal electrodes have been undertaken. From these studies, a picture has evolved which directly links charge transfer mediated cation intercalation processes to surface overlayer crystal structure, and overlayer structure to critical charge transfer parameters. We have discovered that a photoelectrochemical cell of composition n-CdSe/(1M) KCN provides a relatively unique environment for testing the dynamic effects of chemisorption processes on heterogeneous charge transfer at the semiconductor-liquid junction. Thus, our retrospective studies have provided for new insight into semiconductor photochemistry. In parallel with our photoelectrochemical projects we have also introduced work on the spatially resolved photodeposition of platinum metal on nonconducting and semiconducting substrates. This chemistry provides new opportunities for the design of semiconductor (or insulator)-metal heterostructures which have applications in solar energy conversion. DOE

N92-26641# California Univ., Berkeley. Lawrence Berkeley Lab.
A SURFACE SCIENCE INVESTIGATION OF SILICON CARBIDE: OXIDATION, CRYSTAL GROWTH AND SURFACE STRUCTURAL ANALYSIS Ph.D. Thesis
J. M. Powers Nov. 1991 150 p
(Contract DE-AC03-76SF-00098)
(DE92-010286; LBL-31541) Avail: NTIS HC/MF A07

For the semiconductor SiC to fulfill its potential as an electronic material, methods must be developed to produce insulating surface oxide layers in a reproducible fashion. Auger electron spectroscopy (AES), low energy electron diffraction (LEED) and x ray photoelectron spectroscopy (XPS) were used to investigate the oxidation of single crystal alpha-SiC over a wide temperature and O2 pressure range. The alpha-SiC surface becomes graphitic at high temperatures and low O2 pressures due to Si and SiO sublimation from the surface. Amorphous SiO2 surface layers from on alpha-SiC at elevated O2 pressures and temperatures. Both the graphitization and oxidation of alpha-SiC appears to be enhanced by surface roughness. Chemical vapor deposition (CVD) is currently the preferred method of producing single crystal SiC, although the method is slow and prone to contamination. We have attempted to produce SiC films at lower temperatures and higher deposition rates using plasma enhanced CVD with CH3SiH3. Scanning AES, XPS and scanning electron microscopy (SEM) were utilized to study the composition and morphology of the deposited Si(x)C(y)H(z) films as a function of substrate temperature, plasma power and ion flux bombardment of the film during deposition. High energy ion bombardment during deposition was found to increase film density and substrate adhesion while simultaneously reducing hydrogen and oxygen incorporation in the film. Under all deposition conditions the Si(x)C(y)H(z) films were found to be amorphous, with the ion bombarded films showing promise as hard protective coatings. Studies with LEED and AES have shown that beta-SiC (100) exhibits multiple surface reconstructions, depending on the surface composition. These surface reconstructions possess substantially different surface reactivities at elevated temperatures, which can complicate the fabrication of metal on SiC junctions. DOE

N92-26648# Cornell Univ., Ithaca, NY. Dept. of Materials Science and Engineering.
CRYSTALLINE-AMORPHOUS INTERFACES AND THEIR RELATION TO GRAIN BOUNDARY FILMS
C. B. Carter 3 Feb. 1992 9 p
(Contract DE-FG02-89ER-45381)
(DE92-009812; DOE/ER-45381/3) Avail: NTIS HC/MF A02

In presence of glass in grain boundaries greatly enhances sintering, in part, because transport of matter along and across the intergranular regions is faster. The glass does not simply act as a catalyst but also changes the character of the interfacial regions. In particular, it tends to encourage faceting of the grains; the scale of this faceting may vary from nanometers to microns. After processing, the glass may remain as a thin layer in the interface during preparation of the polycrystalline compact as was initially demonstrated for Si3N4 and proposed for other ceramics. The glass may also crystallize to form an intergranular crystalline layer or it may withdraw from the planar interfaces into 'three grain' and 'four grain' junctions (the dewetting process). The present program has begun to examine how glass affects and interacts with crystalline ceramics. The main aim of the program is to examine how glass moves into and out of grain boundaries and why this movement takes. By understanding this process, this important aspect of many ceramic materials will be better controlled. Since TEM is the main tool used, methods will be developed for analyzing interfaces as part of this program. DOE

N92-26672# International Centre for Theoretical Physics, Trieste (Italy).
PERCOLATION EFFECTS IN THE V-I CHARACTERISTICS OF GRANULAR YBa2Cu3O(7-DELTA)
E. Babic, M. Prester, D. Babic, P. Nozar, P. Stastny, and F. C. Matacotta Oct. 1991 12 p
(DE92-617541; IC-91/346) Avail: NTIS HC/MF A03

V-I characteristics of granular YBa2Cu3O(7-delta) samples with very different grain size and thickness have been studied in the temperature range 65-85 K and magnetic fields up to 35 Oe. The results present clear evidence of percolation effects in a 3D network of weakly linked superconducting grains. The onset of dissipation follows a V proportional to (I - I(sub c))(exp n) power law n assumes values between 2 and 2.6 and does not depend on microstructure or thickness. It shows a very weak dependence, if any, on the external magnetic field, H, and temperature, T. This suggests that the shape of the low current side of the distribution of critical

currents of the links is also quite insensitive to H and T. It also shows that the transition to the coherent state takes place at T greater than 85 K. Peculiar percolation effects have been observed when the thickness of the sample approaches the grain size. V proportional to (I - I(sub c))(exp n) onsets of dissipation with exponent n practically the same as in other granular superconductors (both conventional and high temperature ones) present clear evidence for the percolation effects in 3D network of intergrain links. DOE

N92-26684# Washington State Univ., Pullman. Dept. of Chemistry.
CROSSOVERS OF THE DENSITY OF STATES IN TWO-DIRECTION DOUBLE-BARRIER RESONANT-TUNNELING STRUCTURES
S. J. Lee, N. H. Shin, J. J. Ko, C. I. Um, and Thomas F. George Jan. 1992 21 p
(Contract N00014-90-J-1193)
(AD-A246124) Avail: NTIS HC/MF A03

The density of states in delta profiled 2D and 1D quantum systems is calculated. It is shown that there are smooth crossovers in the density of states from a 3D square-root behavior to a 2D steplike behavior, and from a 2D to a 1D sawtooth-like behavior, as the confinements increase. Quantum well structures are being extensively studied for applications in ultra large scale integrated circuits and high-speed optoelectronics. As for these systems, the lateral confinement of originally quasi-2D (Q2D) electron layers to submicron dimensions has made possible the realization of quasi-1D (Q1D) electron systems. Among them, resonant tunneling structures are of great interest not only because of their potential applications, but also for the underlying basic physics. GRA

N92-26763# Worcester Polytechnic Inst., MA. Dept. of Physics.
BAND STRUCTURE AND OPTICAL PROPERTIES OF SEMICONDUCTOR SUPERLATTICES Final Report
L. R. Ram-Mohan 17 Dec. 1991 5 p
(Contract N00014-89-J-2038)
(AD-A246076) Avail: NTIS HC/MF A01

This period has been very productive in terms of research results, as evidenced by 13 publications on magneto-optics and magneto-transport in collaboration with the NRL research group. The theoretical development of the transfer matrix method (TMM) has provided a compact and efficient algorithm for the band structure of superlattices. GRA

N92-26774 Minnesota Univ., Minneapolis.
A STUDY OF BUCKMINSTERFULLERENE USING NEW PSEUDOPOTENTIALS Ph.D. Thesis
Norman Joseph Troullier, Jr. 1991 139 p
Avail: Univ. Microfilms Order No. DA9207810

We present pseudopotential plane-wave local-density calculations of the electronic and structural properties of solid C-60 (fullerite). The calculated molecular bond lengths, lattice constant, bulk modulus, enthalpy of formation, and the equation of state for compression are in good agreement with experiment. The shape of the theoretical density of states is in excellent agreement with the experimental photoemission and inverse photoemission spectra. We also present the calculated band-structure for the states near the fundamental gap. We have made a thorough analysis of the electronic states of C-60 and found that they can be conveniently classified according to their angular character, and use it to identify the origin of the peaks in the electronic density of states. In order to perform accurate plane-wave converged C-60 calculations, we have developed a simple procedure to generate first-principles norm-conserving pseudopotentials, which are designed to be smooth and therefore save computational resources when used with a plane-wave basis. We found these pseudopotentials to be extremely efficient for cases where the plane-wave expansion has a slow convergence, in particular for systems containing first row elements such as carbon, transition metals and rare-earth elements. The wide applicability of the pseudopotentials are exemplified with plane-wave calculations for copper, zincblende, diamond, alpha-quartz, rutile and cerium. The large number of atoms in the C-60 system imposes a heavy computational load on both storage and cpu time requirements. Therefore, we have investigated the computational requirements for the pseudopotential plane-wave method as a function of the number of atoms per unit cell. For systems containing a large number of atoms the computational load can be reduced if the pseudopotential operator is of a suitable form, such that it can be efficiently calculated in the position representation. The pseudopotentials we have examined include local pseudopotentials, position dependent electron mass pseudopotentials, and separable non-local pseudopotentials.
Dissert. Abstr.

N92-26826# Sandia National Labs., Albuquerque, NM.
ETCHING EFFECTS IN ION IMPLANTED SiO2
G. Battaglin, A. Boscolo-Boscoletto, F. Caccavale, G. DeMarchi, P. Mazzoldi (Padua Univ., Italy), and G. W. Arnold 1992 6 p Presented at the Fall Meeting of the European Materials Research Society, Strasbourg, France, 5-8 Nov. 1991
(Contract DE-AC04-76DP-00789)
(DE92-011150; SAND-92-0437C; CONF-911109-9) Avail: NTIS HC/MF A02

Chemical and physical transformations involved in ion implantation processes in glasses determine changes in mechanical and tribological properties, in network dilatation, in induced optical absorption and luminescence and in the composition and chemical behavior as a function of different experimental conditions (ion, energy, dose, target temperature). Variations of chemical etch rate in HF are related to radiation damages and formation of compounds. A systematic study of the etch rate changes in silica due to Ar, N, Si plus N implants has been performed. Structure modifications at depths greater than the corresponding implanted ion ranges are evidenced for nuclear deposited energy greater than 10(exp 22) keV cm(exp -3). Formation of silicon oxynitrides reduces the etch rate values. DOE

N92-26842# Argonne National Lab., IL.
STRUCTURAL COHERENCE OF THE CuO2 PLANES OF OXIDE SUPERCONDUCTORS: IS IT A REQUIREMENT FOR SUPERCONDUCTIVITY?
J. D. Jorgensen, D. G. Hinks, B. A. Hunter, R. L. Hitterman, A. W. Mitchell, P. G. Radaelli, B. Dabrowski, J. L. Wagner, H. Takahashi, and E. C. Larson Feb. 1992 11 p Presented at the Lattice Effects in High (Tc) Superconductors, Santa Fe, NM, 13-15 Jan. 1992
(Contract W-31-109-eng-38)
(DE92-009724; ANL/CP-74854; CONF-920141-3) Avail: NTIS HC/MF A03

The CuO2 planes of copper-oxide superconductors are not perfectly flat. The oxygen atoms are displaced out of the plane of the copper atoms. In some compounds the pattern of corrugation exhibits long-range translational symmetry; in others, it does not. We describe structures of the first type as coherent and those of the second type as incoherent. In the context of this definition, the orthorhombic phases of compounds based on YBa2Cu3O(6+x) and La2CuO4 are coherent, while the tetragonal phases are probably incoherent as a result of random oxygen atom displacements that give rise to average tetragonal symmetry. The latter structures are more appropriately called disordered tetragonal structures. When data for these two systems are interpreted in terms of a model that admits short-range orthorhombic order in structures that exhibit average tetragonal symmetry, we are led to conclude that there is no evidence for superconductivity in compounds with disordered tetragonal symmetry. We are led to propose that structural coherence of the CuO2 planes is a requirement for superconductivity in layered copper-oxide compounds. DOE

N92-26843# Oak Ridge National Lab., TN.
THE PRODUCTION AND PROPERTIES OF MELT-ZONE TEXTURED Y1Ba2Cu3O(7-DELTA) FILAMENTS Abstract Only
D. K. Christen, C. E. Klabunde, B. C. Chakoumakos, A. Goyal, D. M. Kroeger, M. J. Neal, M. V. Parish, and D. B. Chandler (CPS

Superconductors, Inc., Milford, MA.) 1992 1 p Presented at the International Workshop on Superconductivity, Honolulu, HI, 23-26 Jun. 1992
(Contract DE-AC05-84OR-21400)
(DE92-008097; CONF-920648-1-Extd-Abst) Avail: NTIS HC/MF A01

Although the YBa2Cu3O(7-(delta)) (YBCO) high-temperature superconductors are known to possess superior flux pinning properties at high temperatures and in a large magnetic fields, the development of practical conductors is severely limited by the existence of 'weak links' at the grain boundaries. It is now established that strongly-linked, high J(sub c) YBCO materials can be produced in the form of bulk masses by a variety of melt-processing techniques. Here we describe a technique that couples a continuous fiber spinning process with zone-melt-processing, resulting in long lengths of high quality YBCO filaments that have microstructures and high-temperature electrical transport properties similar to those of melt-textured bulk materials. DOE

N92-26851# Oak Ridge National Lab., TN.
SOME EXPERIENCES WITH ABSORPTION, PHONON RAMAN, AND LUMINESCENCE SPECTROSCOPIC PROBES OF CRYSTAL STRUCTURE OF f-ELEMENT COMPOUNDS
J. R. Peterson 1992 3 p Presented at the Conference on Rare Earths, Kyoto, Japan, 1-5 Jun. 1992
(Contracts DE-AC05-84OR-21400; DE-FG05-88ER-13865)
(DE92-007828; CONF-920625-2) Avail: NTIS HC/MF A01

Structural information is crucial to the study and understanding of the basic chemical properties of the f-elements. X-ray diffraction (XRD) techniques are usually used to obtain crystal structure information. However, the transuranium (5f) elements, because of their radioactivity and limited availability, present problems for standard XRD analysis. For some time now we have been developing and using various spectroscopic probes of crystal structure; an overview of our research in this area is presented here. DOE

N92-26857# Los Alamos National Lab., NM.
INDUCED CYCLE STRUCTURES OF THE HYPEROCTAHEDRAL GROUP
W. Y. C. Chen Jun. 1992 16 p Presented at the 4th Conference on Formal Power Series and Algebraic Combinatorics, Montreal, Canada, 15-19 Jun. 1992
(Contract W-7405-eng-36)
(DE92-007570; LA-UR-92-266; CONF-920662-1) Avail: NTIS HC/MF A03

The hyperoctahedral group B(sub n) is treated as the automorphism group of the n-dimensional hypercube, denoted Q(sub n), which is nowadays understood to be a graph on 2(sup n) vertices. It is well known that B(sub n) can be represented by the group of signed permutations. In other words, any signed permutation induces a permutation on the vertices of Q(sub n) which preserves adjacencies. Moreover, signed permutations also induce a permutation group on the edges of Q(sub n), denoted H(sub n). We study the cycle structures of both B(sub n) and H(sub n). The technique proposed here is to determine the induced cycle structure of a signed permutation by the number of fixed vertices or fixed edges of a signed permutation in the cyclic group generated by a signed permutation of given type. Here we directly define the type of a signed permutation by a double partition based on its signed cycle decomposition. In this way, we obtain explicit formulas for the number of induced cycles on vertices as well as edges of Q(sub n) of a signed permutation in terms of its type. By further exploring the connection between cycle indices and the structure of fixed points, we obtain the cycle indices of both B(sub n) and H(sub n). Our formula for the cycle index of B(sub n) is much more natural and considerably simpler than that of Harrison and High. Meanwhile, the cycle structure of H(sub n) seems to have been untouched before, although it is well motivated by nonisomorphic edge colorings of Q(sub n) as well as by the recent interest in symmetries of computer networks. DOE

N92-26927# Technische Univ., Delft (Netherlands).
QUANTUM INTERFERENCE AND CONFINEMENT EFFECTS IN NARROW CHANNEL Si-MOSFET'S Ph.D. Thesis
J. R. Gao 24 Oct. 1991 123 p Sponsored in part by Stichting voor Fundamenteel Onderzoek der Materie, Amsterdam, Netherlands; and Nederlandse Organisatie voor Wetenschappelijk Onderzoek, The Hague
(PB92-150176) Avail: NTIS HC/MF A06

Experimental studies are discussed of the electrical transport phenomena in the mesoscopic regime in two types of narrow channel Si-Metal Oxide Semiconductor Field-Effect Transistor's (MOSFET's), single-channel MOSFET's, and multiple-channel MOSFET's with a dual-gate. Universal conductance fluctuations, weak localization, quantum confinement effects, and lateral superlattice effects in the conductance were investigated. The following topics are discussed: theoretical background; narrow channel Si-MOSFET's for quasi-one-dimensional quantum transport; temperature dependence of universal conductance fluctuations in narrow Si inversion layers; universal fluctuations in the conductance of narrow Si inversion layers as a function of the Fermi energy; one-dimensional subband effects in the conductance of multiple quantum wires in Si-MOSFET's; enhancement of weak localization in a Si lateral superlattice device; and fluctuations in the transconductance of multiple quantum wires in Si-MOSFET's. GRA

N92-27059# Brookhaven National Lab., Upton, NY.
LATTICE INSTABILITIES AND STRUCTURAL PHASE TRANSFORMATIONS IN La2CuO4 SUPERCONDUCTORS AND INSULATORS
J. D. Axe 1991 14 p Presented at the Lattice Effects in High (Tc) Superconductors, Santa Fe, NM, 13-15 Jan. 1992
(Contract DE-AC02-76CH-00016)
(DE92-010045; BNL-47128; CONF-920141-4) Avail: NTIS HC/MF A03

Soft-mode structural phase transformations, common in many perovskite-based materials, are also found in La2CuO4 and structurally related oxides. The resulting phase behavior is rather complex, but is a natural consequence of the degeneracy of the soft phonon order parameters. This paper reviews the structural and lattice-dynamical results and their interpretation based upon mean-field statistical mechanical models. DOE

N92-27064# Michigan Technological Univ., Houghton. Dept. of Physics.
EFFECT OF INTERSTITIALS ON THE TRAPPING OF HYDROGEN IN IRON-SINGLE CRYSTALS Final Report
James T. Waber 1992 41 p Prepared in cooperation with Northwestern University, Evanston, IL
(AD-A246412) Avail: NTIS HC/MF A03

A nondestructive method of determining the densities of edge and screw dislocations was developed. Using it, thermal elimination of dislocation was shown to be a binary and two stage process for both cold rolled and metallographically polished specimens. The process involves the glide of dislocation dipoles rather than vacancy migration and climb. A method of extracting kinetic information from isochronal runs was developed and tested with isothermal runs. The strong effect of surface dislocations on reducing the diffusion of hydrogen and deuterium in iron single crystals was demonstrated. There is not much of an opening of ions at the core of the dislocations. Therefore positrons probably do not annihilate at the normal sites of the core of the dislocations. The idea that there was insufficient room for a positron to be trapped at a dislocation was based on some approximate calculations carried out while they were associated with Argonne National Lab. GRA

N92-26396 Technische Univ., Munich (Germany, F.R.). Dept. of Physics.
SUPERCONDUCTING TUNNEL JUNCTIONS
H. Kraus, J. Jochum, B. Kemmather, M. Gutsche, F. v.Feilitzsch, and R. L. Moessbauer *In* Max-Planck-Inst. fuer Physik und Astrophysik, Cryogenic Detector Development Nov. 1991 9 p

Presented at the 4th International Workshop on Low Temperature Particle Detectors, Oxford, England, 4-7 Sep. 1991 (For primary document see N92-26391 17-35)
Copyright Avail: Max-Planck-Inst. fuer Physik und Astrophysik, Foehringer Ring 6, D-8000 Munich, Fed. Republic of Germany

N92-26397 Max-Planck-Inst. fuer Physik und Astrophysik, Munich (Germany, F.R.).
ELECTRON-PHONON DECOUPLING AND SUPERCONDUCTING GRAINS
P. Freund, H.-J. Gebauer, and L. Stodolsky *In its* Cryogenic Detector Development Nov. 1991 11 p Presented at the 4th International Workshop on Low Temperature Particle Detectors, Oxford, England, 4-7 Sep. 1991 (For primary document see N92-26391 17-35)
Copyright Avail: Max-Planck-Inst. fuer Physik und Astrophysik, Foehringer Ring 6, D-8000 Munich, Fed. Republic of Germany

N92-27127*# Technical Univ. of Denmark, Lyngby. Physics Lab. 3.
RESULTS OF THE TTF-TCNQ AND THE CALCIUM CARBONATE CRYSTALLIZATION ON THE LONG DURATION EXPOSURE FACILITY
Kjeld Flemming Nielsen and M. David Lind (Rockwell International Science Center, Thousand Oaks, CA.) *In* NASA. Langley Research Center, LDEF: 69 Months in Space. First Post-Retrieval Symposium, Part 3 Jan. 1992 p 1675-1685 (For primary document see N92-27083 17-99)
Avail: NTIS HC/MF A21; 1 functional color page

77 THERMODYNAMICS AND STATISTICAL PHYSICS

Includes quantum mechanics; theoretical physics; and Bose and Fermi statistics.

For related information see also *25 Inorganic and Physical Chemistry* and *34 Fluid Mechanics and Heat Transfer.*

N92-26617# Naval Postgraduate School, Monterey, CA.
EFFECTS OF POWER PULSATIONS ON NATURAL CONVECTION FROM DISCRETE HEAT SOURCES M.S. Thesis
Stephen Larsen Dec. 1991 285 p
(AD-A246557) Avail: NTIS HC/MF A13

The natural convection heat transfer response of an array of heaters flush mounted on a vertical test surface in water to periodic input power has been investigated. Two types of periodic input power variations were examined: a triangular wave and an approximate square wave. The resulting heater temperatures over several cycles were measured for mean values of 0.5, 1.0, 2.0, and 3.0 watts and varying amplitudes. The frequency of the input power pattern was also varied, from 0.025 to 0.1 Hz. The measured heater temperatures were compared with the responses for steady input power equal to the mean of the periodic input. GRA

N92-26733 Georgia Inst. of Tech., Atlanta.
HYPERSONIC AEROSPACE VEHICLE LEADING EDGE COOLING USING HEAT PIPE, TRANSPIRATION AND FILM COOLING TECHNIQUES Ph.D. Thesis
James Michael Modlin 1991 131 p
Avail: Univ. Microfilms Order No. DA9136243

An investigation was conducted to study the feasibility of cooling hypersonic vehicle leading edge structures exposed to severe aerodynamic surface heat fluxes using a combination of liquid metal heat pipes and surface mass transfer cooling techniques. A generalized, transient, finite difference based hypersonic leading edge cooling model was developed that incorporated these effects and was demonstrated on an assumed aerospace plane-type wing leading edge section and a SCRAMJET engine inlet leading edge section. The hypersonic leading edge cooling model was developed using an existing, experimentally verified heat pipe model. Two applications of the hypersonic leading edge cooling model were examined. An assumed aerospace plane-type wing leading edge section exposed to a severe laminar, hypersonic aerodynamic surface heat flux was studied. A second application of the hypersonic leading edge cooling model was conducted on an assumed one-quarter inch nose diameter SCRAMJET engine inlet leading edge section exposed to both a transient laminar, hypersonic aerodynamic surface heat flux and a type 4 shock interference surface heat flux. The investigation led to the conclusion that cooling leading edge structures exposed to severe hypersonic flight environments using a combination of liquid metal heat pipe, surface transpiration, and film cooling methods appeared feasible. Dissert. Abstr.

N92-26780 Maryland Univ., College Park.
FINITE TEMPERATURE QUANTUM FIELD THEORY IN CURVED SPACETIME Ph.D. Thesis
Aris Michael Stylianopoulos 1991 236 p
Avail: Univ. Microfilms Order No. DA9133172

Several methods towards the formulation of theories of quantum fields in non equilibrium conditions are presented and applied to the studies of quantum thermal processes in the early Universe. The methods we introduce and problems studied include the zeta function method for static spacetimes, applied to the calculation of the finite temperature effective potential for a lambda phi (exp 4) field in static Taub spacetime. This result is useful for calculating the critical temperature for symmetry restoration of the scalar field. Another problem studied is an extension of the imaginary time formalism, coupled with a quasilocal expansion for slowly varying background fields to derive the one-loop finite temperature effective Lagrangian for lambda phi (exp 4) fields in curved spacetime. For spacetimes with small curvature, we use a Riemann normal coordinate for the metric and a derivative expansion for the background field. For homogeneous cosmologies we consider conformally related fields and the Robertson Walker universe as background to carry a thermal perturbation calculation. In addition, for a Bianchi type-1 universe, we use an expansion in orders of small anisotropy. Also discussed is a two particle irreducible effective action and 1/N approximation for O(N) lambda phi (exp 4) field for the study of symmetry behavior at finite temperature in curved spacetime. We find that for slowly varying fields the critical temperature is increased by an amount proportional to the second time derivative of the background field. For various spacetime dimensions and for static flat spacetime we calculate the finite temperature effective potential both at the one loop level and in a 1/N approximation. In both cases we find failure of dimensional reduction. As transition to quantum kinetic field theory and non equilibrium statistical field theory we calculate the Wigner function for a near thermal massive non conformal free scalar field in the Robertson Walker universe, and the one loop near thermal density matrix of a quasilocal system. To go beyond finite temperature we introduce the closed time patch effective action which is useful for treating non equilibrium quantum processes. As an example, we calculate the viscosity function for the scalar background field due to fermion pair production for the Yukawa interaction. Dissert. Abstr.

N92-26805# Institut des Hautes Etudes Scientifiques, Bures-sur-Yvette (France).
NON-COMPACT WZW CONFORMAL FIELD THEORIES
K. Gawedzki Oct. 1991 34 p
(PB92-125038; IHES/P/91/73) Avail: NTIS HC/MF A03

Non-compact WZW sigma models are considered, especially the ones with symmetric space H(sup C)/H as the target, for H in a compact Lie group. The author offers examples of non-rational conformal field theories. The author notes their relation to the compact WZW models, but stresses their distinctive features such as the continuous spectrum of conformal weights, diverging partition functions, and the presence of two types of operators analogous to the local and non-local insertions recently discussed in the Liouville theory. Gauging non-compact abelian subgroups of H(sup C) leads to non-rational coset theories. In particular, gauging one parameter boosts in the SL(2,C)/SU(2) model gives an alternative, explicitly stable construction of a conformal sigma model with the euclidean 2D black hole target. The author computes the

(regularized) toroidal partition function and discusses the spectrum of the theory. A comparison is made with a more standard approach based on the U(1) coset of the SU(1,1) WZW theory where stability is not evident, but where unitarity becomes more transparent.
Author

N92-27058# Naval Postgraduate School, Monterey, CA.
NUCLEATE POOL BOILING OF R-114 AND R-114/OIL MIXTURES FROM SINGLE ENHANCED TUBES M.S. Thesis
Dean C. Sugiyama Sep. 1991 227 p
(AD-A245487) Avail: NTIS HC/MF A11

Nucleate pool boiling heat transfer is an integral part of any vapor-compression refrigeration cycle. With a view to improving overall cycle efficiency, the heat transfer performance in the evaporator can be improved by using enhanced boiling surfaces. This thesis looks at the pool boiling characteristics of R-114 (presently used in large shipboard AC systems) from 10 enhanced single copper tubes and compares performance with a smooth copper tube. Since small amounts of oil escape into the refrigerant as it passes through the compressor of a refrigeration system, tests have also been conducted with up to 10 pct. (by weight) of a miscible oil to see what effect this may have on overall evaporator performance. GRA

N92-27171# Naval Postgraduate School, Monterey, CA.
STUDIES IN CHAOS USING STOCHASTIC METHODS M.S. Thesis
Edward A. Healy, Jr. Jun. 1991 81 p
(AD-A246919) Avail: NTIS HC/MF A05

Methods of chaos have been used to classify many heretofore inexplicable nonlinear dynamical systems in fields as diverse as ecology to engineering and economics to meteorology. This thesis presents the mathematical background needed to understand chaos as well as the engineering techniques used to study the nature of dynamical systems. Several dynamical systems are studied using two probabilistic measures of chaos, fractal correlation dimension, and the multivariate scaling analysis. A new technique for developing a multivariate scaling analysis using a time embedding procedure is presented. The dynamical systems studied include the Lorenz equations, Duffing's equation, and helicopter flight vibrations. GRA

N92-26985# Japan Systems Corp., Kawasaki.
THERMAL ANALYSIS OF EVAPORATIVE COOLERS
Masatoshi Ohuchi, Masao Furukawa (National Space Development Agency, Ibaraki, Japan), and Koichi Oshima *In* ESA, 4th European Symposium on Space Environmental Control Systems, Volume 2 Dec. 1991 p 851-854 (For primary document see N92-26950 17-54)
Avail: NTIS HC/MF A23; ESA, EPD, ESTEC, Noordwijk, Netherlands, HC 150 Dutch guilders (2 vols)

80 SOCIAL SCIENCES (GENERAL)

Includes educational matters.

No abstracts in this category.

81 ADMINISTRATION AND MANAGEMENT

Includes management planning and research.

N92-26250# Technische Univ., Delft (Netherlands).
DEVELOPING AN ADAPTIVE SCHEDULING SUPPORT ENVIRONMENT Ph.D. Thesis
Alexander Verbraeck 21 Nov. 1991 232 p
(ISBN-90-9004609-7; ETN-92-91286) Copyright Avail: NTIS HC/MF A11

In order to have a mode of communication for modeling problems, a general model that describes scheduling problems is presented. This model was developed using literature and experiences with a number of industrial scheduling problems as a basis. The case of an actual scheduling problem at a real life company is detailed. At the company, one of the production planners who is scheduling manually, experiences a number of problems. A descriptive model of the current scheduling situation is presented. Possible solutions for the scheduling problem at the company are described. The most important considerations for the actual implementation of the scheduling support system are given. Using the implementation of the scheduling support environment, a number of experiments were carried out to test the feasibility of the solution. The outline of the experiments and the analysis of the results are given. The original research questions and the experiments and results are discussed and conclusions are drawn. ESA

N92-26353# Small Business Administration, Washington, DC.
US SMALL BUSINESS ADMINISTRATION FY 1990 NATIONAL ACCOMPLISHMENT REPORT AND FY 1991 NATIONAL AFFIRMATIVE EMPLOYMENT PROGRAM PLAN
1991 91 p
(PB92-157064) Avail: NTIS HC/MF A05

The Accomplishment Report reflects action taken at the national level during fiscal year (FY) 1990 to meet Agency program objectives as set forth in the Agency-wide Multi-Year Affirmative Employment Program Plan for Minorities and Women for FY 1988 through FY 1992. The Plan Update reflects the occupational areas where there continues to be conspicuous absence or manifest imbalance of minorities and women in the Agency's work force and, therefore, where affirmative employment efforts need to be directed to ensure continued progress in achieving a representative work force. It describes the Agency's FY 1991 affirmative recruitment and placement goals. GRA

N92-26369# Small Business Administration, Washington, DC. Office of the Chief Counsel for Advocacy.
SMALL BUSINESSES MAKE A DIFFERENCE
Nov. 1991 457 p Presented at the 12th National Legislative Conference on Small Business Issues, Kansas City, MO, 17-20 Nov. 1991
(PB92-160118) Avail: NTIS HC/MF A20

A collection of issue papers prepared on a variety of issues affecting small business, the publication was presented for attendees at the 12th National Legislative Conference on Small Business Issues, which was sponsored by the U.S. Small Business Administration's Office of Advocacy and held in Kansas City, Missouri, on November 17-20, 1991. GRA

N92-26426# Carnegie-Mellon Univ., Pittsburgh, PA. Robotics Inst.
KNOWLEDGE-BASED PRODUCTION MANAGEMENT: APPROACHES, RESULTS, AND PROSPECTS
Stephen F. Smith Dec. 1991 41 p
(AD-A245714; CMU-RI-TR-91-21) Avail: NTIS HC/MF A03

In this paper we provide an overview of research in the field of knowledge-based production management. We begin by examining the important sources of decision-making difficulty in practical production management domains, discussing the requirements implied by each with respect to the development of effective production management tools, and identifying the general opportunities in this regard provided by AI-based technology. We then categorize work in the field along several different dimensions, indicating the principal types of manufacturing domains that have received attention, the particular production management and control activities that are emphasized, and the various perspectives that have emerged with respect to the tradeoff that must be made in practical production management contexts between predictive decision-making to optimize behavior and reactive decision-making to manage executional uncertainty. The bulk of the paper focuses on summarizing the dominant approaches to knowledge-based production management that have emerged. Here, we identify the

general concepts, principles, and techniques that distinguish various paradigms, characterize the strengths and weaknesses of each paradigm from the standpoint of different production management requirements, and indicate the results that work within each paradigm has produced to date. GRA

N92-26523# MO-SCI Corp., Rolla, MO.
SURVEY OF SMALL BUSINESS USE OF INTELLECTUAL PROPERTY PROTECTION
M. S. Koen Feb. 1992 253 p
(Contract SBA-3070-OA-88)
(PB92-151703) Avail: NTIS HC/MF A12

Small and large enterprises use the intellectual property protection system in a variety of ways. The goal was to gain a greater understanding of the forms of intellectual property protection favored by large and small enterprises depending on their circumstances. The difficulties faced with intellectual property protection system and recommendations for improving the system are examined. It is shown that when small enterprises using the intellectual property protection system are compared with large enterprises that also use the system, relationships with other enterprises and organizations are more crucial to the small enterprises than to the large ones. Small enterprises have more problems with infringements of intellectual property, with the Freedom of Information Act, and in meeting patent costs; particularly the fees of private patent attorneys. Both technology licenses granted and licenses received are more important for the operating income of the small enterprises so involved. Author

N92-26552*# Research Inst. for Computing and Information Systems, Houston, TX.
DATA MANAGEMENT SYSTEMS (DMS): COMPLEX DATA TYPES STUDY. VOLUME 1: APPENDICES A-B. VOLUME 2: APPENDICES C1-C5. VOLUME 3: APPENDICES D1-D3 AND E Final Report
T. F. Leibfried, Jr., Sadegh Davari, Swami Natarajan, and Wei Zhao (Texas A&M Univ., College Station.) Apr. 1992 636 p
(Contract NCC9-16)
(NASA-CR-190397; NAS 1.26:190397) Avail: NTIS HC/MF A99

Two categories were chosen for study: the issue of using a preprocessor on Ada code of Application Programs which would interface with the Run-Time Object Data Base Standard Services (RODB STSV), the intent was to catch and correct any mis-registration errors of the program coder between the user declared Objects, their types, their addresses, and the corresponding RODB definitions; and RODB STSV Performance Issues and Identification of Problems with the planned methods for accessing Primitive Object Attributes, this included the study of an alternate storage scheme to the 'store objects by attribute' scheme in the current design of the RODB. The study resulted in essentially three separate documents, an interpretation of the system requirements, an assessment of the preliminary design, and a detailing of the components of a detailed design. Author

N92-26660# Naval Postgraduate School, Monterey, CA.
BEST VALUE CONTRACTING IN THE PROCUREMENT OF ENGINEERING AND TECHNICAL SERVICES M.S. Thesis
Herbert F. Byrns Dec. 1991 118 p
(AD-A245524) Avail: NTIS HC/MF A06

The purpose of this research is to define and discuss the 'best value' concept and how it relates to the procurement of engineering and technical services. The research was conducted by a review of regulations and policy guidance, interviews with Government and defense industry personnel, and visits to Navy Contracting Activities that procure engineering and technical services. The intent of the study was to analyze how the 'best value' concept is currently implemented, problems with implementation, and to offer recommendations to improve 'best value' source selection. This study also recommends areas for future study that may further improve the use of 'best value' in the procurement of professional services. GRA

N92-26790*# National Aeronautics and Space Administration. Ames Research Center, Moffett Field, CA.
PLANNING AND SCHEDULING RESEARCH AT NASA AMES RESEARCH CENTER
Peter Friedland Nov. 1990 8 p
(NASA-TM-107888; FIA-90-11-01-01; NAS 1.15:107888) Avail: NTIS HC/MF A02

Planning and scheduling is the area of artificial intelligence research that focuses on the determination of a series of operations to achieve some set of (possibly) interacting goals and the placement of those operations in a timeline that allows them to be accomplished given available resources. Work in this area at the NASA Ames Research Center ranging from basic research in constrain-based reasoning and machine learning, to the development of efficient scheduling tools, to the application of such tools to complex agency problems is described. Author

N92-26811# Department of Energy, Washington, DC. Research Office.
SMALL BUSINESS INNOVATION RESEARCH: PROGRAM SOLICITATION CLOSING DATE, 27 JANUARY 1992
1992 88 p
(DE92-010132; DOE/ER-0504) Avail: NTIS HC/MF A05

The Department of Energy (DOE) invites small business firms to submit grant applications under this tenth annual solicitation for the Small Business Innovation Research (SBIR) program. Firms with strong research capabilities in science or engineering in any of the topic areas described in Appendix 1 are encouraged to participate. DOE will support high quality research or research and development (R & D) on advanced concepts concerning important energy related scientific or engineering problems and opportunities that could lead to significant public benefit if the research is successful. Objectives of this program include stimulating technological innovation in the private sector, strengthening the role of small business in meeting Federal research and R & D needs, increasing the commercial application of DOE supported research results, and improving the return on investment from Federally funded research for economic and social benefits to the Nation. DOE

N92-26828# General Accounting Office, Washington, DC.
KENNEDY SPACE CENTER: DECISION ON PHOTOGRAPHIC REQUIREMENTS APPEARS JUSTIFIED
Apr. 1992 10 p
(GAO/NSIAD-92-192; B-248197) Avail: NTIS HC/MF A02

NASA's decision to transfer some photography work from the photographic support contractor to the shuttle processing, payload ground operations, and base operations contractors was an attempt to hold the three contractors more fully accountable for accomplishment of their respective missions. Most of the photographic work in question is performed as a minor part of the duties of quality assurance personnel with simple-to-use cameras. According to NASA's Inspector General, the photography costs are less than would be incurred if the photographs were taken by the photographic support contractor. Engineers who use the photographs are generally satisfied with their quality, and in cases where NASA believes that professional quality photographs are needed, it can have the photographic support contractor take them. Author

N92-26863# UFA, Inc., Newton, MA.
EXPERT SYSTEM MANAGEMENT SYSTEM Final Report, Jan. 1987 - Sep. 1990
Arthur Gerstenfeld and Kiet D. Hoang 30 Aug. 1991 43 p
(Contract F33615-88-C-1720)
(AD-A247102; WL-TR-91-1063) Avail: NTIS HC/MF A03

The Expert System Management System (ESMS) Small Business Innovative Research Contract developed a distributed fault-tolerant expert system shell for multiple expert systems in a multiprocessor environment. The ESMS contained four domain specific expert systems called Manager Expert System, Route Planner Expert System, Weapon Expert System, and Situation Awareness and Display Expert System. The ESMS expert system

shell was written in LISP and runs on four Explorer II computers. Each of the expert systems were responsible for their own area of expertise, but each communicated and cooperated with the other experts along with a real-time man-in-the-loop flight simulator. The four expert systems developed were host independent, relocatable, and interruptable when a higher priority task arrived. The ESMS was able to detect network and processor failures, along with being able to reconfigure the system according to the available resources. The system was both event and data driven, and shared global variables. The system was interfaced with a MicroVAX 2 computer to the MIL-STD-1553 data bus in order to receive waypoints and aircraft data from a real-time man-in-the-loop simulation. GRA

N92-27046 Institute for Perception RVO-TNO, Soesterberg (Netherlands). Cognitive Psychology Group.
HUMAN COGNITIVE PROCESSES IN COMMAND AND CONTROL PLANNING. 3: DETERMINING BASIC PROCESSES INVOLVED IN PLANNING IN TIME AND SPACE Final Report [COGNITIEVE PROCESSEN IN COMMAND AND CONTROL PLANNING. 3: BASISPROCESSEN IN PLANNING IN TIJD EN RUIMTE]
Carol A. McCann (Defence and Civil Inst. of Environmental Medicine, North York, Ontario) and P. J. M. D. Essens 7 Aug. 1991 51 p Sponsored by TNO Defence Research
(IZF-1991-B-11; TD91-2171; ETN-92-91234) Copyright Avail: TNO Inst. for Perception, Kampweg 5, P.O. Box 23, 3769 ZG Soesterberg, Netherlands

The ways in which people create plans to accomplish a task that has both temporal and spatial components are investigated. Two goals were addressed to develop a method for determining the cognitive processes associated with planning; and to develop a model for efficient planning for the task used in the study. Two planners gave verbal and graphical protocols while planning the most efficient way for shopping robots to pick up commodities in a grocery store. Each planner created a plan for twelve such problems and the plan was executed after each planning session. The protocols were analyzed to identify the primitive concepts and actions used in the planning process. Observations of planners' behavior in this study indicated that plans were developed in an evolutionary manner. Planners discovered and refined methods for organizing the information and procedures for manipulating it during the course of the sessions. It is shown that planners attended to different levels of detail of information in planning, and used a variety of planning strategies. A hierarchical model for efficient planning for this task is proposed that assumes plans are developed hierarchically at three successive levels of detail. ESA

N92-27080* National Aeronautics and Space Administration, Washington, DC.
MANAGEMENT: A BIBLIOGRAPHY FOR NASA MANAGERS
Mar. 1992 168 p
(NASA-SP-7500(26); NAS 1.21:7500(26)) Avail: NTIS HC A08

This bibliography lists 630 reports, articles and other documents introduced into the NASA Scientific and Technical Information System in 1991. Items are selected and grouped according to their usefulness to the manager as manager. Citations are grouped into ten subject categories: human factors and personnel issues; management theory and techniques; industrial management and manufacturing; robotics and expert systems; computers and information management; research and development; economics, costs and markets; logistics and operations management; reliability and quality control; and legality, legislation, and policy. Author

N92-27190# Department of Defense, Washington, DC.
THE DEPARTMENT OF DEFENSE CRITICAL TECHNOLOGIES PLAN FOR THE COMMITTEES ON ARMED SERVICES, UNITED STATES CONGRESS
1 May 1991 376 p
(AD-A234900) Avail: NTIS HC/MF A17

The critical technologies plan describes 21 technologies considered essential for maintaining the qualitative superiority of U.S. weapon systems and an investment strategy is outlined to manage and promote the development of these technologies. This 3rd annual plan has a new section added which documents funding levels for individual Defense Critical Technologies for relevant programs. The orderly, evolutionary improvements is sought in weapon systems. Innovative, highly leveraged breakthrough technology is sought along with the insertion of this technology into the military capability. Also, technology trump cards are sought to sustain long term dominance in the technological arms race. The Science and Technology program is the principal vehicle for implementing these objectives. This year's planning process confirms the priority placed on these technologies by DoD in the 1990 Critical Technologies Plan. The Defense Critical Technologies are discussed further and brief technology plan summaries are presented. The funding is summarized. Author

N92-26990# Compagnia Italiana Servizi Tecnici, Rome. Space Div.
LOGISTICS IN SPACE: TOOLS TO SUPPORT ASTRONAUTS
G. F. DeLuca, S. Masullo, and A. Schisano *In* ESA, 4th European Symposium on Space Environmental Control Systems, Volume 2 Dec. 1991 p 893-898 (For primary document see N92-26950 17-54)
Avail: NTIS HC/MF A23; ESA, EPD, ESTEC, Noordwijk, Netherlands, HC 150 Dutch guilders (2 vols)

82 DOCUMENTATION AND INFORMATION SCIENCE

Includes information management; information storage and retrieval technology; technical writing; graphic arts; and micrography.

For computer documentation see *61 Computer Programming and Software.*

N92-26174# North Atlantic Treaty Organization, Brussels (Belgium).
EXECUTIVE SUMMARY OF THE TECHNICAL PROCEEDINGS ON MILITARY INFORMATION SYSTEM ENGINEERING (DEFENCE RESEARCH GROUP PANEL 11 ON INFORMATION PROCESSING TECHNOLOGY)
13 Jan. 1992 8 p Symposium held in Brussels, Belgium, 13 Jan. 1992
(AD-A245656; AC/243-N/347) Avail: NTIS HC/MF A02

The symposium provided a forum for information exchange and discussion of current research in information processing technology and its application to the engineering of military information systems. The objectives were: (1) To assess the problems of engineering information processing systems for military use; (2) To identify emerging technologies and techniques for system engineering and evaluate the benefits offered; and (3) To determine the research needed to facilitate the introduction and application of beneficial techniques to the engineering of future military systems. GRA

N92-26176# Naval Postgraduate School, Monterey, CA.
THE DEVELOPMENT OF A DESIGN DATABASE FOR THE COMPUTER AIDED PROTOTYPING SYSTEM M.S. Thesis
Andrew P. Dwyer and Garry W. Lewis Sep. 1991 376 p
(AD-A245786) Avail: NTIS HC/MF A17

The Computer Aided Prototyping System (CAPS) was created to rapidly prototype real time systems to determine early in the development cycle whether system requirements can be met. The CAPS consists of several software tools that automatically generate an executable Ada model of the proposed system. This thesis describes the development of a design database (DDB) for the CAPS. The DDB is an engineering database that contains all information related to a prototype software design. The DDB enhances the CAPS environment and the prototyping paradigm by providing to the designer the functions of storage, retrieval, viewing, and versioning of prototype components. GRA

N92-26221# California Univ., Berkeley. Lawrence Berkeley Lab.
INFORMATION TECHNOLOGY RESOURCES ASSESSMENT
D. F. Stevens, ed. Jan. 1992 65 p
(Contract DE-AC03-76SF-00098)
(DE92-009498; LBL-31610) Avail: NTIS HC/MF A04

This year's Information Technology Resources Assessment (ITRA) is something of a departure from traditional practice. Past assessments have concentrated on developments in fundamental technology, particularly with respect to hardware. They form an impressive chronicle of decreasing cycle times, increasing densities, decreasing costs (or, equivalently, increasing capacity and capability per dollar spent), and new system architectures, with a leavening of operating systems and languages. Past assessments have aimed, and succeeded, at putting information technology squarely in the spotlight; by contrast, in the first part of this assessment, we would like to move it to the background, and encourage the reader to reflect less on the continuing technological miracles of miniaturization in space and time and more on the second- and third-order implications of some possible workplace applications of these miracles. This Information Technology Resources Assessment is intended to provide a sense of technological direction for planners in projecting the hardware, software, and human resources necessary to support the diverse IT requirements of the various components of the DOE community. It is also intended to provide a sense of our new understanding of the place of IT in our organizations. DOE

N92-26368# Department of the Treasury, Washington, DC. Office of the Deputy Assistant Secretary for Information Systems.
EXECUTIVE SUMMARY OF INFORMATION SYSTEMS PLANS: FISCAL YEARS 1993 TO 1997
Nov. 1991 108 p
(PB92-158351) Avail: NTIS HC/MF A06

The report outlines the major systems and strategic planning issues in Treasury information systems for fiscal year (FY) 1993-1997. The summary is an overview of the major information systems that the Department expects to implement and maintain over the next five years. It provides Treasury and other government officials, as well as the public, with information on how Treasury addresses strategic issues and plans the development and implementation of information systems that are important not only for Treasury, but for the Federal government as a whole. GRA

N92-26378# Defence Research Establishment, Ottawa (Ontario).
DATA FUSION AND CORRELATION TECHNIQUES TESTBED (DFACTT): FIELD TRIAL 14 JANUARY 1991
Janette D. Hooper and Derek Elsaesser Jul. 1991 60 p
(AD-A245324; DREO-TN-91-11) Avail: NTIS HC/MF A04

The Data Fusion and Correlation Techniques Testbed (DFACTT) is a platform on which to test new methods of data fusion and machine intelligence in the electronic warfare field. With the ability to operate multiple Smalltalk environments as well as independent tasks on a variety of VMEbus based devices, the DFACTT will provide an in-house facility at DREO to quickly prototype new ideas and technologies in the areas of sensor data fusion, parallel processing, and knowledge-based programming. The phase 1 testbed developed under contract was interfaced to real EW sensors from the 2nd (EW) Squadron of the 1st Canadian Division Headquarters and Signals Regiment (CDHSR) for a field trial at Defence Research Establishment Ottawa (DREO), 14 Jan. 1991. One station of the Communications Emitter Locating System (CELS) was connected for location inputs to the DFACTT, as were two WJ8617B receivers for radio intercept input. A scenario was developed and kept secret from those who were to act as operator and analyst on the DFACTT. Three radio networks formed the target for the DFACTT operators. The operators were to intercept and locate the emitters, track them, and determine the objective of the scenario. GRA

N92-26403# Physics and Electronics Lab. TNO, The Hague (Netherlands).
PLAN OF ACTION SURVEY OF FUNCTIONAL REQUIREMENTS FOR A GEOGRAPHICAL INFORMATION SYSTEM Final Report
M. R. Woestenburg 7 Nov. 1991 42 p In DUTCH; ENGLISH summary
(AD-A245622; FEL-91-A286; TDCK-TD91-3272) Avail: NTIS HC/MF A03

This document outlines the action plan for assignment A91KL680, aimed at research on the Digital Geographical Information System (DGIS) which supports command and control within the Royal Army. The research follows two directions. One direction is based on the application of a commercial GIS. The other direction is based on the application of a research GIS. Based on GIS requirements from the users, implementation of those requirements will take place on the most appropriate GIS or on both systems. The study will be concluded with a comparison of both systems. The action plan contains detailed information about the purpose, work packages, schedules and project organization. GRA

N92-26422 Politecnico di Milano (Italy). Dipartimento di Elettronica.
VERIFYING BEHAVIORAL CONSISTENCY OF AN OBJECT-ORIENTED DATABASE SCHEMA
Alberto Coen-Porisini, Luigi Lavazza (Master School CEFRIEL, Milan, Italy), and Roberto Zicari Nov. 1991 25 p
(Rept-91-054; ETN-92-91251) Avail: Politecnico di Milano, Piazza Leonardo da Vinci 32, 20133 Milan, Italy

A simple data flow technique to determine sufficient conditions for ensuring type safeness for an object oriented database system is defined. The technique is based on the notion of 'type sets'; informally speaking a type set is a convenient way to express, at compile time, all types an attribute or a method can possibly be bound to at run time. The static detection of all possible occurrences of run time errors, by looking at the type sets associated to each method and attribute in the schema of an object oriented database, is shown. In particular, this technique is very valuable for verifying the 'behavioral consistency' of the database after some schema modifications are performed. A motivating example is given and the problem of run time type errors is explained. Formal definitions of the fundamental concepts introduced are given. ESA

N92-26453# Cold Spring Harbor Lab., New York, NY.
A COMPUTER SYSTEM FOR ACCESS TO DISTRIBUTED GENOME MAPPING DATA
T. G. Marr Feb. 1992 9 p
(Contract DE-FG02-91ER-61190)
(DE92-008875; DOE/ER-61190/1) Avail: NTIS HC/MF A02

Development of a computer system for access to distributed genome mapping data is continuing. This effort is to develop software which accesses multiple databases and retrieves data which contain information useful for accelerating mapping human chromosomes. For example, the molecular sequence databases (GenBank, EMBL Data Library, PIR, SwissProt) which contain data required for the development of oligonucleotides for probing DNA as well as for extracting data for primer pair development for PCR-based methods. It is also to develop software which qualitatively integrates the following mapping data: (1) markers regionally localized using cytogenetic methods; (2) polymorphic markers ordered by genetic linkage analysis; (3) clones ordered by various 'finger printing' methods; (4) fragments ordered by long range restriction mapping; (5) single genomic fragments or clones that have STSs assigned to them; (6) nucleotide sequences; (7) the associated metadata such as the submitting investigator's name, location, etc; (8) the source organism; (9) the chromosome the element is from; (10) the chromosomal location is whatever detail is available. DOE

N92-26465# Defense Technical Information Center, Alexandria, VA.

CATALOGING GUIDELINES
Gail B. Martens Jan. 1992 147 p
(AD-A246500) Avail: NTIS HC/MF A07

The guidelines for descriptive cataloging is a procedure manual published by the Defense Technical Information Center (DTIC). It outlines the cataloging information to be included in the data fields for online input of technical publications. The text is arranged numerically, by field number, and includes Appendices A through N, with separate sections on special handling and search procedures for duplicate checking. Changes to the security classifications fields have been added to implement DoD 5200.1-R, Information Security Program Regulation. An enhanced version of this guideline for remote input is available as the Shared Bibliographic Input Manual. GRA

N92-26469# Naval Postgraduate School, Monterey, CA.
INFORMATION SYSTEMS PLANNING METHODOLOGIES: A FRAMEWORK FOR COMPARISON AND SELECTION M.S. Thesis
Robert E. Steffensen Sep. 1991 130 p
(AD-A246527) Avail: NTIS HC/MF A07

The success of organizational information systems (IS) depends largely upon effective planning for those information systems. A comprehensive IS plan should provide a coordinated approach to strategic business goals, organizational information requirements, and an overall measure of performance. Acknowledging the importance of comprehensive planning in the process of managing the organization's information resource, a collection of methodologies has been accumulated, to serve in carrying out the IS planning effort. However, a managerial problem that often arises is how to make best use of current planning methodologies. The purpose of this thesis is to survey the existing methodologies, establish a framework for analyzing the IS planning methodologies, and examine some of their advantages and limitations. GRA

N92-26481 Golden Gate Coll., San Francisco, CA.
INFORMATION LIABILITY: NEW INTERPRETATIONS FOR THE ELECTRONIC AGE Ph.D. Thesis
Blodwen Tarter 1991 163 p
Avail: Univ. Microfilms Order No. DA9208142

Information liability hinges on two questions: who is responsible for creating and providing accurate information for third-party consumption; and, to what extent is the creator and/or provider actually liable for the quality of that information? This dissertation examines these questions as they relate to electronic databases. The broad electronic distribution of data appears to have created a demand for a higher standard of quality than is expected of traditional printed materials. This demand for better quality, coupled with the complexity of the electronic information publishing process and the economic value of decisions made based upon online information, has significantly elevated concerns about information liability. The review of the literature falls into four categories: (1) librarian/information specialist malpractice, (2) case law on database producers' and database distributors' liability for accuracy of information, (3) database quality as a conceptual issue, and (4) database quality as a practical issue. Exploratory interviews with selected database producers, distributors, search intermediaries, telecommunications network providers, and end users identified common information liability concerns and possible ways to alleviate those concerns. The dissertation details and categorizes the results of those interviews. The study suggests that the electronic information industry has many ways of limiting its information liability. The judicious use of contracts and disclaimers, careful planning and implementation of quality control and assurance processes and procedures, thorough education of end users, and innovative use of changing technology are logical means to lessen the likelihood of litigation. Each of these tools should be used to the greatest extent possible. The risk/benefit trade off for each organization will determine to what extent these safeguards are implemented. Litigation and damage claims cannot be prevented, but the likelihood of their occurrence can be reduced by careful preventive practices. Emphasis will continue to be upon continual improvement of electronic information delivery as a way to avoid court mandated solutions. However, the drive for profitability, rather than any fear of litigation, is the most compelling reason for maintaining and improving the quality of electronic information. Dissert. Abstr.

N92-26567 Texas A&M Univ., College Station.
NEXUS: A KERNEL COMPLEX OBJECT MANAGEMENT SYSTEM Ph.D. Thesis
Santosh S. Venkatraman 1991 261 p
Avail: Univ. Microfilms Order No. DA9134019

In this research complex objects are captured via a graphical object scheme called the NEXUS scheme. The NEXUS scheme supports aggregation, IS-A, and association relationships along with their constraints. The scheme is particularly designed to capture different types of IS-A relationships, in addition to aggregation and association. A formalism is developed for the NEXUS scheme which precisely describes the scheme and its semantics. The formalism describes both the static (structural), as well as the dynamic (updates) aspects of the NEXUS scheme. The plausibility of using the nested relational model to support the objects and semantics portrayed in the NEXUS scheme is studied. It turns out that the nested relational model has to be extended to accommodate complex objects. An algorithm is presented which translates a NEXUS scheme into such an 'extended' nested relational scheme. An architecture is proposed to implement a complex object management based on NEXUS. Finally, a part of the NEXUS system is implemented using LEX and YACC tools on a SUN 3/160 workstation running under UNIX. Dissert. Abstr.

N92-26575# Sandia National Labs., Albuquerque, NM.
TECHNICAL SPECIFICATION FOR THE SANDIA MANAGEMENT RESTRUCTURE STUDY TEAM (MRST) PROTOTYPE INFORMATION SYSTEM
T. R. Wyatt, R. C. Hall, L. T. Davis, E. J. Klamerus, and I. Thurston Jan. 1992 112 p
(Contract DE-AC04-76DP-00789)
(DE92-010360; SAND-91-1575) Avail: NTIS HC/MF A06

This document contains implementation details for the Sandia Management Restructure Study Team (MRST) Prototype Information System, which resides on a Sun SPARC 2 workstation employing the INGRES RDBMS. The INGRES/Windows 4GL application editor was used to define the components of the two user applications which comprise the system. These specifications together with the MRST information model and corresponding database definition constitute the MRST Prototype Information System technical specification and implementation description presented herein. The MRST Prototype Information System represents a completed software product which has been presented to the Management Restructure Study Team to support the management restructing processes at Sandia National Laboratories. DOE

N92-26614 Case Western Reserve Univ., Cleveland, OH.
THE EFFECT OF COLLECTION HOMOGENEITY ON TERM ASSOCIATION AS A METHOD OF REQUEST EXPANSION IN INFORMATION RETRIEVAL Ph.D. Thesis
Elsuni Sidahmed Elkalifa 1991 122 p
Avail: Univ. Microfilms Order No. DA9202263

Statistical techniques have been proposed as alternatives to traditional methods of request expansion or feedback mechanisms. These statistical measures are derived from formulas which attempt to correlate two given index terms on the basis of their frequency of co-occurrence in the documents of a given collection. These techniques attempt to relax the retrieval requirement that the request terms should exactly match the document descriptors before the documents can be judged relevant to the request. Though simple the concept seems to be, the complexity of the natural language and the irregularities that govern the syntactic and sematic structure make the application of such techniques rather complicated. Due to this most of the previous investigations failed to produce any efficient alternatives to traditional information retrieval systems. A major problem is false or spurious association

between semantically and conceptually independent terms. It is believed that the failure of these studies is mainly due to the heterogeneity of the collections used rather than to the inefficiency of the techniques themselves. A combination of two techniques is used to create a more powerful request expansion technique. Cluster analysis techniques are used to subdivide the document collection into small more homogeneous collections; then term association techniques are applied to determine which terms could be used to expand the original request. A method used to compute the degree of association between original request terms and document descriptors is based on the formula, R(sub J1) = (N(W(sub J)W(sub 1)))/(N(W(sub J)) + N(W(sub 1)) - N(W(sub J)W(sub 1))) where: R(sub J1) is the coefficient of association between term W(sub J) and term W(sub 1); N(WPVjPVW(sub 1)) = number of documents which both term W(sub J) and term W(sub 1) appeared; N(W(sub J)) = number of documents in which term W(sub J) occurred; N(W(sub 1)) = number of documents in which term W(sub 1) occurred. The document file consisted of the significant words in the titles, abstracts, and identifiers of 150 documents. Three search strategies were formulated for each request: the first consisted of the original search terms, the second included terms extracted from the entire collection while the third consisted of a combination of terms extracted from specific clusters and the original request terms. Dissert. Abstr.

N92-26689# Department of Energy, Oak Ridge, TN. Office of Scientific and Technical Information.
DOE NEW TECHNOLOGY
A. Tamura, ed. and L. Kane, ed. Jan. 1992 190 p
(DE92-001619; DOE/ER-0535P) Avail: NTIS HC/MF A09

The purpose of DOE New Technology is to provide information on how to access specific technologies developed through research sponsored by the U.S. Department of Energy (DOE) and performed by DOE laboratories or by contracted researchers. This document describes technologies identified as having potential for commercial applications, in addition to a catalog of current patent applications and patents available for licensing from DOE and DOE contractors. DOE New Technology is divided into three sections. The first section, 'New Technology from DOE', consists of technology assessments which are prepared by DOE laboratories whenever a research project is judged as having potential for commercial applications. These entries describe each technology and give a point of contact for more information. The second and third sections, 'Patents Available for Licensing from DOE', and 'Other Patents from Technologies Funded by DOE' include both current technologies' patents and patent applications. Technologies owned by DOE are announced at both the application and the patent stage, while technologies funded but not owned by DOE are announced at patent stage only. DOE

N92-26762# Naval Postgraduate School, Monterey, CA.
MEASURING THE EFFECTIVENESS OF INFORMATION SYSTEMS M.S. Thesis
Angela W. Cyrus Jun. 1991 70 p
(AD-A246007) Avail: NTIS HC/MF A04

Measuring the effectiveness of information systems (IS) is an issue that has generated debate and research among academics and practitioners. This thesis consolidates the numerous and various approaches to measuring IS effectiveness into six general schools of thought: user satisfaction, system usage, performance/usefulness, productivity, value analysis, and cost-benefit analysis. It then presents a model for examining the various linkages that exist among the IS effectiveness measures. These linkages include: user satisfaction and system usage, system usage and performance, performance and productivity, and productivity and cost justification. This research provides the user a summary of the IS effectiveness literature of the past two decades and a consolidated reference for measuring the effectiveness of information systems. GRA

N92-26765# Naval Postgraduate School, Monterey, CA.
A PROTOTYPE SEMANTIC INTEGRITY FRONT END EXPERT SYSTEM FOR A RELATIONAL DATABASE M.S. Thesis
George J. Salitsky 26 Sep. 1991 141 p
(AD-A246084) Avail: NTIS HC/MF A07

Information is a critical resource in today's enterprises. Whether they are industrial, commercial, educational, or military, these organizations maintain an ever increasing amount of information in databases. Ensuring the accuracy of information in a database is paramount to the organizations that maintain these databases. Many decisions are made from the information extracted from the database, and incorrect data will lead to incorrect decision making. This thesis examines the feasibility of using expert systems for enforcing semantic integrity constraints to relational databases. To accomplish this goal, the thesis develops a classification for semantic integrity constraints, applies it to develop rules for the Navy's Naval Aircraft Flight Record application, and builds a front end expert system to enforce these rules dynamically. The expert system enforces integrity rules for all maintenance operations. GRA

N92-26767# Logistics Management Inst., Bethesda, MD.
DOD IMPLEMENTATION GUIDELINES FOR ELECTRONIC DATA INTERCHANGE (EDI), VOLUME 2 Final Report
Morey M. Henderson and Ann P. Lewis Dec. 1991 446 p
(Contract MDA903-90-C-0006)
(AD-A246614; LMI-DL001-01R1-Vol-2) Avail: NTIS HC/MF A19

This document establishes a baseline of DoD's conventions for implementing the American National Standards Institute (ANSI) Accredited Standards Committee (ASC) X12 uniform standard for the electronic interchange of business transaction. The DoD transaction set conventions are defined. It includes the instructions for implementing the control structure and definitions of the usage indicators and applicable codes. In addition to the communication control structure, the EDI structure provides the standards user with multiple levels of control to ensure data integrity. It does so by using header and trailer control segments designed to uniquely identify the start and end of the interchange functional groups and transaction sets. GRA

N92-26776 Claremont Graduate School, CA.
USER INTERFACE CONSISTENCY ACROSS END-USER APPLICATION PROGRAMS: EFFECT ON LEARNING AND SATISFACTION Ph.D. Thesis
John W. Satzinger 1991 292 p
Avail: Univ. Microfilms Order No. DA9123660

Some assumptions of the consistency guideline were tested by manipulating the consistency of the interface across applications. The two independent variables were degree of consistency of the command language and degree of consistency of the appearance of the display screen. A laboratory experiment was conducted where participants learned and used two applications in one training session. Four experimental conditions resulted from the two-by-two factorial design. The dependent variables were amount learned, which included user knowledge and the ability to use the applications, and satisfaction, which included subjective evaluations of the application designs, ease of use, and perceived usefulness. The applications learned were modules in a cooperative work system developed specifically for the study to carefully manipulate interface consistency across applications. All combinations of interfaces used direct manipulation, color graphics, and selection with a mouse. No differences were found in user knowledge about the applications, but inconsistent command languages across applications required more user actions, providing support for the benefits of consistent command languages. Inconsistent screen appearance, however, led to greater accuracy and higher satisfaction ratings, which were surprising results. Overall, the findings provide support for the consistency guideline for command languages, but a distinctive appearance for the interface of an application might reduce complexity for an end-user working with multiple applications in a work session. Dissert. Abstr.

N92-26830# Wichita State Univ., KS. National Inst. for Aviation Research.
TEST PLAN FOR THE INTERNATIONAL AIRCRAFT OPERATOR INFORMATION SYSTEM
John J. Hutchinson, John Ellis, Barbara K. Smith, and Jim North Feb. 1992 10 p
(Contract DTFA03-89-C-00057)
(DOT/FAA/CT-91/18) Avail: NTIS HC/MF A02

This test plan outlines a methodology for determining whether the International Aircraft Operator Information System is ready to become fully operational as a prototype system. The system was operational on a very limited basis beginning in Aug. 1990. During the review, Federal Aviation Administration (FAA) personnel will be able to examine information system documentation, data base contents, information system processes, and reports. The actual tests will consist of entering the system, generating queries, and reviewing audits. In the course of carrying out these activities it will be possible to review all of the aspects of the system.
Author

N92-26875 Physics and Electronics Lab. TNO, The Hague (Netherlands).
BUILDING A GIS ON TOP OF THE OPEN DBMS POSTGRES Final Report [HET BOUWEN VAN EEN GIS OP BASIS VAN HET OPEN DBMS POSTGRES]
P. J. M. vanOosterom and C. Vijlbrief Aug. 1991 27 p Presented at the 2nd European Conference on Geographical Information Systems, Brussels, Belgium, 2-5 Apr. 1991 Prepared in cooperation with Institute for Perception RVO-TNO, Soesterberg, Netherlands
(FEL-91-B183; TD91-2613; ETN-92-91222) Copyright Avail: TNO Physics and Electronics Lab., P.O. Box 96864, 2509 JG The Hague, Netherlands

Many commercial Geographic Information Systems (GIS) have a dual architecture: the thematic information is stored in a relational Data Base Management System (DBMS) and the spatial information is stored on a separate subsystem capable of dealing with spatial data and spatial queries. Besides being conceptually inelegant, this dual architecture also reduces the performance, because objects must be retrieved and compiled from components that may be stored far apart in the two subsystems. A solution based on the extendable database management system 'Postgres', in which thematic and spatial data are stored together, is presented.
ESA

N92-26926# Office of Management and Budget, Washington, DC.
MANAGING FEDERAL INFORMATION RESOURCES: UNDER THE PAPERWORK REDUCTION ACT OF 1980 Annual Report No. 9
Jan. 1992 58 p
(PB92-154905) Avail: NTIS HC/MF A04

The report describes the Office of Management and Budget's (OMB's) implementation of the Paperwork Reduction Act of 1980 objectives during 1990. It discusses OMB management and oversight of the major Federal information gathering, processing, and dissemination activities.
GRA

N92-27081* National Aeronautics and Space Administration, Washington, DC.
NASA PATENT ABSTRACTS BIBLIOGRAPHY: A CONTINUING BIBLIOGRAPHY. SECTION 2: INDEXES (SUPPLEMENT 40)
Jan. 1992 564 p
(NASA-SP-7039(40)-Sect-2; NAS 1.21:7039(40)-Sect-2) Avail: NTIS HC A24; NTIS standing order as PB92-911100, A03

A subject index is provided for over 5100 patents and patent applications for the period May 1969 through December 1991. Additional indexes list personal authors, corporate authors, contract numbers, NASA case numbers, U.S. patent class numbers, U.S. patent numbers, and NASA accession numbers.
Author

N92-27170*# National Aeronautics and Space Administration. Langley Research Center, Hampton, VA.
NASA/DOD AEROSPACE KNOWLEDGE DIFFUSION RESEARCH PROJECT: AN INITIAL INVESTIGATION INTO THE PRODUCTION AND USE OF SCIENTIFIC AND TECHNICAL INFORMATION (STI) AT 5 NASA CENTERS. RESULTS OF A TELEPHONE SURVEY
Nanci A. Glassman and Thomas E. Pinelli Jun. 1992 81 p Sponsored in part by DoD and Indiana Univ.
(NASA-TM-104173; NAS 1.15:104173; Rept-12) Avail: NTIS HC/MF A05

A study was conducted to provide NASA management with an 'initial' look at the production and use of scientific and technical information (STI) at five NASA centers (Ames, Goddard, Langley, Lewis, and Marshall). The 550 respondents who were interviewed by telephone held favorable views regarding the NASA STI system. About 65 percent of the respondents stated that it is either very or somewhat important for them to publish their work through the NASA STI system. About 10 percent of those respondents encountered problems using the NASA STI system services for publication. The most frequently reported problem was 'the process is too time consuming' (8.6 percent). Overall, those respondents using the NASA STI system to publish their work rated the system as excellent (24.6 percent) or good (37.6 percent). About 79 percent of the respondents stated that it is either very or somewhat important for them to use the NASA STI system to access information. The most frequently reported problems were 'the time and effort it takes to locate and obtain information through the system' (14.4 percent). Overall, about 83 percent of the respondents stated that the NASA STI system is important to performing their work. Overall, about 73 percent of the respondents stated that the NASA STI system meets their information needs.
Author

83 ECONOMICS AND COST ANALYSIS

Includes cost effectiveness studies.

N92-26730# Office of Technology Assessment, Washington, DC.
COMPETING ECONOMIES: AMERICA, EUROPE, AND THE PACIFIC RIM
Oct. 1991 382 p
(PB92-115757; OTA-ITE-498; ISBN-0-16-035933-3) Avail: NTIS HC/MF A17; also available SOD HC $17.00 as 052-003-01260-0

Examined here is how the economic environment of the United States can be made more conducive to improving manufacturing performance. How Federal institutions, in cooperation with industry, can develop competitiveness strategies for high tech, fast growing industries, is considered, as well as how trade, financial, and technology policies could be combined into a strategic competitiveness policy.
Author

84 LAW, POLITICAL SCIENCE AND SPACE POLICY

Includes NASA appropriation hearings; aviation law; space law and policy; international law; international cooperation; and patent policy.

N92-26761# Naval Postgraduate School, Monterey, CA.
AN ANALYSIS OF THE ROLE OF THE BUDGET COMMITTEES IN THE CONGRESSIONAL BUDGET PROCESS M.S. Thesis
Stephen G. West Dec. 1991 107 p
(AD-A246005) Avail: NTIS HC/MF A06

Congress assumed a more active role in the federal budget process with the Congressional Budget and Impoundment Control Act of 1974 (CBA), legislation which created the House and Senate Budget Committees. During the first years of the CBA, these committees were effective in establishing the budget process. In

1981, they contributed to a dramatic shift in fiscal policy. Consequently, the budget process assumed a magnitude which was beyond the purview of a single set of committees. The remainder of decade was dominated by large coalitions of budget summits, obscuring the role of the Budget Committees. In the mid-1980's, concern over the deficit shifted the focus of the budget process further from the budget Committees. Gramm-Rudman-Hollings legislated deficit totals and instituted the sequester to cut spending when Congress could not. The most recent revision of the budget process is the Budget Enforcement Act of 1990 (BEA), which further displaces the Budget Committees. Past trends suggest the BEA will be superseded by legislation which may further diminish the role of the Budget Committees.
GRA

85 URBAN TECHNOLOGY AND TRANSPORTATION

Includes applications of space technology to urban problems; technology transfer; technology assessment; and surface and mass transportation.

For related information see also *03 Air Transportation and Safety, 16 Space Transportation,* and *44 Energy Production and Conversion.*

N92-27051# Air Force Systems Command, Wright-Patterson AFB, OH. Foreign Technology Div.
CHINESE SPACE TECHNOLOGY'S SPIN-OFFS AND APPLICATIONS
Jiachi Yang, Fangwen Xu, and Peijian Ye 10 Dec. 1991 15 p Transl. into ENGLISH from Shisie Daodan Yu Hangtian (China), no. 5, 1990 p 3-6
(AD-A246375; FTD-ID(RS)T-0574-91) Avail: NTIS HC/MF A03

China, in the area of space technology, has already achieved successes which are the focus of attention throughout the world. At the same time, space technology has also gone through spin-offs and applications in what we call 'engineering for civilian uses' in various areas such as industry, agriculture, geology, medical science, and so on. Because of this, we have produced a good number of new products and high technologies. This has also been a very great advantage to the development of China's society and economy. The Chinese Academy of Space Technology (CAST), for many years, has consistently devoted itself to the work of taking space projects in such areas as electronics technology, measurement or surveying technology, control technology, temperature control technology, vacuum technology, and other similar fields, and turning them into engineering for civilian uses, effectively promoting spin-offs. GRA

88 SPACE SCIENCES (GENERAL)

No abstracts in this category.

89 ASTRONOMY

Includes radio, gamma-ray, and infrared astronomy, and astrometry.

N92-26184*# Smithsonian Astrophysical Observatory, Cambridge, MA.
MAPPING THE GREAT ATTRACTOR REGION IN X RAYS AND DIFFUSE X RAY EMISSION: A POSSIBLE GALACTIC WIND IN THE BULGE OF M31 Final Report, 1 Aug. 1989 - 31 Jul. 1991
W. R. Forman May 1992 5 p
(Grant NAG5-1204)
(NASA-CR-190402; NAS 1.26:190402) Avail: NTIS HC/MF A01

The NASA ADP Program to study the x ray emission in the direction of the Great Attractor and from the core of M31 has resulted in four papers; three on the Shapley Supercluster which is the dominant x ray feature in the Great Attractor region and one on the diffuse emission in M31. The results of these papers are summarized. Author

N92-26477 Wyoming Univ., Laramie.
AN INFRARED MICHELSON STELLAR INTERFEROMETER AND ITS APPLICATIONS Ph.D. Thesis
James Arthur Benson 1991 97 p
Avail: Univ. Microfilms Order No. DA9202115

A new two-telescope infrared Michelson interferometer is described. IRMA (Infrared Michelson Array) is a prototype near-infrared, broad-band, two-telescope interferometer that was constructed during the course of this thesis. The variable baseline interferometer is now a fully functioning instrument operating in the plains, a few kilometers from the University of Wyoming. Different telescope baselines can easily be achieved by varying the separation between the telescopes from a minimum of 2.5 meters to a maximum separation of 19.5 meters. Earth's own rotation is utilized in order to scan the broad-band fringe packet past the detectors. The general layout of the instrument, the method of data acquisition, and data analysis are described. Finally, the successful operation of this instrument is demonstrated by our use of it to provide the first direct angular diameter measurements at 2.2 microns of the star Alpha Herculis. Dissert. Abstr.

N92-26760 Princeton Univ., NJ.
HIGH PRECISION TIMING OF MILLISECOND PULSARS Ph.D. Thesis
Martin F. Ryba 1991 172 p
Avail: Univ. Microfilms Order No. DA9135859

Described here is the development of our third-generation timing system, and its use at Arecibo Observatory. This system utilizes four real-time coherent dedispersers, which remove pulse smearing caused by interstellar dispersion. The data taken using the dedispersers along with that from regular filter bank spectrometers provide the most precise pulsar TOA's obtainable. To yield any physics, raw TOA's must be precisely referenced to terrestrial time standards, and transformed to an inertial reference frame located at the solar system barycenter using an accurate model of the earth's rotation and motion. The barycentric TOA's must then be fit into a model of the pulsar's spin, position, proper motion, and binary motion. The submicrosecond precision of our measurements puts stringent requirements on each of these steps, and provides some of the most accurate astrometric and binary measurements available, including the measurement of annual parallax and general relativistic effects that allow us to measure the mass of pulsar. The differences between the predicted and measured TOA's can themselves be used, for example, to constrain the energy density of long wavelength gravitational radiation. The arrival times from our most precise timing measurements, those of PSR 1937 + 21, clearly show deviations from the model far greater than our measurement errors, with greater power at very long wavelengths. The analysis of this steep-spectrum noise cannot be done with standard Fourier algorithms. We have developed a spectral estimation technique that is a valid estimator of the true power spectrum and useful with unevenly sampled data. We use the measured spectrum to characterize the likely sources of the timing noise and to place a limit on the cosmic gravitational wave background. Dissert. Abstr.

N92-26886*# National Aeronautics and Space Administration. Ames Research Center, Moffett Field, CA.
APPLYING ARTIFICIAL INTELLIGENCE TO THE CONTROL OF SPACE TELESCOPES (EXTENDED ABSTRACT)
Mark Drummond, Keith Swanson, John Bresina, Andrew Philips, and Rich Levinson Mar. 1992 8 p Presented at the International Symposium on Artificial Intelligence, Robotics, and Automation in Space (i-SAIRAS), Toulouse, France, 30 Sep. - 2 Oct. 1992

Submitted for publication
(NASA-TM-107913; FIA-92-05; NAS 1.15:107913) Avail: NTIS HC/MF A02

The field of astronomy has recently benefited from the availability of space telescopes. The Hubble Space Telescope (HST), for instance, despite its problems, provides a unique and valuable view of the universe. However, unlike HST, a telescope need not be in low Earth orbit to escape our thickening atmosphere: it is currently technologically feasible to put a telescope on the moon, and there are excellent reasons for doing this. Either in low Earth orbit or on the moon, a space telescope represents an expensive and sought-after resource. Thus, the planning, scheduling, and control of these telescopes is an important problem that must be seriously studied. Author

N92-27049 Max-Planck-Inst. fuer Physik und Astrophysik, Garching (Germany, F.R.). Inst. fuer Extraterrestrische Physik.
THE HUS SOLAR FLARE AND COSMIC GAMMA RAY BURST DETECTOR ABOARD THE ULYSSES SPACECRAFT
Michel Boer, Michael Sommer, and K. Hurley (California Univ., Berkeley.) Feb. 1990 15 p Previously announced in IAA as A91-14631 Submitted for publication
(MPE-Preprint-175; ETN-92-98599) Avail:
Fachinformationszentrum Karlsruhe, 7514
Leopoldshafen-Eggenstein 2, Fed. Republic of Germany

An overview of the instruments and scientific objectives is given of the HUS experiment aboard the ESA-NASA Ulysses spacecraft. The primary objective is the detection of cosmic gamma ray bursts and solar hard x ray flares. Details of the Si sensors and CsI detectors used in the experiment are given as well as their position aboard the spacecraft and details of the journey being made. The impulsive energy release, the heating and particle acceleration, the storage, and the energy transport of solar flares will be observed using multispacecraft and multiwavelength observations. Partial distribution and classification of the sources of gamma ray bursts are examined as well as soft gamma ray repeaters and the Jovian hard x ray emission. Author

N92-27077# Naval Postgraduate School, Monterey, CA. Dept. of Physics.
MEASUREMENT OF SURFACE LAYER OPTICAL TURBULENCE ABOVE AMOS M.S. Thesis
Dec. 1991 124 p
(AD-A246387; NPS-PH-92-005) Avail: NTIS HC/MF A06

Temperature fluctuations in the atmosphere severely limit the angular resolution of earth bound observation facilities to around 1 arcsecond. This corresponds to an effective, coherent, aperture size of 10 cm even though the telescope may have a 2 to 4 m primary mirror. Understanding the spatial and temporal distribution of atmospheric optical turbulence is essential to maximize the performance of large astronomical telescopes. This thesis made use of a 5 kHz high frequency, short range Doppler acoustic sounder to investigate the first 100 meters of the mountain boundary layer turbulence above the Air Force Maui Observation Site, AMOS, Haleakala, HI. These measurements were part of a coordinated site evaluation for a proposed 4 m telescope to be built at AMOS in the near future. Tentative results revealed significant layering, 15 to 20 m and occasionally thicker, in the turbulent surface layers above AMOS. Additionally, a comparison of two proposed construction sites near the top of Haleakala showed that the turbulent surface layer tends to follow the contours of the mountain. GRA

N92-26976# Dornier System G.m.b.H., Friedrichshafen (Germany, F.R.).
THERMAL CONTROL OF TELESCOPE APERTURES BY OPTIMIZED BAFFLE HEATING
R. Gessner, K. Eckert, and F. Zilly *In* ESA, 4th European Symposium on Space Environmental Control Systems, Volume 2 Dec. 1991 p 791-796 (For primary document see N92-26950 17-54)
Avail: NTIS HC/MF A23; ESA, EPD, ESTEC, Noordwijk, Netherlands, HC 150 Dutch guilders (2 vols)

N92-27001# European Space Agency. European Space Research and Technology Center, ESTEC, Noordwijk (Netherlands). Thermal Control and Life Support Div.
THERMAL IMPLICATIONS FROM THE HUBBLE SPACE TELESCOPE SOLAR ARRAY BI-STEM BOOM IN-ORBIT DISTURBANCE
P. Poinas and G. I. M. Beere *In its* 4th European Symposium on Space Environmental Control Systems, Volume 2 Dec. 1991 p 961-967 (For primary document see N92-26950 17-54)
Avail: NTIS HC/MF A23; ESA, EPD, ESTEC, Noordwijk, Netherlands, HC 150 Dutch guilders (2 vols)

90 ASTROPHYSICS

Includes cosmology; celestial mechanics; space plasmas; and interstellar and interplanetary gases and dust.
For related information see also *75 Plasma Physics.*

N92-26436*# Fermi National Accelerator Lab., Batavia, IL.
EUCLIDEAN BLACK HOLE VORTICES
Fay Dowker, Ruth Gregory, and Jennie Traschen (Massachusetts Univ., Amherst.) Dec. 1991 25 p Sponsored in part by DOE (Grants NAGw-2381; NSF PHY-89-18388)
(NASA-CR-190117; NAS 1.26:190117; FERMILAB-Pub-91/332-A; EFI-91-70; UMHEP-361) Avail: NTIS HC/MF A03

We argue the existence of solutions of the Euclidean Einstein equations that correspond to a vortex sitting at the horizon of a black hole. We find the asymptotic behaviors, at the horizon and at infinity, of vortex solutions for the gauge and scalar fields in an abelian Higgs model on a Euclidean Schwarzschild background and interpolate between them by integrating the equations numerically. Calculating the backreaction shows that the effect of the vortex is to cut a slice out of the Schwarzschild geometry. Consequences of these solutions for black hole thermodynamics are discussed. Author

N92-26476 Cornell Univ., Ithaca, NY.
DESTRUCTION AND EXCITATION OF ACCRETED NUCLEI IN NEUTRON STAR ATMOSPHERES: GAMMA RAY LINES AND X RAY BURSTS Ph.D. Thesis
Lars Bildsten 1991 180 p
Avail: Univ. Microfilms Order No. DA9203944

The fate of incident C-12, N-14, and O-16 (CNO) in accreting neutron star atmospheres is described. When the accreting material is stopped by Coulomb collisions with atmospheric electrons, all incoming elements heavier than Helium thermalize at higher altitudes in the atmosphere than the accreting protons. The incoming protons and Helium then destroy the elements via nuclear spallation reactions. A small fraction of the nuclear reactions cause nuclear excitation and subsequent gamma-ray emission. The probability for a nucleus to survive this bombardment depends on how long it spends in the hazardous region of the atmosphere. The fractions of incident C-12, N-14, and O-16 that survive proton bombardment are calculated as a function of the accretion rate, and the mass and radius of the neutron star. The subsequent paucity of CNO nuclei decreases hydrogen burning rates in the deep regions of the atmosphere, thereby reducing the amount of Helium available for the unstable nuclear flashes that cause Type 1 X-ray bursts. The gamma-ray line emission from this collisional deceleration scenario is determined. For accretion of material with solar abundances of CNO elements, the flux in the 4.438 MeV gamma-ray line is always far below the observational limits of the Gamma-Ray Observatory (GRO). Many previously unaddressed properties of an accreting neutron star atmosphere prove important when solving the heavy element diffusion problem. Specifically, we show that the incident electrons are crucial in determining the macroscopic electric field present in the atmosphere.
Dissert. Abstr.

N92-26491 Minnesota Univ., Minneapolis.
SUPERSYMMETRY AND DARK MATTER, A NEW CANDIDATE

Ph.D. Thesis
David Thomas 1991 86 p
Avail: Univ. Microfilms Order No. DA9209443

The neutral supersymmetric fermion sector of the model obtained by adding an SU(2) times U(1) gauge singlet Higgs superfield to the minimal supersymmetric standard model, is discussed in the context of the dark matter problem. While the theory contains many of the same dark matter candidates as the minimal model, it also includes a new state D, comprised of a combination of higgsinos, the partners of the Higgs scalars. Unlike other neutralinos however, the new state is light (below 30 GeV) for a significant part of the parameter space, improving chances for detection with existing detectors. The neutralino and Higgs sectors are discussed, leading to a calculation of the annihilation cross-section, and hence the relic density of the new state. The density parameter due to the D varies from a value too low to represent a solution to the dark matter problem, to a point where the Universe is overclosed. For a variety of masses, a set of parameters are chosen to close the Universe, and the rate for scattering off nuclear matter is calculated. For a large number of nuclei the detection rate can reach over 1 event (kg center dot day)(exp -1). Dissert. Abstr.

N92-26522 California Inst. of Tech., Pasadena.
DYNAMICS OF NEUTRON STARS AND BINARIES IN GLOBULAR CLUSTERS OR, MENAGES A TROIS: REVITALIZING BURNT OUT DEGENERATES THROUGH PARTNER SWAPPING Ph.D. Thesis
Steinn Sigurdsson 1992 245 p
Avail: Univ. Microfilms Order No. DA9209484

Interaction cross-sections and collision cross-sections for a set of hard multi-mass binary-single star interactions are calculated in order to estimate three-body collision cross-sections in galactic globular clusters. The cross-sections are calculated by direct integration of binary-single star encounters, using Monte Carlo sampling to average over the three-body phase space. A number of mass-ratios physically relevant to the globular cluster environment are used. Differential energy transfer rates due to three-body interactions are calculated. Parametric approximations for the various cross-sections calculated are found. The results of the cross-sections are used to evaluate various formation scenarios for the pulsars PSR2127 + 11C (M15C) and PSR1744-24A (TER5A). In addition, the contribution of the globular cluster system to the galactic birthrate of PSR1913 + 16 type systems is estimated. The dynamics and interactions of a test binary population in a number of globular cluster models are calculated in a static background. The cluster method used is isotropic multi-mass King models of varying concentration and density. The developed model is generalizable to an arbitrary cluster distribution function, including one evolving in time. Relative probabilities of different encounters are found for binaries on arbitrary trajectories in the various cluster models. The actual interaction rates of the test population are calculated by direct integration, using Monte Carlo sampling to average over the initial binary parameters. The number of neutron stars expected to be recycled in different concentration clusters is estimated with a particular view to understanding the pulsar population observed in clusters 47Tuc and M15. Dissert. Abstr.

N92-26554 California Univ., Los Angeles.
EVIDENCE FOR CLUSTER MAGNETIC FIELDS AROUND RADIO GALAXIES Ph.D. Thesis
Gregory Benjamin Taylor 1991 217 p
Avail: Univ. Microfilms Order No. DA9200901

The researchers undertook a detailed, high resolution study of four sources with large rotation measures: Hydra A, 3C 295, 3C 194, and 3C 318. Much of the effort was dedicated to the study of Hydra A, which is a relatively nearby, bright radio galaxy of large physical size (700 kpc). Through a detailed study of this object, one can learn more about the class of high rotation measure sources as a whole. In order to learn more about this remarkable radio source and its environment, the researchers observed it extensively in the 2, 3.6, 6, 20, and 90 cm bands with the Very Large Array (VLA), and in the H alpha with the Calar Alto 3.5 m telescope. In Hydra A and 3C 295, the researchers found Faraday rotation measures of 12000 radians m(exp -2) and more, with large gradients and frequent sign reversals. With the exception of 3C 194, all the high resolution measure sources found to date reside in dense cooling flow clusters. The observations presented here, along with recent observations of Cygnus A, A 1795, A 2052, and A 2199 (Ge 1991) are most readily explained by the existence of cluster magnetic fields around some radio galaxies. The observations of Hydra A indicated that there exists both a tangled and an organized component to the cluster magnetic field with strengths of approximately 50 and approximately 6 micron G, respectively. These magnetic fields may play an important role in cluster evolution. Dissert. Abstr.

N92-26576 Arizona Univ., Tucson.
ATMOSPHERIC PARAMETERS OF A SOFT X RAY SELECTED SET OF HOT DA WHITE DWARFS Ph.D. Thesis
Kenneth Mark Kidder 1991 154 p
Avail: Univ. Microfilms Order No. DA9210327

Soft x-ray/EUV observations provide a sensitive means of probing the structure and composition of the atmospheres of hot hydrogen-rich (DA) white dwarf stars. This is due to the fact that soft x-rays originate from hotter, deeper layers of the photosphere than do longer wavelengths. A primary aim of this research is to expand the sample of DA's observed with soft x-ray instrumentation through a search for serendipitous observations of catalogued hot DA white dwarfs in existing soft x-ray databases. The positional coincidences of 31 catalogued DA's (McCook and Sion 1987) were examined in Einstein IPC and EXOSAT LE fields. As a result, three soft x-ray sources have been identified corresponding to the white dwarfs (WD0631 + 107, WD1113 + 413 and WD0425 + 168) and a fourth source which is probably not due to photospheric thermal emission from the coincident white dwarf. The three detected DA's have relatively low effective temperatures (27,200 +/- 400 K, 26,200 +/- 1100 K and 24,000 +/- 500 K, respectively), as determined independently using complementary optical and UV spectroscopy. Applying these temperature constraints to the soft x-ray photometric data, the photospheres of these stars must be composed of effectively pure hydrogen (n(He)/n(H) less than 10 exp -5), although the hottest star, WD0631 + 107, can have trace levels of homogeneously mixed helium less than 10 exp -4.2. The analysis of the soft x-ray observations are supplemented with independent determinations of temperature, gravity, and V magnitude. The method of determination employed is to fit the well-sampled wings of the broad hydrogen absorption profiles with self-consistent model atmosphere predictions. Precise temperatures and gravities are obtained by fitting the observed profiles independently, then jointly determining a consistent solution for each object. In this effort, a ground-based observation program was established to obtain high quality spectra of the Balmer delta and gamma lines and in some cases the Balmer beta line. IUE spectrophotometry of the Lyman alpha line, when available, was also incorporated into the determination of the temperature and gravity. Dissert. Abstr.

N92-26578 Florida Univ., Gainesville.
ANALYTICAL AND NUMERICAL INVESTIGATION OF NONLINEAR GRAVITATIONAL CLUSTERING Ph.D. Thesis
Laddawan Ruamsuwan 1991 116 p
Avail: Univ. Microfilms Order No. DA9209070

An approach to nonlinear gravitational clustering is developed using the one-particle Vlasov equation and the velocity moments. Results of this approach agree with those derived earlier from the cosmological BBGKY hierarchy in the fluid limit. The set of equations is closed by using a hierarchical model suggested by perturbation theory. In this approach one need not assume vanishing skewness of the velocity dispersion. Scale invariant and self-similar solutions were obtained in the strong clustering regime, but such solutions are found to be not stable to small perturbations. Numerical solutions to the Davis-Peebles equations without the stability assumption were obtained for three sets of initial condition. The two-point correlation function was found to agree with linear

perturbation theory. As the two-point correlation function became large, the numerical results were found to be unstable, which agree with the earlier analytic result. Dissert. Abstr.

N92-26723 Illinois Univ., Urbana-Champaign.
A SELF-CONTAMINATION MODEL FOR THE FORMATION OF GLOBULAR STAR CLUSTERS Ph.D. Thesis
James Howard Brown 1991 110 p
Avail: Univ. Microfilms Order No. DA9136554

Described here is a model of globular cluster formation which allows the self contamination of the cluster by an earlier generation of massive stars. It is first shown that such self-contamination naturally produces an Fe/H in the range from -2.5 to -1.0, precisely the same range observed in the metal poor (halo) globular clusters; this also seems to require that the disk clusters started with a substantial initial metallicity. To minimize the problem of creating homogeneous globular clusters, the second (currently observed) generation of stars is assumed to form in the expanding supershell around the first generation stars. Both numerical and analytic models are used to address this problem. The most important result of this investigation was that the late evolution of the supershell is the most important, and that this phase of the evolution is dominated by the external medium in which the cloud is embedded. This result and the requirement that only the most tightly bound systems may become globular clusters lead to the conclusion that a globular cluster with the mass and binding energy typically observed can be formed at star formation efficiences as low as 10-20 percent. Furthermore, self contamination requires that the typical Fe/H of a bound system be about -1.6, independent of the free parameters of the model, allowing the clusters and field stars to form with different metallicity distributions in spite of their forming at the same time. Since the formation of globular clusters in this model is tied to the external pressure, the halo globular cluster masses and distribution can be used as probes of the early galactic structure. In particular, this model requires an increase in the typical globular cluster mass as one moves out from the galactic center; the masses of the halo clusters are examined, and they show considerable evidence for such a gradient. Based on a pressure distribution derived from this data, the effect of the galactic tidal field on the model is also investigated using an N-body simulation. Dissert. Abstr.

N92-26725 Illinois Univ., Urbana-Champaign.
THE GALACTIC EVOLUTION OF s-PROCESS ELEMENTS VIA ASYMPTOTIC GIANT BRANCH STARS Ph.D. Thesis
Grant Bazan 1991 267 p
Avail: Univ. Microfilms Order No. DA9136540

We attempt to study the ability of asymptotic giant branch stars to produce s-process elements as a function of initial mass and metallicity. The normal methods of extracting information from spectroscopic observations of the surfaces of these stars are reviewed and it is shown how misleading some of the past claims are and which methods of analysis might eliminate the current confusion. Results from stellar evolution models are brought together in order to establish trends of certain parameters as functions of one or two other parameters. Using these parameterizations, we have determined the s-process abundances created by these stars for different scenarios, and we have related them to surface features that are observable. It is found that the two commonly advocated sources for s-process neutrons cannot produce observational features of MS and S stars as the scenarios are put forth in the literature. It is found, however, that perturbations of these models within the physical limitations of the more popular scenarios can result in observational features of MS and S stars. We also look at the limitations put upon various s-process scenarios by galactic chemical evolution, where we find that AGB stars as an s-process source are consistent with the trends in the heavy elements as a function of the metallicity history of the galaxy. It is also realized that the nucleosynthetic yield of any s-process source must be relatively insensitive to the initial composition of the progenitor star. Dissert. Abstr.

N92-26757 Michigan Univ., Ann Arbor.
POLYCYCLIC AROMATIC HYDROCARBON RADIATIVE PROPERTIES AND FORMATION IN CARBON-RICH STELLAR OUTFLOWS Ph.D. Thesis
Isabelle Marie Chercheneff 1991 183 p
Avail: Univ. Microfilms Order No. DA9135569

The infrared emission and radiative properties of gas-phase polycyclic aromatic hydrocarbon (PAH) molecules are investigated: the infrared fluorescence spectrum of azulene (C10H8) is measured experimentally, and the optical constants for several other small PAHs are estimated theoretically. It was found that small aromatic molecules experience an 'inverse greenhouse' effect that favors their survival close to the photosphere. The formation of PAH molecules in carbon-rich stellar outflows is modelled by a detailed chemical kinetic approach. This method uses a complete and up-to-date chemical scheme based on soot formation in combustion systems. Strong periodic shocks in the inner stellar envelope are considered, and their effects on the gas density and flow velocity are evaluated. The boundary molecular concentrations at the shock formation radius are derived from thermal equilibrium calculations including PAHs. The 'inverse greenhouse' effect is included, and calculations are carried out for aromatics up to the size of pyrene. PAH concentration profiles are obtained for several envelope models. The PAH formation yields are small compared to values derived from the observed dust content of stellar envelopes. Furthermore, the yields are extremely sensitive to gas density and temperature. It is therefore unlikely that aromatic molecules are generated in the stellar outflow, itself. However, another mechanism is suggested: PAHs may form and accumulate in gas parcels subjected to quasi-ballistic trajectories induced by shocks, close to the photosphere. Dissert. Abstr.

N92-26833# Institut des Hautes Etudes Scientifiques, Bures-sur-Yvette (France).
QUANTUM BLACK HOLES AND HAWKING'S RADIATION
V. Berezin Nov. 1991 31 p Prepared in cooperation with Academy of Sciences, (USSR), Moscow
(PB92-152313; IHES/P/91/76) Avail: NTIS HC/MF A03

A black hole model with a self-gravitating charged spherical dust thin shell as a source is considered. The Schrodinger-type equation for such a model is derived. The equation appears to be a finite difference equation. A method for solving such an equation is proposed and the discrete spectrum of the bound state energy levels is found. The quantum black hole states are selected and investigated. It is shown that the black hole spectrum obtained is compatible with the existence of Hawking's radiation in the limit of low temperatures both for large and nearly extreme Reissner-Nordstrom black holes. Author

N92-26946# Max-Planck-Inst. fuer Physik und Astrophysik, Munich (Germany, F.R.). Inst. fuer Astrophysik.
AN ANISOTROPIC HOMOLOGOUS MODEL FOR THE CORE-COLLAPSE IN STAR CLUSTERS Ph.D. Thesis - Technische Univ. [EIN ANISOTROPES HOMOLOGES MODELL FUER DEN CORE-KOLLAPS IN STERNHAUFEN]
Peter D. Louis 1990 88 p In GERMAN; ENGLISH summary
(ETN-92-90826) Avail: NTIS HC/MF A05

A new method for computing the quasi stationary evolution of spherical star clusters based on moment equations of Boltzmann's equation is described. The deficiency of high velocity stars and the anisotropic velocity distribution, both of which are distinctive features of real stellar systems, are approximated by single parameters. The effects of gravitational encounters between individual stars are represented by collision terms in the moment equations, which are considered up to fourth order in this treatment, and which are closed at fifth order. The model is applied to the phenomenon of core collapse in one component star clusters. The effects of modifying the equations of the approximate model are discussed in detail. ESA

N92-27048 Max-Planck-Inst. fuer Physik und Astrophysik, Garching (Germany, F.R.). Inst. fuer Extraterrestrische Physik.
X RAY OBSERVATIONS OF GAMMA RAY BURST SOURCES

Michel Boer, M. Gottardi, K. Hurley, and G. Pizzichini (Consiglio Nazionale delle Ricerche, Bologna, Italy) Feb. 1990 16 p Previously announced in IAA as A90-52674 Submitted for publication
(MPE-Preprint-174; ETN-92-98598) Avail: Fachinformationszentrum Karlsruhe, 7514 Leopoldshafen-Eggenstein 2, Fed. Republic of Germany

Preliminary results of Exosat observations of three gamma ray burst error boxes are reported. No source was detected down to a limit of 10 to the -10th erg/sq cm s, assuming a blackbody spectrum for the burst counterpart. Results are interpreted in the framework of current theoretical models. Author

91 LUNAR AND PLANETARY EXPLORATION

Includes planetology; and manned and unmanned flights.

For spacecraft design or space stations see *18 Spacecraft Design, Testing and Performance.*

N92-26438*# Georgia Inst. of Tech., Atlanta. School of Electrical Engineering.
LABORATORY EVALUATION AND APPLICATION OF MICROWAVE ABSORPTION PROPERTIES UNDER SIMULATED CONDITIONS FOR PLANETARY ATMOSPHERES Semiannual Status Report No. 17, 1 Nov. 1991 - 30 Apr. 1992
Paul G. Steffes 20 Apr. 1992 35 p
(Grant NAGw-533)
(NASA-CR-190211; NAS 1.26:190211) Avail: NTIS HC/MF A03

Radio absorptivity data for planetary atmospheres obtained from spacecraft radio occultation experiments and earth-based radio astronomical observations can be used to infer abundances of microwave absorbing atmospheric constituents in those atmospheres, as long as reliable information regarding the microwave absorbing properties of potential constituents is available. The use of theoretically derived microwave absorption properties for such atmospheric constituents, or using laboratory measurements of such properties under environmental conditions which are significantly different than those of the planetary atmosphere being studied, often leads to significant misinterpretation of available opacity data. The recognition of the need to make such laboratory measurements of simulated planetary atmospheres over a range of temperatures and pressures which correspond to the altitudes probed by both radio occultation experiments and radio astronomical observations, and over a range of frequencies which correspond to those used in both radio occultation experiments and radio astronomical observations, has led to the development of a facility at Georgia Tech which is capable of making such measurements. The goal of this investigation was to conduct such measurements and to apply the results to a wide range of planetary observations, both spacecraft and earth-based, in order to determine the identity and abundance profiles of constituents in those planetary atmospheres. Author

N92-26778 Washington Univ., Seattle.
RADAR SCATTERING AS A SOURCE OF GEOLOGICAL INFORMATION ON VENUS AND EARTH Ph.D. Thesis
Jeffrey Jonathan Plaut 1991 357 p
Avail: Univ. Microfilms Order No. DA9134398

Recent years have seen a rapid increase in the use of radar remote sensing as a tool for geological investigation. The intent of the research is to conduct geological interpretations of this type of data by exploring the mechanisms of radar scattering as they relate to geologic surfaces, and finding the means to extract the most geologically useful information from the data. The primary data sets used are, for Venus, the Earth-based Goldstone observations and early Magellan orbital observations, and for Earth, airborne NASA AIRSAR data for the Mojave Desert. The desert sites provide the necessary 'ground truth' to understand the radar properties of surfaces and to extend this understanding to the interpretation of the planetary data. Multiwave length polarimetric radar (AIRSAR) data were obtained for several geologically diverse sites in the Mojave Desert. This study is among the first to apply radiometric calibrations to such data for geological analysis. Polarimetric data were found to be extremely useful for distinguishing active and stable sand dune features. The wavelength diversity of AIRSAR can be used to distinguish roughness characteristics of lava flows, alluvial deposits and bedrock outcrops. Radar signatures of lava flows are seen to vary significantly as a function of exposure age of the flow, due to changes in roughness caused by weathering and erosion. Comparison of radar scattering coefficients from lava flows on Venus and Earth indicates that flow surfaces on Venus are generally smoother than those on Earth. Dissert. Abstr.

N92-26819# RAND Corp., Santa Monica, CA.
THE PRELIMINARY GEODETIC CONTROL NETWORK OF VENUS
Merton E. Davies and Patricia G. Rogers 1991 23 p
(Contract JPL-953613)
(RAND-N-3437-JPL) Avail: NTIS HC/MF A03

This brief note describes the coordinate system of Venus adopted by the Magellan project, Venus coordinate transformations, the control point numbering system, and the preliminary control network of Venus. Figures and tables that provide greater detail are presented. Author

92 SOLAR PHYSICS

Includes solar activity, solar flares, solar radiation and sunspots.

For related information see *93 Space Radiation.*

N92-26191*# National Aeronautics and Space Administration. Goddard Space Flight Center, Greenbelt, MD.
HANDBOOK OF SOLAR-TERRESTRIAL DATA SYSTEMS, VERSION 1
Nov. 1991 176 p
(NASA-TM-107810; NSSDC/WDC-A-R/S-91-26; NAS 1.15:107810) Avail: NTIS HC/MF A09

The interaction between the solar wind and the earth's magnetic field creates a large magnetic cavity which is termed the magnetosphere. Energy derived from the solar wind is ultimately dissipated by particle acceleration-precipitation and Joule heating in the magnetosphere-ionosphere. The rate of energy dissipation is highly variable, with peak levels during geomagnetic storms and substorms. The degree to which solar wind and magnetospheric conditions control the energy dissipation processes remains one of the major outstanding questions in magnetospheric physics. A conference on Solar Wind-Magnetospheric Coupling was convened to discuss these issues and this handbook is the result. Author

N92-26247*# Smithsonian Astrophysical Observatory, Cambridge, MA.
OBSERVATIONAL AND THEORETICAL INVESTIGATIONS IN SOLAR SEISMOLOGY Final Semiannual Reports No. 1-3, 1 Mar. 1989 - 31 Aug. 1990 and 1 Mar. 1989 - 28 Feb. 1991
Robert W. Noyes Mar. 1992 40 p
(Grant NAGw-1677)
(NASA-CR-190245; NAS 1.26:190245) Avail: NTIS HC/MF A03

This is the final report on a project to develop a theoretical basis for interpreting solar oscillation data in terms of the interior dynamics and structure of the Sun. The topics covered include the following: (1) studies of the helioseismic signatures of differential rotation and convection in the solar interior; (2) wave generation by turbulent convection; and (3) the study of antipodal sunspot imaging of an active region tomography. Author

N92-26385# California Univ., Berkeley. Lawrence Berkeley Lab.
TOPICS IN PARTICLE PHYSICS AND COSMOLOGY Ph.D. Thesis

S. D. H. Hsu 2 Aug. 1991 40 p
(Contract DE-AC03-76SF-00098)
(DE92-010478; LBL-31107; UCB-PTH-91/38) Avail: NTIS HC/MF A03

The Standard Model of particle physics, together with the Big Bang model of the early universe, constitute a framework which encompasses our current understanding of fundamental laws and beginning of our universe. Despite recent speculative trends, quantum field theory remains the theoretical tool of choice for investigating new physics either at high energy colliders, or in the early universe. In this dissertation, several field theoretic phenomena relevant to cosmology or particle physics are explored. A common theme in these explorations is the structure of the vacuum state in quantum field theory. First, we discuss first-order phase transitions in the early universe, in which the effective vacuum state of the universe shifts discontinuously as the temperature drops below some critical point. We find that the dynamics of a certain type of first-order phase transition can lead to production of primordial black holes, which could constitute the dark matter of our universe. Alternatively, supercooled first-order phase transitions may be the cause of an extended inflationary epoch in the early universe, which is generally regarded as necessary to solve several cosmological puzzles. We derive limits on such scenarios based on nearly model-independent percolation properties of the transition. We also study some nonperturbative aspects of the field theory vacuum. We show that non-topological solitons of a single fermion and Higgs fields can only exist in strongly coupled theories. In particular, we find that at the lowest fermionic excitations in the Standard Model are single fermions, and not bound states of fermion plugs Higgs. Finally, we investigate the intriguing behavior of instanton-induced cross sections. We discover Higgs-Higgs cross sections which increase exponentially with center of mass energy due to the presence of instanton solutions related to vacuum instability. DOE

N92-26437*# National Academy of Sciences - National Research Council, Washington, DC.
WORKSHOP ON SOLAR ACTIVITY, SOLAR WIND, TERRESTRIAL EFFECTS, AND SOLAR ACCELERATION Final Report
10 Apr. 1992 38 p Presented at the Interacademy Workshop on Solar Terrestrial Physics, USSR, 15-20 Oct. 1990
(Grant NAGw-2261)
(NASA-CR-190195; NAS 1.26:190195) Avail: NTIS HC/MF A03

A summary of the proceedings from the workshop are presented. The areas covered were solar activity, solar wind, terrestrial effects, and solar acceleration. Specific topics addressed include: (1) solar cycle manifestations, both large and small scale, as well as long-term and short-term changes, including transients such as flares; (2) sources of solar wind, as identified by interplanetary observations including coronal mass ejections (CME's) or x-ray bright points, and the theory for and evolution of large-scale and small-scale structures; (3) magnetosphere responses, as observed by spacecraft, to variable solar wind and transient energetic particle emissions; and (4) origin and propagation of solar cosmic rays as related to solar activity and terrestrial effects, and solar wind coronal-hole relationships and dynamics. Author

N92-26566# Brookhaven National Lab., Upton, NY.
THE STATUS OF GALLEX
R. Wink (Max-Planck-Inst. fuer Kernphysik, Heidelberg, Germany, F.R.) 1991 14 p Presented at the International School on Particles and Cosmology, Baksan, USSR, 6-12 May 1991
(Contract DE-AC02-76CH-00016)
(DE92-010077; BNL-47155; CONF-9105319-1) Avail: NTIS HC/MF A03

We describe the status of GALLEX solar neutrino experiment until the end of June 1991. Since June 1990, 31 desorptions with the full equipment have been done. The results of the first 27 desorptions are presented. We also describe our low level proportional counters including the counting system. DOE

N92-26779 California Univ., Los Angeles.
SOLAR WIND INTERACTION WITH VENUS AND MARS Ph.D. Thesis
Tie-Long Zhang 1991 178 p
Avail: Univ. Microfilms Order No. DA9134040

We present the results of studies of the solar wind interaction with Venus and Mars. In the Venus studies, we examine the magnetic barrier, bow shock and associated solar wind properties. First, we determine the average solar wind properties at 0.72 AU and their variation with the solar cycle. Second, we construct altitude profiles of the magnetic barrier and find out where in the magnetosheath agreement with the gas dynamic model breaks down. We find that the magnetic barrier transfers most of the solar wind dynamic pressure to the ionosphere via the enhanced magnetic pressure. The existence of a north-south asymmetry in the barrier strength is also demonstrated by our analysis. Third, we study the bow shock position and its variation with the solar cycle. We find that the shape of the bow shock remains constant and only the size varies during the solar cycle. Using a gas dynamic model and the observed bow shock location, we infer the variation in the size of the effective obstacle during the solar cycle. During solar maximum, the magnetic barrier acts as the effective obstacle deflecting the magnetosheath plasma. During solar minimum the effective obstacle is well below the subsolar ionopause and some absorption of the solar wind plasma by the Venus neutral atmosphere is implied by our observations. The dependence of the solar cycle variation of the shock position on the orientation of the interplanetary magnetic field reinforces the idea that planetary ion pickup is important in the interaction of the solar wind with Venus. In the Mars studies, we examine the variation in the position of the bow shock with the solar wind dynamic pressure, magnetosonic Mach number and the interplanetary magnetic field. Observations show that the position of the terminator bow shock varies with interplanetary magnetic field (IMF) orientation in the same way as at Venus. We find that the shock cross section at the terminator plane is asymmetric and is controlled by the interplanetary magnetic field. As at Venus, the Mars shock position in the terminator plane varies little with solar wind dynamic pressure; rather, the major controlling factor is solar wind Mach number. We conclude that the solar wind interaction with Mars appears to be Venus-like, with a magnetic moment too small to affect significantly the solar wind interaction. Dissert. Abstr.

93 SPACE RADIATION

Includes cosmic radiation; and inner and outer earth's radiation belts.

For biological effects of radiation see *52 Aerospace Medicine*. For theory see *73 Nuclear and High-Energy Physics*.

N92-26211# Argonne National Lab., IL. High Energy Physics Div.
SIMULTANEOUS OBSERVATIONS OF EXTENSIVE AIR SHOWERS AND UNDERGROUND MUONS AT SOUDAN 2
W. W. M. Allison, G. D. Barr, C. B. Brooks, J. H. Cobb, R. H. Giles, D. H. Perkins, P. D. Shield, M. A. Thomson, L. M. Tupper, and N. West (Oxford Univ., England) et al Aug. 1991 5 p Presented at the International Cosmic Ray Conference, Dublin, Ireland, 11-23 Aug. 1991
(Contract W-31-109-eng-38)
(DE92-010282; ANL/HEP/CP-91-117; CONF-9108141-9) Avail: NTIS HC/MF A01

We have built a small proportional tube air shower array on the surface above the Soudan 2 proton decay detector in Soudan, Minnesota, USA. This array, in coincidence with the underground detector, allows simultaneous surface and underground observations of high energy cosmic ray showers. These observations, still in their initial stages, may eventually be able to provide information about the composition of cosmic ray primaries in the 'knee' region of the energy spectrum. DOE

N92-26215# Argonne National Lab., IL. High Energy Physics Div.
UNDERGROUND MUONS FROM THE DIRECTION OF CYGNUS X-3 DURING THE JANUARY 1991 RADIO FLARE
Aug. 1991 8 p Presented at the International Cosmic Ray Conference, Dublin, Ireland, 11-23 Aug. 1991
(Contract W-31-109-eng-38)
(DE92-010346; ANL/HEP/CP-91-116; CONF-9108141-6) Avail: NTIS HC/MF A02

Muons recorded in the Soudan 2 underground nucleon decay detector from January 1989 to February 1991 have been examined for any correlation with the radio flares of Cyguns X-3 observed during this period. On two nearby days during the radio flare of January 1991, a total of 32 muons within 2.0 degrees of the Cyguns X-3 direction were observed when 11.4 were expected. DOE

N92-26216# Argonne National Lab., IL. High Energy Physics Div.
A SEARCH FOR MAGNETIC MONOPOLES WITH THE SOUDAN 2 DETECTOR
W. W. M. Allison, G. D. Warr, C. B. Brooks, J. H. Cobb, L. M. Kirby-Gallagher, R. H. Giles, G. L. Giller, D. H. Perkins, P. D. Shield, and M. A. Thomson et al Aug. 1991 5 p Presented at the International Cosmic Ray Conference, Dublin, Ireland, 11-23 Aug. 1991
(Contract W-31-109-eng-38)
(DE92-010347; ANL/HEP/CP-91-115; CONF-9108141-7) Avail: NTIS HC/MF A01

A search for GUT magnetic monopoles has been conducted using the Soudan 2 nucleon decay detector. This detector is a fine-grained tracking calorimeter. Monopole candidates were selected on the basis of significantly higher ionization than through-going cosmic ray muons. Preliminary results, using data taken over approximately one year with no monopoles observed, correspond to a flux limit of 2.4 x 10 exp -24/(sq. cm)(sr)(s) over a velocity range of 10(exp -3) less than beta less than 0.95. DOE

N92-26218# Argonne National Lab., IL. High Energy Physics Div.
MUON/ELECTRON SEPARATION FOR ATMOSPHERIC NEUTRINO INTERACTIONS
W. W. M. Allison, G. D. Barr, C. B. Brooks, J. H. Cobb, L. M. Kirby-Gallagher, R. H. Giles, G. L. Giller, D. H. Perkins, P. D. Shield, and M. A. Thomson et al Aug. 1991 4 p Presented at the International Cosmic Ray Conference, Dublin, Ireland, 11-23 Aug. 1991
(Contract W-31-109-eng-38)
(DE92-010349; ANL/HEP/CP-91-112; CONF-9108141-8) Avail: NTIS HC/MF A01

A study has been made of the ability of the Soudan 2 nucleon decay detector to distinguish between showering and non-showering particles, utilizing several different pattern recognition techniques. This work has direct application in the determination of the nu(sub mu)/nu(sub e) ratio for atmospheric neutrino induced events. The results of the application of these techniques to Monte Carlo data and to calibration data from the ISIS test beam are presented. DOE

N92-26253# Argonne National Lab., IL. High Energy Physics Div.
COMPOSITION STUDIES BASED ON COINCIDENT AIR SHOWER ARRAY AND UNDERGROUND MUON DATA
U. DasGupta, K. Ruddick (Minnesota Univ., Minneapolis.), and T. H. Fields Aug. 1991 5 p Presented at the International Cosmic Ray Conference, Dublin, Ireland, 11-23 Aug. 1991
(Contract W-31-109-eng-38)
(DE92-010345; ANL/HEP/CP-91-119; CONF-9108141-5) Avail: NTIS HC/MF A01

We report on a final analysis of coincident underground muon data measured by the Soudan 1 proton decay detector and air shower data measured by an associated proportional tube array. These data were reported first at the 21st ICRC, Adelaide. We have done further analysis to determine the principal sources of systematic errors in such measurements, including different models of the primary interaction. DOE

N92-26264# Argonne National Lab., IL. High Energy Physics Div.
UNDERGROUND MUONS OBSERVED IN THE SOUDAN 2 DETECTOR FROM THE DIRECTIONS OF X RAY SOURCES
W. W. M. Allison, G. D. Barr, C. B. Brooks, J. H. Cobb, R. H. Giles, D. H. Perkins, P. D. Shield, M. A. Thomson, L. M. Tupper, and N. West et al Aug. 1991 5 p Presented at the International Cosmic Ray Conference, Dublin, Ireland, 11-23 Aug. 1991
(Contract W-31-109-eng-38)
(DE92-010344; ANL/HEP/CP-91-118; CONF-9108141-4) Avail: NTIS HC/MF A01

We report on observations of underground muons made with the Soudan 2 proton decay detector at a depth of 2090 mwe from the directions of the binaries Hercules X-1 and 1E2259+586 and the Crab pulsar. DOE

N92-26544# Oak Ridge National Lab., TN.
A USER'S MANUAL FOR MASH 1.0: A MONTE CARLO ADJOINT SHIELDING CODE SYSTEM
J. O. Johnson, ed. Mar. 1992 437 p
(Contract DE-AC05-84OR-21400)
(DE92-010375; ORNL/TM-11778) Avail: NTIS HC/MF A19

The Monte Carlo Adjoint Shielding Code System, MASH, calculates neutron and gamma-ray environments and radiation protection factors for armored military vehicles, structures, trenches, and other shielding configurations by coupling a forward discrete ordinates air-over-ground transport calculation with an adjoint Monte Carlo treatment of the shielding geometry. Efficiency and optimum use of computer time are emphasized. The code system include the GRTUNCL and DORT codes for air-over-ground transport calculations, the MORSE code with the GIFT5 combinatorial geometry package for adjoint shielding calculations, and several peripheral codes that perform the required data preparations, transformations, and coupling functions. MASH is the successor to the Vehicle Code System (VCS) initially developed at Oak Ridge National Laboratory (ORNL). The discrete ordinates calculation determines the fluence on a coupling surface surrounding the shielding geometry due to an external neutron/gamma-ray source. The Monte Carlo calculation determines the effectiveness of the fluence at that surface in causing a response in a detector within the shielding geometry, i.e., the 'dose importance' of the coupling surface fluence. A coupling code folds the fluence together with the dose importance, giving the desired dose response. The coupling code can determine the dose response as a function of the shielding geometry orientation relative to the source, distance from the source, and energy response of the detector. This user's manual includes a short description of each code, the input required to execute the code along with some helpful input data notes, and a representative sample problem (input data and selected output edits) for each code. DOE

N92-26804# Academy of Sciences of the Armenian SSR, Erivan.
INTERPRETATION OF DISTRIBUTIONS ON K(SUB pi)(SUP 0) IN pFe, nFe, AND piFe INTERACTIONS AT 0.5-5.0 TeV IN THE FRAMEWORK OF CONTEMPORARY MODELS
V. V. Avakyan, A. P. Garyaka, and G. Z. Zazyan 1991 34 p In RUSSIAN; ENGLISH summary
(DE92-621189; EFI-1326-21-91) Avail: NTIS HC/MF A03

Fluctuations of the observable parameters of nuclear electromagnetic cascades induced by 0.5-5.0 TeV cosmic ray protons, neutrons and pions are studied by the ionization calorimeter of the PION setup. The distributions of the inelasticity coefficient K(sub pi)(sup 0) are measured for pFe, nFe and (pi)Fe interactions and compared with the predictions of various models. The probability of the inelastic charge exchange reaction in the (pi)Fe interactions is defined. DOE

99 GENERAL

N92-26640# Department of Energy, Washington, DC. Office of Research.
ABSTRACTS OF PHASE 1 AWARDS, 1991
1991 107 p
(DE92-010133; DOE/ER-0505) Avail: NTIS HC/MF A06

Contained in this booklet are abstracts of the Phase 1 awards made in Fiscal Year 1991 under the Small Business Innovation Research (SBIR) program in the Department of Energy (DOE). This program, now completing its ninth year, was established in compliance with the Small Business Innovation Development Act, Public Law 97-219. The 173 Phase 1 projects described here were selected in a highly competitive process from a total of 1401 grant applications received in response to the 1991 Solicitation. The work described in the abstracts represents high-risk research, but the benefits will also be potentially high if the objectives are met. Brief comments on the potential applications, as described by the awardee, are given after each abstract. Individuals and organizations, including venture capital and larger industrial firms, with an interest in the research described in any of the abstracts are encouraged to contact the appropriate small business directly. Topics include biomass, electric vehicle batteries, fuel cells, HCl Electrolysis, innovative appliances, enhanced oil recovery, natural gas, fossil resource utilization, environmental control technology, alternative fuels, coal utilization, coal liquefaction, robotics, remote sensing, nuclear fuel cycle, geotechnology, computers, atmospheric sciences, and other topics. DOE

N92-26664# Naval Academy, Annapolis, MD.
SUMMARY OF RESEARCH: ACADEMIC DEPARTMENTS, 1990-1991 Annual Report, Jul. 1990 - Jun. 1991
Fred Fetrow Oct. 1991 316 p
(AD-A245533; USNA-3910-3; Rept-16) Avail: NTIS HC/MF A14

This annual report summarizes the research work of the Naval Academy faculty and midshipmen for the period July 1990 through June 1991. Sponsored and independent research projects are listed by title, followed by the names of the investigators and an abstract. A list of publications and their abstracts are included as well as presentations at professional meeting, conferences, and seminars. GRA

N92-26824*# National Aeronautics and Space Administration. Goddard Space Flight Center, Greenbelt, MD.
RESEARCH AND TECHNOLOGY, 1990: GODDARD SPACE FLIGHT CENTER
1990 222 p
(NASA-TM-107792; NAS 1.15:107792; PB92-155951) Avail: NTIS HC/MF A10; 25 functional color p ages

Goddard celebrates 1990 as a banner year in space based astronomy. From above the Earth's obscuring atmosphere, four major orbiting observatories examined the heavens at wavelengths that spanned the electromagnetic spectrum. In the infrared and microwave, the Cosmic Background Explorer (COBE), measured the spectrum and angular distribution of the cosmic background radiation to extraordinary precision. In the optical and UV, the Hubble Space Telescope has returned spectacular high resolution images and spectra of a wealth of astronomical objects. The Goddard High Resolution Spectrograph has resolved dozens of UV spectral lines which are as yet unidentified because they have never before been seen in any astronomical spectrum. In x rays, the Roentgen Satellite has begun returning equally spectacular images of high energy objects within our own and other galaxies. Author

N92-27083*# National Aeronautics and Space Administration. Langley Research Center, Hampton, VA.
LDEF: 69 MONTHS IN SPACE. FIRST POST-RETRIEVAL SYMPOSIUM, PART 3
Arlene S. Levine, ed. Washington Jan. 1992 485 p Symposium held in Kissimmee, FL, 2-8 Jun. 1991; sponsored by NASA, Washington Original contains color illustrations
(RTOP 196-88-00-03)
(NASA-CP-3134-Pt-3; L-17042-Pt-3; NAS 1.55:3134-Pt-3) Avail: NTIS HC/MF A21; 1 functional color page

A compilation of papers presented at the First Long Duration Exposure Facility (LDEF) Post-Retrieval Symposium is presented. The papers represent the preliminary data analysis of the 57 experiments flown on the LDEF. The experiments include materials, coatings, thermal systems, power and propulsion, science (cosmic ray, interstellar gas, heavy ions, and micrometeoroid), electronics, optics, and life sciences. For individual titles, see N92-27084 through N92-27129.

N92-27084*# National Aeronautics and Space Administration. Goddard Space Flight Center, Greenbelt, MD.
SYSTEMS SPECIAL INVESTIGATION GROUP OVERVIEW c23
James B. Mason, Harry Dursch, and Joel Edelman (Long Duration Exposure Facility Newsletter, Silver Spring, MD.) *In* NASA. Langley Research Center, LDEF: 69 Months in Space. First Post-Retrieval Symposium, Part 3 Jan. 1992 p 1217-1223 (For primary document see N92-27083 17-99)
Avail: NTIS HC/MF A21; 1 functional color page

The Systems Special Investigation Group (SIG) has undertaken investigations in the four major engineering disciplines represented by LDEF hardware: electrical, mechanical, thermal, and optical systems. Testing was planned for the highest possible level of assembly, and top level system tests for nearly all systems were performed at this time. Testing to date was performed on a mix of LDEF and individual experimenter systems. No electrical or mechanical system level failures attributed to the spaceflight environment were detected by the Systems SIG. Some low cost electrical components were used successfully, although relays were a continuing problem. Extensive mechanical galling was observed, but no evidence of coldwelding was identified. A working index of observed systems anomalies was created and will be used to support the tracking and resolution of these effects. LDEF hardware currently available to the Systems SIG includes most of the LDEF facility systems hardware, and some significant experimenter hardware as well. A series of work packages was developed for each of several subsystem types where further testing is of critical interest. The Systems SIG is distributing a regular newsletter to the greater LDEF community in order to maintain coherence in an investigation which is widely scattered both in subject matter and in geography. Circulation of this informal document has quadrupled in its first year. Author

N92-27085*# Thiokol Corp., Brigham City, UT.
SPACE AGING OF SOLID ROCKET MATERIALS Abstract Only c28
Dean M. Lester, Leon L. Jones, R. B. Smalley, Jr., and R. Neil Ord *In* NASA. Langley Research Center, LDEF: 69 Months in Space. First Post-Retrieval Symposium, Part 3 Jan. 1992 p 1225 (For primary document see N92-27083 17-99)
Avail: NTIS HC/MF A21; 1 functional color page

Solid rocket propellant and rocket motor components were aged in a vented container on the interior of the LDEF. This paper will present the results of aging the Improved Performance Space Motor-II/Payload Assist Module-Delta II (IPSM-II/PAM-DII) space motor components. Ballistic and mechanical properties of the space aged main propellant, igniter propellant, and ignition system were compared with similar data from preflight and ground aged samples. Mechanical properties of the composite materials and bonded joints used in the motor case, insulation, liner, nozzle, exit cone, and skirt were similarly evaluated. The space aging results will be compared to data collected in a ground based vacuum aging program on similar components. The operation of the vacuum actuated venting valve and pressure actuated resealing of the container will also be addressed. The materials tested showed no significant changes due to space aging. These results indicate that properly designed solid rocket motors can be expected to perform reliably after extended periods of exposure to a space environment. Author

N92-27086*# Grumman Aerospace Corp., Bethpage, NY. Corporate Research Center.

EFFECTS OF THE SPACE ENVIRONMENT ON SPACE-BASED RADAR PHASED-ARRAY ANTENNA; STATUS AND PRELIMINARY OBSERVATIONS (LDEF EXPERIMENT A0133) **c27**

J. B. Whiteside, D. Giangano, R. L. Heuer, E. Kamykowski, M. Kesselman, W. D. Rooney, R. Schulte, and M. Stauber *In* NASA. Langley Research Center, LDEF: 69 Months in Space. First Post-Retrieval Symposium, Part 3 Jan. 1992 p 1227-1240 (For primary document see N92-27083 17-99)

Avail: NTIS HC/MF A21; 1 functional color page

The overall objective of the experiment was to evaluate the effect of the space environment on components considered for a Space-Based Radar (SBR) Phased-Array Antenna. Of primary interest was a study of the degradation of the polyimide film Kapton (DuPont trademark), the material considered for use in the antenna plane. The most striking result of the experiment was the overall good condition of the Kapton antenna planes and Kapton tensile specimens, despite nearly six years of exposure to the space environment. This was largely attributable to the orientation of the Kapton (parallel and flush on the space end) and the stability of the Long Duration Exposure Facility (LDEF) in orbit. However, weathering of exposed Kapton surfaces was not insignificant. Results on elongation and mechanical properties of the plain and the fiberglass-reinforced Kapton are presented. Reduction in strain to failure of flight-exposed Kapton is attributed to surface defects of these specimens. Physical property testing of the materials to date reveals no significant difference between flight-exposed and control material. The second objective was to investigate the interaction between high-voltage electrodes and typical spacecraft contaminants in simulation of discharge triggering across differentially charged dielectric surfaces (spacecraft charging conditions). Electronic data acquisition and memory systems appeared to operate correctly, but very few discharges were recorded. Induced radioactivity, contamination, impacts, and orientation features of atomic oxygen erosion were observed.

Author

N92-27087*# National Aeronautics and Space Administration. Marshall Space Flight Center, Huntsville, AL.

AN OVERVIEW OF THE FIRST RESULTS ON THE SOLAR ARRAY MATERIALS PASSIVE LDEF EXPERIMENT (SAMPLE), A0171 **c44**

Ann F. Whitaker and Leighton E. Young *In* NASA. Langley Research Center, LDEF: 69 Months in Space. First Post-Retrieval Symposium, Part 3 Jan. 1992 p 1241-1254 (For primary document see N92-27083 17-99)

Avail: NTIS HC/MF A21; 1 functional color page

Power degradation in the solar cells was consistent with the exposure environment and appears to be produced principally by the radiation and atomic oxygen environments. Atomic oxygen erosion was generally as expected; atomic oxygen effects dominated for the most part in materials that were both atomic oxygen and ultraviolet vulnerable. Silicone coatings appear to protect Kapton, and adhesive systems contained under photon opaque materials were surprisingly environmentally resistant. A high density of small micro-meteroid/space debris impacts were observed on mirrors, protective coatings, paints, and composites. New synergistic effects of the space environment were noted in the interaction of atomic oxygen and copious amounts of contamination and in the induced luminescence of many materials.

Author

N92-27088*# Wright Lab., Wright-Patterson AFB, OH. Aerospace Power Div.

EXPERIMENT M0003-4: ADVANCED SOLAR CELL AND COVERGLASS ANALYSIS, AN OVERVIEW **c44**

Terry M. Trumble *In* NASA. Langley Research Center, LDEF: 69 Months in Space. First Post-Retrieval Symposium, Part 3 Jan. 1992 p 1255-1256 (For primary document see N92-27083 17-99)

Avail: NTIS HC/MF A21; 1 functional color page

The experiment consists of 51 coverglass samples and 12 solar cell strings. Sixteen (16) of the coverglass samples were on the leading edge and 16 on the trailing edge. An additional 16 samples were used as control samples and were not flown. The scenario for analysis was established for the coverglasses as follows. A photographic and a Nomarski survey were taken. Selected sites were then analyzed in their 'dirty' condition for optical transmission, reflectance, and absorbance. The coverglass samples have yet to be cleaned and resulting residue analyzed. The next stage of the analysis of the filters will be by probing through their layers to evaluate the multilayers used in their design. The solar cells were visually inspected and photographed. Tape recorder data is being analyzed and selected cell strings are being evaluated for their electrical properties. The first phase of the optical studies were completed.

Author

N92-27089*# Phillips Lab., Kirkland AFB, NM. Optoelectronics Section.

PRELIMINARY ANALYSES OF WL EXPERIMENT NO. 701, SPACE ENVIRONMENT EFFECTS ON OPERATING FIBER OPTIC SYSTEMS **c74**

E. W. Taylor, J. N. Berry, A. D. Sanchez, R. J. Padden, and S. P. Chapman *In* NASA. Langley Research Center, LDEF: 69 Months in Space. First Post-Retrieval Symposium, Part 3 Jan. 1992 p 1257-1282 (For primary document see N92-27083 17-99)

Avail: NTIS HC/MF A21; 1 functional color page

A brief overview of the analyses performed to date on WL Experiment-701 is presented. Four active digital fiber optic links were directly exposed to the space environment for a period of 2114 days. The links were situated aboard the Long Duration Exposure Facility (LDEF) with the cabled, single fiber windings atop an experimental tray containing instrumentation for exercising the experiment in orbit. Despite the unplanned and prolonged exposure to trapped and galactic radiation, wide temperature extremes, atomic oxygen interactions, and micro-meteorite and debris impacts, in most instances the optical data links performed well within the experimental limits. Analysis of the recorded orbital data clearly indicates that fiber optic applications in space will meet with success. Ongoing tests and analysis of the experiment at the Phillips Laboratory's Optoelectronics Laboratory will expand this premise, and establish the first known and extensive database of active fiber optic link performance during prolonged space exposure. WL Exp-701 was designed as a feasibility demonstration for fiber optic technology in space applications, and to study the performance of operating fiber systems exposed to space environmental factors such as galactic radiation, and wide temperature cycling. WL Exp-701 is widely acknowledged as a benchmark accomplishment that clearly demonstrates, for the first time, that fiber optic technology can be successfully used in a variety of space applications.

Author

N92-27090*# Jet Propulsion Lab., California Inst. of Tech., Pasadena.

LDEF FIBER OPTIC EXPOSURE EXPERIMENT NO. S-0109 **c74**

A. R. Johnston, L. A. Bergman, and R. Hartmayer *In* NASA. Langley Research Center, LDEF: 69 Months in Space. First Post-Retrieval Symposium, Part 3 Jan. 1992 p 1283-1298 (For primary document see N92-27083 17-99)

Avail: NTIS HC/MF A21; 1 functional color page

Ten fiber optic cable samples of different types were exposed in low-earth orbit for over 5.5 years on the Long-Duration Exposure Facility (LDEF). Four of the samples were mounted externally, and the remaining six were internal, under approximately 0.5 g cm(exp -2) of aluminum. The experiment was recovered in Jan. 1990, and laboratory evaluation of the effects of the exposure has continued since. An increase in fiber loss, presumed to be from radiation darkening, aging effects on polymer materials used in cabling, unique contamination effects on connector terminations, and micrometeoroid impacts were observed. In addition, the sample loss was measured for each sample as a function of temperature before and after the flight. All cable samples were functional, and the best exhibited no measurable change in performance, indicating

that conventional fiber optic cables can perform satisfactorily in spacecraft. Experimental results obtained to date are presented and discussed. D.R.D.

N92-27091*# Optical Coating Lab., Inc., Santa Rosa, CA.
OPTICAL PERFORMANCE OF EXPOSED SOLAR CELL COVERS Abstract Only **c74**
Thomas H. Allen, Bryant P. Hichwa, Steven R. Selee, Jerry Dodds, and Greg S. Long *In* NASA. Langley Research Center, LDEF: 69 Months in Space. First Post-Retrieval Symposium, Part 3 Jan. 1992 p 1299 (For primary document see N92-27083 17-99)
Avail: NTIS HC/MF A21; 1 functional color page

This paper discusses the characterization results of samples flown on the Long Duration Exposure Facility (LDEF). These samples included both coated and uncoated fused silica and ceria glass substrates used in the manufacture of solar cell covers. The coatings comprised a single-layer magnesium fluoride antireflection coating and an all-dielectric high-reflector multilayer coating centered at 350 nm. Samples were mounted on both the leading and trailing surfaces of the LDEF for exposure to the environment of space. The optical properties of the coatings will be compared to control samples which were stored on the ground during the LDEF Mission. Results of Auger Electron Spectroscopy and Rutherford Backscatter Spectroscopy measurements made on several of the coatings will be presented to explain the effects of space on the chemical composition of the coatings. Author

N92-27092*# Instruments Service Aerodynamique, Longjumeau (France).
RULED AND HOLOGRAPHIC DIFFRACTION GRATINGS EXPERIMENT (AO 138-5) **c35**
Francis Bonnemason *In* NASA. Langley Research Center, LDEF: 69 Months in Space. First Post-Retrieval Symposium, Part 3 Jan. 1992 p 1301-1314 (For primary document see N92-27083 17-99)
Avail: NTIS HC/MF A21; 1 functional color page

Ruled and Holographic Gratings (originals and replicas) proposed for use in loaded spectroscopic experiments are discussed. The optical performance of the gratings was tested in the low-earth orbital environment. Comparisons were made with identical components, which had been stored on the earth for the duration of the experiment. The following tests were performed: wavefront planeity, light efficiency, and stray-light level. Author

N92-27093*# McDonnell-Douglas Electronics Co., Saint Louis, MO.
POST-FLIGHT CHARACTERIZATION OF OPTICAL SYSTEM SAMPLES, THERMAL CONTROL SAMPLES, AND DETECTORS FROM LDEF EXPERIMENT M0003, SUB-EXPERIMENTS 6 AND 13 Abstract Only **c74**
Randall R. Hodgson, James N. Holsen, and Robert A. Drerup, Jr. (Wright Lab., Wright-Patterson AFB, OH.) *In* NASA. Langley Research Center, LDEF: 69 Months in Space. First Post-Retrieval Symposium, Part 3 Jan. 1992 p 1315 (For primary document see N92-27083 17-99)
Avail: NTIS HC/MF A21; 1 functional color page

Flight samples and control samples of optical and thermal control coatings were measured for hemispheric reflectance and transmission. Data was recorded for wavelengths from .25 to 18 microns. The samples were exposed directly to the orbital environment, but were on the trailing edge of the LDEF satellite. Preliminary analysis shows no significant change in the reflectance or transmission values of most of the samples. Author

N92-27094*# Georgia Inst. of Tech., Atlanta.
LDEF ACTIVE OPTICAL SYSTEM COMPONENTS EXPERIMENT **c74**
M. D. Blue *In* NASA. Langley Research Center, LDEF: 69 Months in Space. First Post-Retrieval Symposium, Part 3 Jan. 1992 p 1317-1326 (For primary document see N92-27083 17-99)
Avail: NTIS HC/MF A21; 1 functional color page

A preliminary report on the Active Optical System Components Experiment is presented. This experiment contained 136 components in a six inch deep tray including lasers, infrared detectors and arrays, ultraviolet light detectors, light-emitting diodes, a light modulator, flash lamps, optical filters, glasses, and samples of surface finishes. Thermal, mechanical, and structural considerations leading to the design of the tray hardware are discussed. In general, changes in the retested component characteristics appear as much related to the passage of time as to the effects of the space environment, but organic materials, multilayer optical interference filters, and extreme-infrared reflectivity of black paints show unexpected changes. Author

N92-27095*# National Aeronautics and Space Administration. Langley Research Center, Hampton, VA.
EFFECTS OF LONG-DURATION EXPOSURE ON OPTICAL SYSTEM COMPONENTS **c74**
Gale A. Harvey *In its* LDEF: 69 Months in Space. First Post-Retrieval Symposium, Part 3 Jan. 1992 p 1327-1340 (For primary document see N92-27083 17-99)
Avail: NTIS HC/MF A21; 1 functional color page

The optical materials and UV detectors experiment (SOO50-1) was a set of 15 optical windows, filters, and ultraviolet detectors. The optical specimens were all retrieved in excellent condition. No discoloration of the bulk optical window materials occurred, but the optical windows did experience several types of contamination. The most notable degradation of the optics were the deposition of an organic film on both surfaces. The films' absorptions were measured using a Fourier Transform Infrared Spectrometer and UV spectrometers. The UV absorptions were almost 100 percent at 200 nm and about 50 percent at 380 nm. Author

N92-27096*# Eastman Kodak Co., Rochester, NY.
EFFECTS OF LONG TERM EXPOSURE ON OPTICAL SUBSTRATES AND COATINGS (SOO50-2) **c74**
John Vallimont and Keith Havey *In* NASA. Langley Research Center, LDEF: 69 Months in Space. First Post-Retrieval Symposium, Part 3 Jan. 1992 p 1341-1342 (For primary document see N92-27083 17-99)
Avail: NTIS HC/MF A21; 1 functional color page

Kodak included 12 substrate and coating samples on the Long Duration Exposure Facility (LDEF) structure. There were 3 fused silica and 3 ultra low expansion (ULE(tm)) uncoated glass samples, 2 ULE(tm) samples with a high reflectance silver coating, 2 fused silica samples with an antireflectance coating, and 2 fused silica samples with a solar rejection coating. The sample dimensions were 32 mm diameter by 1 mm thick. A set of duplicate control samples was also manufactured and stored in a controlled environment for comparison purposes. A preliminary evaluation of the flight samples for effects from the 5 year mission showed that a contaminant was deposited on the samples, a micrometeroid impact occurred on one of the samples, and the radiation darkening which was expected for the glass did not occur. The results are presented in more detail. Author

N92-27097*# MATRA Service Aerodynamique, Velizy-Villacoublay (France).
VACUUM DEPOSITED OPTICAL COATINGS EXPERIMENT **c74**
Jean Charlier *In* NASA. Langley Research Center, LDEF: 69 Months in Space. First Post-Retrieval Symposium, Part 3 Jan. 1992 p 1343-1360 (For primary document see N92-27083 17-99)
Avail: NTIS HC/MF A21; 1 functional color page

The 138-4 Frecopa experiment consisted of 20 sorts of optical components and coatings subjected to space exposure. They covered a large range of use from the UV to IR spectrum: filters, mirrors, dichroics, beam splitters, and antireflection coatings made of several different materials as layers and substrates. By comparing pre- and post-flight spectral performances, it was possible to put into evidence the alterations due to space exposure. Author

N92-27098*# Naval Weapons Center, China Lake, CA.
SPACE ENVIRONMENTAL EFFECTS ON COATED OPTICS **c74**
T. M. Donovan, J. M. Bennett, R. Z. Dalbey, D. K. Burge, and S. Gyetvay (Aerospace Corp., Los Angeles, CA.) *In* NASA. Langley Research Center, LDEF: 69 Months in Space. First Post-Retrieval Symposium, Part 3 Jan. 1992 p 1361-1375 (For primary document see N92-27083 17-99)
(DARPA Order 3154)
Avail: NTIS HC/MF A21; 1 functional color page

Several high reflectance mirrors and an output window were selected for the Long Duration Exposure Facility (LDEF) by pre-flight screening using laboratory simulation of natural space radiation. One mirror, a silicon/aluminum oxide design, showed expected excellent stability in orbit and a long shelf life. An aluminum oxide coated calcium fluoride window also showed good stability. Less stable but more interesting behavior was observed in the zinc sulfide based mirrors that showed contamination effects and related dendrite formation. These samples, which were located on both leading and trailing edges, also had interesting impact sites.
Author

N92-27099*# National Aeronautics and Space Administration. Marshall Space Flight Center, Huntsville, AL.
CONTAMINATION OF OPTICAL SURFACES IN EARTH ORBIT Abstract Only **c74**
Donald L. Kinser, Robert A. Weller, M. H. Mendenhall, D. E. Wiedlocher (Vanderbilt Univ., Nashville, TN.), R. Nichols, D. Tucker, and A. Whitaker *In* NASA. Langley Research Center, LDEF: 69 Months in Space. First Post-Retrieval Symposium, Part 3 Jan. 1992 p 1377 (For primary document see N92-27083 17-99)
Avail: NTIS HC/MF A21; 1 functional color page

Glass and glass ceramic samples exposed to the low earth orbit environment for approximately 5.5 years on the Long Duration Exposure Facility (LDEF) were found to display limited degradation in optical transmission. Commercial optical quality fused silica samples display decreases in transmission in the 200 to 400 nm wavelength region, and this degradation appears to be a consequence of surface contamination. The contamination, found only on internal surfaces of samples, was measured by medium energy backscattering spectrometry and found to be primarily carbon. Additional thin film contamination by a species with atomic mass near 64, which was present at the level of about 8 x 10 exp 14/sq. cm has not been identified. These observations are consistent with the interpretation that organic binders used in the black absorbing paint (Chem Glaze Z-306) inside the sample holding tray were concentrated in the vicinity of the samples and photolytically cracked by solar UV radiation. The resulting decomposition products were deposited on the interior sample surface and gave rise to the optical transmission loss. No detectable contamination was observed on the external or space exposed surface of the samples. No measurable damage was detected which could be attributed to the direct action of gamma or UV radiation on the glass samples. These results emphasize the need for special precautions in the preparation of spacecraft carrying precision optical components on long duration missions.
Author

N92-27100*# National Aeronautics and Space Administration. Lewis Research Center, Cleveland, OH.
DURABILITY EVALUATION OF PHOTOVOLTAIC BLANKET MATERIALS EXPOSED ON LDEF TRAY S1003 **c27**
Sharon K. Rutledge and Raymond M. Olle (Cleveland State Univ., OH.) *In* NASA. Langley Research Center, LDEF: 69 Months in Space. First Post-Retrieval Symposium, Part 3 Jan. 1992 p 1379-1394 (For primary document see N92-27083 17-99)
Avail: NTIS HC/MF A21; 1 functional color page

Several candidate protective coatings on Kapton and uncoated Kapton were exposed to the low Earth orbital (LEO) environment on the Long Duration Exposure Facility (LDEF) to determine if the coatings could be used to protect polymeric substrates from degradation in the LEO environment. The coatings that were evaluated were 700 A of aluminum oxide, 650 A of silicon dioxide, and 650 A of a 4 percent polytetrafluoroethylene-96 percent silicon dioxide mixed coating. All of the coatings evaluated were ion beam sputter deposited. These materials were exposed to a very low atomic oxygen fluence (4.8 x 10 exp 19 atoms/sq. cm) as a result of the experiment tray being located 98 degrees from the ram direction. As a result of the low atomic oxygen fluence, determination of a change in mass was not possible for any of the samples including the uncoated Kapton. There was no evidence of spalling of any of the coatings after the approximately 33,600 thermal cycles recorded for LDEF. The surface of the uncoated Kapton, however, did show evidence of grazing incidence texturing. There was a 7-8 percent increase in solar absorptance for the silicon dioxide and aluminum oxide coated Kapton and only a 4 percent increase for the mixed coating. It appears that the addition of a small amount of fluoropolymer may reduce the magnitude of absorptance increase due to environmental exposure. Thermal emittance did not change significantly for any of the exposed samples. Scanning electron microscopy revealed few micrometeoroid or debris impacts, but the impact sites found indicated that the extent of damage or cracking of the coating around the defect site did not extend beyond a factor of three of the impact crater diameter. This limiting of impact damage is of great significance for the durability of thin film coatings used for protection against the LEO environment.
Author

N92-27101*# National Aeronautics and Space Administration. Lewis Research Center, Cleveland, OH.
ADVANCED PHOTOVOLTAIC EXPERIMENT, S0014: PRELIMINARY FLIGHT RESULTS AND POST-FLIGHT FINDINGS **c44**
David J. Brinker, John R. Hickey (Eppley Lab., Inc., Newport, RI.), and David A. Scheiman *In* NASA. Langley Research Center, LDEF: 69 Months in Space. First Post-Retrieval Symposium, Part 3 Jan. 1992 p 1395-1404 (For primary document see N92-27083 17-99)
Avail: NTIS HC/MF A21; 1 functional color page

The Advanced Photovoltaic Experiment is a Long Duration Exposure Facility (LDEF) experiment originally designed to provide reference solar cell standards for laboratory measurements as well as to investigate the solar spectrum and the effects of long term exposure of space solar cells to the low earth orbit (LEO) environment. The experiment functioned on-orbit as designed, successfully measuring and recording cell performance and solar insolation data over the first 325 days. The objectives and design of the experiment are presented as well as the preliminary flight results and postflight findings.
Author

N92-27102*# Messerschmitt-Boelkow G.m.b.H., Munich (Germany, F.R.).
EVALUATION OF LDEF EXPERIMENT S1002 **c27**
Ludwig Preuss *In* NASA. Langley Research Center, LDEF: 69 Months in Space. 1st Post-Retrieval Symposium, Part 3 Jan. 1992 p 1405-1417 (For primary document see N92-27083 17-99)
Avail: NTIS HC/MF A21; 1 functional color page

Thermal control coatings, solar cells, and micrometeoroid capture cells developed under government contract have been flown on the experiment to investigate both the behavior of these components under space conditions and to collect micrometeoroids and debris. The visual inspections, electrical and thermo-optical measurements as well as chemical and metallurgical investigations conducted on the complete experiment and on individual components are described, analyzed, and discussed. The postflight results of the thermal control coatings proved to be in good accordance with laboratory results.
Author

N92-27103*# TRW Space Technology Labs., Redondo Beach, CA.
LDEF SP-HVDE (SPACE PLASMA-HIGH VOLTAGE DRAINAGE EXPERIMENT) POST-FLIGHT RESULTS: LEAKAGE CURRENT AND DISCHARGE **c33**
J. Y. Yaung, W. C. Wong, B. K. Blakkolb, L. E. Ryan, J. E. Chedotte, and W. W. L. Taylor *In* NASA. Langley Research Center, LDEF:

69 Months in Space. First Post-Retrieval Symposium, Part 3 Jan. 1992 p 1419-1429 (For primary document see N92-27083 17-99)
Avail: NTIS HC/MF A21; 1 functional color page

TRW designed and fabricated two identical SP-HVDE trays which were flown in the NASA LDEF (Long Duration Exposure Facility) for 5.75 years in the LEO (low earth orbit) environment. One tray was placed near the leading edge and one near the trailing edge, and investigations were performed to compare the environmental interactions on the dielectric samples of the two trays. Each tray consisted of six assemblies with Kapton dielectric samples of varying thicknesses (i.e., 2 mils, 3 mil, and 5 mils) biased under +/- 300 V, +/- 500 V, and +/- 1000 V. The original objective was successfully achieved by measuring the first in-flight average leakage current through the samples. Less than 5 percent of the post-flight coulometers behaved anomalously. The data should be valuable to the design and evaluation of spacecraft with high voltage systems. M/D (micrometeoroid and debris) impacts over the dielectric samples were examined using a SEM (Scanning Electron Microscope) and an EDS (Energy Dispersive x-ray Spectrometer). These impact sites were sprayed by silver which were most likely caused either by the impact or a 'local ESD' (electrostatic discharge). Author

N92-27104*# National Aeronautics and Space Administration. Goddard Space Flight Center, Greenbelt, MD.
LONG DURATION EXPOSURE FACILITY (LDEF) LOW TEMPERATURE HEAT PIPE EXPERIMENT PACKAGE (HEPP) FLIGHT RESULTS c34
Roy McIntosh, Craig McCreight, and Patrick J. Brennan (OAO Corp., Greenbelt, MD.) *In* NASA. Langley Research Center, LDEF: 69 Months in Space. First Post-Retrieval Symposium, Part 3 Jan. 1992 p 1431-1439 (For primary document see N92-27083 17-99)
Avail: NTIS HC/MF A21; 1 functional color page

The Low Temperature Heat Pipe Flight Experiment (HEPP) is a fairly complicated thermal control experiment that was designed to evaluate the performance of two different low temperature ethan heat pipes. A total of 388 days of continuous operation with an axially grooved aluminum transporter heat pipe and an axially grooved stainless steel heat pipe diode was demonstrated before the EPDS batteries lost power. Preliminary postflight tests showed that the heat pipes are still functioning. A summary of the flight data analysis for the heat pipes and the related support systems is presented. Author

N92-27105*# National Aeronautics and Space Administration. Goddard Space Flight Center, Greenbelt, MD.
LONG DURATION EXPOSURE FACILITY (LDEF) LOW-TEMPERATURE HEAT PIPE EXPERIMENT PACKAGE POWER SYSTEM RESULTS c34
Smith E. Tiller and David Sullivan *In* NASA. Langley Research Center, LDEF: 69 Months in Space. First Post-Retrieval Symposium, Part 3 Jan. 1992 p 1441-1454 (For primary document see N92-27083 17-99)
Avail: NTIS HC/MF A21; 1 functional color page

An overview of a self-contained Direct Energy Transfer Power System which was developed to provide power to the Long Duration Exposure Facility (LDEF) Low-Temperature Heat Pipe Experiment Package is presented. The power system operated successfully for the entire mission. Data recorded by the onboard recorder shows that the system operated within design specifications. Other than unanticipated overcharging of the battery, the power system operated as expected for nearly 32,000 low earth orbit cycles, and was still operational when tested after the LDEF recovery. Some physical damage was sustained by the solar array panels due to micrometeoroid hits, but there were not electrical failures. Author

N92-27106*# McDonnell-Douglas Electronics Co., Saint Louis, MO. Laser and Electronics Systems Div.
RESULTS FROM THE LDEF/A0076 CASCADED VARIABLE CONDUCTANCE HEATPIPE EXPERIMENT c34
Michael G. Grote *In* NASA. Langley Research Center, LDEF: 69 Months in Space. First Post-Retrieval Symposium, Part 3 Jan. 1992 p 1455-1466 (For primary document see N92-27083 17-99)
Avail: NTIS HC/MF A21; 1 functional color page

The A0076 Variable Conductance Heat Pipe Experiment (CVCHPE) on the Long Duration Exposure Facility (LDEF) demonstrated temperature control better than +/- 0.3 C during fifty days on on-orbit data collection in a widely varying external environment. The experiment used two series connected, dry reservoir variable conductance heat pipes which require no electrical power for operation. The heat pipes used a central artery design with ammonia working fluid and nitrogen control gas. The LDEF was in orbit for almost six years rather than the planned one year mission. Although no additional data were taken during this extended period, post-test data indicated that the set point drifted upward less than 1 C per year. There were significant changes to the appearance of all external thermal control surfaces primarily due to atomic oxygen degradation, and one small anomaly in the electronics. These changes, though, had little effect on the CVCHPE performance. Author

N92-27107*# National Aeronautics and Space Administration. Marshall Space Flight Center, Huntsville, AL.
TRANSVERSE FLAT PLATE HEAT PIPE EXPERIMENT c34
David Shular *In* NASA. Langley Research Center, LDEF: 69 Months in Space. First Post-Retrieval Symposium, Part 3 Jan. 1992 p 1467-1475 (For primary document see N92-27083 17-99)
Avail: NTIS HC/MF A21; 1 functional color page

The Transverse Flat Plate Heat Pipe is a thermal control device that serves the dual function of temperature control and mounting base for electronic equipment. In its ultimate application, the heat pipe would be a lightweight structural member that could be configured in a platform or enclosure, and provide temperature control for large space structures, flight experiments, and equipment. The purpose of this experiment is to evaluate the zero g performance of several heat pipe modules. Performance assessment will include: (1) the systems heat transport capability; (2) temperature drop between evaporator and condensor; and (3) the ability to maintain temperature over varying duty cycles and environments. Also, performance degradation, if any, will be monitored over the length of the LDEF mission. The objective of this experiment is to demonstrate that a self-regulated heat pipe thermal control system can maintain hardware temperatures within tolerances of + or - 9 F or less with varying heat inputs, independent of vehicle payload orientation. Author

N92-27108*# Reading Univ. (England). Infrared Multilayer Lab.
EXPOSURE TO SPACE RADIATION OF HIGH-PERFORMANCE INFRARED MULTILAYER FILTERS AND MATERIALS TECHNOLOGY EXPERIMENT (A0056) c74
Gary J. Hawkins, John S. Seeley, and Roger Hunneman *In* NASA. Langley Research Center, LDEF: 69 Months in Space. First Post-Retrieval Symposium, Part 3 Jan. 1992 p 1477-1491 (For primary document see N92-27083 17-99)
Avail: NTIS HC/MF A21; 1 functional color page

Infrared optical multilayer filters and materials were exposed to the space environment of low Earth orbit on LDEF. The effects are summarized of that environment on the physical and optical properties of the filters and materials flown. Author

N92-27109*# Eppley Lab., Inc., Newport, RI.
PASSIVE EXPOSURE OF EARTH RADIATION BUDGET EXPERIMENT COMPONENTS. LDEF EXPERIMENT AO-147: POST-FLIGHT EXAMINATIONS AND TESTS c35
John R. Hickey *In* NASA. Langley Research Center, LDEF: 69 Months in Space. First Post-Retrieval Symposium, Part 3 Jan. 1992 p 1493-1509 (For primary document see N92-27083 17-99)
(Contracts NAS1-15350; NAS3-25958)
Avail: NTIS HC/MF A21; 1 functional color page

The flight spare sensors of the Earth Radiation Budget (ERB)

experiment of the Nimbus 6 and 7 missions were flown aboard the LDEF. The preliminary post retrieval examination and test results are presented here for the sensor windows and filters, the thermopile sensors and a cavity radiometer. Author

N92-27110*# Barr Associates, Inc., Westford, MA.
TRANSMITTANCE MEASUREMENTS OF ULTRAVIOLET AND VISIBLE WAVELENGTH FILTERS FLOWN ABOARD LDEF **c74**

Thomas A. Mooney and Ali Smajkiewicz *In* NASA. Langley Research Center, LDEF: 69 Months in Space. First Post-Retrieval Symposium, Part 3 Jan. 1992 p 1511-1521 (For primary document see N92-27083 17-99)
Avail: NTIS HC/MF A21; 1 functional color page

A set of ten interference filters were supplied to be mounted on experiment no. A0-147 of LDEF. The results of spectral transmission measurements before delivery and after recovery are presented. Included are descriptions of the construction and materials included in the filters. Additional results from photographic microscopic and surface analytical observations are being gathered and will be presented later. Author

N92-27111*# Martin Marietta Labs., Baltimore, MD.
RADIATION SENSITIVITY OF QUARTZ CRYSTAL OSCILLATORS EXPERIMENT FOR THE LONG DURATION EXPOSURE FACILITY (LDEF) **c33**

J. S. Ahearn and J. D. Venables *In* NASA. Langley Research Center, LDEF: 69 Months in Space. First Post-Retrieval Symposium, Part 3 Jan. 1992 p 1523-1531 (For primary document see N92-27083 17-99)
Avail: NTIS HC/MF A21; 1 functional color page

Factors determining the radiation sensitivity of quartz crystal oscillators were studied on NASA's LDEF. Quartz materials were examined in the transmission electron microscope (TEM) and classified as to their sensitivity to radiation damage by establishing the rate of damage caused by the electron beam in the microscope. Two types of materials, i.e., swept premium Q quartz and natural quartz were chosen because clear differences were observed in their response to the electron beam in the TEM studies. Quartz resonators were then fabricated from them, tested for frequency stability over a greater than 6 mo. period and flown on the LDEF satellite. After retrieval (more than 7 yrs in space) the stability of the resonators was again determined. All of the space exposed resonators fabricated with swept premium Q material exhibited a frequency shift above that of the control resonators: none of the resonators fabricated from the natural quartz materials exhibited such a shift. The significant differences observed between the two types of materials in both the ground-based TEM studies and the space radiation induced frequency changes suggest that there may be a correlation between the two observations. Author

N92-27112*# Boeing Co., Seattle, WA. Defense and Space Group.
LDEF ELECTRONIC SYSTEMS: SUCCESSES, FAILURES AND LESSONS **c33**

E. A. Miller, L. K. Brooks, C. J. Johnson, J. L. Levorsen, O. R. Mulkey, D. C. Porter, and D. W. Smith *In* NASA. Langley Research Center, LDEF: 69 Months in Space. First Post-Retrieval Symposium, Part 3 Jan. 1992 p 1533-1546 (For primary document see N92-27083 17-99)
(Contract NAS1-19224)
Avail: NTIS HC/MF A21; 1 functional color page

Following LDEF retrieval, a series of tests were performed of various NASA and experimenter electronics, including the NASA provided data and initiate systems. The post-flight test program objectives and observations are discussed, as well as the 'lessons learned' from these examinations. Results are also included of an evaluation of electronic hardware flown on Boeing's LDEF experiment. Overall the electronic systems performed remarkably well, even though most were developed under budget restraints and used some non-space qualified components. Several anomalies were observed, however, including some which resulted in loss of data. Suggestions for avoiding similar problems on future programs are presented. Author

N92-27113*# National Aeronautics and Space Administration. Langley Research Center, Hampton, VA.
EFFECT OF SPACE EXPOSURE OF PYROELECTRIC INFRARED DETECTORS **c35**

James B. Robertson *In its* LDEF: 69 Months in Space. First Post-Retrieval Symposium, Part 3 Jan. 1992 p 1547-1548 (For primary document see N92-27083 17-99)
Avail: NTIS HC/MF A21; 1 functional color page

Pyroelectric detectors are one of many different types of infrared radiation detectors. The pyroelectric detectors are of interest for long term space use because they do not require cooling during operation. Also, they can detect at very long wavelengths and they have a relatively flat spectral response. A disadvantage is that the radiation must be chopped in order to be detected by a pyroelectric detector. The objective was to determine the effects of launch and space exposure on the performance of commercially available pyroelectric detectors. The approach was to measure certain detector parameters before and after flight and try to determine the amount and cause of the degradation. The experiment was passive: no data was taken during flight. It is concluded that lithium-tantalate and strontium-barium-niobate are suitable materials for pyroelectric detectors for long term space applications. Author

N92-27114*# Boeing Co., Seattle, WA. Defense and Space Group.
LDEF MECHANICAL SYSTEMS **c37**

W. Steve Spear and Harry W. Dursch *In* NASA. Langley Research Center, LDEF: 69 Months in Space. First Post-Retrieval Symposium, Part 3 Jan. 1992 p 1549-1564 (For primary document see N92-27083 17-99)
(Contract NAS1-18224)
Avail: NTIS HC/MF A21; 1 functional color page

Following LDEF retrieval, a number of studies were made of mechanical hardware and structure flown on the LDEF. The primary objectives are to determine the effects of long term space exposure on (1) mechanisms either used on LDEF or as part of individual experiments; (2) LDEF structural components; and (3) fasteners. Results from examination and testing of LDEF structure, fasteners, LDEF end support beam, environment exposure control canisters, experiment tray clamps, LDEF grapple fixtures, and viscous damper are presented. The most significant finding is the absence of space exposure related cold welding. The instances of seizure or removal difficulties initially attributed to cold welding were shown to have resulted from installation galling damage or improper removal techniques. Widespread difficulties encountered with removal of stainless steel fasteners underscore the need for effective thread lubrication schemes to ensure successful application of proposed orbital replacement units onboard Space Station Freedom. Author

N92-27115*# Boeing Co., Seattle, WA. Defense and Space Group.
ON-ORBIT COLDWELDING: FACT OR FRICTION? **c26**

Harry Dursch and Steve Spear *In* NASA. Langley Research Center, LDEF: 69 Months in Space. First Post-Retrieval Symposium, Part 3 Jan. 1992 p 1565-1576 (For primary document see N92-27083 17-99)
(Contract NAS1-18224)
Avail: NTIS HC/MF A21; 1 functional color page

A study into the potential of on-orbit coldwelding occurring was completed. No instances of cold welding were found during deintegration and subsequent testing and analysis of LDEF hardware. This finding generated wide interest and indicated the need to review previous on-orbit coldwelding experiments and on-orbit spacecraft anomalies to determine whether the absence of coldwelding on LDEF was to be expected. Results show that even though there have been no documented cases of significant on-orbit coldwelding events occurring, precautions should be taken

to ensure that neither coldwelding nor galling occurs in the space or prelaunch environment. Author

N92-27116*# National Aeronautics and Space Administration. Marshall Space Flight Center, Huntsville, AL.
THERMAL CONTROL SURFACES EXPERIMENT FLIGHT SYSTEM PERFORMANCE **c18**
Donald R. Wilkes, Leigh L. Hummer (AZ Technology, Huntsville, AL.), and James M. Zwiener *In* NASA. Langley Research Center, LDEF: 69 Months in Space. First Post-Retrieval Symposium, Part 3 Jan. 1992 p 1577-1591 (For primary document see N92-27083 17-99)
Avail: NTIS HC/MF A21; 1 functional color page

The Thermal Control Surfaces Experiment (TCSE) is the most complex system retrieved after long term space exposure. The TCSE is a microcosm of complex electro-optical payloads being developed and flown. The objective of the TCSE on the LDEF was to determine the effects of the near-Earth orbital environment and the LDEF induced environment on spacecraft thermal control surfaces. The TCSE was a comprehensive experiment that combined in-space measurements with extensive post-flight analyses of thermal control surfaces to determine the effects of exposure to the low Earth orbit space environment. The TCSE was the first space experiment to measure the optical properties of thermal control surfaces the way they are routinely measured in the lab. The performance of the TCSE flight system on the LDEF was excellent. Author

N92-27117*# Centre National d'Etudes Spatiales, Toulouse (France).
FRENCH COOPERATIVE PASSIVE PAYLOAD (FRECOPA) **c23**
Christian Durin *In* NASA. Langley Research Center, LDEF: 69 Months in Space. First Post-Retrieval Symposium, Part 3 Jan. 1992 p 1593-1605 (For primary document see N92-27083 17-99)
Avail: NTIS HC/MF A21; 1 functional color page

The fact that the LDEF satellite mission was extended resulted in a study of FRECOPA system elements. These tests were run on materials, electronics, wiring, and motor drives. It is worthwhile studying these elements as they have been exposed to the low earth orbit for nearly six years, whereas the experimental specimens were exposed for ten months. No functional damage was observed which was induced by impacts or erosion. A decrease in thermal, optical, and mechanical properties for DELRIN and teflon glass fabric induced by erosion and thermal environment was observed. The most important damage parameters are UV radiation and thermal cycling. Author

N92-27118*# Aerospatiale, Cannes (France). Space and Strategic Systems Div.
EFFECTS OF ULTRA-VACUUM AND SPACE ENVIRONMENT ON CONTACT OHMIC RESISTANCE: LDEF EXPERIMENT AO 138-11 **c33**
Jean-Pierre Assie and Alfred Perotto *In* NASA. Langley Research Center, LDEF: 69 Months in Space. First Post-Retrieval Symposium, Part 3 Jan. 1992 p 1607-1611 (For primary document see N92-27083 17-99)
Avail: NTIS HC/MF A21; 1 functional color page

The FRECOPA experimentation of chemical resistance of electrical connector contacts, as described, has evidenced the detrimental time variations of nickel plated conductors and gilded copper contacts, irrespective of crimping storage or metal peening conditions. With a view to reorient aluminum technology a silvered aluminum conductor/gilded aluminum contact solution was evaluated. Author

N92-27119*# Aerospatiale, Cannes (France). Space and Strategic Systems Div.
MICROWELDING (OR COLD-WELDING) OF VARIOUS METALLIC MATERIALS UNDER THE ULTRA-VACUUM LDEF EXPERIMENT AO 138-10 **c26**
Jean-Pierre Assie and Eric Conde (Centre National d'Etudes Spatiales, Toulouse, France) *In* NASA. Langley Research Center, LDEF: 69 Months in Space. First Post-Retrieval Symposium, Part 3 Jan. 1992 p 1613-1623 (For primary document see N92-27083 17-99)
Avail: NTIS HC/MF A21; 1 functional color page

The FRECOPA experimentation, as part of the Long Duration Exposure Facility (LDEF) mission, of mechanical and electrical parts of spacecraft in space ultra-vacuum has demonstrated freedom from any cold welding including microweld effects. This, as theorized, is due to integrity in space of the earthly grown oxygen layer. A further experimentation, a dynamic one this time, could provide a wealth of scientific data, yielding reliable material selecting criteria. Author

N92-27120*# Park (George W.) Seed Co., Inc., Greenwood, SC.
SEEDS IN SPACE EXPERIMENT **c51**
Jim A. Alston *In* NASA. Langley Research Center, LDEF: 69 Months in Space. First Post-Retrieval Symposium, Part 3 Jan. 1992 p 1625-1634 (For primary document see N92-27083 17-99)
Avail: NTIS HC/MF A21; 1 functional color page

Two million seeds of 120 different varieties representing 106 species, 97 genera, and 55 plant families were flown aboard the Long Duration Exposure Facility (LDEF). The seeds were housed in one sealed canister and in two small vented canisters. After being returned to earth, the seeds were germinated and the germination rates and development of the resulting plants were compared to the performance of the control seeds that stayed in the Park Seed's seed storage facility. There was a better survival rate in the sealed canister in space than at the storage facility at Park Seed. At least some of the seeds in each of the vented canisters survived the exposure to vacuum for almost six years. The number of observed apparent mutations was very low.
Author

N92-27121*# Oklahoma State Univ., Stillwater.
SPACE EXPOSED EXPERIMENT DEVELOPED FOR STUDENTS (SEEDS) (P0004-2) **c51**
Doris K. Grigsby and Nelson J. Ehrlich *In* NASA. Langley Research Center, LDEF: 69 Months in Space. First Post-Retrieval Symposium, Part 3 Jan. 1992 p 1635-1636 (For primary document see N92-27083 17-99)
Avail: NTIS HC/MF A21; 1 functional color page

SEEDS, a cooperative endeavor of NASA Headquarters, the NASA Langley Research Center, and the George W. Park Seed Company, resulted in the distribution of approximately 132,000 SEEDS kits to 3.3 million students. Kits contained Rutger's tomato seeds that had flown on the Long Duration Exposure Facility (LDEF), as well as seeds that had been stored in a climate controlled warehouse for the same time period. Preliminary data indicates the germination rate for space exposed seeds was 73.8 percent while Earth based seeds germinated at a rate of 70.3 percent. Tests conducted within the first six months after retrieval indicated space exposed seeds germinated in an average of 8.0 days, while Earth based seeds' average germination time was 8.3 days. Some mutations (assumed to be radiation induced) include plants that added a leaf instead of the usual flower at the end of the flower frond. Also, fruit produced from a flower with a variegated calyx bore seeds producing albino plants, while fruit from a flower with a green calyx from the same plant bore seeds producing green plants. Author

N92-27122*# The Research Inst. of the Gulf of Maine, South Portland.
SURVIVAL OF EPIPHYTIC BACTERIA FROM SEED STORED ON THE LONG DURATION EXPOSURE FACILITY (LDEF)
Abstract Only **c51**
Andrew C. Schuerger, Bret L. Norman, and Joseph A. Angelo, Jr. (Science Applications International Corp., Melbourne, FL.) *In* NASA. Langley Research Center, LDEF: 69 Months in Space. First Post-Retrieval Symposium, Part 3 Jan. 1992 p 1637

(For primary document see N92-27083 17-99)
Avail: NTIS HC/MF A21; 1 functional color page

Microbial contamination in American spacecraft has previously been documented, however, potential risks to plants and humans in future space based controlled ecological life support systems (CELSS) have yet to be addressed directly. The current study was designed to determine the survival of microorganisms exposed to the relatively harsh conditions found in low Earth orbit (LEO). Total mean dosage for flight and ground control seeds were 210.2 and 0.9 rads, respectively. Bacteria were isolated by plating samples of seedwashings onto dilute tryptic soy agar. Pure isolates of morphologically distinct bacteria were obtained by standard microbiological procedures. Bacteria were grouped according to colony type and preliminary identification was completed using a fatty acid analysis system. Bacillus spp. were the primary microorganisms that survived on seed during the experiment. Results support the hypothesis that terrestrial microorganisms can survive long periods of time in relatively harsh LEO environments. Author

N92-27123*# Deutsche Forschungsanstalt fuer Luft- und Raumfahrt, Cologne (Germany, F.R.). Inst. for Aerospace Medicine.

PRELIMINARY TOTAL DOSE MEASUREMENTS ON LDEF c51

G. Reitz *In* NASA. Langley Research Center, LDEF: 69 months in Space. First Post-Retrieval Symposium, Part 3 p1643-1649 (SEE N92-27083 17-99) Jan. 1992 (For primary document see N92-27083 17-99)
Avail: NTIS HC/MF A21; 1 functional color page

After spending nearly six years in Earth's orbit twenty stacks consisting of radiation detectors and biological objects are now back on Earth. These Free Flyer Biostack experiments are part of the Long Duration Exposure Facility (LDEF). The major objective of the experiments are to investigate the biological effectiveness of single heavy ions of the cosmic radiation in various biological systems and to provide information about the spectral composition of the radiation field and the total dose received in the LDEF orbit. The preliminary analysis of the thermoluminescence dosimeters (TLD) yields maximum absorbed dose rates of 2.24 mGy day(exp -1) behind 0.7 g cm(exp -2) shielding and 1.17 mGy day(exp -1) behind 12 g cm(exp -2) shielding. A thermal neutron fluence of 1.7 n cm(exp -2)s(exp -1) is determined from the differences in absorbed dose for different isotopic mixtures of lithium. The results of this experiment on LDEF are especially valuable since LDEF stayed for almost six years in the prospected orbit of the Space Station Freedom. Author

N92-27124*# Johann-Wolfgang-Goethe-Univ., Frankfurt am Main (Germany, F.R.). Botanical Inst.

TOTAL DOSE EFFECTS (TDE) OF HEAVY IONIZING RADIATION IN FUNGUS SPORES AND PLANT SEEDS: PRELIMINARY INVESTIGATIONS c51

A. R. Kranz, M. W. Zimmermann, R. Stadler, K. E. Gartenbach, and M. Pickert *In* NASA. Langley Research Center, LDEF: 69 Months in Space. First Post-Retrieval Symposium, Part 3 Jan. 1992 p 1651-1660 (For primary document see N92-27083 17-99)
Avail: NTIS HC/MF A21; 1 functional color page

The opportunity to compare cosmic radiation effects caused during long and short duration exposure flights in biological objects are limited until now, and data obtained so far are very rare and insufficient. Because of the very long exposure of the experiment during the Long Duration Exposure Facility (LDEF) mission (approximately 2000 days) structural changes of the hardware material can be expected which will influence its biocompatibility and, thus, will interact with the radiobiological effects. The aim of the experiment flown on LDEF was a detailed investigation of biological effects caused by cosmic radiation especially of particles of high atomic number Z and high energy. The flight hardware consisted of standard BIOSTACK containers; in these containers a special sandwich construction consisted of visual plastic detectors with seed rsp. spore layers interlocked. H.A.

N92-27125*# Marburg Univ. (Germany, F.R.). Dept. of Environmental Sciences and Space Medicine.

PRELIMINARY RESULTS OF THE ARTEMIA SALINA EXPERIMENTS IN BIOSTACK ON LDEF c51

E. H. Graul, W. Ruether, and C. O. Hiendl *In* NASA. Langley Research Center, LDEF: 69 Months in Space. First Post-Retrieval Symposium, Part 3 Jan. 1992 p 1661-1665 (For primary document see N92-27083 17-99)
Avail: NTIS HC/MF A21; 1 functional color page

The mosaic egg of the brine shrimp, Artemia salina, resting in blastula or gastrula state represents a system that during further development, proceeds without any further development to the larval stage, the free swimming nauplius. Therefore, injury to a single cell of the egg will be manifest in the larvae. In several experiments, it was shown that the passage of a single heavy ion through the shrimp egg damaged a cellular area large enough to disturb either embryogenesis or further development of the larvae, or the integrity of the adult individual. Emergence from the egg shell was heavily disturbed by the heavy ions as was hatching. Additional late effects, due to a hit by a heavy ion, are delayed of growth and of sexual maturity, and reduced fertility. Anomalies in the body and the extremities could be observed more frequently for the nauplii which had developed from eggs hit by heavy ions. H.A.

N92-27126*# Deutsche Forschungsanstalt fuer Luft- und Raumfahrt, Cologne (Germany, F.R.). Inst. of Aerospace Medicine.

LONG-TERM EXPOSURE OF BACTERIAL SPORES TO SPACE c51

G. Horneck, H. Buecker, and G. Reitz *In* NASA. Langley Research Center, LDEF: 69 Months in Space. First Post-Retrieval Symposium, Part 3 Jan. 1992 p 1667-1673 (For primary document see N92-27083 17-99)
Avail: NTIS HC/MF A21; 1 functional color page

With the NASA mission of the Long Duration Exposure Facility (LDEF), the authors have obtained the opportunity to expose Bacillus subtilis spores for nearly six years to the space environment and to analyze their responses after retrieval. The experiment was mounted onto a side tray of LDEF facing space. Data shows that the chances of microorganisms surviving in free space will be greatly increased by adequate shielding against solar ultraviolet light. H.A.

N92-27127*# Technical Univ. of Denmark, Lyngby. Physics Lab. 3.

RESULTS OF THE TTF-TCNQ AND THE CALCIUM CARBONATE CRYSTALLIZATION ON THE LONG DURATION EXPOSURE FACILITY c76

Kjeld Flemming Nielsen and M. David Lind (Rockwell International Science Center, Thousand Oaks, CA.) *In* NASA. Langley Research Center, LDEF: 69 Months in Space. First Post-Retrieval Symposium, Part 3 Jan. 1992 p 1675-1685 (For primary document see N92-27083 17-99)
Avail: NTIS HC/MF A21; 1 functional color page

Experiment A0139A on the Long Duration Exposure Facility (LDEF) carried four large containers into orbit five years with crystal growth solutions for lead sulfide, calcium carbonate, and TTF-TCNQ. Although temperature data was lost, the experimental program had been working since the valves in all containers had been opened. All four experiments produced crystals of varying quality. The calcium carbonate crystals had the best appearance. The TTF-TCNQ crystals were packed together near the valve openings of the container. When taken apart, the single crystals showed some unusual morphological properties. X ray investigations as well as conductivity measurements on long duration space grown TTF-TCNQ crystals will be presented. Comparisons will be made with our previous space solution growth experiments. The TTF-TCNQ crystals are no longer of the highest interest, so this activity has been terminated in favor of calcium carbonate and calcium phosphate crystallizations. Author

N92-27128*# NASA Space Station Program Office, Reston, VA.
THE ROLE OF THE LONG DURATION EXPOSURE FACILITY IN THE DEVELOPMENT OF SPACE SYSTEMS **c23**
Sally A. Little *In* NASA. Langley Research Center, LDEF: 69 Months in Space. First Post-Retrieval Symposium, Part 3 Jan. 1992 p 1687-1690 (For primary document see N92-27083 17-99)
Avail: NTIS HC/MF A21; 1 functional color page

The Long Duration Exposure Facility (LDEF) presents the international, aerospace community with an unprecedented opportunity to examine the synergistic, long term, space environmental effects on systems and materials. The analysis of the data within appropriate environmental contexts is essential to the overall process of advancing the understanding of space environmental effects needed for the continuing development of strategies to improve the reliability and durability of space systems and to effectively deal with the future challenges that new space initiatives will likely present. Author

N92-27129*# American Space Technology, Inc., Santa Monica, CA.
RETRIEVABLE PAYLOAD CARRIER: NEXT GENERATION LONG DURATION EXPOSURE FACILITY **c18**
Arthur T. Perry *In* NASA. Langley Research Center, LDEF: 69 Months in Space. First Post-Retrieval Symposium, Part 3 Jan. 1992 p 1691-1700 (For primary document see N92-27083 17-99)
Avail: NTIS HC/MF A21; 1 functional color page

This paper describes the Retrievable Payload Carrier (RPC), which is a multi-experiment, free flyer spacecraft being privately developed to make in-space experimentation more accessible and economically feasible for research and development organizations. The carrier concept was derived from NASA's highly successful and flight proven Long Duration Exposure Facility (LDEF). The LDEF capabilities have been enhanced to meet new customer requirements. This reusable payload carrier is planned for launch and retrieval by the space shuttle on a regular basis. The RPC's flexible design will facilitate manifesting of the shuttle cargo bay space. The vehicle is designed so that either the entire vehicle or only individual experiments can be removed and replaced. A fully operational RPC program consists of: (1) a carrier spacecraft; (2) a ground control station; (3) a ground processing facility; and (4) the personnel required to support both the development and operational phases of the program. Author

Typical Subject Index Listing

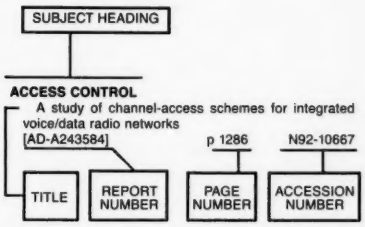

The subject heading is a key to the subject content of the document. Titles, report numbers, and accession numbers of pertinent documents are provided under each subject heading. When the title is insufficiently descriptive of the document content, a title extension has been added, separated from the title by three hyphens. The report number helps to indicate the type of document cited (e.g., NASA report, NASA translation, NASA contractor report). The accession number is the number by which the document abstracts are arranged in this journal and by which the document is sold or requested. The page number helps you locate the the citation in the abstract section. The titles, with title extensions if present, are arranged under each subject heading in ascending accession number order. The subject headings have been selected from the latest revision of the *NASA Thesaurus*.

A

ABLATION
The importance of chemical reactions with environment for ablation process of thermal protection and structural materials p 2883 N92-27015

ABRASION RESISTANCE
The effect of sandstorms on PV arrays and components --- photovoltaic cells
[DE92-001240] p 2927 N92-26686

ABSORBENTS
Activation and characterization of some molecular sieve catalysts
[ETN-92-91306] p 2871 N92-26261
Metal oxide absorbents for regenerative carbon dioxide and water vapor removal for advanced portable life support systems p 2968 N92-27021

ABSORBERS (EQUIPMENT)
Tests on various arrangements of liquid column vibration absorbers
[PB92-152610] p 2896 N92-26506

ABSORPTION SPECTRA
Water vapor information content of absorption lines observed in the Sun's infrared radiance p 2942 N92-26490

ABSORPTION SPECTROSCOPY
Spectroscopy and kinetics of combustion gases at high temperatures
[DE92-011216] p 2872 N92-26281

ABSTRACTS
Abstracts of phase 1 awards, 1991
[DE92-010133] p 3022 N92-26640
Summary of research: Academic departments, 1990-1991
[AD-A245533] p 3022 N92-26664

ACCELERATED LIFE TESTS
Life testing of secondary Ag-Zn cells p 2865 N92-27153
Accelerated cycle life performance for ovonic nickel-metal hydride cells p 2865 N92-27155

ACCELERATION (PHYSICS)
Non-compact WZW conformal field theories
[PB92-125038] p 3007 N92-26805

ACCELEROMETERS
The development of an optical fiber accelerometer
[DE92-008680] p 2997 N92-26452
Fiber-optic flexural disk accelerometer
[AD-A246203] p 2908 N92-26459

ACCESS CONTROL
A modeling strategy for large-scale optimization based on analysis and visualization principles
[AD-A246570] p 2987 N92-26620

ACCURACY
An adaptive correction technique for Differential Global Positioning System p 2851 N92-26623

ACETONITRILE
Neutron powder diffraction study of deuterated beta-acetonitrile p 3002 N92-26324
Solvation effects on the electronic structure of 4-N,N-Dimethylaminobenzonitrile: Mixing of the local pipi* and charge transfer states
[AD-A245814] p 2874 N92-26608

ACOUSTIC EMISSION
Source location in thin plates using crosscorrelation
[AD-A245521] p 2992 N92-26678

ACOUSTIC PROPAGATION
Description of the Rayflux ray tracing program and comparison with other models and measurements
[AD-A245413] p 2944 N92-26877

ACOUSTIC PROPERTIES
The modeling and control of acoustic/structure interaction problems via piezoceramic actuators: 2-D numerical examples
[NASA-CR-189639] p 2987 N92-26668

ACOUSTIC SOUNDING
Description of the Rayflux ray tracing program and comparison with other models and measurements
[AD-A245413] p 2944 N92-26877

ACOUSTIC VELOCITY
Recursive ray acoustics for three-dimensional sound-speed profiles
[AD-A245613] p 2991 N92-26228
The utility of acoustic travel times in locating the north wall of the Gulf Stream
[AD-A246219] p 2949 N92-26463
Symbolic solution of a multilayer ocean waveguide problem with arbitrary depth dependent ambient density and sound speed profiles
[AD-A245476] p 2949 N92-26533
A compendium of environmental data collected during the southwest Florida shallow-water acoustic sea test
[AD-A246143] p 2950 N92-27071

ACOUSTICAL HOLOGRAPHY
Optical hidden layer network
[AD-A246162] p 2992 N92-26413

ACOUSTICS
Computational methods for problems of acoustics with particular reference to exterior domains p 2992 N92-26558
Apparatus for measuring the absorption of sound by noise in one dimension
[AD-A246442] p 2992 N92-27031
The 3D rocket combustor acoustics model
[NASA-TM-105734] p 2861 N92-27035

ACTIVATED CARBON
GAC adsorption of a mixture of natural organic matter and VOCs in the presence and absence of molecular oxygen
[PB92-153782] p 2928 N92-26354
Differential Scanning Calorimetry (DSC) for the analysis of activated carbon
[AD-A245899] p 2872 N92-26404

ACTIVATION
Conversion of ethane and of propane to higher olefin hydrocarbons
[DE92-009487] p 2870 N92-26209

ACTIVE CONTROL
The modeling and control of acoustic/structure interaction problems via piezoceramic actuators: 2-D numerical examples
[NASA-CR-189639] p 2987 N92-26668
Conjugating binary systems: Advanced cooling liquids for use in spacecraft ATCS p 2905 N92-27027

ACTS
Report for neutral buoyancy simulations of transfer orbit stage contingency extravehicular activities
[NASA-TM-103583] p 2857 N92-26268

ACTUATOR DISKS
Powder processing of aero-engine components
[PNR-90813] p 2880 N92-27044

ACTUATORS
The modeling and control of acoustic/structure interaction problems via piezoceramic actuators: 2-D numerical examples
[NASA-CR-189639] p 2987 N92-26668
Experiments in modelling and end-point control of two-link flexible manipulators p 2915 N92-26731

ADA (PROGRAMMING LANGUAGE)
Distributed and parallel Ada and the Ada 9X recommendations
[NASA-CR-190392] p 2978 N92-26199
Reconfiguration in robust distributed real-time systems based on global checkpoints
[AD-A245615] p 2970 N92-26382
Data Management Systems (DMS): Complex data types study. Volume 1: Appendices A-B. Volume 2: Appendices C1-C5. Volume 3: Appendices D1-D3 and E
[NASA-CR-190397] p 3009 N92-26552
An Ada object oriented missile flight simulation
[AD-A246378] p 2977 N92-27052

ADAPTIVE CONTROL
An adaptive, packet-switched HF data terminal: Functional overview and initial performance
[AD-A246318] p 2973 N92-26292
Dynamic control of a space robot system with no thrust jets controlled base
[AD-A245711] p 2981 N92-26356
Adaptive control of robotic manipulators with structural flexibility p 2914 N92-26475
Adaptive regulation of the boiler-turbine unit of a Combined Heat and Power (CHP) system
[RR-417] p 2887 N92-26752
Adaptive control of nonlinear and stochastic systems
[AD-A247204] p 2985 N92-27169

ADDITIVES
Method for implanting impurities in semiconductors and semiconductor implanted with impurities
[AD-D015196] p 3003 N92-26433

ADENOSINE TRIPHOSPHATE
Study of hydrazine metabolism and toxicity
[AD-A245755] p 2884 N92-26589

ADHESION
Computational techniques in tribology and material science at the atomic level
[NASA-TM-105573] p 2990 N92-26671
An electroplater's view of PVD processing
[DE92-009052] p 2878 N92-26732

ADSORPTION
GAC adsorption of a mixture of natural organic matter and VOCs in the presence and absence of molecular oxygen
[PB92-153782] p 2928 N92-26354
A new phase in palladium hydride technology
[DE92-009852] p 2875 N92-26718

ADVANCED LAUNCH SYSTEM (STS)
Utilization of a bipolar lead acid battery for the advanced launch system p 2865 N92-27157

ADVANCED VERY HIGH RESOLUTION RADIOMETER
Cirrus clouds and condensation trail on 18 Oct. 1989 over the North sea (ICE '89). Determination of height and optical depth using ALEX, AVHRR and HIRS p 2940 N92-26340

ADVECTION
Tracer transport in the middle atmosphere p 2928 N92-26473
Nonexpansive prolongations and difference schemes for the advection equation
[PB92-141530] p 2986 N92-26502

AERODYNAMIC BRAKES
Critical soft landing technology issues for future US space missions
[NASA-CR-185673] p 2858 N92-26884
AERODYNAMIC COEFFICIENTS
Rarefied-flow aerodynamics
[NASA-CR-190452] p 2850 N92-27191
AERODYNAMIC CONFIGURATIONS
High-alpha vortex decoupling investigations on a chine forebody/Delta wing configuration at transonic Mach numbers
[NASA-CR-189642] p 2849 N92-26651
Distributed acoustic receptivity in laminar flow control configurations
[NASA-CR-4438] p 2898 N92-26680
AERODYNAMIC DRAG
Reynolds number dependence of the drag coefficient for laminar flow through fine-scale screens
[DE92-002930] p 2899 N92-26698
Aerodynamic drag on the bullet trains
p 2902 N92-26911
Flow around an isolated surface roughness in the laminar boundary layer p 2903 N92-26913
Application of riblet surface to pipe flow
p 2903 N92-26915
AERODYNAMIC FORCES
Aerodynamic interference between stores
[AD-A247207] p 2850 N92-27172
AERODYNAMIC INTERFERENCE
Aerodynamic interference between stores
[AD-A247207] p 2850 N92-27172
AERODYNAMIC LOADS
Computer program for calculating in-flight aircraft-store interface reaction loads
[AD-A245782] p 2852 N92-26896
Computational method to predict thermodynamic, transport, and flow properties for the modified Langley 8-foot high-temperature tunnel
[NASA-TM-4374] p 2905 N92-27193
AERODYNAMICS
Theoretical principles of a Euler method for the calculation of three dimensional flows
[F+W-TF-2012] p 2905 N92-27045
Rarefied-flow aerodynamics
[NASA-CR-190452] p 2850 N92-27191
AERONAUTICAL ENGINEERING
Naval Postgraduate School aircraft synthesis program (user's manual)
[AD-A246198] p 2974 N92-26458
AEROSOLS
Remote sensing of atmosphere with aircraft borne lidar systems p 2941 N92-26347
Parameterization of water-soluble component of aerosol particles in numerical cloud models
[NASA-CR-190225] p 2945 N92-26474
AEROSPACE ENGINEERING
Advanced materials aspects of concurrent engineering
[AD-A245437] p 2880 N92-26275
COSMIC software catalog, 1992 edition
[NASA-CR-188973] p 2977 N92-26868
Chinese space technology's spin-offs and applications
[AD-A246375] p 3015 N92-27051
NASA patent abstracts bibliography: A continuing bibliography. Section 2: Indexes (supplement 40)
[NASA-SP-7039(40)-SECT-2] p 3014 N92-27081
LDEF mechanical systems p 2916 N92-27114
The role of the Long Duration Exposure Facility in the development of space systems p 2867 N92-27128
The 1990 NASA Aerospace Battery Workshop
[NASA-CP-3119] p 2862 N92-27130
Rarefied-flow aerodynamics
[NASA-CR-190452] p 2850 N92-27191
AEROSPACE ENVIRONMENTS
Space aging of solid rocket materials
p 2884 N92-27085
Effects of the space environment on space-based radar phased-array antenna; status and preliminary observations (LDEF Experiment A0133) p 2883 N92-27086
Preliminary analyses of WL experiment No. 701, space environment effects on operating fiber optic systems
p 2998 N92-27089
Exposure to space radiation of high-performance infrared multilayer filters and materials technology experiment (A0056) p 2999 N92-27108
On-orbit coldwelding: Fact or friction?
p 2880 N92-27115
Thermal control surfaces experiment flight system performance p 2860 N92-27116
Effects of ultra-vacuum and space environment on contact ohmic resistance: LDEF experiment AO 138-11
p 2895 N92-27118
AEROSPACE MEDICINE
Space life sciences strategic plan, 1991
[NASA-TM-107856] p 2950 N92-26266
Aerospace medicine and biology: A continuing bibliography with indexes (supplement 362)
[NASA-SP-7011(362)] p 2953 N92-27068
AEROSPACE PLANES
An experimental investigation of a 2-D scramjet inlet at flow Mach numbers of 8 to 25 and stagnation temperatures of 800 to 4,100 K p 2854 N92-26586
AEROSPACE SAFETY
NASA. Johnson Space Center primary battery applications p 2863 N92-27142
AEROSPACE SCIENCES
COSMIC software catalog, 1992 edition
[NASA-CR-188973] p 2977 N92-26868
AEROSPACE SYSTEMS
The transpirator, an efficient and light evaporative cooler for space technology p 2887 N92-26986
The role of the Long Duration Exposure Facility in the development of space systems p 2867 N92-27128
Multiple cell CPV nickel-hydrogen battery
p 2866 N92-27166
AEROSPACE VEHICLES
Hypersonic aerospace vehicle leading edge cooling using heat pipe, transpiration and film cooling techniques
p 3007 N92-26733
Human round trip to Mars: Six months and radiation safe
[DE92-010160] p 2857 N92-26818
AEROTHERMODYNAMICS
Computational method to predict thermodynamic, transport, and flow properties for the modified Langley 8-foot high-temperature tunnel
[NASA-TM-4374] p 2905 N92-27193
AGGREGATES
Experimental study of shear fracture and aggregate interlock in cementbased composites
[PB92-151521] p 2868 N92-26525
Quantum dynamics of helium clusters
[AD-A245752] p 2995 N92-26588
AGING (MATERIALS)
Aging effects in palladium and LaNi(4.25)Al(0.75) tritides
[DE92-009945] p 2870 N92-26217
Assessment of diagnostic methods for solenoid-operated valves
[DE92-009379] p 2913 N92-26234
Space aging of solid rocket materials
p 2884 N92-27085
Chemical evaluation of non-woven nylon separators used in Ni/Cd cells p 2863 N92-27140
AGRICULTURE
An assessment of satellite remote sensing for land cover classification p 2922 N92-26625
AIR CONDITIONING EQUIPMENT
The centrifugal mass exchange apparatus in air-conditioning system of isolated, inhabited object and its work control p 2957 N92-26956
AIR CURRENTS
Undulatory airflow over the Spanish southern central highplain with northern winds p 2940 N92-26339
AIR FILTERS
Biodegradation studies with space cabin contaminants to determine the feasibility of Biological Air Filtration (BAF) in space cabins p 2962 N92-26983
AIR MASSES
Mean and turbulent structure of the marine atmospheric boundary layer during cold air outbreaks of different intensities: Observational and modelling analyses
p 2942 N92-26489
Study of entrainment mechanisms in convective clouds
[NASA-CR-190223] p 2946 N92-26735
Analysis of mixing mechanisms in numerically simulated convective clouds
[NASA-CR-190222] p 2946 N92-26736
AIR NAVIGATION
An adaptive correction technique for Differential Global Positioning System p 2851 N92-26623
AIR POLLUTION
Noxious matter transportation in the Alpine regions
p 2934 N92-26332
Plume trajectory validation study: Brown cloud support project overview
[DE92-006911] p 2928 N92-26390
Running a conference as a clean product. International Conference on Pollution Prevention: Clean technologies and clean products
[PB92-109099] p 2930 N92-26495
Organic carbon in soil and the global carbon cycle
[DE92-010289] p 2931 N92-26580
The impact of climate upon variation in air pollution using a synoptic climatological approach p 2931 N92-26590
Assessment of computer models for estimating vehicle emission factors. Volume 2: Description and comparison of the MOBILE4 and EMFAC7E models
[PB92-113067] p 2932 N92-26803
Rule-based expert system for evaluating the quality of long-term, in-situ, gas chromatographic measurements of atmospheric methane
[PB92-128560] p 2876 N92-26812
Evaluation of carbon dioxide emission control strategies in New York State
[DE92-010162] p 2932 N92-26825
A finite element/finite difference approach for modeling three-dimensional flow and pollutant dispersion around structures
[DE92-007322] p 2934 N92-26935
AIR PURIFICATION
Biodegradation studies with space cabin contaminants to determine the feasibility of Biological Air Filtration (BAF) in space cabins p 2962 N92-26983
AIR QUALITY
The impact of climate upon variation in air pollution using a synoptic climatological approach p 2931 N92-26590
Assessment of computer models for estimating vehicle emission factors. Volume 1: Executive summary
[PB92-113059] p 2931 N92-26802
AIR TO AIR MISSILES
An Ada object oriented missile flight simulation
[AD-A246378] p 2977 N92-27052
AIR WATER INTERACTIONS
Theoretical and modeling studies of the marine planetary boundary layer
[AD-A245903] p 2942 N92-26432
Mean and turbulent structure of the marine atmospheric boundary layer during cold air outbreaks of different intensities: Observational and modelling analyses
p 2942 N92-26489
AIRBORNE EQUIPMENT
Analysis of thermal infrared data acquired over playas: Silver Lake and Deep Springs Lake, California and Lunar Lake, Nevada p 2926 N92-26864
AIRCRAFT CONTROL
F-111C flight dynamic model aerodynamic data-base development and verification
[AD-A246356] p 2850 N92-26947
High lift aircraft
[AD-D015215] p 2853 N92-27185
AIRCRAFT DESIGN
Gamma Group-The Pale Horse: A proposal in response to a commercial air transportation study ort study
[NASA-CR-190019] p 2852 N92-26435
Naval Postgraduate School aircraft synthesis program (user's manual)
[AD-A246198] p 2974 N92-26458
AIRCRAFT DETECTION
The Lockheed F-117A
[RAND-P-7746-RGS] p 2852 N92-26673
AIRCRAFT EQUIPMENT
Aircraft photovoltaic power-generating system
p 2926 N92-26581
AIRCRAFT FUEL SYSTEMS
Separation of external stores: Comparison of results
[F+W-TF-2058] p 2853 N92-26944
AIRCRAFT ICING
The icing of the wing upper side and bottom side of the icing research aircraft of the DLR
p 2850 N92-26349
AIRCRAFT INSTRUMENTS
Remote sensing of atmosphere with aircraft borne lidar systems p 2941 N92-26347
AIRCRAFT LANDING
High lift aircraft
[AD-D015215] p 2853 N92-27185
AIRCRAFT MODELS
Development and testing of an unmanned air vehicle telemetry system
[AD-A246577] p 2858 N92-26621
AIRCRAFT PERFORMANCE
F-111C flight dynamic model aerodynamic data-base development and verification
[AD-A246356] p 2850 N92-26947
AIRCRAFT RELIABILITY
Test plan for the international aircraft operator information system
[DOT/FAA/CT-91/18] p 3014 N92-26830
AIRCRAFT STABILITY
F-111C flight dynamic model aerodynamic data-base development and verification
[AD-A246356] p 2850 N92-26947
Hot-gas reingestion engine response considerations
[PNR-90810] p 2855 N92-27042
AIRFOILS
An outline of a numerical scheme for calculating two-dimensional time linearised transonic flow using the Green's function method
[AD-A246349] p 2895 N92-26258
Distributed acoustic receptivity in laminar flow control configurations
[NASA-CR-4438] p 2898 N92-26680

AIRGLOW
U.S. ground-based space research programs in Svalbard (Norway) p 2935 N92-26296
ALBEDO
Theoretical and modeling studies of the marine planetary boundary layer
[AD-A245903] p 2942 N92-26432
ALCOHOLS
High octane ethers from synthesis gas-derived alcohols
[DE92-010480] p 2884 N92-26548
ALGEBRA
Algorithms for capacity computations and algebraic cascade coding with applications to data storage p 2977 N92-27053
ALGORITHMS
Comparison of one-way wave propagation algorithms in underwater acoustics-error estimates and sensitivity
[AD-A245660] p 2991 N92-26175
On the design of VLSI circuits for the Winograd Fourier transform algorithm
[AD-A246317] p 2892 N92-26244
The state of multiple sensor, multiple target tracking in ballistic missile defense
[AD-A245433] p 2850 N92-26272
Software maturity model applied to SDI
[AD-A245439] p 2972 N92-26276
Modeling node bandwidth limits and their effects on vector combining algorithms
[DE92-010829] p 2979 N92-26277
Description of a global shallow water model based on the spectral transform method
[PB92-155258] p 2928 N92-26352
The joint US/UK 1990 epoch world magnetic model
[NASA-CR-190424] p 2942 N92-26406
Neural network error correction for solving coupled ordinary differential equations
[NASA-TM-101796] p 2986 N92-26407
A computational analysis of properties and limitations of neural networks: Toward new parallel architectures for learning
[AD-A246156] p 2981 N92-26410
Optical hidden layer network
[AD-A246162] p 2992 N92-26413
Design and implementation of a toolbox of modularized C programs to construct, analyze, and test network optimization algorithms
[AD-A246191] p 2979 N92-26417
Finding a best subtree of a tree
[REPT-91-041] p 2986 N92-26420
Ocean bottom simulation using fractal geometry
[AD-A245477] p 2949 N92-26423
A comparison of direction finding results from an FFT peak identification technique with those from the music algorithm
[AD-A245675] p 2888 N92-26424
Hybrid efficient control algorithms for robot manipulators
[AD-A245716] p 2981 N92-26428
Theoretical issues in adaptive Set-Membership-Based signal processing.
[AD-A245721] p 2980 N92-26430
A random polynomial algorithm for the matroid parity base problem
[REPT-91-079] p 2974 N92-26449
Performance analysis of image motion analysis algorithms
[AD-A246522] p 2974 N92-26468
Algorithms for blending surface generation
[AD-A245686] p 2975 N92-26524
N-learners problem: Learning Boolean combinations of halfspaces
[DE92-010390] p 2987 N92-26545
The minimization of multiple valued logic expressions using parallel processors
[AD-A245763] p 2980 N92-26596
Radar target identification by natural resonances: Evaluation of signal processing algorithms
[AD-A246566] p 2889 N92-26619
A boundary integral method for steady unsaturated flow in nonhomogeneous media
[DE92-009066] p 2897 N92-26644
Iterative system modeling using multigrid techniques
[AD-A245522] p 2976 N92-26658
Development of TRMM radar rainfall retrieval algorithms
[TW-7] p 2923 N92-26708
A supervisory control strategy for navigation of mobile robots in dynamic environments p 2983 N92-26734
Explanation-based generalization of partially ordered plans
[NASA-TM-107869] p 2983 N92-26789
On increasing the capabilities of the SMART adaptive random number generator
[DE92-621106] p 2976 N92-26835
Solution of the first-order form of the 3-D discrete ordinates equations on a massively parallel machine
[DE92-004575] p 2981 N92-26854
A real-time synthetic aperture radar processor: Introduction and project description
[AD-A245370] p 2890 N92-26876
Monthly mean global satellite data sets available in CCM history tape format
[NASA-CR-190344] p 2933 N92-26878
Downdating of Szego polynomials and data fitting applications
[AD-A245825] p 2988 N92-26900
Proximal minimization algorithms with cutting planes
[AD-A246436] p 2977 N92-26949
Kalman smoother applied to lace
[AD-A246439] p 2859 N92-27030
Rocket engine diagnostics using qualitative modeling techniques
[NASA-TM-105714] p 2861 N92-27033
Interface of an uncoupled boundary layer algorithm with an inviscid core flow algorithm for unsteady supersonic engine inlets
[NASA-TM-105684] p 2855 N92-27037
Algorithms for capacity computations and algebraic cascade coding with applications to data storage p 2977 N92-27053
Complementary metal oxide silicon cyclic redundancy check generators
[AD-A246140] p 2894 N92-27061
NPSNET: Hierarchical data structures for real-time three-dimensional visual simulation
[AD-A246380] p 2978 N92-27073
ALIGNMENT
Application of decentralized control to a laser alignment system
[DE92-009692] p 2912 N92-26646
ALKALIES
Photocathode transfer and storage techniques using alkali vapor feedback control
[DE92-008449] p 2891 N92-26202
ALKENES
Conversion of ethane and of propane to higher olefin hydrocarbons
[DE92-009487] p 2870 N92-26209
ALKYL COMPOUNDS
Comparison of laser models
[NASA-CR-190302] p 2913 N92-26870
ALLOCATIONS
The fidelity enhancement process
[AD-A245388] p 2977 N92-26840
ALLOYS
Why first-principles calculations for alloys?
[DE92-010285] p 2877 N92-26213
ALPHA PARTICLES
Calorimetric particle detectors with superconducting absorber materials p 2907 N92-26393
Scenarios for the nonlinear evolution of alpha particle induced Alfven wave instability
[DE92-010549] p 3000 N92-26550
ALPS MOUNTAINS (EUROPE)
Noxious matter transportation in the Alpine regions p 2934 N92-26332
ALTITUDE TESTS
Acoustic interactions between an altitude test facility and jet engine plumes: Theory and experiments
[NASA-CR-190423] p 2853 N92-26405
ALUMINUM
Elevated temperature properties of a dispersion strengthened Al-(Fe, V, Si) alloy
[AD-A246427] p 2880 N92-27067
ALUMINUM ALLOYS
Dynamic restoration mechanisms in Al-5.8 at. percent Mg deformed to large strains in the solute drag regime
[DE92-009529] p 2877 N92-26223
Atomistic studies of grain boundaries in alloys and compounds
[DE92-010792] p 2877 N92-26251
Fundamental mechanisms affecting friction welding under vacuum
[AD-A245685] p 2877 N92-26520
Deformation behavior of an age-hardenable Beta + Alpha-Two titanium alloy
[AD-A246362] p 2879 N92-26939
Elevated temperature properties of a dispersion strengthened Al-(Fe, V, Si) alloy
[AD-A246427] p 2880 N92-27067
ALUMINUM ARSENIDES
Generation of nonequilibrium optical phonons in GaAs/AlAs quantum wells by intrasubband and intersubband scatterings
[DE92-010264] p 2993 N92-26207
ALUMINUM GALLIUM ARSENIDE LASERS
Innovative techniques for the production of low cost 2D laser diode arrays
[AD-A247282] p 2913 N92-27178
ALUMINUM GALLIUM ARSENIDES
Studies of deep level transient spectroscopy of DX centers in GaAlAs: Te under uniaxial stress
[DE92-010258] p 3001 N92-26204
Investigation of kinetics of MOCVD systems
[AD-A246090] p 2893 N92-26540
High-speed pulse detection room-temperature optical nonlinearities for GaInAs/A1InAs and GaA1InAs/A1InAs multiple quantum wells and integrated mirror etalon at 1.3 micrometers
[AD-A246369] p 2998 N92-26943
ALUMINUM HYDRIDES
Aging effects in palladium and LaNi(4.25)Al(0.75) tritides
[DE92-009945] p 2870 N92-26217
ALUMINUM OXIDES
Slip casting and green body evaluation of 6 percent yttria, 2 percent alumina silicon nitride
[AD-A245817] p 2881 N92-26283
Compressive damage and fracture modeling of ceramic subjected to high-velocity impact p 2881 N92-26492
Comparison of ceramic uniaxial compression specimens through detailed finite element modelling
[AD-A245816] p 2882 N92-26609
Study and analysis of the stress state in a ceramic, button-head, tensile specimen
[DE92-007794] p 2918 N92-26784
ALUMINUM-LITHIUM ALLOYS
Retention and release of tritium in aluminum clad, Al-Li alloys
[DE92-009905] p 2878 N92-26635
AMBIENT TEMPERATURE
Cycle life characteristics of Li-TiS2 cells p 2865 N92-27154
AMMONIUM SULFATES
Evaluation of the Fourier transform infrared spectrometer for particle-associated ammonium sulfate determination
[PB92-160084] p 2910 N92-26830
AMORPHOUS MATERIALS
Fabrication and characterization of amorphous lithium electrolyte thin films and rechargeable thin-film batteries
[DE92-010108] p 2893 N92-26636
New amorphous thin-film lithium electrolyte and rechargeable microbattery
[DE92-010110] p 2893 N92-26637
Crystalline-amorphous interfaces and their relation to grain boundary films
[DE92-009812] p 3004 N92-26648
AMORPHOUS SILICON
Photovoltaic manufacturing technology, phase 1
[DE92-001199] p 2926 N92-26190
AMPLITUDE MODULATION
Synchronous detection in monolithically integrated AM upconversion receivers
[ETN-92-91305] p 2892 N92-26260
ANALOG TO DIGITAL CONVERTERS
Effect of gyro noise on ADKEM gyro-only missile system performance
[AD-A246150] p 2852 N92-26408
ANALOGIES
On the existence of a capital similarity p 2941 N92-26344
ANATOMY
User manual for Natick's Footwear Database
[AD-A246275] p 2954 N92-26243
ANELASTICITY
Ensuring mass conversion in a heavy-gas dispersion model using the generalized anelastic equations
[DE92-007323] p 2934 N92-26936
ANGLE OF ATTACK
High-alpha vortex decoupling investigations on a chine forebody/Delta wing configuration at transonic Mach numbers
[NASA-CR-189642] p 2849 N92-26651
ANGULAR DISTRIBUTION
Li-6,d reaction on sd-, fp- and g-shell nuclei in ZR- and FR-DWBA formalisms
[DE92-614353] p 2994 N92-26365
ANGULAR MOMENTUM
Dynamic control of a space robot system with no thrust jets controlled base
[AD-A245711] p 2981 N92-26356
ANGULAR RESOLUTION
Measurement of surface layer optical turbulence above AMOS
[AD-A246387] p 3016 N92-27077
ANILINE
Vibrational dynamics of aniline (N2)1 clusters in their first excited singlet state
[AD-A245812] p 2872 N92-26431
ANIMALS
Clinical investigation program, fiscal year 1991
[AD-A246558] p 2992 N92-26618

ANIONS
Measurements of scattering processes in negative ion-atom collisions
[DE92-010319] p 2995 N92-26574
NASA Li/CF(x) cell problem analysis: Anion exchange chromatography analysis p 2864 N92-27145

ANISOTROPIC MEDIA
Transient diffusive electromagnetic fields in layered anisotropic media
[ISBN-90-6275-722-7] p 2887 N92-26254

ANISOTROPY
Magnetic anisotropy from first principles
[ISBN-90-9004483-3] p 2877 N92-26252
An anisotropic homologous model for the core-collapse in star clusters
[ETN-92-90826] p 3018 N92-26946

ANNEALING
Stochastic versions of the EM algorithm
[AD-A246929] p 2989 N92-27174

ANNIHILATION REACTIONS
Supersymmetry and dark matter, a new candidate p 3016 N92-26491

ANNUAL VARIATIONS
Undulatory airflow over the Spanish southern central highplain with northern winds p 2940 N92-26339
Comparison of wind profiles in close proximity to each other
[AD-A246152] p 2945 N92-26409

ANODES
Development of a 300 Amp-hr high rate lithium thionyl chloride cell p 2864 N92-27149
Zinc-oxygen battery development program p 2865 N92-27152

ANTARCTIC REGIONS
Antarctic studies of the cusp p 2936 N92-26301

ANTENNA ARRAYS
A comparison of direction finding results from an FFT peak identification technique with those from the music algorithm
[AD-A245675] p 2888 N92-26424

ANTENNA DESIGN
An antenna design for PANSAT using NEC
[AD-A245482] p 2888 N92-26399

ANTENNA RADIATION PATTERNS
An antenna design for PANSAT using NEC
[AD-A245482] p 2888 N92-26399
Status of TRMM project: Rain radar in the Tropical Rainfall Measuring Mission
[TW-2] p 2922 N92-26703
Storm model and beam filling problem for rain retrievals
[TW-6] p 2923 N92-26707

ANTHROPOMETRY
Design guide for saddle seating on small high-speed craft
[ISVR-TR-205] p 2956 N92-26891

ANTIREFLECTION COATINGS
Optical performance of exposed solar cell covers p 2998 N92-27091
Post-flight characterization of optical system samples, thermal control samples, and detectors from LDEF experiment M0003, sub-experiments 6 and 13 p 2998 N92-27093
Effects of long term exposure on optical substrates and coatings (SOO50-2) p 2998 N92-27096
Vacuum deposited optical coatings experiment p 2999 N92-27097

ANTISUBMARINE WARFARE
The utility of acoustic travel times in locating the north wall of the Gulf Stream
[AD-A246219] p 2949 N92-26463

APERTURES
Fractal characteristics of fracture roughness and aperture data
[DE92-010302] p 2895 N92-26214
Early risk reduction phase 1 FLIR/laser designator window
[AD-A246352] p 2911 N92-26293
Large coherent arrays for laser radars, phase 1
[AD-A245528] p 2912 N92-26663

APEXES
Cell vertex methods for compressible gas flows p 2897 N92-26599

APPLICATIONS PROGRAMS (COMPUTERS)
Description of and users manual for TUBA: A computer code for generating two-dimensional random fields via the turning bands method
[DE92-001020] p 2971 N92-26189
Description of a global shallow water model based on the spectral transform method
[PB92-155258] p 2928 N92-26352
A computer program for the calculation of daubechies wavelets
[AD-A245461] p 2975 N92-26529
A FORTRAN 90 code for magnetohydrodynamics
[DE92-010362] p 3000 N92-26577
Analysis of EMP response of structures using frequency domain electromagnetic interaction codes
[AD-A245758] p 2889 N92-26592
The development of a model builder for a microcircuit substrate
[AD-A245765] p 2893 N92-26606
User's guide to WPL microwave radiative transfer software
[PB92-129931] p 2890 N92-26809
Bayesian classification theory
[NASA-TM-107885] p 2988 N92-26894

APPROXIMATION
Comparison of one-way wave propagation algorithms in underwater acoustics-error estimates and sensitivity
[AD-A245660] p 2991 N92-26175
Electromagnetic scattering by a moving object: Theory and experiment
[PB92-150911] p 2889 N92-26511
Asymptotic analysis of the vibrations of variable length cantilever beams p 2918 N92-26739

AQUATIC PLANTS
Differentiation on genus of aquatic macrophytes through remote sensing in the Tucurui Reservoir, Para State, Brazil
[INPE-5315-PRE/1712] p 2951 N92-26721

AQUEOUS SOLUTIONS
The use of ion chromatography-dc plasma atomic emission spectrometry for the speciation of trace metals
[DE92-010317] p 2871 N92-26236

ARC SPRAYING
Evaluation of plasma sprayed crucible coatings for melt processing copper-refractory metal alloys
[DE92-008912] p 2878 N92-26727

ARCHES
Weight optimum arch structures
[AD-A246001] p 2918 N92-26759

ARCHITECTURE
Fourth European Symposium on Space Environment Control Systems, volume 2
[ESA-SP-324-VOL-2] p 2956 N92-26950
New perspectives of living in space: Habitability guidelines for future manned space systems p 2968 N92-27022
Influence of architecture on the definition of a space station configuration p 2860 N92-27024

ARCHITECTURE (COMPUTERS)
Scalable coherent interface: Links to the future
[DE92-010728] p 2887 N92-26267
Selection and specification of a data link protocol for VSAT based inter-LAN communications
[AD-A246289] p 2979 N92-26361
A computational analysis of properties and limitations of neural networks: Toward new parallel architectures for learning
[AD-A246156] p 2981 N92-26410
Hardware synthesis using high-level Petri nets
[REPT-91-071] p 2970 N92-26439
Architecture flow diagrams under Teamwork
[DE92-010482] p 2922 N92-26534
An object-oriented approach to computer architecture simulation
[AD-A246597] p 2970 N92-26773
Building a GIS on top of the open DBMS Postgres
[FEL-91-B183] p 3014 N92-26875
Software architecture for a distributed real-time system in Ada, with application to telerobotics
[NASA-TM-4367] p 2977 N92-26904
UT40 - Asset Library Open Architecture Framework (ALOAF)
[AD-A247268] p 2978 N92-27177

ARCTIC OCEAN
Numerical investigation of the circulation of an ice-covered Arctic Ocean p 2949 N92-26568

ARCTIC REGIONS
Cluster Dayside Polar Cusp
[ESA-SP-330] p 2935 N92-26294
The Norwegian upper atmosphere programme in Svalbard (Norway) p 2935 N92-26295
Research programmes at Svalbard (Norway) p 2935 N92-26297
Optical ground-based network p 2937 N92-26313

ARMED FORCES (UNITED STATES)
Apogee, perigee, and recovery: Chronology of Army exploitation of space
[RAND-N-3103-A] p 2856 N92-26192
Summary of research: Academic departments, 1990-1991
[AD-A245533] p 3022 N92-26664

AROMATIC COMPOUNDS
Aromatic-radical oxidation kinetics
[DE92-010821] p 2871 N92-26274
High melting aromatic nitrate esters
[AD-D015190] p 2884 N92-26880

ARRAYS
Composition studies based on coincident air shower array and underground muon data
[DE92-010345] p 3021 N92-26253
Field-emission arrays: A potentially bright source
[AD-A246561] p 2893 N92-26741

ARTEMIA
Preliminary results of the Artemia salina experiments in biostack on LDEF p 2952 N92-27125

ARTIFICIAL GRAVITY
Critical technologies: Spacecraft habitability, an update p 2966 N92-27010

ARTIFICIAL INTELLIGENCE
Constrained neural network architectures for target recognition
[DE92-011159] p 2982 N92-26434
A design rationale for NASA TileWorld
[NASA-TM-107882] p 2982 N92-26627
Principal investigator in a box: Version 1.2 documentation
[NASA-TM-107886] p 2982 N92-26628
Computer modeling of human decision making
[NASA-TM-107868] p 2983 N92-26630
Two papers on feed-forward networks
[NASA-TM-107840] p 2983 N92-26631
An analysis of commitment strategies in planning: The details
[NASA-TM-107881] p 2983 N92-26643
Explanation-based generalization of partially ordered plans
[NASA-TM-107869] p 2983 N92-26789
Planning and scheduling research at NASA Ames Research Center
[NASA-TM-107888] p 3009 N92-26790
Discrete sequence prediction and its applications
[NASA-TM-107865] p 2984 N92-26791
Applying artificial intelligence to the control of space telescopes (extended abstract)
[NASA-TM-107913] p 3015 N92-26886
The 1990 progress report and future plans
[NASA-TM-107911] p 2984 N92-26887
Modelling default and likelihood reasoning as probabilistic
[NASA-TM-107889] p 2984 N92-26893
Bayesian classification theory
[NASA-TM-107885] p 2988 N92-26894
The APT/ERE planning and scheduling manifesto
[NASA-TM-107906] p 2984 N92-27055
The structure and formation of natural categories
[NASA-TM-107896] p 2985 N92-27056

ARTIFICIAL SATELLITES
The effect of switched array battery charge control on CRRES spacecraft: 3 + month data summary p 2862 N92-27134
Low cost battery designs for small satellite applications p 2866 N92-27160

ASIA
TRMM and Asian monsoon --- tropical rainfall measuring mission
[TW-12] p 2924 N92-26713
Competing economies: America, Europe, and the Pacific rim
[PB92-115757] p 3014 N92-26730

ASPECT RATIO
Study of the transition to turbulence within a curved rectangular channel with 40 to 1 aspect ratio
[AD-A246314] p 2896 N92-26290

ASTROMETRY
High precision timing of millisecond pulsars p 3015 N92-26760

ASTRONAUT PERFORMANCE
Development of the suit enclosure soft joints of the European EVA space suit p 2965 N92-27005

ASTRONAUT TRAINING
CBT: Role and future application for crew training --- computer based training p 2953 N92-26992

ASTRONAUTS
Logistics in space: Tools to support astronauts p 2963 N92-26990
Multi-cultural components and keys for European worldwide space programs p 2857 N92-27008

ASTRONOMICAL SATELLITES
ROSAT: Measured temperatures versus thermal analysis results p 2859 N92-26997

ASTRONOMY
Research and technology, 1990: Goddard Space Flight Center
[NASA-TM-107792] p 3022 N92-26824
Measurement of surface layer optical turbulence above AMOS
[AD-A246387] p 3016 N92-27077

ASTROPHYSICS
Tensor-multi-scalar theories of gravitation
[PB92-152305] p 2943 N92-26820

ASYMMETRY
Numerical simulations of gun-launched kinetic energy projectiles subjected to asymmetric projectile base pressure
[DE92-005065] p 2857 N92-26693
ASYMPTOTIC GIANT BRANCH STARS
The galactic evolution of s-process elements via asymptotic giant branch stars p 3018 N92-26725
ASYMPTOTIC METHODS
Bias robust estimation of scale
[AD-A245698] p 2985 N92-26229
Asymptotic analysis of the vibrations of variable length cantilever beams p 2918 N92-26739
Lyapunov equation for infinite-dimensional discrete bilinear systems
[DE92-621066] p 2988 N92-26831
ASYMPTOTIC SERIES
Effects of video bandwidth on the performance of a square law detector with Gaussian IF and video filters
[AD-A246506] p 2989 N92-26467
Developments of solutions of some special elliptic equations at a corner
[PB92-148741] p 2986 N92-26503
Asymptotic analysis of the vibrations of variable length cantilever beams p 2918 N92-26739
ATLANTIC OCEAN
Proceedings of 6th Hawaiian Winter Workshop on Dynamics of Oceanic Internal Gravity Waves
[AD-A245650] p 2948 N92-26173
Investigation of carbon dioxide in the South Atlantic and northern Weddell Sea areas (WOCE Sections A-12 and A-21) during the METEOR expedition 11/5, January - March 1990
[DE92-010027] p 2928 N92-26231
Meridional zonation of the Barents Sea ecosystem inferred from satellite remote sensing and in situ bio-optical observations
[AD-A246323] p 2948 N92-26245
Quantitative assessment of the slope resolution of seafloor mapping systems
[AD-A246158] p 2949 N92-26411
ATMOSPHERIC ATTENUATION
User's guide to WPL microwave radiative transfer software
[PB92-129931] p 2890 N92-26809
Passive determination of temperature and range using spectral band measurements of photon emittance
[AD-A247147] p 2910 N92-27181
ATMOSPHERIC BOUNDARY LAYER
The Norwegian upper atmosphere programme in Svalbard (Norway) p 2935 N92-26295
Research programmes at Svalbard (Norway) p 2935 N92-26297
Polar cap boundary and structure of dayside cusp as determined by ion precipitation p 2936 N92-26300
The present understanding of the cusp p 2936 N92-26306
Solar wind-magnetosphere coupling processes observed near the dayside cusp/cleft p 2937 N92-26307
The composite structure of thermals as derived from aircraft observations p 2941 N92-26346
Measurements in the inhomogeneous convective boundary layer using three powered gliders p 2942 N92-26350
Characteristics of upper-level and boundary layer forcing in Western Pacific cyclones
[AD-A246301] p 2945 N92-26364
Theoretical and modeling studies of the marine planetary boundary layer
[AD-A245903] p 2942 N92-26432
A second-order bulk boundary layer model, revision
[AD-A245828] p 2905 N92-26934
ATMOSPHERIC CHEMISTRY
Investigation of carbon dioxide in the South Atlantic and northern Weddell Sea areas (WOCE Sections A-12 and A-21) during the METEOR expedition 11/5, January - March 1990
[DE92-010027] p 2928 N92-26231
ATMOSPHERIC CIRCULATION
Geochemical constraints on ocean general circulation models
[DE92-010805] p 2948 N92-26270
A reformulation of the Eady model p 2939 N92-26330
Comparison of frontogenetical structures for different cases of frontal development p 2939 N92-26333
The stability of barotropic vortices: Implications for tropical cyclone motion p 2940 N92-26335
Convection wave studies over land and sea p 2940 N92-26341
The objective determination of front lines p 2941 N92-26343
The composite structure of thermals as derived from aircraft observations p 2941 N92-26346
Plume trajectory validation study: Brown cloud support project overview
[DE92-006911] p 2928 N92-26390
Comparison of wind profiles in close proximity to each other
[AD-A246152] p 2945 N92-26409
Tracer transport in the middle atmosphere p 2928 N92-26473
Research plan for utilizing TRMM data in MRI --- tropical rainfall measuring mission
[TW-13] p 2924 N92-26714
Investigations of a single point temperature probe for measurement of atmospheric turbulence
[AD-A246563] p 2909 N92-26794
Observations of wind forced circulation on the continental shelf off Point Sur, California from a self-contained acoustic Doppler current profiler
[AD-A246437] p 2950 N92-27029
Measurement of surface layer optical turbulence above AMOS
[AD-A246387] p 3016 N92-27077
ATMOSPHERIC COMPOSITION
Remote sensing of atmosphere with aircraft borne lidar systems p 2941 N92-26347
Laboratory evaluation and application of microwave absorption properties under simulated conditions for planetary atmospheres
[NASA-CR-190211] p 3019 N92-26438
Tracer transport in the middle atmosphere p 2928 N92-26473
The impact of climate upon variation in air pollution using a synoptic climatological approach p 2931 N92-26590
Improved procedures for quantifying key meteorological effects on ambient ozone data
[PB92-163278] p 2931 N92-26793
ATMOSPHERIC DENSITY
An analysis of middle ultraviolet emissions of molecular nitrogen and nitric oxide and vacuum calibration of an ultraviolet spectrograph
[AD-A245984] p 2943 N92-26753
ATMOSPHERIC GENERAL CIRCULATION MODELS
Equilibrium-analysis of projected climate change effects on the global soil organic matter pool
[PB92-153022] p 2930 N92-26509
Development of an advanced finite-difference atmospheric general circulation model
[DE92-010923] p 2944 N92-26937
ATMOSPHERIC HEATING
Tracer transport in the middle atmosphere p 2928 N92-26473
ATMOSPHERIC MODELS
Energy transfer properties and mechanisms
[DE92-011215] p 2994 N92-26240
Geochemical constraints on ocean general circulation models
[DE92-010805] p 2948 N92-26270
Contributions to atmospheric physics in honor of Dr. Manfred Reinhardt on his 65th birthday
[DLR-FB-91-30] p 2939 N92-26329
A reformulation of the Eady model p 2939 N92-26330
Noxious matter transportation in the Alpine regions p 2934 N92-26332
A simple model for the convective boundary layer over wavy terrain with variable heat flux p 2934 N92-26334
The stability of barotropic vortices: Implications for tropical cyclone motion p 2940 N92-26335
Theoretical and modeling studies of the marine planetary boundary layer
[AD-A245903] p 2942 N92-26432
Tracer transport in the middle atmosphere p 2928 N92-26473
Mean and turbulent structure of the marine atmospheric boundary layer during cold air outbreaks of different intensities: Observational and modelling analyses p 2942 N92-26489
Atmospheric parameters of a soft x ray selected set of hot DA white dwarfs p 3017 N92-26576
Monthly mean global satellite data sets available in CCM history tape format
[NASA-CR-190344] p 2933 N92-26878
A second-order bulk boundary layer model, revision
[AD-A245828] p 2905 N92-26934
ATMOSPHERIC MOISTURE
Water vapor information content of absorption lines observed in the Sun's infrared radiance p 2942 N92-26490
Water cycles around the subtropical frontal zone in East Asia
[TW-9] p 2923 N92-26710
Research program on hydrology
[TW-14] p 2924 N92-26715
Water recovery from condensate of crew respiration products aboard the Space Station p 2956 N92-26951
ATMOSPHERIC OPTICS
A high repetition rate lidar
[AD-A245382] p 2890 N92-26872
ATMOSPHERIC PHYSICS
Contributions to atmospheric physics in honor of Dr. Manfred Reinhardt on his 65th birthday
[DLR-FB-91-30] p 2939 N92-26329
ATMOSPHERIC PRESSURE
Atmospheric environment for Space Shuttle Columbia (STS-40) launch
[NASA-TM-103585] p 2945 N92-26288
ATMOSPHERIC RADIATION
Muon/electron separation for atmospheric neutrino interactions
[DE92-010349] p 3021 N92-26218
Passive exposure of Earth radiation budget experiment components. LDEF experiment AO-147: Post-flight examinations and tests p 2910 N92-27109
ATMOSPHERIC SOUNDING
Undulatory airflow over the Spanish southern central highplain with northern winds p 2940 N92-26339
Cirrus clouds and condensation trail on 18 Oct. 1989 over the North sea (ICE '89). Determination of height and optical depth using ALEX, AVHRR and HIRS p 2940 N92-26340
Ozone trends --- atmospheric ozone variations p 2934 N92-26345
European Earth Observation Program p 2925 N92-26745
Description of the Rayflux ray tracing program and comparison with other models and measurements
[AD-A245413] p 2944 N92-26877
ATMOSPHERIC TEMPERATURE
Atmospheric environment for Space Shuttle Columbia (STS-40) launch
[NASA-TM-103585] p 2945 N92-26288
Water vapor information content of absorption lines observed in the Sun's infrared radiance p 2942 N92-26490
Utilization of tropical convection data for meteorological operation
[TW-11] p 2924 N92-26712
ATMOSPHERIC TURBULENCE
Mean and turbulent structure of the marine atmospheric boundary layer during cold air outbreaks of different intensities: Observational and modelling analyses p 2942 N92-26489
Investigations of a single point temperature probe for measurement of atmospheric turbulence
[AD-A246563] p 2909 N92-26794
Measurement of surface layer optical turbulence above AMOS
[AD-A246387] p 3016 N92-27077
ATOMIC SPECTRA
The use of ion chromatography-dc plasma atomic emission spectrometry for the speciation of trace metals
[DE92-010317] p 2871 N92-26236
ATOMIC STRUCTURE
Spectroscopic imaging, diffraction, and holography with x ray photoemission
[DE92-009142] p 2996 N92-26187
Atomistic studies of grain boundaries in alloys and compounds
[DE92-010792] p 2877 N92-26251
Neutron powder diffraction study on Eu-substituted Bi2Sr2CaCu2O(8+y) high temperature superconductor p 3003 N92-26328
Solvation effects on the electronic structure of 4-N,N-Dimethylaminobenzonitrile: Mixing of the local pipi* and charge transfer states
[AD-A245814] p 2874 N92-26608
Computational techniques in tribology and material science at the atomic level
[NASA-TM-105573] p 2990 N92-26671
New theoretical methods for electronic structure and gas-phase state specific oxidation/reduction studies
[AD-A246127] p 2875 N92-26687
ATOMIC WEIGHTS
Dynamic restoration mechanisms in Al-5.8 at. percent Mg deformed to large strains in the solute drag regime
[DE92-009529] p 2877 N92-26223
ATOMS
Spontaneous and induced coherent radiation generation in atomic vapors
[AD-A246078] p 2890 N92-26764
Laser cooling and trapping of atoms and particles
[AD-A247208] p 2913 N92-27173
ATTITUDE (INCLINATION)
Dynamic control of a space robot system with no thrust jets controlled base
[AD-A245711] p 2981 N92-26356
AUGMENTATION
The fidelity enhancement process
[AD-A245388] p 2977 N92-26840

AURORA 7
Research programmes at Svalbard (Norway) p 2935 N92-26297
AURORAL ARCS
A model of the dayside magnetosphere and breakups in the cusp region p 2937 N92-26312
AURORAL ELECTROJETS
The dynamic response of the westward auroral electrojet and polar cap currents to solar wind-magnetosphere coupling p 2943 N92-26622
AURORAL ZONES
The effects of magnetic storm phases on F-layer irregularities from auroral to equatorial latitudes [AD-A245495] p 2943 N92-26675
AURORAS
The Norwegian upper atmosphere programme in Svalbard (Norway) p 2935 N92-26295
U.S. ground-based space research programs in Svalbard (Norway) p 2935 N92-26296
Optical ground-based network p 2937 N92-26313
AUTOMATIC CONTROL
Perception for outdoor navigation [AD-A245715] p 2851 N92-26427
A design rationale for NASA TileWorld [NASA-TM-107882] p 2982 N92-26627
Applying knowledge compilation techniques to model-based reasoning [NASA-TM-107876] p 2984 N92-26885
AUTOMATION
Investigating the utility of coupling COCOMO with a system dynamics simulation of software development [AD-A245484] p 2973 N92-26400
AUTOMOBILE ENGINES
Development of natural gas rotary engines [PB92-149665] p 2915 N92-26816
AUTONOMOUS NAVIGATION
Perception for outdoor navigation [AD-A245715] p 2851 N92-26427
Dead reckoning navigation for walking robots [NASA-CR-190296] p 2982 N92-26429
AUTOROTATION
Coning motion and flat spinning of slender bodies at high angles of attack p 2902 N92-26912
AWARDS
Small business innovation research: Program solicitation closing date, 27 January 1992 [DE92-010132] p 3009 N92-26811
AXIAL STRAIN
Application of neutron diffraction to measure residual strains in high temperature composites [DE91-014021] p 2869 N92-26679
AXISYMMETRIC BODIES
Large-scale structures and the spatial evolution of wakes behind axisymmetric bluff bodies p 2901 N92-26871
AXISYMMETRIC FLOW
An experimental study of natural and forced modes in an axisymmetric jet p 2897 N92-26600
AZULENE
Polycyclic aromatic hydrocarbon radiative properties and formation in carbon-rich stellar outflows p 3018 N92-26757

B

BACILLUS
Survival of epiphytic bacteria from seed stored on the Long Duration Exposure Facility (LDEF) p 2952 N92-27122
Long-term exposure of bacterial spores to space p 2952 N92-27126
BACKGROUND RADIATION
Infrared clutter measurements of marine backgrounds [AD-A245422] p 2932 N92-26873
BACKSCATTERING
Microwave backscattering fuel/air ratio control and flame monitoring device [PB92-141779] p 2876 N92-26783
Modeling 3-D objects with planar surfaces for prediction of electromagnetic scattering [NASA-TM-107598] p 2891 N92-27189
BACTERIA
Time-resolved laser studies on the proton pump mechanism of bacteriorhodopsin [DE92-003218] p 2951 N92-26493
The application of XPS to the study of MIC [DE92-010156] p 2879 N92-26813
Carbon monoxide metabolism by the photosynthetic bacterium Rhodospirillum rubrum [DE92-010953] p 2951 N92-26938
Thiocapsa roseopersicina, a bacterium for sulfur-recycling in microbial ecosystems designed for CELSS and space purposes p 2951 N92-26977
Chemolithotropic hydrogen-oxidizing bacteria and their possible functions in closed ecological life-support systems p 2951 N92-26979
BAFFLES
Thermal control of telescope apertures by optimized baffle heating p 2961 N92-26976
The 3D rocket combustor acoustics model [NASA-TM-105734] p 2861 N92-27035
BALLISTIC MISSILES
The state of multiple sensor, multiple target tracking in ballistic missile defense [AD-A245433] p 2850 N92-26272
BALLOON-BORNE INSTRUMENTS
Balloons for conjugate cusp studies in the 1990's p 2938 N92-26315
French space programmes related to global change p 2925 N92-26746
BALTIC SEA
The effect of global change and long period tides on the Earth's rotation and gravitational potential p 2925 N92-26781
BANACH SPACE
Dvoretzky's theorem: 30 years later [PB92-153212] p 2988 N92-26788
BAND STRUCTURE OF SOLIDS
Band structure and optical properties of semiconductor superlattices [AD-A246076] p 3005 N92-26763
BANDPASS FILTERS
Estimation of peak intensities from frequency filtered total scattering data of neutrons obtained by the reverse Fourier method p 3002 N92-26321
Experimental results for inductive strips in inhomogeneous finline [AD-A247254] p 2895 N92-27176
BANDWIDTH
Modeling node bandwidth limits and their effects on vector combining algorithms [DE92-010829] p 2979 N92-26277
Effects of video bandwidth on the performance of a square law detector with Gaussian IF and video filters [AD-A246506] p 2989 N92-26467
Experimental results for inductive strips in inhomogeneous finline [AD-A247254] p 2895 N92-27176
BARENTS SEA
Meridional zonation of the Barents Sea ecosystem inferred from satellite remote sensing and in situ bio-optical observations [AD-A246323] p 2948 N92-26245
BARIUM OXIDES
Recent results in characterization of melt-grown and quench-melt-grown YBCO superconductors [DE92-010281] p 3001 N92-26210
Analysis of Yttrium-Barium-Copper-Oxide by x ray diffraction and mechanical characterization [NASA-TM-104562] p 2869 N92-26650
Percolation effects in the V-I characteristics of granular YBa2Cu3O(7-delta) [DE92-617541] p 3004 N92-26672
BAROCLINIC INSTABILITY
A reformulation of the Eady model p 2939 N92-26330
BAROCLINIC WAVES
A reformulation of the Eady model p 2939 N92-26330
Upper/lower vortex interaction and potential vorticity inversion p 2939 N92-26331
BAROTROPIC FLOW
The stability of barotropic vortices: Implications for tropical cyclone motion p 2940 N92-26335
BARYONS
Open problems and future prospects for hypernuclear physics [DE92-010158] p 2995 N92-26815
BASE PRESSURE
Numerical simulations of gun-launched kinetic energy projectiles subjected to asymmetric projectile base pressure [DE92-005065] p 2857 N92-26693
An experimental investigation of high-speed water entry for full size and scale-model pointed nose vehicle [DE92-004363] p 2899 N92-26716
BATCH PROCESSING
Numerical modeling of silicon photodiodes for high-accuracy applications with PC-1D [PB92-148279] p 2894 N92-26821
BATHYMETERS
Ocean bottom modeling for ray acoustics [AD-A246287] p 2948 N92-26360
BATTERY CHARGERS
Exploring possible relationships between plate pore size character and cell performance p 2863 N92-27141
BAYES THEOREM
Introduction in IND and recursive partitioning [NASA-TM-107879] p 2983 N92-26629
Two papers on feed-forward networks [NASA-TM-107840] p 2983 N92-26631
A Bayes-Maximum Entropy method for multi-sensor data fusion [DE92-000680] p 2983 N92-26657
Modelling default and likelihood reasoning as probabilistic [NASA-TM-107889] p 2984 N92-26893
Bayesian classification theory [NASA-TM-107885] p 2988 N92-26894
BBGKY HIERARCHY
Analytical and numerical investigation of nonlinear gravitational clustering p 3017 N92-26578
BEAM INTERACTIONS
Operation of a Smith-Purcell free-electron laser at submillimeter wavelengths p 2912 N92-26626
BEAM WAVEGUIDES
Erosion of a relativistic electron beam propagating in a plasma channel [DE92-009059] p 3000 N92-26666
BEAMS (SUPPORTS)
Optical strain monitoring in composite materials [AD-A245474] p 2868 N92-26532
Dimensional analysis of structural steel beam design [AD-A245759] p 2917 N92-26593
Reliability and failure analyses of composite beams and plates containing stress concentrations p 2918 N92-26598
The modeling and control of acoustic/structure interaction problems via piezoceramic actuators: 2-D numerical examples [NASA-CR-189639] p 2987 N92-26668
Sensitivity of sensors for characterizing chaos [AD-A246423] p 2921 N92-27066
BEARINGS
Ceramic bearing technology: Proceedings of the NIST/DARPA Workshop [PB92-137553] p 2914 N92-26366
Full-scale transmission testing to evaluate advanced lubricants [NASA-TM-105668] p 2915 N92-26560
BEDROCK
A comparative assessment of radiological impact due to nuclear waste disposal in hard crystalline bedrock, appendix 1 [IAEA-CN-43/449] p 2929 N92-26483
BEND TESTS
Degradation and buckling of metal tubes under cyclic bending and external pressure p 2920 N92-26869
BENDING
Optical strain monitoring in composite materials [AD-A245474] p 2868 N92-26532
Degradation and buckling of metal tubes under cyclic bending and external pressure p 2920 N92-26869
BENDING FATIGUE
An investigation of the behavior of the clamp-induced bending stresses [DE92-006504] p 2918 N92-26694
BENZENE
Aromatic-radical oxidation kinetics [DE92-010821] p 2871 N92-26274
BERKELIUM
Gas phase chromatography of halides of elements 104 and 105 [DE92-010284] p 2870 N92-26212
BIAS
Bias robust estimation of scale [AD-A245698] p 2985 N92-26229
BIBLIOGRAPHIES
Cataloging guidelines [AD-A246500] p 3011 N92-26465
Abstracts of phase 1 awards, 1991 [DE92-010133] p 3022 N92-26640
DOE new technology [DE92-001619] p 3013 N92-26689
Aerospace medicine and biology: A continuing bibliography with indexes (supplement 362) [NASA-SP-7011(362)] p 2953 N92-27068
Management: A bibliography for NASA managers [NASA-SP-7500(26)] p 3010 N92-27080
NASA patent abstracts bibliography: A continuing bibliography. Section 2: Indexes (supplement 40) [NASA-SP-7039(40)-SECT-2] p 3014 N92-27081
BINARY ALLOYS
Atomistic studies of grain boundaries in alloys and compounds [DE92-010792] p 2877 N92-26251
X ray scattering studies of non-equilibrium ordering processes [DE92-010311] p 2877 N92-26542
Numerical formulation for the prediction of solid/liquid change of a binary alloy [NASA-CR-188468] p 2878 N92-26642
BINARY MIXTURES
Conjugating binary systems: Advanced cooling liquids for use in spacecraft ATCS p 2905 N92-27027

BINARY STARS
Dynamics of neutron stars and binaries in globular clusters or, menages a trois: Revitalizing burnt out degenerates through partner swapping
p 3017 N92-26522
BINARY SYSTEMS (MATERIALS)
The influence of pressure on the phase behaviour of water + oil + surfactant systems
[ISBN-90-6275-732-4] p 2871 N92-26257
Failure studies of bimaterial interfaces and constrained ductile layers p 2868 N92-26559
BINAURAL HEARING
Binaural ultrasound detector and imager
[AD-D015214] p 2993 N92-27184
BIOASTRONAUTICS
Aerospace medicine and biology: A continuing bibliography with indexes (supplement 362)
[NASA-SP-7011(362)] p 2953 N92-27068
BIOCHEMISTRY
Biochemical, endocrine, and hematological factors in human oxygen tolerance extension: Predictive studies 6
[NASA-CR-190341] p 2952 N92-26263
BIOCONVERSION
Environmental implications of increased biomass energy use
[DE92-001219] p 2932 N92-26810
BIODEGRADATION
Biodegradation studies with space cabin contaminants to determine the feasibility of Biological Air Filtration (BAF) in space cabins p 2962 N92-26983
BIODYNAMICS
Maintenance manual for Natick's Footwear Database
[AD-A246273] p 2954 N92-26242
User manual for Natick's Footwear Database
[AD-A246275] p 2954 N92-26243
Correlation and prediction of dynamic human isolated joint strength from lean body mass
[NASA-TP-3207] p 2956 N92-26682
BIOLOGICAL EFFECTS
Life sciences and environmental sciences
[DE92-010254] p 2950 N92-26203
Aerospace medicine and biology: A continuing bibliography with indexes (supplement 362)
[NASA-SP-7011(362)] p 2953 N92-27068
Total Dose Effects (TDE) of heavy ionizing radiation in fungus spores and plant seeds: Preliminary investigations p 2952 N92-27124
Preliminary results of the Artemia salina experiments in biostack on LDEF p 2952 N92-27125
BIOMASS
Global assessment of promising forest management practices for sequestration of carbon
[PB92-153006] p 2930 N92-26510
High-yield hydrogen production by catalytic gasification of coal or biomass
[DE92-008770] p 2875 N92-26724
Environmental implications of increased biomass energy use
[DE92-001219] p 2932 N92-26810
Thiocapsa roseopersicina, a bacterium for sulfur-recycling in microbial ecosystems designed for CELSS and space purposes p 2951 N92-26977
BIOMASS ENERGY PRODUCTION
Environmental implications of increased biomass energy use
[DE92-001219] p 2932 N92-26810
BIOMEDICAL DATA
Parabolic flight: Reports of microgravity experiments by aircraft, volume 1, no. 2
[EG-910045] p 2884 N92-26440
Biomedical data acquisition and processing technology p 2885 N92-26446
BIOPROCESSING
Life support research and development for the Department of Energy Space Exploration Initiative
[DE92-007239] p 2955 N92-26494
BIOREACTORS
Modelling light transfer inside photobiofermentors: Applications to the photosynthetic compartments of CELSS p 2952 N92-26982
BIOSPHERE
Model studies of the transfer of radionuclides in the Finnish environment
[VTT-PUBL-81] p 2929 N92-26482
Assessment of biospheric behaviour of releases from nuclear waste repositories, appendix 2
p 2929 N92-26484
Assessment of radiation doses due to releases to the biosphere from nuclear waste repositories, appendix 3
p 2929 N92-26485
Sensitivity analysis of biospheric behaviour of radionuclides released from nuclear waste repositories, appendix 4 p 2929 N92-26486
Biosphere model validation by intercomparison to observed behaviour of fallout radionuclides in the aquatic environment, appendix 5 p 2930 N92-26487
Equilibrium-analysis of projected climate change effects on the global soil organic matter pool
[PB92-153022] p 2930 N92-26509
BIOTECHNOLOGY
Life sciences and environmental sciences
[DE92-010254] p 2950 N92-26203
Biotechnology for the 21st century, FY 1993
[DE92-007757] p 2951 N92-26850
Biodegradation studies with space cabin contaminants to determine the feasibility of Biological Air Filtration (BAF) in space cabins p 2962 N92-26983
BIPOLARITY
Utilization of a bipolar lead acid battery for the advanced launch system p 2865 N92-27157
BIRTH
Sturm-Liouville eigenfunctions expressed in determinant form
[AD-A245991] p 2987 N92-26755
BISMUTH ALLOYS
Atomistic studies of grain boundaries in alloys and compounds
[DE92-010792] p 2877 N92-26251
BIT ERROR RATE
A measuring facility for testing radio communication equipment
[AD-A245621] p 2890 N92-26874
BLACK HOLES (ASTRONOMY)
Topics in particle physics and cosmology
[DE92-010478] p 3019 N92-26385
Euclidean black hole vortices
[NASA-CR-190117] p 3016 N92-26436
Non-compact WZW conformal field theories
[PB92-125038] p 3007 N92-26805
Quantum black holes and Hawking's radiation
[PB92-152313] p 3018 N92-26833
BLOCKING
Modeling 3-D objects with planar surfaces for prediction of electromagnetic scattering
[NASA-TM-107598] p 2891 N92-27189
BLUFF BODIES
Large-scale structures and the spatial evolution of wakes behind axisymmetric bluff bodies p 2901 N92-26871
BLUNT BODIES
Wave viscosity interaction in nonlinear roll motion
[AD-A245756] p 2897 N92-26591
BODY MEASUREMENT (BIOLOGY)
Parabolic flight: Reports of microgravity experiments by aircraft, volume 1, no. 2
[EG-910045] p 2884 N92-26440
Biomedical data acquisition and processing technology p 2885 N92-26446
BODY-WING CONFIGURATIONS
Observation and measurements of flow structures in the stagnation region of a wing-body junction
p 2849 N92-26616
Subsonic investigations of vortex interaction control for enhanced high-alpha aerodynamics of a chine forebody/Delta wing configuration
[NASA-CR-189641] p 2849 N92-26652
BOILER PLATE
Progress in the development of lightweight nickel electrode
[NASA-TM-105638] p 2875 N92-26670
BOILERS
Fuel staging and its implementation in a novel internally staged burner
[ETN-92-91307] p 2872 N92-26285
Adaptive regulation of the boiler-turbine unit of a Combined Heat and Power (CHP) system
[RR-417] p 2887 N92-26752
Progress in the development of the Hermes evaporators p 2962 N92-26984
Post-test examination of a pool boiler receiver
[NASA-TM-105635] p 2880 N92-27192
BOMBER AIRCRAFT
The role of the B-2 in the new US defense strategy
[RAND-P-7744] p 2990 N92-26194
Man-machine interface analyses for bomber flight management system
[AD-A245707] p 2955 N92-26355
BOOLEAN ALGEBRA
N-learners problem: Learning Boolean combinations of halfspaces
[DE92-010390] p 2987 N92-26545
BOOSTER ROCKET ENGINES
Performances of 250 Amp-hr lithium/thionyl chloride cells p 2864 N92-27148
BOOSTERS (EXPLOSIVES)
High melting aromatic nitrate esters
[AD-D015190] p 2884 N92-26880
BOOTS (FOOTWEAR)
Maintenance manual for Natick's Footwear Database
[AD-A246273] p 2954 N92-26242
User manual for Natick's Footwear Database
[AD-A246275] p 2954 N92-26243
BORON
Novel molecular sources for dispersing boron in carbon-carbon composites
[AD-A246999] p 2870 N92-26882
BOUNDARY CONDITIONS
Computational methods for problems of acoustics with particular reference to exterior domains
p 2992 N92-26558
Spectral boundary conditions and index theorem for 2-dimensional compact manifold with boundary
[DE92-621115] p 2990 N92-26798
Plasma dynamics of the Earth magnetopause-boundary layer and its coupling to the polar ionosphere
p 2944 N92-26865
BOUNDARY ELEMENT METHOD
Computational methods for problems of acoustics with particular reference to exterior domains
p 2992 N92-26558
Turbulent mixing in supersonic jets
p 2850 N92-27054
BOUNDARY INTEGRAL METHOD
Computations of nonlinear gravity waves by a desingularized boundary integral method
p 2942 N92-26583
BOUNDARY LAYER CONTROL
Distributed acoustic receptivity in laminar flow control configurations
[NASA-CR-4438] p 2898 N92-26680
Proceedings of the 5th and 6th Seminars on Investigation and Control of Boundary-Layer Transition
[NAL-SP-12] p 2901 N92-26906
BOUNDARY LAYER EQUATIONS
On the subject of geometric spacing of meteorological sensors
[AD-A245824] p 2946 N92-26899
BOUNDARY LAYER FLOW
Observation and measurements of flow structures in the stagnation region of a wing-body junction
p 2849 N92-26616
Boundary-layer receptivity due to distributed surface imperfections of a deterministic or random nature
[NASA-CR-4439] p 2898 N92-26681
Interface of an uncoupled boundary layer algorithm with an inviscid core flow algorithm for unsteady supersonic engine inlets
[NASA-TM-105684] p 2855 N92-27037
BOUNDARY LAYER TRANSITION
Proceedings of the 5th and 6th Seminars on Investigation and Control of Boundary-Layer Transition
[NAL-SP-12] p 2901 N92-26906
Pattern search in turbulent field p 2901 N92-26907
Research activities on CFD at the Ship Research Institute p 2902 N92-26908
Three dimensional boundary layer transition on a yawed cylinder p 2902 N92-26909
An evolutional process of three dimensional disturbances in laminar boundary layers
p 2902 N92-26910
Aerodynamic drag on the bullet trains
p 2902 N92-26911
Coning motion and flat spinning of slender bodies at high angles of attack p 2902 N92-26912
Flow around an isolated surface roughness in the laminar boundary layer p 2903 N92-26913
Experimental studies on the flat plate boundary layer transition using hydrogen bubble method
p 2903 N92-26914
Application of riblet surface to pipe flow
p 2903 N92-26915
Numerical studies on laminar turbulent transition at the Stuttgart University, Germany p 2903 N92-26916
Investigation on the boundary layer transition of alternately oscillating flow in deceleration phase
p 2903 N92-26917
Vortex structure in wake of a circular cylinder
p 2904 N92-26918
Control of turbulent mixing in hypersonic flow
p 2904 N92-26919
Numerical simulation of the laminar turbulent transition in a stratified flow p 2904 N92-26920
Responses of boundary layers to strong external disturbances p 2904 N92-26921
Cross-flow instabilities and pressure gradients in boundary layers p 2904 N92-26922
BOUNDARY LAYERS
A simple model for the convective boundary layer over wavy terrain with variable heat flux
p 2934 N92-26334
Mean and turbulent structure of the marine atmospheric boundary layer during cold air outbreaks of different intensities: Observational and modelling analyses
p 2942 N92-26489
Boundary-layer receptivity due to distributed surface imperfections of a deterministic or random nature
[NASA-CR-4439] p 2898 N92-26681

Physical processes within the nocturnal stratus-topped boundary layer, revision
[AD-A245829] p 2947 N92-26901
Development of an advanced finite-difference atmospheric general circulation model
[DE92-010923] p 2944 N92-26937

BOUNDARY VALUE PROBLEMS
Developments of solutions of some special elliptic equations at a corner
[PB92-148741] p 2986 N92-26503
On the stochastic fatigue crack growth problem p 2917 N92-26557
A boundary integral method for steady unsaturated flow in nonhomogeneous media
[DE92-009066] p 2897 N92-26644

BOW WAVES
Solar wind interaction with Venus and Mars p 3020 N92-26779

BRAGG ANGLE
Higher order parametric x rays
[AD-A247148] p 2991 N92-27182

BRAZIL
Differentiation on genus of aquatic macrophytes through remote sensing in the Tucurui Reservoir, Para State, Brazil
[INPE-5315-PRE/1712] p 2951 N92-26721

BREADBOARD MODELS
Software requirements document for the netCDF interface within ECMOP, version 1.0
[AD-A246220] p 2974 N92-26464
EVA life support design and technology developments p 2965 N92-27002
Fan/pump/separator technology development for EVA p 2966 N92-27006

BREAKWATERS
Hindcast wave information for the Great Lakes: Lake Huron. Wave information studies of US coastlines
[AD-A246326] p 2949 N92-26387

BREEDER REACTORS
An investigation of the behavior of the clamp-induced bending stresses
[DE92-006504] p 2918 N92-26694

BRIGHTNESS TEMPERATURE
Storm model and beam filling problem for rain retrievals
[TW-6] p 2923 N92-26707
User's guide to WPL microwave radiative transfer software
[PB92-129931] p 2890 N92-26809

BRILLOUIN EFFECT
Fail safe system for suppressing stimulated Brillouin scattering in large optics on the Nova laser
[DE92-008608] p 2911 N92-26505

BRISTOL-SIDDELEY BS 53 ENGINE
VSTOL engine design evolution: Growth of the Pegasus engine for Harrier
[PNR-90805] p 2855 N92-27039

BRITTLENESS
Improving the fracture resistance of irradiated martensitic steels
[DE92-008387] p 2879 N92-26848

BROMINE COMPOUNDS
Calorimetric determination of the thermoneutral potential for Li/BrCl in SOCl2 (BCX) cells p 2864 N92-27146

BUBBLES
Helium bubble flow visualization of the spanwise separation on a NACA 0012 with simulated glaze ice
[NASA-TM-105742] p 2849 N92-26612

BUCKLING
Buckling of unidirectional graphite/epoxy composite plates at low temperatures
[AD-A246602] p 2869 N92-26796
Degradation and buckling of metal tubes under cyclic bending and external pressure p 2920 N92-26869

BUCKMINSTERFULLERENE
A study of buckminsterfullerene using new pseudopotentials p 3005 N92-26774

BUDGETING
An analysis of the role of the budget committees in the Congressional budget process
[AD-A246005] p 3014 N92-26761

BUILDINGS
Tests on various arrangements of liquid column vibration absorbers
[PB92-152610] p 2896 N92-26506
A finite element/finite difference approach for modeling three-dimensional flow and pollutant dispersion around structures
[DE92-007322] p 2934 N92-26935

BUOYANCY
Report for neutral buoyancy simulations of transfer orbit stage contingency extravehicular activities
[NASA-TM-103583] p 2857 N92-26268

BURN-IN
RF vacuum microelectronics
[AD-A246579] p 2893 N92-26771

BURNERS
Fuel staging and its implementation in a novel internally staged burner
[ETN-92-91307] p 2872 N92-26285

BURNING RATE
Burn-rate studies with iron/potassium perchlorate heat pellets
[DE92-008524] p 2875 N92-26722
Microwave backscattering fuel/air ratio control and flame monitoring device
[PB92-141779] p 2876 N92-26783
The 3D rocket combustor acoustics model
[NASA-TM-105734] p 2861 N92-27035

BUTT JOINTS
Post-test examination of a pool boiler receiver
[NASA-TM-105635] p 2880 N92-27192

C

C (PROGRAMMING LANGUAGE)
Design and implementation of a toolbox of modularized C programs to construct, analyze, and test network optimization algorithms
[AD-A246191] p 2979 N92-26417

C++ (PROGRAMMING LANGUAGE)
Experiences in using C++ to develop a next generation strong shock wave physics code
[DE92-006675] p 2976 N92-26696

CADMIUM SELENIDES
Photoinduced charge separation in solid-state and molecular systems
[DE92-010130] p 3004 N92-26639

CADMIUM SULFIDES
Photoinduced charge separation in solid-state and molecular systems
[DE92-010130] p 3004 N92-26639

CADMIUM TELLURIDES
Cadmium telluride thin films on silicon substrates
[AD-A245309] p 3001 N92-26226

CALCIUM CARBONATES
Results of the TTF-TCNQ and the calcium carbonate crystallization on the Long Duration Exposure Facility p 3007 N92-27127

CALIBRATING
Calibration of CR-39 for detecting fusion neutrons
[DE92-009063] p 2993 N92-26225
Hindcast wave information for the Great Lakes: Lake Huron. Wave information studies of US coastlines
[AD-A246326] p 2949 N92-26387
Fiber-optic flexural disk accelerometer
[AD-A246203] p 2908 N92-26459
An analysis of middle ultraviolet emissions of molecular nitrogen and nitric oxide and vacuum calibration of an ultraviolet spectrograph
[AD-A245984] p 2943 N92-26753
Radar scattering as a source of geological information on Venus and Earth p 3019 N92-26778

CALIFORNIUM COMPOUNDS
Comparison of laser and conventional heating in TLD dosemapping
[DE92-010773] p 2910 N92-26269

CALORIMETERS
A search for magnetic monopoles with the Soudan 2 detector
[DE92-010347] p 3021 N92-26216
Cryogenic detector development
[MPI-PHE/91-07] p 2906 N92-26391
Cryogenic calorimeters for dark matter and neutrinos p 2907 N92-26392
Calorimetric particle detectors with superconducting absorber materials p 2907 N92-26393
Recent progress in calorimeters with transition edge thermometers p 2907 N92-26394
Signal-to-noise ratio expected for a calorimeter with transition edge thermometer p 2907 N92-26395
Electron-phonon decoupling and superconducting grains p 2907 N92-26397
Differential Scanning Calorimetry (DSC) for the analysis of activated carbon
[AD-A245899] p 2872 N92-26404
Calorimetric determination of the thermoneutral potential for Li/BrCl in SOCl2 (BCX) cells p 2864 N92-27146

CAMERAS
Dynamic lens compensation for active color imaging and constant magnification focusing
[AD-A245713] p 2997 N92-26425
Representations in visual motion
[PB92-148287] p 2984 N92-26814

CANADIAN SPACE PROGRAM
Canadian Earth Observation Program p 2925 N92-26747
Environmental projects at the Canada Centre for Remote Sensing p 2925 N92-26748

CANOPIES (VEGETATION)
Surface energy budget and evapotranspiration measurement support
[NASA-CR-190059] p 2944 N92-26185

CANTILEVER BEAMS
Asymptotic analysis of the vibrations of variable length cantilever beams p 2918 N92-26739

CAPACITORS
Transportable 5 MW power supply system for gyrotron operation
[DE92-009051] p 2892 N92-26224

CARBON
Equilibrium-analysis of projected climate change effects on the global soil organic matter pool
[PB92-153022] p 2930 N92-26509
Global assessment of promising forest management practices for sequestration of carbon
[PB92-153006] p 2930 N92-26510
Factors influencing the microstructural and mechanical properties of ULCB steel weldments
[AD-A245523] p 2878 N92-26659
STS lithium/CF(x) battery p 2863 N92-27143

CARBON CYCLE
Investigation of carbon dioxide in the South Atlantic and northern Weddell Sea areas (WOCE Sections A-12 and A-21) during the METEOR expedition 11/5, January - March 1990
[DE92-010027] p 2928 N92-26231
Organic carbon in soil and the global carbon cycle
[DE92-010289] p 2931 N92-26580

CARBON DIOXIDE
Investigation of carbon dioxide in the South Atlantic and northern Weddell Sea areas (WOCE Sections A-12 and A-21) during the METEOR expedition 11/5, January - March 1990
[DE92-010027] p 2928 N92-26231
Energy transfer properties and mechanisms
[DE92-011215] p 2994 N92-26240
Geochemical constraints on ocean general circulation models
[DE92-010805] p 2948 N92-26270
Use of the Edmonds-Reilly Model to model energy-related greenhouse gas emissions
[DE92-010035] p 2931 N92-26633
Evaluation of carbon dioxide emission control strategies in New York State
[DE92-010162] p 2932 N92-26825
Technology for reduction of CO2 emissions from the transportation sector
[PB92-153733] p 2933 N92-26929
Investigation on a partial pressure carbon dioxide sensor p 2968 N92-27019

CARBON DIOXIDE CONCENTRATION
Investigation of carbon dioxide in the South Atlantic and northern Weddell Sea areas (WOCE Sections A-12 and A-21) during the METEOR expedition 11/5, January - March 1990
[DE92-010027] p 2928 N92-26231

CARBON DIOXIDE LASERS
Comparison of laser and conventional heating in TLD dosemapping
[DE92-010773] p 2910 N92-26269
Construction and function of a multifunction CO2-Laser system
[AD-A245425] p 2910 N92-26271

CARBON DIOXIDE REMOVAL
Metal oxide absorbents for regenerative carbon dioxide and water vapor removal for advanced portable life support systems p 2968 N92-27021

CARBON MONOXIDE
Carbon monoxide metabolism by the photosynthetic bacterium Rhodospirillum rubrum
[DE92-010953] p 2951 N92-26938

CARBON TETRACHLORIDE
Static, microwave, infrared, and visible permittivity related to chemical structure: N-methylacetamide, N-dimethylacetamide and their mixtures in CCl4 at 32 C
[AD-A246364] p 2991 N92-26940

CARBON 13
The carbon isotopic compositions of individual compounds from ancient and modern depositional environments p 2921 N92-26478

CARBON-CARBON COMPOSITES
Reliability and failure analyses of composite beams and plates containing stress concentrations p 2918 N92-26598
Novel molecular sources for dispersing boron in carbon-carbon composites
[AD-A246999] p 2870 N92-26882

CARBONYL COMPOUNDS
Selective metallization of carbonyl-containing polymer films
[AD-D015219] p 2883 N92-27187

CARBORANE
Novel molecular sources for dispersing boron in carbon-carbon composites
[AD-A246999] p 2870 N92-26882
CARCINOGENS
Life sciences and environmental sciences
[DE92-010254] p 2950 N92-26203
CARRIER MOBILITY
Mobility of electrons and holes in semiconductors
[DE92-010125] p 3004 N92-26638
CATALOGS (PUBLICATIONS)
Cataloging guidelines
[AD-A246500] p 3011 N92-26465
DOE new technology
[DE92-001619] p 3013 N92-26689
COSMIC software catalog, 1992 edition
[NASA-CR-188973] p 2977 N92-26868
The study on a directory of human performance models for system design (Defence Research Group Panel 8 on the defence applications of human and bio-medical sciences)
[AD-A247346] p 2970 N92-27179
CATALYSIS
Conversion of ethane and of propane to higher olefin hydrocarbons
[DE92-009487] p 2870 N92-26209
Low severity upgrading of F-T waxes with solid superacids
[DE92-009081] p 2873 N92-26457
Reaction/separation process for enhanced methane conversion
[PB92-149657] p 2873 N92-26508
Enhance methane reactivity
[PB92-154822] p 2873 N92-26516
High-yield hydrogen production by catalytic gasification of coal or biomass
[DE92-008770] p 2875 N92-26724
CATALYSTS
Activation and characterization of some molecular sieve catalysts
[ETN-92-91306] p 2871 N92-26261
Conceptual design study for the use of COBE rocket engines on the Tropical Rainfall Measuring Mission
[NASA-CR-190383] p 2945 N92-26535
A novel process for methanol synthesis
[DE92-010465] p 2883 N92-26547
Catalytic wet-oxidation of human waste produced in a space habitat: Purification of the oxidized liquor for human drinking p 2957 N92-26954
CATALYTIC ACTIVITY
Electrocatalysts for oxygen electrodes
[DE92-009491] p 2871 N92-26220
CATHODE GLOW
Field-emission arrays: A potentially bright source
[AD-A246561] p 2893 N92-26741
CATHODES
Development of a 300 Amp-hr high rate lithium thionyl chloride cell p 2864 N92-27149
Zinc-oxygen battery development program p 2865 N92-27152
CATIONS
High-yield hydrogen production by catalytic gasification of coal or biomass
[DE92-008770] p 2875 N92-26724
CAUCHY PROBLEM
Performance prediction and design of maximum thrust planar supersonic nozzles using a flux-difference-splitting technique p 2853 N92-26480
Wave structure in one and two dimensional fluid flow
[DE92-007421] p 2900 N92-26855
CAVITATION FLOW
Helium bubble flow visualization of the spanwise separation on a NACA 0012 with simulated glaze ice
[NASA-TM-105742] p 2849 N92-26612
An experimental investigation of high-speed water entry for full size and scale-model pointed nose vehicle
[DE92-004363] p 2899 N92-26716
Numerical simulation of two-dimensional single- and multiple-material flow fields
[DE92-007428] p 2901 N92-26856
CAVITY RESONATORS
Exact solutions for a mode of the electromagnetic field in a resonator with time-dependent characteristics of the internal medium
[AD-A245700] p 2888 N92-26374
CELL CATHODES
Examination of the discharge mechanism of Li/CF(x) cells: Comparison of the electrochemical reduction mechanisms of PTFE and (CF(x))n by lithium p 2865 N92-27151
CELLS (BIOLOGY)
Life sciences and environmental sciences
[DE92-010254] p 2950 N92-26203
CEMENTS
Experimental study of shear fracture and aggregate interlock in cementbased composites
[PB92-151521] p 2868 N92-26525
CENTRAL NERVOUS SYSTEM
Low power laser irradiation effect with emphasis on injured neural tissues
[AD-A246410] p 2953 N92-27063
CENTRIFUGAL COMPRESSORS
Turbocharged pressurized combustion system
[PB92-142579] p 2873 N92-26521
CENTRIFUGAL PUMPS
CPA: A controlled pump assembly for two-phase loops applications p 2916 N92-26987
CENTRIFUGING
The centrifugal mass exchange apparatus in air-conditioning system of isolated, inhabited object and its work control p 2957 N92-26956
CERAMIC MATRIX COMPOSITES
Failure studies of bimaterial interfaces and constrained ductile layers p 2868 N92-26559
Analysis and modeling of high-temperature performance of advanced fiber composites p 2868 N92-26564
Ceramic composites: Experimental and analytical study of SiC/Si3N4 composites p 2882 N92-26859
CERAMIC NUCLEAR FUELS
An investigation of the mechanical properties and microscopic structure of extruded powder aluminum subjected to biaxial loadings at elevated temperature p 2879 N92-26770
CERAMICS
Advanced materials aspects of concurrent engineering
[AD-A245437] p 2880 N92-26275
Slip casting and green body evaluation of 6 percent yttria, 2 percent alumina silicon nitride
[AD-A245817] p 2881 N92-26283
Ceramic bearing technology: Proceedings of the NIST/DARPA Workshop
[PB92-137553] p 2914 N92-26366
Compressive damage and fracture modeling of ceramic subjected to high-velocity impact p 2881 N92-26492
High temperature furnace modeling and performance verifications
[NASA-CR-190403] p 2908 N92-26536
Comparison of ceramic uniaxial compression specimens through detailed finite element modelling
[AD-A245816] p 2882 N92-26609
Crystalline-amorphous interfaces and their relation to grain boundary films
[DE92-009812] p 3004 N92-26648
Analysis of Yttrium-Barium-Copper-Oxide by x ray diffraction and mechanical characterization
[NASA-TM-104562] p 2869 N92-26650
Studies of rain erosion mechanisms in a range of IR transmitting ceramics including coated samples
[AD-A245299] p 2882 N92-26751
Fracture of structural ceramics in combined mode 1 and mode 2 loading p 2882 N92-26775
Study and analysis of the stress state in a ceramic, button-head, tensile specimen
[DE92-007794] p 2918 N92-26784
Contamination of optical surfaces in Earth orbit p 2999 N92-27099
CESIUM 137
Modeling transfer of Cs-137 fallout in a large Finnish watercourse, appendix 6 p 2930 N92-26488
CHANGE DETECTION
Report of the CC1 working group on climate change detection
[WCDMP-14] p 2947 N92-26923
CHANNEL CAPACITY
Optical communications with number states p 2889 N92-26604
Algorithms for capacity computations and algebraic cascade coding with applications to data storage p 2977 N92-27053
CHANNEL FLOW
Study of the transition to turbulence within a curved rectangular channel with 40 to 1 aspect ratio
[AD-A246314] p 2896 N92-26290
Systematic study of Reynolds stress closure models in the computations of plane channel flows
[NASA-CR-189646] p 2898 N92-26649
Heat transfer in oscillating flows with sudden change in cross section
[NASA-TM-105692] p 2861 N92-26654
Numerical simulation of the laminar turbulent transition in a stratified flow p 2904 N92-26920
CHANNELS
Algorithms for capacity computations and algebraic cascade coding with applications to data storage p 2977 N92-27053
CHANNELS (DATA TRANSMISSION)
An adaptive, packet-switched HF data terminal: Functional overview and initial performance
[AD-A246318] p 2973 N92-26292
Optical communications with number states p 2889 N92-26604
CHAOS
Mesh and torus chaotic routing (updated version)
[AD-A246284] p 2979 N92-26359
Fractals and chaos
[AD-A246502] p 2990 N92-26466
Sensitivity of sensors for characterizing chaos
[AD-A246423] p 2921 N92-27066
Studies in chaos using stochastic methods
[AD-A246919] p 3008 N92-27171
CHARACTER RECOGNITION
Massively parallel implementation of character recognition systems
[PB92-149863] p 2980 N92-26501
CHARACTERIZATION
Activation and characterization of some molecular sieve catalysts
[ETN-92-91306] p 2871 N92-26261
Differential Scanning Calorimetry (DSC) for the analysis of activated carbon
[AD-A245899] p 2872 N92-26404
Optical performance of exposed solar cell covers p 2998 N92-27091
CHARGE COUPLED DEVICES
Description of the multispectral CCD-camera
[AD-A245681] p 2908 N92-26517
CHARGE EFFICIENCY
New amorphous thin-film lithium electrolyte and rechargeable microbattery
[DE92-010110] p 2893 N92-26637
A constant current charge technique for low Earth orbit life testing p 2863 N92-27139
Li/BCX, SVO, and CSC cells: Power sources for aerospace applications p 2864 N92-27147
Life testing of secondary Ag-Zn cells p 2865 N92-27153
CHARGE EXCHANGE
Interpretation of distributions on K(sub pi)(sup 0) in pFe, nFe, and piFe interactions at 0.5-5.0 TeV in the framework of contemporary models
[DE92-621189] p 3021 N92-26804
CHARGE TRANSFER
Solvation effects on the electronic structure of 4-N,N-Dimethylaminobenzonitrile: Mixing of the local pipi* and charge transfer states
[AD-A245814] p 2874 N92-26608
Photoinduced charge separation in solid-state and molecular systems
[DE92-010130] p 3004 N92-26639
CHARGED PARTICLES
Diffraction phenomena in spontaneous and stimulated radiation by relativistic particles in crystals (review)
[DE92-009501] p 3001 N92-26222
New description of multiplicity distribution in inelastic meson-proton interactions
[DE92-621167] p 2995 N92-26800
Dielectric tensor of strongly coupled plasmas
[DE92-621524] p 3001 N92-26807
On increasing the capabilities of the SMART adaptive random number generator
[DE92-621106] p 2976 N92-26835
CHEMICAL ANALYSIS
Bis (pentamethylcyclopentadienyl) ytterbium: Electron-transfer reactions with organotransition metal complexes
[DE92-010300] p 2994 N92-26235
Investigation of kinetics of MOCVD systems
[AD-A246090] p 2893 N92-26540
A surface science investigation of silicon carbide: Oxidation, crystal growth and surface structural analysis
[DE92-010286] p 3004 N92-26641
Technology transfer and application of SERS continuous monitor for trace organic compounds
[DE92-008900] p 2875 N92-26726
Chemical evaluation of non-woven nylon separators used in Ni/Cd cells p 2863 N92-27140
CHEMICAL BONDS
Bis (pentamethylcyclopentadienyl) ytterbium: Electron-transfer reactions with organotransition metal complexes
[DE92-010300] p 2994 N92-26235
The computation of C-C and N-N bond dissociation energies for singly, doubly, and triply bonded systems
[NASA-CR-190254] p 2994 N92-26539
Fundamental studies of the chemical vapor deposition of diamond
[DE92-010327] p 2881 N92-26543
A study of buckminsterfullerene using new pseudopotentials p 3005 N92-26774
CHEMICAL COMPOSITION
Relationship between composition, structure, properties, thermo-mechanical processing and ballistic performance of tungsten heavy alloys
[AD-A245649] p 2876 N92-26172

Non-destructive analysis for hydrogen concentrations in materials
[AD-A246098] p 2874 N92-26541
The Debye temperature of YBa2Cu3O(7-(delta)) and its dependence on the volume fraction of superconductivity
[DE92-010305] p 3003 N92-26584
Optical performance of exposed solar cell covers p 2998 N92-27091

CHEMICAL EQUILIBRIUM
Investigation of kinetics of MOCVD systems
[AD-A246090] p 2893 N92-26540

CHEMICAL EVOLUTION
The galactic evolution of s-process elements via asymptotic giant branch stars p 3018 N92-26725

CHEMICAL REACTIONS
Conversion of ethane and of propane to higher olefin hydrocarbons
[DE92-009487] p 2870 N92-26209
Gas phase chromatography of halides of elements 104 and 105
[DE92-010284] p 2870 N92-26212
Differential Scanning Calorimetry (DSC) for the analysis of activated carbon
[AD-A245899] p 2872 N92-26404
Comparison of laser models
[NASA-CR-190302] p 2913 N92-26870
The importance of chemical reactions with environment for ablation process of thermal protection and structural materials p 2883 N92-27015

CHEMICAL REACTORS
Aromatic-radical oxidation kinetics
[DE92-010821] p 2871 N92-26274
Reaction/separation process for enhanced methane conversion
[PB92-149657] p 2873 N92-26508
A novel process for methanol synthesis
[DE92-010465] p 2883 N92-26547

CHEMISORPTION
Photoinduced charge separation in solid-state and molecular systems
[DE92-010130] p 3004 N92-26639

CHINESE SPACE PROGRAM
Chinese space technology's spin-offs and applications
[AD-A246375] p 3015 N92-27051

CHIPS
Stresses in solder joints of electronic packages
[AD-A245799] p 2894 N92-26897

CHIPS (ELECTRONICS)
Complementary metal oxide silicon cyclic redundancy check generators
[AD-A246140] p 2894 N92-27061

CHLORIDES
NASA Li/CF(x) cell problem analysis: Anion exchange chromatography analysis p 2864 N92-27145

CHLORINE COMPOUNDS
Calorimetric determination of the thermoneutral potential for Li/BrCl in SOCl2 (BCX) cells p 2864 N92-27146

CHLORINE FLUORIDES
NASA Li/CF(x) cell problem analysis: Scanning electron microscopy with energy dispersive x ray spectrometry p 2863 N92-27144

CHROMATOGRAPHY
The use of ion chromatography-dc plasma atomic emission spectrometry for the speciation of trace metals
[DE92-010317] p 2871 N92-26236
NASA Li/CF(x) cell problem analysis: Anion exchange chromatography analysis p 2864 N92-27145

CHROMITES
A novel process for methanol synthesis
[DE92-010465] p 2883 N92-26547

CHROMIUM ISOTOPES
Gamma-ray spectrometry of LDEF samples
[DE92-009947] p 2874 N92-26632

CHROMIUM OXIDES
Evaluation of plasma sprayed crucible coatings for melt processing copper-refractory metal alloys
[DE92-008912] p 2878 N92-26727

CHROMOSOMES
A computer system for access to distributed genome mapping data
[DE92-008875] p 3011 N92-26453

CHRONOLOGY
Apogee, perigee, and recovery: Chronology of Army exploitation of space
[RAND-N-3103-A] p 2856 N92-26192

CIRCULAR CYLINDERS
Vortex structure in wake of a circular cylinder p 2904 N92-26918

CIRRUS CLOUDS
Cirrus clouds and condensation trail on 18 Oct. 1989 over the North sea (ICE '89). Determination of height and optical depth using ALEX, AVHRR and HIRS p 2940 N92-26340

CIVIL AVIATION
An adaptive correction technique for Differential Global Positioning System p 2851 N92-26623

CLADDING
Retention and release of tritium in aluminum clad, Al-Li alloys
[DE92-009905] p 2878 N92-26635

CLAMPS
An investigation of the behavior of the clamp-induced bending stresses
[DE92-006504] p 2918 N92-26694

CLASSIFICATIONS
Cataloging guidelines
[AD-A246500] p 3011 N92-26465
Differentiation on genus of aquatic macrophytes through remote sensing in the Tucurui Reservoir, Para State, Brazil
[INPE-5315-PRE/1712] p 2951 N92-26721
Bayesian classification theory
[NASA-TM-107885] p 2988 N92-26894

CLASSIFIERS
Introduction in IND and recursive partitioning
[NASA-TM-107879] p 2983 N92-26629
Feature discovery via neural networks for object recognition in SAR imagery
[DE92-007046] p 2891 N92-26902

CLEAVAGE
Improving the fracture resistance of irradiated martensitic steels
[DE92-008387] p 2879 N92-26848

CLIMATE
Contributions to atmospheric physics in honor of Dr. Manfred Reinhardt on his 65th birthday
[DLR-FB-91-30] p 2939 N92-26329
Equilibrium-analysis of projected climate change effects on the global soil organic matter pool
[PB92-153022] p 2930 N92-26509
Role of climate in forest monitoring and assessment: A New England example
[PB92-132885] p 2930 N92-26519
Organic carbon in soil and the global carbon cycle
[DE92-010289] p 2931 N92-26580
The impact of climate upon variation in air pollution using a synoptic climatological approach p 2931 N92-26590
Research plan for utilizing TRMM data in MRI --- tropical rainfall measuring mission
[TW-13] p 2924 N92-26714
Climate research at regional climate centers in 1991
[PB92-160399] p 2946 N92-26822
Report of the CC1 working group on climate change detection
[WCDMP-14] p 2947 N92-26923
CC1 experts meeting on CLIMAT code adaptation
[WCDMP-15] p 2947 N92-26924
Report of the CC1 experts meeting on tracking and transmission of climate system monitoring information
[WCDMP-16] p 2947 N92-26925

CLIMATE CHANGE
Equilibrium-analysis of projected climate change effects on the global soil organic matter pool
[PB92-153022] p 2930 N92-26509
Monthly mean global satellite data sets available in CCM history tape format
[NASA-CR-190344] p 2933 N92-26878
Report of the CC1 working group on climate change detection
[WCDMP-14] p 2947 N92-26923
PAGES. Past global changes project: Proposed implementation plans for research activities
[IGBP-REPT-19-ATTACH-10] p 2934 N92-27082

CLIMATOLOGY
The objective determination of front lines p 2941 N92-26343
Role of climate in forest monitoring and assessment: A New England example
[PB92-132885] p 2930 N92-26519
The impact of climate upon variation in air pollution using a synoptic climatological approach p 2931 N92-26590
Research and technology, 1990: Goddard Space Flight Center
[NASA-TM-107792] p 3022 N92-26824
Report of the CC1 working group on climate change detection
[WCDMP-14] p 2947 N92-26923
CC1 experts meeting on CLIMAT code adaptation
[WCDMP-15] p 2947 N92-26924
Report of the CC1 experts meeting on tracking and transmission of climate system monitoring information
[WCDMP-16] p 2947 N92-26925

CLINICAL MEDICINE
Clinical investigation program, fiscal year 1991
[AD-A246558] p 2992 N92-26618

CLOCKS
Characterization of the clock in a new inexpensive GPS receiver: The Magnavox MX 4200
[AD-A246165] p 2851 N92-26415

CLOSED ECOLOGICAL SYSTEMS
Human support issues and systems for the space exploration initiative: Results from Project Outreach
[NASA-CR-190320] p 2954 N92-26193
Life support research and development, a Department of Energy program for the Space Exploration Initiative
[DE92-007681] p 2955 N92-26375
Fourth European Symposium on Space Environment Control Systems, volume 2
[ESA-SP-324-VOL-2] p 2956 N92-26950
Thiocapsa roseopersicina, a bacterium for sulfur-recycling in microbial ecosystems designed for CELSS and space purposes p 2951 N92-26977
Higher plant growth in closed environment: Preliminary experiments in life support facility at ESA-ESTEC p 2951 N92-26978
Chemolithotropic hydrogen-oxidizing bacteria and their possible functions in closed ecological life-support systems p 2951 N92-26979
MELISSA: Physical links of compartments Nitrobacter/Spirulina p 2961 N92-26981
Modelling light transfer inside photobiofermentors: Applications to the photosynthetic compartments of CELSS p 2952 N92-26982
Study on the requirements for the installation of a CES and habitability centre p 2966 N92-27007

CLOSURE LAW
On testing models for the pressure-strain correlation of turbulence using direct simulations
[NASA-CR-189638] p 2901 N92-26883

CLOSURES
Subgraphs, closures and Hamiltonicity
[PB92-148766] p 2987 N92-26737

CLOTHING
Maintenance manual for Natick's Footwear Database
[AD-A246273] p 2954 N92-26242

CLOUD COVER
Theoretical and modeling studies of the marine planetary boundary layer
[AD-A245903] p 2942 N92-26432

CLOUD PHYSICS
Plume trajectory validation study: Brown cloud support project overview
[DE92-006911] p 2928 N92-26390

CLOUDS (METEOROLOGY)
Atmospheric environment for Space Shuttle Columbia (STS-40) launch
[NASA-TM-103585] p 2945 N92-26288
Investigation of convection over sea by aircraft observations p 2926 N92-26337
Convection wave studies over land and sea p 2940 N92-26341
Remote sensing of atmosphere with aircraft borne lidar systems p 2941 N92-26347

CLUMPS
Analytical and numerical investigation of nonlinear gravitational clustering p 3017 N92-26578

CLUSTER ANALYSIS
The effect of collection homogeneity on term association as a method of request expansion in information retrieval p 3012 N92-26614

CLUSTER MISSION
Cluster Dayside Polar Cusp
[ESA-SP-330] p 2935 N92-26294
Cusp and cleft studies in Greenland p 2935 N92-26299
Lesson learned from GEOS and ISEE p 2936 N92-26302
The requirements for data exchange between Cluster and ground-based observatories, using EISCAT as an illustrative example p 2938 N92-26316
Requirements for coordinated Cluster and ground-based observations of the cusp p 2938 N92-26318

CLUSTERS
Toluene-water clusters: Ion fragmentation and chemistry
[AD-A245813] p 2874 N92-26526

CLUTTER
Description of the multispectral CCD-camera
[AD-A245681] p 2908 N92-26517
Infrared clutter measurements of marine backgrounds
[AD-A245422] p 2932 N92-26873
Feature discovery via neural networks for object recognition in SAR imagery
[DE92-007046] p 2891 N92-26902

COAL
Fuel staging and its implementation in a novel internally staged burner
[ETN-92-91307] p 2872 N92-26285

COAL DERIVED GASES
Fuel staging and its implementation in a novel internally staged burner
[ETN-92-91307] p 2872 N92-26285

COAL GASIFICATION
High-yield hydrogen production by catalytic gasification of coal or biomass
[DE92-008770] p 2875 N92-26724
COASTAL WATER
Hydrographic data from the Coastal Transition Zone (CTZ) program, 5-19 July 1988
[AD-A245517] p 2950 N92-27069
COASTAL ZONE COLOR SCANNER
Meridional zonation of the Barents Sea ecosystem inferred from satellite remote sensing and in situ bio-optical observations
[AD-A246323] p 2948 N92-26245
COASTS
Hindcast wave information for the Great Lakes: Lake Huron. Wave information studies of US coastlines
[AD-A246326] p 2949 N92-26387
COATINGS
An electroplater's view of PVD processing
[DE92-009052] p 2878 N92-26732
Studies of rain erosion mechanisms in a range of IR transmitting ceramics including coated samples
[AD-A245299] p 2882 N92-26751
COBALT
Relationship between composition, structure, properties, thermo-mechanical processing and ballistic performance of tungsten heavy alloys
[AD-A245649] p 2876 N92-26172
Magneto-optical multilayers --- optical data storage
[DE92-009726] p 2997 N92-26565
COBALT ISOTOPES
Gamma-ray spectrometry of LDEF samples
[DE92-009947] p 2874 N92-26632
CODING
A comparison of direction finding results from an FFT peak identification technique with those from the music algorithm
[AD-A245675] p 2888 N92-26424
CC1 experts meeting on CLIMAT code adaptation
[WCDMP-15] p 2947 N92-26924
COEFFICIENTS
Recognition of 3-D symmetric objects from range images in automated assembly tasks
[NASA-CR-187664] p 2886 N92-26656
COGENERATION
Adaptive regulation of the boiler-turbine unit of a Combined Heat and Power (CHP) system
[RR-417] p 2887 N92-26752
COGNITION
MoCog1: A computer simulation of recognition-primed human decision making
[NASA-TM-107872] p 2984 N92-26888
Human cognitive processes in command and control planning. 3: Determining basic processes involved in planning in time and space
[IZF-1991-B-11] p 3010 N92-27046
The structure and formation of natural categories
[NASA-TM-107896] p 2985 N92-27056
COGNITIVE PSYCHOLOGY
The structure and formation of natural categories
[NASA-TM-107896] p 2985 N92-27056
COHERENT RADAR
Cusp studies with HF radars p 2936 N92-26304
Large coherent arrays for laser radars, phase 1
[AD-A245528] p 2912 N92-26663
COHERENT RADIATION
Operation of a Smith-Purcell free-electron laser at submillimeter wavelengths p 2912 N92-26626
Spontaneous and induced coherent radiation generation in atomic vapors
[AD-A246078] p 2890 N92-26764
COLD FRONTS
Mesoscale observations of a cold front associated with a prefrontal hailstorm p 2940 N92-26338
High frequency analyses of coastal meteorological phenomena affecting refractivity
[AD-A246383] p 2947 N92-27075
COLD NEUTRONS
Acquired polarization in fundamental symmetry experiments
[AD-A245646] p 2993 N92-26171
COLD TOLERANCE
Physiological design goals and proposed thermal limits for US Navy thermal garments: Proceedings of 2 conferences sponsored by the Naval Medical Research and Development Command
[AD-A245543] p 2956 N92-26665
COLD WATER
Hydrographic data from the Coastal Transition Zone (CTZ) program, 5-19 July 1988
[AD-A245517] p 2950 N92-27069
COLD WELDING
On-orbit coldwelding: Fact or friction?
p 2880 N92-27115
Microwelding (or cold-welding) of various metallic materials under the ultra-vacuum LDEF experiment AO 138-10 p 2880 N92-27119
COLLISION AVOIDANCE
A supervisory control strategy for navigation of mobile robots in dynamic environments p 2983 N92-26734
COLLISIONLESS PLASMAS
Kinetic theory of toroidicity-induced Alfven eigenmode
[DE92-010424] p 2999 N92-26546
Dynamic properties of quasi-two-dimensional one component plasmas
[DE92-621523] p 3000 N92-26806
COLLISIONS
Dynamics of neutron stars and binaries in globular clusters or, menages a trois: Revitalizing burnt out degenerates through partner swapping
p 3017 N92-26522
COLLOCATION
Estimation of geopotential differences over intercontinental locations using satellite and terrestrial measurements p 2924 N92-26728
COLLOIDS
Fundamentals of electrokinetics
[DE92-008326] p 2894 N92-26847
COLOR
Dynamic lens compensation for active color imaging and constant magnification focusing
[AD-A245713] p 2997 N92-26425
Color image processing and object tracking workstation
[NASA-TM-105561] p 2886 N92-26611
COLOR CENTERS
Optimization of a color center Q-switched Nd:YLF laser
[DE92-621612] p 2910 N92-26287
COLOR VISION
Selective search for the target properties color and form
[IZF-1991-B-13] p 2953 N92-27047
COLUMBIA (ORBITER)
Atmospheric environment for Space Shuttle Columbia (STS-40) launch
[NASA-TM-103585] p 2945 N92-26288
COLUMBUS SPACE STATION
Space Station Freedom regenerative water recovery system configuration selection p 2957 N92-26953
Battery thermal control of the Columbus Free Flyer
p 2859 N92-26970
CAD system for HFE analyses: Zero-g posture in optimisation of Columbus APM crew workstations --- human factors engineering p 2963 N92-26991
Crew support equipment: Identification and definition of additional hardware for Columbus APM laboratory habitability p 2964 N92-26993
Concept for a European Space Station: Habitability, life support, and laboratory facilities p 2969 N92-27023
COMBAT
Using solid modeling techniques to construct three-dimensional icons for a visual simulator
[AD-A245784] p 2971 N92-26195
System evaluation of a frequency hopping combat net radio
[AD-A246365] p 2891 N92-26941
COMBINATORIAL ANALYSIS
Universal R-matrix for quantized (super)algebras
[DE92-621067] p 2988 N92-26834
COMBUSTION
Burn-rate studies with iron/potassium perchlorate heat pellets
[DE92-008524] p 2875 N92-26722
Development of natural gas rotary engines
[PB92-149665] p 2915 N92-26816
Microgravity combustion science: Progress, plans, and opportunities
[NASA-TM-105410] p 2886 N92-27197
COMBUSTION CHAMBERS
A model for aerodynamically-valved pulse combustion
[DE92-009887] p 2871 N92-26262
Turbocharged pressurized combustion system
[PB92-142579] p 2873 N92-26521
A parametric numerical study of mixing in a cylindrical duct
[NASA-TM-105695] p 2854 N92-26553
The 3D rocket combustor acoustics model
[NASA-TM-105734] p 2861 N92-27035
COMBUSTION CHEMISTRY
Aromatic-radical oxidation kinetics
[DE92-010821] p 2871 N92-26274
Spectroscopy and kinetics of combustion gases at high temperatures
[DE92-011216] p 2872 N92-26281
Advancing natural gas combustion science and technology-low NOx
[PB92-137652] p 2876 N92-26782
COMBUSTION CONTROL
Control of turbulent mixing in hypersonic flow
p 2904 N92-26919
COMBUSTION EFFICIENCY
Effect of model selection on combustor performance and stability predictions using ROCCID
[NASA-TM-105750] p 2861 N92-27036
COMBUSTION PHYSICS
Theoretical and numerical study of flame propagation and transition to detonation --- detonation transition
p 2874 N92-26615
Computational method to predict thermodynamic, transport, and flow properties for the modified Langley 8-foot high-temperature tunnel
[NASA-TM-4374] p 2905 N92-27193
COMBUSTION PRODUCTS
Spectroscopy and kinetics of combustion gases at high temperatures
[DE92-011216] p 2872 N92-26281
Fuel staging and its implementation in a novel internally staged burner
[ETN-92-91307] p 2872 N92-26285
Advancing natural gas combustion science and technology-low NOx
[PB92-137652] p 2876 N92-26782
Assessment of computer models for estimating vehicle emission factors. Volume 1: Executive summary
[PB92-113059] p 2931 N92-26802
Assessment of computer models for estimating vehicle emission factors. Volume 2: Description and comparison of the MOBILE4 and EMFAC7E models
[PB92-113067] p 2932 N92-26803
Technology for reduction of CO2 emissions from the transportation sector
[PB92-153733] p 2933 N92-26929
COMBUSTION STABILITY
The 3D rocket combustor acoustics model
[NASA-TM-105734] p 2861 N92-27035
Effect of model selection on combustor performance and stability predictions using ROCCID
[NASA-TM-105750] p 2861 N92-27036
COMMAND AND CONTROL
Plan of action survey of functional requirements for a geographical information system
[AD-A245622] p 3011 N92-26403
System evaluation of a frequency hopping combat net radio
[AD-A246365] p 2891 N92-26941
Human cognitive processes in command and control planning. 3: Determining basic processes involved in planning in time and space
[IZF-1991-B-11] p 3010 N92-27046
COMMAND LANGUAGES
User interface consistency across end-user application programs: Effect on learning and satisfaction
p 3013 N92-26776
COMMERCE
US Small Business Administration FY 1990 national accomplishment report and FY 1991 national affirmative employment program plan
[PB92-157064] p 3008 N92-26353
Small Businesses Make a Difference
[PB92-160118] p 3008 N92-26369
Survey of small business use of intellectual property protection
[PB92-151703] p 3009 N92-26523
Small business innovation research: Program solicitation closing date, 27 January 1992
[DE92-010132] p 3009 N92-26811
COMMERCIAL AIRCRAFT
Gamma Group-The Pale Horse: A proposal in response to a commercial air transportation study ort study
[NASA-CR-190019] p 2852 N92-26435
COMMUNICATION
Reference model for frameworks of software engineering environments
[PB92-158328] p 2973 N92-26370
COMMUNICATION EQUIPMENT
A measuring facility for testing radio communication equipment
[AD-A245621] p 2890 N92-26874
COMMUNICATION NETWORKS
Modeling node bandwidth limits and their effects on vector combining algorithms
[DE92-010829] p 2979 N92-26277
An adaptive, packet-switched HF data terminal: Functional overview and initial performance
[AD-A246318] p 2973 N92-26292
Data fusion and correlation techniques testbed (DFACTT): Field trial 14 January 1991
[AD-A245324] p 3011 N92-26378
System evaluation of a frequency hopping combat net radio
[AD-A246365] p 2891 N92-26941

COMMUNICATION SATELLITES
Requirements analysis and design for implementation of a satellite link for a local area computer network
[AD-A245610] p 2978 N92-26227
A comparison of the UHF Follow-On and MILSTAR satellite communication systems
[AD-A245806] p 2891 N92-26933
Italsat thermal control: The in-orbit performances p 2859 N92-26996
Eutelsat 2: SAR-10009 nickel-hydrogen battery p 2866 N92-27159

COMPARISON
Comparison of frontogenetical structures for different cases of frontal development p 2939 N92-26333
Comparison of wind profiles in close proximity to each other
[AD-A246152] p 2945 N92-26409
Comparison of ceramic uniaxial compression specimens through detailed finite element modelling
[AD-A245816] p 2882 N92-26609
An electroplater's view of PVD processing
[DE92-009052] p 2878 N92-26732

COMPATIBILITY
Materials compatibility and wall stresses in hydride storage beds
[DE92-009432] p 2870 N92-26201

COMPILERS
Model compilation: An approach to automated model derivation
[NASA-TM-107895] p 2985 N92-27057

COMPLEX COMPOUNDS
Bis (pentamethylcyclopentadienyl) ytterbium: Electron-transfer reactions with organotransition metal complexes
[DE92-010300] p 2994 N92-26235

COMPLEX SYSTEMS
NEXUS: A kernel complex object management system p 3012 N92-26567

COMPLEXITY
A random polynomial algorithm for the matroid parity base problem
[REPT-91-079] p 2974 N92-26449

COMPOSITE MATERIALS
Composite strength statistics from fiber strength statistics
[AD-A245616] p 2867 N92-26383
Experimental study of shear fracture and aggregate interlock in cementbased composites
[PB92-151521] p 2868 N92-26525
Optical strain monitoring in composite materials
[AD-A245474] p 2868 N92-26532
Finite element modeling of static indentation damage in laminated composites p 2869 N92-26827
Penetration of laminated composites by projectiles p 2869 N92-26861

COMPOSITE PROPELLANTS
Solid fuel ramjet infrared signature
[AD-A246299] p 2860 N92-26362

COMPOSITE STRUCTURES
Optical strain monitoring in composite materials
[AD-A245474] p 2868 N92-26532
Reliability and failure analyses of composite beams and plates containing stress concentrations p 2918 N92-26598
Composite fuselage technology (summary of year 2)
[NASA-CR-190434] p 2852 N92-26655
A finite element method including transverse stresses for thick laminated plates and shells p 2920 N92-26860

COMPOSITION (PROPERTY)
The carbon isotopic compositions of individual compounds from ancient and modern depositional environments p 2921 N92-26478

COMPRESSIBLE FLOW
Cell vertex methods for compressible gas flows p 2897 N92-26599
A parametric study of the hydrodynamic stability theory of 3-D compressible free shear flows p 2900 N92-26849
Wave structure in one and two dimensional fluid flow
[DE92-007421] p 2900 N92-26855
Numerical simulation of two-dimensional single- and multiple-material flow fields
[DE92-007428] p 2901 N92-26856
Interface of an uncoupled boundary layer algorithm with an inviscid core flow algorithm for unsteady supersonic engine inlets
[NASA-TM-105684] p 2855 N92-27037
Turbulent mixing in supersonic jets p 2850 N92-27054

COMPRESSION LOADS
Effect of thermal residual stresses on the stress-strain behavior of metal-matrix composites
[AD-A246136] p 2868 N92-26386
Buckling of unidirectional graphite/epoxy composite plates at low temperatures
[AD-A246602] p 2869 N92-26796
Recent advances in shock and quasi-isentropic compression techniques for dynamic material property studies
[DE92-007988] p 2919 N92-26852

COMPRESSION TESTS
Compressive damage and fracture modeling of ceramic subjected to high-velocity impact p 2881 N92-26492
Comparison of ceramic uniaxial compression specimens through detailed finite element modelling
[AD-A245816] p 2882 N92-26609

COMPRESSIVE STRENGTH
Computational modelling of rubberlike materials
[ETN-92-91304] p 2916 N92-26259
A method to improve post impact compressive strength in graphite/epoxy composite materials after low temperature impact
[AD-A245395] p 2867 N92-26380
Comparison of ceramic uniaxial compression specimens through detailed finite element modelling
[AD-A245816] p 2882 N92-26609

COMPUTATION
A FORTRAN 90 code for magnetohydrodynamics
[DE92-010362] p 3000 N92-26577

COMPUTATIONAL FLUID DYNAMICS
Numerical simulation of two-dimensional single- and multiple-material flow fields
[DE92-007428] p 2901 N92-26856
Proceedings of the 5th and 6th Seminars on Investigation and Control of Boundary-Layer Transition
[NAL-SP-12] p 2901 N92-26906
Pattern search in turbulent field p 2901 N92-26907
Research activities on CFD at the Ship Research Institute p 2902 N92-26908
Three dimensional boundary layer transition on a yawed cylinder p 2902 N92-26909
An evolutional process of three dimensional disturbances in laminar boundary layers p 2902 N92-26910
Aerodynamic drag on the bullet trains p 2902 N92-26911
Coning motion and flat spinning of slender bodies at high angles of attack p 2902 N92-26912
Flow around an isolated surface roughness in the laminar boundary layer p 2903 N92-26913
Experimental studies on the flat plate boundary layer transition using hydrogen bubble method p 2903 N92-26914
Application of riblet surface to pipe flow p 2903 N92-26915
Numerical studies on laminar turbulent transition at the Stuttgart University, Germany p 2903 N92-26916
Investigation on the boundary layer transition of alternately oscillating flow in deceleration phase p 2903 N92-26917
Vortex structure in wake of a circular cylinder p 2904 N92-26918
Control of turbulent mixing in hypersonic flow p 2904 N92-26919
Numerical simulation of the laminar turbulent transition in a stratified flow p 2904 N92-26920
Responses of boundary layers to strong external disturbances p 2904 N92-26921
Cross-flow instabilities and pressure gradients in boundary layers p 2904 N92-26922
Unified computational method for design of fluid loop systems p 2905 N92-26962
The changing role of experimentation in aeroengine R and D: The point of view of the research worker
[AD-A246372] p 2856 N92-27062

COMPUTATIONAL GRIDS
Description of and users manual for TUBA: A computer code for generating two-dimensional random fields via the turning bands method
[DE92-001020] p 2971 N92-26189
Mesh and torus chaotic routing (updated version)
[AD-A246284] p 2979 N92-26359
Nonexpansive prolongations and difference schemes for the advection equation
[PB92-141530] p 2986 N92-26502
Three-dimensional upwind scheme for solving the Euler equations on unstructured tetrahedral grids --- tetrahedral grids p 2849 N92-26585
Cell vertex methods for compressible gas flows p 2897 N92-26599
Application of parametrized variational principles in the finite element method p 2987 N92-26624
Iterative system modeling using multigrid techniques
[AD-A245522] p 2976 N92-26658
Eulerian computational methods
[DE92-008017] p 2900 N92-26853
Homogenization models for 2-D grid structures
[NASA-CR-190321] p 2920 N92-26892

COMPUTER AIDED DESIGN
The development of a design database for the computer aided prototyping system
[AD-A245786] p 3010 N92-26176
Integrating reverse engineering into Computer-Aided Software Engineering (CASE) p 2974 N92-26479
Algorithms for blending surface generation
[AD-A245686] p 2975 N92-26524
Rule-based expert system for evaluating the quality of long-term, in-situ, gas chromatographic measurements of atmospheric methane
[PB92-128560] p 2876 N92-26812
CAD system for HFE analyses: Zero-g posture in optimisation of Columbus APM crew workstations --- human factors engineering p 2963 N92-26991

COMPUTER DESIGN
Requirements analysis and design for implementation of a satellite link for a local area computer network
[AD-A245610] p 2978 N92-26227

COMPUTER GRAPHICS
Advanced software development workstation. Engineering scripting language graphical editor: DRAFT design document
[NASA-CR-190393] p 2971 N92-26181
Advanced software development workstation. Engineering scripting language graphical editor: DRAFT code documentation
[NASA-CR-190389] p 2971 N92-26182
Advanced software development workstation project: Engineering scripting language. Graphical editor
[NASA-CR-190391] p 2971 N92-26183
Distributed visualization
[DE92-009405] p 2971 N92-26188
Using solid modeling techniques to construct three-dimensional icons for a visual simulator
[AD-A245784] p 2971 N92-26195
Estimation of motion parameters from image sequences
[AD-A246135] p 2986 N92-26358
Fractals and chaos
[AD-A246502] p 2990 N92-26466
Performance analysis of image motion analysis algorithms
[AD-A246522] p 2974 N92-26468
A modeling strategy for large-scale optimization based on analysis and visualization principles
[AD-A246570] p 2987 N92-26620
Scientific documentary animation: How much accuracy is enough?
[DE92-009698] p 2975 N92-26647
User interface consistency across end-user application programs: Effect on learning and satisfaction p 3013 N92-26776
Forging a path with tool and data attributes
[DE92-009800] p 2976 N92-26797
GRABE: A simple graphical back-end for thermal simulation packages p 2958 N92-26961

COMPUTER INFORMATION SECURITY
Reference model for frameworks of software engineering environments
[PB92-158328] p 2973 N92-26370

COMPUTER NETWORKS
Distributed visualization
[DE92-009405] p 2971 N92-26188
Distributed and parallel Ada and the Ada 9X recommendations
[NASA-CR-190392] p 2978 N92-26199
Scalable coherent interface: Links to the future
[DE92-010728] p 2887 N92-26267
Assessments of selected real-time computing technologies
[AD-A245434] p 2972 N92-26273
Paralex: An environment for parallel programming in distributed systems
[AD-A245445] p 2979 N92-26278
Run-time support for dynamic load balancing and debugging in paralex
[AD-A245446] p 2979 N92-26279
Mesh and torus chaotic routing (updated version)
[AD-A246284] p 2979 N92-26359
Executive summary of information systems plans: Fiscal years 1993 to 1997
[PB92-158351] p 3011 N92-26368
A computational analysis of properties and limitations of neural networks: Toward new parallel architectures for learning
[AD-A246156] p 2981 N92-26410
Design and implementation of a toolbox of modularized C programs to construct, analyze, and test network optimization algorithms
[AD-A246191] p 2979 N92-26417
Software requirements document for the netCDF interface within ECMOP, version 1.0
[AD-A246220] p 2974 N92-26464

Automated interpretation of S-invariants of predicate/transition nets: An application of non-classical logics
[PB92-143544] p 2975 N92-26500
Two papers on feed-forward networks
[NASA-TM-107840] p 2983 N92-26631
The Orca Project: Research on high performance parallel computer programming environments
[AD-A234648] p 2980 N92-26801
A security analysis of version 2 of the Network Time Protocol (NTP): A report to the privacy and security research group
[NASA-CR-190428] p 2981 N92-27183

COMPUTER PROGRAMMING

Assessments of selected real-time computing technologies
[AD-A245434] p 2972 N92-26273
Software requirements document for the netCDF interface within ECMOP, version 1.0
[AD-A246220] p 2974 N92-26464
Generation of multi-resolution maps
[PB92-152206] p 2921 N92-26513
Matched field processing on the connection machine
[AD-A245469] p 2980 N92-26531
The 8th IEEE Workshop on Real-Time Operating Systems
[AD-A246126] p 2976 N92-26685
Experiences in using C++ to develop a next generation strong shock wave physics code
[DE92-006675] p 2976 N92-26696

COMPUTER PROGRAMS

The development of a design database for the computer aided prototyping system
[AD-A245786] p 3010 N92-26176
Advanced software development workstation project: Engineering scripting language. Graphical editor
[NASA-CR-190391] p 2971 N92-26183
Requirements analysis and design for implementation of a satellite link for a local area computer network
[AD-A245610] p 2978 N92-26227
Software maturity model applied to SDI
[AD-A245439] p 2972 N92-26276
Performance enhancement of the NPS Transient Electromagnetic Scattering Laboratory
[AD-A246300] p 2888 N92-26363
Investigating the utility of coupling COCOMO with a system dynamics simulation of software development
[AD-A245484] p 2973 N92-26400
Improving CMM software quality
[NPL-DITC-194/92] p 2974 N92-26450
A computer system for access to distributed genome mapping data
[DE92-008875] p 3011 N92-26453
Naval Postgraduate School aircraft synthesis program (user's manual)
[AD-A246198] p 2974 N92-26458
An empirical approach to analysis of similarities between software failure regions
[AD-A246208] p 2974 N92-26461
Software requirements document for the netCDF interface within ECMOP, version 1.0
[AD-A246220] p 2974 N92-26464
Architecture flow diagrams under Teamwork
[DE92-010482] p 2922 N92-26534
Dimensional analysis of structural steel beam design
[AD-A245759] p 2917 N92-26593
Radar target identification by natural resonances: Evaluation of signal processing algorithms
[AD-A246566] p 2889 N92-26619
A modeling strategy for large-scale optimization based on analysis and visualization principles
[AD-A246570] p 2987 N92-26620
Computer modeling of human decision making
[NASA-TM-107868] p 2983 N92-26630
Use of the Edmonds-Reilly Model to model energy-related greenhouse gas emissions
[DE92-010035] p 2931 N92-26633
Real time imaging and infrared background scene analysis using the Naval Postgraduate School infrared search and target designation (NPS-IRSTD) system
[AD-A245527] p 2997 N92-26662
The 8th IEEE Workshop on Real-Time Operating Systems
[AD-A246126] p 2976 N92-26685
Progress towards understanding and predicting convection heat transfer in the turbine gas path
[NASA-TM-105674] p 2898 N92-26690
The navigation data logger for a suitcase navigation system
[AD-A245997] p 2851 N92-26756
Assessment of computer models for estimating vehicle emission factors. Volume 1: Executive summary
[PB92-113059] p 2931 N92-26802
Numerical solution of the equation of neutrons transport on plane geometry by analytical schemes using acceleration by synthetic diffusion
[DE92-621426] p 2995 N92-26844
Numerical simulation of two-dimensional single- and multiple-material flow fields
[DE92-007428] p 2901 N92-26856
COSMIC software catalog, 1992 edition
[NASA-CR-188973] p 2977 N92-26868
Description of the Rayflux ray tracing program and comparison with other models and measurements
[AD-A245413] p 2944 N92-26877
Computer program for calculating in-flight aircraft-store interface reaction loads
[AD-A245782] p 2852 N92-26896
Computer Program Estimate Trend (ESTREND): A system for the detection of trends in water-quality data
[PB92-147727] p 2933 N92-26931
Buffered serial data card
[AD-A246435] p 2852 N92-26948
Integrated communication environment for thermal analysis software p 2958 N92-26959
GRABE: A simple graphical back-end for thermal simulation packages p 2958 N92-26961
CBT: Role and future application for crew training --- computer based training p 2953 N92-26992
Overview of NASA supported Stirling thermodynamic loss research
[NASA-TM-105690] p 2861 N92-27034
The 3D rocket combustor acoustics model
[NASA-TM-105734] p 2861 N92-27035
Effect of model selection on combustor performance and stability predictions using ROCCID
[NASA-TM-105750] p 2861 N92-27036
Documentation for the Semi-Automated Mesoscale Analysis System 1.1
[AD-A246144] p 2985 N92-27072
Computational method to predict thermodynamic, transport, and flow properties for the modified Langley 8-foot high-temperature tunnel
[NASA-TM-4374] p 2905 N92-27193

COMPUTER STORAGE DEVICES

Algorithms for capacity computations and algebraic cascade coding with applications to data storage
p 2977 N92-27053

COMPUTER SYSTEMS DESIGN

Assessments of selected real-time computing technologies
[AD-A245434] p 2972 N92-26273
Software maturity model applied to SDI
[AD-A245439] p 2972 N92-26276
A computer system for access to distributed genome mapping data
[DE92-008875] p 3011 N92-26453

COMPUTER SYSTEMS PERFORMANCE

Assessments of selected real-time computing technologies
[AD-A245434] p 2972 N92-26273
Software maturity model applied to SDI
[AD-A245439] p 2972 N92-26276
Improving CMM software quality
[NPL-DITC-194/92] p 2974 N92-26450
Architecture flow diagrams under Teamwork
[DE92-010482] p 2922 N92-26534
A design rationale for NASA TileWorld
[NASA-TM-107882] p 2982 N92-26627
The Orca Project: Research on high performance parallel computer programming environments
[AD-A234648] p 2980 N92-26801

COMPUTER SYSTEMS PROGRAMS

Implementing error values in applicative languages
[DE92-008927] p 2972 N92-26233

COMPUTER TECHNIQUES

A design rationale for NASA TileWorld
[NASA-TM-107882] p 2982 N92-26627

COMPUTER VISION

Shape from periodic texture using the spectrogram
[AD-A245855] p 2973 N92-26384
Perception for outdoor navigation
[AD-A245715] p 2851 N92-26427
Massively parallel implementation of character recognition systems
[PB92-149863] p 2980 N92-26501

COMPUTERIZED SIMULATION

Distributed visualization
[DE92-009405] p 2971 N92-26188
The state of multiple sensor, multiple target tracking in ballistic missile defense
[AD-A245433] p 2850 N92-26272
A fractal computer model of macromolecule-cell surface interactions
[AD-A245394] p 2950 N92-26289
Investigating the utility of coupling COCOMO with a system dynamics simulation of software development
[AD-A245484] p 2973 N92-26400
A frequency domain based approach to on-line system identification
[AD-A246193] p 2973 N92-26418
Computer modeling of human decision making
[NASA-TM-107868] p 2983 N92-26630
Scientific documentary animation: How much accuracy is enough?
[DE92-009698] p 2975 N92-26647
Evaluation of the computational validity of the image model in predicting the sound field in a wedge-shaped layer using acoustical reciprocity
[AD-A246548] p 2992 N92-26688
Transient gas motion in nuclear-reactor-pumped lasers: Computational and experimental results
[DE92-002357] p 2912 N92-26691
Numerical simulations of gun-launched kinetic energy projectiles subjected to asymmetric projectile base pressure
[DE92-005065] p 2857 N92-26693
Simulation of 3D non-planar fatigue crack growth in a turbine blade root
[DE92-006859] p 2854 N92-26697
Reynolds number dependence of the drag coefficient for laminar flow through fine-scale screens
[DE92-002930] p 2899 N92-26698
Analysis of mixing mechanisms in numerically simulated convective clouds
[NASA-CR-190222] p 2946 N92-26736
An object-oriented approach to computer architecture simulation
[AD-A246597] p 2970 N92-26773
Forging a path with tool and data attributes
[DE92-009800] p 2976 N92-26797
Assessment of computer models for estimating vehicle emission factors. Volume 1: Executive summary
[PB92-113059] p 2931 N92-26802
Assessment of computer models for estimating vehicle emission factors. Volume 2: Description and comparison of the MOBILE4 and EMFAC7E models
[PB92-113067] p 2932 N92-26803
Numerical simulation of two-dimensional single- and multiple-material flow fields
[DE92-007428] p 2901 N92-26856
MoCog1: A computer simulation of recognition-primed human decision making
[NASA-TM-107872] p 2984 N92-26888
Proceedings of the 5th and 6th Seminars on Investigation and Control of Boundary-Layer Transition
[NAL-SP-12] p 2901 N92-26906
Pattern search in turbulent field p 2901 N92-26907
Research activities on CFD at the Ship Research Institute p 2902 N92-26908
Three dimensional boundary layer transition on a yawed cylinder p 2902 N92-26909
An evolutional process of three dimensional disturbances in laminar boundary layers p 2902 N92-26910
Aerodynamic drag on the bullet trains p 2902 N92-26911
Coning motion and flat spinning of slender bodies at high angles of attack p 2902 N92-26912
Flow around an isolated surface roughness in the laminar boundary layer p 2903 N92-26913
Experimental studies on the flat plate boundary layer transition using hydrogen bubble method p 2903 N92-26914
Application of riblet surface to pipe flow p 2903 N92-26915
Numerical studies on laminar turbulent transition at the Stuttgart University, Germany p 2903 N92-26916
Investigation on the boundary layer transition of alternately oscillating flow in deceleration phase p 2903 N92-26917
Vortex structure in wake of a circular cylinder p 2904 N92-26918
Control of turbulent mixing in hypersonic flow p 2904 N92-26919
Numerical simulation of the laminar turbulent transition in a stratified flow p 2904 N92-26920
Responses of boundary layers to strong external disturbances p 2904 N92-26921
Cross-flow instabilities and pressure gradients in boundary layers p 2904 N92-26922
Thermal analysis of evaporative coolers p 2962 N92-26985
An Ada object oriented missile flight simulation
[AD-A246378] p 2977 N92-27052
NPSNET: Hierarchical data structures for real-time three-dimensional visual simulation
[AD-A246380] p 2978 N92-27073

COMPUTERS

Extracting fuzzy rules under uncertainty and measuring definability using rough sets
[NASA-CR-190396] p 2972 N92-26197

Measuring uncertainty by extracting fuzzy rules using rough sets
[NASA-CR-190395] p 2972 N92-26198
Requirements analysis and design for implementation of a satellite link for a local area computer network
[AD-A245610] p 2978 N92-26227

CONCENTRATION (COMPOSITION)
A comparative assessment of radiological impact due to nuclear waste disposal in hard crystalline bedrock, appendix 1
[IAEA-CN-43/449] p 2929 N92-26483
Non-destructive analysis for hydrogen concentrations in materials
[AD-A246098] p 2874 N92-26541

CONCRETES
Experimental study of shear fracture and aggregate interlock in cementbased composites
[PB92-151521] p 2868 N92-26525

CONCURRENT PROCESSING
Advanced materials aspects of concurrent engineering
[AD-A245437] p 2880 N92-26275

CONDENSATES
Water recovery from condensate of crew respiration products aboard the Space Station
p 2956 N92-26951

CONDENSATION NUCLEI
Parameterization of water-soluble component of aerosol particles in numerical cloud models
[NASA-CR-190225] p 2945 N92-26474
Study of entrainment mechanisms in convective clouds
[NASA-CR-190223] p 2946 N92-26735

CONDUCTIVE HEAT TRANSFER
Analysis and modeling of high-temperature performance of advanced fiber composites p 2868 N92-26564
The development of a model builder for a microcircuit substrate
[AD-A245765] p 2893 N92-26606
Results from the LDEF/A0076 cascaded variable conductance heatpipe experiment p 2906 N92-27106
Calorimetric determination of the thermoneutral potential for Li/BrCl in SOCl2 (BCX) cells p 2864 N92-27146

CONFERENCES
Handbook of solar-terrestrial data systems, version 1
[NASA-TM-107810] p 3019 N92-26191
Workshop on Solar Activity, Solar Wind, Terrestrial Effects, and Solar Acceleration
[NASA-CR-190195] p 3020 N92-26437
Running a conference as a clean product. International Conference on Pollution Prevention: Clean technologies and clean products
[PB92-109099] p 2930 N92-26495
SOLTECH 1992 proceedings: Solar Process Heat Program, volume 1
[DE92-001238] p 2927 N92-26683
International Conference on Japanese Earth Observation Programs: TRMM Workshop
[JTN-92-80345] p 2922 N92-26701
International Conference on Japanese Earth Observation Programs: Plenary Session
[JTN-92-80342] p 2924 N92-26742
Proceedings of the 5th and 6th Seminars on Investigation and Control of Boundary-Layer Transition
[NAL-SP-12] p 2901 N92-26906
Report of the CC1 working group on climate change detection
[WCDMP-14] p 2947 N92-26923
CC1 experts meeting on CLIMAT code adaptation
[WCDMP-15] p 2947 N92-26924
Report of the CC1 experts meeting on tracking and transmission of climate system monitoring information
[WCDMP-16] p 2947 N92-26925
LDEF: 69 Months in Space. First Post-Retrieval Symposium, part 3
[NASA-CP-3134-PT-3] p 3022 N92-27083
The 1990 NASA Aerospace Battery Workshop
[NASA-CP-3119] p 2862 N92-27130

CONFIDENCE LIMITS
Lower confidence limit expressions for P(X greater than y) and P(X greater than Y) under normality
[AD-A245787] p 2989 N92-26177

CONICAL BODIES
Focusing x ray transition radiation with cylindrical and elliptical optics
[AD-A245987] p 2997 N92-26754

CONNECTORS
LDEF fiber optic exposure experiment No. S-0109
p 2998 N92-27090

CONSERVATION EQUATIONS
A second-order bulk boundary layer model, revision
[AD-A245828] p 2905 N92-26934

CONSERVATION LAWS
On shock capturing for liquid and gas media
p 2897 N92-26556

CONSISTENCY
Verifying behavioral consistency of an object-oriented database schema
[REPT-91-054] p 3011 N92-26422
User interface consistency across end-user application programs: Effect on learning and satisfaction
p 3013 N92-26776

CONSTANTS
Determination of rates of reaction in the gas phase in the troposphere. Theory and practice. Part 3: Rate of indirect photoreaction
[PB92-150374] p 2944 N92-26838

CONTACT RESISTANCE
Effects of ultra-vacuum and space environment on contact ohmic resistance: LDEF experiment AO 138-11
p 2895 N92-27118

CONTAINERLESS MELTS
The experiment under microgravity by aircraft: The experiment in floating by gas flow p 2886 N92-26447

CONTAMINANTS
Noxious matter transportation in the Alpine regions
p 2934 N92-26332
A finite element/finite difference approach for modeling three-dimensional flow and pollutant dispersion around structures
[DE92-007322] p 2934 N92-26935

CONTAMINATION
The interaction of a vortex ring with a contaminated free surface p 2900 N92-26785
LDEF fiber optic exposure experiment No. S-0109
p 2998 N92-27090
Contamination of optical surfaces in Earth orbit
p 2999 N92-27099

CONTINGENCY
Report for neutral buoyancy simulations of transfer orbit stage contingency extravehicular activities
[NASA-TM-103583] p 2857 N92-26268

CONTINUITY EQUATION
Ensuring mass conversion in a heavy-gas dispersion model using the generalized anelastic equations
[DE92-007323] p 2934 N92-26936

CONTINUOUS RADIATION
Transportable 5 MW power supply system for gyrotron operation
[DE92-009051] p 2892 N92-26224

CONTINUOUS SPECTRA
Non-compact WZW conformal field theories
[PB92-125038] p 3007 N92-26805

CONTINUUM MECHANICS
Hamiltonian lattice field theory: Computer calculations using variational methods
[DE92-010479] p 2985 N92-26232
Compressive damage and fracture modeling of ceramic subjected to high-velocity impact p 2881 N92-26492
Eulerian computational methods
[DE92-008017] p 2900 N92-26853

CONTINUUMS
Mode structure and continuum damping of high-n toroidal Alfven eigenmodes
[DE92-010547] p 2999 N92-26256
Eulerian computational methods
[DE92-008017] p 2900 N92-26853

CONTOURS
Design guide for saddle seating on small high-speed craft
[ISVR-TR-205] p 2956 N92-26891

CONTRACTORS
Kennedy Space Center: Decision on photographic requirements appears justified
[GAO/NSIAD-92-192] p 3009 N92-26828

CONTRAILS
Cirrus clouds and condensation trail on 18 Oct. 1989 over the North sea (ICE '89). Determination of height and optical depth using ALEX, AVHRR and HIRS
p 2940 N92-26340

CONTROL EQUIPMENT
Time optimal trajectories for mobile robots with two independently driven wheels
[DE92-010002] p 2913 N92-26219
DoD implementation guidelines for Electronic Data Interchange (EDI), volume 2
[AD-A246614] p 3013 N92-26767
Nickel-hydrogen LEO cycling at 20 percent - 50 percent DOD p 2867 N92-27168

CONTROL STABILITY
Hybrid efficient control algorithms for robot manipulators
[AD-A245716] p 2981 N92-26428

CONTROL SURFACES
Thermal control surfaces experiment flight system performance p 2860 N92-27116

CONTROL SYSTEMS DESIGN
Adaptive control of robotic manipulators with structural flexibility p 2914 N92-26475
Parameter robust reduced-order control of flexible structures p 2982 N92-26597
A design rationale for NASA TileWorld
[NASA-TM-107882] p 2982 N92-26627
Application of decentralized control to a laser alignment system
[DE92-009692] p 2912 N92-26646
Experiments in modelling and end-point control of two-link flexible manipulators p 2915 N92-26731
Using min-max of torque to resolve redundancy for a mobile manipulator
[DE92-000070] p 2915 N92-26750
DoD implementation guidelines for Electronic Data Interchange (EDI), volume 2
[AD-A246614] p 3013 N92-26767
Structural dynamic interaction with solar tracking control for evolutionary Space Station concepts
[NASA-TM-107629] p 2920 N92-26903
Nickel-hydrogen LEO cycling at 20 percent - 50 percent DOD p 2867 N92-27168

CONTROLLED ATMOSPHERES
Higher plant growth in closed environment: Preliminary experiments in life support facility at ESA-ESTEC
p 2951 N92-26978

CONTROLLERS
Parameter robust reduced-order control of flexible structures p 2982 N92-26597
Experiments in modelling and end-point control of two-link flexible manipulators p 2915 N92-26731

CONVECTION
Surface energy budget and evapotranspiration measurement support
[NASA-CR-190059] p 2944 N92-26185
Incoherent scatter radar measurements of the cusp
p 2936 N92-26303
Cusp studies with HF radars p 2936 N92-26304
Solar wind-magnetosphere coupling processes observed near the dayside cusp/cleft
p 2937 N92-26307
Ground-based studies of sensing magnetosphere/ionosphere interactions: Convection and substorms p 2937 N92-26311
Relationships between ionospheric and tail phenomena p 2938 N92-26317
A simple model for the convective boundary layer over wavy terrain with variable heat flux
p 2934 N92-26334
Investigation of convection over sea by aircraft observations p 2926 N92-26337
Convection wave studies over land and sea
p 2940 N92-26341
Mean and turbulent structure of the marine atmospheric boundary layer during cold air outbreaks of different intensities: Observational and modelling analyses
p 2942 N92-26489
Utilization of tropical convection data for meteorological operation
[TW-11] p 2924 N92-26712
TRMM and Asian monsoon --- tropical rainfall measuring mission
[TW-12] p 2924 N92-26713
Research plan for utilizing TRMM data in MRI --- tropical rainfall measuring mission
[TW-13] p 2924 N92-26714
Study of entrainment mechanisms in convective clouds
[NASA-CR-190223] p 2946 N92-26735

CONVECTION CLOUDS
Analysis of mixing mechanisms in numerically simulated convective clouds
[NASA-CR-190222] p 2946 N92-26736

CONVECTIVE FLOW
A simple model for the convective boundary layer over wavy terrain with variable heat flux
p 2934 N92-26334
Convection wave studies over land and sea
p 2940 N92-26341
Precipitation formation processes in convective and stratiform clouds as deduced by coordinated polarimetric radar and aircraft measurements p 2941 N92-26342
The composite structure of thermals as derived from aircraft observations p 2941 N92-26346
Measurements in the inhomogeneous convective boundary layer using three powered gliders
p 2942 N92-26350
Preliminary experiment of GDEF (Gas Dynamics Experiment Facility) p 2885 N92-26442
Numerical formulation for the prediction of solid/liquid change of a binary alloy
[NASA-CR-188468] p 2878 N92-26642

CONVECTIVE HEAT TRANSFER
The development of a model builder for a microcircuit substrate
[AD-A245765] p 2893 N92-26606
Effects of power pulsations on natural convection from discrete heat sources
[AD-A246557] p 3007 N92-26617

Progress towards understanding and predicting convection heat transfer in the turbine gas path
[NASA-TM-105674] p 2898 N92-26690

CONVERGENCE
Developments of solutions of some special elliptic equations at a corner
[PB92-148741] p 2986 N92-26503
Proximal minimization algorithms with cutting planes
[AD-A246436] p 2977 N92-26949

CONVERGENT NOZZLES
Acoustic interactions between an altitude test facility and jet engine plumes: Theory and experiments
[NASA-CR-190423] p 2853 N92-26405

COOLANTS
Conjugating binary systems: Advanced cooling liquids for use in spacecraft ATCS p 2905 N92-27027

COOLING
Buckling of unidirectional graphite/epoxy composite plates at low temperatures
[AD-A246602] p 2869 N92-26796

COOLING FLOWS (ASTROPHYSICS)
Evidence for cluster magnetic fields around radio galaxies p 3017 N92-26554

COOLING SYSTEMS
Analysis of frozen startup of high-temperature heat pipes and three-dimensional modeling of block-heated heat pipes
[AD-A245327] p 2896 N92-26379
Effectiveness of a selected microclimate cooling system in increasing tolerance time to work in the heat. Application to Navy Physiological Heat Exposure Limits (PHEL) curve 5
[AD-A246529] p 2952 N92-26470
Passive water hammer in pipes due to flashing
[DE92-004180] p 2899 N92-26699
Hypersonic aerospace vehicle leading edge cooling using heat pipe, transpiration and film cooling techniques p 3007 N92-26733
Integrated heat pipe concept for Li/SOCl2 cells cooling p 2895 N92-26974
Thermal analysis of evaporative coolers p 2962 N92-26985
The transpirator, an efficient and light evaporative cooler for space technology p 2887 N92-26986
CPA: A controlled pump assembly for two-phase loops applications p 2916 N92-26987
Flight test results of the passive cooling system p 2860 N92-27000
Conjugating binary systems: Advanced cooling liquids for use in spacecraft ATCS p 2905 N92-27027

COORDINATE TRANSFORMATIONS
Weight optimum arch structures
[AD-A246001] p 2918 N92-26759

COORDINATES
Representations in visual motion
[PB92-148287] p 2984 N92-26814

COPPER ALLOYS
Relationship between composition, structure, properties, thermo-mechanical processing and ballistic performance of tungsten heavy alloys
[AD-A245649] p 2876 N92-26172
Atomistic studies of grain boundaries in alloys and compounds
[DE92-010792] p 2877 N92-26251
Evaluation of plasma sprayed crucible coatings for melt processing copper-refractory metal alloys
[DE92-008912] p 2878 N92-26727

COPPER COMPOUNDS
Bis (pentamethylcyclopentadienyl) ytterbium: Electron-transfer reactions with organotransition metal complexes
[DE92-010300] p 2994 N92-26235
A novel process for methanol synthesis
[DE92-010465] p 2883 N92-26547

COPPER OXIDES
Recent results in characterization of melt-grown and quench-melt-grown YBCO superconductors
[DE92-010281] p 3001 N92-26210
Magnetic flux noise in copper oxide superconductors
[DE92-010299] p 3003 N92-26582
The Debye temperature of YBa2Cu3O(7-(delta)) and its dependence on the volume fraction of superconductivity
[DE92-010305] p 3003 N92-26584
Analysis of Yttrium-Barium-Copper-Oxide by x ray diffraction and mechanical characterization
[NASA-TM-104562] p 2869 N92-26650
Percolation effects in the V-I characteristics of granular YBa2Cu3O(7-delta)
[DE92-617541] p 3004 N92-26672
Structural coherence of the CuO2 planes of oxide superconductors: Is it a requirement for superconductivity?
[DE92-009724] p 3005 N92-26842
Lattice instabilities and structural phase transformations in La2CuO4 superconductors and insulators
[DE92-010045] p 3006 N92-27059

COPYRIGHTS
Survey of small business use of intellectual property protection
[PB92-151703] p 3009 N92-26523

CORE FLOW
Interface of an uncoupled boundary layer algorithm with an inviscid core flow algorithm for unsteady supersonic engine inlets
[NASA-TM-105684] p 2855 N92-27037

CORNERS
Developments of solutions of some special elliptic equations at a corner
[PB92-148741] p 2986 N92-26503

CORONAL HOLES
Workshop on Solar Activity, Solar Wind, Terrestrial Effects, and Solar Acceleration
[NASA-CR-190195] p 3020 N92-26437

CORRELATION DETECTION
Fast envelope correlation for passive ranging
[AD-A246333] p 2886 N92-26388

CORROSION
The application of XPS to the study of MIC
[DE92-010156] p 2879 N92-26813
Post-test examination of a pool boiler receiver
[NASA-TM-105635] p 2880 N92-27192

CORROSION RESISTANCE
Assessment of a hot hydrogen nuclear propulsion fuel test facility
[DE92-004571] p 2995 N92-26692
The application of XPS to the study of MIC
[DE92-010156] p 2879 N92-26813

CORROSION TESTS
Application of in situ x ray absorption and fluorescence measurements to analyze solutions in a simulated pit
[DE92-009159] p 2878 N92-26563

COSINE SERIES
VHDL behavioral description of discrete cosine transform in image compression
[AD-A245389] p 2972 N92-26248

COSMIC BACKGROUND EXPLORER SATELLITE
Conceptual design study for the use of COBE rocket engines on the Tropical Rainfall Measuring Mission
[NASA-CR-190383] p 2945 N92-26535
COBE battery overview: History, handling, and performance p 2882 N92-27131

COSMIC RAY SHOWERS
Simultaneous observations of extensive air showers and underground muons at Soudan 2
[DE92-010282] p 3020 N92-26211
Muon/electron separation for atmospheric neutrino interactions
[DE92-010349] p 3021 N92-26218
Composition studies based on coincident air shower array and underground muon data
[DE92-010345] p 3021 N92-26253
Interpretation of distributions on K(sub pi)(sup 0) in pFe, nFe, and piFe interactions at 0.5-5.0 TeV in the framework of contemporary models
[DE92-621189] p 3021 N92-26804

COSMIC RAYS
Underground muons from the direction of Cygnus X-3 during the January 1991 radio flare
[DE92-010346] p 3021 N92-26215
A search for magnetic monopoles with the Soudan 2 detector
[DE92-010347] p 3021 N92-26216
Composition studies based on coincident air shower array and underground muon data
[DE92-010345] p 3021 N92-26253

COSMIC X RAYS
Underground muons observed in the Soudan 2 detector from the directions of x ray sources
[DE92-010344] p 3021 N92-26264

COSMOLOGY
Topics in particle physics and cosmology
[DE92-010478] p 3019 N92-26385
Analytical and numerical investigation of nonlinear gravitational clustering p 3017 N92-26578
Finite temperature quantum field theory in curved spacetime p 3007 N92-26780

COST ANALYSIS
An analysis of commitment strategies in planning: The details
[NASA-TM-107681] p 2983 N92-26643
Measuring the effectiveness of information systems
[AD-A246007] p 3013 N92-26762

COST EFFECTIVENESS
Information technology resources assessment
[DE92-009498] p 3011 N92-26221
A comparison of heavy lift launch vehicle options for the 1990s
[AD-A245617] p 2857 N92-26402
A prototype multi-media data base for tracking interface relationships and performing cost tradeoffs for the Sea Launch and Recovery (SEALAR) space launch system
[AD-A245481] p 2857 N92-26515

COST ESTIMATES
Investigating the utility of coupling COCOMO with a system dynamics simulation of software development
[AD-A245484] p 2973 N92-26400
Environmental implications of increased biomass energy use
[DE92-001219] p 2932 N92-26810

COST REDUCTION
Kennedy Space Center: Decision on photographic requirements appears justified
[GAO/NSIAD-92-192] p 3009 N92-26828
Innovative techniques for the production of low cost 2D laser diode arrays
[AD-A247282] p 2913 N92-27178

COSTS
An electroplater's view of PVD processing
[DE92-009052] p 2878 N92-26732

COUETTE FLOW
Acoustically probed Taylor-Couette flow apparatus
[AD-A246385] p 2993 N92-27076

COULOMB COLLISIONS
Destruction and excitation of accreted nuclei in neutron star atmospheres: Gamma ray lines and x ray bursts p 3016 N92-26476

COUNTERMEASURES
LBNP as countermeasure: An automated scenario p 2953 N92-27012

CRACK ARREST
Crack arrest and static fracture toughness tests of a ship plate steel
[AD-A245641] p 2916 N92-26282

CRACK GEOMETRY
Crack arrest and static fracture toughness tests of a ship plate steel
[AD-A245641] p 2916 N92-26282

CRACK PROPAGATION
Crack arrest and static fracture toughness tests of a ship plate steel
[AD-A245641] p 2916 N92-26282
On the stochastic fatigue crack growth problem p 2917 N92-26557
Failure studies of bimaterial interfaces and constrained ductile layers p 2868 N92-26559
Simulation of 3D non-planar fatigue crack growth in a turbine blade root
[DE92-006859] p 2854 N92-26697
Studies of rain erosion mechanisms in a range of IR transmitting ceramics including coated samples
[AD-A245299] p 2882 N92-26751
Fracture of structural ceramics in combined mode 1 and mode 2 loading p 2882 N92-26775

CRACK TIPS
Fracture of structural ceramics in combined mode 1 and mode 2 loading p 2882 N92-26775

CRACKS
On the stochastic fatigue crack growth problem p 2917 N92-26557
Fracture of structural ceramics in combined mode 1 and mode 2 loading p 2882 N92-26775
Novel molecular sources for dispersing boron in carbon-carbon composites
[AD-A246999] p 2870 N92-26882

CREEP PROPERTIES
Analysis and modeling of high-temperature performance of advanced fiber composites p 2868 N92-26564
Modeling cycle and time-dependent creep/relaxation effects on fatigue lives of notched members --- creep/relaxation p 2919 N92-26629
Predictability of long-term creep and rupture in a nozzle-to-sphere vessel model
[DE92-008099] p 2919 N92-26845
Improving the fracture resistance of irradiated martensitic steels
[DE92-006387] p 2879 N92-26848

CREW PROCEDURES (INFLIGHT)
Human factors in the conception of the Hermes space vehicle p 2963 N92-26989
Logistics in space: Tools to support astronauts p 2963 N92-26990
Engineering of a new overall system to improve the interaction between the crew and the ground-based scientists and personnel p 2964 N92-26995

CREW WORKSTATIONS
CAD system for HFE analyses: Zero-g posture in optimisation of Columbus APM crew workstations --- human factors engineering p 2963 N92-26991
Crew support equipment: Identification and definition of additional hardware for Columbus APM laboratory habitability p 2964 N92-26993
Engineering of a new overall system to improve the interaction between the crew and the ground-based scientists and personnel p 2964 N92-26995

CRITICAL PRESSURE
Oxygen recombination in the sealed nickel-cadmium cell p 2863 N92-27138

CROSS CORRELATION
Source location in thin plates using crosscorrelation
[AD-A245521] p 2992 N92-26678
CROSS FLOW
CFD mixing analysis of jets injected from straight and slanted slots into confined crossflow in rectangular ducts
[NASA-TM-105699] p 2854 N92-26561
CROSSLINKING
A fractal computer model of macromolecule-cell surface interactions
[AD-A245394] p 2950 N92-26289
CROSSOVERS
Crossovers of the density of states in two-direction double-barrier resonant-tunneling structures
[AD-A246124] p 3005 N92-26684
RF vacuum microelectronics
[AD-A246579] p 2893 N92-26771
CRUCIBLES
Evaluation of plasma sprayed crucible coatings for melt processing copper-refractory metal alloys
[DE92-008912] p 2878 N92-26727
CRYOGENIC COOLING
Laser cooling and trapping of atoms and particles
[AD-A247208] p 2913 N92-27173
CRYOGENIC EQUIPMENT
Cryogenic detector development
[MPI-PHE/91-07] p 2906 N92-26391
Cryogenic calorimeters for dark matter and neutrinos p 2907 N92-26392
CRYSTAL DEFECTS
Why first-principles calculations for alloys?
[DE92-010285] p 2877 N92-26213
Atomistic studies of grain boundaries in alloys and compounds
[DE92-010792] p 2877 N92-26251
Simulation studies for surfaces and materials strength
[NASA-CR-190340] p 3001 N92-26265
Computational techniques in tribology and material science at the atomic level
[NASA-TM-105573] p 2990 N92-26671
CRYSTAL GROWTH
Recent results in characterization of melt-grown and quench-melt-grown YBCO superconductors
[DE92-010281] p 3001 N92-26210
A surface science investigation of silicon carbide: Oxidation, crystal growth and surface structural analysis
[DE92-010286] p 3004 N92-26641
Results of the TTF-TCNQ and the calcium carbonate crystallization on the Long Duration Exposure Facility p 3007 N92-27127
CRYSTAL LATTICES
Hamiltonian lattice field theory: Computer calculations using variational methods
[DE92-010479] p 2985 N92-26232
Simulation studies for surfaces and materials strength
[NASA-CR-190340] p 3001 N92-26265
CRYSTAL OSCILLATORS
Characterization of the clock in a new inexpensive GPS receiver: The Magnavox MX 4200
[AD-A246165] p 2851 N92-26415
Radiation sensitivity of quartz crystal oscillators experiment for the Long Duration Exposure Facility (LDEF) p 2895 N92-27111
CRYSTAL STRUCTURE
Development and applications of the reverse neutron time-of-flight method with Fourier-type beam chopper
[VTT-PUBL-82] p 3001 N92-26320
Determination of the structure of Y(HCOO)3 by the neutron time-of-flight diffraction method p 3002 N92-26325
Anomalous structural behaviour of the high-temperature superconducting compound La(1.8)Sr(0.2)CuO(4-y) p 3003 N92-26327
Neutron powder diffraction study on Eu-substituted Bi2Sr2CaCu2O(8+y) high temperature superconductor p 3003 N92-26328
A comprehensive review of the XRD data of the primary and secondary phases present in the BSCCO superconductor system
[DE92-010363] p 3003 N92-26579
Crystalline-amorphous interfaces and their relation to grain boundary films
[DE92-009812] p 3004 N92-26648
Computational techniques in tribology and material science at the atomic level
[NASA-TM-105573] p 2990 N92-26671
Structural coherence of the CuO2 planes of oxide superconductors: Is it a requirement for superconductivity?
[DE92-009724] p 3005 N92-26842
Some experiences with absorption, phonon Raman, and luminescence spectroscopic probes of crystal structure of f-element compounds
[DE92-007828] p 3006 N92-26851
CRYSTALLINITY
Magnetic anisotropy from first principles
[ISBN-90-9004483-3] p 2877 N92-26252
CRYSTALLIZATION
Results of the TTF-TCNQ and the calcium carbonate crystallization on the Long Duration Exposure Facility p 3007 N92-27127
CRYSTALS
Why first-principles calculations for alloys?
[DE92-010285] p 2877 N92-26213
Design of a high-precision tunable double crystal monochromator
[DE92-010137] p 2909 N92-26572
CULTURE (SOCIAL SCIENCES)
Multi-cultural components and keys for European worldwide space programs p 2857 N92-27008
CURIUM ISOTOPES
Gas phase chromatography of halides of elements 104 and 105
[DE92-010284] p 2870 N92-26212
CURRENT AMPLIFIERS
Silicon drift chambers with integrated amplifiers as low energy detectors p 2908 N92-26398
CURRENT DENSITY
Investigation of deep dielectric charging and subsequent currents on geosynchronous spacecraft
[AD-A245764] p 2858 N92-26605
CURVATURE
Algorithms for blending surface generation
[AD-A245686] p 2975 N92-26524
Recognition of 3-D symmetric objects from range images in automated assembly tasks
[NASA-CR-187664] p 2886 N92-26656
Finite temperature quantum field theory in curved spacetime p 3007 N92-26780
CUTTING
Proximal minimization algorithms with cutting planes
[AD-A246436] p 2977 N92-26949
CYCLES
Cycle life characteristics of Li-TiS2 cells p 2865 N92-27154
Evaluation of sodium-nickel chloride cells for space applications p 2865 N92-27156
Nickel-hydrogen LEO cycling at 20 percent - 50 percent DOD p 2867 N92-27168
CYCLIC HYDROCARBONS
The carbon isotopic compositions of individual compounds from ancient and modern depositional environments p 2921 N92-26478
Polycyclic aromatic hydrocarbon radiative properties and formation in carbon-rich stellar outflows p 3018 N92-26757
CYCLIC LOADS
Degradation and buckling of metal tubes under cyclic bending and external pressure p 2920 N92-26869
CYCLONES
The stability of barotropic vortices: Implications for tropical cyclone motion p 2940 N92-26335
Characteristics of upper-level and boundary layer forcing in Western Pacific cyclones
[AD-A246301] p 2945 N92-26364
CYCLOTRON RESONANCE DEVICES
Transportable 5 MW power supply system for gyrotron operation
[DE92-009051] p 2892 N92-26224
Diagnostic upgrades on MTX
[DE92-009695] p 2906 N92-26230
Installation and operation of the 400 kW 140 GHz gyrotron on the MTX experiment
[DE92-009053] p 2906 N92-26377
CYLINDRICAL BODIES
Materials compatibility and wall stresses in hydride storage beds
[DE92-009432] p 2870 N92-26201
Fiber-optic flexural disk accelerometer
[AD-A246203] p 2908 N92-26459
Focusing x ray transition radiation with cylindrical and elliptical optics
[AD-A245987] p 2997 N92-26754
Three dimensional boundary layer transition on a yawed cylinder p 2902 N92-26909
Acoustically probed Taylor-Couette flow apparatus
[AD-A246385] p 2993 N92-27076
CYLINDRICAL SHELLS
Dynamic response of cylindrical shells to underwater end-on explosion
[AD-A245804] p 2920 N92-26932

D

DAMAGE
Fail safe system for suppressing stimulated Brillouin scattering in large optics on the Nova laser
[DE92-008608] p 2911 N92-26505
DAMAGE ASSESSMENT
Composite fuselage technology (summary of year 2)
[NASA-CR-190434] p 2852 N92-26655
Finite element modeling of static indentation damage in laminated composites p 2869 N92-26827
Penetration of laminated composites by projectiles p 2869 N92-26861
DAMPING
Mode structure and continuum damping of high-n toroidal Alfven eigenmodes
[DE92-010547] p 2999 N92-26256
Scenarios for the nonlinear evolution of alpha particle induced Alfven wave instability
[DE92-010549] p 3000 N92-26550
DARK ADAPTATION
Conquest of darkness by management of the stars
[AD-A245496] p 2997 N92-26676
DARK MATTER
Cryogenic calorimeters for dark matter and neutrinos p 2907 N92-26392
Supersymmetry and dark matter, a new candidate p 3016 N92-26491
DASSAULT AIRCRAFT
The DLR meteorological research aircraft Falcon p 2941 N92-26348
DATA ACQUISITION
Optical ground-based network p 2937 N92-26313
The DLR meteorological research aircraft Falcon p 2941 N92-26348
Biomedical data acquisition and processing technology p 2885 N92-26446
Role of climate in forest monitoring and assessment: A New England example
[PB92-132885] p 2930 N92-26519
The status of GALLEX
[DE92-010077] p 3020 N92-26566
Development and testing of an unmanned air vehicle telemetry system
[AD-A246577] p 2858 N92-26621
An assessment of satellite remote sensing for land cover classification p 2922 N92-26625
Climate research at regional climate centers in 1991
[PB92-160399] p 2946 N92-26822
Managing Federal information resources: Under the Paperwork Reduction Act of 1980
[PB92-154905] p 3014 N92-26926
A processing environment for test and simulation data of thermodynamic systems p 2959 N92-26963
Nickel-hydrogen LEO cycling at 20 percent - 50 percent DOD p 2867 N92-27168
DATA BASE MANAGEMENT SYSTEMS
The requirements for data exchange between Cluster and ground-based observatories, using EISCAT as an illustrative example p 2938 N92-26316
A computer system for access to distributed genome mapping data
[DE92-008875] p 3011 N92-26453
Data Management Systems (DMS): Complex data types study. Volume 1: Appendices A-B. Volume 2: Appendices C1-C5. Volume 3: Appendices D1-D3 and E
[NASA-CR-190397] p 3009 N92-26552
Technical specification for the Sandia Management Restructure Study Team (MRST) Prototype Information System
[DE92-010360] p 3012 N92-26575
Volatile Organic Compound (VOC) and Particulate Matter (PM) speciation data system user's manual, version 1.4
[PB92-105527] p 2932 N92-26823
Building a GIS on top of the open DBMS Postgres
[FEL-91-B183] p 3014 N92-26875
DATA BASES
The development of a design database for the computer aided prototyping system
[AD-A245786] p 3010 N92-26176
Testbank (1.0) user's manual
[AD-A245895] p 2971 N92-26196
Recursive ray acoustics for three-dimensional sound-speed profiles
[AD-A245613] p 2991 N92-26228
Maintenance manual for Natick's Footwear Database
[AD-A246273] p 2954 N92-26242
User manual for Natick's Footwear Database
[AD-A246275] p 2954 N92-26243
Life support research and development, a Department of Energy program for the Space Exploration Initiative
[DE92-007681] p 2955 N92-26375
Composite strength statistics from fiber strength statistics
[AD-A245616] p 2867 N92-26383
Quantitative assessment of the slope resolution of seafloor mapping systems
[AD-A246158] p 2949 N92-26411
The SOL object-oriented database language
[REPT-91-053] p 2973 N92-26421

Verifying behavioral consistency of an object-oriented database schema
[REPT-91-054] p 3011 N92-26422
Cataloging guidelines
[AD-A246500] p 3011 N92-26465
Information liability: New interpretations for the electronic age --- online databases
p 3012 N92-26481
Global assessment of promising forest management practices for sequestration of carbon
[PB92-153006] p 2930 N92-26510
A prototype multi-media data base for tracking interface relationships and performing cost tradeoffs for the Sea Launch and Recovery (SEALAR) space launch system
[AD-A245481] p 2857 N92-26515
Technical specification for the Sandia Management Restructure Study Team (MRST) Prototype Information System
[DE92-010360] p 3012 N92-26575
The effect of collection homogeneity on term association as a method of request expansion in information retrieval p 3012 N92-26614
A modeling strategy for large-scale optimization based on analysis and visualization principles
[AD-A246570] p 2987 N92-26620
A prototype semantic integrity front end expert system for a relational database
[AD-A246084] p 3013 N92-26765
Volatile Organic Compound (VOC) and Particulate Matter (PM) speciation data system user's manual, version 1.4
[PB92-105527] p 2932 N92-26823
Test plan for the international aircraft operator information system
[DOT/FAA/CT-91/18] p 3014 N92-26830
F-111C flight dynamic model aerodynamic data-base development and verification
[AD-A246356] p 2850 N92-26947
Integrated communication environment for thermal analysis software p 2958 N92-26959
AVHRR satellite data: Users guide for accessing NOARL archives
[AD-A246142] p 2926 N92-27070
Documentation for the Semi-Automated Mesoscale Analysis System 1.1
[AD-A246144] p 2985 N92-27072

DATA COMPRESSION

VHDL behavioral description of discrete cosine transform in image compression
[AD-A245389] p 2972 N92-26248
Discrete sequence prediction and its applications
[NASA-TM-107865] p 2984 N92-26791

DATA CORRELATION

Data fusion and correlation techniques testbed (DFACTT): Field trial 14 January 1991
[AD-A245324] p 3011 N92-26378

DATA FLOW ANALYSIS

Verifying behavioral consistency of an object-oriented database schema
[REPT-91-054] p 3011 N92-26422

DATA LINKS

Requirements analysis and design for implementation of a satellite link for a local area computer network
[AD-A245610] p 2978 N92-26227
Scalable coherent interface: Links to the future
[DE92-010728] p 2887 N92-26267
Selection and specification of a data link protocol for VSAT based inter-LAN communications
[AD-A246289] p 2979 N92-26361
Preliminary analyses of WL experiment No. 701, space environment effects on operating fiber optic systems
p 2998 N92-27089

DATA MANAGEMENT

Software requirements document for the netCDF interface within ECMOP, version 1.0
[AD-A246220] p 2974 N92-26464
Data Management Systems (DMS): Complex data types study. Volume 1: Appendices A-B. Volume 2: Appendices C1-C5. Volume 3: Appendices D1-D3 and E
[NASA-CR-190397] p 3009 N92-26552
Dimensional analysis of structural steel beam design
[AD-A245759] p 2917 N92-26593
DoD implementation guidelines for Electronic Data Interchange (EDI), volume 2
[AD-A246614] p 3013 N92-26767

DATA PROCESSING

Optical ground-based network p 2937 N92-26313
Data fusion and correlation techniques testbed (DFACTT): Field trial 14 January 1991
[AD-A245324] p 3011 N92-26378
Development of TRMM radar rainfall retrieval algorithms
[TW-7] p 2923 N92-26708
Forging a path with tool and data attributes
[DE92-009800] p 2976 N92-26797
A processing environment for test and simulation data of thermodynamic systems p 2959 N92-26963

DATA PROCESSING TERMINALS

An adaptive, packet-switched HF data terminal: Functional overview and initial performance
[AD-A246318] p 2973 N92-26292

DATA REDUCTION

Development of TRMM radar rainfall retrieval algorithms
[TW-7] p 2923 N92-26708

DATA STORAGE

Magneto-optical multilayers --- optical data storage
[DE92-009726] p 2997 N92-26565
Building a GIS on top of the open DBMS Postgres
[FEL-91-B183] p 3014 N92-26875
Algorithms for capacity computations and algebraic cascade coding with applications to data storage
p 2977 N92-27053

DATA STRUCTURES

Generation of multi-resolution maps
[PB92-152206] p 2921 N92-26513
Definition of the common structure of data to promote the communication between different thermal software tools p 2958 N92-26960

DATA SYSTEMS

Handbook of solar-terrestrial data systems, version 1
[NASA-TM-107810] p 3019 N92-26191
The requirements for data exchange between Cluster and ground-based observatories, using EISCAT as an illustrative example p 2938 N92-26316
Small Explorer Data System MIL-STD-1773 fiber optic bus
[NASA-TP-3227] p 2858 N92-26667
The navigation data logger for a suitcase navigation system
[AD-A245997] p 2851 N92-26756
Functional requirements document for NASA/MSFC Earth Science and Applications Division: Data and information system (ESAD-DIS). Interoperability, 1992
[NASA-TM-4388] p 2921 N92-26905
Computer Program Estimate Trend (ESTREND): A system for the detection of trends in water-quality data
[PB92-147727] p 2933 N92-26931

DATA TRANSFER (COMPUTERS)

Integrated communication environment for thermal analysis software p 2958 N92-26959
Definition of the common structure of data to promote the communication between different thermal software tools p 2958 N92-26960
A processing environment for test and simulation data of thermodynamic systems p 2959 N92-26963

DATA TRANSMISSION

Parabolic flight: Reports of microgravity experiments by aircraft, volume 1, no. 2
[EG-910045] p 2884 N92-26440
Buffered serial data card
[AD-A246435] p 2852 N92-26948

DAYTIME

A model of the dayside magnetosphere and breakups in the cusp region p 2937 N92-26312
Imaging the Earth's magnetosphere using ground magnetometer arrays p 2938 N92-26314
Mathematical model of physical processes responsible for generation of magnetospheric electric fields and their penetration into the Earth's magnetosphere
p 2938 N92-26319

DEAD RECKONING

Dead reckoning navigation for walking robots
[NASA-CR-190296] p 2982 N92-26429

DEATH

Sturm-Liouville eigenfunctions expressed in determinant form
[AD-A245991] p 2987 N92-26755

DECISION MAKING

Using solid modeling techniques to construct three-dimensional icons for a visual simulator
[AD-A245784] p 2971 N92-26195
Measuring uncertainty by extracting fuzzy rules using rough sets
[NASA-CR-190395] p 2972 N92-26198
Knowledge-based production management: Approaches, results, and prospects
[AD-A245714] p 3008 N92-26426
Computer modeling of human decision making
[NASA-TM-107868] p 2983 N92-26630
MoCog1: A computer simulation of recognition-primed human decision making
[NASA-TM-107872] p 2984 N92-26888

DECISION THEORY

Extracting fuzzy rules under uncertainty and measuring definability using rough sets
[NASA-CR-190396] p 2972 N92-26197

DECODING

Implementation of multi-frequency modulation with Trellis encoding and Viterbi decoding using a digital signal processing board
[AD-A245998] p 2976 N92-26758
Algorithms for capacity computations and algebraic cascade coding with applications to data storage
p 2977 N92-27053

DECOMPOSITION

Equilibrium-analysis of projected climate change effects on the global soil organic matter pool
[PB92-153022] p 2930 N92-26509
Decomposition of bipartite graphs under degree constraints
[PB92-148626] p 2988 N92-26817
On testing models for the pressure-strain correlation of turbulence using direct simulations
[NASA-CR-189638] p 2901 N92-26883

DECOUPLING

High-alpha vortex decoupling investigations on a chine forebody/Delta wing configuration at transonic Mach numbers
[NASA-CR-189642] p 2849 N92-26651

DEFECTS

Simulation of 3D non-planar fatigue crack growth in a turbine blade root
[DE92-006859] p 2854 N92-26697

DEFENSE INDUSTRY

Best value contracting in the procurement of engineering and technical services
[AD-A245524] p 3009 N92-26660

DEFENSE PROGRAM

The role of the B-2 in the new US defense strategy
[RAND-P-7744] p 2990 N92-26194
Cataloging guidelines
[AD-A246500] p 3011 N92-26465
The Department of Defense critical technologies plan for the Committees on Armed Services, United States Congress
[AD-A234900] p 3010 N92-27190

DEFLECTION

Effect of temperature and gap opening rate on the resiliency of candidate solid rocket booster O-ring materials
[NASA-TP-3226] p 2883 N92-27194

DEFORMATION

Deformation behavior of an age-hardenable Beta+Alpha-Two titanium alloy
[AD-A246362] p 2879 N92-26939

DEGRADATION

Degradation and buckling of metal tubes under cyclic bending and external pressure p 2920 N92-26869
An overview of the first results on the solar array materials passive LDEF experiment (sample), A0171
p 2927 N92-27087

DEGREES OF FREEDOM

Man-machine aspects of remotely controlled space manipulators
[ISBN-90-370-0056-8] p 2954 N92-26255

DELAY LINES

Performance enhancement of the NPS Transient Electromagnetic Scattering Laboratory
[AD-A246300] p 2888 N92-26363

DELTA WINGS

High-alpha vortex decoupling investigations on a chine forebody/Delta wing configuration at transonic Mach numbers
[NASA-CR-189642] p 2849 N92-26651
Subsonic investigations of vortex interaction control for enhanced high-alpha aerodynamics of a chine forebody/Delta wing configuration
[NASA-CR-189641] p 2849 N92-26652

DENSIFICATION

Spheroidization and densification of Nickel powders by RF-induction plasma
[PB92-151893] p 2879 N92-26787

DEPLOYMENT

Safety testing of lithium cells p 2864 N92-27150

DEPOLARIZATION

Polarisation effects in fibre lasers
p 2911 N92-26571

DEPOSITION

Photocathode transfer and storage techniques using alkali vapor feedback control
[DE92-008449] p 2891 N92-26202
Investigation of deep dielectric charging and subsequent currents on geosynchronous spacecraft
[AD-A245764] p 2858 N92-26605

DEPTH MEASUREMENT

Quantitative assessment of the slope resolution of seafloor mapping systems
[AD-A246158] p 2949 N92-26411

DESCRIPTIVE GEOMETRY

Geometry and mass model of ionizing radiation experiments on the LDEF satellite
[NASA-CR-184325] p 2993 N92-26200

DESIGN ANALYSIS
Hardware synthesis using high-level Petri nets
[REPT-91-071] p 2970 N92-26439
An infrared Michelson stellar interferometer and its applications p 3015 N92-26477
Design of a high-precision tunable double crystal monochromator
[DE92-010137] p 2909 N92-26572
Dimensional analysis of structural steel beam design
[AD-A245759] p 2917 N92-26593
Zirconia-based fuel cells for power generation
[DE92-009886] p 2927 N92-26719
Rule-based expert system for evaluating the quality of long-term, in-situ, gas chromatographic measurements of atmospheric methane
[PB92-128560] p 2876 N92-26812
Evaluation of integral measurements for the SP-100 space reactor
[DE92-009717] p 2996 N92-26841
Structural dynamic interaction with solar tracking control for evolutionary Space Station concepts
[NASA-TM-107629] p 2920 N92-26903
Unified computational method for design of fluid loop systems p 2905 N92-26962
Heat pipe-based radiative panel p 2859 N92-26968
Impact of diet on the design of waste processors in CELSS p 2961 N92-26980
Magellan battery operations: An overview p 2862 N92-27133
Super NiCd battery program: History and performance p 2862 N92-27135
Hughes advanced nickel-cadmium batteries: An update p 2862 N92-27136

DESORPTION
A new phase in palladium hydride technology
[DE92-009852] p 2875 N92-26718

DESTRUCTION
Destruction and excitation of accreted nuclei in neutron star atmospheres: Gamma ray lines and x ray bursts p 3016 N92-26476

DETECTION
Differentiation on genus of aquatic macrophytes through remote sensing in the Tucurui Reservoir, Para State, Brazil
[INPE-5315-PRE/1712] p 2951 N92-26721

DETERMINANTS
Sturm-Liouville eigenfunctions expressed in determinant form
[AD-A245991] p 2987 N92-26755

DETONATION WAVES
Theoretical and numerical study of flame propagation and transition to detonation --- detonation transition p 2874 N92-26615
Shock-turbulence interactions in a reacting flow
[NASA-CR-189647] p 2905 N92-27032

DEUTERIUM
Calibration of CR-39 for detecting fusion neutrons
[DE92-009063] p 2993 N92-26225
Infrared spectroscopy and hydrogen isotope geochemistry of hydrous silicate glasses
[DE92-008398] p 2881 N92-26451
Metal hydride based isotope separation: Large-scale operations
[DE92-009830] p 2875 N92-26717

DEUTERONS
Li-6,d reaction on sd-, fp- and g-shell nuclei in ZR- and FR-DWBA formalisms
[DE92-614353] p 2994 N92-26365

DIAMOND FILMS
Fundamental studies of the chemical vapor deposition of diamond
[DE92-010327] p 2881 N92-26543
Influence of substrate topography on the nucleation of diamond thin films
[DE92-010777] p 2883 N92-27060

DIAMONDS
Fundamental studies of the chemical vapor deposition of diamond
[DE92-010327] p 2881 N92-26543

DICHROISM
Time-resolved laser studies on the proton pump mechanism of bacteriorhodopsin
[DE92-003218] p 2951 N92-26493

DIELECTRIC PERMEABILITY
Dynamic properties of quasi-two-dimensional one component plasmas
[DE92-621523] p 3000 N92-26806
Dielectric tensor of strongly coupled plasmas
[DE92-621524] p 3001 N92-26807

DIELECTRIC PROPERTIES
Cluster model of polarization reflection from metallic surfaces
[AD-A245781] p 2996 N92-26241
Measurement electronics of industrial microwave resonator sensors
[PB92-152750] p 2909 N92-26786
Static, microwave, infrared, and visible permittivity related to chemical structure: N-methylacetamide, N-dimethylacetamide and their mixtures in CCl4 at 32 C
[AD-A246364] p 2991 N92-26940

DIELECTRICS
Exact solutions for a mode of the electromagnetic field in a resonator with time-dependent characteristics of the internal medium
[AD-A245700] p 2888 N92-26374
Signal-to-noise ratio expected for a calorimeter with transition edge thermometer p 2907 N92-26395
Investigation of deep dielectric charging and subsequent currents on geosynchronous spacecraft
[AD-A245764] p 2858 N92-26605
Analysis of surface wave propagation in a grounded dielectric slab covered by a resistive sheet
[NASA-TM-107583] p 2889 N92-26653
Dielectric tensor of strongly coupled plasmas
[DE92-621524] p 3001 N92-26807

DIETS
Impact of diet on the design of waste processors in CELSS p 2961 N92-26980
An evaluative study of the sensory qualities of selected European and Asian foods for international space missions (a French food study) p 2966 N92-27009

DIFFERENCE EQUATIONS
Quantum black holes and Hawking's radiation
[PB92-152313] p 3018 N92-26833

DIFFERENTIAL EQUATIONS
Recursive ray acoustics for three-dimensional sound-speed profiles
[AD-A245613] p 2991 N92-26228
Neural network error correction for solving coupled ordinary differential equations
[NASA-TM-101796] p 2986 N92-26407
Nonexpansive prolongations and difference schemes for the advection equation
[PB92-141530] p 2986 N92-26502
Three-dimensional upwind scheme for solving the Euler equations on unstructured tetrahedral grids --- tetrahedral grids p 2849 N92-26585
Sturm-Liouville eigenfunctions expressed in determinant form
[AD-A245991] p 2987 N92-26755
Solution of the first-order form of the 3-D discrete ordinates equations on a massively parallel machine
[DE92-004575] p 2981 N92-26854

DIFFRACTION
Spectroscopic imaging, diffraction, and holography with x ray photoemission
[DE92-009142] p 2996 N92-26187

DIFFRACTION PATTERNS
A comprehensive review of the XRD data of the primary and secondary phases present in the BSCCO superconductor system
[DE92-010363] p 3003 N92-26579

DIFFRACTION RADIATION
Diffraction phenomena in spontaneous and stimulated radiation by relativistic particles in crystals (review)
[DE92-009501] p 3001 N92-26222

DIFFRACTOMETERS
The high resolution diffractometer mini-Sfinks p 3002 N92-26322
High-resolution Fourier TOF powder diffraction. 1: Performance of the Mini-Sfinks Facility p 3002 N92-26323

DIFFUSION
Two-phase flow of Newtonian and Non-Newtonian fluids in a porous medium applied to water coning
[PB92-151109] p 2900 N92-26836
Numerical solution of the equation of neutrons transport on plane geometry by analytical schemes using acceleration by synthetic diffusion
[DE92-621426] p 2995 N92-26844
Effect of interstitials on the trapping of hydrogen in iron-single crystals
[AD-A246412] p 3006 N92-27064

DIFFUSION FLAMES
Color image processing and object tracking workstation
[NASA-TM-105561] p 2886 N92-26611
Microwave backscattering fuel/air ratio control and flame monitoring device
[PB92-141779] p 2876 N92-26783

DIFFUSIVITY
GAC adsorption of a mixture of natural organic matter and VOCs in the presence and absence of molecular oxygen
[PB92-153782] p 2928 N92-26354

DIGITAL COMMAND SYSTEMS
Plan of action survey of functional requirements for a geographical information system
[AD-A245622] p 3011 N92-26403

DIGITAL DATA
Differentiation on genus of aquatic macrophytes through remote sensing in the Tucurui Reservoir, Para State, Brazil
[INPE-5315-PRE/1712] p 2951 N92-26721

DIGITAL SIMULATION
Assessment of radiation doses due to releases to the biosphere from nuclear waste repositories, appendix 3 p 2929 N92-26485
Modeling transfer of Cs-137 fallout in a large Finnish watercourse, appendix 6 p 2930 N92-26488

DIGITAL SYSTEMS
Implementation of multi-frequency modulation with Trellis encoding and Viterbi decoding using a digital signal processing board
[AD-A245998] p 2976 N92-26758
A real-time synthetic aperture radar processor: Introduction and project description
[AD-A245370] p 2890 N92-26876
VLSI implementation of fuzzy logic operator unit
[AD-A247146] p 2989 N92-27180

DIGITAL TECHNIQUES
Fast envelope correlation for passive ranging
[AD-A246333] p 2888 N92-26388

DILUTION
CFD mixing analysis of jets injected from straight and slanted slots into confined crossflow in rectangular ducts
[NASA-TM-105699] p 2854 N92-26561

DIMENSIONAL ANALYSIS
Dimensional analysis of structural steel beam design
[AD-A245759] p 2917 N92-26593

DIMENSIONAL MEASUREMENT
Fine scale structure of conserved scalar mixing in turbulent shear flows: Sc much greater than 1 and Sc approximately equal to 1 p 2899 N92-26740

DINING PHILOSOPHERS PROBLEM
Proving properties of real-time systems through logical specifications and Petri net models
[REPT-91-072] p 2973 N92-26448

DIODES
Diode pumped 275 watt average power Nd:YAG slab laser
[DE92-008604] p 2911 N92-26504
Advances in the engineering of high field applied-B ion diodes for inertial confinement fusion
[DE92-006528] p 3000 N92-26695

DIRAC EQUATION
Spectral boundary conditions and index theorem for 2-dimensional compact manifold with boundary
[DE92-621115] p 2990 N92-26798

DIRECT CURRENT
The use of ion chromatography-dc plasma atomic emission spectrometry for the speciation of trace metals
[DE92-010317] p 2871 N92-26236
Tuned-circuit dual-mode Johnson noise thermometers
[DE92-010121] p 2908 N92-26569

DIRECTION FINDING
An evaluation of superresolution methods for tactical radio direction finding
[AD-A246316] p 2851 N92-26291
A comparison of direction finding results from an FFT peak identification technique with those from the music algorithm
[AD-A245675] p 2888 N92-26424

DIRECTIONAL SOLIDIFICATION (CRYSTALS)
High temperature furnace modeling and performance verifications
[NASA-CR-190403] p 2908 N92-26536

DIRECTORIES
The study on a directory of human performance models for system design (Defence Research Group Panel 8 on the defence applications of human and bio-medical sciences)
[AD-A247346] p 2970 N92-27179

DISCRIMINATORS
The sixteen channel CAMAC constant fraction discriminator for APEX
[DE92-010550] p 2970 N92-26551

DISEASES
Differentiation on genus of aquatic macrophytes through remote sensing in the Tucurui Reservoir, Para State, Brazil
[INPE-5315-PRE/1712] p 2951 N92-26721

DISKS
Fiber-optic flexural disk accelerometer
[AD-A246203] p 2908 N92-26459

DISPENSERS
Pneumatically actuated multiple store launcher
[AD-D015237] p 2853 N92-27188

DISPERSING
Diapycnal mixing, gravity-current propagation, and sediment dispersion in turbulent fluids
[AD-A246160] p 2896 N92-26412
Novel molecular sources for dispersing boron in carbon-carbon composites
[AD-A246999] p 2870 N92-26882

DISPLACEMENT
Asymptotic analysis of the vibrations of variable length cantilever beams p 2918 N92-26739
DISPLAY DEVICES
RF vacuum microelectronics
[AD-A246579] p 2893 N92-26771
User interface consistency across end-user application programs: Effect on learning and satisfaction p 3013 N92-26776
Expert system management system
[AD-A247102] p 3009 N92-26863
DISSIPATION
Mutual friction in superfluid He-3: Effects of bound states in the vortex core
[PB92-142231] p 2896 N92-26507
DISSOCIATION
The computation of C-C and N-N bond dissociation energies for singly, doubly, and triply bonded systems
[NASA-CR-190254] p 2994 N92-26539
DISTILLATION EQUIPMENT
The centrifugal mass exchange apparatus in air-conditioning system of isolated, inhabited object and its work control p 2957 N92-26956
DISTORTION
Eulerian computational methods
[DE92-008017] p 2900 N92-26853
DISTRIBUTED PARAMETER SYSTEMS
Reconfiguration in robust distributed real-time systems based on global checkpoints
[AD-A245615] p 2970 N92-26382
Automated interpretation of S-invariants of predicate/transition nets: An application of non-classical logics
[PB92-143544] p 2975 N92-26500
Software architecture for a distributed real-time system in Ada, with application to telerobotics
[NASA-TM-4367] p 2977 N92-26904
DISTRIBUTED PROCESSING
Distributed visualization
[DE92-009405] p 2971 N92-26188
Scalable coherent interface: Links to the future
[DE92-010728] p 2887 N92-26267
Paralex: An environment for parallel programming in distributed systems
[AD-A245445] p 2979 N92-26278
Run-time support for dynamic load balancing and debugging in paralex
[AD-A245446] p 2979 N92-26279
Tools and techniques for adding fault tolerance to distributed and parallel programs
[AD-A245510] p 2980 N92-26677
DIURNAL VARIATIONS
Comparison of wind profiles in close proximity to each other
[AD-A246152] p 2945 N92-26409
DIVING (UNDERWATER)
Physiological design goals and proposed thermal limits for US Navy thermal garments: Proceedings of 2 conferences sponsored by the Naval Medical Research and Development Command
[AD-A245543] p 2956 N92-26665
DOMAINS
A frequency domain based approach to on-line system identification
[AD-A246193] p 2973 N92-26418
Knowledge-based production management: Approaches, results, and prospects
[AD-A245714] p 3008 N92-26426
Computational methods for problems of acoustics with particular reference to exterior domains p 2992 N92-26558
DOMES
Principal investigator in a box: Version 1.2 documentation
[NASA-TM-107886] p 2982 N92-26628
DOPED CRYSTALS
Studies of deep level transient spectroscopy of DX centers in GaAlAs: Te under uniaxial stress
[DE92-010258] p 3001 N92-26204
DOPPLER EFFECT
Kalman smoother applied to lace
[AD-A246439] p 2859 N92-27030
DOPPLER RADAR
Precipitation formation processes in convective and stratiform clouds as deduced by coordinated polarimetric radar and aircraft measurements p 2941 N92-26342
Integrating wind profiler data into forecast and warning operations at NWS field offices
[PB92-146075] p 2945 N92-26514
Kalman smoother applied to lace
[AD-A246439] p 2859 N92-27030
DOSAGE
Study of hydrazine metabolism and toxicity
[AD-A245755] p 2884 N92-26589
DOSIMETERS
Geometry and mass model of ionizing radiation experiments on the LDEF satellite
[NASA-CR-184325] p 2993 N92-26200
Calibration of CR-39 for detecting fusion neutrons
[DE92-009063] p 2993 N92-26225
Comparison of laser and conventional heating in TLD dosemapping
[DE92-010773] p 2910 N92-26269
Preliminary total dose measurements on LDEF --- long duration exposure facility p 2952 N92-27123
DREDGING
Hindcast wave information for the Great Lakes: Lake Huron. Wave information studies of US coastlines
[AD-A246326] p 2949 N92-26387
DROPS (LIQUIDS)
Parameterization of water-soluble component of aerosol particles in numerical cloud models
[NASA-CR-190225] p 2945 N92-26474
The liquid droplet radiator: Status of development p 2905 N92-26969
DROPSONDES
Precision of the long baseline acoustic navigation system used by Pegasus
[AD-A246598] p 2852 N92-26795
DRYING
Application of irradiation techniques to food and foodstuffs
[DE92-614952] p 2954 N92-26186
DUALITY THEOREM
Dvoretzky's theorem: 30 years later
[PB92-153212] p 2988 N92-26788
DUCT GEOMETRY
A parametric numerical study of mixing in a cylindrical duct
[NASA-TM-105695] p 2854 N92-26553
CFD mixing analysis of jets injected from straight and slanted slots into confined crossflow in rectangular ducts
[NASA-TM-105699] p 2854 N92-26561
DUCTED BODIES
Investigation on the boundary layer transition of alternately oscillating flow in deceleration phase p 2903 N92-26917
DUCTED FLOW
Numerical solution of plastic liquids shape factor
[PB92-133958] p 2896 N92-26496
CFD mixing analysis of jets injected from straight and slanted slots into confined crossflow in rectangular ducts
[NASA-TM-105699] p 2854 N92-26561
Numerical simulation of the laminar turbulent transition in a stratified flow p 2904 N92-26920
High lift aircraft
[AD-D015215] p 2853 N92-27185
DUCTILITY
Failure studies of bimaterial interfaces and constrained ductile layers p 2868 N92-26559
DUCTS
A parametric numerical study of mixing in a cylindrical duct
[NASA-TM-105695] p 2854 N92-26553
Effect of type of load on stress analysis of thin-walled ducts
[NASA-TP-3248] p 2918 N92-26669
DUMMIES
The electronic evaluation of the Advanced Dynamic Anthropomorphic Manikin (ADAM) in high temperature environments
[AD-A245459] p 2955 N92-26528
DURABILITY
Durability evaluation of photovoltaic blanket materials exposed on LDEF tray S1003 p 2883 N92-27100
The role of the Long Duration Exposure Facility in the development of space systems p 2867 N92-27128
DUST
Quantum black holes and Hawking's radiation
[PB92-152313] p 3018 N92-26833
DUST STORMS
The effect of sandstorms on PV arrays and components --- photovoltaic cells
[DE92-001240] p 2927 N92-26686
DYNAMIC CHARACTERISTICS
A frequency domain based approach to on-line system identification
[AD-A246193] p 2973 N92-26418
Dynamic lens compensation for active color imaging and constant magnification focusing
[AD-A245713] p 2997 N92-26425
Fractals and chaos
[AD-A246502] p 2990 N92-26466
Dynamics of neutron stars and binaries in globular clusters or, menages a trois: Revitalizing burnt out degenerates through partner swapping p 3017 N92-26522
The modeling and control of acoustic/structure interaction problems via piezoceramic actuators: 2-D numerical examples
[NASA-CR-189639] p 2987 N92-26668
An instrument for engine torque estimation and misfire detection --- torque p 2909 N92-26738
Recent advances in shock and quasi-isentropic compression techniques for dynamic material property studies
[DE92-007988] p 2919 N92-26852
DYNAMIC CONTROL
Dynamic control of a space robot system with no thrust jets controlled base
[AD-A245711] p 2981 N92-26356
Parameter robust reduced-order control of flexible structures p 2982 N92-26597
Adaptive control of nonlinear and stochastic systems
[AD-A247204] p 2985 N92-27169
DYNAMIC LOADS
Results of a portable fiber-optic weigh-in-motion system
[DE92-009011] p 2996 N92-26376
DYNAMIC MODELS
Proceedings of 6th Hawaiian Winter Workshop on Dynamics of Oceanic Internal Gravity Waves
[AD-A245650] p 2948 N92-26173
Investigating the utility of coupling COCOMO with a system dynamics simulation of software development
[AD-A245484] p 2973 N92-26400
Correlation and prediction of dynamic human isolated joint strength from lean body mass
[NASA-TP-3207] p 2956 N92-26682
F-111C flight dynamic model aerodynamic data-base development and verification
[AD-A246356] p 2850 N92-26947
Adaptive control of nonlinear and stochastic systems
[AD-A247204] p 2985 N92-27169
DYNAMIC RANGE
Results of a portable fiber-optic weigh-in-motion system
[DE92-009011] p 2996 N92-26376
DYNAMIC RESPONSE
Optimization of space structures to minimize dynamic response p 2858 N92-26610
The dynamic response of the westward auroral electrojet and polar cap currents to solar wind-magnetosphere coupling p 2943 N92-26622
Role of shock compression technique for scientific and engineering studies
[DE92-008324] p 2919 N92-26846
Homogenization models for 2-D grid structures
[NASA-CR-190321] p 2920 N92-26892
Dynamic response of cylindrical shells to underwater end-on explosion
[AD-A245804] p 2920 N92-26932
DYNAMIC STRUCTURAL ANALYSIS
Homogenization models for 2-D grid structures
[NASA-CR-190321] p 2920 N92-26892
Structural dynamic interaction with solar tracking control for evolutionary Space Station concepts
[NASA-TM-107629] p 2920 N92-26903
DYNAMIC TESTS
Compressive damage and fracture modeling of ceramic subjected to high-velocity impact p 2881 N92-26492
DYNAMICAL SYSTEMS
Studies in chaos using stochastic methods
[AD-A246919] p 3008 N92-27171

E

E REGION
The effects of magnetic storm phases on F-layer irregularities from auroral to equatorial latitudes
[AD-A245495] p 2943 N92-26675
EARTH (PLANET)
The joint US/UK 1990 epoch world magnetic model
[NASA-CR-190424] p 2942 N92-26406
Radar scattering as a source of geological information on Venus and Earth p 3019 N92-26778
EARTH ATMOSPHERE
Water vapor information content of absorption lines observed in the Sun's infrared radiance p 2942 N92-26490
Organic carbon in soil and the global carbon cycle
[DE92-010289] p 2931 N92-26580
Research and technology, 1990: Goddard Space Flight Center
[NASA-TM-107792] p 3022 N92-26824
EARTH ENVIRONMENT
Study on the requirements for the installation of a CES and habitability centre p 2966 N92-27007
EARTH GRAVITATION
The effect of global change and long period tides on the Earth's rotation and gravitational potential p 2925 N92-26781

EARTH IONOSPHERE
Cluster Dayside Polar Cusp
[ESA-SP-330] p 2935 N92-26294
U.S. ground-based space research programs in Svalbard (Norway) p 2935 N92-26296
Research programmes at Svalbard (Norway) p 2935 N92-26297
Polar cap boundary and structure of dayside cusp as determined by ion precipitation p 2936 N92-26300
Antarctic studies of the cusp p 2936 N92-26301
Cusp studies with HF radars p 2936 N92-26304
Plans for the EISCAT Svalbard (Norway) radar p 2936 N92-26305
The ionospheric signature of flux transfer events p 2937 N92-26308
Relationships between ionospheric and tail phenomena p 2938 N92-26317

EARTH MAGNETOSPHERE
Cluster Dayside Polar Cusp
[ESA-SP-330] p 2935 N92-26294
U.S. ground-based space research programs in Svalbard (Norway) p 2935 N92-26296
Research programmes at Svalbard (Norway) p 2935 N92-26297
The Polar Geophysical Institute program of the theoretical and experimental investigation on cusp p 2935 N92-26298
Antarctic studies of the cusp p 2936 N92-26301
Lesson learned from GEOS and ISEE p 2936 N92-26302
The present understanding of the cusp p 2936 N92-26306
Balloons for conjugate cusp studies in the 1990's p 2938 N92-26315
Mathematical model of physical processes responsible for generation of magnetospheric electric fields and their penetration into the Earth's magnetosphere p 2938 N92-26319
The dynamic response of the westward auroral electrojet and polar cap currents to solar wind-magnetosphere coupling p 2943 N92-26622

EARTH MANTLE
Imaging earth's interior: Tomographic inversions for mantle P-wave velocity structure
[DE92-010271] p 2934 N92-26208
Incoherent scatter radar measurements of the cusp p 2936 N92-26303

EARTH OBSERVATIONS (FROM SPACE)
Measurement of surface layer optical turbulence above AMOS
[AD-A246387] p 3016 N92-27077

EARTH ORBITAL ENVIRONMENTS
Ruled and holographic diffraction gratings experiment (AO 138-5) p 2910 N92-27092
LDEF active optical system components experiment p 2998 N92-27094
Effects of long-duration exposure on optical system components p 2998 N92-27095
Effects of long term exposure on optical substrates and coatings (SOO50-2) p 2998 N92-27096
Space environmental effects on coated optics p 2999 N92-27098
Contamination of optical surfaces in Earth orbit p 2999 N92-27099
Durability evaluation of photovoltaic blanket materials exposed on LDEF tray S1003 p 2883 N92-27100
Advanced photovoltaic experiment, S0014: Preliminary flight results and post-flight findings p 2927 N92-27101
LDEF SP-HVDE (Space Plasma-High Voltage Drainage Experiment) post-flight results: Leakage current and discharge p 2895 N92-27103
Survival of epiphytic bacteria from seed stored on the Long Duration Exposure Facility (LDEF) p 2952 N92-27122
The role of the Long Duration Exposure Facility in the development of space systems p 2867 N92-27128
SAFT nickel-cadmium cell performances for GEO and LEO applications p 2863 N92-27137
The evaluation of layered separators for nickel-hydrogen cells p 2866 N92-27161
Nickel-hydrogen LEO cycling at 20 percent - 50 percent DOD p 2867 N92-27168

EARTH ORBITS
Orbital maintenance of endoatmospheric low earth-orbiting satellites
[AD-A246381] p 2859 N92-27074
A constant current charge technique for low Earth orbit life testing p 2863 N92-27139

EARTH RADIATION BUDGET EXPERIMENT
Passive exposure of Earth radiation budget experiment components. LDEF experiment AO-147: Post-flight examinations and tests p 2910 N92-27109

EARTH SCIENCES
Functional requirements document for NASA/MSFC Earth Science and Applications Division: Data and information system (ESAD-DIS). Interoperability, 1992
[NASA-TM-4388] p 2921 N92-26905

EARTH SURFACE
Development of an advanced finite-difference atmospheric general circulation model
[DE92-010923] p 2944 N92-26937

EARTHQUAKES
Imaging earth's interior: Tomographic inversions for mantle P-wave velocity structure
[DE92-010271] p 2934 N92-26208
Fault zone structure determined through the analysis of earthquake arrival times
[DE92-010322] p 2935 N92-26239

EATING
An evaluative study of the sensory qualities of selected European and Asian foods for international space missions (a French food study) p 2966 N92-27009

ECONOMIC DEVELOPMENT
Small Businesses Make a Difference
[PB92-160118] p 3008 N92-26369

ECONOMICS
Competing economies: America, Europe, and the Pacific rim
[PB92-115757] p 3014 N92-26730
Chinese space technology's spin-offs and applications
[AD-A246375] p 3015 N92-27051

ECOSYSTEMS
Meridional zonation of the Barents Sea ecosystem inferred from satellite remote sensing and in situ bio-optical observations
[AD-A246323] p 2948 N92-26245
Life support research and development, a Department of Energy program for the Space Exploration Initiative
[DE92-007681] p 2955 N92-26375
Equilibrium-analysis of projected climate change effects on the global soil organic matter pool
[PB92-153022] p 2930 N92-26509
Organic carbon in soil and the global carbon cycle
[DE92-010289] p 2931 N92-26580
Impact of diet on the design of waste processors in CELSS p 2961 N92-26980
MELISSA: Physical links of compartments Nitrobacter/Spirulina p 2961 N92-26981
PAGES. Past global changes project: Proposed implementation plans for research activities
[IGBP-REPT-19-ATTACH-10] p 2934 N92-27082

EDDY CURRENTS
A simple model for the convective boundary layer over wavy terrain with variable heat flux p 2934 N92-26334

EDGE DETECTION
Color image processing and object tracking workstation
[NASA-TM-105561] p 2886 N92-26611

EDGE DISLOCATIONS
Effect of interstitials on the trapping of hydrogen in iron-single crystals
[AD-A246412] p 3006 N92-27064

EDGE LOADING
Buckling of unidirectional graphite/epoxy composite plates at low temperatures
[AD-A246602] p 2869 N92-26796

EDITING ROUTINES (COMPUTERS)
Testbank (1.0) user's manual
[AD-A245895] p 2971 N92-26196

EDUCATION
Small Businesses Make a Difference
[PB92-160118] p 3008 N92-26369

EFFECTIVENESS
Measuring the effectiveness of information systems
[AD-A246007] p 3013 N92-26762

EGGS
Preliminary results of the Artemia salina experiments in biostack on LDEF p 2952 N92-27125

EIGENVALUES
Mode structure and continuum damping of high-n toroidal Alfven eigenmodes
[DE92-010547] p 2999 N92-26256
Identification of linear systems by an asymptotically stable observer
[NASA-TP-3164] p 2917 N92-26537

EIGENVECTORS
Mode structure and continuum damping of high-n toroidal Alfven eigenmodes
[DE92-010547] p 2999 N92-26256
Optical communications with number states p 2889 N92-26604
Sturm-Liouville eigenfunctions expressed in determinant form
[AD-A245991] p 2987 N92-26755

EINSTEIN EQUATIONS
Euclidean black hole vortices
[NASA-CR-190117] p 3016 N92-26436

EISCAT RADAR SYSTEM (EUROPE)
Plans for the EISCAT Svalbard (Norway) radar p 2936 N92-26305
The requirements for data exchange between Cluster and ground-based observatories, using EISCAT as an illustrative example p 2938 N92-26316

EJECTORS
Use of an approximate similarity principle for the thermal scaling of a full-scale thrust augmenting ejector
[NASA-TM-105724] p 2854 N92-26613

ELASTIC DEFORMATION
Computational aspects of an implicit finite element procedure for elasto-viscoplastic large deformation problems p 2917 N92-26594

ELASTIC PROPERTIES
Computational modelling of rubberlike materials
[ETN-92-91304] p 2916 N92-26259

ELASTIC SCATTERING
Cryogenic detector development
[MPI-PHE/91-07] p 2906 N92-26391
Cryogenic calorimeters for dark matter and neutrinos p 2907 N92-26392
Measurements of scattering processes in negative ion-atom collisions
[DE92-010319] p 2995 N92-26574

ELASTOMERS
Effect of temperature and gap opening rate on the resiliency of candidate solid rocket booster O-ring materials
[NASA-TP-3226] p 2883 N92-27194

ELBOW (ANATOMY)
Development of the suit enclosure soft joints of the European EVA space suit p 2965 N92-27005

ELECTRIC BATTERIES
Fabrication and characterization of amorphous lithium electrolyte thin films and rechargeable thin-film batteries
[DE92-010108] p 2893 N92-26636
New amorphous thin-film lithium electrolyte and rechargeable microbattery
[DE92-010110] p 2893 N92-26637
Long Duration Exposure Facility (LDEF) low-temperature heat pipe experiment package power system results p 2906 N92-27105
COBE battery overview: History, handling, and performance p 2862 N92-27131
End-of-life evaluation of the solar maximum mission batteries p 2862 N92-27132
Magellan battery operations: An overview p 2862 N92-27133
The effect of switched array battery charge control on CRRES spacecraft: 3 + month data summary p 2862 N92-27134
STS lithium/CF(x) battery p 2863 N92-27143
NASA Li/CF(x) cell problem analysis: Scanning electron microscopy with energy dispersive x ray spectrometry p 2863 N92-27144
Evaluation of sodium-nickel chloride cells for space applications p 2865 N92-27156
Low cost battery designs for small satellite applications p 2866 N92-27160

ELECTRIC CONDUCTORS
Analysis of Yttrium-Barium-Copper-Oxide by x ray diffraction and mechanical characterization
[NASA-TM-104562] p 2869 N92-26650

ELECTRIC CONNECTORS
Reduced models for the behavior of VLSI circuits
[ISBN-90-6275-721-9] p 2892 N92-26249
Effects of ultra-vacuum and space environment on contact ohmic resistance: LDEF experiment AO 138-11 p 2895 N92-27118

ELECTRIC CURRENT
Short-wave low-frequency spectra in a current-carrying plasma
[DE92-621529] p 3001 N92-26808
A constant current charge technique for low Earth orbit life testing p 2863 N92-27139

ELECTRIC DIPOLES
Polarisation effects in fibre lasers p 2911 N92-26571

ELECTRIC DISCHARGES
SAFT nickel-cadmium cell performances for GEO and LEO applications p 2863 N92-27137
Life testing of secondary Ag-Zn cells p 2865 N92-27153

ELECTRIC FIELDS
The Polar Geophysical Institute program of the theoretical and experimental investigation on cusp p 2935 N92-26298
Mathematical model of physical processes responsible for generation of magnetospheric electric fields and their penetration into the Earth's magnetosphere p 2938 N92-26319

ELECTRIC GENERATORS
Aircraft photovoltaic power-generating system p 2926 N92-26581

Adaptive regulation of the boiler-turbine unit of a Combined Heat and Power (CHP) system
[RR-417] p 2887 N92-26752

ELECTRIC POTENTIAL
Diode pumped 275 watt average power Nd:YAG slab laser
[DE92-008604] p 2911 N92-26504
Main and auxiliary transformer rectifier system for minimizing line harmonics
[AD-D015209] p 2894 N92-26881
A constant current charge technique for low Earth orbit life testing p 2863 N92-27139
Performances of 250 Amp-hr lithium/thionyl chloride cells p 2864 N92-27148

ELECTRIC POWER PLANTS
Magnetohydrodynamic Electromagnetic Pulse (MHD-EMP) interaction with power transmission and distribution systems
[DE92-010365] p 2887 N92-26237

ELECTRIC POWER TRANSMISSION
Magnetohydrodynamic Electromagnetic Pulse (MHD-EMP) interaction with power transmission and distribution systems
[DE92-010365] p 2887 N92-26237

ELECTRIC SWITCHES
Plasma interactions in a plasma erosion opening switch
[AD-A246179] p 2999 N92-26416

ELECTRICAL GROUNDING
Analysis of surface wave propagation in a grounded dielectric slab covered by a resistive sheet
[NASA-TM-107583] p 2889 N92-26653

ELECTRICAL PROPERTIES
Systems special investigation group overview p 2867 N92-27084
Experiment M0003-4: Advanced solar cell and coverglass analysis, an overview p 2927 N92-27088

ELECTRICAL RESISTANCE
Reduced models for the behavior of VLSI circuits
[ISBN-90-6275-721-9] p 2892 N92-26249

ELECTRICAL RESISTIVITY
Static electricity: A literature review
[AD-A246533] p 2990 N92-26471
Analysis of surface wave propagation in a grounded dielectric slab covered by a resistive sheet
[NASA-TM-107583] p 2889 N92-26653
The production and properties of melt-zone textured Y1Ba2Cu3O(7-delta) filaments
[DE92-008097] p 3005 N92-26843

ELECTRO-OPTICS
Development and testing of a prototype electro-optical phase encoded position transducer
[AD-A245486] p 2908 N92-26401
Crossovers of the density of states in two-direction double-barrier resonant-tunneling structures
[AD-A246124] p 3005 N92-26684
Preliminary analyses of WL experiment No. 701, space environment effects on operating fiber optic systems p 2998 N92-27089

ELECTROCATALYSTS
Electrocatalysts for oxygen electrodes
[DE92-009491] p 2871 N92-26220
Low temperature electrochemical activation of methane
[PB92-152917] p 2872 N92-26351

ELECTROCHEMICAL CELLS
Photoinduced charge separation in solid-state and molecular systems
[DE92-010130] p 3004 N92-26639
Li/BCX, SVO, and CSC cells: Power sources for aerospace applications p 2864 N92-27147
Development of a 300 Amp-hr high rate lithium thionyl chloride cell p 2864 N92-27149
Safety testing of lithium cells p 2864 N92-27150
Examination of the discharge mechanism of Li/CF(x) cells: Comparison of the electrochemical reduction mechanisms of PTFE and (CF(x))n by lithium p 2865 N92-27151

ELECTROCHEMICAL CORROSION
Application of in situ x ray absorption and fluorescence measurements to analyze solutions in a simulated pit
[DE92-009159] p 2878 N92-26563

ELECTROCHEMICAL OXIDATION
Low temperature electrochemical activation of methane
[PB92-152917] p 2872 N92-26351

ELECTRODES
Electrocatalysts for oxygen electrodes
[DE92-009491] p 2871 N92-26220
Proposed model of thermionically assisted breakdown and implementation on electrostatic thrusters
[AD-A246207] p 2990 N92-26460
Progress in the development of lightweight nickel electrode
[NASA-TM-105638] p 2875 N92-26670
Super NiCd battery program: History and performance p 2862 N92-27135
Recent developments in nickel electrode analysis p 2865 N92-27158

ELECTRODYNAMICS
The Polar Geophysical Institute program of the theoretical and experimental investigation on cusp p 2935 N92-26298

ELECTROJETS
Ground-based studies of sensing magnetosphere/ionosphere interactions: Convection and substorms p 2937 N92-26311

ELECTROKINETICS
Fundamentals of electrokinetics
[DE92-008326] p 2894 N92-26847

ELECTROLYTES
Gas-pressure studies with Li(Si)/FeS2 thermal batteries
[DE92-010801] p 2892 N92-26238
The influence of pressure on the phase behaviour of water + oil + surfactant systems
[ISBN-90-6275-732-4] p 2871 N92-26257
Synthesis of novel fluorinated phosphonic acid electrolytes for phosphoric acid fuel cells
[PB92-164300] p 2926 N92-26372
Fabrication and characterization of amorphous lithium electrolyte thin films and rechargeable thin-film batteries
[DE92-010108] p 2893 N92-26636
New amorphous thin-film lithium electrolyte and rechargeable microbattery
[DE92-010110] p 2893 N92-26637
Zirconia-based fuel cells for power generation
[DE92-009886] p 2927 N92-26719
Exploring possible relationships between plate pore size character and cell performance p 2863 N92-27141
Development of a 300 Amp-hr high rate lithium thionyl chloride cell p 2864 N92-27149

ELECTROMAGNETIC FIELDS
Transient diffusive electromagnetic fields in layered anisotropic media
[ISBN-90-6275-722-7] p 2887 N92-26254
Joint services electronics program
[AD-A245636] p 2892 N92-26280
Exact solutions for a mode of the electromagnetic field in a resonator with time-dependent characteristics of the internal medium
[AD-A245700] p 2888 N92-26374
Optical communications with number states p 2889 N92-26604

ELECTROMAGNETIC INTERACTIONS
Analysis of EMP response of structures using frequency domain electromagnetic interaction codes
[AD-A245758] p 2889 N92-26592
Vacuum polarization tensor in 3-dimensional quantum electrodynamics
[DE92-621141] p 2890 N92-26799
Linear and non-linear response of liquid and solid particles to energetic radiation
[AD-A246368] p 2894 N92-26942

ELECTROMAGNETIC INTERFERENCE
Transmittance measurements of ultraviolet and visible wavelength filters flown aboard LDEF p 2999 N92-27110

ELECTROMAGNETIC NOISE
Effect of gyro noise on ADKEM gyro-only missile system performance
[AD-A246150] p 2852 N92-26408
Squeezed light and twin beams generation with a Q-switched laser p 2912 N92-26603

ELECTROMAGNETIC PULSES
Magnetohydrodynamic Electromagnetic Pulse (MHD-EMP) interaction with power transmission and distribution systems
[DE92-010365] p 2887 N92-26237
Analysis of EMP response of structures using frequency domain electromagnetic interaction codes
[AD-A245758] p 2889 N92-26592

ELECTROMAGNETIC RADIATION
Performance enhancement of the NPS Transient Electromagnetic Scattering Laboratory
[AD-A246300] p 2888 N92-26363
Adverse reproductive events and electromagnetic radiation
[PB92-145796] p 2953 N92-26512
Dielectric tensor of strongly coupled plasmas
[DE92-621524] p 3001 N92-26807

ELECTROMAGNETIC SCATTERING
Performance enhancement of the NPS Transient Electromagnetic Scattering Laboratory
[AD-A246300] p 2888 N92-26363
Electromagnetic scattering by a moving object: Theory and experiment
[PB92-150911] p 2889 N92-26511
Modeling 3-D objects with planar surfaces for prediction of electromagnetic scattering
[NASA-TM-107598] p 2891 N92-27189

ELECTROMAGNETISM
An antenna design for PANSAT using NEC
[AD-A245482] p 2888 N92-26399
Analysis of EMP response of structures using frequency domain electromagnetic interaction codes
[AD-A245758] p 2889 N92-26592

ELECTRON ACCELERATORS
Higher order parametric x rays
[AD-A247148] p 2991 N92-27182

ELECTRON BEAMS
Theory of electromagnetic instability of an intense beam in a quadrupole focusing system
[AD-A246560] p 2990 N92-26768
Radiation sensitivity of quartz crystal oscillators experiment for the Long Duration Exposure Facility (LDEF) p 2895 N92-27111
Higher order parametric x rays
[AD-A247148] p 2991 N92-27182

ELECTRON CYCLOTRON HEATING
Transportable 5 MW power supply system for gyrotron operation
[DE92-009051] p 2892 N92-26224
Diagnostic upgrades on MTX
[DE92-009695] p 2906 N92-26230
Installation and operation of the 400 kW 140 GHz gyrotron on the MTX experiment
[DE92-009053] p 2906 N92-26377

ELECTRON DIFFRACTION
Diffraction phenomena in spontaneous and stimulated radiation by relativistic particles in crystals (review)
[DE92-009501] p 3001 N92-26222
A comprehensive review of the XRD data of the primary and secondary phases present in the BSCCO superconductor system
[DE92-010363] p 3003 N92-26579

ELECTRON DISTRIBUTION
Investigation of deep dielectric charging and subsequent currents on geosynchronous spacecraft
[AD-A245764] p 2858 N92-26605

ELECTRON EMISSION
Plasma interactions in a plasma erosion opening switch
[AD-A246179] p 2999 N92-26416
Proposed model of thermionically assisted breakdown and implementation on electrostatic thrusters
[AD-A246207] p 2990 N92-26460

ELECTRON MICROSCOPES
Modification and experimental validation of a combined optical and collection probe for solid propellant exhaust analysis
[AD-A245387] p 2884 N92-26839

ELECTRON MICROSCOPY
Photoinduced charge separation in solid-state and molecular systems
[DE92-010130] p 3004 N92-26639
NASA Li/CF(x) cell problem analysis: Scanning electron microscopy with energy dispersive x ray spectrometry p 2863 N92-27144

ELECTRON PHONON INTERACTIONS
Generation of nonequilibrium optical phonons in GaAs/AlAs quantum wells by intrasubband and intersubband scatterings
[DE92-010264] p 2993 N92-26207
Electron-phonon decoupling and superconducting grains p 2907 N92-26397

ELECTRON PLASMA
High frequency Raman current drive
[PB92-142223] p 2893 N92-26497

ELECTRON SOURCES
Field-emission arrays: A potentially bright source
[AD-A246561] p 2893 N92-26741

ELECTRON STATES
Solvation effects on the electronic structure of 4-N,N-Dimethylaminobenzonitrile: Mixing of the local pipi* and charge transfer states
[AD-A245814] p 2874 N92-26608
A study of buckminsterfullerene using new pseudopotentials p 3005 N92-26774
Dynamic properties of quasi-two-dimensional one component plasmas
[DE92-621523] p 3000 N92-26806

ELECTRON TRANSFER
Bis (pentamethylcyclopentadienyl) ytterbium: Electron-transfer reactions with organotransition metal complexes
[DE92-010300] p 2994 N92-26235
Photochemical energy conversion by membrane-bound photoredox systems
[DE92-008709] p 2927 N92-26858

ELECTRONIC EQUIPMENT
Description of the multispectral CCD-camera
[AD-A245681] p 2908 N92-26517
The development of a model builder for a microcircuit substrate
[AD-A245765] p 2893 N92-26606

ELECTRONIC EQUIPMENT TESTS
LDEF electronic systems: Successes, failures and lessons p 2895 N92-27112
ELECTRONIC FILTERS
Effects of video bandwidth on the performance of a square law detector with Gaussian IF and video filters [AD-A246506] p 2989 N92-26467
ELECTRONIC WARFARE
Data fusion and correlation techniques testbed (DFACTT): Field trial 14 January 1991 [AD-A245324] p 3011 N92-26378
System evaluation of a frequency hopping combat net radio [AD-A246365] p 2891 N92-26941
ELECTROPLATING
An electroplater's view of PVD processing [DE92-009052] p 2878 N92-26732
ELECTROSTATIC CHARGE
Ulysses, one year after the launch p 2860 N92-26999
ELECTROSTATIC PROPULSION
Proposed model of thermionically assisted breakdown and implementation on electrostatic thrusters [AD-A246207] p 2990 N92-26460
ELECTROSTATICS
Short-wave low-frequency spectra in a current-carrying plasma [DE92-621529] p 3001 N92-26808
ELEMENT 104
Gas phase chromatography of halides of elements 104 and 105 [DE92-010284] p 2870 N92-26212
ELEMENT 105
Gas phase chromatography of halides of elements 104 and 105 [DE92-010284] p 2870 N92-26212
ELEMENTARY PARTICLE INTERACTIONS
Open problems and future prospects for hypernuclear physics [DE92-010158] p 2995 N92-26815
ELLIPSES
On certain methods of determining the ellipses and ellipsoids of the positioning accuracy of robot manipulators [ISSN-0208-5658] p 2914 N92-26284
ELLIPSOIDS
On certain methods of determining the ellipses and ellipsoids of the positioning accuracy of robot manipulators [ISSN-0208-5658] p 2914 N92-26284
Theoretical issues in adaptive Set-Membership-Based signal processing. [AD-A245721] p 2980 N92-26430
ELLIPTIC DIFFERENTIAL EQUATIONS
Developments of solutions of some special elliptic equations at a corner [PB92-148741] p 2986 N92-26503
ELLIPTICAL CYLINDERS
Focusing x ray transition radiation with cylindrical and elliptical optics [AD-A245987] p 2997 N92-26754
ELONGATION
Elevated temperature properties of a dispersion strengthened Al-(Fe, V, Si) alloy [AD-A246427] p 2880 N92-27067
EMBRYOLOGY
Preliminary results of the Artemia salina experiments in biostack on LDEF p 2952 N92-27125
EMISSION
A parametric numerical study of mixing in a cylindrical duct [NASA-TM-105695] p 2854 N92-26553
Volatile Organic Compound (VOC) and Particulate Matter (PM) speciation data system user's manual, version 1.4 [PB92-105527] p 2932 N92-26823
EMISSION SPECTRA
The use of ion chromatography-dc plasma atomic emission spectrometry for the speciation of trace metals [DE92-010317] p 2871 N92-26236
Exposure to space radiation of high-performance infrared multilayer filters and materials technology experiment (A0056) p 2999 N92-27108
EMITTANCE
Passive determination of temperature and range using spectral band measurements of photon emittance [AD-A247147] p 2910 N92-27181
EMITTERS
Proposed model of thermionically assisted breakdown and implementation on electrostatic thrusters [AD-A246207] p 2990 N92-26460
EMPLOYMENT
US Small Business Administration FY 1990 national accomplishment report and FY 1991 national affirmative employment program plan [PB92-157064] p 3008 N92-26353
END EFFECTORS
A framework for recognizing grasps [AD-A245712] p 2981 N92-26357
END PLATES
Dynamic response of cylindrical shells to underwater end-on explosion [AD-A245804] p 2920 N92-26932
ENDOCRINOLOGY
Biochemical, endocrine, and hematological factors in human oxygen tolerance extension: Predictive studies 6 [NASA-CR-190341] p 2952 N92-26263
ENERGETIC PARTICLES
Scenarios for the nonlinear evolution of alpha particle induced Alfven wave instability [DE92-010549] p 3000 N92-26550
The status of GALLEX [DE92-010077] p 3020 N92-26566
Linear and non-linear response of liquid and solid particles to energetic radiation [AD-A246368] p 2894 N92-26942
ENERGY BUDGETS
Surface energy budget and evapotranspiration measurement support [NASA-CR-190059] p 2944 N92-26185
Passive exposure of Earth radiation budget experiment components. LDEF experiment AO-147: Post-flight examinations and tests p 2910 N92-27109
ENERGY CONSERVATION
Application of riblet surface to pipe flow p 2903 N92-26915
ENERGY CONSUMPTION
Environmental implications of increased biomass energy use [DE92-001219] p 2932 N92-26810
ENERGY CONVERSION
Environmental implications of increased biomass energy use [DE92-001219] p 2932 N92-26810
ENERGY CONVERSION EFFICIENCY
Inertial fusion energy power plant design using the Compact Torus Accelerator: HYLIFE-CT [DE92-008941] p 3000 N92-26729
ENERGY DISSIPATION
Mean and turbulent structure of the marine atmospheric boundary layer during cold air outbreaks of different intensities: Observational and modelling analyses p 2942 N92-26489
Measurements of scattering processes in negative ion-atom collisions [DE92-010319] p 2995 N92-26574
Quasi-elastic nuclear scattering at high energies [NASA-TM-4362] p 2996 N92-26832
ENERGY DISTRIBUTION
Magnetohydrodynamic Electromagnetic Pulse (MHD-EMP) interaction with power transmission and distribution systems [DE92-010365] p 2887 N92-26237
ENERGY LEVELS
Mutual friction in superfluid He-3: Effects of bound states in the vortex core [PB92-142231] p 2896 N92-26507
Quantum black holes and Hawking's radiation [PB92-152313] p 3018 N92-26833
ENERGY POLICY
SOLTECH 1992 proceedings: Solar Process Heat Program, volume 1 [DE92-001238] p 2927 N92-26683
ENERGY SPECTRA
Simultaneous observations of extensive air showers and underground muons at Soudan 2 [DE92-010282] p 3020 N92-26211
Interpretation of distributions on K(sub pi)(sup 0) in pFe, nFe, and piFe interactions at 0.5-5.0 TeV in the framework of contemporary models [DE92-621189] p 3021 N92-26804
ENERGY TECHNOLOGY
Fusion energy and Canada's role [DE92-621553] p 2999 N92-26286
SOLTECH 1992 proceedings: Solar Process Heat Program, volume 1 [DE92-001238] p 2927 N92-26683
DOE new technology [DE92-001619] p 3013 N92-26689
Passive water hammer in pipes due to flashing [DE92-004180] p 2899 N92-26699
Water hammer due to the sudden stopping of a flashing flow [DE92-004181] p 2899 N92-26700
Inertial fusion energy power plant design using the Compact Torus Accelerator: HYLIFE-CT [DE92-008941] p 3000 N92-26729
ENERGY TRANSFER
Energy transfer properties and mechanisms [DE92-011215] p 2994 N92-26240
Mean and turbulent structure of the marine atmospheric boundary layer during cold air outbreaks of different intensities: Observational and modelling analyses p 2942 N92-26489
Numerical formulation for the prediction of solid/liquid change of a binary alloy [NASA-CR-188468] p 2878 N92-26642
Role of shock compression technique for scientific and engineering studies [DE92-008324] p 2919 N92-26846
Vibrational spectroscopy in shock-compressed liquids [DE92-007713] p 2876 N92-26867
The HUS solar flare and cosmic gamma ray burst detector aboard the Ulysses spacecraft [MPE-PREPRINT-175] p 3016 N92-27049
ENGINE CONTROL
ASTOVL engine control [PNR-90808] p 2855 N92-27040
ENGINE DESIGN
Throttleless Otto-cycle natural gas engines [PB92-164482] p 2914 N92-26371
Theoretical and experimental study of thermoacoustic engines [AD-A246334] p 2914 N92-26389
Development of natural gas rotary engines [PB92-149665] p 2915 N92-26816
VSTOL engine design evolution: Growth of the Pegasus engine for Harrier [PNR-90805] p 2855 N92-27039
ASTOVL engine control [PNR-90808] p 2855 N92-27040
Simultaneous engineering in aero-gas turbine design and manufacture [PNR-90811] p 2856 N92-27043
The changing role of experimentation in aeroengine R and D: The point of view of the research worker [AD-A246372] p 2856 N92-27062
ENGINE INLETS
Hypersonic aerospace vehicle leading edge cooling using heat pipe, transpiration and film cooling techniques p 3007 N92-26733
Interface of an uncoupled boundary layer algorithm with an invisicd core flow algorithm for unsteady supersonic engine inlets [NASA-TM-105684] p 2855 N92-27037
ENGINE MONITORING INSTRUMENTS
Rocket engine diagnostics using qualitative modeling techniques [NASA-TM-105714] p 2861 N92-27033
ENGINE PARTS
Powder processing of aero-engine components [PNR-90813] p 2880 N92-27044
The changing role of experimentation in aeroengine R and D: The point of view of the research worker [AD-A246372] p 2856 N92-27062
ENGINE TESTS
Acoustic interactions between an altitude test facility and jet engine plumes: Theory and experiments [NASA-CR-190423] p 2853 N92-26405
VSTOL engine design evolution: Growth of the Pegasus engine for Harrier [PNR-90805] p 2855 N92-27039
The changing role of experimentation in aeroengine R and D: The point of view of the research worker [AD-A246372] p 2856 N92-27062
ENGINEERING MANAGEMENT
Simultaneous engineering in aero-gas turbine design and manufacture [PNR-90811] p 2856 N92-27043
ENTHALPY
On shock capturing for liquid and gas media p 2897 N92-26556
A study of buckminsterfullerene using new pseudopotentials p 3005 N92-26774
ENTIRE FUNCTIONS
Studies of inertio-gravity waves induced by geostrophic adjustment of the atmospheric jet stream p 2944 N92-26866
ENTOMOLOGY
A one-dimensional temperature model for a snow cover: Technical documentation for SNTHERM.89 [AD-A245493] p 2922 N92-26674
ENTRAINMENT
Theoretical and modeling studies of the marine planetary boundary layer [AD-A245903] p 2942 N92-26432
Study of entrainment mechanisms in convective clouds [NASA-CR-190223] p 2946 N92-26735
Analysis of mixing mechanisms in numerically simulated convective clouds [NASA-CR-190222] p 2946 N92-26736
Physical processes within the nocturnal stratus-topped boundary layer, revision [AD-A245829] p 2947 N92-26901

ENTROPY
The APT/ERE planning and scheduling manifesto
(NASA-TM-107906) p 2984 N92-27055
ENVIRONMENT EFFECTS
Life sciences and environmental sciences
(DE92-010254) p 2950 N92-26203
Environmental implications of increased biomass energy use
(DE92-001219) p 2932 N92-26810
Climate research at regional climate centers in 1991
(PB92-160399) p 2946 N92-26822
Evaluation of carbon dioxide emission control strategies in New York State
(DE92-010162) p 2932 N92-26825
PAGES. Past global changes project: Proposed implementation plans for research activities
(IGBP-REPT-19-ATTACH-10) p 2934 N92-27082
Preliminary analyses of WL experiment No. 701, space environment effects on operating fiber optic systems
p 2998 N92-27089
The role of the Long Duration Exposure Facility in the development of space systems p 2857 N92-27128
ENVIRONMENT MODELS
The development of a design database for the computer aided prototyping system
(AD-A245786) p 3010 N92-26176
Model studies of the transfer of radionuclides in the Finnish environment
(VTT-PUBL-81) p 2929 N92-26482
A comparative assessment of radiological impact due to nuclear waste disposal in hard crystalline bedrock, appendix 1
(IAEA-CN-43/449) p 2929 N92-26483
Assessment of radiation doses due to releases to the biosphere from nuclear waste repositories, appendix 3
p 2929 N92-26485
Biosphere model validation by intercomparison to observed behaviour of fallout radionuclides in the aquatic environment, appendix 5 p 2930 N92-26487
Modeling transfer of Cs-137 fallout in a large Finnish watercourse, appendix 6 p 2930 N92-26488
ENVIRONMENT POLLUTION
Model studies of the transfer of radionuclides in the Finnish environment
(VTT-PUBL-81) p 2929 N92-26482
ENVIRONMENT PROTECTION
Role of climate in forest monitoring and assessment: A New England example
(PB92-132885) p 2930 N92-26519
The impact of climate upon variation in air pollution using a synoptic climatological approach p 2931 N92-26590
Assessment of computer models for estimating vehicle emission factors. Volume 1: Executive summary
(PB92-113059) p 2931 N92-26802
Assessment of computer models for estimating vehicle emission factors. Volume 2: Description and comparison of the MOBILE4 and EMFAC7E models
(PB92-113067) p 2932 N92-26803
Environmental Protection Agency's municipal solid waste landfill liner design criteria
(PB92-153766) p 2933 N92-26928
ENVIRONMENTAL CONTROL
Fourth European Symposium on Space Environment Control Systems, volume 2
(ESA-SP-324-VOL-2) p 2956 N92-26950
Design of JEM temperature and humidity control system p 2958 N92-26957
A processing environment for test and simulation data of thermodynamic systems p 2959 N92-26963
Higher plant growth in closed environment: Preliminary experiments in life support facility at ESA-ESTEC
p 2961 N92-26978
Impact of diet on the design of waste processors in CELSS p 2961 N92-26980
Moon base habitability aspects p 2969 N92-27026
ENVIRONMENTAL MONITORING
Role of climate in forest monitoring and assessment: A New England example
(PB92-132885) p 2930 N92-26519
Environmental radiation data
(PB92-164706) p 2933 N92-26890
ENVIRONMENTAL TESTS
Ruled and holographic diffraction gratings experiment (AO 138-5) p 2910 N92-27092
LDEF active optical system components experiment
p 2998 N92-27094
Effects of long-duration exposure on optical system components p 2998 N92-27095
Effects of long term exposure on optical substrates and coatings (SOO50-2) p 2998 N92-27096
Space environmental effects on coated optics
p 2999 N92-27098
Contamination of optical surfaces in Earth orbit
p 2999 N92-27099
Durability evaluation of photovoltaic blanket materials exposed on LDEF tray S1003 p 2883 N92-27100
Advanced photovoltaic experiment, S0014: Preliminary flight results and post-flight findings
p 2927 N92-27101
LDEF SP-HVDE (Space Plasma-High Voltage Drainage Experiment) post-flight results: Leakage current and discharge p 2895 N92-27103
The evaluation of layered separators for nickel-hydrogen cells p 2866 N92-27161
ENZYMES
Carbon monoxide metabolism by the photosynthetic bacterium Rhodospirillum rubrum
(DE92-010953) p 2951 N92-26938
EPIDEMIOLOGY
Adverse reproductive events and electromagnetic radiation
(PB92-145796) p 2953 N92-26512
EPITAXY
Cadmium telluride thin films on silicon substrates
(AD-A245309) p 3001 N92-26226
EQUATIONS OF STATE
On shock capturing for liquid and gas media
p 2897 N92-26556
A study of buckminsterfullerene using new pseudopotentials p 3005 N92-26774
Wave structure in one and two dimensional fluid flow
(DE92-007421) p 2900 N92-26855
EQUIVALENT CIRCUITS
Measurement electronics of industrial microwave resonator sensors
(PB92-152750) p 2909 N92-26786
ERGODIC PROCESS
Stochastic versions of the EM algorithm
(AD-A246929) p 2989 N92-27174
EROSION
Plasma interactions in a plasma erosion opening switch
(AD-A246179) p 2999 N92-26416
Erosion of a relativistic electron beam propagating in a plasma channel
(DE92-009059) p 3000 N92-26666
French Cooperative Passive Payload (FRECOPA)
p 2867 N92-27117
ERROR ANALYSIS
Comparison of one-way wave propagation algorithms in underwater acoustics-error estimates and sensitivity
(AD-A245660) p 2991 N92-26175
Implementing error values in applicative languages
(DE92-008927) p 2972 N92-26233
Neural network error correction for solving coupled ordinary differential equations
(NASA-TM-101796) p 2986 N92-26407
Effects of non-uniform windowing on the performance of a fast frequency-hopped noncoherent MFSK receiver over Rician fading channels with partial-band interference and Doppler shift
(AD-A245762) p 2889 N92-26595
Estimation of geopotential differences over intercontinental locations using satellite and terrestrial measurements p 2924 N92-26726
ERROR CORRECTING DEVICES
Neural network error correction for solving coupled ordinary differential equations
(NASA-TM-101796) p 2986 N92-26407
ERRORS
Implementing error values in applicative languages
(DE92-008927) p 2972 N92-26233
Neural network error correction for solving coupled ordinary differential equations
(NASA-TM-101796) p 2986 N92-26407
Evaluation of integral measurements for the SP-100 space reactor
(DE92-009717) p 2996 N92-26841
ESA SATELLITES
European Earth Observation Program
p 2925 N92-26745
ESTIMATES
Bias robust estimation of scale
(AD-A245698) p 2985 N92-26229
Assessment of computer models for estimating vehicle emission factors. Volume 2: Description and comparison of the MOBILE4 and EMFAC7E models
(PB92-113067) p 2932 N92-26803
Computer Program Estimate Trend (ESTREND): A system for the detection of trends in water-quality data
(PB92-147727) p 2933 N92-26931
A finite element/finite difference approach for modeling three-dimensional flow and pollutant dispersion around structures
(DE92-007322) p 2934 N92-26935
ESTIMATING
Estimating mesoscale, orographically enhanced precipitation using synoptic scale data
(AD-A245749) p 2946 N92-26562
An instrument for engine torque estimation and misfire detection --- torque p 2909 N92-26738
Assessment of computer models for estimating vehicle emission factors. Volume 1: Executive summary
(PB92-113059) p 2931 N92-26802
Assessment of computer models for estimating vehicle emission factors. Volume 2: Description and comparison of the MOBILE4 and EMFAC7E models
(PB92-113067) p 2932 N92-26803
Computer Program Estimate Trend (ESTREND): A system for the detection of trends in water-quality data
(PB92-147727) p 2933 N92-26931
ETALONS
High-speed pulse detection room-temperature optical nonlinearities for GaInAs/AlInAs and GaAlInAs/AlInAs multiple quantum wells and integrated mirror etalon at 1.3 micrometers
(AD-A246369) p 2998 N92-26943
ETCHING
Calibration of CR-39 for detecting fusion neutrons
(DE92-009063) p 2993 N92-26225
Etching effects in ion implanted SiO2
(DE92-011150) p 3005 N92-26826
ETHANE
Conversion of ethane and of propane to higher olefin hydrocarbons
(DE92-009487) p 2870 N92-26209
ETHERS
High octane ethers from synthesis gas-derived alcohols
(DE92-010480) p 2884 N92-26548
EUCLIDEAN GEOMETRY
Euclidean black hole vortices
(NASA-CR-190117) p 3016 N92-26436
EULER EQUATIONS OF MOTION
Cell vertex methods for compressible gas flows
p 2897 N92-26599
Theoretical principles of a Euler method for the calculation of three dimensional flows
(F+W-TF-2012) p 2905 N92-27045
EUROPE
Competing economies: America, Europe, and the Pacific rim
(PB92-115757) p 3014 N92-26730
EUROPEAN SPACE AGENCY
European Earth Observation Program
p 2925 N92-26745
EUROPIUM COMPOUNDS
Neutron powder diffraction study on Eu-substituted Bi2Sr2CaCu2O(8+y) high temperature superconductor
p 3003 N92-26328
EVALUATION
Testbank (1.0) user's manual
(AD-A245895) p 2971 N92-26196
CBT: Role and future application for crew training --- computer based training p 2953 N92-26992
EVAPORATION
High frequency analyses of coastal meteorological phenomena effecting refractivity
(AD-A246383) p 2947 N92-27075
EVAPORATIVE COOLING
Thermal analysis of evaporative coolers
p 2962 N92-26985
The transpirator, an efficient and light evaporative cooler for space technology p 2887 N92-26986
EVAPORATORS
A processing environment for test and simulation data of thermodynamic systems p 2959 N92-26963
Progress in the development of the Hermes evaporators p 2962 N92-26984
Nucleate pool boiling of R-114 and R-114/oil mixtures from single enhanced tubes
(AD-A245487) p 3008 N92-27058
EVAPOTRANSPIRATION
Surface energy budget and evapotranspiration measurement support
(NASA-CR-190059) p 2944 N92-26185
EVENT HORIZON
Euclidean black hole vortices
(NASA-CR-190117) p 3016 N92-26436
EXCIMER LASERS
Linear and non-linear response of liquid and solid particles to energetic radiation
(AD-A246366) p 2894 N92-26942
EXCITATION
Vibrational dynamics of aniline (N2)1 clusters in their first excited singlet state
(AD-A245812) p 2872 N92-26431
Destruction and excitation of accreted nuclei in neutron star atmospheres: Gamma ray lines and x ray bursts
p 3016 N92-26476
The computation of C-C and N-N bond dissociation energies for singly, doubly, and triply bonded systems
(NASA-CR-190254) p 2994 N92-26539
Dynamic properties of quasi-two-dimensional one component plasmas
(DE92-621523) p 3000 N92-26806

EXHAUST EMISSION
Summary of NOx control technologies and their availability and extent of application
[PB92-158260] p 2928 N92-26373
Use of the Edmonds-Reilly Model to model energy-related greenhouse gas emissions
[DE92-010035] p 2931 N92-26633
Assessment of computer models for estimating vehicle emission factors. Volume 1: Executive summary
[PB92-113059] p 2931 N92-26802
EXHAUST GASES
Summary of NOx control technologies and their availability and extent of application
[PB92-158260] p 2928 N92-26373
Use of the Edmonds-Reilly Model to model energy-related greenhouse gas emissions
[DE92-010035] p 2931 N92-26633
Assessment of computer models for estimating vehicle emission factors. Volume 2: Description and comparison of the MOBILE4 and EMFAC7E models
[PB92-113067] p 2932 N92-26803
Modification and experimental validation of a combined optical and collection probe for solid propellant exhaust analysis
[AD-A245387] p 2884 N92-26839
EXOBIOLOGY
Aerospace medicine and biology: A continuing bibliography with indexes (supplement 362)
[NASA-SP-7011(362)] p 2953 N92-27068
EXPERIMENT DESIGN
Feasibility study of an expert system for the design of fusion/solidification experiment boarding on space furnace p 2886 N92-26964
Advanced photovoltaic experiment, S0014: Preliminary flight results and post-flight findings p 2927 N92-27101
EXPERIMENTATION
Toluene-water clusters: Ion fragmentation and chemistry
[AD-A245813] p 2874 N92-26526
EXPERT SYSTEMS
Advanced software development workstation project: Engineering scripting language. Graphical editor
[NASA-CR-190391] p 2971 N92-26183
Data fusion and correlation techniques testbed (DFACTT): Field trial 14 January 1991
[AD-A245324] p 3011 N92-26378
Knowledge-based production management: Approaches, results, and prospects
[AD-A245714] p 3008 N92-26426
Research accomplished at the Knowledge Based Systems Lab: IDEF3, version 1.0
[NASA-CR-190279] p 2975 N92-26587
Principal investigator in a box: Version 1.2 documentation
[NASA-TM-107886] p 2982 N92-26628
A prototype semantic integrity front end expert system for a relational database
[AD-A246084] p 3013 N92-26765
Rule-based expert system for evaluating the quality of long-term, in-situ, gas chromatographic measurements of atmospheric methane
[PB92-128560] p 2876 N92-26812
Expert system management system
[AD-A247102] p 3009 N92-26863
Applying knowledge compilation techniques to model-based reasoning
[NASA-TM-107876] p 2984 N92-26885
Feasibility study of an expert system for the design of fusion/solidification experiment boarding on space furnace p 2886 N92-26964
Model compilation: An approach to automated model derivation
[NASA-TM-107895] p 2985 N92-27057
Documentation for the Semi-Automated Mesoscale Analysis System 1.1
[AD-A246144] p 2985 N92-27072
EXPLORER SATELLITES
Small Explorer Data System MIL-STD-1773 fiber optic bus
[NASA-TP-3227] p 2858 N92-26667
EXPLOSIONS
An explosively driven, fast shock tube
[DE92-008437] p 2856 N92-26720
EXPLOSIVES
Role of shock compression technique for scientific and engineering studies
[DE92-008324] p 2919 N92-26846
High melting aromatic nitrate esters
[AD-D015190] p 2884 N92-26880
EXPOSURE
The effect of sandstorms on PV arrays and components --- photovoltaic cells
[DE92-001240] p 2927 N92-26686
An overview of the first results on the solar array materials passive LDEF experiment (sample), A0171 p 2927 N92-27087
LDEF fiber optic exposure experiment No. S-0109 p 2998 N92-27090
Optical performance of exposed solar cell covers p 2998 N92-27091
EXTERNAL STORE SEPARATION
Separation of external stores: Comparison of results [F+W-TF-2058] p 2853 N92-26944
Aerodynamic interference between stores
[AD-A247207] p 2850 N92-27172
EXTERNAL STORES
Computer program for calculating in-flight aircraft-store interface reaction loads
[AD-A245782] p 2852 N92-26896
Aerodynamic interference between stores
[AD-A247207] p 2850 N92-27172
Pneumatically actuated multiple store launcher
[AD-D015237] p 2853 N92-27188
EXTRACTION
Radar scattering as a source of geological information on Venus and Earth p 3019 N92-26778
EXTRATERRESTRIAL ENVIRONMENTS
Study on the requirements for the installation of a CES and habitability centre p 2966 N92-27007
EXTRATERRESTRIAL RADIATION
Space environmental effects on coated optics p 2999 N92-27098
Exposure to space radiation of high-performance infrared multilayer filters and materials technology experiment (A0056) p 2999 N92-27108
Transmittance measurements of ultraviolet and visible wavelength filters flown aboard LDEF p 2999 N92-27110
Radiation sensitivity of quartz crystal oscillators experiment for the Long Duration Exposure Facility (LDEF) p 2895 N92-27111
LDEF electronic systems: Successes, failures and lessons p 2895 N92-27112
Effect of space exposure of pyroelectric infrared detectors p 2910 N92-27113
LDEF mechanical systems p 2916 N92-27114
EXTRAVEHICULAR ACTIVITY
Report for neutral buoyancy simulations of transfer orbit stage contingency extravehicular activities
[NASA-TM-103583] p 2857 N92-26268
Genesis and evaluation of an ergonomic architecture for the ESA EVA suit p 2965 N92-27003
Determination of ventilation requirements for a space suit helmet p 2968 N92-27017
EXTRAVEHICULAR MOBILITY UNITS
Fourth European Symposium on Space Environment Control Systems, volume 2
[ESA-SP-324-VOL-2] p 2956 N92-26950
EVA life support design and technology developments p 2965 N92-27002
Genesis and evaluation of an ergonomic architecture for the ESA EVA suit p 2965 N92-27003
EVA space suit thermal control and micrometeoroid protection p 2965 N92-27004
Development of the suit enclosure soft joints of the European EVA space suit p 2965 N92-27005
Development of European sublimator technology for EVA p 2968 N92-27018
Investigation on a partial pressure carbon dioxide sensor p 2968 N92-27019
Heat rejection system for an advanced extravehicular mobility unit portable life support system p 2968 N92-27020
EXTRUDING
An investigation of the mechanical properties and microscopic structure of extruded powder aluminum subjected to biaxial loadings at elevated temperature p 2879 N92-26770

F

F REGION
The effects of magnetic storm phases on F-layer irregularities from auroral to equatorial latitudes
[AD-A245495] p 2943 N92-26675
F-1 ROCKET ENGINE
A comparison of heavy lift launch vehicle options for the 1990s
[AD-A245617] p 2857 N92-26402
F-117A AIRCRAFT
The Lockheed F-117A
[RAND-P-7746-RGS] p 2852 N92-26673
F-16 AIRCRAFT
Development and testing of an unmanned air vehicle telemetry system
[AD-A246577] p 2858 N92-26621
FABRICATION
An investigation of the mechanical properties and microscopic structure of extruded powder aluminum subjected to biaxial loadings at elevated temperature p 2879 N92-26770
RF vacuum microelectronics
[AD-A246579] p 2893 N92-26771
Stresses in solder joints of electronic packages
[AD-A245799] p 2894 N92-26897
FACTORIAL DESIGN
User interface consistency across end-user application programs: Effect on learning and satisfaction p 3013 N92-26776
FAILURE
Fail safe system for suppressing stimulated Brillouin scattering in large optics on the Nova laser
[DE92-008608] p 2911 N92-26505
Failure studies of bimaterial interfaces and constrained ductile layers p 2868 N92-26559
Analysis and modeling of high-temperature performance of advanced fiber composites p 2868 N92-26564
FAILURE ANALYSIS
Assessment of diagnostic methods for solenoid-operated valves
[DE92-009379] p 2913 N92-26234
Reconfiguration in robust distributed real-time systems based on global checkpoints
[AD-A245615] p 2970 N92-26382
An empirical approach to analysis of similarities between software failure regions
[AD-A246208] p 2974 N92-26461
Reliability and failure analyses of composite beams and plates containing stress concentrations p 2918 N92-26598
Composite fuselage technology (summary of year 2)
[NASA-CR-190434] p 2852 N92-26655
Ceramic composites: Experimental and analytical study of SiC/Si3N4 composites p 2882 N92-26859
Applying knowledge compilation techniques to model-based reasoning
[NASA-TM-107876] p 2984 N92-26885
FAILURE MODES
Mixed Weibull distributions in reliability engineering: Statistical models for the lifetime of units with multiple modes of failure p 2916 N92-26602
FALLOUT
Biosphere model validation by intercomparison to observed behaviour of fallout radionuclides in the aquatic environment, appendix 5 p 2930 N92-26487
Modeling transfer of Cs-137 fallout in a large Finnish watercourse, appendix 6 p 2930 N92-26488
Environmental radiation data
[PB92-164706] p 2933 N92-26890
FALSE ALARMS
Fast envelope correlation for passive ranging
[AD-A246333] p 2888 N92-26388
FAST FOURIER TRANSFORMATIONS
Estimation of motion parameters from image sequences
[AD-A246135] p 2986 N92-26358
A frequency domain based approach to on-line system identification
[AD-A246193] p 2973 N92-26418
A comparison of direction finding results from an FFT peak identification technique with those from the music algorithm
[AD-A245675] p 2888 N92-26424
FAST NUCLEAR REACTORS
An investigation of the behavior of the clamp-induced bending stresses
[DE92-006504] p 2918 N92-26694
Evaluation of integral measurements for the SP-100 space reactor
[DE92-009717] p 2996 N92-26841
FATIGUE (MATERIALS)
On the stochastic fatigue crack growth problem p 2917 N92-26557
Simulation of 3D non-planar fatigue crack growth in a turbine blade root
[DE92-006859] p 2854 N92-26697
FATIGUE LIFE
Simulation of 3D non-planar fatigue crack growth in a turbine blade root
[DE92-006859] p 2854 N92-26697
The changing role of experimentation in aeroengine R and D: The point of view of the research worker
[AD-A246372] p 2856 N92-27062
FAULT TOLERANCE
Reconfiguration in robust distributed real-time systems based on global checkpoints
[AD-A245615] p 2970 N92-26382
Tools and techniques for adding fault tolerance to distributed and parallel programs
[AD-A245510] p 2980 N92-26677
Expert system management system
[AD-A247102] p 3009 N92-26863

Applying knowledge compilation techniques to model-based reasoning
[NASA-TM-107876] p 2984 N92-26885
Use of Markov methods in analysis of fault-tolerant systems with flexible repair policies
[PNR-90801] p 2916 N92-27038

FEASIBILITY
A feasibility study: California Department of Forestry and Fire Protection utilization of infrared technologies for wildland fire suppression and management
[NASA-CR-190458] p 2926 N92-27195

FEASIBILITY ANALYSIS
Fundamental mechanisms affecting friction welding under vacuum
[AD-A245685] p 2877 N92-26520
A prototype semantic integrity front end expert system for a relational database
[AD-A246084] p 3013 N92-26765
Environmental implications of increased biomass energy use
[DE92-001219] p 2932 N92-26810
Feasibility study of an expert system for the design of fusion/solidification experiment boarding on space furnace p 2886 N92-26964
Biodegradation studies with space cabin contaminants to determine the feasibility of Biological Air Filtration (BAF) in space cabins p 2962 N92-26983
Aerodynamic interference between stores
[AD-A247207] p 2850 N92-27172

FEDERAL BUDGETS
An analysis of the role of the budget committees in the Congressional budget process
[AD-A246005] p 3014 N92-26761
Biotechnology for the 21st century, FY 1993
[DE92-007757] p 2951 N92-26850

FEEDBACK CONTROL
Photocathode transfer and storage techniques using alkali vapor feedback control
[DE92-008449] p 2891 N92-26202
Adaptive control of robotic manipulators with structural flexibility p 2914 N92-26475
Parameter robust reduced-order control of flexible structures p 2982 N92-26597
Application of decentralized control to a laser alignment system
[DE92-009692] p 2912 N92-26646
The modeling and control of acoustic/structure interaction problems via piezoceramic actuators: 2-D numerical examples
[NASA-CR-189639] p 2987 N92-26668

FEEDFORWARD CONTROL
Two papers on feed-forward networks
[NASA-TM-107840] p 2983 N92-26631

FEET (ANATOMY)
Maintenance manual for Natick's Footwear Database
[AD-A246273] p 2954 N92-26242
User manual for Natick's Footwear Database
[AD-A246275] p 2954 N92-26243

FERMIONS
Supersymmetry and dark matter, a new candidate p 3016 N92-26491

FIBER COMPOSITES
Analysis and modeling of high-temperature performance of advanced fiber composites p 2868 N92-26564
Mesomechanics of viscoplastic metal matrix composites p 2869 N92-26607
Application of neutron diffraction to measure residual strains in high temperature composites
[DE91-014021] p 2869 N92-26679
Ceramic composites: Experimental and analytical study of SiC/Si3N4 composites p 2882 N92-26859

FIBER OPTICS
Results of a portable fiber-optic weigh-in-motion system
[DE92-009011] p 2996 N92-26376
Optical hidden layer network
[AD-A246162] p 2992 N92-26413
Fiber-optic flexural disk accelerometer
[AD-A246203] p 2908 N92-26459
Small Explorer Data System MIL-STD-1773 fiber optic bus
[NASA-TP-3227] p 2858 N92-26667
Technology transfer and application of SERS continuous monitor for trace organic compounds
[DE92-008900] p 2875 N92-26726
Preliminary analyses of WL experiment No. 701, space environment effects on operating fiber optic systems p 2998 N92-27089
LDEF fiber optic exposure experiment No. S-0109 p 2998 N92-27090
Differential polarimetric fiber optic sensor
[AD-D015218] p 2998 N92-27186

FIBER ORIENTATION
Analysis and modeling of high-temperature performance of advanced fiber composites p 2868 N92-26564

FIBER STRENGTH
Composite strength statistics from fiber strength statistics
[AD-A245616] p 2867 N92-26383
Ceramic composites: Experimental and analytical study of SiC/Si3N4 composites p 2882 N92-26859

FIELD EFFECT TRANSISTORS
Quantum interference and confinement effects in narrow channel Si-MOSFET's
[PB92-150176] p 3006 N92-26927

FIELD EMISSION
Field-emission arrays: A potentially bright source
[AD-A246561] p 2893 N92-26741

FIELD THEORY (ALGEBRA)
Universal R-matrix for quantized (super)algebras
[DE92-621067] p 2988 N92-26834

FIELD THEORY (PHYSICS)
Hamiltonian lattice field theory: Computer calculations using variational methods
[DE92-010479] p 2985 N92-26232
Topics in particle physics and cosmology
[DE92-010478] p 3019 N92-26385
Finite temperature quantum field theory in curved spacetime p 3007 N92-26780
Non-compact WZW conformal field theories
[PB92-125038] p 3007 N92-26805
Tensor-multi-scalar theories of gravitation
[PB92-152305] p 2943 N92-26820

FILE MAINTENANCE (COMPUTERS)
Integrating reverse engineering into Computer-Aided Software Engineering (CASE) p 2974 N92-26479

FILLETS
Algorithms for blending surface generation
[AD-A245686] p 2975 N92-26524

FILM COOLING
Hypersonic aerospace vehicle leading edge cooling using heat pipe, transpiration and film cooling techniques p 3007 N92-26733

FINITE DIFFERENCE THEORY
Mode structure and continuum damping of high-n toroidal Alfven eigenmodes
[DE92-010547] p 2999 N92-26256
Performance analysis of image motion analysis algorithms
[AD-A246522] p 2974 N92-26468
Tracer transport in the middle atmosphere p 2928 N92-26473
Numerical solution of plastic liquids shape factor
[PB92-133958] p 2896 N92-26496
Nonexpansive prolongations and difference schemes for the advection equation
[PB92-141530] p 2986 N92-26502
On the stochastic fatigue crack growth problem p 2917 N92-26557
Precision of the long baseline acoustic navigation system used by Pegasus
[AD-A246598] p 2852 N92-26795
Eulerian computational methods
[DE92-008017] p 2900 N92-26853
Penetration of laminated composites by projectiles p 2869 N92-26861
A finite element/finite difference approach for modeling three-dimensional flow and pollutant dispersion around structures
[DE92-007322] p 2934 N92-26935
Development of an advanced finite-difference atmospheric general circulation model
[DE92-010923] p 2944 N92-26937

FINITE ELEMENT METHOD
Effect of thermal residual stresses on the stress-strain behavior of metal-matrix composites
[AD-A246136] p 2868 N92-26386
On the stochastic fatigue crack growth problem p 2917 N92-26557
Computational methods for problems of acoustics with particular reference to exterior domains p 2992 N92-26558
Computational aspects of an implicit finite element procedure for elasto-viscoplastic large deformation problems p 2917 N92-26594
Reliability and failure analyses of composite beams and plates containing stress concentrations p 2918 N92-26598
Mesomechanics of viscoplastic metal matrix composites p 2869 N92-26607
Comparison of ceramic uniaxial compression specimens through detailed finite element modelling
[AD-A245816] p 2882 N92-26609
Application of parametrized variational principles in the finite element method p 2987 N92-26624
Weight optimum arch structures
[AD-A246001] p 2918 N92-26759
Finite element modeling of static indentation damage in laminated composites p 2869 N92-26827
Modeling cycle and time-dependent creep/relaxation effects on fatigue lives of notched members --- creep/relaxation p 2919 N92-26829
A finite element method including transverse stresses for thick laminated plates and shells p 2920 N92-26860
Structural dynamic interaction with solar tracking control for evolutionary Space Station concepts
[NASA-TM-107629] p 2920 N92-26903

FINITE VOLUME METHOD
Three-dimensional upwind scheme for solving the Euler equations on unstructured tetrahedral grids --- tetrahedral grids p 2849 N92-26585
Cell vertex methods for compressible gas flows p 2897 N92-26599

FINLAND
Model studies of the transfer of radionuclides in the Finnish environment
[VTT-PUBL-81] p 2929 N92-26482
Modeling transfer of Cs-137 fallout in a large Finnish watercourse, appendix 6 p 2930 N92-26488

FIRE PREVENTION
Static electricity: A literature review
[AD-A246533] p 2990 N92-26471
A feasibility study: California Department of Forestry and Fire Protection utilization of infrared technologies for wildland fire suppression and management
[NASA-CR-190458] p 2926 N92-27195
Microgravity combustion science: Progress, plans, and opportunities
[NASA-TM-105410] p 2886 N92-27197

FIRES
Numerical field model simulation of full-scale fire tests in a closed spherical/cylindrical vessel using advanced computer graphics techniques
[AD-A245810] p 2887 N92-26898

FISHES
Application of irradiation techniques to food and foodstuffs
[DE92-614952] p 2954 N92-26186

FISSION PRODUCTS
Environmental radiation data
[PB92-164706] p 2933 N92-26890

FITTING
Downdating of Szego polynomials and data fitting applications
[AD-A245825] p 2988 N92-26900

FLAME PROPAGATION
Color image processing and object tracking workstation
[NASA-TM-105561] p 2886 N92-26611
Theoretical and numerical study of flame propagation and transition to detonation --- detonation transition p 2874 N92-26615

FLAME RETARDANTS
Static electricity: A literature review
[AD-A246533] p 2990 N92-26471

FLAME STABILITY
Theoretical and numerical study of flame propagation and transition to detonation --- detonation transition p 2874 N92-26615

FLAMMABILITY
Static electricity: A literature review
[AD-A246533] p 2990 N92-26471
Microgravity combustion science: Progress, plans, and opportunities
[NASA-TM-105410] p 2886 N92-27197

FLAMMABLE GASES
Static electricity: A literature review
[AD-A246533] p 2990 N92-26471

FLAT PLATES
Experimental studies on the flat plate boundary layer transition using hydrogen bubble method p 2903 N92-26914
Numerical studies on laminar turbulent transition at the Stuttgart University, Germany p 2903 N92-26916
Responses of boundary layers to strong external disturbances p 2904 N92-26921
Transverse flat plate heat pipe experiment p 2906 N92-27107

FLEXIBILITY
Adaptive control of robotic manipulators with structural flexibility p 2914 N92-26475

FLEXIBLE BODIES
Fiber-optic flexural disk accelerometer
[AD-A246203] p 2908 N92-26459
Parameter robust reduced-order control of flexible structures p 2982 N92-26597
Homogenization models for 2-D grid structures
[NASA-CR-190321] p 2920 N92-26892

FLIGHT CHARACTERISTICS
Outlines of parabolic flight p 2884 N92-26441

FLIGHT CONTROL
F-111C flight dynamic model aerodynamic data-base development and verification
[AD-A246356] p 2850 N92-26947

FLIGHT MANAGEMENT SYSTEMS
Man-machine interface analyses for bomber flight management system
[AD-A245707] p 2955 N92-26355
FLIGHT OPERATIONS
Outlines of parabolic flight p 2884 N92-26441
FLIGHT OPTIMIZATION
Man-machine interface analyses for bomber flight management system
[AD-A245707] p 2955 N92-26355
FLIGHT SAFETY
NASA. Johnson Space Center primary battery applications p 2863 N92-27142
FLIGHT SIMULATION
Microcomputer-based instrument flight simulation: Undergraduate pilot training student attitude assessment
[AD-A245449] p 2856 N92-26527
An Ada object oriented missile flight simulation
[AD-A246378] p 2977 N92-27052
FLIGHT SIMULATORS
Expert system management system
[AD-A247102] p 3009 N92-26863
FLIGHT TESTS
Development and testing of an unmanned air vehicle telemetry system
[AD-A246577] p 2858 N92-26621
Separation of external stores: Comparison of results
[F+W-TF-2058] p 2853 N92-26944
Flight test results of the passive cooling system p 2860 N92-27000
FLIR DETECTORS
Early risk reduction phase 1 FLIR/laser designator window
[AD-A246352] p 2911 N92-26293
FLOAT ZONES
The experiment under microgravity by aircraft: The experiment in floating by gas flow p 2886 N92-26447
FLOATING
The experiment under microgravity by aircraft: The experiment in floating by gas flow p 2886 N92-26447
FLOQUET THEOREM
Multiquanta photodetachment from the H(-) ion
[DE92-010306] p 2911 N92-26573
FLOW CHARACTERISTICS
Upper/lower vortex interaction and potential vorticity inversion p 2939 N92-26331
FLOW CHARTS
Architecture flow diagrams under Teamwork
[DE92-010482] p 2922 N92-26534
FLOW DISTORTION
An evolutional process of three dimensional disturbances in laminar boundary layers p 2902 N92-26910
FLOW DISTRIBUTION
Performance prediction and design of maximum thrust planar supersonic nozzles using a flux-difference-splitting technique p 2853 N92-26480
CFD mixing analysis of jets injected from straight and slanted slots into confined crossflow in rectangular ducts
[NASA-TM-105699] p 2854 N92-26561
An experimental investigation of a 2-D scramjet inlet at flow Mach numbers of 8 to 25 and stagnation temperatures of 800 to 4,100 K p 2854 N92-26586
Use of an approximate similarity principle for the thermal scaling of a full-scale thrust augmenting ejector
[NASA-TM-105724] p 2854 N92-26613
Theoretical and numerical study of flame propagation and transition to detonation --- detonation transition p 2874 N92-26615
Observation and measurements of flow structures in the stagnation region of a wing-body junction p 2849 N92-26616
Systematic study of Reynolds stress closure models in the computations of plane channel flows
[NASA-CR-189646] p 2898 N92-26649
The interaction of a vortex ring with a contaminated free surface p 2900 N92-26785
A parametric study of the hydrodynamic stability theory of 3-D compressible free shear flows p 2900 N92-26849
Numerical simulation of two-dimensional single- and multiple-material flow fields
[DE92-007428] p 2901 N92-26856
Large-scale structures and the spatial evolution of wakes behind axisymmetric bluff bodies p 2901 N92-26871
Pattern search in turbulent field p 2901 N92-26907
Vortex structure in wake of a circular cylinder p 2904 N92-26918
Numerical simulation of the laminar turbulent transition in a stratified flow p 2904 N92-26920
Overview of NASA supported Stirling thermodynamic loss research
[NASA-TM-105690] p 2861 N92-27034
Subscale solid rocket motor infrared signature and particle behavior
[AD-A246416] p 2862 N92-27065
High lift aircraft
[AD-D015215] p 2853 N92-27185
Computational method to predict thermodynamic, transport, and flow properties for the modified Langley 8-foot high-temperature tunnel
[NASA-TM-4374] p 2905 N92-27193
FLOW EQUATIONS
Wave structure in one and two dimensional fluid flow
[DE92-007421] p 2900 N92-26855
FLOW MEASUREMENT
Optical flow sensor
[AD-D015200] p 2997 N92-26862
Experimental studies on the flat plate boundary layer transition using hydrogen bubble method p 2903 N92-26914
Investigation on the boundary layer transition of alternately oscillating flow in deceleration phase p 2903 N92-26917
FLOW STABILITY
The stability of barotropic vortices: Implications for tropical cyclone motion p 2940 N92-26335
An experimental study of natural and forced modes in an axisymmetric jet p 2897 N92-26600
Distributed acoustic receptivity in laminar flow control configurations
[NASA-CR-4438] p 2898 N92-26680
Boundary-layer receptivity due to distributed surface imperfections of a deterministic or random nature
[NASA-CR-4439] p 2898 N92-26681
A parametric study of the hydrodynamic stability theory of 3-D compressible free shear flows p 2900 N92-26849
Three dimensional boundary layer transition on a yawed cylinder p 2902 N92-26909
Numerical studies on laminar turbulent transition at the Stuttgart University, Germany p 2903 N92-26916
Turbulent mixing in supersonic jets p 2850 N92-27054
FLOW VELOCITY
Polycyclic aromatic hydrocarbon radiative properties and formation in carbon-rich stellar outflows p 3018 N92-26757
Optical flow sensor
[AD-D015200] p 2997 N92-26862
FLOW VISUALIZATION
Helium bubble flow visualization of the spanwise separation on a NACA 0012 with simulated glaze ice
[NASA-TM-105742] p 2849 N92-26612
Observation and measurements of flow structures in the stagnation region of a wing-body junction p 2849 N92-26616
The interaction of a vortex ring with a contaminated free surface p 2900 N92-26785
Large-scale structures and the spatial evolution of wakes behind axisymmetric bluff bodies p 2901 N92-26871
Proceedings of the 5th and 6th Seminars on Investigation and Control of Boundary-Layer Transition
[NAL-SP-12] p 2901 N92-26906
Experimental studies on the flat plate boundary layer transition using hydrogen bubble method p 2903 N92-26914
FLUENCE
Preliminary total dose measurements on LDEF --- long duration exposure facility p 2952 N92-27123
FLUID BOUNDARIES
Symbolic solution of a multilayer ocean waveguide problem with arbitrary depth dependent ambient density and sound speed profiles
[AD-A245476] p 2949 N92-26533
FLUID DYNAMICS
On the existence of a capital similarity p 2941 N92-26344
FLUID FLOW
A model for aerodynamically-valved pulse combustion
[DE92-009687] p 2871 N92-26262
Diapycnal mixing, gravity-current propagation, and sediment dispersion in turbulent fluids
[AD-A246160] p 2896 N92-26412
Parabolic flight experiments on bubble migration under reduced gravity p 2885 N92-26443
Liquid motion analysis with lateral impacts under low gravity p 2885 N92-26445
FLUID MANAGEMENT
Liquid motion analysis with lateral impacts under low gravity p 2885 N92-26445
FLUORESCENCE
Polarisation effects in fibre lasers p 2911 N92-26571
Application of fluorescent-particle imaging to measuring flow in complex media
[DE92-009121] p 2898 N92-26645
Polycyclic aromatic hydrocarbon radiative properties and formation in carbon-rich stellar outflows p 3018 N92-26757
FLUORIDES
Comparison of laser and conventional heating in TLD dosemapping
[DE92-010773] p 2910 N92-26269
NASA Li/CF(x) cell problem analysis: Anion exchange chromatography analysis p 2864 N92-27145
FLUORO COMPOUNDS
Synthesis of novel fluorinated phosphonic acid electrolytes for phosphoric acid fuel cells
[PB92-164300] p 2926 N92-26372
FLUX DENSITY
Mapping of the auroral oval to the tail p 2937 N92-26309
FLUX PINNING
The production and properties of melt-zone textured Y1Ba2Cu3O(7-delta) filaments
[DE92-008097] p 3005 N92-26843
FLYING PERSONNEL
Test plan for the international aircraft operator information system
[DOT/FAA/CT-91/18] p 3014 N92-26830
FOCUSING
Focusing x ray transition radiation with cylindrical and elliptical optics
[AD-A245987] p 2997 N92-26754
Theory of electromagnetic instability of an intense beam in a quadrupole focusing system
[AD-A246560] p 2990 N92-26768
FOOD PROCESSING
Application of irradiation techniques to food and foodstuffs
[DE92-614952] p 2954 N92-26186
Critical technologies: Spacecraft habitability, an update p 2966 N92-27010
FOOTPRINTS
Cusp studies with HF radars p 2936 N92-26304
FOREBODIES
High-alpha vortex decoupling investigations on a chine forebody/Delta wing configuration at transonic Mach numbers
[NASA-CR-189642] p 2849 N92-26651
FOREST MANAGEMENT
Global assessment of promising forest management practices for sequestration of carbon
[PB92-153006] p 2930 N92-26510
Waste minimization for non-agricultural pesticide applicators: EPA's pollution prevention guide
[PB92-153774] p 2933 N92-26889
A feasibility study: California Department of Forestry and Fire Protection utilization of infrared technologies for wildland fire suppression and management
[NASA-CR-190458] p 2926 N92-27195
FORESTS
Global assessment of promising forest management practices for sequestration of carbon
[PB92-153006] p 2930 N92-26510
Role of climate in forest monitoring and assessment: A New England example
[PB92-132885] p 2930 N92-26519
FORMALISM
NEXUS: A kernel complex object management system p 3012 N92-26567
FORMAT
Software requirements document for the netCDF interface within ECMOP, version 1.0
[AD-A246220] p 2974 N92-26464
FORMATES
Determination of the structure of Y(HCOO)3 by the neutron time-of-flight diffraction method p 3002 N92-26325
FORTRAN
A FORTRAN 90 code for magnetohydrodynamics
[DE92-010362] p 3000 N92-26577
FOURIER ANALYSIS
Development and applications of the reverse neutron time-of-flight method with Fourier-type beam chopper
[VTT-PUBL-82] p 3001 N92-26320
Estimation of peak intensities from frequency filtered total scattering data of neutrons obtained by the reverse Fourier method p 3002 N92-26321
High-resolution Fourier TOF powder diffraction. 1: Performance of the Mini-Sfinks Facility p 3002 N92-26323
Neutron powder diffraction study of deuterated beta-acetonitrile p 3002 N92-26324
FOURIER SERIES
Recursive ray acoustics for three-dimensional sound-speed profiles
[AD-A245613] p 2991 N92-26228
Ocean bottom modeling for ray acoustics
[AD-A246287] p 2948 N92-26360
FOURIER TRANSFORMATION
On the design of VLSI circuits for the Winograd Fourier transform algorithm
[AD-A246317] p 2892 N92-26244

Evaluation of the Fourier transform infrared spectrometer for particle-associated ammonium sulfate determination
[PB92-160084] p 2910 N92-26930

FOVEA
Modeling of explorative procedures for remote object identification
[AD-A245525] p 2922 N92-26661

FRACTALS
Fractal characteristics of fracture roughness and aperture data
[DE92-010302] p 2895 N92-26214
A fractal computer model of macromolecule-cell surface interactions
[AD-A245394] p 2950 N92-26289
Ocean bottom simulation using fractal geometry
[AD-A245477] p 2949 N92-26423
Fractals and chaos
[AD-A246502] p 2990 N92-26466
Studies in chaos using stochastic methods
[AD-A246919] p 3008 N92-27171

FRACTIONATION
The carbon isotopic compositions of individual compounds from ancient and modern depositional environments p 2921 N92-26478

FRACTURE MECHANICS
Failure studies of bimaterial interfaces and constrained ductile layers p 2868 N92-26559
Simulation of 3D non-planar fatigue crack growth in a turbine blade root
[DE92-006859] p 2854 N92-26697
Fracture of structural ceramics in combined mode 1 and mode 2 loading p 2882 N92-26775
Study and analysis of the stress state in a ceramic, button-head, tensile specimen
[DE92-007794] p 2918 N92-26784

FRACTURE STRENGTH
Crack arrest and static fracture toughness tests of a ship plate steel
[AD-A245641] p 2916 N92-26282
Experimental study of shear fracture and aggregate interlock in cementbased composites
[PB92-151521] p 2868 N92-26525
Fracture of structural ceramics in combined mode 1 and mode 2 loading p 2882 N92-26775
Improving the fracture resistance of irradiated martensitic steels
[DE92-008387] p 2879 N92-26848

FRACTURES (MATERIALS)
Fractal characteristics of fracture roughness and aperture data
[DE92-010302] p 2895 N92-26214

FRACTURING
Fractal characteristics of fracture roughness and aperture data
[DE92-010302] p 2895 N92-26214
Experimental study of shear fracture and aggregate interlock in cementbased composites
[PB92-151521] p 2868 N92-26525
Fracture of structural ceramics in combined mode 1 and mode 2 loading p 2882 N92-26775

FRAGMENTATION
Toluene-water clusters: Ion fragmentation and chemistry
[AD-A245813] p 2874 N92-26526

FRANCK-CONDON PRINCIPLE
An analysis of middle ultraviolet emissions of molecular nitrogen and nitric oxide and vacuum calibration of an ultraviolet spectrograph
[AD-A245984] p 2943 N92-26753

FREE CONVECTION
Preliminary experiment of GDEF (Gas Dynamics Experiment Facility) p 2885 N92-26442
Effects of power pulsations on natural convection from discrete heat sources
[AD-A246557] p 3007 N92-26617

FREE ELECTRON LASERS
Diagnostic upgrades on MTX
[DE92-009695] p 2906 N92-26230
High frequency Raman current drive
[PB92-142223] p 2893 N92-26497
Operation of a Smith-Purcell free-electron laser at submillimeter wavelengths p 2912 N92-26626

FRENCH SPACE PROGRAM
French space programmes related to global change p 2925 N92-26746

FREQUENCIES
Mutual friction in superfluid He-3: Effects of bound states in the vortex core
[PB92-142231] p 2896 N92-26507
Analysis of EMP response of structures using frequency domain electromagnetic interaction codes
[AD-A245758] p 2889 N92-26592

FREQUENCY CONVERTERS
Binaural ultrasound detector and imager
[AD-D015214] p 2993 N92-27184

FREQUENCY DISTRIBUTION
Estimation of peak intensities from frequency filtered total scattering data of neutrons obtained by the reverse Fourier method p 3002 N92-26321

FREQUENCY HOPPING
Effects of non-uniform windowing on the performance of a fast frequency-hopped noncoherent MFSK receiver over Rician fading channels with partial-band interference and Doppler shift
[AD-A245762] p 2889 N92-26595
System evaluation of a frequency hopping combat net radio
[AD-A246365] p 2891 N92-26941

FREQUENCY MODULATION
Implementation of multi-frequency modulation with Trellis encoding and Viterbi decoding using a digital signal processing board
[AD-A245998] p 2976 N92-26758

FREQUENCY RANGES
Analysis of EMP response of structures using frequency domain electromagnetic interaction codes
[AD-A245758] p 2889 N92-26592

FREQUENCY RESPONSE
A frequency domain based approach to on-line system identification
[AD-A246193] p 2973 N92-26418
Spontaneous and induced coherent radiation generation in atomic vapors
[AD-A246078] p 2890 N92-26764

FREQUENCY SHIFT KEYING
Effects of non-uniform windowing on the performance of a fast frequency-hopped noncoherent MFSK receiver over Rician fading channels with partial-band interference and Doppler shift
[AD-A245762] p 2889 N92-26595

FREQUENCY STABILITY
Radiation sensitivity of quartz crystal oscillators experiment for the Long Duration Exposure Facility (LDEF) p 2895 N92-27111

FRESNEL INTEGRALS
Cluster model of polarization reflection from metallic surfaces
[AD-A245781] p 2996 N92-26241

FRICTION
Ceramic bearing technology: Proceedings of the NIST/DARPA Workshop
[PB92-137553] p 2914 N92-26366
Mutual friction in superfluid He-3: Effects of bound states in the vortex core
[PB92-142231] p 2896 N92-26507
Computational techniques in tribology and material science at the atomic level
[NASA-TM-105573] p 2990 N92-26671

FRICTION FACTOR
On-orbit coldwelding: Fact or friction? p 2880 N92-27115

FRICTION WELDING
Fundamental mechanisms affecting friction welding under vacuum
[AD-A245685] p 2877 N92-26520

FRONTS (METEOROLOGY)
Contributions to atmospheric physics in honor of Dr. Manfred Reinhardt on his 65th birthday
[DLR-FB-91-30] p 2939 N92-26329
Comparison of frontogenetical structures for different cases of frontal development p 2939 N92-26333
The objective determination of front lines p 2941 N92-26343

FUEL CELLS
Zirconia-based fuel cells for power generation
[DE92-009886] p 2927 N92-26719

FUEL COMBUSTION
A model for aerodynamically-valved pulse combustion
[DE92-009887] p 2871 N92-26262
Fuel staging and its implementation in a novel internally staged burner
[ETN-92-91307] p 2872 N92-26285
Turbocharged pressurized combustion system
[PB92-142579] p 2873 N92-26521
Advancing natural gas combustion science and technology-low NOx
[PB92-137652] p 2876 N92-26782
Microwave backscattering fuel/air ratio control and flame monitoring device
[PB92-141779] p 2876 N92-26783
Technology for reduction of CO2 emissions from the transportation sector
[PB92-153733] p 2933 N92-26929

FUEL CONSUMPTION
Throttleless Otto-cycle natural gas engines
[PB92-164482] p 2914 N92-26371

FUEL INJECTION
Fuel staging and its implementation in a novel internally staged burner
[ETN-92-91307] p 2872 N92-26285

FUEL TANKS
Separation of external stores: Comparison of results
[F+W-TF-2058] p 2853 N92-26944

FUEL TESTS
Assessment of a hot hydrogen nuclear propulsion fuel test facility
[DE92-004571] p 2995 N92-26692

FUEL-AIR RATIO
Microwave backscattering fuel/air ratio control and flame monitoring device
[PB92-141779] p 2876 N92-26783

FUELS
A model for aerodynamically-valved pulse combustion
[DE92-009887] p 2871 N92-26262

FULL SCALE TESTS
Acoustic interactions between an altitude test facility and jet engine plumes: Theory and experiments
[NASA-CR-190423] p 2853 N92-26405
Numerical field model simulation of full-scale fire tests in a closed spherical/cylindrical vessel using advanced computer graphics techniques
[AD-A245810] p 2887 N92-26898

FUNCTIONAL ANALYSIS
Dvoretzky's theorem: 30 years later
[PB92-153212] p 2988 N92-26788

FUNCTIONAL DESIGN SPECIFICATIONS
Requirements analysis and design for implementation of a satellite link for a local area computer network
[AD-A245610] p 2978 N92-26227
Plan of action survey of functional requirements for a geographical information system
[AD-A245622] p 3011 N92-26403
Functional requirements document for NASA/MSFC Earth Science and Applications Division: Data and information system (ESAD-DIS). Interoperability, 1992
[NASA-TM-4388] p 2921 N92-26905

FUNCTIONS (MATHEMATICS)
A computer program for the calculation of daubechies wavelets
[AD-A245461] p 2975 N92-26529

FUNGI
Total Dose Effects (TDE) of heavy ionizing radiation in fungus spores and plant seeds: Preliminary investigations p 2952 N92-27124

FURNACES
High temperature furnace modeling and performance verifications
[NASA-CR-190403] p 2908 N92-26536
Feasibility study of an expert system for the design of fusion/solidification experiment boarding on space furnace p 2886 N92-26964

FUSELAGES
Composite fuselage technology (summary of year 2)
[NASA-CR-190434] p 2852 N92-26655

FUSION (MELTING)
Feasibility study of an expert system for the design of fusion/solidification experiment boarding on space furnace p 2886 N92-26964

FUSION REACTORS
Inertial fusion energy power plant design using the Compact Torus Accelerator: HYLIFE-CT
[DE92-008941] p 3000 N92-26729

FUSION WELDING
Factors influencing the microstructural and mechanical properties of ULCB steel weldments
[AD-A245523] p 2878 N92-26659

FUZZY SETS
Extracting fuzzy rules under uncertainty and measuring definability using rough sets
[NASA-CR-190396] p 2972 N92-26197
Measuring uncertainty by extracting fuzzy rules using rough sets
[NASA-CR-190395] p 2972 N92-26198
VLSI implementation of fuzzy logic operator unit
[AD-A247146] p 2989 N92-27180

FUZZY SYSTEMS
VLSI implementation of fuzzy logic operator unit
[AD-A247146] p 2989 N92-27180

G

GALACTIC BULGE
Mapping the great attractor region in x rays and diffuse x ray emission: A possible galactic wind in the bulge of M31
[NASA-CR-190402] p 3015 N92-26184

GALACTIC CLUSTERS
Mapping the great attractor region in x rays and diffuse x ray emission: A possible galactic wind in the bulge of M31
[NASA-CR-190402] p 3015 N92-26184
Evidence for cluster magnetic fields around radio galaxies p 3017 N92-26554

GALACTIC EVOLUTION
The galactic evolution of s-process elements via asymptotic giant branch stars p 3018 N92-26725
GALACTIC STRUCTURE
A self-contamination model for the formation of globular star clusters p 3018 N92-26723
GALERKIN METHOD
Computational methods for problems of acoustics with particular reference to exterior domains p 2992 N92-26558
GALLIUM ARSENIDES
Generation of nonequilibrium optical phonons in GaAs/AlAs quantum wells by intrasubband and intersubband scatterings [DE92-010264] p 2993 N92-26207
Method for implanting impurities in semiconductors and semiconductor implanted with impurities [AD-D015196] p 3003 N92-26433
GAMMA RAY ASTRONOMY
X ray observations of gamma ray burst sources [MPE-PREPRINT-174] p 3018 N92-27048
GAMMA RAY BURSTS
X ray observations of gamma ray burst sources [MPE-PREPRINT-174] p 3018 N92-27048
The HUS solar flare and cosmic gamma ray burst detector aboard the Ulysses spacecraft [MPE-PREPRINT-175] p 3016 N92-27049
GAMMA RAY SPECTRA
New approaches to studies of exotic nuclei [DE92-010127] p 2994 N92-26570
Gamma-ray spectrometry of LDEF samples [DE92-009947] p 2874 N92-26632
GAMMA RAYS
Destruction and excitation of accreted nuclei in neutron star atmospheres: Gamma ray lines and x ray bursts p 3016 N92-26476
A user's manual for MASH 1.0: A Monte Carlo adjoint shielding code system [DE92-010375] p 3021 N92-26544
GANGLIA
Low power laser irradiation effect with emphasis on injured neural tissues [AD-A246410] p 2953 N92-27063
GAS ANALYSIS
Gravimetric gas determinations for volume calibrations [DE92-010041] p 2874 N92-26634
GAS CHROMATOGRAPHY
Gas phase chromatography of halides of elements 104 and 105 [DE92-010284] p 2870 N92-26212
Gas-pressure studies with Li(Si)/FeS2 thermal batteries [DE92-010801] p 2892 N92-26238
Metal hydride based isotope separation: Large-scale operations [DE92-009830] p 2875 N92-26717
Rule-based expert system for evaluating the quality of long-term, in-situ, gas chromatographic measurements of atmospheric methane [PB92-128560] p 2876 N92-26812
GAS COMPOSITION
Improved procedures for quantifying key meteorological effects on ambient ozone data [PB92-163278] p 2931 N92-26793
GAS DENSITY
Polycyclic aromatic hydrocarbon radiative properties and formation in carbon-rich stellar outflows p 3018 N92-26757
GAS DYNAMICS
On shock capturing for liquid and gas media p 2897 N92-26556
GAS FLOW
Cell vertex methods for compressible gas flows p 2897 N92-26599
Microwave backscattering fuel/air ratio control and flame monitoring device [PB92-141779] p 2876 N92-26783
Ensuring mass conversion in a heavy-gas dispersion model using the generalized anelastic equations [DE92-007323] p 2934 N92-26936
GAS JETS
Turbulent mixing in supersonic jets p 2850 N92-27054
GAS LASERS
Transient gas motion in nuclear-reactor-pumped lasers: Computational and experimental results [DE92-002357] p 2912 N92-26691
GAS PATH ANALYSIS
Progress towards understanding and predicting convection heat transfer in the turbine gas path [NASA-TM-105674] p 2898 N92-26690
GAS PRESSURE
Gas-pressure studies with Li(Si)/FeS2 thermal batteries [DE92-010801] p 2892 N92-26238
Oxygen recombination in the sealed nickel-cadmium cell p 2863 N92-27138
Pneumatically actuated multiple store launcher [AD-D015237] p 2853 N92-27188
GAS SPECTROSCOPY
Spectroscopy and kinetics of combustion gases at high temperatures [DE92-011216] p 2872 N92-26281
GAS STREAMS
A parametric study of the hydrodynamic stability theory of 3-D compressible free shear flows p 2900 N92-26849
GAS TURBINE ENGINES
Aircraft photovoltaic power-generating system p 2926 N92-26581
GAS TURBINES
Turbocharged pressurized combustion system [PB92-142579] p 2873 N92-26521
A parametric numerical study of mixing in a cylindrical duct [NASA-TM-105695] p 2854 N92-26553
CFD mixing analysis of jets injected from straight and slanted slots into confined crossflow in rectangular ducts [NASA-TM-105699] p 2854 N92-26561
Progress towards understanding and predicting convection heat transfer in the turbine gas path [NASA-TM-105674] p 2898 N92-26690
Advancing natural gas combustion science and technology-low NOx [PB92-137652] p 2876 N92-26782
Simultaneous engineering in aero-gas turbine design and manufacture [PNR-90811] p 2856 N92-27043
The changing role of experimentation in aeroengine R and D: The point of view of the research worker [AD-A246372] p 2856 N92-27062
GAS-SOLID INTERACTIONS
The importance of chemical reactions with environment for ablation process of thermal protection and structural materials p 2883 N92-27015
GASIFICATION
High octane ethers from synthesis gas-derived alcohols [DE92-010480] p 2884 N92-26548
GATES (CIRCUITS)
High-speed pulse detection room-temperature optical nonlinearities for GaInAs/AlInAs and GaA1InAs/A1InAs multiple quantum wells and integrated mirror etalon at 1.3 micrometers [AD-A246369] p 2998 N92-26943
GEAR TEETH
Gear tooth stress measurements of two helicopter planetary stages [NASA-TM-105651] p 2915 N92-26555
GEARS
Full-scale transmission testing to evaluate advanced lubricants [NASA-TM-105668] p 2915 N92-26560
GENETIC CODE
A computer system for access to distributed genome mapping data [DE92-008875] p 3011 N92-26453
GENETIC ENGINEERING
Biotechnology for the 21st century, FY 1993 [DE92-007757] p 2951 N92-26850
GEOCHEMISTRY
Geochemical constraints on ocean general circulation models [DE92-010805] p 2948 N92-26270
Infrared spectroscopy and hydrogen isotope geochemistry of hydrous silicate glasses [DE92-008398] p 2881 N92-26451
GEODESY
Characterization of the clock in a new inexpensive GPS receiver: The Magnavox MX 4200 [AD-A246165] p 2851 N92-26415
GEODETIC COORDINATES
The preliminary geodetic control network of Venus [RAND-N-3437-JPL] p 3019 N92-26819
GEOGRAPHIC INFORMATION SYSTEMS
Plan of action survey of functional requirements for a geographical information system [AD-A245622] p 3011 N92-26403
Generation of multi-resolution maps [PB92-152206] p 2921 N92-26513
Role of climate in forest monitoring and assessment: A New England example [PB92-132885] p 2930 N92-26519
Building a GIS on top of the open DBMS Postgres [FEL-91-B183] p 3014 N92-26875
GEOIDS
The geoid, GPS, and levelling p 2925 N92-26777
GEOLOGICAL FAULTS
Fault zone structure determined through the analysis of earthquake arrival times [DE92-010322] p 2935 N92-26239
GEOLOGICAL SURVEYS
Fault zone structure determined through the analysis of earthquake arrival times [DE92-010322] p 2935 N92-26239
Radar scattering as a source of geological information on Venus and Earth p 3019 N92-26778
GEOLOGY
Radar scattering as a source of geological information on Venus and Earth p 3019 N92-26778
GEOMAGNETIC LATITUDE
The effects of magnetic storm phases on F-layer irregularities from auroral to equatorial latitudes [AD-A245495] p 2943 N92-26675
GEOMAGNETIC TAIL
Mapping of the auroral oval to the tail p 2937 N92-26309
Relationships between ionospheric and tail phenomena p 2938 N92-26317
GEOMAGNETISM
Handbook of solar-terrestrial data systems, version 1 [NASA-TM-107810] p 3019 N92-26191
Lesson learned from GEOS and ISEE p 2936 N92-26302
The joint US/UK 1990 epoch world magnetic model [NASA-CR-190424] p 2942 N92-26406
GEOMETRICAL ACOUSTICS
Recursive ray acoustics for three-dimensional sound-speed profiles [AD-A245613] p 2991 N92-26228
Ocean bottom modeling for ray acoustics [AD-A246287] p 2948 N92-26360
GEOMETRY
Ocean bottom simulation using fractal geometry [AD-A245477] p 2949 N92-26423
On the subject of geometric spacing of meteorological sensors [AD-A245824] p 2946 N92-26899
GEOPHYSICAL OBSERVATORIES
Cluster Dayside Polar Cusp [ESA-SP-330] p 2935 N92-26294
The Norwegian upper atmosphere programme in Svalbard (Norway) p 2935 N92-26295
Antarctic studies of the cusp p 2936 N92-26301
The need of coordinated observations in space and from ground p 2937 N92-26310
GEOPHYSICS
On the existence of a capital similarity p 2941 N92-26344
GEOPOTENTIAL
Estimation of geopotential differences over intercontinental locations using satellite and terrestrial measurements p 2924 N92-26728
GEOS SATELLITES (ESA)
Lesson learned from GEOS and ISEE p 2936 N92-26302
GEOSTROPHIC WIND
A reformulation of the Eady model p 2939 N92-26330
Studies of inertio-gravity waves induced by geostrophic adjustment of the atmospheric jet stream p 2944 N92-26866
GERMANY
The DLR meteorological research aircraft Falcon p 2941 N92-26348
GERMINATION
Space Exposed Experiment Developed for Students (SEEDS) (P0004-2) p 2952 N92-27121
GIANT STARS
The galactic evolution of s-process elements via asymptotic giant branch stars p 3018 N92-26725
GLACIERS
The effect of global change and long period tides on the Earth's rotation and gravitational potential p 2925 N92-26781
GLASS
Infrared spectroscopy and hydrogen isotope geochemistry of hydrous silicate glasses [DE92-008398] p 2881 N92-26451
Crystalline-amorphous interfaces and their relation to grain boundary films [DE92-009812] p 3004 N92-26648
Fracture of structural ceramics in combined mode 1 and mode 2 loading p 2882 N92-26775
Etching effects in ion implanted SiO2 [DE92-011150] p 3005 N92-26826
Contamination of optical surfaces in Earth orbit p 2999 N92-27099
GLASS FIBERS
Lightweight fiber insulations performance and application p 2883 N92-27016
GLIDE LANDINGS
Critical soft landing technology issues for future US space missions [NASA-CR-185673] p 2858 N92-26884

GLIDERS
Measurements in the inhomogeneous convective boundary layer using three powered gliders
p 2942 N92-26350
GLOBAL POSITIONING SYSTEM
Characterization of the clock in a new inexpensive GPS receiver: The Magnavox MX 4200
[AD-A246165] p 2851 N92-26415
An adaptive correction technique for Differential Global Positioning System p 2851 N92-26623
Estimation of geopotential differences over intercontinental locations using satellite and terrestrial measurements p 2924 N92-26728
The geoid, GPS, and levelling p 2925 N92-26777
Buffered serial data card
[AD-A246435] p 2852 N92-26948
GLOBAL WARMING
Equilibrium-analysis of projected climate change effects on the global soil organic matter pool
[PB92-153022] p 2930 N92-26509
The effect of global change and long period tides on the Earth's rotation and gravitational potential
p 2925 N92-26781
GLOBULAR CLUSTERS
Dynamics of neutron stars and binaries in globular clusters or, menages a trois: Revitalizing burnt out degenerates through partner swapping
p 3017 N92-26522
A self-contamination model for the formation of globular star clusters p 3018 N92-26723
GOLD
Simulation studies for surfaces and materials strength
[NASA-CR-190340] p 3001 N92-26265
GOVERNMENT/INDUSTRY RELATIONS
US Small Business Administration FY 1990 national accomplishment report and FY 1991 national affirmative employment program plan
[PB92-157064] p 3008 N92-26353
Small Businesses Make a Difference
[PB92-160118] p 3008 N92-26369
GRAIN BOUNDARIES
Dynamic restoration mechanisms in Al-5.8 at. percent Mg deformed to large strains in the solute drag regime
[DE92-009529] p 2877 N92-26223
Atomistic studies of grain boundaries in alloys and compounds
[DE92-010792] p 2877 N92-26251
Crystalline-amorphous interfaces and their relation to grain boundary films
[DE92-009812] p 3004 N92-26648
The production and properties of melt-zone textured Y1Ba2Cu3O(7-delta) filaments
[DE92-008097] p 3005 N92-26843
GRAND UNIFIED THEORY
A search for magnetic monopoles with the Soudan 2 detector
[DE92-010347] p 3021 N92-26216
GRANTS
Small business innovation research: Program solicitation closing date, 27 January 1992
[DE92-010132] p 3009 N92-26811
GRANULAR MATERIALS
Computation of hydrodynamics using kinetic theory
[DE92-009079] p 2896 N92-26456
GRAPH THEORY
Subgraphs, closures and Hamiltonicity
[PB92-148766] p 2987 N92-26737
Decomposition of bipartite graphs under degree constraints
[PB92-148626] p 2988 N92-26817
GRAPHITE
Higher order parametric x rays
[AD-A247148] p 2991 N92-27182
GRAPHITE-EPOXY COMPOSITES
A method to improve post impact compressive strength in graphite/epoxy composite materials after low temperature impact
[AD-A245395] p 2867 N92-26380
Buckling of unidirectional graphite/epoxy composite plates at low temperatures
[AD-A246602] p 2869 N92-26796
GRAPHS (CHARTS)
Subgraphs, closures and Hamiltonicity
[PB92-148766] p 2987 N92-26737
Decomposition of bipartite graphs under degree constraints
[PB92-148626] p 2988 N92-26817
GRATINGS (SPECTRA)
Ruled and holographic diffraction gratings experiment (AO 138-5) p 2910 N92-27092
GRAVIMETRY
Gravimetric gas determinations for volume calibrations
[DE92-010041] p 2874 N92-26634
GRAVITATION
The effect of global change and long period tides on the Earth's rotation and gravitational potential
p 2925 N92-26781
GRAVITATION THEORY
Euclidean black hole vortices
[NASA-CR-190117] p 3016 N92-26436
Tensor-multi-scalar theories of gravitation
[PB92-152305] p 2943 N92-26820
GRAVITATIONAL COLLAPSE
An anisotropic homologous model for the core-collapse in star clusters
[ETN-92-90826] p 3018 N92-26946
GRAVITATIONAL FIELDS
The effect of global change and long period tides on the Earth's rotation and gravitational potential
p 2925 N92-26781
Tensor-multi-scalar theories of gravitation
[PB92-152305] p 2943 N92-26820
GRAVITATIONAL WAVES
High precision timing of millisecond pulsars
p 3015 N92-26760
Tensor-multi-scalar theories of gravitation
[PB92-152305] p 2943 N92-26820
GRAVITY WAVES
Proceedings of 6th Hawaiian Winter Workshop on Dynamics of Oceanic Internal Gravity Waves
[AD-A245650] p 2948 N92-26173
Cusp studies with HF radars p 2936 N92-26304
Computations of nonlinear gravity waves by a desingularized boundary integral method
p 2942 N92-26583
Studies of inertio-gravity waves induced by geostrophic adjustment of the atmospheric jet stream
p 2944 N92-26866
GRAZING INCIDENCE
Cluster model of polarization reflection from metallic surfaces
[AD-A245781] p 2996 N92-26241
GREEN'S FUNCTIONS
Hamiltonian lattice field theory: Computer calculations using variational methods
[DE92-010479] p 2985 N92-26232
An outline of a numerical scheme for calculating two-dimensional time linearised transonic flow using the Green's function method
[AD-A246349] p 2895 N92-26258
Mutual friction in superfluid He-3: Effects of bound states in the vortex core
[PB92-142231] p 2896 N92-26507
GREENHOUSE EFFECT
Use of the Edmonds-Reilly Model to model energy-related greenhouse gas emissions
[DE92-010035] p 2931 N92-26633
Report of the CC1 working group on climate change detection
[WCDMP-14] p 2947 N92-26923
GREENHOUSES
Waste minimization for non-agricultural pesticide applicators: EPA's pollution prevention guide
[PB92-153774] p 2933 N92-26889
GREENLAND
Cusp and cleft studies in Greenland
p 2935 N92-26299
GRID GENERATION (MATHEMATICS)
Wave viscosity interaction in nonlinear roll motion
[AD-A245756] p 2897 N92-26591
Application of parametrized variational principles in the finite element method p 2987 N92-26624
GRINDING (COMMINUTION)
Study and analysis of the stress state in a ceramic, button-head, tensile specimen
[DE92-007794] p 2918 N92-26784
GROUND BASED CONTROL
The preliminary geodetic control network of Venus
[RAND-N-3437-JPL] p 3019 N92-26819
GROUND STATIONS
Cluster Dayside Polar Cusp
[ESA-SP-330] p 2935 N92-26294
The need of coordinated observations in space and from ground p 2937 N92-26310
Optical ground-based network p 2937 N92-26313
Retrievable payload carrier: Next generation Long Duration Exposure Facility p 2860 N92-27129
GROUND TRUTH
Radar scattering as a source of geological information on Venus and Earth p 3019 N92-26778
GROUP THEORY
Induced cycle structures of the hyperoctahedral group
[DE92-007570] p 3006 N92-26857
GULF STREAM
The utility of acoustic travel times in locating the north wall of the Gulf Stream
[AD-A246219] p 2949 N92-26463
Mean and turbulent structure of the marine atmospheric boundary layer during cold air outbreaks of different intensities: Observational and modelling analyses
p 2942 N92-26489
GUN LAUNCHERS
Numerical simulations of gun-launched kinetic energy projectiles subjected to asymmetric projectile base pressure
[DE92-005065] p 2857 N92-26693
GYROSCOPES
Effect of gyro noise on ADKEM gyro-only missile system performance
[AD-A246150] p 2852 N92-26408
GYROSTABILIZERS
Effect of gyro noise on ADKEM gyro-only missile system performance
[AD-A246150] p 2852 N92-26408

H

HABITABILITY
Fourth European Symposium on Space Environment Control Systems, volume 2
[ESA-SP-324-VOL-2] p 2956 N92-26950
Human factors in the conception of the Hermes space vehicle p 2963 N92-26989
Crew support equipment: Identification and definition of additional hardware for Columbus APM laboratory habitability p 2964 N92-26993
Study on the requirements for the installation of a CES and habitability centre p 2966 N92-27007
Critical technologies: Spacecraft habitability, an update p 2966 N92-27010
New perspectives of living in space: Habitability guidelines for future manned space systems
p 2968 N92-27022
Concept for a European Space Station: Habitability, life support, and laboratory facilities p 2969 N92-27023
Moon base habitability aspects p 2969 N92-27026
HAILSTORMS
Mesoscale observations of a cold front associated with a prefrontal hailstorm p 2940 N92-26338
Precipitation formation processes in convective and stratiform clouds as deduced by coordinated polarimetric radar and aircraft measurements p 2941 N92-26342
HALIDES
Gas phase chromatography of halides of elements 104 and 105
[DE92-010284] p 2870 N92-26212
HALOS
A self-contamination model for the formation of globular star clusters p 3018 N92-26723
HAMILTONIAN FUNCTIONS
Hamiltonian lattice field theory: Computer calculations using variational methods
[DE92-010479] p 2985 N92-26232
Subgraphs, closures and Hamiltonicity
[PB92-148766] p 2987 N92-26737
HANDBOOKS
Handbook of solar-terrestrial data systems, version 1
[NASA-TM-107810] p 3019 N92-26191
HARDWARE
Hardware synthesis using high-level Petri nets
[REPT-91-071] p 2970 N92-26439
Crew support equipment: Identification and definition of additional hardware for Columbus APM laboratory habitability p 2964 N92-26993
HARMONIC OSCILLATION
Wave viscosity interaction in nonlinear roll motion
[AD-A245756] p 2897 N92-26591
HARMONIC OSCILLATORS
Exact solutions for a mode of the electromagnetic field in a resonator with time-dependent characteristics of the internal medium
[AD-A245700] p 2888 N92-26374
HARMONICS
Main and auxiliary transformer rectifier system for minimizing line harmonics
[AD-D015209] p 2894 N92-26881
HARRIER AIRCRAFT
VSTOL engine design evolution: Growth of the Pegasus engine for Harrier
[PNR-90805] p 2855 N92-27039
HEALTH
Life sciences and environmental sciences
[DE92-010254] p 2950 N92-26203
HEALTH PHYSICS
Human round trip to Mars: Six months and radiation safe
[DE92-010160] p 2857 N92-26818
HEAT AFFECTED ZONE
Post-test examination of a pool boiler receiver
[NASA-TM-105635] p 2880 N92-27192

HEAT EXCHANGERS
Theoretical and experimental study of thermoacoustic engines
[AD-A246334] p 2914 N92-26389
Progress in the development of the Hermes evaporators p 2962 N92-26984
The transpirator, an efficient and light evaporative cooler for space technology p 2887 N92-26986
Thermo-hydraulic investigations on heat exchangers for Columbus hybrid radiators p 2887 N92-26988
Development of European sublimator technology for EVA p 2968 N92-27018

HEAT FLUX
Surface energy budget and evapotranspiration measurement support
[NASA-CR-190059] p 2944 N92-26185
A simple model for the convective boundary layer over wavy terrain with variable heat flux p 2934 N92-26334
Performances of 250 Amp-hr lithium/thionyl chloride cells p 2864 N92-27148

HEAT GENERATION
Adaptive regulation of the boiler-turbine unit of a Combined Heat and Power (CHP) system
[RR-417] p 2887 N92-26752
Calorimetric determination of the thermoneutral potential for Li/BrCl in SOCl2 (BCX) cells p 2864 N92-27146

HEAT MEASUREMENT
Differential Scanning Calorimetry (DSC) for the analysis of activated carbon
[AD-A245899] p 2872 N92-26404

HEAT PIPES
Analysis of frozen startup of high-temperature heat pipes and three-dimensional modeling of block-heated heat pipes
[AD-A245327] p 2896 N92-26379
Hypersonic aerospace vehicle leading edge cooling using heat pipe, transpiration and film cooling techniques p 3007 N92-26733
Design and performance of the Spacelab Astro-1 mission heat pipe radiator p 2859 N92-26965
SIGMA VCHP radiator: In-orbit performance p 2859 N92-26966
Heat pipe-based radiative panel p 2859 N92-26968
Battery thermal control of the Columbus Free Flyer p 2859 N92-26970
Passive thermostate system with application of gas-filled heat pipes and thermal energy of solar radiation p 2905 N92-26972
Integrated heat pipe concept for Li/SOCl2 cells cooling p 2895 N92-26974
Thermo-hydraulic investigations on heat exchangers for Columbus hybrid radiators p 2887 N92-26988
Long Duration Exposure Facility (LDEF) low temperature heat pipe experiment package (HEPP) flight results p 2906 N92-27104
Long Duration Exposure Facility (LDEF) low-temperature heat pipe experiment package power system results p 2906 N92-27105
Results from the LDEF/A0076 cascaded variable conductance heatpipe experiment p 2906 N92-27106
Transverse flat plate heat pipe experiment p 2906 N92-27107

HEAT PUMPS
Theoretical and experimental study of thermoacoustic engines
[AD-A246334] p 2914 N92-26389

HEAT RADIATORS
Heat rejection system for an advanced extravehicular mobility unit portable life support system p 2968 N92-27020

HEAT SHIELDING
Thermal implications from the Hubble Space Telescope solar array bi-stem boom in-orbit disturbance p 2965 N92-27001
Lightweight fiber insulations performance and application p 2883 N92-27016
Heatshield concepts for the Rosetta Aerocapsule p 2860 N92-27028

HEAT SINKS
Heat rejection system for an advanced extravehicular mobility unit portable life support system p 2968 N92-27020

HEAT SOURCES
Effects of power pulsations on natural convection from discrete heat sources
[AD-A246557] p 3007 N92-26617
Burn-rate studies with iron/potassium perchlorate heat pellets
[DE92-008524] p 2875 N92-26722

HEAT STORAGE
Heat receivers for solar dynamic space power systems p 2860 N92-26601

HEAT TOLERANCE
Effectiveness of a selected microclimate cooling system in increasing tolerance time to work in the heat. Application to Navy Physiological Heat Exposure Limits (PHEL) curve 5
[AD-A246529] p 2952 N92-26470
Physiological design goals and proposed thermal limits for US Navy thermal garments: Proceedings of 2 conferences sponsored by the Naval Medical Research and Development Command
[AD-A245543] p 2956 N92-26665

HEAT TRANSFER
Heat receivers for solar dynamic space power systems p 2860 N92-26601
A one-dimensional temperature model for a snow cover: Technical documentation for SNTHERM.89
[AD-A245493] p 2922 N92-26674
Numerical field model simulation of full-scale fire tests in a closed spherical/cylindrical vessel using advanced computer graphics techniques
[AD-A245810] p 2887 N92-26898
The centrifugal mass exchange apparatus in air-conditioning system of isolated, inhabited object and its work control p 2957 N92-26956
Thermo-hydraulic investigations on heat exchangers for Columbus hybrid radiators p 2887 N92-26988
Conjugating binary systems: Advanced cooling liquids for use in spacecraft ATCS p 2905 N92-27027
Nucleate pool boiling of R-114 and R-114/oil mixtures from single enhanced tubes
[AD-A245487] p 3008 N92-27058
Transverse flat plate heat pipe experiment p 2906 N92-27107

HEAT TRANSFER COEFFICIENTS
Heat transfer in oscillating flows with sudden change in cross section
[NASA-TM-105692] p 2861 N92-26654

HEATERS
Effects of power pulsations on natural convection from discrete heat sources
[AD-A246557] p 3007 N92-26617
Optical flow sensor
[AD-D015200] p 2997 N92-26862

HEATING
Transient gas motion in nuclear-reactor-pumped lasers: Computational and experimental results
[DE92-002357] p 2912 N92-26691

HEATING EQUIPMENT
Heat receivers for solar dynamic space power systems p 2860 N92-26601

HEAVY IONS
Li-6,d reaction on sd-, fp- and g-shell nuclei in ZR- and FR-DWBA formalisms
[DE92-614353] p 2994 N92-26365
Preliminary total dose measurements on LDEF --- long duration exposure facility p 2952 N92-27123
Preliminary results of the Artemia salina experiments in biostack on LDEF p 2952 N92-27125

HEAVY LIFT LAUNCH VEHICLES
A comparison of heavy lift launch vehicle options for the 1990s
[AD-A245617] p 2857 N92-26402

HEISENBERG THEORY
Universal R-matrix for quantized (super)algebras
[DE92-621067] p 2988 N92-26834

HELICOPTER PROPELLER DRIVE
Full-scale transmission testing to evaluate advanced lubricants
[NASA-TM-105668] p 2915 N92-26560

HELIOSEISMOLOGY
Observational and theoretical investigations in solar seismology
[NASA-CR-190245] p 3019 N92-26247

HELIUM
Mutual friction in superfluid He-3: Effects of bound states in the vortex core
[PB92-142231] p 2896 N92-26507
Helium bubble flow visualization of the spanwise separation on a NACA 0012 with simulated glaze ice
[NASA-TM-105742] p 2849 N92-26612

HELIUM ISOTOPES
Helium-3 mass spectrometry for low-level tritium analysis of environmental samples
[DE92-008937] p 2873 N92-26454
Quantum dynamics of helium clusters
[AD-A245752] p 2995 N92-26588

HELMET MOUNTED DISPLAYS
Advanced technology for portable personal visualization
[AD-A245819] p 2954 N92-26179

HELMETS
Determination of ventilation requirements for a space suit helmet p 2968 N92-27017

HEMODYNAMIC RESPONSES
LBNP as countermeasure: An automated scenario p 2953 N92-27012

HERMES MANNED SPACEPLANE
A processing environment for test and simulation data of thermodynamic systems p 2959 N92-26963
Progress in the development of the Hermes evaporators p 2962 N92-26984
Human factors in the conception of the Hermes space vehicle p 2963 N92-26989
Warm structures and thermal protection of the European spaceplane Hermes p 2860 N92-27014

HEURISTIC METHODS
Integrating reverse engineering into Computer-Aided Software Engineering (CASE) p 2974 N92-26479
The minimization of multiple valued logic expressions using parallel processors
[AD-A245763] p 2980 N92-26596

HIERARCHIES
Generation of multi-resolution maps
[PB92-152206] p 2921 N92-26513
A modeling strategy for large-scale optimization based on analysis and visualization principles
[AD-A246570] p 2987 N92-26620

HIGH ACCELERATION
An explosively driven, fast shock tube
[DE92-008437] p 2856 N92-26720

HIGH ALTITUDE
Estimation of geopotential differences over intercontinental locations using satellite and terrestrial measurements p 2924 N92-26728

HIGH ENERGY INTERACTIONS
Muon/electron separation for atmospheric neutrino interactions
[DE92-010349] p 3021 N92-26218

HIGH FIELD MAGNETS
Advances in the engineering of high field applied-B ion diodes for inertial confinement fusion
[DE92-006528] p 3000 N92-26695

HIGH FREQUENCIES
An evaluation of superresolution methods for tactical radio direction finding
[AD-A246316] p 2851 N92-26291
An adaptive, packet-switched HF data terminal: Functional overview and initial performance
[AD-A246318] p 2973 N92-26292
High frequency Raman current drive
[PB92-142223] p 2893 N92-26497

HIGH IMPULSE
An explosively driven, fast shock tube
[DE92-008437] p 2856 N92-26720

HIGH LEVEL LANGUAGES
Advanced software development workstation. Engineering scripting language graphical editor: DRAFT design document
[NASA-CR-190393] p 2971 N92-26181

HIGH POWER LASERS
High frequency Raman current drive
[PB92-142223] p 2893 N92-26497
Innovative techniques for the production of low cost 2D laser diode arrays
[AD-A247282] p 2913 N92-27178

HIGH PRESSURE
Role of shock compression technique for scientific and engineering studies
[DE92-008324] p 2919 N92-26846
Vibrational spectroscopy in shock-compressed liquids
[DE92-007713] p 2876 N92-26867

HIGH RESOLUTION
An evaluation of superresolution methods for tactical radio direction finding
[AD-A246316] p 2851 N92-26291
The high resolution diffractometer mini-Sfinks p 3002 N92-26322
High-resolution Fourier TOF powder diffraction. 1: Performance of the Mini-Sfinks Facility p 3002 N92-26323
A high-resolution neutron powder diffraction study in high-T(sub c) superconductor YBa2Cu3O7 p 3002 N92-26326
Anomalous structural behaviour of the high-temperature superconducting compound La(1.8)Sr(0.2)CuO(4-y) p 3003 N92-26327
Quantitative assessment of the slope resolution of seafloor mapping systems
[AD-A246158] p 2949 N92-26411
Design of a high-precision tunable double crystal monochromator
[DE92-010137] p 2909 N92-26572
Open problems and future prospects for hypernuclear physics
[DE92-010158] p 2995 N92-26815

HIGH REYNOLDS NUMBER
An experimental study of natural and forced modes in an axisymmetric jet p 2897 N92-26600

HIGH SPEED
Compressive damage and fracture modeling of ceramic subjected to high-velocity impact p 2881 N92-26492

An experimental investigation of high-speed water entry for full size and scale-model pointed nose vehicle
[DE92-004363] p 2899 N92-26716
Design guide for saddle seating on small high-speed craft
[ISVR-TR-205] p 2956 N92-26891

HIGH STRENGTH STEELS
Factors influencing the microstructural and mechanical properties of ULCB steel weldments
[AD-A245523] p 2878 N92-26659

HIGH TEMPERATURE
Analysis of frozen startup of high-temperature heat pipes and three-dimensional modeling of block-heated heat pipes
[AD-A245327] p 2896 N92-26379
Analysis and modeling of high-temperature performance of advanced fiber composites p 2868 N92-26564
Tuned-circuit dual-mode Johnson noise thermometers
[DE92-010121] p 2908 N92-26569
Zirconia-based fuel cells for power generation
[DE92-009886] p 2927 N92-26719
Vibrational spectroscopy in shock-compressed liquids
[DE92-007713] p 2876 N92-26867

HIGH TEMPERATURE ENVIRONMENTS
The electronic evaluation of the Advanced Dynamic Anthropomorphic Manikin (ADAM) in high temperature environments
[AD-A245459] p 2955 N92-26528

HIGH TEMPERATURE GASES
Spectroscopy and kinetics of combustion gases at high temperatures
[DE92-011216] p 2872 N92-26281
Hot-gas reingestion engine response considerations
[PNR-90810] p 2855 N92-27042

HIGH TEMPERATURE PLASMAS
High frequency Raman current drive
[PB92-142223] p 2893 N92-26497

HIGH TEMPERATURE SUPERCONDUCTORS
Thin-film high temperature superconducting flux transformers coupled to SQUIDS
[DE92-010260] p 2891 N92-26205
Recent results in characterization of melt-grown and quench-melt-grown YBCO superconductors
[DE92-010281] p 3001 N92-26210
A high-resolution neutron powder diffraction study in high-T(sub c) superconductor YBa2Cu3O7
p 3002 N92-26326
Anomalous structural behaviour of the high-temperature superconducting compound La(1.8)Sr(0.2)CuO(4-y)
p 3003 N92-26327
Neutron powder diffraction study on Eu-substituted Bi2Sr2CaCu2O(8+y) high temperature superconductor
p 3003 N92-26328
A comprehensive review of the XRD data of the primary and secondary phases present in the BSCCO superconductor system
[DE92-010363] p 3003 N92-26579
Magnetic flux noise in copper oxide superconductors
[DE92-010299] p 3003 N92-26582
The Debye temperature of YBa2Cu3O(7-(delta)) and its dependence on the volume fraction of superconductivity
[DE92-010305] p 3003 N92-26584
Analysis of Yttrium-Barium-Copper-Oxide by x ray diffraction and mechanical characterization
[NASA-TM-104562] p 2869 N92-26650
Percolation effects in the V-I characteristics of granular YBa2Cu3O(7-delta)
[DE92-617541] p 3004 N92-26672
Structural coherence of the CuO2 planes of oxide superconductors: Is it a requirement for superconductivity?
[DE92-009724] p 3005 N92-26842
The production and properties of melt-zone textured Y1Ba2Cu3O(7-delta) filaments
[DE92-008097] p 3005 N92-26843
Lattice instabilities and structural phase transformations in La2CuO4 superconductors and insulators
[DE92-010045] p 3006 N92-27059

HIGH TEMPERATURE TESTS
The electronic evaluation of the Advanced Dynamic Anthropomorphic Manikin (ADAM) in high temperature environments
[AD-A245459] p 2955 N92-26528
Application of neutron diffraction to measure residual strains in high temperature composites
[DE91-014021] p 2869 N92-26679
Assessment of a hot hydrogen nuclear propulsion fuel test facility
[DE92-004571] p 2995 N92-26692
Predictability of long-term creep and rupture in a nozzle-to-sphere vessel model
[DE92-008099] p 2919 N92-26845

HIGH VACUUM
Microwelding (or cold-welding) of various metallic materials under the ultra-vacuum LDEF experiment AO 138-10 p 2880 N92-27119
Seeds in space experiment --- long duration exposure facility p 2952 N92-27120

HILBERT SPACE
Hyperspaces of infinite-dimensional compacta
[PB92-149335] p 2986 N92-26367
Lyapunov equation for infinite-dimensional discrete bilinear systems
[DE92-621066] p 2988 N92-26831

HOLDING
A framework for recognizing grasps
[AD-A245712] p 2981 N92-26357

HOLE MOBILITY
Mobility of electrons and holes in semiconductors
[DE92-010125] p 3004 N92-26638

HOLOGRAPHY
Spectroscopic imaging, diffraction, and holography with x ray photoemission
[DE92-009142] p 2996 N92-26187
Ruled and holographic diffraction gratings experiment (AO 138-5) p 2910 N92-27092

HOMOGENEITY
The effect of collection homogeneity on term association as a method of request expansion in information retrieval p 3012 N92-26614

HOMOGENEOUS TURBULENCE
On testing models for the pressure-strain correlation of turbulence using direct simulations
[NASA-CR-189638] p 2901 N92-26883

HOMOGENIZING
Homogenization models for 2-D grid structures
[NASA-CR-190321] p 2920 N92-26892

HOMOLOGY
Hyperspaces of infinite-dimensional compacta
[PB92-149335] p 2986 N92-26367
An anisotropic homologous model for the core-collapse in star clusters
[ETN-92-90826] p 3018 N92-26946

HOMOTOPY THEORY
Hyperspaces of infinite-dimensional compacta
[PB92-149335] p 2986 N92-26367

HOT ELECTRONS
Generation of nonequilibrium optical phonons in GaAs/AlAs quantum wells by intrasubband and intersubband scatterings
[DE92-010264] p 2993 N92-26207

HTPB PROPELLANTS
Solid fuel ramjet infrared signature
[AD-A246299] p 2860 N92-26362

HUBBLE SPACE TELESCOPE
Applying artificial intelligence to the control of space telescopes (extended abstract)
[NASA-TM-107913] p 3015 N92-26886
Thermal implications from the Hubble Space Telescope solar array bi-stem boom in-orbit disturbance
p 2965 N92-27001
Hubble Space Telescope battery background
p 2866 N92-27163
Hubble Space Telescope NiH2 six battery test
p 2866 N92-27164
Hubble Space Telescope nickel-hydrogen flight spare battery test p 2866 N92-27165
Results of a technical analysis of the Hubble Space Telescope nickel-cadmium and nickel-hydrogen batteries
p 2867 N92-27167

HUGONIOT EQUATION OF STATE
Role of shock compression technique for scientific and engineering studies
[DE92-008324] p 2919 N92-26846

HUMAN BEHAVIOR
Computer modeling of human decision making
[NASA-TM-107868] p 2983 N92-26630
MoCog1: A computer simulation of recognition-primed human decision making
[NASA-TM-107872] p 2984 N92-26888

HUMAN BEINGS
Clinical investigation program, fiscal year 1991
[AD-A246558] p 2992 N92-26618
Correlation and prediction of dynamic human isolated joint strength from lean body mass
[NASA-TP-3207] p 2956 N92-26682

HUMAN FACTORS ENGINEERING
Design guide for saddle seating on small high-speed craft
[ISVR-TR-205] p 2956 N92-26891
Human factors in the conception of the Hermes space vehicle p 2963 N92-26989
CAD system for HFE analyses: Zero-g posture in optimisation of Columbus APM crew workstations --- human factors engineering p 2963 N92-26991
Crew support equipment: Identification and definition of additional hardware for Columbus APM laboratory habitability p 2964 N92-26993
Engineering of a new overall system to improve the interaction between the crew and the ground-based scientists and personnel p 2964 N92-26995
EVA life support design and technology developments
p 2965 N92-27002
Genesis and evaluation of an ergonomic architecture for the ESA EVA suit p 2965 N92-27003
Development of the suit enclosure soft joints of the European EVA space suit p 2965 N92-27005
Fan/pump/separator technology development for EVA
p 2966 N92-27006
Architectural studies relating to human body motion morphology in microgravity p 2953 N92-27011
New perspectives of living in space: Habitability guidelines for future manned space systems
p 2968 N92-27022
Influence of architecture on the definition of a space station configuration p 2860 N92-27024
Moon base habitability aspects p 2969 N92-27026

HUMAN PERFORMANCE
The validation of a human force model to predict dynamic forces resulting from multi-joint motions
[NASA-TP-3206] p 2956 N92-26538
Genesis and evaluation of an ergonomic architecture for the ESA EVA suit p 2965 N92-27003
The study on a directory of human performance models for system design (Defence Research Group Panel 8 on the defence applications of human and bio-medical sciences)
[AD-A247346] p 2970 N92-27179

HUMAN RESOURCES
Information technology resources assessment
[DE92-009498] p 3011 N92-26221

HUMAN TOLERANCES
Biochemical, endocrine, and hematological factors in human oxygen tolerance extension: Predictive studies 6
[NASA-CR-190341] p 2952 N92-26263

HUMAN WASTES
Catalytic wet-oxidation of human waste produced in a space habitat: Purification of the oxidized liquor for human drinking p 2957 N92-26954

HUMIDITY
Atmospheric environment for Space Shuttle Columbia (STS-40) launch
[NASA-TM-103585] p 2945 N92-26288
Design of JEM temperature and humidity control system p 2958 N92-26957
Development of European sublimator technology for EVA p 2968 N92-27018

HUMIDITY MEASUREMENT
Measurement electronics of industrial microwave resonator sensors
[PB92-152750] p 2909 N92-26786

HYDRAULIC EQUIPMENT
Passive water hammer in pipes due to flashing
[DE92-004180] p 2899 N92-26699
Water hammer due to the sudden stopping of a flashing flow
[DE92-004181] p 2899 N92-26700

HYDRAULIC TEST TUNNELS
Observation and measurements of flow structures in the stagnation region of a wing-body junction
p 2849 N92-26616

HYDRAZINES
Conceptual design study for the use of COBE rocket engines on the Tropical Rainfall Measuring Mission
[NASA-CR-190383] p 2945 N92-26535
Study of hydrazine metabolism and toxicity
[AD-A245755] p 2884 N92-26589

HYDRIDES
Materials compatibility and wall stresses in hydride storage beds
[DE92-009432] p 2870 N92-26201

HYDROBALLISTICS
An experimental investigation of high-speed water entry for full size and scale-model pointed nose vehicle
[DE92-004363] p 2899 N92-26716

HYDROCRACKING
Low severity upgrading of F-T waxes with solid superacids
[DE92-009081] p 2873 N92-26457

HYDRODYNAMICS
Computation of hydrodynamics using kinetic theory
[DE92-009079] p 2896 N92-26456
Wave viscosity interaction in nonlinear roll motion
[AD-A245756] p 2897 N92-26591
An explosively driven, fast shock tube
[DE92-008437] p 2856 N92-26720
Numerical simulation of two-dimensional single- and multiple-material flow fields
[DE92-007428] p 2901 N92-26656

HYDROGEN
Non-destructive analysis for hydrogen concentrations in materials
[AD-A246098] p 2874 N92-26541

HYDROGEN FUELS
Assessment of a hot hydrogen nuclear propulsion fuel test facility
[DE92-004571] p 2995 N92-26692

HYDROGEN IONS
Multiquanta photodetachment from the H(-) ion
[DE92-010306] p 2911 N92-26573
Measurements of scattering processes in negative ion-atom collisions
[DE92-010319] p 2995 N92-26574
Effect of interstitials on the trapping of hydrogen in iron-single crystals
[AD-A246412] p 3006 N92-27064
HYDROGEN ISOTOPES
A new phase in palladium hydride technology
[DE92-009852] p 2875 N92-26718
HYDROGEN PRODUCTION
High-yield hydrogen production by catalytic gasification of coal or biomass
[DE92-008770] p 2875 N92-26724
HYDROGENOLYSIS
A novel process for methanol synthesis
[DE92-010465] p 2883 N92-26547
HYDROGRAPHY
Meridional zonation of the Barents Sea ecosystem inferred from satellite remote sensing and in situ bio-optical observations
[AD-A246323] p 2948 N92-26245
Hydrographic data from the Coastal Transition Zone (CTZ) program, 5-19 July 1988
[AD-A245517] p 2950 N92-27069
HYDROLOGICAL CYCLE
Water cycles around the subtropical frontal zone in East Asia
[TW-9] p 2923 N92-26710
Rainfall pattern over the tropical rain forest
[TW-10] p 2923 N92-26711
Research program on hydrology
[TW-14] p 2924 N92-26715
HYDROLOGY
Description of and users manual for TUBA: A computer code for generating two-dimensional random fields via the turning bands method
[DE92-001020] p 2971 N92-26189
HYDROLOGY MODELS
Validation of numerical models by TRMM and validation of TRMM by numerical models
[TW-8] p 2923 N92-26709
HYPERGEOMETRIC FUNCTIONS
Sturm-Liouville eigenfunctions expressed in determinant form
[AD-A245991] p 2987 N92-26755
HYPERNUCLEI
Open problems and future prospects for hypernuclear physics
[DE92-010158] p 2995 N92-26815
HYPERONS
Open problems and future prospects for hypernuclear physics
[DE92-010158] p 2995 N92-26815
HYPERSONIC FLOW
An experimental investigation of a 2-D scramjet inlet at flow Mach numbers of 8 to 25 and stagnation temperatures of 800 to 4,100 K p 2854 N92-26586
Control of turbulent mixing in hypersonic flow p 2904 N92-26919
HYPERSONIC VEHICLES
Analysis of frozen startup of high-temperature heat pipes and three-dimensional modeling of block-heated heat pipes
[AD-A245327] p 2896 N92-26379
An experimental investigation of a 2-D scramjet inlet at flow Mach numbers of 8 to 25 and stagnation temperatures of 800 to 4,100 K p 2854 N92-26586
Hypersonic aerospace vehicle leading edge cooling using heat pipe, transpiration and film cooling techniques p 3007 N92-26733
Computational method to predict thermodynamic, transport, and flow properties for the modified Langley 8-foot high-temperature tunnel
[NASA-TM-4374] p 2905 N92-27193
HYPERSPACES
Hyperspaces of infinite-dimensional compacta
[PB92-149335] p 2986 N92-26367

I

ICE FORMATION
Helium bubble flow visualization of the spanwise separation on a NACA 0012 with simulated glaze ice
[NASA-TM-105742] p 2849 N92-26612
IDEAL GAS
On shock capturing for liquid and gas media p 2817 N92-26556
IGNITION
Proposed model of thermionically assisted breakdown and implementation on electrostatic thrusters
[AD-A246207] p 2990 N92-26460
Static electricity: A literature review
[AD-A246533] p 2990 N92-26471
IMAGE ANALYSIS
Estimation of motion parameters from image sequences
[AD-A246135] p 2986 N92-26358
Shape from periodic texture using the spectrogram
[AD-A245855] p 2973 N92-26384
Dynamic lens compensation for active color imaging and constant magnification focusing
[AD-A245713] p 2997 N92-26425
IMAGE INTENSIFIERS
Conquest of darkness by management of the stars
[AD-A245496] p 2997 N92-26676
IMAGE MOTION COMPENSATION
Estimation of motion parameters from image sequences
[AD-A246135] p 2986 N92-26358
Performance analysis of image motion analysis algorithms
[AD-A246522] p 2974 N92-26468
IMAGE PROCESSING
VHDL behavioral description of discrete cosine transform in image compression
[AD-A245389] p 2972 N92-26248
Imaging the Earth's magnetosphere using ground magnetometer arrays p 2938 N92-26314
Estimation of motion parameters from image sequences
[AD-A246135] p 2986 N92-26358
Applications of wavelets to signal processing held in Wright-Patterson AFB, Ohio on 20-22 March 1991. Volume 2: Tutorial notes
[AD-A245567] p 2888 N92-26381
Performance analysis of image motion analysis algorithms
[AD-A246522] p 2974 N92-26468
Massively parallel implementation of character recognition systems
[PB92-149863] p 2980 N92-26501
Generation of multi-resolution maps
[PB92-152206] p 2921 N92-26513
Description of the multispectral CCD-camera
[AD-A245681] p 2908 N92-26517
Color image processing and object tracking workstation
[NASA-TM-105561] p 2886 N92-26611
Application of fluorescent-particle imaging to measuring flow in complex media
[DE92-009121] p 2898 N92-26645
AVHRR satellite data: Users guide for accessing NOARL archives
[AD-A246142] p 2926 N92-27070
IMAGE RESOLUTION
On the construction of multivariate (pre)wavelets
[AD-A247105] p 2989 N92-27175
IMAGE TRANSDUCERS
Binaural ultrasound detector and imager
[AD-D015214] p 2993 N92-27184
IMAGING TECHNIQUES
Spectroscopic imaging, diffraction, and holography with x ray photoemission
[DE92-009142] p 2996 N92-26187
Spatially variant tomographic imaging: Estimation, identification, and optimization
[DE92-010262] p 2921 N92-26206
Imaging earth's interior: Tomographic inversions for mantle P-wave velocity structure
[DE92-010271] p 2934 N92-26208
Dynamic lens compensation for active color imaging and constant magnification focusing
[AD-A245713] p 2997 N92-26425
Real time imaging and infrared background scene analysis using the Naval Postgraduate School infrared search and target designation (NPS-IRSTD) system
[AD-A245527] p 2997 N92-26662
Investigations of a single point temperature probe for measurement of atmospheric turbulence
[AD-A246563] p 2909 N92-26794
IMPACT DAMAGE
Compressive damage and fracture modeling of ceramic subjected to high-velocity impact p 2881 N92-26492
IMPACT STRENGTH
A method to improve post impact compressive strength in graphite/epoxy composite materials after low temperature impact
[AD-A245395] p 2867 N92-26380
IMPACT TESTS
A method to improve post impact compressive strength in graphite/epoxy composite materials after low temperature impact
[AD-A245395] p 2867 N92-26380
Compressive damage and fracture modeling of ceramic subjected to high-velocity impact p 2881 N92-26492
An experimental investigation of high-speed water entry for full size and scale-model pointed nose vehicle
[DE92-004363] p 2899 N92-26716
IMPEDANCE MEASUREMENT
Life testing of secondary Ag-Zn cells p 2865 N92-27153
IMPLOSIONS
An explosively driven, fast shock tube
[DE92-008437] p 2856 N92-26720
IMPURITIES
Method for implanting impurities in semiconductors and semiconductor implanted with impurities
[AD-D015196] p 3003 N92-26433
INCOHERENT SCATTER RADAR
Incoherent scatter radar measurements of the cusp p 2936 N92-26303
INCOHERENT SCATTERING
Plans for the EISCAT Svalbard (Norway) radar p 2936 N92-26305
INCOMPRESSIBLE FLUIDS
Two-phase flow of Newtonian and Non-Newtonian fluids in a porous medium applied to water coning
[PB92-151109] p 2900 N92-26836
INDENTATION
Finite element modeling of static indentation damage in laminated composites p 2869 N92-26827
INDEXES (DOCUMENTATION)
COSMIC software catalog, 1992 edition
[NASA-CR-188973] p 2977 N92-26868
NASA patent abstracts bibliography: A continuing bibliography. Section 2: Indexes (supplement 40)
[NASA-SP-7039(40)-SECT-2] p 3014 N92-27081
INDIUM ARSENIDES
High-speed pulse detection room-temperature optical nonlinearities for GaInAs/A1InAs and GaA1InAs/A1InAs multiple quantum wells and integrated mirror etalon at 1.3 micrometers
[AD-A246369] p 2998 N92-26943
INDIUM PHOSPHIDES
Investigation of kinetics of MOCVD systems
[AD-A246090] p 2893 N92-26540
INDUSTRIAL MANAGEMENT
Small Businesses Make a Difference
[PB92-160118] p 3008 N92-26369
INDUSTRIES
Competing economies: America, Europe, and the Pacific rim
[PB92-115757] p 3014 N92-26730
The 1990 progress report and future plans
[NASA-TM-107911] p 2984 N92-26887
INELASTIC SCATTERING
New description of multiplicity distribution in inelastic meson-proton interactions
[DE92-621167] p 2995 N92-26800
INERTIAL CONFINEMENT FUSION
Advances in the engineering of high field applied-B ion diodes for inertial confinement fusion
[DE92-006528] p 3000 N92-26695
Inertial fusion energy power plant design using the Compact Torus Accelerator: HYLIFE-CT
[DE92-008941] p 3000 N92-26729
INFORMATION DISSEMINATION
Information liability: New interpretations for the electronic age --- online databases p 3012 N92-26481
DOE new technology
[DE92-001619] p 3013 N92-26689
DoD implementation guidelines for Electronic Data Interchange (EDI), volume 2
[AD-A246614] p 3013 N92-26767
Climate research at regional climate centers in 1991
[PB92-160399] p 2946 N92-26822
CC1 experts meeting on CLIMAT code adaptation
[WCDMP-15] p 2947 N92-26924
Managing Federal information resources: Under the Paperwork Reduction Act of 1980
[PB92-154905] p 3014 N92-26926
NASA/DoD Aerospace Knowledge Diffusion Research Project: An initial investigation into the production and use of Scientific and Technical Information (STI) at 5 NASA centers. Results of a telephone survey
[NASA-TM-104173] p 3014 N92-27170
INFORMATION MANAGEMENT
Executive summary of information systems plans: Fiscal years 1993 to 1997
[PB92-158351] p 3011 N92-26368
Cataloging guidelines
[AD-A246500] p 3011 N92-26465
Information systems planning methodologies: A framework for comparison and selection
[AD-A246527] p 3012 N92-26469
Information liability: New interpretations for the electronic age --- online databases p 3012 N92-26481

Managing Federal information resources: Under the Paperwork Reduction Act of 1980
[PB92-154905] p 3014 N92-26926
Logistics in space: Tools to support astronauts
p 2963 N92-26990

INFORMATION RETRIEVAL
The effect of collection homogeneity on term association as a method of request expansion in information retrieval p 3012 N92-26614
AVHRR satellite data: Users guide for accessing NOARL archives
[AD-A246142] p 2926 N92-27070

INFORMATION SYSTEMS
Executive summary of the technical proceedings on Military Information System Engineering (Defence Research Group Panel 11 on Information Processing Technology)
[AD-A245656] p 3010 N92-26174
Information technology resources assessment
[DE92-009498] p 3011 N92-26221
Executive summary of information systems plans: Fiscal years 1993 to 1997
[PB92-158351] p 3011 N92-26368
Information liability: New interpretations for the electronic age --- online databases
p 3012 N92-26481
The effect of collection homogeneity on term association as a method of request expansion in information retrieval p 3012 N92-26614
Measuring the effectiveness of information systems
[AD-A246007] p 3013 N92-26762
Test plan for the international aircraft operator information system
[DOT/FAA/CT-91/18] p 3014 N92-26830
Functional requirements document for NASA/MSFC Earth Science and Applications Division: Data and information system (ESAD-DIS). Interoperability, 1992
[NASA-TM-4388] p 2921 N92-26905
Managing Federal information resources: Under the Paperwork Reduction Act of 1980
[PB92-154905] p 3014 N92-26926
NASA/DoD Aerospace Knowledge Diffusion Research Project: An initial investigation into the production and use of Scientific and Technical Information (STI) at 5 NASA centers. Results of a telephone survey
[NASA-TM-104173] p 3014 N92-27170

INFORMATION TRANSFER
Executive summary of information systems plans: Fiscal years 1993 to 1997
[PB92-158351] p 3011 N92-26368
DoD implementation guidelines for Electronic Data Interchange (EDI), volume 2
[AD-A246614] p 3013 N92-26767
NASA/DoD Aerospace Knowledge Diffusion Research Project: An initial investigation into the production and use of Scientific and Technical Information (STI) at 5 NASA centers. Results of a telephone survey
[NASA-TM-104173] p 3014 N92-27170

INFRARED DETECTORS
Effect of space exposure of pyroelectric infrared detectors p 2910 N92-27113

INFRARED FILTERS
Exposure to space radiation of high-performance infrared multilayer filters and materials technology experiment (A0056) p 2999 N92-27108

INFRARED IMAGERY
The utility of acoustic travel times in locating the north wall of the Gulf Stream
[AD-A246219] p 2949 N92-26463
Description of the multispectral CCD-camera
[AD-A245681] p 2908 N92-26517
A feasibility study: California Department of Forestry and Fire Protection utilization of infrared technologies for wildland fire suppression and management
[NASA-CR-190458] p 2926 N92-27195

INFRARED INTERFEROMETERS
An infrared Michelson stellar interferometer and its applications p 3015 N92-26477

INFRARED RADIATION
An infrared Michelson stellar interferometer and its applications p 3015 N92-26477
Water vapor information content of absorption lines observed in the Sun's infrared radiance
p 2942 N92-26490
Real time imaging and infrared background scene analysis using the Naval Postgraduate School infrared search and target designation (NPS-IRSTD) system
[AD-A245527] p 2997 N92-26662
Research and technology, 1990: Goddard Space Flight Center
[NASA-TM-107792] p 3022 N92-26824
Analysis of thermal infrared data acquired over playas: Silver Lake and Deep Springs Lake, California and Lunar Lake, Nevada p 2926 N92-26864
Infrared clutter measurements of marine backgrounds
[AD-A245422] p 2932 N92-26873
Modeling for improved minimum resolvable temperature difference measurements
[AD-A246389] p 2991 N92-27078
Effect of space exposure of pyroelectric infrared detectors p 2910 N92-27113
A feasibility study: California Department of Forestry and Fire Protection utilization of infrared technologies for wildland fire suppression and management
[NASA-CR-190458] p 2926 N92-27195

INFRARED SCANNERS
Analysis of thermal infrared data acquired over playas: Silver Lake and Deep Springs Lake, California and Lunar Lake, Nevada p 2926 N92-26864

INFRARED SIGNATURES
Solid fuel ramjet infrared signature
[AD-A246299] p 2860 N92-26382
Subscale solid rocket motor infrared signature and particle behavior
[AD-A246416] p 2862 N92-27065

INFRARED SPECTRA
Infrared spectroscopy and hydrogen isotope geochemistry of hydrous silicate glasses
[DE92-008398] p 2881 N92-26451
Polycyclic aromatic hydrocarbon radiative properties and formation in carbon-rich stellar outflows
p 3018 N92-26757
Analysis of thermal infrared data acquired over playas: Silver Lake and Deep Springs Lake, California and Lunar Lake, Nevada p 2926 N92-26864
Evaluation of the Fourier transform infrared spectrometer for particle-associated ammonium sulfate determination
[PB92-160084] p 2910 N92-26930
Modeling for improved minimum resolvable temperature difference measurements
[AD-A246389] p 2991 N92-27078

INFRARED SPECTROMETERS
Evaluation of the Fourier transform infrared spectrometer for particle-associated ammonium sulfate determination
[PB92-160084] p 2910 N92-26930

INFRARED WINDOWS
Studies of rain erosion mechanisms in a range of IR transmitting ceramics including coated samples
[AD-A245299] p 2882 N92-26751

INGESTION (ENGINES)
Hot-gas reingestion engine response considerations
[PNR-90810] p 2855 N92-27042

INHOMOGENEITY
Measurements in the inhomogeneous convective boundary layer using three powered gliders
p 2942 N92-26350

INLAND WATERS
Modeling transfer of Cs-137 fallout in a large Finnish watercourse, appendix 6 p 2930 N92-26488

INLET FLOW
An experimental investigation of a 2-D scramjet inlet at flow Mach numbers of 8 to 25 and stagnation temperatures of 800 to 4,100 K p 2854 N92-26586

INSPECTION
Assessment of diagnostic methods for solenoid-operated valves
[DE92-009379] p 2913 N92-26234

INSTALLING
Installation and operation of the 400 kW 140 GHz gyrotron on the MTX experiment
[DE92-009053] p 2906 N92-26377

INSULATORS
Lattice instabilities and structural phase transformations in La2CuO4 superconductors and insulators
[DE92-010045] p 3006 N92-27059

INTEGERS
Decomposition of bipartite graphs under degree constraints
[PB92-148626] p 2988 N92-26817

INTEGRAL EQUATIONS
Joint services electronics program
[AD-A245636] p 2892 N92-26280
Computations of nonlinear gravity waves by a desingularized boundary integral method
p 2942 N92-26583

INTEGRATED CIRCUITS
The sixteen channel CAMAC constant fraction discriminator for APEX
[DE92-010550] p 2970 N92-26551

INTELLECT
Survey of small business use of intellectual property protection
[PB92-151703] p 3009 N92-26523

INTERACTIONAL AERODYNAMICS
Subsonic investigations of vortex interaction control for enhanced high-alpha aerodynamics of a chine forebody/Delta wing configuration
[NASA-CR-189641] p 2849 N92-26652

INTERFACE STABILITY
Parabolic flight: Reports of microgravity experiments by aircraft, volume 1, no. 2
[EG-910045] p 2884 N92-26440
Parabolic flight experiments on bubble migration under reduced gravity p 2885 N92-26443
Micro-gravity experiment of vapor/liquid reorientation induced by capillary force p 2885 N92-26444
Liquid motion analysis with lateral impacts under low gravity p 2885 N92-26445

INTERMETALLICS
Advanced materials aspects of concurrent engineering
[AD-A245437] p 2880 N92-26275

INTERNAL COMBUSTION ENGINES
Throttleless Otto-cycle natural gas engines
[PB92-164482] p 2914 N92-26371
An instrument for engine torque estimation and misfire detection --- torque p 2909 N92-26738
Development of natural gas rotary engines
[PB92-149665] p 2915 N92-26816

INTERNAL ENERGY
On shock capturing for liquid and gas media
p 2897 N92-26556

INTERNAL WAVES
Proceedings of 6th Hawaiian Winter Workshop on Dynamics of Oceanic Internal Gravity Waves
[AD-A245650] p 2948 N92-26173

INTERNATIONAL COOPERATION
Tropical Rainfall Measuring Mission (TRMM) science report
[TW-5] p 2923 N92-26706
Multi-cultural components and keys for European worldwide space programs p 2857 N92-27008

INTERNATIONAL SUN EARTH EXPLORERS
Lesson learned from GEOS and ISEE
p 2936 N92-26302

INTERPLANETARY MAGNETIC FIELDS
Incoherent scatter radar measurements of the cusp
p 2936 N92-26303
Ground-based studies of sensing magnetosphere/ionosphere interactions: Convection and substorms p 2937 N92-26311
The dynamic response of the westward auroral electrojet and polar cap currents to solar wind-magnetosphere coupling p 2943 N92-26622
Solar wind interaction with Venus and Mars
p 3020 N92-26779

INTERPLANETARY SPACECRAFT
Human round trip to Mars: Six months and radiation safe
[DE92-010160] p 2857 N92-26818

INTERSTITIALS
Effect of interstitials on the trapping of hydrogen in iron-single crystals
[AD-A246412] p 3006 N92-27064

INTRAVEHICULAR ACTIVITY
Microgravity simulation p 2964 N92-26994
Crew-friendly support systems for internal vehicular activities in zero gravity, experimented underwater for the Columbus programme p 2969 N92-27025

INVARIANCE
Characterization of discrete-time linear periodically time-varying systems
[AD-A245822] p 2989 N92-26180

INVERSE KINEMATICS
The validation of a human force model to predict dynamic forces resulting from multi-joint motions
[NASA-TP-3206] p 2956 N92-26538

INVERSE SCATTERING
Nonlinear waves and inverse scattering
[AD-A246164] p 2986 N92-26414

INVERSIONS
Imaging earth's interior: Tomographic inversions for mantle P-wave velocity structure
[DE92-010271] p 2934 N92-26208

INVISCID FLOW
Performance prediction and design of maximum thrust planar supersonic nozzles using a flux-difference-splitting technique p 2853 N92-26480
Cross-flow instabilities and pressure gradients in boundary layers p 2904 N92-26922
Interface of an uncoupled boundary layer algorithm with an inviscid core flow algorithm for unsteady supersonic engine inlets
[NASA-TM-105684] p 2855 N92-27037
Aerodynamic interference between stores
[AD-A247207] p 2850 N92-27172

ION ACCELERATORS
New approaches to studies of exotic nuclei
[DE92-010127] p 2994 N92-26570

ION BEAMS
Theory of electromagnetic instability of an intense beam in a quadrupole focusing system
[AD-A246560] p 2990 N92-26768

ION DENSITY (CONCENTRATION)
Polar cap boundary and structure of dayside cusp as determined by ion precipitation p 2936 N92-26300
ION EMISSION
The use of ion chromatography-dc plasma atomic emission spectrometry for the speciation of trace metals
[DE92-010317] p 2871 N92-26236
The onset of breakdown in a fast pulsed vacuum diode
[AD-A246395] p 2895 N92-27079
ION IMPLANTATION
Method for implanting impurities in semiconductors and semiconductor implanted with impurities
[AD-D015196] p 3003 N92-26433
Etching effects in ion implanted SiO2
[DE92-011150] p 3005 N92-26826
IONIC REACTIONS
Toluene-water clusters: Ion fragmentation and chemistry
[AD-A245813] p 2874 N92-26526
IONIZATION CHAMBERS
Cryogenic detector development
[MPI-PHE/91-07] p 2906 N92-26391
Silicon drift chambers with integrated amplifiers as low energy detectors p 2908 N92-26398
Proposed model of thermionically assisted breakdown and implementation on electrostatic thrusters
[AD-A246207] p 2990 N92-26460
IONIZED GASES
Preliminary experiment of GDEF (Gas Dynamics Experiment Facility) p 2885 N92-26442
IONIZING RADIATION
Geometry and mass model of ionizing radiation experiments on the LDEF satellite
[NASA-CR-184325] p 2993 N92-26200
Total Dose Effects (TDE) of heavy ionizing radiation in fungus spores and plant seeds: Preliminary investigations p 2952 N92-27124
IONOSPHERIC CONDUCTIVITY
Plasma dynamics of the Earth magnetopause-boundary layer and its coupling to the polar ionosphere p 2944 N92-26865
IONOSPHERIC PROPAGATION
The effects of magnetic storm phases on F-layer irregularities from auroral to equatorial latitudes
[AD-A245495] p 2943 N92-26675
IONS
Etching effects in ion implanted SiO2
[DE92-011150] p 3005 N92-26826
IRON
Relationship between composition, structure, properties, thermo-mechanical processing and ballistic performance of tungsten heavy alloys
[AD-A245649] p 2876 N92-26172
Elevated temperature properties of a dispersion strengthened Al-(Fe, V, Si) alloy
[AD-A246427] p 2880 N92-27067
IRON COMPOUNDS
Gas-pressure studies with Li(Si)/FeS2 thermal batteries
[DE92-010801] p 2892 N92-26238
Burn-rate studies with iron/potassium perchlorate heat pellets
[DE92-008524] p 2875 N92-26722
IRRADIATION
Application of irradiation techniques to food and foodstuffs
[DE92-614952] p 2954 N92-26186
Low power laser irradiation effect with emphasis on injured neural tissues
[AD-A246410] p 2953 N92-27063
Selective metallization of carbonyl-containing polymer films
[AD-D015219] p 2883 N92-27187
ISOMERIZATION
Low severity upgrading of F-T waxes with solid superacids
[DE92-009081] p 2873 N92-26457
ISOMORPHISM
Induced cycle structures of the hyperoctahedral group
[DE92-007570] p 3006 N92-26857
ISOPARAMETRIC FINITE ELEMENTS
Finite element modeling of static indentation damage in laminated composites p 2869 N92-26827
ISOTOPE SEPARATION
Metal hydride based isotope separation: Large-scale operations
[DE92-009830] p 2875 N92-26717
ISOTOPES
Gas phase chromatography of halides of elements 104 and 105
[DE92-010284] p 2870 N92-26212
ISOTOPIC ENRICHMENT
Metal hydride based isotope separation: Large-scale operations
[DE92-009830] p 2875 N92-26717
ISOTOPIC LABELING
The carbon isotopic compositions of individual compounds from ancient and modern depositional environments p 2921 N92-26478
ISOTROPIC MEDIA
Transient diffusive electromagnetic fields in layered anisotropic media
[ISBN-90-6275-722-7] p 2887 N92-26254
ISOTROPIC TURBULENCE
Shock-turbulence interactions in a reacting flow
[NASA-CR-189647] p 2905 N92-27032
ITERATION
Nonexpansive prolongations and difference schemes for the advection equation
[PB92-141530] p 2986 N92-26502
Iterative system modeling using multigrid techniques
[AD-A245522] p 2976 N92-26658
ITERATIVE SOLUTION
Neural network error correction for solving coupled ordinary differential equations
[NASA-TM-101796] p 2986 N92-26407
Euclidean black hole vortices
[NASA-CR-190117] p 3016 N92-26436
Computational methods for problems of acoustics with particular reference to exterior domains p 2992 N92-26558
Computations of nonlinear gravity waves by a desingularized boundary integral method p 2942 N92-26583
Computational aspects of an implicit finite element procedure for elasto-viscoplastic large deformation problems p 2917 N92-26594
Cell vertex methods for compressible gas flows p 2897 N92-26599
Numerical solution of the equation of neutrons transport on plane geometry by analytical schemes using acceleration by synthetic diffusion
[DE92-621426] p 2995 N92-26844
Solution of the first-order form of the 3-D discrete ordinates equations on a massively parallel machine
[DE92-004575] p 2981 N92-26854

J

JAMMING
Effects of non-uniform windowing on the performance of a fast frequency-hopped noncoherent MFSK receiver over Rician fading channels with partial-band interference and Doppler shift
[AD-A245762] p 2889 N92-26595
JAPANESE SPACECRAFT
International Conference on Japanese Earth Observation Programs: TRMM Workshop
[JTN-92-80345] p 2922 N92-26701
The Tropical Rainfall Measuring Mission (TRMM) program at the Goddard Space Flight Center (GSFC)
[TW-1] p 2922 N92-26702
Status of TRMM project: Rain radar in the Tropical Rainfall Measuring Mission
[TW-2] p 2922 N92-26703
Status of TRMM (NASDA) --- tropical rainfall measuring mission
[TW-3] p 2923 N92-26704
TRMM Mission Team --- tropical rainfall measuring mission
[TW-4] p 2923 N92-26705
Tropical Rainfall Measuring Mission (TRMM) science report
[TW-5] p 2923 N92-26706
Storm model and beam filling problem for rain retrievals
[TW-6] p 2923 N92-26707
Development of TRMM radar rainfall retrieval algorithms
[TW-7] p 2923 N92-26708
Validation of numerical models by TRMM and validation of TRMM by numerical models
[TW-8] p 2923 N92-26709
Water cycles around the subtropical frontal zone in East Asia
[TW-9] p 2923 N92-26710
Rainfall pattern over the tropical rain forest
[TW-10] p 2923 N92-26711
Utilization of tropical convection data for meteorological operation
[TW-11] p 2924 N92-26712
TRMM and Asian monsoon --- tropical rainfall measuring mission
[TW-12] p 2924 N92-26713
Research plan for utilizing TRMM data in MRI --- tropical rainfall measuring mission
[TW-13] p 2924 N92-26714
Research program on hydrology
[TW-14] p 2924 N92-26715
International Conference on Japanese Earth Observation Programs: Plenary Session
[JTN-92-80342] p 2924 N92-26742
Japanese Earth Observation Program p 2924 N92-26743
MOS-1 activity report p 2925 N92-26749
JET AIRCRAFT
Aircraft photovoltaic power-generating system p 2926 N92-26581
JET ENGINES
Acoustic interactions between an altitude test facility and jet engine plumes: Theory and experiments
[NASA-CR-190423] p 2853 N92-26405
Aircraft photovoltaic power-generating system p 2926 N92-26581
Use of Markov methods in analysis of fault-tolerant systems with flexible repair policies
[PNR-90801] p 2916 N92-27038
JET FLOW
Spinning jets from shaped charges with flow turned liners
[MBB-UA-1197-90-PUB] p 2886 N92-26246
An experimental study of natural and forced modes in an axisymmetric jet p 2897 N92-26600
JET MIXING FLOW
A parametric numerical study of mixing in a cylindrical duct
[NASA-TM-105695] p 2854 N92-26553
CFD mixing analysis of jets injected from straight and slanted slots into confined crossflow in rectangular ducts
[NASA-TM-105699] p 2854 N92-26561
JET PROPULSION
Powder processing of aero-engine components
[PNR-90813] p 2880 N92-27044
JOINTS (ANATOMY)
Correlation and prediction of dynamic human isolated joint strength from lean body mass
[NASA-TP-3207] p 2956 N92-26682
JOINTS (JUNCTIONS)
Using min-max of torque to resolve redundancy for a mobile manipulator
[DE92-000070] p 2915 N92-26750

K

KALMAN FILTERS
Estimation of motion parameters from image sequences
[AD-A246135] p 2986 N92-26358
Performance analysis of image motion analysis algorithms
[AD-A246522] p 2974 N92-26468
An adaptive correction technique for Differential Global Positioning System p 2851 N92-26623
Kalman smoother applied to lace
[AD-A246439] p 2859 N92-27030
KAPTON (TRADEMARK)
Effects of the space environment on space-based radar phased-array antenna; status and preliminary observations (LDEF Experiment A0133) p 2883 N92-27086
An overview of the first results on the solar array materials passive LDEF experiment (sample), A0171 p 2927 N92-27087
Durability evaluation of photovoltaic blanket materials exposed on LDEF tray S1003 p 2883 N92-27100
KELVIN-HELMHOLTZ INSTABILITY
Plasma dynamics of the Earth magnetopause-boundary layer and its coupling to the polar ionosphere p 2944 N92-26865
KERNEL FUNCTIONS
NEXUS: A kernel complex object management system p 3012 N92-26567
KEVLAR (TRADEMARK)
Penetration of laminated composites by projectiles p 2869 N92-26861
KINEMATICS
On increasing the capabilities of the SMART adaptive random number generator
[DE92-621106] p 2976 N92-26835
KINETIC ENERGY
Numerical simulations of gun-launched kinetic energy projectiles subjected to asymmetric projectile base pressure
[DE92-005065] p 2857 N92-26693
Ensuring mass conversion in a heavy-gas dispersion model using the generalized anelastic equations
[DE92-007323] p 2934 N92-26936
KINETIC THEORY
Computation of hydrodynamics using kinetic theory
[DE92-009079] p 2896 N92-26456
Kinetic theory of toroidicity-induced Alfven eigenmode
[DE92-010424] p 2999 N92-26546
Finite temperature quantum field theory in curved spacetime p 3007 N92-26780

KINETICS
Modelling light transfer inside photobiofermentors: Applications to the photosynthetic compartments of CELSS p 2952 N92-26982
KNOWLEDGE BASES (ARTIFICIAL INTELLIGENCE)
Knowledge-based production management: Approaches, results, and prospects
[AD-A245714] p 3008 N92-26426
Applying knowledge compilation techniques to model-based reasoning
[NASA-TM-107876] p 2984 N92-26885
Model compilation: An approach to automated model derivation
[NASA-TM-107895] p 2985 N92-27057
KNOWLEDGE REPRESENTATION
Research accomplished at the Knowledge Based Systems Lab: IDEF3, version 1.0
[NASA-CR-190279] p 2975 N92-26587
KOLMOGOROFF THEORY
On the stochastic fatigue crack growth problem p 2917 N92-26557

L

LAGRANGE MULTIPLIERS
Application of parametrized variational principles in the finite element method p 2987 N92-26624
LAKE HURON
Hindcast wave information for the Great Lakes: Lake Huron. Wave information studies of US coastlines
[AD-A246326] p 2949 N92-26387
LAKES
Analysis of thermal infrared data acquired over playas: Silver Lake and Deep Springs Lake, California and Lunar Lake, Nevada p 2926 N92-26864
LAMINAR BOUNDARY LAYER
Distributed acoustic receptivity in laminar flow control configurations
[NASA-CR-4438] p 2898 N92-26680
LAMINAR FLOW
Aromatic-radical oxidation kinetics
[DE92-010821] p 2871 N92-26274
Study of the transition to turbulence within a curved rectangular channel with 40 to 1 aspect ratio
[AD-A246314] p 2896 N92-26290
Heat transfer in oscillating flows with sudden change in cross section
[NASA-TM-105692] p 2861 N92-26654
Reynolds number dependence of the drag coefficient for laminar flow through fine-scale screens
[DE92-002930] p 2899 N92-26698
Overview of NASA supported Stirling thermodynamic loss research
[NASA-TM-105690] p 2861 N92-27034
LAMINAR HEAT TRANSFER
Heat transfer in oscillating flows with sudden change in cross section
[NASA-TM-105692] p 2861 N92-26654
LAMINATES
Application of irradiation techniques to food and foodstuffs
[DE92-614952] p 2954 N92-26186
Analysis and modeling of high-temperature performance of advanced fiber composites p 2868 N92-26564
Reflection of x rays from repeated multilayer structures
[AD-A246562] p 2991 N92-26769
Buckling of unidirectional graphite/epoxy composite plates at low temperatures
[AD-A246602] p 2869 N92-26796
Finite element modeling of static indentation damage in laminated composites p 2869 N92-26827
A finite element method including transverse stresses for thick laminated plates and shells p 2920 N92-26860
Penetration of laminated composites by projectiles p 2869 N92-26861
LAND
Convection wave studies over land and sea p 2940 N92-26341
LANDAU DAMPING
Kinetic theory of toroidicity-induced Alfven eigenmode
[DE92-010424] p 2999 N92-26546
LANDFILLS
Environmental Protection Agency's municipal solid waste landfill liner design criteria
[PB92-153766] p 2933 N92-26928
LANDING AIDS
Critical soft landing technology issues for future US space missions
[NASA-CR-185673] p 2858 N92-26884
LANGUAGE PROGRAMMING
Distributed and parallel Ada and the Ada 9X recommendations
[NASA-CR-190392] p 2978 N92-26199
The SOL object-oriented database language
[REPT-91-053] p 2973 N92-26421
LANGUAGES
Information technology resources assessment
[DE92-009498] p 3011 N92-26221
LANTHANUM COMPOUNDS
Aging effects in palladium and LaNi(4.25)Al(0.75) tritides
[DE92-009945] p 2870 N92-26217
Anomalous structural behaviour of the high-temperature superconducting compound La(1.8)Sr(0.2)CuO(4-y) p 3003 N92-26327
Lattice instabilities and structural phase transformations in La2CuO4 superconductors and insulators
[DE92-010045] p 3006 N92-27059
LARGE SCALE INTEGRATION
Crossovers of the density of states in two-direction double-barrier resonant-tunneling structures
[AD-A246124] p 3005 N92-26684
LARGE SPACE STRUCTURES
Optimization of space structures to minimize dynamic response p 2858 N92-26610
Transverse flat plate heat pipe experiment p 2906 N92-27107
LASER APPLICATIONS
Time-resolved laser studies on the proton pump mechanism of bacteriorhodopsin
[DE92-003218] p 2951 N92-26493
Investigations of a single point temperature probe for measurement of atmospheric turbulence
[AD-A246563] p 2909 N92-26794
Laser cooling and trapping of atoms and particles
[AD-A247208] p 2913 N92-27173
LASER BEAMS
Construction and function of a multifunction CO2-Laser system
[AD-A245425] p 2910 N92-26271
Operation of a Smith-Purcell free-electron laser at submillimeter wavelengths p 2912 N92-26626
Application of fluorescent-particle imaging to measuring flow in complex media
[DE92-009121] p 2898 N92-26645
Application of decentralized control to a laser alignment system
[DE92-009692] p 2912 N92-26646
Erosion of a relativistic electron beam propagating in a plasma channel
[DE92-009059] p 3000 N92-26666
Linear and non-linear response of liquid and solid particles to energetic radiation
[AD-A246368] p 2894 N92-26942
Laser glittering in the relatively stable propagation layer near the sea surface
[AD-A246374] p 2913 N92-27050
LASER DAMAGE
Energy threshold for laser induced breakdown on a metal surface under high and ultra high vacuum conditions
[AD-A246212] p 2911 N92-26462
Low power laser irradiation effect with emphasis on injured neural tissues
[AD-A246410] p 2953 N92-27063
LASER HEATING
Diagnostic upgrades on MTX
[DE92-009695] p 2906 N92-26230
Comparison of laser and conventional heating in TLD dosemapping
[DE92-010773] p 2910 N92-26269
LASER MATERIALS
Photocathode transfer and storage techniques using alkali vapor feedback control
[DE92-008449] p 2891 N92-26202
LASER RANGE FINDERS
Construction and function of a multifunction CO2-Laser system
[AD-A245425] p 2910 N92-26271
LASER SPECTROSCOPY
Spectroscopy and kinetics of combustion gases at high temperatures
[DE92-011216] p 2872 N92-26281
LASER TARGET DESIGNATORS
Early risk reduction phase 1 FLIR/laser designator window
[AD-A246352] p 2911 N92-26293
LASER TARGETS
Large coherent arrays for laser radars, phase 1
[AD-A245528] p 2912 N92-26663
LASER WINDOWS
Early risk reduction phase 1 FLIR/laser designator window
[AD-A246352] p 2911 N92-26293
LASERS
Fail safe system for suppressing stimulated Brillouin scattering in large optics on the Nova laser
[DE92-008608] p 2911 N92-26505
LATENT HEAT
Surface energy budget and evapotranspiration measurement support
[NASA-CR-190059] p 2944 N92-26185
LATTICE PARAMETERS
Cadmium telluride thin films on silicon substrates
[AD-A245309] p 3001 N92-26226
LAUNCH VEHICLE CONFIGURATIONS
A comparison of heavy lift launch vehicle options for the 1990s
[AD-A245617] p 2857 N92-26402
LAUNCHERS
Role of shock compression technique for scientific and engineering studies
[DE92-008324] p 2919 N92-26846
Pneumatically actuated multiple store launcher
[AD-D015237] p 2853 N92-27188
LAUNCHING
A comparison of heavy lift launch vehicle options for the 1990s
[AD-A245617] p 2857 N92-26402
Retrievable payload carrier: Next generation Long Duration Exposure Facility p 2860 N92-27129
LAW (JURISPRUDENCE)
An analysis of the role of the budget committees in the Congressional budget process
[AD-A246005] p 3014 N92-26761
LAY-UP
Composite fuselage technology (summary of year 2)
[NASA-CR-190434] p 2852 N92-26655
Penetration of laminated composites by projectiles p 2869 N92-26861
LEAD ACID BATTERIES
Utilization of a bipolar lead acid battery for the advanced launch system p 2865 N92-27157
LEAD SULFIDES
Results of the TTF-TCNQ and the calcium carbonate crystallization on the Long Duration Exposure Facility p 3007 N92-27127
LEADING EDGES
Analysis of frozen startup of high-temperature heat pipes and three-dimensional modeling of block-heated heat pipes
[AD-A245327] p 2896 N92-26379
Hypersonic aerospace vehicle leading edge cooling using heat pipe, transpiration and film cooling techniques p 3007 N92-26733
LDEF SP-HVDE (Space Plasma-High Voltage Drainage Experiment) post-flight results: Leakage current and discharge p 2895 N92-27103
LEAKAGE
Post-test examination of a pool boiler receiver
[NASA-TM-105635] p 2880 N92-27192
LEARNING
N-learners problem: Learning Boolean combinations of halfspaces
[DE92-010390] p 2987 N92-26545
LEAST SQUARES METHOD
Correlation and prediction of dynamic human isolated joint strength from lean body mass
[NASA-TP-3207] p 2956 N92-26682
LEE WAVES
Undulatory airflow over the Spanish southern central highplain with northern winds p 2940 N92-26339
LEGAL LIABILITY
Information liability: New interpretations for the electronic age --- online databases p 3012 N92-26481
Survey of small business use of intellectual property protection
[PB92-151703] p 3009 N92-26523
LEGENDRE FUNCTIONS
Sturm-Liouville eigenfunctions expressed in determinant form
[AD-A245991] p 2987 N92-26755
LENSES
Dynamic lens compensation for active color imaging and constant magnification focusing
[AD-A245713] p 2997 N92-26425
LEVELING
The geoid, GPS, and levelling p 2925 N92-26777
LIAPUNOV FUNCTIONS
Lyapunov equation for infinite-dimensional discrete bilinear systems
[DE92-621066] p 2988 N92-26831
LIBRARIES
UT40 - Asset Library Open Architecture Framework (ALOAF)
[AD-A247268] p 2978 N92-27177
LIE GROUPS
Non-compact WZW conformal field theories
[PB92-125038] p 3007 N92-26805
Universal R-matrix for quantized (super)algebras
[DE92-821067] p 2988 N92-26834

On the evaluation of the U(3) content of the matrix elements of 1- and 2-body operators
[DE92-621113] p 2988 N92-26837
Induced cycle structures of the hyperoctahedral group
[DE92-007570] p 3006 N92-26857

LIFE (DURABILITY)
Life testing of secondary Ag-Zn cells
p 2865 N92-27153
Cycle life characteristics of Li-TiS2 cells
p 2865 N92-27154
Accelerated cycle life performance for ovonic nickel-metal hydride cells p 2865 N92-27155
Evaluation of sodium-nickel chloride cells for space applications p 2865 N92-27156
Update of a nickel-hydrogen cycle life model
p 2866 N92-27162

LIFE SCIENCES
Human support issues and systems for the space exploration initiative: Results from Project Outreach
[NASA-CR-190320] p 2954 N92-26193
Space life sciences strategic plan, 1991
[NASA-TM-107856] p 2950 N92-26266
Aerospace medicine and biology: A continuing bibliography with indexes (supplement 362)
[NASA-SP-7011(362)] p 2953 N92-27068
LDEF: 69 Months in Space. First Post-Retrieval Symposium, part 3
[NASA-CP-3134-PT-3] p 3022 N92-27083

LIFE SUPPORT SYSTEMS
Human support issues and systems for the space exploration initiative: Results from Project Outreach
[NASA-CR-190320] p 2954 N92-26193
Life support research and development, a Department of Energy program for the Space Exploration Initiative
[DE92-007681] p 2955 N92-26375
Life support research and development for the Department of Energy Space Exploration Initiative
[DE92-007239] p 2955 N92-26494
Higher plant growth in closed environment: Preliminary experiments in life support facility at ESA-ESTEC
p 2951 N92-26978
Chemolithotropic hydrogen-oxidizing bacteria and their possible functions in closed ecological life-support systems p 2951 N92-26979
Impact of diet on the design of waste processors in CELSS p 2961 N92-26980
MELISSA: Physical links of compartments Nitrobacter/Spirulina p 2961 N92-26981
EVA life support design and technology developments
p 2965 N92-27002
Fan/pump/separator technology development for EVA
p 2966 N92-27006
Determination of ventilation requirements for a space suit helmet p 2968 N92-27017
Concept for a European Space Station: Habitability, life support, and laboratory facilities p 2969 N92-27023
Moon base habitability aspects p 2969 N92-27026

LIFT
Use of an approximate similarity principle for the thermal scaling of a full-scale thrust augmenting ejector
[NASA-TM-105724] p 2854 N92-26613
High lift aircraft
[AD-D015215] p 2853 N92-27185

LIFTING REENTRY VEHICLES
Rarefied-flow aerodynamics
[NASA-CR-190452] p 2850 N92-27191

LIGHT (VISIBLE RADIATION)
Application of decentralized control to a laser alignment system
[DE92-009692] p 2912 N92-26646

LIGHT BEAMS
Squeezed light and twin beams generation with a Q-switched laser p 2912 N92-26603
Liquid level and volume measurement device
[AD-D015189] p 2909 N92-26879
Laser glittering in the relatively stable propagation layer near the sea surface
[AD-A246374] p 2913 N92-27050

LIGHT IONS
Advances in the engineering of high field applied-B ion diodes for inertial confinement fusion
[DE92-006528] p 3000 N92-26695

LIGHT MODULATION
Optical hidden layer network
[AD-A246162] p 2992 N92-26413

LIGHT SOURCES
Liquid level and volume measurement device
[AD-D015189] p 2909 N92-26879

LIGHT TRANSMISSION
Modelling light transfer inside photobiofermentors: Applications to the photosynthetic compartments of CELSS p 2952 N92-26982
Laser glittering in the relatively stable propagation layer near the sea surface
[AD-A246374] p 2913 N92-27050
Experiment M0003-4: Advanced solar cell and coverglass analysis, an overview p 2927 N92-27088
Contamination of optical surfaces in Earth orbit
p 2999 N92-27099
Differential polarimetric fiber optic sensor
[AD-D015218] p 2998 N92-27186

LIGHT WATER
Metal hydride based isotope separation: Large-scale operations
[DE92-009830] p 2875 N92-26717

LIKELIHOOD RATIO
Mixed Weibull distributions in reliability engineering: Statistical models for the lifetime of units with multiple modes of failure p 2916 N92-26602

LINE SPECTRA
Research and technology, 1990: Goddard Space Flight Center
[NASA-TM-107792] p 3022 N92-26824

LINEAR ACCELERATORS
Focusing x ray transition radiation with cylindrical and elliptical optics
[AD-A245987] p 2997 N92-26754
Higher order parametric x rays
[AD-A247148] p 2991 N92-27182

LINEAR EQUATIONS
Nonexpansive prolongations and difference schemes for the advection equation
[PB92-141530] p 2986 N92-26502

LINEAR PROGRAMMING
Evaluation of carbon dioxide emission control strategies in New York State
[DE92-010162] p 2932 N92-26825
Proximal minimization algorithms with cutting planes
[AD-A246436] p 2977 N92-26949

LINEAR QUADRATIC GAUSSIAN CONTROL
Parameter robust reduced-order control of flexible structures p 2982 N92-26597
Experiments in modelling and end-point control of two-link flexible manipulators p 2915 N92-26731

LINEAR QUADRATIC REGULATOR
The modeling and control of acoustic/structure interaction problems via piezoceramic actuators: 2-D numerical examples
[NASA-CR-189639] p 2987 N92-26668

LINEAR SYSTEMS
Characterization of discrete-time linear periodically time-varying systems
[AD-A245822] p 2989 N92-26180
Identification of linear systems by an asymptotically stable observer
[NASA-TP-3164] p 2917 N92-26537

LININGS
Spinning jets from shaped charges with flow turned liners
[MBB-UA-1197-90-PUB] p 2886 N92-26246
Environmental Protection Agency's municipal solid waste landfill liner design criteria
[PB92-153766] p 2933 N92-26928

LIPID METABOLISM
Study of hydrazine metabolism and toxicity
[AD-A245755] p 2884 N92-26589

LIQUID HELIUM
Dynamic properties of quasi-two-dimensional one component plasmas
[DE92-621523] p 3000 N92-26806

LIQUID LEVELS
Liquid level and volume measurement device
[AD-D015189] p 2909 N92-26879

LIQUID PROPELLANT ROCKET ENGINES
Effect of model selection on combustor performance and stability predictions using ROCCID
[NASA-TM-105750] p 2861 N92-27036

LIQUID SLOSHING
Parabolic flight experiments on bubble migration under reduced gravity p 2885 N92-26443
Liquid motion analysis with lateral impacts under low gravity p 2885 N92-26445

LIQUID SURFACES
The interaction of a vortex ring with a contaminated free surface p 2900 N92-26785

LIQUID-VAPOR INTERFACES
Parabolic flight: Reports of microgravity experiments by aircraft, volume 1, no. 2
[EG-910045] p 2884 N92-26440
Parabolic flight experiments on bubble migration under reduced gravity p 2885 N92-26443
Micro-gravity experiment of vapor/liquid reorientation induced by capillary force p 2885 N92-26444
Liquid motion analysis with lateral impacts under low gravity p 2885 N92-26445
Color image processing and object tracking workstation
[NASA-TM-105561] p 2886 N92-26611

LIQUIDS
Vibrational spectroscopy in shock-compressed liquids
[DE92-007713] p 2876 N92-26867

LITHIUM
Gas-pressure studies with Li(Si)/FeS2 thermal batteries
[DE92-010801] p 2892 N92-26238
Safety testing of lithium cells p 2864 N92-27150
Examination of the discharge mechanism of Li/CF(x) cells: Comparison of the electrochemical reduction mechanisms of PTFE and (CF(x))n by lithium
p 2865 N92-27151

LITHIUM CHLORIDES
Development of a 300 Amp-hr high rate lithium thionyl chloride cell p 2864 N92-27149

LITHIUM COMPOUNDS
Fabrication and characterization of amorphous lithium electrolyte thin films and rechargeable thin-film batteries
[DE92-010108] p 2893 N92-26636
New amorphous thin-film lithium electrolyte and rechargeable microbattery
[DE92-010110] p 2893 N92-26637
Integrated heat pipe concept for Li/SOCl2 cells cooling p 2895 N92-26974
NASA Li/CF(x) cell problem analysis: Scanning electron microscopy with energy dispersive x ray spectrometry
p 2863 N92-27144
Calorimetric determination of the thermoneutral potential for Li/BrCl in SOCl2 (BCX) cells p 2864 N92-27146
Li/BCX, SVO, and CSC cells: Power sources for aerospace applications p 2864 N92-27147

LITHIUM FLUORIDES
Optimization of a color center Q-switched Nd:YLF laser
[DE92-621612] p 2910 N92-26287
STS lithium/CF(x) battery p 2863 N92-27143

LITHIUM ISOTOPES
Li-6,d reaction on sd-, fp- and g-shell nuclei in ZR- and FR-DWBA formalisms
[DE92-614353] p 2994 N92-26365

LITHIUM SULFUR BATTERIES
Integrated heat pipe concept for Li/SOCl2 cells cooling p 2895 N92-26974
The 1990 NASA Aerospace Battery Workshop
[NASA-CP-3119] p 2862 N92-27130
Performances of 250 Amp-hr lithium/thionyl chloride cells p 2864 N92-27148
Cycle life characteristics of Li-TiS2 cells
p 2865 N92-27154

LOAD DISTRIBUTION (FORCES)
Gear tooth stress measurements of two helicopter planetary stages
[NASA-TM-105651] p 2915 N92-26555

LOADING RATE
Recent advances in shock and quasi-isentropic compression techniques for dynamic material property studies
[DE92-007988] p 2919 N92-26852

LOADS (FORCES)
Effect of type of load on stress analysis of thin-walled ducts
[NASA-TP-3248] p 2918 N92-26669
Fracture of structural ceramics in combined mode 1 and mode 2 loading p 2882 N92-26775

LOCAL AREA NETWORKS
Requirements analysis and design for implementation of a satellite link for a local area computer network
[AD-A245610] p 2978 N92-26227
Scalable coherent interface: Links to the future
[DE92-010728] p 2887 N92-26267
Selection and specification of a data link protocol for VSAT based inter-LAN communications
[AD-A246289] p 2979 N92-26361

LOCOMOTION
Architectural studies relating to human body motion morphology in microgravity p 2953 N92-27011

LOFTING
Algorithms for blending surface generation
[AD-A245686] p 2975 N92-26524

LOGIC PROGRAMMING
Proving properties of real-time systems through logical specifications and Petri net models
[REPT-91-072] p 2973 N92-26448

LOGISTICS MANAGEMENT
Logistics in space: Tools to support astronauts
p 2963 N92-26990

LONG DURATION EXPOSURE FACILITY
Geometry and mass model of ionizing radiation experiments on the LDEF satellite
[NASA-CR-184325] p 2993 N92-26200
LDEF: 69 Months in Space. First Post-Retrieval Symposium, part 3
[NASA-CP-3134-PT-3] p 3022 N92-27083
Systems special investigation group overview
p 2867 N92-27084
Space aging of solid rocket materials
p 2884 N92-27085

Effects of the space environment on space-based radar phased-array antenna; status and preliminary observations (LDEF Experiment A0133) p 2883 N92-27086
An overview of the first results on the solar array materials passive LDEF experiment (sample), A0171 p 2927 N92-27087
Preliminary analyses of WL experiment No. 701, space environment effects on operating fiber optic systems p 2998 N92-27089
LDEF fiber optic exposure experiment No. S-0109 p 2998 N92-27090
Optical performance of exposed solar cell covers p 2998 N92-27091
Ruled and holographic diffraction gratings experiment (AO 138-5) p 2910 N92-27092
Post-flight characterization of optical system samples, thermal control samples, and detectors from LDEF experiment M0003, sub-experiments 6 and 13 p 2998 N92-27093
LDEF active optical system components experiment p 2998 N92-27094
Effects of long-duration exposure on optical system components p 2998 N92-27095
Effects of long term exposure on optical substrates and coatings (SOO50-2) p 2998 N92-27096
Vacuum deposited optical coatings experiment p 2999 N92-27097
Space environmental effects on coated optics p 2999 N92-27098
Contamination of optical surfaces in Earth orbit p 2999 N92-27099
Durability evaluation of photovoltaic blanket materials exposed on LDEF tray S1003 p 2883 N92-27100
Advanced photovoltaic experiment, S0014: Preliminary flight results and post-flight findings p 2927 N92-27101
Evaluation of LDEF experiment S1002 p 2883 N92-27102
LDEF SP-HVDE (Space Plasma-High Voltage Drainage Experiment) post-flight results: Leakage current and discharge p 2895 N92-27103
Long Duration Exposure Facility (LDEF) low temperature heat pipe experiment package (HEPP) flight results p 2906 N92-27104
Long Duration Exposure Facility (LDEF) low-temperature heat pipe experiment package power system results p 2906 N92-27105
Results from the LDEF/A0076 cascaded variable conductance heatpipe experiment p 2906 N92-27106
Radiation sensitivity of quartz crystal oscillators experiment for the Long Duration Exposure Facility (LDEF) p 2895 N92-27111
LDEF electronic systems: Successes, failures and lessons p 2895 N92-27112
LDEF mechanical systems p 2916 N92-27114
On-orbit coldwelding: Fact or friction? p 2880 N92-27115
Thermal control surfaces experiment flight system performance p 2860 N92-27116
French Cooperative Passive Payload (FRECOPA) p 2867 N92-27117
Effects of ultra-vacuum and space environment on contact ohmic resistance: LDEF experiment AO 138-11 p 2895 N92-27118
Microwelding (or cold-welding) of various metallic materials under the ultra-vacuum LDEF experiment AO 138-10 p 2880 N92-27119
Seeds in space experiment --- long duration exposure facility p 2952 N92-27120
Space Exposed Experiment Developed for Students (SEEDS) (P0004-2) p 2952 N92-27121
Survival of epiphytic bacteria from seed stored on the Long Duration Exposure Facility (LDEF) p 2952 N92-27122
Preliminary total dose measurements on LDEF --- long duration exposure facility p 2952 N92-27123
Total Dose Effects (TDE) of heavy ionizing radiation in fungus spores and plant seeds: Preliminary investigations p 2952 N92-27124
Preliminary results of the Artemia salina experiments in biostack on LDEF p 2952 N92-27125
Long-term exposure of bacterial spores to space p 2952 N92-27126
Results of the TTF-TCNQ and the calcium carbonate crystallization on the Long Duration Exposure Facility p 3007 N92-27127
The role of the Long Duration Exposure Facility in the development of space systems p 2867 N92-27128
Retrievable payload carrier: Next generation Long Duration Exposure Facility p 2860 N92-27129

LONG RANGE WEATHER FORECASTING
Utilization of tropical convection data for meteorological operation
[TW-11] p 2924 N92-26712

LOOPS
Unified computational method for design of fluid loop systems p 2905 N92-26962
Development of fluid loop and hybrid radiators: Test results p 2859 N92-26967

LORENTZ FORCE
Research activities on CFD at the Ship Research Institute p 2902 N92-26908

LOSSES
Overview of NASA supported Stirling thermodynamic loss research
[NASA-TM-105690] p 2861 N92-27034

LOW ALTITUDE
A refined maximum likelihood method for tracking low-altitude targets over the sea: Results of simulation and experiments
[AD-A246534] p 2888 N92-26419

LOW COST
Innovative techniques for the production of low cost 2D laser diode arrays
[AD-A247282] p 2913 N92-27178

LOW FREQUENCIES
Short-wave low-frequency spectra in a current-carrying plasma
[DE92-621529] p 3001 N92-26808

LOW GRAVITY MANUFACTURING
Parabolic flight: Reports of microgravity experiments by aircraft, volume 1, no. 2
[EG-910045] p 2884 N92-26440

LOW PASS FILTERS
Estimation of peak intensities from frequency filtered total scattering data of neutrons obtained by the reverse Fourier method p 3002 N92-26321
An adaptive correction technique for Differential Global Positioning System p 2851 N92-26623
Observations of wind forced circulation on the continental shelf off Point Sur, California from a self-contained acoustic Doppler current profiler
[AD-A246437] p 2950 N92-27029

LOW SPEED
Observation and measurements of flow structures in the stagnation region of a wing-body junction p 2849 N92-26616

LOW TEMPERATURE
A method to improve post impact compressive strength in graphite/epoxy composite materials after low temperature impact
[AD-A245395] p 2867 N92-26380
Long Duration Exposure Facility (LDEF) low-temperature heat pipe experiment package power system results p 2906 N92-27105

LOW TEMPERATURE TESTS
Low temperature electrochemical activation of methane
[PB92-152917] p 2872 N92-26351

LOWER ATMOSPHERE
Studies of inertio-gravity waves induced by geostrophic adjustment of the atmospheric jet stream p 2944 N92-26866

LOWER BODY NEGATIVE PRESSURE
LBNP as countermeasure: An automated scenario p 2953 N92-27012

LUBRICANTS
Full-scale transmission testing to evaluate advanced lubricants
[NASA-TM-105668] p 2915 N92-26560

LUBRICATING OILS
Full-scale transmission testing to evaluate advanced lubricants
[NASA-TM-105668] p 2915 N92-26560

LUMINESCENCE
Etching effects in ion implanted SiO2
[DE92-011150] p 3005 N92-26826
Some experiences with absorption, phonon Raman, and luminescence spectroscopic probes of crystal structure of f-element compounds
[DE92-007828] p 3006 N92-26851

LUNAR BASES
New perspectives of living in space: Habitability guidelines for future manned space systems p 2968 N92-27022
Moon base habitability aspects p 2969 N92-27026

LUNAR TIDES
The effect of global change and long period tides on the Earth's rotation and gravitational potential p 2925 N92-26781

M

MACHINE LEARNING
Neural network error correction for solving coupled ordinary differential equations
[NASA-TM-101796] p 2986 N92-26407
Introduction to IND and recursive partitioning
[NASA-TM-107879] p 2983 N92-26629
Computer modeling of human decision making
[NASA-TM-107868] p 2983 N92-26630
Explanation-based generalization of partially ordered plans
[NASA-TM-107869] p 2983 N92-26789
Planning and scheduling research at NASA Ames Research Center
[NASA-TM-107888] p 3009 N92-26790
Discrete sequence prediction and its applications
[NASA-TM-107865] p 2984 N92-26791
Bayesian classification theory
[NASA-TM-107885] p 2988 N92-26894
The structure and formation of natural categories
[NASA-TM-107896] p 2985 N92-27056

MACROMOLECULES
A fractal computer model of macromolecule-cell surface interactions
[AD-A245394] p 2950 N92-26289

MAGELLAN PROJECT (NASA)
Magellan battery operations: An overview p 2862 N92-27133

MAGNESIUM ALLOYS
Dynamic restoration mechanisms in Al-5.8 at. percent Mg deformed to large strains in the solute drag regime
[DE92-009529] p 2877 N92-26223

MAGNET COILS
Advances in the engineering of high field applied-B ion diodes for inertial confinement fusion
[DE92-006528] p 3000 N92-26695

MAGNETIC DIFFUSION
Transient diffusive electromagnetic fields in layered anisotropic media
[ISBN-90-6275-722-7] p 2887 N92-26254

MAGNETIC FIELD RECONNECTION
The ionospheric signature of flux transfer events p 2937 N92-26308
A model of the dayside magnetosphere and breakups in the cusp region p 2937 N92-26312
Mathematical model of physical processes responsible for generation of magnetospheric electric fields and their penetration into the Earth's magnetosphere p 2938 N92-26319

MAGNETIC FIELDS
The Polar Geophysical Institute program of the theoretical and experimental investigation on cusp p 2935 N92-26298
Mapping of the auroral oval to the tail p 2937 N92-26309
The joint US/UK 1990 epoch world magnetic model
[NASA-CR-190424] p 2942 N92-26406
Evidence for cluster magnetic fields around radio galaxies p 3017 N92-26554
Erosion of a relativistic electron beam propagating in a plasma channel
[DE92-009059] p 3000 N92-26666
Spectral boundary conditions and index theorem for 2-dimensional compact manifold with boundary
[DE92-621115] p 2990 N92-26798

MAGNETIC FLUX
The present understanding of the cusp p 2936 N92-26306
Magnetic flux noise in copper oxide superconductors
[DE92-010299] p 3003 N92-26582

MAGNETIC LEVITATION VEHICLES
National MAGLEV initiative. Moving America: New directions, new opportunities
[PB92-163237] p 2914 N92-26518

MAGNETIC MATERIALS
Magnetic anisotropy from first principles
[ISBN-90-9004483-3] p 2877 N92-26252

MAGNETIC MOMENTS
The Debye temperature of YBa2Cu3O(7-(delta)) and its dependence on the volume fraction of superconductivity
[DE92-010305] p 3003 N92-26584

MAGNETIC MONOPOLES
A search for magnetic monopoles with the Soudan 2 detector
[DE92-010347] p 3021 N92-26216

MAGNETIC PERMEABILITY
Bis (pentamethylcyclopentadienyl) ytterbium: Electron-transfer reactions with organotransition metal complexes
[DE92-010300] p 2994 N92-26235
Transient diffusive electromagnetic fields in layered anisotropic media
[ISBN-90-6275-722-7] p 2887 N92-26254

MAGNETIC SIGNATURES
The ionospheric signature of flux transfer events p 2937 N92-26308
Ground-based studies of sensing magnetosphere/ionosphere interactions: Convection and substorms p 2937 N92-26311
Imaging the Earth's magnetosphere using ground magnetometer arrays p 2938 N92-26314

MAGNETIC STORMS
Magnetohydrodynamic Electromagnetic Pulse (MHD-EMP) interaction with power transmission and distribution systems
[DE92-010365] p 2887 N92-26237
Mapping of the auroral oval to the tail
p 2937 N92-26309
Ground-based studies of sensing magnetosphere/ionosphere interactions: Convection and substorms p 2937 N92-26311
Relationships between ionospheric and tail phenomena p 2938 N92-26317
The effects of magnetic storm phases on F-layer irregularities from auroral to equatorial latitudes
[AD-A245495] p 2943 N92-26675

MAGNETIC SUSPENSION
National MAGLEV initiative. Moving America: New directions, new opportunities
[PB92-163237] p 2914 N92-26518

MAGNETO-OPTICS
Magneto-optical multilayers --- optical data storage
[DE92-009726] p 2997 N92-26565
Band structure and optical properties of semiconductor superlattices
[AD-A246076] p 3005 N92-26763

MAGNETOHYDRODYNAMIC FLOW
Plasma dynamics of the Earth magnetopause-boundary layer and its coupling to the polar ionosphere
p 2944 N92-26865

MAGNETOHYDRODYNAMIC STABILITY
Preliminary experiment of GDEF (Gas Dynamics Experiment Facility) p 2885 N92-26442
Kinetic theory of toroidicity-induced Alfven eigenmode
[DE92-010424] p 2999 N92-26546
Scenarios for the nonlinear evolution of alpha particle induced Alfven wave instability
[DE92-010549] p 3000 N92-26550
Theory of electromagnetic instability of an intense beam in a quadrupole focusing system
[AD-A246560] p 2990 N92-26768

MAGNETOHYDRODYNAMIC WAVES
Magnetohydrodynamic Electromagnetic Pulse (MHD-EMP) interaction with power transmission and distribution systems
[DE92-010365] p 2887 N92-26237
Mode structure and continuum damping of high-n toroidal Alfven eigenmodes
[DE92-010547] p 2999 N92-26256
Kinetic theory of toroidicity-induced Alfven eigenmode
[DE92-010424] p 2999 N92-26546
Scenarios for the nonlinear evolution of alpha particle induced Alfven wave instability
[DE92-010549] p 3000 N92-26550

MAGNETOHYDRODYNAMICS
Magnetohydrodynamic Electromagnetic Pulse (MHD-EMP) interaction with power transmission and distribution systems
[DE92-010365] p 2887 N92-26237
A FORTRAN 90 code for magnetohydrodynamics
[DE92-010362] p 3000 N92-26577

MAGNETOMETERS
Thin-film high temperature superconducting flux transformers coupled to SQUIDS
[DE92-010260] p 2891 N92-26205
U.S. ground-based space research programs in Svalbard (Norway) p 2935 N92-26296
Imaging the Earth's magnetosphere using ground magnetometer arrays p 2938 N92-26314

MAGNETOPAUSE
The ionospheric signature of flux transfer events
p 2937 N92-26308
A model of the dayside magnetosphere and breakups in the cusp region p 2937 N92-26312
Plasma dynamics of the Earth magnetopause-boundary layer and its coupling to the polar ionosphere
p 2944 N92-26865

MAGNETOSHEATH
A model of the dayside magnetosphere and breakups in the cusp region p 2937 N92-26312
Solar wind interaction with Venus and Mars
p 3020 N92-26779

MAGNETOSPHERE-IONOSPHERE COUPLING
Handbook of solar-terrestrial data systems, version 1
[NASA-TM-107810] p 3019 N92-26191
Solar wind-magnetosphere coupling processes observed near the dayside cusp/cleft
p 2937 N92-26307
Ground-based studies of sensing magnetosphere/ionosphere interactions: Convection and substorms p 2937 N92-26311
Plasma dynamics of the Earth magnetopause-boundary layer and its coupling to the polar ionosphere
p 2944 N92-26865

MAGNETOSTATICS
Dielectric tensor of strongly coupled plasmas
[DE92-621524] p 3001 N92-26807
Short-wave low-frequency spectra in a current-carrying plasma
[DE92-621529] p 3001 N92-26808

MAGNIFICATION
Dynamic lens compensation for active color imaging and constant magnification focusing
[AD-A245713] p 2997 N92-26425

MAINTENANCE
Maintenance manual for Natick's Footwear Database
[AD-A246273] p 2954 N92-26242
A prototype semantic integrity front end expert system for a relational database
[AD-A246084] p 3013 N92-26765

MAN ENVIRONMENT INTERACTIONS
Equilibrium-analysis of projected climate change effects on the global soil organic matter pool
[PB92-153022] p 2930 N92-26509
Monthly mean global satellite data sets available in CCM history tape format
[NASA-CR-190344] p 2933 N92-26878

MAN MACHINE SYSTEMS
Man-machine aspects of remotely controlled space manipulators
[ISBN-90-370-0056-8] p 2954 N92-26255
Man-machine interface analyses for bomber flight management system
[AD-A245707] p 2955 N92-26355
Logistics in space: Tools to support astronauts
p 2963 N92-26990
CAD system for HFE analyses: Zero-g posture in optimisation of Columbus APM crew workstations --- human factors engineering p 2963 N92-26991
Engineering of a new overall system to improve the interaction between the crew and the ground-based scientists and personnel p 2964 N92-26995

MAN TENDED FREE FLYERS
Battery thermal control of the Columbus Free Flyer
p 2859 N92-26970

MAN-COMPUTER INTERFACE
Naval Postgraduate School aircraft synthesis program (user's manual)
[AD-A246198] p 2974 N92-26458
User interface consistency across end-user application programs: Effect on learning and satisfaction
p 3013 N92-26776
Engineering of a new overall system to improve the interaction between the crew and the ground-based scientists and personnel p 2964 N92-26995

MANAGEMENT
Management: A bibliography for NASA managers
[NASA-SP-7500(26)] p 3010 N92-27080

MANAGEMENT INFORMATION SYSTEMS
Information systems planning methodologies: A framework for comparison and selection
[AD-A246527] p 3012 N92-26469
Technical specification for the Sandia Management Restructure Study Team (MRST) Prototype Information System
[DE92-010360] p 3012 N92-26575

MANAGEMENT METHODS
Management: A bibliography for NASA managers
[NASA-SP-7500(26)] p 3010 N92-27080

MANAGEMENT PLANNING
Executive summary of information systems plans: Fiscal years 1993 to 1997
[PB92-158351] p 3011 N92-26368
Applying artificial intelligence to the control of space telescopes (extended abstract)
[NASA-TM-107913] p 3015 N92-26886
The 1990 progress report and future plans
[NASA-TM-107911] p 2984 N92-26887
Management: A bibliography for NASA managers
[NASA-SP-7500(26)] p 3010 N92-27080

MANAGEMENT SYSTEMS
NEXUS: A kernel complex object management system
p 3012 N92-26567
Expert system management system
[AD-A247102] p 3009 N92-26863

MANGANESE ISOTOPES
Gamma-ray spectrometry of LDEF samples
[DE92-009947] p 2874 N92-26632

MANIPULATORS
Man-machine aspects of remotely controlled space manipulators
[ISBN-90-370-0056-8] p 2954 N92-26255
On certain methods of determining the ellipses an d ellipsoids of the positioning accuracy of robot manipulators
[ISSN-0208-5658] p 2914 N92-26284
A framework for recognizing grasps
[AD-A245712] p 2981 N92-26357
Hybrid efficient control algorithms for robot manipulators
[AD-A245716] p 2981 N92-26428
Adaptive control of robotic manipulators with structural flexibility p 2914 N92-26475
A Bayes-Maximum Entropy method for multi-sensor data fusion
[DE92-000680] p 2983 N92-26657
Experiments in modelling and end-point control of two-link flexible manipulators p 2915 N92-26731
Using min-max of torque to resolve redundancy for a mobile manipulator
[DE92-000070] p 2915 N92-26750

MANNED MARS MISSIONS
Human round trip to Mars: Six months and radiation safe
[DE92-010160] p 2857 N92-26818

MANNED SPACE FLIGHT
Life support research and development for the Department of Energy Space Exploration Initiative
[DE92-007239] p 2955 N92-26494

MANNED SPACECRAFT
New perspectives of living in space: Habitability guidelines for future manned space systems
p 2968 N92-27022

MANUAL CONTROL
Man-machine aspects of remotely controlled space manipulators
[ISBN-90-370-0056-8] p 2954 N92-26255

MANUALS
Cataloging guidelines
[AD-A246500] p 3011 N92-26465
Introduction in IND and recursive partitioning
[NASA-TM-107879] p 2983 N92-26629
Waste minimization for non-agricultural pesticide applicators: EPA's pollution prevention guide
[PB92-153774] p 2933 N92-26889

MANUFACTURING
Photovoltaic manufacturing technology, phase 1
[DE92-001199] p 2926 N92-26190
Simultaneous engineering in aero-gas turbine design and manufacture
[PNR-90811] p 2856 N92-27043

MANY BODY PROBLEM
Simulation studies for surfaces and materials strength
[NASA-CR-190340] p 3001 N92-26265

MAPPING
Mapping of the auroral oval to the tail
p 2937 N92-26309
Relationships between ionospheric and tail phenomena p 2938 N92-26317
Quantitative assessment of the slope resolution of seafloor mapping systems
[AD-A246158] p 2949 N92-26411

MAPS
Generation of multi-resolution maps
[PB92-152206] p 2921 N92-26513

MARINE ENVIRONMENTS
Biosphere model validation by intercomparison to observed behaviour of fallout radionuclides in the aquatic environment, appendix 5 p 2930 N92-26487
Infrared clutter measurements of marine backgrounds
[AD-A245422] p 2932 N92-26873

MARINE PROPULSION
Algorithms for blending surface generation
[AD-A245686] p 2975 N92-26524

MARINE TECHNOLOGY
The utility of acoustic travel times in locating the north wall of the Gulf Stream
[AD-A246219] p 2949 N92-26463

MARKOV CHAINS
Adaptive control of nonlinear and stochastic systems
[AD-A247204] p 2985 N92-27169
Stochastic versions of the EM algorithm
[AD-A246929] p 2989 N92-27174

MARKOV PROCESSES
Identification of linear systems by an asymptotically stable observer
[NASA-TP-3164] p 2917 N92-26537
On the stochastic fatigue crack growth problem
p 2917 N92-26557
Use of Markov methods in analysis of fault-tolerant systems with flexible repair policies
[PNR-90801] p 2916 N92-27038

MARS (PLANET)
Solar wind interaction with Venus and Mars
p 3020 N92-26779

MARS ATMOSPHERE
Solar wind interaction with Venus and Mars
p 3020 N92-26779

MARTENSITIC STAINLESS STEELS
Improving the fracture resistance of irradiated martensitic steels
[DE92-008387] p 2879 N92-26848

MASS
A one-dimensional temperature model for a snow cover: Technical documentation for SNTHERM.89
[AD-A245493] p 2922 N92-26674

MASS FLOW
A parametric numerical study of mixing in a cylindrical duct
[NASA-TM-105695] p 2854 N92-26553
MASS SPECTROMETERS
New approaches to studies of exotic nuclei
[DE92-010127] p 2994 N92-26570
MASS SPECTROSCOPY
Helium-3 mass spectrometry for low-level tritium analysis of environmental samples
[DE92-008937] p 2873 N92-26454
MASS TRANSFER
The centrifugal mass exchange apparatus in air-conditioning system of isolated, inhabited object and its work control p 2957 N92-26956
MASSIVE STARS
A self-contamination model for the formation of globular star clusters p 3018 N92-26723
MASSIVELY PARALLEL PROCESSORS
Massively parallel implementation of character recognition systems
[PB92-149863] p 2980 N92-26501
Matched field processing on the connection machine
[AD-A245469] p 2980 N92-26531
A FORTRAN 90 code for magnetohydrodynamics
[DE92-010362] p 3000 N92-26577
Experiences in using C++ to develop a next generation strong shock wave physics code
[DE92-006675] p 2976 N92-26696
The Orca Project: Research on high performance parallel computer programming environments
[AD-A234648] p 2980 N92-26801
Solution of the first-order form of the 3-D discrete ordinates equations on a massively parallel machine
[DE92-004575] p 2981 N92-26854
MATHEMATICAL LOGIC
Automated interpretation of S-invariants of predicate/transition nets: An application of non-classical logics
[PB92-143544] p 2975 N92-26500
Modelling default and likelihood reasoning as probabilistic
[NASA-TM-107889] p 2984 N92-26893
VLSI implementation of fuzzy logic operator unit
[AD-A247146] p 2989 N92-27180
MATHEMATICAL MODELS
Recursive ray acoustics for three-dimensional sound-speed profiles
[AD-A245613] p 2991 N92-26228
Fault zone structure determined through the analysis of earthquake arrival times
[DE92-010322] p 2935 N92-26239
A model for aerodynamically-valved pulse combustion
[DE92-009887] p 2871 N92-26262
Modeling node bandwidth limits and their effects on vector combining algorithms
[DE92-010629] p 2979 N92-26277
The Polar Geophysical Institute program of the theoretical and experimental investigation on cusp p 2935 N92-26298
Contributions to atmospheric physics in honor of Dr. Manfred Reinhardt on his 65th birthday
[DLR-FB-91-30] p 2939 N92-26329
A reformulation of the Eady model p 2939 N92-26330
Upper/lower vortex interaction and potential vorticity inversion p 2939 N92-26331
Noxious matter transportation in the Alpine regions p 2934 N92-26332
Comparison of frontogenetical structures for different cases of frontal development p 2939 N92-26333
A simple model for the convective boundary layer over wavy terrain with variable heat flux p 2934 N92-26334
Investigation of convection over sea by aircraft observations p 2926 N92-26337
Description of a global shallow water model based on the spectral transform method
[PB92-155258] p 2928 N92-26352
Ocean bottom modeling for ray acoustics
[AD-A246287] p 2948 N92-26360
Composite strength statistics from fiber strength statistics
[AD-A245616] p 2867 N92-26383
Hindcast wave information for the Great Lakes: Lake Huron. Wave information studies of US coastlines
[AD-A246326] p 2949 N92-26387
Acoustic interactions between an altitude test facility and jet engine plumes: Theory and experiments
[NASA-CR-190423] p 2853 N92-26405
Effect of gyro noise on ADKEM gyro-only missile system performance
[AD-A246150] p 2852 N92-26408
Parameterization of water-soluble component of aerosol particles in numerical cloud models
[NASA-CR-190225] p 2945 N92-26474
Compressive damage and fracture modeling of ceramic subjected to high-velocity impact p 2881 N92-26492
Fundamental mechanisms affecting friction welding under vacuum
[AD-A245685] p 2877 N92-26520
Polarisation effects in fibre lasers p 2911 N92-26571
Analysis of EMP response of structures using frequency domain electromagnetic interaction codes
[AD-A245758] p 2889 N92-26592
Dimensional analysis of structural steel beam design
[AD-A245759] p 2917 N92-26593
Computational aspects of an implicit finite element procedure for elasto-viscoplastic large deformation problems p 2917 N92-26594
Parameter robust reduced-order control of flexible structures p 2982 N92-26597
Mixed Weibull distributions in reliability engineering: Statistical models for the lifetime of units with multiple modes of failure p 2916 N92-26602
Mesomechanics of viscoplastic metal matrix composites p 2869 N92-26607
Optimization of space structures to minimize dynamic response p 2858 N92-26610
Theoretical and numerical study of flame propagation and transition to detonation --- detonation transition p 2874 N92-26615
A modeling strategy for large-scale optimization based on analysis and visualization principles
[AD-A246570] p 2987 N92-26620
Computer modeling of human decision making
[NASA-TM-107868] p 2983 N92-26630
Use of the Edmonds-Reilly Model to model energy-related greenhouse gas emissions
[DE92-010035] p 2931 N92-26633
Retention and release of tritium in aluminum clad, Al-Li alloys
[DE92-009905] p 2878 N92-26635
Numerical formulation for the prediction of solid/liquid change of a binary alloy
[NASA-CR-188468] p 2878 N92-26642
Computational techniques in tribology and material science at the atomic level
[NASA-TM-105573] p 2990 N92-26671
A one-dimensional temperature model for a snow cover: Technical documentation for SNTHERM.89
[AD-A245493] p 2922 N92-26674
Evaluation of the computational validity of the image model in predicting the sound field in a wedge-shaped layer using acoustical reciprocity
[AD-A246548] p 2992 N92-26688
Transient gas motion in nuclear-reactor-pumped lasers: Computational and experimental results
[DE92-002357] p 2912 N92-26691
Experiences in using C++ to develop a next generation strong shock wave physics code
[DE92-006675] p 2976 N92-26696
Validation of numerical models by TRMM and validation of TRMM by numerical models
[TW-8] p 2923 N92-26709
Rainfall pattern over the tropical rain forest
[TW-10] p 2923 N92-26711
Research plan for utilizing TRMM data in MRI --- tropical rainfall measuring mission
[TW-13] p 2924 N92-26714
An experimental investigation of high-speed water entry for full size and scale-model pointed nose vehicle
[DE92-004363] p 2899 N92-26716
Estimation of geopotential differences over intercontinental locations using satellite and terrestrial measurements p 2924 N92-26728
Experiments in modelling and end-point control of two-link flexible manipulators p 2915 N92-26731
Forging a path with tool and data attributes
[DE92-009800] p 2976 N92-26797
Assessment of computer models for estimating vehicle emission factors. Volume 1: Executive summary
[PB92-113059] p 2931 N92-26802
Dielectric tensor of strongly coupled plasmas
[DE92-621524] p 3001 N92-26807
Numerical modeling of silicon photodiodes for high-accuracy applications with PC-1D
[PB92-148279] p 2894 N92-26821
Evaluation of carbon dioxide emission control strategies in New York State
[DE92-010162] p 2932 N92-26825
Finite element modeling of static indentation damage in laminated composites p 2869 N92-26827
On the evaluation of the U(3) content of the matrix elements of 1- and 2-body operators
[DE92-621113] p 2988 N92-26837
Comparison of laser models
[NASA-CR-190302] p 2913 N92-26870
Description of the Rayflux ray tracing program and comparison with other models and measurements
[AD-A245413] p 2944 N92-26877
Homogenization models for 2-D grid structures
[NASA-CR-190321] p 2920 N92-26892
Modelling default and likelihood reasoning as probabilistic
[NASA-TM-107889] p 2984 N92-26893
Bayesian classification theory
[NASA-TM-107885] p 2988 N92-26894
Numerical field model simulation of full-scale fire tests in a closed spherical/cylindrical vessel using advanced computer graphics techniques
[AD-A245810] p 2887 N92-26898
An anisotropic homologous model for the core-collapse in star clusters
[ETN-92-90826] p 3018 N92-26946
Unified computational method for design of fluid loop systems p 2905 N92-26962
Heat pipe-based radiative panel p 2859 N92-26968
Development of a thermal control concept for the optical system of the SUMER experiment on SOHO p 2960 N92-26975
Modelling light transfer inside photobiofermentors: Applications to the photosynthetic compartments of CELSS p 2952 N92-26982
Thermal analysis of evaporative coolers p 2962 N92-26985
Thermo-hydraulic investigations on heat exchangers for Columbus hybrid radiators p 2887 N92-26988
Italsat thermal control: The in-orbit performances p 2859 N92-26996
ROSAT: Measured temperatures versus thermal analysis results p 2859 N92-26997
Ulysses, one year after the launch p 2860 N92-26999
Thermal implications from the Hubble Space Telescope solar array bi-stem boom in-orbit disturbance p 2965 N92-27001
X ray observations of gamma ray burst sources
[MPE-PREPRINT-174] p 3018 N92-27048
The changing role of experimentation in aeroengine R and D: The point of view of the research worker
[AD-A246372] p 2856 N92-27062
Modeling for improved minimum resolvable temperature difference measurements
[AD-A246389] p 2991 N92-27078
Modeling 3-D objects with planar surfaces for prediction of electromagnetic scattering
[NASA-TM-107598] p 2891 N92-27189
MATRICES (MATHEMATICS)
On the evaluation of the U(3) content of the matrix elements of 1- and 2-body operators
[DE92-621113] p 2988 N92-26837
MATTER (PHYSICS)
Supersymmetry and dark matter, a new candidate p 3016 N92-26491
MAXIMUM ENTROPY METHOD
A Bayes-Maximum Entropy method for multi-sensor data fusion
[DE92-000680] p 2983 N92-26657
MAXIMUM LIKELIHOOD ESTIMATES
A refined maximum likelihood method for tracking low-altitude targets over the sea: Results of simulation and experiments
[AD-A246534] p 2888 N92-26419
Mixed Weibull distributions in reliability engineering: Statistical models for the lifetime of units with multiple modes of failure p 2916 N92-26602
Modelling default and likelihood reasoning as probabilistic
[NASA-TM-107889] p 2984 N92-26893
Stochastic versions of the EM algorithm
[AD-A246929] p 2989 N92-27174
MEASUREMENT
A high-resolution neutron powder diffraction study in high-T(sub c) superconductor YBa2Cu3O7 p 3002 N92-26326
Aircraft observation of a small-scale solitary wave near the tropopause p 2940 N92-26336
Measurements in the inhomogeneous convective boundary layer using three powered gliders p 2942 N92-26350
Measurements of scattering processes in negative ion-atom collisions
[DE92-010319] p 2995 N92-26574
MECHANICAL PROPERTIES
Simulation studies for surfaces and materials strength
[NASA-CR-190340] p 3001 N92-26265
Composite strength statistics from fiber strength statistics
[AD-A245616] p 2867 N92-26383
Comparison of ceramic uniaxial compression specimens through detailed finite element modelling
[AD-A245816] p 2882 N92-26609
Analysis of Yttrium-Barium-Copper-Oxide by x ray diffraction and mechanical characterization
[NASA-TM-104562] p 2869 N92-26650

Study and analysis of the stress state in a ceramic, button-head, tensile specimen
[DE92-007794] p 2918 N92-26784
Modeling cycle and time-dependent creep/relaxation effects on fatigue lives of notched members --- creep/relaxation p 2919 N92-26829
Ceramic composites: Experimental and analytical study of SiC/Si3N4 composites p 2882 N92-26859
Systems special investigation group overview p 2867 N92-27084

MEDICAL PERSONNEL
Adverse reproductive events and electromagnetic radiation
[PB92-145796] p 2953 N92-26512

MEDICAL SCIENCE
The study on a directory of human performance models for system design (Defence Research Group Panel 8 on the defence applications of human and bio-medical sciences)
[AD-A247346] p 2970 N92-27179

MEDICAL SERVICES
Clinical investigation program, fiscal year 1991
[AD-A246558] p 2992 N92-26618

MELTING
The effect of global change and long period tides on the Earth's rotation and gravitational potential p 2925 N92-26781

MELTS (CRYSTAL GROWTH)
Recent results in characterization of melt-grown and quench-melt-grown YBCO superconductors
[DE92-010281] p 3001 N92-26210

MEMBRANE STRUCTURES
Reaction/separation process for enhanced methane conversion
[PB92-149657] p 2873 N92-26508

MEMBRANES
Photochemical energy conversion by membrane-bound photoredox systems
[DE92-008709] p 2927 N92-26858

MEMORY (COMPUTERS)
Algorithms for capacity computations and algebraic cascade coding with applications to data storage p 2977 N92-27053

MENTAL PERFORMANCE
MoCog1: A computer simulation of recognition-primed human decision making
[NASA-TM-107872] p 2984 N92-26888

MERCURY AMALGAMS
Examination of the discharge mechanism of Li/CF(x) cells: Comparison of the electrochemical reduction mechanisms of PTFE and (CF(x))n by lithium p 2865 N92-27151

MERIDIONAL FLOW
Meridional zonation of the Barents Sea ecosystem inferred from satellite remote sensing and in situ bio-optical observations
[AD-A246323] p 2948 N92-26245

MESOMETEOROLOGY
The objective determination of front lines p 2941 N92-26343

MESON-MESON INTERACTIONS
Interpretation of distributions on K(sub pi)(sup 0) in pFe, nFe, and piFe interactions at 0.5-5.0 TeV in the framework of contemporary models
[DE92-621189] p 3021 N92-26804

MESON-NUCLEON INTERACTIONS
New description of multiplicity distribution in inelastic meson-proton interactions
[DE92-621167] p 2995 N92-26800

MESOSCALE PHENOMENA
Noxious matter transportation in the Alpine regions p 2934 N92-26332
Comparison of frontogenetical structures for different cases of frontal development p 2939 N92-26333
Mesoscale observations of a cold front associated with a prefrontal hailstorm p 2940 N92-26338
The objective determination of front lines p 2941 N92-26343
Estimating mesoscale, orographically enhanced precipitation using synoptic scale data
[AD-A245749] p 2946 N92-26562
Documentation for the Semi-Automated Mesoscale Analysis System 1.1
[AD-A246144] p 2985 N92-27072

MESSAGE PROCESSING
Mesh and torus chaotic routing (updated version)
[AD-A246284] p 2979 N92-26359
Expert system management system
[AD-A247102] p 3009 N92-26863

METABOLISM
Carbon monoxide metabolism by the photosynthetic bacterium Rhodospirillum rubrum
[DE92-010953] p 2951 N92-26938

METABOLITES
Study of hydrazine metabolism and toxicity
[AD-A245755] p 2884 N92-26589

METAL COMPOUNDS
Magnetic anisotropy from first principles
[ISBN-90-9004483-3] p 2877 N92-26252

METAL FATIGUE
Predictability of long-term creep and rupture in a nozzle-to-sphere vessel model
[DE92-008099] p 2919 N92-26845

METAL FIBERS
Application of neutron diffraction to measure residual strains in high temperature composites
[DE91-014021] p 2869 N92-26679

METAL FILMS
Selective metallization of carbonyl-containing polymer films
[AD-D015219] p 2883 N92-27187

METAL FOILS
Failure studies of bimaterial interfaces and constrained ductile layers p 2868 N92-26559

METAL HYDRIDES
Aging effects in palladium and LaNi(4.25)Al(0.75) tritides
[DE92-009945] p 2870 N92-26217
Metal hydride based isotope separation: Large-scale operations
[DE92-009830] p 2875 N92-26717
A new phase in palladium hydride technology
[DE92-009852] p 2875 N92-26718
Accelerated cycle life performance for ovonic nickel-metal hydride cells p 2865 N92-27155
Low cost battery designs for small satellite applications p 2866 N92-27160

METAL IONS
Application of in situ x ray absorption and fluorescence measurements to analyze solutions in a simulated pit
[DE92-009159] p 2878 N92-26563
Polarisation effects in fibre lasers p 2911 N92-26571
High-yield hydrogen production by catalytic gasification of coal or biomass
[DE92-008770] p 2875 N92-26724
The application of XPS to the study of MIC
[DE92-010156] p 2879 N92-26813
Recent developments in nickel electrode analysis p 2865 N92-27158

METAL MATRIX COMPOSITES
Advanced materials aspects of concurrent engineering
[AD-A245437] p 2880 N92-26275
Effect of thermal residual stresses on the stress-strain behavior of metal-matrix composites
[AD-A246136] p 2868 N92-26386
Mesomechanics of viscoplastic metal matrix composites p 2869 N92-26607
Application of neutron diffraction to measure residual strains in high temperature composites
[DE91-014021] p 2869 N92-26679

METAL OXIDE SEMICONDUCTORS
Quantum interference and confinement effects in narrow channel Si-MOSFET's
[PB92-150176] p 3006 N92-26927

METAL OXIDES
Metal oxide absorbents for regenerative carbon dioxide and water vapor removal for advanced portable life support systems p 2968 N92-27021
Complementary metal oxide silicon cyclic redundancy check generators
[AD-A246140] p 2894 N92-27061

METAL PLATES
Crack arrest and static fracture toughness tests of a ship plate steel
[AD-A245641] p 2916 N92-26282
Energy threshold for laser induced breakdown on a metal surface under high and ultra high vacuum conditions
[AD-A246212] p 2911 N92-26462

METAL POWDER
Neutron powder diffraction study on Eu-substituted Bi2Sr2CaCu2O(8+y) high temperature superconductor p 3003 N92-26328
Spheroidization and densification of Nickel powders by RF-induction plasma
[PB92-151893] p 2879 N92-26787
Powder processing of aero-engine components
[PNR-90813] p 2880 N92-27044

METAL PROPELLANTS
Solid fuel ramjet infrared signature
[AD-A246299] p 2860 N92-26362

METAL SURFACES
Cluster model of polarization reflection from metallic surfaces
[AD-A245781] p 2996 N92-26241
Energy threshold for laser induced breakdown on a metal surface under high and ultra high vacuum conditions
[AD-A246212] p 2911 N92-26462
Computational techniques in tribology and material science at the atomic level
[NASA-TM-105573] p 2990 N92-26671
The application of XPS to the study of MIC
[DE92-010156] p 2879 N92-26813
Selective metallization of carbonyl-containing polymer films
[AD-D015219] p 2883 N92-27187

METAL VAPORS
Spontaneous and induced coherent radiation generation in atomic vapors
[AD-A246078] p 2890 N92-26764

METAL-METAL BONDING
Microwelding (or cold-welding) of various metallic materials under the ultra-vacuum LDEF experiment AO 138-10 p 2880 N92-27119

METALLICITY
A self-contamination model for the formation of globular star clusters p 3018 N92-26723
The galactic evolution of s-process elements via asymptotic giant branch stars p 3018 N92-26725

METALLIZING
RF vacuum microelectronics
[AD-A246579] p 2893 N92-26771
Selective metallization of carbonyl-containing polymer films
[AD-D015219] p 2883 N92-27187

METALORGANIC CHEMICAL VAPOR DEPOSITION
Investigation of kinetics of MOCVD systems
[AD-A246090] p 2893 N92-26540

METALS
The use of ion chromatography-dc plasma atomic emission spectrometry for the speciation of trace metals
[DE92-010317] p 2871 N92-26236

METEORITIC DAMAGE
Long Duration Exposure Facility (LDEF) low-temperature heat pipe experiment package power system results p 2906 N92-27105

METEOROID PROTECTION
EVA space suit thermal control and micrometeoroid protection p 2965 N92-27004

METEOROLOGICAL CHARTS
Climate research at regional climate centers in 1991
[PB92-160399] p 2946 N92-26822

METEOROLOGICAL INSTRUMENTS
The DLR meteorological research aircraft Falcon p 2941 N92-26348
On the subject of geometric spacing of meteorological sensors
[AD-A245824] p 2946 N92-26899

METEOROLOGICAL PARAMETERS
Integrating wind profiler data into forecast and warning operations at NWS field offices
[PB92-146075] p 2945 N92-26514
Atmospheric parameters of a soft x ray selected set of hot DA white dwarfs p 3017 N92-26576
The impact of climate upon variation in air pollution using a synoptic climatological approach p 2931 N92-26590
International Conference on Japanese Earth Observation Programs: TRMM Workshop
[JTN-92-80345] p 2922 N92-26701
Status of TRMM project: Rain radar in the Tropical Rainfall Measuring Mission
[TW-2] p 2922 N92-26703
TRMM Mission Team --- tropical rainfall measuring mission
[TW-4] p 2923 N92-26705
TRMM and Asian monsoon --- tropical rainfall measuring mission
[TW-12] p 2924 N92-26713
Research plan for utilizing TRMM data in MRI --- tropical rainfall measuring mission
[TW-13] p 2924 N92-26714
Improved procedures for quantifying key meteorological effects on ambient ozone data
[PB92-163278] p 2931 N92-26793
Monthly mean global satellite data sets available in CCM history tape format
[NASA-CR-190344] p 2933 N92-26878
Report of the CC1 experts meeting on tracking and transmission of climate system monitoring information
[WCDMP-16] p 2947 N92-26925
High frequency analyses of coastal meteorological phenomena affecting refractivity
[AD-A246383] p 2947 N92-27075

METEOROLOGICAL RADAR
International Conference on Japanese Earth Observation Programs: TRMM Workshop
[JTN-92-80345] p 2922 N92-26701
Status of TRMM project: Rain radar in the Tropical Rainfall Measuring Mission
[TW-2] p 2922 N92-26703
Status of TRMM (NASDA) --- tropical rainfall measuring mission
[TW-3] p 2923 N92-26704

METEOROLOGICAL SERVICES
Climate research at regional climate centers in 1991
[PB92-160399] p 2946 N92-26822

METEOROLOGY
Atmospheric environment for Space Shuttle Columbia (STS-40) launch
[NASA-TM-103585] p 2945 N92-26288
Remote sensing of atmosphere with aircraft borne lidar systems p 2941 N92-26347
Improved procedures for quantifying key meteorological effects on ambient ozone data
[PB92-163278] p 2931 N92-26793
CC1 experts meeting on CLIMAT code adaptation
[WCDMP-15] p 2947 N92-26924
METHANE
Low temperature electrochemical activation of methane
[PB92-152917] p 2872 N92-26351
Reaction/separation process for enhanced methane conversion
[PB92-149657] p 2873 N92-26508
Enhance methane reactivity
[PB92-154822] p 2873 N92-26516
Rule-based expert system for evaluating the quality of long-term, in-situ, gas chromatographic measurements of atmospheric methane
[PB92-128560] p 2876 N92-26812
METHOD OF MOMENTS
Dynamic properties of quasi-two-dimensional one component plasmas
[DE92-621523] p 3000 N92-26806
METHYL ALCOHOL
Reaction/separation process for enhanced methane conversion
[PB92-149657] p 2873 N92-26508
Enhance methane reactivity
[PB92-154822] p 2873 N92-26516
A novel process for methanol synthesis
[DE92-010465] p 2883 N92-26547
High octane ethers from synthesis gas-derived alcohols
[DE92-010480] p 2884 N92-26548
Technology for reduction of CO2 emissions from the transportation sector
[PB92-153733] p 2933 N92-26929
METHYL COMPOUNDS
Synthesis of novel fluorinated phosphonic acid electrolytes for phosphoric acid fuel cells
[PB92-164300] p 2926 N92-26372
METRIC SPACE
Hyperspaces of infinite-dimensional compacta
[PB92-149335] p 2986 N92-26367
Finite temperature quantum field theory in curved spacetime p 3007 N92-26780
MICHELSON INTERFEROMETERS
Fiber-optic flexural disk accelerometer
[AD-A246203] p 2908 N92-26459
An infrared Michelson stellar interferometer and its applications p 3015 N92-26477
Optical flow sensor
[AD-D015200] p 2997 N92-26862
MICROCOMPUTERS
Microcomputer-based instrument flight simulation: Undergraduate pilot training student attitude assessment
[AD-A245449] p 2856 N92-26527
MICROELECTRONICS
The development of a model builder for a microcircuit substrate
[AD-A245765] p 2893 N92-26606
RF vacuum microelectronics
[AD-A246579] p 2893 N92-26771
Fracture of structural ceramics in combined mode 1 and mode 2 loading p 2882 N92-26775
MICROGRAVITY APPLICATIONS
Microwelding (or cold-welding) of various metallic materials under the ultra-vacuum LDEF experiment AO 138-10 p 2880 N92-27119
Microgravity combustion science: Progress, plans, and opportunities
[NASA-TM-105410] p 2886 N92-27197
MICROMETEOROIDS
Evaluation of LDEF experiment S1002 p 2883 N92-27102
Long Duration Exposure Facility (LDEF) low-temperature heat pipe experiment package power system results p 2906 N92-27105
MICROORGANISMS
Application of irradiation techniques to food and foodstuffs
[DE92-614952] p 2954 N92-26186
Biodegradation studies with space cabin contaminants to determine the feasibility of Biological Air Filtration (BAF) in space cabins p 2962 N92-26983
MICROSCOPY
Spectroscopic imaging, diffraction, and holography with x ray photoemission
[DE92-009142] p 2996 N92-26187
MICROSTRUCTURE
Microstructural evaluation of as-solidified and heat treated gamma-TiAl based powders
[DE92-008956] p 2881 N92-26455
Mesomechanics of viscoplastic metal matrix composites p 2869 N92-26607
Factors influencing the microstructural and mechanical properties of ULCB steel weldments
[AD-A245523] p 2878 N92-26659
An investigation of the mechanical properties and microscopic structure of extruded powder aluminum subjected to biaxial loadings at elevated temperature p 2879 N92-26770
The production and properties of melt-zone textured Y1Ba2Cu3O(7-delta) filaments
[DE92-008097] p 3005 N92-26843
Development of a microstructural-related description for the high temperature stress-strain behaviour of the turbine blade material IN 738 LC
[JUEL-2466] p 2880 N92-26945
MICROWAVE ABSORPTION
Laboratory evaluation and application of microwave absorption properties under simulated conditions for planetary atmospheres
[NASA-CR-190211] p 3019 N92-26438
MICROWAVE AMPLIFIERS
Transportable 5 MW power supply system for gyrotron operation
[DE92-009051] p 2892 N92-26224
Diagnostic upgrades on MTX
[DE92-009695] p 2906 N92-26230
Installation and operation of the 400 kW 140 GHz gyrotron on the MTX experiment
[DE92-009053] p 2906 N92-26377
MICROWAVE EQUIPMENT
Photovoltaic manufacturing technology, phase 1
[DE92-001199] p 2926 N92-26190
MICROWAVE OSCILLATORS
Measurement electronics of industrial microwave resonator sensors
[PB92-152750] p 2909 N92-26786
MICROWAVE RADIOMETERS
User's guide to WPL microwave radiative transfer software
[PB92-129931] p 2890 N92-26809
MICROWAVE RESONANCE
Measurement electronics of industrial microwave resonator sensors
[PB92-152750] p 2909 N92-26786
MICROWAVE SCATTERING
Microwave backscattering fuel/air ratio control and flame monitoring device
[PB92-141779] p 2876 N92-26783
MICROWAVE SENSORS
Measurement electronics of industrial microwave resonator sensors
[PB92-152750] p 2909 N92-26786
MICROWAVE TUBES
Operation of a Smith-Purcell free-electron laser at submillimeter wavelengths p 2912 N92-26626
MICROWAVES
User's guide to WPL microwave radiative transfer software
[PB92-129931] p 2890 N92-26809
Research and technology, 1990: Goddard Space Flight Center
[NASA-TM-107792] p 3022 N92-26824
MIDDLE ATMOSPHERE
Tracer transport in the middle atmosphere p 2928 N92-26473
Studies of inertio-gravity waves induced by geostrophic adjustment of the atmospheric jet stream p 2944 N92-26866
MILITARY AIRCRAFT
A prototype semantic integrity front end expert system for a relational database
[AD-A246084] p 3013 N92-26765
MILITARY HELICOPTERS
A modeling strategy for large-scale optimization based on analysis and visualization principles
[AD-A246570] p 2987 N92-26620
MILITARY OPERATIONS
Apogee, perigee, and recovery: Chronology of Army exploitation of space
[RAND-N-3103-A] p 2856 N92-26192
The role of the B-2 in the new US defense strategy
[RAND-P-7744] p 2990 N92-26194
MILITARY TECHNOLOGY
Executive summary of the technical proceedings on Military Information System Engineering (Defence Research Group Panel 11 on Information Processing Technology)
[AD-A245656] p 3010 N92-26174
Apogee, perigee, and recovery: Chronology of Army exploitation of space
[RAND-N-3103-A] p 2856 N92-26192
The Department of Defense critical technologies plan for the Committees on Armed Services, United States Congress
[AD-A234900] p 3010 N92-27190
MINIMAX TECHNIQUE
Bias robust estimation of scale
[AD-A245698] p 2985 N92-26229
Using min-max of torque to resolve redundancy for a mobile manipulator
[DE92-000070] p 2915 N92-26750
MIR SPACE STATION
Water recovery from condensate of crew respiration products aboard the Space Station p 2956 N92-26951
Water reclamation from urine aboard the Space Station p 2957 N92-26952
Hygiene water recovery aboard the Space Station p 2957 N92-26955
MIRRORS
High-speed pulse detection room-temperature optical nonlinearities for GaInAs/A1InAs and GaA1InAs/A1InAs multiple quantum wells and integrated mirror etalon at 1.3 micrometers
[AD-A246369] p 2998 N92-26943
Space environmental effects on coated optics p 2999 N92-27098
MISALIGNMENT
Dynamic restoration mechanisms in Al-5.8 at. percent Mg deformed to large strains in the solute drag regime
[DE92-009529] p 2877 N92-26223
Ceramic composites: Experimental and analytical study of SiC/Si3N4 composites p 2882 N92-26859
MISSILE DETECTION
The state of multiple sensor, multiple target tracking in ballistic missile defense
[AD-A245433] p 2850 N92-26272
MISSILE SYSTEMS
Effect of gyro noise on ADKEM gyro-only missile system performance
[AD-A246150] p 2852 N92-26408
MISSILE TRACKING
The state of multiple sensor, multiple target tracking in ballistic missile defense
[AD-A245433] p 2850 N92-26272
MISSILES
Spinning jets from shaped charges with flow turned liners
[MBB-UA-1197-90-PUB] p 2886 N92-26246
Effect of gyro noise on ADKEM gyro-only missile system performance
[AD-A246150] p 2852 N92-26408
MISSION PLANNING
The Tropical Rainfall Measuring Mission (TRMM) program at the Goddard Space Flight Center (GSFC)
[TW-1] p 2922 N92-26702
MIXED OXIDES
Recent results in characterization of melt-grown and quench-melt-grown YBCO superconductors
[DE92-010281] p 3001 N92-26210
Percolation effects in the V-I characteristics of granular YBa2Cu3O(7-delta)
[DE92-617541] p 3004 N92-26672
MIXING
Diapycnal mixing, gravity-current propagation, and sediment dispersion in turbulent fluids
[AD-A246160] p 2896 N92-26412
MIXING LAYERS (FLUIDS)
The composite structure of thermals as derived from aircraft observations p 2941 N92-26346
Fine scale structure of conserved scalar mixing in turbulent shear flows: Sc much greater than 1 and Sc approximately equal to 1 p 2899 N92-26740
MODELS
Reference model for frameworks of software engineering environments
[PB92-158328] p 2973 N92-26370
The development of a model builder for a microcircuit substrate
[AD-A245765] p 2893 N92-26606
Integrated heat pipe concept for Li/SOCl2 cells cooling p 2895 N92-26974
Model compilation: An approach to automated model derivation
[NASA-TM-107895] p 2985 N92-27057
MODULES
Principal investigator in a box: Version 1.2 documentation
[NASA-TM-107886] p 2982 N92-26628
Utilization of a bipolar lead acid battery for the advanced launch system p 2865 N92-27157
MOISTURE
Study of entrainment mechanisms in convective clouds
[NASA-CR-190223] p 2946 N92-26735

MOISTURE CONTENT
The icing of the wing upper side and bottom side of the icing research aircraft of the DLR
p 2850 N92-26349
Measurement electronics of industrial microwave resonator sensors
[PB92-152750] p 2909 N92-26786
MOJAVE DESERT (CA)
Radar scattering as a source of geological information on Venus and Earth p 3019 N92-26778
MOLECULAR ABSORPTION
Vibrational dynamics of aniline (N2)1 clusters in their first excited singlet state
[AD-A245812] p 2872 N92-26431
MOLECULAR BEAM EPITAXY
Innovative techniques for the production of low cost 2D laser diode arrays
[AD-A247282] p 2913 N92-27178
MOLECULAR BIOLOGY
Life sciences and environmental sciences
[DE92-010254] p 2950 N92-26203
MOLECULAR CHAINS
Static, microwave, infrared, and visible permittivity related to chemical structure: N-methylacetamide, N-dimethylacetamide and their mixtures in CCl4 at 32 C
[AD-A246364] p 2991 N92-26940
MOLECULAR COLLISIONS
Energy transfer properties and mechanisms
[DE92-011215] p 2994 N92-26240
MOLECULAR ENERGY LEVELS
The computation of C-C and N-N bond dissociation energies for singly, doubly, and triply bonded systems
[NASA-CR-190254] p 2994 N92-26539
MOLECULAR EXCITATION
Solvation effects on the electronic structure of 4-N,N-Dimethylaminobenzonitrile: Mixing of the local pipi* and charge transfer states
[AD-A245814] p 2874 N92-26608
MOLECULAR GASES
An analysis of middle ultraviolet emissions of molecular nitrogen and nitric oxide and vacuum calibration of an ultraviolet spectrograph
[AD-A245984] p 2943 N92-26753
MOLECULAR STRUCTURE
Bis (pentamethylcyclopentadienyl) ytterbium: Electron-transfer reactions with organotransition metal complexes
[DE92-010300] p 2994 N92-26235
Quantum dynamics of helium clusters
[AD-A245752] p 2995 N92-26588
A surface science investigation of silicon carbide: Oxidation, crystal growth and surface structural analysis
[DE92-010286] p 3004 N92-26641
MOLECULES
Laser cooling and trapping of atoms and particles
[AD-A247208] p 2913 N92-27173
MOLYBDENUM
Calorimetric particle detectors with superconducting absorber materials p 2907 N92-26393
MOMENTS OF INERTIA
Adaptive control of robotic manipulators with structural flexibility p 2914 N92-26475
New approaches to studies of exotic nuclei
[DE92-010127] p 2994 N92-26570
MOMENTUM TRANSFER
Quasi-elastic nuclear scattering at high energies
[NASA-TM-4362] p 2996 N92-26832
MONATOMIC GASES
Measurements of scattering processes in negative ion-atom collisions
[DE92-010319] p 2995 N92-26574
MONITORS
Technology transfer and application of SERS continuous monitor for trace organic compounds
[DE92-008900] p 2875 N92-26726
Microwave backscattering fuel/air ratio control and flame monitoring device
[PB92-141779] p 2876 N92-26783
Report of the CC1 experts meeting on tracking and transmission of climate system monitoring information
[WCDMP-16] p 2947 N92-26925
MONOCHROMATORS
Design of a high-precision tunable double crystal monochromator
[DE92-010137] p 2909 N92-26572
MONSOONS
TRMM and Asian monsoon --- tropical rainfall measuring mission
[TW-12] p 2924 N92-26713
MONTE CARLO METHOD
Muon/electron separation for atmospheric neutrino interactions
[DE92-010349] p 3021 N92-26218
Bias robust estimation of scale
[AD-A245698] p 2985 N92-26229
Effect of gyro noise on ADKEM gyro-only missile system performance
[AD-A246150] p 2852 N92-26408
A refined maximum likelihood method for tracking low-altitude targets over the sea: Results of simulation and experiments
[AD-A246534] p 2888 N92-26419
Dynamics of neutron stars and binaries in globular clusters or, menages a trois: Revitalizing burnt out degenerates through partner swapping
p 3017 N92-26522
A user's manual for MASH 1.0: A Monte Carlo adjoint shielding code system
[DE92-010375] p 3021 N92-26544
Mixed Weibull distributions in reliability engineering: Statistical models for the lifetime of units with multiple modes of failure p 2916 N92-26602
On increasing the capabilities of the SMART adaptive random number generator
[DE92-621106] p 2976 N92-26835
Stochastic versions of the EM algorithm
[AD-A246929] p 2989 N92-27174
MORPHOLOGY
Fundamental studies of the chemical vapor deposition of diamond
[DE92-010327] p 2881 N92-26543
Architectural studies relating to human body motion morphology in microgravity p 2953 N92-27011
Influence of substrate topography on the nucleation of diamond thin films
[DE92-010777] p 2883 N92-27060
MOTION SICKNESS
Critical technologies: Spacecraft habitability, an update
p 2966 N92-27010
MOTION SIMULATION
Description of a global shallow water model based on the spectral transform method
[PB92-155258] p 2928 N92-26352
MOTOR VEHICLES
Assessment of computer models for estimating vehicle emission factors. Volume 1: Executive summary
[PB92-113059] p 2931 N92-26802
Assessment of computer models for estimating vehicle emission factors. Volume 2: Description and comparison of the MOBILE4 and EMFAC7E models
[PB92-113067] p 2932 N92-26803
Technology for reduction of CO2 emissions from the transportation sector
[PB92-153733] p 2933 N92-26929
MULTIGRID METHODS
Cell vertex methods for compressible gas flows
p 2897 N92-26599
MULTILAYER INSULATION
Development of a thermal control concept for the optical system of the SUMER experiment on SOHO
p 2960 N92-26975
MULTIPATH TRANSMISSION
A refined maximum likelihood method for tracking low-altitude targets over the sea: Results of simulation and experiments
[AD-A246534] p 2888 N92-26419
MULTIPHASE FLOW
Application of fluorescent-particle imaging to measuring flow in complex media
[DE92-009121] p 2898 N92-26645
MULTIPHOTON ABSORPTION
Energy transfer properties and mechanisms
[DE92-011215] p 2994 N92-26240
Multiquanta photodetachment from the H(-) ion
[DE92-010306] p 2911 N92-26573
MULTIPLE TARGET TRACKING
The state of multiple sensor, multiple target tracking in ballistic missile defense
[AD-A245433] p 2850 N92-26272
MULTIPROCESSING (COMPUTERS)
Scalable coherent interface: Links to the future
[DE92-010728] p 2887 N92-26267
Modeling node bandwidth limits and their effects on vector combining algorithms
[DE92-010829] p 2979 N92-26277
Mesh and torus chaotic routing (updated version)
[AD-A246284] p 2979 N92-26359
Reconfiguration in robust distributed real-time systems based on global checkpoints
[AD-A245615] p 2970 N92-26382
Expert system management system
[AD-A247102] p 3009 N92-26863
Software architecture for a distributed real-time system in Ada, with application to telerobotics
[NASA-TM-4367] p 2977 N92-26904
MULTISENSOR APPLICATIONS
A Bayes-Maximum Entropy method for multi-sensor data fusion
[DE92-000680] p 2983 N92-26657
MULTISPECTRAL BAND CAMERAS
Description of the multispectral CCD-camera
[AD-A245681] p 2908 N92-26517
MULTISPECTRAL BAND SCANNERS
Analysis of thermal infrared data acquired over playas: Silver Lake and Deep Springs Lake, California and Lunar Lake, Nevada p 2926 N92-26864
MULTISTATIC RADAR
Large coherent arrays for laser radars, phase 1
[AD-A245528] p 2912 N92-26663
MULTIVARIATE STATISTICAL ANALYSIS
A computational analysis of properties and limitations of neural networks: Toward new parallel architectures for learning
[AD-A246156] p 2981 N92-26410
Studies in chaos using stochastic methods
[AD-A246919] p 3008 N92-27171
On the construction of multivariate (pre)wavelets
[AD-A247105] p 2989 N92-27175
MUONS
Simultaneous observations of extensive air showers and underground muons at Soudan 2
[DE92-010282] p 3020 N92-26211
Underground muons from the direction of Cygnus X-3 during the January 1991 radio flare
[DE92-010346] p 3021 N92-26215
A search for magnetic monopoles with the Soudan 2 detector
[DE92-010347] p 3021 N92-26216
Composition studies based on coincident air shower array and underground muon data
[DE92-010345] p 3021 N92-26253
Underground muons observed in the Soudan 2 detector from the directions of x ray sources
[DE92-010344] p 3021 N92-26264
MUSCULAR STRENGTH
The validation of a human force model to predict dynamic forces resulting from multi-joint motions
[NASA-TP-3206] p 2956 N92-26538
MUTATIONS
Space Exposed Experiment Developed for Students (SEEDS) (P0004-2) p 2952 N92-27121

N

NASA PROGRAMS
Space life sciences strategic plan, 1991
[NASA-TM-107856] p 2950 N92-26266
COSMIC software catalog, 1992 edition
[NASA-CR-188973] p 2977 N92-26868
The 1990 progress report and future plans
[NASA-TM-107911] p 2984 N92-26887
NASA patent abstracts bibliography: A continuing bibliography. Section 2: Indexes (supplement 40)
[NASA-SP-7039(40)-SECT-2] p 3014 N92-27081
NASA/DoD Aerospace Knowledge Diffusion Research Project: An initial investigation into the production and use of Scientific and Technical Information (STI) at 5 NASA centers. Results of a telephone survey
[NASA-TM-104173] p 3014 N92-27170
NATIONAL AEROSPACE PLANE PROGRAM
An experimental investigation of a 2-D scramjet inlet at flow Mach numbers of 8 to 25 and stagnation temperatures of 800 to 4,100 K p 2854 N92-26586
NATURAL GAS
Turbocharged pressurized combustion system
[PB92-142579] p 2873 N92-26521
Advancing natural gas combustion science and technology-low NOx
[PB92-137652] p 2876 N92-26782
Microwave backscattering fuel/air ratio control and flame monitoring device
[PB92-141779] p 2876 N92-26783
Development of natural gas rotary engines
[PB92-149665] p 2915 N92-26816
NAVIER-STOKES EQUATION
Proceedings of the 5th and 6th Seminars on Investigation and Control of Boundary-Layer Transition
[NAL-SP-12] p 2901 N92-26906
NAVIGATION
A supervisory control strategy for navigation of mobile robots in dynamic environments p 2983 N92-26734
NAVIGATION AIDS
Time optimal trajectories for mobile robots with two independently driven wheels
[DE92-010002] p 2913 N92-26219
The navigation data logger for a suitcase navigation system
[AD-A245997] p 2851 N92-26756
Precision of the long baseline acoustic navigation system used by Pegasus
[AD-A246598] p 2852 N92-26795
NAVIGATION SATELLITES
An adaptive correction technique for Differential Global Positioning System p 2851 N92-26623

Estimation of geopotential differences over intercontinental locations using satellite and terrestrial measurements p 2924 N92-26728

NEODYMIUM LASERS

Optimization of a color center Q-switched Nd:YLF laser
[DE92-621612] p 2910 N92-26287

Diode pumped 275 watt average power Nd:YAG slab laser
[DE92-008604] p 2911 N92-26504

NEPTUNIUM ISOTOPES

A comparative assessment of radiological impact due to nuclear waste disposal in hard crystalline bedrock, appendix 1
[IAEA-CN-43/449] p 2929 N92-26483

NETWORK ANALYSIS

Design and implementation of a toolbox of modularized C programs to construct, analyze, and test network optimization algorithms
[AD-A246191] p 2979 N92-26417

Constrained neural network architectures for target recognition
[DE92-011159] p 2982 N92-26434

NETWORK CONTROL

Two papers on feed-forward networks
[NASA-TM-107840] p 2983 N92-26631

NETWORKS

The preliminary geodetic control network of Venus
[RAND-N-3437-JPL] p 3019 N92-26819

NEUMANN PROBLEM

Computational methods for problems of acoustics with particular reference to exterior domains p 2992 N92-26558

NEURAL NETS

Neural network error correction for solving coupled ordinary differential equations
[NASA-TM-101796] p 2986 N92-26407

A computational analysis of properties and limitations of neural networks: Toward new parallel architectures for learning
[AD-A246156] p 2981 N92-26410

Optical hidden layer network
[AD-A246162] p 2992 N92-26413

Perception for outdoor navigation
[AD-A245715] p 2851 N92-26427

Constrained neural network architectures for target recognition
[DE92-011159] p 2982 N92-26434

Feature discovery via neural networks for object recognition in SAR imagery
[DE92-007046] p 2891 N92-26902

NEUTRAL BUOYANCY SIMULATION

Microgravity simulation p 2964 N92-26994

NEUTRINOS

Muon/electron separation for atmospheric neutrino interactions
[DE92-010349] p 3021 N92-26218

Cryogenic calorimeters for dark matter and neutrinos p 2907 N92-26392

NEUTRON ACTIVATION ANALYSIS

Determination of the structure of Y(HCOO)3 by the neutron time-of-flight diffraction method p 3002 N92-26325

NEUTRON BEAMS

Acquired polarization in fundamental symmetry experiments
[AD-A245646] p 2993 N92-26171

NEUTRON DIFFRACTION

Development and applications of the reverse neutron time-of-flight method with Fourier-type beam chopper
[VTT-PUBL-82] p 3001 N92-26320

Estimation of peak intensities from frequency filtered total scattering data of neutrons obtained by the reverse Fourier method p 3002 N92-26321

The high resolution diffractometer mini-Sfinks p 3002 N92-26322

High-resolution Fourier TOF powder diffraction. 1: Performance of the Mini-Sfinks Facility p 3002 N92-26323

Neutron powder diffraction study of deuterated beta-acetonitrile p 3002 N92-26324

Determination of the structure of Y(HCOO)3 by the neutron time-of-flight diffraction method p 3002 N92-26325

A high-resolution neutron powder diffraction study in high-T(sub c) superconductor YBa2Cu3O7 p 3002 N92-26326

Anomalous structural behaviour of the high-temperature superconducting compound La(1.8)Sr(0.2)CuO(4-y) p 3003 N92-26327

Neutron powder diffraction study on Eu-substituted Bi2Sr2CaCu2O(8+y) high temperature superconductor p 3003 N92-26328

Application of neutron diffraction to measure residual strains in high temperature composites
[DE91-014021] p 2869 N92-26679

NEUTRON DISTRIBUTION

Numerical solution of the equation of neutrons transport on plane geometry by analytical schemes using acceleration by synthetic diffusion
[DE92-621426] p 2995 N92-26844

NEUTRON EMISSION

Calibration of CR-39 for detecting fusion neutrons
[DE92-009063] p 2993 N92-26225

NEUTRON IRRADIATION

Improving the fracture resistance of irradiated martensitic steels
[DE92-008387] p 2879 N92-26848

NEUTRON SCATTERING

Estimation of peak intensities from frequency filtered total scattering data of neutrons obtained by the reverse Fourier method p 3002 N92-26321

Non-destructive analysis for hydrogen concentrations in materials
[AD-A246098] p 2874 N92-26541

X ray scattering studies of non-equilibrium ordering processes
[DE92-010311] p 2877 N92-26542

NEUTRON STARS

Destruction and excitation of accreted nuclei in neutron star atmospheres: Gamma ray lines and x ray bursts p 3016 N92-26476

Dynamics of neutron stars and binaries in globular clusters or, menages a trois: Revitalizing burnt out degenerates through partner swapping p 3017 N92-26522

Tensor-multi-scalar theories of gravitation
[PB92-152305] p 2943 N92-26820

X ray observations of gamma ray burst sources
[MPE-PREPRINT-174] p 3018 N92-27048

NEUTRONS

Calibration of CR-39 for detecting fusion neutrons
[DE92-009063] p 2993 N92-26225

A user's manual for MASH 1.0: A Monte Carlo adjoint shielding code system
[DE92-010375] p 3021 N92-26544

Numerical solution of the equation of neutrons transport on plane geometry by analytical schemes using acceleration by synthetic diffusion
[DE92-621426] p 2995 N92-26844

NEW ENGLAND (US)

Role of climate in forest monitoring and assessment: A New England example
[PB92-132885] p 2930 N92-26519

NEW YORK

Evaluation of carbon dioxide emission control strategies in New York State
[DE92-010162] p 2932 N92-26825

NEWTON-RAPHSON METHOD

Computational aspects of an implicit finite element procedure for elasto-viscoplastic large deformation problems p 2917 N92-26594

NEWTONIAN FLUIDS

Two-phase flow of Newtonian and Non-Newtonian fluids in a porous medium applied to water coning
[PB92-151109] p 2900 N92-26836

NICKEL

Relationship between composition, structure, properties, thermo-mechanical processing and ballistic performance of tungsten heavy alloys
[AD-A245649] p 2876 N92-26172

Progress in the development of lightweight nickel electrode
[NASA-TM-105638] p 2875 N92-26670

Spheroidization and densification of Nickel powders by RF-induction plasma
[PB92-151893] p 2879 N92-26787

Effects of ultra-vacuum and space environment on contact ohmic resistance: LDEF experiment AO 138-11 p 2895 N92-27118

Evaluation of sodium-nickel chloride cells for space applications p 2865 N92-27156

NICKEL ALLOYS

Atomistic studies of grain boundaries in alloys and compounds
[DE92-010792] p 2877 N92-26251

NICKEL CADMIUM BATTERIES

The 1990 NASA Aerospace Battery Workshop
[NASA-CP-3119] p 2862 N92-27130

Magellan battery operations: An overview p 2862 N92-27133

Super NiCd battery program: History and performance p 2862 N92-27135

Hughes advanced nickel-cadmium batteries: An update p 2862 N92-27136

SAFT nickel-cadmium cell performances for GEO and LEO applications p 2863 N92-27137

Oxygen recombination in the sealed nickel-cadmium cell p 2863 N92-27138

A constant current charge technique for low Earth orbit life testing p 2863 N92-27139

Chemical evaluation of non-woven nylon separators used in Ni/Cd cells p 2863 N92-27140

Exploring possible relationships between plate pore size character and cell performance p 2863 N92-27141

Accelerated cycle life performance for ovonic nickel-metal hydride cells p 2865 N92-27155

Recent developments in nickel electrode analysis p 2865 N92-27158

Results of a technical analysis of the Hubble Space Telescope nickel-cadmium and nickel-hydrogen batteries p 2867 N92-27167

NICKEL COMPOUNDS

Aging effects in palladium and LaNi(4.25)Al(0.75) tritides
[DE92-009945] p 2870 N92-26217

NICKEL HYDROGEN BATTERIES

Progress in the development of lightweight nickel electrode
[NASA-TM-105638] p 2875 N92-26670

Battery thermal control of the Columbus Free Flyer p 2859 N92-26970

The 1990 NASA Aerospace Battery Workshop
[NASA-CP-3119] p 2862 N92-27130

Recent developments in nickel electrode analysis p 2865 N92-27158

Eutelsat 2: SAR-10009 nickel-hydrogen battery p 2866 N92-27159

Low cost battery designs for small satellite applications p 2866 N92-27160

Update of a nickel-hydrogen cycle life model p 2866 N92-27162

Hubble Space Telescope battery background p 2866 N92-27163

Hubble Space Telescope NiH2 six battery test p 2866 N92-27164

Hubble Space Telescope nickel-hydrogen flight spare battery test p 2866 N92-27165

Multiple cell CPV nickel-hydrogen battery p 2866 N92-27166

Results of a technical analysis of the Hubble Space Telescope nickel-cadmium and nickel-hydrogen batteries p 2867 N92-27167

Nickel-hydrogen LEO cycling at 20 percent - 50 percent DOD p 2867 N92-27168

NIGHT VISION

Conquest of darkness by management of the stars
[AD-A245496] p 2997 N92-26676

NIOBIUM ALLOYS

Deformation behavior of an age-hardenable Beta+Alpha-Two titanium alloy
[AD-A246362] p 2879 N92-26939

NITRATE ESTERS

High melting aromatic nitrate esters
[AD-D015190] p 2884 N92-26880

NITRIC OXIDE

An analysis of middle ultraviolet emissions of molecular nitrogen and nitric oxide and vacuum calibration of an ultraviolet spectrograph
[AD-A245984] p 2943 N92-26753

NITROBACTER

MELISSA: Physical links of compartments Nitrobacter/Spirulina p 2961 N92-26981

NITROGEN

An analysis of middle ultraviolet emissions of molecular nitrogen and nitric oxide and vacuum calibration of an ultraviolet spectrograph
[AD-A245984] p 2943 N92-26753

NITROGEN OXIDES

Summary of NOx control technologies and their availability and extent of application
[PB92-158260] p 2928 N92-26373

Advancing natural gas combustion science and technology-low NOx
[PB92-137652] p 2876 N92-26782

NOISE (SOUND)

Symbolic solution of a multilayer ocean waveguide problem with arbitrary depth dependent ambient density and sound speed profiles
[AD-A245476] p 2949 N92-26533

NOISE INTENSITY

Characterization of the clock in a new inexpensive GPS receiver: The Magnavox MX 4200
[AD-A246165] p 2851 N92-26415

NOISE REDUCTION

Squeezed light and twin beams generation with a Q-switched laser p 2912 N92-26603

NOISE TEMPERATURE

Tuned-circuit dual-mode Johnson noise thermometers
[DE92-010121] p 2908 N92-26569

NONDESTRUCTIVE TESTS

Non-destructive analysis for hydrogen concentrations in materials
[AD-A246098] p 2874 N92-26541

NONLINEAR EQUATIONS

Nonlinear waves and inverse scattering
[AD-A246164] p 2986 N92-26414

NONLINEAR SYSTEMS
Nonlinear waves and inverse scattering
[AD-A246164] p 2986 N92-26414
Two papers on feed-forward networks
[NASA-TM-107840] p 2983 N92-26631
An analysis of commitment strategies in planning: The details
[NASA-TM-107881] p 2983 N92-26643
Adaptive regulation of the boiler-turbine unit of a Combined Heat and Power (CHP) system
[RR-417] p 2887 N92-26752
Adaptive control of nonlinear and stochastic systems
[AD-A247204] p 2985 N92-27169
Studies in chaos using stochastic methods
[AD-A246919] p 3008 N92-27171
NONLINEARITY
Analytical and numerical investigation of nonlinear gravitational clustering p 3017 N92-26578
Computations of nonlinear gravity waves by a desingularized boundary integral method p 2942 N92-26583
Wave viscosity interaction in nonlinear roll motion
[AD-A245756] p 2897 N92-26591
Numerical formulation for the prediction of solid/liquid change of a binary alloy
[NASA-CR-188468] p 2878 N92-26642
A boundary integral method for steady unsaturated flow in nonhomogeneous media
[DE92-009066] p 2897 N92-26644
Short-wave low-frequency spectra in a current-carrying plasma
[DE92-621529] p 3001 N92-26808
NONUNIFORMITY
Effects of non-uniform windowing on the performance of a fast frequency-hopped noncoherent MFSK receiver over Rician fading channels with partial-band interference and Doppler shift
[AD-A245762] p 2889 N92-26595
Transient gas motion in nuclear-reactor-pumped lasers: Computational and experimental results
[DE92-002357] p 2912 N92-26691
NORMAL DENSITY FUNCTIONS
Lower confidence limit expressions for P(X greater than y) and P(X greater than Y) under normality
[AD-A245787] p 2989 N92-26177
Description of and users manual for TUBA: A computer code for generating two-dimensional random fields via the turning bands method
[DE92-001020] p 2971 N92-26189
On certain methods of determining the ellipses an d ellipsoids of the positioning accuracy of robot manipulators
[ISSN-0208-5658] p 2914 N92-26284
NORTH SEA
Investigation of convection over sea by aircraft observations p 2926 N92-26337
Cirrus clouds and condensation trail on 18 Oct. 1989 over the North sea (ICE '89). Determination of height and optical depth using ALEX, AVHRR and HIRS p 2940 N92-26340
The effect of global change and long period tides on the Earth's rotation and gravitational potential p 2925 N92-26781
NOSE CONES
Analysis of frozen startup of high-temperature heat pipes and three-dimensional modeling of block-heated heat pipes
[AD-A245327] p 2896 N92-26379
NOTCH TESTS
Modeling cycle and time-dependent creep/relaxation effects on fatigue lives of notched members --- creep/relaxation p 2919 N92-26829
NOZZLE DESIGN
Performance prediction and design of maximum thrust planar supersonic nozzles using a flux-difference-splitting technique p 2853 N92-26480
NOZZLE FLOW
An experimental study of natural and forced modes in an axisymmetric jet p 2897 N92-26600
Subscale solid rocket motor infrared signature and particle behavior
[AD-A246416] p 2862 N92-27065
NUCLEAR BINDING ENERGY
Vibrational dynamics of aniline (N2)1 clusters in their first excited singlet state
[AD-A245812] p 2872 N92-26431
The computation of C-C and N-N bond dissociation energies for singly, doubly, and triply bonded systems
[NASA-CR-190254] p 2994 N92-26539
Multiquanta photodetachment from the H(-) ion
[DE92-010306] p 2911 N92-26573
Quantum dynamics of helium clusters
[AD-A245752] p 2995 N92-26588
A self-contamination model for the formation of globular star clusters p 3018 N92-26723
NUCLEAR DEFORMATION
New approaches to studies of exotic nuclei
[DE92-010127] p 2994 N92-26570
NUCLEAR DEVICES
Environmental radiation data
[PB92-164706] p 2933 N92-26890
NUCLEAR ELECTRIC PROPULSION
NASA/DOE/DOD nuclear propulsion technology planning: Summary of FY 1991 interagency panel results
[NASA-TM-105703] p 2861 N92-26792
NUCLEAR EXPLOSIONS
Effect of textile test sample size on assessment of protection to skin from thermal radiation
[AD-A246535] p 2955 N92-26472
NUCLEAR FUELS
An investigation of the mechanical properties and microscopic structure of extruded powder aluminum subjected to biaxial loadings at elevated temperature p 2879 N92-26770
NUCLEAR FUSION
Calibration of CR-39 for detecting fusion neutrons
[DE92-009063] p 2993 N92-26225
NUCLEAR MAGNETIC RESONANCE
Acquired polarization in fundamental symmetry experiments
[AD-A245646] p 2993 N92-26171
Activation and characterization of some molecular sieve catalysts
[ETN-92-91306] p 2871 N92-26261
NUCLEAR MEDICINE
Life sciences and environmental sciences
[DE92-010254] p 2950 N92-26203
NUCLEAR PARTICLES
X ray observations of gamma ray burst sources
[MPE-PREPRINT-174] p 3018 N92-27048
NUCLEAR PHYSICS
Open problems and future prospects for hypernuclear physics
[DE92-010158] p 2995 N92-26815
NUCLEAR POWER PLANTS
Assessment of diagnostic methods for solenoid-operated valves
[DE92-009379] p 2913 N92-26234
NUCLEAR PROPULSION
Assessment of a hot hydrogen nuclear propulsion fuel test facility
[DE92-004571] p 2995 N92-26692
NASA/DOE/DOD nuclear propulsion technology planning: Summary of FY 1991 interagency panel results
[NASA-TM-105703] p 2861 N92-26792
NUCLEAR PUMPING
Transient gas motion in nuclear-reactor-pumped lasers: Computational and experimental results
[DE92-002357] p 2912 N92-26691
NUCLEAR RADIATION
Life sciences and environmental sciences
[DE92-010254] p 2950 N92-26203
NUCLEAR RADIATION SPECTROSCOPY
Acquired polarization in fundamental symmetry experiments
[AD-A245646] p 2993 N92-26171
NUCLEAR REACTIONS
Li-6,d reaction on sd-, fp- and g-shell nuclei in ZR- and FR-DWBA formalisms
[DE92-614353] p 2994 N92-26365
Destruction and excitation of accreted nuclei in neutron star atmospheres: Gamma ray lines and x ray bursts p 3016 N92-26476
Interpretation of distributions on K(sub pi)(sup 0) in pFe, nFe, and piFe interactions at 0.5-5.0 TeV in the framework of contemporary models
[DE92-621189] p 3021 N92-26804
NUCLEAR REACTORS
Fusion energy and Canada's role
[DE92-621553] p 2999 N92-26286
Transient gas motion in nuclear-reactor-pumped lasers: Computational and experimental results
[DE92-002357] p 2912 N92-26691
NUCLEAR SCATTERING
Quasi-elastic nuclear scattering at high energies
[NASA-TM-4362] p 2996 N92-26832
NUCLEAR STRUCTURE
New approaches to studies of exotic nuclei
[DE92-010127] p 2994 N92-26570
Open problems and future prospects for hypernuclear physics
[DE92-010158] p 2995 N92-26815
On the evaluation of the U(3) content of the matrix elements of 1- and 2-body operators
[DE92-621113] p 2988 N92-26837
NUCLEATE BOILING
Nucleate pool boiling of R-114 and R-114/oil mixtures from single enhanced tubes
[AD-A245487] p 3008 N92-27058
NUCLEATION
Fundamental studies of the chemical vapor deposition of diamond
[DE92-010327] p 2881 N92-26543
Influence of substrate topography on the nucleation of diamond thin films
[DE92-010777] p 2883 N92-27060
NUCLEONS
Underground muons from the direction of Cygnus X-3 during the January 1991 radio flare
[DE92-010346] p 3021 N92-26215
A search for magnetic monopoles with the Soudan 2 detector
[DE92-010347] p 3021 N92-26216
Muon/electron separation for atmospheric neutrino interactions
[DE92-010349] p 3021 N92-26218
Supersymmetry and dark matter, a new candidate p 3016 N92-26491
Quasi-elastic nuclear scattering at high energies
[NASA-TM-4362] p 2996 N92-26832
NUCLIDES
Sensitivity analysis of biospheric behaviour of radionuclides released from nuclear waste repositories, appendix 4 p 2929 N92-26486
NUMERICAL ANALYSIS
Diapycnal mixing, gravity-current propagation, and sediment dispersion in turbulent fluids
[AD-A246160] p 2896 N92-26412
Algorithms for blending surface generation
[AD-A245686] p 2975 N92-26524
A FORTRAN 90 code for magnetohydrodynamics
[DE92-010362] p 3000 N92-26577
NUMERICAL CONTROL
Installation and operation of the 400 kW 140 GHz gyrotron on the MTX experiment
[DE92-009053] p 2906 N92-26377
An investigation of the mechanical properties and microscopic structure of extruded powder aluminum subjected to biaxial loadings at elevated temperature p 2879 N92-26770
Nickel-hydrogen LEO cycling at 20 percent - 50 percent DOD p 2867 N92-27168
NUMERICAL STABILITY
Identification of linear systems by an asymptotically stable observer
[NASA-TP-3164] p 2917 N92-26537
NYLON (TRADEMARK)
Chemical evaluation of non-woven nylon separators used in Ni/Cd cells p 2863 N92-27140

O

O RING SEALS
Effect of temperature and gap opening rate on the resiliency of candidate solid rocket booster O-ring materials
[NASA-TP-3226] p 2883 N92-27194
OBJECT PROGRAMS
Experiences in using C++ to develop a next generation strong shock wave physics code
[DE92-006675] p 2976 N92-26696
OBJECT-ORIENTED PROGRAMMING
The SOL object-oriented database language
[REPT-91-053] p 2973 N92-26421
A prototype multi-media data base for tracking interface relationships and performing cost tradeoffs for the Sea Launch and Recovery (SEALAR) space launch system
[AD-A245481] p 2857 N92-26515
An object-oriented approach to computer architecture simulation
[AD-A246597] p 2970 N92-26773
Forging a path with tool and data attributes
[DE92-009800] p 2976 N92-26797
An Ada object oriented missile flight simulation
[AD-A246378] p 2977 N92-27052
OBSERVATION
Optical ground-based network p 2937 N92-26313
Contributions to atmospheric physics in honor of Dr. Manfred Reinhardt on his 65th birthday
[DLR-FB-91-30] p 2939 N92-26329
Mesoscale observations of a cold front associated with a prefrontal hailstorm p 2940 N92-26338
OBSERVATION AIRCRAFT
Aircraft observation of a small-scale solitary wave near the tropopause p 2940 N92-26336
Investigation of convection over sea by aircraft observations p 2926 N92-26337
Precipitation formation processes in convective and stratiform clouds as deduced by coordinated polarimetric radar and aircraft measurements p 2941 N92-26342
The composite structure of thermals as derived from aircraft observations p 2941 N92-26346

OBSTACLE AVOIDANCE
A supervisory control strategy for navigation of mobile robots in dynamic environments p 2983 N92-26734
OCEAN BOTTOM
Proceedings of 6th Hawaiian Winter Workshop on Dynamics of Oceanic Internal Gravity Waves
[AD-A245650] p 2948 N92-26173
Geochemical constraints on ocean general circulation models
[DE92-010805] p 2948 N92-26270
Ocean bottom modeling for ray acoustics
[AD-A246287] p 2948 N92-26360
Quantitative assessment of the slope resolution of seafloor mapping systems
[AD-A246158] p 2949 N92-26411
Ocean bottom simulation using fractal geometry
[AD-A245477] p 2949 N92-26423
Precision of the long baseline acoustic navigation system used by Pegasus
[AD-A246598] p 2852 N92-26795
OCEAN CURRENTS
Investigation of carbon dioxide in the South Atlantic and northern Weddell Sea areas (WOCE Sections A-12 and A-21) during the METEOR expedition 11/5, January - March 1990
[DE92-010027] p 2928 N92-26231
Meridional zonation of the Barents Sea ecosystem inferred from satellite remote sensing and in situ bio-optical observations
[AD-A246323] p 2948 N92-26245
Geochemical constraints on ocean general circulation models
[DE92-010805] p 2948 N92-26270
Numerical investigation of the circulation of an ice-covered Arctic Ocean p 2949 N92-26568
Precision of the long baseline acoustic navigation system used by Pegasus
[AD-A246598] p 2852 N92-26795
Observations of wind forced circulation on the continental shelf off Point Sur, California from a self-contained acoustic Doppler current profiler
[AD-A246437] p 2950 N92-27029
OCEAN MODELS
Geochemical constraints on ocean general circulation models
[DE92-010805] p 2948 N92-26270
Ocean bottom simulation using fractal geometry
[AD-A245477] p 2949 N92-26423
Software requirements document for the netCDF interface within ECMOP, version 1.0
[AD-A246220] p 2974 N92-26464
Numerical investigation of the circulation of an ice-covered Arctic Ocean p 2949 N92-26568
OCEAN SURFACE
Laser glittering in the relatively stable propagation layer near the sea surface
[AD-A246374] p 2913 N92-27050
OCEANOGRAPHIC PARAMETERS
A compendium of environmental data collected during the southwest Florida shallow-water acoustic sea test
[AD-A246143] p 2950 N92-27071
Documentation for the Semi-Automated Mesoscale Analysis System 1.1
[AD-A246144] p 2985 N92-27072
OCEANOGRAPHY
Investigation of carbon dioxide in the South Atlantic and northern Weddell Sea areas (WOCE Sections A-12 and A-21) during the METEOR expedition 11/5, January - March 1990
[DE92-010027] p 2928 N92-26231
Geochemical constraints on ocean general circulation models
[DE92-010805] p 2948 N92-26270
OCEANS
Symbolic solution of a multilayer ocean waveguide problem with arbitrary depth dependent ambient density and sound speed profiles
[AD-A245476] p 2949 N92-26533
The effect of global change and long period tides on the Earth's rotation and gravitational potential p 2925 N92-26781
OCTANES
High octane ethers from synthesis gas-derived alcohols
[DE92-010480] p 2884 N92-26548
OFF-ON CONTROL
Time optimal trajectories for mobile robots with two independently driven wheels
[DE92-010002] p 2913 N92-26219
OH-58 HELICOPTER
Gear tooth stress measurements of two helicopter planetary stages
[NASA-TM-105651] p 2915 N92-26555
OILS
The influence of pressure on the phase behaviour of water + oil + surfactant systems
[ISBN-90-6275-732-4] p 2871 N92-26257
Two-phase flow of Newtonian and Non-Newtonian fluids in a porous medium applied to water coning
[PB92-151109] p 2900 N92-26836
Nucleate pool boiling of R-114 and R-114/oil mixtures from single enhanced tubes
[AD-A245487] p 3008 N92-27058
OLFACTORY PERCEPTION
An evaluative study of the sensory qualities of selected European and Asian foods for international space missions (a French food study) p 2966 N92-27009
ON-LINE SYSTEMS
A frequency domain based approach to on-line system identification
[AD-A246193] p 2973 N92-26418
Cataloging guidelines
[AD-A246500] p 3011 N92-26465
Information liability: New interpretations for the electronic age --- online databases p 3012 N92-26481
ONE DIMENSIONAL FLOW
Wave structure in one and two dimensional fluid flow
[DE92-007421] p 2900 N92-26855
OPEN CIRCUIT VOLTAGE
Li/BCX, SVO, and CSC cells: Power sources for aerospace applications p 2864 N92-27147
OPERATING SYSTEMS (COMPUTERS)
Assessments of selected real-time computing technologies
[AD-A245434] p 2972 N92-26273
Tools and techniques for adding fault tolerance to distributed and parallel programs
[AD-A245510] p 2980 N92-26677
The 8th IEEE Workshop on Real-Time Operating Systems
[AD-A246126] p 2976 N92-26685
OPERATING TEMPERATURE
Li/BCX, SVO, and CSC cells: Power sources for aerospace applications p 2864 N92-27147
Examination of the discharge mechanism of Li/CF(x) cells: Comparison of the electrochemical reduction mechanisms of PTFE and (CF(x))n by lithium p 2865 N92-27151
OPERATORS (MATHEMATICS)
Lyapunov equation for infinite-dimensional discrete bilinear systems
[DE92-621066] p 2988 N92-26831
On the evaluation of the U(3) content of the matrix elements of 1- and 2-body operators
[DE92-621113] p 2988 N92-26837
OPTICAL COMMUNICATION
Optical communications with number states p 2889 N92-26604
High-speed pulse detection room-temperature optical nonlinearities for GaInAs/A1InAs and GaA1InAs/A1InAs multiple quantum wells and integrated mirror etalon at 1.3 micrometers
[AD-A246369] p 2998 N92-26943
Laser glittering in the relatively stable propagation layer near the sea surface
[AD-A246374] p 2913 N92-27050
OPTICAL EQUIPMENT
LDEF active optical system components experiment p 2998 N92-27094
Effects of long-duration exposure on optical system components p 2998 N92-27095
Vacuum deposited optical coatings experiment p 2999 N92-27097
Space environmental effects on coated optics p 2999 N92-27098
OPTICAL FIBERS
The development of an optical fiber accelerometer
[DE92-008680] p 2997 N92-26452
Optical strain monitoring in composite materials
[AD-A245474] p 2868 N92-26532
Polarisation effects in fibre lasers p 2911 N92-26571
High-speed pulse detection room-temperature optical nonlinearities for GaInAs/A1InAs and GaA1InAs/A1InAs multiple quantum wells and integrated mirror etalon at 1.3 micrometers
[AD-A246369] p 2998 N92-26943
OPTICAL FILTERS
Effects of long-duration exposure on optical system components p 2998 N92-27095
Exposure to space radiation of high-performance infrared multilayer filters and materials technology experiment (A0056) p 2999 N92-27108
Passive exposure of Earth radiation budget experiment components. LDEF experiment AO-147: Post-flight examinations and tests p 2910 N92-27109
OPTICAL MATERIALS
Effects of long-duration exposure on optical system components p 2998 N92-27095
Effects of long term exposure on optical substrates and coatings (SOO50-2) p 2998 N92-27096
OPTICAL MEASUREMENT
Determination of the structure of Y(HCOO)3 by the neutron time-of-flight diffraction method p 3002 N92-26325
OPTICAL MEASURING INSTRUMENTS
Comparison of laser and conventional heating in TLD dosemapping
[DE92-010773] p 2910 N92-26269
U.S. ground-based space research programs in Svalbard (Norway) p 2935 N92-26296
Results of a portable fiber-optic weigh-in-motion system
[DE92-009011] p 2996 N92-26376
Optical flow sensor
[AD-D015200] p 2997 N92-26862
Liquid level and volume measurement device
[AD-D015189] p 2909 N92-26879
Investigation on a partial pressure carbon dioxide sensor p 2968 N92-27019
Differential polarimetric fiber optic sensor
[AD-D015218] p 2998 N92-27186
OPTICAL PATHS
Laser glittering in the relatively stable propagation layer near the sea surface
[AD-A246374] p 2913 N92-27050
OPTICAL POLARIZATION
Differential polarimetric fiber optic sensor
[AD-D015218] p 2998 N92-27186
OPTICAL PROPERTIES
Band structure and optical properties of semiconductor superlattices
[AD-A246076] p 3005 N92-26763
Quasi-elastic nuclear scattering at high energies
[NASA-TM-4362] p 2996 N92-26832
Systems special investigation group overview p 2867 N92-27084
OPTICAL PUMPING
Diode pumped 275 watt average power Nd:YAG slab laser
[DE92-008604] p 2911 N92-26504
OPTICAL RADAR
Cirrus clouds and condensation trail on 18 Oct. 1989 over the North sea (ICE '89). Determination of height and optical depth using ALEX, AVHRR and HIRS p 2940 N92-26340
Remote sensing of atmosphere with aircraft borne lidar systems p 2941 N92-26347
Large coherent arrays for laser radars, phase 1
[AD-A245528] p 2912 N92-26663
A high repetition rate lidar
[AD-A245382] p 2890 N92-26872
OPTICAL SWITCHING
High-speed pulse detection room-temperature optical nonlinearities for GaInAs/A1InAs and GaA1InAs/A1InAs multiple quantum wells and integrated mirror etalon at 1.3 micrometers
[AD-A246369] p 2998 N92-26943
OPTICAL THICKNESS
Cirrus clouds and condensation trail on 18 Oct. 1989 over the North sea (ICE '89). Determination of height and optical depth using ALEX, AVHRR and HIRS p 2940 N92-26340
OPTICAL TRACKING
The state of multiple sensor, multiple target tracking in ballistic missile defense
[AD-A245433] p 2850 N92-26272
OPTIMAL CONTROL
A modeling strategy for large-scale optimization based on analysis and visualization principles
[AD-A246570] p 2987 N92-26620
Principal investigator in a box: Version 1.2 documentation
[NASA-TM-107886] p 2982 N92-26628
A supervisory control strategy for navigation of mobile robots in dynamic environments p 2983 N92-26734
Adaptive control of nonlinear and stochastic systems
[AD-A247204] p 2985 N92-27169
OPTIMIZATION
Design and implementation of a toolbox of modularized C programs to construct, analyze, and test network optimization algorithms
[AD-A246191] p 2979 N92-26417
The minimization of multiple valued logic expressions using parallel processors
[AD-A245763] p 2980 N92-26596
Optimization of space structures to minimize dynamic response p 2858 N92-26610
Proximal minimization algorithms with cutting planes
[AD-A246436] p 2977 N92-26949
Thermal control of telescope apertures by optimized baffle heating p 2961 N92-26976

Rarefied-flow aerodynamics
[NASA-CR-190452] p 2850 N92-27191
OPTOELECTRONIC DEVICES
Liquid level and volume measurement device
[AD-D015189] p 2909 N92-26879
ORBITAL ASSEMBLY
Fundamental mechanisms affecting friction welding under vacuum
[AD-A245685] p 2877 N92-26520
ORBITAL MECHANICS
On-orbit coldwelding: Fact or friction?
p 2880 N92-27115
ORDER-DISORDER TRANSFORMATIONS
X ray scattering studies of non-equilibrium ordering processes
[DE92-010311] p 2877 N92-26542
Structural coherence of the CuO2 planes of oxide superconductors: Is it a requirement for superconductivity?
[DE92-009724] p 3005 N92-26842
ORDNANCE
The geoid, GPS, and levelling p 2925 N92-26777
ORGANIC COMPOUNDS
Energy transfer properties and mechanisms
[DE92-011215] p 2994 N92-26240
Technology transfer and application of SERS continuous monitor for trace organic compounds
[DE92-008900] p 2875 N92-26726
Volatile Organic Compound (VOC) and Particulate Matter (PM) speciation data system user's manual, version 1.4
[PB92-105527] p 2932 N92-26823
ORGANIC MATERIALS
GAC adsorption of a mixture of natural organic matter and VOCs in the presence and absence of molecular oxygen
[PB92-153782] p 2928 N92-26354
Equilibrium-analysis of projected climate change effects on the global soil organic matter pool
[PB92-153022] p 2930 N92-26509
ORGANIC PEROXIDES
Study of hydrazine metabolism and toxicity
[AD-A245755] p 2884 N92-26589
ORGANIZATIONS
Information technology resources assessment
[DE92-009498] p 3011 N92-26221
ORGANOMETALLIC COMPOUNDS
Electrocatalysts for oxygen electrodes
[DE92-009491] p 2871 N92-26220
Bis (pentamethylcyclopentadienyl) ytterbium: Electron-transfer reactions with organotransition metal complexes
[DE92-010300] p 2994 N92-26235
ORIFICES
A parametric numerical study of mixing in a cylindrical duct
[NASA-TM-105695] p 2854 N92-26553
OROGRAPHY
Estimating mesoscale, orographically enhanced precipitation using synoptic scale data
[AD-A245749] p 2946 N92-26562
OSCILLATING CYLINDERS
Dynamic response of cylindrical shells to underwater end-on explosion
[AD-A245804] p 2920 N92-26932
OSCILLATING FLOW
Heat transfer in oscillating flows with sudden change in cross section
[NASA-TM-105692] p 2861 N92-26654
Investigation on the boundary layer transition of alternately oscillating flow in deceleration phase
p 2903 N92-26917
Overview of NASA supported Stirling thermodynamic loss research
[NASA-TM-105690] p 2861 N92-27034
OSCILLATION DAMPERS
Tests on various arrangements of liquid column vibration absorbers
[PB92-152610] p 2896 N92-26506
OSCILLATIONS
Mutual friction in superfluid He-3: Effects of bound states in the vortex core
[PB92-142231] p 2896 N92-26507
OSCILLATORS
Diffraction phenomena in spontaneous and stimulated radiation by relativistic particles in crystals (review)
[DE92-009501] p 3001 N92-26222
Development and testing of a prototype electro-optical phase encoded position transducer
[AD-A245486] p 2908 N92-26401
OTTO CYCLE
Throttleless Otto-cycle natural gas engines
[PB92-164482] p 2914 N92-26371
OVERPRESSURE
Theoretical and numerical study of flame propagation and transition to detonation --- detonation transition
p 2874 N92-26615
OXIDATION
Aromatic-radical oxidation kinetics
[DE92-010821] p 2871 N92-26274
Reaction/separation process for enhanced methane conversion
[PB92-149657] p 2873 N92-26508
Enhance methane reactivity
[PB92-154822] p 2873 N92-26516
Study of hydrazine metabolism and toxicity
[AD-A245755] p 2884 N92-26589
A surface science investigation of silicon carbide: Oxidation, crystal growth and surface structural analysis
[DE92-010286] p 3004 N92-26641
New theoretical methods for electronic structure and gas-phase state specific oxidation/reduction studies
[AD-A246127] p 2875 N92-26687
Novel molecular sources for dispersing boron in carbon-carbon composites
[AD-A246999] p 2870 N92-26882
Catalytic wet-oxidation of human waste produced in a space habitat: Purification of the oxidized liquor for human drinking p 2957 N92-26954
Thiocapsa roseopersicina, a bacterium for sulfur-recycling in microbial ecosystems designed for CELSS and space purposes p 2951 N92-26977
OXIDATION RESISTANCE
Novel molecular sources for dispersing boron in carbon-carbon composites
[AD-A246999] p 2870 N92-26882
OXIDATION-REDUCTION REACTIONS
New theoretical methods for electronic structure and gas-phase state specific oxidation/reduction studies
[AD-A246127] p 2875 N92-26687
Photochemical energy conversion by membrane-bound photoredox systems
[DE92-008709] p 2927 N92-26858
Carbon monoxide metabolism by the photosynthetic bacterium Rhodospirillum rubrum
[DE92-010953] p 2951 N92-26938
OXIDES
Carbon monoxide metabolism by the photosynthetic bacterium Rhodospirillum rubrum
[DE92-010953] p 2951 N92-26938
OXIDIZERS
Enhance methane reactivity
[PB92-154822] p 2873 N92-26516
OXYGEN
Electrocatalysts for oxygen electrodes
[DE92-009491] p 2871 N92-26220
Biochemical, endocrine, and hematological factors in human oxygen tolerance extension: Predictive studies 6
[NASA-CR-190341] p 2952 N92-26263
GAC adsorption of a mixture of natural organic matter and VOCs in the presence and absence of molecular oxygen
[PB92-153782] p 2928 N92-26354
Synthesis of novel fluorinated phosphonic acid electrolytes for phosphoric acid fuel cells
[PB92-164300] p 2926 N92-26372
Microwelding (or cold-welding) of various metallic materials under the ultra-vacuum LDEF experiment AO 138-10 p 2880 N92-27119
OXYGEN ATOMS
Structural coherence of the CuO2 planes of oxide superconductors: Is it a requirement for superconductivity?
[DE92-009724] p 3005 N92-26842
An overview of the first results on the solar array materials passive LDEF experiment (sample), A0171
p 2927 N92-27087
Preliminary analyses of WL experiment No. 701, space environment effects on operating fiber optic systems
p 2998 N92-27089
OXYGEN PRODUCTION
Higher plant growth in closed environment: Preliminary experiments in life support facility at ESA-ESTEC
p 2951 N92-26978
OXYGEN RECOMBINATION
Oxygen recombination in the sealed nickel-cadmium cell p 2863 N92-27138
OXYGEN SUPPLY EQUIPMENT
Investigation on a partial pressure carbon dioxide sensor p 2968 N92-27019
OXYGENATION
The importance of chemical reactions with environment for ablation process of thermal protection and structural materials p 2883 N92-27015
OZONE
Ozone trends --- atmospheric ozone variations
p 2934 N92-26345
Improved procedures for quantifying key meteorological effects on ambient ozone data
[PB92-163278] p 2931 N92-26793
Report of the CC1 experts meeting on tracking and transmission of climate system information
[WCDMP-16] p 2947 N92-26925
OZONE DEPLETION
Ozone trends --- atmospheric ozone variations
p 2934 N92-26345
Tracer transport in the middle atmosphere
p 2928 N92-26473
OZONOSPHERE
Ozone trends --- atmospheric ozone variations
p 2934 N92-26345

P

P WAVES
Imaging earth's interior: Tomographic inversions for mantle P-wave velocity structure
[DE92-010271] p 2934 N92-26208
Fault zone structure determined through the analysis of earthquake arrival times
[DE92-010322] p 2935 N92-26239
PACIFIC OCEAN
Characteristics of upper-level and boundary layer forcing in Western Pacific cyclones
[AD-A246301] p 2945 N92-26364
PACKAGING
Application of irradiation techniques to food and foodstuffs
[DE92-614952] p 2954 N92-26186
PACKET SWITCHING
An adaptive, packet-switched HF data terminal: Functional overview and initial performance
[AD-A246318] p 2973 N92-26292
PAIR PRODUCTION
The sixteen channel CAMAC constant fraction discriminator for APEX
[DE92-010550] p 2970 N92-26551
PALEOCLIMATOLOGY
PAGES. Past global changes project: Proposed implementation plans for research activities
[IGBP-REPT-19-ATTACH-10] p 2934 N92-27082
PALEONTOLOGY
The carbon isotopic compositions of individual compounds from ancient and modern depositional environments p 2921 N92-26478
PALLADIUM
Aging effects in palladium and LaNi(4.25)Al(0.75) tritides
[DE92-009945] p 2870 N92-26217
PALLADIUM COMPOUNDS
Aging effects in palladium and LaNi(4.25)Al(0.75) tritides
[DE92-009945] p 2870 N92-26217
A new phase in palladium hydride technology
[DE92-009852] p 2875 N92-26718
PANELS
Heat pipe-based radiative panel p 2859 N92-26968
PARABOLIC FLIGHT
Parabolic flight: Reports of microgravity experiments by aircraft, volume 1, no. 2
[EG-910045] p 2884 N92-26440
Outlines of parabolic flight p 2884 N92-26441
Preliminary experiment of GDEF (Gas Dynamics Experiment Facility) p 2885 N92-26442
Parabolic flight experiments on bubble migration under reduced gravity p 2885 N92-26443
Micro-gravity experiment of vapor/liquid reorientation induced by capillary force p 2885 N92-26444
Biomedical data acquisition and processing technology p 2885 N92-26446
The experiment under microgravity by aircraft: The experiment in floating by gas flow p 2886 N92-26447
Microgravity simulation p 2964 N92-26994
Crew-friendly support systems for internal vehicular activities in zero gravity, experimented underwater for the Columbus programme p 2969 N92-27025
PARACHUTE DESCENT
Critical soft landing technology issues for future US space missions
[NASA-CR-185673] p 2858 N92-26884
PARALLEL PLATES
Heat transfer in oscillating flows with sudden change in cross section
[NASA-TM-105692] p 2861 N92-26654
Development of a 300 Amp-hr high rate lithium thionyl chloride cell p 2864 N92-27149
PARALLEL PROCESSING (COMPUTERS)
Distributed visualization
[DE92-009405] p 2971 N92-26188
Distributed and parallel Ada and the Ada 9X recommendations
[NASA-CR-190392] p 2978 N92-26199

Modeling node bandwidth limits and their effects on vector combining algorithms
[DE92-010829] p 2979 N92-26277
Run-time support for dynamic load balancing and debugging in paralex
[AD-A245446] p 2979 N92-26279
A computational analysis of properties and limitations of neural networks: Toward new parallel architectures for learning
[AD-A246156] p 2981 N92-26410
Massively parallel implementation of character recognition systems
[PB92-149863] p 2980 N92-26501
Matched field processing on the connection machine
[AD-A245469] p 2980 N92-26531
The minimization of multiple valued logic expressions using parallel processors
[AD-A245763] p 2980 N92-26596
The Orca Project: Research on high performance parallel computer programming environments
[AD-A234648] p 2980 N92-26801
Solution of the first-order form of the 3-D discrete ordinates equations on a massively parallel machine
[DE92-004575] p 2981 N92-26854

PARALLEL PROGRAMMING
Distributed and parallel Ada and the Ada 9X recommendations
[NASA-CR-190392] p 2978 N92-26199
Paralex: An environment for parallel programming in distributed systems
[AD-A245445] p 2979 N92-26278
Data fusion and correlation techniques testbed (DFACTT): Field trial 14 January 1991
[AD-A245324] p 3011 N92-26378
The minimization of multiple valued logic expressions using parallel processors
[AD-A245763] p 2980 N92-26596
Tools and techniques for adding fault tolerance to distributed and parallel programs
[AD-A245510] p 2980 N92-26677
The Orca Project: Research on high performance parallel computer programming environments
[AD-A234648] p 2980 N92-26801

PARAMETERIZATION
Investigation of convection over sea by aircraft observations p 2926 N92-26337
Dynamic control of a space robot system with no thrust jets controlled base
[AD-A245711] p 2981 N92-26356
Parameterization of water-soluble component of aerosol particles in numerical cloud models
[NASA-CR-190225] p 2945 N92-26474
Application of parametrized variational principles in the finite element method p 2987 N92-26624
Development of an advanced finite-difference atmospheric general circulation model
[DE92-010923] p 2944 N92-26937

PARAMETRIC AMPLIFIERS
Squeezed light and twin beams generation with a Q-switched laser p 2912 N92-26603

PARITY
A random polynomial algorithm for the matroid parity base problem
[REPT-91-079] p 2974 N92-26449

PARTIAL PRESSURE
Investigation on a partial pressure carbon dioxide sensor p 2968 N92-27019

PARTICLE ACCELERATION
The HUS solar flare and cosmic gamma ray burst detector aboard the Ulysses spacecraft
[MPE-PREPRINT-175] p 3016 N92-27049

PARTICLE ACCELERATOR TARGETS
Fail safe system for suppressing stimulated Brillouin scattering in large optics on the Nova laser
[DE92-008608] p 2911 N92-26505
The status of GALLEX
[DE92-010077] p 3020 N92-26566
Higher order parametric x rays
[AD-A247148] p 2991 N92-27182

PARTICLE ACCELERATORS
Advances in the engineering of high field applied-B ion diodes for inertial confinement fusion
[DE92-006528] p 3000 N92-26695

PARTICLE PRECIPITATION
Polar cap boundary and structure of dayside cusp as determined by ion precipitation p 2936 N92-26300

PARTICLE PRODUCTION
New description of multiplicity distribution in inelastic meson-proton interactions
[DE92-621167] p 2995 N92-26800
Interpretation of distributions on K(sub pi)(sup 0) in pFe, nFe, and piFe interactions at 0.5-5.0 TeV in the framework of contemporary models
[DE92-621189] p 3021 N92-26804

PARTICLE SIZE DISTRIBUTION
Microstructural evaluation of as-solidified and heat treated gamma-TiAl based powders
[DE92-008956] p 2881 N92-26455
Modification and experimental validation of a combined optical and collection probe for solid propellant exhaust analysis
[AD-A245387] p 2884 N92-26839
Development of a microstructural-related description for the high temperature stress-strain behaviour of the turbine blade material IN 738 LC
[JUEL-2466] p 2880 N92-26945
Subscale solid rocket motor infrared signature and particle behavior
[AD-A246416] p 2862 N92-27065

PARTICLE THEORY
Topics in particle physics and cosmology
[DE92-010478] p 3019 N92-26385
Interpretation of distributions on K(sub pi)(sup 0) in pFe, nFe, and piFe interactions at 0.5-5.0 TeV in the framework of contemporary models
[DE92-621189] p 3021 N92-26804

PARTICLES
Modification and experimental validation of a combined optical and collection probe for solid propellant exhaust analysis
[AD-A245387] p 2884 N92-26839
Laser cooling and trapping of atoms and particles
[AD-A247208] p 2913 N92-27173

PARTICULATES
Volatile Organic Compound (VOC) and Particulate Matter (PM) speciation data system user's manual, version 1.4
[PB92-105527] p 2932 N92-26823
Evaluation of the Fourier transform infrared spectrometer for particle-associated ammonium sulfate determination
[PB92-160084] p 2910 N92-26930

PARTITIONS (MATHEMATICS)
Introduction in IND and recursive partitioning
[NASA-TM-107879] p 2983 N92-26629

PASSENGER AIRCRAFT
Gamma Group-The Pale Horse: A proposal in response to a commercial air transportation study ort study
[NASA-CR-190019] p 2852 N92-26435

PATENT APPLICATIONS
NASA patent abstracts bibliography: A continuing bibliography. Section 2: Indexes (supplement 40)
[NASA-SP-7039(40)-SECT-2] p 3014 N92-27081

PATENT POLICY
Survey of small business use of intellectual property protection
[PB92-151703] p 3009 N92-26523

PATENTS
NASA patent abstracts bibliography: A continuing bibliography. Section 2: Indexes (supplement 40)
[NASA-SP-7039(40)-SECT-2] p 3014 N92-27081

PATTERN RECOGNITION
Muon/electron separation for atmospheric neutrino interactions
[DE92-010349] p 3021 N92-26218
Perception for outdoor navigation
[AD-A245715] p 2851 N92-26427
Recognition of 3-D symmetric objects from range images in automated assembly tasks
[NASA-CR-187664] p 2886 N92-26656
Feature discovery via neural networks for object recognition in SAR imagery
[DE92-007046] p 2891 N92-26902

PENETRATION
Penetration of laminated composites by projectiles p 2869 N92-26661

PERCOLATION
Percolation effects in the V-I characteristics of granular YBa2Cu3O(7-delta)
[DE92-617541] p 3004 N92-26672

PERFLUORO COMPOUNDS
Comparison of laser models
[NASA-CR-190302] p 2913 N92-26870

PERFORMANCE PREDICTION
An antenna design for PANSAT using NEC
[AD-A245482] p 2888 N92-26399
Effect of gyro noise on ADKEM gyro-only missile system performance
[AD-A246150] p 2852 N92-26408
Performance prediction and design of maximum thrust planar supersonic nozzles using a flux-difference-splitting technique p 2853 N92-26480
Nonstationary higher order spectral analysis
[AD-A246580] p 2991 N92-26772
Hubble Space Telescope nickel-hydrogen flight spare battery test p 2866 N92-27165
The study on a directory of human performance models for system design (Defence Research Group Panel 8 on the defence applications of human and bio-medical sciences)
[AD-A247346] p 2970 N92-27179

PERFORMANCE TESTS
Testbank (1.0) user's manual
[AD-A245895] p 2971 N92-26196
Software requirements document for the netCDF interface within ECMOP, version 1.0
[AD-A246220] p 2974 N92-26464
Effect of textile test sample size on assessment of protection to skin from thermal radiation
[AD-A246535] p 2955 N92-26472
Measuring the effectiveness of information systems
[AD-A246007] p 3013 N92-26762
Rule-based expert system for evaluating the quality of long-term, in-situ, gas chromatographic measurements of atmospheric methane
[PB92-128560] p 2876 N92-26812
A measuring facility for testing radio communication equipment
[AD-A245821] p 2890 N92-26874
Progress in the development of the Hermes evaporators p 2962 N92-26984
The transpirator, an efficient and light evaporative cooler for space technology p 2887 N92-26986
CPA: A controlled pump assembly for two-phase loops applications p 2916 N92-26987
Thermo-hydraulic investigations on heat exchangers for Columbus hybrid radiators p 2887 N92-26988
Italsat thermal control: The in-orbit performances p 2859 N92-26996
Transverse flat plate heat pipe experiment p 2906 N92-27107
COBE battery overview: History, handling, and performance p 2862 N92-27131
End-of-life evaluation of the solar maximum mission batteries p 2862 N92-27132
Magellan battery operations: An overview p 2862 N92-27133
Super NiCd battery program: History and performance p 2862 N92-27135
Hughes advanced nickel-cadmium batteries: An update p 2862 N92-27136
SAFT nickel-cadmium cell performances for GEO and LEO applications p 2863 N92-27137
Oxygen recombination in the sealed nickel-cadmium cell p 2863 N92-27138
Safety testing of lithium cells p 2864 N92-27150
The evaluation of layered separators for nickel-hydrogen cells p 2866 N92-27161
Hubble Space Telescope NiH2 six battery test p 2866 N92-27164
Hubble Space Telescope nickel-hydrogen flight spare battery test p 2866 N92-27165

PERIODIC FUNCTIONS
Downdating of Szego polynomials and data fitting applications
[AD-A245825] p 2988 N92-26900

PERIODIC VARIATIONS
Characterization of discrete-time linear periodically time-varying systems
[AD-A245822] p 2989 N92-26180
Homogenization models for 2-D grid structures
[NASA-CR-190321] p 2920 N92-26892
PAGES. Past global changes project: Proposed implementation plans for research activities
[IGBP-REPT-19-ATTACH-10] p 2934 N92-27092

PERIPHERAL NERVOUS SYSTEM
Low power laser irradiation effect with emphasis on injured neural tissues
[AD-A246410] p 2953 N92-27063

PERMEABILITY
Retention and release of tritium in aluminum clad, Al-Li alloys
[DE92-009905] p 2878 N92-26635

PERMITTIVITY
Static, microwave, infrared, and visible permittivity related to chemical structure: N-methylacetamide, N-dimethylacetamide and their mixtures in CCl4 at 32 C
[AD-A246364] p 2991 N92-26940

PERMUTATIONS
Induced cycle structures of the hyperoctahedral group
[DE92-007570] p 3006 N92-26857

PEROXIDES
Low temperature electrochemical activation of methane
[PB92-152917] p 2872 N92-26951

PERSONNEL MANAGEMENT
US Small Business Administration FY 1990 national accomplishment report and FY 1991 national affirmative employment program plan
[PB92-157064] p 3008 N92-26353

Test plan for the international aircraft operator information system
[DOT/FAA/CT-91/18] p 3014 N92-26830

PERTURBATION
Analytical and numerical investigation of nonlinear gravitational clustering p 3017 N92-26578

PERTURBATION THEORY
Upper/lower vortex interaction and potential vorticity inversion p 2939 N92-26331
Analytical and numerical investigation of nonlinear gravitational clustering p 3017 N92-26578
A boundary integral method for steady unsaturated flow in nonhomogeneous media
[DE92-009066] p 2897 N92-26644
Turbulent mixing in supersonic jets p 2850 N92-27054

PESTICIDES
Waste minimization for non-agricultural pesticide applicators: EPA's pollution prevention guide
[PB92-153774] p 2933 N92-26889

PETRI NETS
Hardware synthesis using high-level Petri nets
[REPT-91-071] p 2970 N92-26439
Proving properties of real-time systems through logical specifications and Petri net models
[REPT-91-072] p 2973 N92-26448
Automated interpretation of S-invariants of predicate/transition nets: An application of non-classical logics
[PB92-143544] p 2975 N92-26500

PHASE CHANGE MATERIALS
Heat receivers for solar dynamic space power systems p 2860 N92-26601
Numerical formulation for the prediction of solid/liquid change of a binary alloy
[NASA-CR-188468] p 2878 N92-26642

PHASE DIAGRAMS
Lattice instabilities and structural phase transformations in La2CuO4 superconductors and insulators
[DE92-010045] p 3006 N92-27059

PHASE SHIFT
A comparison of direction finding results from an FFT peak identification technique with those from the music algorithm
[AD-A245675] p 2888 N92-26424

PHASE TRANSFORMATIONS
Why first-principles calculations for alloys?
[DE92-010285] p 2877 N92-26213
Neutron powder diffraction study of deuterated beta-acetonitrile p 3002 N92-26324
Recent progress in calorimeters with transition edge thermometers p 2907 N92-26394
Microstructural evaluation of as-solidified and heat treated gamma-TiAl based powders
[DE92-008956] p 2881 N92-26455
A one-dimensional temperature model for a snow cover: Technical documentation for SNTHERM.89
[AD-A245493] p 2922 N92-26674
A new phase in palladium hydride technology
[DE92-009852] p 2875 N92-26718
Lattice instabilities and structural phase transformations in La2CuO4 superconductors and insulators
[DE92-010045] p 3006 N92-27059

PHASED ARRAYS
Large coherent arrays for laser radars, phase 1
[AD-A245528] p 2912 N92-26663
Effects of the space environment on space-based radar phased-array antenna; status and preliminary observations (LDEF Experiment A0133) p 2883 N92-27086

PHONONS
Generation of nonequilibrium optical phonons in GaAs/AlAs quantum wells by intrasubband and intersubband scatterings
[DE92-010264] p 2993 N92-26207
Some experiences with absorption, phonon Raman, and luminescence spectroscopic probes of crystal structure of f-element compounds
[DE92-007828] p 3006 N92-26851

PHOSPHORIC ACID
Synthesis of novel fluorinated phosphonic acid electrolytes for phosphoric acid fuel cells
[PB92-164300] p 2926 N92-26372

PHOTOCATHODES
Photocathode transfer and storage techniques using alkali vapor feedback control
[DE92-008449] p 2891 N92-26202

PHOTOCHEMICAL REACTIONS
Photoinduced charge separation in solid-state and molecular systems
[DE92-010130] p 3004 N92-26639
Determination of rates of reaction in the gas phase in the troposphere. Theory and practice. Part 3: Rate of indirect photoreaction
[PB92-150374] p 2944 N92-26838
Photochemical energy conversion by membrane-bound photoredox systems
[DE92-008709] p 2927 N92-26858

PHOTODETACHMENT
Multiquanta photodetachment from the H(-) ion
[DE92-010306] p 2911 N92-26573

PHOTODIODES
Numerical modeling of silicon photodiodes for high-accuracy applications with PC-1D
[PB92-148279] p 2894 N92-26821

PHOTODISSOCIATION
Comparison of laser models
[NASA-CR-190302] p 2913 N92-26870

PHOTOELECTRIC EMISSION
Spectroscopic imaging, diffraction, and holography with x ray photoemission
[DE92-009142] p 2996 N92-26187
Investigation of deep dielectric charging and subsequent currents on geosynchronous spacecraft
[AD-A245764] p 2858 N92-26605
A study of buckminsterfullerene using new pseudopotentials p 3005 N92-26774

PHOTOELECTRON SPECTROSCOPY
The application of XPS to the study of MIC
[DE92-010156] p 2879 N92-26813

PHOTOGRAPHS
Kennedy Space Center: Decision on photographic requirements appears justified
[GAO/NSIAD-92-192] p 3009 N92-26828

PHOTOGRAPHY
Kennedy Space Center: Decision on photographic requirements appears justified
[GAO/NSIAD-92-192] p 3009 N92-26828

PHOTOIONIZATION
Energy transfer properties and mechanisms
[DE92-011215] p 2994 N92-26240
Multiquanta photodetachment from the H(-) ion
[DE92-010306] p 2911 N92-26573

PHOTOLITHOGRAPHY
Fracture of structural ceramics in combined mode 1 and mode 2 loading p 2882 N92-26775

PHOTOMETRY
Passive determination of temperature and range using spectral band measurements of photon emittance
[AD-A247147] p 2910 N92-27181

PHOTONICS
High-speed pulse detection room-temperature optical nonlinearities for GaInAs/A1InAs and GaA1InAs/A1InAs multiple quantum wells and integrated mirror etalon at 1.3 micrometers
[AD-A246369] p 2998 N92-26943

PHOTONS
Vibrational dynamics of aniline (N2)1 clusters in their first excited singlet state
[AD-A245812] p 2872 N92-26431
Multiquanta photodetachment from the H(-) ion
[DE92-010306] p 2911 N92-26573
Optical communications with number states p 2889 N92-26604
Reflection of x rays from repeated multilayer structures
[AD-A246562] p 2991 N92-26769
Passive determination of temperature and range using spectral band measurements of photon emittance
[AD-A247147] p 2910 N92-27181
Higher order parametric x rays
[AD-A247148] p 2991 N92-27182

PHOTOSPHERE
Polycyclic aromatic hydrocarbon radiative properties and formation in carbon-rich stellar outflows p 3018 N92-26757

PHOTOSYNTHESIS
Photochemical energy conversion by membrane-bound photoredox systems
[DE92-008709] p 2927 N92-26858
Carbon monoxide metabolism by the photosynthetic bacterium Rhodospirillum rubrum
[DE92-010953] p 2951 N92-26938
Modelling light transfer inside photobiofermentors: Applications to the photosynthetic compartments of CELSS p 2952 N92-26982

PHOTOVOLTAIC CELLS
Aircraft photovoltaic power-generating system p 2926 N92-26581
The effect of sandstorms on PV arrays and components --- photovoltaic cells
[DE92-001240] p 2927 N92-26686

PHOTOVOLTAIC CONVERSION
Aircraft photovoltaic power-generating system p 2926 N92-26581
The effect of sandstorms on PV arrays and components --- photovoltaic cells
[DE92-001240] p 2927 N92-26686

PHYSICAL PROPERTIES
An electroplater's view of PVD processing
[DE92-009052] p 2878 N92-26732

PHYSIOLOGICAL EFFECTS
Biomedical data acquisition and processing technology p 2885 N92-26446
Physiological design goals and proposed thermal limits for US Navy thermal garments: Proceedings of 2 conferences sponsored by the Naval Medical Research and Development Command
[AD-A245543] p 2956 N92-26665
Microgravity simulation p 2964 N92-26994

PHYSIOLOGICAL RESPONSES
LBNP as countermeasure: An automated scenario p 2953 N92-27012

PHYSIOLOGY
User manual for Natick's Footwear Database
[AD-A246275] p 2954 N92-26243

PIEZOELECTRIC CERAMICS
The modeling and control of acoustic/structure interaction problems via piezoceramic actuators: 2-D numerical examples
[NASA-CR-189639] p 2987 N92-26668

PILOT TRAINING
Microcomputer-based instrument flight simulation: Undergraduate pilot training student attitude assessment
[AD-A245449] p 2856 N92-26527

PILOTS (PERSONNEL)
Microcomputer-based instrument flight simulation: Undergraduate pilot training student attitude assessment
[AD-A245449] p 2856 N92-26527

PIONS
Interpretation of distributions on K(sub pi)(sup 0) in pFe, nFe, and piFe interactions at 0.5-5.0 TeV in the framework of contemporary models
[DE92-621189] p 3021 N92-26804

PIPE FLOW
Numerical solution of plastic liquids shape factor
[PB92-133958] p 2896 N92-26496
Passive water hammer in pipes due to flashing
[DE92-004180] p 2899 N92-26699
Water hammer due to the sudden stopping of a flashing flow
[DE92-004181] p 2899 N92-26700
Application of riblet surface to pipe flow p 2903 N92-26915

PIPELINES
Application of riblet surface to pipe flow p 2903 N92-26915

PIPES (TUBES)
Effect of type of load on stress analysis of thin-walled ducts
[NASA-TP-3248] p 2918 N92-26669
Degradation and buckling of metal tubes under cyclic bending and external pressure p 2920 N92-26869

PITTING
Full-scale transmission testing to evaluate advanced lubricants
[NASA-TM-105668] p 2915 N92-26560

PLANE STRAIN
Computational aspects of an implicit finite element procedure for elasto-viscoplastic large deformation problems p 2917 N92-26594

PLANE WAVES
Reflection of x rays from repeated multilayer structures
[AD-A246562] p 2991 N92-26769
A study of buckminsterfullerene using new pseudopotentials p 3005 N92-26774

PLANETARY ATMOSPHERES
Laboratory evaluation and application of microwave absorption properties under simulated conditions for planetary atmospheres
[NASA-CR-190211] p 3019 N92-26438

PLANETARY BOUNDARY LAYER
Theoretical and modeling studies of the marine planetary boundary layer
[AD-A245903] p 2942 N92-26432
A second-order bulk boundary layer model, revision
[AD-A245828] p 2905 N92-26934

PLANETARY MAGNETIC FIELDS
The joint US/UK 1990 epoch world magnetic model
[NASA-CR-190424] p 2942 N92-26406

PLANETARY MAPPING
The joint US/UK 1990 epoch world magnetic model
[NASA-CR-190424] p 2942 N92-26406
The preliminary geodetic control network of Venus
[RAND-N-3437-JPL] p 3019 N92-26819

PLANNING
Information systems planning methodologies: A framework for comparison and selection
[AD-A246527] p 3012 N92-26469
An analysis of commitment strategies in planning: The details
[NASA-TM-107881] p 2983 N92-26643
Explanation-based generalization of partially ordered plans
[NASA-TM-107869] p 2983 N92-26789

Planning and scheduling research at NASA Ames Research Center
[NASA-TM-107888] p 3009 N92-26790
Human cognitive processes in command and control planning. 3: Determining basic processes involved in planning in time and space
[IZF-1991-B-11] p 3010 N92-27046
The APT/ERE planning and scheduling manifesto
[NASA-TM-107906] p 2984 N92-27055

PLANS
Explanation-based generalization of partially ordered plans
[NASA-TM-107869] p 2983 N92-26789

PLANT DESIGN
Inertial fusion energy power plant design using the Compact Torus Accelerator: HYLIFE-CT
[DE92-008941] p 3000 N92-26729

PLANTS (BOTANY)
Higher plant growth in closed environment: Preliminary experiments in life support facility at ESA-ESTEC
p 2951 N92-26978

PLASMA ACCELERATION
Research activities on CFD at the Ship Research Institute p 2902 N92-26908

PLASMA CONTROL
Fusion energy and Canada's role
[DE92-621553] p 2999 N92-26286

PLASMA CURRENTS
The use of ion chromatography-dc plasma atomic emission spectrometry for the speciation of trace metals
[DE92-010317] p 2871 N92-26236
The onset of breakdown in a fast pulsed vacuum diode
[AD-A246395] p 2895 N92-27079

PLASMA DENSITY
The onset of breakdown in a fast pulsed vacuum diode
[AD-A246395] p 2895 N92-27079

PLASMA DIAGNOSTICS
Diagnostic upgrades on MTX
[DE92-009695] p 2906 N92-26230
Preliminary experiment of GDEF (Gas Dynamics Experiment Facility) p 2885 N92-26442

PLASMA DIODES
The onset of breakdown in a fast pulsed vacuum diode
[AD-A246395] p 2895 N92-27079

PLASMA DYNAMICS
Plasma dynamics of the Earth magnetopause-boundary layer and its coupling to the polar ionosphere
p 2944 N92-26865

PLASMA HEATING
Diagnostic upgrades on MTX
[DE92-009695] p 2906 N92-26230
Spheroidization and densification of Nickel powders by RF-induction plasma
[PB92-151893] p 2879 N92-26787
The onset of breakdown in a fast pulsed vacuum diode
[AD-A246395] p 2895 N92-27079

PLASMA INTERACTIONS
Plasma interactions in a plasma erosion opening switch
[AD-A246179] p 2999 N92-26416
Solar wind interaction with Venus and Mars
p 3020 N92-26779

PLASMA RADIATION
The use of ion chromatography-dc plasma atomic emission spectrometry for the speciation of trace metals
[DE92-010317] p 2871 N92-26236

PLASMA WAVES
High frequency Raman current drive
[PB92-142223] p 2893 N92-26497
Scenarios for the nonlinear evolution of alpha particle induced Alfven wave instability
[DE92-010549] p 3000 N92-26550

PLASMAGUIDES
Diagnostic upgrades on MTX
[DE92-009695] p 2906 N92-26230

PLASMAS (PHYSICS)
High frequency Raman current drive
[PB92-142223] p 2893 N92-26497
Short-wave low-frequency spectra in a current-carrying plasma
[DE92-621529] p 3001 N92-26808

PLASTIC DEFORMATION
Failure studies of bimaterial interfaces and constrained ductile layers p 2868 N92-26559
Computational aspects of an implicit finite element procedure for elasto-viscoplastic large deformation problems p 2917 N92-26594
An investigation of the mechanical properties and microscopic structure of extruded powder aluminum subjected to biaxial loadings at elevated temperature
p 2879 N92-26770

PLASTIC FLOW
Numerical solution of plastic liquids shape factor
[PB92-133958] p 2896 N92-26496

PLATES (STRUCTURAL MEMBERS)
Buckling of unidirectional graphite/epoxy composite plates at low temperatures
[AD-A246602] p 2869 N92-26796

PLATINUM
Magneto-optical multilayers — optical data storage
[DE92-009726] p 2997 N92-26565

PLAYAS
Analysis of thermal infrared data acquired over playas: Silver Lake and Deep Springs Lake, California and Lunar Lake, Nevada p 2926 N92-26864

PLUMES
The composite structure of thermals as derived from aircraft observations p 2941 N92-26346
Plume trajectory validation study: Brown cloud support project overview
[DE92-006911] p 2928 N92-26390
Acoustic interactions between an altitude test facility and jet engine plumes: Theory and experiments
[NASA-CR-190423] p 2853 N92-26405

PLY ORIENTATION
Analysis and modeling of high-temperature performance of advanced fiber composites p 2868 N92-26564

PNEUMATIC EQUIPMENT
Pneumatically actuated multiple store launcher
[AD-D015237] p 2853 N92-27188

POISSON EQUATION
Numerical solution of plastic liquids shape factor
[PB92-133958] p 2896 N92-26496

POLAR CAPS
Polar cap boundary and structure of dayside cusp as determined by ion precipitation p 2936 N92-26300
Plans for the EISCAT Svalbard (Norway) radar
p 2936 N92-26305
Balloons for conjugate cusp studies in the 1990's
p 2938 N92-26315
The dynamic response of the westward auroral electrojet and polar cap currents to solar wind-magnetosphere coupling p 2943 N92-26622

POLAR CUSPS
Cluster Dayside Polar Cusp
[ESA-SP-330] p 2935 N92-26294
The Norwegian upper atmosphere programme in Svalbard (Norway) p 2935 N92-26295
Research programmes at Svalbard (Norway)
p 2935 N92-26297
The Polar Geophysical Institute program of the theoretical and experimental investigation on cusp
p 2935 N92-26298
Cusp and cleft studies in Greenland
p 2935 N92-26299
Polar cap boundary and structure of dayside cusp as determined by ion precipitation p 2936 N92-26300
Antarctic studies of the cusp p 2936 N92-26301
Incoherent scatter radar measurements of the cusp
p 2936 N92-26303
Cusp studies with HF radars p 2936 N92-26304
Plans for the EISCAT Svalbard (Norway) radar
p 2936 N92-26305
The present understanding of the cusp
p 2936 N92-26306
Solar wind-magnetosphere coupling processes observed near the dayside cusp/cleft
p 2937 N92-26307
The ionospheric signature of flux transfer events
p 2937 N92-26308
A model of the dayside magnetosphere and breakups in the cusp region p 2937 N92-26312
Imaging the Earth's magnetosphere using ground magnetometer arrays p 2938 N92-26314
Requirements for coordinated Cluster and ground-based observations of the cusp p 2938 N92-26318
Mathematical model of physical processes responsible for generation of magnetospheric electric fields and their penetration into the Earth's magnetosphere
p 2938 N92-26319

POLARIMETRY
Radar scattering as a source of geological information on Venus and Earth p 3019 N92-26778

POLARIZATION (CHARGE SEPARATION)
Photoinduced charge separation in solid-state and molecular systems
[DE92-010130] p 3004 N92-26639

POLARIZATION CHARACTERISTICS
Vacuum polarization tensor in 3-dimensional quantum electrodynamics
[DE92-621141] p 2890 N92-26799

POLARIZED LIGHT
Cluster model of polarization reflection from metallic surfaces
[AD-A245781] p 2996 N92-26241

POLARIZED RADIATION
An antenna design for PANSAT using NEC
[AD-A245482] p 2888 N92-26399

POLARIZERS
Polarisation effects in fibre lasers
p 2911 N92-26571

POLICIES
Competing economies: America, Europe, and the Pacific rim
[PB92-115757] p 3014 N92-26730
An analysis of the role of the budget committees in the Congressional budget process
[AD-A246005] p 3014 N92-26761
NASA/DOE/DOD nuclear propulsion technology planning: Summary of FY 1991 interagency panel results
[NASA-TM-105703] p 2861 N92-26792
Managing Federal information resources: Under the Paperwork Reduction Act of 1980
[PB92-154905] p 3014 N92-26926

POLLUTION CONTROL
Summary of NOx control technologies and their availability and extent of application
[PB92-158260] p 2928 N92-26373
Running a conference as a clean product. International Conference on Pollution Prevention: Clean technologies and clean products
[PB92-109099] p 2930 N92-26495
Environmental implications of increased biomass energy use
[DE92-001219] p 2932 N92-26810
Evaluation of carbon dioxide emission control strategies in New York State
[DE92-010162] p 2932 N92-26825
Waste minimization for non-agricultural pesticide applicators: EPA's pollution prevention guide
[PB92-153774] p 2933 N92-26889
Technology for reduction of CO2 emissions from the transportation sector
[PB92-153733] p 2933 N92-26929

POLLUTION MONITORING
Noxious matter transportation in the Alpine regions
p 2934 N92-26332

POLLUTION TRANSPORT
Noxious matter transportation in the Alpine regions
p 2934 N92-26332
Model studies of the transfer of radionuclides in the Finnish environment
[VTT-PUBL-81] p 2929 N92-26482
Assessment of biospheric behaviour of releases from nuclear waste repositories, appendix 2
p 2929 N92-26484
Sensitivity analysis of biospheric behaviour of radionuclides released from nuclear waste repositories, appendix 4 p 2929 N92-26486
Biosphere model validation by intercomparison to observed behaviour of fallout radionuclides in the aquatic environment, appendix 5 p 2930 N92-26487
Modeling transfer of Cs-137 fallout in a large Finnish watercourse, appendix 6 p 2930 N92-26488
A finite element/finite difference approach for modeling three-dimensional flow and pollutant dispersion around structures
[DE92-007322] p 2934 N92-26935

POLYESTERS
Penetration of laminated composites by projectiles
p 2869 N92-26861

POLYMERIC FILMS
Selective metallization of carbonyl-containing polymer films
[AD-D015219] p 2883 N92-27187

POLYMERS
Numerical solution of plastic liquids shape factor
[PB92-133958] p 2896 N92-26496
X ray scattering studies of non-equilibrium ordering processes
[DE92-010311] p 2877 N92-26542

POLYMETHYL METHACRYLATE
Solid fuel ramjet infrared signature
[AD-A246299] p 2860 N92-26362

POLYNOMIALS
Ocean bottom modeling for ray acoustics
[AD-A246287] p 2948 N92-26360
Finding a best subtree of a tree
[REPT-91-041] p 2986 N92-26420
A random polynomial algorithm for the matroid parity base problem
[REPT-91-079] p 2974 N92-26449
N-learners problem: Learning Boolean combinations of halfspaces
[DE92-010390] p 2987 N92-26545
Decomposition of bipartite graphs under degree constraints
[PB92-148626] p 2988 N92-26817
Downdating of Szego polynomials and data fitting applications
[AD-A245825] p 2988 N92-26900

POLYNUCLEOTIDES
A computer system for access to distributed genome mapping data
[DE92-008875] p 3011 N92-26453
PONDEROMOTIVE FORCES
Multiquanta photodetachment from the H(-) ion
[DE92-010306] p 2911 N92-26573
POROSITY
Spheroidization and densification of Nickel powders by RF-induction plasma
[PB92-151893] p 2879 N92-26787
Two-phase flow of Newtonian and Non-Newtonian fluids in a porous medium applied to water coning
[PB92-151109] p 2900 N92-26836
Exploring possible relationships between plate pore size character and cell performance p 2863 N92-27141
POROUS MATERIALS
A boundary integral method for steady unsaturated flow in nonhomogeneous media
[DE92-009066] p 2897 N92-26644
Application of fluorescent-particle imaging to measuring flow in complex media
[DE92-009121] p 2898 N92-26645
POROUS PLATES
Development of European sublimator technology for EVA p 2968 N92-27018
PORTABLE EQUIPMENT
Advanced technology for portable personal visualization
[AD-A245819] p 2954 N92-26179
Engineering of a new overall system to improve the interaction between the crew and the ground-based scientists and personnel p 2964 N92-26995
PORTABLE LIFE SUPPORT SYSTEMS
Heat rejection system for an advanced extravehicular mobility unit portable life support system p 2968 N92-27020
Metal oxide absorbents for regenerative carbon dioxide and water vapor removal for advanced portable life support systems p 2968 N92-27021
POSITION (LOCATION)
Dead reckoning navigation for walking robots
[NASA-CR-190296] p 2982 N92-26429
Estimation of geopotential differences over intercontinental locations using satellite and terrestrial measurements p 2924 N92-26728
POSITION INDICATORS
Development and testing of a prototype electro-optical phase encoded position transducer
[AD-A245486] p 2908 N92-26401
POSITION SENSING
Development and testing of a prototype electro-optical phase encoded position transducer
[AD-A245486] p 2908 N92-26401
POSITIONING
On certain methods of determining the ellipses an d ellipsoids of the positioning accuracy of robot manipulators
[ISSN-0208-5658] p 2914 N92-26284
An adaptive correction technique for Differential Global Positioning System p 2851 N92-26623
POSITIVE FEEDBACK
Equilibrium-analysis of projected climate change effects on the global soil organic matter pool
[PB92-153022] p 2930 N92-26509
POSITIVE IONS
Recent developments in nickel electrode analysis p 2865 N92-27158
POSITRONS
The sixteen channel CAMAC constant fraction discriminator for APEX
[DE92-010550] p 2970 N92-26551
Effect of interstitials on the trapping of hydrogen in iron-single crystals
[AD-A246412] p 3006 N92-27064
POSTFLIGHT ANALYSIS
Development and testing of an unmanned air vehicle telemetry system
[AD-A246577] p 2858 N92-26621
Space environmental effects on coated optics p 2999 N92-27098
Advanced photovoltaic experiment, S0014: Preliminary flight results and post-flight findings p 2927 N92-27101
Evaluation of LDEF experiment S1002 p 2883 N92-27102
LDEF SP-HVDE (Space Plasma-High Voltage Drainage Experiment) post-flight results: Leakage current and discharge p 2895 N92-27103
Long Duration Exposure Facility (LDEF) low temperature heat pipe experiment package (HEPP) flight results p 2906 N92-27104
Results from the LDEF/A0076 cascaded variable conductance heatpipe experiment p 2906 N92-27106
POSTMISSION ANALYSIS (SPACECRAFT)
Design and performance of the Spacelab Astro-1 mission heat pipe radiator p 2859 N92-26965
SPOT multimission platform thermal control: Five years of in-flight results p 2860 N92-26998
POSTURE
CAD system for HFE analyses: Zero-g posture in optimisation of Columbus APM crew workstations --- human factors engineering p 2963 N92-26991
Architectural studies relating to human body motion morphology in microgravity p 2953 N92-27011
POTABLE WATER
Catalytic wet-oxidation of human waste produced in a space habitat: Purification of the oxidized liquor for human drinking p 2957 N92-26954
POTASSIUM
Recent developments in nickel electrode analysis p 2865 N92-27158
POTASSIUM PERCHLORATES
Burn-rate studies with iron/potassium perchlorate heat pellets
[DE92-008524] p 2875 N92-26722
POTENTIAL ENERGY
Simulation studies for surfaces and materials strength
[NASA-CR-190340] p 3001 N92-26265
POTENTIAL FIELDS
A supervisory control strategy for navigation of mobile robots in dynamic environments p 2983 N92-26734
POWDER (PARTICLES)
Materials compatibility and wall stresses in hydride storage beds
[DE92-009432] p 2870 N92-26201
Neutron powder diffraction study of deuterated beta-acetonitrile p 3002 N92-26324
Microstructural evaluation of as-solidified and heat treated gamma-TiAl based powders
[DE92-008956] p 2881 N92-26455
POWDER METALLURGY
Microstructural evaluation of as-solidified and heat treated gamma-TiAl based powders
[DE92-008956] p 2881 N92-26455
An investigation of the mechanical properties and microscopic structure of extruded powder aluminum subjected to biaxial loadings at elevated temperature p 2879 N92-26770
Spheroidization and densification of Nickel powders by RF-induction plasma
[PB92-151893] p 2879 N92-26787
Powder processing of aero-engine components
[PNR-90813] p 2880 N92-27044
POWDERED ALUMINUM
An investigation of the mechanical properties and microscopic structure of extruded powder aluminum subjected to biaxial loadings at elevated temperature p 2879 N92-26770
POWER EFFICIENCY
Throttleless Otto-cycle natural gas engines
[PB92-164482] p 2914 N92-26371
POWER SPECTRA
Kalman smoother applied to lace
[AD-A246439] p 2859 N92-27030
PRECIPITATION (METEOROLOGY)
Precipitation formation processes in convective and stratiform clouds as deduced by coordinated polarimetric radar and aircraft measurements p 2941 N92-26342
Estimating mesoscale, orographically enhanced precipitation using synoptic scale data
[AD-A245749] p 2946 N92-26562
Validation of numerical models by TRMM and validation of TRMM by numerical models
[TW-8] p 2923 N92-26709
Water cycles around the subtropical frontal zone in East Asia
[TW-9] p 2923 N92-26710
PRECIPITATION HARDENING
Deformation behavior of an age-hardenable Beta + Alpha-Two titanium alloy
[AD-A246362] p 2879 N92-26939
PRECISION
High precision timing of millisecond pulsars p 3015 N92-26760
Precision of the long baseline acoustic navigation system used by Pegasus
[AD-A246598] p 2852 N92-26795
PREDICTION ANALYSIS TECHNIQUES
Atmospheric parameters of a soft x ray selected set of hot DA white dwarfs p 3017 N92-26576
The dynamic response of the westward auroral electrojet and polar cap currents to solar wind-magnetosphere coupling p 2943 N92-26622
Correlation and prediction of dynamic human isolated joint strength from lean body mass
[NASA-TP-3207] p 2956 N92-26682
Evaluation of the computational validity of the image model in predicting the sound field in a wedge-shaped layer using acoustical reciprocity
[AD-A246548] p 2992 N92-26688
Progress towards understanding and predicting convection heat transfer in the turbine gas path
[NASA-TM-105674] p 2898 N92-26690
A supervisory control strategy for navigation of mobile robots in dynamic environments p 2983 N92-26734
Nonstationary higher order spectral analysis
[AD-A246580] p 2991 N92-26772
Discrete sequence prediction and its applications
[NASA-TM-107865] p 2984 N92-26791
Penetration of laminated composites by projectiles p 2869 N92-26861
Degradation and buckling of metal tubes under cyclic bending and external pressure p 2920 N92-26869
Modelling default and likelihood reasoning as probabilistic
[NASA-TM-107889] p 2984 N92-26893
Computer Program Estimate Trend (ESTREND): A system for the detection of trends in water-quality data
[PB92-147727] p 2933 N92-26931
Update of a nickel-hydrogen cycle life model p 2866 N92-27162
PREDICTIONS
Predictability of long-term creep and rupture in a nozzle-to-sphere vessel model
[DE92-008099] p 2919 N92-26845
PREGNANCY
Adverse reproductive events and electromagnetic radiation
[PB92-145796] p 2953 N92-26512
PREMIXED FLAMES
Advancing natural gas combustion science and technology-low NOx
[PB92-137652] p 2876 N92-26782
PRESERVING
Application of irradiation techniques to food and foodstuffs
[DE92-614952] p 2954 N92-26186
PRESSING (FORMING)
Relationship between composition, structure, properties, thermo-mechanical processing and ballistic performance of tungsten heavy alloys
[AD-A245649] p 2876 N92-26172
PRESSURE DEPENDENCE
Recent advances in shock and quasi-isentropic compression techniques for dynamic material property studies
[DE92-007988] p 2919 N92-26852
PRESSURE DISTRIBUTION
Use of an approximate similarity principle for the thermal scaling of a full-scale thrust augmenting ejector
[NASA-TM-105724] p 2854 N92-26613
Subsonic investigations of vortex interaction control for enhanced high-alpha aerodynamics of a chine forebody/Delta wing configuration
[NASA-CR-189641] p 2849 N92-26652
Evaluation of the computational validity of the image model in predicting the sound field in a wedge-shaped layer using acoustical reciprocity
[AD-A246548] p 2992 N92-26688
PRESSURE EFFECTS
Recent advances in shock and quasi-isentropic compression techniques for dynamic material property studies
[DE92-007988] p 2919 N92-26852
Degradation and buckling of metal tubes under cyclic bending and external pressure p 2920 N92-26869
PRESSURE GRADIENTS
Study of entrainment mechanisms in convective clouds
[NASA-CR-190223] p 2946 N92-26735
Observations of wind forced circulation on the continental shelf off Point Sur, California from a self-contained acoustic Doppler current profiler
[AD-A246437] p 2950 N92-27029
PRESSURE MEASUREMENT
Gas-pressure studies with Li(Si)/FeS2 thermal batteries
[DE92-010801] p 2892 N92-26238
Water hammer due to the sudden stopping of a flashing flow
[DE92-004181] p 2899 N92-26700
PRESSURE RATIO
Evaluation of the computational validity of the image model in predicting the sound field in a wedge-shaped layer using acoustical reciprocity
[AD-A246548] p 2992 N92-26688
PRESSURE SENSORS
Investigation on a partial pressure carbon dioxide sensor p 2968 N92-27019
PRESSURE VESSELS
Turbocharged pressurized combustion system
[PB92-142579] p 2873 N92-26521

PREVENTION
Running a conference as a clean product. International Conference on Pollution Prevention: Clean technologies and clean products
[PB92-109099] p 2930 N92-26495
PRIMARY BATTERIES
NASA. Johnson Space Center primary battery applications p 2863 N92-27142
PRIMITIVE EQUATIONS
Description of a global shallow water model based on the spectral transform method
[PB92-155258] p 2928 N92-26352
PROBABILITY DISTRIBUTION FUNCTIONS
Characterization of discrete-time linear periodically time-varying systems
[AD-A245822] p 2989 N92-26180
PROBABILITY THEORY
Lower confidence limit expressions for P(X greater than y) and P(X greater than Y) under normality
[AD-A245787] p 2989 N92-26177
Extracting fuzzy rules under uncertainty and measuring definability using rough sets
[NASA-CR-190396] p 2972 N92-26197
Measuring uncertainty by extracting fuzzy rules using rough sets
[NASA-CR-190395] p 2972 N92-26198
On certain methods of determining the ellipses an d ellipsoids of the positioning accuracy of robot manipulators
[ISSN-0208-5658] p 2914 N92-26284
Composite strength statistics from fiber strength statistics
[AD-A245616] p 2867 N92-26383
Effects of video bandwidth on the performance of a square law detector with Gaussian IF and video filters
[AD-A246506] p 2989 N92-26467
STATLIB/PC users guide
[AD-A245462] p 2975 N92-26530
On the stochastic fatigue crack growth problem p 2917 N92-26557
Introduction in IND and recursive partitioning
[NASA-TM-107879] p 2983 N92-26629
Tools and techniques for adding fault tolerance to distributed and parallel programs
[AD-A245510] p 2980 N92-26677
Sturm-Liouville eigenfunctions expressed in determinant form
[AD-A245991] p 2987 N92-26755
Modelling default and likelihood reasoning as probabilistic
[NASA-TM-107889] p 2984 N92-26893
Bayesian classification theory
[NASA-TM-107885] p 2988 N92-26894
Stochastic versions of the EM algorithm
[AD-A246929] p 2989 N92-27174
PROBLEM SOLVING
Applying knowledge compilation techniques to model-based reasoning
[NASA-TM-107876] p 2984 N92-26885
Applying artificial intelligence to the control of space telescopes (extended abstract)
[NASA-TM-107913] p 3015 N92-26886
Institute for Computational Mechanics in Propulsion (ICOMP)
[NASA-TM-105612] p 2989 N92-27196
PROCESS CONTROL (INDUSTRY)
Developing an adaptive scheduling support environment
[ISBN-90-9004609-7] p 3008 N92-26250
PROCUREMENT POLICY
Best value contracting in the procurement of engineering and technical services
[AD-A245524] p 3009 N92-26660
PRODUCT DEVELOPMENT
The 1990 progress report and future plans
[NASA-TM-107911] p 2984 N92-26887
PRODUCTION MANAGEMENT
Knowledge-based production management: Approaches, results, and prospects
[AD-A245714] p 3008 N92-26426
PRODUCTION PLANNING
Developing an adaptive scheduling support environment
[ISBN-90-9004609-7] p 3008 N92-26250
PRODUCTIVITY
Global assessment of promising forest management practices for sequestration of carbon
[PB92-153006] p 2930 N92-26510
Measuring the effectiveness of information systems
[AD-A246007] p 3013 N92-26762
PROGRAM VERIFICATION (COMPUTERS)
Software maturity model applied to SDI
[AD-A245439] p 2972 N92-26276
Paralex: An environment for parallel programming in distributed systems
[AD-A245445] p 2979 N92-26278
Run-time support for dynamic load balancing and debugging in paralex
[AD-A245446] p 2979 N92-26279
An empirical approach to analysis of similarities between software failure regions
[AD-A246208] p 2974 N92-26461
Automated interpretation of S-invariants of predicate/transition nets: An application of non-classical logics
[PB92-143544] p 2975 N92-26500
PROGRAMMING LANGUAGES
Advanced software development workstation project: Engineering scripting language. Graphical editor
[NASA-CR-190391] p 2971 N92-26183
Implementing error values in applicative languages
[DE92-008927] p 2972 N92-26233
The SOL object-oriented database language
[REPT-91-053] p 2973 N92-26421
Matched field processing on the connection machine
[AD-A245469] p 2980 N92-26531
Research accomplished at the Knowledge Based Systems Lab: IDEF3, version 1.0
[NASA-CR-190279] p 2975 N92-26587
The 8th IEEE Workshop on Real-Time Operating Systems
[AD-A246126] p 2976 N92-26685
Evaluation criteria for real-time specification languages
[AD-A246612] p 2976 N92-26766
PROGRAMS
Small business innovation research: Program solicitation closing date, 27 January 1992
[DE92-010132] p 3009 N92-26811
PROJECT MANAGEMENT
The Tropical Rainfall Measuring Mission (TRMM) program at the Goddard Space Flight Center (GSFC)
[TW-1] p 2922 N92-26702
Status of TRMM (NASDA) --- tropical rainfall measuring mission
[TW-3] p 2923 N92-26704
Small business innovation research: Program solicitation closing date, 27 January 1992
[DE92-010132] p 3009 N92-26811
Institute for Computational Mechanics in Propulsion (ICOMP)
[NASA-TM-105612] p 2989 N92-27196
PROJECT PLANNING
US Small Business Administration FY 1990 national accomplishment report and FY 1991 national affirmative employment program plan
[PB92-157064] p 3008 N92-26353
Tropical Rainfall Measuring Mission (TRMM) science report
[TW-5] p 2923 N92-26706
NASA/DOE/DOD nuclear propulsion technology planning: Summary of FY 1991 interagency panel results
[NASA-TM-105703] p 2861 N92-26792
PAGES. Past global changes project: Proposed implementation plans for research activities
[IGBP-REPT-19-ATTACH-10] p 2934 N92-27082
PROJECTILES
Spinning jets from shaped charges with flow turned liners
[MBB-UA-1197-90-PUB] p 2886 N92-26246
Numerical simulations of gun-launched kinetic energy projectiles subjected to asymmetric projectile base pressure
[DE92-005065] p 2857 N92-26693
PROPAGATION VELOCITY
Imaging earth's interior: Tomographic inversions for mantle P-wave velocity structure
[DE92-010271] p 2934 N92-26208
Fault zone structure determined through the analysis of earthquake arrival times
[DE92-010322] p 2935 N92-26239
PROPANE
Conversion of ethane and of propane to higher olefin hydrocarbons
[DE92-009487] p 2870 N92-26209
PROPELLER BLADES
Algorithms for blending surface generation
[AD-A245686] p 2975 N92-26524
PROPRIOCEPTION
Modeling of explorative procedures for remote object identification
[AD-A245525] p 2922 N92-26661
PROPULSION
LDEF: 69 Months in Space. First Post-Retrieval Symposium, part 3
[NASA-CP-3134-PT-3] p 3022 N92-27083
PROPULSION SYSTEM CONFIGURATIONS
ASTOVL propulsion systems: Configuration and concept choice
[PNR-90809] p 2855 N92-27041
PROPULSION SYSTEM PERFORMANCE
Conceptual design study for the use of COBE rocket engines on the Tropical Rainfall Measuring Mission
[NASA-CR-190383] p 2945 N92-26535
An instrument for engine torque estimation and misfire detection --- torque p 2909 N92-26738
Rocket engine diagnostics using qualitative modeling techniques
[NASA-TM-105714] p 2861 N92-27033
ASTOVL propulsion systems: Configuration and concept choice
[PNR-90809] p 2855 N92-27041
PROTECTIVE CLOTHING
Effectiveness of a selected microclimate cooling system in increasing tolerance time to work in the heat. Application to Navy Physiological Heat Exposure Limits (PHEL) curve 5
[AD-A246529] p 2952 N92-26470
Effect of textile test sample size on assessment of protection to skin from thermal radiation
[AD-A246535] p 2955 N92-26472
Physiological design goals and proposed thermal limits for US Navy thermal garments: Proceedings of 2 conferences sponsored by the Naval Medical Research and Development Command
[AD-A245543] p 2956 N92-26665
PROTECTIVE COATINGS
The effect of sandstorms on PV arrays and components --- photovoltaic cells
[DE92-001240] p 2927 N92-26686
Novel molecular sources for dispersing boron in carbon-carbon composites
[AD-A246999] p 2870 N92-26882
The importance of chemical reactions with environment for ablation process of thermal protection and structural materials p 2883 N92-27015
Space environmental effects on coated optics p 2999 N92-27098
Durability evaluation of photovoltaic blanket materials exposed on LDEF tray S1003 p 2883 N92-27100
PROTEINS
Chemolithotropic hydrogen-oxidizing bacteria and their possible functions in closed ecological life-support systems p 2951 N92-26979
PROTOCOL (COMPUTERS)
An adaptive, packet-switched HF data terminal: Functional overview and initial performance
[AD-A246318] p 2973 N92-26292
Selection and specification of a data link protocol for VSAT based inter-LAN communications
[AD-A246289] p 2979 N92-26361
A security analysis of version 2 of the Network Time Protocol (NTP): A report to the privacy and security research group
[NASA-CR-190428] p 2981 N92-27183
PROTONS
Simultaneous observations of extensive air showers and underground muons at Soudan 2
[DE92-010282] p 3020 N92-26211
Composition studies based on coincident air shower array and underground muon data
[DE92-010345] p 3021 N92-26253
Time-resolved laser studies on the proton pump mechanism of bacteriorhodopsin
[DE92-003218] p 2951 N92-26493
PROTOTYPES
The development of a design database for the computer aided prototyping system
[AD-A245786] p 3010 N92-26176
Development and testing of a prototype electro-optical phase encoded position transducer
[AD-A245486] p 2908 N92-26401
A prototype multi-media data base for tracking interface relationships and performing cost tradeoffs for the Sea Launch and Recovery (SEALAR) space launch system
[AD-A245481] p 2857 N92-26515
Technical specification for the Sandia Management Restructure Study Team (MRST) Prototype Information System
[DE92-010360] p 3012 N92-26575
A prototype semantic integrity front end expert system for a relational database
[AD-A246084] p 3013 N92-26765
Progress in the development of the Hermes evaporators p 2962 N92-26984
Hughes advanced nickel-cadmium batteries: An update p 2862 N92-27136
PROVING
Proving properties of real-time systems through logical specifications and Petri net models
[REPT-91-072] p 2973 N92-26448
PROXIMITY EFFECT (ELECTRICITY)
Recent progress in calorimeters with transition edge thermometers p 2907 N92-26394

PSEUDOPOTENTIALS
A study of buckminsterfullerene using new pseudopotentials p 3005 N92-26774
PSYCHOLOGICAL FACTORS
Multi-cultural components and keys for European worldwide space programs p 2857 N92-27008
PULSARS
Underground muons observed in the Soudan 2 detector from the directions of x ray sources
[DE92-010344] p 3021 N92-26264
High precision timing of millisecond pulsars p 3015 N92-26760
Tensor-multi-scalar theories of gravitation
[PB92-152305] p 2943 N92-26820
PULSE POSITION MODULATION
Optical communications with number states p 2889 N92-26604
PULSE REPETITION RATE
A high repetition rate lidar
[AD-A245382] p 2890 N92-26872
PULSED LASERS
Energy threshold for laser induced breakdown on a metal surface under high and ultra high vacuum conditions
[AD-A246212] p 2911 N92-26462
A high repetition rate lidar
[AD-A245382] p 2890 N92-26872
PULSES
A model for aerodynamically-valved pulse combustion
[DE92-009887] p 2871 N92-26262
Plasma interactions in a plasma erosion opening switch
[AD-A246179] p 2999 N92-26416
PUMPS
Fan/pump/separator technology development for EVA p 2966 N92-27006
PUNCHED CARDS
Buffered serial data card
[AD-A246435] p 2852 N92-26948
PURIFICATION
Water recovery from condensate of crew respiration products aboard the Space Station p 2956 N92-26951
Space Station Freedom regenerative water recovery system configuration selection p 2957 N92-26953
Catalytic wet-oxidation of human waste produced in a space habitat: Purification of the oxidized liquor for human drinking p 2957 N92-26954
PUSH-PULL AMPLIFIERS
Fiber-optic flexural disk accelerometer
[AD-A246203] p 2908 N92-26459
PYROLYSIS
Aromatic-radical oxidation kinetics
[DE92-010821] p 2871 N92-26274
PYROTECHNICS
Pyrotechnic device reliability
[AD-A245818] p 2883 N92-26178
Burn-rate studies with iron/potassium perchlorate heat pellets
[DE92-008524] p 2875 N92-26722

Q

Q SWITCHED LASERS
Optimization of a color center Q-switched Nd:YLF laser
[DE92-621612] p 2910 N92-26287
Energy threshold for laser induced breakdown on a metal surface under high and ultra high vacuum conditions
[AD-A246212] p 2911 N92-26462
Polarisation effects in fibre lasers p 2911 N92-26571
Squeezed light and twin beams generation with a Q-switched laser p 2912 N92-26603
QUADRUPOLES
Theory of electromagnetic instability of an intense beam in a quadrupole focusing system
[AD-A246560] p 2990 N92-26768
QUALIFICATIONS
NASA. Johnson Space Center primary battery applications p 2863 N92-27142
QUALITY CONTROL
Improving CMM software quality
[NPL-DITC-194/92] p 2974 N92-26450
Rule-based expert system for evaluating the quality of long-term, in-situ, gas chromatographic measurements of atmospheric methane
[PB92-128560] p 2876 N92-26812
Kennedy Space Center: Decision on photographic requirements appears justified
[GAO/NSIAD-92-192] p 3009 N92-26828
QUANTITATIVE ANALYSIS
Non-destructive analysis for hydrogen concentrations in materials
[AD-A246098] p 2874 N92-26541
QUANTUM EFFICIENCY
Quantum dynamics of helium clusters
[AD-A245752] p 2995 N92-26588
QUANTUM ELECTRODYNAMICS
Vacuum polarization tensor in 3-dimensional quantum electrodynamics
[DE92-621141] p 2890 N92-26799
QUANTUM ELECTRONICS
Crossovers of the density of states in two-direction double-barrier resonant-tunneling structures
[AD-A246124] p 3005 N92-26684
QUANTUM MECHANICS
Quantum dynamics of helium clusters
[AD-A245752] p 2995 N92-26588
QUANTUM OPTICS
Squeezed light and twin beams generation with a Q-switched laser p 2912 N92-26603
Optical communications with number states p 2889 N92-26604
QUANTUM STATISTICS
Non-compact WZW conformal field theories
[PB92-125038] p 3007 N92-26805
QUANTUM THEORY
Hamiltonian lattice field theory: Computer calculations using variational methods
[DE92-010479] p 2985 N92-26232
Topics in particle physics and cosmology
[DE92-010478] p 3019 N92-26385
Finite temperature quantum field theory in curved spacetime p 3007 N92-26780
Dynamic properties of quasi-two-dimensional one component plasmas
[DE92-621523] p 3000 N92-26806
QUANTUM WELLS
Generation of nonequilibrium optical phonons in GaAs/AlAs quantum wells by intrasubband and intersubband scatterings
[DE92-010264] p 2993 N92-26207
Crossovers of the density of states in two-direction double-barrier resonant-tunneling structures
[AD-A246124] p 3005 N92-26684
High-speed pulse detection room-temperature optical nonlinearities for GaInAs/A1InAs and GaA1InAs/A1InAs multiple quantum wells and integrated mirror etalon at 1.3 micrometers
[AD-A246369] p 2998 N92-26943
QUARTZ CRYSTALS
Radiation sensitivity of quartz crystal oscillators experiment for the Long Duration Exposure Facility (LDEF) p 2895 N92-27111

R

RADAR ANTENNAS
Effects of the space environment on space-based radar phased-array antenna; status and preliminary observations (LDEF Experiment A0133) p 2883 N92-27086
RADAR DATA
Radar scattering as a source of geological information on Venus and Earth p 3019 N92-26778
RADAR DETECTION
The Lockheed F-117A
[RAND-P-7746-RGS] p 2852 N92-26673
RADAR EQUIPMENT
Status of TRMM project: Rain radar in the Tropical Rainfall Measuring Mission
[TW-2] p 2922 N92-26703
RADAR IMAGERY
Feature discovery via neural networks for object recognition in SAR imagery
[DE92-007046] p 2891 N92-26902
RADAR MAPS
Incoherent scatter radar measurements of the cusp p 2936 N92-26303
RADAR MEASUREMENT
Precipitation formation processes in convective and stratiform clouds as deduced by coordinated polarimetric radar and aircraft measurements p 2941 N92-26342
Remote sensing of atmosphere with aircraft borne lidar systems p 2941 N92-26347
International Conference on Japanese Earth Observation Programs: TRMM Workshop
[JTN-92-80345] p 2922 N92-26701
The Tropical Rainfall Measuring Mission (TRMM) program at the Goddard Space Flight Center (GSFC)
[TW-1] p 2922 N92-26702
Status of TRMM (NASDA) --- tropical rainfall measuring mission
[TW-3] p 2923 N92-26704
TRMM Mission Team --- tropical rainfall measuring mission
[TW-4] p 2923 N92-26705
Tropical Rainfall Measuring Mission (TRMM) science report
[TW-5] p 2923 N92-26706
Storm model and beam filling problem for rain retrievals
[TW-6] p 2923 N92-26707
Development of TRMM radar rainfall retrieval algorithms
[TW-7] p 2923 N92-26708
Validation of numerical models by TRMM and validation of TRMM by numerical models
[TW-8] p 2923 N92-26709
Water cycles around the subtropical frontal zone in East Asia
[TW-9] p 2923 N92-26710
Rainfall pattern over the tropical rain forest
[TW-10] p 2923 N92-26711
Utilization of tropical convection data for meteorological operation
[TW-11] p 2924 N92-26712
TRMM and Asian monsoon --- tropical rainfall measuring mission
[TW-12] p 2924 N92-26713
Research plan for utilizing TRMM data in MRI --- tropical rainfall measuring mission
[TW-13] p 2924 N92-26714
Research program on hydrology
[TW-14] p 2924 N92-26715
RADAR RANGE
Fast envelope correlation for passive ranging
[AD-A246333] p 2888 N92-26388
RADAR SCATTERING
Radar target identification by natural resonances: Evaluation of signal processing algorithms
[AD-A246566] p 2889 N92-26619
Radar scattering as a source of geological information on Venus and Earth p 3019 N92-26778
RADAR SIGNATURES
Radar target identification by natural resonances: Evaluation of signal processing algorithms
[AD-A246566] p 2889 N92-26619
RADAR TARGETS
Performance enhancement of the NPS Transient Electromagnetic Scattering Laboratory
[AD-A246300] p 2888 N92-26363
Radar target identification by natural resonances: Evaluation of signal processing algorithms
[AD-A246566] p 2889 N92-26619
RADAR TRACKING
A refined maximum likelihood method for tracking low-altitude targets over the sea: Results of simulation and experiments
[AD-A246534] p 2888 N92-26419
RADIANCE
Water vapor information content of absorption lines observed in the Sun's infrared radiance p 2942 N92-26490
RADIANT COOLING
Physical processes within the nocturnal stratus-topped boundary layer, revision
[AD-A245829] p 2947 N92-26901
RADIANT FLUX DENSITY
Aircraft photovoltaic power-generating system p 2926 N92-26581
RADIATION ABSORPTION
Transmittance measurements of ultraviolet and visible wavelength filters flown aboard LDEF p 2999 N92-27110
RADIATION COUNTERS
Cryogenic detector development
[MPI-PHE/91-07] p 2906 N92-26391
Calorimetric particle detectors with superconducting absorber materials p 2907 N92-26393
Superconducting tunnel junctions p 2907 N92-26396
Silicon drift chambers with integrated amplifiers as low energy detectors p 2908 N92-26398
RADIATION DAMAGE
Adverse reproductive events and electromagnetic radiation
[PB92-145796] p 2953 N92-26512
LDEF mechanical systems p 2916 N92-27114
French Cooperative Passive Payload (FRECOPA) p 2867 N92-27117
RADIATION DETECTORS
A search for magnetic monopoles with the Soudan 2 detector
[DE92-010347] p 3021 N92-26216
Composition studies based on coincident air shower array and underground muon data
[DE92-010345] p 3021 N92-26253
Underground muons observed in the Soudan 2 detector from the directions of x ray sources
[DE92-010344] p 3021 N92-26264
The status of GALLEX
[DE92-010077] p 3020 N92-26566
Focusing x ray transition radiation with cylindrical and elliptical optics
[AD-A245987] p 2997 N92-26754

Effect of space exposure of pyroelectric infrared detectors p 2910 N92-27113

RADIATION DOSAGE

A comparative assessment of radiological impact due to nuclear waste disposal in hard crystalline bedrock, appendix 1
[IAEA-CN-43/449] p 2929 N92-26483

Assessment of biospheric behaviour of releases from nuclear waste repositories, appendix 2
p 2929 N92-26484

Assessment of radiation doses due to releases to the biosphere from nuclear waste repositories, appendix 3
p 2929 N92-26485

Human round trip to Mars: Six months and radiation safe
[DE92-010160] p 2857 N92-26818

Exposure to space radiation of high-performance infrared multilayer filters and materials technology experiment (A0056) p 2999 N92-27108

Passive exposure of Earth radiation budget experiment components. LDEF experiment AO-147: Post-flight examinations and tests p 2910 N92-27109

Effect of space exposure of pyroelectric infrared detectors p 2910 N92-27113

LDEF mechanical systems p 2916 N92-27114

Thermal control surfaces experiment flight system performance p 2860 N92-27116

Preliminary total dose measurements on LDEF --- long duration exposure facility p 2952 N92-27123

Total Dose Effects (TDE) of heavy ionizing radiation in fungus spores and plant seeds: Preliminary investigations p 2952 N92-27124

Preliminary results of the Artemia salina experiments in biostack on LDEF p 2952 N92-27125

Long-term exposure of bacterial spores to space
p 2952 N92-27126

RADIATION EFFECTS

Application of irradiation techniques to food and foodstuffs
[DE92-614952] p 2954 N92-26186

Geometry and mass model of ionizing radiation experiments on the LDEF satellite
[NASA-CR-184325] p 2993 N92-26200

Adverse reproductive events and electromagnetic radiation
[PB92-145796] p 2953 N92-26512

Etching effects in ion implanted SiO2
[DE92-011150] p 3005 N92-26826

Linear and non-linear response of liquid and solid particles to energetic radiation
[AD-A246368] p 2894 N92-26942

Critical technologies: Spacecraft habitability, an update
p 2966 N92-27010

LDEF fiber optic exposure experiment No. S-0109
p 2998 N92-27090

Radiation sensitivity of quartz crystal oscillators experiment for the Long Duration Exposure Facility (LDEF) p 2895 N92-27111

LDEF electronic systems: Successes, failures and lessons p 2895 N92-27112

Effect of space exposure of pyroelectric infrared detectors p 2910 N92-27113

LDEF mechanical systems p 2916 N92-27114

Seeds in space experiment --- long duration exposure facility p 2952 N92-27120

Survival of epiphytic bacteria from seed stored on the Long Duration Exposure Facility (LDEF)
p 2952 N92-27122

Total Dose Effects (TDE) of heavy ionizing radiation in fungus spores and plant seeds: Preliminary investigations p 2952 N92-27124

Long-term exposure of bacterial spores to space
p 2952 N92-27126

RADIATION HAZARDS

Adverse reproductive events and electromagnetic radiation
[PB92-145796] p 2953 N92-26512

RADIATION INJURIES

Preliminary results of the Artemia salina experiments in biostack on LDEF p 2952 N92-27125

RADIATION MEASUREMENT

Simultaneous observations of extensive air showers and underground muons at Soudan 2
[DE92-010282] p 3020 N92-26211

Underground muons from the direction of Cygnus X-3 during the January 1991 radio flare
[DE92-010346] p 3021 N92-26215

Calibration of CR-39 for detecting fusion neutrons
[DE92-009063] p 2993 N92-26225

Preliminary total dose measurements on LDEF --- long duration exposure facility p 2952 N92-27123

RADIATION PROTECTION

Human round trip to Mars: Six months and radiation safe
[DE92-010160] p 2857 N92-26818

RADIATION SHIELDING

Geometry and mass model of ionizing radiation experiments on the LDEF satellite
[NASA-CR-184325] p 2993 N92-26200

A user's manual for MASH 1.0: A Monte Carlo adjoint shielding code system
[DE92-010375] p 3021 N92-26544

Preliminary total dose measurements on LDEF --- long duration exposure facility p 2952 N92-27123

Long-term exposure of bacterial spores to space
p 2952 N92-27126

RADIATION SOURCES

Spontaneous and induced coherent radiation generation in atomic vapors
[AD-A246078] p 2890 N92-26764

RADIATION TRANSPORT

Numerical solution of the equation of neutrons transport on plane geometry by analytical schemes using acceleration by synthetic diffusion
[DE92-621426] p 2995 N92-26844

RADIATIVE HEAT TRANSFER

High temperature furnace modeling and performance verifications
[NASA-CR-190403] p 2908 N92-26536

The development of a model builder for a microcircuit substrate
[AD-A245765] p 2893 N92-26606

Thermal control of telescope apertures by optimized baffle heating p 2961 N92-26976

RADIATIVE TRANSFER

Water vapor information content of absorption lines observed in the Sun's infrared radiance
p 2942 N92-26490

User's guide to WPL microwave radiative transfer software
[PB92-129931] p 2890 N92-26809

Modelling light transfer inside photobiofermentors: Applications to the photosynthetic compartments of CELSS p 2952 N92-26982

RADIATORS

Flight test results of the passive cooling system
p 2860 N92-27000

RADICALS

Spectroscopy and kinetics of combustion gases at high temperatures
[DE92-011216] p 2872 N92-26281

RADIO ASTRONOMY

Laboratory evaluation and application of microwave absorption properties under simulated conditions for planetary atmospheres
[NASA-CR-190211] p 3019 N92-26438

An infrared Michelson stellar interferometer and its applications p 3015 N92-26477

RADIO COMMUNICATION

A measuring facility for testing radio communication equipment
[AD-A245621] p 2890 N92-26874

System evaluation of a frequency hopping combat net radio
[AD-A246365] p 2891 N92-26941

RADIO DIRECTION FINDERS

An evaluation of superresolution methods for tactical radio direction finding
[AD-A246316] p 2851 N92-26291

RADIO EQUIPMENT

Joint services electronics program
[AD-A245636] p 2892 N92-26280

Data fusion and correlation techniques testbed (DFACTT): Field trial 14 January 1991
[AD-A245324] p 3011 N92-26378

The fidelity enhancement process
[AD-A245388] p 2977 N92-26840

A measuring facility for testing radio communication equipment
[AD-A245621] p 2890 N92-26874

RADIO FREQUENCIES

RF vacuum microelectronics
[AD-A246579] p 2893 N92-26771

RADIO FREQUENCY HEATING

Spheroidization and densification of Nickel powders by RF-induction plasma
[PB92-151893] p 2879 N92-26787

RADIO GALAXIES

Evidence for cluster magnetic fields around radio galaxies p 3017 N92-26554

RADIO OBSERVATION

Laboratory evaluation and application of microwave absorption properties under simulated conditions for planetary atmospheres
[NASA-CR-190211] p 3019 N92-26438

RADIO OCCULTATION

Laboratory evaluation and application of microwave absorption properties under simulated conditions for planetary atmospheres
[NASA-CR-190211] p 3019 N92-26438

RADIO RECEPTION

Data fusion and correlation techniques testbed (DFACTT): Field trial 14 January 1991
[AD-A245324] p 3011 N92-26378

RADIO SOURCES (ASTRONOMY)

Underground muons from the direction of Cygnus X-3 during the January 1991 radio flare
[DE92-010346] p 3021 N92-26215

RADIO TELESCOPES

An infrared Michelson stellar interferometer and its applications p 3015 N92-26477

RADIOACTIVE CONTAMINANTS

Environmental radiation data
[PB92-164706] p 2933 N92-26890

RADIOACTIVE DECAY

A search for magnetic monopoles with the Soudan 2 detector
[DE92-010347] p 3021 N92-26216

Composition studies based on coincident air shower array and underground muon data
[DE92-010345] p 3021 N92-26253

New approaches to studies of exotic nuclei
[DE92-010127] p 2994 N92-26570

RADIOACTIVE ISOTOPES

Model studies of the transfer of radionuclides in the Finnish environment
[VTT-PUBL-81] p 2929 N92-26482

Assessment of radiation doses due to releases to the biosphere from nuclear waste repositories, appendix 3
p 2929 N92-26485

Sensitivity analysis of biospheric behaviour of radionuclides released from nuclear waste repositories, appendix 4 p 2929 N92-26486

Biosphere model validation by intercomparison to observed behaviour of fallout radionuclides in the aquatic environment, appendix 5 p 2930 N92-26487

RADIOACTIVE WASTES

Model studies of the transfer of radionuclides in the Finnish environment
[VTT-PUBL-81] p 2929 N92-26482

A comparative assessment of radiological impact due to nuclear waste disposal in hard crystalline bedrock, appendix 1
[IAEA-CN-43/449] p 2929 N92-26483

Assessment of biospheric behaviour of releases from nuclear waste repositories, appendix 2
p 2929 N92-26484

Assessment of radiation doses due to releases to the biosphere from nuclear waste repositories, appendix 3
p 2929 N92-26485

Sensitivity analysis of biospheric behaviour of radionuclides released from nuclear waste repositories, appendix 4 p 2929 N92-26486

An investigation of the mechanical properties and microscopic structure of extruded powder aluminum subjected to biaxial loadings at elevated temperature
p 2879 N92-26770

RADIOMETERS

MOS-1 activity report p 2925 N92-26749

Radar scattering as a source of geological information on Venus and Earth p 3019 N92-26778

Passive exposure of Earth radiation budget experiment components. LDEF experiment AO-147: Post-flight examinations and tests p 2910 N92-27109

RADIOSONDES

High frequency analyses of coastal meteorological phenomena affecting refractivity
[AD-A246383] p 2947 N92-27075

RAIL TRANSPORTATION

National MAGLEV initiative. Moving America: New directions, new opportunities
[PB92-163237] p 2914 N92-26518

Aerodynamic drag on the bullet trains
p 2902 N92-26911

RAIN

The Tropical Rainfall Measuring Mission (TRMM) program at the Goddard Space Flight Center (GSFC)
[TW-1] p 2922 N92-26702

Status of TRMM project: Rain radar in the Tropical Rainfall Measuring Mission
[TW-2] p 2922 N92-26703

Status of TRMM (NASDA) --- tropical rainfall measuring mission
[TW-3] p 2923 N92-26704

TRMM Mission Team --- tropical rainfall measuring mission
[TW-4] p 2923 N92-26705

Tropical Rainfall Measuring Mission (TRMM) science report
[TW-5] p 2923 N92-26706

Storm model and beam filling problem for rain retrievals
[TW-6] p 2923 N92-26707

Development of TRMM radar rainfall retrieval algorithms
[TW-7] p 2923 N92-26708

Rainfall pattern over the tropical rain forest
[TW-10] p 2923 N92-26711
Research program on hydrology
[TW-14] p 2924 N92-26715

RAIN EROSION
Studies of rain erosion mechanisms in a range of IR transmitting ceramics including coated samples
[AD-A245299] p 2882 N92-26751

RAIN FORESTS
Equilibrium-analysis of projected climate change effects on the global soil organic matter pool
[PB92-153022] p 2930 N92-26509
Rainfall pattern over the tropical rain forest
[TW-10] p 2923 N92-26711

RAMAN SPECTRA
Technology transfer and application of SERS continuous monitor for trace organic compounds
[DE92-008900] p 2875 N92-26726
Some experiences with absorption, phonon Raman, and luminescence spectroscopic probes of crystal structure of f-element compounds
[DE92-007828] p 3006 N92-26851

RAMAN SPECTROSCOPY
Some experiences with absorption, phonon Raman, and luminescence spectroscopic probes of crystal structure of f-element compounds
[DE92-007828] p 3006 N92-26851
Vibrational spectroscopy in shock-compressed liquids
[DE92-007713] p 2876 N92-26867

RAMJET ENGINES
Solid fuel ramjet infrared signature
[AD-A246299] p 2860 N92-26362

RANDOM NUMBERS
On increasing the capabilities of the SMART adaptive random number generator
[DE92-621106] p 2976 N92-26835

RANDOM PROCESSES
A random polynomial algorithm for the matroid parity base problem
[REPT-91-079] p 2974 N92-26449
Boundary-layer receptivity due to distributed surface imperfections of a deterministic or random nature
[NASA-CR-4439] p 2898 N92-26681

RANGE FINDERS
Description of the multispectral CCD-camera
[AD-A245681] p 2908 N92-26517

RANGE SAFETY
STS lithium/CF(x) battery p 2863 N92-27143

RANGEFINDING
Fast envelope correlation for passive ranging
[AD-A246333] p 2888 N92-26388
Recognition of 3-D symmetric objects from range images in automated assembly tasks
[NASA-CR-187664] p 2886 N92-26656
Passive determination of temperature and range using spectral band measurements of photon emittance
[AD-A247147] p 2910 N92-27181

RAPID TRANSIT SYSTEMS
National MAGLEV initiative. Moving America: New directions, new opportunities
[PB92-163237] p 2914 N92-26518
Aerodynamic drag on the bullet trains
p 2902 N92-26911

RARE EARTH ELEMENTS
Polarisation effects in fibre lasers
p 2911 N92-26571

RAREFIED GAS DYNAMICS
Rarefied-flow aerodynamics
[NASA-CR-190452] p 2850 N92-27191

RAREFIED PLASMAS
Parabolic flight: Reports of microgravity experiments by aircraft, volume 1, no. 2
[EG-910045] p 2884 N92-26440
Preliminary experiment of GDEF (Gas Dynamics Experiment Facility) p 2885 N92-26442

RAY TRACING
Description of the Rayflux ray tracing program and comparison with other models and measurements
[AD-A245413] p 2944 N92-26877

RAYLEIGH-RITZ METHOD
Hamiltonian lattice field theory: Computer calculations using variational methods
[DE92-010479] p 2985 N92-26232

REACTING FLOW
Shock-turbulence interactions in a reacting flow
[NASA-CR-189647] p 2905 N92-27032

REACTION KINETICS
Electrocatalysts for oxygen electrodes
[DE92-009491] p 2871 N92-26220
Aromatic-radical oxidation kinetics
[DE92-010821] p 2871 N92-26274
Spectroscopy and kinetics of combustion gases at high temperatures
[DE92-011216] p 2872 N92-26281
Time-resolved laser studies on the proton pump mechanism of bacteriorhodopsin
[DE92-003218] p 2951 N92-26493
Toluene-water clusters: Ion fragmentation and chemistry
[AD-A245813] p 2874 N92-26526
High-yield hydrogen production by catalytic gasification of coal or biomass
[DE92-008770] p 2875 N92-26724
Polycyclic aromatic hydrocarbon radiative properties and formation in carbon-rich stellar outflows
p 3018 N92-26757
Advancing natural gas combustion science and technology-low NOx
[PB92-137652] p 2876 N92-26782
Determination of rates of reaction in the gas phase in the troposphere. Theory and practice. Part 3: Rate of indirect photoreaction
[PB92-150374] p 2944 N92-26838

REACTIVITY
Enhance methane reactivity
[PB92-154822] p 2873 N92-26516

REACTOR DESIGN
Reaction/separation process for enhanced methane conversion
[PB92-149657] p 2873 N92-26508
Inertial fusion energy power plant design using the Compact Torus Accelerator: HYLIFE-CT
[DE92-008941] p 3000 N92-26729
Evaluation of integral measurements for the SP-100 space reactor
[DE92-009717] p 2996 N92-26841

REACTOR MATERIALS
Predictability of long-term creep and rupture in a nozzle-to-sphere vessel model
[DE92-008099] p 2919 N92-26845

REACTOR SAFETY
Assessment of diagnostic methods for solenoid-operated valves
[DE92-009379] p 2913 N92-26234

REAL TIME OPERATION
The development of a design database for the computer aided prototyping system
[AD-A245786] p 3010 N92-26176
Assessments of selected real-time computing technologies
[AD-A245434] p 2972 N92-26273
An adaptive, packet-switched HF data terminal: Functional overview and initial performance
[AD-A246318] p 2973 N92-26292
Reconfiguration in robust distributed real-time systems based on global checkpoints
[AD-A245615] p 2970 N92-26382
Optical hidden layer network
[AD-A246162] p 2992 N92-26413
Proving properties of real-time systems through logical specifications and Petri net models
[REPT-91-072] p 2973 N92-26448
Real time imaging and infrared background scene analysis using the Naval Postgraduate School infrared search and target designation (NPS-IRSTD) system
[AD-A245527] p 2997 N92-26662
The 8th IEEE Workshop on Real-Time Operating Systems
[AD-A246126] p 2976 N92-26685
Evaluation criteria for real-time specification languages
[AD-A246612] p 2976 N92-26766
Expert system management system
[AD-A247102] p 3009 N92-26863
Software architecture for a distributed real-time system in Ada, with application to telerobotics
[NASA-TM-4367] p 2977 N92-26904
NPSNET: Hierarchical data structures for real-time three-dimensional visual simulation
[AD-A246380] p 2978 N92-27073

RECEIVERS
Synchronous detection in monolithically integrated AM upconversion receivers
[ETN-92-91305] p 2892 N92-26260
Characterization of the clock in a new inexpensive GPS receiver: The Magnavox MX 4200
[AD-A246165] p 2851 N92-26415
Effects of video bandwidth on the performance of a square law detector with Gaussian IF and video filters
[AD-A246506] p 2989 N92-26467
Effects of non-uniform windowing on the performance of a fast frequency-hopped noncoherent MFSK receiver over Rician fading channels with partial-band interference and Doppler shift
[AD-A245762] p 2889 N92-26595
Heat receivers for solar dynamic space power systems p 2860 N92-26601
Post-test examination of a pool boiler receiver
[NASA-TM-105635] p 2880 N92-27192

RECHARGING
Cycle life characteristics of Li-TiS2 cells
p 2865 N92-27154

RECOVERABLE LAUNCH VEHICLES
Winged launcher thermal design aspects
p 2858 N92-27013

RECRYSTALLIZATION
Dynamic restoration mechanisms in Al-5.8 at. percent Mg deformed to large strains in the solute drag regime
[DE92-009529] p 2877 N92-26223

RECTANGULAR PLATES
Buckling of unidirectional graphite/epoxy composite plates at low temperatures
[AD-A246602] p 2869 N92-26796

RECTIFIERS
Main and auxiliary transformer rectifier system for minimizing line harmonics
[AD-D015209] p 2894 N92-26881

RECURSIVE FUNCTIONS
Recursive ray acoustics for three-dimensional sound-speed profiles
[AD-A245613] p 2991 N92-26228
Theoretical issues in adaptive Set-Membership-Based signal processing.
[AD-A245721] p 2980 N92-26430
Introduction in IND and recursive partitioning
[NASA-TM-107879] p 2983 N92-26629

RECYCLING
Life support research and development for the Department of Energy Space Exploration Initiative
[DE92-007239] p 2955 N92-26494
Waste minimization for non-agricultural pesticide applicators: EPA's pollution prevention guide
[PB92-153774] p 2933 N92-26889
Thiocapsa roseopersicina, a bacterium for sulfur-recycling in microbial ecosystems designed for CELSS and space purposes p 2951 N92-26977
Chemolithotropic hydrogen-oxidizing bacteria and their possible functions in closed ecological life-support systems p 2951 N92-26979
Impact of diet on the design of waste processors in CELSS p 2961 N92-26980

REDUCED GRAVITY
Parabolic flight: Reports of microgravity experiments by aircraft, volume 1, no. 2
[EG-910045] p 2884 N92-26440
Outlines of parabolic flight p 2884 N92-26441
Preliminary experiment of GDEF (Gas Dynamics Experiment Facility) p 2885 N92-26442
Parabolic flight experiments on bubble migration under reduced gravity p 2885 N92-26443
Micro-gravity experiment of vapor/liquid reorientation induced by capillary force p 2885 N92-26444
Liquid motion analysis with lateral impacts under low gravity p 2885 N92-26445
Biomedical data acquisition and processing technology p 2885 N92-26446
The experiment under microgravity by aircraft: The experiment in floating by gas flow p 2886 N92-26447
Microgravity simulation p 2964 N92-26994
Architectural studies relating to human body motion morphology in microgravity p 2953 N92-27011
Crew-friendly support systems for internal vehicular activities in zero gravity, experimented underwater for the Columbus programme p 2969 N92-27025
Microgravity combustion science: Progress, plans, and opportunities
[NASA-TM-105410] p 2886 N92-27197

REDUCTION (CHEMISTRY)
New theoretical methods for electronic structure and gas-phase state specific oxidation/reduction studies
[AD-A246127] p 2875 N92-26687

REDUNDANCY
Complementary metal oxide silicon cyclic redundancy check generators
[AD-A246140] p 2894 N92-27061

REENTRY
Lightweight fiber insulations performance and application p 2883 N92-27016

REENTRY VEHICLES
Analysis of frozen startup of high-temperature heat pipes and three-dimensional modeling of block-heated heat pipes
[AD-A245327] p 2896 N92-26379

REFLECTANCE
Cluster model of polarization reflection from metallic surfaces
[AD-A245781] p 2996 N92-26241
Reflection of x rays from repeated multilayer structures
[AD-A246562] p 2991 N92-26769
Experiment M0003-4: Advanced solar cell and coverglass analysis, an overview p 2927 N92-27088

REFLECTED WAVES
Cluster model of polarization reflection from metallic surfaces
[AD-A245781] p 2996 N92-26241
REFLECTION
Apparatus for measuring the absorption of sound by noise in one dimension
[AD-A246442] p 2992 N92-27031
REFRACTIVITY
Application of fluorescent-particle imaging to measuring flow in complex media
[DE92-009121] p 2898 N92-26645
Transient gas motion in nuclear-reactor-pumped lasers: Computational and experimental results
[DE92-002357] p 2912 N92-26691
Reflection of x rays from repeated multilayer structures
[AD-A246562] p 2991 N92-26769
Investigations of a single point temperature probe for measurement of atmospheric turbulence
[AD-A246563] p 2909 N92-26794
Static, microwave, infrared, and visible permittivity related to chemical structure: N-methylacetamide, N-dimethylacetamide and their mixtures in CCl4 at 32 C
[AD-A246364] p 2991 N92-26940
High frequency analyses of coastal meteorological phenomena affecting refractivity
[AD-A246383] p 2947 N92-27075
REFRACTORY MATERIALS
High temperature furnace modeling and performance verifications
[NASA-CR-190403] p 2908 N92-26536
Application of neutron diffraction to measure residual strains in high temperature composites
[DE91-014021] p 2869 N92-26679
Powder processing of aero-engine components
[PNR-90813] p 2880 N92-27044
REFRACTORY METAL ALLOYS
Evaluation of plasma sprayed crucible coatings for melt processing copper-refractory metal alloys
[DE92-008912] p 2878 N92-26727
REFRIGERATORS
Theoretical and experimental study of thermoacoustic engines
[AD-A246334] p 2914 N92-26389
Nucleate pool boiling of R-114 and R-114/oil mixtures from single enhanced tubes
[AD-A245487] p 3008 N92-27058
REGENERATION (ENGINEERING)
Metal oxide absorbents for regenerative carbon dioxide and water vapor removal for advanced portable life support systems p 2968 N92-27021
REGRESSION ANALYSIS
Correlation and prediction of dynamic human isolated joint strength from lean body mass
[NASA-TP-3207] p 2956 N92-26682
REGULATIONS
Environmental Protection Agency's municipal solid waste landfill liner design criteria
[PB92-153766] p 2933 N92-26928
REJECTION
The liquid droplet radiator: Status of development p 2905 N92-26969
RELATIVISTIC ELECTRON BEAMS
Operation of a Smith-Purcell free-electron laser at submillimeter wavelengths p 2912 N92-26626
Erosion of a relativistic electron beam propagating in a plasma channel
[DE92-009059] p 3000 N92-26666
RELATIVISTIC PARTICLES
Diffraction phenomena in spontaneous and stimulated radiation by relativistic particles in crystals (review)
[DE92-009501] p 3001 N92-26222
RELAXATION METHOD (MATHEMATICS)
Numerical solution of plastic liquids shape factor
[PB92-133958] p 2896 N92-26496
RELIABILITY
An adaptive correction technique for Differential Global Positioning System p 2851 N92-26623
The role of the Long Duration Exposure Facility in the development of space systems p 2867 N92-27128
STS lithium/CF(x) battery p 2863 N92-27143
RELIABILITY ANALYSIS
Pyrotechnic device reliability
[AD-A245818] p 2883 N92-26178
Reliability and failure analyses of composite beams and plates containing stress concentrations p 2918 N92-26598
Use of Markov methods in analysis of fault-tolerant systems with flexible repair policies
[PNR-90801] p 2916 N92-27038
RELIABILITY ENGINEERING
Pyrotechnic device reliability
[AD-A245818] p 2883 N92-26178
Composite strength statistics from fiber strength statistics
[AD-A245616] p 2867 N92-26383
Mixed Weibull distributions in reliability engineering: Statistical models for the lifetime of units with multiple modes of failure p 2916 N92-26602
REMOTE CONTROL
Man-machine aspects of remotely controlled space manipulators
[ISBN-90-370-0056-8] p 2954 N92-26255
REMOTE SENSING
Meridional zonation of the Barents Sea ecosystem inferred from satellite remote sensing and in situ bio-optical observations
[AD-A246323] p 2948 N92-26245
Remote sensing of atmosphere with aircraft borne lidar systems p 2941 N92-26347
An assessment of satellite remote sensing for land cover classification p 2922 N92-26625
A Bayes-Maximum Entropy method for multi-sensor data fusion
[DE92-000680] p 2983 N92-26657
International Conference on Japanese Earth Observation Programs: TRMM Workshop
[JTN-92-80345] p 2922 N92-26701
The Tropical Rainfall Measuring Mission (TRMM) program at the Goddard Space Flight Center (GSFC)
[TW-1] p 2922 N92-26702
Status of TRMM project: Rain radar in the Tropical Rainfall Measuring Mission
[TW-2] p 2922 N92-26703
Status of TRMM (NASDA) --- tropical rainfall measuring mission
[TW-3] p 2923 N92-26704
TRMM Mission Team --- tropical rainfall measuring mission
[TW-4] p 2923 N92-26705
Tropical Rainfall Measuring Mission (TRMM) science report
[TW-5] p 2923 N92-26706
Storm model and beam filling problem for rain retrievals
[TW-6] p 2923 N92-26707
Development of TRMM radar rainfall retrieval algorithms
[TW-7] p 2923 N92-26708
Validation of numerical models by TRMM and validation of TRMM by numerical models
[TW-8] p 2923 N92-26709
Water cycles around the subtropical frontal zone in East Asia
[TW-9] p 2923 N92-26710
Rainfall pattern over the tropical rain forest
[TW-10] p 2923 N92-26711
Utilization of tropical convection data for meteorological operation
[TW-11] p 2924 N92-26712
TRMM and Asian monsoon --- tropical rainfall measuring mission
[TW-12] p 2924 N92-26713
Research plan for utilizing TRMM data in MRI --- tropical rainfall measuring mission
[TW-13] p 2924 N92-26714
Research program on hydrology
[TW-14] p 2924 N92-26715
Differentiation on genus of aquatic macrophytes through remote sensing in the Tucurui Reservoir, Para State, Brazil
[INPE-5315-PRE/1712] p 2951 N92-26721
International Conference on Japanese Earth Observation Programs: Plenary Session
[JTN-92-80342] p 2924 N92-26742
Japanese Earth Observation Program p 2924 N92-26743
Distribution of proposed Earth probes and other related missions p 2925 N92-26744
European Earth Observation Program p 2925 N92-26745
French space programmes related to global change p 2925 N92-26746
Canadian Earth Observation Program p 2925 N92-26747
Environmental projects at the Canada Centre for Remote Sensing p 2925 N92-26748
MOS-1 activity report p 2925 N92-26749
Radar scattering as a source of geological information on Venus and Earth p 3019 N92-26778
A high repetition rate lidar
[AD-A245382] p 2890 N92-26872
REMOTE SENSORS
Description of the multispectral CCD-camera
[AD-A245681] p 2908 N92-26517
Modeling of explorative procedures for remote object identification
[AD-A245525] p 2922 N92-26661
International Conference on Japanese Earth Observation Programs: Plenary Session
[JTN-92-80342] p 2924 N92-26742
Distribution of proposed Earth probes and other related missions p 2925 N92-26744
Environmental projects at the Canada Centre for Remote Sensing p 2925 N92-26748
Differential polarimetric fiber optic sensor
[AD-D015218] p 2998 N92-27186
REMOTELY PILOTED VEHICLES
Gamma Group-The Pale Horse: A proposal in response to a commercial air transportation study ort study
[NASA-CR-190019] p 2852 N92-26435
Development and testing of an unmanned air vehicle telemetry system
[AD-A246577] p 2858 N92-26621
REPRODUCTION (BIOLOGY)
Adverse reproductive events and electromagnetic radiation
[PB92-145796] p 2953 N92-26512
REQUIREMENTS
A comparison of heavy lift launch vehicle options for the 1990s
[AD-A245617] p 2857 N92-26402
Software requirements document for the netCDF interface within ECMOP, version 1.0
[AD-A246220] p 2974 N92-26464
CBT: Role and future application for crew training --- computer based training p 2953 N92-26992
RESEARCH AIRCRAFT
The DLR meteorological research aircraft Falcon p 2941 N92-26348
The icing of the wing upper side and bottom side of the icing research aircraft of the DLR p 2850 N92-26349
RESEARCH AND DEVELOPMENT
SOLTECH 1992 proceedings. Solar Process Heat Program, volume 1
[DE92-001238] p 2927 N92-26683
DOE new technology
[DE92-001619] p 3013 N92-26689
Small business innovation research: Program solicitation closing date, 27 January 1992
[DE92-010132] p 3009 N92-26811
Climate research at regional climate centers in 1991
[PB92-160399] p 2946 N92-26822
Development of fluid loop and hybrid radiators: Test results p 2859 N92-26967
EVA life support design and technology developments p 2965 N92-27002
RESEARCH FACILITIES
New approaches to studies of exotic nuclei
[DE92-010127] p 2994 N92-26570
Experiences in using C++ to develop a next generation strong shock wave physics code
[DE92-006675] p 2976 N92-26696
Microgravity simulation p 2964 N92-26994
RESEARCH MANAGEMENT
Abstracts of phase 1 awards, 1991
[DE92-010133] p 3022 N92-26640
Summary of research: Academic departments, 1990-1991
[AD-A245533] p 3022 N92-26664
Biotechnology for the 21st century, FY 1993
[DE92-007757] p 2951 N92-26850
RESERVOIRS
Differentiation on genus of aquatic macrophytes through remote sensing in the Tucurui Reservoir, Para State, Brazil
[INPE-5315-PRE/1712] p 2951 N92-26721
RESIDUAL STRESS
Effect of thermal residual stresses on the stress-strain behavior of metal-matrix composites
[AD-A246136] p 2868 N92-26386
Application of neutron diffraction to measure residual strains in high temperature composites
[DE91-014021] p 2869 N92-26679
RESIDUES
Experiment M0003-4: Advanced solar cell and coverglass analysis, an overview p 2927 N92-27088
RESILIENCE
Effect of temperature and gap opening rate on the resiliency of candidate solid rocket booster O-ring materials
[NASA-TP-3226] p 2883 N92-27194
RESISTANCE THERMOMETERS
Tuned-circuit dual-mode Johnson noise thermometers
[DE92-010121] p 2908 N92-26569
RESOLUTION
The high resolution diffractometer mini-Sfinks p 3002 N92-26322
Generation of multi-resolution maps
[PB92-152206] p 2921 N92-26513

RESONANCE
Radar target identification by natural resonances: Evaluation of signal processing algorithms
[AD-A246566] p 2889 N92-26619
Modeling 3-D objects with planar surfaces for prediction of electromagnetic scattering
[NASA-TM-107598] p 2891 N92-27189
RESONANT FREQUENCIES
Optimization of space structures to minimize dynamic response p 2858 N92-26610
Radar target identification by natural resonances: Evaluation of signal processing algorithms
[AD-A246566] p 2889 N92-26619
Experimental results for inductive strips in inhomogeneous finline
[AD-A247254] p 2895 N92-27176
RESONANT TUNNELING
Crossovers of the density of states in two-direction double-barrier resonant-tunneling structures
[AD-A246124] p 3005 N92-26684
RESONATORS
Measurement electronics of industrial microwave resonator sensors
[PB92-152750] p 2909 N92-26786
Experimental results for inductive strips in inhomogeneous finline
[AD-A247254] p 2895 N92-27176
RESPIRATION
Water recovery from condensate of crew respiration products aboard the Space Station
p 2956 N92-26951
RESPIRATORY PHYSIOLOGY
Physiological design goals and proposed thermal limits for US Navy thermal garments: Proceedings of 2 conferences sponsored by the Naval Medical Research and Development Command
[AD-A245543] p 2956 N92-26665
RETINA
Low power laser irradiation effect with emphasis on injured neural tissues
[AD-A246410] p 2953 N92-27063
RETROREFLECTORS
Kalman smoother applied to lace
[AD-A246439] p 2859 N92-27030
RETURN TO EARTH SPACE FLIGHT
LBNP as countermeasure: An automated scenario
p 2953 N92-27012
Heatshield concepts for the Rosetta Aerocapsule
p 2860 N92-27028
REUSABLE SPACECRAFT
Retrievable payload carrier: Next generation Long Duration Exposure Facility p 2860 N92-27129
REVERBERATION
A compendium of environmental data collected during the southwest Florida shallow-water acoustic sea test
[AD-A246143] p 2950 N92-27071
REYNOLDS NUMBER
Reynolds number dependence of the drag coefficient for laminar flow through fine-scale screens
[DE92-002930] p 2899 N92-26698
REYNOLDS STRESS
Systematic study of Reynolds stress closure models in the computations of plane channel flows
[NASA-CR-189646] p 2898 N92-26649
RIBLETS
Application of riblet surface to pipe flow
p 2903 N92-26915
RIEMANN MANIFOLD
Spectral boundary conditions and index theorem for 2-dimensional compact manifold with boundary
[DE92-621115] p 2990 N92-26798
RIEMANN WAVES
Wave structure in one and two dimensional fluid flow
[DE92-007421] p 2900 N92-26855
RIGID STRUCTURES
Asymptotic analysis of the vibrations of variable length cantilever beams p 2918 N92-26739
ROBOT ARMS
Man-machine aspects of remotely controlled space manipulators
[ISBN-90-370-0056-8] p 2954 N92-26255
Hybrid efficient control algorithms for robot manipulators
[AD-A245716] p 2981 N92-26428
Adaptive control of robotic manipulators with structural flexibility p 2914 N92-26475
ROBOT CONTROL
Time optimal trajectories for mobile robots with two independently driven wheels
[DE92-010002] p 2913 N92-26219
Dynamic control of a space robot system with no thrust jets controlled base
[AD-A245711] p 2981 N92-26356
A framework for recognizing grasps
[AD-A245712] p 2981 N92-26357
Perception for outdoor navigation
[AD-A245715] p 2851 N92-26427
Experiments in modelling and end-point control of two-link flexible manipulators p 2915 N92-26731
A supervisory control strategy for navigation of mobile robots in dynamic environments p 2983 N92-26734
Using min-max of torque to resolve redundancy for a mobile manipulator
[DE92-000070] p 2915 N92-26750
ROBOT DYNAMICS
Dynamic control of a space robot system with no thrust jets controlled base
[AD-A245711] p 2981 N92-26356
A supervisory control strategy for navigation of mobile robots in dynamic environments p 2983 N92-26734
Using min-max of torque to resolve redundancy for a mobile manipulator
[DE92-000070] p 2915 N92-26750
ROBOTICS
Using min-max of torque to resolve redundancy for a mobile manipulator
[DE92-000070] p 2915 N92-26750
Representations in visual motion
[PB92-148287] p 2984 N92-26814
Software architecture for a distributed real-time system in Ada, with application to telerobotics
[NASA-TM-4367] p 2977 N92-26904
ROBOTS
Time optimal trajectories for mobile robots with two independently driven wheels
[DE92-010002] p 2913 N92-26219
A framework for recognizing grasps
[AD-A245712] p 2981 N92-26357
Dead reckoning navigation for walking robots
[NASA-CR-190296] p 2982 N92-26429
A Bayes-Maximum Entropy method for multi-sensor data fusion
[DE92-000680] p 2983 N92-26657
Representations in visual motion
[PB92-148287] p 2984 N92-26814
ROBUSTNESS (MATHEMATICS)
Bias robust estimation of scale
[AD-A245698] p 2985 N92-26229
Reconfiguration in robust distributed real-time systems based on global checkpoints
[AD-A245615] p 2970 N92-26382
Dead reckoning navigation for walking robots
[NASA-CR-190296] p 2982 N92-26429
Parameter robust reduced-order control of flexible structures p 2982 N92-26597
ROCKET ENGINE DESIGN
Effect of model selection on combustor performance and stability predictions using ROCCID
[NASA-TM-105750] p 2861 N92-27036
ROCKET ENGINES
Conceptual design study for the use of COBE rocket engines on the Tropical Rainfall Measuring Mission
[NASA-CR-190383] p 2945 N92-26535
Space aging of solid rocket materials
p 2884 N92-27085
ROCKET THRUST
Effect of model selection on combustor performance and stability predictions using ROCCID
[NASA-TM-105750] p 2861 N92-27036
ROCKS
Fractal characteristics of fracture roughness and aperture data
[DE92-010302] p 2895 N92-26214
ROOM TEMPERATURE
Low temperature electrochemical activation of methane
[PB92-152917] p 2872 N92-26351
Deformation behavior of an age-hardenable Beta + Alpha-Two titanium alloy
[AD-A246362] p 2879 N92-26939
ROSAT MISSION
ROSAT: Measured temperatures versus thermal analysis results p 2859 N92-26997
ROTARY ENGINES
Development of natural gas rotary engines
[PB92-149665] p 2915 N92-26816
ROTATING BODIES
Spinning jets from shaped charges with flow turned liners
[MBB-UA-1197-90-PUB] p 2886 N92-26246
Principal investigator in a box: Version 1.2 documentation
[NASA-TM-107886] p 2982 N92-26628
An instrument for engine torque estimation and misfire detection --- torque p 2909 N92-26738
ROTATING FLUIDS
Acoustically probed Taylor-Couette flow apparatus
[AD-A246385] p 2993 N92-27076
RUBBER
Computational modelling of rubberlike materials
[ETN-92-91304] p 2916 N92-26259
RUN TIME (COMPUTERS)
Run-time support for dynamic load balancing and debugging in paralex
[AD-A245446] p 2979 N92-26279
RUNGE-KUTTA METHOD
Three-dimensional upwind scheme for solving the Euler equations on unstructured tetrahedral grids --- tetrahedral grids p 2849 N92-26585

S

S STARS
The galactic evolution of s-process elements via asymptotic giant branch stars p 3018 N92-26725
S WAVES
Fault zone structure determined through the analysis of earthquake arrival times
[DE92-010322] p 2935 N92-26239
SAFETY
Safety testing of lithium cells p 2864 N92-27150
SAFETY DEVICES
Static electricity: A literature review
[AD-A246533] p 2990 N92-26471
SAMPLED DATA SYSTEMS
High precision timing of millisecond pulsars
p 3015 N92-26760
SAMPLING
Environmental radiation data
[PB92-164706] p 2933 N92-26890
SATELLITE ANTENNAS
An antenna design for PANSAT using NEC
[AD-A245482] p 2888 N92-26399
SATELLITE COMMUNICATION
A comparison of the UHF Follow-On and MILSTAR satellite communication systems
[AD-A245806] p 2891 N92-26933
SATELLITE DRAG
Orbital maintenance of endoatmospheric low earth-orbiting satellites
[AD-A246381] p 2859 N92-27074
SATELLITE IMAGERY
Meridional zonation of the Barents Sea ecosystem inferred from satellite remote sensing and in situ bio-optical observations
[AD-A246323] p 2948 N92-26245
International Conference on Japanese Earth Observation Programs: Plenary Session
[JTN-92-80342] p 2924 N92-26742
Japanese Earth Observation Program
p 2924 N92-26743
MOS-1 activity report p 2925 N92-26749
SATELLITE NETWORKS
Requirements analysis and design for implementation of a satellite link for a local area computer network
[AD-A245610] p 2978 N92-26227
A comparison of the UHF Follow-On and MILSTAR satellite communication systems
[AD-A245806] p 2891 N92-26933
SATELLITE OBSERVATION
Research programmes at Svalbard (Norway)
p 2935 N92-26297
The need of coordinated observations in space and from ground p 2937 N92-26310
Requirements for coordinated Cluster and ground-based observations of the cusp p 2938 N92-26318
Cirrus clouds and condensation trail on 18 Oct. 1989 over the North sea (ICE '89). Determination of height and optical depth using ALEX, AVHRR and HIRS
p 2940 N92-26340
Tracer transport in the middle atmosphere
p 2928 N92-26473
An assessment of satellite remote sensing for land cover classification p 2922 N92-26625
International Conference on Japanese Earth Observation Programs: Plenary Session
[JTN-92-80342] p 2924 N92-26742
Japanese Earth Observation Program
p 2924 N92-26743
Distribution of proposed Earth probes and other related missions p 2925 N92-26744
European Earth Observation Program
p 2925 N92-26745
French space programmes related to global change
p 2925 N92-26746
Canadian Earth Observation Program
p 2925 N92-26747
Environmental projects at the Canada Centre for Remote Sensing p 2925 N92-26748
MOS-1 activity report p 2925 N92-26749
Monthly mean global satellite data sets available in CCM history tape format
[NASA-CR-190344] p 2933 N92-26878
AVHRR satellite data: Users guide for accessing NOARL archives
[AD-A246142] p 2926 N92-27070

SATELLITE SOUNDING
International Conference on Japanese Earth Observation Programs: Plenary Session
[JTN-92-80342] p 2924 N92-26742
Japanese Earth Observation Program
p 2924 N92-26743
Distribution of proposed Earth probes and other related missions p 2925 N92-26744
European Earth Observation Program
p 2925 N92-26745
French space programmes related to global change
p 2925 N92-26746
Canadian Earth Observation Program
p 2925 N92-26747
Environmental projects at the Canada Centre for Remote Sensing p 2925 N92-26748

SATELLITE TEMPERATURE
Italsat thermal control: The in-orbit performances
p 2859 N92-26996
ROSAT: Measured temperatures versus thermal analysis results p 2859 N92-26997
SPOT multimission platform thermal control: Five years of in-flight results p 2860 N92-26998
LDEF: 69 Months in Space. First Post-Retrieval Symposium, part 3
[NASA-CP-3134-PT-3] p 3022 N92-27083

SATELLITE-BORNE INSTRUMENTS
Japanese Earth Observation Program
p 2924 N92-26743
Distribution of proposed Earth probes and other related missions p 2925 N92-26744

SATELLITE-BORNE RADAR
International Conference on Japanese Earth Observation Programs: TRMM Workshop
[JTN-92-80345] p 2922 N92-26701
The Tropical Rainfall Measuring Mission (TRMM) program at the Goddard Space Flight Center (GSFC)
[TW-1] p 2922 N92-26702
Status of TRMM project: Rain radar in the Tropical Rainfall Measuring Mission
[TW-2] p 2922 N92-26703
Status of TRMM (NASDA) --- tropical rainfall measuring mission
[TW-3] p 2923 N92-26704
Storm model and beam filling problem for rain retrievals
[TW-6] p 2923 N92-26707
Development of TRMM radar rainfall retrieval algorithms
[TW-7] p 2923 N92-26708
Validation of numerical models by TRMM and validation of TRMM by numerical models
[TW-8] p 2923 N92-26709
Water cycles around the subtropical frontal zone in East Asia
[TW-9] p 2923 N92-26710
Rainfall pattern over the tropical rain forest
[TW-10] p 2923 N92-26711
Utilization of tropical convection data for meteorological operation
[TW-11] p 2924 N92-26712
TRMM and Asian monsoon --- tropical rainfall measuring mission
[TW-12] p 2924 N92-26713
Research plan for utilizing TRMM data in MRI --- tropical rainfall measuring mission
[TW-13] p 2924 N92-26714
Research program on hydrology
[TW-14] p 2924 N92-26715
International Conference on Japanese Earth Observation Programs: Plenary Session
[JTN-92-80342] p 2924 N92-26742
Canadian Earth Observation Program
p 2925 N92-26747

SATELLITE-TO-SATELLITE TRACKING
Estimation of geopotential differences over intercontinental locations using satellite and terrestrial measurements p 2924 N92-26728

SCALE MODELS
Development and testing of an unmanned air vehicle telemetry system
[AD-A246577] p 2858 N92-26621

SCALING LAWS
On the subject of geometric spacing of meteorological sensors
[AD-A245824] p 2946 N92-26899

SCANDIUM ISOTOPES
Gamma-ray spectrometry of LDEF samples
[DE92-009947] p 2874 N92-26632

SCATTERING
Electromagnetic scattering by a moving object: Theory and experiment
[PB92-150911] p 2889 N92-26511
Measurements of scattering processes in negative ion-atom collisions
[DE92-010319] p 2995 N92-26574
Higher order parametric x rays
[AD-A247148] p 2991 N92-27182

SCATTERING AMPLITUDE
Hamiltonian lattice field theory: Computer calculations using variational methods
[DE92-010479] p 2985 N92-26232

SCATTERING CROSS SECTIONS
Development and applications of the reverse neutron time-of-flight method with Fourier-type beam chopper
[VTT-PUBL-82] p 3001 N92-26320
Quasi-elastic nuclear scattering at high energies
[NASA-TM-4362] p 2996 N92-26832

SCENE ANALYSIS
Real time imaging and infrared background scene analysis using the Naval Postgraduate School infrared search and target designation (NPS-IRSTD) system
[AD-A245527] p 2997 N92-26662

SCHEDULING
Developing an adaptive scheduling support environment
[ISBN-90-9004609-7] p 3008 N92-26250
Knowledge-based production management: Approaches, results, and prospects
[AD-A245714] p 3008 N92-26426
A design rationale for NASA TileWorld
[NASA-TM-107882] p 2982 N92-26627
Planning and scheduling research at NASA Ames Research Center
[NASA-TM-107888] p 3009 N92-26790
Applying artificial intelligence to the control of space telescopes (extended abstract)
[NASA-TM-107913] p 3015 N92-26886
The APT/ERE planning and scheduling manifesto
[NASA-TM-107906] p 2984 N92-27055

SCIENTIFIC SATELLITES
Thermal design for the space-exposed instruments for the scientific satellite SAX p 2860 N92-26973

SCREENS
Reynolds number dependence of the drag coefficient for laminar flow through fine-scale screens
[DE92-002930] p 2899 N92-26698

SEA LAUNCHING
A prototype multi-media data base for tracking interface relationships and performing cost tradeoffs for the Sea Launch and Recovery (SEALAR) space launch system
[AD-A245481] p 2857 N92-26515

SEA LEVEL
The effect of global change and long period tides on the Earth's rotation and gravitational potential
p 2925 N92-26781

SEA STATES
Infrared clutter measurements of marine backgrounds
[AD-A245422] p 2932 N92-26873

SEA SURFACE TEMPERATURE
Theoretical and modeling studies of the marine planetary boundary layer
[AD-A245903] p 2942 N92-26432
Mean and turbulent structure of the marine atmospheric boundary layer during cold air outbreaks of different intensities: Observational and modelling analyses
p 2942 N92-26489
Utilization of tropical convection data for meteorological operation
[TW-11] p 2924 N92-26712

SEA WATER
Investigation of carbon dioxide in the South Atlantic and northern Weddell Sea areas (WOCE Sections A-12 and A-21) during the METEOR expedition 11/5, January - March 1990
[DE92-010027] p 2928 N92-26231

SEALING
Effect of temperature and gap opening rate on the resiliency of candidate solid rocket booster O-ring materials
[NASA-TP-3226] p 2883 N92-27194

SEALS (STOPPERS)
Rocket engine diagnostics using qualitative modeling techniques
[NASA-TM-105714] p 2861 N92-27033

SEARCH PROFILES
The effect of collection homogeneity on term association as a method of request expansion in information retrieval p 3012 N92-26614

SEAS
Convection wave studies over land and sea
p 2940 N92-26341

SEATS
Design guide for saddle seating on small high-speed craft
[ISVR-TR-205] p 2956 N92-26891

SECURITY
A security analysis of version 2 of the Network Time Protocol (NTP): A report to the privacy and security research group
[NASA-CR-190428] p 2981 N92-27183

SEDIMENTS
Diapycnal mixing, gravity-current propagation, and sediment dispersion in turbulent fluids
[AD-A246160] p 2896 N92-26412
The carbon isotopic compositions of individual compounds from ancient and modern depositional environments p 2921 N92-26478

SEEDS
Seeds in space experiment --- long duration exposure facility p 2952 N92-27120
Space Exposed Experiment Developed for Students (SEEDS) (P0004-2) p 2952 N92-27121
Survival of epiphytic bacteria from seed stored on the Long Duration Exposure Facility (LDEF)
p 2952 N92-27122
Total Dose Effects (TDE) of heavy ionizing radiation in fungus spores and plant seeds: Preliminary investigations p 2952 N92-27124

SEISMIC WAVES
Observational and theoretical investigations in solar seismology
[NASA-CR-190245] p 3019 N92-26247

SELECTIVITY
Selective search for the target properties color and form
[IZF-1991-B-13] p 2953 N92-27047

SEMANTICS
Research accomplished at the Knowledge Based Systems Lab: IDEF3, version 1.0
[NASA-CR-190279] p 2975 N92-26587
A prototype semantic integrity front end expert system for a relational database
[AD-A246084] p 3013 N92-26765

SEMICONDUCTOR DEVICES
Silicon drift chambers with integrated amplifiers as low energy detectors p 2908 N92-26398

SEMICONDUCTOR DIODES
Innovative techniques for the production of low cost 2D laser diode arrays
[AD-A247282] p 2913 N92-27178

SEMICONDUCTOR LASERS
Innovative techniques for the production of low cost 2D laser diode arrays
[AD-A247282] p 2913 N92-27178

SEMICONDUCTORS (MATERIALS)
Studies of deep level transient spectroscopy of DX centers in GaAlAs: Te under uniaxial stress
[DE92-010258] p 3001 N92-26204
Generation of nonequilibrium optical phonons in GaAs/AlAs quantum wells by intrasubband and intersubband scatterings
[DE92-010264] p 2993 N92-26207
Method for implanting impurities in semiconductors and semiconductor implanted with impurities
[AD-D015196] p 3003 N92-26433
Investigation of kinetics of MOCVD systems
[AD-A246090] p 2893 N92-26540
Mobility of electrons and holes in semiconductors
[DE92-010125] p 3004 N92-26638
Photoinduced charge separation in solid-state and molecular systems
[DE92-010130] p 3004 N92-26639
Band structure and optical properties of semiconductor superlattices
[AD-A246076] p 3005 N92-26763

SENSITIVITY
Sensitivity analysis of biospheric behaviour of radionuclides released from nuclear waste repositories, appendix 4 p 2929 N92-26486

SENSORS
Optical flow sensor
[AD-D015200] p 2997 N92-26862

SEPARATED FLOW
Wave viscosity interaction in nonlinear roll motion
[AD-A245756] p 2897 N92-26591
Helium bubble flow visualization of the spanwise separation on a NACA 0012 with simulated glaze ice
[NASA-TM-105742] p 2849 N92-26612

SEPARATORS
Fan/pump/separator technology development for EVA
p 2966 N92-27006
Super NiCd battery program: History and performance
p 2862 N92-27135
Hughes advanced nickel-cadmium batteries: An update p 2862 N92-27136
Chemical evaluation of non-woven nylon separators used in Ni/Cd cells p 2863 N92-27140
Utilization of a bipolar lead acid battery for the advanced launch system p 2865 N92-27157
The evaluation of layered separators for nickel-hydrogen cells p 2866 N92-27161

SEQUENCING
Estimation of motion parameters from image sequences
[AD-A246135] p 2986 N92-26358

Discrete sequence prediction and its applications
[NASA-TM-107865] p 2984 N92-26791

SERIES EXPANSION
Effects of video bandwidth on the performance of a square law detector with Gaussian IF and video filters
[AD-A246506] p 2989 N92-26467
Developments of solutions of some special elliptic equations at a corner
[PB92-148741] p 2986 N92-26503

SERVICE LIFE
COBE battery overview: History, handling, and performance p 2862 N92-27131
End-of-life evaluation of the solar maximum mission batteries p 2862 N92-27132
Chemical evaluation of non-woven nylon separators used in Ni/Cd cells p 2863 N92-27140

SET THEORY
Extracting fuzzy rules under uncertainty and measuring definability using rough sets
[NASA-CR-190396] p 2972 N92-26197
Measuring uncertainty by extracting fuzzy rules using rough sets
[NASA-CR-190395] p 2972 N92-26198
Finding a best subtree of a tree
[REPT-91-041] p 2986 N92-26420
Verifying behavioral consistency of an object-oriented database schema
[REPT-91-054] p 3011 N92-26422
Theoretical issues in adaptive Set-Membership-Based signal processing.
[AD-A245721] p 2980 N92-26430
N-learners problem: Learning Boolean combinations of halfspaces
[DE92-010390] p 2987 N92-26545
Dvoretzky's theorem: 30 years later
[PB92-153212] p 2988 N92-26788

SHALES
The carbon isotopic compositions of individual compounds from ancient and modern depositional environments p 2921 N92-26478

SHALLOW WATER
Description of a global shallow water model based on the spectral transform method
[PB92-155258] p 2928 N92-26352
A compendium of environmental data collected during the southwest Florida shallow-water acoustic sea test
[AD-A246143] p 2950 N92-27071

SHAPED CHARGES
Spinning jets from shaped charges with flow turned liners
[MBB-UA-1197-90-PUB] p 2886 N92-26246

SHAPES
Shape from periodic texture using the spectrogram
[AD-A245855] p 2973 N92-26384
Numerical solution of plastic liquids shape factor
[PB92-133958] p 2896 N92-26496

SHEAR
Spinning jets from shaped charges with flow turned liners
[MBB-UA-1197-90-PUB] p 2886 N92-26246

SHEAR FLOW
Fine scale structure of conserved scalar mixing in turbulent shear flows: Sc much greater than 1 and Sc approximately equal to 1 p 2899 N92-26740
A parametric study of the hydrodynamic stability theory of 3-D compressible free shear flows p 2900 N92-26849
On testing models for the pressure-strain correlation of turbulence using direct simulations
[NASA-CR-189638] p 2901 N92-26883
Numerical simulation of the laminar turbulent transition in a stratified flow p 2904 N92-26920

SHEAR LAYERS
An experimental study of natural and forced modes in an axisymmetric jet p 2897 N92-26600
Vortex structure in wake of a circular cylinder p 2904 N92-26918
Turbulent mixing in supersonic jets p 2850 N92-27054

SHEAR PROPERTIES
Computational modelling of rubberlike materials
[ETN-92-91304] p 2916 N92-26259

SHEAR STRESS
A finite element method including transverse stresses for thick laminated plates and shells p 2920 N92-26860

SHELLS (STRUCTURAL FORMS)
A finite element method including transverse stresses for thick laminated plates and shells p 2920 N92-26860

SHIPS
Numerical field model simulation of full-scale fire tests in a closed spherical/cylindrical vessel using advanced computer graphics techniques
[AD-A245810] p 2887 N92-26898

SHOCK LOADS
An explosively driven, fast shock tube
[DE92-008437] p 2856 N92-26720
Role of shock compression technique for scientific and engineering studies
[DE92-008324] p 2919 N92-26846
Recent advances in shock and quasi-isentropic compression techniques for dynamic material property studies
[DE92-007988] p 2919 N92-26852

SHOCK RESISTANCE
Analysis and modeling of high-temperature performance of advanced fiber composites p 2868 N92-26564

SHOCK TESTS
Dynamic response of cylindrical shells to underwater end-on explosion
[AD-A245804] p 2920 N92-26932

SHOCK TUBES
An explosively driven, fast shock tube
[DE92-008437] p 2856 N92-26720

SHOCK WAVE INTERACTION
Shock-turbulence interactions in a reacting flow
[NASA-CR-189647] p 2905 N92-27032

SHOCK WAVE PROPAGATION
Comparison of one-way wave propagation algorithms in underwater acoustics-error estimates and sensitivity
[AD-A245660] p 2991 N92-26175

SHOCK WAVES
Experiences in using C++ to develop a next generation strong shock wave physics code
[DE92-006675] p 2976 N92-26696
Vibrational spectroscopy in shock-compressed liquids
[DE92-007713] p 2876 N92-26867
Control of turbulent mixing in hypersonic flow p 2904 N92-26919

SHOES
Maintenance manual for Natick's Footwear Database
[AD-A246273] p 2954 N92-26242
User manual for Natick's Footwear Database
[AD-A246275] p 2954 N92-26243

SHORT CIRCUITS
Safety testing of lithium cells p 2864 N92-27150

SHORT WAVE RADIATION
Short-wave low-frequency spectra in a current-carrying plasma
[DE92-621529] p 3001 N92-26808

SHOULDERS
The validation of a human force model to predict dynamic forces resulting from multi-joint motions
[NASA-TP-3206] p 2956 N92-26538

SIGNAL DETECTION
Synchronous detection in monolithically integrated AM upconversion receivers
[ETN-92-91305] p 2892 N92-26260
Nonstationary higher order spectral analysis
[AD-A246580] p 2991 N92-26772

SIGNAL DETECTORS
Data fusion and correlation techniques testbed (DFACTT): Field trial 14 January 1991
[AD-A245324] p 3011 N92-26378

SIGNAL ENCODING
Implementation of multi-frequency modulation with Trellis encoding and Viterbi decoding using a digital signal processing board
[AD-A245998] p 2976 N92-26758
Algorithms for capacity computations and algebraic cascade coding with applications to data storage p 2977 N92-27053

SIGNAL FLOW GRAPHS
Pattern search in turbulent field p 2901 N92-26907

SIGNAL PROCESSING
Spatially variant tomographic imaging: Estimation, identification, and optimization
[DE92-010262] p 2921 N92-26206
Applications of wavelets to signal processing held in Wright-Patterson AFB, Ohio on 20-22 March 1991. Volume 2: Tutorial notes
[AD-A245567] p 2888 N92-26381
Fast envelope correlation for passive ranging
[AD-A246333] p 2888 N92-26388
Optical hidden layer network
[AD-A246162] p 2992 N92-26413
Theoretical issues in adaptive Set-Membership-Based signal processing.
[AD-A245721] p 2980 N92-26430
Matched field processing on the connection machine
[AD-A245469] p 2980 N92-26531
Radar target identification by natural resonances: Evaluation of signal processing algorithms
[AD-A246586] p 2889 N92-26619
Source location in thin plates using crosscorrelation
[AD-A245521] p 2992 N92-26678
Implementation of multi-frequency modulation with Trellis encoding and Viterbi decoding using a digital signal processing board
[AD-A245998] p 2976 N92-26758
A real-time synthetic aperture radar processor: Introduction and project description
[AD-A245370] p 2890 N92-26876
High-speed pulse detection room-temperature optical nonlinearities for GaInAs/A1InAs and GaA1InAs/A1InAs multiple quantum wells and integrated mirror etalon at 1.3 micrometers
[AD-A246369] p 2998 N92-26943

SIGNAL TO NOISE RATIOS
Fast envelope correlation for passive ranging
[AD-A246333] p 2888 N92-26388
Signal-to-noise ratio expected for a calorimeter with transition edge thermometer p 2907 N92-26395
Performance analysis of image motion analysis algorithms
[AD-A246522] p 2974 N92-26468
A measuring facility for testing radio communication equipment
[AD-A245621] p 2890 N92-26874
Modeling for improved minimum resolvable temperature difference measurements
[AD-A246389] p 2991 N92-27078

SILANES
A surface science investigation of silicon carbide: Oxidation, crystal growth and surface structural analysis
[DE92-010286] p 3004 N92-26641

SILICA GLASS
Lightweight fiber insulations performance and application p 2883 N92-27016
Optical performance of exposed solar cell covers p 2998 N92-27091
Effects of long term exposure on optical substrates and coatings (SOO50-2) p 2998 N92-27096

SILICATES
Infrared spectroscopy and hydrogen isotope geochemistry of hydrous silicate glasses
[DE92-008398] p 2881 N92-26451

SILICON
Cadmium telluride thin films on silicon substrates
[AD-A245309] p 3001 N92-26226
Gas-pressure studies with Li(Si)/FeS2 thermal batteries
[DE92-010801] p 2892 N92-26238
Simulation studies for surfaces and materials strength
[NASA-CR-190340] p 3001 N92-26265
Silicon drift chambers with integrated amplifiers as low energy detectors p 2908 N92-26398
Method for implanting impurities in semiconductors and semiconductor implanted with impurities
[AD-D015196] p 3003 N92-26433
Numerical modeling of silicon photodiodes for high-accuracy applications with PC-1D
[PB92-148279] p 2894 N92-26821
Complementary metal oxide silicon cyclic redundancy check generators
[AD-A246140] p 2894 N92-27061

SILICON ALLOYS
Elevated temperature properties of a dispersion strengthened Al-(Fe, V, Si) alloy
[AD-A246427] p 2880 N92-27067

SILICON CARBIDES
A surface science investigation of silicon carbide: Oxidation, crystal growth and surface structural analysis
[DE92-010286] p 3004 N92-26641
Ceramic composites: Experimental and analytical study of SiC/Si3N4 composites p 2882 N92-26859

SILICON DIOXIDE
Etching effects in ion implanted SiO2
[DE92-011150] p 3005 N92-26826

SILICON NITRIDES
Slip casting and green body evaluation of 6 percent yttria, 2 percent alumina silicon nitride
[AD-A245817] p 2881 N92-26283
Study and analysis of the stress state in a ceramic, button-head, tensile specimen
[DE92-007794] p 2918 N92-26784
Ceramic composites: Experimental and analytical study of SiC/Si3N4 composites p 2882 N92-26859

SILVER ZINC BATTERIES
The 1990 NASA Aerospace Battery Workshop
[NASA-CP-3119] p 2862 N92-27130
Life testing of secondary Ag-Zn cells p 2865 N92-27153

SILVICULTURE
Global assessment of promising forest management practices for sequestration of carbon
[PB92-153006] p 2930 N92-26510

SIMILARITY THEOREM
On the existence of a capital similarity p 2941 N92-26344
Use of an approximate similarity principle for the thermal scaling of a full-scale thrust augmenting ejector
[NASA-TM-105724] p 2854 N92-26613

SIMULATION
Report for neutral buoyancy simulations of transfer orbit stage contingency extravehicular activities
[NASA-TM-103583] p 2857 N92-26268
Numerical investigation of the circulation of an ice-covered Arctic Ocean p 2949 N92-26568
Numerical simulations of gun-launched kinetic energy projectiles subjected to asymmetric projectile base pressure
[DE92-005065] p 2857 N92-26693
SAFT nickel-cadmium cell performances for GEO and LEO applications p 2863 N92-27137
Hubble Space Telescope nickel-hydrogen flight spare battery test p 2866 N92-27165

SIMULATORS
A design rationale for NASA TileWorld
[NASA-TM-107882] p 2982 N92-26627
An object-oriented approach to computer architecture simulation
[AD-A246597] p 2970 N92-26773

SINGLE CRYSTALS
Magnetic flux noise in copper oxide superconductors
[DE92-010299] p 3003 N92-26582
Effect of interstitials on the trapping of hydrogen in iron-single crystals
[AD-A246412] p 3006 N92-27064
Results of the TTF-TCNQ and the calcium carbonate crystallization on the Long Duration Exposure Facility
p 3007 N92-27127

SINTERING
Relationship between composition, structure, properties, thermo-mechanical processing and ballistic performance of tungsten heavy alloys
[AD-A245649] p 2876 N92-26172
Crystalline-amorphous interfaces and their relation to grain boundary films
[DE92-009812] p 3004 N92-26648

SKIN (ANATOMY)
Effect of textile test sample size on assessment of protection to skin from thermal radiation
[AD-A246535] p 2955 N92-26472

SLABS
Analysis of surface wave propagation in a grounded dielectric slab covered by a resistive sheet
[NASA-TM-107583] p 2889 N92-26653

SLENDER BODIES
Coning motion and flat spinning of slender bodies at high angles of attack p 2902 N92-26912

SLIDING
Hybrid efficient control algorithms for robot manipulators
[AD-A245716] p 2981 N92-26428

SLIP CASTING
Slip casting and green body evaluation of 6 percent yttria, 2 percent alumina silicon nitride
[AD-A245817] p 2881 N92-26283

SLOPES
Quantitative assessment of the slope resolution of seafloor mapping systems
[AD-A246158] p 2949 N92-26411

SLOTS
CFD mixing analysis of jets injected from straight and slanted slots into confined crossflow in rectangular ducts
[NASA-TM-105699] p 2854 N92-26561

SMALL SCIENTIFIC SATELLITES
Small Explorer Data System MIL-STD-1773 fiber optic bus
[NASA-TP-3227] p 2858 N92-26667

SNOW COVER
A one-dimensional temperature model for a snow cover: Technical documentation for SNTHERM.89
[AD-A245493] p 2922 N92-26674

SOCIAL FACTORS
Multi-cultural components and keys for European worldwide space programs p 2857 N92-27008

SODIUM
Spontaneous and induced coherent radiation generation in atomic vapors
[AD-A246078] p 2890 N92-26764

SODIUM CHLORIDES
Evaluation of sodium-nickel chloride cells for space applications p 2865 N92-27156

SODIUM 22
Gamma-ray spectrometry of LDEF samples
[DE92-009947] p 2874 N92-26632

SOFT LANDING
Critical soft landing technology issues for future US space missions
[NASA-CR-185673] p 2858 N92-26884

SOFTWARE ENGINEERING
Advanced software development workstation. Engineering scripting language graphical editor: DRAFT design document
[NASA-CR-190393] p 2971 N92-26181
Advanced software development workstation. Engineering scripting language graphical editor: DRAFT code documentation
[NASA-CR-190389] p 2971 N92-26182
Advanced software development workstation project: Engineering scripting language. Graphical editor
[NASA-CR-190391] p 2971 N92-26183
Software maturity model applied to SDI
[AD-A245439] p 2972 N92-26276
Reference model for frameworks of software engineering environments
[PB92-158328] p 2973 N92-26370
Investigating the utility of coupling COCOMO with a system dynamics simulation of software development
[AD-A245484] p 2973 N92-26400
Integrating reverse engineering into Computer-Aided Software Engineering (CASE) p 2974 N92-26479
Research accomplished at the Knowledge Based Systems Lab: IDEF3, version 1.0
[NASA-CR-190279] p 2975 N92-26587
Research and technology, 1990: Goddard Space Flight Center
[NASA-TM-107792] p 3022 N92-26824
The 1990 progress report and future plans
[NASA-TM-107911] p 2984 N92-26887
Software architecture for a distributed real-time system in Ada, with application to telerobotics
[NASA-TM-4367] p 2977 N92-26904
Integrated communication environment for thermal analysis software p 2958 N92-26959
UT40 - Asset Library Open Architecture Framework (ALOAF)
[AD-A247268] p 2978 N92-27177

SOFTWARE TOOLS
The development of a design database for the computer aided prototyping system
[AD-A245786] p 3010 N92-26176
Reference model for frameworks of software engineering environments
[PB92-158328] p 2973 N92-26370
Integrating reverse engineering into Computer-Aided Software Engineering (CASE) p 2974 N92-26479
Architecture flow diagrams under Teamwork
[DE92-010482] p 2922 N92-26534
Tools and techniques for adding fault tolerance to distributed and parallel programs
[AD-A245510] p 2980 N92-26677
Forging a path with tool and data attributes
[DE92-009800] p 2976 N92-26797
The fidelity enhancement process
[AD-A245388] p 2977 N92-26840
COSMIC software catalog, 1992 edition
[NASA-CR-188973] p 2977 N92-26868
FIESTA: An integrated approach to thermal model processing p 2958 N92-26958
Definition of the common structure of data to promote the communication between different thermal software tools p 2958 N92-26960

SOHO MISSION
Development of a thermal control concept for the optical system of the SUMER experiment on SOHO
p 2960 N92-26975

SOIL SCIENCE
Organic carbon in soil and the global carbon cycle
[DE92-010289] p 2931 N92-26580
Fundamentals of electrokinetics
[DE92-008326] p 2894 N92-26847

SOILS
Equilibrium-analysis of projected climate change effects on the global soil organic matter pool
[PB92-153022] p 2930 N92-26509

SOLAR ACTIVITY
Workshop on Solar Activity, Solar Wind, Terrestrial Effects, and Solar Acceleration
[NASA-CR-190195] p 3020 N92-26437

SOLAR ACTIVITY EFFECTS
Workshop on Solar Activity, Solar Wind, Terrestrial Effects, and Solar Acceleration
[NASA-CR-190195] p 3020 N92-26437
Solar wind interaction with Venus and Mars
p 3020 N92-26779

SOLAR ARRAYS
The effect of sandstorms on PV arrays and components --- photovoltaic cells
[DE92-001240] p 2927 N92-26686
MILSTAR's flexible substrate solar array: Lessons learned, addendum
[NASA-CP-3147-ADD] p 2927 N92-26895
Thermal implications from the Hubble Space Telescope solar array bi-stem boom in-orbit disturbance
p 2965 N92-27001
An overview of the first results on the solar array materials passive LDEF experiment (sample), A0171
p 2927 N92-27087
Long Duration Exposure Facility (LDEF) low-temperature heat pipe experiment package power system results
p 2906 N92-27105
The effect of switched array battery charge control on CRRES spacecraft: 3 + month data summary
p 2862 N92-27134

SOLAR BLANKETS
Ulysses, one year after the launch
p 2860 N92-26999
Durability evaluation of photovoltaic blanket materials exposed on LDEF tray S1003 p 2883 N92-27100

SOLAR CELLS
Photovoltaic manufacturing technology, phase 1
[DE92-001199] p 2926 N92-26190
Numerical modeling of silicon photodiodes for high-accuracy applications with PC-1D
[PB92-148279] p 2894 N92-26821
An overview of the first results on the solar array materials passive LDEF experiment (sample), A0171
p 2927 N92-27087
Experiment M0003-4: Advanced solar cell and coverglass analysis, an overview p 2927 N92-27088
Optical performance of exposed solar cell covers
p 2998 N92-27091
Advanced photovoltaic experiment, S0014: Preliminary flight results and post-flight findings
p 2927 N92-27101
Evaluation of LDEF experiment S1002
p 2883 N92-27102

SOLAR COSMIC RAYS
Workshop on Solar Activity, Solar Wind, Terrestrial Effects, and Solar Acceleration
[NASA-CR-190195] p 3020 N92-26437

SOLAR CYCLES
Workshop on Solar Activity, Solar Wind, Terrestrial Effects, and Solar Acceleration
[NASA-CR-190195] p 3020 N92-26437
Solar wind interaction with Venus and Mars
p 3020 N92-26779

SOLAR DYNAMIC POWER SYSTEMS
Heat receivers for solar dynamic space power systems p 2860 N92-26601

SOLAR ENERGY
SOLTECH 1992 proceedings: Solar Process Heat Program, volume 1
[DE92-001238] p 2927 N92-26683
Passive thermostate system with application of gas-filled heat pipes and thermal energy of solar radiation
p 2905 N92-26972

SOLAR ENERGY CONVERSION
SOLTECH 1992 proceedings: Solar Process Heat Program, volume 1
[DE92-001238] p 2927 N92-26683
Photochemical energy conversion by membrane-bound photoredox systems
[DE92-008709] p 2927 N92-26858

SOLAR FLARES
The HUS solar flare and cosmic gamma ray burst detector aboard the Ulysses spacecraft
[MPE-PREPRINT-175] p 3016 N92-27049

SOLAR HEATING
Physical processes within the nocturnal stratus-topped boundary layer, revision
[AD-A245829] p 2947 N92-26901

SOLAR INTERIOR
Observational and theoretical investigations in solar seismology
[NASA-CR-190245] p 3019 N92-26247

SOLAR MAXIMUM MISSION
End-of-life evaluation of the solar maximum mission batteries p 2862 N92-27132

SOLAR NEUTRINOS
The status of GALLEX
[DE92-010077] p 3020 N92-26566

SOLAR OSCILLATIONS
Observational and theoretical investigations in solar seismology
[NASA-CR-190245] p 3019 N92-26247

SOLAR RADIATION
The effects of magnetic storm phases on F-layer irregularities from auroral to equatorial latitudes
[AD-A245495] p 2943 N92-26675

SOLAR TERRESTRIAL INTERACTIONS
Cusp and cleft studies in Greenland
p 2935 N92-26299
The present understanding of the cusp
p 2936 N92-26306
Solar wind-magnetosphere coupling processes observed near the dayside cusp/cleft
p 2937 N92-26307
The need of coordinated observations in space and from ground p 2937 N92-26310
Mathematical model of physical processes responsible for generation of magnetospheric electric fields and their penetration into the Earth's magnetosphere
p 2938 N92-26319

SOLAR WIND
Handbook of solar-terrestrial data systems, version 1 [NASA-TM-107810] p 3019 N92-26191
Antarctic studies of the cusp p 2936 N92-26301
Solar wind-magnetosphere coupling processes observed near the dayside cusp/cleft p 2937 N92-26307
Workshop on Solar Activity, Solar Wind, Terrestrial Effects, and Solar Acceleration [NASA-CR-190195] p 3020 N92-26437
The dynamic response of the westward auroral electrojet and polar cap currents to solar wind-magnetosphere coupling p 2943 N92-26622
Solar wind interaction with Venus and Mars p 3020 N92-26779

SOLAR X-RAYS
Workshop on Solar Activity, Solar Wind, Terrestrial Effects, and Solar Acceleration [NASA-CR-190195] p 3020 N92-26437
The HUS solar flare and cosmic gamma ray burst detector aboard the Ulysses spacecraft [MPE-PREPRINT-175] p 3016 N92-27049

SOLAR-PUMPED LASERS
Comparison of laser models [NASA-CR-190302] p 2913 N92-26870

SOLDERED JOINTS
Stresses in solder joints of electronic packages [AD-A245799] p 2894 N92-26897

SOLDERING
Stresses in solder joints of electronic packages [AD-A245799] p 2894 N92-26897

SOLDERS
Stresses in solder joints of electronic packages [AD-A245799] p 2894 N92-26897

SOLENOIDS
Assessment of diagnostic methods for solenoid-operated valves [DE92-009379] p 2913 N92-26234

SOLID LUBRICANTS
Ceramic bearing technology: Proceedings of the NIST/DARPA Workshop [PB92-137553] p 2914 N92-26366

SOLID PROPELLANT ROCKET ENGINES
Report for neutral buoyancy simulations of transfer orbit stage contingency extravehicular activities [NASA-TM-103583] p 2857 N92-26268
Modification and experimental validation of a combined optical and collection probe for solid propellant exhaust analysis [AD-A245387] p 2884 N92-26839
Subscale solid rocket motor infrared signature and particle behavior [AD-A246416] p 2862 N92-27065

SOLID PROPELLANTS
Modification and experimental validation of a combined optical and collection probe for solid propellant exhaust analysis [AD-A245387] p 2884 N92-26839

SOLID ROCKET PROPELLANTS
Space aging of solid rocket materials p 2884 N92-27085

SOLID WASTES
Environmental Protection Agency's municipal solid waste landfill liner design criteria [PB92-153766] p 2933 N92-26928

SOLIDIFICATION
Microstructural evaluation of as-solidified and heat treated gamma-TiAl based powders [DE92-008956] p 2881 N92-26455
Feasibility study of an expert system for the design of fusion/solidification experiment boarding on space furnace p 2886 N92-26964

SOLIDS
Eulerian computational methods [DE92-008017] p 2900 N92-26853

SOLITARY WAVES
Aircraft observation of a small-scale solitary wave near the tropopause p 2940 N92-26336

SOLUBILITY
Retention and release of tritium in aluminum clad, Al-Li alloys [DE92-009905] p 2878 N92-26635

SOLVATION
Solvation effects on the electronic structure of 4-N,N-Dimethylaminobenzonitrile: Mixing of the local pipi* and charge transfer states [AD-A245814] p 2874 N92-26608

SOLVENTS
Solvation effects on the electronic structure of 4-N,N-Dimethylaminobenzonitrile: Mixing of the local pipi* and charge transfer states [AD-A245814] p 2874 N92-26608

SONAR
Precision of the long baseline acoustic navigation system used by Pegasus [AD-A246598] p 2852 N92-26795

SOUND FIELDS
Evaluation of the computational validity of the image model in predicting the sound field in a wedge-shaped layer using acoustical reciprocity [AD-A246548] p 2992 N92-26688
Acoustically probed Taylor-Couette flow apparatus [AD-A246385] p 2993 N92-27076

SOUND GENERATORS
Theoretical and experimental study of thermoacoustic engines [AD-A246334] p 2914 N92-26389

SOUND TRANSDUCERS
Optical hidden layer network [AD-A246162] p 2992 N92-26413
Binaural ultrasound detector and imager [AD-D015214] p 2993 N92-27184

SOUND TRANSMISSION
The utility of acoustic travel times in locating the north wall of the Gulf Stream [AD-A246219] p 2949 N92-26463
Apparatus for measuring the absorption of sound by noise in one dimension [AD-A246442] p 2992 N92-27031

SOUND WAVES
Ocean bottom modeling for ray acoustics [AD-A246287] p 2948 N92-26360
Theoretical and experimental study of thermoacoustic engines [AD-A246334] p 2914 N92-26389
Optical hidden layer network [AD-A246162] p 2992 N92-26413
Distributed acoustic receptivity in laminar flow control configurations [NASA-CR-4438] p 2898 N92-26680
Boundary-layer receptivity due to distributed surface imperfections of a deterministic or random nature [NASA-CR-4439] p 2898 N92-26681
Apparatus for measuring the absorption of sound by noise in one dimension [AD-A246442] p 2992 N92-27031

SPACE BASED RADAR
Effects of the space environment on space-based radar phased-array antenna; status and preliminary observations (LDEF Experiment A0133) p 2883 N92-27086

SPACE CAPSULES
Heatshield concepts for the Rosetta Aerocapsule p 2860 N92-27028

SPACE DEBRIS
Evaluation of LDEF experiment S1002 p 2883 N92-27102

SPACE ENVIRONMENT SIMULATION
Critical technologies: Spacecraft habitability, an update p 2966 N92-27010

SPACE EXPLORATION
Human support issues and systems for the space exploration initiative: Results from Project Outreach [NASA-CR-190320] p 2954 N92-26193
Life support research and development, a Department of Energy program for the Space Exploration Initiative [DE92-007681] p 2955 N92-26375
Life support research and development for the Department of Energy Space Exploration Initiative [DE92-007239] p 2955 N92-26494
Assessment of a hot hydrogen nuclear propulsion fuel test facility [DE92-004571] p 2995 N92-26692
NASA/DOE/DOD nuclear propulsion technology planning: Summary of FY 1991 interagency panel results [NASA-TM-105703] p 2861 N92-26792

SPACE FLIGHT
Orbital maintenance of endoatmospheric low earth-orbiting satellites [AD-A246381] p 2859 N92-27074

SPACE FLIGHT FEEDING
An evaluative study of the sensory qualities of selected European and Asian foods for international space missions (a French food study) p 2966 N92-27009

SPACE FLIGHT TRAINING
CBT: Role and future application for crew training --- computer based training p 2953 N92-26992

SPACE LOGISTICS
Logistics in space: Tools to support astronauts p 2963 N92-26990

SPACE MANUFACTURING
Microwelding (or cold-welding) of various metallic materials under the ultra-vacuum LDEF experiment AO 138-10 p 2880 N92-27119

SPACE MISSIONS
Apogee, perigee, and recovery: Chronology of Army exploitation of space [RAND-N-3103-A] p 2856 N92-26192
Critical soft landing technology issues for future US space missions [NASA-CR-185673] p 2858 N92-26884
Multi-cultural components and keys for European worldwide space programs p 2857 N92-27008
Heatshield concepts for the Rosetta Aerocapsule p 2860 N92-27028

SPACE PLASMAS
LDEF SP-HVDE (Space Plasma-High Voltage Drainage Experiment) post-flight results: Leakage current and discharge p 2895 N92-27103

SPACE POWER REACTORS
Tuned-circuit dual-mode Johnson noise thermometers [DE92-010121] p 2908 N92-26569
Evaluation of integral measurements for the SP-100 space reactor [DE92-009717] p 2996 N92-26841

SPACE PROBES
Development of a thermal control concept for the optical system of the SUMER experiment on SOHO p 2960 N92-26975

SPACE RATIONS
An evaluative study of the sensory qualities of selected European and Asian foods for international space missions (a French food study) p 2966 N92-27009

SPACE SHUTTLE MAIN ENGINE
Effect of type of load on stress analysis of thin-walled ducts [NASA-TP-3248] p 2918 N92-26669
Rocket engine diagnostics using qualitative modeling techniques [NASA-TM-105714] p 2861 N92-27033

SPACE SHUTTLE PAYLOADS
Retrievable payload carrier: Next generation Long Duration Exposure Facility p 2860 N92-27129

SPACE SHUTTLES
Atmospheric environment for Space Shuttle Columbia (STS-40) launch [NASA-TM-103585] p 2945 N92-26288
Thermal analysis of evaporative coolers p 2962 N92-26985

SPACE STATION FREEDOM
MILSTAR's flexible substrate solar array: Lessons learned, addendum [NASA-CP-3147-ADD] p 2927 N92-26895
Structural dynamic interaction with solar tracking control for evolutionary Space Station concepts [NASA-TM-107629] p 2920 N92-26903

SPACE STATION POWER SUPPLIES
SPOT multimission platform thermal control: Five years of in-flight results p 2860 N92-26998

SPACE STATIONS
Structural dynamic interaction with solar tracking control for evolutionary Space Station concepts [NASA-TM-107629] p 2920 N92-26903
Fourth European Symposium on Space Environment Control Systems, volume 2 [ESA-SP-324-VOL-2] p 2956 N92-26950
Influence of architecture on the definition of a space station configuration p 2860 N92-27024

SPACE SUITS
Genesis and evaluation of an ergonomic architecture for the ESA EVA suit p 2965 N92-27003
EVA space suit thermal control and micrometeoroid protection p 2965 N92-27004
Development of the suit enclosure soft joints of the European EVA space suit p 2965 N92-27005
Fan/pump/separator technology development for EVA p 2966 N92-27006

SPACE-TIME FUNCTIONS
Finite temperature quantum field theory in curved spacetime p 3007 N92-26780
Human cognitive processes in command and control planning. 3: Determining basic processes involved in planning in time and space [IZF-1991-B-11] p 3010 N92-27046

SPACEBORNE EXPERIMENTS
Laboratory evaluation and application of microwave absorption properties under simulated conditions for planetary atmospheres [NASA-CR-190211] p 3019 N92-26438
Principal investigator in a box: Version 1.2 documentation [NASA-TM-107886] p 2982 N92-26628
Space aging of solid rocket materials p 2884 N92-27085
LDEF active optical system components experiment p 2998 N92-27094
Effects of long-duration exposure on optical system components p 2998 N92-27095
Vacuum deposited optical coatings experiment p 2999 N92-27097
Durability evaluation of photovoltaic blanket materials exposed on LDEF tray S1003 p 2883 N92-27100
Advanced photovoltaic experiment, S0014: Preliminary flight results and post-flight findings p 2927 N92-27101
Evaluation of LDEF experiment S1002 p 2883 N92-27102

LDEF SP-HVDE (Space Plasma-High Voltage Drainage Experiment) post-flight results: Leakage current and discharge p 2895 N92-27103
Long Duration Exposure Facility (LDEF) low temperature heat pipe experiment package (HEPP) flight results p 2906 N92-27104
Results from the LDEF/A0076 cascaded variable conductance heatpipe experiment p 2906 N92-27106
Seeds in space experiment --- long duration exposure facility p 2952 N92-27120
Space Exposed Experiment Developed for Students (SEEDS) (P0004-2) p 2952 N92-27121
Retrievable payload carrier: Next generation Long Duration Exposure Facility p 2860 N92-27129

SPACEBORNE TELESCOPES
SIGMA VCHP radiator: In-orbit performance p 2859 N92-26966
Thermal control of telescope apertures by optimized baffle heating p 2961 N92-26976

SPACECRAFT CABINS
Biodegradation studies with space cabin contaminants to determine the feasibility of Biological Air Filtration (BAF) in space cabins p 2962 N92-26983

SPACECRAFT CHARGING
Investigation of deep dielectric charging and subsequent currents on geosynchronous spacecraft [AD-A245764] p 2858 N92-26605

SPACECRAFT CONFIGURATIONS
Influence of architecture on the definition of a space station configuration p 2860 N92-27024

SPACECRAFT CONTROL
Structural dynamic interaction with solar tracking control for evolutionary Space Station concepts [NASA-TM-107629] p 2920 N92-26903

SPACECRAFT DESIGN
Design of JEM temperature and humidity control system p 2958 N92-26957
The liquid droplet radiator: Status of development p 2905 N92-26969
Human factors in the conception of the Hermes space vehicle p 2963 N92-26989
CAD system for HFE analyses: Zero-g posture in optimisation of Columbus APM crew workstations --- human factors engineering p 2963 N92-26991
Italsat thermal control: The in-orbit performances p 2859 N92-26996
Architectural studies relating to human body motion morphology in microgravity p 2953 N92-27011
Warm structures and thermal protection of the European spaceplane Hermes p 2860 N92-27014
New perspectives of living in space: Habitability guidelines for future manned space systems p 2968 N92-27022
Concept for a European Space Station: Habitability, life support, and laboratory facilities p 2969 N92-27023
Rarefied-flow aerodynamics [NASA-CR-190452] p 2850 N92-27191

SPACECRAFT ENVIRONMENTS
Catalytic wet-oxidation of human waste produced in a space habitat: Purification of the oxidized liquor for human drinking p 2957 N92-26954
Design of JEM temperature and humidity control system p 2958 N92-26957
Systems special investigation group overview p 2867 N92-27084

SPACECRAFT EQUIPMENT
Small Explorer Data System MIL-STD-1773 fiber optic bus [NASA-TP-3227] p 2858 N92-26667
The centrifugal mass exchange apparatus in air-conditioning system of isolated, inhabited object and its work control p 2957 N92-26956
Crew support equipment: Identification and definition of additional hardware for Columbus APM laboratory habitability p 2964 N92-26993
Microgravity simulation p 2964 N92-26994

SPACECRAFT INSTRUMENTS
Passive thermostate system with application of gas-filled heat pipes and thermal energy of solar radiation p 2905 N92-26972
Thermal design for the space-exposed instruments for the scientific satellite SAX p 2860 N92-26973

SPACECRAFT LAUNCHING
Atmospheric environment for Space Shuttle Columbia (STS-40) launch [NASA-TM-103585] p 2945 N92-26288
A prototype multi-media data base for tracking interface relationships and performing cost tradeoffs for the Sea Launch and Recovery (SEALAR) space launch system [AD-A245481] p 2857 N92-26515

SPACECRAFT MODULES
Design of JEM temperature and humidity control system p 2958 N92-26957
Crew support equipment: Identification and definition of additional hardware for Columbus APM laboratory habitability p 2964 N92-26993

SPACECRAFT MOTION
Sensitivity of sensors for characterizing chaos [AD-A246423] p 2921 N92-27066

SPACECRAFT PERFORMANCE
International Conference on Japanese Earth Observation Programs: TRMM Workshop [JTN-92-80345] p 2922 N92-26701
Japanese Earth Observation Program p 2924 N92-26743
SIGMA VCHP radiator: In-orbit performance p 2859 N92-26966
Ulysses, one year after the launch p 2860 N92-26999

SPACECRAFT POWER SUPPLIES
Heat receivers for solar dynamic space power systems p 2860 N92-26601
Integrated heat pipe concept for Li/SOCl2 cells cooling p 2895 N92-26974
Concept for a European Space Station: Habitability, life support, and laboratory facilities p 2969 N92-27023
The 1990 NASA Aerospace Battery Workshop [NASA-CP-3119] p 2862 N92-27130
COBE battery overview: History, handling, and performance p 2862 N92-27131
End-of-life evaluation of the solar maximum mission batteries p 2862 N92-27132
Magellan battery operations: An overview p 2862 N92-27133
The effect of switched array battery charge control on CRRES spacecraft: 3 + month data summary p 2862 N92-27134
Super NiCd battery program: History and performance p 2862 N92-27135
Hughes advanced nickel-cadmium batteries: An update p 2862 N92-27136
SAFT nickel-cadmium cell performances for GEO and LEO applications p 2863 N92-27137
Zinc-oxygen battery development program p 2865 N92-27152
Evaluation of sodium-nickel chloride cells for space applications p 2865 N92-27156
Eutelsat 2: SAR-10009 nickel-hydrogen battery p 2866 N92-27159
Low cost battery designs for small satellite applications p 2866 N92-27160
Hubble Space Telescope NiH2 six battery test p 2866 N92-27164
Nickel-hydrogen LEO cycling at 20 percent - 50 percent DOD p 2867 N92-27168

SPACECRAFT RADIATORS
Unified computational method for design of fluid loop systems p 2905 N92-26962
Design and performance of the Spacelab Astro-1 mission heat pipe radiator p 2859 N92-26965
SIGMA VCHP radiator: In-orbit performance p 2859 N92-26966
Development of fluid loop and hybrid radiators: Test results p 2859 N92-26967
Heat pipe-based radiative panel p 2859 N92-26968
The liquid droplet radiator: Status of development p 2905 N92-26969
Thermo-hydraulic investigations on heat exchangers for Columbus hybrid radiators p 2887 N92-26988
Flight test results of the passive cooling system p 2860 N92-27000

SPACECRAFT RECOVERY
A prototype multi-media data base for tracking interface relationships and performing cost tradeoffs for the Sea Launch and Recovery (SEALAR) space launch system [AD-A245481] p 2857 N92-26515

SPACECRAFT STRUCTURES
Optimization of space structures to minimize dynamic response p 2858 N92-26610

SPACECRAFT TEMPERATURE
Thermal analysis of evaporative coolers p 2962 N92-26985
CPA: A controlled pump assembly for two-phase loops applications p 2916 N92-26987
Ulysses, one year after the launch p 2860 N92-26999
Flight test results of the passive cooling system p 2860 N92-27000
Lightweight fiber insulations performance and application p 2883 N92-27016

SPACECRAFT TRAJECTORIES
Orbital maintenance of endoatmospheric low earth-orbiting satellites [AD-A246381] p 2859 N92-27074

SPACELAB
Design and performance of the Spacelab Astro-1 mission heat pipe radiator p 2859 N92-26965
Thermal analysis of the Spacelab mission D2 utility support structure and its payloads p 2859 N92-26971

SPACELAB PAYLOADS
Thermal analysis of the Spacelab mission D2 utility support structure and its payloads p 2859 N92-26971

SPACING
On the subject of geometric spacing of meteorological sensors [AD-A245824] p 2946 N92-26899

SPAIN
Undulatory airflow over the Spanish southern central highplain with northern winds p 2940 N92-26339

SPARK IGNITION
An instrument for engine torque estimation and misfire detection --- torque p 2909 N92-26738

SPATIAL DISTRIBUTION
Spatially variant tomographic imaging: Estimation, identification, and optimization [DE92-010262] p 2921 N92-26206
Recursive ray acoustics for three-dimensional sound-speed profiles [AD-A245613] p 2991 N92-26228
Improved procedures for quantifying key meteorological effects on ambient ozone data [PB92-163278] p 2931 N92-26793

SPATIAL FILTERING
Estimation of peak intensities from frequency filtered total scattering data of neutrons obtained by the reverse Fourier method p 3002 N92-26321

SPATIAL RESOLUTION
Requirements for coordinated Cluster and ground-based observations of the cusp p 2938 N92-26318
NPSNET: Hierarchical data structures for real-time three-dimensional visual simulation [AD-A246380] p 2978 N92-27073

SPECIFIC HEAT
The Debye temperature of YBa2Cu3O(7-(delta)) and its dependence on the volume fraction of superconductivity [DE92-010305] p 3003 N92-26584

SPECIFICATIONS
Technical specification for the Sandia Management Restructure Study Team (MRST) Prototype Information System [DE92-010360] p 3012 N92-26575
COBE battery overview: History, handling, and performance p 2862 N92-27131
The effect of switched array battery charge control on CRRES spacecraft: 3 + month data summary p 2862 N92-27134

SPECTRA
Spectral boundary conditions and index theorem for 2-dimensional compact manifold with boundary [DE92-621115] p 2990 N92-26798
Short-wave low-frequency spectra in a current-carrying plasma [DE92-621529] p 3001 N92-26808

SPECTRAL BANDS
Differentiation on genus of aquatic macrophytes through remote sensing in the Tucurui Reservoir, Para State, Brazil [INPE-5315-PRE/1712] p 2951 N92-26721
Passive determination of temperature and range using spectral band measurements of photon emittance [AD-A247147] p 2910 N92-27181

SPECTRAL CORRELATION
Fast envelope correlation for passive ranging [AD-A246333] p 2888 N92-26388

SPECTRAL SENSITIVITY
Sensitivity of sensors for characterizing chaos [AD-A246423] p 2921 N92-27066

SPECTROGRAMS
Shape from periodic texture using the spectrogram [AD-A245855] p 2973 N92-26384

SPECTROMETERS
Composition studies based on coincident air shower array and underground muon data [DE92-010345] p 3021 N92-26253
Underground muons observed in the Soudan 2 detector from the directions of x ray sources [DE92-010344] p 3021 N92-26264
High precision timing of millisecond pulsars p 3015 N92-26760

SPECTROSCOPIC ANALYSIS
Studies of deep level transient spectroscopy of DX centers in GaAlAs: Te under uniaxial stress [DE92-010258] p 3001 N92-26204
The use of ion chromatography-dc plasma atomic emission spectrometry for the speciation of trace metals [DE92-010317] p 2871 N92-26236

SPECTROSCOPY
Studies of deep level transient spectroscopy of DX centers in GaAlAs: Te under uniaxial stress [DE92-010258] p 3001 N92-26204
The galactic evolution of s-process elements via asymptotic giant branch stars p 3018 N92-26725
Open problems and future prospects for hypernuclear physics [DE92-010158] p 2995 N92-26815

SPECTRUM ANALYSIS
Development and applications of the reverse neutron time-of-flight method with Fourier-type beam chopper
[VTT-PUBL-82] p 3001 N92-26320
Water vapor information content of absorption lines observed in the Sun's infrared radiance
p 2942 N92-26490
Nonstationary higher order spectral analysis
[AD-A246580] p 2991 N92-26772
SPEECH RECOGNITION
Applications of wavelets to signal processing held in Wright-Patterson AFB, Ohio on 20-22 March 1991. Volume 2: Tutorial notes
[AD-A245567] p 2888 N92-26381
SPENT FUELS
Assessment of biospheric behaviour of releases from nuclear waste repositories, appendix 2
p 2929 N92-26484
Assessment of radiation doses due to releases to the biosphere from nuclear waste repositories, appendix 3
p 2929 N92-26485
SPHERICAL COORDINATES
Description of a global shallow water model based on the spectral transform method
[PB92-155258] p 2928 N92-26352
SPHERICAL SHELLS
Quantum black holes and Hawking's radiation
[PB92-152313] p 3018 N92-26833
SPHEROIDS
Spheroidization and densification of Nickel powders by RF-induction plasma
[PB92-151893] p 2879 N92-26787
SPIN
Spinning jets from shaped charges with flow turned liners
[MBB-UA-1197-90-PUB] p 2886 N92-26246
SPLINE FUNCTIONS
Recursive ray acoustics for three-dimensional sound-speed profiles
[AD-A245613] p 2991 N92-26228
Ocean bottom modeling for ray acoustics
[AD-A246287] p 2948 N92-26360
On the construction of multivariate (pre)wavelets
[AD-A247105] p 2989 N92-27175
SPONTANEOUS EMISSION
Spontaneous and induced coherent radiation generation in atomic vapors
[AD-A246078] p 2890 N92-26764
SPORES
Total Dose Effects (TDE) of heavy ionizing radiation in fungus spores and plant seeds: Preliminary investigations p 2952 N92-27124
Long-term exposure of bacterial spores to space
p 2952 N92-27126
SPOT (FRENCH SATELLITE)
SPOT multimission platform thermal control: Five years of in-flight results p 2860 N92-26998
SPRAYED COATINGS
Evaluation of plasma sprayed crucible coatings for melt processing copper-refractory metal alloys
[DE92-008912] p 2878 N92-26727
SPREAD SPECTRUM TRANSMISSION
Effects of non-uniform windowing on the performance of a fast frequency-hopped noncoherent MFSK receiver over Rician fading channels with partial-band interference and Doppler shift
[AD-A245762] p 2889 N92-26595
SQUEEZED STATES (QUANTUM THEORY)
Squeezed light and twin beams generation with a Q-switched laser p 2912 N92-26603
SQUID (DETECTORS)
Thin-film high temperature superconducting flux transformers coupled to SQUIDS
[DE92-010260] p 2891 N92-26205
Magnetic flux noise in copper oxide superconductors
[DE92-010299] p 3003 N92-26582
STABILITY
Lyapunov equation for infinite-dimensional discrete bilinear systems
[DE92-621066] p 2988 N92-26831
STACKING FAULT ENERGY
Dynamic restoration mechanisms in Al-5.8 at. percent Mg deformed to large strains in the solute drag regime
[DE92-009529] p 2877 N92-26223
STAGNATION POINT
Observation and measurements of flow structures in the stagnation region of a wing-body junction
p 2849 N92-26616
STAGNATION TEMPERATURE
An experimental investigation of a 2-D scramjet inlet at flow Mach numbers of 8 to 25 and stagnation temperatures of 800 to 4,100 K p 2854 N92-26586
STAINLESS STEELS
Predictability of long-term creep and rupture in a nozzle-to-sphere vessel model
[DE92-008099] p 2919 N92-26845
STANDARD DEVIATION
Testbank (1.0) user's manual
[AD-A245895] p 2971 N92-26196
Comparison of wind profiles in close proximity to each other
[AD-A246152] p 2945 N92-26409
STANDARDS
Improving CMM software quality
[NPL-DITC-194/92] p 2974 N92-26450
DoD implementation guidelines for Electronic Data Interchange (EDI), volume 2
[AD-A246614] p 3013 N92-26767
STAR CLUSTERS
An anisotropic homologous model for the core-collapse in star clusters
[ETN-92-90826] p 3018 N92-26946
STAR FORMATION
A self-contamination model for the formation of globular star clusters p 3018 N92-26723
STAR TRACKERS
Structural dynamic interaction with solar tracking control for evolutionary Space Station concepts
[NASA-TM-107629] p 2920 N92-26903
STARS
Polycyclic aromatic hydrocarbon radiative properties and formation in carbon-rich stellar outflows
p 3018 N92-26757
STATIC ELECTRICITY
Static electricity: A literature review
[AD-A246533] p 2990 N92-26471
STATISTICAL ANALYSIS
Spatially variant tomographic imaging: Estimation, identification, and optimization
[DE92-010262] p 2921 N92-26206
Ozone trends --- atmospheric ozone variations
p 2934 N92-26345
Hindcast wave information for the Great Lakes: Lake Huron. Wave information studies of US coastlines
[AD-A246326] p 2949 N92-26387
STATLIB/PC users guide
[AD-A245462] p 2975 N92-26530
Mixed Weibull distributions in reliability engineering: Statistical models for the lifetime of units with multiple modes of failure p 2916 N92-26602
The effect of collection homogeneity on term association as a method of request expansion in information retrieval p 3012 N92-26614
High precision timing of millisecond pulsars
p 3015 N92-26760
STATISTICAL CORRELATION
Correlation and prediction of dynamic human isolated joint strength from lean body mass
[NASA-TP-3207] p 2956 N92-26682
STATISTICAL DISTRIBUTIONS
Spatially variant tomographic imaging: Estimation, identification, and optimization
[DE92-010262] p 2921 N92-26206
STEADY FLOW
An outline of a numerical scheme for calculating two-dimensional time linearised transonic flow using the Green's function method
[AD-A246349] p 2895 N92-26258
A boundary integral method for steady unsaturated flow in nonhomogeneous media
[DE92-009066] p 2897 N92-26644
STEADY STATE CREEP
Elevated temperature properties of a dispersion strengthened Al-(Fe, V, Si) alloy
[AD-A246427] p 2880 N92-27067
STEAM FLOW
Adaptive regulation of the boiler-turbine unit of a Combined Heat and Power (CHP) system
[RR-417] p 2887 N92-26752
STEELS
Crack arrest and static fracture toughness tests of a ship plate steel
[AD-A245641] p 2916 N92-26282
Dimensional analysis of structural steel beam design
[AD-A245759] p 2917 N92-26593
STELLAR ATMOSPHERES
Energy transfer properties and mechanisms
[DE92-011215] p 2994 N92-26240
Atmospheric parameters of a soft x ray selected set of hot DA white dwarfs p 3017 N92-26576
STELLAR CORES
An anisotropic homologous model for the core-collapse in star clusters
[ETN-92-90826] p 3018 N92-26946
STELLAR ENVELOPES
Polycyclic aromatic hydrocarbon radiative properties and formation in carbon-rich stellar outflows
p 3018 N92-26757
STELLAR EVOLUTION
The galactic evolution of s-process elements via asymptotic giant branch stars p 3018 N92-26725
STELLAR GRAVITATION
Tensor-multi-scalar theories of gravitation
[PB92-152305] p 2943 N92-26820
STELLAR MASS EJECTION
Workshop on Solar Activity, Solar Wind, Terrestrial Effects, and Solar Acceleration
[NASA-CR-190195] p 3020 N92-26437
STELLAR MODELS
Dynamics of neutron stars and binaries in globular clusters or, menages a trois: Revitalizing burnt out degenerates through partner swapping
p 3017 N92-26522
STELLAR STRUCTURE
Observational and theoretical investigations in solar seismology
[NASA-CR-190245] p 3019 N92-26247
STELLAR TEMPERATURE
X ray observations of gamma ray burst sources
[MPE-PREPRINT-174] p 3018 N92-27048
STELLARATORS
Effects of orbit squeezing on ion transport in the banana regime in tokamaks
[DE92-010548] p 3000 N92-26549
STIFFNESS MATRIX
Application of parametrized variational principles in the finite element method p 2987 N92-26624
Weight optimum arch structures
[AD-A246001] p 2918 N92-26759
STIRLING CYCLE
Overview of NASA supported Stirling thermodynamic loss research
[NASA-TM-105690] p 2861 N92-27034
STOCHASTIC PROCESSES
Adaptive control of nonlinear and stochastic systems
[AD-A247204] p 2985 N92-27169
Studies in chaos using stochastic methods
[AD-A246919] p 3008 N92-27171
Stochastic versions of the EM algorithm
[AD-A246929] p 2989 N92-27174
STOICHIOMETRY
A high-resolution neutron powder diffraction study in high-T(sub c) superconductor YBa2Cu3O7
p 3002 N92-26326
STORAGE BATTERIES
Zinc-oxygen battery development program
p 2865 N92-27152
STRAIN ENERGY METHODS
Computational modelling of rubberlike materials
[ETN-92-91304] p 2916 N92-26259
STRAIN ENERGY RELEASE RATE
Computational modelling of rubberlike materials
[ETN-92-91304] p 2916 N92-26259
Fracture of structural ceramics in combined mode 1 and mode 2 loading p 2882 N92-26775
STRAIN GAGE ACCELEROMETERS
Sensitivity of sensors for characterizing chaos
[AD-A246423] p 2921 N92-27066
STRAIN MEASUREMENT
Optical strain monitoring in composite materials
[AD-A245474] p 2868 N92-26532
STRAIN RATE
Elevated temperature properties of a dispersion strengthened Al-(Fe, V, Si) alloy
[AD-A246427] p 2880 N92-27067
STRATEGY
The role of the B-2 in the new US defense strategy
[RAND-P-7744] p 2990 N92-26194
STRATIFIED FLOW
Precipitation formation processes in convective and stratiform clouds as deduced by coordinated polarimetric radar and aircraft measurements p 2941 N92-26342
Numerical simulation of the laminar turbulent transition in a stratified flow p 2904 N92-26920
STRATOCUMULUS CLOUDS
Parameterization of water-soluble component of aerosol particles in numerical cloud models
[NASA-CR-190225] p 2945 N92-26474
STRATUS CLOUDS
Precipitation formation processes in convective and stratiform clouds as deduced by coordinated polarimetric radar and aircraft measurements p 2941 N92-26342
STRESS ANALYSIS
Studies of deep level transient spectroscopy of DX centers in GaAlAs: Te under uniaxial stress
[DE92-010258] p 3001 N92-26204
Reliability and failure analyses of composite beams and plates containing stress concentrations
p 2918 N92-26598
Systematic study of Reynolds stress closure models in the computations of plane channel flows
[NASA-CR-189646] p 2898 N92-26649
Effect of type of load on stress analysis of thin-walled ducts
[NASA-TP-3248] p 2918 N92-26669

An investigation of the behavior of the clamp-induced bending stresses
[DE92-006504] p 2918 N92-26694
Weight optimum arch structures
[AD-A246001] p 2918 N92-26759
Study and analysis of the stress state in a ceramic, button-head, tensile specimen
[DE92-007794] p 2918 N92-26784
A finite element method including transverse stresses for thick laminated plates and shells
p 2920 N92-26860

STRESS CONCENTRATION
Gear tooth stress measurements of two helicopter planetary stages
[NASA-TM-105651] p 2915 N92-26555
Reliability and failure analyses of composite beams and plates containing stress concentrations
p 2918 N92-26598

STRESS CORROSION
Studies of rain erosion mechanisms in a range of IR transmitting ceramics including coated samples
[AD-A245299] p 2882 N92-26751

STRESS DISTRIBUTION
Gear tooth stress measurements of two helicopter planetary stages
[NASA-TM-105651] p 2915 N92-26555

STRESS MEASUREMENT
Gear tooth stress measurements of two helicopter planetary stages
[NASA-TM-105651] p 2915 N92-26555

STRESS RELAXATION
Modeling cycle and time-dependent creep/relaxation effects on fatigue lives of notched members --- creep/relaxation p 2919 N92-26829

STRESS-STRAIN RELATIONSHIPS
Effect of thermal residual stresses on the stress-strain behavior of metal-matrix composites
[AD-A246136] p 2868 N92-26386
Application of parametrized variational principles in the finite element method p 2987 N92-26624
Modeling cycle and time-dependent creep/relaxation effects on fatigue lives of notched members --- creep/relaxation p 2919 N92-26829
Ceramic composites: Experimental and analytical study of SiC/Si3N4 composites p 2882 N92-26859
Development of a microstructural-related description for the high temperature stress-strain behaviour of the turbine blade material IN 738 LC
[JUEL-2466] p 2880 N92-26945

STRESSES
Materials compatibility and wall stresses in hydride storage beds
[DE92-009432] p 2870 N92-26201

STRONGLY COUPLED PLASMAS
Dielectric tensor of strongly coupled plasmas
[DE92-621524] p 3001 N92-26807

STRUCTURAL ANALYSIS
Analysis of EMP response of structures using frequency domain electromagnetic interaction codes
[AD-A245758] p 2889 N92-26592
Winged launcher thermal design aspects
p 2858 N92-27013

STRUCTURAL DESIGN
Composite fuselage technology (summary of year 2)
[NASA-CR-190434] p 2852 N92-26655
Design guide for saddle seating on small high-speed craft
[ISVR-TR-205] p 2956 N92-26891
Concept for a European Space Station: Habitability, life support, and laboratory facilities p 2969 N92-27023
Influence of architecture on the definition of a space station configuration p 2860 N92-27024
LDEF mechanical systems p 2916 N92-27114

STRUCTURAL FAILURE
Composite fuselage technology (summary of year 2)
[NASA-CR-190434] p 2852 N92-26655
Weight optimum arch structures
[AD-A246001] p 2918 N92-26759

STRUCTURAL PROPERTIES (GEOLOGY)
A compendium of environmental data collected during the southwest Florida shallow-water acoustic sea test
[AD-A246143] p 2950 N92-27071

STRUCTURAL VIBRATION
Tests on various arrangements of liquid column vibration absorbers
[PB92-152610] p 2896 N92-26506
Asymptotic analysis of the vibrations of variable length cantilever beams p 2918 N92-26739
Design guide for saddle seating on small high-speed craft
[ISVR-TR-205] p 2956 N92-26891

SUBLIMATION
Development of European sublimator technology for EVA p 2968 N92-27018

SUBMARINES
Numerical field model simulation of full-scale fire tests in a closed spherical/cylindrical vessel using advanced computer graphics techniques
[AD-A245810] p 2887 N92-26898

SUBMILLIMETER WAVES
Operation of a Smith-Purcell free-electron laser at submillimeter wavelengths p 2912 N92-26626

SUBROUTINES
STATLIB/PC users guide
[AD-A245462] p 2975 N92-26530

SUBSONIC FLOW
An outline of a numerical scheme for calculating two-dimensional time linearised transonic flow using the Green's function method
[AD-A246349] p 2895 N92-26258
Subsonic investigations of vortex interaction control for enhanced high-alpha aerodynamics of a chine forebody/Delta wing configuration
[NASA-CR-189641] p 2849 N92-26652

SUBSTRATES
Photovoltaic manufacturing technology, phase 1
[DE92-001199] p 2926 N92-26190
Cadmium telluride thin films on silicon substrates
[AD-A245309] p 3001 N92-26226
Magneto-optical multilayers --- optical data storage
[DE92-009726] p 2997 N92-26565
Influence of substrate topography on the nucleation of diamond thin films
[DE92-010777] p 2883 N92-27060
Effects of long term exposure on optical substrates and coatings (SOO50-2) p 2998 N92-27096

SULFIDES
Gas-pressure studies with Li(Si)/FeS2 thermal batteries
[DE92-010801] p 2892 N92-26238

SULFUR
Method for implanting impurities in semiconductors and semiconductor implanted with impurities
[AD-D015196] p 3003 N92-26433

SULFUR CHLORIDES
Performances of 250 Amp-hr lithium/thionyl chloride cells p 2864 N92-27148

SULFUR COMPOUNDS
Thiocapsa roseopersicina, a bacterium for sulfur-recycling in microbial ecosystems designed for CELSS and space purposes p 2951 N92-26977

SULFUR DIOXIDES
NASA Li/CF(x) cell problem analysis: Anion exchange chromatography analysis p 2864 N92-27145

SUN
Observational and theoretical investigations in solar seismology
[NASA-CR-190245] p 3019 N92-26247
Water vapor information content of absorption lines observed in the Sun's infrared radiance
p 2942 N92-26490
Structural dynamic interaction with solar tracking control for evolutionary Space Station concepts
[NASA-TM-107629] p 2920 N92-26903

SUPERCHARGERS
Turbocharged pressurized combustion system
[PB92-142579] p 2873 N92-26521

SUPERCONDUCTING FILMS
Thin-film high temperature superconducting flux transformers coupled to SQUIDS
[DE92-010260] p 2891 N92-26205
Cryogenic detector development
[MPI-PHE/91-07] p 2906 N92-26391
Signal-to-noise ratio expected for a calorimeter with transition edge thermometer p 2907 N92-26395
Superconducting tunnel junctions
p 2907 N92-26396

SUPERCONDUCTING MAGNETS
Installation and operation of the 400 kW 140 GHz gyrotron on the MTX experiment
[DE92-009053] p 2906 N92-26377

SUPERCONDUCTIVITY
Electron-phonon decoupling and superconducting grains p 2907 N92-26397

SUPERCONDUCTORS
Calorimetric particle detectors with superconducting absorber materials p 2907 N92-26393
Analysis of Yttrium-Barium-Copper-Oxide by x ray diffraction and mechanical characterization
[NASA-TM-104562] p 2869 N92-26650

SUPERFLUIDITY
Mutual friction in superfluid He-3: Effects of bound states in the vortex core
[PB92-142231] p 2896 N92-26507
Quantum dynamics of helium clusters
[AD-A245752] p 2995 N92-26588

SUPERHIGH FREQUENCIES
Experimental results for inductive strips in inhomogeneous finline
[AD-A247254] p 2895 N92-27176

SUPERLATTICES
Magneto-optical multilayers --- optical data storage
[DE92-009726] p 2997 N92-26565
Band structure and optical properties of semiconductor superlattices
[AD-A246076] p 3005 N92-26763
Quantum interference and confinement effects in narrow channel Si-MOSFET's
[PB92-150176] p 3006 N92-26927

SUPERPRESSURE BALLOONS
Plume trajectory validation study: Brown cloud support project overview
[DE92-006911] p 2928 N92-26390

SUPERSONIC COMBUSTION RAMJET ENGINES
An experimental investigation of a 2-D scramjet inlet at flow Mach numbers of 8 to 25 and stagnation temperatures of 800 to 4,100 K p 2854 N92-26586
Hypersonic aerospace vehicle leading edge cooling using heat pipe, transpiration and film cooling techniques
p 3007 N92-26733
Control of turbulent mixing in hypersonic flow
p 2904 N92-26919

SUPERSONIC FLIGHT
ASTOVL engine control
[PNR-90808] p 2855 N92-27040

SUPERSONIC FLOW
Performance prediction and design of maximum thrust planar supersonic nozzles using a flux-difference-splitting technique p 2853 N92-26480
A parametric study of the hydrodynamic stability theory of 3-D compressible free shear flows
p 2900 N92-26849

SUPERSONIC INLETS
Interface of an uncoupled boundary layer algorithm with an inviscid core flow algorithm for unsteady supersonic engine inlets
[NASA-TM-105684] p 2855 N92-27037

SUPERSONIC JET FLOW
Acoustic interactions between an altitude test facility and jet engine plumes: Theory and experiments
[NASA-CR-190423] p 2853 N92-26405
Turbulent mixing in supersonic jets
p 2850 N92-27054

SUPERSONIC NOZZLES
Performance prediction and design of maximum thrust planar supersonic nozzles using a flux-difference-splitting technique p 2853 N92-26480

SUPERSYMMETRY
Supersymmetry and dark matter, a new candidate
p 3016 N92-26491

SUPPORT SYSTEMS
Engineering of a new overall system to improve the interaction between the crew and the ground-based scientists and personnel p 2964 N92-26995
Crew-friendly support systems for internal vehicular activities in zero gravity, experimented underwater for the Columbus programme p 2969 N92-27025

SUPPORTS
Thermal analysis of the Spacelab mission D2 utility support structure and its payloads p 2859 N92-26971

SURFACE DEFECTS
Boundary-layer receptivity due to distributed surface imperfections of a deterministic or random nature
[NASA-CR-4439] p 2898 N92-26681

SURFACE ENERGY
Surface energy budget and evapotranspiration measurement support
[NASA-CR-190059] p 2944 N92-26185
Computational techniques in tribology and material science at the atomic level
[NASA-TM-105573] p 2990 N92-26671

SURFACE LAYERS
The composite structure of thermals as derived from aircraft observations p 2941 N92-26346

SURFACE PROPERTIES
Ceramic bearing technology: Proceedings of the NIST/DARPA Workshop
[PB92-137553] p 2914 N92-26366
Shape from periodic texture using the spectrogram
[AD-A245855] p 2973 N92-26384
Experiment M0003-4: Advanced solar cell and coverglass analysis, an overview p 2927 N92-27088

SURFACE REACTIONS
A fractal computer model of macromolecule-cell surface interactions
[AD-A245394] p 2950 N92-26289
Energy threshold for laser induced breakdown on a metal surface under high and ultra high vacuum conditions
[AD-A246212] p 2911 N92-26462

SURFACE ROUGHNESS
Fractal characteristics of fracture roughness and aperture data
[DE92-010302] p 2895 N92-26214
Boundary-layer receptivity due to distributed surface imperfections of a deterministic or random nature
[NASA-CR-4439] p 2898 N92-26681

Flow around an isolated surface roughness in the laminar boundary layer p 2903 N92-26913
SURFACE WATER
Investigation of carbon dioxide in the South Atlantic and northern Weddell Sea areas (WOCE Sections A-12 and A-21) during the METEOR expedition 11/5, January - March 1990
[DE92-010027] p 2928 N92-26231
SURFACE WAVES
Analysis of surface wave propagation in a grounded dielectric slab covered by a resistive sheet
[NASA-TM-107583] p 2889 N92-26653
SURFACTANTS
The influence of pressure on the phase behaviour of water + oil + surfactant systems
[ISBN-90-6275-732-4] p 2871 N92-26257
The interaction of a vortex ring with a contaminated free surface p 2900 N92-26785
SURVEYS
Plan of action survey of functional requirements for a geographical information system
[AD-A245622] p 3011 N92-26403
The geoid, GPS, and levelling p 2925 N92-26777
Experiment M0003-4: Advanced solar cell and coverglass analysis, an overview p 2927 N92-27088
NASA/DoD Aerospace Knowledge Diffusion Research Project: An initial investigation into the production and use of Scientific and Technical Information (STI) at 5 NASA centers. Results of a telephone survey
[NASA-TM-104173] p 3014 N92-27170
SURVIVAL
Survival of epiphytic bacteria from seed stored on the Long Duration Exposure Facility (LDEF)
p 2952 N92-27122
SWEAT COOLING
Hypersonic aerospace vehicle leading edge cooling using heat pipe, transpiration and film cooling techniques
p 3007 N92-26733
SWELLING
Examination of the discharge mechanism of Li/CF(x) cells: Comparison of the electrochemical reduction mechanisms of PTFE and (CF(x))n by lithium
p 2865 N92-27151
SWEPTBACK WINGS
Three dimensional boundary layer transition on a yawed cylinder p 2902 N92-26909
Cross-flow instabilities and pressure gradients in boundary layers p 2904 N92-26922
SWITCHING
The effect of switched array battery charge control on CRRES spacecraft: 3 + month data summary
p 2862 N92-27134
SYNCHRONISM
Synchronous detection in monolithically integrated AM upconversion receivers
[ETN-92-91305] p 2892 N92-26260
SYNCHRONOUS SATELLITES
Investigation of deep dielectric charging and subsequent currents on geosynchronous spacecraft
[AD-A245764] p 2858 N92-26605
SAFT nickel-cadmium cell performances for GEO and LEO applications p 2863 N92-27137
SYNOPTIC MEASUREMENT
The objective determination of front lines
p 2941 N92-26343
SYNOPTIC METEOROLOGY
Comparison of frontogenetical structures for different cases of frontal development p 2939 N92-26333
Mesoscale observations of a cold front associated with a prefrontal hailstorm p 2940 N92-26338
The impact of climate upon variation in air pollution using a synoptic climatological approach p 2931 N92-26590
SYNTHESIS (CHEMISTRY)
Conversion of ethane and of propane to higher olefin hydrocarbons
[DE92-009487] p 2870 N92-26209
Synthesis of novel fluorinated phosphonic acid electrolytes for phosphoric acid fuel cells
[PB92-164300] p 2926 N92-26372
Computation of hydrodynamics using kinetic theory
[DE92-009079] p 2896 N92-26456
Low severity upgrading of F-T waxes with solid superacids
[DE92-009081] p 2873 N92-26457
Reaction/separation process for enhanced methane conversion
[PB92-149657] p 2873 N92-26508
High octane ethers from synthesis gas-derived alcohols
[DE92-010480] p 2884 N92-26548
SYNTHETIC APERTURE RADAR
A real-time synthetic aperture radar processor: Introduction and project description
[AD-A245370] p 2890 N92-26876
Feature discovery via neural networks for object recognition in SAR imagery
[DE92-007046] p 2891 N92-26902
SYSTEM IDENTIFICATION
A frequency domain based approach to on-line system identification
[AD-A246193] p 2973 N92-26418
Identification of linear systems by an asymptotically stable observer
[NASA-TP-3164] p 2917 N92-26537
Iterative system modeling using multigrid techniques
[AD-A245522] p 2976 N92-26658
SYSTEMS ENGINEERING
Executive summary of the technical proceedings on Military Information System Engineering (Defence Research Group Panel 11 on Information Processing Technology)
[AD-A245656] p 3010 N92-26174
Investigating the utility of coupling COCOMO with a system dynamics simulation of software development
[AD-A245484] p 2973 N92-26400
Water reclamation from urine aboard the Space Station p 2957 N92-26952
Space Station Freedom regenerative water recovery system configuration selection p 2957 N92-26953
Hygiene water recovery aboard the Space Station
p 2957 N92-26955
Design of JEM temperature and humidity control system p 2958 N92-26957
FIESTA: An integrated approach to thermal model processing p 2958 N92-26958
Design and performance of the Spacelab Astro-1 mission heat pipe radiator p 2859 N92-26965
Thermal design for the space-exposed instruments for the scientific satellite SAX p 2860 N92-26973
Development of a thermal control concept for the optical system of the SUMER experiment on SOHO
p 2960 N92-26975
MELISSA: Physical links of compartments Nitrobacter/Spirulina p 2961 N92-26981
Progress in the development of the Hermes evaporators p 2962 N92-26984
Thermo-hydraulic investigations on heat exchangers for Columbus hybrid radiators p 2887 N92-26988
Winged launcher thermal design aspects
p 2858 N92-27013
SYSTEMS INTEGRATION
Computer program for calculating in-flight aircraft-store interface reaction loads
[AD-A245782] p 2852 N92-26896
SYSTEMS SIMULATION
Reduced models for the behavior of VLSI circuits
[ISBN-90-6275-721-9] p 2892 N92-26249
Developing an adaptive scheduling support environment
[ISBN-90-9004609-7] p 3008 N92-26250
Adaptive regulation of the boiler-turbine unit of a Combined Heat and Power (CHP) system
[RR-417] p 2887 N92-26752
Thiocapsa roseopersicina, a bacterium for sulfur-recycling in microbial ecosystems designed for CELSS and space purposes p 2951 N92-26977
MELISSA: Physical links of compartments Nitrobacter/Spirulina p 2961 N92-26981

T

TAIL ASSEMBLIES
Composite strength statistics from fiber strength statistics
[AD-A245616] p 2867 N92-26383
TANTALUM
Evaluation of plasma sprayed crucible coatings for melt processing copper-refractory metal alloys
[DE92-008912] p 2878 N92-26727
TANTALUM CARBIDES
Evaluation of plasma sprayed crucible coatings for melt processing copper-refractory metal alloys
[DE92-008912] p 2878 N92-26727
TARGET ACQUISITION
Selective search for the target properties color and form
[IZF-1991-B-13] p 2953 N92-27047
TARGET RECOGNITION
Performance enhancement of the NPS Transient Electromagnetic Scattering Laboratory
[AD-A246300] p 2888 N92-26363
Constrained neural network architectures for target recognition
[DE92-011159] p 2982 N92-26434
Radar target identification by natural resonances: Evaluation of signal processing algorithms
[AD-A246566] p 2889 N92-26619
Real time imaging and infrared background scene analysis using the Naval Postgraduate School infrared search and target designation (NPS-IRSTD) system
[AD-A245527] p 2997 N92-26662
Large coherent arrays for laser radars, phase 1
[AD-A245528] p 2912 N92-26663
Selective search for the target properties color and form
[IZF-1991-B-13] p 2953 N92-27047
TARGET THICKNESS
Acquired polarization in fundamental symmetry experiments
[AD-A245646] p 2993 N92-26171
TARGETS
Electromagnetic scattering by a moving object: Theory and experiment
[PB92-150911] p 2889 N92-26511
TASKS
A framework for recognizing grasps
[AD-A245712] p 2981 N92-26357
TASTE
An evaluative study of the sensory qualities of selected European and Asian foods for international space missions (a French food study) p 2966 N92-27009
TAYLOR INSTABILITY
Acoustically probed Taylor-Couette flow apparatus
[AD-A246385] p 2993 N92-27076
TEAMS
TRMM Mission Team --- tropical rainfall measuring mission
[TW-4] p 2923 N92-26705
TECHNOLOGY ASSESSMENT
Information technology resources assessment
[DE92-009498] p 3011 N92-26221
Ceramic bearing technology: Proceedings of the NIST/DARPA Workshop
[PB92-137553] p 2914 N92-26366
Small Businesses Make a Difference
[PB92-160118] p 3008 N92-26369
SOLTECH 1992 proceedings: Solar Process Heat Program, volume 1
[DE92-001238] p 2927 N92-26683
DOE new technology
[DE92-001619] p 3013 N92-26689
Assessment of a hot hydrogen nuclear propulsion fuel test facility
[DE92-004571] p 2995 N92-26692
An electroplater's view of PVD processing
[DE92-009052] p 2878 N92-26732
The liquid droplet radiator: Status of development
p 2905 N92-26969
MELISSA: Physical links of compartments Nitrobacter/Spirulina p 2961 N92-26981
EVA life support design and technology developments
p 2965 N92-27002
The 1990 NASA Aerospace Battery Workshop
[NASA-CP-3119] p 2862 N92-27130
The Department of Defense critical technologies plan for the Committees on Armed Services, United States Congress
[AD-A234900] p 3010 N92-27190
TECHNOLOGY TRANSFER
DOE new technology
[DE92-001619] p 3013 N92-26689
Advances in the engineering of high field applied-B ion diodes for inertial confinement fusion
[DE92-006528] p 3000 N92-26695
Technology transfer and application of SERS continuous monitor for trace organic compounds
[DE92-008900] p 2875 N92-26726
TECHNOLOGY UTILIZATION
Advanced technology for portable personal visualization
[AD-A245819] p 2954 N92-26179
A new phase in palladium hydride technology
[DE92-009852] p 2875 N92-26718
Technology transfer and application of SERS continuous monitor for trace organic compounds
[DE92-008900] p 2875 N92-26726
Evaluation of carbon dioxide emission control strategies in New York State
[DE92-010162] p 2932 N92-26825
Managing Federal information resources: Under the Paperwork Reduction Act of 1980
[PB92-154905] p 3014 N92-26926
Chinese space technology's spin-offs and applications
[AD-A246375] p 3015 N92-27051
The Department of Defense critical technologies plan for the Committees on Armed Services, United States Congress
[AD-A234900] p 3010 N92-27190
TELECOMMUNICATION
Executive summary of information systems plans: Fiscal years 1993 to 1997
[PB92-158351] p 3011 N92-26368

The fidelity enhancement process
[AD-A245388] p 2977 N92-26840
A comparison of the UHF Follow-On and MILSTAR satellite communication systems
[AD-A245806] p 2891 N92-26933

TELEMETRY
Development and testing of an unmanned air vehicle telemetry system
[AD-A246577] p 2858 N92-26621

TELEOPERATORS
Man-machine aspects of remotely controlled space manipulators
[ISBN-90-370-0056-8] p 2954 N92-26255
Software architecture for a distributed real-time system in Ada, with application to telerobotics
[NASA-TM-4367] p 2977 N92-26904

TELEROBOTICS
Software architecture for a distributed real-time system in Ada, with application to telerobotics
[NASA-TM-4367] p 2977 N92-26904

TELESCOPES
Measurement of surface layer optical turbulence above AMOS
[AD-A246387] p 3016 N92-27077

TELLURIUM
Studies of deep level transient spectroscopy of DX centers in GaAlAs: Te under uniaxial stress
[DE92-010258] p 3001 N92-26204

TEMPERATE REGIONS
Water cycles around the subtropical frontal zone in East Asia
[TW-9] p 2923 N92-26710

TEMPERATURE
The icing of the wing upper side and bottom side of the icing research aircraft of the DLR
p 2850 N92-26349

TEMPERATURE CONTROL
Conceptual design study for the use of COBE rocket engines on the Tropical Rainfall Measuring Mission
[NASA-CR-190383] p 2945 N92-26535
Fourth European Symposium on Space Environment Control Systems, volume 2
[ESA-SP-324-VOL-2] p 2956 N92-26950
Design of JEM temperature and humidity control system p 2958 N92-26957
FIESTA: An integrated approach to thermal model processing p 2958 N92-26958
Unified computational method for design of fluid loop systems p 2905 N92-26962
Design and performance of the Spacelab Astro-1 mission heat pipe radiator p 2859 N92-26965
SIGMA VCHP radiator: In-orbit performance p 2859 N92-26966
Development of fluid loop and hybrid radiators: Test results p 2859 N92-26967
Battery thermal control of the Columbus Free Flyer p 2859 N92-26970
Thermal analysis of the Spacelab mission D2 utility support structure and its payloads p 2859 N92-26971
Passive thermostate system with application of gas-filled heat pipes and thermal energy of solar radiation p 2905 N92-26972
Thermal design for the space-exposed instruments for the scientific satellite SAX p 2860 N92-26973
Development of a thermal control concept for the optical system of the SUMER experiment on SOHO p 2960 N92-26975
Thermal control of telescope apertures by optimized baffle heating p 2961 N92-26976
Progress in the development of the Hermes evaporators p 2962 N92-26984
Thermal analysis of evaporative coolers p 2962 N92-26985
The transpirator, an efficient and light evaporative cooler for space technology p 2887 N92-26986
CPA: A controlled pump assembly for two-phase loops applications p 2916 N92-26987
Italsat thermal control: The in-orbit performances p 2859 N92-26996
ROSAT: Measured temperatures versus thermal analysis results p 2859 N92-26997
SPOT multimission platform thermal control: Five years of in-flight results p 2860 N92-26998
Ulysses, one year after the launch p 2860 N92-26999
Flight test results of the passive cooling system p 2860 N92-27000
Thermal implications from the Hubble Space Telescope solar array bi-stem boom in-orbit disturbance p 2965 N92-27001
EVA space suit thermal control and micrometeoroid protection p 2965 N92-27004
Development of European sublimator technology for EVA p 2968 N92-27018
Heat rejection system for an advanced extravehicular mobility unit portable life support system p 2968 N92-27020
Conjugating binary systems: Advanced cooling liquids for use in spacecraft ATCS p 2905 N92-27027
LDEF: 69 Months in Space. First Post-Retrieval Symposium, part 3
[NASA-CP-3134-PT-3] p 3022 N92-27083
Post-flight characterization of optical system samples, thermal control samples, and detectors from LDEF experiment M0003, sub-experiments 6 and 13 p 2998 N92-27093
Results from the LDEF/A0076 cascaded variable conductance heatpipe experiment p 2906 N92-27106
Transverse flat plate heat pipe experiment p 2906 N92-27107
Thermal control surfaces experiment flight system performance p 2860 N92-27116

TEMPERATURE DEPENDENCE
Use of an approximate similarity principle for the thermal scaling of a full-scale thrust augmenting ejector
[NASA-TM-105724] p 2854 N92-26613
Mobility of electrons and holes in semiconductors
[DE92-010125] p 3004 N92-26638
A new phase in palladium hydride technology
[DE92-009852] p 2875 N92-26718
Quantum interference and confinement effects in narrow channel Si-MOSFET's
[PB92-150176] p 3006 N92-26927
Passive determination of temperature and range using spectral band measurements of photon emittance
[AD-A247147] p 2910 N92-27181

TEMPERATURE DISTRIBUTION
Theoretical and modeling studies of the marine planetary boundary layer
[AD-A245903] p 2942 N92-26432
Finite temperature quantum field theory in curved spacetime p 3007 N92-26780

TEMPERATURE EFFECTS
The electronic evaluation of the Advanced Dynamic Anthropomorphic Manikin (ADAM) in high temperature environments
[AD-A245459] p 2955 N92-26528
Deformation behavior of an age-hardenable Beta + Alpha-Two titanium alloy
[AD-A246362] p 2879 N92-26939
Thermal implications from the Hubble Space Telescope solar array bi-stem boom in-orbit disturbance p 2965 N92-27001
Shock-turbulence interactions in a reacting flow
[NASA-CR-189647] p 2905 N92-27032
Hot-gas reingestion engine response considerations
[PNR-90810] p 2855 N92-27042
Seeds in space experiment --- long duration exposure facility p 2952 N92-27120
Oxygen recombination in the sealed nickel-cadmium cell p 2863 N92-27138
Effect of temperature and gap opening rate on the resiliency of candidate solid rocket booster O-ring materials
[NASA-TP-3226] p 2883 N92-27194

TEMPERATURE GRADIENTS
Modeling for improved minimum resolvable temperature difference measurements
[AD-A246389] p 2991 N92-27078

TEMPERATURE MEASUREMENT
Differential Scanning Calorimetry (DSC) for the analysis of activated carbon
[AD-A245899] p 2872 N92-26404
Tuned-circuit dual-mode Johnson noise thermometers
[DE92-010121] p 2908 N92-26569
Effects of power pulsations on natural convection from discrete heat sources
[AD-A246557] p 3007 N92-26617
Investigations of a single point temperature probe for measurement of atmospheric turbulence
[AD-A246563] p 2909 N92-26794
ROSAT: Measured temperatures versus thermal analysis results p 2859 N92-26997
SPOT multimission platform thermal control: Five years of in-flight results p 2860 N92-26998
Passive determination of temperature and range using spectral band measurements of photon emittance
[AD-A247147] p 2910 N92-27181

TEMPERATURE MEASURING INSTRUMENTS
Differential Scanning Calorimetry (DSC) for the analysis of activated carbon
[AD-A245899] p 2872 N92-26404

TEMPERATURE PROBES
Investigations of a single point temperature probe for measurement of atmospheric turbulence
[AD-A246563] p 2909 N92-26794

TEMPERATURE PROFILES
The electronic evaluation of the Advanced Dynamic Anthropomorphic Manikin (ADAM) in high temperature environments
[AD-A245459] p 2955 N92-26528

TEMPERATURE SENSORS
Tuned-circuit dual-mode Johnson noise thermometers
[DE92-010121] p 2908 N92-26569

TEMPORAL RESOLUTION
Requirements for coordinated Cluster and ground-based observations of the cusp p 2938 N92-26318

TENSILE STRENGTH
Study and analysis of the stress state in a ceramic, button-head, tensile specimen
[DE92-007794] p 2918 N92-26784

TENSORS
Vacuum polarization tensor in 3-dimensional quantum electrodynamics
[DE92-621141] p 2890 N92-26799
Dielectric tensor of strongly coupled plasmas
[DE92-621524] p 3001 N92-26807

TERMINAL BALLISTICS
Penetration of laminated composites by projectiles p 2869 N92-26861

TERNARY SYSTEMS
A comprehensive review of the XRD data of the primary and secondary phases present in the BSCCO superconductor system
[DE92-010363] p 3003 N92-26579

TERRAIN
Quantitative assessment of the slope resolution of seafloor mapping systems
[AD-A246158] p 2949 N92-26411

TERRAIN ANALYSIS
An assessment of satellite remote sensing for land cover classification p 2922 N92-26625
NPSNET: Hierarchical data structures for real-time three-dimensional visual simulation
[AD-A246380] p 2978 N92-27073

TEST FACILITIES
Acoustic interactions between an altitude test facility and jet engine plumes: Theory and experiments
[NASA-CR-190423] p 2853 N92-26405
Assessment of a hot hydrogen nuclear propulsion fuel test facility
[DE92-004571] p 2995 N92-26692
An investigation of the behavior of the clamp-induced bending stresses
[DE92-006504] p 2918 N92-26694
Study on the requirements for the installation of a CES and habitability centre p 2966 N92-27007
Computational method to predict thermodynamic, transport, and flow properties for the modified Langley 8-foot high-temperature tunnel
[NASA-TM-4374] p 2905 N92-27193

TEST PATTERN GENERATORS
Complementary metal oxide silicon cyclic redundancy check generators
[AD-A246140] p 2894 N92-27061

TESTS
Development and testing of a prototype electro-optical phase encoded position transducer
[AD-A245486] p 2908 N92-26401

TETRAHEDRONS
Three-dimensional upwind scheme for solving the Euler equations on unstructured tetrahedral grids --- tetrahedral grids p 2849 N92-26585

TEXTILES
Static electricity: A literature review
[AD-A246533] p 2990 N92-26471
Effect of textile test sample size on assessment of protection to skin from thermal radiation
[AD-A246535] p 2955 N92-26472

TEXTURES
Shape from periodic texture using the spectrogram
[AD-A245855] p 2973 N92-26384

THAILAND
MOS-1 activity report p 2925 N92-26749

THEMATIC MAPPING
The present understanding of the cusp p 2936 N92-26306
Building a GIS on top of the open DBMS Postgres
[FEL-91-B183] p 3014 N92-26875

THEOREM PROVING
Spectral boundary conditions and index theorem for 2-dimensional compact manifold with boundary
[DE92-621115] p 2990 N92-26798
Lyapunov equation for infinite-dimensional discrete bilinear systems
[DE92-621066] p 2988 N92-26831
Universal R-matrix for quantized (super)algebras
[DE92-621067] p 2988 N92-26834
Induced cycle structures of the hyperoctahedral group
[DE92-007570] p 3006 N92-26857

THERMAL ANALYSIS
The development of a model builder for a microcircuit substrate
[AD-A245765] p 2893 N92-26606
FIESTA: An integrated approach to thermal model processing p 2958 N92-26958
Integrated communication environment for thermal analysis software p 2958 N92-26959
Definition of the common structure of data to promote the communication between different thermal software tools p 2958 N92-26960
The liquid droplet radiator: Status of development p 2905 N92-26969
Thermal analysis of the Spacelab mission D2 utility support structure and its payloads p 2859 N92-26971
Development of a thermal control concept for the optical system of the SUMER experiment on SOHO p 2960 N92-26975
Thermal analysis of evaporative coolers p 2962 N92-26985
ROSAT: Measured temperatures versus thermal analysis results p 2859 N92-26997
Thermal implications from the Hubble Space Telescope solar array bi-stem boom in-orbit disturbance p 2965 N92-27001
Winged launcher thermal design aspects p 2858 N92-27013
Systems special investigation group overview p 2867 N92-27084

THERMAL BATTERIES
Gas-pressure studies with Li(Si)/FeS2 thermal batteries
[DE92-010801] p 2892 N92-26238
Burn-rate studies with iron/potassium perchlorate heat pellets
[DE92-008524] p 2875 N92-26722
Calorimetric determination of the thermoneutral potential for Li/BrCl in SOCl2 (BCX) cells p 2864 N92-27146

THERMAL BLOOMING
Linear and non-linear response of liquid and solid particles to energetic radiation
[AD-A246368] p 2894 N92-26942

THERMAL CONDUCTIVITY
Effects of orbit squeezing on ion transport in the banana regime in tokamaks
[DE92-010548] p 3000 N92-26549

THERMAL CONTROL COATINGS
LDEF: 69 Months in Space. First Post-Retrieval Symposium, part 3
[NASA-CP-3134-PT-3] p 3022 N92-27083
Post-flight characterization of optical system samples, thermal control samples, and detectors from LDEF experiment M0003, sub-experiments 6 and 13 p 2998 N92-27093
Evaluation of LDEF experiment S1002 p 2883 N92-27102

THERMAL CYCLING TESTS
French Cooperative Passive Payload (FRECOPA) p 2867 N92-27117
Effects of ultra-vacuum and space environment on contact ohmic resistance: LDEF experiment AO 138-11 p 2895 N92-27118

THERMAL EMISSION
Atmospheric parameters of a soft x ray selected set of hot DA white dwarfs p 3017 N92-26576

THERMAL ENVIRONMENTS
French Cooperative Passive Payload (FRECOPA) p 2867 N92-27117

THERMAL EXPANSION
Buckling of unidirectional graphite/epoxy composite plates at low temperatures
[AD-A246602] p 2869 N92-26796

THERMAL INSULATION
Warm structures and thermal protection of the European spaceplane Hermes p 2860 N92-27014
Lightweight fiber insulations performance and application p 2883 N92-27016

THERMAL NEUTRONS
Preliminary total dose measurements on LDEF --- long duration exposure facility p 2952 N92-27123

THERMAL PROTECTION
Effect of textile test sample size on assessment of protection to skin from thermal radiation
[AD-A246535] p 2955 N92-26472
Fourth European Symposium on Space Environment Control Systems, volume 2
[ESA-SP-324-VOL-2] p 2956 N92-26950
Winged launcher thermal design aspects p 2858 N92-27013
Warm structures and thermal protection of the European spaceplane Hermes p 2860 N92-27014
The importance of chemical reactions with environment for ablation process of thermal protection and structural materials p 2883 N92-27015
Heatshield concepts for the Rosetta Aerocapsule p 2860 N92-27028
Thermal control surfaces experiment flight system performance p 2860 N92-27116

THERMAL SHOCK
Analysis and modeling of high-temperature performance of advanced fiber composites p 2868 N92-26564

THERMAL SIMULATION
GRABE: A simple graphical back-end for thermal simulation packages p 2958 N92-26961
Development of a thermal control concept for the optical system of the SUMER experiment on SOHO p 2960 N92-26975
Italsat thermal control: The in-orbit performances p 2859 N92-26996

THERMAL STRESSES
Effect of thermal residual stresses on the stress-strain behavior of metal-matrix composites
[AD-A246136] p 2868 N92-26386
The electronic evaluation of the Advanced Dynamic Anthropomorphic Manikin (ADAM) in high temperature environments
[AD-A245459] p 2955 N92-26528
Analysis and modeling of high-temperature performance of advanced fiber composites p 2868 N92-26564
Physiological design goals and proposed thermal limits for US Navy thermal garments: Proceedings of 2 conferences sponsored by the Naval Medical Research and Development Command
[AD-A245543] p 2956 N92-26665

THERMAL VACUUM TESTS
Development of fluid loop and hybrid radiators: Test results p 2859 N92-26967

THERMODYNAMIC COUPLING
Electron-phonon decoupling and superconducting grains p 2907 N92-26397

THERMODYNAMIC CYCLES
Development of fluid loop and hybrid radiators: Test results p 2859 N92-26967
CPA: A controlled pump assembly for two-phase loops applications p 2916 N92-26987

THERMODYNAMIC EQUILIBRIUM
Magnetic flux noise in copper oxide superconductors
[DE92-010299] p 3003 N92-26582

THERMODYNAMIC PROPERTIES
Study of entrainment mechanisms in convective clouds
[NASA-CR-190223] p 2946 N92-26735
Computational method to predict thermodynamic, transport, and flow properties for the modified Langley 8-foot high-temperature tunnel
[NASA-TM-4374] p 2905 N92-27193

THERMODYNAMICS
Analysis and modeling of high-temperature performance of advanced fiber composites p 2868 N92-26564
A processing environment for test and simulation data of thermodynamic systems p 2959 N92-26963
Overview of NASA supported Stirling thermodynamic loss research
[NASA-TM-105690] p 2861 N92-27034

THERMOELASTICITY
Stresses in solder joints of electronic packages
[AD-A245799] p 2894 N92-26897

THERMOLUMINESCENCE
Comparison of laser and conventional heating in TLD dosemapping
[DE92-010773] p 2910 N92-26269

THERMOMETERS
Cryogenic detector development
[MPI-PHE/91-07] p 2906 N92-26391
Recent progress in calorimeters with transition edge thermometers p 2907 N92-26394
Signal-to-noise ratio expected for a calorimeter with transition edge thermometer p 2907 N92-26395

THERMONUCLEAR REACTIONS
Fusion energy and Canada's role
[DE92-621553] p 2999 N92-26286

THERMOPHYSICAL PROPERTIES
Theoretical and experimental study of thermoacoustic engines
[AD-A246334] p 2914 N92-26389

THERMOSTATS
Passive thermostate system with application of gas-filled heat pipes and thermal energy of solar radiation p 2905 N92-26972

THICK PLATES
A finite element method including transverse stresses for thick laminated plates and shells p 2920 N92-26860

THIN FILMS
Thin-film high temperature superconducting flux transformers coupled to SQUIDS
[DE92-010260] p 2891 N92-26205
Cadmium telluride thin films on silicon substrates
[AD-A245309] p 3001 N92-26226
Magneto-optical multilayers --- optical data storage
[DE92-009726] p 2997 N92-26565
Fabrication and characterization of amorphous lithium electrolyte thin films and rechargeable thin-film batteries
[DE92-010108] p 2893 N92-26636
New amorphous thin-film lithium electrolyte and rechargeable microbattery
[DE92-010110] p 2893 N92-26637
Influence of substrate topography on the nucleation of diamond thin films
[DE92-010777] p 2883 N92-27060

THIN PLATES
Fiber-optic flexural disk accelerometer
[AD-A246203] p 2908 N92-26459
Source location in thin plates using crosscorrelation
[AD-A245521] p 2992 N92-26678

THIN WALLED SHELLS
Quantum black holes and Hawking's radiation
[PB92-152313] p 3018 N92-26833

THIN WALLS
Effect of type of load on stress analysis of thin-walled ducts
[NASA-TP-3248] p 2918 N92-26669

THREE DIMENSIONAL BODIES
Recognition of 3-D symmetric objects from range images in automated assembly tasks
[NASA-CR-187664] p 2886 N92-26656
Modeling 3-D objects with planar surfaces for prediction of electromagnetic scattering
[NASA-TM-107598] p 2891 N92-27189

THREE DIMENSIONAL BOUNDARY LAYER
Three dimensional boundary layer transition on a yawed cylinder p 2902 N92-26909
An evolutional process of three dimensional disturbances in laminar boundary layers p 2902 N92-26910
Investigation on the boundary layer transition of alternately oscillating flow in deceleration phase p 2903 N92-26917
Responses of boundary layers to strong external disturbances p 2904 N92-26921
Cross-flow instabilities and pressure gradients in boundary layers p 2904 N92-26922

THREE DIMENSIONAL FLOW
Reynolds number dependence of the drag coefficient for laminar flow through fine-scale screens
[DE92-002930] p 2899 N92-26698
Fine scale structure of conserved scalar mixing in turbulent shear flows: Sc much greater than 1 and Sc approximately equal to 1 p 2899 N92-26740
A parametric study of the hydrodynamic stability theory of 3-D compressible free shear flows p 2900 N92-26849
A finite element/finite difference approach for modeling three-dimensional flow and pollutant dispersion around structures
[DE92-007322] p 2934 N92-26935
Theoretical principles of a Euler method for the calculation of three dimensional flows
[F+W-TF-2012] p 2905 N92-27045

THREE DIMENSIONAL MODELS
Using solid modeling techniques to construct three-dimensional icons for a visual simulator
[AD-A245784] p 2971 N92-26195
Reduced models for the behavior of VLSI circuits
[ISBN-90-6275-721-9] p 2892 N92-26249
Analysis of frozen startup of high-temperature heat pipes and three-dimensional modeling of block-heated heat pipes
[AD-A245327] p 2896 N92-26379
Simulation of 3D non-planar fatigue crack growth in a turbine blade root
[DE92-006859] p 2854 N92-26697
Study of entrainment mechanisms in convective clouds
[NASA-CR-190223] p 2946 N92-26735
Solution of the first-order form of the 3-D discrete ordinates equations on a massively parallel machine
[DE92-004575] p 2981 N92-26854
Numerical field model simulation of full-scale fire tests in a closed spherical/cylindrical vessel using advanced computer graphics techniques
[AD-A245810] p 2887 N92-26898
Coning motion and flat spinning of slender bodies at high angles of attack p 2902 N92-26912
CAD system for HFE analyses: Zero-g posture in optimisation of Columbus APM crew workstations --- human factors engineering p 2963 N92-26991

THREE DIMENSIONAL MOTION
Vacuum polarization tensor in 3-dimensional quantum electrodynamics
[DE92-621141] p 2890 N92-26799

THRESHOLDS
Energy threshold for laser induced breakdown on a metal surface under high and ultra high vacuum conditions
[AD-A246212] p 2911 N92-26462

THROTTLING
Throttleless Otto-cycle natural gas engines
[PB92-164482] p 2914 N92-26371
THRUST
Performance prediction and design of maximum thrust planar supersonic nozzles using a flux-difference-splitting technique p 2853 N92-26480
THRUST AUGMENTATION
Use of an approximate similarity principle for the thermal scaling of a full-scale thrust augmenting ejector
[NASA-TM-105724] p 2854 N92-26613
THRUST CONTROL
ASTOVL engine control
[PNR-90808] p 2855 N92-27040
THRUST VECTOR CONTROL
Hot-gas reingestion engine response considerations
[PNR-90810] p 2855 N92-27042
TIDES
The effect of global change and long period tides on the Earth's rotation and gravitational potential p 2925 N92-26781
TIME
Characterization of discrete-time linear periodically time-varying systems
[AD-A245822] p 2989 N92-26180
A computer program for the calculation of daubechies wavelets
[AD-A245461] p 2975 N92-26529
Sensitivity of sensors for characterizing chaos
[AD-A246423] p 2921 N92-27066
A security analysis of version 2 of the Network Time Protocol (NTP): A report to the privacy and security research group
[NASA-CR-190428] p 2981 N92-27183
TIME DEPENDENCE
Exact solutions for a mode of the electromagnetic field in a resonator with time-dependent characteristics of the internal medium
[AD-A245700] p 2888 N92-26374
Modeling cycle and time-dependent creep/relaxation effects on fatigue lives of notched members --- creep/relaxation p 2919 N92-26829
Pattern search in turbulent field p 2901 N92-26907
Ensuring mass conversion in a heavy-gas dispersion model using the generalized anelastic equations
[DE92-007323] p 2934 N92-26936
TIME DIVISION MULTIPLEXING
High-speed pulse detection room-temperature optical nonlinearities for GaInAs/A1InAs and GaA1InAs/A1InAs multiple quantum wells and integrated mirror etalon at 1.3 micrometers
[AD-A246369] p 2998 N92-26943
TIME MARCHING
Computations of nonlinear gravity waves by a desingularized boundary integral method p 2942 N92-26583
Three-dimensional upwind scheme for solving the Euler equations on unstructured tetrahedral grids --- tetrahedral grids p 2849 N92-26585
Cell vertex methods for compressible gas flows p 2897 N92-26599
TIME MEASUREMENT
The sixteen channel CAMAC constant fraction discriminator for APEX
[DE92-010550] p 2970 N92-26551
High precision timing of millisecond pulsars p 3015 N92-26760
TIME OF FLIGHT SPECTROMETERS
Development and applications of the reverse neutron time-of-flight method with Fourier-type beam chopper
[VTT-PUBL-82] p 3001 N92-26320
The high resolution diffractometer mini-Sfinks p 3002 N92-26322
High-resolution Fourier TOF powder diffraction. 1: Performance of the Mini-Sfinks Facility p 3002 N92-26323
Neutron powder diffraction study of deuterated beta-acetonitrile p 3002 N92-26324
Determination of the structure of Y(HCOO)3 by the neutron time-of-flight diffraction method p 3002 N92-26325
TIME SHARING
Scalable coherent interface: Links to the future
[DE92-010728] p 2887 N92-26267
TITANIUM ALLOYS
Deformation behavior of an age-hardenable Beta + Alpha-Two titanium alloy
[AD-A246362] p 2879 N92-26939
Cycle life characteristics of Li-TiS2 cells p 2865 N92-27154
TOKAMAK DEVICES
Diagnostic upgrades on MTX
[DE92-009695] p 2906 N92-26230
Mode structure and continuum damping of high-n toroidal Alfven eigenmodes
[DE92-010547] p 2999 N92-26256
Installation and operation of the 400 kW 140 GHz gyrotron on the MTX experiment
[DE92-009053] p 2906 N92-26377
High frequency Raman current drive
[PB92-142223] p 2893 N92-26497
Kinetic theory of toroidicity-induced Alfven eigenmode
[DE92-010424] p 2999 N92-26546
Effects of orbit squeezing on ion transport in the banana regime in tokamaks
[DE92-010548] p 3000 N92-26549
TOLERANCES (MECHANICS)
Composite fuselage technology (summary of year 2)
[NASA-CR-190434] p 2852 N92-26655
TOLERANCES (PHYSIOLOGY)
Biochemical, endocrine, and hematological factors in human oxygen tolerance extension: Predictive studies 6
[NASA-CR-190341] p 2952 N92-26263
TOLLMIEN-SCHLICHTING WAVES
An evolutional process of three dimensional disturbances in laminar boundary layers p 2902 N92-26910
Experimental studies on the flat plate boundary layer transition using hydrogen bubble method p 2903 N92-26914
TOLUENE
Aromatic-radical oxidation kinetics
[DE92-010821] p 2871 N92-26274
Toluene-water clusters: Ion fragmentation and chemistry
[AD-A245813] p 2874 N92-26526
TOMATOES
Space Exposed Experiment Developed for Students (SEEDS) (P0004-2) p 2952 N92-27121
TOMOGRAPHY
Spatially variant tomographic imaging: Estimation, identification, and optimization
[DE92-010262] p 2921 N92-26206
Imaging earth's interior: Tomographic inversions for mantle P-wave velocity structure
[DE92-010271] p 2934 N92-26208
The utility of acoustic travel times in locating the north wall of the Gulf Stream
[AD-A246219] p 2949 N92-26463
TOPOGRAPHY
The geoid, GPS, and levelling p 2925 N92-26777
TOROIDAL PLASMAS
Mode structure and continuum damping of high-n toroidal Alfven eigenmodes
[DE92-010547] p 2999 N92-26256
Inertial fusion energy power plant design using the Compact Torus Accelerator: HYLIFE-CT
[DE92-008941] p 3000 N92-26729
TORQUE
The validation of a human force model to predict dynamic forces resulting from multi-joint motions
[NASA-TP-3206] p 2956 N92-26538
Correlation and prediction of dynamic human isolated joint strength from lean body mass
[NASA-TP-3207] p 2956 N92-26682
An instrument for engine torque estimation and misfire detection --- torque p 2909 N92-26738
TORUSES
Mesh and torus chaotic routing (updated version)
[AD-A246284] p 2979 N92-26359
Inertial fusion energy power plant design using the Compact Torus Accelerator: HYLIFE-CT
[DE92-008941] p 3000 N92-26729
TOUGHNESS
Improving the fracture resistance of irradiated martensitic steels
[DE92-008387] p 2879 N92-26848
TOXICITY
Study of hydrazine metabolism and toxicity
[AD-A245755] p 2884 N92-26589
TRACE CONTAMINANTS
Technology transfer and application of SERS continuous monitor for trace organic compounds
[DE92-008900] p 2875 N92-26726
Biodegradation studies with space cabin contaminants to determine the feasibility of Biological Air Filtration (BAF) in space cabins p 2962 N92-26983
TRACKING (POSITION)
Color image processing and object tracking workstation
[NASA-TM-105561] p 2886 N92-26611
TRADEOFFS
A comparison of heavy lift launch vehicle options for the 1990s
[AD-A245617] p 2857 N92-26402
A prototype multi-media data base for tracking interface relationships and performing cost tradeoffs for the Sea Launch and Recovery (SEALAR) space launch system
[AD-A245481] p 2857 N92-26515
TRAILING EDGES
LDEF SP-HVDE (Space Plasma-High Voltage Drainage Experiment) post-flight results: Leakage current and discharge p 2895 N92-27103
TRAINING DEVICES
CBT: Role and future application for crew training --- computer based training p 2953 N92-26992
TRAINING EVALUATION
Microcomputer-based instrument flight simulation: Undergraduate pilot training student attitude assessment
[AD-A245449] p 2856 N92-26527
TRAINING SIMULATORS
Using solid modeling techniques to construct three-dimensional icons for a visual simulator
[AD-A245784] p 2971 N92-26195
CBT: Role and future application for crew training --- computer based training p 2953 N92-26992
TRAJECTORIES
Plume trajectory validation study: Brown cloud support project overview
[DE92-006911] p 2928 N92-26390
Analysis of mixing mechanisms in numerically simulated convective clouds
[NASA-CR-190222] p 2946 N92-26736
TRAJECTORY ANALYSIS
Study of entrainment mechanisms in convective clouds
[NASA-CR-190223] p 2946 N92-26735
TRAJECTORY CONTROL
Experiments in modelling and end-point control of two-link flexible manipulators p 2915 N92-26731
TRAJECTORY OPTIMIZATION
Time optimal trajectories for mobile robots with two independently driven wheels
[DE92-010002] p 2913 N92-26219
Orbital maintenance of endoatmospheric low earth-orbiting satellites
[AD-A246381] p 2859 N92-27074
TRANSDUCERS
Development and testing of a prototype electro-optical phase encoded position transducer
[AD-A245486] p 2908 N92-26401
TRANSFER ORBITS
Report for neutral buoyancy simulations of transfer orbit stage contingency extravehicular activities
[NASA-TM-103583] p 2857 N92-26268
TRANSFORMATIONS (MATHEMATICS)
VHDL behavioral description of discrete cosine transform in image compression
[AD-A245389] p 2972 N92-26248
TRANSFORMERS
Thin-film high temperature superconducting flux transformers coupled to SQUIDS
[DE92-010260] p 2891 N92-26205
Magnetohydrodynamic Electromagnetic Pulse (MHD-EMP) interaction with power transmission and distribution systems
[DE92-010365] p 2887 N92-26237
Main and auxiliary transformer rectifier system for minimizing line harmonics
[AD-D015209] p 2894 N92-26881
TRANSIENT RESPONSE
Thermal implications from the Hubble Space Telescope solar array bi-stem boom in-orbit disturbance p 2965 N92-27001
TRANSIT TIME
Pattern search in turbulent field p 2901 N92-26907
TRANSITION
Focusing x ray transition radiation with cylindrical and elliptical optics
[AD-A245987] p 2997 N92-26754
TRANSITION FLOW
Study of the transition to turbulence within a curved rectangular channel with 40 to 1 aspect ratio
[AD-A246314] p 2896 N92-26290
Distributed acoustic receptivity in laminar flow control configurations
[NASA-CR-4438] p 2898 N92-26680
Boundary-layer receptivity due to distributed surface imperfections of a deterministic or random nature
[NASA-CR-4439] p 2898 N92-26681
Numerical simulation of the laminar turbulent transition in a stratified flow p 2904 N92-26920
TRANSITION METALS
Electrocatalysts for oxygen electrodes
[DE92-009491] p 2871 N92-26220
Bis (pentamethylcyclopentadienyl) ytterbium: Electron-transfer reactions with organotransition metal complexes
[DE92-010300] p 2994 N92-26235
TRANSITION TEMPERATURE
A high-resolution neutron powder diffraction study in high-T(sub c) superconductor YBa2Cu3O7 p 3002 N92-26326
Recent progress in calorimeters with transition edge thermometers p 2907 N92-26394

Signal-to-noise ratio expected for a calorimeter with transition edge thermometer p 2907 N92-26395
The production and properties of melt-zone textured Y1Ba2Cu3O(7-delta) filaments
[DE92-008097] p 3005 N92-26843

TRANSLATIONAL MOTION
Representations in visual motion
[PB92-148287] p 2984 N92-26814

TRANSMISSION
Studies of rain erosion mechanisms in a range of IR transmitting ceramics including coated samples
[AD-A245299] p 2882 N92-26751

TRANSMISSION LINES
Magnetohydrodynamic Electromagnetic Pulse (MHD-EMP) interaction with power transmission and distribution systems
[DE92-010365] p 2887 N92-26237

TRANSMISSION LOSS
A compendium of environmental data collected during the southwest Florida shallow-water acoustic sea test
[AD-A246143] p 2950 N92-27071
Contamination of optical surfaces in Earth orbit p 2999 N92-27099

TRANSMISSIONS (MACHINE ELEMENTS)
Gear tooth stress measurements of two helicopter planetary stages
[NASA-TM-105651] p 2915 N92-26555
Full-scale transmission testing to evaluate advanced lubricants
[NASA-TM-105668] p 2915 N92-26560

TRANSMITTANCE
Water vapor information content of absorption lines observed in the Sun's infrared radiance p 2942 N92-26490
Passive exposure of Earth radiation budget experiment components. LDEF experiment AO-147: Post-flight examinations and tests p 2910 N92-27109
Transmittance measurements of ultraviolet and visible wavelength filters flown aboard LDEF p 2999 N92-27110

TRANSONIC FLOW
An outline of a numerical scheme for calculating two-dimensional time linearised transonic flow using the Green's function method
[AD-A246349] p 2895 N92-26258

TRANSONIC SPEED
High-alpha vortex decoupling investigations on a chine forebody/Delta wing configuration at transonic Mach numbers
[NASA-CR-189642] p 2849 N92-26651

TRANSPIRATION
The transpirator, an efficient and light evaporative cooler for space technology p 2887 N92-26986

TRANSPONDERS
Plume trajectory validation study: Brown cloud support project overview
[DE92-006911] p 2928 N92-26390

TRANSPORT PROPERTIES
Band structure and optical properties of semiconductor superlattices
[AD-A246076] p 3005 N92-26763
Computational method to predict thermodynamic, transport, and flow properties for the modified Langley 8-foot high-temperature tunnel
[NASA-TM-4374] p 2905 N92-27193

TRANSPORT THEORY
Effects of orbit squeezing on ion transport in the banana regime in tokamaks
[DE92-010548] p 3000 N92-26549
Numerical solution of the equation of neutrons transport on plane geometry by analytical schemes using acceleration by synthetic diffusion
[DE92-621426] p 2995 N92-26844

TRANSVERSE WAVES
Cross-flow instabilities and pressure gradients in boundary layers p 2904 N92-26922

TRAPPED PARTICLES
Effects of orbit squeezing on ion transport in the banana regime in tokamaks
[DE92-010548] p 3000 N92-26549

TRAPPING
Effects of orbit squeezing on ion transport in the banana regime in tokamaks
[DE92-010548] p 3000 N92-26549
Effect of interstitials on the trapping of hydrogen in iron-single crystals
[AD-A246412] p 3006 N92-27064

TRAVELING WAVE TUBES
Apparatus for measuring the absorption of sound by noise in one dimension
[AD-A246442] p 2992 N92-27031

TRAYS
LDEF active optical system components experiment p 2998 N92-27094
LDEF SP-HVDE (Space Plasma-High Voltage Drainage Experiment) post-flight results: Leakage current and discharge p 2895 N92-27103

TREES (MATHEMATICS)
Finding a best subtree of a tree
[REPT-91-041] p 2986 N92-26420
Introduction in IND and recursive partitioning
[NASA-TM-107879] p 2983 N92-26629

TRELLIS CODING
Implementation of multi-frequency modulation with Trellis encoding and Viterbi decoding using a digital signal processing board
[AD-A245998] p 2976 N92-26758

TRENDS
Ozone trends --- atmospheric ozone variations p 2934 N92-26345
Global assessment of promising forest management practices for sequestration of carbon
[PB92-153006] p 2930 N92-26510
Computer Program Estimate Trend (ESTREND): A system for the detection of trends in water-quality data
[PB92-147727] p 2933 N92-26931

TRIANGULATION
Fast envelope correlation for passive ranging
[AD-A246333] p 2888 N92-26388

TRIBOLOGY
Ceramic bearing technology: Proceedings of the NIST/DARPA Workshop
[PB92-137553] p 2914 N92-26366
Computational techniques in tribology and material science at the atomic level
[NASA-TM-105573] p 2990 N92-26671
Etching effects in ion implanted SiO2
[DE92-011150] p 3005 N92-26826

TRIGONOMETRIC FUNCTIONS
Downdating of Szego polynomials and data fitting applications
[AD-A245825] p 2988 N92-26900

TRITIUM
Materials compatibility and wall stresses in hydride storage beds
[DE92-009432] p 2870 N92-26201
Aging effects in palladium and LaNi(4.25)Al(0.75) tritides
[DE92-009945] p 2870 N92-26217
Helium-3 mass spectrometry for low-level tritium analysis of environmental samples
[DE92-008937] p 2873 N92-26454
Retention and release of tritium in aluminum clad, Al-Li alloys
[DE92-009905] p 2878 N92-26635
Metal hydride based isotope separation: Large-scale operations
[DE92-009830] p 2875 N92-26717

TROPICAL METEOROLOGY
International Conference on Japanese Earth Observation Programs: TRMM Workshop
[JTN-92-80345] p 2922 N92-26701
Status of TRMM project: Rain radar in the Tropical Rainfall Measuring Mission
[TW-2] p 2922 N92-26703
Status of TRMM (NASDA) --- tropical rainfall measuring mission
[TW-3] p 2923 N92-26704
Tropical Rainfall Measuring Mission (TRMM) science report
[TW-5] p 2923 N92-26706
Storm model and beam filling problem for rain retrievals
[TW-6] p 2923 N92-26707
Development of TRMM radar rainfall retrieval algorithms
[TW-7] p 2923 N92-26708
Water cycles around the subtropical frontal zone in East Asia
[TW-9] p 2923 N92-26710
Utilization of tropical convection data for meteorological operation
[TW-11] p 2924 N92-26712

TROPICAL REGIONS
Global assessment of promising forest management practices for sequestration of carbon
[PB92-153006] p 2930 N92-26510
The Tropical Rainfall Measuring Mission (TRMM) program at the Goddard Space Flight Center (GSFC)
[TW-1] p 2922 N92-26702
TRMM Mission Team --- tropical rainfall measuring mission
[TW-4] p 2923 N92-26705
Rainfall pattern over the tropical rain forest
[TW-10] p 2923 N92-26711

TROPICAL STORMS
The stability of barotropic vortices: Implications for tropical cyclone motion p 2940 N92-26335

TROPOPAUSE
Aircraft observation of a small-scale solitary wave near the tropopause p 2940 N92-26336

TROPOSPHERE
Contributions to atmospheric physics in honor of Dr. Manfred Reinhardt on his 65th birthday
[DLR-FB-91-30] p 2939 N92-26329
Integrating wind profiler data into forecast and warning operations at NWS field offices
[PB92-146075] p 2945 N92-26514
Determination of rates of reaction in the gas phase in the troposphere. Theory and practice. Part 3: Rate of indirect photoreaction
[PB92-150374] p 2944 N92-26838

TUNABLE LASERS
Design of a high-precision tunable double crystal monochromator
[DE92-010137] p 2909 N92-26572

TUNGSTEN ALLOYS
Relationship between composition, structure, properties, thermo-mechanical processing and ballistic performance of tungsten heavy alloys
[AD-A245649] p 2876 N92-26172

TUNNEL DIODES
Superconducting tunnel junctions p 2907 N92-26396

TURBINE BLADES
Simulation of 3D non-planar fatigue crack growth in a turbine blade root
[DE92-006859] p 2854 N92-26697
Development of a microstructural-related description for the high temperature stress-strain behaviour of the turbine blade material IN 738 LC
[JUEL-2466] p 2880 N92-26945

TURBINE PUMPS
Rocket engine diagnostics using qualitative modeling techniques
[NASA-TM-105714] p 2861 N92-27033

TURBINES
Adaptive regulation of the boiler-turbine unit of a Combined Heat and Power (CHP) system
[RR-417] p 2887 N92-26752

TURBOCOMPRESSORS
Turbocharged pressurized combustion system
[PB92-142579] p 2873 N92-26521

TURBULENCE
Study of the transition to turbulence within a curved rectangular channel with 40 to 1 aspect ratio
[AD-A246314] p 2896 N92-26290
Aircraft observation of a small-scale solitary wave near the tropopause p 2940 N92-26336
Measurements in the inhomogeneous convective boundary layer using three powered gliders p 2942 N92-26350
Systematic study of Reynolds stress closure models in the computations of plane channel flows
[NASA-CR-189646] p 2898 N92-26649
Reynolds number dependence of the drag coefficient for laminar flow through fine-scale screens
[DE92-002930] p 2899 N92-26698
On the subject of geometric spacing of meteorological sensors
[AD-A245824] p 2946 N92-26899
A second-order bulk boundary layer model, revision
[AD-A245828] p 2905 N92-26934

TURBULENCE MODELS
Systematic study of Reynolds stress closure models in the computations of plane channel flows
[NASA-CR-189646] p 2898 N92-26649
On testing models for the pressure-strain correlation of turbulence using direct simulations
[NASA-CR-189638] p 2901 N92-26883
Physical processes within the nocturnal stratus-topped boundary layer, revision
[AD-A245829] p 2947 N92-26901

TURBULENT BOUNDARY LAYER
Diapycnal mixing, gravity-current propagation, and sediment dispersion in turbulent fluids
[AD-A246160] p 2896 N92-26412

TURBULENT DIFFUSION
Systematic study of Reynolds stress closure models in the computations of plane channel flows
[NASA-CR-189646] p 2898 N92-26649

TURBULENT FLOW
Study of the transition to turbulence within a curved rectangular channel with 40 to 1 aspect ratio
[AD-A246314] p 2896 N92-26290
Diapycnal mixing, gravity-current propagation, and sediment dispersion in turbulent fluids
[AD-A246160] p 2896 N92-26412
Systematic study of Reynolds stress closure models in the computations of plane channel flows
[NASA-CR-189646] p 2898 N92-26649
Fine scale structure of conserved scalar mixing in turbulent shear flows: Sc much greater than 1 and Sc approximately equal to 1 p 2899 N92-26740

On testing models for the pressure-strain correlation of turbulence using direct simulations
[NASA-CR-189638] p 2901 N92-26883
Pattern search in turbulent field p 2901 N92-26907
Shock-turbulence interactions in a reacting flow
[NASA-CR-189647] p 2905 N92-27032

TURBULENT JETS
An experimental study of natural and forced modes in an axisymmetric jet p 2897 N92-26600

TURBULENT MIXING
Analysis of mixing mechanisms in numerically simulated convective clouds
[NASA-CR-190222] p 2946 N92-26736
Fine scale structure of conserved scalar mixing in turbulent shear flows: Sc much greater than 1 and Sc approximately equal to 1 p 2899 N92-26740
Advancing natural gas combustion science and technology-low NOx
[PB92-137652] p 2876 N92-26782
Control of turbulent mixing in hypersonic flow p 2904 N92-26919
Turbulent mixing in supersonic jets p 2850 N92-27054

TURNSTILE ANTENNAS
An antenna design for PANSAT using NEC
[AD-A245482] p 2888 N92-26399

TWO DIMENSIONAL BODIES
Recognition of 3-D symmetric objects from range images in automated assembly tasks
[NASA-CR-187664] p 2886 N92-26656

TWO DIMENSIONAL FLOW
An outline of a numerical scheme for calculating two-dimensional time linearised transonic flow using the Green's function method
[AD-A246349] p 2895 N92-26258
A parametric study of the hydrodynamic stability theory of 3-D compressible free shear flows p 2900 N92-26849
Wave structure in one and two dimensional fluid flow
[DE92-007421] p 2900 N92-26855
Numerical simulation of two-dimensional single- and multiple-material flow fields
[DE92-007428] p 2901 N92-26856

TWO PHASE FLOW
Passive water hammer in pipes due to flashing
[DE92-004180] p 2899 N92-26699
Two-phase flow of Newtonian and Non-Newtonian fluids in a porous medium applied to water coning
[PB92-151109] p 2900 N92-26836
CPA: A controlled pump assembly for two-phase loops applications p 2916 N92-26987

U

ULTRAHIGH FREQUENCIES
An evaluation of superresolution methods for tactical radio direction finding
[AD-A246316] p 2851 N92-26291
A comparison of the UHF Follow-On and MILSTAR satellite communication systems
[AD-A245806] p 2891 N92-26933

ULTRASONICS
A Bayes-Maximum Entropy method for multi-sensor data fusion
[DE92-000680] p 2983 N92-26657
Binaural ultrasound detector and imager
[AD-D015214] p 2993 N92-27184

ULTRAVIOLET ABSORPTION
Time-resolved laser studies on the proton pump mechanism of bacteriorhodopsin
[DE92-003218] p 2951 N92-26493

ULTRAVIOLET DETECTORS
Effects of long-duration exposure on optical system components p 2998 N92-27095

ULTRAVIOLET EMISSION
An analysis of middle ultraviolet emissions of molecular nitrogen and nitric oxide and vacuum calibration of an ultraviolet spectrograph
[AD-A245984] p 2943 N92-26753

ULTRAVIOLET FILTERS
Transmittance measurements of ultraviolet and visible wavelength filters flown aboard LDEF p 2999 N92-27110

ULTRAVIOLET PHOTOGRAPHY
A feasibility study: California Department of Forestry and Fire Protection utilization of infrared technologies for wildland fire suppression and management
[NASA-CR-190458] p 2926 N92-27195

ULTRAVIOLET RADIATION
French Cooperative Passive Payload (FRECOPA) p 2867 N92-27117

ULTRAVIOLET SPECTRA
Research and technology, 1990: Goddard Space Flight Center
[NASA-TM-107792] p 3022 N92-26824

ULTRAVIOLET SPECTROMETERS
Development of a thermal control concept for the optical system of the SUMER experiment on SOHO p 2960 N92-26975

ULTRAVIOLET TELESCOPES
Research and technology, 1990: Goddard Space Flight Center
[NASA-TM-107792] p 3022 N92-26824

ULYSSES MISSION
Ulysses, one year after the launch p 2860 N92-26999
The HUS solar flare and cosmic gamma ray burst detector aboard the Ulysses spacecraft
[MPE-PREPRINT-175] p 3016 N92-27049

UNDERWATER ACOUSTICS
Comparison of one-way wave propagation algorithms in underwater acoustics-error estimates and sensitivity
[AD-A245660] p 2991 N92-26175
Ocean bottom modeling for ray acoustics
[AD-A246287] p 2948 N92-26360
The utility of acoustic travel times in locating the north wall of the Gulf Stream
[AD-A246219] p 2949 N92-26463
Evaluation of the computational validity of the image model in predicting the sound field in a wedge-shaped layer using acoustical reciprocity
[AD-A246548] p 2992 N92-26688
Precision of the long baseline acoustic navigation system used by Pegasus
[AD-A246598] p 2852 N92-26795
A compendium of environmental data collected during the southwest Florida shallow-water acoustic sea test
[AD-A246143] p 2950 N92-27071

UNDERWATER EXPLOSIONS
On shock capturing for liquid and gas media p 2897 N92-26556
Dynamic response of cylindrical shells to underwater end-on explosion
[AD-A245804] p 2920 N92-26932

UNDERWATER TESTS
Dynamic response of cylindrical shells to underwater end-on explosion
[AD-A245804] p 2920 N92-26932
Crew-friendly support systems for internal vehicular activities in zero gravity, experimented underwater for the Columbus programme p 2969 N92-27025

UNITED STATES
Competing economies: America, Europe, and the Pacific rim
[PB92-115757] p 3014 N92-26730

UNIVERSE
Topics in particle physics and cosmology
[DE92-010478] p 3019 N92-26385
Supersymmetry and dark matter, a new candidate p 3016 N92-26491
Finite temperature quantum field theory in curved spacetime p 3007 N92-26780

UNIX (OPERATING SYSTEM)
Distributed visualization
[DE92-009405] p 2971 N92-26188
NEXUS: A kernel complex object management system p 3012 N92-26567

UNSTEADY FLOW
Effects of power pulsations on natural convection from discrete heat sources
[AD-A246557] p 3007 N92-26617
An experimental investigation of high-speed water entry for full size and scale-model pointed nose vehicle
[DE92-004363] p 2899 N92-26716

UP-CONVERTERS
Synchronous detection in monolithically integrated AM upconversion receivers
[ETN-92-91305] p 2892 N92-26260

UPPER ATMOSPHERE
The Norwegian upper atmosphere programme in Svalbard (Norway) p 2935 N92-26295
Cusp and cleft studies in Greenland p 2935 N92-26299
Mean and turbulent structure of the marine atmospheric boundary layer during cold air outbreaks of different intensities: Observational and modelling analyses p 2942 N92-26489

URBAN DEVELOPMENT
An assessment of satellite remote sensing for land cover classification p 2922 N92-26625

URINE
Water reclamation from urine aboard the Space Station p 2957 N92-26952

USER MANUALS (COMPUTER PROGRAMS)
Description of and users manual for TUBA: A computer code for generating two-dimensional random fields via the turning bands method
[DE92-001020] p 2971 N92-26189
Testbank (1.0) user's manual
[AD-A245895] p 2971 N92-26196
Maintenance manual for Natick's Footwear Database
[AD-A246273] p 2954 N92-26242
User manual for Natick's Footwear Database
[AD-A246275] p 2954 N92-26243
Naval Postgraduate School aircraft synthesis program (user's manual)
[AD-A246198] p 2974 N92-26458
STATLIB/PC users guide
[AD-A245462] p 2975 N92-26530
A user's manual for MASH 1.0: A Monte Carlo adjoint shielding code system
[DE92-010375] p 3021 N92-26544
User's guide to WPL microwave radiative transfer software
[PB92-129931] p 2890 N92-26809
Volatile Organic Compound (VOC) and Particulate Matter (PM) speciation data system user's manual, version 1.4
[PB92-105527] p 2932 N92-26823
Computer program for calculating in-flight aircraft-store interface reaction loads
[AD-A245782] p 2852 N92-26896

USER REQUIREMENTS
Information systems planning methodologies: A framework for comparison and selection
[AD-A246527] p 3012 N92-26469
NASA/DoD Aerospace Knowledge Diffusion Research Project: An initial investigation into the production and use of Scientific and Technical Information (STI) at 5 NASA centers. Results of a telephone survey
[NASA-TM-104173] p 3014 N92-27170

V

V/STOL AIRCRAFT
VSTOL engine design evolution: Growth of the Pegasus engine for Harrier
[PNR-90805] p 2855 N92-27039
ASTOVL engine control
[PNR-90808] p 2855 N92-27040
ASTOVL propulsion systems: Configuration and concept choice
[PNR-90809] p 2855 N92-27041

VACUUM
An analysis of middle ultraviolet emissions of molecular nitrogen and nitric oxide and vacuum calibration of an ultraviolet spectrograph
[AD-A245984] p 2943 N92-26753
RF vacuum microelectronics
[AD-A246579] p 2893 N92-26771
Vacuum polarization tensor in 3-dimensional quantum electrodynamics
[DE92-621141] p 2890 N92-26799
The onset of breakdown in a fast pulsed vacuum diode
[AD-A246395] p 2895 N92-27079

VACUUM DEPOSITION
Vacuum deposited optical coatings experiment p 2999 N92-27097

VACUUM EFFECTS
Photocathode transfer and storage techniques using alkali vapor feedback control
[DE92-008449] p 2891 N92-26202
Energy threshold for laser induced breakdown on a metal surface under high and ultra high vacuum conditions
[AD-A246212] p 2911 N92-26462
Fundamental mechanisms affecting friction welding under vacuum
[AD-A245685] p 2877 N92-26520
Microwelding (or cold-welding) of various metallic materials under the ultra-vacuum LDEF experiment AO 138-10 p 2880 N92-27119
Seeds in space experiment — long duration exposure facility p 2952 N92-27120

VALENCE
The computation of C-C and N-N bond dissociation energies for singly, doubly, and triply bonded systems
[NASA-CR-190254] p 2994 N92-26539

VALUE ENGINEERING
Best value contracting in the procurement of engineering and technical services
[AD-A245524] p 3009 N92-26660

VALVES
Assessment of diagnostic methods for solenoid-operated valves
[DE92-009379] p 2913 N92-26234
Water hammer due to the sudden stopping of a flashing flow
[DE92-004181] p 2899 N92-26700

VANADIUM
Calorimetric particle detectors with superconducting absorber materials p 2907 N92-26393

VANADIUM OXIDES
Fabrication and characterization of amorphous lithium electrolyte thin films and rechargeable thin-film batteries
[DE92-010108] p 2893 N92-26636
New amorphous thin-film lithium electrolyte and rechargeable microbattery
[DE92-010110] p 2893 N92-26637
VAPOR DEPOSITION
Photovoltaic manufacturing technology, phase 1
[DE92-001199] p 2926 N92-26190
Fundamental studies of the chemical vapor deposition of diamond
[DE92-010327] p 2881 N92-26543
A surface science investigation of silicon carbide: Oxidation, crystal growth and surface structural analysis
[DE92-010286] p 3004 N92-26641
An electroplater's view of PVD processing
[DE92-009052] p 2878 N92-26732
VAPOR PHASES
New theoretical methods for electronic structure and gas-phase state specific oxidation/reduction studies
[AD-A246127] p 2875 N92-26687
Polycyclic aromatic hydrocarbon radiative properties and formation in carbon-rich stellar outflows
p 3018 N92-26757
Determination of rates of reaction in the gas phase in the troposphere. Theory and practice. Part 3: Rate of indirect photoreaction
[PB92-150374] p 2944 N92-26838
VAPORS
Photocathode transfer and storage techniques using alkali vapor feedback control
[DE92-008449] p 2891 N92-26202
VARIANCE (STATISTICS)
Lower confidence limit expressions for P(X greater than y) and P(X greater than Y) under normality
[AD-A245787] p 2989 N92-26177
VARIATIONAL PRINCIPLES
Application of parametrized variational principles in the finite element method p 2987 N92-26624
VATOL AIRCRAFT
High lift aircraft
[AD-D015215] p 2853 N92-27185
VEGETATION
Equilibrium-analysis of projected climate change effects on the global soil organic matter pool
[PB92-153022] p 2930 N92-26509
VEGETATION GROWTH
Higher plant growth in closed environment: Preliminary experiments in life support facility at ESA-ESTEC
p 2951 N92-26978
VELOCITY DISTRIBUTION
Aircraft observation of a small-scale solitary wave near the tropopause p 2940 N92-26336
Symbolic solution of a multilayer ocean waveguide problem with arbitrary depth dependent ambient density and sound speed profiles
[AD-A245476] p 2949 N92-26533
Studies of inertio-gravity waves induced by geostrophic adjustment of the atmospheric jet stream
p 2944 N92-26866
Large-scale structures and the spatial evolution of wakes behind axisymmetric bluff bodies p 2901 N92-26871
VELOCITY MEASUREMENT
Construction and function of a multifunction CO2-Laser system
[AD-A245425] p 2910 N92-26271
VENTILATION
Determination of ventilation requirements for a space suit helmet p 2968 N92-27017
VENTILATION FANS
Fan/pump/separator technology development for EVA
p 2966 N92-27006
VENUS (PLANET)
Radar scattering as a source of geological information on Venus and Earth p 3019 N92-26778
Solar wind interaction with Venus and Mars
p 3020 N92-26779
The preliminary geodetic control network of Venus
[RAND-N-3437-JPL] p 3019 N92-26819
VENUS ATMOSPHERE
Solar wind interaction with Venus and Mars
p 3020 N92-26779
VENUS SURFACE
The preliminary geodetic control network of Venus
[RAND-N-3437-JPL] p 3019 N92-26819
VERTICAL AIR CURRENTS
The composite structure of thermals as derived from aircraft observations p 2941 N92-26346
Study of entrainment mechanisms in convective clouds
[NASA-CR-190223] p 2946 N92-26735
Analysis of mixing mechanisms in numerically simulated convective clouds
[NASA-CR-190222] p 2946 N92-26736
Physical processes within the nocturnal stratus-topped boundary layer, revision
[AD-A245829] p 2947 N92-26901
VERY LARGE SCALE INTEGRATION
On the design of VLSI circuits for the Winograd Fourier transform algorithm
[AD-A246317] p 2892 N92-26244
Reduced models for the behavior of VLSI circuits
[ISBN-90-6275-721-9] p 2892 N92-26249
The minimization of multiple valued logic expressions using parallel processors
[AD-A245763] p 2980 N92-26596
A real-time synthetic aperture radar processor: Introduction and project description
[AD-A245370] p 2890 N92-26876
VLSI implementation of fuzzy logic operator unit
[AD-A247146] p 2989 N92-27180
VESTS
Effectiveness of a selected microclimate cooling system in increasing tolerance time to work in the heat. Application to Navy Physiological Heat Exposure Limits (PHEL) curve 5
[AD-A246529] p 2952 N92-26470
VHSIC (CIRCUITS)
VHDL behavioral description of discrete cosine transform in image compression
[AD-A245389] p 2972 N92-26248
VIBRATION
Vibrational dynamics of aniline (N2)1 clusters in their first excited singlet state
[AD-A245812] p 2872 N92-26431
Vibrational spectroscopy in shock-compressed liquids
[DE92-007713] p 2876 N92-26867
VIBRATION DAMPING
Tests on various arrangements of liquid column vibration absorbers
[PB92-152610] p 2896 N92-26506
VIBRATION ISOLATORS
Tests on various arrangements of liquid column vibration absorbers
[PB92-152610] p 2896 N92-26506
Optimization of space structures to minimize dynamic response p 2858 N92-26610
VIBRATION MEASUREMENT
Construction and function of a multifunction CO2-Laser system
[AD-A245425] p 2910 N92-26271
VIBRATION TESTS
Optimization of space structures to minimize dynamic response p 2858 N92-26610
VIBRATIONAL SPECTRA
The computation of C-C and N-N bond dissociation energies for singly, doubly, and triply bonded systems
[NASA-CR-190254] p 2994 N92-26539
Kalman smoother applied to lace
[AD-A246439] p 2859 N92-27030
VIDEO COMMUNICATION
Effects of video bandwidth on the performance of a square law detector with Gaussian IF and video filters
[AD-A246506] p 2989 N92-26467
VIDEO EQUIPMENT
Effects of video bandwidth on the performance of a square law detector with Gaussian IF and video filters
[AD-A246506] p 2989 N92-26467
VIRTUAL MEMORY SYSTEMS
Description of and users manual for TUBA: A computer code for generating two-dimensional random fields via the turning bands method
[DE92-001020] p 2971 N92-26189
VIRTUAL REALITY
Advanced technology for portable personal visualization
[AD-A245819] p 2954 N92-26179
VISCOPLASTICITY
Computational aspects of an implicit finite element procedure for elasto-viscoplastic large deformation problems p 2917 N92-26594
Mesomechanics of viscoplastic metal matrix composites p 2869 N92-26607
VISCOSITY
Computation of hydrodynamics using kinetic theory
[DE92-009079] p 2896 N92-26456
VISCOUS DAMPING
Wave viscosity interaction in nonlinear roll motion
[AD-A245756] p 2897 N92-26591
VISCOUS FLOW
Wave viscosity interaction in nonlinear roll motion
[AD-A245756] p 2897 N92-26591
Aerodynamic interference between stores
[AD-A247207] p 2850 N92-27172
VISCOUS FLUIDS
Wave viscosity interaction in nonlinear roll motion
[AD-A245756] p 2897 N92-26591
VISION
Man-machine aspects of remotely controlled space manipulators
[ISBN-90-370-0056-8] p 2954 N92-26255
Representations in visual motion
[PB92-148287] p 2984 N92-26814
VISUAL PERCEPTION
Modeling of explorative procedures for remote object identification
[AD-A245525] p 2922 N92-26661
NPSNET: Hierarchical data structures for real-time three-dimensional visual simulation
[AD-A246380] p 2978 N92-27073
VITERBI DECODERS
Implementation of multi-frequency modulation with Trellis encoding and Viterbi decoding using a digital signal processing board
[AD-A245998] p 2976 N92-26758
VOICE DATA PROCESSING
Applications of wavelets to signal processing held in Wright-Patterson AFB, Ohio on 20-22 March 1991. Volume 2: Tutorial notes
[AD-A245567] p 2888 N92-26381
VOLT-AMPERE CHARACTERISTICS
Percolation effects in the V-I characteristics of granular YBa2Cu3O(7-delta)
[DE92-617541] p 3004 N92-26672
Cycle life characteristics of Li-TiS2 cells
p 2865 N92-27154
VOLUME
Gravimetric gas determinations for volume calibrations
[DE92-010041] p 2874 N92-26634
Liquid level and volume measurement device
[AD-D015189] p 2909 N92-26879
VORTEX ALLEVIATION
Subsonic investigations of vortex interaction control for enhanced high-alpha aerodynamics of a chine forebody/Delta wing configuration
[NASA-CR-189641] p 2849 N92-26652
VORTEX FILAMENTS
The interaction of a vortex ring with a contaminated free surface p 2900 N92-26785
VORTEX RINGS
The interaction of a vortex ring with a contaminated free surface p 2900 N92-26785
VORTICES
Study of the transition to turbulence within a curved rectangular channel with 40 to 1 aspect ratio
[AD-A246314] p 2896 N92-26290
Contributions to atmospheric physics in honor of Dr. Manfred Reinhardt on his 65th birthday
[DLR-FB-91-30] p 2939 N92-26329
Upper/lower vortex interaction and potential vorticity inversion p 2939 N92-26331
The stability of barotropic vortices: Implications for tropical cyclone motion p 2940 N92-26335
Convection wave studies over land and sea
p 2940 N92-26341
Diapycnal mixing, gravity-current propagation, and sediment dispersion in turbulent fluids
[AD-A246160] p 2896 N92-26412
Euclidean black hole vortices
[NASA-CR-190117] p 3016 N92-26436
Mutual friction in superfluid He-3: Effects of bound states in the vortex core
[PB92-142231] p 2896 N92-26507
High-alpha vortex decoupling investigations on a chine forebody/Delta wing configuration at transonic Mach numbers
[NASA-CR-189642] p 2849 N92-26651
Physical processes within the nocturnal stratus-topped boundary layer, revision
[AD-A245829] p 2947 N92-26901
Vortex structure in wake of a circular cylinder
p 2904 N92-26918
A second-order bulk boundary layer model, revision
[AD-A245828] p 2905 N92-26934
VORTICITY
Upper/lower vortex interaction and potential vorticity inversion p 2939 N92-26331
The interaction of a vortex ring with a contaminated free surface p 2900 N92-26785
VSAT (NETWORK)
Selection and specification of a data link protocol for VSAT based inter-LAN communications
[AD-A246289] p 2979 N92-26361

W

WAKES
Large-scale structures and the spatial evolution of wakes behind axisymmetnc bluff bodies p 2901 N92-26871
WALKING MACHINES
Dead reckoning navigation for walking robots
[NASA-CR-190296] p 2982 N92-26429

WALL FLOW
Theoretical principles of a Euler method for the calculation of three dimensional flows
[F+W-TF-2012] p 2905 N92-27045
WALLS
Materials compatibility and wall stresses in hydride storage beds
[DE92-009432] p 2870 N92-26201
WASTE DISPOSAL
Assessment of biospheric behaviour of releases from nuclear waste repositories, appendix 2
p 2929 N92-26484
Assessment of radiation doses due to releases to the biosphere from nuclear waste repositories, appendix 3
p 2929 N92-26485
Sensitivity analysis of biospheric behaviour of radionuclides released from nuclear waste repositories, appendix 4 p 2929 N92-26486
Running a conference as a clean product. International Conference on Pollution Prevention: Clean technologies and clean products
[PB92-109099] p 2930 N92-26495
Fundamentals of electrokinetics
[DE92-008326] p 2894 N92-26847
Environmental Protection Agency's municipal solid waste landfill liner design criteria
[PB92-153766] p 2933 N92-26928
WASTE HEAT
The liquid droplet radiator: Status of development
p 2905 N92-26969
Progress in the development of the Hermes evaporators p 2962 N92-26984
WASTE TREATMENT
Life support research and development for the Department of Energy Space Exploration Initiative
[DE92-007239] p 2955 N92-26494
Fundamentals of electrokinetics
[DE92-008326] p 2894 N92-26847
Space Station Freedom regenerative water recovery system configuration selection p 2957 N92-26953
Catalytic wet-oxidation of human waste produced in a space habitat: Purification of the oxidized liquor for human drinking p 2957 N92-26954
Thiocapsa roseopersicina, a bacterium for sulfur-recycling in microbial ecosystems designed for CELSS and space purposes p 2951 N92-26977
Chemolithotropic hydrogen-oxidizing bacteria and their possible functions in closed ecological life-support systems p 2951 N92-26979
Impact of diet on the design of waste processors in CELSS p 2961 N92-26980
WASTE UTILIZATION
Life support research and development for the Department of Energy Space Exploration Initiative
[DE92-007239] p 2955 N92-26494
WATER
The influence of pressure on the phase behaviour of water + oil + surfactant systems
[ISBN-90-6275-732-4] p 2871 N92-26257
Toluene-water clusters: Ion fragmentation and chemistry
[AD-A245813] p 2874 N92-26526
On shock capturing for liquid and gas media
p 2897 N92-26556
Solvation effects on the electronic structure of 4-N,N-Dimethylaminobenzonitrile: Mixing of the local pipi* and charge transfer states
[AD-A245814] p 2874 N92-26608
Two-phase flow of Newtonian and Non-Newtonian fluids in a porous medium applied to water coning
[PB92-151109] p 2900 N92-26836
WATER CIRCULATION
Observations of wind forced circulation on the continental shelf off Point Sur, California from a self-contained acoustic Doppler current profiler
[AD-A246437] p 2950 N92-27029
WATER HAMMER
Passive water hammer in pipes due to flashing
[DE92-004180] p 2899 N92-26699
Water hammer due to the sudden stopping of a flashing flow
[DE92-004181] p 2899 N92-26700
WATER QUALITY
Computer Program Estimate Trend (ESTREND): A system for the detection of trends in water-quality data
[PB92-147727] p 2933 N92-26931
WATER RECLAMATION
Fourth European Symposium on Space Environment Control Systems, volume 2
[ESA-SP-324-VOL-2] p 2956 N92-26950
Water recovery from condensate of crew respiration products aboard the Space Station
p 2956 N92-26951
Water reclamation from urine aboard the Space Station p 2957 N92-26952
Space Station Freedom regenerative water recovery system configuration selection p 2957 N92-26953
Hygiene water recovery aboard the Space Station
p 2957 N92-26955
Chemolithotropic hydrogen-oxidizing bacteria and their possible functions in closed ecological life-support systems p 2951 N92-26979
WATER RESOURCES
Description of and users manual for TUBA: A computer code for generating two-dimensional random fields via the turning bands method
[DE92-001020] p 2971 N92-26189
WATER TEMPERATURE
Effects of power pulsations on natural convection from discrete heat sources
[AD-A246557] p 3007 N92-26617
WATER TREATMENT
Hygiene water recovery aboard the Space Station
p 2957 N92-26955
WATER TUNNEL TESTS
Observation and measurements of flow structures in the stagnation region of a wing-body junction
p 2849 N92-26616
WATER VAPOR
Water vapor information content of absorption lines observed in the Sun's infrared radiance
p 2942 N92-26490
Metal oxide absorbents for regenerative carbon dioxide and water vapor removal for advanced portable life support systems p 2968 N92-27021
WATER VEHICLES
An experimental investigation of high-speed water entry for full size and scale-model pointed nose vehicle
[DE92-004363] p 2899 N92-26716
WAVE DISPERSION
Theory of electromagnetic instability of an intense beam in a quadrupole focusing system
[AD-A246560] p 2990 N92-26768
WAVE DRAG
Development of an advanced finite-difference atmospheric general circulation model
[DE92-010923] p 2944 N92-26937
WAVE EQUATIONS
Nonlinear waves and inverse scattering
[AD-A246164] p 2986 N92-26414
Computational methods for problems of acoustics with particular reference to exterior domains
p 2992 N92-26558
WAVE FRONTS
Ruled and holographic diffraction gratings experiment (AO 138-5) p 2910 N92-27092
WAVE GENERATION
An evolutional process of three dimensional disturbances in laminar boundary layers
p 2902 N92-26910
WAVE INTERACTION
Proceedings of 6th Hawaiian Winter Workshop on Dynamics of Oceanic Internal Gravity Waves
[AD-A245650] p 2948 N92-26173
A reformulation of the Eady model
p 2939 N92-26330
Upper/lower vortex interaction and potential vorticity inversion p 2939 N92-26331
Wave viscosity interaction in nonlinear roll motion
[AD-A245756] p 2897 N92-26591
WAVE PROPAGATION
Imaging earth's interior: Tomographic inversions for mantle P-wave velocity structure
[DE92-010271] p 2934 N92-26208
Analysis of surface wave propagation in a grounded dielectric slab covered by a resistive sheet
[NASA-TM-107583] p 2889 N92-26653
Source location in thin plates using crosscorrelation
[AD-A245521] p 2992 N92-26678
User's guide to WPL microwave radiative transfer software
[PB92-129931] p 2890 N92-26809
Eulerian computational methods
[DE92-008017] p 2900 N92-26853
Wave structure in one and two dimensional fluid flow
[DE92-007421] p 2900 N92-26855
WAVEFORMS
Wave structure in one and two dimensional fluid flow
[DE92-007421] p 2900 N92-26855
WAVEGUIDES
Symbolic solution of a multilayer ocean waveguide problem with arbitrary depth dependent ambient density and sound speed profiles
[AD-A245476] p 2949 N92-26533
Theory of electromagnetic instability of an intense beam in a quadrupole focusing system
[AD-A246560] p 2990 N92-26768
Experimental results for inductive strips in inhomogeneous finline
[AD-A247254] p 2895 N92-27176
WAVES
Convection wave studies over land and sea
p 2940 N92-26341
WAXES
Low severity upgrading of F-T waxes with solid superacids
[DE92-009081] p 2873 N92-26457
WEAK ENERGY INTERACTIONS
Proceedings of 6th Hawaiian Winter Workshop on Dynamics of Oceanic Internal Gravity Waves
[AD-A245650] p 2948 N92-26173
WEAPON SYSTEMS
Expert system management system
[AD-A247102] p 3009 N92-26863
Computer program for calculating in-flight aircraft-store interface reaction loads
[AD-A245782] p 2852 N92-26896
The Department of Defense critical technologies plan for the Committees on Armed Services, United States Congress
[AD-A234900] p 3010 N92-27190
WEAR
Ceramic bearing technology: Proceedings of the NIST/DARPA Workshop
[PB92-137553] p 2914 N92-26366
The effect of sandstorms on PV arrays and components -- photovoltaic cells
[DE92-001240] p 2927 N92-26686
WEATHER
Improved procedures for quantifying key meteorological effects on ambient ozone data
[PB92-163278] p 2931 N92-26793
Report of the CC1 experts meeting on tracking and transmission of climate system monitoring information
[WCDMP-16] p 2947 N92-26925
WEATHER FORECASTING
Integrating wind profiler data into forecast and warning operations at NWS field offices
[PB92-146075] p 2945 N92-26514
Estimating mesoscale, orographically enhanced precipitation using synoptic scale data
[AD-A245749] p 2946 N92-26562
High frequency analyses of coastal meteorological phenomena affecting refractivity
[AD-A246383] p 2947 N92-27075
WEATHER STATIONS
Comparison of wind profiles in close proximity to each other
[AD-A246152] p 2945 N92-26409
WEIBULL DENSITY FUNCTIONS
Reliability and failure analyses of composite beams and plates containing stress concentrations
p 2918 N92-26598
Mixed Weibull distributions in reliability engineering: Statistical models for the lifetime of units with multiple modes of failure p 2916 N92-26602
WEIGHT MEASUREMENT
Results of a portable fiber-optic weigh-in-motion system
[DE92-009011] p 2996 N92-26376
WEIGHTLESSNESS
Parabolic flight: Reports of microgravity experiments by aircraft, volume 1, no. 2
[EG-910045] p 2884 N92-26440
Outlines of parabolic flight p 2884 N92-26441
Preliminary experiment of GDEF (Gas Dynamics Experiment Facility) p 2885 N92-26442
Micro-gravity experiment of vapor/liquid reorientation induced by capillary force p 2885 N92-26444
Biomedical data acquisition and processing technology p 2885 N92-26446
The experiment under microgravity by aircraft: The experiment in floating by gas flow p 2886 N92-26447
Transverse flat plate heat pipe experiment
p 2906 N92-27107
WELD TESTS
Fundamental mechanisms affecting friction welding under vacuum
[AD-A245685] p 2877 N92-26520
WELDABILITY
Factors influencing the microstructural and mechanical properties of ULCB steel weldments
[AD-A245523] p 2878 N92-26659
Microwelding (or cold-welding) of various metallic materials under the ultra-vacuum LDEF experiment AO 138-10 p 2880 N92-27119
WELDED JOINTS
Fundamental mechanisms affecting friction welding under vacuum
[AD-A245685] p 2877 N92-26520
Factors influencing the microstructural and mechanical properties of ULCB steel weldments
[AD-A245523] p 2878 N92-26659

WHEELS
Time optimal trajectories for mobile robots with two independently driven wheels
[DE92-010002] p 2913 N92-26219
WHISKER COMPOSITES
Effect of thermal residual stresses on the stress-strain behavior of metal-matrix composites
[AD-A246136] p 2868 N92-26386
WHITE DWARF STARS
Atmospheric parameters of a soft x ray selected set of hot DA white dwarfs p 3017 N92-26576
WIND (METEOROLOGY)
Undulatory airflow over the Spanish southern central highplain with northern winds p 2940 N92-26339
WIND DIRECTION
Comparison of wind profiles in close proximity to each other
[AD-A246152] p 2945 N92-26409
WIND EFFECTS
Observations of wind forced circulation on the continental shelf off Point Sur, California from a self-contained acoustic Doppler current profiler
[AD-A246437] p 2950 N92-27029
WIND EROSION
Hindcast wave information for the Great Lakes: Lake Huron. Wave information studies of US coastlines
[AD-A246326] p 2949 N92-26387
WIND PROFILES
Comparison of wind profiles in close proximity to each other
[AD-A246152] p 2945 N92-26409
Integrating wind profiler data into forecast and warning operations at NWS field offices
[PB92-146075] p 2945 N92-26514
WIND TUNNEL MODELS
High-alpha vortex decoupling investigations on a chine forebody/Delta wing configuration at transonic Mach numbers
[NASA-CR-189642] p 2849 N92-26651
WIND TUNNEL TESTS
High-alpha vortex decoupling investigations on a chine forebody/Delta wing configuration at transonic Mach numbers
[NASA-CR-189642] p 2849 N92-26651
WIND VELOCITY
Comparison of wind profiles in close proximity to each other
[AD-A246152] p 2945 N92-26409
Integrating wind profiler data into forecast and warning operations at NWS field offices
[PB92-146075] p 2945 N92-26514
WINDOWS (APERTURES)
Effects of long-duration exposure on optical system components p 2998 N92-27095
WINDS ALOFT
Atmospheric environment for Space Shuttle Columbia (STS-40) launch
[NASA-TM-103585] p 2945 N92-26288
WINGS
The icing of the wing upper side and bottom side of the icing research aircraft of the DLR p 2850 N92-26349
WOOD
High-yield hydrogen production by catalytic gasification of coal or biomass
[DE92-008770] p 2875 N92-26724
WORKSTATIONS
Advanced software development workstation. Engineering scripting language graphical editor: DRAFT design document
[NASA-CR-190393] p 2971 N92-26181
Advanced software development workstation. Engineering scripting language graphical editor: DRAFT code documentation
[NASA-CR-190389] p 2971 N92-26182
Advanced software development workstation project: Engineering scripting language. Graphical editor
[NASA-CR-190391] p 2971 N92-26183
Distributed visualization
[DE92-009405] p 2971 N92-26188
Color image processing and object tracking workstation
[NASA-TM-105561] p 2886 N92-26611
WORLD METEOROLOGICAL ORGANIZATION
Report of the CC1 experts meeting on tracking and transmission of climate system monitoring information
[WCDMP-16] p 2947 N92-26925
WRIST
The validation of a human force model to predict dynamic forces resulting from multi-joint motions
[NASA-TP-3206] p 2956 N92-26538

X

X RAY ABSORPTION
Application of in situ x ray absorption and fluorescence measurements to analyze solutions in a simulated pit
[DE92-009159] p 2878 N92-26563
X RAY ASTRONOMY
Thermal design for the space-exposed instruments for the scientific satellite SAX p 2860 N92-26973
X RAY DIFFRACTION
Diffraction phenomena in spontaneous and stimulated radiation by relativistic particles in crystals (review)
[DE92-009501] p 3001 N92-26222
Joint services electronics program
[AD-A245636] p 2892 N92-26280
Anomalous structural behaviour of the high-temperature superconducting compound La(1.8)Sr(0.2)CuO(4-y)
p 3003 N92-26327
A comprehensive review of the XRD data of the primary and secondary phases present in the BSCCO superconductor system
[DE92-010363] p 3003 N92-26579
Some experiences with absorption, phonon Raman, and luminescence spectroscopic probes of crystal structure of f-element compounds
[DE92-007828] p 3006 N92-26851
X RAY FLUORESCENCE
Application of in situ x ray absorption and fluorescence measurements to analyze solutions in a simulated pit
[DE92-009159] p 2878 N92-26563
X RAY SCATTERING
X ray scattering studies of non-equilibrium ordering processes
[DE92-010311] p 2877 N92-26542
X RAY SOURCES
Underground muons observed in the Soudan 2 detector from the directions of x ray sources
[DE92-010344] p 3021 N92-26264
Atmospheric parameters of a soft x ray selected set of hot DA white dwarfs p 3017 N92-26576
X RAY SPECTROSCOPY
Spectroscopic imaging, diffraction, and holography with x ray photoemission
[DE92-009142] p 2996 N92-26187
Superconducting tunnel junctions
p 2907 N92-26396
Application of in situ x ray absorption and fluorescence measurements to analyze solutions in a simulated pit
[DE92-009159] p 2878 N92-26563
The application of XPS to the study of MIC
[DE92-010156] p 2879 N92-26813
NASA Li/CF(x) cell problem analysis: Scanning electron microscopy with energy dispersive x ray spectrometry
p 2863 N92-27144
X RAYS
Mapping the great attractor region in x rays and diffuse x ray emission: A possible galactic wind in the bulge of M31
[NASA-CR-190402] p 3015 N92-26184
Comparison of laser and conventional heating in TLD dosemapping
[DE92-010773] p 2910 N92-26269
Destruction and excitation of accreted nuclei in neutron star atmospheres: Gamma ray lines and x ray bursts
p 3016 N92-26476
Atmospheric parameters of a soft x ray selected set of hot DA white dwarfs p 3017 N92-26576
Focusing x ray transition radiation with cylindrical and elliptical optics
[AD-A245987] p 2997 N92-26754
Reflection of x rays from repeated multilayer structures
[AD-A246562] p 2991 N92-26769
Higher order parametric x rays
[AD-A247148] p 2991 N92-27182

Y

YAG LASERS
Photocathode transfer and storage techniques using alkali vapor feedback control
[DE92-008449] p 2891 N92-26202
Diode pumped 275 watt average power Nd:YAG slab laser
[DE92-008604] p 2911 N92-26504
YTTRIUM
Determination of the structure of Y(HCOO)3 by the neutron time-of-flight diffraction method
p 3002 N92-26325
YTTRIUM COMPOUNDS
A high-resolution neutron powder diffraction study in high-T(sub c) superconductor YBa2Cu3O7
p 3002 N92-26326
YTTRIUM OXIDES
Recent results in characterization of melt-grown and quench-melt-grown YBCO superconductors
[DE92-010281] p 3001 N92-26210
Slip casting and green body evaluation of 6 percent yttria, 2 percent alumina silicon nitride
[AD-A245817] p 2881 N92-26283
The Debye temperature of YBa2Cu3O(7-(delta)) and its dependence on the volume fraction of superconductivity
[DE92-010305] p 3003 N92-26584
Analysis of Yttrium-Barium-Copper-Oxide by x ray diffraction and mechanical characterization
[NASA-TM-104562] p 2869 N92-26650
Percolation effects in the V-I characteristics of granular YBa2Cu3O(7-delta)
[DE92-617541] p 3004 N92-26672
Zirconia-based fuel cells for power generation
[DE92-009886] p 2927 N92-26719

Z

ZINC SULFIDES
Studies of rain erosion mechanisms in a range of IR transmitting ceramics including coated samples
[AD-A245299] p 2882 N92-26751
ZINC-OXYGEN BATTERIES
Zinc-oxygen battery development program
p 2865 N92-27152
ZIRCONIUM OXIDES
High temperature furnace modeling and performance verifications
[NASA-CR-190403] p 2908 N92-26536
Zirconia-based fuel cells for power generation
[DE92-009886] p 2927 N92-26719
Evaluation of plasma sprayed crucible coatings for melt processing copper-refractory metal alloys
[DE92-008912] p 2878 N92-26727
Hughes advanced nickel-cadmium batteries: An update p 2862 N92-27136
ZONE MELTING
The experiment under microgravity by aircraft: The experiment in floating by gas flow p 2886 N92-26447

Typical Personal Author Index Listing

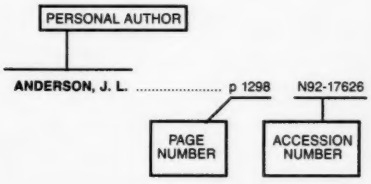

Listings in this index are arranged alphabetically by personal author. The page number helps you locate the citation in the abstract section. The accession number denotes the number by which the citation is identified.

A

AARONS, JULES ..... p 2943 N92-26675
ABBOTT, CHRISTOPHER L. ..... p 2950 N92-27029
ABDON, MYRIAN DEMOURA ..... p 2951 N92-26721
ABLOWITZ, MARK J. ..... p 2986 N92-26414
ABRAMOV, G. K. ..... p 2956 N92-26951
ABRAMOV, L. K. ..... p 2957 N92-26955
ABROSIMOV, A. I. ..... p 2860 N92-27000
ACOSTA, JUAN C. ..... p 2922 N92-26661
ADAMS, LOYCE ..... p 2980 N92-26801
ADAMS, T. A. ..... p 2980 N92-26531
ADOLPH, JURINE ..... p 2982 N92-26628
AFFOLTER, H. ..... p 2853 N92-26944
AGGARWAL, P. K. ..... p 2918 N92-26669
AHEARN, J. S. ..... p 2895 N92-27111
AHMED, S. ..... p 2966 N92-27009
AHUJA, K. K. ..... p 2853 N92-26405
AKSU, IBRAHIM ..... p 2974 N92-26468
ALBRECHT, G. ..... p 2911 N92-26504
ALBUS, J. S. ..... p 2984 N92-26814
ALCARAS, J. A. C. ..... p 2988 N92-26837
ALCOUFFE, R. E. ..... p 2981 N92-26854
ALDRIDGE, ANN M. ..... p 2956 N92-26538
p 2956 N92-26682
ALET, IRENEE ..... p 2860 N92-26998
ALEXANDER, DENNIS R. ..... p 2894 N92-26942
ALEXANDER, R. B. ..... p 2933 N92-26931
ALEXANDRE, A. ..... p 2895 N92-26974
ALF, M. ..... p 2887 N92-26986
ALLEN, P. B. ..... p 3004 N92-26638
ALLEN, THOMAS H. ..... p 2998 N92-27091
ALLISON, W. W. M. ..... p 3020 N92-26211
p 3021 N92-26216
p 3021 N92-26218
p 3021 N92-26264
ALONSO-VARGAS, G. ..... p 2995 N92-26844
ALSTON, JIM A. ..... p 2952 N92-27120
ALVERTOS, NICOLAS ..... p 2886 N92-26656
ALVISI, LORENZO ..... p 2979 N92-26278
p 2979 N92-26279
AMIDIEU, M. ..... p 2859 N92-26967
AMMANN, K. ..... p 2968 N92-27019
AMMAR, GREG ..... p 2988 N92-26900
AMOROSO, ALESSANDRO ..... p 2979 N92-26278
p 2979 N92-26279
ANDERSEN, N. H. ..... p 3002 N92-26324
ANDERSON, DANA Z. ..... p 2992 N92-26413
ANDERSON, TIMOTHY J. ..... p 2893 N92-26540
ANFIMOV, N. A. ..... p 2883 N92-27015
ANGEL, S. M. ..... p 2898 N92-26645
ANGELO, JOSEPH A., JR. ..... p 2952 N92-27122
ANGOEV, MICHAEL D. ..... p 2946 N92-26562
ANIKEEVA, V. A. ..... p 2976 N92-26835
ANTONENKO, J. ..... p 2883 N92-27016
ANTSON, OLLI K. ..... p 3001 N92-26320
p 3002 N92-26321
p 3002 N92-26323
p 3002 N92-26324
p 3002 N92-26325
p 3002 N92-26326
p 3003 N92-26328
AOYAGI, T. ..... p 2957 N92-26954
ARAPOSTATHIS, ARISTOTLE ..... p 2985 N92-27169
ARIF, ABUL FAZAL MUHAMMAD ..... p 2917 N92-26594
ARMSTRONG, T. W. ..... p 2993 N92-26200
ARNOLD, G. W. ..... p 3005 N92-26826
ARNOLD, NEIL F. ..... p 2928 N92-26473
ARNOLD, T. R. ..... p 2971 N92-26188
ARNOTT, W. P. ..... p 2914 N92-26389
AROESTY, J. ..... p 2954 N92-26193
ARRIAGA, ARLINDO JOSE CLAUDINO ..... p 2942 N92-26490
ARSENOVIC, PETAR ..... p 2869 N92-26650
ASAI, MASAHITO ..... p 2902 N92-26910
p 2904 N92-26921
ASAY, J. R. ..... p 2919 N92-26846
p 2919 N92-26852
ASSIE, JEAN-PIERRE ..... p 2895 N92-27118
p 2880 N92-27119
ATTIA, E. H. ..... p 2912 N92-26663
AUMEIER, S. E. ..... p 2996 N92-26841
AVAKYAN, V. V. ..... p 3021 N92-26804
AVELLINI, BARBARA A. ..... p 2952 N92-26470
AXE, J. D. ..... p 3006 N92-27059
AYERS, J. KIRK ..... p 2920 N92-26903
AYTUR, ORHAN B. ..... p 2912 N92-26603
AZGUI, F. ..... p 2907 N92-26393

B

BABAOGLU, OZALP ..... p 2979 N92-26278
p 2979 N92-26279
p 2980 N92-26677
BABENKO, V. A. ..... p 2859 N92-26968
BABIC, D. ..... p 3004 N92-26672
BABIC, E. ..... p 3004 N92-26672
BADER, S. D. ..... p 2997 N92-26565
BAILEY, MICHAEL P. ..... p 2883 N92-26178
BAIN, D. B. ..... p 2854 N92-26561
BAISCH, FRIEDHELM ..... p 2953 N92-27012
BAKER, J. R. ..... p 2921 N92-26206
BAKER, JOHN ..... p 2863 N92-27144
BAKER, K. B. ..... p 2936 N92-26304
BAKER, R. S. ..... p 2981 N92-26854
BALACHANDRAN, U. ..... p 3001 N92-26210
BALDOCHI, S. L. ..... p 2910 N92-26287
BALDWIN, CRAIG W. ..... p 2996 N92-26241
BANKS, H. T. ..... p 2987 N92-26668
p 2920 N92-26892
BANNISTER, C. E. ..... p 2870 N92-26201
BARABASH, P. A. ..... p 2957 N92-26956
BARANKIEWICZ, WENDY S. ..... p 2854 N92-26613
BARGATZE, LEE FROST ..... p 2943 N92-26622
BARKER, J. R. ..... p 2994 N92-26240
BARNES, P. R. ..... p 2887 N92-26237
BARNS, D. W. ..... p 2931 N92-26633
BARR, G. D. ..... p 3020 N92-26211
p 3021 N92-26218
p 3021 N92-26264
BARRERA, TOM P. ..... p 2863 N92-27138
BARRON, C. I. ..... p 2935 N92-26294
BARTOLOTTA, PAUL A. ..... p 2880 N92-27192
BARTON, JOHN P. ..... p 2894 N92-26942
BARYSHEV, O. V. ..... p 2860 N92-27000
BARYSHEVSKY, V. G. ..... p 3001 N92-26222
BASS, HENRY E. ..... p 2914 N92-26389
BATES, J. B. ..... p 2893 N92-26636
p 2893 N92-26637
BATTAGLIN, G. ..... p 3005 N92-26826
BATTISTE, R. L. ..... p 2919 N92-26845
BATTS, G. W. ..... p 2945 N92-26288
BATURKIN, V. M. ..... p 2905 N92-26972
BATY, R. S. ..... p 2901 N92-26856
BAUDIN, CATHERINE ..... p 2985 N92-27057
BAUGH, KEVIN W. ..... p 2989 N92-26180
BAUSCHLICHER, CHARLES W., JR. ..... p 2994 N92-26539
BAXAM, CARL C. ..... p 2865 N92-27151
BAZAN, GRANT ..... p 3018 N92-26725
BEACH, R. ..... p 2911 N92-26504
BEAVER, PHILIP F. ..... p 2990 N92-26466
BECK, F. B. ..... p 2891 N92-27189
BECK, LUIS ..... p 2953 N92-27012
BECKERMAN, M. ..... p 2983 N92-26657
BECKMAN, E. L. ..... p 2956 N92-26665
BEERE, G. I. M. ..... p 2965 N92-27001
BELKIN, MICHAEL ..... p 2953 N92-27063
BELL, WALTER J. ..... p 2990 N92-26460
BENETT, B. ..... p 2911 N92-26504
BENNETT, J. M. ..... p 2999 N92-27098
BENSEL, CAROLYN K. ..... p 2954 N92-26242
p 2954 N92-26243
BENSON, JAMES ARTHUR ..... p 3015 N92-26477
BENTVELSEN, P. H. ..... p 2910 N92-26271
BENVENUTTI, EUGENE S., JR. ..... p 2979 N92-26361
BEREZIN, V. ..... p 3018 N92-26833
BERGMAN, L. A. ..... p 2998 N92-27090
BERK, H. L. ..... p 2999 N92-26256
p 3000 N92-26550
BERLIN, A. A. ..... p 2957 N92-26955
BERMAN, C. H. ..... p 2876 N92-26783
BERNIER, JEAN D. ..... p 2997 N92-26662
BERNSTEIN, E. R. ..... p 2872 N92-26431
p 2874 N92-26608
BERNSTEIN, ELLIOT R. ..... p 2874 N92-26526
BERRY, J. N. ..... p 2998 N92-27089
BERUTI, V. ..... p 2925 N92-26745
BETTS, EDWARD E. ..... p 2853 N92-27185
BHAT, M. K. ..... p 2849 N92-26651
p 2849 N92-26652
BHATNAGAR, RAJIV ..... p 2982 N92-26628
BHATTACHARRYYA, SAMIT K. ..... p 2861 N92-26792
BIERENS, L. H. J. ..... p 2890 N92-26876
BIERI, R. L. ..... p 3000 N92-26729
BILDSTEN, LARS ..... p 3016 N92-26476
BINDER, MICHAEL ..... p 2861 N92-27033
BINOT, R. A. ..... p 2961 N92-26981
p 2962 N92-26983
BINOT, ROGER ..... p 2951 N92-26978
BISCARAT, JEAN-CLAUDE ..... p 2989 N92-27174
BISHOP, MATT ..... p 2981 N92-27183
BITHER, CHERYL A. ..... p 2987 N92-26620
BLAKKOLB, B. K. ..... p 2895 N92-27103
BLALOCK, T. V. ..... p 2908 N92-26569
BLAZYE, CHRISTOPHER J. ..... p 2922 N92-26625
BLISS, E. S. ..... p 2912 N92-26646
BLOCK, D. R. ..... p 2930 N92-26519
BLUE, J. L. ..... p 2980 N92-26501
BLUE, M. D. ..... p 2998 N92-27094
BLUM, KEVIN M. ..... p 2993 N92-27076
BOBBA, FABIANA ..... p 2963 N92-26991
BOBE, L. S. ..... p 2956 N92-26951
p 2957 N92-26952
p 2957 N92-26956
BOCARSLY, A. B. ..... p 3004 N92-26639
BOCHAROV, S. S. ..... p 2957 N92-26952
p 2957 N92-26955
BODVARSSON, G. S. ..... p 2895 N92-26214
BOER, MICHEL ..... p 3018 N92-27048
p 3016 N92-27049
BOERNGE, J. ..... p 2895 N92-26214
BOGNER, R. SAM ..... p 2862 N92-27136
BOHLEN, R. ..... p 2962 N92-26984
BOITEL, V. ..... p 2966 N92-27006
BOLDING, KEVIN ..... p 2979 N92-26359
BOLOTOVSKII, R. L. ..... p 3003 N92-26327
BONCEK, RAYMOND K. ..... p 2998 N92-26943
BONINO, GIANFRANCO ..... p 2860 N92-26973
BONNEMASON, FRANCIS ..... p 2910 N92-27092
BORGHESE, JOSEPH B. ..... p 2968 N92-27021
BORGWARDT, R. H. ..... p 2933 N92-26929
BOS, JAN FRANS TONNIS ..... p 2954 N92-26255
BOSCOLO-BOSCOLETTO, A. ..... p 3005 N92-26826
BOSSE, ELOI ..... p 2888 N92-26419
BOTICARIO, LUIS A. ..... p 2920 N92-26932
BOURASSA, MARY E. ..... p 2930 N92-26495
BOURLAND, DEBORAH S. ..... p 2865 N92-27152
BOWMAN, C. T. ..... p 2872 N92-26281
BOYLE, GERARD H. ..... p 2864 N92-27149
BOZZOLO, G. H. ..... p 2990 N92-26671
BRADINI, LUCA ..... p 2860 N92-27024
BRAGG, BOB J. ..... p 2863 N92-27142
BRAGG, M. ..... p 2849 N92-26612

BRAIG, ALBERT p 2859 N92-26997
BREGER, D. p 2928 N92-26231
BREISACHER, KEVIN J. p 2861 N92-27035
BREIZMAN, B. N. p 3000 N92-26550
BREKKE, A. p 2935 N92-26295
BRENNAN, PATRICK J. p 2906 N92-27104
BRESANI, ALDO E. p 2888 N92-26363
BRESINA, JOHN p 2983 N92-26643
p 3015 N92-26886
p 2984 N92-27055
BRESINA, JOHN L. p 2982 N92-26627
BREVEGLIERI, LUCA p 2974 N92-26449
BREWER, JEFFREY C. p 2865 N92-27153
p 2866 N92-27165
BRILL, JACK p 2866 N92-27160
BRINKER, DAVID J. p 2927 N92-27101
BRITE, C. p 2909 N92-26572
BRITTEN, R. A. p 2926 N92-27195
BRITTON, DORIS L. p 2875 N92-26670
BRODY, ERIC A. p 2948 N92-26245
BROECKER, W. S. p 2948 N92-26270
BROERSMA, H. J. p 2987 N92-26737
p 2988 N92-26817
BRONSTEIN, LEON p 2925 N92-26747
BROOKES, DANIEL p 2888 N92-26419
BROOKS, C. B. p 3020 N92-26211
p 3021 N92-26216
p 3021 N92-26218
p 3021 N92-26264
BROOKS, FREDERICK P., JR. p 2954 N92-26179
BROOKS, L. K. p 2895 N92-27112
BROUGHTON, T. p 2856 N92-27043
BROWN-STRATTAN, M. A. p 2928 N92-26390
BROWN, DENNIS B. p 2991 N92-26769
BROWN, GAIR D. p 2909 N92-26879
BROWN, JAMES HOWARD p 3018 N92-26723
BROWNING, D. F. p 2911 N92-26505
BUCCA, P. J. p 2950 N92-27071
BUCH, KENNETH ALVAN, JR. p 2899 N92-26740
BUCHANAN, DAVID LEIGH p 2869 N92-26607
BUDGE, K. G. p 2976 N92-26696
BUECKER, H. p 2952 N92-27126
BULKIN, A. P. p 3002 N92-26322
p 3002 N92-26323
p 3002 N92-26325
p 3003 N92-26327
BUNTINE, WRAY p 2983 N92-26629
p 2984 N92-26893
BUNTINE, WRAY L. p 2983 N92-26631
BURCH, I. A. p 2916 N92-26282
BURGE, D. K. p 2999 N92-27098
BURTON, D. J. p 2926 N92-26372
BYRNS, HERBERT F. p 3009 N92-26660
BYTELLA, JOSEPH p 2864 N92-27145
BYUN, MYUNG WOO p 2954 N92-26186

C

CACACE, F. p 2973 N92-26421
CACCAVALE, F. p 3005 N92-26826
CALCOTE, H. F. p 2876 N92-26783
CAMERON, B. J. p 2891 N92-26202
CAMERON, L. E. p 2872 N92-26404
CAMPBELL, G. GARRETT p 2933 N92-26878
CANDELA, G. T. p 2980 N92-26501
CANNON, STEVEN CARY p 2901 N92-26871
CAO, YUSONG p 2942 N92-26583
CAPELLI, C. p 2973 N92-26421
CARPENTER, P. p 2993 N92-26225
CARROLL, R. M. p 2908 N92-26569
CARTER, A. F. p 2873 N92-26521
CARTER, C. B. p 3004 N92-26648
CARUANA, RICH p 2983 N92-26629
CASALNUOVO, S. A. p 2997 N92-26452
CASPER, T. p 2906 N92-26230
CAVALLARO, PAUL V. p 2882 N92-26609
CELEUX, GILLES p 2989 N92-27174
CHAKOUMAKOS, B. C. p 3005 N92-26843
CHAN, S. T. p 2934 N92-26936
CHANCHAI, P. p 2925 N92-26749
CHANDLER-HOROWITZ, D. p 2894 N92-26821
CHANDLER, D. B. p 3005 N92-26843
CHANG, CRAIG H. p 2968 N92-27021
CHANG, WEE L. p 2989 N92-26467
CHAO, CHI-SHUN p 2973 N92-26418
CHAPMAN, S. P. p 2998 N92-27089
CHAR, K. p 2891 N92-26205
CHARLIER, JEAN p 2999 N92-27097
CHASE, CHARLES A., VII p 2977 N92-26840
CHEDOTTE, J. E. p 2895 N92-27103
CHEESEMAN, PETER p 2988 N92-26894
CHEN, C. C. p 2872 N92-26351
CHEN, PHILIP S. p 2870 N92-26882
CHEN, TZE JANG p 2897 N92-26556
CHEN, W. Y. C. p 3006 N92-26857
CHENUT, G. p 2958 N92-26959
CHERCHENEFF, ISABELLE MARIE p 3018 N92-26757
CHHABILDAS, L. C. p 2919 N92-26846
p 2919 N92-26852
CHI, Y. T. p 3001 N92-26226
CHIARELLI, C. p 2860 N92-27028
CHIKILEV, O. G. p 2995 N92-26800
CHIN, MIAO p 2894 N92-27061
CHIN, YU-CHI p 2851 N92-26756
CHIPMAN, D. W. p 2928 N92-26231
CHO, HAN OK p 2954 N92-26186
CHO, J. H. p 2878 N92-26563
CHOU, HSING-TUNG p 2851 N92-26623
CHOUDHARI, MEELAN p 2898 N92-26680
p 2898 N92-26681
CHOUDHURY, A. p 2893 N92-26636
CHRISTEN, D. K. p 3005 N92-26843
CHU, STEVEN p 2913 N92-27173
CHUN, CLAYTON K. S. p 2852 N92-26673
CIORANESCU, D. p 2920 N92-26892
CISSEL, MATTHEW B. p 2880 N92-27067
CLARK, E. A. p 2870 N92-26201
CLARK, J. M. p 2952 N92-26263
CLARK, JOHN S. p 2861 N92-26792
CLARK, SHANG-YING p 2982 N92-26434
CLARK, WILLIAM D. K. p 2864 N92-27147
CLARKE, J. p 2891 N92-26205
CLAYTON, C. R. p 2879 N92-26813
CLEMENTS, PAUL C. p 2976 N92-26766
COBB, J. H. p 3020 N92-26211
p 3021 N92-26216
p 3021 N92-26218
p 3021 N92-26264
COCKRELL, C. R. p 2891 N92-27189
COEN-PORISINI, ALBERTO p 3011 N92-26422
COLASSON, M. p 2969 N92-27023
COLBORN, B. L. p 2993 N92-26200
COLCLOUGH, M. S. p 2891 N92-26205
COLE, J. K. p 2899 N92-26716
COLEMAN, RACHEL J. p 2942 N92-26406
COLLINS, P. J. p 2996 N92-26841
COLLOPY, M. T. p 2993 N92-26225
COLOMBANO, SILVANO P. p 2982 N92-26628
COMASKEY, B. p 2911 N92-26504
COMBEE, LEENDERT p 2887 N92-26254
COMISO, JOSEFINA p 2948 N92-26245
COMPTON, MICHAEL p 2982 N92-26628
p 2984 N92-26887
CONDE, ERIC p 2880 N92-27119
COOK, MICHAEL J. p 2913 N92-27178
COOK, WILLIAM HOWARD p 2881 N92-26492
COOPER, G. W. p 2993 N92-26225
COOPER, M. I. p 2850 N92-26947
COOPER, PAUL A. p 2920 N92-26903
COOPER, S. p 2906 N92-26391
COOPER, SUSAN p 2907 N92-26392
p 2907 N92-26394
COOTER, E. J. p 2930 N92-26519
CORNET, J. F. p 2961 N92-26981
p 2952 N92-26982
CORNISH, P. V. p 2966 N92-27009
CORONA, EDMUNDO p 2920 N92-26869
CORREA, S. M. p 2876 N92-26782
CORUM, J. M. p 2919 N92-26845
COSTA, F. E. p 2910 N92-26287
COSTA, O. L. V. p 2988 N92-26831
COWLEY, S. W. H. p 2937 N92-26308
COX, M. G. p 2974 N92-26450
CRAWFORD, ROBYN L. p 2955 N92-26355
CROW, RITA M. p 2990 N92-26471
CRUZE, STEPHEN PAUL p 2889 N92-26604
CUCINOTTA, FRANCIS A. p 2996 N92-26832
CUDDIHY, EDWARD F. p 2863 N92-27140
CULAS, DONALD E. p 2972 N92-26197
CURDT, W. p 2960 N92-26975
CYRUS, ANGELA W. p 3013 N92-26762
CZERWINSKI, K. R. p 2870 N92-26212

D

DAALDEROP, GERARDUS HENRICUS OTTO p 2877 N92-26252
DABROWSKI, B. p 3005 N92-26842
DALBEY, R. Z. p 2999 N92-27098
DALY, C. p 2931 N92-26793
DAMAN, M. E. p 2865 N92-27158
DAMOUR, T. p 2943 N92-26820
DAMS, R. A. J. p 2966 N92-27010
DARCY, ERIC C. p 2864 N92-27146
DARLING, DOUGLAS p 2855 N92-27037
DARSEY, J. A. p 2986 N92-26407
DASGUPTA, U. p 3021 N92-26253
DAVARI, SADEGH p 3009 N92-26552
DAVENPORT, A. J. p 2878 N92-26563
DAVIES, HUW C. p 2939 N92-26330
DAVIES, MERTON E. p 3019 N92-26819
DAVIS, L. T. p 3012 N92-26575
DAVOLI, RENZO p 2979 N92-26278
p 2979 N92-26279
DAWSON, L. p 2958 N92-26961
DCUNHA, IVAN p 2886 N92-26656
DEBOOR, CARL p 2989 N92-27175
DECHAMBURE, DANIEL p 2951 N92-26978
DECKER, HARRY J. p 2915 N92-26560
DEEHR, C. p 2935 N92-26296
DEFONTAINE, D. p 2877 N92-26213
DEKONING, J. P. A. p 2958 N92-26958
DELIGIANNIS, FRANK p 2865 N92-27154
DELL, R. DAN p 2863 N92-27141
DELLER, JOHN R. p 2980 N92-26430
DELUCA, G. F. p 2963 N92-26990
DEMARCHI, G. p 3005 N92-26826
DEMMEL, JOHANN p 2850 N92-26349
DEMUREN, A. O. p 2898 N92-26649
DENG, AN-TE p 2972 N92-26248
DENISENKO, V. V. p 2938 N92-26319
DENNIG, P. A. p 2883 N92-27060
DEPAROLIS, M. N. p 2916 N92-26987
DESAUNETTES, B. p 2886 N92-26964
DESAUNETTES, BRUNO p 2958 N92-26960
DESNOYER, D. p 2860 N92-27028
DEVORE, RONALD A. p 2989 N92-27175
DEWA, ISMAIL B. p 2989 N92-27180
DEWOLF, H. p 2958 N92-26958
DIEBOLT, JEAN p 2989 N92-27174
DIENER, M. p 2965 N92-27003
DIETRICH, HARRY B. p 3003 N92-26433
DINI, J. W. p 2878 N92-26732
DION, MARC p 2889 N92-26592
DIXON, R. K. p 2930 N92-26510
DODDS, JERRY p 2998 N92-27091
DODGE, JEFFREY S. p 2950 N92-26289
DODONOV, V. V. p 2888 N92-26374
DOELLNER, OSCAR LEONARD p 2926 N92-26581
DOHERTY, MICHAEL P. p 2861 N92-26792
DONG, YIBING p 2909 N92-26738
DONOHUE, GEORGE L. p 2990 N92-26194
DONOVAN, T. M. p 2999 N92-27098
DORESWAMY, RAJIV p 2865 N92-27153
DORFF, STEPHEN J. p 2992 N92-27031
DOTY, JOHN HOWARD p 2853 N92-26480
DOUGHERTY, F. C. p 2850 N92-27172
DOUGHERTY, JULIE A. p 2987 N92-26620
DOVER, C. B. p 2995 N92-26815
DOWKER, FAY p 3016 N92-26436
DRERUP, ROBERT A., JR. p 2998 N92-27093
DRESHFIELD, ROBERT L. p 2880 N92-27192
DRIVER, D. p 2880 N92-27044
DROLET, T. S. p 2999 N92-26286
DRUMHELLER, DAVID M. p 2975 N92-26529
DRUMMOND, MARK p 2983 N92-26643
p 3015 N92-26886
p 2984 N92-27055
DRUMMOND, MARK E. p 2982 N92-26627
DUBERTRET, G. p 2952 N92-26982
DUBOVSKAYA, I. YA. p 3001 N92-26222
DUDENEY, J. R. p 2936 N92-26304
DUDENHOEFER, JAMES E. p 2861 N92-26654
DUDLEY, G. J. p 2865 N92-27156
DUDNEY, N. J. p 2893 N92-26636
p 2893 N92-26637
DUFFAR, T. p 2886 N92-26964
DUMMER, D. p 2906 N92-26391
p 2907 N92-26394
p 2907 N92-26395
DUNFORD, E. p 2938 N92-26316
DUNHAM, J. p 2856 N92-27062
DUNN, DEROME OSMOND p 2919 N92-26829
DUNN, K. A. p 2870 N92-26201
DUNN, ROBERT C. p 2867 N92-26380
DURBIN, E. J. p 2914 N92-26371
DURIN, CHRISTIAN p 2867 N92-27117
DURSCH, HARRY p 2867 N92-27084
p 2880 N92-27115
DURSCH, HARRY W. p 2916 N92-27114
DUSSAP, C. G. p 2952 N92-26982
DUTTA, PIYUSH K. p 2869 N92-26796
DWYER, ANDREW P. p 3010 N92-26176

E

EBELING, W.-D. p 2887 N92-26988
p 2883 N92-27016
p 2905 N92-27027
ECKERT, K. p 2961 N92-26976
ECKLES, STEVEN p 2865 N92-27157
EDDY, JOHN A. p 2934 N92-27082
EDELMAN, JOEL p 2867 N92-27084
EDGAR, TIM p 2862 N92-27135

EDMONDS, J. A. p 2931 N92-26633
EDWARDS, J. p 2957 N92-26953
EGGER, JOSEPH p 2939 N92-26331
EHLER, T. p 2852 N92-26435
EHRET, GERHARD p 2941 N92-26347
EHRLICH, NELSON J. p 2952 N92-27121
EIDEN, M. p 2860 N92-27028
EL-SAYED, M. A. p 2951 N92-26493
ELIZONDO, MICHAEL A. p 2917 N92-26593
ELKALIFA, ELSUNI SIDAHMED p 3012 N92-26614
ELLIS, JOHN p 3014 N92-26830
ELLRICK, DANIEL A. p 2888 N92-26399
ELSAESSER, DEREK p 3011 N92-26378
ENNEKING, THOMAS JOSEPH p 2917 N92-26557
ENTSTRASSER, NORBERT p 2942 N92-26350
EPSTEIN, S. p 2881 N92-26451
ERKAEV, N. V. p 2938 N92-26319
ERNST, G. p 2887 N92-26986
ESENWEIN, GEORGE F. p 2925 N92-26744
ESPOSITO-FARESE, G. p 2943 N92-26820
ESSENS, P. J. M. D. p 3010 N92-27046
EUSTACE, R. W. p 2850 N92-26947
EYRING, EDWARD M. p 2991 N92-26940

F

FAGHRI, AMIR p 2896 N92-26379
FAILOR, R. A. p 2873 N92-26454
FALCONER, J. L. p 2873 N92-26508
FALTER, D. D. p 2908 N92-26569
FARAFONOV, N. S. p 2956 N92-26951
p 2957 N92-26955
FARMER, W. S. p 2913 N92-26234
FAUDREE, R. J. p 2988 N92-26817
FAUQUET, REGIS p 2953 N92-27011
FEELEY, O. C. p 2884 N92-26548
FEENSTRA, P. p 2890 N92-26874
FEHL, D. L. p 2910 N92-26269
FEILER, CHARLES E. p 2989 N92-27196
FELDER, MIGUEL p 2973 N92-26448
FELKER, B. p 2906 N92-26377
FELLOUS, J. L. p 2925 N92-26746
FERBER, M. K. p 2918 N92-26784
FERGER, P. p 2907 N92-26393
FERGUSON, S. W. p 2906 N92-26377
FERNANDO, H. J. p 2896 N92-26412
FERRANTE, J. p 2990 N92-26671
FERRARI, M. J. p 2891 N92-26205
p 3003 N92-26582
FERRARIO, M. T. p 2899 N92-26716
FERRARIS, SIMONA p 2964 N92-26993
FETROW, FRED p 3022 N92-26664
FIELD, J. E. p 2882 N92-26751
FIELDS, T. H. p 3021 N92-26253
FIELKE, G. p 2852 N92-26948
FILKINS, PETER C. p 2975 N92-26524
FILONENKO, V. B. p 2957 N92-26952
p 2957 N92-26955
p 2957 N92-26956
FIMPEL, HANS P. p 2941 N92-26348
FIRMAN, PAUL p 2991 N92-26940
FIRMIN, J. L. p 2895 N92-26974
FISCHER, W. p 2887 N92-26988
FISHER, DOUGLAS p 2985 N92-27056
FISHER, R. A. p 3003 N92-26584
FISHMAN, LOUIS p 2991 N92-26175
FLANEGAN, MARK p 2858 N92-26667
FLEMING, A. J. p 2853 N92-26405
FLORIS, F. J. T. p 2900 N92-26836
FOGLER, R. J. p 2891 N92-26902
FONTES, KEVIN A. p 2970 N92-26773
FOOTE, J. p 2906 N92-26230
FORMAN, W. R. p 3015 N92-26184
FORSTER, G. p 2907 N92-26393
FOSTER, MICHAEL S. p 2949 N92-26463
FRAINER, RICHARD p 2982 N92-26628
FRANCIS, A. J. p 2879 N92-26813
FRANK, M. p 2906 N92-26391
p 2907 N92-26394
FREEMAN, KATHERINE HAINES p 2921 N92-26478
FREEMAN, M. P. p 2937 N92-26308
FREITAS, B. p 2911 N92-26504
FRESE, K. W. p 2872 N92-26351
FREUND, P. p 2906 N92-26391
p 2907 N92-26397
FRIDLING, BARRY E. p 2850 N92-26272
FRIEDLAND, PETER p 3009 N92-26790
p 2984 N92-26887
FRIIS-CHRISTENSEN, E. p 2935 N92-26299
p 2937 N92-26307
p 2938 N92-26314
FRINK, NEAL TILSON p 2849 N92-26585
FUCHS, G. E. p 2881 N92-26455
FUCHS, HENRY p 2954 N92-26179
FUEHNE, JOSEPH PATRICK p 2920 N92-26860
FUJIMORI, NAOJI p 2885 N92-26442
FUKUI, MASAHIRO p 2885 N92-26445
FUKUNISHI, YU p 2903 N92-26917
FUNKE, H. p 2966 N92-27006
FUQUA, STEVEN J. p 2896 N92-26290
FURDAK, U. G. p 2860 N92-27000
FURMANOVA, N. G. p 3002 N92-26325
FURUKAWA, MASAO p 2885 N92-26444
p 2905 N92-26962
p 2962 N92-26985

G

GAHN, RANDALL F. p 2866 N92-27161
GAIA, ENRICO p 2963 N92-26991
p 2964 N92-26993
GALIPO, A. p 2973 N92-26421
GALOFARO, LUCA p 2860 N92-27024
GANGOPADHYAY, A. K. p 3001 N92-26210
GAO, J. R. p 3006 N92-26927
GARNER, D. R. p 2892 N92-26224
GARRIS, M. D. p 2980 N92-26501
GARRISON, J. C. p 2873 N92-26454
GARTENBACH, K. E. p 2952 N92-27124
GARYAKA, A. P. p 3021 N92-26804
GASARCH, CAROLYN E. p 2976 N92-26766
GATSKI, T. B. p 2901 N92-26883
GAWEDZKI, K. p 3007 N92-26805
GAYRARD, JOEL p 2859 N92-26966
GEBAUER, H.-J. p 2906 N92-26391
p 2907 N92-26397
p 2908 N92-26398
GEDIK, ABDULLAH p 2911 N92-26462
GEIST, J. p 2894 N92-26821
GEMMER, R. V. p 2876 N92-26782
GENERAL, VOLKER p 2968 N92-27018
GENG, STEVEN M. p 2861 N92-27034
GENTRY, WILLIAM O. p 2865 N92-27157
GEORGE, T. F. p 2888 N92-26374
GEORGE, THOMAS F. p 3005 N92-26684
GERA, GIANLUIGI p 2965 N92-27004
GERRARD, SARA MARGARET ELIZABETH
p 2925 N92-26777
GERSTENFELD, ARTHUR p 3009 N92-26863
GESSNER, R. p 2961 N92-26976
GEVARTER, WILLIAM B. p 2983 N92-26630
p 2984 N92-26888
GHOSH, P. K. p 3001 N92-26226
GIACHINI, LUIGI A. p 2979 N92-26278
p 2979 N92-26279
GIALLORENZI, THOMAS G. p 2997 N92-26862
GIANGANO, D. p 2883 N92-27086
GIBB, JOHN p 2927 N92-26895
GIBBS, P. W. p 2874 N92-26634
GIDASPOW, D. p 2896 N92-26456
GILES, R. H. p 3020 N92-26211
p 3021 N92-26216
p 3021 N92-26218
p 3021 N92-26264
GILLER, G. L. p 3021 N92-26216
p 3021 N92-26218
GILLOW, J. B. p 2879 N92-26813
GINN, LELON L. p 2974 N92-26461
GIOMMI, MARCO p 2859 N92-26996
GIORGI, PIER LUIGI p 2963 N92-26991
GITELSON, J. G. p 2951 N92-26979
GIULIANI, JAMES E. p 2861 N92-27036
GLADDINES, H. p 2986 N92-26367
GLASSMAN, NANCI A. p 3014 N92-27170
GLASSMEIER, K. H. p 2937 N92-26307
p 2938 N92-26314
GLOVER, C. W. p 2987 N92-26545
GLUECK, PETER p 2863 N92-27139
GLUECK, PETER R. p 2862 N92-27133
GLUSHENKO, P. I. p 2956 N92-26951
GMEHLING, J. p 2905 N92-27027
GNACEK, DEE p 2863 N92-27143
GOEHRE, C. p 2962 N92-26984
GOLDSACK, STEPHEN J. p 2978 N92-26199
GOLDSTEIN, G. p 2932 N92-26825
GOLIYAD, N. N. p 2957 N92-26956
GOMES, B. R. p 2950 N92-27071
GORDEYEV, V. M. p 2956 N92-26951
GORDON, J. E. p 3003 N92-26584
GORDON, KAREN D. p 2972 N92-26273
GOSHOZONO, TOSHIKAZU p 2885 N92-26443
GOTTARDI, M. p 3018 N92-27048
GOUALARD, JACQUES p 2864 N92-27148
GOYAL, A. p 3005 N92-26843
GRAF, JUTTA p 2934 N92-26332
GRAGG, WILLIAM p 2988 N92-26900
GRANLUND, S. p 2896 N92-26496
GRANT, GEORGE A. p 2955 N92-26472
GRASSESCHI, G. L. p 2996 N92-26841
GRAUL, E. H. p 2952 N92-27125
GRAVES, MICHAEL J. p 2852 N92-26655
GRAY, L. J. p 2854 N92-26697
GREENWALD, R. A. p 2936 N92-26304
GREGORICH, K. E. p 2870 N92-26212
GREGORY, RUTH p 3016 N92-26436
GRESHO, P. M. p 2934 N92-26936
GRETCHINA, N. K. p 2905 N92-26972
GRIDER, GARY W. p 2921 N92-26905
GRIFFIN, M. J. p 2956 N92-26891
GRIFFITH, P. p 2899 N92-26699
p 2899 N92-26700
GRIGSBY, DORIS K. p 2952 N92-27121
GROLEAU, NICOLAS p 2982 N92-26628
GROS, J. B. p 2952 N92-26982
GROSSMANN, ROBERT p 2940 N92-26341
GROTE, MICHAEL G. p 2906 N92-27106
GROTHER, P. p 2980 N92-26501
GRUNDY, I. H. p 2895 N92-26258
GRUZALSKI, G. R. p 2893 N92-26636
p 2893 N92-26637
GUERRAZZI, A. p 2953 N92-26992
GUIDOTTI, R. A. p 2892 N92-26238
p 2875 N92-26722
GUSTAFSSON, GEORG p 2937 N92-26309
GUSTAVSON, D. B. p 2887 N92-26267
GUTIERREZ, W. T. p 2899 N92-26716
GUTSCHE, M. p 2907 N92-26396
GUYENNE, T.-DUC p 2956 N92-26950
GYETVAY, S. p 2999 N92-27098

H

HACK, JAMES J. p 2928 N92-26352
HACKER, JOERG M. p 2941 N92-26346
HADFIELD, STEVEN M. p 2971 N92-26196
HAGEN, MARTIN p 2941 N92-26342
HAILEY, C. E. p 2899 N92-26716
HALADA, G. P. p 2879 N92-26813
HALICIOGLU, TIMUR p 3001 N92-26265
HALL, R. C. p 3012 N92-26575
HALLAL, MICHAEL P., JR. p 2895 N92-27079
HAMILTON, J. H. p 2994 N92-26570
HAMMER, J. H. p 3000 N92-26729
HAMMOND, RUSSELL E. p 2894 N92-26881
HAMNER, RICHARD M. p 2859 N92-26965
HANNINK, N. J. p 2870 N92-26212
HANSON, R. K. p 2872 N92-26281
HANSON, ROBIN p 2988 N92-26894
HARA, V. p 2896 N92-26496
HARARI, ISAAC p 2992 N92-26558
HARDWICKE, KEITH R. p 2991 N92-26772
HARMON, C. D. p 2993 N92-26225
HARRISON, BRIAN H. p 2955 N92-26472
HART, JOAN M. p 2968 N92-27021
HARTEN, T. M. p 2933 N92-26889
HARTMAN, C. W. p 3000 N92-26729
HARTMANN, SVEN R. p 2890 N92-26764
HARTMAYER, R. p 2998 N92-27090
HARUYAMA, YUKIO p 2924 N92-26743
HARVEY, GALE A. p 2998 N92-27095
HASHIM, WAQAR p 2861 N92-26654
HASKELL, MARGARET F. p 2852 N92-26795
HASSON, SCOTT M. p 2956 N92-26538
p 2956 N92-26682
HATTORI, AKIRA p 2958 N92-26957
HAUF, THOMAS p 2940 N92-26336
HAUSERMAN, W. B. p 2875 N92-26724
HAVEY, KEITH p 2998 N92-27096
HAWKINS, GARY J. p 2999 N92-27108
HAWKINS, J. p 2852 N92-26435
HAYAKAWA, JUNJI p 2886 N92-26447
HAYDEN, JEFF p 2862 N92-27135
HAYDEN, S. Z. p 2881 N92-26455
HAZELTINE, R. D. p 3000 N92-26549
HEALY, EDWARD A., JR. p 3008 N92-27171
HEIMANN, DIETER p 2934 N92-26332
HEINBOCKEL, JOHN H. p 2913 N92-26870
HEINEMANN, H. p 2870 N92-26209
HEINONEN, O. J. p 2929 N92-26483
HELD, MANFRED p 2886 N92-26246
HENDEL, B. p 2865 N92-27156
HENDERSON, DIANE p 2948 N92-26173
HENDERSON, MOREY M. p 3013 N92-26767
HENDERSON, R. A. p 2870 N92-26212
HENSHALL, G. A. p 2877 N92-26223
HERMAN, R. G. p 2884 N92-26548
HEUER, R. L. p 2883 N92-27086
HICHWA, BRYANT P. p 2998 N92-27091
HICKEY, JOHN R. p 2927 N92-27101
p 2910 N92-27109
HIENDL, C. O. p 2952 N92-27125
HIISMAEKI, P. p 3002 N92-26321
p 3002 N92-26322
p 3002 N92-26325
HIISMAEKI, P. E. p 3002 N92-26323
p 3002 N92-26326

HILL, D. ..... p 2932 N92-26825
HILL, MELVIN ..... p 2863 N92-27141
HINEMAN, M. F. ..... p 2872 N92-26431
HINKS, D. G. ..... p 3005 N92-26842
HINZPETER, HANS ..... p 2926 N92-26337
HIRAKAWA, SHINJI ..... p 2910 N92-27181
HIRATA, YUTAKA ..... p 2885 N92-26446
HITTERMAN, R. L. ..... p 3005 N92-26842
HOANG, KIET D. ..... p 3009 N92-26863
HODGSON, RANDALL R. ..... p 2998 N92-27093
HOELLER, HARTMUT ..... p 2941 N92-26342
HOFFMAN, D. C. ..... p 2870 N92-26212
HOFFMANN, HANS-EBERHARD . p 2850 N92-26349
HOINKA, KLAUS P. ..... p 2940 N92-26338
HOINKA, KLAUS-PETER ..... p 2939 N92-26329
HOLDEMAN, J. D. ..... p 2854 N92-26553
p 2854 N92-26561
HOLDEN, KRITINA ..... p 2982 N92-26628
HOLLAND, R. C. ..... p 2873 N92-26454
HOLSEN, JAMES N. ..... p 2998 N92-27093
HOLTET, J. A. ..... p 2935 N92-26295
HOLZBACHER-VALERO, A. A. ... p 2978 N92-26199
HOOPER, JANETTE D. ..... p 3011 N92-26378
HOOVER, CLOYES R. ..... p 2909 N92-26794
HOREN, A. S. ..... p 2875 N92-26717
HORNECK, G. ..... p 2952 N92-27126
HORNSBY, LINDA S. ..... p 2859 N92-26965
HORTA, LUCAS G. ..... p 2917 N92-26537
HOSHINO, K. ..... p 2906 N92-26230
HOSTETLER, L. D. ..... p 2891 N92-26902
HOWE, S. D. ..... p 2995 N92-26692
HRASTAR, JOHN ..... p 2922 N92-26702
HSU, S. D. H. ..... p 3019 N92-26385
HUANG, C. K. ..... p 2865 N92-27154
HUANG, F. H. ..... p 2879 N92-26848
HUANG, S. N. ..... p 2918 N92-26694
HUBBARD, C. R. ..... p 3003 N92-26579
HUDISCHEWSKYJ, A. B. ..... p 2931 N92-26793
HUDSON, G. B. ..... p 2873 N92-26454
HUERTH, M. ..... p 2905 N92-27027
HUI, DAVID ..... p 2869 N92-26796
HULTQVIST, BENGT ..... p 2937 N92-26310
HUMMER, LEIGH L. ..... p 2860 N92-27116
HUNNEMAN, ROGER ..... p 2999 N92-27108
HUNT, JAMES J. ..... p 2956 N92-26950
HUNT, L. ROANE ..... p 2905 N92-27193
HUNTER, B. A. ..... p 3005 N92-26842
HURLEY, K. ..... p 3018 N92-27048
p 3016 N92-27049
HURRELL, JAMES W. ..... p 2933 N92-26878
HUSH, D. R. ..... p 2982 N92-26434
p 2891 N92-26902
HUSSAIN, SYED A. ..... p 2891 N92-26941
HUSSAINI, M. Y. ..... p 2905 N92-27032
HUTCHINSON, JOHN J. ..... p 3014 N92-26830
HUTTENBACH, R. C. ..... p 2969 N92-27023

I

IBRAHIM, MOUNIR ..... p 2861 N92-26654
IBRAHIM, MOUNIR B. ..... p 2854 N92-26613
IGALSON, J. ..... p 2906 N92-26391
p 2907 N92-26393
IIDA, TOORU ..... p 2885 N92-26444
IKEUCHI, KATSUSHI ..... p 2981 N92-26357
ILDIZ, FATIH ..... p 2986 N92-26358
IM, EASTWOOD ..... p 2923 N92-26706
INGRAFFEA, A. R. ..... p 2854 N92-26697
INUZUKA, TADAO ..... p 2885 N92-26442
ISAACS, H. S. ..... p 2878 N92-26563
ISHIDA, NORIYASU ..... p 2903 N92-26914
ISHII, SHINYA ..... p 2885 N92-26443
ISHII, YASUO ..... p 2885 N92-26444
ISHIKAWA, KAZUKO ..... p 2886 N92-26447
ISHIKAWA, MASAMICHI ..... p 2885 N92-26442
p 2885 N92-26443
ISHIKURA, SEIZOU ..... p 2885 N92-26443
p 2885 N92-26445
ITO, NOBUTAKE ..... p 2904 N92-26922
IVERSEN, IVER B. ..... p 2938 N92-26315
IWASAKI, YUMI ..... p 2985 N92-27057
IZU, M. ..... p 2926 N92-26190

J

JACKSON, M. C. ..... p 2892 N92-26224
p 2906 N92-26377
JACKSON, T. L. ..... p 2905 N92-27032
JACOBSON, A. K. ..... p 2875 N92-26722
JACOBY, BENEDICTA R. ..... p 2877 N92-26520
JAGER, D. ..... p 2962 N92-26983
JAHANMIR, S. ..... p 2914 N92-26366
JAKOB, RUEDIGER ..... p 2928 N92-26352
JALLICE, DORIS ..... p 2862 N92-27132
JAMES, C. E. ..... p 2997 N92-26452
JAMES, C. R. ..... p 2894 N92-26821
JANSEN, P. ..... p 2951 N92-26977
JASPER, G. L. ..... p 2945 N92-26288
JEFFORDS, RALPH D. ..... p 2976 N92-26766
JELTSCH, R. ..... p 2986 N92-26502
JENKINS, M. G. ..... p 2918 N92-26784
JENKINS, V. T. ..... p 2918 N92-26784
JESSEN, PAUL F. ..... p 2950 N92-27069
JIANG, SIYUAN ..... p 2916 N92-26602
JOCHUM, ANNE M. ..... p 2942 N92-26350
JOCHUM, J. ..... p 2907 N92-26396
JOHANSSON, M. ..... p 2884 N92-26548
JOHNS, STEVEN T. ..... p 2998 N92-26943
JOHNSON, C. J. ..... p 2895 N92-27112
JOHNSON, D. W. ..... p 2858 N92-26884
JOHNSON, ERIC P. ..... p 2867 N92-26383
JOHNSON, GARY ..... p 2975 N92-26530
JOHNSON, J. O. ..... p 3021 N92-26544
JOHNSON, L. J. ..... p 2955 N92-26375
JOHNSON, LAMAR J. ..... p 2955 N92-26494
JOHNSON, LEOPOLD J. ..... p 2894 N92-26881
JOHNSTON, A. R. ..... p 2998 N92-27090
JONES, KEN R. ..... p 2866 N92-27166
JONES, LEON L. ..... p 2884 N92-27085
JONES, R. R., III ..... p 2853 N92-26405
JONES, S. C. ..... p 2910 N92-26269
JONES, STEPHEN H. ..... p 2982 N92-26597
JONES, TREVOR N. ..... p 2948 N92-26360
JORDAN, J. K. ..... p 2996 N92-26376
JORDAN, RACHEL ..... p 2922 N92-26674
JORGENSEN, J. D. ..... p 3005 N92-26842
JUANG, JER-NAN ..... p 2917 N92-26537
JULVE, JAIME ..... p 2940 N92-26339
JUNG, HAN SOO ..... p 2869 N92-26827
JUNGERT, E. ..... p 2921 N92-26513

K

KABRISKY, M. ..... p 2888 N92-26381
KACHER, C. D. ..... p 2870 N92-26212
KACHMAN, NICHOLAS JAMES .. p 2900 N92-26785
KADKHODAYAN, B. ..... p 2870 N92-26212
KAESTNER, MARTINA ..... p 2940 N92-26340
KAGEYAMA, TAROU ..... p 2884 N92-26441
KAILA, K. ..... p 2937 N92-26313
KAISER, E. Q. ..... p 2865 N92-27158
KALEPS, INTS ..... p 2955 N92-26528
KALU, ERIC E. ..... p 2864 N92-27146
KAMBHAMPATI, SUBBARAO ..... p 2983 N92-26789
KAMEI, SHINICHI ..... p 2885 N92-26442
KAMIDE, Y. ..... p 2937 N92-26311
KAMIMURA, KAZUHIDE ..... p 2885 N92-26445
KAMIYAMA, MASAKI ..... p 2885 N92-26446
KAMYKOWSKI, E. ..... p 2883 N92-27086
KANADE, TAKEO ..... p 2851 N92-26427
KANE, L. ..... p 3013 N92-26689
KANEKO, SAYUMI ..... p 2885 N92-26446
KANEVSKY, VALERY ..... p 2961 N92-26980
KANG, SING B. ..... p 2981 N92-26357
KANONCHIK, L. E. ..... p 2859 N92-26968
KARLEMO, T. T. ..... p 3003 N92-26328
KARPPINEN, M. J. ..... p 3003 N92-26328
KARRARI, M. ..... p 2887 N92-26752
KARTTUNEN, S. J. ..... p 2893 N92-26497
KASHIWA, B. A. ..... p 2901 N92-26856
KASHYAP, SATISH ..... p 2889 N92-26592
KASSNER, M. E. ..... p 2877 N92-26223
KATO, KURANOSHIN ..... p 2923 N92-26710
KEARNS, J. R. ..... p 2879 N92-26813
KEDAR, SMADAR ..... p 2983 N92-26789
KELLER, K. ..... p 2858 N92-27013
KELLER, RICHARD M. ..... p 2984 N92-26885
p 2985 N92-27057
KELLEY, D. F. ..... p 2872 N92-26431
KELLMAN, LYLE J. ..... p 2884 N92-26839
KEMMATHER, B. ..... p 2907 N92-26396
KEMP, R. A. ..... p 2908 N92-26517
KENNEDY, LEWIS M. ..... p 2862 N92-27130
KERHO, M. ..... p 2849 N92-26612
KERSEY, ALAN D. ..... p 2998 N92-27186
KESSACI, A. ..... p 2886 N92-26964
KESSELMAN, M. ..... p 2883 N92-27086
KEUNING, S. ..... p 2962 N92-26983
KHORONENKO, V. A. ..... p 2860 N92-27000
KHOROSHKIN, S. M. ..... p 2988 N92-26834
KHRUSTALEV, D. K. ..... p 2859 N92-26968
KIDDER, KENNETH MARK ..... p 3017 N92-26576
KIEMLE, CHRISTIAN ..... p 2941 N92-26347
KIM, DAI-SIK ..... p 2993 N92-26207
KIM, S. K. ..... p 2872 N92-26431
KIM, SANGHO ..... p 2849 N92-26616
KIM, SUC WON ..... p 2954 N92-26186
KING, PETER SAMUEL ..... p 2900 N92-26849
KINGSTON, J. J. ..... p 2891 N92-26205
KINOSHITA, TAKEO ..... p 2924 N92-26715
KINSER, DONALD L. ..... p 2999 N92-27099
KIPPES, ADAM A. ..... p 2945 N92-26364
KIRBY-GALLAGHER, L. M. ..... p 3021 N92-26216
p 3021 N92-26218
KIRCHNER, FRANK ..... p 2953 N92-27012
KIRKPATRICK, THOMAS I. ..... p 2993 N92-27184
KITAEV, A. V. ..... p 2938 N92-26319
KLABUNDE, C. E. ..... p 3005 N92-26843
KLAMERUS, E. J. ..... p 3012 N92-26575
KLEBELSBERG, ANJA ..... p 2942 N92-26350
KLEINERT-ALVARADO, G. ..... p 2959 N92-26963
KLEM, MARK D. ..... p 2861 N92-27036
KLIER, K. ..... p 2884 N92-26548
KLIMEK, ROBERT B. ..... p 2886 N92-26611
KLINGELE, S. ..... p 2966 N92-27006
KNILL, KEVIN JAMES ..... p 2872 N92-26285
KO, J. J. ..... p 3005 N92-26684
KOBAYASHI, YOSHIO ..... p 2885 N92-26445
KOCH, K. R. ..... p 2981 N92-26854
KOCH, M. B. ..... p 2891 N92-27189
KOCH, M. W. ..... p 2891 N92-26902
KODAMA, YOSHIAKI ..... p 2902 N92-26908
KOEN, M. S. ..... p 3009 N92-26523
KOGAN, YEFIM L. ..... p 2945 N92-26474
p 2946 N92-26735
p 2946 N92-26736
KOHAMA, YASUAKI ..... p 2902 N92-26909
KOHLER, R. ..... p 2894 N92-26821
KOJIMA, TEIRYOU ..... p 2885 N92-26446
KOMOLOV, V. V. ..... p 2957 N92-26952
p 2957 N92-26955
KOMORI, MINORU ..... p 2885 N92-26444
KOPNIN, N. B. ..... p 2896 N92-26507
KORHONEN, RIITTA ..... p 2929 N92-26482
p 2929 N92-26483
p 2929 N92-26484
p 2929 N92-26485
p 2929 N92-26486
p 2930 N92-26487
p 2930 N92-26488
KORNREICH, P. G. ..... p 3001 N92-26226
KOROTKOVA, T. K. ..... p 3002 N92-26322
p 3002 N92-26323
KOSS, D. A. ..... p 2879 N92-26939
KOTIL, TEMEL ..... p 2882 N92-26859
KOZAK, M. W. ..... p 2894 N92-26847
KOZU, TOSHIAKI ..... p 2923 N92-26708
KRALL, J. ..... p 2990 N92-26768
KRANTZ, TIMOTHY L. ..... p 2915 N92-26555
KRANZ, A. R. ..... p 2952 N92-27124
KRAUS, H. ..... p 2907 N92-26396
KRAUS, HELMUT ..... p 2939 N92-26333
KREEK, S. A. ..... p 2870 N92-26212
KREMER, PETER ..... p 2968 N92-27018
KRIEBEL, KARL-THEODOR ..... p 2940 N92-26340
KRISHNAMOORTHY, RAJEEV .... p 2977 N92-27053
KRISTIANSEN, E. ..... p 2887 N92-26267
KROEGER, D. M. ..... p 3005 N92-26843
KROL, MARK F. ..... p 2998 N92-26943
KROST, K. J. ..... p 2910 N92-26930
KROTKOV, ERIC P. ..... p 2982 N92-26429
KRUMM, JOHN ..... p 2973 N92-26384
KRUTOV, G. A. ..... p 3003 N92-26327
KRYTER, R. C. ..... p 2913 N92-26234
KUBRUSLY, C. S. ..... p 2988 N92-26831
KUCIAUSKAS, ARUNAS P. ..... p 2926 N92-27070
KUDRYASHEV, V. A. ..... p 3002 N92-26322
p 3002 N92-26323
p 3002 N92-26325
p 3003 N92-26327
KUETTNER, JOACHIM ..... p 2940 N92-26341
KUKKONEN, H. S. ..... p 3002 N92-26323
KULP, T. J. ..... p 2898 N92-26645
KUMAR, S. ..... p 2895 N92-26214
KUNZ, G. J. ..... p 2890 N92-26872
KUO, T. C. ..... p 3001 N92-26226
KUPERMAN, GILBERT G. ..... p 2955 N92-26355
KUPPERMAN, D. S. ..... p 2869 N92-26679
KURIYAMA, YOSHIO ..... p 2885 N92-26444
KVALE, T. J. ..... p 2995 N92-26574
KWON, JOONG HO ..... p 2954 N92-26186
KYRIAKOPOULOS, KANSTANTINOS J. p 2983 N92-26734

L

LABEL, KEN ..... p 2858 N92-26667
LACH, CYNTHIA L. ..... p 2883 N92-27194
LAGACE, PAUL A. ..... p 2852 N92-26655
LAI, SEN-HAO ..... p 2982 N92-26628
LAIRD, PHILIP ..... p 2984 N92-26791
LAM, CHIH-CHAO ..... p 2982 N92-26628
LAMBERTSEN, C. J. ..... p 2952 N92-26263
LAMPERTI, G. ..... p 2973 N92-26421

LANDRETH, R. E. p 2933 N92-26928
LANG, P. M. p 2876 N92-26812
LANGHOFF, STEPHEN R. p 2994 N92-26539
LANGLEY, PAT p 2985 N92-27056
LANIER, J. ROY p 2866 N92-27164
LANTERI, A. p 2859 N92-26970
LARSEN, STEPHEN p 3007 N92-26617
LARSON, E. C. p 3005 N92-26842
LARSON, PAUL A. p 2993 N92-26171
LARTER, NICK p 2969 N92-27023
LASNIER, C. p 2906 N92-26230
LASSEUR, C. p 2961 N92-26981
LASSUS, J. M. p 2966 N92-27006
LAUBER, STEPHEN E. p 2942 N92-26406
LAVAZZA, LUIGI p 3011 N92-26422
LAVITOLA, MARIA STELLA p 2968 N92-27022
LAVOIE, PIERRE p 2892 N92-26244
LAVROV, I. V. p 2956 N92-26951
LAWPHONGPANICH, SIRIPHONG
p 2977 N92-26949
LAZARAKOS, GREGORY A. p 2889 N92-26619
LAZARETH, O. W. p 2857 N92-26818
LE, SHIXIAO p 2913 N92-27050
LEAKE, STEPHEN p 2977 N92-26904
LEBER, R. L. p 3000 N92-26729
LECUYER, P. p 2958 N92-26959
LEDUC, S. K. p 2930 N92-26519
LEE, CHONG OH p 2874 N92-26615
LEE, D. M. p 2870 N92-26212
LEE, J. p 2932 N92-26825
LEE, JU-JANG p 2981 N92-26428
LEE, KYUNG T. p 2992 N92-26688
LEE, MYUNG W. p 2875 N92-26717
LEE, R. L. p 2934 N92-26935
LEE, S. J. p 3005 N92-26684
LEEMANS, R. p 2930 N92-26509
LEFEVRE, VICKI C. p 2852 N92-26408
LEIBFRIED, T. F., JR. p 3009 N92-26552
LEIDINGER, B. J. G. p 2962 N92-26984
LEIFER, A. p 2944 N92-26838
LEONOV, V. A. p 2957 N92-26952
LEROU, R. J. p 2910 N92-26271
LESTER, DEAN M. p 2884 N92-27085
LEVINE, ARLENE S. p 3022 N92-27083
LEVINSON, RICH p 3015 N92-26886
p 2984 N92-27055
LEVITT, LARRY J. p 2945 N92-26409
LEVORSEN, J. L. p 2895 N92-27112
LEWICKI, DAVID G. p 2915 N92-26560
LEWIS, ANN P. p 3013 N92-26767
LEWIS, GARRY W. p 3010 N92-26176
LI, MING-FU p 3001 N92-26204
LI, SHIJIAN p 2874 N92-26526
LIANG, S. H. p 2872 N92-26404
LIBERTO, NICK p 2864 N92-27150
LIM, TAE W. p 2920 N92-26903
LIN, JIN-TONG p 2911 N92-26571
LIND, M. DAVID p 3007 N92-27127
LINDBERG, D. M. p 2999 N92-26256
LITTLE, SALLY A. p 2867 N92-27128
LITTLEFIELD, R. J. p 2979 N92-26277
LIVERANI, STEFANO p 2859 N92-26996
LOCKWOOD, MIKE p 2936 N92-26303
p 2937 N92-26308
p 2938 N92-26316
LOGAN, B. G. p 3000 N92-26729
LOGAN, J. p 2954 N92-26193
LONDSCHIEN, B. p 2880 N92-26945
LONG, GREG S. p 2998 N92-27091
LONG, T. W. p 2912 N92-26646
LONGMAN, RICHARD W. p 2917 N92-26537
LONGSTAFF, T. A. p 2976 N92-26797
LOPEZ, A. R. p 2901 N92-26856
LOPEZ, P. p 2906 N92-26230
LORD, ROBERT J. p 2911 N92-26293
LORENTZEN, RICHARD B. p 2978 N92-26227
LOSHMANOV, A. A. p 3002 N92-26325
LOUIS, PETER D. p 3018 N92-26946
LOUTHAN, M. R., JR. p 2878 N92-26635
LOWERY, JOHN E. p 2867 N92-27168
LOYOLA, DIEGO p 2953 N92-27012
LUCK, C. F. p 2893 N92-26636
p 2893 N92-26637
LUDDEN, P. W. p 2951 N92-26938
LUDEWIG, H. p 2857 N92-26818
LUEHRSEN, RUSSELL P. p 2860 N92-26362
LUNDIN, R. p 2936 N92-26306
LUO, ZHANGAI p 2944 N92-26866
LYNCH, SUSAN K. p 2932 N92-26823

M

MACDONALD, KEN C. p 2949 N92-26411
MACHA, J. M. p 2858 N92-26884
MACHIDA, TSUNEO p 2886 N92-26447
MACIASZEK, T. p 2859 N92-26967
MACK, BRYAN D. p 2943 N92-26753
MACK, J. R. p 2915 N92-26816
MACKEY, RANDALL L. p 2978 N92-27073
MACLEAN, S. C. p 2873 N92-26454
MAEDA, TATSUO p 2902 N92-26911
MAESEN, THEODORUS LUDOVICUS MICHEAL
p 2871 N92-26261
MAFFIOLI, FRANCESCO p 2986 N92-26420
MAHAJAN, S. M. p 2999 N92-26546
MAHAN, G. D. p 3004 N92-26638
MAIDA, JAMES C. p 2956 N92-26538
p 2956 N92-26682
MAIER, M. R. p 2970 N92-26551
MAIN, L. A. p 2955 N92-26472
MALEYEV, S. V. p 3003 N92-26327
MALYSHEV, A. L. p 3003 N92-26327
MANAHAN, MEERA p 2982 N92-26628
MANDIN, C. p 2965 N92-27003
MANDRIOLI, DINO p 2973 N92-26448
MANIKANAHALLY, DHANESHKUMAR NARASIMHAIAH
p 2858 N92-26610
MANKO, O. V. p 2888 N92-26374
MANZO, MICHELLE A. p 2867 N92-27167
MARCHETTI, ANDREA p 2991 N92-26940
MARCUS, STEVEN I. p 2985 N92-27169
MARGALIT, N. p 2865 N92-27151
MARK, JOSEPH F. p 2857 N92-26515
MARR, T. G. p 3011 N92-26453
MARSH, S. p 2856 N92-26720
MARSHALL, ALBERT p 2861 N92-26792
MARSHALL, FRANK P. p 2853 N92-27188
MARTENS, GAIL B. p 3011 N92-26465
MARTIN, C. A. p 2850 N92-26947
MARTIN, R. D. p 2985 N92-26229
MARTIN, R. L. p 2918 N92-26784
MARTINEAU, SERGE p 2892 N92-26244
MARTINEZ, ANTHONY A. p 2947 N92-27075
MARTINEZ, M. J. p 2897 N92-26644
MASARIE, K. A. p 2876 N92-26812
MASON, JAMES B. p 2867 N92-27084
MASSEY, K. C. p 2853 N92-26405
MASULLO, S. p 2963 N92-26990
p 2953 N92-26992
MATACOTTA, F. C. p 3004 N92-26672
MATSUI, TATSUYA p 2903 N92-26914
p 2904 N92-26918
MATSUMOTO, HIROAKI p 2885 N92-26443
MATSUNAGA, P. T. p 2994 N92-26235
MATVEENKOV, I. T. p 2938 N92-26319
MAUL, WILLIAM p 2861 N92-27033
MAX, N. L. p 2975 N92-26647
MAYER, GEORGE p 2880 N92-26275
MAYER, PAULA S. D. p 2975 N92-26587
MAYER, RICHARD J. p 2975 N92-26587
MAZZOLDI, P. p 3005 N92-26826
MCBRIDE, D. D. p 2858 N92-26884
MCCANN, CAROL A. p 3010 N92-27046
MCCARTHY, TIMOTHY G. p 2887 N92-26898
MCCLAIN, CHARLES p 2948 N92-26245
MCCREIGHT, CRAIG p 2906 N92-27104
MCGLAUN, M. p 2900 N92-26853
MCHALE, PAUL F. p 2878 N92-26659
MCINTOSH, ROY p 2906 N92-27104
MCKILLIP, S. T. p 2870 N92-26201
MCQUEEN, H. J. p 2877 N92-26223
MECKING, M. p 2994 N92-26365
MEERKOETTER, RALF p 2940 N92-26340
MEISCHNER, PETER p 2941 N92-26342
MELIOPOULOS, A. P. S. p 2887 N92-26237
MELVIN, R. A. D. p 2958 N92-26961
MENDENHALL, M. H. p 2999 N92-27099
MENDILLO, MICHAEL p 2943 N92-26675
MENENDEZ, V. p 2965 N92-27005
MENIKOFF, R. p 2900 N92-26855
MENN, F. p 2883 N92-27016
MENZEL, CHRISTOPHER P. p 2975 N92-26587
MENZIES, MARGARET A. p 2918 N92-26759
MERCHIE, B. p 2966 N92-27006
MERGEAY, M. p 2951 N92-26977
MESSENGER, A. J. p 2956 N92-26891
MESSIORA, STEVE p 2977 N92-26904
METT, R. R. p 2999 N92-26546
MEYER, CLAUDIA p 2861 N92-27033
MEYER, MARION p 2951 N92-26721
MEYER, R. p 2887 N92-26988
MEYER, WALTER p 2874 N92-26541
MEZENTSEV, A. V. p 2938 N92-26319
MICHELINI, A. p 2935 N92-26239
MIEDZA, B. p 2859 N92-26970
MIKA, FRANK J. p 2888 N92-26388
MIKLICH, A. H. p 2891 N92-26205
MILES, RONALD p 2865 N92-27157
MILES, T. R., JR. p 2932 N92-26810
MILES, T. R., SR. p 2932 N92-26810
MILITELLO, CARMELO p 2987 N92-26624
MILLER, E. A. p 2895 N92-27112
MILLER, LEE p 2866 N92-27159
MILLER, P. J. p 2972 N92-26233
MILLER, WILLIAM H. p 2874 N92-26541
MILMAN, V. p 2988 N92-26788
MIN, J. B. p 2918 N92-26669
MINTON, STEVEN p 2983 N92-26643
MISHCHENKO, A. V. p 2990 N92-26798
MITCHELL, A. W. p 3005 N92-26842
MITCHELL, B. G. p 2948 N92-26245
MITCHELL, EDDIE p 2856 N92-26192
MITCHELL, N. A. p 2855 N92-27041
MIWA, SABUROU p 2958 N92-26957
MIYAMOTO, AKIRA p 2885 N92-26448
MIYAZAKI, YOSHIROU p 2885 N92-26444
MODLIN, JAMES MICHAEL p 3007 N92-26733
MODZELEWSKI, STEPHEN A. p 2852 N92-26896
MOELLER, P. p 2859 N92-26970
MOENG, CHIN-HOH p 2947 N92-26901
p 2905 N92-26934
MOESSBAUER, R. L. p 2907 N92-26393
p 2907 N92-26396
MOIR, R. W. p 3000 N92-26729
MONGIA, H. C. p 2854 N92-26553
MONSERRAT, G. p 2966 N92-27007
MONTBRIAND, L. E. p 2888 N92-26424
MOONEY, THOMAS A. p 2999 N92-27110
MOORE, D. S. p 2876 N92-26867
MOORE, FREDERICK G. p 3003 N92-26433
MOORE, THOMAS J. p 2880 N92-27192
MORATO, S. P. p 2910 N92-26287
MORRIS, S. C. p 2932 N92-26825
MORZENTI, ANGELO p 2973 N92-26448
MOSCATELLI, ANTONIO p 2965 N92-27004
MOSKALENKO, O. P. p 2905 N92-26972
MOSLEMIE, A. p 2975 N92-26500
MOTOHASHI, TATSUO p 2903 N92-26913
p 2903 N92-26916
MOYA, M. M. p 2982 N92-26434
p 2891 N92-26902
MUELLER-REMMERS, P. p 2962 N92-26984
MUELLER-REMMERS, P. L. p 2905 N92-27027
MUELLER, PETER p 2948 N92-26173
MUELLER, R. p 2959 N92-26963
p 2962 N92-26984
MUHS, J. D. p 2996 N92-26376
MUIR, JOHN p 2895 N92-27176
MULKEY, O. R. p 2895 N92-27112
MULLENDORE, JAMES A. p 2876 N92-26172
MUNDINGER, D. p 2911 N92-26504
MURAKAMI, KEIJI p 2885 N92-26442
MURAKAMI, MASATO p 2924 N92-26713
MURATA, KEIJI p 2885 N92-26444
MURATOV, V. G. p 3002 N92-26322
p 3002 N92-26323
MUSSO, GIORGIO p 2964 N92-26993
MUTKA, H. p 3002 N92-26325
MUURINEN, A. p 2929 N92-26483

N

NAGAOKA, SHUNJI p 2885 N92-26445
p 2885 N92-26446
NAGLER, S. E. p 2877 N92-26542
NAKAMURA, KENJI p 2923 N92-26707
NAKAMURA, SHIN p 2886 N92-26447
NAKAO, SHINICHI p 2903 N92-26915
NAKAZAWA, TETSUO p 2924 N92-26714
NAKI, MINORU p 2885 N92-26443
p 2886 N92-26447
NARAYANASWAMI, L. L. p 2871 N92-26262
NATARAJAN, SWAMI p 3009 N92-26552
NAYAK, PANDURANG p 2985 N92-27057
NAYERI, MAJID p 2980 N92-26430
NEAL, D. R. p 2912 N92-26691
NEAL, M. J. p 3005 N92-26843
NEVANLINNA, O. p 2986 N92-26502
NEVEU, D. p 2958 N92-26959
NEWELL, J. p 2852 N92-26435
NGUYEN, THOI K. p 2961 N92-26980
NICHOLS, J. D. p 2926 N92-27195
NICHOLS, R. p 2999 N92-27099
NICHOLSON, H. p 2887 N92-26752
NICINSKI, T. p 2922 N92-26534
NICKEL, H. p 2880 N92-26945
NIELSEN, KJELD FLEMMING p 3007 N92-27127
NILSON, D. p 2906 N92-26230
NISHIOKA, MICHIO p 2904 N92-26919
NITTA, TSUYOSHI p 2924 N92-26712
NIXON, D. A. p 2969 N92-27023
NOBILE, A. p 2870 N92-26217
NOBLE, R. D. p 2873 N92-26508
NODA, A. M. p 2931 N92-26793
NOID, D. W. p 2986 N92-26407
NOORU-MOHAMED, M. B. p 2868 N92-26525

NORMAN, BRET L. ..... p 2952 N92-27122
NORTH, JIM ..... p 3014 N92-26830
NORTHRUP, M. A. ..... p 2898 N92-26645
NOTKIN, DAVID ..... p 2980 N92-26801
NOURRY, GERARD R. ..... p 2973 N92-26292
NOVIKOV, V. M. ..... p 2956 N92-26951
p 2957 N92-26952
NOYES, ROBERT W. ..... p 3019 N92-26247
NOZAR, P. ..... p 3004 N92-26672
NULL, J. M. ..... p 2950 N92-27071

O

OAKLEY, CELIA MARIE ..... p 2915 N92-26731
OBLOW, E. M. ..... p 2987 N92-26545
ODA, T. ..... p 2906 N92-26230
ODAJIMA, K. ..... p 2906 N92-26230
OECHSLE, V. L. ..... p 2854 N92-26553
OGUTI, TAKASI ..... p 2935 N92-26297
OHARA, M. ..... p 2852 N92-26435
OHE, D. J. ..... p 2933 N92-26931
OHERN, T. J. ..... p 2899 N92-26698
OHUCHI, MASATOSHI ..... p 2962 N92-26985
OKAMOTE, KENICHI ..... p 2922 N92-26703
OKUDE, MUNESHIGE ..... p 2903 N92-26914
p 2904 N92-26918
OKUSHI, JUN ..... p 2953 N92-27011
OKUYAMA, TSUNEO ..... p 2885 N92-26445
OLBERT, PHIL ..... p 2862 N92-27134
OLCOTT, JOANNE E. ..... p 2908 N92-26459
OLIVEIRA, HOMERO FERNANDES
p 2979 N92-26417
OLLE, RAYMOND M. ..... p 2883 N92-27100
OLLIVIER, Y. ..... p 2965 N92-27003
p 2965 N92-27005
OLSEN, DOUGLAS R. ..... p 2977 N92-26904
ONEIL, R. ..... p 2925 N92-26748
OOTA, NOBUHIRO ..... p 2885 N92-26442
OOYAMA, MASARU ..... p 2885 N92-26443
p 2885 N92-26445
ORAL, SABRI O. ..... p 2980 N92-26596
ORAM, S. D. ..... p 2969 N92-27023
ORD, R. NEIL ..... p 2884 N92-27085
ORLANDO, R. ..... p 2876 N92-26783
ORTNER, J. ..... p 3000 N92-26806
OSBORNE, MICHAEL J. ..... p 2991 N92-27182
OSHIMA, KOICHI ..... p 2962 N92-26985
OTAGURO, TOSHIO ..... p 2901 N92-26907
OTZINGER, BURTON M. ..... p 2865 N92-27155
OUELLET-HELLSTROM, R. ..... p 2953 N92-26512
OXLEY, M. ..... p 2888 N92-26381

P

PADDEN, R. J. ..... p 2998 N92-27089
PADILLA, E. H. ..... p 2911 N92-26505
PAETIKANGAS, T. J. H. ..... p 2893 N92-26497
PALEVSKY, ALAN ..... p 2893 N92-26771
PANDYA, ABHILASH K. ..... p 2956 N92-26538
p 2956 N92-26682
PAPADIMAS, S. P. ..... p 2928 N92-26354
PAPENBERG, H. ..... p 2905 N92-27027
PARDO, MANUEL ..... p 2851 N92-26415
PARISH, M. V. ..... p 3005 N92-26843
PARKER, JOHN T. ..... p 2974 N92-26458
PARKS, G. S. ..... p 2926 N92-27195
PARRIOTT, GARY R. ..... p 2908 N92-26401
PASTOR, M. ..... p 2966 N92-27007
PAUL, P. G. ..... p 2962 N92-26983
PAULICK, MICHAEL J. ..... p 2886 N92-26611
PAULS, DAVID D. ..... p 2859 N92-27074
PAVLIS, NIKOLAOS KONSTANTINOS
p 2924 N92-26728
PAWLOWSKI, PETER ..... p 2859 N92-26997
PECK, MICHAEL R. ..... p 2942 N92-26406
PEDERSEN, ARNE ..... p 2936 N92-26302
PEERY, J. S. ..... p 2976 N92-26696
PEIO, KAREN J. ..... p 2955 N92-26355
PELLINEN, R. ..... p 2937 N92-26313
PELTONEN, E. K. ..... p 2929 N92-26483
PENKALLA, H. J. ..... p 2880 N92-26945
PERERA, P. A. A. ..... p 2970 N92-26551
PEREZ-DAVIS, MARLA ESTHER ..... p 2860 N92-26601
PERINO, MARIA ANTONIETTA ..... p 2969 N92-27026
PERKINS, CLIFTON E., JR. ..... p 2891 N92-26933
PERKINS, D. H. ..... p 3020 N92-26211
p 3021 N92-26216
p 3021 N92-26218
p 3021 N92-26264
PERKINS, LOUISE ..... p 2974 N92-26464
PEROTTO, ALFRED ..... p 2895 N92-27118
PERRAUT, S. ..... p 2938 N92-26317
PERRY, ARTHUR T. ..... p 2860 N92-27129
PERSSON, J. ..... p 2921 N92-26513
p 2905 N92-26969
PERUSEK, GAIL P. ..... p 2854 N92-26613
PETERS, LEON, JR. ..... p 2892 N92-26280
PETERSEN, D. E. ..... p 2906 N92-26377
PETERSEN, H. ..... p 2860 N92-26999
PETERSON, J. R. ..... p 3006 N92-26851
PETROY, SHELLEY BOUGAN ..... p 2926 N92-26864
PETRUCCI, SERGIO ..... p 2991 N92-26940
PETTY, C. ..... p 2911 N92-26504
PETZOLDT, R. W. ..... p 3000 N92-26729
PEYGHAMBARIAN, N. ..... p 2998 N92-26943
PHAN, MINH Q. ..... p 2917 N92-26537
PHILIPS, ANDREW ..... p 3015 N92-26886
PHILIPS, ANDREW B. ..... p 2982 N92-26627
p 2983 N92-26643
PHILIPS, ANDY ..... p 2984 N92-27055
PHILLIPS, MICHAEL D. ..... p 2987 N92-26755
PHILLIPS, N. E. ..... p 3003 N92-26584
PICKERT, M. ..... p 2952 N92-27124
PIDGEON, A. N. ..... p 2958 N92-26961
PIMENTAL, NANCY A. ..... p 2952 N92-26470
PIMENTEL, B. M. ..... p 2890 N92-26799
PIN, F. G. ..... p 2913 N92-26219
PINELLI, THOMAS E. ..... p 3014 N92-27170
PINNOCK, M. ..... p 2936 N92-26304
PINOTTI, ROBERTO ..... p 2857 N92-27008
p 2968 N92-27022
PINSKI, B. J. ..... p 2957 N92-26952
PIROVANO, A. ..... p 2973 N92-26421
PIVOVAROV, V. G. ..... p 2935 N92-26298
p 2938 N92-26319
PIZZICHINI, G. ..... p 3018 N92-27048
PLANERT, CHRISTINE ..... p 2968 N92-27018
PLAUT, JEFFREY JONATHAN ..... p 3019 N92-26778
POEPPEL, R. B. ..... p 3001 N92-26210
POEYRY, H. ..... p 3002 N92-26322
p 3002 N92-26325
POEYRY, H. O. ..... p 3002 N92-26323
p 3002 N92-26326
POGGIO, T. A. ..... p 2981 N92-26410
POIDOMANI, GAETANO ..... p 2860 N92-26973
POINAS, P. ..... p 2965 N92-27001
POLCRACK, JANE S. ..... p 2971 N92-26195
POLNICKY, F. W. ..... p 2991 N92-26228
POOLE, PAULA M. ..... p 2954 N92-26242
p 2954 N92-26243
PORTER, D. C. ..... p 2895 N92-27112
PORTMAN, KIM ..... p 2970 N92-26439
POST, W. M., III ..... p 2931 N92-26580
POTTER, J. LEITH ..... p 2850 N92-27191
POTYONDY, D. O. ..... p 2854 N92-26697
POWELL, J. R. ..... p 2857 N92-26818
POWERS, J. M. ..... p 3004 N92-26641
POWLEY, JANE FENG ..... p 2931 N92-26590
PRABHU, RAMADAS K. ..... p 2905 N92-27193
PRESTER, M. ..... p 3004 N92-26672
PREUSS, LUDWIG ..... p 2883 N92-27102
PRICE, EDWIN JAMES ..... p 2912 N92-26626
PRIEM, RICHARD J. ..... p 2861 N92-27035
PROEBST, F. ..... p 2906 N92-26391
p 2907 N92-26394
p 2907 N92-26395
PROTASOV, N. N. ..... p 2956 N92-26951
p 2957 N92-26952
p 2957 N92-26955
PUDOVKIN, M. I. ..... p 2937 N92-26312
PUETT, RONNIE D. ..... p 2970 N92-26382
PUIG, OLIVIER ..... p 2863 N92-27137
PULLIAM, R. J. ..... p 2934 N92-26208

Q

QIAN, WEN ..... p 2974 N92-26464
QUATTROCCHI, L. S. ..... p 2879 N92-26939
QUINN, B. J. ..... p 2855 N92-27040
QUINN, JANET ..... p 2881 N92-26283
QUINN, JOHN M. ..... p 2942 N92-26406

R

RABERN, D. A. ..... p 2857 N92-26693
RACHELE, HENRY ..... p 2946 N92-26899
RACINE, JOHN A. ..... p 2862 N92-27065
RADAELLI, P. G. ..... p 3005 N92-26842
RAHMAN, M. A. ..... p 2994 N92-26365
RAM-MOHAN, L. R. ..... p 3005 N92-26763
RAMAMRITHAM, KRITHI ..... p 2976 N92-26685
RAMAN, GANESH GANAPATHI ..... p 2897 N92-26600
RAMP, STEVEN R. ..... p 2950 N92-27069
RANDALL, D. A. ..... p 2944 N92-26937
RANDALL, DAVID A. ..... p 2942 N92-26432
p 2947 N92-26901
p 2905 N92-26934
RANDISI, S. ..... p 2953 N92-26992
RANELLI, PETER HENRY ..... p 2949 N92-26568
RAO, DHANVADA M. ..... p 2849 N92-26651
p 2849 N92-26652
RAO, N. S. V. ..... p 2987 N92-26545
RAPPOPORT, KEVIN J. ..... p 2972 N92-26273
RAPSET, RICHARD ..... p 2914 N92-26389
RASMUSSEN, ROY R. ..... p 2955 N92-26528
RATHJEN, H. ..... p 2960 N92-26975
RATIER, A. ..... p 2925 N92-26746
RAVENSCROFT, D. S. ..... p 2892 N92-26224
RAVIV, D. ..... p 2984 N92-26814
READ, WILLIAM J. ..... p 2851 N92-26291
REARDON, B. J. ..... p 3003 N92-26579
REBNORD, D. A. ..... p 2920 N92-26892
REED, J. W. ..... p 2875 N92-26722
REICHEL, LOTHER ..... p 2988 N92-26900
REILLYN, J. M. ..... p 2931 N92-26633
REINHARDT, F. W. ..... p 2892 N92-26238
REISTER, D. B. ..... p 2913 N92-26219
p 2915 N92-26750
REITZ, G. ..... p 2952 N92-27123
p 2952 N92-27126
RENGER, WOLFGANG ..... p 2940 N92-26340
p 2941 N92-26347
REUSSER, PETER ..... p 2916 N92-26987
REYES, P. ..... p 2993 N92-26225
REYSA, R. ..... p 2957 N92-26953
RIBNER, H. S. ..... p 2905 N92-27032
RICE, B. ..... p 2906 N92-26230
RICH, STEPHEN T. ..... p 2945 N92-26514
RICHARDS, G. A. ..... p 2871 N92-26262
RICHMOND, A. D. ..... p 2937 N92-26311
RICHTER, DEAN A. ..... p 2976 N92-26658
RIEDLER, W. ..... p 2938 N92-26315
RIFERT, V. G. ..... p 2957 N92-26956
RITTER, J. C. ..... p 2916 N92-26282
RIVERS, M. L. ..... p 2878 N92-26563
RIVEST, R. ..... p 2981 N92-26410
ROBERTS, G. P. ..... p 2951 N92-26938
ROBERTS, M. J. ..... p 2908 N92-26569
ROBERTSON, CANDACE J. ..... p 2949 N92-26423
ROBERTSON, J. D. ..... p 2893 N92-26636
ROBERTSON, JAMES B. ..... p 2910 N92-27113
ROBERTSON, M. ..... p 2970 N92-26551
ROBINSON, A. M. ..... p 2894 N92-26821
ROBINSON, DANIEL B. ..... p 2868 N92-26532
RODGER, A. S. ..... p 2936 N92-26301
ROESCH, PATRIC K. ..... p 2893 N92-26606
ROESLER, UWE ..... p 2941 N92-26347
ROETTGER, J. ..... p 2936 N92-26305
ROGERS, BRIAN K. ..... p 2856 N92-26527
ROGERS, PATRICIA G. ..... p 3019 N92-26819
ROGERS, S. ..... p 2888 N92-26381
ROHR, R. ..... p 2962 N92-26984
ROLAND, CHARLES M. ..... p 2883 N92-27187
ROMBOLI, A. ..... p 2973 N92-26421
RON, AMOS ..... p 2989 N92-27175
RONNEY, P. D. ..... p 2914 N92-26371
ROONEY, W. D. ..... p 2883 N92-27086
ROSENBLUTH, M. N. ..... p 2999 N92-26256
ROSENFELD, ALFRED ..... p 2911 N92-26293
ROSENSTEIN, RICHARD M. ..... p 2954 N92-26242
p 2954 N92-26243
ROSENSTOCK, HERBERT B. ..... p 2991 N92-26769
ROSSI, W. ..... p 2910 N92-26287
ROSTON, GERALD P. ..... p 2982 N92-26429
ROTELA, E. ..... p 2909 N92-26572
ROVANG, D. C. ..... p 3000 N92-26695
RUAMSUWAN, LADDAWAN ..... p 3017 N92-26578
RUDDICK, K. ..... p 3021 N92-26253
RUDGYARD, MICHAEL A. ..... p 2897 N92-26599
RUETHER, W. ..... p 2952 N92-27125
RUIZ, C. L. ..... p 2993 N92-26225
RULOFS, A. ..... p 2906 N92-26391
RUOHONIEMI, J. M. ..... p 2936 N92-26304
RUPPERSBERG, GERHARD ..... p 2940 N92-26340
p 2941 N92-26347
RUTLEDGE, SHARON K. ..... p 2883 N92-27100
RYAN, L. E. ..... p 2895 N92-27103
RYBA, MARTIN F. ..... p 3015 N92-26760
RYLYUK, V. M. ..... p 3001 N92-26807

S

SACCHI, ENRICO ..... p 2859 N92-26996
SAIGAL, A. ..... p 2869 N92-26679
SAKOWSKI, BARBARA ..... p 2855 N92-27037
SALA, E. ..... p 2953 N92-26992
SALAMINUCCI, MARCO ANTONIO
p 2854 N92-26586
SALINAS, DAVID ..... p 2894 N92-26897
SALITSKY, GEORGE J. ..... p 3013 N92-26765
SALOMAA, M. M. ..... p 2896 N92-26507
SALOMAA, R. R. E. ..... p 2893 N92-26497
SAMEJIMA, HIROTO ..... p 2885 N92-26443
p 2886 N92-26447

SAMSONOV, N. M. p 2956 N92-26951
p 2957 N92-26952
p 2957 N92-26955
SANBORN, B. A. p 3004 N92-26638
SANCHEZ, A. D. p 2998 N92-27089
SARKAR, S. p 2898 N92-26649
p 2901 N92-26883
SASSEN, CORNELIS LAURENTIUS
p 2871 N92-26257
SATO, HIROSHI p 2901 N92-26907
SATOU, YOUICHIROU p 2885 N92-26442
SATZINGER, JOHN W. p 3013 N92-26776
SAUVAUD, J. A. p 2938 N92-26317
SAVOLAINEN, I. p 2929 N92-26483
p 2929 N92-26484
p 2929 N92-26485
p 2929 N92-26486
SCHAMILOGLU, E. p 3000 N92-26666
SCHEIMAN, DAVID A. p 2927 N92-27101
SCHERTZ, T. L. p 2933 N92-26931
SCHERTZ, W. W. p 2955 N92-26375
SCHERTZ, WILLIAM W. p 2955 N92-26494
SCHIERMEYER, I. p 2987 N92-26737
SCHISANO, A. p 2963 N92-26990
SCHLEICHER, MARCEL p 2905 N92-27045
SCHMIDLAPP, A. p 2993 N92-26225
SCHMIDT, E. p 2857 N92-26818
SCHMIDT, R. p 2938 N92-26316
SCHMIDT, S. C. p 2876 N92-26867
SCHNEIDER, G. E. p 2878 N92-26642
SCHREIBER, JONATHAN K. p 2857 N92-26402
SCHROEDER, J. A. p 2890 N92-26809
SCHROEDER, P. E. p 2930 N92-26510
SCHUBERT, F. p 2880 N92-26945
SCHUDT, KARL p 2852 N92-26435
SCHUERGER, ANDREW C. p 2952 N92-27122
SCHULTE, R. p 2883 N92-27086
SCHUMANN, ULRICH p 2939 N92-26329
p 2934 N92-26334
SCHWARTZ, MICHAEL p 2953 N92-27063
SCHWARZ, B. p 2883 N92-27016
SCHWERING, P. B. W. p 2932 N92-26873
SCHYDLOWER, MANUEL p 2992 N92-26618
SCOTT, C. D. p 2955 N92-26375
SCOTT, CHARLES D. p 2955 N92-26494
SCOTT, T. C. p 2955 N92-26375
SCUDIERE, M. B. p 2996 N92-26376
SEELEY, JOHN S. p 2999 N92-27108
SEIDEL, W. p 2906 N92-26391
p 2907 N92-26394
p 2907 N92-26395
SEIGENTHALER, DANIEL M. p 2868 N92-26386
SELEE, STEVEN R. p 2998 N92-27091
SEN, A. p 2873 N92-26516
SEURIG, R. p 2968 N92-27017
SEWALL, N. R. p 2906 N92-26377
SEXTON, J. D. p 2857 N92-26268
SEXTON, PHILIP p 2956 N92-26665
SHAFER, STEVEN A. p 2973 N92-26384
p 2997 N92-26425
SHAING, K. C. p 3000 N92-26549
SHANG, Q.-Y. p 2874 N92-26608
SHAO, QINGQIU p 2905 N92-26934
SHARMA, S. p 2909 N92-26572
SHCHEBETOV, A. F. p 3002 N92-26322
p 3002 N92-26323
SHELTON, R. O. p 2986 N92-26407
SHEN, D. p 2865 N92-27154
SHEN, SHAOHUA p 2947 N92-26901
SHEPARD, R. L. p 2908 N92-26569
SHIBUKAWA, KIWAO p 2885 N92-26442
SHIBUTANI, SYOZO p 2958 N92-26957
SHIELD, P. D. p 3020 N92-26211
p 3021 N92-26216
p 3021 N92-26218
p 3021 N92-26264
SHIMIZU, MORIO p 2885 N92-26445
p 2885 N92-26446
SHIMSKI, JOHN T. p 2915 N92-26560
SHIN, J. p 2849 N92-26612
SHIN, N. H. p 3005 N92-26684
SHIN, PHILIP Y. p 2894 N92-26897
SHIVELY, DAVID G. p 2889 N92-26653
SHKODA, K. N. p 2905 N92-26972
SHLEIFER, M. p 2909 N92-26572
SHLYAPNIKOV, P. V. p 2995 N92-26800
SHODA, M. p 2914 N92-26371
SHULAR, DAVID p 2906 N92-27107
SHUM, HEUNG-YEUNG p 2981 N92-26356
SIDKO, F. Y. p 2951 N92-26979
SIGURDSSON, STEINN p 3017 N92-26522
SILCOX, R. J. p 2987 N92-26668
SIMMET, GEORG p 2941 N92-26347
SIMON, FREDERICK F. p 2898 N92-26690
SIMONEAU, ROBERT J. p 2898 N92-26690
SIMONS, JACK p 2875 N92-26687
SIMS, J. M. p 2873 N92-26454
SINGH, DILEEP p 2882 N92-26775
SINGHAL, S. C. p 2927 N92-26719
SINJAK, J. E. p 2956 N92-26951
SIPILAE, S. K. p 2893 N92-26497
SITENKO, YU. A. p 2990 N92-26798
SITZMANN, MICHAEL E. p 2884 N92-26880
SKOOG, A. I. p 2965 N92-27002
SLEEFE, G. E. p 2997 N92-26452
SMAJKIEWICZ, ALI p 2999 N92-27110
SMALLEY, R. B., JR. p 2884 N92-27085
SMITH, A. p 2860 N92-27028
SMITH, BARBARA K. p 3014 N92-26830
SMITH, C. E. p 2854 N92-26561
SMITH, D. W. p 2895 N92-27112
SMITH, DONALD S. p 2858 N92-26605
SMITH, ERIC A. p 2944 N92-26185
SMITH, J. R. p 3000 N92-26666
SMITH, JAMES E., JR. p 2908 N92-26536
SMITH, M. F. p 2937 N92-26308
SMITH, R. C. p 2987 N92-26668
SMITH, R. W. p 2935 N92-26296
SMITH, RICHARD W. p 2973 N92-26400
SMITH, ROGER K. p 2940 N92-26335
SMITH, STEPHEN F. p 3008 N92-26426
SNYDER, LAWRENCE p 2979 N92-26359
p 2980 N92-26801
SOHA, G. p 2852 N92-26435
SOLARZ, R. p 2911 N92-26504
SOMMER, MICHAEL p 3016 N92-27049
SOMORJAI, G. A. p 2870 N92-26209
SONNENSCHEIN, MARK F. p 2883 N92-27187
SORIAL, G. A. p 2928 N92-26354
SOVIE, AMY p 2861 N92-27033
SPEAR, STEVE p 2880 N92-27115
SPEAR, W. STEVE p 2916 N92-27114
SPENCER, JAMES R. p 2876 N92-26172
SPETH, T. F. p 2928 N92-26354
SPEZIALE, C. G. p 2901 N92-26883
SPITTLE, ERIC K. p 2955 N92-26528
SPRINGER, R. W. p 2891 N92-26202
SPRINGSTEEN, BETH p 2972 N92-26276
STACY, JOHN L. p 2998 N92-26943
STADLER, R. p 2952 N92-27124
STANDLEE, DAN p 2866 N92-27163
STASTNY, P. p 3004 N92-26672
STAUBER, M. p 2883 N92-27086
STEELE, L. P. p 2876 N92-26812
STEFFENSEN, ROBERT E. p 3012 N92-26469
STEFFES, PAUL G. p 3019 N92-26438
STEINACKER, REINHOLD p 2941 N92-26343
STEPHENS, J. BRISCOE p 2921 N92-26905
STEVENS, D. F. p 3011 N92-26221
STEVENS, WARD C. p 2870 N92-26882
STEVENSON, D. A. p 2881 N92-26543
p 2883 N92-27060
STEVER, R. p 2906 N92-26230
STEVER, R. D. p 2906 N92-26377
STEWART, DORATHY A. p 2945 N92-26409
STEWART, W. p 2953 N92-26512
STILL, G. J. p 2986 N92-26503
STODOLSKY, L. p 2906 N92-26391
p 2907 N92-26397
STOECKENIUS, T. E. p 2931 N92-26793
STOLPER, E. p 2881 N92-26451
STONE, KENNETH R. p 2930 N92-26495
STONESIFER, GREG T. p 2968 N92-27021
STREET, A. B. p 2855 N92-27039
STROHBUSCH, U. p 2994 N92-26365
STROOM, C. p 2958 N92-26959
p 2958 N92-26961
STRUMPF, HAL J. p 2968 N92-27020
STUTZ, JOHN p 2988 N92-26894
STYGAR, W. A. p 2993 N92-26225
STYLIANOPOULOS, ARIS MICHAEL
p 3007 N92-26780
SUGIYAMA, DEAN C. p 3008 N92-27058
SUIDAN, M. T. p 2928 N92-26354
SUJKA, B. R. p 2910 N92-26269
SULEIMAN, A. p 2895 N92-26974
SULLIVAN, DAVID p 2906 N92-27105
p 2862 N92-27131
SUMI, AKIYOSHI p 2923 N92-26709
SUMPTER, B. G. p 2986 N92-26407
SUOLANEN, V. p 2929 N92-26486
SUPPER, W. p 2905 N92-27027
SURAMPUDI, S. p 2865 N92-27154
SURANO, K. A. p 2873 N92-26454
SUTER, B. p 2888 N92-26381
SUTHERLAND, S. C. p 2928 N92-26231
SUTTON, S. R. p 2878 N92-26563
SUZUKI, A. T. p 2890 N92-26799
SUZUKI, KEISUKE p 2885 N92-26446
SUZUKI, TADASHI p 2958 N92-26957
SWANSON, KEITH p 3015 N92-26886
p 2984 N92-27055
SWANSON, KEITH J. p 2982 N92-26627
SWEENEY, E. p 2899 N92-26699
SWEENEY, E. J. p 2899 N92-26700
SWEET, J. A. p 2910 N92-26269
SWINDLE, D. W., JR. p 2875 N92-26726
SWYDEN, T. p 2990 N92-26768
SWYDEN, THOMAS p 2893 N92-26741
SZCZEPINSKI, WOJCIECH p 2914 N92-26284

T

TABAK, M. p 3000 N92-26729
TAKAGISHI, MASAHARU p 2958 N92-26957
TAKAHASHI, H. p 3005 N92-26842
TAKAHASHI, TARO p 2928 N92-26231
TAKAHASHI, Y. p 2957 N92-26954
TAKAOKI, MUNEO p 2885 N92-26445
TAKEDA, N. p 2957 N92-26954
TAKEDA, TAKAO p 2923 N92-26710
TAKHTAMYSHEV, G. G. p 2976 N92-26835
TALJA, J. p 2879 N92-26787
TAM, C. K. p 2853 N92-26405
TAMPONNET, C. p 2961 N92-26981
TAMPONNET, CHRISTIAN p 2951 N92-26978
TAMURA, A. p 3013 N92-26689
TAN, T. H. p 2856 N92-26720
TANAKA, HIROSHI p 2923 N92-26711
TANAKA, K. p 2957 N92-26954
TANAKA, KAZUO p 2985 N92-27057
TANAKA, KIYOSHI p 2886 N92-26447
TANG, CHA-MEI p 2893 N92-26741
p 2990 N92-26768
TANG, CHEN-YAU p 2911 N92-26573
TARTER, BLODWEN p 3012 N92-26481
TASKINEN, P. p 2879 N92-26787
TATE, ATSUSHI p 2902 N92-26912
TAYLOR, E. W. p 2998 N92-27089
TAYLOR, GREGORY BENJAMIN p 3017 N92-26554
TAYLOR, PETER R. p 2994 N92-26539
TAYLOR, W. W. L. p 2895 N92-27103
TENNERY, V. J. p 2918 N92-26784
TESCHE, F. M. p 2887 N92-26237
TEW, ROY C. p 2861 N92-26654
p 2861 N92-27034
THALLER, LAWRENCE H. p 2863 N92-27141
p 2866 N92-27162
THEEUWES, J. p 2953 N92-27047
THEON, JOHN p 2923 N92-26706
THERIAULT, R. p 2978 N92-26199
THOMAS, CHRISTOPHER B. p 2999 N92-26416
THOMAS, DAVID p 3016 N92-26491
THOMPSON, C. E. p 2911 N92-26505
THOMSON, M. A. p 3020 N92-26211
p 3021 N92-26216
p 3021 N92-26218
p 3021 N92-26264
THORNGREN, FRANK R. p 2859 N92-27030
THORNTON, J. P. p 2927 N92-26686
THORPE, CHARLES p 2851 N92-26427
THURSTON, I. p 3012 N92-26575
TIERNEY, J. W. p 2873 N92-26457
p 2883 N92-26547
TIITTA, A. p 3002 N92-26322
TIITTA, A. T. p 3002 N92-26323
p 3002 N92-26326
TILLER, SMITH p 2862 N92-27131
TILLER, SMITH E. p 2906 N92-27105
TILLI, K. J. p 3002 N92-26324
TIMBRELL, J. A. p 2884 N92-26589
TIMMERMAN, PAUL J. p 2862 N92-27133
TIMMERS, G. p 2868 N92-26525
TING, ANTONIO C. p 2893 N92-26741
TINKER, LAWRENCE A. p 2863 N92-27141
TIWARI, S. N. p 2878 N92-26642
TKACHENKO, I. M. p 3000 N92-26806
p 3001 N92-26807
TOBIN, K. W., JR. p 2996 N92-26376
TOBIN, M. T. p 3000 N92-26729
TOLLIN, G. p 2927 N92-26858
TOLSTOJ, V. N. p 2988 N92-26834
TOMAS, A. p 2966 N92-27007
TOMATIS, CARLO p 2968 N92-27022
TOMAZELLI, J. L. p 2890 N92-26799
TOPERVERG, B. P. p 3003 N92-26327
TORCZYNSKI, J. R. p 2912 N92-26691
p 2899 N92-26698
TORKAR, K. M. p 2938 N92-26315
TOSI, MARIA CRISTINA p 2965 N92-27004
TOWNSEND, LAWRENCE W. p 2996 N92-26832
TRASCHEN, JENNIE p 3016 N92-26436
TRAVOR, BRUCE W. p 2853 N92-27188
TRAYNHAM, YVONNE M. p 2869 N92-26796
TROSHICHEV, O. A. p 2936 N92-26300
TROULLIER, NORMAN JOSEPH, JR.
p 3005 N92-26774

TRUBACHEV, I. N. p 2951 N92-26979
TRUMBLE, TERRY M. p 2927 N92-27088
TRUNOV, V. A. p 3002 N92-26322
p 3002 N92-26325
p 3002 N92-26326
p 3003 N92-26327
TRUPIN, ANDREW SETH p 2925 N92-26781
TRUPPI, L. p 2930 N92-26519
TUCKER, D. p 2999 N92-27099
TUERLER, A. p 2870 N92-26212
TUNICK, ARNOLD p 2946 N92-26899
TUPPER, L. M. p 3020 N92-26211
p 3021 N92-26264
TURNER, D. P. p 2930 N92-26509
TURNER, ROSS M. p 2888 N92-26419

U

UGARTE, ALEJANDRO R. p 2991 N92-27078
ULLAKKO, K. M. p 3002 N92-26326
p 3003 N92-26328
ULYANOV, V. A. p 3002 N92-26322
p 3002 N92-26325
p 3002 N92-26326
p 3003 N92-26327
UM, C. I. p 2888 N92-26374
p 3005 N92-26684
UNDERWOOD, J. H. p 2916 N92-26282
UPADHYE, RAVI p 2961 N92-26980
URASA, I. T. p 2871 N92-26236
USAMI, RON p 2885 N92-26445
USOWICZ, THADDEUS W. p 2974 N92-26479
USUI, SHIROU p 2885 N92-26446

V

V.FEILITZSCH, F. p 2907 N92-26393
p 2907 N92-26396
VAETH, R. p 2965 N92-27002
VAINIKAINEN, P. V. p 2909 N92-26786
VAKHRUSHEV, S. B. p 3003 N92-26327
VAKULENKO, M. O. p 3001 N92-26808
VALENTIAN, D. p 2886 N92-26964
VALETTE, F. R. p 2886 N92-26964
VALKIAINEN, M. p 2929 N92-26483
VALLIMONT, JOHN p 2998 N92-27096
VANAGAS, V. p 2988 N92-26837
VANDAM, J. W. p 2999 N92-26256
VANDENBERG, J. p 2993 N92-26225
VANDENBERG, S. p 2852 N92-26435
VANDENBOGERT, PETRUS ANTONIUS JOHANNES p 2916 N92-26259
VANDENHEUVEL, J. p 2988 N92-26817
VANDERPLAS, JACOB p 2892 N92-26260
VANDERSEE, WINFRIED p 2934 N92-26345
VANGENDEREN, ARIE JOHANNES p 2892 N92-26249
VANKOERSEL, A. C. p 2944 N92-26877
VANLUE, D. p 2911 N92-26504
VANMIER, J. G. M. p 2868 N92-26525
VANMILL, J. p 2986 N92-26367
VANOOSTEROM, P. J. M. p 3014 N92-26875
VARIAS, ANDREW GEORGE p 2868 N92-26559
VASILIEV, L. L. p 2859 N92-26968
VAUGHAN, ROBERT G. p 2921 N92-27066
VAUGHN, W. S. p 2956 N92-26665
VECE, THOMAS W. p 2889 N92-26595
VEHAR, D. W. p 2910 N92-26269
VELDMAN, H. J. p 2988 N92-26817
VENABLES, J. D. p 2895 N92-27111
VENKATESWARAN, S. p 2905 N92-27193
VENKATRAMAN, SANTOSH S. p 3012 N92-26567
VERBRAECK, ALEXANDER p 3008 N92-26250
VERGE-DEPRE, K. p 2964 N92-26994
VERNEUIL, J. C. p 2860 N92-27014
VIALANEIX, J. P. p 2860 N92-27014
VIBERTI, CARLO p 2964 N92-26995
p 2969 N92-27025
VIDAS, ROBIN p 2865 N92-27157
VIDIC, R. D. p 2928 N92-26354
VIEIRAJUNIOR, N. D. p 2910 N92-26287
VIGUIER, CHRISTIAN p 2958 N92-26960
VIJLBRIEF, C. p 3014 N92-26875
VISWANATHAN, KRISHNAMURTHY p 2850 N92-27054
VITEK, V. p 2877 N92-26251
VO-DINH, T. p 2875 N92-26726
VOGEL, M. H. p 2889 N92-26511
VOLKERT, HANS p 2941 N92-26344
VOLOVA, T. G. p 2951 N92-26979
VOLZ, RICHARD A. p 2978 N92-26199
VOSS, J. M. p 2926 N92-27195
VOTRUBA, PAUL M. p 2997 N92-26754
VUIGNER, A. A. p 2968 N92-27020
VUORI, SEPPO p 2930 N92-26487

W

WABER, JAMES T. p 3006 N92-27064
WADA, KUNIHISA p 2904 N92-26918
WAGNER, J. L. p 3005 N92-26842
WAITE, JOHN V. p 2977 N92-27052
WALD, K. R. p 2993 N92-26207
WALDROP, RAYMOND S. p 2978 N92-26199
WALEH, AHMAD p 2961 N92-26980
WALKER, D. W. p 3000 N92-26577
WALTERS, R. R. p 2875 N92-26722
WALTERS, R. T. p 2870 N92-26217
p 2875 N92-26718
WANG, F. p 2872 N92-26351
WANG, YUAN RUO p 2868 N92-26564
WANTUCK, P. J. p 2995 N92-26692
WARHOLA, G. p 2888 N92-26381
WARR, G. D. p 3021 N92-26216
WARREN, JOHN p 2861 N92-26792
WATANABE, H. H. p 2995 N92-26692
WATANABE, SATORU p 2885 N92-26446
WATKINS, R. D. p 2896 N92-26506
WAYLAND, ROBERT JAMES p 2942 N92-26489
WEBB, PAUL W. p 2956 N92-26665
WEBER, HARRY C. p 2940 N92-26335
WEGE, KLAUS p 2934 N92-26345
WEI, CHANG-QUAN p 2944 N92-26865
WEIGEND, ANDREAS S. p 2983 N92-26631
WEILAND, T. L. p 2911 N92-26505
WEISS, W. C. p 2892 N92-26224
WELLER, ROBERT A. p 2999 N92-27099
WELLSTOOD, F. C. p 2891 N92-26205
WENDER, I. p 2873 N92-26457
p 2883 N92-26547
WENDLING, PETER p 2940 N92-26340
WERLING, E. p 2860 N92-27014
WERMER, J. R. p 2870 N92-26217
WERNER, P. W. p 3000 N92-26666
WESOLOWSKI, ZBIGNIEW p 2914 N92-26284
WESSELS, W. p 2859 N92-26971
WEST, N. p 3020 N92-26211
p 3021 N92-26264
WEST, STEPHEN G. p 3014 N92-26761
WESTFALL, R. L. p 2910 N92-26269
WESTWATER, E. R. p 2890 N92-26809
WHALEY, K. B. p 2995 N92-26588
WHITAKER, A. p 2999 N92-27099
WHITAKER, ANN F. p 2927 N92-27087
WHITAKER, LYN R. p 2883 N92-26178
WHITE, PAUL p 2916 N92-27038
WHITE, RALPH E. p 2864 N92-27146
WHITELEY, RICHARD V. p 2865 N92-27158
WHITESIDE, J. B. p 2883 N92-27086
WHITT, THOMAS H. p 2866 N92-27164
p 2866 N92-27165
WICKENHEISER, TIMOTHY J. p 2861 N92-26792
WIEDLOCHER, D. E. p 2999 N92-27099
WILHELM, KEVIN T. p 2858 N92-26621
WILKES, DONALD R. p 2860 N92-27116
WILLEKE, HERMANN p 2942 N92-26350
WILLIAMS, ALASTAIR G. p 2941 N92-26346
WILLIAMS, D. D. p 2855 N92-27042
WILLIS, D. M. p 2938 N92-26316
WILLSON, REG G. p 2997 N92-26425
WILSON, C. L. p 2980 N92-26501
WILSON, GARY R. p 2991 N92-26772
WILSON, J. L. p 2971 N92-26189
WILSON, JOHN W. p 2996 N92-26832
WINISDOERFFER, F. p 2963 N92-26989
WINJUM, J. K. p 2930 N92-26510
WINK, R. p 3020 N92-26566
WINN, W. G. p 2874 N92-26632
WINTEMUTE, J. D. p 2911 N92-26505
WISE, J. A. p 2955 N92-26375
WISE, JAMES A. p 2955 N92-26494
WISEMAN, ROBERT S. p 2997 N92-26676
WISNIEWSKI, JOHN W. p 2976 N92-26758
WITT, J. p 2966 N92-27006
p 2968 N92-27017
p 2968 N92-27019
WITT, JOHANNES p 2968 N92-27018
WOCH, J. p 2936 N92-26306
WOERMANN, D. p 2905 N92-27027
WOESTENBURG, M. R. p 3011 N92-26403
WOLF, A. R. p 2899 N92-26699
WOLFS, F. L. H. p 2970 N92-26551
WONG, W. C. p 2895 N92-27103
WOODS, TERRY ORISKA p 2879 N92-26770
WOODS, W. M. p 2989 N92-26177
WOOLFORD, BARBARA J. p 2956 N92-26538
p 2956 N92-26682
WORM, JEFFREY A. p 2972 N92-26198
WU, SIJUN p 2914 N92-26475
WYATT, T. R. p 3012 N92-26575
WYDEVEN, THEODORE p 2961 N92-26980
WYMAN, CHARLES E. p 2955 N92-26494

X

XU, FANGWEN p 3015 N92-27051
XU, MEIZHEN p 2991 N92-26940
XU, YANGSHENG p 2981 N92-26356

Y

YALCINTAS, M. G. p 2875 N92-26726
YAMAMOTO, KIYOSHI p 2904 N92-26920
YAMAMOTO, SHIZUO p 2923 N92-26704
p 2923 N92-26705
YAMAUCHI, M. p 2936 N92-26306
YAMAZAKI, TSUTOMU p 2885 N92-26444
YANG, JAE SEUNG p 2954 N92-26186
YANG, JIACHI p 3015 N92-27051
YANG, Y. p 2879 N92-26787
YAUNG, J. Y. p 2895 N92-27103
YE, HUANCHUN p 3000 N92-26550
YE, PEIJIAN p 3015 N92-27051
YEAGER, E. B. p 2871 N92-26220
YEH, EUENG-NAN p 2948 N92-26245
YEO, INCHEOL p 2918 N92-26598
YEON, K. H. p 2888 N92-26374
YI, THOMAS p 2862 N92-27131
p 2862 N92-27132
YOSHINAGA, TAKASHI p 2902 N92-26912
YOSHITOMI, SUSUMU p 2885 N92-26443
p 2886 N92-26447
YOUNG, CHARLES J., JR. p 2949 N92-26533
YOUNG, LEIGHTON E. p 2927 N92-27087
YOUNIS, MAHMOUD ALY p 2918 N92-26739
YU, P. Y. p 2993 N92-26207
YU, Y. P. p 3001 N92-26204
YUM, SEONG SOO p 2945 N92-26474

Z

ZAGRODNIK, JEFFREY P. p 2866 N92-27166
ZAHARCHUK, G. p 2891 N92-26205
ZAKO, R. L. p 2985 N92-26232
ZAMAR, RUBEN H. p 2985 N92-26229
ZAMAY, S. S. p 2938 N92-26319
ZAZYAN, G. Z. p 3021 N92-26804
ZHANG, TIE-LONG p 3020 N92-26779
ZHAO, WEI p 3009 N92-26552
ZHU, GUOQI p 2869 N92-26861
ZICARI, R. p 2973 N92-26421
ZICARI, ROBERTO p 3011 N92-26422
ZILLY, F. p 2961 N92-26976
ZIMMERMAN, AL H. p 2863 N92-27138
ZIMMERMAN, D. A. p 2971 N92-26189
ZIMMERMAN, R. p 2954 N92-26193
ZIMMERMANN, M. W. p 2952 N92-27124
ZIOLA, STEVEN M. p 2992 N92-26678
ZUHR, R. A. p 2893 N92-26636
ZWEBEN, MONTE p 2984 N92-26887
ZWIENER, JAMES M. p 2860 N92-27116

CORPORATE SOURCE INDEX

Typical Corporate Source Index Listing

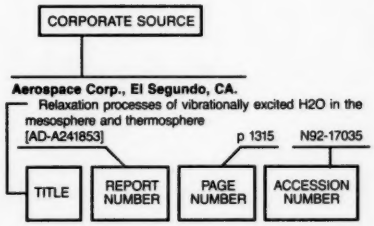

Listings in this index are arranged alphabetically by corporate source. The title of the document provides the user with a brief description of the subject matter. The report number helps to indicate the type of document cited (e.g., NASA report, translation, NASA contractor report). The accession number denotes the number by which the citation is identified. The page number helps you locate the citation in the abstract section. The titles are arranged under each corporate source in ascending accession number order.

A

ACADEMY OF PEDAGOGICAL SCIENCES OF THE USSR, MOSCOW.
Universal R-matrix for quantized (super)algebras
[DE92-621067] p 2988 N92-26834

ACADEMY OF SCIENCES, GRAZ (AUSTRIA).
Balloons for conjugate cusp studies in the 1990's
p 2938 N92-26315

ACADEMY OF SCIENCES OF THE ARMENIAN SSR, ERIVAN.
Interpretation of distributions on K(sub pi)(sup 0) in pFe, nFe, and piFe interactions at 0.5-5.0 TeV in the framework of contemporary models
[DE92-621189] p 3021 N92-26804

ACADEMY OF SCIENCES OF THE UKRAINIAN SSR, KIEV.
Spectral boundary conditions and index theorem for 2-dimensional compact manifold with boundary
[DE92-621115] p 2990 N92-26798
Dynamic properties of quasi-two-dimensional one component plasmas
[DE92-621523] p 3000 N92-26806
Dielectric tensor of strongly coupled plasmas
[DE92-621524] p 3001 N92-26807
Short-wave low-frequency spectra in a current-carrying plasma
[DE92-621529] p 3001 N92-26808

ACADEMY OF SCIENCES (USSR), APATITY.
The Polar Geophysical Institute program of the theoretical and experimental investigation on cusp
p 2935 N92-26298

ACADEMY OF SCIENCES (USSR), KRASNOYARSK.
Chemolithotropic hydrogen-oxidizing bacteria and their possible functions in closed ecological life-support systems p 2951 N92-26979

ACADEMY OF SCIENCES (USSR), LENINGRAD.
Polar cap boundary and structure of dayside cusp as determined by ion precipitation p 2936 N92-26300

ACADEMY OF SCIENCES (USSR), MOSCOW.
Quantum black holes and Hawking's radiation
[PB92-152313] p 3018 N92-26833

ACADEMY OF SCIENCES (USSR), NOVOSIBIRSK.
Mathematical model of physical processes responsible for generation of magnetospheric electric fields and their penetration into the Earth's magnetosphere
p 2938 N92-26319

ADVANCED TECHNOLOGY MATERIALS, INC., DANBURY, CT.
Novel molecular sources for dispersing boron in carbon-carbon composites
[AD-A246999] p 2870 N92-26882

AEROCHEM RESEARCH LABS., INC., PRINCETON, NJ.
Microwave backscattering fuel/air ratio control and flame monitoring device
[PB92-141779] p 2876 N92-26783

AERONAUTICAL RESEARCH LABS., MELBOURNE (AUSTRALIA).
An outline of a numerical scheme for calculating two-dimensional time linearised transonic flow using the Green's function method
[AD-A246349] p 2895 N92-26258
F-111C flight dynamic model aerodynamic data-base development and verification
[AD-A246356] p 2850 N92-26947

AEROSPACE CORP., EL SEGUNDO, CA.
Oxygen recombination in the sealed nickel-cadmium cell p 2863 N92-27138

AEROSPACE CORP., LOS ANGELES, CA.
Exploring possible relationships between plate pore size character and cell performance p 2863 N92-27141
Update of a nickel-hydrogen cycle life model
p 2866 N92-27162

AEROSPACE MEDICAL RESEARCH LABS., BROOKS AFB, TX.
Microcomputer-based instrument flight simulation: Undergraduate pilot training student attitude assessment
[AD-A245449] p 2856 N92-26527
The electronic evaluation of the Advanced Dynamic Anthropomorphic Manikin (ADAM) in high temperature environments
[AD-A245459] p 2955 N92-26528

AEROSPATIALE, CANNES (FRANCE).
Development of fluid loop and hybrid radiators: Test results p 2859 N92-26967
Effects of ultra-vacuum and space environment on contact ohmic resistance: LDEF experiment AO 138-11
p 2895 N92-27118
Microwelding (or cold-welding) of various metallic materials under the ultra-vacuum LDEF experiment AO 138-10 p 2880 N92-27119

AEROSPATIALE, LES MUREAUX (FRANCE).
Human factors in the conception of the Hermes space vehicle p 2963 N92-26989

AIR FORCE ACADEMY, CO.
Testbank (1.0) user's manual
[AD-A245895] p 2971 N92-26196

AIR FORCE INST. OF TECH., WRIGHT-PATTERSON AFB, OH.
Applications of wavelets to signal processing held in Wright-Patterson AFB, Ohio on 20-22 March 1991. Volume 2: Tutorial notes
[AD-A245567] p 2888 N92-26381

AIR FORCE SYSTEMS COMMAND, WRIGHT-PATTERSON AFB, OH.
Laser glittering in the relatively stable propagation layer near the sea surface
[AD-A246374] p 2913 N92-27050
Chinese space technology's spin-offs and applications
[AD-A246375] p 3015 N92-27051

AIRESEARCH MFG. CO., TORRANCE, CA.
Heat rejection system for an advanced extravehicular mobility unit portable life support system
p 2968 N92-27020
Metal oxide absorbents for regenerative carbon dioxide and water vapor removal for advanced portable life support systems p 2968 N92-27021

AKADEMIYA NAUK BSSR, MINSK.
Heat pipe-based radiative panel p 2859 N92-26968

ALABAMA UNIV., HUNTSVILLE.
High temperature furnace modeling and performance verifications
[NASA-CR-190403] p 2908 N92-26536

ALASKA UNIV., FAIRBANKS.
U.S. ground-based space research programs in Svalbard (Norway) p 2935 N92-26296
Plasma dynamics of the Earth magnetopause-boundary layer and its coupling to the polar ionosphere
p 2944 N92-26865
Studies of inertio-gravity waves induced by geostrophic adjustment of the atmospheric jet stream
p 2944 N92-26866

ALBERTA UNIV., EDMONTON.
Numerical modeling of silicon photodiodes for high-accuracy applications with PC-1D
[PB92-148279] p 2894 N92-26821

ALENIA SPAZIO S.P.A., ROME (ITALY).
Italsat thermal control: The in-orbit performances
p 2859 N92-26996

ALENIA SPAZIO S.P.A., TURIN (ITALY).
Thermal design for the space-exposed instruments for the scientific satellite SAX p 2860 N92-26973
CAD system for HFE analyses: Zero-g posture in optimisation of Columbus APM crew workstations
p 2963 N92-26991
Crew support equipment: Identification and definition of additional hardware for Columbus APM laboratory habitability p 2964 N92-26993
EVA space suit thermal control and micrometeoroid protection p 2965 N92-27004
New perspectives of living in space: Habitability guidelines for future manned space systems
p 2968 N92-27022
Moon base habitability aspects p 2969 N92-27026

ALL-UNION RESEARCH INST. OF ELECTROMECHANICS, MOSCOW (USSR).
Flight test results of the passive cooling system
p 2860 N92-27000

AMERICAN SPACE TECHNOLOGY, INC., SANTA MONICA, CA.
Retrievable payload carrier: Next generation Long Duration Exposure Facility p 2860 N92-27129

AMES LAB., IA.
Evaluation of plasma sprayed crucible coatings for melt processing copper-refractory metal alloys
[DE92-008912] p 2878 N92-26727

ARGONNE NATIONAL LAB., IL.
Recent results in characterization of melt-grown and quench-melt-grown YBCO superconductors
[DE92-010281] p 3001 N92-26210
Simultaneous observations of extensive air showers and underground muons at Soudan 2
[DE92-010282] p 3020 N92-26211
Underground muons from the direction of Cygnus X-3 during the January 1991 radio flare
[DE92-010346] p 3021 N92-26215
A search for magnetic monopoles with the Soudan 2 detector
[DE92-010347] p 3021 N92-26216
Muon/electron separation for atmospheric neutrino interactions
[DE92-010349] p 3021 N92-26218
Composition studies based on coincident air shower array and underground muon data
[DE92-010345] p 3021 N92-26253
Underground muons observed in the Soudan 2 detector from the directions of x ray sources
[DE92-010344] p 3021 N92-26264
Magneto-optical multilayers
[DE92-009726] p 2997 N92-26565
Application of neutron diffraction to measure residual strains in high temperature composites
[DE91-014021] p 2869 N92-26679
Evaluation of integral measurements for the SP-100 space reactor
[DE92-009717] p 2996 N92-26841
Structural coherence of the CuO2 planes of oxide superconductors: Is it a requirement for superconductivity?
[DE92-009724] p 3005 N92-26842

ARIZONA STATE UNIV., TEMPE.
Diapycnal mixing, gravity-current propagation, and sediment dispersion in turbulent fluids
[AD-A246160] p 2896 N92-26412
ARIZONA UNIV., TUCSON.
Atmospheric parameters of a soft x ray selected set of hot DA white dwarfs p 3017 N92-26576
Aircraft photovoltaic power-generating system p 2926 N92-26581
Mixed Weibull distributions in reliability engineering: Statistical models for the lifetime of units with multiple modes of failure p 2916 N92-26602
Photochemical energy conversion by membrane-bound photoredox systems
[DE92-008709] p 2927 N92-26858
Large-scale structures and the spatial evolution of wakes behind axisymmetric bluff bodies p 2901 N92-26871
High-speed pulse detection room-temperature optical nonlinearities for GaInAs/A1InAs and GaA1InAs/A1InAs multiple quantum wells and integrated mirror etalon at 1.3 micrometers
[AD-A246369] p 2998 N92-26943
ARMY ARMAMENT RESEARCH, DEVELOPMENT AND ENGINEERING CENTER, WATERVLIET, NY.
Crack arrest and static fracture toughness tests of a ship plate steel
[AD-A245641] p 2916 N92-26282
ARMY COLD REGIONS RESEARCH AND ENGINEERING LAB., HANOVER, NH.
A one-dimensional temperature model for a snow cover: Technical documentation for SNTHERM.89
[AD-A245493] p 2922 N92-26674
Buckling of unidirectional graphite/epoxy composite plates at low temperatures
[AD-A246602] p 2869 N92-26796
ARMY LAB. COMMAND, WHITE SANDS MISSILE RANGE, NM.
On the subject of geometric spacing of meteorological sensors
[AD-A245824] p 2946 N92-26899
ARMY MATERIALS TECHNOLOGY LAB., WATERTOWN, MA.
Slip casting and green body evaluation of 6 percent yttria, 2 percent alumina silicon nitride
[AD-A245817] p 2881 N92-26283
Comparison of ceramic uniaxial compression specimens through detailed finite element modelling
[AD-A245816] p 2882 N92-26609
ARMY MISSILE COMMAND, REDSTONE ARSENAL, AL.
Effect of gyro noise on ADKEM gyro-only missile system performance
[AD-A246150] p 2852 N92-26408
Comparison of wind profiles in close proximity to each other
[AD-A246152] p 2945 N92-26409
ARMY NATICK LABS., MA.
Maintenance manual for Natick's Footwear Database
[AD-A246273] p 2954 N92-26242
User manual for Natick's Footwear Database
[AD-A246275] p 2954 N92-26243
ATOMIC ENERGY RESEARCH INST., DAEDUK (REPUBLIC OF KOREA).
Application of irradiation techniques to food and foodstuffs
[DE92-614952] p 2954 N92-26186
AUBURN UNIV., AL.
Optimization of space structures to minimize dynamic response p 2858 N92-26610
AVIONS MARCEL DASSAULT-BREGUET AVIATION, SAINT-CLOUD (FRANCE).
Genesis and evaluation of an ergonomic architecture for the ESA EVA suit p 2965 N92-27003

B

BALL AEROSPACE SYSTEMS DIV., BOULDER, CO.
The effect of switched array battery charge control on CRRES spacecraft: 3 + month data summary p 2862 N92-27134
BARR ASSOCIATES, INC., WESTFORD, MA.
Transmittance measurements of ultraviolet and visible wavelength filters flown aboard LDEF p 2999 N92-27110
BERTIN ET CIE., PLAISIR (FRANCE).
Integrated communication environment for thermal analysis software p 2958 N92-26959
BIOCLEAR ENVIRONMENTAL BIOTECHNOLOGY, GRONINGEN (NETHERLANDS).
Biodegradation studies with space cabin contaminants to determine the feasibility of Biological Air Filtration (BAF) in space cabins p 2962 N92-26983
BOEING CO., HOUSTON, TX.
Space Station Freedom regenerative water recovery system configuration selection p 2957 N92-26953
BOEING CO., SEATTLE, WA.
LDEF electronic systems: Successes, failures and lessons p 2895 N92-27112
LDEF mechanical systems p 2916 N92-27114
On-orbit coldwelding: Fact or friction? p 2880 N92-27115
BONN UNIV. (GERMANY, F.R.).
Comparison of frontogenetical structures for different cases of frontal development p 2939 N92-26333
BOSTON UNIV., MA.
The effects of magnetic storm phases on F-layer irregularities from auroral to equatorial latitudes
[AD-A245495] p 2943 N92-26675
BRITISH ANTARCTIC SURVEY, CAMBRIDGE (ENGLAND).
Antarctic studies of the cusp p 2936 N92-26301
BROOKHAVEN NATIONAL LAB., UPTON, NY.
Application of in situ x ray absorption and fluorescence measurements to analyze solutions in a simulated pit
[DE92-009159] p 2878 N92-26563
The status of GALLEX
[DE92-010077] p 3020 N92-26566
Design of a high-precision tunable double crystal monochromator
[DE92-010137] p 2909 N92-26572
The application of XPS to the study of MIC
[DE92-010156] p 2879 N92-26813
Open problems and future prospects for hypernuclear physics
[DE92-010158] p 2995 N92-26815
Human round trip to Mars: Six months and radiation safe
[DE92-010160] p 2857 N92-26818
Evaluation of carbon dioxide emission control strategies in New York State
[DE92-010162] p 2932 N92-26825
Lattice instabilities and structural phase transformations in La2CuO4 superconductors and insulators
[DE92-010045] p 3006 N92-27059
BROWN UNIV., PROVIDENCE, RI.
Failure studies of bimaterial interfaces and constrained ductile layers p 2868 N92-26559
BUREAU INTERNATIONAL DES POIDS ET MESURES, SEVRES (FRANCE).
Numerical modeling of silicon photodiodes for high-accuracy applications with PC-1D
[PB92-148279] p 2894 N92-26821

C

CALIFORNIA INST. OF TECH., PASADENA.
Infrared spectroscopy and hydrogen isotope geochemistry of hydrous silicate glasses
[DE92-008398] p 2881 N92-26451
Dynamics of neutron stars and binaries in globular clusters or, menages a trois: Revitalizing burnt out degenerates through partner swapping p 3017 N92-26522
CALIFORNIA UNIV., BERKELEY.
Diagnostic upgrades on MTX
[DE92-009695] p 2908 N92-26230
Quantum dynamics of helium clusters
[AD-A245752] p 2995 N92-26588
Wave viscosity interaction in nonlinear roll motion
[AD-A245756] p 2897 N92-26591
Penetration of laminated composites by projectiles p 2869 N92-26861
CALIFORNIA UNIV., BERKELEY. LAWRENCE BERKELEY LAB.
Spectroscopic imaging, diffraction, and holography with x ray photoemission
[DE92-009142] p 2996 N92-26187
Life sciences and environmental sciences
[DE92-010254] p 2950 N92-26203
Studies of deep level transient spectroscopy of DX centers in GaAlAs: Te under uniaxial stress
[DE92-010258] p 3001 N92-26204
Thin-film high temperature superconducting flux transformers coupled to SQUIDS
[DE92-010260] p 2891 N92-26205
Spatially variant tomographic imaging: Estimation, identification, and optimization
[DE92-010262] p 2921 N92-26206
Generation of nonequilibrium optical phonons in GaAs/AlAs quantum wells by intrasubband and intersubband scatterings
[DE92-010264] p 2993 N92-26207
Imaging earth's interior: Tomographic inversions for mantle P-wave velocity structure
[DE92-010271] p 2934 N92-26208
Conversion of ethane and of propane to higher olefin hydrocarbons
[DE92-009487] p 2870 N92-26209
Gas phase chromatography of halides of elements 104 and 105
[DE92-010284] p 2870 N92-26212
Why first-principles calculations for alloys?
[DE92-010285] p 2877 N92-26213
Fractal characteristics of fracture roughness and aperture data
[DE92-010302] p 2895 N92-26214
Electrocatalysts for oxygen electrodes
[DE92-009491] p 2871 N92-26220
Information technology resources assessment
[DE92-009498] p 3011 N92-26221
Diffraction phenomena in spontaneous and stimulated radiation by relativistic particles in crystals (review)
[DE92-009501] p 3001 N92-26222
Hamiltonian lattice field theory: Computer calculations using variational methods
[DE92-010479] p 2985 N92-26232
Bis (pentamethylcyclopentadienyl) ytterbium: Electron-transfer reactions with organotransition metal complexes
[DE92-010300] p 2994 N92-26235
Fault zone structure determined through the analysis of earthquake arrival times
[DE92-010322] p 2935 N92-26239
Topics in particle physics and cosmology
[DE92-010478] p 3019 N92-26385
The sixteen channel CAMAC constant fraction discriminator for APEX
[DE92-010550] p 2970 N92-26551
Magnetic flux noise in copper oxide superconductors
[DE92-010299] p 3003 N92-26582
The Debye temperature of YBa2Cu3O(7-(delta)) and its dependence on the volume fraction of superconductivity
[DE92-010305] p 3003 N92-26584
A surface science investigation of silicon carbide: Oxidation, crystal growth and surface structural analysis
[DE92-010286] p 3004 N92-26641
CALIFORNIA UNIV., LOS ANGELES.
Time-resolved laser studies on the proton pump mechanism of bacteriorhodopsin
[DE92-003218] p 2951 N92-26493
Evidence for cluster magnetic fields around radio galaxies p 3017 N92-26554
The dynamic response of the westward auroral electrojet and polar cap currents to solar wind-magnetosphere coupling p 2943 N92-26622
Solar wind interaction with Venus and Mars p 3020 N92-26779
CALIFORNIA UNIV., SAN FRANCISCO.
Integrating reverse engineering into Computer-Aided Software Engineering (CASE) p 2974 N92-26479
CALIFORNIA UNIV., SANTA BARBARA.
Quantitative assessment of the slope resolution of seafloor mapping systems
[AD-A246158] p 2949 N92-26411
CAMBRIDGE UNIV. (ENGLAND).
Studies of rain erosion mechanisms in a range of IR transmitting ceramics including coated samples
[AD-A245299] p 2882 N92-26751
CANADA CENTRE FOR REMOTE SENSING, OTTAWA (ONTARIO).
Canadian Earth Observation Program p 2925 N92-26747
Environmental projects at the Canada Centre for Remote Sensing p 2925 N92-26748
CANADIAN FUSION FUELS TECHNOLOGY PROJECT, TORONTO (ONTARIO).
Fusion energy and Canada's role
[DE92-621553] p 2999 N92-26286
CARNEGIE-MELLON UNIV., PITTSBURGH, PA.
Dynamic control of a space robot system with no thrust jets controlled base
[AD-A245711] p 2981 N92-26356
A framework for recognizing grasps
[AD-A245712] p 2981 N92-26357
Shape from periodic texture using the spectrogram
[AD-A245855] p 2973 N92-26384
Dynamic lens compensation for active color imaging and constant magnification focusing
[AD-A245713] p 2997 N92-26425
Knowledge-based production management: Approaches, results, and prospects
[AD-A245714] p 3008 N92-26426
Perception for outdoor navigation
[AD-A245715] p 2851 N92-26427
Hybrid efficient control algorithms for robot manipulators
[AD-A245716] p 2981 N92-26428
Dead reckoning navigation for walking robots
[NASA-CR-190296] p 2982 N92-26429
CASE WESTERN RESERVE UNIV., CLEVELAND, OH.
An experimental study of natural and forced modes in an axisymmetric jet p 2897 N92-
Heat receivers for solar dynamic [illegible] power systems p [illegible] N92-26601

The effect of collection homogeneity on term association as a method of request expansion in information retrieval p 3012 N92-26614

CATALYST RESEARCH CORP., SPARKS, MD.
NASA Li/CF(x) cell problem analysis: Scanning electron microscopy with energy dispersive x ray spectrometry p 2863 N92-27144
NASA Li/CF(x) cell problem analysis: Anion exchange chromatography analysis p 2864 N92-27145
Safety testing of lithium cells p 2864 N92-27150

CENTRAL RESEARCH INST. OF TECH. AND MACHINE BUILDING, MOSCOW (USSR).
The importance of chemical reactions with environment for ablation process of thermal protection and structural materials p 2883 N92-27015

CENTRE D'ETUDE DE L'ENERGIE NUCLEAIRE, MOL (BELGIUM).
Thiocapsa roseopersicina, a bacterium for sulfur-recycling in microbial ecosystems designed for CELSS and space purposes p 2951 N92-26977

CENTRE DE RECHERCHES EN PHYSIQUE DE L'ENVIRONNEMENT, ISSY-LES-MOULINEAUX (FRANCE).
Relationships between ionospheric and tail phenomena p 2938 N92-26317

CENTRE NATIONAL D'ETUDES SPATIALES, PARIS (FRANCE).
French space programmes related to global change p 2925 N92-26746

CENTRE NATIONAL D'ETUDES SPATIALES, TOULOUSE (FRANCE).
Definition of the common structure of data to promote the communication between different thermal software tools p 2958 N92-26960
Feasibility study of an expert system for the design of fusion/solidification experiment boarding on space furnace p 2886 N92-26964
SIGMA VCHP radiator: In-orbit performance p 2859 N92-26966
Development of fluid loop and hybrid radiators: Test results p 2859 N92-26967
SPOT multimission platform thermal control: Five years of in-flight results p 2860 N92-26998
French Cooperative Passive Payload (FRECOPA) p 2867 N92-27117

CENTRE NATIONAL DE LA RECHERCHE SCIENTIFIQUE, MARSEILLES (FRANCE).
Tensor-multi-scalar theories of gravitation [PB92-152305] p 2943 N92-26820

CINCINNATI UNIV., OH.
GAC adsorption of a mixture of natural organic matter and VOCs in the presence and absence of molecular oxygen [PB92-153782] p 2928 N92-26354

CJB DEVELOPMENTS LTD., PORTSMOUTH (ENGLAND).
Critical technologies: Spacecraft habitability, an update p 2966 N92-27010

CLAREMONT GRADUATE SCHOOL, CA.
User interface consistency across end-user application programs: Effect on learning and satisfaction p 3013 N92-26776

COASTAL ENGINEERING RESEARCH CENTER, VICKSBURG, MS.
Hindcast wave information for the Great Lakes: Lake Huron. Wave information studies of US coastlines [AD-A246326] p 2949 N92-26387

COLD SPRING HARBOR LAB., NEW YORK, NY.
A computer system for access to distributed genome mapping data [DE92-008875] p 3011 N92-26453

COLOGNE UNIV. (GERMANY, F.R.).
Imaging the Earth's magnetosphere using ground magnetometer arrays p 2938 N92-26314

COLORADO SCHOOL OF MINES, GOLDEN.
Comparison of one-way wave propagation algorithms in underwater acoustics-error estimates and sensitivity [AD-A245660] p 2991 N92-26175

COLORADO STATE UNIV., FORT COLLINS.
Vibrational dynamics of aniline (N2)1 clusters in their first excited singlet state [AD-A245812] p 2872 N92-26431
Theoretical and modeling studies of the marine planetary boundary layer [AD-A245903] p 2942 N92-26432
Toluene-water clusters: Ion fragmentation and chemistry [AD-A245813] p 2874 N92-26526
Solvation effects on the electronic structure of 4-N,N-Dimethylaminobenzonitrile: Mixing of the local pipi* and charge transfer states [AD-A245814] p 2874 N92-26608
Physical processes within the nocturnal stratus-topped boundary layer, revision [AD-A245829] p 2947 N92-26901
A second-order bulk boundary layer model, revision [AD-A245828] p 2905 N92-26934
Development of an advanced finite-difference atmospheric general circulation model [DE92-010923] p 2944 N92-26937

COLORADO UNIV., BOULDER.
Optical hidden layer network [AD-A246162] p 2992 N92-26413
Nonlinear waves and inverse scattering [AD-A246164] p 2986 N92-26414
Reaction/separation process for enhanced methane conversion [PB92-149657] p 2873 N92-26508
Application of parametrized variational principles in the finite element method p 2987 N92-26624
The effect of global change and long period tides on the Earth's rotation and gravitational potential p 2925 N92-26781
Aerodynamic interference between stores [AD-A247207] p 2850 N92-27172

COLUMBIA UNIV., NEW YORK, NY.
Spontaneous and induced coherent radiation generation in atomic vapors [AD-A246078] p 2890 N92-26764

COMMUNICATIONS RESEARCH CENTRE, OTTAWA (ONTARIO).
An adaptive, packet-switched HF data terminal: Functional overview and initial performance [AD-A246318] p 2973 N92-26292
A comparison of direction finding results from an FFT peak identification technique with those from the music algorithm [AD-A245675] p 2888 N92-26424

COMPAGNIA ITALIANA SERVIZI TECNICI, ROME.
Logistics in space: Tools to support astronauts p 2963 N92-26990
CBT: Role and future application for crew training p 2953 N92-26992

CONSEJO SUPERIOR DE INVESTIGACIONES CIENTIFICAS, MADRID (SPAIN).
Undulatory airflow over the Spanish southern central highplain with northern winds p 2940 N92-26339

CORNELL UNIV., ITHACA, NY.
Paralex: An environment for parallel programming in distributed systems [AD-A245445] p 2979 N92-26278
Run-time support for dynamic load balancing and debugging in paralex [AD-A245446] p 2979 N92-26279
Destruction and excitation of accreted nuclei in neutron star atmospheres: Gamma ray lines and x ray bursts p 3016 N92-26476
Crystalline-amorphous interfaces and their relation to grain boundary films [DE92-009812] p 3004 N92-26648
Tools and techniques for adding fault tolerance to distributed and parallel programs [AD-A245510] p 2980 N92-26677
Algorithms for capacity computations and algebraic cascade coding with applications to data storage p 2977 N92-27053

CORPS OF ENGINEERS, WASHINGTON, DC.
National MAGLEV initiative. Moving America: New directions, new opportunities [PB92-163237] p 2914 N92-26518

CORVALLIS ENVIRONMENTAL RESEARCH LAB., OR.
Global assessment of promising forest management practices for sequestration of carbon [PB92-153006] p 2930 N92-26510

D

DANISH METEOROLOGICAL INST., COPENHAGEN.
Cusp and cleft studies in Greenland p 2935 N92-26299
Solar wind-magnetosphere coupling processes observed near the dayside cusp/cleft p 2937 N92-26307

DARTMOUTH COLL., HANOVER, NH.
Numerical investigation of the circulation of an ice-covered Arctic Ocean p 2949 N92-26568
Operation of a Smith-Purcell free-electron laser at submillimeter wavelengths p 2912 N92-26626
A security analysis of version 2 of the Network Time Protocol (NTP): A report to the privacy and security research group [NASA-CR-190428] p 2981 N92-27183

DEFENCE RESEARCH ESTABLISHMENT, OTTAWA (ONTARIO).
On the design of VLSI circuits for the Winograd Fourier transform algorithm [AD-A246317] p 2892 N92-26244
An evaluation of superresolution methods for tactical radio direction finding [AD-A246316] p 2851 N92-26291
Data fusion and correlation techniques testbed (DFACTT): Field trial 14 January 1991 [AD-A245324] p 3011 N92-26378
Differential Scanning Calorimetry (DSC) for the analysis of activated carbon [AD-A245899] p 2872 N92-26404
A refined maximum likelihood method for tracking low-altitude targets over the sea: Results of simulation and experiments [AD-A246534] p 2888 N92-26419
Static electricity: A literature review [AD-A246533] p 2990 N92-26471
Effect of textile test sample size on assessment of protection to skin from thermal radiation [AD-A246535] p 2955 N92-26472
Analysis of EMP response of structures using frequency domain electromagnetic interaction codes [AD-A245758] p 2889 N92-26592

DEFENSE TECHNICAL INFORMATION CENTER, ALEXANDRIA, VA.
Cataloging guidelines [AD-A246500] p 3011 N92-26465

DELAWARE UNIV., NEWARK.
Analysis and modeling of high-temperature performance of advanced fiber composites p 2868 N92-26564
The impact of climate upon variation in air pollution using a synoptic climatological approach p 2931 N92-26590

DEPARTMENT OF DEFENSE, WASHINGTON, DC.
The Department of Defense critical technologies plan for the Committees on Armed Services, United States Congress [AD-A234900] p 3010 N92-27190

DEPARTMENT OF ENERGY, MORGANTOWN, WV.
A model for aerodynamically-valved pulse combustion [DE92-009887] p 2871 N92-26262

DEPARTMENT OF ENERGY, OAK RIDGE, TN.
DOE new technology [DE92-001619] p 3013 N92-26689

DEPARTMENT OF ENERGY, WASHINGTON, DC.
National MAGLEV initiative. Moving America: New directions, new opportunities [PB92-163237] p 2914 N92-26518
Abstracts of phase 1 awards, 1991 [DE92-010133] p 3022 N92-26640
SOLTECH 1992 proceedings: Solar Process Heat Program, volume 1 [DE92-001238] p 2927 N92-26683
Small business innovation research: Program solicitation closing date, 27 January 1992 [DE92-010132] p 3009 N92-26811

DEPARTMENT OF THE NAVY, WASHINGTON, DC.
Method for implanting impurities in semiconductors and semiconductor implanted with impurities [AD-D015196] p 3003 N92-26433
Optical flow sensor [AD-D015200] p 2997 N92-26862
Liquid level and volume measurement device [AD-D015189] p 2909 N92-26879
High melting aromatic nitrate esters [AD-D015190] p 2884 N92-26880
Main and auxiliary transformer rectifier system for minimizing line harmonics [AD-D015209] p 2894 N92-26881
Binaural ultrasound detector and imager [AD-D015214] p 2993 N92-27184
High lift aircraft [AD-D015215] p 2853 N92-27185
Differential polarimetric fiber optic sensor [AD-D015218] p 2998 N92-27186
Selective metallization of carbonyl-containing polymer films [AD-D015219] p 2883 N92-27187
Pneumatically actuated multiple store launcher [AD-D015237] p 2853 N92-27188

DEPARTMENT OF THE TREASURY, WASHINGTON, DC.
Executive summary of information systems plans: Fiscal years 1993 to 1997 [PB92-158351] p 3011 N92-26368

DESIGN MODELS, INC., LOS ANGELES, CA.
Architectural studies relating to human body motion morphology in microgravity p 2953 N92-27011

DEUTSCHE FORSCHUNGSANSTALT FUER LUFT- UND RAUMFAHRT, COLOGNE (GERMANY, F.R.).
LBNP as countermeasure: An automated scenario p 2953 N92-27012
Preliminary total dose measurements on LDEF p 2952 N92-27123
Long-term exposure of bacterial spores to space p 2952 N92-27126

DEUTSCHE FORSCHUNGSANSTALT FUER LUFT- UND RAUMFAHRT, OBERPFAFFENHOFEN (GERMANY, F.R.).
Contributions to atmospheric physics in honor of Dr. Manfred Reinhardt on his 65th birthday [DLR-FB-91-30] p 2939 N92-26329

Noxious matter transportation in the Alpine regions
p 2934 N92-26332
A simple model for the convective boundary layer over wavy terrain with variable heat flux
p 2934 N92-26334
Aircraft observation of a small-scale solitary wave near the tropopause p 2940 N92-26336
Mesoscale observations of a cold front associated with a prefrontal hailstorm p 2940 N92-26338
Cirrus clouds and condensation trail on 18 Oct. 1989 over the North sea (ICE '89). Determination of height and optical depth using ALEX, AVHRR and HIRS
p 2940 N92-26340
Precipitation formation processes in convective and stratiform clouds as deduced by coordinated polarimetric radar and aircraft measurements p 2941 N92-26342
On the existence of a capital similarity
p 2941 N92-26344
Remote sensing of atmosphere with aircraft borne lidar systems p 2941 N92-26347
The DLR meteorological research aircraft Falcon
p 2941 N92-26348
The icing of the wing upper side and bottom side of the icing research aircraft of the DLR
p 2850 N92-26349
Measurements in the inhomogeneous convective boundary layer using three powered gliders
p 2942 N92-26350

DIAMOND AIR SERVICE, INC. (JAPAN).
Outlines of parabolic flight p 2884 N92-26441

DORNIER SYSTEM G.M.B.H., FRIEDRICHSHAFEN (GERMANY, F.R.).
Thermal control of telescope apertures by optimized baffle heating p 2961 N92-26976
ROSAT: Measured temperatures versus thermal analysis results p 2859 N92-26997
EVA life support design and technology developments
p 2965 N92-27002

DRAEGERWERK A.G., LUEBECK (GERMANY, F.R.).
Investigation on a partial pressure carbon dioxide sensor p 2968 N92-27019

E

EAGLE-PICHER INDUSTRIES, INC., COLORADO SPRINGS, CO.
Super NiCd battery program: History and performance
p 2862 N92-27135

EAGLE-PICHER INDUSTRIES, INC., JOPLIN, MO.
Eutelsat 2: SAR-10009 nickel-hydrogen battery
p 2866 N92-27159
Low cost battery designs for small satellite applications p 2866 N92-27160
Hubble Space Telescope battery background
p 2866 N92-27163

EASTMAN KODAK CO., ROCHESTER, NY.
Effects of long term exposure on optical substrates and coatings (SOO50-2) p 2998 N92-27096

ECOLE NATIONALE SUPERIEURE DE MECANIQUE ET D'AEROTECHNIQUE, POITIERS (FRANCE).
Integrated heat pipe concept for Li/SOCl2 cells cooling p 2895 N92-26974

EG AND G ROCKY FLATS, INC., GOLDEN, CO.
Plume trajectory validation study: Brown cloud support project overview
[DE92-006911] p 2928 N92-26390

EIDGENOESSISCHE TECHNISCHE HOCHSCHULE, ZURICH (SWITZERLAND).
A reformulation of the Eady model
p 2939 N92-26330
Nonexpansive prolongations and difference schemes for the advection equation
[PB92-141530] p 2986 N92-26502

EIDGENOESSISCHES FLUGZEUGWERK, EMMEN (SWITZERLAND).
Separation of external stores: Comparison of results
[F+W-TF-2058] p 2853 N92-26944
Theoretical principles of a Euler method for the calculation of three dimensional flows
[F+W-TF-2012] p 2905 N92-27045

EISCAT SCIENTIFIC ASSOCIATION, KIRUNA (SWEDEN).
Plans for the EISCAT Svalbard (Norway) radar
p 2936 N92-26305

ELORET CORP., SUNNYVALE, CA.
Simulation studies for surfaces and materials strength
[NASA-CR-190340] p 3001 N92-26265

ENERGY AND ENVIRONMENTAL ANALYSIS, INC., ARLINGTON, VA.
Assessment of computer models for estimating vehicle emission factors. Volume 2: Description and comparison of the MOBILE4 and EMFAC7E models
[PB92-113067] p 2932 N92-26803

ENVIRONMENTAL PROTECTION AGENCY, CINCINNATI, OH.
GAC adsorption of a mixture of natural organic matter and VOCs in the presence and absence of molecular oxygen
[PB92-153782] p 2928 N92-26354
Running a conference as a clean product. International Conference on Pollution Prevention: Clean technologies and clean products
[PB92-109099] p 2930 N92-26495
Waste minimization for non-agricultural pesticide applicators: EPA's pollution prevention guide
[PB92-153774] p 2933 N92-26889
Environmental Protection Agency's municipal solid waste landfill liner design criteria
[PB92-153766] p 2933 N92-26928

ENVIRONMENTAL PROTECTION AGENCY, RESEARCH TRIANGLE PARK, NC.
Role of climate in forest monitoring and assessment: A New England example
[PB92-132885] p 2930 N92-26519
Technology for reduction of CO2 emissions from the transportation sector
[PB92-153733] p 2933 N92-26929
Evaluation of the Fourier transform infrared spectrometer for particle-associated ammonium sulfate determination
[PB92-160084] p 2910 N92-26930

ENVIRONMENTAL PROTECTION AGENCY, WASHINGTON, DC.
Determination of rates of reaction in the gas phase in the troposphere. Theory and practice. Part 3: Rate of indirect photoreaction
[PB92-150374] p 2944 N92-26838
Environmental radiation data
[PB92-164706] p 2933 N92-26890

EPPLEY LAB., INC., NEWPORT, RI.
Passive exposure of Earth radiation budget experiment components. LDEF experiment AO-147: Post-flight examinations and tests p 2910 N92-27109

ERNO RAUMFAHRTTECHNIK G.M.B.H. BREMEN (GERMANY, F.R.).
A processing environment for test and simulation data of thermodynamic systems p 2959 N92-26963
Battery thermal control of the Columbus Free Flyer
p 2859 N92-26970
Thermal analysis of the Spacelab mission D2 utility support structure and its payloads p 2859 N92-26971
Development of a thermal control concept for the optical system of the SUMER experiment on SOHO
p 2960 N92-26975
Progress in the development of the Hermes evaporators p 2962 N92-26984
Thermo-hydraulic investigations on heat exchangers for Columbus hybrid radiators p 2887 N92-26988
Lightweight fiber insulations performance and application p 2883 N92-27016
Conjugating binary systems: Advanced cooling liquids for use in spacecraft ATCS p 2905 N92-27027

EUROPEAN SPACE AGENCY, PARIS (FRANCE).
Cluster Dayside Polar Cusp
[ESA-SP-330] p 2935 N92-26294
European Earth Observation Program
p 2925 N92-26745
Fourth European Symposium on Space Environment Control Systems, volume 2
[ESA-SP-324-VOL-2] p 2956 N92-26950

EUROPEAN SPACE AGENCY. CENTRE SPATIAL DE TOULOUSE (FRANCE).
Warm structures and thermal protection of the European spaceplane Hermes p 2860 N92-27014

EUROPEAN SPACE AGENCY. EUROPEAN SPACE RESEARCH AND TECHNOLOGY CENTER, ESTEC, NOORDWIJK (NETHERLANDS).
Lesson learned from GEOS and ISEE
p 2936 N92-26302
The requirements for data exchange between Cluster and ground-based observatories, using EISCAT as an illustrative example p 2938 N92-26316
The liquid droplet radiator: Status of development
p 2905 N92-26969
Higher plant growth in closed environment: Preliminary experiments in life support facility at ESA-ESTEC
p 2951 N92-26978
MELISSA: Physical links of compartments Nitrobacter/Spirulina p 2961 N92-26981
CPA: A controlled pump assembly for two-phase loops applications p 2916 N92-26987
Microgravity simulation p 2964 N92-26994
Engineering of a new overall system to improve the interaction between the crew and the ground-based scientists and personnel p 2964 N92-26995
Thermal implications from the Hubble Space Telescope solar array bi-stem boom in-orbit disturbance
p 2965 N92-27001
Winged launcher thermal design aspects
p 2856 N92-27013
Determination of ventilation requirements for a space suit helmet p 2968 N92-27017
Crew-friendly support systems for internal vehicular activities in zero gravity, experimented underwater for the Columbus programme p 2969 N92-27025
Heatshield concepts for the Rosetta Aerocapsule
p 2860 N92-27028
Evaluation of sodium-nickel chloride cells for space applications p 2865 N92-27156

F

FEDERAL COORDINATING COUNCIL FOR SCIENCE, ENGINEERING AND TECHNOLOGY, WASHINGTON, DC.
Biotechnology for the 21st century, FY 1993
[DE92-007757] p 2951 N92-26850

FEDERAL RAILROAD ADMINISTRATION, WASHINGTON, DC.
National MAGLEV initiative. Moving America: New directions, new opportunities
[PB92-163237] p 2914 N92-26518

FERMI NATIONAL ACCELERATOR LAB., BATAVIA, IL.
Euclidean black hole vortices
[NASA-CR-190117] p 3016 N92-26436
Architecture flow diagrams under Teamwork
[DE92-010482] p 2922 N92-26534

FINNISH METEOROLOGICAL INST., HELSINKI.
Optical ground-based network p 2937 N92-26313

FLINDERS UNIV., ADELAIDE (AUSTRALIA).
The composite structure of thermals as derived from aircraft observations p 2941 N92-26346

FLORIDA ATLANTIC UNIV., BOCA RATON.
Representations in visual motion
[PB92-148287] p 2984 N92-26814

FLORIDA STATE UNIV., TALLAHASSEE.
Surface energy budget and evapotranspiration measurement support
[NASA-CR-190059] p 2944 N92-26185

FLORIDA UNIV., GAINESVILLE.
Compressive damage and fracture modeling of ceramic subjected to high-velocity impact p 2881 N92-26492
Investigation of kinetics of MOCVD systems
[AD-A246090] p 2893 N92-26540
X ray scattering studies of non-equilibrium ordering processes
[DE92-010311] p 2877 N92-26542
Analytical and numerical investigation of nonlinear gravitational clustering p 3017 N92-26578
Finite element modeling of static indentation damage in laminated composites p 2869 N92-26827

FOKKER SPACE AND SYSTEMS, AMSTERDAM (NETHERLANDS).
FIESTA: An integrated approach to thermal model processing p 2958 N92-26958
Ulysses, one year after the launch
p 2860 N92-26999

FORSCHUNGSZENTRUM JUELICH G.M.B.H. (GERMANY, F.R.).
Development of a microstructural-related description for the high temperature stress-strain behaviour of the turbine blade material IN 738 LC
[JUEL-2466] p 2880 N92-26945

FUTURO S.R.L., FLORENCE (ITALY).
Multi-cultural components and keys for European worldwide space programs p 2857 N92-27008

G

GENERAL ACCOUNTING OFFICE, WASHINGTON, DC.
Kennedy Space Center: Decision on photographic requirements appears justified
[GAO/NSIAD-92-192] p 3009 N92-26828

GENERAL ELECTRIC CO., SCHENECTADY, NY.
Microstructural evaluation of as-solidified and heat treated gamma-TiAl based powders
[DE92-008956] p 2881 N92-26455
Advancing natural gas combustion science and technology-low NOx
[PB92-137652] p 2876 N92-26782

GEOLOGICAL SURVEY, RESTON, VA.
Computer Program Estimate Trend (ESTREND): A system for the detection of trends in water-quality data
[PB92-147727] p 2933 N92-26931

GEORGIA INST. OF TECH., ATLANTA.
Magnetohydrodynamic Electromagnetic Pulse (MHD-EMP) interaction with power transmission and distribution systems
[DE92-010365] p 2887 N92-26237

Laboratory evaluation and application of microwave absorption properties under simulated conditions for planetary atmospheres
[NASA-CR-190211] p 3019 N92-26438
Hypersonic aerospace vehicle leading edge cooling using heat pipe, transpiration and film cooling techniques p 3007 N92-26733
An investigation of the mechanical properties and microscopic structure of extruded powder aluminum subjected to biaxial loadings at elevated temperature p 2879 N92-26770
LDEF active optical system components experiment p 2998 N92-27094

GEORGIA TECH RESEARCH INST., ATLANTA.
Acoustic interactions between an altitude test facility and jet engine plumes: Theory and experiments
[NASA-CR-190423] p 2853 N92-26405

GEORGIA UNIV., ATHENS.
COSMIC software catalog, 1992 edition
[NASA-CR-188973] p 2977 N92-26868

GIFU UNIV. (JAPAN).
Experimental studies on the flat plate boundary layer transition using hydrogen bubble method p 2903 N92-26914

GOLDEN GATE COLL., SAN FRANCISCO, CA.
Information liability: New interpretations for the electronic age p 3012 N92-26481

GOSUDARSTVENNYI KOMITET PO ISPOLZOVANIYU ATOMNOI ENERGII, SERPUKHOV (USSR).
New description of multiplicity distribution in inelastic meson-proton interactions
[DE92-621167] p 2995 N92-26800
On increasing the capabilities of the SMART adaptive random number generator
[DE92-621106] p 2976 N92-26835

GRUMMAN AEROSPACE CORP., BETHPAGE, NY.
Effects of the space environment on space-based radar phased-array antenna; status and preliminary observations (LDEF Experiment A0133) p 2883 N92-27086

GTE SYLVANIA, INC., TOWANDA, PA.
Relationship between composition, structure, properties, thermo-mechanical processing and ballistic performance of tungsten heavy alloys
[AD-A245649] p 2876 N92-26172

H

HAMBURG UNIV. (GERMANY, F.R.).
Investigation of convection over sea by aircraft observations p 2926 N92-26337

HAMILTON STANDARD, WINDSOR LOCKS, CT.
Conceptual design study for the use of COBE rocket engines on the Tropical Rainfall Measuring Mission
[NASA-CR-190383] p 2945 N92-26535

HAMPTON UNIV., VA.
The use of ion chromatography-dc plasma atomic emission spectrometry for the speciation of trace metals
[DE92-010317] p 2871 N92-26236

HAWAII UNIV., HONOLULU.
Proceedings of 6th Hawaiian Winter Workshop on Dynamics of Oceanic Internal Gravity Waves
[AD-A245650] p 2948 N92-26173

HELSINKI UNIV. OF TECHNOLOGY, ESPOO (FINLAND).
Numerical solution of plastic liquids shape factor
[PB92-133958] p 2896 N92-26496
High frequency Raman current drive
[PB92-142223] p 2893 N92-26497
Automated interpretation of S-invariants of predicate/transition nets: An application of non-classical logics
[PB92-143544] p 2975 N92-26500
Nonexpansive prolongations and difference schemes for the advection equation
[PB92-141530] p 2986 N92-26502
Mutual friction in superfluid He-3: Effects of bound states in the vortex core
[PB92-142231] p 2896 N92-26507
Measurement electronics of industrial microwave resonator sensors
[PB92-152750] p 2909 N92-26786
Spheroidization and densification of Nickel powders by RF-induction plasma
[PB92-151893] p 2879 N92-26787

HIGH TECHNOLOGY CORP., HAMPTON, VA.
Distributed acoustic receptivity in laminar flow control configurations
[NASA-CR-4438] p 2898 N92-26680
Boundary-layer receptivity due to distributed surface imperfections of a deterministic or random nature
[NASA-CR-4439] p 2898 N92-26681

HUGHES AIRCRAFT CO., TORRANCE, CA.
Hughes advanced nickel-cadmium batteries: An update p 2862 N92-27136

I

ILLINOIS INST. OF TECH., CHICAGO.
Computation of hydrodynamics using kinetic theory
[DE92-009079] p 2896 N92-26456

ILLINOIS UNIV., CHICAGO.
Adaptive control of robotic manipulators with structural flexibility p 2914 N92-26475

ILLINOIS UNIV., URBANA-CHAMPAIGN.
A self-contamination model for the formation of globular star clusters p 3018 N92-26723
The galactic evolution of s-process elements via asymptotic giant branch stars p 3018 N92-26725

INDIANA UNIV., BLOOMINGTON.
The carbon isotopic compositions of individual compounds from ancient and modern depositional environments p 2921 N92-26478

INFERENCE CORP., EL SEGUNDO, CA.
Advanced software development workstation. Engineering scripting language graphical editor: DRAFT design document
[NASA-CR-190393] p 2971 N92-26181
Advanced software development workstation. Engineering scripting language graphical editor: DRAFT code documentation
[NASA-CR-190389] p 2971 N92-26182
Advanced software development workstation project: Engineering scripting language. Graphical editor
[NASA-CR-190391] p 2971 N92-26183

INNSBRUCK UNIV. (AUSTRIA).
The objective determination of front lines p 2941 N92-26343

INSTITUT DES HAUTES ETUDES SCIENTIFIQUES, BURES-SUR-YVETTE (FRANCE).
Dvoretzky's theorem: 30 years later
[PB92-153212] p 2988 N92-26788
Non-compact WZW conformal field theories
[PB92-125038] p 3007 N92-26805
Tensor-multi-scalar theories of gravitation
[PB92-152305] p 2943 N92-26820
Quantum black holes and Hawking's radiation
[PB92-152313] p 3018 N92-26833

INSTITUTE FOR COMPUTER APPLICATIONS IN SCIENCE AND ENGINEERING, HAMPTON, VA.
Systematic study of Reynolds stress closure models in the computations of plane channel flows
[NASA-CR-189646] p 2898 N92-26649
The modeling and control of acoustic/structure interaction problems via piezoceramic actuators: 2-D numerical examples
[NASA-CR-189639] p 2987 N92-26668
On testing models for the pressure-strain correlation of turbulence using direct simulations
[NASA-CR-189638] p 2901 N92-26883
Shock-turbulence interactions in a reacting flow
[NASA-CR-189647] p 2905 N92-27032

INSTITUTE FOR DEFENSE ANALYSES, ALEXANDRIA, VA.
The state of multiple sensor, multiple target tracking in ballistic missile defense
[AD-A245433] p 2850 N92-26272
Assessments of selected real-time computing technologies
[AD-A245434] p 2972 N92-26273
Advanced materials aspects of concurrent engineering
[AD-A245437] p 2880 N92-26275
Software maturity model applied to SDI
[AD-A245439] p 2972 N92-26276

INSTITUTE FOR NAVAL OCEANOGRAPHY, BAY SAINT LOUIS, MS.
The utility of acoustic travel times in locating the north wall of the Gulf Stream
[AD-A246219] p 2949 N92-26463
Software requirements document for the netCDF interface within ECMOP, version 1.0
[AD-A246220] p 2974 N92-26464

INSTITUTE FOR PERCEPTION RVO-TNO, SOESTERBERG (NETHERLANDS).
Building a GIS on top of the open DBMS Postgres
[FEL-91-B183] p 3014 N92-26875
Human cognitive processes in command and control planning. 3: Determining basic processes involved in planning in time and space
[IZF-1991-B-11] p 3010 N92-27046
Selective search for the target properties color and form
[IZF-1991-B-13] p 2953 N92-27047

INSTITUTE OF FLOW RESEARCH (JAPAN).
Pattern search in turbulent field p 2901 N92-26907

INSTITUTE OF SOUND AND VIBRATION RESEARCH, SOUTHAMPTON (ENGLAND).
Design guide for saddle seating on small high-speed craft
[ISVR-TR-205] p 2956 N92-26891

INSTITUTO DE FISICA TEORICA, SAO PAULO (BRAZIL).
Vacuum polarization tensor in 3-dimensional quantum electrodynamics
[DE92-621141] p 2890 N92-26799
On the evaluation of the U(3) content of the matrix elements of 1- and 2-body operators
[DE92-621113] p 2988 N92-26837

INSTITUTO DE PESQUISAS ENERGETICAS E NUCLEARES, SAO PAULO (BRAZIL).
Optimization of a color center Q-switched Nd:YLF laser
[DE92-621612] p 2910 N92-26287

INSTITUTO DE PESQUISAS ESPACIAIS, SAO JOSE DOS CAMPOS (BRAZIL).
Differentiation on genus of aquatic macrophytes through remote sensing in the Tucurui Reservoir, Para State, Brazil
[INPE-5315-PRE/1712] p 2951 N92-26721

INSTITUTO POLITECNICO NACIONAL, MEXICO CITY.
Numerical solution of the equation of neutrons transport on plane geometry by analytical schemes using acceleration by synthetic diffusion
[DE92-621426] p 2995 N92-26844

INSTITUUT TNO VOOR BOUWMATERIALEN EN BOUWCONSTRUCTIES, DELFT (NETHERLANDS).
Experimental study of shear fracture and aggregate interlock in cementbased composites
[PB92-151521] p 2868 N92-26525

INSTRUMENTS SERVICE AERODYNAMIQUE, LONGJUMEAU (FRANCE).
Ruled and holographic diffraction gratings experiment (AO 138-5) p 2910 N92-27092

INTERFACIAL SCIENCES, INC., SANTA CLARA, CA.
Low temperature electrochemical activation of methane
[PB92-152917] p 2872 N92-26351

INTERNATIONAL CENTRE FOR THEORETICAL PHYSICS, TRIESTE (ITALY).
Li-6,d reaction on sd-, fp- and g-shell nuclei in ZR- and FR-DWBA formalisms
[DE92-614353] p 2994 N92-26365
Percolation effects in the V-I characteristics of granular YBa2Cu3O(7-delta)
[DE92-617541] p 3004 N92-26672

INTERNATIONAL COUNCIL OF SCIENTIFIC UNIONS, STOCKHOLM (SWEDEN).
PAGES. Past global changes project: Proposed implementation plans for research activities
[IGBP-REPT-19-ATTACH-10] p 2934 N92-27082

INTERNATIONAL FLAME RESEARCH FOUNDATION, IJMUIDEN (NETHERLANDS).
Fuel staging and its implementation in a novel internally staged burner
[ETN-92-91307] p 2872 N92-26285

INTERSPEC, INC., AMBLER, PA.
Large coherent arrays for laser radars, phase 1
[AD-A245528] p 2912 N92-26663

IOWA UNIV., IOWA CITY.
Synthesis of novel fluorinated phosphonic acid electrolytes for phosphoric acid fuel cells
[PB92-164300] p 2926 N92-26372

J

JAPAN METEOROLOGICAL AGENCY, TOKYO.
Utilization of tropical convection data for meteorological operation
[TW-11] p 2924 N92-26712

JAPAN SYSTEMS CORP., KAWASAKI.
Thermal analysis of evaporative coolers p 2962 N92-26985

JET PROPULSION LAB., CALIFORNIA INST. OF TECH., PASADENA.
LDEF fiber optic exposure experiment No. S-0109 p 2998 N92-27090
Magellan battery operations: An overview p 2862 N92-27133
A constant current charge technique for low Earth orbit life testing p 2863 N92-27139
Chemical evaluation of non-woven nylon separators used in Ni/Cd cells p 2863 N92-27140
Cycle life characteristics of Li-TiS2 cells p 2865 N92-27154
A feasibility study: California Department of Forestry and Fire Protection utilization of infrared technologies for wildland fire suppression and management
[NASA-CR-190458] p 2926 N92-27195

JOHANN-WOLFGANG-GOETHE-UNIV., FRANKFURT AM MAIN (GERMANY, F.R.).
Total Dose Effects (TDE) of heavy ionizing radiation in fungus spores and plant seeds: Preliminary investigations p 2952 N92-27124

JOHN DEERE TECHNOLOGIES INTERNATIONAL, INC., WOOD-RIDGE, NJ.
Development of natural gas rotary engines
[PB92-149665] p 2915 N92-26816
JOHNS HOPKINS UNIV., BALTIMORE, MD.
Adverse reproductive events and electromagnetic radiation
[PB92-145796] p 2953 N92-26512
JOHNS HOPKINS UNIV., LAUREL, MD.
Cusp studies with HF radars p 2936 N92-26304
JOHNSON CONTROLS, INC., MILWAUKEE, WI.
Utilization of a bipolar lead acid battery for the advanced launch system p 2865 N92-27157
Multiple cell CPV nickel-hydrogen battery p 2866 N92-27166

K

KARLSRUHE UNIV. (GERMANY, F.R.).
The transpirator, an efficient and light evaporative cooler for space technology p 2887 N92-26986
KIEV POLYTECHNIC (USSR).
The centrifugal mass exchange apparatus in air-conditioning system of isolated, inhabited object and its work control p 2957 N92-26956
Passive thermostate system with application of gas-filled heat pipes and thermal energy of solar radiation p 2905 N92-26972

L

LABORATORIO DE COMPUTACAO CIENTIFICA, RIO DE JANEIRO (BRAZIL).
Lyapunov equation for infinite-dimensional discrete bilinear systems
[DE92-621066] p 2988 N92-26831
LAMONT-DOHERTY GEOLOGICAL INST., PALISADES, NY.
Investigation of carbon dioxide in the South Atlantic and northern Weddell Sea areas (WOCE Sections A-12 and A-21) during the METEOR expedition 11/5, January - March 1990
[DE92-010027] p 2928 N92-26231
LAWRENCE LIVERMORE NATIONAL LAB., CA.
Dynamic restoration mechanisms in Al-5.8 at. percent Mg deformed to large strains in the solute drag regime
[DE92-009529] p 2877 N92-26223
Transportable 5 MW power supply system for gyrotron operation
[DE92-009051] p 2892 N92-26224
Implementing error values in applicative languages
[DE92-008927] p 2972 N92-26233
Geochemical constraints on ocean general circulation models
[DE92-010805] p 2948 N92-26270
Installation and operation of the 400 kW 140 GHz gyrotron on the MTX experiment
[DE92-009053] p 2906 N92-26377
Helium-3 mass spectrometry for low-level tritium analysis of environmental samples
[DE92-008937] p 2873 N92-26454
Diode pumped 275 watt average power Nd:YAG slab laser
[DE92-008604] p 2911 N92-26504
Fail safe system for suppressing stimulated Brillouin scattering in large optics on the Nova laser
[DE92-008608] p 2911 N92-26505
Application of fluorescent-particle imaging to measuring flow in complex media
[DE92-009121] p 2898 N92-26645
Application of decentralized control to a laser alignment system
[DE92-009692] p 2912 N92-26646
Scientific documentary animation: How much accuracy is enough?
[DE92-009698] p 2975 N92-26647
Inertial fusion energy power plant design using the Compact Torus Accelerator: HYLIFE-CT
[DE92-008941] p 3000 N92-26729
An electroplater's view of PVD processing
[DE92-009052] p 2878 N92-26732
Forging a path with tool and data attributes
[DE92-009800] p 2976 N92-26797
A finite element/finite difference approach for modeling three-dimensional flow and pollutant dispersion around structures
[DE92-007322] p 2934 N92-26935
Ensuring mass conversion in a heavy-gas dispersion model using the generalized anelastic equations
[DE92-007323] p 2934 N92-26936
LEHIGH UNIV., BETHLEHEM, PA.
High octane ethers from synthesis gas-derived alcohols
[DE92-010480] p 2884 N92-26548
LENINGRAD NUCLEAR PHYSICS INST. (USSR).
The high resolution diffractometer mini-Sfinks p 3002 N92-26322
Determination of the structure of Y(HCOO)3 by the neutron time-of-flight diffraction method p 3002 N92-26325
Anomalous structural behaviour of the high-temperature superconducting compound La(1.8)Sr(0.2)CuO(4-y) p 3003 N92-26327
LENINGRAD STATE UNIV. (USSR).
A model of the dayside magnetosphere and breakups in the cusp region p 2937 N92-26312
LOCKHEED MISSILES AND SPACE CO., SUNNYVALE, CA.
MILSTAR's flexible substrate solar array: Lessons learned, addendum
[NASA-CP-3147-ADD] p 2927 N92-26895
LOGICON, INC., DAYTON, OH.
Man-machine interface analyses for bomber flight management system
[AD-A245707] p 2955 N92-26355
LOGISTICS MANAGEMENT INST., BETHESDA, MD.
DoD implementation guidelines for Electronic Data Interchange (EDI), volume 2
[AD-A246614] p 3013 N92-26767
LONDON UNIV. (ENGLAND).
Study of hydrazine metabolism and toxicity
[AD-A245755] p 2884 N92-26589
LOS ALAMOS NATIONAL LAB., NM.
Photocathode transfer and storage techniques using alkali vapor feedback control
[DE92-008449] p 2891 N92-26202
Multiquanta photodetachment from the H(-) ion
[DE92-010306] p 2911 N92-26573
Assessment of a hot hydrogen nuclear propulsion fuel test facility
[DE92-004571] p 2995 N92-26692
Numerical simulations of gun-launched kinetic energy projectiles subjected to asymmetric projectile base pressure
[DE92-005065] p 2857 N92-26693
An explosively driven, fast shock tube
[DE92-008437] p 2856 N92-26720
Solution of the first-order form of the 3-D discrete ordinates equations on a massively parallel machine
[DE92-004575] p 2981 N92-26854
Wave structure in one and two dimensional fluid flow
[DE92-007421] p 2900 N92-26855
Numerical simulation of two-dimensional single- and multiple-material flow fields
[DE92-007428] p 2901 N92-26856
Induced cycle structures of the hyperoctahedral group
[DE92-007570] p 3006 N92-26857
Vibrational spectroscopy in shock-compressed liquids
[DE92-007713] p 2876 N92-26867

M

MANTECH ENVIRONMENTAL TECHNOLOGY, INC., CORVALLIS, OR.
Equilibrium-analysis of projected climate change effects on the global soil organic matter pool
[PB92-153022] p 2930 N92-26509
MARBURG UNIV. (GERMANY, F.R.).
Preliminary results of the Artemia salina experiments in biostack on LDEF p 2952 N92-27125
MARTIN MARIETTA CORP., ORLANDO, FL.
Conquest of darkness by management of the stars
[AD-A245496] p 2997 N92-26676
MARTIN MARIETTA LABS., BALTIMORE, MD.
Radiation sensitivity of quartz crystal oscillators experiment for the Long Duration Exposure Facility (LDEF) p 2895 N92-27111
MARYLAND UNIV., COLLEGE PARK.
Finite temperature quantum field theory in curved spacetime p 3007 N92-26780
MASSACHUSETTS INST. OF TECH., CAMBRIDGE.
A computational analysis of properties and limitations of neural networks: Toward new parallel architectures for learning
[AD-A246156] p 2981 N92-26410
Fundamental mechanisms affecting friction welding under vacuum
[AD-A245685] p 2877 N92-26520
Algorithms for blending surface generation
[AD-A245686] p 2975 N92-26524
Composite fuselage technology (summary of year 2)
[NASA-CR-190434] p 2852 N92-26655
Passive water hammer in pipes due to flashing
[DE92-004180] p 2899 N92-26699
Water hammer due to the sudden stopping of a flashing flow
[DE92-004181] p 2899 N92-26700
MASSACHUSETTS UNIV., AMHERST.
The 8th IEEE Workshop on Real-Time Operating Systems
[AD-A246126] p 2976 N92-26685
MATRA ESPACE, PARIS-VELIZY (FRANCE).
Modelling light transfer inside photobiofermentors: Applications to the photosynthetic compartments of CELSS p 2952 N92-26982
MATRA SERVICE AERODYNAMIQUE, VELIZY-VILLACOUBLAY (FRANCE).
Vacuum deposited optical coatings experiment p 2999 N92-27097
MAX-PLANCK-INST. FUER AERONOMIE, KATLENBURG-LINDAU (GERMANY, F.R.).
Development of a thermal control concept for the optical system of the SUMER experiment on SOHO p 2960 N92-26975
MAX-PLANCK-INST. FUER PHYSIK UND ASTROPHYSIK, GARCHING (GERMANY, F.R.).
Cryogenic detector development
[MPI-PHE/91-07] p 2906 N92-26391
X ray observations of gamma ray burst sources
[MPE-PREPRINT-174] p 3018 N92-27048
The HUS solar flare and cosmic gamma ray burst detector aboard the Ulysses spacecraft
[MPE-PREPRINT-175] p 3016 N92-27049
MAX-PLANCK-INST. FUER PHYSIK UND ASTROPHYSIK, MUNICH (GERMANY, F.R.).
Cryogenic calorimeters for dark matter and neutrinos p 2907 N92-26392
Recent progress in calorimeters with transition edge thermometers p 2907 N92-26394
Signal-to-noise ratio expected for a calorimeter with transition edge thermometer p 2907 N92-26395
Electron-phonon decoupling and superconducting grains p 2907 N92-26397
Silicon drift chambers with integrated amplifiers as low energy detectors p 2908 N92-26398
An anisotropic homologous model for the core-collapse in star clusters
[ETN-92-90826] p 3018 N92-26946
MCDONNELL AIRCRAFT CO., SAINT LOUIS, MO.
Early risk reduction phase 1 FLIR/laser designator window
[AD-A246352] p 2911 N92-26293
MCDONNELL-DOUGLAS ELECTRONICS CO., SAINT LOUIS, MO.
Post-flight characterization of optical system samples, thermal control samples, and detectors from LDEF experiment M0003, sub-experiments 6 and 13 p 2998 N92-27093
Results from the LDEF/A0076 cascaded variable conductance heatpipe experiment p 2906 N92-27106
MEIJO UNIV., NAGOYA (JAPAN).
Vortex structure in wake of a circular cylinder p 2904 N92-26918
MEMPHIS STATE UNIV., TN.
Decomposition of bipartite graphs under degree constraints
[PB92-148626] p 2988 N92-26817
MESSERSCHMITT-BOELKOW-BLOHM G.M.B.H., SCHROBENHAUSEN (GERMANY, F.R.).
Spinning jets from shaped charges with flow turned liners
[MBB-UA-1197-90-PUB] p 2886 N92-26246
MESSERSCHMITT-BOELKOW G.M.B.H., MUNICH (GERMANY, F.R.).
Evaluation of LDEF experiment S1002 p 2883 N92-27102
METEOROLOGICAL RESEARCH INST., TSUKUBA (JAPAN).
TRMM and Asian monsoon
[TW-12] p 2924 N92-26713
Research plan for utilizing TRMM data in MRI
[TW-13] p 2924 N92-26714
METEOROLOGISCHES OBSERVATORIUM, HOHENPEISSENBERG (GERMANY, F.R.).
Ozone trends p 2934 N92-26345
MICHIGAN STATE UNIV., EAST LANSING.
Theoretical issues in adaptive Set-Membership-Based signal processing.
[AD-A245721] p 2980 N92-26430
MICHIGAN TECHNOLOGICAL UNIV., HOUGHTON.
Effect of interstitials on the trapping of hydrogen in iron-single crystals
[AD-A246412] p 3006 N92-27064
MICHIGAN UNIV., ANN ARBOR.
Energy transfer properties and mechanisms
[DE92-011215] p 2994 N92-26240
Computations of nonlinear gravity waves by a desingularized boundary integral method p 2942 N92-26583
Theoretical and numerical study of flame propagation and transition to detonation p 2874 N92-26615
An instrument for engine torque estimation and misfire detection p 2909 N92-26738

Fine scale structure of conserved scalar mixing in turbulent shear flows: Sc much greater than 1 and Sc approximately equal to 1 p 2899 N92-26740

Polycyclic aromatic hydrocarbon radiative properties and formation in carbon-rich stellar outflows p 3018 N92-26757

The interaction of a vortex ring with a contaminated free surface p 2900 N92-26785

Ceramic composites: Experimental and analytical study of SiC/Si3N4 composites p 2882 N92-26859

MIDWEST RESEARCH INST., CARY, NC.

Summary of NOx control technologies and their availability and extent of application
[PB92-158260] p 2928 N92-26373

MIDWEST RESEARCH INST., GOLDEN, CO.

Photovoltaic manufacturing technology, phase 1
[DE92-001199] p 2926 N92-26190

SOLTECH 1992 proceedings: Solar Process Heat Program, volume 1
[DE92-001238] p 2927 N92-26683

The effect of sandstorms on PV arrays and components
[DE92-001240] p 2927 N92-26686

Environmental implications of increased biomass energy use
[DE92-001219] p 2932 N92-26810

MINISTRY OF POSTS AND TELECOMMUNICATIONS, TOKYO (JAPAN).

Status of TRMM project: Rain radar in the Tropical Rainfall Measuring Mission
[TW-2] p 2922 N92-26703

Storm model and beam filling problem for rain retrievals
[TW-6] p 2923 N92-26707

Development of TRMM radar rainfall retrieval algorithms
[TW-7] p 2923 N92-26708

MINNESOTA UNIV., MINNEAPOLIS.

Supersymmetry and dark matter, a new candidate p 3016 N92-26491

Computational aspects of an implicit finite element procedure for elasto-viscoplastic large deformation problems p 2917 N92-26594

A study of buckminsterfullerene using new pseudopotentials p 3005 N92-26774

MISSISSIPPI UNIV., UNIVERSITY.

Theoretical and experimental study of thermoacoustic engines
[AD-A246334] p 2914 N92-26389

MO-SCI CORP., ROLLA, MO.

Survey of small business use of intellectual property protection
[PB92-151703] p 3009 N92-26523

N

NAGOYA UNIV. (JAPAN).

Water cycles around the subtropical frontal zone in East Asia
[TW-9] p 2923 N92-26710

Rainfall pattern over the tropical rain forest
[TW-10] p 2923 N92-26711

NAGOYA UNIV., TOYOKAWA (JAPAN).

Research programmes at Svalbard (Norway) p 2935 N92-26297

NASA SPACE STATION PROGRAM OFFICE, RESTON, VA.

The role of the Long Duration Exposure Facility in the development of space systems p 2867 N92-27128

NATIONAL ACADEMY OF SCIENCES - NATIONAL RESEARCH COUNCIL, WASHINGTON, DC.

Workshop on Solar Activity, Solar Wind, Terrestrial Effects, and Solar Acceleration
[NASA-CR-190195] p 3020 N92-26437

NATIONAL AERONAUTICS AND SPACE ADMINISTRATION, WASHINGTON, DC.

Space life sciences strategic plan, 1991
[NASA-TM-107856] p 2950 N92-26266

Tropical Rainfall Measuring Mission (TRMM) science report
[TW-5] p 2923 N92-26706

Distribution of proposed Earth probes and other related missions p 2925 N92-26744

Aerospace medicine and biology: A continuing bibliography with indexes (supplement 362)
[NASA-SP-7011(362)] p 2953 N92-27068

Management: A bibliography for NASA managers
[NASA-SP-7500(26)] p 3010 N92-27080

NASA patent abstracts bibliography: A continuing bibliography. Section 2: Indexes (supplement 40)
[NASA-SP-7039(40)-SECT-2] p 3014 N92-27081

NATIONAL AERONAUTICS AND SPACE ADMINISTRATION. AMES RESEARCH CENTER, MOFFETT FIELD, CA.

The computation of C-C and N-N bond dissociation energies for singly, doubly, and triply bonded systems
[NASA-CR-190254] p 2994 N92-26539

A design rationale for NASA TileWorld
[NASA-TM-107882] p 2982 N92-26627

Principal investigator in a box: Version 1.2 documentation
[NASA-TM-107886] p 2982 N92-26628

Introduction in IND and recursive partitioning
[NASA-TM-107879] p 2983 N92-26629

Computer modeling of human decision making
[NASA-TM-107868] p 2983 N92-26630

Two papers on feed-forward networks
[NASA-TM-107840] p 2983 N92-26631

An analysis of commitment strategies in planning: The details
[NASA-TM-107881] p 2983 N92-26643

Explanation-based generalization of partially ordered plans
[NASA-TM-107869] p 2983 N92-26789

Planning and scheduling research at NASA Ames Research Center
[NASA-TM-107888] p 3009 N92-26790

Discrete sequence prediction and its applications
[NASA-TM-107865] p 2984 N92-26791

Applying knowledge compilation techniques to model-based reasoning
[NASA-TM-107876] p 2984 N92-26885

Applying artificial intelligence to the control of space telescopes (extended abstract)
[NASA-TM-107913] p 3015 N92-26886

The 1990 progress report and future plans
[NASA-TM-107911] p 2984 N92-26887

MoCog1: A computer simulation of recognition-primed human decision making
[NASA-TM-107872] p 2984 N92-26888

Modelling default and likelihood reasoning as probabilistic
[NASA-TM-107889] p 2984 N92-26893

Bayesian classification theory
[NASA-TM-107885] p 2988 N92-26894

Impact of diet on the design of waste processors in CELSS p 2961 N92-26980

The APT/ERE planning and scheduling manifesto
[NASA-TM-107906] p 2984 N92-27055

The structure and formation of natural categories
[NASA-TM-107896] p 2985 N92-27056

Model compilation: An approach to automated model derivation
[NASA-TM-107895] p 2985 N92-27057

NATIONAL AERONAUTICS AND SPACE ADMINISTRATION. GODDARD SPACE FLIGHT CENTER, GREENBELT, MD.

Handbook of solar-terrestrial data systems, version 1
[NASA-TM-107810] p 3019 N92-26191

The ionospheric signature of flux transfer events p 2937 N92-26308

Analysis of Yttrium-Barium-Copper-Oxide by x ray diffraction and mechanical characterization
[NASA-TM-104562] p 2869 N92-26650

Small Explorer Data System MIL-STD-1773 fiber optic bus
[NASA-TP-3227] p 2858 N92-26667

The Tropical Rainfall Measuring Mission (TRMM) program at the Goddard Space Flight Center (GSFC)
[TW-1] p 2922 N92-26702

Research and technology, 1990: Goddard Space Flight Center
[NASA-TM-107792] p 3022 N92-26824

Software architecture for a distributed real-time system in Ada, with application to telerobotics
[NASA-TM-4367] p 2977 N92-26904

Systems special investigation group overview p 2867 N92-27084

Long Duration Exposure Facility (LDEF) low temperature heat pipe experiment package (HEPP) flight results p 2906 N92-27104

Long Duration Exposure Facility (LDEF) low-temperature heat pipe experiment package power system results p 2906 N92-27105

COBE battery overview: History, handling, and performance p 2862 N92-27131

End-of-life evaluation of the solar maximum mission batteries p 2862 N92-27132

NATIONAL AERONAUTICS AND SPACE ADMINISTRATION. LYNDON B. JOHNSON SPACE CENTER, HOUSTON, TX.

Neural network error correction for solving coupled ordinary differential equations
[NASA-TM-101796] p 2986 N92-26407

The validation of a human force model to predict dynamic forces resulting from multi-joint motions
[NASA-TP-3206] p 2956 N92-26538

Correlation and prediction of dynamic human isolated joint strength from lean body mass
[NASA-TP-3207] p 2956 N92-26682

NASA, Johnson Space Center primary battery applications p 2863 N92-27142

Calorimetric determination of the thermoneutral potential for Li/BrCl in SOCl2 (BCX) cells p 2864 N92-27146

Zinc-oxygen battery development program p 2865 N92-27152

NATIONAL AERONAUTICS AND SPACE ADMINISTRATION. LANGLEY RESEARCH CENTER, HAMPTON, VA.

Identification of linear systems by an asymptotically stable observer
[NASA-TP-3164] p 2917 N92-26537

Analysis of surface wave propagation in a grounded dielectric slab covered by a resistive sheet
[NASA-TM-107583] p 2889 N92-26653

Quasi-elastic nuclear scattering at high energies
[NASA-TM-4362] p 2996 N92-26832

Structural dynamic interaction with solar tracking control for evolutionary Space Station concepts
[NASA-TM-107629] p 2920 N92-26903

LDEF: 69 Months in Space. First Post-Retrieval Symposium, part 3
[NASA-CP-3134-PT-3] p 3022 N92-27083

Effects of long-duration exposure on optical system components p 2998 N92-27095

Effect of space exposure of pyroelectric infrared detectors p 2910 N92-27113

NASA/DoD Aerospace Knowledge Diffusion Research Project: An initial investigation into the production and use of Scientific and Technical Information (STI) at 5 NASA centers. Results of a telephone survey
[NASA-TM-104173] p 3014 N92-27170

Modeling 3-D objects with planar surfaces for prediction of electromagnetic scattering
[NASA-TM-107598] p 2891 N92-27189

Computational method to predict thermodynamic, transport, and flow properties for the modified Langley 8-foot high-temperature tunnel
[NASA-TM-4374] p 2905 N92-27193

Effect of temperature and gap opening rate on the resiliency of candidate solid rocket booster O-ring materials
[NASA-TP-3226] p 2883 N92-27194

NATIONAL AERONAUTICS AND SPACE ADMINISTRATION. LEWIS RESEARCH CENTER, CLEVELAND, OH.

A parametric numerical study of mixing in a cylindrical duct
[NASA-TM-105695] p 2854 N92-26553

Gear tooth stress measurements of two helicopter planetary stages
[NASA-TM-105651] p 2915 N92-26555

Full-scale transmission testing to evaluate advanced lubricants
[NASA-TM-105668] p 2915 N92-26560

CFD mixing analysis of jets injected from straight and slanted slots into confined crossflow in rectangular ducts
[NASA-TM-105699] p 2854 N92-26561

Color image processing and object tracking workstation
[NASA-TM-105561] p 2886 N92-26611

Helium bubble flow visualization of the spanwise separation on a NACA 0012 with simulated glaze ice
[NASA-TM-105742] p 2849 N92-26612

Use of an approximate similarity principle for the thermal scaling of a full-scale thrust augmenting ejector
[NASA-TM-105724] p 2854 N92-26613

Heat transfer in oscillating flows with sudden change in cross section
[NASA-TM-105692] p 2861 N92-26654

Progress in the development of lightweight nickel electrode
[NASA-TM-105638] p 2875 N92-26670

Computational techniques in tribology and material science at the atomic level
[NASA-TM-105573] p 2990 N92-26671

Progress towards understanding and predicting convection heat transfer in the turbine gas path
[NASA-TM-105674] p 2898 N92-26690

NASA/DOE/DOD nuclear propulsion technology planning: Summary of FY 1991 interagency panel results
[NASA-TM-105703] p 2861 N92-26792

Rocket engine diagnostics using qualitative modeling techniques
[NASA-TM-105714] p 2861 N92-27033

Overview of NASA supported Stirling thermodynamic loss research
[NASA-TM-105690] p 2861 N92-27034

The 3D rocket combustor acoustics model
[NASA-TM-105734] p 2861 N92-27035

Effect of model selection on combustor performance and stability predictions using ROCCID
[NASA-TM-105750] p 2861 N92-27036

Interface of an uncoupled boundary layer algorithm with an inviscid core flow algorithm for unsteady supersonic engine inlets
[NASA-TM-105684] p 2855 N92-27037
Durability evaluation of photovoltaic blanket materials exposed on LDEF tray S1003 p 2883 N92-27100
Advanced photovoltaic experiment, S0014: Preliminary flight results and post-flight findings p 2927 N92-27101
The evaluation of layered separators for nickel-hydrogen cells p 2866 N92-27161
Results of a technical analysis of the Hubble Space Telescope nickel-cadmium and nickel-hydrogen batteries p 2867 N92-27167
Post-test examination of a pool boiler receiver
[NASA-TM-105635] p 2880 N92-27192
Institute for Computational Mechanics in Propulsion (ICOMP)
[NASA-TM-105612] p 2989 N92-27196
Microgravity combustion science: Progress, plans, and opportunities
[NASA-TM-105410] p 2886 N92-27197

NATIONAL AERONAUTICS AND SPACE ADMINISTRATION. MARSHALL SPACE FLIGHT CENTER, HUNTSVILLE, AL.
Report for neutral buoyancy simulations of transfer orbit stage contingency extravehicular activities
[NASA-TM-103583] p 2857 N92-26268
Atmospheric environment for Space Shuttle Columbia (STS-40) launch
[NASA-TM-103585] p 2945 N92-26288
Effect of type of load on stress analysis of thin-walled ducts
[NASA-TP-3248] p 2918 N92-26669
Functional requirements document for NASA/MSFC Earth Science and Applications Division: Data and information system (ESAD-DIS). Interoperability, 1992
[NASA-TM-4388] p 2921 N92-26905
An overview of the first results on the solar array materials passive LDEF experiment (sample), A0171 p 2927 N92-27087
Contamination of optical surfaces in Earth orbit p 2999 N92-27099
Transverse flat plate heat pipe experiment p 2906 N92-27107
Thermal control surfaces experiment flight system performance p 2860 N92-27116
The 1990 NASA Aerospace Battery Workshop
[NASA-CP-3119] p 2862 N92-27130
Life testing of secondary Ag-Zn cells p 2865 N92-27153
Hubble Space Telescope NiH2 six battery test p 2866 N92-27164
Hubble Space Telescope nickel-hydrogen flight spare battery test p 2866 N92-27165
Nickel-hydrogen LEO cycling at 20 percent - 50 percent DOD p 2867 N92-27168

NATIONAL AEROSPACE LAB., TOKYO (JAPAN).
Proceedings of the 5th and 6th Seminars on Investigation and Control of Boundary-Layer Transition
[NAL-SP-12] p 2901 N92-26906
Coning motion and flat spinning of slender bodies at high angles of attack p 2902 N92-26912
Numerical simulation of the laminar turbulent transition in a stratified flow p 2904 N92-26920
Cross-flow instabilities and pressure gradients in boundary layers p 2904 N92-26922

NATIONAL CENTER FOR ATMOSPHERIC RESEARCH, BOULDER, CO.
Ground-based studies of sensing magnetosphere/ionosphere interactions: Convection and substorms p 2937 N92-26311
Convection wave studies over land and sea p 2940 N92-26341
Description of a global shallow water model based on the spectral transform method
[PB92-155258] p 2928 N92-26352
Monthly mean global satellite data sets available in CCM history tape format
[NASA-CR-190344] p 2933 N92-26878

NATIONAL INST. OF STANDARDS AND TECHNOLOGY, GAITHERSBURG, MD.
Ceramic bearing technology: Proceedings of the NIST/DARPA Workshop
[PB92-137553] p 2914 N92-26366
Reference model for frameworks of software engineering environments
[PB92-158328] p 2973 N92-26370
Massively parallel implementation of character recognition systems
[PB92-149863] p 2980 N92-26501
Representations in visual motion
[PB92-148287] p 2984 N92-26814
Numerical modeling of silicon photodiodes for high-accuracy applications with PC-1D
[PB92-148279] p 2894 N92-26821

NATIONAL METEOROLOGICAL CENTER, WASHINGTON, DC.
Climate research at regional climate centers in 1991
[PB92-160399] p 2946 N92-26822

NATIONAL OCEANIC AND ATMOSPHERIC ADMINISTRATION, BOULDER, CO.
User's guide to WPL microwave radiative transfer software
[PB92-129931] p 2890 N92-26809
Rule-based expert system for evaluating the quality of long-term, in-situ, gas chromatographic measurements of atmospheric methane
[PB92-128560] p 2876 N92-26812

NATIONAL PHYSICAL LAB., TEDDINGTON (ENGLAND).
Improving CMM software quality
[NPL-DITC-194/92] p 2974 N92-26450

NATIONAL RESEARCH COUNCIL, BANGKOK (THAILAND).
MOS-1 activity report p 2925 N92-26749

NATIONAL RESEARCH INST. FOR EARTH SCIENCE AND DISASTER PREVENTION, IBARAKI (JAPAN).
Research program on hydrology
[TW-14] p 2924 N92-26715

NATIONAL RESEARCH LAB. OF METROLOGY, TOKYO (JAPAN).
Application of riblet surface to pipe flow p 2903 N92-26915

NATIONAL SPACE DEVELOPMENT AGENCY, IBARAKI (JAPAN).
Micro-gravity experiment of vapor/liquid reorientation induced by capillary force p 2885 N92-26444

NATIONAL SPACE DEVELOPMENT AGENCY, TOKYO (JAPAN).
Parabolic flight: Reports of microgravity experiments by aircraft, volume 1, no. 2
[EG-910045] p 2884 N92-26440
Preliminary experiment of GDEF (Gas Dynamics Experiment Facility) p 2885 N92-26442
Parabolic flight experiments on bubble migration under reduced gravity p 2885 N92-26443
Liquid motion analysis with lateral impacts under low gravity p 2885 N92-26445
Biomedical data acquisition and processing technology p 2885 N92-26446
The experiment under microgravity by aircraft: The experiment in floating by gas flow p 2886 N92-26447
International Conference on Japanese Earth Observation Programs: TRMM Workshop
[JTN-92-80345] p 2922 N92-26701
Status of TRMM (NASDA)
[TW-3] p 2923 N92-26704
TRMM Mission Team
[TW-4] p 2923 N92-26705
International Conference on Japanese Earth Observation Programs: Plenary Session
[JTN-92-80342] p 2924 N92-26742
Japanese Earth Observation Program p 2924 N92-26743
Design of JEM temperature and humidity control system p 2958 N92-26957

NATIONAL WEATHER SERVICE, FORT WORTH, TX.
Integrating wind profiler data into forecast and warning operations at NWS field offices
[PB92-146075] p 2945 N92-26514

NATURAL ENVIRONMENTAL RESEARCH COUNCIL, LONDON (ENGLAND).
The joint US/UK 1990 epoch world magnetic model
[NASA-CR-190424] p 2942 N92-26406

NAUCHNO-PROIZVODSTVENNOE OBEDINENIE NIICHIMMASH, MOSCOW (USSR).
Water recovery from condensate of crew respiration products aboard the Space Station p 2956 N92-26951
Water reclamation from urine aboard the Space Station p 2957 N92-26952
Hygiene water recovery aboard the Space Station p 2957 N92-26955

NAVAL ACADEMY, ANNAPOLIS, MD.
Acquired polarization in fundamental symmetry experiments
[AD-A245646] p 2993 N92-26171
A fractal computer model of macromolecule-cell surface interactions
[AD-A245394] p 2950 N92-26289
A method to improve post impact compressive strength in graphite/epoxy composite materials after low temperature impact
[AD-A245395] p 2867 N92-26380
Optical strain monitoring in composite materials
[AD-A245474] p 2868 N92-26532
Summary of research: Academic departments, 1990-1991
[AD-A245533] p 3022 N92-26664

NAVAL MEDICAL RESEARCH INST., BETHESDA, MD.
Physiological design goals and proposed thermal limits for US Navy thermal garments: Proceedings of 2 conferences sponsored by the Naval Medical Research and Development Command
[AD-A245543] p 2956 N92-26665

NAVAL OCEAN SYSTEMS CENTER, SAN DIEGO, CA.
Matched field processing on the connection machine
[AD-A245469] p 2980 N92-26531

NAVAL OCEANOGRAPHIC AND ATMOSPHERIC RESEARCH LAB., BAY SAINT LOUIS, MS.
A compendium of environmental data collected during the southwest Florida shallow-water acoustic sea test
[AD-A246143] p 2950 N92-27071
Documentation for the Semi-Automated Mesoscale Analysis System 1.1
[AD-A246144] p 2985 N92-27072

NAVAL OCEANOGRAPHIC AND ATMOSPHERIC RESEARCH LAB., MONTEREY, CA.
AVHRR satellite data: Users guide for accessing NOARL archives
[AD-A246142] p 2926 N92-27070

NAVAL OCEANOGRAPHIC OFFICE, BAY SAINT LOUIS, MS.
The joint US/UK 1990 epoch world magnetic model
[NASA-CR-190424] p 2942 N92-26406

NAVAL POSTGRADUATE SCHOOL, MONTEREY, CA.
The development of a design database for the computer aided prototyping system
[AD-A245786] p 3010 N92-26176
Lower confidence limit expressions for P(X greater than y) and P(X greater than Y) under normality
[AD-A245787] p 2989 N92-26177
Pyrotechnic device reliability
[AD-A245818] p 2883 N92-26178
Using solid modeling techniques to construct three-dimensional icons for a visual simulator
[AD-A245784] p 2971 N92-26195
Requirements analysis and design for implementation of a satellite link for a local area computer network
[AD-A245610] p 2978 N92-26227
Recursive ray acoustics for three-dimensional sound-speed profiles
[AD-A245613] p 2991 N92-26228
Cluster model of polarization reflection from metallic surfaces
[AD-A245781] p 2996 N92-26241
VHDL behavioral description of discrete cosine transform in image compression
[AD-A245389] p 2972 N92-26248
Study of the transition to turbulence within a curved rectangular channel with 40 to 1 aspect ratio
[AD-A246314] p 2896 N92-26290
Estimation of motion parameters from image sequences
[AD-A246135] p 2986 N92-26358
Ocean bottom modeling for ray acoustics
[AD-A246287] p 2948 N92-26360
Selection and specification of a data link protocol for VSAT based inter-LAN communications
[AD-A246289] p 2979 N92-26361
Solid fuel ramjet infrared signature
[AD-A246299] p 2860 N92-26362
Performance enhancement of the NPS Transient Electromagnetic Scattering Laboratory
[AD-A246300] p 2888 N92-26363
Characteristics of upper-level and boundary layer forcing in Western Pacific cyclones
[AD-A246301] p 2945 N92-26364
Reconfiguration in robust distributed real-time systems based on global checkpoints
[AD-A245615] p 2970 N92-26382
Composite strength statistics from fiber strength statistics
[AD-A245616] p 2867 N92-26383
Effect of thermal residual stresses on the stress-strain behavior of metal-matrix composites
[AD-A246136] p 2868 N92-26386
Fast envelope correlation for passive ranging
[AD-A246333] p 2888 N92-26388
An antenna design for PANSAT using NEC
[AD-A245482] p 2888 N92-26399
Investigating the utility of coupling COCOMO with a system dynamics simulation of software development
[AD-A245484] p 2973 N92-26400
Development and testing of a prototype electro-optical phase encoded position transducer
[AD-A245486] p 2908 N92-26401
A comparison of heavy lift launch vehicle options for the 1990s
[AD-A245617] p 2857 N92-26402
Characterization of the clock in a new inexpensive GPS receiver: The Magnavox MX 4200
[AD-A246165] p 2851 N92-26415

Plasma interactions in a plasma erosion opening switch
[AD-A246179] p 2999 N92-26416
Design and implementation of a toolbox of modularized C programs to construct, analyze, and test network optimization algorithms
[AD-A246191] p 2979 N92-26417
A frequency domain based approach to on-line system identification
[AD-A246193] p 2973 N92-26418
Ocean bottom simulation using fractal geometry
[AD-A245477] p 2949 N92-26423
Naval Postgraduate School aircraft synthesis program (user's manual)
[AD-A246198] p 2974 N92-26458
Fiber-optic flexural disk accelerometer
[AD-A246203] p 2908 N92-26459
Proposed model of thermionically assisted breakdown and implementation on electrostatic thrusters
[AD-A246207] p 2990 N92-26460
An empirical approach to analysis of similarities between software failure regions
[AD-A246208] p 2974 N92-26461
Energy threshold for laser induced breakdown on a metal surface under high and ultra high vacuum conditions
[AD-A246212] p 2911 N92-26462
Fractals and chaos
[AD-A246502] p 2990 N92-26466
Effects of video bandwidth on the performance of a square law detector with Gaussian IF and video filters
[AD-A246506] p 2989 N92-26467
Performance analysis of image motion analysis algorithms
[AD-A246522] p 2974 N92-26468
Information systems planning methodologies: A framework for comparison and selection
[AD-A246527] p 3012 N92-26469
A prototype multi-media data base for tracking interface relationships and performing cost tradeoffs for the Sea Launch and Recovery (SEALAR) space launch system
[AD-A245481] p 2857 N92-26515
Symbolic solution of a multilayer ocean waveguide problem with arbitrary depth dependent ambient density and sound speed profiles
[AD-A245476] p 2949 N92-26533
Estimating mesoscale, orographically enhanced precipitation using synoptic scale data
[AD-A245749] p 2946 N92-26562
Dimensional analysis of structural steel beam design
[AD-A245759] p 2917 N92-26593
Effects of non-uniform windowing on the performance of a fast frequency-hopped noncoherent MFSK receiver over Rician fading channels with partial-band interference and Doppler shift
[AD-A245762] p 2889 N92-26595
The minimization of multiple valued logic expressions using parallel processors
[AD-A245763] p 2980 N92-26596
Investigation of deep dielectric charging and subsequent currents on geosynchronous spacecraft
[AD-A245764] p 2858 N92-26605
The development of a model builder for a microcircuit substrate
[AD-A245765] p 2893 N92-26606
Effects of power pulsations on natural convection from discrete heat sources
[AD-A246557] p 3007 N92-26617
Radar target identification by natural resonances: Evaluation of signal processing algorithms
[AD-A246566] p 2889 N92-26619
A modeling strategy for large-scale optimization based on analysis and visualization principles
[AD-A246570] p 2987 N92-26620
Development and testing of an unmanned air vehicle telemetry system
[AD-A246577] p 2858 N92-26621
Iterative system modeling using multigrid techniques
[AD-A245522] p 2976 N92-26658
Factors influencing the microstructural and mechanical properties of ULCB steel weldments
[AD-A245523] p 2878 N92-26659
Best value contracting in the procurement of engineering and technical services
[AD-A245524] p 3009 N92-26660
Modeling of explorative procedures for remote object identification
[AD-A245525] p 2922 N92-26661
Real time imaging and infrared background scene analysis using the Naval Postgraduate School infrared search and target designation (NPS-IRSTD) system
[AD-A245527] p 2997 N92-26662
Source location in thin plates using crosscorrelation
[AD-A245521] p 2992 N92-26678
Evaluation of the computational validity of the image model in predicting the sound field in a wedge-shaped layer using acoustical reciprocity
[AD-A246548] p 2992 N92-26688
An analysis of middle ultraviolet emissions of molecular nitrogen and nitric oxide and vacuum calibration of an ultraviolet spectrograph
[AD-A245984] p 2943 N92-26753
Focusing x ray transition radiation with cylindrical and elliptical optics
[AD-A245987] p 2997 N92-26754
Sturm-Liouville eigenfunctions expressed in determinant form
[AD-A245991] p 2987 N92-26755
The navigation data logger for a suitcase navigation system
[AD-A245997] p 2851 N92-26756
Implementation of multi-frequency modulation with Trellis encoding and Viterbi decoding using a digital signal processing board
[AD-A245998] p 2976 N92-26758
Weight optimum arch structures
[AD-A246001] p 2918 N92-26759
An analysis of the role of the budget committees in the Congressional budget process
[AD-A246005] p 3014 N92-26761
Measuring the effectiveness of information systems
[AD-A246007] p 3013 N92-26762
A prototype semantic integrity front end expert system for a relational database
[AD-A246084] p 3013 N92-26765
An object-oriented approach to computer architecture simulation
[AD-A246597] p 2970 N92-26773
Investigations of a single point temperature probe for measurement of atmospheric turbulence
[AD-A246563] p 2909 N92-26794
Precision of the long baseline acoustic navigation system used by Pegasus
[AD-A246598] p 2852 N92-26795
Modification and experimental validation of a combined optical and collection probe for solid propellant exhaust analysis
[AD-A245387] p 2884 N92-26839
The fidelity enhancement process
[AD-A245388] p 2977 N92-26840
Computer program for calculating in-flight aircraft-store interface reaction loads
[AD-A245782] p 2852 N92-26896
Stresses in solder joints of electronic packages
[AD-A245799] p 2894 N92-26897
Numerical field model simulation of full-scale fire tests in a closed spherical/cylindrical vessel using advanced computer graphics techniques
[AD-A245810] p 2887 N92-26898
Downdating of Szego polynomials and data fitting applications
[AD-A245825] p 2988 N92-26900
Dynamic response of cylindrical shells to underwater end-on explosion
[AD-A245804] p 2920 N92-26932
A comparison of the UHF Follow-On and MILSTAR satellite communication systems
[AD-A245806] p 2891 N92-26933
System evaluation of a frequency hopping combat net radio
[AD-A246365] p 2891 N92-26941
Proximal minimization algorithms with cutting planes
[AD-A246436] p 2977 N92-26949
Observations of wind forced circulation on the continental shelf off Point Sur, California from a self-contained acoustic Doppler current profiler
[AD-A246437] p 2950 N92-27029
Kalman smoother applied to lace
[AD-A246439] p 2859 N92-27030
Apparatus for measuring the absorption of sound by noise in one dimension
[AD-A246442] p 2992 N92-27031
An Ada object oriented missile flight simulation
[AD-A246378] p 2977 N92-27052
Nucleate pool boiling of R-114 and R-114/oil mixtures from single enhanced tubes
[AD-A245487] p 3008 N92-27058
Complementary metal oxide silicon cyclic redundancy check generators
[AD-A246140] p 2894 N92-27061
Subscale solid rocket motor infrared signature and particle behavior
[AD-A246416] p 2862 N92-27065
Sensitivity of sensors for characterizing chaos
[AD-A246423] p 2921 N92-27066
Elevated temperature properties of a dispersion strengthened Al-(Fe, V, Si) alloy
[AD-A246427] p 2880 N92-27067
Hydrographic data from the Coastal Transition Zone (CTZ) program, 5-19 July 1988
[AD-A245517] p 2950 N92-27069
NPSNET: Hierarchical data structures for real-time three-dimensional visual simulation
[AD-A246380] p 2978 N92-27073
Orbital maintenance of endoatmospheric low earth-orbiting satellites
[AD-A246381] p 2859 N92-27074
High frequency analyses of coastal meteorological phenomena affecting refractivity
[AD-A246383] p 2947 N92-27075
Acoustically probed Taylor-Couette flow apparatus
[AD-A246385] p 2993 N92-27076
Measurement of surface layer optical turbulence above AMOS
[AD-A246387] p 3016 N92-27077
Modeling for improved minimum resolvable temperature difference measurements
[AD-A246389] p 2991 N92-27078
The onset of breakdown in a fast pulsed vacuum diode
[AD-A246395] p 2895 N92-27079
Studies in chaos using stochastic methods
[AD-A246919] p 3008 N92-27171
Experimental results for inductive strips in inhomogeneous finline
[AD-A247254] p 2895 N92-27176
VLSI implementation of fuzzy logic operator unit
[AD-A247146] p 2989 N92-27180
Passive determination of temperature and range using spectral band measurements of photon emittance
[AD-A247147] p 2910 N92-27181
Higher order parametric x rays
[AD-A247148] p 2991 N92-27182

NAVAL RESEARCH LAB., WASHINGTON, DC.
A computer program for the calculation of daubechies wavelets
[AD-A245461] p 2975 N92-26529
Field-emission arrays: A potentially bright source
[AD-A246561] p 2893 N92-26741
Evaluation criteria for real-time specification languages
[AD-A246612] p 2976 N92-26766
Theory of electromagnetic instability of an intense beam in a quadrupole focusing system
[AD-A246560] p 2990 N92-26768
Reflection of x rays from repeated multilayer structures
[AD-A246562] p 2991 N92-26769

NAVAL SURFACE WARFARE CENTER, DAHLGREN, VA.
STATLIB/PC users guide
[AD-A245462] p 2975 N92-26530

NAVAL WEAPONS CENTER, CHINA LAKE, CA.
Space environmental effects on coated optics p 2999 N92-27098

NAVY CLOTHING AND TEXTILE RESEARCH FACILITY, NATICK, MA.
Effectiveness of a selected microclimate cooling system in increasing tolerance time to work in the heat. Application to Navy Physiological Heat Exposure Limits (PHEL) curve 5
[AD-A246529] p 2952 N92-26470

NEBRASKA UNIV., LINCOLN.
Linear and non-linear response of liquid and solid particles to energetic radiation
[AD-A246368] p 2894 N92-26942

NELSON SPACE SERVICES LTD., LONDON (ENGLAND).
Concept for a European Space Station: Habitability, life support, and laboratory facilities p 2969 N92-27023

NEW MEXICO INST. OF MINING AND TECHNOLOGY, SOCORRO.
Description of and users manual for TUBA: A computer code for generating two-dimensional random fields via the turning bands method
[DE92-001020] p 2971 N92-26189

NIHON UNIV., TOKYO (JAPAN).
Flow around an isolated surface roughness in the laminar boundary layer p 2903 N92-26913
Numerical studies on laminar turbulent transition at the Stuttgart University, Germany p 2903 N92-26916

NIIGATA UNIV. (JAPAN).
Catalytic wet-oxidation of human waste produced in a space habitat: Purification of the oxidized liquor for human drinking p 2957 N92-26954

NOKIA RESEARCH CENTER, ESPOO (FINLAND).
Numerical solution of plastic liquids shape factor
[PB92-133958] p 2896 N92-26496

NORD-MICRO ELEKTRONIC FEINMECHANIK G.M.B.H., FRANKFORT (GERMANY, F.R.).
Development of European sublimator technology for EVA p 2968 N92-27018

NORTH ATLANTIC TREATY ORGANIZATION, BRUSSELS (BELGIUM).
Executive summary of the technical proceedings on Military Information System Engineering (Defence Research Group Panel 11 on Information Processing Technology)
[AD-A245656] p 3010 N92-26174
The study on a directory of human performance models for system design (Defence Research Group Panel 8 on the defence applications of human and bio-medical sciences)
[AD-A247346] p 2970 N92-27179
NORTH CAROLINA STATE UNIV., RALEIGH.
Mean and turbulent structure of the marine atmospheric boundary layer during cold air outbreaks of different intensities: Observational and modelling analyses
p 2942 N92-26489
Homogenization models for 2-D grid structures
[NASA-CR-190321] p 2920 N92-26892
NORTH CAROLINA UNIV., CHAPEL HILL.
Advanced technology for portable personal visualization
[AD-A245819] p 2954 N92-26179
NORTH DAKOTA UNIV., GRAND FORKS.
High-yield hydrogen production by catalytic gasification of coal or biomass
[DE92-008770] p 2875 N92-26724
NORTHEAST SEMICONDUCTOR, INC., ITHACA, NY.
Innovative techniques for the production of low cost 2D laser diode arrays
[AD-A247282] p 2913 N92-27178
NORTHERN RESEARCH AND ENGINEERING CORP., WOBURN, MA.
Turbocharged pressurized combustion system
[PB92-142579] p 2873 N92-26521
NORTHWESTERN UNIV., EVANSTON, IL.
Squeezed light and twin beams generation with a Q-switched laser p 2912 N92-26603
Optical communications with number states
p 2889 N92-26604
Effect of interstitials on the trapping of hydrogen in iron-single crystals
[AD-A246412] p 3006 N92-27064
NOTRE DAME UNIV., IN.
Gamma Group-The Pale Horse: A proposal in response to a commercial air transportation study ort study
[NASA-CR-190019] p 2852 N92-26435
On the stochastic fatigue crack growth problem
p 2917 N92-26557
NOTTINGHAM UNIV. (ENGLAND).
An assessment of satellite remote sensing for land cover classification p 2922 N92-26625
The geoid, GPS, and levelling p 2925 N92-26777
NUEVAS TECNOLOGIAS ESPACIALES S.A., LLISSA D'AMUNT (SPAIN).
Study on the requirements for the installation of a CES and habitability centre p 2966 N92-27007

O

OAK RIDGE NATIONAL LAB., TN.
Time optimal trajectories for mobile robots with two independently driven wheels
[DE92-010002] p 2913 N92-26219
Assessment of diagnostic methods for solenoid-operated valves
[DE92-009379] p 2913 N92-26234
Magnetohydrodynamic Electromagnetic Pulse (MHD-EMP) interaction with power transmission and distribution systems
[DE92-010365] p 2887 N92-26237
Life support research and development, a Department of Energy program for the Space Exploration Initiative
[DE92-007681] p 2955 N92-26375
Results of a portable fiber-optic weigh-in-motion system
[DE92-009011] p 2996 N92-26376
Life support research and development for the Department of Energy Space Exploration Initiative
[DE92-007239] p 2955 N92-26494
A user's manual for MASH 1.0: A Monte Carlo adjoint shielding code system
[DE92-010375] p 3021 N92-26544
N-learners problem: Learning Boolean combinations of halfspaces
[DE92-010390] p 2987 N92-26545
Tuned-circuit dual-mode Johnson noise thermometers
[DE92-010121] p 2908 N92-26569
A FORTRAN 90 code for magnetohydrodynamics
[DE92-010362] p 3000 N92-26577
A comprehensive review of the XRD data of the primary and secondary phases present in the BSCCO superconductor system
[DE92-010363] p 3003 N92-26579
Organic carbon in soil and the global carbon cycle
[DE92-010289] p 2931 N92-26580
Fabrication and characterization of amorphous lithium electrolyte thin films and rechargeable thin-film batteries
[DE92-010108] p 2893 N92-26636
New amorphous thin-film lithium electrolyte and rechargeable microbattery
[DE92-010110] p 2893 N92-26637
Mobility of electrons and holes in semiconductors
[DE92-010125] p 3004 N92-26638
A Bayes-Maximum Entropy method for multi-sensor data fusion
[DE92-000680] p 2983 N92-26657
Simulation of 3D non-planar fatigue crack growth in a turbine blade root
[DE92-006859] p 2854 N92-26697
Technology transfer and application of SERS continuous monitor for trace organic compounds
[DE92-008900] p 2875 N92-26726
Using min-max of torque to resolve redundancy for a mobile manipulator
[DE92-000070] p 2915 N92-26750
Study and analysis of the stress state in a ceramic, button-head, tensile specimen
[DE92-007794] p 2918 N92-26784
The production and properties of melt-zone textured Y1Ba2Cu3O(7-delta) filaments
[DE92-008097] p 3005 N92-26843
Predictability of long-term creep and rupture in a nozzle-to-sphere vessel model
[DE92-008099] p 2919 N92-26845
Some experiences with absorption, phonon Raman, and luminescence spectroscopic probes of crystal structure of f-element compounds
[DE92-007828] p 3006 N92-26851
OBSERVATOIRE DE PARIS (FRANCE).
Tensor-multi-scalar theories of gravitation
[PB92-152305] p 2943 N92-26820
OFFICE OF MANAGEMENT AND BUDGET, WASHINGTON, DC.
Managing Federal information resources: Under the Paperwork Reduction Act of 1980
[PB92-154905] p 3014 N92-26926
OFFICE OF TECHNOLOGY ASSESSMENT, WASHINGTON, DC.
Competing economies: America, Europe, and the Pacific rim
[PB92-115757] p 3014 N92-26730
OHIO STATE UNIV., COLUMBUS.
Joint services electronics program
[AD-A245636] p 2892 N92-26280
Estimation of geopotential differences over intercontinental locations using satellite and terrestrial measurements p 2924 N92-26728
Dvoretzky's theorem: 30 years later
[PB92-153212] p 2988 N92-26788
OKLAHOMA STATE UNIV., STILLWATER.
Space Exposed Experiment Developed for Students (SEEDS) (P0004-2) p 2952 N92-27121
OKLAHOMA UNIV., NORMAN.
Parameterization of water-soluble component of aerosol particles in numerical cloud models
[NASA-CR-190225] p 2945 N92-26474
Study of entrainment mechanisms in convective clouds
[NASA-CR-190223] p 2946 N92-26735
Analysis of mixing mechanisms in numerically simulated convective clouds
[NASA-CR-190222] p 2946 N92-26736
OLD DOMINION UNIV., NORFOLK, VA.
On shock capturing for liquid and gas media
p 2897 N92-26556
Numerical formulation for the prediction of solid/liquid change of a binary alloy
[NASA-CR-188468] p 2878 N92-26642
Recognition of 3-D symmetric objects from range images in automated assembly tasks
[NASA-CR-187664] p 2886 N92-26656
Comparison of laser models
[NASA-CR-190302] p 2913 N92-26870
OPTICAL COATING LAB., INC., SANTA ROSA, CA.
Optical performance of exposed solar cell covers
p 2998 N92-27091
OSAKA UNIV. (JAPAN).
An evolutional process of three dimensional disturbances in laminar boundary layers
p 2902 N92-26910
Control of turbulent mixing in hypersonic flow
p 2904 N92-26919
Responses of boundary layers to strong external disturbances p 2904 N92-26921
OSLO UNIV. (NORWAY).
The Norwegian upper atmosphere programme in Svalbard (Norway) p 2935 N92-26295
OXFORD UNIV. (ENGLAND).
Tracer transport in the middle atmosphere
p 2928 N92-26473
Cell vertex methods for compressible gas flows
p 2897 N92-26599

P

PACIFIC NORTHWEST LAB., RICHLAND, WA.
Modeling node bandwidth limits and their effects on vector combining algorithms
[DE92-010829] p 2979 N92-26277
Use of the Edmonds-Reilly Model to model energy-related greenhouse gas emissions
[DE92-010035] p 2931 N92-26633
PARK (GEORGE W.) SEED CO., INC., GREENWOOD, SC.
Seeds in space experiment p 2952 N92-27120
PENNSYLVANIA STATE UNIV., UNIVERSITY PARK.
Enhance methane reactivity
[PB92-154822] p 2873 N92-26516
Deformation behavior of an age-hardenable Beta+Alpha-Two titanium alloy
[AD-A246362] p 2879 N92-26939
Turbulent mixing in supersonic jets
p 2850 N92-27054
PENNSYLVANIA UNIV., PHILADELPHIA.
Atomistic studies of grain boundaries in alloys and compounds
[DE92-010792] p 2877 N92-26251
Biochemical, endocrine, and hematological factors in human oxygen tolerance extension: Predictive studies 6
[NASA-CR-190341] p 2952 N92-26263
PHILIPS GLOEILAMPENFABRIEKEN N.V., EINDHOVEN (NETHERLANDS).
Magnetic anisotropy from first principles
[ISBN-90-9004483-3] p 2877 N92-26252
PHILLIPS LAB., KIRKLAND AFB, NM.
Preliminary analyses of WL experiment No. 701, space environment effects on operating fiber optic systems
p 2998 N92-27089
PHYSICS AND ELECTRONICS LAB. TNO, THE HAGUE (NETHERLANDS).
Construction and function of a multifunction CO2-Laser system
[AD-A245425] p 2910 N92-26271
Plan of action survey of functional requirements for a geographical information system
[AD-A245622] p 3011 N92-26403
Description of the multispectral CCD-camera
[AD-A245681] p 2908 N92-26517
A high repetition rate lidar
[AD-A245382] p 2890 N92-26872
Infrared clutter measurements of marine backgrounds
[AD-A245422] p 2932 N92-26873
A measuring facility for testing radio communication equipment
[AD-A245621] p 2890 N92-26874
Building a GIS on top of the open DBMS Postgres
[FEL-91-B183] p 3014 N92-26875
A real-time synthetic aperture radar processor: Introduction and project description
[AD-A245370] p 2890 N92-26876
Description of the Rayflux ray tracing program and comparison with other models and measurements
[AD-A245413] p 2944 N92-26877
PITTSBURGH UNIV., PA.
Low severity upgrading of F-T waxes with solid superacids
[DE92-009081] p 2873 N92-26457
A novel process for methanol synthesis
[DE92-010465] p 2883 N92-26547
POLISH ACADEMY OF SCIENCES, WARSAW.
On certain methods of determining the ellipses an d ellipsoids of the positioning accuracy of robot manipulators
[ISSN-0208-5658] p 2914 N92-26284
POLITECNICO DI MILANO (ITALY).
Finding a best subtree of a tree
[REPT-91-041] p 2986 N92-26420
The SOL object-oriented database language
[REPT-91-053] p 2973 N92-26421
Verifying behavioral consistency of an object-oriented database schema
[REPT-91-054] p 3011 N92-26422
Hardware synthesis using high-level Petri nets
[REPT-91-071] p 2970 N92-26439
Proving properties of real-time systems through logical specifications and Petri net models
[REPT-91-072] p 2973 N92-26448
A random polynomial algorithm for the matroid parity base problem
[REPT-91-079] p 2974 N92-26449

PRINCETON UNIV., NJ.
Aromatic-radical oxidation kinetics
[DE92-010821] p 2871 N92-26274
Throttleless Otto-cycle natural gas engines
[PB92-164482] p 2914 N92-26371
Photoinduced charge separation in solid-state and molecular systems
[DE92-010130] p 3004 N92-26639
High precision timing of millisecond pulsars
p 3015 N92-26760
PROGETTO AREA, ROME (ITALY).
Influence of architecture on the definition of a space station configuration p 2860 N92-27024
PURDUE UNIV., WEST LAFAYETTE, IN.
Performance prediction and design of maximum thrust planar supersonic nozzles using a flux-difference-splitting technique p 2853 N92-26480

R

RADIAN CORP., RESEARCH TRIANGLE PARK, NC.
Volatile Organic Compound (VOC) and Particulate Matter (PM) speciation data system user's manual, version 1.4
[PB92-105527] p 2932 N92-26823
RAILWAY TECHNICAL RESEARCH INST., TOKYO (JAPAN).
Aerodynamic drag on the bullet trains
p 2902 N92-26911
RAND CORP., SANTA MONICA, CA.
Apogee, perigee, and recovery: Chronology of Army exploitation of space
[RAND-N-3103-A] p 2856 N92-26192
Human support issues and systems for the space exploration initiative: Results from Project Outreach
[NASA-CR-190320] p 2954 N92-26193
The role of the B-2 in the new US defense strategy
[RAND-P-7744] p 2990 N92-26194
The preliminary geodetic control network of Venus
[RAND-N-3437-JPL] p 3019 N92-26819
RAND GRADUATE INST. FOR POLICIES STUDY, SANTA MONICA, CA.
The Lockheed F-117A
[RAND-P-7746-RGS] p 2852 N92-26673
RAYTHEON CO., LEXINGTON, MA.
RF vacuum microelectronics
[AD-A246579] p 2893 N92-26771
READING UNIV. (ENGLAND).
Exposure to space radiation of high-performance infrared multilayer filters and materials technology experiment (A0056) p 2999 N92-27108
RENSSELAER POLYTECHNIC INST., TROY, NY.
An experimental investigation of a 2-D scramjet inlet at flow Mach numbers of 8 to 25 and stagnation temperatures of 800 to 4,100 K p 2854 N92-26586
A supervisory control strategy for navigation of mobile robots in dynamic environments p 2983 N92-26734
RESEARCH INST. FOR COMPUTING AND INFORMATION SYSTEMS, HOUSTON, TX.
Advanced software development workstation. Engineering scripting language graphical editor: DRAFT design document
[NASA-CR-190393] p 2971 N92-26181
Advanced software development workstation. Engineering scripting language graphical editor: DRAFT code documentation
[NASA-CR-190389] p 2971 N92-26182
Advanced software development workstation project: Engineering scripting language. Graphical editor
[NASA-CR-190391] p 2971 N92-26183
Extracting fuzzy rules under uncertainty and measuring definability using rough sets
[NASA-CR-190396] p 2972 N92-26197
Measuring uncertainty by extracting fuzzy rules using rough sets
[NASA-CR-190395] p 2972 N92-26198
Distributed and parallel Ada and the Ada 9X recommendations
[NASA-CR-190392] p 2978 N92-26199
Data Management Systems (DMS): Complex data types study. Volume 1: Appendices A-B. Volume 2: Appendices C1-C5. Volume 3: Appendices D1-D3 and E
[NASA-CR-190397] p 3009 N92-26552
RESEARCH INST. OF NATIONAL DEFENCE, LINKOEPING (SWEDEN).
Generation of multi-resolution maps
[PB92-152206] p 2921 N92-26513
ROCKWELL INTERNATIONAL CORP., CANOGA PARK, CA.
Accelerated cycle life performance for ovonic nickel-metal hydride cells p 2865 N92-27155
ROLLS-ROYCE LTD., BRISTOL (ENGLAND).
VSTOL engine design evolution: Growth of the Pegasus engine for Harrier
[PNR-90805] p 2855 N92-27039
ASTOVL engine control
[PNR-90808] p 2855 N92-27040
Hot-gas reingestion engine response considerations
[PNR-90810] p 2855 N92-27042
ROLLS-ROYCE LTD., DERBY (ENGLAND).
Use of Markov methods in analysis of fault-tolerant systems with flexible repair policies
[PNR-90801] p 2916 N92-27038
ASTOVL propulsion systems: Configuration and concept choice
[PNR-90809] p 2855 N92-27041
Simultaneous engineering in aero-gas turbine design and manufacture
[PNR-90811] p 2856 N92-27043
Powder processing of aero-engine components
[PNR-90813] p 2880 N92-27044
ROYAL AIRCRAFT ESTABLISHMENT, FARNBOROUGH (ENGLAND).
The changing role of experimentation in aeroengine R and D: The point of view of the research worker
[AD-A246372] p 2856 N92-27062
RUTGERS - THE STATE UNIV., NEW BRUNSWICK, NJ.
A design rationale for NASA TileWorld
[NASA-TM-107882] p 2982 N92-26627
RUTHERFORD HIGH ENERGY LAB., CHILTON (ENGLAND).
Incoherent scatter radar measurements of the cusp
p 2936 N92-26303
Requirements for coordinated Cluster and ground-based observations of the cusp p 2938 N92-26318

S

SANDIA NATIONAL LABS., ALBUQUERQUE, NM.
Calibration of CR-39 for detecting fusion neutrons
[DE92-009063] p 2993 N92-26225
Gas-pressure studies with Li(Si)/FeS2 thermal batteries
[DE92-010801] p 2892 N92-26238
Comparison of laser and conventional heating in TLD dosemapping
[DE92-010773] p 2910 N92-26269
Constrained neural network architectures for target recognition
[DE92-011159] p 2982 N92-26434
The development of an optical fiber accelerometer
[DE92-008680] p 2997 N92-26452
Technical specification for the Sandia Management Restructure Study Team (MRST) Prototype Information System
[DE92-010360] p 3012 N92-26575
A boundary integral method for steady unsaturated flow in nonhomogeneous media
[DE92-009066] p 2897 N92-26644
Erosion of a relativistic electron beam propagating in a plasma channel
[DE92-009059] p 3000 N92-26666
SOLTECH 1992 proceedings: Solar Process Heat Program, volume 1
[DE92-001238] p 2927 N92-26683
Transient gas motion in nuclear-reactor-pumped lasers: Computational and experimental results
[DE92-002357] p 2912 N92-26691
Advances in the engineering of high field applied-B ion diodes for inertial confinement fusion
[DE92-006528] p 3000 N92-26695
Experiences in using C++ to develop a next generation strong shock wave physics code
[DE92-006675] p 2976 N92-26696
Reynolds number dependence of the drag coefficient for laminar flow through fine-scale screens
[DE92-002930] p 2899 N92-26698
An experimental investigation of high-speed water entry for full size and scale-model pointed nose vehicle
[DE92-004363] p 2899 N92-26716
Burn-rate studies with iron/potassium perchlorate heat pellets
[DE92-008524] p 2875 N92-26722
Etching effects in ion implanted SiO2
[DE92-011150] p 3005 N92-26826
Role of shock compression technique for scientific and engineering studies
[DE92-008324] p 2919 N92-26846
Fundamentals of electrokinetics
[DE92-008326] p 2894 N92-26847
Recent advances in shock and quasi-isentropic compression techniques for dynamic material property studies
[DE92-007988] p 2919 N92-26852
Eulerian computational methods
[DE92-008017] p 2900 N92-26853
Critical soft landing technology issues for future US space missions
[NASA-CR-185673] p 2858 N92-26884
Feature discovery via neural networks for object recognition in SAR imagery
[DE92-007046] p 2891 N92-26902
SCIENCE APPLICATIONS INTERNATIONAL CORP., PROSPECT, TN.
Geometry and mass model of ionizing radiation experiments on the LDEF satellite
[NASA-CR-184325] p 2993 N92-26200
SCRIPPS INSTITUTION OF OCEANOGRAPHY, LA JOLLA, CA.
Meridional zonation of the Barents Sea ecosystem inferred from satellite remote sensing and in situ bio-optical observations
[AD-A246323] p 2948 N92-26245
SHEFFIELD UNIV. (ENGLAND).
Adaptive regulation of the boiler-turbine unit of a Combined Heat and Power (CHP) system
[RR-417] p 2887 N92-26752
SHIP RESEARCH INST., TOKYO (JAPAN).
Research activities on CFD at the Ship Research Institute p 2902 N92-26908
SMALL BUSINESS ADMINISTRATION, WASHINGTON, DC.
US Small Business Administration FY 1990 national accomplishment report and FY 1991 national affirmative employment program plan
[PB92-157064] p 3008 N92-26353
Small Businesses Make a Difference
[PB92-160118] p 3008 N92-26369
SMITHSONIAN ASTROPHYSICAL OBSERVATORY, CAMBRIDGE, MA.
Mapping the great attractor region in x rays and diffuse x ray emission: A possible galactic wind in the bulge of M31
[NASA-CR-190402] p 3015 N92-26184
Observational and theoretical investigations in solar seismology
[NASA-CR-190245] p 3019 N92-26247
SOCIETE DES ACCUMULATEURS FIXES ET DE TRACTION, ROMAINVILLE (FRANCE).
SAFT nickel-cadmium cell performances for GEO and LEO applications p 2863 N92-27137
Performances of 250 Amp-hr lithium/thionyl chloride cells p 2864 N92-27148
SOUTHAMPTON UNIV. (ENGLAND).
Polarisation effects in fibre lasers
p 2911 N92-26571
STANFORD LINEAR ACCELERATOR CENTER, CA.
Scalable coherent interface: Links to the future
[DE92-010728] p 2887 N92-26267
STANFORD UNIV., CA.
Spectroscopy and kinetics of combustion gases at high temperatures
[DE92-011216] p 2872 N92-26281
Fundamental studies of the chemical vapor deposition of diamond
[DE92-010327] p 2881 N92-26543
Computational methods for problems of acoustics with particular reference to exterior domains
p 2992 N92-26558
An adaptive correction technique for Differential Global Positioning System p 2851 N92-26623
Experiments in modelling and end-point control of two-link flexible manipulators p 2915 N92-26731
Influence of substrate topography on the nucleation of diamond thin films
[DE92-010777] p 2883 N92-27060
Laser cooling and trapping of atoms and particles
[AD-A247208] p 2913 N92-27173
SURVEILLANCE RESEARCH LAB., SALISBURY (AUSTRALIA).
Buffered serial data card
[AD-A246435] p 2852 N92-26948
SWEDISH INST. OF SPACE PHYSICS, KIRUNA.
The present understanding of the cusp
p 2936 N92-26306
The need of coordinated observations in space and from ground p 2937 N92-26310
SWEDISH INST. OF SPACE PHYSICS, UPPSALA.
Mapping of the auroral oval to the tail
p 2937 N92-26309
SYDNEY UNIV. (AUSTRALIA).
Tests on various arrangements of liquid column vibration absorbers
[PB92-152610] p 2896 N92-26506
SYRACUSE UNIV., NY.
Cadmium telluride thin films on silicon substrates
[AD-A245309] p 3001 N92-26226
Non-destructive analysis for hydrogen concentrations in materials
[AD-A246098] p 2874 N92-26541
SYSTEMS APPLICATIONS, INC., SAN RAFAEL, CA.
Assessment of computer models for estimating vehicle emission factors. Volume 1: Executive summary
[PB92-113059] p 2931 N92-26802

Assessment of computer models for estimating vehicle emission factors. Volume 2: Description and comparison of the MOBILE4 and EMFAC7E models
[PB92-113067] p 2932 N92-26803

SYSTEMS APPLICATIONS INTERNATIONAL, SAN RAFAEL, CA.
Improved procedures for quantifying key meteorological effects on ambient ozone data
[PB92-163278] p 2931 N92-26793

T

TECHNICAL RESEARCH CENTRE OF FINLAND, ESPOO.
Development and applications of the reverse neutron time-of-flight method with Fourier-type beam chopper
[VTT-PUBL-82] p 3001 N92-26320
Estimation of peak intensities from frequency filtered total scattering data of neutrons obtained by the reverse Fourier method p 3002 N92-26321
High-resolution Fourier TOF powder diffraction. 1: Performance of the Mini-Sfinks Facility p 3002 N92-26323
Neutron powder diffraction study of deuterated beta-acetonitrile p 3002 N92-26324
A high-resolution neutron powder diffraction study in high-T(sub c) superconductor YBa2Cu3O7 p 3002 N92-26326
Neutron powder diffraction study on Eu-substituted Bi2Sr2CaCu2O(8+y) high temperature superconductor p 3003 N92-26328
Model studies of the transfer of radionuclides in the Finnish environment
[VTT-PUBL-81] p 2929 N92-26482
A comparative assessment of radiological impact due to nuclear waste disposal in hard crystalline bedrock, appendix 1
[IAEA-CN-43/449] p 2929 N92-26483
Numerical solution of plastic liquids shape factor
[PB92-133958] p 2896 N92-26496

TECHNICAL RESEARCH CENTRE OF FINLAND, HELSINKI.
Assessment of biospheric behaviour of releases from nuclear waste repositories, appendix 2 p 2929 N92-26484
Assessment of radiation doses due to releases to the biosphere from nuclear waste repositories, appendix 3 p 2929 N92-26485
Sensitivity analysis of biospheric behaviour of radionuclides released from nuclear waste repositories, appendix 4 p 2929 N92-26486
Biosphere model validation by intercomparison to observed behaviour of fallout radionuclides in the aquatic environment, appendix 5 p 2930 N92-26487
Modeling transfer of Cs-137 fallout in a large Finnish watercourse, appendix 6 p 2930 N92-26488

TECHNICAL UNIV. OF DENMARK, LYNGBY.
Results of the TTF-TCNQ and the calcium carbonate crystallization on the Long Duration Exposure Facility p 3007 N92-27127

TECHNISCHE HOCHSCHULE, AACHEN (GERMANY, F.R.).
Subgraphs, closures and Hamiltonicity
[PB92-148766] p 2987 N92-26737

TECHNISCHE HOGESCHOOL, DELFT (NETHERLANDS).
Experimental study of shear fracture and aggregate interlock in cementbased composites
[PB92-151521] p 2868 N92-26525

TECHNISCHE UNIV., DELFT (NETHERLANDS).
Reduced models for the behavior of VLSI circuits
[ISBN-90-6275-721-9] p 2892 N92-26249
Developing an adaptive scheduling support environment
[ISBN-90-9004609-7] p 3008 N92-26250
Magnetic anisotropy from first principles
[ISBN-90-9004483-3] p 2877 N92-26252
Transient diffusive electromagnetic fields in layered anisotropic media
[ISBN-90-6275-722-7] p 2887 N92-26254
Man-machine aspects of remotely controlled space manipulators
[ISBN-90-370-0056-8] p 2954 N92-26255
The influence of pressure on the phase behaviour of water + oil + surfactant systems
[ISBN-90-6275-732-4] p 2871 N92-26257
Computational modelling of rubberlike materials
[ETN-92-91304] p 2916 N92-26259
Synchronous detection in monolithically integrated AM upconversion receivers
[ETN-92-91305] p 2892 N92-26260
Activation and characterization of some molecular sieve catalysts
[ETN-92-91306] p 2871 N92-26261
Fuel staging and its implementation in a novel internally staged burner
[ETN-92-91307] p 2872 N92-26285
Electromagnetic scattering by a moving object: Theory and experiment
[PB92-150911] p 2889 N92-26511
Two-phase flow of Newtonian and Non-Newtonian fluids in a porous medium applied to water coning
[PB92-151109] p 2900 N92-26836
Quantum interference and confinement effects in narrow channel Si-MOSFET's
[PB92-150176] p 3006 N92-26927

TECHNISCHE UNIV., MUNICH (GERMANY, F.R.).
Upper/lower vortex interaction and potential vorticity inversion p 2939 N92-26331
The stability of barotropic vortices: Implications for tropical cyclone motion p 2940 N92-26335
Calorimetric particle detectors with superconducting absorber materials p 2907 N92-26393
Superconducting tunnel junctions p 2907 N92-26396

TECHNISCHE UNIV., TWENTE (NETHERLANDS).
Developments of solutions of some special elliptic equations at a corner
[PB92-148741] p 2986 N92-26503
Subgraphs, closures and Hamiltonicity
[PB92-148766] p 2987 N92-26737
Decomposition of bipartite graphs under degree constraints
[PB92-148626] p 2988 N92-26817

TECHNOFAN, BLAGNAC (FRANCE).
Fan/pump/separator technology development for EVA p 2966 N92-27006

TEL-AVIV UNIV. (ISRAEL).
Dvoretzky's theorem: 30 years later
[PB92-153212] p 2988 N92-26788

TELEDYNE BROWN ENGINEERING, HUNTSVILLE, AL.
Design and performance of the Spacelab Astro-1 mission heat pipe radiator p 2859 N92-26965

TEXAS A&M UNIV., COLLEGE STATION.
NEXUS: A kernel complex object management system p 3012 N92-26567
Research accomplished at the Knowledge Based Systems Lab: IDEF3, version 1.0
[NASA-CR-190279] p 2975 N92-26587
A finite element method including transverse stresses for thick laminated plates and shells p 2920 N92-26860

TEXAS SOUTHERN UNIV., HOUSTON.
An evaluative study of the sensory qualities of selected European and Asian foods for international space missions (a French food study) p 2966 N92-27009

TEXAS UNIV., AUSTIN.
Characterization of discrete-time linear periodically time-varying systems
[AD-A245822] p 2989 N92-26180
Mode structure and continuum damping of high-n toroidal Alfven eigenmodes
[DE92-010547] p 2999 N92-26256
Kinetic theory of toroidicity-induced Alfven eigenmode
[DE92-010424] p 2999 N92-26546
Effects of orbit squeezing on ion transport in the banana regime in tokamaks
[DE92-010548] p 3000 N92-26549
Scenarios for the nonlinear evolution of alpha particle induced Alfven wave instability
[DE92-010549] p 3000 N92-26550
Evaluation criteria for real-time specification languages
[AD-A246612] p 2976 N92-26766
Nonstationary higher order spectral analysis
[AD-A246580] p 2991 N92-26772
Degradation and buckling of metal tubes under cyclic bending and external pressure p 2920 N92-26869
Adaptive control of nonlinear and stochastic systems
[AD-A247204] p 2985 N92-27169

THE RESEARCH INST. OF THE GULF OF MAINE, SOUTH PORTLAND.
Survival of epiphytic bacteria from seed stored on the Long Duration Exposure Facility (LDEF) p 2952 N92-27122

THIOKOL CORP., BRIGHAM CITY, UT.
Space aging of solid rocket materials p 2884 N92-27085

TOHOKU UNIV., SENDAI (JAPAN).
Three dimensional boundary layer transition on a yawed cylinder p 2902 N92-26909
Investigation on the boundary layer transition of alternately oscillating flow in deceleration phase p 2903 N92-26917

TOKYO UNIV. (JAPAN).
Validation of numerical models by TRMM and validation of TRMM by numerical models
[TW-8] p 2923 N92-26709

TOLEDO UNIV., OH.
Measurements of scattering processes in negative ion-atom collisions
[DE92-010319] p 2995 N92-26574

TRACOR BATTERY TECHNOLOGY CENTER, ROCKVILLE, MD.
Examination of the discharge mechanism of Li/CF(x) cells: Comparison of the electrochemical reduction mechanisms of PTFE and (CF(x))n by lithium p 2865 N92-27151

TRW SPACE TECHNOLOGY LABS., REDONDO BEACH, CA.
LDEF SP-HVDE (Space Plasma-High Voltage Drainage Experiment) post-flight results: Leakage current and discharge p 2895 N92-27103

TSUKUBA SPACE CENTER, IBARAGI (JAPAN).
Unified computational method for design of fluid loop systems p 2905 N92-26962

TURING INST., GLASGOW (SCOTLAND).
Modelling default and likelihood reasoning as probabilistic
[NASA-TM-107889] p 2984 N92-26893

U

UFA, INC., NEWTON, MA.
Expert system management system
[AD-A247102] p 3009 N92-26863

UNISYS CORP., RESTON, VA.
UT40 - Asset Library Open Architecture Framework (ALOAF)
[AD-A247268] p 2978 N92-27177

UNITED TECHNOLOGIES CORP., HUNTSVILLE, AL.
STS lithium/CF(x) battery p 2863 N92-27143

UNIVERSITY OF TECHNOLOGY, SYDNEY (AUSTRALIA).
Modelling default and likelihood reasoning as probabilistic
[NASA-TM-107889] p 2984 N92-26893

UNIVERSITY OF THE PACIFIC, FOREST GROVE, OR.
Recent developments in nickel electrode analysis p 2865 N92-27158

UTAH UNIV., SALT LAKE CITY.
New theoretical methods for electronic structure and gas-phase state specific oxidation/reduction studies
[AD-A246127] p 2875 N92-26687
Fracture of structural ceramics in combined mode 1 and mode 2 loading p 2882 N92-26775
Static, microwave, infrared, and visible permittivity related to chemical structure: N-methylacetamide, N-dimethylacetamide and their mixtures in CCl4 at 32 C
[AD-A246364] p 2991 N92-26940

V

VANDERBILT UNIV., NASHVILLE, TN.
New approaches to studies of exotic nuclei
[DE92-010127] p 2994 N92-26570
Rarefied-flow aerodynamics
[NASA-CR-190452] p 2850 N92-27191

VEGA SPACE SYSTEMS ENGINEERING LTD., HARPENDEN (ENGLAND).
GRABE: A simple graphical back-end for thermal simulation packages p 2958 N92-26961

VIGYAN RESEARCH ASSOCIATES, INC., HAMPTON, VA.
High-alpha vortex decoupling investigations on a chine forebody/Delta wing configuration at transonic Mach numbers
[NASA-CR-189642] p 2849 N92-26651
Subsonic investigations of vortex interaction control for enhanced high-alpha aerodynamics of a chine forebody/Delta wing configuration
[NASA-CR-189641] p 2849 N92-26652

VIRGINIA POLYTECHNIC INST. AND STATE UNIV., BLACKSBURG.
Three-dimensional upwind scheme for solving the Euler equations on unstructured tetrahedral grids p 2849 N92-26585
Parameter robust reduced-order control of flexible structures p 2982 N92-26597
Reliability and failure analyses of composite beams and plates containing stress concentrations p 2918 N92-26598
Observation and measurements of flow structures in the stagnation region of a wing-body junction p 2849 N92-26616
Modeling cycle and time-dependent creep/relaxation effects on fatigue lives of notched members p 2919 N92-26829
A parametric study of the hydrodynamic stability theory of 3-D compressible free shear flows p 2900 N92-26849

VRIJE UNIV., AMSTERDAM (NETHERLANDS).
Hyperspaces of infinite-dimensional compacta
[PB92-149335] p 2986 N92-26367

W

WASHINGTON STATE UNIV., PULLMAN.
Exact solutions for a mode of the electromagnetic field in a resonator with time-dependent characteristics of the internal medium
[AD-A245700] p 2888 N92-26374
Crossovers of the density of states in two-direction double-barrier resonant-tunneling structures
[AD-A246124] p 3005 N92-26684
WASHINGTON UNIV., SAINT LOUIS, MO.
Mesomechanics of viscoplastic metal matrix composites p 2869 N92-26607
Analysis of thermal infrared data acquired over playas: Silver Lake and Deep Springs Lake, California and Lunar Lake, Nevada p 2926 N92-26864
WASHINGTON UNIV., SEATTLE.
Bias robust estimation of scale
[AD-A245698] p 2985 N92-26229
Mesh and torus chaotic routing (updated version)
[AD-A246284] p 2979 N92-26359
Radar scattering as a source of geological information on Venus and Earth p 3019 N92-26778
The Orca Project: Research on high performance parallel computer programming environments
[AD-A234648] p 2980 N92-26801
Stochastic versions of the EM algorithm
[AD-A246929] p 2989 N92-27174
WEIZMANN INST. OF SCIENCE, REHOVOTH (ISRAEL).
Low power laser irradiation effect with emphasis on injured neural tissues
[AD-A246410] p 2953 N92-27063
WESTINGHOUSE ELECTRIC CORP., PITTSBURGH, PA.
Zirconia-based fuel cells for power generation
[DE92-009886] p 2927 N92-26719
WESTINGHOUSE HANFORD CO., RICHLAND, WA.
An investigation of the behavior of the clamp-induced bending stresses
[DE92-006504] p 2918 N92-26694
Improving the fracture resistance of irradiated martensitic steels
[DE92-008387] p 2879 N92-26848
WESTINGHOUSE SAVANNAH RIVER CO., AIKEN, SC.
Distributed visualization
[DE92-009405] p 2971 N92-26188
Materials compatibility and wall stresses in hydride storage beds
[DE92-009432] p 2870 N92-26201
Aging effects in palladium and LaNi(4.25)Al(0.75) tritides
[DE92-009945] p 2870 N92-26217
Gamma-ray spectrometry of LDEF samples
[DE92-009947] p 2874 N92-26632
Gravimetric gas determinations for volume calibrations
[DE92-010041] p 2874 N92-26634
Retention and release of tritium in aluminum clad, Al-Li alloys
[DE92-009905] p 2878 N92-26635
Metal hydride based isotope separation: Large-scale operations
[DE92-009830] p 2875 N92-26717
A new phase in palladium hydride technology
[DE92-009852] p 2875 N92-26718
WICHITA STATE UNIV., KS.
Test plan for the international aircraft operator information system
[DOT/FAA/CT-91/18] p 3014 N92-26830
WILLIAM BEAUMONT ARMY HOSPITAL, EL PASO, TX.
Clinical investigation program, fiscal year 1991
[AD-A246558] p 2992 N92-26618
WILSON GREATBATCH LTD., CLARENCE, NY.
Li/BCX, SVO, and CSC cells: Power sources for aerospace applications p 2864 N92-27147
WISCONSIN UNIV., MADISON.
Water vapor information content of absorption lines observed in the Sun's infrared radiance p 2942 N92-26490
Asymptotic analysis of the vibrations of variable length cantilever beams p 2918 N92-26739
Carbon monoxide metabolism by the photosynthetic bacterium Rhodospirillum rubrum
[DE92-010953] p 2951 N92-26938
On the construction of multivariate (pre)wavelets
[AD-A247105] p 2989 N92-27175
WORCESTER POLYTECHNIC INST., MA.
Band structure and optical properties of semiconductor superlattices
[AD-A246076] p 3005 N92-26763
WORLD METEOROLOGICAL ORGANIZATION, GENEVA (SWITZERLAND).
Report of the CC1 working group on climate change detection
[WCDMP-14] p 2947 N92-26923
CC1 experts meeting on CLIMAT code adaptation
[WCDMP-15] p 2947 N92-26924
Report of the CC1 experts meeting on tracking and transmission of climate system monitoring information
[WCDMP-16] p 2947 N92-26925
WRIGHT LAB., WRIGHT-PATTERSON AFB, OH.
Experiment M0003-4: Advanced solar cell and coverglass analysis, an overview p 2927 N92-27088
WRIGHT STATE UNIV., DAYTON, OH.
Analysis of frozen startup of high-temperature heat pipes and three-dimensional modeling of block-heated heat pipes
[AD-A245327] p 2896 N92-26379
WYOMING UNIV., LARAMIE.
An infrared Michelson stellar interferometer and its applications p 3015 N92-26477

Y

YARDNEY TECHNICAL PRODUCTS, INC., PAWCATUCK, CT.
Development of a 300 Amp-hr high rate lithium thionyl chloride cell p 2864 N92-27149

Z

ZODIAC ESPANOLA S.A., FIGUERAS (SPAIN).
Development of the suit enclosure soft joints of the European EVA space suit p 2965 N92-27005

Typical Contract Number Index Listing

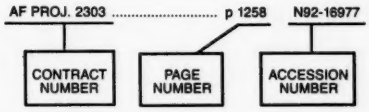

Listings in this index are arranged alphanumerically by contract number. Under each contract number the accession numbers denoting documents that have been produced as a result of research done under that contract are arranged in ascending order. The page number helps to locate the citation in the abstract section. The accession number denotes the number by which the citation is identified.

AF PROJ. 1123 ..... p 2656 N92-26527
AF PROJ. 2304 ..... p 2980 N92-26801
AF PROJ. 7231 ..... p 2955 N92-26528
AF-AFOSR-0033-91 ..... p 2985 N92-27169
AF-AFOSR-0091-90 ..... p 2987 N92-26668
p 2920 N92-26892
AF-AFOSR-0180-91 ..... p 2905 N92-27032
AF-AFOSR-0235-89 ..... p 2850 N92-27172
AF-AFOSR-0282-89 ..... p 2980 N92-26801
AF-AFOSR-0313-88 ..... p 2884 N92-26589
AF-AFOSR-0349-88 ..... p 2913 N92-27173
AF-AFOSR-0384-87 ..... p 2882 N92-26751
AF-4732/4014/89 ..... p 3003 N92-26328
ARB-A832-134 ..... p 2931 N92-26793
ARPA ORDER 7597 ..... p 2981 N92-26357
p 2997 N92-26425
ARPA ORDER 8162 ..... p 2893 N92-26771
A84KL122 ..... p 2890 N92-26872
A88KM637 ..... p 2932 N92-26873
A89KL641 ..... p 2890 N92-26874
A89KL661 ..... p 2944 N92-26877
DA PROJ. 1L1-62211-A-47-A ..... p 2915 N92-26555
p 2915 N92-26560
DA PROJ. 3M1-62787-A-878 ..... p 2953 N92-27063
DA PROJ. 4A1-61102-AT-24 ..... p 2922 N92-26674
DA PROJ. 4A7-62784-AT-42 ..... p 2869 N92-26796
DAAL03-87-K-0105 ..... p 2874 N92-26541
DAAL03-87-K-0138 ..... p 2894 N92-26942
DAAL03-87-K-0140 ..... p 2992 N92-26413
DAAL03-89-K-0148 ..... p 2991 N92-26940
DAAL03-90-G-0090 ..... p 2989 N92-27175
DAAL04-86-C-0023 ..... p 2876 N92-26172
DACA76-89-C-0014 ..... p 2851 N92-26427
DAEA18-90-C-0044 ..... p 2954 N92-26179
DAMD17-90-Z-0008 ..... p 2953 N92-27063
DARPA ORDER 3154 ..... p 2999 N92-27098
DE-AC02-76CH-00016 ..... p 2878 N92-26563
p 3020 N92-26566
p 2909 N92-26572
p 2879 N92-26813
p 2995 N92-26815
p 2857 N92-26818
p 2932 N92-26825
p 3006 N92-27059
DE-AC02-76CH-03000 ..... p 2922 N92-26534
DE-AC02-83CH-10093 ..... p 2926 N92-26190
p 2955 N92-26494
p 2927 N92-26683
p 2927 N92-26686
p 2932 N92-26810
DE-AC03-76SF-00098 ..... p 2996 N92-26187
p 2950 N92-26203
p 3001 N92-26204
p 2891 N92-26205
p 2921 N92-26206
p 2993 N92-26207
p 2934 N92-26208
p 2870 N92-26209
p 2870 N92-26212
p 2877 N92-26213
p 2895 N92-26214
p 2871 N92-26220
p 3011 N92-26221
p 3001 N92-26222
p 2985 N92-26232
p 2994 N92-26235
p 2935 N92-26239
p 3019 N92-26385
p 2970 N92-26551
p 3003 N92-26582
p 3003 N92-26584
p 3004 N92-26641
DE-AC03-76SF-00515 ..... p 2887 N92-26267
DE-AC04-76DP-00789 ..... p 2993 N92-26225
p 2892 N92-26238
p 2910 N92-26269
p 2982 N92-26434
p 2997 N92-26452
p 3012 N92-26575
p 2897 N92-26644
p 3000 N92-26666
p 2927 N92-26683
p 2912 N92-26691
p 3000 N92-26695
p 2976 N92-26696
p 2899 N92-26698
p 2899 N92-26716
p 2875 N92-26722
p 3005 N92-26826
p 2919 N92-26846
p 2894 N92-26847
p 2919 N92-26852
p 2900 N92-26853
p 2901 N92-26856
p 2891 N92-26902
DE-AC05-76OR-00033 ..... p 2994 N92-26570
DE-AC05-84OR-21400 ..... p 2913 N92-26219
p 2913 N92-26234
p 2887 N92-26237
p 2955 N92-26375
p 2996 N92-26376
p 2986 N92-26407
p 2955 N92-26494
p 3021 N92-26544
p 2987 N92-26545
p 3000 N92-26549
p 2908 N92-26569
p 2994 N92-26570
p 3000 N92-26577
p 3003 N92-26579
p 2931 N92-26580
p 2893 N92-26636
p 2893 N92-26637
p 3004 N92-26638
p 2983 N92-26657
p 2854 N92-26697
p 2875 N92-26726
p 2915 N92-26750
p 2918 N92-26784
p 3005 N92-26843
p 2919 N92-26845
p 3006 N92-26851
DE-AC06-76RL-01830 ..... p 2979 N92-26277
p 2931 N92-26633
DE-AC06-87RL-10930 ..... p 2918 N92-26694
p 2879 N92-26848
DE-AC07-76ID-01570 ..... p 2955 N92-26494
DE-AC09-89SR-18035 ..... p 2971 N92-26188
p 2870 N92-26201
p 2870 N92-26217
p 2874 N92-26632
p 2874 N92-26634
p 2878 N92-26635
p 2875 N92-26717
p 2875 N92-26718
DE-AC12-76SN-00052 ..... p 2881 N92-26455
DE-AC22-85BC-10850 ..... p 2971 N92-26189
DE-AC22-90PC-90044 ..... p 2884 N92-26548
DE-AC34-90DP-62349 ..... p 2926 N92-26390
DE-AI04-85AL-33408 ..... p 2880 N92-27192
DE-FC21-86MC-10637 ..... p 2875 N92-26724
DE-FC21-91MC-28055 ..... p 2927 N92-26719
DE-FG02-85ER-13438 ..... p 3004 N92-26639
DE-FG02-85ER-13442 ..... p 2994 N92-26240
DE-FG02-86ER-13554 ..... p 2871 N92-26274
DE-FG02-86ER-13631 ..... p 2927 N92-26858
DE-FG02-87ER-13691 ..... p 2951 N92-26938
DE-FG02-87ER-45295 ..... p 2877 N92-26251
DE-FG02-89ER-45381 ..... p 3004 N92-26648
DE-FG02-90ER-60943 ..... p 2928 N92-26231
DE-FG02-91ER-61190 ..... p 3011 N92-26453
DE-FG02-91ER-61218 ..... p 2944 N92-26937
DE-FG03-85ER-13445 ..... p 2881 N92-26451
DE-FG03-88ER-13826 ..... p 2951 N92-26493
DE-FG03-88ER-13857 ..... p 2872 N92-26281
DE-FG03-88ER-53275 ..... p 2999 N92-26256
DE-FG05-80ET-53088 ..... p 2999 N92-26256
p 2999 N92-26546
p 3000 N92-26549
p 3000 N92-26550
DE-FG05-86ER-13589 ..... p 2871 N92-26236
DE-FG05-86ER-45280 ..... p 2877 N92-26542
DE-FG05-88ER-13865 ..... p 3006 N92-26851
DE-FG05-88ER-13971 ..... p 2995 N92-26574
DE-FG05-88ER-40407 ..... p 2994 N92-26570
DE-FG05-88ER-45345 ..... p 2881 N92-26543
p 2883 N92-27060
DE-FG07-88ER-12822 ..... p 2899 N92-26699
p 2899 N92-26700
DE-FG22-89PC-89769 ..... p 2896 N92-26456
DE-FG22-89PC-89786 ..... p 2883 N92-26547
DE-FG22-91PC-91304 ..... p 2873 N92-26457
DTFA03-89-C-00057 ..... p 3014 N92-26830
EEC-991 ..... p 2892 N92-26249
EPA-68-C8-0006 ..... p 2930 N92-26509
EPA-68-C8-0062 ..... p 2930 N92-26495
EPA-68-DO-0125 ..... p 2932 N92-26823
EPA-68-D1-0115 ..... p 2928 N92-26373
ESTEC-8757/90/NL/PP(SC) ..... p 2905 N92-27027
F19628-86-K-0012 ..... p 2893 N92-26540
F19628-88-D-0031 ..... p 2978 N92-27177
F30602-88-D-0026 ..... p 2998 N92-26943
F30602-88-D-0027 ..... p 3001 N92-26226
F33615-86-C-2720 ..... p 2896 N92-26379
F33615-88-C-1720 ..... p 3009 N92-26863
F33615-89-C-0532 ..... p 2955 N92-26355
F33615-90-C-1465 ..... p 2981 N92-26357
p 2973 N92-26384
p 2997 N92-26425
F49620-86-C-0008 ..... p 2954 N92-26193
F49620-91-C-0046 ..... p 2870 N92-26882
GRI-5084-260-1081 ..... p 2926 N92-26372
GRI-5086-233-1262 ..... p 2915 N92-26816
GRI-5087-234-1608 ..... p 2873 N92-26521
GRI-5088-260-1671 ..... p 2914 N92-26371
GRI-5089-260-1912 ..... p 2876 N92-26782
GRI-5090-260-1973 ..... p 2872 N92-26351
GRI-5090-260-2005 ..... p 2873 N92-26508
GRI-5090-260-2014 ..... p 2876 N92-26783
GRI-5091-260-2184 ..... p 2873 N92-26516
IOP-IC-45-009 ..... p 2892 N92-26249
JPL-953613 ..... p 3019 N92-26819
MDA903-86-C-0059 ..... p 2856 N92-26192
MDA903-89-C-0003 ..... p 2850 N92-26272
p 2972 N92-26273
p 2880 N92-26275
p 2972 N92-26276
MDA903-90-C-0006 ..... p 3013 N92-26767
MDA972-91-C-0032 ..... p 2893 N92-26771
NAGW-1175 ..... p 2982 N92-26429
NAGW-1677 ..... p 3019 N92-26247
NAGW-2261 ..... p 3020 N92-26437
NAGW-2381 ..... p 3016 N92-26436
NAGW-533 ..... p 3019 N92-26438
NAG1-1116 ..... p 2987 N92-26668
p 2920 N92-26892
NAG1-115 ..... p 2940 N92-26341
NAG1-757 ..... p 2913 N92-26870
NAG1-921 ..... p 2850 N92-27191
NAG1-991 ..... p 2852 N92-26655
NAG2-628 ..... p 2981 N92-27183
NAG5-1204 ..... p 3015 N92-26184
NAG5-1528 ..... p 2945 N92-26474
p 2946 N92-26735
p 2946 N92-26736
NAG8-708 ..... p 2908 N92-26536
NAG8-881 ..... p 2944 N92-26185

NAG9-342 ..... p 2952 N92-26263
NASA ORDER T-9317R ..... p 2858 N92-26884
NASW-17214 ..... p 2933 N92-26878
NASW-17384 ..... p 2937 N92-26311
NASW-4435 ..... p 2852 N92-26435
NAS1-15350 ..... p 2910 N92-27109
NAS1-18107 ..... p 2987 N92-26668
NAS1-18224 ..... p 2916 N92-27114
p 2880 N92-27115
NAS1-18240 ..... p 2898 N92-26680
p 2898 N92-26681
NAS1-18584 ..... p 2878 N92-26642
p 2886 N92-26656
NAS1-18605 ..... p 2898 N92-26649
p 2987 N92-26668
p 2901 N92-26883
p 2905 N92-27032
NAS1-18856 ..... p 2849 N92-26651
p 2849 N92-26652
NAS1-19061 ..... p 2853 N92-26405
NAS1-19224 ..... p 2895 N92-27112
NAS2-11555 ..... p 2985 N92-27057
NAS2-12952 ..... p 2985 N92-27057
NAS2-13210 ..... p 2984 N92-26885
NAS2-13260 ..... p 2961 N92-26980
NAS3-25266 ..... p 2861 N92-27033
NAS3-25958 ..... p 2910 N92-27109
NAS5-31889 ..... p 2945 N92-26535
NAS7-918 ..... p 2926 N92-27195
NAS8-39121 ..... p 2993 N92-26200
NAS8-50000 ..... p 2957 N92-26953
NAS9-17900 ..... p 2956 N92-26538
p 2956 N92-26682
p 2968 N92-27021
NATO-RG-85-0240 ..... p 2986 N92-26420
NCC2-297 ..... p 3001 N92-26265
NCC2-371 ..... p 2994 N92-26539
NCC2-537 ..... p 2984 N92-26885
NCC3-206 ..... p 2886 N92-26611
NCC3-233 ..... p 2989 N92-27196
NCC9-16 ..... p 2971 N92-26181
p 2971 N92-26182
p 2971 N92-26183
p 2972 N92-26197
p 2972 N92-26198
p 2978 N92-26199
p 3009 N92-26552
NIOSH-R01-OH-02373 ..... p 2953 N92-26512
NPSOR-92-010 ..... p 2989 N92-26177
NR PROJ. RM3-5-G-87 ..... p 2926 N92-27070
NR PROJ. RR0-3103 ..... p 2950 N92-27069
NR PROJ. R10-300 ..... p 2974 N92-26464
NSF ATM-89-18879 ..... p 2940 N92-26341
NSF DMS-88-18530 ..... p 2920 N92-26892
NSF DMS-90-00053 ..... p 2989 N92-27175
NSF INT-90-08726 ..... p 2984 N92-26791
NSF PHY-89-18388 ..... p 3016 N92-26436
N00014-72-C-0057 ..... p 2956 N92-26665
N00014-80-C-0193 ..... p 2956 N92-26665
N00014-87-WR-24018 ..... p 2950 N92-27069
N00014-88-K-0299 ..... p 2890 N92-26764
N00014-88-K-0629 ..... p 2897 N92-26591
N00014-89-J-1007 ..... p 2892 N92-26280
N00014-89-J-1237 ..... p 2872 N92-26431
p 2874 N92-26526
p 2874 N92-26608
N00014-89-J-1364 ..... p 2942 N92-26432
p 2947 N92-26901
p 2905 N92-26934
N00014-89-J-1497 ..... p 2875 N92-26687
N00014-89-J-1639 ..... p 2948 N92-26245
N00014-89-J-1754 ..... p 2943 N92-26675
N00014-89-J-1755 ..... p 2995 N92-26588
N00014-89-J-1967 ..... p 2991 N92-26772
N00014-89-J-2038 ..... p 3005 N92-26763
N00014-89-J-3087 ..... p 2914 N92-26389
N00014-90-J-1023 ..... p 2991 N92-26175
N00014-90-J-1193 ..... p 2888 N92-26374
p 3005 N92-26684
N00014-90-J-1218 ..... p 2986 N92-26414
N00014-90-J-1487 ..... p 2940 N92-26335
N00014-90-J-1598 ..... p 2896 N92-26412
N00014-90-J-1737 ..... p 2949 N92-26411
N00014-90-J-4010 ..... p 2948 N92-26173
N00014-91-C-0150 ..... p 2912 N92-26663
N00014-91-C-0222 ..... p 2913 N92-27178
N00014-91-J-1074 ..... p 2985 N92-26229
p 2989 N92-27174
N00014-91-J-1219 ..... p 2979 N92-26279
N00014-91-J-1329 ..... p 2980 N92-26430
N00014-91-J-1369 ..... p 2976 N92-26685
N00014-91-J-1414 ..... p 2879 N92-26939
N00014-91-J-4041 ..... p 2979 N92-26359
N00019-88-C-0051 ..... p 2911 N92-26293
N00123-89-G-0580 ..... p 2877 N92-26520
p 2975 N92-26524
RICIS PROJ. SE-35 ..... p 2978 N92-26199
RICIS PROJ. SE-41 ..... p 2971 N92-26181
p 2971 N92-26182
p 2971 N92-26183
RICIS PROJ. SR-01 ..... p 2972 N92-26197
p 2972 N92-26198
RTOP 196-88-00-03 ..... p 3022 N92-27083
RTOP 505-62-20 ..... p 2855 N92-27037
RTOP 505-62-21 ..... p 2989 N92-27196
RTOP 505-62-52 ..... p 2898 N92-26690
RTOP 505-62-71 ..... p 2854 N92-26613
RTOP 505-63-36 ..... p 2915 N92-26555
p 2915 N92-26560
RTOP 505-63-50-03 ..... p 2883 N92-27194
RTOP 505-64-20-54 ..... p 2889 N92-26653
RTOP 505-64-70-01 ..... p 2891 N92-27189
RTOP 505-68-10 ..... p 2849 N92-26612
RTOP 505-68-30-03 ..... p 2849 N92-26651
p 2849 N92-26652
RTOP 505-90-52-01 ..... p 2898 N92-26649
p 2987 N92-26668
p 2901 N92-26883
p 2905 N92-27032
RTOP 505-90-53 ..... p 2990 N92-26671
RTOP 506-41-21 ..... p 2875 N92-26670
RTOP 506-43-31-05 ..... p 2905 N92-27193
RTOP 537-02-02 ..... p 2854 N92-26553
RTOP 537-02-20 ..... p 2854 N92-26561
RTOP 537-03-23-03 ..... p 2898 N92-26680
p 2898 N92-26681
RTOP 549-02-41-50 ..... p 2886 N92-26656
RTOP 578-41-29-03 ..... p 2933 N92-26878
RTOP 590-13-11 ..... p 2861 N92-26654
p 2861 N92-27034
p 2880 N92-27192
RTOP 590-14-31-01 ..... p 2920 N92-26903
RTOP 590-14-61-01 ..... p 2917 N92-26537
RTOP 590-21-21 ..... p 2861 N92-27035
p 2861 N92-27036
RTOP 593-12-21 ..... p 2861 N92-27033
RTOP 593-42-21-01 ..... p 2996 N92-26832
RTOP 593-71-00 ..... p 2861 N92-26792
RTOP 674-22-05 ..... p 2886 N92-27197
RTOP 694-03-00 ..... p 2886 N92-26611
RTOP 694-80-70-01 ..... p 2878 N92-26642
SBA-3070-OA-88 ..... p 3009 N92-26523
W-31-109-ENG-38 ..... p 3001 N92-26210
p 3020 N92-26211
p 3021 N92-26215
p 3021 N92-26216
p 3021 N92-26218
p 3021 N92-26253
p 3021 N92-26264
p 2955 N92-26494
p 2997 N92-26565
p 2869 N92-26679
p 2996 N92-26841
p 3005 N92-26842
W-7405-ENG-36 ..... p 2891 N92-26202
p 2911 N92-26573
p 2995 N92-26692
p 2857 N92-26693
p 2856 N92-26720
p 2981 N92-26854
p 2900 N92-26855
p 2901 N92-26856
p 3006 N92-26857
p 2876 N92-26867
W-7405-ENG-48 ..... p 2877 N92-26223
p 2892 N92-26224
p 2906 N92-26230
p 2972 N92-26233
p 2948 N92-26270
p 2906 N92-26377
p 2873 N92-26454
p 2911 N92-26504
p 2911 N92-26505
p 2898 N92-26645
p 2912 N92-26646
p 2975 N92-26647
p 3000 N92-26729
p 2878 N92-26732
p 2976 N92-26797
p 2934 N92-26935
p 2934 N92-26936
W-7405-ENG-82 ..... p 2878 N92-26727

Typical Report Number Index Listing

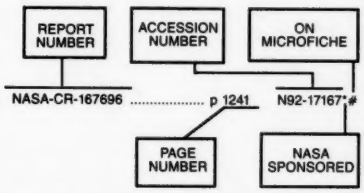

Listings in this index are arranged alphanumerically by report number. The accession number denotes the number by which the citation is identified. The page number helps to locate the citation in the abstract section. An asterisk (*) indicates that the item is a NASA report. A pound sign (#) indicates that the item is available on microfiche.

AC/243(PANEL 8)TR/1 ..... p 2970 N92-27179 #
AC/243-N/347 ..... p 3010 N92-26174 #

AD-A234648 ..... p 2980 N92-26801 #
AD-A234900 ..... p 3010 N92-27190 #
AD-A245299 ..... p 2882 N92-26751 #
AD-A245309 ..... p 3001 N92-26226 #
AD-A245324 ..... p 3011 N92-26378 #
AD-A245327 ..... p 2896 N92-26379 #
AD-A245370 ..... p 2890 N92-26876
AD-A245382 ..... p 2890 N92-26872
AD-A245387 ..... p 2884 N92-26839 #
AD-A245388 ..... p 2977 N92-26840 #
AD-A245389 ..... p 2972 N92-26248 #
AD-A245394 ..... p 2950 N92-26289 #
AD-A245395 ..... p 2867 N92-26380 #
AD-A245413 ..... p 2944 N92-26877
AD-A245422 ..... p 2932 N92-26873
AD-A245425 ..... p 2910 N92-26271 #
AD-A245433 ..... p 2850 N92-26272 #
AD-A245434 ..... p 2972 N92-26273 #
AD-A245437 ..... p 2880 N92-26275 #
AD-A245439 ..... p 2972 N92-26276 #
AD-A245445 ..... p 2979 N92-26278 #
AD-A245446 ..... p 2979 N92-26279 #
AD-A245449 ..... p 2856 N92-26527 #
AD-A245459 ..... p 2955 N92-26528 #
AD-A245461 ..... p 2975 N92-26529 #
AD-A245462 ..... p 2975 N92-26530 #
AD-A245463 ..... p 2853 N92-26405 * #
AD-A245469 ..... p 2980 N92-26531 #
AD-A245474 ..... p 2868 N92-26532 #
AD-A245476 ..... p 2949 N92-26533 #
AD-A245477 ..... p 2949 N92-26423 #
AD-A245481 ..... p 2857 N92-26515 #
AD-A245482 ..... p 2888 N92-26399 #
AD-A245484 ..... p 2973 N92-26400 #
AD-A245486 ..... p 2908 N92-26401 #
AD-A245487 ..... p 3008 N92-27058 #
AD-A245493 ..... p 2922 N92-26674 #
AD-A245495 ..... p 2943 N92-26675 #
AD-A245496 ..... p 2997 N92-26676 #
AD-A245510 ..... p 2980 N92-26677 #
AD-A245517 ..... p 2950 N92-27069 #
AD-A245521 ..... p 2992 N92-26678 #
AD-A245522 ..... p 2976 N92-26658 #
AD-A245523 ..... p 2878 N92-26659 #
AD-A245524 ..... p 3009 N92-26660 #
AD-A245525 ..... p 2922 N92-26661 #
AD-A245527 ..... p 2997 N92-26662 #
AD-A245528 ..... p 2912 N92-26663 #
AD-A245533 ..... p 3022 N92-26664 #
AD-A245543 ..... p 2956 N92-26665 #
AD-A245567 ..... p 2888 N92-26381 #
AD-A245610 ..... p 2978 N92-26227 #
AD-A245613 ..... p 2991 N92-26228 #
AD-A245615 ..... p 2970 N92-26382 #
AD-A245616 ..... p 2867 N92-26383 #
AD-A245617 ..... p 2857 N92-26402 #
AD-A245621 ..... p 2890 N92-26874
AD-A245622 ..... p 3011 N92-26403 #
AD-A245636 ..... p 2892 N92-26280 #
AD-A245641 ..... p 2916 N92-26282 #
AD-A245646 ..... p 2993 N92-26171 #
AD-A245649 ..... p 2876 N92-26172 #
AD-A245650 ..... p 2948 N92-26173 #
AD-A245656 ..... p 3010 N92-26174 #
AD-A245660 ..... p 2991 N92-26175 #
AD-A245675 ..... p 2888 N92-26424 #
AD-A245681 ..... p 2908 N92-26517 #
AD-A245685 ..... p 2877 N92-26520 #
AD-A245686 ..... p 2975 N92-26524 #
AD-A245698 ..... p 2985 N92-26229 #
AD-A245700 ..... p 2888 N92-26374 #
AD-A245707 ..... p 2955 N92-26355 #
AD-A245711 ..... p 2981 N92-26356 #
AD-A245712 ..... p 2981 N92-26357 #
AD-A245713 ..... p 2997 N92-26425 #
AD-A245714 ..... p 3008 N92-26426 #
AD-A245715 ..... p 2851 N92-26427 #
AD-A245716 ..... p 2981 N92-26428 #
AD-A245717 ..... p 2982 N92-26429 * #
AD-A245721 ..... p 2980 N92-26430 #
AD-A245749 ..... p 2946 N92-26562 #
AD-A245752 ..... p 2995 N92-26588 #
AD-A245755 ..... p 2884 N92-26589 #
AD-A245756 ..... p 2897 N92-26591 #
AD-A245758 ..... p 2889 N92-26592 #
AD-A245759 ..... p 2917 N92-26593 #
AD-A245762 ..... p 2889 N92-26595 #
AD-A245763 ..... p 2980 N92-26596 #
AD-A245764 ..... p 2858 N92-26605 #
AD-A245765 ..... p 2893 N92-26606 #
AD-A245781 ..... p 2996 N92-26241 #
AD-A245782 ..... p 2852 N92-26896 #
AD-A245784 ..... p 2971 N92-26195 #
AD-A245786 ..... p 3010 N92-26176 #
AD-A245787 ..... p 2989 N92-26177 #
AD-A245799 ..... p 2894 N92-26897 #
AD-A245804 ..... p 2920 N92-26932 #
AD-A245806 ..... p 2891 N92-26933 #
AD-A245810 ..... p 2887 N92-26898 #
AD-A245812 ..... p 2872 N92-26431 #
AD-A245813 ..... p 2874 N92-26526 #
AD-A245814 ..... p 2874 N92-26608 #
AD-A245816 ..... p 2882 N92-26609 #
AD-A245817 ..... p 2881 N92-26283 #
AD-A245818 ..... p 2883 N92-26178 #
AD-A245819 ..... p 2954 N92-26179 #
AD-A245822 ..... p 2989 N92-26180 #
AD-A245824 ..... p 2946 N92-26899 #
AD-A245825 ..... p 2988 N92-26900 #
AD-A245828 ..... p 2905 N92-26934 #
AD-A245829 ..... p 2947 N92-26901 #
AD-A245855 ..... p 2973 N92-26384 #
AD-A245860 ..... p 2942 N92-26406 * #
AD-A245895 ..... p 2971 N92-26196 #
AD-A245899 ..... p 2872 N92-26404 #
AD-A245903 ..... p 2942 N92-26432 #
AD-A245984 ..... p 2943 N92-26753 #
AD-A245987 ..... p 2997 N92-26754 #
AD-A245991 ..... p 2987 N92-26755 #
AD-A245997 ..... p 2851 N92-26756 #
AD-A245998 ..... p 2976 N92-26758 #
AD-A246001 ..... p 2918 N92-26759 #
AD-A246005 ..... p 3014 N92-26761 #
AD-A246007 ..... p 3013 N92-26762 #
AD-A246076 ..... p 3005 N92-26763 #
AD-A246078 ..... p 2890 N92-26764 #
AD-A246084 ..... p 3013 N92-26765 #
AD-A246090 ..... p 2893 N92-26540 #
AD-A246098 ..... p 2874 N92-26541 #
AD-A246124 ..... p 3005 N92-26684 #
AD-A246126 ..... p 2976 N92-26685 #
AD-A246127 ..... p 2875 N92-26687 #
AD-A246135 ..... p 2986 N92-26358 #
AD-A246136 ..... p 2868 N92-26386 #
AD-A246140 ..... p 2894 N92-27061 #
AD-A246142 ..... p 2926 N92-27070 #
AD-A246143 ..... p 2950 N92-27071 #
AD-A246144 ..... p 2985 N92-27072 #
AD-A246150 ..... p 2852 N92-26408 #
AD-A246152 ..... p 2945 N92-26409 #
AD-A246156 ..... p 2981 N92-26410 #
AD-A246158 ..... p 2949 N92-26411 #
AD-A246160 ..... p 2896 N92-26412 #
AD-A246162 ..... p 2992 N92-26413 #
AD-A246164 ..... p 2986 N92-26414 #
AD-A246165 ..... p 2851 N92-26415 #
AD-A246179 ..... p 2999 N92-26416 #
AD-A246191 ..... p 2979 N92-26417 #
AD-A246193 ..... p 2973 N92-26418 #
AD-A246198 ..... p 2974 N92-26458 #
AD-A246203 ..... p 2908 N92-26459 #
AD-A246207 ..... p 2990 N92-26460 #
AD-A246208 ..... p 2974 N92-26461 #
AD-A246212 ..... p 2911 N92-26462 #
AD-A246219 ..... p 2949 N92-26463 #
AD-A246220 ..... p 2974 N92-26464 #
AD-A246273 ..... p 2954 N92-26242 #
AD-A246275 ..... p 2954 N92-26243 #
AD-A246284 ..... p 2979 N92-26359 #
AD-A246287 ..... p 2948 N92-26360 #
AD-A246289 ..... p 2979 N92-26361 #
AD-A246299 ..... p 2860 N92-26362 #
AD-A246300 ..... p 2888 N92-26363 #
AD-A246301 ..... p 2945 N92-26364 #
AD-A246314 ..... p 2896 N92-26290 #
AD-A246316 ..... p 2851 N92-26291 #
AD-A246317 ..... p 2892 N92-26244 #
AD-A246318 ..... p 2973 N92-26292 #
AD-A246323 ..... p 2948 N92-26245 #
AD-A246326 ..... p 2949 N92-26387 #
AD-A246333 ..... p 2888 N92-26388 #
AD-A246334 ..... p 2914 N92-26389 #
AD-A246349 ..... p 2895 N92-26258 #
AD-A246352 ..... p 2911 N92-26293 #
AD-A246356 ..... p 2850 N92-26947 #
AD-A246362 ..... p 2879 N92-26939 #
AD-A246364 ..... p 2991 N92-26940 #
AD-A246365 ..... p 2891 N92-26941 #
AD-A246368 ..... p 2894 N92-26942 #
AD-A246369 ..... p 2998 N92-26943 #
AD-A246372 ..... p 2856 N92-27062 #
AD-A246374 ..... p 2913 N92-27050 #
AD-A246375 ..... p 3015 N92-27051 #
AD-A246378 ..... p 2977 N92-27052 #
AD-A246380 ..... p 2978 N92-27073 #
AD-A246381 ..... p 2859 N92-27074 #
AD-A246383 ..... p 2947 N92-27075 #
AD-A246385 ..... p 2993 N92-27076 #
AD-A246387 ..... p 3016 N92-27077 #
AD-A246389 ..... p 2991 N92-27078 #
AD-A246395 ..... p 2895 N92-27079 #
AD-A246410 ..... p 2953 N92-27063 #
AD-A246412 ..... p 3006 N92-27064 #
AD-A246416 ..... p 2862 N92-27065 #
AD-A246423 ..... p 2921 N92-27066 #
AD-A246427 ..... p 2880 N92-27067 #
AD-A246435 ..... p 2852 N92-26948 #
AD-A246436 ..... p 2977 N92-26949 #
AD-A246437 ..... p 2950 N92-27029 #
AD-A246439 ..... p 2859 N92-27030 #
AD-A246442 ..... p 2992 N92-27031 #
AD-A246500 ..... p 3011 N92-26465 #
AD-A246502 ..... p 2990 N92-26466 #
AD-A246506 ..... p 2989 N92-26467 #
AD-A246522 ..... p 2974 N92-26468 #
AD-A246527 ..... p 3012 N92-26469 #
AD-A246529 ..... p 2952 N92-26470 #
AD-A246533 ..... p 2990 N92-26471 #
AD-A246534 ..... p 2888 N92-26419 #
AD-A246535 ..... p 2955 N92-26472 #
AD-A246548 ..... p 2992 N92-26688 #
AD-A246557 ..... p 3007 N92-26617 #
AD-A246558 ..... p 2992 N92-26618 #
AD-A246560 ..... p 2990 N92-26768 #
AD-A246561 ..... p 2893 N92-26741 #
AD-A246562 ..... p 2991 N92-26769 #
AD-A246563 ..... p 2909 N92-26794 #
AD-A246566 ..... p 2889 N92-26619 #

AD-A246570 ..... p 2987 N92-26620 #
AD-A246577 ..... p 2858 N92-26621 #
AD-A246579 ..... p 2893 N92-26771 #
AD-A246580 ..... p 2991 N92-26772 #
AD-A246597 ..... p 2970 N92-26773 #
AD-A246598 ..... p 2852 N92-26795 #
AD-A246602 ..... p 2869 N92-26796 #
AD-A246612 ..... p 2976 N92-26766 #
AD-A246614 ..... p 3013 N92-26767 #
AD-A246919 ..... p 3008 N92-27171 #
AD-A246929 ..... p 2989 N92-27174 #
AD-A246999 ..... p 2870 N92-26882 #
AD-A247102 ..... p 3009 N92-26863 #
AD-A247105 ..... p 2989 N92-27175 #
AD-A247146 ..... p 2989 N92-27180 #
AD-A247147 ..... p 2910 N92-27181 #
AD-A247148 ..... p 2991 N92-27182 #
AD-A247204 ..... p 2985 N92-27169 #
AD-A247207 ..... p 2850 N92-27172 #
AD-A247208 ..... p 2913 N92-27173 #
AD-A247254 ..... p 2895 N92-27176 #
AD-A247268 ..... p 2978 N92-27177 #
AD-A247282 ..... p 2913 N92-27178 #
AD-A247346 ..... p 2970 N92-27179 #

AD-D015189 ..... p 2909 N92-26879
AD-D015190 ..... p 2884 N92-26880
AD-D015196 ..... p 3003 N92-26433 #
AD-D015200 ..... p 2997 N92-26862 #
AD-D015209 ..... p 2894 N92-26881
AD-D015214 ..... p 2993 N92-27184
AD-D015215 ..... p 2853 N92-27185 #
AD-D015218 ..... p 2998 N92-27186
AD-D015219 ..... p 2883 N92-27187
AD-D015237 ..... p 2853 N92-27188

AD-E040167 ..... p 2985 N92-27072 #
AD-E040172 ..... p 2926 N92-27070 #
AD-E040175 ..... p 2950 N92-27071 #
AD-E040177 ..... p 2949 N92-26463 #
AD-E040179 ..... p 2974 N92-26464 #
AD-E501456 ..... p 2972 N92-26273 #
AD-E501463 ..... p 2880 N92-26275 #
AD-E501470 ..... p 2850 N92-26272 #
AD-E501471 ..... p 2972 N92-26276 #
AD-E951742 ..... p 2945 N92-26409 #
AD-E951752 ..... p 2852 N92-26408 #

AEDC-TR-91-20 ..... p 2853 N92-26405 * #

AEROCHEM-TP-497 ..... p 2876 N92-26783 #

AFIT/EN-TM-91-1-VOL-2 ..... p 2888 N92-26381 #

AFOSR-91-0263TR ..... p 2980 N92-26801 #
AFOSR-92-0086TR ..... p 2850 N92-27172 #
AFOSR-92-0093TR ..... p 2913 N92-27173 #
AFOSR-92-0118TR ..... p 2985 N92-27169 #

AIAA PAPER 92-0413 ..... p 2849 N92-26612 * #
AIAA PAPER 92-3087 ..... p 2854 N92-26561 * #
AIAA PAPER 92-3792 ..... p 2854 N92-26613 * #

AIAA-92-3083 ..... p 2855 N92-27037 * #
AIAA-92-3164 ..... p 2861 N92-27033 * #
AIAA-92-3226 ..... p 2861 N92-27036 * #
AIAA-92-3228 ..... p 2861 N92-27035 * #

AL-TR-1991-0018 ..... p 2955 N92-26355 #
AL-TR-1991-0039 ..... p 2856 N92-26527 #
AL-TR-1991-0079 ..... p 2955 N92-26528 #

AMSMI/TR-RD-GC-91-6 ..... p 2852 N92-26408 #

AMSMI/TR-RD-WS-91-9 ..... p 2945 N92-26409 #

ANL/CP-73148 ..... p 2996 N92-26841 #
ANL/CP-73280 ..... p 2869 N92-26679 #
ANL/CP-74854 ..... p 3005 N92-26842 #
ANL/CP-75188 ..... p 3001 N92-26210 #
ANL/CP-75618 ..... p 2997 N92-26565 #

ANL/HEP/CP-91-112 ..... p 3021 N92-26218 #
ANL/HEP/CP-91-115 ..... p 3021 N92-26216 #
ANL/HEP/CP-91-116 ..... p 3021 N92-26215 #
ANL/HEP/CP-91-117 ..... p 3020 N92-26211 #
ANL/HEP/CP-91-118 ..... p 3021 N92-26264 #
ANL/HEP/CP-91-119 ..... p 3021 N92-26253 #

ARB-R-92-478 ..... p 2931 N92-26793 #

ARCCB-TR-91035 ..... p 2916 N92-26282 #

ARL-FLIGHT-MECH-TM-437 ..... p 2850 N92-26947 #

ARL-STRUC-TM-527 ..... p 2895 N92-26258 #

ARL-TR-91-20 ..... p 2989 N92-26180 #
ARL-TR-91-8 ..... p 2991 N92-26772 #

ARO-25199.3-MS ..... p 2874 N92-26541 #
ARO-25273.6-PH ..... p 2992 N92-26413 #
ARO-26636.2-CH ..... p 2991 N92-26940 #

ASL-TMR-0011 ..... p 2946 N92-26899 #

AVSCOM-TR-91-C-035 ..... p 2915 N92-26560 * #
AVSCOM-TR-91-C-038 ..... p 2915 N92-26555 * #

B-248197 ..... p 3009 N92-26828 #

BNL-45092 ..... p 2879 N92-26813 #
BNL-46287-REV ..... p 2857 N92-26818 #
BNL-47110 ..... p 2932 N92-26825 #
BNL-47115 ..... p 2995 N92-26815 #
BNL-47128 ..... p 3006 N92-27059 #
BNL-47155 ..... p 3020 N92-26566 #
BNL-47180 ..... p 2878 N92-26563 #
BNL-47194 ..... p 2909 N92-26572 #

CERC-WIS-26 ..... p 2949 N92-26387 #

CESAR-91/24 ..... p 2987 N92-26545 #
CESAR-92/09 ..... p 2913 N92-26219 #

CMS-TSR-92-09 ..... p 2989 N92-27175 #

CMU-RI-TR-91-21 ..... p 3008 N92-26426 #
CMU-RI-TR-91-24 ..... p 2981 N92-26357 #
CMU-RI-TR-91-26 ..... p 2997 N92-26425 #
CMU-RI-TR-91-27 ..... p 2982 N92-26429 * #
CMU-RI-TR-91-28 ..... p 2851 N92-26427 #
CMU-RI-TR-91-29 ..... p 2973 N92-26384 #
CMU-RI-TR-91-30 ..... p 2981 N92-26428 #
CMU-RI-TR-91-33 ..... p 2981 N92-26356 #

CONF-910422-8 ..... p 2873 N92-26454 #
CONF-910422-9 ..... p 2870 N92-26212 #
CONF-9104246-2 ..... p 2870 N92-26201 #
CONF-9104435-94 ..... p 2895 N92-26214 #
CONF-9105317-1 ..... p 2898 N92-26645 #
CONF-9105319-1 ..... p 3020 N92-26566 #
CONF-9106105-1 ..... p 2993 N92-26207 #
CONF-9106224-3 ..... p 2891 N92-26205 #
CONF-9106275-6 ..... p 2877 N92-26213 #
CONF-9107146-4 ..... p 3001 N92-26204 #
CONF-910774-102 ..... p 2874 N92-26634 #
CONF-9108118-46 ..... p 2891 N92-26202 #
CONF-9108141-4 ..... p 3021 N92-26264 #
CONF-9108141-5 ..... p 3021 N92-26253 #
CONF-9108141-6 ..... p 3021 N92-26215 #
CONF-9108141-7 ..... p 3021 N92-26216 #
CONF-9108141-8 ..... p 3021 N92-26218 #
CONF-9108141-9 ..... p 3020 N92-26211 #
CONF-9108191 ..... p 2996 N92-26187 #
CONF-9108202-1 ..... p 2972 N92-26233 #
CONF-910854-3 ..... p 2883 N92-27060 #
CONF-910920-19 ..... p 2870 N92-26217 #
CONF-910920-22 ..... p 2875 N92-26717 #
CONF-910920-25 ..... p 2875 N92-26718 #
CONF-910920-27 ..... p 2878 N92-26635 #
CONF-9109230-11 ..... p 2996 N92-26376 #
CONF-9109276-9 ..... p 2971 N92-26188 #
CONF-9109332-4 ..... p 2994 N92-26570 #
CONF-9109340-3 ..... p 2931 N92-26580 #
CONF-910938-9 ..... p 2881 N92-26455 #
CONF-910968-73 ..... p 2906 N92-26377 #
CONF-910968-76 ..... p 2892 N92-26224 #
CONF-910968-77 ..... p 2906 N92-26230 #
CONF-911047-20 ..... p 2878 N92-26563 #
CONF-911106-90 ..... p 2970 N92-26551 #
CONF-911109-9 ..... p 3005 N92-26826 #
CONF-911208-7 ..... p 2995 N92-26815 #
CONF-920104-6-REV ..... p 2857 N92-26818 #
CONF-920124-13 ..... p 2911 N92-26505 #
CONF-920124-14 ..... p 2911 N92-26504 #
CONF-920141-3 ..... p 3005 N92-26842 #
CONF-920141-4 ..... p 3006 N92-27059 #
CONF-920141-6 ..... p 3003 N92-26584 #
CONF-920168-2 ..... p 2894 N92-26847 #
CONF-920212-2 ..... p 2997 N92-26565 #
CONF-920237-2 ..... p 2887 N92-26267 #
CONF-920240-2 ..... p 3001 N92-26210 #
CONF-920263-1 ..... p 2955 N92-26375 #
CONF-920290-VOL-1 ..... p 2927 N92-26683 #
CONF-920308-16 ..... p 2996 N92-26841 #
CONF-920309-1 ..... p 3004 N92-26638 #
CONF-9203102-1 ..... p 2927 N92-26719 #
CONF-920362-2 ..... p 2993 N92-26225 #
CONF-920362-7 ..... p 2910 N92-26269 #
CONF-920367-6 ..... p 2997 N92-26452 #
CONF-920375-3 ..... p 2913 N92-26234 #
CONF-9204103-1 ..... p 2871 N92-26262 #

CONF-920423-2 ..... p 2908 N92-26569 #
CONF-920458-3 ..... p 2879 N92-26813 #
CONF-920471-3 ..... p 2982 N92-26434 #
CONF-920473-1 ..... p 2955 N92-26494 #
CONF-9205121-2 ..... p 2875 N92-26726 #
CONF-9205128-1 ..... p 2922 N92-26534 #
CONF-920540-13 ..... p 2983 N92-26657 #
CONF-920540-5 ..... p 2915 N92-26750 #
CONF-920581-1 ..... p 2893 N92-26636 #
CONF-920605-1 ..... p 2912 N92-26691 #
CONF-920605-2 ..... p 2899 N92-26698 #
CONF-920605-3 ..... p 2934 N92-26936 #
CONF-920605-4 ..... p 2934 N92-26935 #
CONF-920606-2 ..... p 2981 N92-26854 #
CONF-920607-1 ..... p 3000 N92-26695 #
CONF-920607-2 ..... p 3000 N92-26729 #
CONF-9206101-1 ..... p 2976 N92-26696 #
CONF-9206102-1 ..... p 2891 N92-26902 #
CONF-9206102-2 ..... p 2986 N92-26407 * #
CONF-9206129-2 ..... p 2878 N92-26732 #
CONF-9206134-1 ..... p 3000 N92-26666 #
CONF-9206135-1 ..... p 2878 N92-26727 #
CONF-9206136-1 ..... p 2975 N92-26647 #
CONF-9206137-1 ..... p 2912 N92-26646 #
CONF-920624-1 ..... p 2869 N92-26679 #
CONF-920625-2 ..... p 3006 N92-26851 #
CONF-920631-2 ..... p 2899 N92-26699 #
CONF-920631-4 ..... p 2899 N92-26700 #
CONF-920631-6 ..... p 2918 N92-26694 #
CONF-920631-7 ..... p 2854 N92-26697 #
CONF-920631-8 ..... p 2919 N92-26845 #
CONF-920643-1 ..... p 2995 N92-26692 #
CONF-920643-2 ..... p 2875 N92-26724 #
CONF-920648-1-EXTD-ABST ..... p 3005 N92-26843 #
CONF-920662-1 ..... p 3006 N92-26857 #
CONF-920664-1 ..... p 2897 N92-26644 #
CONF-920669-1 ..... p 2875 N92-26722 #
CONF-920669-2 ..... p 2893 N92-26637 #
CONF-920669-3 ..... p 2892 N92-26238 #
CONF-920673-2 ..... p 2879 N92-26848 #
CONF-920678-1 ..... p 2927 N92-26686 #
CONF-920685-1 ..... p 2899 N92-26716 #
CONF-920685-2 ..... p 2901 N92-26856 #
CONF-920688-2 ..... p 2900 N92-26855 #
CONF-920688-3 ..... p 2876 N92-26867 #
CONF-920688-4 ..... p 2919 N92-26852 #
CONF-920688-5 ..... p 2900 N92-26853 #
CONF-920688-6 ..... p 2919 N92-26846 #
CONF-920688-7 ..... p 2856 N92-26720 #
CONF-920689-1 ..... p 2857 N92-26693 #

CRC-TR-1423 ..... p 2973 N92-26292 #

CRC-1438 ..... p 2888 N92-26424 #

CRREL-SR-91-16 ..... p 2922 N92-26674 #
CRREL-SR-91-20 ..... p 2869 N92-26796 #

DE91-014021 ..... p 2869 N92-26679 #
DE92-000070 ..... p 2915 N92-26750 #
DE92-000680 ..... p 2983 N92-26657 #
DE92-001020 ..... p 2971 N92-26189 #
DE92-001199 ..... p 2926 N92-26190 #
DE92-001219 ..... p 2932 N92-26810 #
DE92-001238 ..... p 2927 N92-26683 #
DE92-001240 ..... p 2927 N92-26686 #
DE92-001619 ..... p 3013 N92-26689 #
DE92-002357 ..... p 2912 N92-26691 #
DE92-002930 ..... p 2899 N92-26698 #
DE92-003218 ..... p 2951 N92-26493 #
DE92-004180 ..... p 2899 N92-26699 #
DE92-004181 ..... p 2899 N92-26700 #
DE92-004363 ..... p 2899 N92-26716 #
DE92-004571 ..... p 2995 N92-26692 #
DE92-004575 ..... p 2981 N92-26854 #
DE92-005065 ..... p 2857 N92-26693 #
DE92-006504 ..... p 2918 N92-26694 #
DE92-006528 ..... p 3000 N92-26695 #
DE92-006675 ..... p 2976 N92-26696 #
DE92-006859 ..... p 2854 N92-26697 #
DE92-006911 ..... p 2928 N92-26390 #
DE92-007046 ..... p 2891 N92-26902 #
DE92-007239 ..... p 2955 N92-26494 #
DE92-007241 ..... p 2986 N92-26407 * #
DE92-007322 ..... p 2934 N92-26935 #
DE92-007323 ..... p 2934 N92-26936 #
DE92-007421 ..... p 2900 N92-26855 #
DE92-007428 ..... p 2901 N92-26856 #
DE92-007570 ..... p 3006 N92-26857 #
DE92-007681 ..... p 2955 N92-26375 #
DE92-007713 ..... p 2876 N92-26867 #
DE92-007757 ..... p 2951 N92-26850 #
DE92-007794 ..... p 2918 N92-26784 #
DE92-007828 ..... p 3006 N92-26851 #
DE92-007988 ..... p 2919 N92-26852 #
DE92-008017 ..... p 2900 N92-26853 #

DE92-008097 ..... p 3005 N92-26843 #
DE92-008099 ..... p 2919 N92-26845 #
DE92-008324 ..... p 2919 N92-26846 #
DE92-008326 ..... p 2894 N92-26847 #
DE92-008387 ..... p 2879 N92-26848 #
DE92-008398 ..... p 2881 N92-26451 #
DE92-008437 ..... p 2856 N92-26720 #
DE92-008449 ..... p 2891 N92-26202 #
DE92-008524 ..... p 2875 N92-26722 #
DE92-008604 ..... p 2911 N92-26504 #
DE92-008608 ..... p 2911 N92-26505 #
DE92-008680 ..... p 2997 N92-26452 #
DE92-008709 ..... p 2927 N92-26858 #
DE92-008770 ..... p 2875 N92-26724 #
DE92-008875 ..... p 3011 N92-26453 #
DE92-008900 ..... p 2875 N92-26726 #
DE92-008912 ..... p 2878 N92-26727 #
DE92-008927 ..... p 2972 N92-26233 #
DE92-008937 ..... p 2873 N92-26454 #
DE92-008941 ..... p 3000 N92-26729 #
DE92-008956 ..... p 2881 N92-26455 #
DE92-009011 ..... p 2996 N92-26376 #
DE92-009051 ..... p 2892 N92-26224 #
DE92-009052 ..... p 2878 N92-26732 #
DE92-009053 ..... p 2906 N92-26377 #
DE92-009059 ..... p 3000 N92-26666 #
DE92-009063 ..... p 2993 N92-26225 #
DE92-009066 ..... p 2897 N92-26644 #
DE92-009079 ..... p 2896 N92-26456 #
DE92-009081 ..... p 2873 N92-26457 #
DE92-009121 ..... p 2898 N92-26645 #
DE92-009142 ..... p 2996 N92-26187 #
DE92-009159 ..... p 2878 N92-26563 #
DE92-009379 ..... p 2913 N92-26234 #
DE92-009405 ..... p 2971 N92-26188 #
DE92-009432 ..... p 2870 N92-26201 #
DE92-009487 ..... p 2870 N92-26209 #
DE92-009491 ..... p 2871 N92-26220 #
DE92-009498 ..... p 3011 N92-26221 #
DE92-009501 ..... p 3001 N92-26222 #
DE92-009529 ..... p 2877 N92-26223 #
DE92-009692 ..... p 2912 N92-26646 #
DE92-009695 ..... p 2906 N92-26230 #
DE92-009698 ..... p 2975 N92-26647 #
DE92-009717 ..... p 2996 N92-26841 #
DE92-009724 ..... p 3005 N92-26842 #
DE92-009726 ..... p 2997 N92-26565 #
DE92-009800 ..... p 2976 N92-26797 #
DE92-009812 ..... p 3004 N92-26648 #
DE92-009830 ..... p 2875 N92-26717 #
DE92-009852 ..... p 2875 N92-26718 #
DE92-009886 ..... p 2927 N92-26719 #
DE92-009887 ..... p 2871 N92-26262 #
DE92-009905 ..... p 2878 N92-26635 #
DE92-009945 ..... p 2870 N92-26217 #
DE92-009947 ..... p 2874 N92-26632 #
DE92-010002 ..... p 2913 N92-26219 #
DE92-010027 ..... p 2928 N92-26231 #
DE92-010035 ..... p 2931 N92-26633 #
DE92-010041 ..... p 2874 N92-26634 #
DE92-010045 ..... p 3006 N92-27059 #
DE92-010077 ..... p 3020 N92-26566 #
DE92-010108 ..... p 2893 N92-26636 #
DE92-010110 ..... p 2893 N92-26637 #
DE92-010121 ..... p 2908 N92-26569 #
DE92-010125 ..... p 3004 N92-26638 #
DE92-010127 ..... p 2994 N92-26570 #
DE92-010130 ..... p 3004 N92-26639 #
DE92-010132 ..... p 3009 N92-26811 #
DE92-010133 ..... p 3022 N92-26640 #
DE92-010137 ..... p 2909 N92-26572 #
DE92-010156 ..... p 2879 N92-26813 #
DE92-010158 ..... p 2995 N92-26815 #
DE92-010160 ..... p 2857 N92-26818 #
DE92-010162 ..... p 2932 N92-26825 #
DE92-010254 ..... p 2950 N92-26203 #
DE92-010258 ..... p 3001 N92-26204 #
DE92-010260 ..... p 2891 N92-26205 #
DE92-010262 ..... p 2921 N92-26206 #
DE92-010264 ..... p 2993 N92-26207 #
DE92-010271 ..... p 2934 N92-26208 #
DE92-010281 ..... p 3001 N92-26210 #
DE92-010282 ..... p 3020 N92-26211 #
DE92-010284 ..... p 2870 N92-26212 #
DE92-010285 ..... p 2877 N92-26213 #
DE92-010286 ..... p 3004 N92-26641 #
DE92-010289 ..... p 2931 N92-26580 #
DE92-010299 ..... p 3003 N92-26582 #
DE92-010300 ..... p 2994 N92-26235 #
DE92-010302 ..... p 2895 N92-26214 #
DE92-010305 ..... p 3003 N92-26584 #
DE92-010306 ..... p 2911 N92-26573 #
DE92-010311 ..... p 2877 N92-26542 #
DE92-010317 ..... p 2871 N92-26236 #
DE92-010319 ..... p 2995 N92-26574 #
DE92-010322 ..... p 2935 N92-26239 #
DE92-010327 ..... p 2881 N92-26543 #
DE92-010344 ..... p 3021 N92-26264 #
DE92-010345 ..... p 3021 N92-26253 #
DE92-010346 ..... p 3021 N92-26215 #
DE92-010347 ..... p 3021 N92-26216 #
DE92-010349 ..... p 3021 N92-26218 #
DE92-010360 ..... p 3012 N92-26575 #
DE92-010362 ..... p 3000 N92-26577 #
DE92-010363 ..... p 3003 N92-26579 #
DE92-010365 ..... p 2887 N92-26237 #
DE92-010375 ..... p 3021 N92-26544 #
DE92-010390 ..... p 2987 N92-26545 #
DE92-010424 ..... p 2999 N92-26546 #
DE92-010465 ..... p 2883 N92-26547 #
DE92-010478 ..... p 3019 N92-26385 #
DE92-010479 ..... p 2985 N92-26232 #
DE92-010480 ..... p 2884 N92-26548 #
DE92-010482 ..... p 2922 N92-26534 #
DE92-010547 ..... p 2999 N92-26256 #
DE92-010548 ..... p 3000 N92-26549 #
DE92-010549 ..... p 3000 N92-26550 #
DE92-010550 ..... p 2970 N92-26551 #
DE92-010728 ..... p 2887 N92-26267 #
DE92-010773 ..... p 2910 N92-26269 #
DE92-010777 ..... p 2883 N92-27060 #
DE92-010792 ..... p 2877 N92-26251 #
DE92-010801 ..... p 2892 N92-26238 #
DE92-010805 ..... p 2948 N92-26270 #
DE92-010821 ..... p 2871 N92-26274 #
DE92-010829 ..... p 2979 N92-26277 #
DE92-010923 ..... p 2944 N92-26937 #
DE92-010953 ..... p 2951 N92-26938 #
DE92-011150 ..... p 3005 N92-26826 #
DE92-011159 ..... p 2982 N92-26434 #
DE92-011215 ..... p 2994 N92-26240 #
DE92-011216 ..... p 2872 N92-26281 #
DE92-614353 ..... p 2994 N92-26365 #
DE92-614952 ..... p 2954 N92-26186 #
DE92-617541 ..... p 3004 N92-26672 #
DE92-621066 ..... p 2988 N92-26831 #
DE92-621067 ..... p 2988 N92-26834 #
DE92-621106 ..... p 2976 N92-26835 #
DE92-621113 ..... p 2988 N92-26837 #
DE92-621115 ..... p 2990 N92-26798 #
DE92-621141 ..... p 2890 N92-26799 #
DE92-621167 ..... p 2995 N92-26800 #
DE92-621189 ..... p 3021 N92-26804 #
DE92-621426 ..... p 2995 N92-26844 #
DE92-621523 ..... p 3000 N92-26806 #
DE92-621524 ..... p 3001 N92-26807 #
DE92-621529 ..... p 3001 N92-26808 #
DE92-621553 ..... p 2999 N92-26286 #
DE92-621612 ..... p 2910 N92-26287 #

DLR-FB-91-30 ..... p 2939 N92-26329 #

DODA-AR-006-091 ..... p 2895 N92-26258 #
DODA-AR-006-440 ..... p 2852 N92-26948 #
DODA-AR-006-595 ..... p 2850 N92-26947 #

DOE-92007757 ..... p 2951 N92-26850 #

DOE/BC-10850/19 ..... p 2971 N92-26189 #

DOE/ER-0504 ..... p 3009 N92-26811 #
DOE/ER-0505 ..... p 3022 N92-26640 #
DOE/ER-0535P ..... p 3013 N92-26689 #
DOE/ER-13438/3 ..... p 3004 N92-26639 #
DOE/ER-13442/6 ..... p 2994 N92-26240 #
DOE/ER-13445/T1 ..... p 2881 N92-26451 #
DOE/ER-13554/6 ..... p 2871 N92-26274 #
DOE/ER-13589/4 ..... p 2871 N92-26236 #
DOE/ER-13631/18 ..... p 2927 N92-26858 #
DOE/ER-13691/T2 ..... p 2951 N92-26938 #
DOE/ER-13828/4 ..... p 2951 N92-26493 #
DOE/ER-13857/T2 ..... p 2872 N92-26281 #
DOE/ER-13971/13 ..... p 2995 N92-26574 #
DOE/ER-45280/T3 ..... p 2877 N92-26542 #
DOE/ER-45295/2 ..... p 2877 N92-26251 #
DOE/ER-45345/T1 ..... p 2881 N92-26543 #
DOE/ER-45381/3 ..... p 3004 N92-26648 #
DOE/ER-60943/1 ..... p 2928 N92-26231 #
DOE/ER-61190/1 ..... p 3011 N92-26453 #
DOE/ER-61218/1 ..... p 2944 N92-26937 #

DOE/ET-53088/537 ..... p 2999 N92-26256 #
DOE/ET-53088/539 ..... p 3000 N92-26549 #
DOE/ET-53088/542 ..... p 3000 N92-26550 #
DOE/ET-53088/543 ..... p 2999 N92-26546 #

DOE/MC-10637/92/C0002 ..... p 2875 N92-26724 #
DOE/MC-28055/92/C0001 ..... p 2927 N92-26719 #

DOE/METC-C/92/7006 ..... p 2871 N92-26262 #

DOE/NASA/33408-6 ..... p 2880 N92-27192 * #

DOE/PC-89769/T8 ..... p 2896 N92-26456 #
DOE/PC-89786/T8 ..... p 2883 N92-26547 #
DOE/PC-90044/5 ..... p 2884 N92-26548 #
DOE/PC-91304/T1 ..... p 2873 N92-26457 #

DOT/FAA/CT-91/18 ..... p 3014 N92-26830 #

DREO-TN-91-11 ..... p 3011 N92-26378 #
DREO-TN-91-28 ..... p 2990 N92-26471 #

DREO-1078 ..... p 2889 N92-26592 #
DREO-1091 ..... p 2851 N92-26291 #
DREO-1096 ..... p 2955 N92-26472 #
DREO-1098 ..... p 2872 N92-26404 #
DREO-1103 ..... p 2888 N92-26419 #
DREO-1108 ..... p 2892 N92-26244 #

DRIC-BR-307984 ..... p 2856 N92-27062 #

E-6777 ..... p 2990 N92-26671 * #
E-6816 ..... p 2886 N92-27197 * #
E-6885 ..... p 2886 N92-26611 * #
E-6950 ..... p 2989 N92-27196 * #
E-6978 ..... p 2880 N92-27192 * #
E-6984 ..... p 2875 N92-26670 * #
E-7015 ..... p 2915 N92-26555 * #
E-7032 ..... p 2915 N92-26560 * #
E-7043 ..... p 2898 N92-26690 * #
E-7063 ..... p 2855 N92-27037 * #
E-7071 ..... p 2861 N92-27034 * #
E-7077 ..... p 2861 N92-26654 * #
E-7083 ..... p 2854 N92-26553 * #
E-7087 ..... p 2854 N92-26561 * #
E-7092 ..... p 2861 N92-26792 * #
E-7108 ..... p 2861 N92-27033 * #
E-7124 ..... p 2854 N92-26613 * #
E-7137 ..... p 2861 N92-27035 * #
E-7147 ..... p 2849 N92-26612 * #
E-7154 ..... p 2861 N92-27036 * #

ECMA-TR/55-ED-2 ..... p 2973 N92-26370 #

EFI-1326-21-91 ..... p 3021 N92-26804 #
EFI-91-70 ..... p 3016 N92-26436 * #

EG-910045 ..... p 2884 N92-26440 #

EOARD-TR-92-01 ..... p 2882 N92-26751 #
EOARD-TR-92-03 ..... p 2884 N92-26589 #

EPA/SW/DK-92/016A ..... p 2932 N92-26823 #

EPA/450/4-91/027 ..... p 2932 N92-26823 #
EPA/520/5-91/025 ..... p 2933 N92-26890 #
EPA/600/A-92/037 ..... p 2930 N92-26510 #
EPA/600/A-92/039 ..... p 2930 N92-26509 #
EPA/600/A-92/047 ..... p 2933 N92-26929 #
EPA/600/A-92/050 ..... p 2933 N92-26928 #
EPA/600/A-92/051 ..... p 2933 N92-26889 #
EPA/600/A-92/052 ..... p 2928 N92-26354 #
EPA/600/R-92/050 ..... p 2910 N92-26930 #
EPA/600/2-91/026 ..... p 2930 N92-26495 #
EPA/600/3-91/074 ..... p 2930 N92-26519 #
EPA/700/R-92/002 ..... p 2944 N92-26838 #

ERC-92038 ..... p 2896 N92-26412 #

ESA-SP-324-VOL-2 ..... p 2956 N92-26950 #
ESA-SP-330 ..... p 2935 N92-26294 #

ETN-92-90774 ..... p 2916 N92-27038 #
ETN-92-90775 ..... p 2855 N92-27039 #
ETN-92-90777 ..... p 2855 N92-27040 #
ETN-92-90778 ..... p 2855 N92-27041 #
ETN-92-90779 ..... p 2855 N92-27042 #
ETN-92-90780 ..... p 2856 N92-27043 #
ETN-92-90781 ..... p 2880 N92-27044 #
ETN-92-90819 ..... p 2905 N92-27045 #
ETN-92-90820 ..... p 2853 N92-26944 #
ETN-92-90823 ..... p 2880 N92-26945 #
ETN-92-90826 ..... p 3018 N92-26946 #
ETN-92-91212 ..... p 2890 N92-26872
ETN-92-91213 ..... p 2932 N92-26873
ETN-92-91217 ..... p 2890 N92-26874
ETN-92-91222 ..... p 3014 N92-26875
ETN-92-91225 ..... p 2890 N92-26876
ETN-92-91227 ..... p 2944 N92-26877
ETN-92-91234 ..... p 3010 N92-27046
ETN-92-91236 ..... p 2953 N92-27047
ETN-92-91249 ..... p 2986 N92-26420
ETN-92-91250 ..... p 2973 N92-26421
ETN-92-91251 ..... p 3011 N92-26422
ETN-92-91263 ..... p 2929 N92-26482 #
ETN-92-91264 ..... p 3001 N92-26320 #
ETN-92-91285 ..... p 2892 N92-26249 #
ETN-92-91286 ..... p 3008 N92-26250 #

ETN-92-91288 ..... p 2877 N92-26252 #
ETN-92-91290 ..... p 2887 N92-26254 #
ETN-92-91291 ..... p 2954 N92-26255 #
ETN-92-91303 ..... p 2871 N92-26257 #
ETN-92-91304 ..... p 2916 N92-26259 #
ETN-92-91305 ..... p 2892 N92-26260 #
ETN-92-91306 ..... p 2871 N92-26261 #
ETN-92-91307 ..... p 2872 N92-26285 #
ETN-92-91356 ..... p 2956 N92-26950 #
ETN-92-91358 ..... p 2970 N92-26439
ETN-92-91359 ..... p 2973 N92-26448
ETN-92-91360 ..... p 2974 N92-26449
ETN-92-91372 ..... p 2974 N92-26450
ETN-92-91389 ..... p 2939 N92-26329 #
ETN-92-91714 ..... p 2935 N92-26294 #
ETN-92-91736 ..... p 2906 N92-26391
ETN-92-98598 ..... p 3018 N92-27048
ETN-92-98599 ..... p 3016 N92-27049
ETN-92-98819 ..... p 2886 N92-26246 #
ETN-92-98850 ..... p 2887 N92-26752 #

F+W-TF-2012 ..... p 2905 N92-27045 #
F+W-TF-2058 ..... p 2853 N92-26944 #

FEL-90-A352 ..... p 2890 N92-26872
FEL-91-A073 ..... p 2932 N92-26873
FEL-91-A161 ..... p 2910 N92-26271 #
FEL-91-A171 ..... p 2890 N92-26874
FEL-91-A286 ..... p 3011 N92-26403 #
FEL-91-B183 ..... p 3014 N92-26875
FEL-91-B234 ..... p 2908 N92-26517 #
FEL-91-B295 ..... p 2890 N92-26876
FEL-91-B335 ..... p 2944 N92-26877

FERMILAB-PUB-91/332-A ..... p 3016 N92-26436 * #

FIA-90-04-06-01 ..... p 2985 N92-27057 * #
FIA-90-09-11-01 ..... p 2984 N92-26893 * #
FIA-90-11-01-01 ..... p 3009 N92-26790 * #
FIA-90-11-05-1 ..... p 2982 N92-26628 * #
FIA-90-12-7-01 ..... p 2988 N92-26894 * #
FIA-91-01 ..... p 2984 N92-26885 * #
FIA-91-04 ..... p 2982 N92-26627 * #
FIA-91-08 ..... p 2983 N92-26643 * #
FIA-91-15 ..... p 2983 N92-26789 * #
FIA-91-22 ..... p 2983 N92-26631 * #
FIA-91-23 ..... p 2984 N92-26888 * #
FIA-91-24 ..... p 2984 N92-27055 * #
FIA-91-28 ..... p 2983 N92-26629 * #
FIA-91-32 ..... p 2983 N92-26630 * #
FIA-92-05 ..... p 3015 N92-26886 * #

FNAL/C-92/58 ..... p 2922 N92-26534 #

FOA-C-30609-3.4 ..... p 2921 N92-26513 #

FTD-ID(RS)T-0574-91 ..... p 3015 N92-27051 #
FTD-ID(RS)T-0688-91 ..... p 2913 N92-27050 #

GAO/NSIAD-92-192 ..... p 3009 N92-26828 #

GR-7670-1317(NP) ..... p 2978 N92-27177 #

GRI-90/0246 ..... p 2914 N92-26371 #
GRI-91/0180 ..... p 2873 N92-26521 #
GRI-91/0290 ..... p 2915 N92-26816 #
GRI-91/0313 ..... p 2876 N92-26782 #
GRI-91/0345 ..... p 2872 N92-26351 #
GRI-91/0383 ..... p 2873 N92-26516 #
GRI-91/0402 ..... p 2876 N92-26783 #
GRI-92/0011 ..... p 2873 N92-26508 #
GRI-92/0066 ..... p 2926 N92-26372 #

GTRI-A8612-001 ..... p 2853 N92-26405 * #

IAEA-CN-43/449 ..... p 2929 N92-26483 #

IC-91/130 ..... p 2994 N92-26365 #
IC-91/346 ..... p 3004 N92-26672 #

ICASE-92-16 ..... p 2901 N92-26883 * #
ICASE-92-17 ..... p 2987 N92-26668 * #
ICASE-92-19 ..... p 2898 N92-26649 * #
ICASE-92-20 ..... p 2905 N92-27032 * #

ICOMP-92-01 ..... p 2989 N92-27196 * #

IDA-D-1033 ..... p 2880 N92-26275 #
IDA-D-1042 ..... p 2972 N92-26276 #

IDA-P-2422 ..... p 2972 N92-26273 #
IDA-P-2590 ..... p 2850 N92-26272 #

IDA/HQ-90-035650 ..... p 2972 N92-26273 #
IDA/HQ-91-38012 ..... p 2850 N92-26272 #
IDA/HQ-91-40225 ..... p 2880 N92-26275 #
IDA/HQ-91-40280 ..... p 2972 N92-26276 #

IFSR-537 ..... p 2999 N92-26256 #
IFSR-539 ..... p 3000 N92-26549 #
IFSR-542 ..... p 3000 N92-26550 #
IFSR-543 ..... p 2999 N92-26546 #

IFT-P-028/91 ..... p 2890 N92-26799 #
IFT-P-031/91 ..... p 2988 N92-26837 #

IFVE-OMVT-91-12 ..... p 2976 N92-26835 #

IFVE-ONF-91-34 ..... p 2995 N92-26800 #

IGBP-REPT-19-ATTACH-10 ..... p 2934 N92-27082

IHES/M/92/1 ..... p 2988 N92-26788 #

IHES/P/91/73 ..... p 3007 N92-26805 #
IHES/P/91/76 ..... p 3018 N92-26833 #
IHES/P/91/93 ..... p 2943 N92-26820 #

INIS-BR-2897 ..... p 2910 N92-26287 #

INIS-MF-13116 ..... p 2999 N92-26286 #
INIS-MF-13134 ..... p 2995 N92-26844 #

INO-TM-3 ..... p 2974 N92-26464 #
INO-TM-5 ..... p 2949 N92-26463 #

INPE-5315-PRE/1712 ..... p 2951 N92-26721 #

IS-M-698 ..... p 2878 N92-26727 #

ISBN-0-16-035933-3 ..... p 3014 N92-26730 #
ISBN-90-370-0056-8 ..... p 2954 N92-26255 #
ISBN-90-6275-721-9 ..... p 2892 N92-26249 #
ISBN-90-6275-722-7 ..... p 2887 N92-26254 #
ISBN-90-6275-732-4 ..... p 2871 N92-26257 #
ISBN-90-9004419-1 ..... p 2900 N92-26836 #
ISBN-90-9004483-3 ..... p 2877 N92-26252 #
ISBN-90-9004609-7 ..... p 3008 N92-26250 #
ISBN-92-9092-138-2 ..... p 2956 N92-26950 #
ISBN-92-9092-162-5 ..... p 2935 N92-26294 #
ISBN-951-22-0472-X ..... p 2893 N92-26497 #
ISBN-951-22-0670-6 ..... p 2986 N92-26502 #
ISBN-951-22-0722-2 ..... p 2909 N92-26786 #
ISBN-951-22-0724-9 ..... p 2896 N92-26496 #
ISBN-951-22-0814-8 ..... p 2975 N92-26500 #
ISBN-951-22-0850-4 ..... p 2879 N92-26787 #
ISBN-951-38-3956-7 ..... p 3001 N92-26320 #
ISBN-951-38-4060-3 ..... p 2929 N92-26482 #

ISSN-0208-5658 ..... p 2914 N92-26284 #
ISSN-0262-5369 ..... p 2974 N92-26450
ISSN-0284-8015 ..... p 2934 N92-27082
ISSN-0289-260X ..... p 2901 N92-26906 #
ISSN-0357-5069 ..... p 3001 N92-26320 #
ISSN-0358-5069 ..... p 2929 N92-26482 #
ISSN-0366-0885 ..... p 2880 N92-26945 #
ISSN-0379-6566 ..... p 2956 N92-26950 #
ISSN-0939-2963 ..... p 2939 N92-26329 #

ISVR-TR-205 ..... p 2956 N92-26891 #

ITF-91-11 ..... p 3001 N92-26808 #
ITF-91-14 ..... p 3000 N92-26806 #

ITP-91-16 ..... p 2990 N92-26798 #
ITP-91-19 ..... p 3001 N92-26807 #

IZF-1991-B-11 ..... p 3010 N92-27046
IZF-1991-B-13 ..... p 2953 N92-27047

JPL-PUBL-90-33 ..... p 2926 N92-27195 * #

JTN-92-80307 ..... p 2901 N92-26906 #
JTN-92-80342 ..... p 2924 N92-26742 #
JTN-92-80345 ..... p 2922 N92-26701 #
JTN-92-80348 ..... p 2884 N92-26440 #

JUEL-2466 ..... p 2880 N92-26945 #

KAERI/RR-976/90 ..... p 2954 N92-26186 #

KAPL-4730 ..... p 2881 N92-26455 #

L-16940 ..... p 2917 N92-26537 * #
L-17013 ..... p 2905 N92-27193 * #
L-17023 ..... p 2883 N92-27194 * #
L-17036 ..... p 2996 N92-26832 * #
L-17042-PT-3 ..... p 3022 N92-27083 * #

LA-UR-91-3988 ..... p 2857 N92-26693 #
LA-UR-91-4157 ..... p 2981 N92-26854 #
LA-UR-91-4177 ..... p 2995 N92-26692 #
LA-UR-92-120 ..... p 2876 N92-26867 #
LA-UR-92-266 ..... p 3006 N92-26857 #
LA-UR-92-356 ..... p 2856 N92-26720 #
LA-UR-92-3 ..... p 2901 N92-26856 #
LA-UR-92-474 ..... p 2891 N92-26202 #
LA-UR-92-49 ..... p 2900 N92-26855 #

LA-12254T ..... p 2911 N92-26573 #

LBL-PUB-696 ..... p 2950 N92-26203 #

LBL-31101 ..... p 2895 N92-26214 #
LBL-31107 ..... p 3019 N92-26385 #
LBL-31158 ..... p 2891 N92-26205 #
LBL-31230 ..... p 2870 N92-26209 #
LBL-31278 ..... p 2871 N92-26220 #
LBL-31377 ..... p 2934 N92-26208 #
LBL-31442 ..... p 2870 N92-26212 #
LBL-31450 ..... p 2970 N92-26551 #
LBL-31480 ..... p 3001 N92-26204 #
LBL-31481 ..... p 2993 N92-26207 #
LBL-31491 ..... p 2994 N92-26235 #
LBL-31512 ..... p 2877 N92-26213 #
LBL-31534 ..... p 2935 N92-26239 #
LBL-31541 ..... p 3004 N92-26641 #
LBL-31553 ..... p 3003 N92-26582 #
LBL-31561 ..... p 2921 N92-26206 #
LBL-31589 ..... p 2985 N92-26232 #
LBL-31610 ..... p 3011 N92-26221 #
LBL-31663 ..... p 3003 N92-26584 #
LBL-31695 ..... p 3001 N92-26222 #
LBL-31853 ..... p 2996 N92-26187 #

LMI-DL001-01R1-VOL-2 ..... p 3013 N92-26767 #

LNCC-004/91 ..... p 2988 N92-26831 #

M-661 ..... p 2862 N92-27130 * #
M-688 ..... p 2918 N92-26669 * #
M-690 ..... p 2921 N92-26905 * #

MBB-UA-1197-90-PUB ..... p 2886 N92-26246 #

MDC-86PR0869-REV ..... p 2911 N92-26293 #

MEMO-984 ..... p 2988 N92-26817 #
MEMO-996 ..... p 2986 N92-26503 #
MEMO-998 ..... p 2987 N92-26737 #

MPE-PREPRINT-174 ..... p 3018 N92-27048
MPE-PREPRINT-175 ..... p 3016 N92-27049

MPI-PHE/91-07 ..... p 2906 N92-26391

MTL-TR-91-44 ..... p 2876 N92-26172 #
MTL-TR-91-50 ..... p 2882 N92-26609 #
MTL-TR-91-52 ..... p 2881 N92-26283 #

NAL-SP-12 ..... p 2901 N92-26906 #

NAS 1.15:101796 ..... p 2986 N92-26407 * #
NAS 1.15:103583 ..... p 2857 N92-26268 * #
NAS 1.15:103585 ..... p 2945 N92-26288 * #
NAS 1.15:104173 ..... p 3014 N92-27170 * #
NAS 1.15:104582 ..... p 2869 N92-26650 * #
NAS 1.15:105410 ..... p 2886 N92-27197 * #
NAS 1.15:105561 ..... p 2886 N92-26611 * #
NAS 1.15:105573 ..... p 2990 N92-26671 * #
NAS 1.15:105612 ..... p 2989 N92-27196 * #
NAS 1.15:105635 ..... p 2880 N92-27192 * #
NAS 1.15:105638 ..... p 2875 N92-26670 * #
NAS 1.15:105651 ..... p 2915 N92-26555 * #
NAS 1.15:105668 ..... p 2915 N92-26560 * #
NAS 1.15:105674 ..... p 2898 N92-26690 * #
NAS 1.15:105684 ..... p 2855 N92-27037 * #
NAS 1.15:105690 ..... p 2861 N92-27034 * #
NAS 1.15:105692 ..... p 2861 N92-26654 * #
NAS 1.15:105695 ..... p 2854 N92-26553 * #
NAS 1.15:105699 ..... p 2854 N92-26561 * #
NAS 1.15:105703 ..... p 2861 N92-26792 * #
NAS 1.15:105714 ..... p 2861 N92-27033 * #
NAS 1.15:105724 ..... p 2854 N92-26613 * #
NAS 1.15:105734 ..... p 2861 N92-27035 * #
NAS 1.15:105742 ..... p 2849 N92-26612 * #
NAS 1.15:105750 ..... p 2861 N92-27036 * #
NAS 1.15:107583 ..... p 2889 N92-26653 * #
NAS 1.15:107598 ..... p 2891 N92-27189 * #
NAS 1.15:107629 ..... p 2920 N92-26903 * #
NAS 1.15:107792 ..... p 3022 N92-26824 * #
NAS 1.15:107810 ..... p 3019 N92-26191 * #
NAS 1.15:107840 ..... p 2983 N92-26631 * #
NAS 1.15:107856 ..... p 2950 N92-26266 * #
NAS 1.15:107865 ..... p 2984 N92-26791 * #
NAS 1.15:107868 ..... p 2983 N92-26630 * #
NAS 1.15:107869 ..... p 2983 N92-26789 * #
NAS 1.15:107872 ..... p 2984 N92-26888 * #

NAS 1.15:107876 ..... p 2984 N92-26885 * #
NAS 1.15:107879 ..... p 2983 N92-26629 * #
NAS 1.15:107881 ..... p 2983 N92-26643 * #
NAS 1.15:107882 ..... p 2982 N92-26627 * #
NAS 1.15:107885 ..... p 2988 N92-26894 * #
NAS 1.15:107886 ..... p 2982 N92-26628 * #
NAS 1.15:107888 ..... p 3009 N92-26790 * #
NAS 1.15:107889 ..... p 2984 N92-26893 * #
NAS 1.15:107895 ..... p 2985 N92-27057 * #
NAS 1.15:107896 ..... p 2985 N92-27056 * #
NAS 1.15:107906 ..... p 2984 N92-27055 * #
NAS 1.15:107911 ..... p 2984 N92-26887 * #
NAS 1.15:107913 ..... p 3015 N92-26886 * #
NAS 1.15:4362 ..... p 2996 N92-26832 * #
NAS 1.15:4367 ..... p 2977 N92-26904 * #
NAS 1.15:4374 ..... p 2905 N92-27193 * #
NAS 1.15:4388 ..... p 2921 N92-26905 * #
NAS 1.21:7011(362) ..... p 2953 N92-27068 *
NAS 1.21:7039(40)-SECT-2 ..... p 3014 N92-27081 *
NAS 1.21:7500(26) ..... p 3010 N92-27080 *
NAS 1.26:184325 ..... p 2993 N92-26200 * #
NAS 1.26:185673 ..... p 2858 N92-26884 * #
NAS 1.26:187664 ..... p 2886 N92-26656 * #
NAS 1.26:188468 ..... p 2878 N92-26642 * #
NAS 1.26:188973 ..... p 2977 N92-26868 *
NAS 1.26:189638 ..... p 2901 N92-26883 * #
NAS 1.26:189639 ..... p 2987 N92-26668 * #
NAS 1.26:189641 ..... p 2849 N92-26652 * #
NAS 1.26:189642 ..... p 2849 N92-26651 * #
NAS 1.26:189646 ..... p 2898 N92-26649 * #
NAS 1.26:189647 ..... p 2905 N92-27032 * #
NAS 1.26:190019 ..... p 2852 N92-26435 * #
NAS 1.26:190059 ..... p 2944 N92-26185 * #
NAS 1.26:190117 ..... p 3016 N92-26436 * #
NAS 1.26:190195 ..... p 3020 N92-26437 * #
NAS 1.26:190211 ..... p 3019 N92-26438 * #
NAS 1.26:190222 ..... p 2946 N92-26736 *
NAS 1.26:190223 ..... p 2946 N92-26735 *
NAS 1.26:190225 ..... p 2945 N92-26474 *
NAS 1.26:190245 ..... p 3019 N92-26247 * #
NAS 1.26:190254 ..... p 2994 N92-26539 * #
NAS 1.26:190279 ..... p 2975 N92-26587 * #
NAS 1.26:190296 ..... p 2982 N92-26429 * #
NAS 1.26:190302 ..... p 2913 N92-26870 * #
NAS 1.26:190320 ..... p 2954 N92-26193 * #
NAS 1.26:190321 ..... p 2920 N92-26892 *
NAS 1.26:190340 ..... p 3001 N92-26265 * #
NAS 1.26:190341 ..... p 2952 N92-26263 * #
NAS 1.26:190344 ..... p 2933 N92-26878 * #
NAS 1.26:190383 ..... p 2945 N92-26535 * #
NAS 1.26:190389 ..... p 2971 N92-26182 * #
NAS 1.26:190391 ..... p 2971 N92-26183 * #
NAS 1.26:190392 ..... p 2978 N92-26199 * #
NAS 1.26:190393 ..... p 2971 N92-26181 * #
NAS 1.26:190395 ..... p 2972 N92-26198 * #
NAS 1.26:190396 ..... p 2972 N92-26197 * #
NAS 1.26:190397 ..... p 3009 N92-26552 * #
NAS 1.26:190402 ..... p 3015 N92-26184 * #
NAS 1.26:190403 ..... p 2908 N92-26536 * #
NAS 1.26:190423 ..... p 2853 N92-26405 * #
NAS 1.26:190424 ..... p 2942 N92-26406 * #
NAS 1.26:190428 ..... p 2981 N92-27183 * #
NAS 1.26:190434 ..... p 2852 N92-26655 * #
NAS 1.26:190452 ..... p 2850 N92-27191 * #
NAS 1.26:190458 ..... p 2926 N92-27195 * #
NAS 1.26:4438 ..... p 2898 N92-26680 * #
NAS 1.26:4439 ..... p 2898 N92-26681 * #
NAS 1.55:3119 ..... p 2862 N92-27130 * #
NAS 1.55:3134-PT-3 ..... p 3022 N92-27083 * #
NAS 1.55:3147-ADD ..... p 2927 N92-26895 * #
NAS 1.60:3164 ..... p 2917 N92-26537 * #
NAS 1.60:3206 ..... p 2956 N92-26538 * #
NAS 1.60:3207 ..... p 2956 N92-26682 * #
NAS 1.60:3226 ..... p 2883 N92-27194 * #
NAS 1.60:3227 ..... p 2858 N92-26667 * #
NAS 1.60:3248 ..... p 2918 N92-26669 * #

NASA-CP-3119 ..... p 2862 N92-27130 * #
NASA-CP-3134-PT-3 ..... p 3022 N92-27083 * #
NASA-CP-3147-ADD ..... p 2927 N92-26895 * #

NASA-CR-184325 ..... p 2993 N92-26200 * #
NASA-CR-185673 ..... p 2858 N92-26884 * #
NASA-CR-187664 ..... p 2886 N92-26656 * #
NASA-CR-188468 ..... p 2878 N92-26642 * #
NASA-CR-188973 ..... p 2977 N92-26868 *
NASA-CR-189638 ..... p 2901 N92-26883 * #
NASA-CR-189639 ..... p 2987 N92-26668 * #
NASA-CR-189641 ..... p 2849 N92-26652 * #
NASA-CR-189642 ..... p 2849 N92-26651 * #
NASA-CR-189646 ..... p 2898 N92-26649 * #
NASA-CR-189647 ..... p 2905 N92-27032 * #
NASA-CR-190019 ..... p 2852 N92-26435 * #
NASA-CR-190059 ..... p 2944 N92-26185 * #
NASA-CR-190117 ..... p 3016 N92-26436 * #
NASA-CR-190195 ..... p 3020 N92-26437 * #
NASA-CR-190211 ..... p 3019 N92-26438 * #
NASA-CR-190222 ..... p 2946 N92-26736 *
NASA-CR-190223 ..... p 2946 N92-26735 *
NASA-CR-190225 ..... p 2945 N92-26474 *
NASA-CR-190245 ..... p 3019 N92-26247 * #
NASA-CR-190254 ..... p 2994 N92-26539 * #
NASA-CR-190279 ..... p 2975 N92-26587 * #
NASA-CR-190296 ..... p 2982 N92-26429 * #
NASA-CR-190302 ..... p 2913 N92-26870 * #
NASA-CR-190320 ..... p 2954 N92-26193 * #
NASA-CR-190321 ..... p 2920 N92-26892 *
NASA-CR-190340 ..... p 3001 N92-26265 * #
NASA-CR-190341 ..... p 2952 N92-26263 * #
NASA-CR-190344 ..... p 2933 N92-26878 * #
NASA-CR-190383 ..... p 2945 N92-26535 * #
NASA-CR-190389 ..... p 2971 N92-26182 * #
NASA-CR-190391 ..... p 2971 N92-26183 * #
NASA-CR-190392 ..... p 2978 N92-26199 * #
NASA-CR-190393 ..... p 2971 N92-26181 * #
NASA-CR-190395 ..... p 2972 N92-26198 * #
NASA-CR-190396 ..... p 2972 N92-26197 * #
NASA-CR-190397 ..... p 3009 N92-26552 * #
NASA-CR-190402 ..... p 3015 N92-26184 * #
NASA-CR-190403 ..... p 2908 N92-26536 * #
NASA-CR-190423 ..... p 2853 N92-26405 * #
NASA-CR-190424 ..... p 2942 N92-26406 * #
NASA-CR-190428 ..... p 2981 N92-27183 * #
NASA-CR-190434 ..... p 2852 N92-26655 * #
NASA-CR-190452 ..... p 2850 N92-27191 * #
NASA-CR-190458 ..... p 2926 N92-27195 * #
NASA-CR-4438 ..... p 2898 N92-26680 * #
NASA-CR-4439 ..... p 2898 N92-26681 * #

NASA-FIA-92-01 ..... p 2984 N92-26791 * #

NASA-SP-7011(362) ..... p 2953 N92-27068 *
NASA-SP-7039(40)-SECT-2 ..... p 3014 N92-27081 *
NASA-SP-7500(26) ..... p 3010 N92-27080 *

NASA-TM-101796 ..... p 2986 N92-26407 * #
NASA-TM-103583 ..... p 2857 N92-26268 * #
NASA-TM-103585 ..... p 2945 N92-26288 * #
NASA-TM-104173 ..... p 3014 N92-27170 * #
NASA-TM-104562 ..... p 2869 N92-26650 * #
NASA-TM-105410 ..... p 2886 N92-27197 * #
NASA-TM-105561 ..... p 2886 N92-26611 * #
NASA-TM-105573 ..... p 2990 N92-26671 * #
NASA-TM-105612 ..... p 2989 N92-27196 * #
NASA-TM-105635 ..... p 2880 N92-27192 * #
NASA-TM-105638 ..... p 2875 N92-26670 * #
NASA-TM-105651 ..... p 2915 N92-26555 * #
NASA-TM-105668 ..... p 2915 N92-26560 * #
NASA-TM-105674 ..... p 2898 N92-26690 * #
NASA-TM-105684 ..... p 2855 N92-27037 * #
NASA-TM-105690 ..... p 2861 N92-27034 * #
NASA-TM-105692 ..... p 2861 N92-26654 * #
NASA-TM-105695 ..... p 2854 N92-26553 * #
NASA-TM-105699 ..... p 2854 N92-26561 * #
NASA-TM-105703 ..... p 2861 N92-26792 * #
NASA-TM-105714 ..... p 2861 N92-27033 * #
NASA-TM-105724 ..... p 2854 N92-26613 * #
NASA-TM-105734 ..... p 2861 N92-27035 * #
NASA-TM-105742 ..... p 2849 N92-26612 * #
NASA-TM-105750 ..... p 2861 N92-27036 * #
NASA-TM-107583 ..... p 2889 N92-26653 * #
NASA-TM-107598 ..... p 2891 N92-27189 * #
NASA-TM-107629 ..... p 2920 N92-26903 * #
NASA-TM-107792 ..... p 3022 N92-26824 * #
NASA-TM-107810 ..... p 3019 N92-26191 * #
NASA-TM-107840 ..... p 2983 N92-26631 * #
NASA-TM-107856 ..... p 2950 N92-26266 * #
NASA-TM-107865 ..... p 2984 N92-26791 * #
NASA-TM-107868 ..... p 2983 N92-26630 * #
NASA-TM-107869 ..... p 2983 N92-26789 * #
NASA-TM-107872 ..... p 2984 N92-26888 * #
NASA-TM-107876 ..... p 2984 N92-26885 * #
NASA-TM-107879 ..... p 2983 N92-26629 * #
NASA-TM-107881 ..... p 2983 N92-26643 * #
NASA-TM-107882 ..... p 2982 N92-26627 * #
NASA-TM-107885 ..... p 2988 N92-26894 * #
NASA-TM-107886 ..... p 2982 N92-26628 * #
NASA-TM-107888 ..... p 3009 N92-26790 * #
NASA-TM-107889 ..... p 2984 N92-26893 * #
NASA-TM-107895 ..... p 2985 N92-27057 * #
NASA-TM-107896 ..... p 2985 N92-27056 * #
NASA-TM-107906 ..... p 2984 N92-27055 * #
NASA-TM-107911 ..... p 2984 N92-26887 * #
NASA-TM-107913 ..... p 3015 N92-26886 * #
NASA-TM-4362 ..... p 2996 N92-26832 * #
NASA-TM-4367 ..... p 2977 N92-26904 * #
NASA-TM-4374 ..... p 2905 N92-27193 * #
NASA-TM-4388 ..... p 2921 N92-26905 * #

NASA-TP-3164 ..... p 2917 N92-26537 * #
NASA-TP-3206 ..... p 2958 N92-26538 * #
NASA-TP-3207 ..... p 2956 N92-26682 * #
NASA-TP-3226 ..... p 2883 N92-27194 * #
NASA-TP-3227 ..... p 2858 N92-26667 * #
NASA-TP-3248 ..... p 2918 N92-26669 * #

NATICK/TR-92/015 ..... p 2954 N92-26242 #
NATICK/TR-92/016 ..... p 2954 N92-26243 #

NAVSWC-TR-91-549 ..... p 2975 N92-26530 #

NAVY-CASE-70938 ..... p 2997 N92-26862 #
NAVY-CASE-72812 ..... p 3003 N92-26433 #

NCAR/TN-343+STR ..... p 2928 N92-26352 #
NCAR/TN-371+STR ..... p 2933 N92-26878 * #

NCTRF-181 ..... p 2952 N92-26470 #

NIIYAF-MGV-91-13-217 ..... p 2988 N92-26834 #

NIST/SP-500/201 ..... p 2973 N92-26370 #
NIST/SP-824 ..... p 2914 N92-26366 #

NISTIR-4592 ..... p 2894 N92-26821 #
NISTIR-4747 ..... p 2984 N92-26814 #
NISTIR-4750 ..... p 2980 N92-26501 #

NMRI-91-85 ..... p 2956 N92-26665 #

NOAA-TM-ERL-CMDL-3 ..... p 2876 N92-26812 #

NOAA-TM-ERL-WPL-213 ..... p 2890 N92-26809 #

NOAA-TM-NWS-SR-141 ..... p 2945 N92-26514 #

NOARL-TN-164 ..... p 2926 N92-27070 #
NOARL-TN-193 ..... p 2985 N92-27072 #
NOARL-TN-208 ..... p 2950 N92-27071 #

NOO-TR-304 ..... p 2942 N92-26406 * #

NOSC-TR-1440 ..... p 2980 N92-26531 #

NPL-DITC-194/92 ..... p 2974 N92-26450

NPS-MA-92-002 ..... p 2988 N92-26900 #

NPS-ME-92-001 ..... p 2894 N92-26897 #

NPS-OC-91-004 ..... p 2851 N92-26415 #
NPS-OC-92-002 ..... p 2950 N92-27069 #

NPS-OR-92-011 ..... p 2977 N92-26949 #

NPS-PH-92-005 ..... p 3016 N92-27077 #

NPSOR-92-005 ..... p 2883 N92-26178 #

NREC-1656-1 ..... p 2873 N92-26521 #

NREL/TP-214-4579-PHASE-1 ..... p 2926 N92-26190 #
NREL/TP-230-4633 ..... p 2932 N92-26810 #
NREL/TP-411-4787 ..... p 2927 N92-26686 #
NREL/TP-432-4804-VOL-1 ..... p 2927 N92-26683 #

NRL-MR-6910 ..... p 2893 N92-26741 #
NRL-MR-6914 ..... p 2990 N92-26768 #
NRL-MR-6923 ..... p 2975 N92-26529 #
NRL-MR-6935 ..... p 2976 N92-26766 #
NRL-MR-6942 ..... p 2991 N92-26769 #

NSSDC/WDC-A-R/S-91-26 ..... p 3019 N92-26191 * #

ORNL/SUB-90-SG828/1 ..... p 2887 N92-26237 #

ORNL/TM-11767 ..... p 2918 N92-26784 #
ORNL/TM-11778 ..... p 3021 N92-26544 #
ORNL/TM-11905 ..... p 2987 N92-26545 #
ORNL/TM-11949 ..... p 3003 N92-26579 #
ORNL/TM-12032 ..... p 3000 N92-26577 #
ORNL/TM-12070 ..... p 2913 N92-26219 #

OTA-ITE-498 ..... p 3014 N92-26730 #

PARGUM-91-08 ..... p 2914 N92-26389 #

PB92-105527 ..... p 2932 N92-26823 #
PB92-109099 ..... p 2930 N92-26495 #
PB92-113059 ..... p 2931 N92-26802 #
PB92-113067 ..... p 2932 N92-26803 #
PB92-115757 ..... p 3014 N92-26730 #
PB92-125038 ..... p 3007 N92-26805 #
PB92-128560 ..... p 2876 N92-26812 #
PB92-129931 ..... p 2890 N92-26809 #
PB92-132885 ..... p 2930 N92-26519 #
PB92-133958 ..... p 2896 N92-26496 #
PB92-137553 ..... p 2914 N92-26366 #

PB92-137652 ..... p 2876 N92-26782 #
PB92-141530 ..... p 2986 N92-26502 #
PB92-141779 ..... p 2876 N92-26783 #
PB92-142223 ..... p 2893 N92-26497 #
PB92-142231 ..... p 2896 N92-26507 #
PB92-142579 ..... p 2873 N92-26521 #
PB92-143544 ..... p 2975 N92-26500 #
PB92-145796 ..... p 2953 N92-26512 #
PB92-146075 ..... p 2945 N92-26514 #
PB92-147727 ..... p 2933 N92-26931 #
PB92-148279 ..... p 2894 N92-26821 #
PB92-148287 ..... p 2984 N92-26814 #
PB92-148626 ..... p 2988 N92-26817 #
PB92-148741 ..... p 2986 N92-26503 #
PB92-148766 ..... p 2987 N92-26737 #
PB92-149335 ..... p 2986 N92-26367 #
PB92-149657 ..... p 2873 N92-26508 #
PB92-149665 ..... p 2915 N92-26816 #
PB92-149863 ..... p 2980 N92-26501 #
PB92-150176 ..... p 3006 N92-26927 #
PB92-150374 ..... p 2944 N92-26838 #
PB92-150911 ..... p 2889 N92-26511 #
PB92-151109 ..... p 2900 N92-26836 #
PB92-151521 ..... p 2868 N92-26525 #
PB92-151703 ..... p 3009 N92-26523 #
PB92-151893 ..... p 2879 N92-26787 #
PB92-152206 ..... p 2921 N92-26513 #
PB92-152305 ..... p 2943 N92-26820 #
PB92-152313 ..... p 3018 N92-26833 #
PB92-152610 ..... p 2896 N92-26506 #
PB92-152750 ..... p 2909 N92-26786 #
PB92-152917 ..... p 2872 N92-26351 #
PB92-153006 ..... p 2930 N92-26510 #
PB92-153022 ..... p 2930 N92-26509 #
PB92-153212 ..... p 2988 N92-26788 #
PB92-153733 ..... p 2933 N92-26929 #
PB92-153766 ..... p 2933 N92-26928 #
PB92-153774 ..... p 2933 N92-26689 #
PB92-153782 ..... p 2928 N92-26354 #
PB92-154822 ..... p 2873 N92-26516 #
PB92-154905 ..... p 3014 N92-26926 #
PB92-155258 ..... p 2928 N92-26352 #
PB92-155951 ..... p 3022 N92-26824 * #
PB92-157064 ..... p 3008 N92-26353 #
PB92-158260 ..... p 2928 N92-26373 #
PB92-158328 ..... p 2973 N92-26370 #
PB92-158351 ..... p 3011 N92-26368 #
PB92-160084 ..... p 2910 N92-26930 #
PB92-160118 ..... p 3008 N92-26369 #
PB92-160399 ..... p 2946 N92-26822 #
PB92-163237 ..... p 2914 N92-26518 #
PB92-163278 ..... p 2931 N92-26793 #
PB92-164300 ..... p 2926 N92-26372 #
PB92-164482 ..... p 2914 N92-26371 #
PB92-164706 ..... p 2933 N92-26890 #

PCS-TR91-154 ..... p 2981 N92-27183 * #

PNL-SA-20425 ..... p 2979 N92-26277 #
PNL-SA-20478 ..... p 2931 N92-26633 #

PNR-90801 ..... p 2916 N92-27038 #
PNR-90805 ..... p 2855 N92-27039 #
PNR-90808 ..... p 2855 N92-27040 #
PNR-90809 ..... p 2855 N92-27041 #
PNR-90810 ..... p 2855 N92-27042 #
PNR-90811 ..... p 2856 N92-27043 #
PNR-90813 ..... p 2880 N92-27044 #

R-639 ..... p 2896 N92-26506 #

RAE-TM-P1216 ..... p 2856 N92-27062 #

RAND-N-3103-A ..... p 2856 N92-26192 #
RAND-N-3287-AF/NASA ..... p 2954 N92-26193 * #
RAND-N-3437-JPL ..... p 3019 N92-26819 #

RAND-P-7744 ..... p 2990 N92-26194 #
RAND-P-7746-RGS ..... p 2852 N92-26673 #

REPT-12 ..... p 3014 N92-27170 * #
REPT-153425 ..... p 2986 N92-26414 #
REPT-16 ..... p 3022 N92-26664 #
REPT-721563-4 ..... p 2892 N92-26280 #
REPT-91-041 ..... p 2986 N92-26420
REPT-91-053 ..... p 2973 N92-26421
REPT-91-054 ..... p 3011 N92-26422
REPT-91-071 ..... p 2970 N92-26439
REPT-91-072 ..... p 2973 N92-26448
REPT-91-079 ..... p 2974 N92-26449
REPT-92A01664 ..... p 2869 N92-26650 * #
REPT-92B00041 ..... p 2858 N92-26667 * #
REPT-92B00063 ..... p 2977 N92-26904 * #

RFP-4533 ..... p 2928 N92-26390 #

RIA-90-02-15-1 ..... p 2985 N92-27056 * #
RIA-90-4-27-1 ..... p 2984 N92-26887 * #

RL-TR-91-266 ..... p 3001 N92-26226 #
RL-TR-91-325 ..... p 2893 N92-26540 #
RL-TR-91-341 ..... p 2998 N92-26943 #

RR-A295 ..... p 2986 N92-26502 #
RR-A297 ..... p 2896 N92-26496 #

RR-417 ..... p 2887 N92-26752 #

S-194 ..... p 2909 N92-26786 #
S-670 ..... p 2956 N92-26538 * #
S-671 ..... p 2956 N92-26682 * #

SAIC-TN-9202 ..... p 2993 N92-26200 * #

SAND-91-1429C ..... p 2899 N92-26698 #
SAND-91-1441C ..... p 2912 N92-26691 #
SAND-91-1575 ..... p 3012 N92-26575 #
SAND-91-2347C ..... p 2875 N92-26722 #
SAND-91-2348C ..... p 2892 N92-26238 #
SAND-91-2555C ..... p 2897 N92-26644 #
SAND-91-2739C ..... p 2894 N92-26847 #
SAND-91-2751C ..... p 2997 N92-26452 #
SAND-91-2788C ..... p 2901 N92-26856 #
SAND-91-2803C ..... p 2899 N92-26716 #
SAND-91-2815C ..... p 2919 N92-26852 #
SAND-91-2817C ..... p 2919 N92-26846 #
SAND-91-2865C ..... p 2900 N92-26853 #
SAND-92-0033C ..... p 2976 N92-26696 #
SAND-92-0063C ..... p 2993 N92-26225 #
SAND-92-0089C ..... p 2910 N92-26269 #
SAND-92-0103C ..... p 3000 N92-26695 #
SAND-92-0134C ..... p 2891 N92-26902 #
SAND-92-0437C ..... p 3005 N92-26826 #
SAND-92-0648C ..... p 2982 N92-26434 #
SAND-92-7070C ..... p 3000 N92-26666 #

SER-A-15 ..... p 2975 N92-26500 #

SLAC-PUB-5699 ..... p 2887 N92-26267 #

SRL-0058-TM ..... p 2852 N92-26948 #

STARS-TC-04041/001/00 ..... p 2978 N92-27177 #

SVHSER-14841 ..... p 2945 N92-26535 * #

SYSAPP-91/091A ..... p 2931 N92-26802 #
SYSAPP-91/091B ..... p 2932 N92-26803 #

TDCK-TD-91-2909 ..... p 2910 N92-26271 #

TDCK-TD91-2901 ..... p 2908 N92-26517 #
TDCK-TD91-3272 ..... p 3011 N92-26403 #

TD90-4059 ..... p 2890 N92-26872
TD91-0993 ..... p 2932 N92-26873
TD91-2171 ..... p 3010 N92-27046
TD91-2232 ..... p 2890 N92-26874
TD91-2613 ..... p 3014 N92-26875
TD91-3276 ..... p 2890 N92-26876
TD91-3298 ..... p 2953 N92-27047
TD91-3980 ..... p 2944 N92-26877

TELAC-91-17 ..... p 2852 N92-26655 * #

TKK-F-A671 ..... p 2893 N92-26497 #
TKK-F-A673 ..... p 2896 N92-26507 #

TKK-V-B65 ..... p 2879 N92-26787 #

TR-227 ..... p 2989 N92-27174 #
TR-3 ..... p 2879 N92-26939 #
TR-75 ..... p 2872 N92-26431 #
TR-76 ..... p 2874 N92-26526 #
TR-77 ..... p 2874 N92-26608 #
TR-91-04-04 ..... p 2979 N92-26359 #
TR-91-1249 ..... p 2980 N92-26677 #
TR-91-1250 ..... p 2979 N92-26278 #
TR-91-1251 ..... p 2979 N92-26279 #

TRMM-SER-705 ..... p 2945 N92-26535 * #

TW-10 ..... p 2923 N92-26711 #
TW-11 ..... p 2924 N92-26712 #
TW-12 ..... p 2924 N92-26713 #
TW-13 ..... p 2924 N92-26714 #
TW-14 ..... p 2924 N92-26715 #
TW-1 ..... p 2922 N92-26702 * #
TW-2 ..... p 2922 N92-26703 #
TW-3 ..... p 2923 N92-26704 #
TW-4 ..... p 2923 N92-26705 #
TW-5 ..... p 2923 N92-26706 * #
TW-6 ..... p 2923 N92-26707 #
TW-7 ..... p 2923 N92-26708 #
TW-8 ..... p 2923 N92-26709 #
TW-9 ..... p 2923 N92-26710 #

UCB-PTH-91/38 ..... p 3019 N92-26385 #
UCB-PTH-91/69 ..... p 2985 N92-26232 #

UCRL-CR-107026 ..... p 2877 N92-26223 #
UCRL-CR-109689 ..... p 2948 N92-26270 #

UCRL-JC-106539 ..... p 2972 N92-26233 #
UCRL-JC-107042 ..... p 2873 N92-26454 #
UCRL-JC-107241 ..... p 2906 N92-26230 #
UCRL-JC-107249 ..... p 2892 N92-26224 #
UCRL-JC-107251 ..... p 2906 N92-26377 #
UCRL-JC-107359 ..... p 2898 N92-26645 #
UCRL-JC-107535 ..... p 2934 N92-26936 #
UCRL-JC-107758 ..... p 2934 N92-26935 #
UCRL-JC-107974 ..... p 2911 N92-26505 #
UCRL-JC-108317 ..... p 2912 N92-26646 #
UCRL-JC-109185 ..... p 2911 N92-26504 #
UCRL-JC-109419 ..... p 2878 N92-26732 #
UCRL-JC-109680 ..... p 3000 N92-26729 #
UCRL-JC-109767 ..... p 2975 N92-26647 #

UCRL-LR-108508 ..... p 2976 N92-26797 #

UMHEP-361 ..... p 3016 N92-26436 * #

US-PATENT-APPL-SN-453658 ..... p 2853 N92-27185 #
US-PATENT-APPL-SN-465677 ..... p 2998 N92-27186
US-PATENT-APPL-SN-481421 ..... p 2993 N92-27184
US-PATENT-APPL-SN-497387 ..... p 2894 N92-26881
US-PATENT-APPL-SN-500979 ..... p 2883 N92-27187
US-PATENT-APPL-SN-561413 ..... p 2909 N92-26879
US-PATENT-APPL-SN-605902 ..... p 2853 N92-27188
US-PATENT-APPL-SN-704561 ..... p 2884 N92-26880
US-PATENT-APPL-SN-749825 ..... p 3003 N92-26433 #
US-PATENT-APPL-SN-767189 ..... p 2997 N92-26862 #

US-PATENT-CLASS-G015-15.00 . p 2993 N92-27184

US-PATENT-CLASS-204-192-19 . p 2883 N92-27187
US-PATENT-CLASS-244-12.1 ..... p 2853 N92-27185 #
US-PATENT-CLASS-250-577 ..... p 2909 N92-26879
US-PATENT-CLASS-356-345 ..... p 2998 N92-27186
US-PATENT-CLASS-363-3 ..... p 2894 N92-26881
US-PATENT-CLASS-548-145 ..... p 2884 N92-26880
US-PATENT-CLASS-89-1.51 ..... p 2853 N92-27188

US-PATENT-5,054,922 ..... p 2998 N92-27186
US-PATENT-5,062,939 ..... p 2883 N92-27187
US-PATENT-5,063,487 ..... p 2894 N92-26881
US-PATENT-5,068,832 ..... p 2993 N92-27184
US-PATENT-5,070,760 ..... p 2853 N92-27188
US-PATENT-5,071,088 ..... p 2853 N92-27185 #
US-PATENT-5,073,720 ..... p 2909 N92-26879
US-PATENT-5,081,255 ..... p 2884 N92-26880

USAFA-TR-91-18 ..... p 2971 N92-26196 #

USGS/WRI-91-4040 ..... p 2933 N92-26931 #

USNA-TSPR-178 ..... p 2950 N92-26289 #
USNA-TSPR-179 ..... p 2867 N92-26380 #
USNA-TSPR-183 ..... p 2993 N92-26171 #
USNA-TSPR-186 ..... p 2868 N92-26532 #

USNA-3910-3 ..... p 3022 N92-26664 #

VTT-PUBL-81 ..... p 2929 N92-26482 #
VTT-PUBL-82 ..... p 3001 N92-26320 #

WCDMP-14 ..... p 2947 N92-26923 #
WCDMP-15 ..... p 2947 N92-26924 #
WCDMP-16 ..... p 2947 N92-26925 #

WHC-SA-1375 ..... p 2918 N92-26694 #
WHC-SA-1432 ..... p 2879 N92-26848 #

WL-TR-91-1063 ..... p 3009 N92-26863 #
WL-TR-91-2086 ..... p 2896 N92-26379 #

WMO-TD-465 ..... p 2947 N92-26925 #
WMO-TD-466 ..... p 2947 N92-26923 #
WMO-TD-468 ..... p 2947 N92-26924 #

WS-382 ..... p 2986 N92-26367 #

WSRC-MS-91-008 ..... p 2875 N92-26718 #
WSRC-MS-91-016 ..... p 2875 N92-26717 #
WSRC-MS-91-062 ..... p 2874 N92-26634 #
WSRC-MS-91-076 ..... p 2870 N92-26217 #
WSRC-MS-91-110 ..... p 2878 N92-26635 #
WSRC-MS-91-142 ..... p 2870 N92-26201 #

WSRC-MS-91-305 ..... p 2971 N92-26188 #

WSRC-RD-91-16 ..... p 2874 N92-26632 #

WSU-TR-88-001 ..... p 2896 N92-26379 #

WSU/DC/92/TR-77 ..... p 2888 N92-26374 #

Typical Accession Number Index Listing

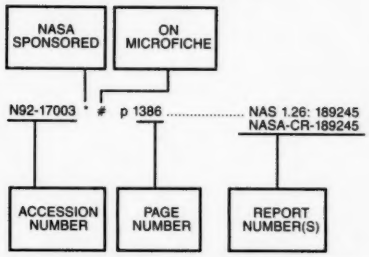

Listings in this index are arranged alphanumerically by accession number. The page number helps to locate the citation in the abstract section. An asterisk (*) indicates that the item is a NASA report. A pound sign (#) indicates that the item is available on microfiche.

N92-26171 # p 2993 ..... AD-A245646
N92-26171 # p 2993 ..... USNA-TSPR-183
N92-26172 # p 2876 ..... AD-A245649
MTL-TR-91-44
N92-26173 # p 2948 ..... AD-A245650
N92-26174 # p 3010 ..... AC/243-N/347
AD-A245656
N92-26175 # p 2991 ..... AD-A245660
N92-26176 # p 3010 ..... AD-A245786
N92-26177 # p 2989 ..... AD-A245787
N92-26178 # p 2883 ..... AD-A245818
NPSOR-92-005
N92-26179 # p 2954 ..... AD-A245819
N92-26180 # p 2989 ..... AD-A245822
ARL-TR-91-20
N92-26181* # p 2971 ..... NAS 1.26:190393
NASA-CR-190393
N92-26182* # p 2971 ..... NAS 1.26:190389
NASA-CR-190389
N92-26183* # p 2971 ..... NAS 1.26:190391
NASA-CR-190391
N92-26184* # p 3015 ..... NAS 1.26:190402
NASA-CR-190402
N92-26185* # p 2944 ..... NAS 1.26:190059
NASA-CR-190059
N92-26186 # p 2954 ..... DE92-614952
KAERI/RR-976/90
N92-26187 # p 2996 ..... CONF-9108191
DE92-009142
LBL-31853
N92-26188 # p 2971 ..... CONF-9109276-9
DE92-009405
WSRC-MS-91-305
N92-26189 # p 2971 ..... DE92-001020
DOE/BC-10850/19
N92-26190 # p 2926 ..... DE92-001199
NREL/TP-214-4579-PHASE-1
N92-26191* # p 3019 ..... NAS 1.15:107810
NASA-TM-107810
NSSDC/WDC-A-R/S-91-26
N92-26192 # p 2856 ..... RAND-N-3103-A
N92-26193* # p 2954 ..... NAS 1.26:190320
NASA-CR-190320
RAND-N-3287-AF/NASA
N92-26194 # p 2990 ..... RAND-P-7744
N92-26195 # p 2971 ..... AD-A245784
N92-26196 # p 2971 ..... AD-A245895
USAFA-TR-91-18
N92-26197* # p 2972 ..... NAS 1.26:190396
NASA-CR-190396
N92-26198* # p 2972 ..... NAS 1.26:190395
NASA-CR-190395
N92-26199* # p 2978 ..... NAS 1.26:190392
NASA-CR-190392
N92-26200* # p 2993 ..... NAS 1.26:184325
NASA-CR-184325
SAIC-TN-9202
N92-26201 # p 2870 ..... CONF-9104246-2
DE92-009432
WSRC-MS-91-142
N92-26202 # p 2891 ..... CONF-9108118-46
DE92-008449
LA-UR-92-474
N92-26203 # p 2950 ..... DE92-010254
LBL-PUB-696
N92-26204 # p 3001 ..... CONF-9107146-4
DE92-010258
LBL-31480
N92-26205 # p 2891 ..... CONF-9106224-3
DE92-010260
LBL-31158
N92-26206 # p 2921 ..... DE92-010262
LBL-31561
N92-26207 # p 2993 ..... CONF-9106105-1
DE92-010264
LBL-31481
N92-26208 # p 2934 ..... DE92-010271
LBL-31377
N92-26209 # p 2870 ..... DE92-009487
LBL-31230
N92-26210 # p 3001 ..... ANL/CP-75188
CONF-920240-2
DE92-010281
N92-26211 # p 3020 ..... ANL/HEP/CP-91-117
CONF-9108141-9
DE92-010282
N92-26212 # p 2870 ..... CONF-910422-9
DE92-010284
LBL-31442
N92-26213 # p 2877 ..... CONF-9106275-6
DE92-010285
LBL-31512
N92-26214 # p 2895 ..... CONF-910435-94
DE92-010302
LBL-31101
N92-26215 # p 3021 ..... ANL/HEP/CP-91-116
CONF-9108141-6
DE92-010346
N92-26216 # p 3021 ..... ANL/HEP/CP-91-115
CONF-9108141-7
DE92-010347
N92-26217 # p 2870 ..... CONF-910920-19
DE92-009945
WSRC-MS-91-076
N92-26218 # p 3021 ..... ANL/HEP/CP-91-112
CONF-9108141-8
DE92-010349
N92-26219 # p 2913 ..... CESAR-92/09
DE92-010002
ORNL/TM-12070
N92-26220 # p 2871 ..... DE92-009491
LBL-31278
N92-26221 # p 3011 ..... DE92-009498
LBL-31610
N92-26222 # p 3001 ..... DE92-009501
LBL-31695
N92-26223 # p 2877 ..... DE92-009529
UCRL-CR-107026
N92-26224 # p 2892 ..... CONF-910968-76
DE92-009051
UCRL-JC-107249
N92-26225 # p 2993 ..... CONF-920362-2
DE92-009063
SAND-92-0063C
N92-26226 # p 3001 ..... AD-A245309
RL-TR-91-266
N92-26227 # p 2978 ..... AD-A245610
N92-26228 # p 2991 ..... AD-A245613
N92-26229 # p 2985 ..... AD-A245698
N92-26230 # p 2906 ..... CONF-910968-77
DE92-009695
UCRL-JC-107241
N92-26231 # p 2928 ..... DE92-010027
DOE/ER-60943/1
N92-26232 # p 2985 ..... DE92-010479
LBL-31589
UCB-PTH-91/69
N92-26233 # p 2972 ..... CONF-9108202-1
DE92-008927
UCRL-JC-106539
N92-26234 # p 2913 ..... CONF-920375-3
DE92-009379
N92-26235 # p 2994 ..... DE92-010300
LBL-31491
N92-26236 # p 2871 ..... DE92-010317
DOE/ER-13589/4
N92-26237 # p 2887 ..... DE92-010365
ORNL/SUB-90-SG828/1
N92-26238 # p 2892 ..... CONF-920669-3
DE92-010801
SAND-91-2348C
N92-26239 # p 2935 ..... DE92-010322
LBL-31534
N92-26240 # p 2994 ..... DE92-011215
DOE/ER-13442/6
N92-26241 # p 2996 ..... AD-A245781
N92-26242 # p 2954 ..... AD-A246273
NATICK/TR-92/015
N92-26243 # p 2954 ..... AD-A246275
NATICK/TR-92/016
N92-26244 # p 2892 ..... AD-A246317
DREO-1108
N92-26245 # p 2948 ..... AD-A246323
N92-26246 # p 2886 ..... ETN-92-98819
MBB-UA-1197-90-PUB
N92-26247* # p 3019 ..... NAS 1.26:190245
NASA-CR-190245
N92-26248 # p 2972 ..... AD-A245389
N92-26249 # p 2892 ..... ETN-92-91285
ISBN-90-6275-721-9
N92-26250 # p 3008 ..... ETN-92-91286
ISBN-90-9004609-7
N92-26251 # p 2877 ..... DE92-010792
DOE/ER-45295/2
N92-26252 # p 2877 ..... ETN-92-91288
ISBN-90-9004483-3
N92-26253 # p 3021 ..... ANL/HEP/CP-91-119
CONF-9108141-5
DE92-010345
N92-26254 # p 2887 ..... ETN-92-91290
ISBN-90-6275-722-7
N92-26255 # p 2954 ..... ETN-92-91291
ISBN-90-370-0056-8
N92-26256 # p 2999 ..... DE92-010547
DOE/ET-53088/537
IFSR-537
N92-26257 # p 2871 ..... ETN-92-91303
ISBN-90-6275-732-4
N92-26258 # p 2895 ..... AD-A246349
ARL-STRUC-TM-527
DODA-AR-006-091
N92-26259 # p 2916 ..... ETN-92-91304
N92-26260 # p 2892 ..... ETN-92-91305
N92-26261 # p 2871 ..... ETN-92-91306
N92-26262 # p 2871 ..... CONF-9204103-1
DE92-009887
DOE/METC-C/92/7006
N92-26263* # p 2952 ..... NAS 1.26:190341
NASA-CR-190341
N92-26264 # p 3021 ..... ANL/HEP/CP-91-118
CONF-9108141-4
DE92-010344
N92-26265* # p 3001 ..... NAS 1.26:190340
NASA-CR-190340
N92-26266* # p 2950 ..... NAS 1.15:107856
NASA-TM-107856
N92-26267 # p 2887 ..... CONF-920237-2
DE92-010728
SLAC-PUB-5699
N92-26268* # p 2857 ..... NAS 1.15:103583
NASA-TM-103583
N92-26269 # p 2910 ..... CONF-920362-7
DE92-010773
SAND-92-0089C
N92-26270 # p 2948 ..... DE92-010805
UCRL-CR-109689
N92-26271 # p 2910 ..... AD-A245425
FEL-91-A161
TDCK-TD-91-2909
N92-26272 # p 2850 ..... AD-A245433
AD-E501470

IDA-P-2590
IDA/HQ-91-38012
N92-26273 # p 2972 ..... AD-A245434
AD-E501456
IDA-P-2422
IDA/HQ-90-035650
N92-26274 # p 2871 ..... DE92-010821
DOE/ER-13554/6
N92-26275 # p 2880 ..... AD-A245437
AD-E501463
IDA-D-1033
IDA/HQ-91-40225
N92-26276 # p 2972 ..... AD-A245439
AD-E501471
IDA-D-1042
IDA/HQ-91-40280
N92-26277 # p 2979 ..... DE92-010829
PNL-SA-20425
N92-26278 # p 2979 ..... AD-A245445
TR-91-1250
N92-26279 # p 2979 ..... AD-A245446
TR-91-1251
N92-26280 # p 2892 ..... AD-A245636
REPT-721563-4
N92-26281 # p 2872 ..... DE92-011216
DOE/ER-13857/T2
N92-26282 # p 2916 ..... AD-A245641
ARCCB-TR-91035
N92-26283 # p 2881 ..... AD-A245817
MTL-TR-91-52
N92-26284 # p 2914 ..... ISSN-0208-5658
N92-26285 # p 2872 ..... ETN-92-91307
N92-26286 # p 2999 ..... DE92-621553
INIS-MF-13116
N92-26287 # p 2910 ..... DE92-621612
INIS-BR-2897
N92-26288*# p 2945 ..... NAS 1.15:103585
NASA-TM-103585
N92-26289 # p 2950 ..... AD-A245394
USNA-TSPR-178
N92-26290 # p 2896 ..... AD-A246314
N92-26291 # p 2851 ..... AD-A246316
DREO-1091
N92-26292 # p 2973 ..... AD-A246318
CRC-TR-1423
N92-26293 # p 2911 ..... AD-A246352
MDC-86PR0869-REV
N92-26294 # p 2935 ..... ESA-SP-330
ETN-92-91714
ISBN-92-9092-162-5
N92-26295 # p 2935 ..... NO REPORT NUMBER
N92-26296 # p 2935 ..... NO REPORT NUMBER
N92-26297 # p 2935 ..... NO REPORT NUMBER
N92-26298 # p 2935 ..... NO REPORT NUMBER
N92-26299 # p 2935 ..... NO REPORT NUMBER
N92-26300 # p 2936 ..... NO REPORT NUMBER
N92-26301 # p 2936 ..... NO REPORT NUMBER
N92-26302 # p 2936 ..... NO REPORT NUMBER
N92-26303 # p 2936 ..... NO REPORT NUMBER
N92-26304 # p 2936 ..... NO REPORT NUMBER
N92-26305 # p 2936 ..... NO REPORT NUMBER
N92-26306 # p 2936 ..... NO REPORT NUMBER
N92-26307 # p 2937 ..... NO REPORT NUMBER
N92-26308 # p 2937 ..... NO REPORT NUMBER
N92-26309 # p 2937 ..... NO REPORT NUMBER
N92-26310 # p 2937 ..... NO REPORT NUMBER
N92-26311 # p 2937 ..... NO REPORT NUMBER
N92-26312 # p 2937 ..... NO REPORT NUMBER
N92-26313 # p 2937 ..... NO REPORT NUMBER
N92-26314 # p 2938 ..... NO REPORT NUMBER
N92-26315 # p 2938 ..... NO REPORT NUMBER
N92-26316 # p 2938 ..... NO REPORT NUMBER
N92-26317 # p 2938 ..... NO REPORT NUMBER
N92-26318 # p 2938 ..... NO REPORT NUMBER
N92-26319 # p 2938 ..... NO REPORT NUMBER
N92-26320 # p 3001 ..... ETN-92-91264
ISBN-951-38-3956-7
ISSN-0357-5069
VTT-PUBL-82
N92-26321 # p 3002 ..... NO REPORT NUMBER
N92-26322 # p 3002 ..... NO REPORT NUMBER
N92-26323 # p 3002 ..... NO REPORT NUMBER
N92-26324 # p 3002 ..... NO REPORT NUMBER
N92-26325 # p 3002 ..... NO REPORT NUMBER
N92-26326 # p 3002 ..... NO REPORT NUMBER
N92-26327 # p 3003 ..... NO REPORT NUMBER
N92-26328 # p 3003 ..... NO REPORT NUMBER
N92-26329 # p 2939 ..... DLR-FB-91-30
ETN-92-91389
ISSN-0939-2963
N92-26330 # p 2939 ..... NO REPORT NUMBER
N92-26331 # p 2939 ..... NO REPORT NUMBER
N92-26332 # p 2934 ..... NO REPORT NUMBER
N92-26333 # p 2939 ..... NO REPORT NUMBER
N92-26334 # p 2934 ..... NO REPORT NUMBER
N92-26335 # p 2940 ..... NO REPORT NUMBER
N92-26336 # p 2940 ..... NO REPORT NUMBER
N92-26337 # p 2926 ..... NO REPORT NUMBER
N92-26338 # p 2940 ..... NO REPORT NUMBER
N92-26339 # p 2940 ..... NO REPORT NUMBER
N92-26340 # p 2940 ..... NO REPORT NUMBER
N92-26341*# p 2940 ..... NO REPORT NUMBER
N92-26342 # p 2941 ..... NO REPORT NUMBER
N92-26343 # p 2941 ..... NO REPORT NUMBER
N92-26344 # p 2941 ..... NO REPORT NUMBER
N92-26345 # p 2934 ..... NO REPORT NUMBER
N92-26346 # p 2941 ..... NO REPORT NUMBER
N92-26347 # p 2941 ..... NO REPORT NUMBER
N92-26348 # p 2941 ..... NO REPORT NUMBER
N92-26349 # p 2850 ..... NO REPORT NUMBER
N92-26350 # p 2942 ..... NO REPORT NUMBER
N92-26351 # p 2872 ..... GRI-91/0345
PB92-152917
N92-26352 # p 2928 ..... NCAR/TN-343+STR
PB92-155258
N92-26353 # p 3008 ..... PB92-157064
N92-26354 # p 2928 ..... EPA/600/A-92/052
PB92-153782
N92-26355 # p 2955 ..... AD-A245707
AL-TR-1991-0018
N92-26356 # p 2981 ..... AD-A245711
CMU-RI-TR-91-33
N92-26357 # p 2981 ..... AD-A245712
CMU-RI-TR-91-24
N92-26358 # p 2986 ..... AD-A246135
N92-26359 # p 2979 ..... AD-A246284
TR-91-04-04
N92-26360 # p 2948 ..... AD-A246287
N92-26361 # p 2979 ..... AD-A246289
N92-26362 # p 2860 ..... AD-A246299
N92-26363 # p 2888 ..... AD-A246300
N92-26364 # p 2945 ..... AD-A246301
N92-26365 # p 2994 ..... DE92-614353
IC-91/130
N92-26366 # p 2914 ..... NIST/SP-824
PB92-137553
N92-26367 # p 2986 ..... PB92-149335
WS-382
N92-26368 # p 3011 ..... PB92-158351
N92-26369 # p 3008 ..... PB92-160118
N92-26370 # p 2973 ..... ECMA-TR/55-ED-2
NIST/SP-500/201
PB92-158328
N92-26371 # p 2914 ..... GRI-90/0246
PB92-164482
N92-26372 # p 2926 ..... GRI-92/0066
PB92-164300
N92-26373 # p 2928 ..... PB92-158260
N92-26374 # p 2888 ..... AD-A245700
WSU/DC/92/TR-77
N92-26375 # p 2955 ..... CONF-920263-1
DE92-007681
N92-26376 # p 2996 ..... CONF-9109230-11
DE92-009011
N92-26377 # p 2906 ..... CONF-910968-73
DE92-009053
UCRL-JC-107251
N92-26378 # p 3011 ..... AD-A245324
DREO-TN-91-11
N92-26379 # p 2896 ..... AD-A245327
WL-TR-91-2086
WSU-TR-88-001
N92-26380 # p 2867 ..... AD-A245395
USNA-TSPR-179
N92-26381 # p 2888 ..... AD-A245567
AFIT/EN-TM-91-1-VOL-2
N92-26382 # p 2970 ..... AD-A245615
N92-26383 # p 2867 ..... AD-A245616
N92-26384 # p 2973 ..... AD-A245855
CMU-RI-TR-91-29
N92-26385 # p 3019 ..... DE92-010478
LBL-31107
UCB-PTH-91/38
N92-26386 # p 2868 ..... AD-A246136
N92-26387 # p 2949 ..... AD-A246326
CERC-WIS-26
N92-26388 # p 2888 ..... AD-A246333
N92-26389 # p 2914 ..... AD-A246334
PARGUM-91-08
N92-26390 # p 2928 ..... DE92-006911
RFP-4533
N92-26391 p 2906 ..... ETN-92-91736
MPI-PHE/91-07
N92-26392 p 2907 ..... NO REPORT NUMBER
N92-26393 p 2907 ..... NO REPORT NUMBER
N92-26394 p 2907 ..... NO REPORT NUMBER
N92-26395 p 2907 ..... NO REPORT NUMBER
N92-26396 p 2907 ..... NO REPORT NUMBER
N92-26397 p 2907 ..... NO REPORT NUMBER
N92-26398 p 2908 ..... NO REPORT NUMBER
N92-26399 # p 2888 ..... AD-A245482
N92-26400 # p 2973 ..... AD-A245484
N92-26401 # p 2908 ..... AD-A245486
N92-26402 # p 2857 ..... AD-A245617
N92-26403 # p 3011 ..... AD-A245622
FEL-91-A286
TDCK-TD91-3272
N92-26404 # p 2872 ..... AD-A245899
DREO-1098
N92-26405*# p 2853 ..... AD-A245463
AEDC-TR-91-20
GTRI-A8612-001
NAS 1.26:190423
NASA-CR-190423
N92-26406*# p 2942 ..... AD-A245860
NAS 1.26:190424
NASA-CR-190424
NOO-TR-304
N92-26407*# p 2986 ..... CONF-9206102-2
DE92-007241
NAS 1.15:101796
NASA-TM-101796
N92-26408 # p 2852 ..... AD-A246150
AD-E951752
AMSMI/TR-RD-GC-91-6
N92-26409 # p 2945 ..... AD-A246152
AD-E951742
AMSMI/TR-RD-WS-91-9
N92-26410 # p 2981 ..... AD-A246156
N92-26411 # p 2949 ..... AD-A246158
N92-26412 # p 2896 ..... AD-A246160
ERC-92038
N92-26413 # p 2992 ..... AD-A246162
ARO-25273.6-PH
N92-26414 # p 2986 ..... AD-A246164
REPT-153425
N92-26415 # p 2851 ..... AD-A246165
NPS-OC-91-004
N92-26416 # p 2999 ..... AD-A246179
N92-26417 # p 2979 ..... AD-A246191
N92-26418 # p 2973 ..... AD-A246193
N92-26419 # p 2888 ..... AD-A246534
DREO-1103
N92-26420 p 2986 ..... ETN-92-91249
REPT-91-041
N92-26421 p 2973 ..... ETN-92-91250
REPT-91-053
N92-26422 p 3011 ..... ETN-92-91251
REPT-91-054
N92-26423 # p 2949 ..... AD-A245477
N92-26424 # p 2888 ..... AD-A245675
CRC-1438
N92-26425 # p 2997 ..... AD-A245713
CMU-RI-TR-91-26
N92-26426 # p 3008 ..... AD-A245714
CMU-RI-TR-91-21
N92-26427 # p 2851 ..... AD-A245715
CMU-RI-TR-91-28
N92-26428 # p 2981 ..... AD-A245716
CMU-RI-TR-91-30
N92-26429*# p 2982 ..... AD-A245717
CMU-RI-TR-91-27
NAS 1.26:190296
NASA-CR-190296
N92-26430 # p 2980 ..... AD-A245721
N92-26431 # p 2872 ..... AD-A245812
TR-75
N92-26432 # p 2942 ..... AD-A245903
N92-26433 # p 3003 ..... AD-D015196
NAVY-CASE-72812
US-PATENT-APPL-SN-749825
N92-26434 # p 2982 ..... CONF-920471-3
DE92-011159
SAND-92-0648C
N92-26435*# p 2852 ..... NAS 1.26:190019
NASA-CR-190019
N92-26436*# p 3016 ..... EFI-91-70
FERMILAB-PUB-91/332-A
NAS 1.26:190117
NASA-CR-190117
UMHEP-361
N92-26437*# p 3020 ..... NAS 1.26:190195
NASA-CR-190195
N92-26438*# p 3019 ..... NAS 1.26:190211
NASA-CR-190211
N92-26439 p 2970 ..... ETN-92-91358
REPT-91-071
N92-26440 # p 2884 ..... EG-910045
JTN-92-80348
N92-26441 # p 2884 ..... NO REPORT NUMBER
N92-26442 # p 2885 ..... NO REPORT NUMBER
N92-26443 # p 2885 ..... NO REPORT NUMBER
N92-26444 # p 2885 ..... NO REPORT NUMBER
N92-26445 # p 2885 ..... NO REPORT NUMBER
N92-26446 # p 2885 ..... NO REPORT NUMBER
N92-26447 # p 2886 ..... NO REPORT NUMBER
N92-26448 p 2973 ..... ETN-92-91359
REPT-91-072

N92-26449 p 2974 ETN-92-91360
REPT-91-079
N92-26450 p 2974 ETN-92-91372
ISSN-0262-5369
NPL-DITC-194/92
N92-26451 # p 2881 DE92-008398
DOE/ER-13445/T1
N92-26452 # p 2997 CONF-920367-6
DE92-008680
SAND-91-2751C
N92-26453 # p 3011 DE92-008875
DOE/ER-61190/1
N92-26454 # p 2873 CONF-910422-8
DE92-008937
UCRL-JC-107042
N92-26455 # p 2881 CONF-910938-9
DE92-008956
KAPL-4730
N92-26456 # p 2896 DE92-009079
DOE/PC-89769/T8
N92-26457 # p 2873 DE92-009081
DOE/PC-91304/T1
N92-26458 # p 2974 AD-A246198
N92-26459 # p 2908 AD-A246203
N92-26460 # p 2990 AD-A246207
N92-26461 # p 2974 AD-A246208
N92-26462 # p 2911 AD-A246212
N92-26463 # p 2949 AD-A246219
AD-E040177
INO-TM-5
N92-26464 # p 2974 AD-A246220
AD-E040179
INO-TM-3
N92-26465 # p 3011 AD-A246500
N92-26466 # p 2990 AD-A246502
N92-26467 # p 2989 AD-A246506
N92-26468 # p 2974 AD-A246522
N92-26469 # p 3012 AD-A246527
N92-26470 # p 2952 AD-A246529
NCTRF-181
N92-26471 # p 2990 AD-A246533
DREO-TN-91-28
N92-26472 # p 2955 AD-A246535
DREO-1096
N92-26473 p 2928 NO REPORT NUMBER
N92-26474* p 2945 NAS 1.26:190225
NASA-CR-190225
N92-26475 p 2914 NO REPORT NUMBER
N92-26476 p 3016 NO REPORT NUMBER
N92-26477 p 3015 NO REPORT NUMBER
N92-26478 p 2921 NO REPORT NUMBER
N92-26479 p 2974 NO REPORT NUMBER
N92-26480 p 2853 NO REPORT NUMBER
N92-26481 p 3012 NO REPORT NUMBER
N92-26482 # p 2929 ETN-92-91263
ISBN-951-38-4060-3
ISSN-0358-5069
VTT-PUBL-81
N92-26483 # p 2929 IAEA-CN-43/449
N92-26484 # p 2929 NO REPORT NUMBER
N92-26485 # p 2929 NO REPORT NUMBER
N92-26486 # p 2929 NO REPORT NUMBER
N92-26487 # p 2930 NO REPORT NUMBER
N92-26488 # p 2930 NO REPORT NUMBER
N92-26489 p 2942 NO REPORT NUMBER
N92-26490 p 2942 NO REPORT NUMBER
N92-26491 p 3016 NO REPORT NUMBER
N92-26492 p 2881 NO REPORT NUMBER
N92-26493 # p 2951 DE92-003218
DOE/ER-13828/4
N92-26494 # p 2955 CONF-920473-1
DE92-007239
N92-26495 # p 2930 EPA/600/2-91/026
PB92-109099
N92-26496 # p 2896 ISBN-951-22-0724-9
PB92-133958
RR-A297
N92-26497 # p 2893 ISBN-951-22-0472-X
PB92-142223
TKK-F-A671
N92-26500 # p 2975 ISBN-951-22-0814-8
PB92-143544
SER-A-15
N92-26501 # p 2980 NISTIR-4750
PB92-149863
N92-26502 # p 2986 ISBN-951-22-0670-6
PB92-141530
RR-A295
N92-26503 # p 2986 MEMO-996
PB92-148741
N92-26504 # p 2911 CONF-920124-14
DE92-008604
UCRL-JC-109185
N92-26505 # p 2911 CONF-920124-13
DE92-008608
UCRL-JC-107974
N92-26506 # p 2896 PB92-152610
R-639
N92-26507 # p 2896 PB92-142231
TKK-F-A673
N92-26508 # p 2873 GRI-92/0011
PB92-149657
N92-26509 # p 2930 EPA/600/A-92/039
PB92-153022
N92-26510 # p 2930 EPA/600/A-92/037
PB92-153006
N92-26511 # p 2889 PB92-150911
N92-26512 # p 2953 PB92-145796
N92-26513 # p 2921 FOA-C-30609-3.4
PB92-152206
N92-26514 # p 2945 NOAA-TM-NWS-SR-141
PB92-146075
N92-26515 # p 2857 AD-A245481
N92-26516 # p 2873 GRI-91/0383
PB92-154822
N92-26517 # p 2908 AD-A245681
FEL-91-B234
TDCK-TD91-2901
N92-26518 # p 2914 PB92-163237
N92-26519 # p 2930 EPA/600/3-91/074
PB92-132885
N92-26520 # p 2877 AD-A245685
N92-26521 # p 2873 GRI-91/0180
NREC-1656-1
PB92-142579
N92-26522 p 3017 NO REPORT NUMBER
N92-26523 # p 3009 PB92-151703
N92-26524 # p 2975 AD-A245686
N92-26525 # p 2868 PB92-151521
N92-26526 # p 2874 AD-A245813
TR-76
N92-26527 # p 2856 AD-A245449
AL-TR-1991-0039
N92-26528 # p 2955 AD-A245459
AL-TR-1991-0079
N92-26529 # p 2975 AD-A245461
NRL-MR-6923
N92-26530 # p 2975 AD-A245462
NAVSWC-TR-91-549
N92-26531 # p 2980 AD-A245469
NOSC-TR-1440
N92-26532 # p 2868 AD-A245474
USNA-TSPR-186
N92-26533 # p 2949 AD-A245476
N92-26534 # p 2922 CONF-9205128-1
DE92-010482
FNAL/C-92/58
N92-26535*# p 2945 NAS 1.26:190383
NASA-CR-190383
SVHSER-14841
TRMM-SER-705
N92-26536*# p 2908 NAS 1.26:190403
NASA-CR-190403
N92-26537*# p 2917 L-16940
NAS 1.60:3164
NASA-TP-3164
N92-26538*# p 2956 NAS 1.60:3206
NASA-TP-3206
S-670
N92-26539*# p 2994 NAS 1.26:190254
NASA-CR-190254
N92-26540 # p 2893 AD-A246090
RL-TR-91-325
N92-26541 # p 2874 AD-A246098
ARO-25199.3-MS
N92-26542 # p 2877 DE92-010311
DOE/ER-45280/T3
N92-26543 # p 2881 DE92-010327
DOE/ER-45345/T1
N92-26544 # p 3021 DE92-010375
ORNL/TM-11778
N92-26545 # p 2987 CESAR-91/24
DE92-010390
ORNL/TM-11905
N92-26546 # p 2999 DE92-010424
DOE/ET-53088/543
IFSR-543
N92-26547 # p 2883 DE92-010465
DOE/PC-89786/T8
N92-26548 # p 2884 DE92-010480
DOE/PC-90044/5
N92-26549 # p 3000 DE92-010548
DOE/ET-53088/539
IFSR-539
N92-26550 # p 3000 DE92-010549
DOE/ET-53088/542
IFSR-542
N92-26551 # p 2970 CONF-911106-90
DE92-010550
LBL-31450
N92-26552*# p 3009 NAS 1.26:190397
NASA-CR-190397
N92-26553*# p 2854 E-7083
NAS 1.15:105695
NASA-TM-105695
N92-26554 p 3017 NO REPORT NUMBER
N92-26555*# p 2915 AVSCOM-TR-91-C-038
E-7015
NAS 1.15:105651
NASA-TM-105651
N92-26556 p 2897 NO REPORT NUMBER
N92-26557 p 2917 NO REPORT NUMBER
N92-26558 p 2992 NO REPORT NUMBER
N92-26559 p 2868 NO REPORT NUMBER
N92-26560*# p 2915 AVSCOM-TR-91-C-035
E-7032
NAS 1.15:105668
NASA-TM-105668
N92-26561*# p 2854 AIAA PAPER 92-3087
E-7087
NAS 1.15:105699
NASA-TM-105699
N92-26562 # p 2946 AD-A245749
N92-26563 # p 2878 BNL-47180
CONF-911047-20
DE92-009159
N92-26564 p 2868 NO REPORT NUMBER
N92-26565 # p 2997 ANL/CP-75618
CONF-920212-2
DE92-009726
N92-26566 # p 3020 BNL-47155
CONF-9105319-1
DE92-010077
N92-26567 p 3012 NO REPORT NUMBER
N92-26568 p 2949 NO REPORT NUMBER
N92-26569 # p 2908 CONF-920423-2
DE92-010121
N92-26570 # p 2994 CONF-9109332-4
DE92-010127
N92-26571 p 2911 NO REPORT NUMBER
N92-26572 # p 2909 BNL-47194
DE92-010137
N92-26573 # p 2911 DE92-010306
LA-12254T
N92-26574 # p 2995 DE92-010319
DOE/ER-13971/13
N92-26575 # p 3012 DE92-010360
SAND-91-1575
N92-26576 p 3017 NO REPORT NUMBER
N92-26577 # p 3000 DE92-010362
ORNL/TM-12032
N92-26578 p 3017 NO REPORT NUMBER
N92-26579 # p 3003 DE92-010363
ORNL/TM-11949
N92-26580 # p 2931 CONF-9109340-3
DE92-010289
N92-26581 p 2926 NO REPORT NUMBER
N92-26582 # p 3003 DE92-010299
LBL-31553
N92-26583 p 2942 NO REPORT NUMBER
N92-26584 # p 3003 CONF-920141-6
DE92-010305
LBL-31663
N92-26585 p 2849 NO REPORT NUMBER
N92-26586 p 2854 NO REPORT NUMBER
N92-26587*# p 2975 NAS 1.26:190279
NASA-CR-190279
N92-26588 # p 2995 AD-A245752
N92-26589 # p 2884 AD-A245755
EOARD-TR-92-03
N92-26590 p 2931 NO REPORT NUMBER
N92-26591 # p 2897 AD-A245756
N92-26592 # p 2889 AD-A245758
DREO-1078
N92-26593 # p 2917 AD-A245759
N92-26594 p 2917 NO REPORT NUMBER
N92-26595 # p 2889 AD-A245762
N92-26596 # p 2980 AD-A245763
N92-26597 p 2982 NO REPORT NUMBER
N92-26598 p 2918 NO REPORT NUMBER
N92-26599 p 2897 NO REPORT NUMBER
N92-26600 p 2897 NO REPORT NUMBER
N92-26601 p 2860 NO REPORT NUMBER
N92-26602 p 2916 NO REPORT NUMBER
N92-26603 p 2912 NO REPORT NUMBER
N92-26604 p 2889 NO REPORT NUMBER
N92-26605 # p 2858 AD-A245764
N92-26606 # p 2893 AD-A245765
N92-26607 p 2869 NO REPORT NUMBER
N92-26608 # p 2874 AD-A245814
TR-77
N92-26609 # p 2882 AD-A245816
MTL-TR-91-50
N92-26610 p 2858 NO REPORT NUMBER
N92-26611*# p 2886 E-6885
NAS 1.15:105561
NASA-TM-105561
N92-26612*# p 2849 AIAA PAPER 92-0413

E-7147
NAS 1.15:105742
NASA-TM-105742
N92-26613* # p 2854 ..... AIAA PAPER 92-3792
E-7124
NAS 1.15:105724
NASA-TM-105724
N92-26614 p 3012 ..... NO REPORT NUMBER
N92-26615 p 2874 ..... NO REPORT NUMBER
N92-26616 p 2849 ..... NO REPORT NUMBER
N92-26617 # p 3007 ..... AD-A246557
N92-26618 # p 2992 ..... AD-A246558
N92-26619 # p 2889 ..... AD-A246566
N92-26620 # p 2987 ..... AD-A246570
N92-26621 # p 2858 ..... AD-A246577
N92-26622 p 2943 ..... NO REPORT NUMBER
N92-26623 p 2851 ..... NO REPORT NUMBER
N92-26624 p 2987 ..... NO REPORT NUMBER
N92-26625 p 2922 ..... NO REPORT NUMBER
N92-26626 p 2912 ..... NO REPORT NUMBER
N92-26627* # p 2982 ..... FIA-91-04
NAS 1.15:107882
NASA-TM-107882
N92-26628* # p 2982 ..... FIA-90-11-05-1
NAS 1.15:107886
NASA-TM-107886
N92-26629* # p 2983 ..... FIA-91-28
NAS 1.15:107879
NASA-TM-107879
N92-26630* # p 2983 ..... FIA-91-32
NAS 1.15:107868
NASA-TM-107868
N92-26631* # p 2983 ..... FIA-91-22
NAS 1.15:107840
NASA-TM-107840
N92-26632 # p 2874 ..... DE92-009947
WSRC-RD-91-16
N92-26633 # p 2931 ..... DE92-010035
PNL-SA-20478
N92-26634 # p 2874 ..... CONF-910774-102
DE92-010041
WSRC-MS-91-062
N92-26635 # p 2878 ..... CONF-910920-27
DE92-009905
WSRC-MS-91-110
N92-26636 # p 2893 ..... CONF-920581-1
DE92-010108
N92-26637 # p 2893 ..... CONF-920669-2
DE92-010110
N92-26638 # p 3004 ..... CONF-920309-1
DE92-010125
N92-26639 # p 3004 ..... DE92-010130
DOE/ER-13438/3
N92-26640 # p 3022 ..... DE92-010133
DOE/ER-0505
N92-26641 # p 3004 ..... DE92-010286
LBL-31541
N92-26642* # p 2878 ..... NAS 1.26:188468
NASA-CR-188468
N92-26643* # p 2983 ..... FIA-91-08
NAS 1.15:107881
NASA-TM-107881
N92-26644 # p 2897 ..... CONF-920664-1
DE92-009066
SAND-91-2555C
N92-26645 # p 2898 ..... CONF-9105317-1
DE92-009121
UCRL-JC-107359
N92-26646 # p 2912 ..... CONF-9206137-1
DE92-009692
UCRL-JC-108317
N92-26647 # p 2975 ..... CONF-9206136-1
DE92-009698
UCRL-JC-109767
N92-26648 # p 3004 ..... DE92-009812
DOE/ER-45381/3
N92-26649* # p 2898 ..... ICASE-92-19
NAS 1.26:189646
NASA-CR-189646
N92-26650* # p 2869 ..... NAS 1.15:104562
NASA-TM-104562
REPT-92A01664
N92-26651* # p 2849 ..... NAS 1.26:189642
NASA-CR-189642
N92-26652* # p 2849 ..... NAS 1.26:189641
NASA-CR-189641
N92-26653* # p 2889 ..... NAS 1.15:107583
NASA-TM-107583
N92-26654* # p 2861 ..... E-7077
NAS 1.15:105692
NASA-TM-105692
N92-26655* # p 2852 ..... NAS 1.26:190434
NASA-CR-190434
TELAC-91-17
N92-26656* # p 2886 ..... NAS 1.26:187664
NASA-CR-187664
N92-26657 # p 2983 ..... CONF-920540-13
DE92-000680
N92-26658 # p 2976 ..... AD-A245522
N92-26659 # p 2878 ..... AD-A245523
N92-26660 # p 3009 ..... AD-A245524
N92-26661 # p 2922 ..... AD-A245525
N92-26662 # p 2997 ..... AD-A245527
N92-26663 # p 2912 ..... AD-A245528
N92-26664 # p 3022 ..... AD-A245533
REPT-16
USNA-3910-3
N92-26665 # p 2956 ..... AD-A245543
NMRI-91-85
N92-26666 # p 3000 ..... CONF-9206134-1
DE92-009059
SAND-92-7070C
N92-26667* # p 2858 ..... NAS 1.60:3227
NASA-TP-3227
REPT-92B00041
N92-26668* # p 2987 ..... ICASE-92-17
NAS 1.26:189639
NASA-CR-189639
N92-26669* # p 2918 ..... M-688
NAS 1.60:3248
NASA-TP-3248
N92-26670* # p 2875 ..... E-6984
NAS 1.15:105638
NASA-TM-105638
N92-26671* # p 2990 ..... E-6777
NAS 1.15:105573
NASA-TM-105573
N92-26672 # p 3004 ..... DE92-617541
IC-91/346
N92-26673 # p 2852 ..... RAND-P-7746-RGS
N92-26674 # p 2922 ..... AD-A245493
CRREL-SR-91-16
N92-26675 # p 2943 ..... AD-A245495
N92-26676 # p 2997 ..... AD-A245496
N92-26677 # p 2980 ..... AD-A245510
TR-91-1249
N92-26678 # p 2992 ..... AD-A245521
N92-26679 # p 2869 ..... ANL/CP-73280
CONF-920624-1
DE91-014021
N92-26680* # p 2898 ..... NAS 1.26:4438
NASA-CR-4438
N92-26681* # p 2898 ..... NAS 1.26:4439
NASA-CR-4439
N92-26682* # p 2956 ..... NAS 1.60:3207
NASA-TP-3207
S-671
N92-26683 # p 2927 ..... CONF-920290-VOL-1
DE92-001238
NREL/TP-432-4804-VOL-1
N92-26684 # p 3005 ..... AD-A246124
N92-26685 # p 2976 ..... AD-A246126
N92-26686 # p 2927 ..... CONF-920678-1
DE92-001240
NREL/TP-411-4787
N92-26687 # p 2875 ..... AD-A246127
N92-26688 # p 2992 ..... AD-A246548
N92-26689 # p 3013 ..... DE92-001619
DOE/ER-0535P
N92-26690* # p 2898 ..... E-7043
NAS 1.15:105674
NASA-TM-105674
N92-26691 # p 2912 ..... CONF-920605-1
DE92-002357
SAND-91-1441C
N92-26692 # p 2995 ..... CONF-920643-1
DE92-004571
LA-UR-91-4177
N92-26693 # p 2857 ..... CONF-920689-1
DE92-005065
LA-UR-91-3988
N92-26694 # p 2918 ..... CONF-920631-6
DE92-006504
WHC-SA-1375
N92-26695 # p 3000 ..... CONF-920607-1
DE92-006528
SAND-92-0103C
N92-26696 # p 2976 ..... CONF-9206101-1
DE92-006675
SAND-92-0033C
N92-26697 # p 2854 ..... CONF-920631-7
DE92-006859
N92-26698 # p 2899 ..... CONF-920605-2
DE92-002930
SAND-91-1429C
N92-26699 # p 2899 ..... CONF-920631-2
DE92-004180
N92-26700 # p 2899 ..... CONF-920631-4
DE92-004181
N92-26701 # p 2922 ..... JTN-92-80345
N92-26702* # p 2922 ..... TW-1
N92-26703 # p 2922 ..... TW-2
N92-26704 # p 2923 ..... TW-3
N92-26705 # p 2923 ..... TW-4
N92-26706* # p 2923 ..... TW-5
N92-26707 # p 2923 ..... TW-6
N92-26708 # p 2923 ..... TW-7
N92-26709 # p 2923 ..... TW-8
N92-26710 # p 2923 ..... TW-9
N92-26711 # p 2923 ..... TW-10
N92-26712 # p 2924 ..... TW-11
N92-26713 # p 2924 ..... TW-12
N92-26714 # p 2924 ..... TW-13
N92-26715 # p 2924 ..... TW-14
N92-26716 # p 2899 ..... CONF-920685-1
DE92-004363
SAND-91-2803C
N92-26717 # p 2875 ..... CONF-910920-22
DE92-009830
WSRC-MS-91-016
N92-26718 # p 2875 ..... CONF-910920-25
DE92-009852
WSRC-MS-91-008
N92-26719 # p 2927 ..... CONF-9203102-1
DE92-009886
DOE/MC-28055/92/C0001
N92-26720 # p 2856 ..... CONF-920688-7
DE92-008437
LA-UR-92-356
N92-26721 # p 2951 ..... INPE-5315-PRE/1712
N92-26722 # p 2875 ..... CONF-920669-1
DE92-008524
SAND-91-2347C
N92-26723 p 3018 ..... NO REPORT NUMBER
N92-26724 # p 2875 ..... CONF-920643-2
DE92-008770
DOE/MC-10637/92/C0002
N92-26725 p 3018 ..... NO REPORT NUMBER
N92-26726 # p 2875 ..... CONF-9205121-2
DE92-008900
N92-26727 # p 2878 ..... CONF-9206135-1
DE92-008912
IS-M-698
N92-26728 p 2924 ..... NO REPORT NUMBER
N92-26729 # p 3000 ..... CONF-920607-2
DE92-008941
UCRL-JC-109680
N92-26730 # p 3014 ..... ISBN-0-16-035933-3
OTA-ITE-498
PB92-115757
N92-26731 p 2915 ..... NO REPORT NUMBER
N92-26732 # p 2878 ..... CONF-9206129-2
DE92-009052
UCRL-JC-109419
N92-26733 p 3007 ..... NO REPORT NUMBER
N92-26734 p 2983 ..... NO REPORT NUMBER
N92-26735* p 2946 ..... NAS 1.26:190223
NASA-CR-190223
N92-26736* p 2946 ..... NAS 1.26:190222
NASA-CR-190222
N92-26737 # p 2987 ..... MEMO-998
PB92-148766
N92-26738 p 2909 ..... NO REPORT NUMBER
N92-26739 p 2918 ..... NO REPORT NUMBER
N92-26740 p 2899 ..... NO REPORT NUMBER
N92-26741 # p 2893 ..... AD-A246561
NRL-MR-6910
N92-26742 # p 2924 ..... JTN-92-80342
N92-26743 # p 2924 ..... NO REPORT NUMBER
N92-26744* # p 2925 ..... NO REPORT NUMBER
N92-26745 # p 2925 ..... NO REPORT NUMBER
N92-26746 # p 2925 ..... NO REPORT NUMBER
N92-26747 # p 2925 ..... NO REPORT NUMBER
N92-26748 # p 2925 ..... NO REPORT NUMBER
N92-26749 # p 2925 ..... NO REPORT NUMBER
N92-26750 # p 2915 ..... CONF-920540-5
DE92-000070
N92-26751 # p 2882 ..... AD-A245299
EOARD-TR-92-01
N92-26752 # p 2887 ..... ETN-92-98850
RR-417
N92-26753 # p 2943 ..... AD-A245984
N92-26754 # p 2997 ..... AD-A245987
N92-26755 # p 2987 ..... AD-A245991
N92-26756 # p 2851 ..... AD-A245997
N92-26757 p 3018 ..... NO REPORT NUMBER
N92-26758 # p 2976 ..... AD-A245998
N92-26759 # p 2918 ..... AD-A246001
N92-26760 p 3015 ..... NO REPORT NUMBER
N92-26761 # p 3014 ..... AD-A246005
N92-26762 # p 3013 ..... AD-A246007
N92-26763 # p 3005 ..... AD-A246076
N92-26764 # p 2890 ..... AD-A246078
N92-26765 # p 3013 ..... AD-A246084
N92-26766 # p 2976 ..... AD-A246612
NRL-MR-6935
N92-26767 # p 3013 ..... AD-A246614
LMI-DL001-01R1-VOL-2

N92-26768 # p 2990 ..... AD-A246560
NRL-MR-6914
N92-26769 # p 2991 ..... AD-A246562
NRL-MR-6942
N92-26770 p 2879 ..... NO REPORT NUMBER
N92-26771 # p 2893 ..... AD-A246579
N92-26772 # p 2991 ..... AD-A246580
ARL-TR-91-8
N92-26773 # p 2970 ..... AD-A246597
N92-26774 p 3005 ..... NO REPORT NUMBER
N92-26775 p 2882 ..... NO REPORT NUMBER
N92-26776 p 3013 ..... NO REPORT NUMBER
N92-26777 p 2925 ..... NO REPORT NUMBER
N92-26778 p 3019 ..... NO REPORT NUMBER
N92-26779 p 3020 ..... NO REPORT NUMBER
N92-26780 p 3007 ..... NO REPORT NUMBER
N92-26781 p 2925 ..... NO REPORT NUMBER
N92-26782 # p 2876 ..... GRI-91/0313
PB92-137652
N92-26783 # p 2876 ..... AEROCHEM-TP-497
GRI-91/0402
PB92-141779
N92-26784 # p 2918 ..... DE92-007794
ORNL/TM-11767
N92-26785 p 2900 ..... NO REPORT NUMBER
N92-26786 # p 2909 ..... ISBN-951-22-0722-2
PB92-152750
S-194
N92-26787 # p 2879 ..... ISBN-951-22-0850-4
PB92-151893
TKK-V-B65
N92-26788 # p 2988 ..... IHES/M/92/1
PB92-153212
N92-26789* # p 2983 ..... FIA-91-15
NAS 1.15:107869
NASA-TM-107869
N92-26790* # p 3009 ..... FIA-90-11-01-01
NAS 1.15:107888
NASA-TM-107888
N92-26791* # p 2984 ..... NAS 1.15:107865
NASA-FIA-92-01
NASA-TM-107865
N92-26792* # p 2861 ..... E-7092
NAS 1.15:105703
NASA-TM-105703
N92-26793 # p 2931 ..... ARB-R-92-478
PB92-163278
N92-26794 # p 2909 ..... AD-A246563
N92-26795 # p 2852 ..... AD-A246598
N92-26796 # p 2869 ..... AD-A246602
CRREL-SR-91-20
N92-26797 # p 2976 ..... DE92-009800
UCRL-LR-108508
N92-26798 # p 2990 ..... DE92-621115
ITP-91-16
N92-26799 # p 2890 ..... DE92-621141
IFT-P-028/91
N92-26800 # p 2995 ..... DE92-621167
IFVE-ONF-91-34
N92-26801 # p 2980 ..... AD-A234648
AFOSR-91-0263TR
N92-26802 # p 2931 ..... PB92-113059
SYSAPP-91/091A
N92-26803 # p 2932 ..... PB92-113067
SYSAPP-91/091B
N92-26804 # p 3021 ..... DE92-621189
EFI-1326-21-91
N92-26805 # p 3007 ..... IHES/P/91/73
PB92-125038
N92-26806 # p 3000 ..... DE92-621523
ITF-91-14
N92-26807 # p 3001 ..... DE92-621524
ITP-91-19
N92-26808 # p 3001 ..... DE92-621529
ITF-91-11
N92-26809 # p 2890 ..... NOAA-TM-ERL-WPL-213
PB92-129931
N92-26810 # p 2932 ..... DE92-001219
NREL/TP-230-4633
N92-26811 # p 3009 ..... DE92-010132
DOE/ER-0504
N92-26812 # p 2876 ..... NOAA-TM-ERL-CMDL-3
PB92-128560
N92-26813 # p 2879 ..... BNL-45092
CONF-920458-3
DE92-010156
N92-26814 # p 2984 ..... NISTIR-4747
PB92-148287
N92-26815 # p 2995 ..... BNL-47115
CONF-911208-7
DE92-010158
N92-26816 # p 2915 ..... GRI-91/0290
PB92-149665
N92-26817 # p 2988 ..... MEMO-984
PB92-148626
N92-26818 # p 2857 ..... BNL-46287-REV
CONF-920104-6-REV
DE92-010160
N92-26819 # p 3019 ..... RAND-N-3437-JPL
N92-26820 # p 2943 ..... IHES/P/91/93
PB92-152305
N92-26821 # p 2894 ..... NISTIR-4592
PB92-148279
N92-26822 # p 2946 ..... PB92-160399
N92-26823 # p 2932 ..... EPA/SW/DK-92/016A
EPA/450/4-91/027
PB92-105527
N92-26824* # p 3022 ..... NAS 1.15:107792
NASA-TM-107792
PB92-155951
N92-26825 # p 2932 ..... BNL-47110
DE92-010162
N92-26826 # p 3005 ..... CONF-911109-9
DE92-011150
SAND-92-0437C
N92-26827 p 2869 ..... NO REPORT NUMBER
N92-26828 # p 3009 ..... B-248197
GAO/NSIAD-92-192
N92-26829 p 2919 ..... NO REPORT NUMBER
N92-26830 # p 3014 ..... DOT/FAA/CT-91/18
N92-26831 # p 2988 ..... DE92-621066
LNCC-004/91
N92-26832* # p 2996 ..... L-17036
NAS 1.15:4362
NASA-TM-4362
N92-26833 # p 3018 ..... IHES/P/91/76
PB92-152313
N92-26834 # p 2988 ..... DE92-621067
NIIYAF-MGV-91-13-217
N92-26835 # p 2976 ..... DE92-621106
IFVE-OMVT-91-12
N92-26836 # p 2900 ..... ISBN-90-9004419-1
PB92-151109
N92-26837 # p 2988 ..... DE92-621113
IFT-P-031/91
N92-26838 # p 2944 ..... EPA/700/R-92/002
PB92-150374
N92-26839 # p 2884 ..... AD-A245387
N92-26840 # p 2977 ..... AD-A245388
N92-26841 # p 2996 ..... ANL/CP-73148
CONF-920308-16
DE92-009717
N92-26842 # p 3005 ..... ANL/CP-74854
CONF-920141-3
DE92-009724
N92-26843 # p 3005 ..... CONF-920648-1-EXTD-ABST
DE92-008097
N92-26844 # p 2995 ..... DE92-621426
INIS-MF-13134
N92-26845 # p 2919 ..... CONF-920631-8
DE92-008099
N92-26846 # p 2919 ..... CONF-920688-6
DE92-008324
SAND-91-2817C
N92-26847 # p 2894 ..... CONF-920168-2
DE92-008326
SAND-91-2739C
N92-26848 # p 2879 ..... CONF-920673-2
DE92-008387
WHC-SA-1432
N92-26849 p 2900 ..... NO REPORT NUMBER
N92-26850 # p 2951 ..... DE92-007757
DOE-92007757
N92-26851 # p 3006 ..... CONF-920625-2
DE92-007828
N92-26852 # p 2919 ..... CONF-920688-4
DE92-007988
SAND-91-2815C
N92-26853 # p 2900 ..... CONF-920688-5
DE92-008017
SAND-91-2865C
N92-26854 # p 2981 ..... CONF-920606-2
DE92-004575
LA-UR-91-4157
N92-26855 # p 2900 ..... CONF-920688-2
DE92-007421
LA-UR-92-49
N92-26856 # p 2901 ..... CONF-920685-2
DE92-007428
LA-UR-92-3
SAND-91-2788C
N92-26857 # p 3006 ..... CONF-920662-1
DE92-007570
LA-UR-92-266
N92-26858 # p 2927 ..... DE92-008709
DOE/ER-13631/18
N92-26859 p 2882 ..... NO REPORT NUMBER
N92-26860 p 2920 ..... NO REPORT NUMBER
N92-26861 p 2869 ..... NO REPORT NUMBER
N92-26862 # p 2997 ..... AD-D015200
NAVY-CASE-70938
US-PATENT-APPL-SN-767189
N92-26863 # p 3009 ..... AD-A247102
WL-TR-91-1063
N92-26864 p 2926 ..... NO REPORT NUMBER
N92-26865 p 2944 ..... NO REPORT NUMBER
N92-26866 p 2944 ..... NO REPORT NUMBER
N92-26867 # p 2876 ..... CONF-920688-3
DE92-007713
LA-UR-92-120
N92-26868* p 2977 ..... NAS 1.26:188973
NASA-CR-188973
N92-26869 p 2920 ..... NO REPORT NUMBER
N92-26870* # p 2913 ..... NAS 1.26:190302
NASA-CR-190302
N92-26871 p 2901 ..... NO REPORT NUMBER
N92-26872 p 2890 ..... AD-A245382
ETN-92-91212
FEL-90-A352
TD90-4059
N92-26873 p 2932 ..... AD-A245422
ETN-92-91213
FEL-91-A073
TD91-0993
N92-26874 p 2890 ..... AD-A245621
ETN-92-91217
FEL-91-A171
TD91-2232
N92-26875 p 3014 ..... ETN-92-91222
FEL-91-B183
TD91-2613
N92-26876 p 2890 ..... AD-A245370
ETN-92-91225
FEL-91-B295
TD91-3276
N92-26877 p 2944 ..... AD-A245413
ETN-92-91227
FEL-91-B335
TD91-3980
N92-26878* # p 2933 ..... NAS 1.26:190344
NASA-CR-190344
NCAR/TN-371+STR
N92-26879 p 2909 ..... AD-D015189
US-PATENT-APPL-SN-561413
US-PATENT-CLASS-250-577
US-PATENT-5,073,720
N92-26880 p 2884 ..... AD-D015190
US-PATENT-APPL-SN-704561
US-PATENT-CLASS-548-145
US-PATENT-5,081,255
N92-26881 p 2894 ..... AD-D015209
US-PATENT-APPL-SN-497387
US-PATENT-CLASS-363-3
US-PATENT-5,063,487
N92-26882 # p 2870 ..... AD-A246999
N92-26883* # p 2901 ..... ICASE-92-16
NAS 1.26:189638
NASA-CR-189638
N92-26884* # p 2858 ..... NAS 1.26:185673
NASA-CR-185673
N92-26885* # p 2984 ..... FIA-91-01
NAS 1.15:107876
NASA-TM-107876
N92-26886* # p 3015 ..... FIA-92-05
NAS 1.15:107913
NASA-TM-107913
N92-26887* # p 2984 ..... NAS 1.15:107911
NASA-TM-107911
RIA-90-4-27-1
N92-26888* # p 2984 ..... FIA-91-23
NAS 1.15:107872
NASA-TM-107872
N92-26889 # p 2933 ..... EPA/600/A-92/051
PB92-153774
N92-26890 # p 2933 ..... EPA/520/5-91/025
PB92-164706
N92-26891 # p 2956 ..... ISVR-TR-205
N92-26892* p 2920 ..... NAS 1.26:190321
NASA-CR-190321
N92-26893* # p 2984 ..... FIA-90-09-11-01
NAS 1.15:107889
NASA-TM-107889
N92-26894* # p 2988 ..... FIA-90-12-7-01
NAS 1.15:107885
NASA-TM-107885
N92-26895* # p 2927 ..... NAS 1.55:3147-ADD
NASA-CP-3147-ADD
N92-26896 # p 2852 ..... AD-A245782
N92-26897 # p 2894 ..... AD-A245799
NPS-ME-92-001
N92-26898 # p 2887 ..... AD-A245810
N92-26899 # p 2946 ..... AD-A245824
ASL-TMR-0011
N92-26900 # p 2988 ..... AD-A245825
NPS-MA-92-002
N92-26901 # p 2947 ..... AD-A245829
N92-26902 # p 2891 ..... CONF-9206102-1
DE92-007046

SAND-92-0134C
N92-26903* # p 2920 ..... NAS 1.15:107629
NASA-TM-107629
N92-26904* # p 2977 ..... NAS 1.15:4367
NASA-TM-4367
REPT-92B00063
N92-26905* # p 2921 ..... M-690
NAS 1.15:4388
NASA-TM-4388
N92-26906 # p 2901 ..... ISSN-0289-260X
JTN-92-80307
NAL-SP-12
N92-26907 # p 2901 ..... NO REPORT NUMBER
N92-26908 # p 2902 ..... NO REPORT NUMBER
N92-26909 # p 2902 ..... NO REPORT NUMBER
N92-26910 # p 2902 ..... NO REPORT NUMBER
N92-26911 # p 2902 ..... NO REPORT NUMBER
N92-26912 # p 2902 ..... NO REPORT NUMBER
N92-26913 # p 2903 ..... NO REPORT NUMBER
N92-26914 # p 2903 ..... NO REPORT NUMBER
N92-26915 # p 2903 ..... NO REPORT NUMBER
N92-26916 # p 2903 ..... NO REPORT NUMBER
N92-26917 # p 2903 ..... NO REPORT NUMBER
N92-26918 # p 2904 ..... NO REPORT NUMBER
N92-26919 # p 2904 ..... NO REPORT NUMBER
N92-26920 # p 2904 ..... NO REPORT NUMBER
N92-26921 # p 2904 ..... NO REPORT NUMBER
N92-26922 # p 2904 ..... NO REPORT NUMBER
N92-26923 # p 2947 ..... WCDMP-14
WMO-TD-466
N92-26924 # p 2947 ..... WCDMP-15
WMO-TD-468
N92-26925 # p 2947 ..... WCDMP-16
WMO-TD-465
N92-26926 # p 3014 ..... PB92-154905
N92-26927 # p 3006 ..... PB92-150176
N92-26928 # p 2933 ..... EPA/600/A-92/050
PB92-153766
N92-26929 # p 2933 ..... EPA/600/A-92/047
PB92-153733
N92-26930 # p 2910 ..... EPA/600/R-92/050
PB92-160084
N92-26931 # p 2933 ..... PB92-147727
USGS/WRI-91-4040
N92-26932 # p 2920 ..... AD-A245804
N92-26933 # p 2891 ..... AD-A245806
N92-26934 # p 2905 ..... AD-A245828
N92-26935 # p 2934 ..... CONF-920605-4
DE92-007322
UCRL-JC-107758
N92-26936 # p 2934 ..... CONF-920605-3
DE92-007323
UCRL-JC-107535
N92-26937 # p 2944 ..... DE92-010923
DOE/ER-61218/1
N92-26938 # p 2951 ..... DE92-010953
DOE/ER-13691/T2
N92-26939 # p 2879 ..... AD-A246362
TR-3
N92-26940 # p 2991 ..... AD-A246364
ARO-26636.2-CH
N92-26941 # p 2891 ..... AD-A246365
N92-26942 # p 2894 ..... AD-A246368
N92-26943 # p 2998 ..... AD-A246369
RL-TR-91-341
N92-26944 # p 2853 ..... ETN-92-90820
F+W-TF-2058
N92-26945 # p 2880 ..... ETN-92-90823
ISSN-0366-0885
JUEL-2466
N92-26946 # p 3018 ..... ETN-92-90826
N92-26947 # p 2850 ..... AD-A246356
ARL-FLIGHT-MECH-TM-437
DODA-AR-008-595
N92-26948 # p 2852 ..... AD-A246435
DODA-AR-008-440
SRL-0058-TM
N92-26949 # p 2977 ..... AD-A246436
NPS-OR-92-011
N92-26950 # p 2956 ..... ESA-SP-324-VOL-2
ETN-92-91356
ISBN-92-9092-138-2
ISSN-0379-6566
N92-26951 # p 2956 ..... NO REPORT NUMBER
N92-26952 # p 2957 ..... NO REPORT NUMBER
N92-26953* # p 2957 ..... NO REPORT NUMBER
N92-26954 # p 2957 ..... NO REPORT NUMBER
N92-26955 # p 2957 ..... NO REPORT NUMBER
N92-26956 # p 2957 ..... NO REPORT NUMBER
N92-26957 # p 2958 ..... NO REPORT NUMBER
N92-26958 # p 2958 ..... NO REPORT NUMBER
N92-26959 # p 2958 ..... NO REPORT NUMBER
N92-26960 # p 2958 ..... NO REPORT NUMBER
N92-26961 # p 2958 ..... NO REPORT NUMBER
N92-26962 # p 2905 ..... NO REPORT NUMBER
N92-26963 # p 2959 ..... NO REPORT NUMBER
N92-26964 # p 2886 ..... NO REPORT NUMBER
N92-26965 # p 2859 ..... NO REPORT NUMBER
N92-26966 # p 2859 ..... NO REPORT NUMBER
N92-26967 # p 2859 ..... NO REPORT NUMBER
N92-26968 # p 2859 ..... NO REPORT NUMBER
N92-26969 # p 2905 ..... NO REPORT NUMBER
N92-26970 # p 2859 ..... NO REPORT NUMBER
N92-26971 # p 2859 ..... NO REPORT NUMBER
N92-26972 # p 2905 ..... NO REPORT NUMBER
N92-26973 # p 2860 ..... NO REPORT NUMBER
N92-26974 # p 2895 ..... NO REPORT NUMBER
N92-26975 # p 2960 ..... NO REPORT NUMBER
N92-26976 # p 2961 ..... NO REPORT NUMBER
N92-26977 # p 2951 ..... NO REPORT NUMBER
N92-26978 # p 2951 ..... NO REPORT NUMBER
N92-26979 # p 2951 ..... NO REPORT NUMBER
N92-26980* # p 2961 ..... NO REPORT NUMBER
N92-26981 # p 2961 ..... NO REPORT NUMBER
N92-26982 # p 2952 ..... NO REPORT NUMBER
N92-26983 # p 2962 ..... NO REPORT NUMBER
N92-26984 # p 2962 ..... NO REPORT NUMBER
N92-26985 # p 2962 ..... NO REPORT NUMBER
N92-26986 # p 2887 ..... NO REPORT NUMBER
N92-26987 # p 2916 ..... NO REPORT NUMBER
N92-26988 # p 2887 ..... NO REPORT NUMBER
N92-26989 # p 2963 ..... NO REPORT NUMBER
N92-26990 # p 2963 ..... NO REPORT NUMBER
N92-26991 # p 2963 ..... NO REPORT NUMBER
N92-26992 # p 2953 ..... NO REPORT NUMBER
N92-26993 # p 2964 ..... NO REPORT NUMBER
N92-26994 # p 2964 ..... NO REPORT NUMBER
N92-26995 # p 2964 ..... NO REPORT NUMBER
N92-26996 # p 2859 ..... NO REPORT NUMBER
N92-26997 # p 2859 ..... NO REPORT NUMBER
N92-26998 # p 2860 ..... NO REPORT NUMBER
N92-26999 # p 2860 ..... NO REPORT NUMBER
N92-27000 # p 2860 ..... NO REPORT NUMBER
N92-27001 # p 2965 ..... NO REPORT NUMBER
N92-27002 # p 2965 ..... NO REPORT NUMBER
N92-27003 # p 2965 ..... NO REPORT NUMBER
N92-27004 # p 2965 ..... NO REPORT NUMBER
N92-27005 # p 2965 ..... NO REPORT NUMBER
N92-27006 # p 2966 ..... NO REPORT NUMBER
N92-27007 # p 2966 ..... NO REPORT NUMBER
N92-27008 # p 2857 ..... NO REPORT NUMBER
N92-27009 # p 2966 ..... NO REPORT NUMBER
N92-27010 # p 2966 ..... NO REPORT NUMBER
N92-27011 # p 2953 ..... NO REPORT NUMBER
N92-27012 # p 2953 ..... NO REPORT NUMBER
N92-27013 # p 2858 ..... NO REPORT NUMBER
N92-27014 # p 2860 ..... NO REPORT NUMBER
N92-27015 # p 2883 ..... NO REPORT NUMBER
N92-27016 # p 2883 ..... NO REPORT NUMBER
N92-27017 # p 2968 ..... NO REPORT NUMBER
N92-27018 # p 2968 ..... NO REPORT NUMBER
N92-27019 # p 2968 ..... NO REPORT NUMBER
N92-27020 # p 2968 ..... NO REPORT NUMBER
N92-27021* # p 2968 ..... NO REPORT NUMBER
N92-27022 # p 2968 ..... NO REPORT NUMBER
N92-27023 # p 2969 ..... NO REPORT NUMBER
N92-27024 # p 2860 ..... NO REPORT NUMBER
N92-27025 # p 2969 ..... NO REPORT NUMBER
N92-27026 # p 2969 ..... NO REPORT NUMBER
N92-27027 # p 2905 ..... NO REPORT NUMBER
N92-27028 # p 2860 ..... NO REPORT NUMBER
N92-27029 # p 2950 ..... AD-A246437
N92-27030 # p 2859 ..... AD-A246439
N92-27031 # p 2992 ..... AD-A246442
N92-27032* # p 2905 ..... ICASE-92-20
NAS 1.26:189647
NASA-CR-189647
N92-27033* # p 2861 ..... AIAA-92-3164
E-7108
NAS 1.15:105714
NASA-TM-105714
N92-27034* # p 2861 ..... E-7071
NAS 1.15:105690
NASA-TM-105690
N92-27035* # p 2861 ..... AIAA-92-3228
E-7137
NAS 1.15:105734
NASA-TM-105734
N92-27036* # p 2861 ..... AIAA-92-3226
E-7154
NAS 1.15:105750
NASA-TM-105750
N92-27037* # p 2855 ..... AIAA-92-3083
E-7063
NAS 1.15:105684
NASA-TM-105684
N92-27038 # p 2916 ..... ETN-92-90774
PNR-90801
N92-27039 # p 2855 ..... ETN-92-90775
PNR-90805
N92-27040 # p 2855 ..... ETN-92-90777
PNR-90808
N92-27041 # p 2855 ..... ETN-92-90778
PNR-90809
N92-27042 # p 2855 ..... ETN-92-90779
PNR-90810
N92-27043 # p 2856 ..... ETN-92-90780
PNR-90811
N92-27044 # p 2880 ..... ETN-92-90781
PNR-90813
N92-27045 # p 2905 ..... ETN-92-90819
F+W-TF-2012
N92-27046 p 3010 ..... ETN-92-91234
IZF-1991-B-11
TD91-2171
N92-27047 p 2953 ..... ETN-92-91236
IZF-1991-B-13
TD91-3298
N92-27048 p 3018 ..... ETN-92-98598
MPE-PREPRINT-174
N92-27049 p 3016 ..... ETN-92-98599
MPE-PREPRINT-175
N92-27050 # p 2913 ..... AD-A246374
FTD-ID(RS)T-0688-91
N92-27051 # p 3015 ..... AD-A246375
FTD-ID(RS)T-0574-91
N92-27052 # p 2977 ..... AD-A246378
N92-27053 p 2977 ..... NO REPORT NUMBER
N92-27054 p 2850 ..... NO REPORT NUMBER
N92-27055* # p 2984 ..... FIA-91-24
NAS 1.15:107906
NASA-TM-107906
N92-27056* # p 2985 ..... NAS 1.15:107896
NASA-TM-107896
RIA-90-02-15-1
N92-27057* # p 2985 ..... FIA-90-04-06-01
NAS 1.15:107895
NASA-TM-107895
N92-27058 # p 3008 ..... AD-A245487
N92-27059 # p 3006 ..... BNL-47128
CONF-920141-4
DE92-010045
N92-27060 # p 2883 ..... CONF-910854-3
DE92-010777
N92-27061 # p 2894 ..... AD-A246140
N92-27062 # p 2856 ..... AD-A246372
DRIC-BR-307984
RAE-TM-P1216
N92-27063 # p 2953 ..... AD-A246410
N92-27064 # p 3006 ..... AD-A246412
N92-27065 # p 2862 ..... AD-A246416
N92-27066 # p 2921 ..... AD-A246423
N92-27067 # p 2880 ..... AD-A246427
N92-27068* p 2953 ..... NAS 1.21:7011(362)
NASA-SP-7011(362)
N92-27069 # p 2950 ..... AD-A245517
NPS-OC-92-002
N92-27070 # p 2926 ..... AD-A246142
AD-E040172
NOARL-TN-164
N92-27071 # p 2950 ..... AD-A246143
AD-E040175
NOARL-TN-208
N92-27072 # p 2985 ..... AD-A246144
AD-E040167
NOARL-TN-193
N92-27073 # p 2978 ..... AD-A246380
N92-27074 # p 2859 ..... AD-A246381
N92-27075 # p 2947 ..... AD-A246383
N92-27076 # p 2993 ..... AD-A246385
N92-27077 # p 3016 ..... AD-A246387
NPS-PH-92-005
N92-27078 # p 2991 ..... AD-A246389
N92-27079 # p 2895 ..... AD-A246395
N92-27080* p 3010 ..... NAS 1.21:7500(26)
NASA-SP-7500(26)
N92-27081* p 3014 ..... NAS 1.21:7039(40)-SECT-2
NASA-SP-7039(40)-SECT-2
N92-27082 p 2934 ..... IGBP-REPT-19-ATTACH-10
ISSN-0284-8015
N92-27083* # p 3022 ..... L-17042-PT-3
NAS 1.55:3134-PT-3
NASA-CP-3134-PT-3
N92-27084* # p 2867 ..... NO REPORT NUMBER
N92-27085* # p 2884 ..... NO REPORT NUMBER
N92-27086* # p 2883 ..... NO REPORT NUMBER
N92-27087* # p 2927 ..... NO REPORT NUMBER
N92-27088* # p 2927 ..... NO REPORT NUMBER
N92-27089* # p 2998 ..... NO REPORT NUMBER
N92-27090* # p 2998 ..... NO REPORT NUMBER
N92-27091* # p 2998 ..... NO REPORT NUMBER
N92-27092* # p 2910 ..... NO REPORT NUMBER
N92-27093* # p 2998 ..... NO REPORT NUMBER
N92-27094* # p 2998 ..... NO REPORT NUMBER
N92-27095* # p 2998 ..... NO REPORT NUMBER
N92-27096* # p 2998 ..... NO REPORT NUMBER
N92-27097* # p 2999 ..... NO REPORT NUMBER
N92-27098* # p 2999 ..... NO REPORT NUMBER

N92-27099* # p 2999 ..... NO REPORT NUMBER
N92-27100* # p 2883 ..... NO REPORT NUMBER
N92-27101* # p 2927 ..... NO REPORT NUMBER
N92-27102* # p 2883 ..... NO REPORT NUMBER
N92-27103* # p 2895 ..... NO REPORT NUMBER
N92-27104* # p 2906 ..... NO REPORT NUMBER
N92-27105* # p 2906 ..... NO REPORT NUMBER
N92-27106* # p 2906 ..... NO REPORT NUMBER
N92-27107* # p 2906 ..... NO REPORT NUMBER
N92-27108* # p 2999 ..... NO REPORT NUMBER
N92-27109* # p 2910 ..... NO REPORT NUMBER
N92-27110* # p 2999 ..... NO REPORT NUMBER
N92-27111* # p 2895 ..... NO REPORT NUMBER
N92-27112* # p 2895 ..... NO REPORT NUMBER
N92-27113* # p 2910 ..... NO REPORT NUMBER
N92-27114* # p 2916 ..... NO REPORT NUMBER
N92-27115* # p 2880 ..... NO REPORT NUMBER
N92-27116* # p 2860 ..... NO REPORT NUMBER
N92-27117* # p 2867 ..... NO REPORT NUMBER
N92-27118* # p 2895 ..... NO REPORT NUMBER
N92-27119* # p 2880 ..... NO REPORT NUMBER
N92-27120* # p 2952 ..... NO REPORT NUMBER
N92-27121* # p 2952 ..... NO REPORT NUMBER
N92-27122* # p 2952 ..... NO REPORT NUMBER
N92-27123* # p 2952 ..... NO REPORT NUMBER
N92-27124* # p 2952 ..... NO REPORT NUMBER
N92-27125* # p 2952 ..... NO REPORT NUMBER
N92-27126* # p 2952 ..... NO REPORT NUMBER
N92-27127* # p 3007 ..... NO REPORT NUMBER
N92-27128* # p 2867 ..... NO REPORT NUMBER
N92-27129* # p 2860 ..... NO REPORT NUMBER
N92-27130* # p 2862 ..... M-661
NAS 1.55:3119
NASA-CP-3119
N92-27131* # p 2862 ..... NO REPORT NUMBER
N92-27132* # p 2862 ..... NO REPORT NUMBER
N92-27133* # p 2862 ..... NO REPORT NUMBER
N92-27134* # p 2862 ..... NO REPORT NUMBER
N92-27135* # p 2862 ..... NO REPORT NUMBER
N92-27136* # p 2862 ..... NO REPORT NUMBER
N92-27137* # p 2863 ..... NO REPORT NUMBER
N92-27138* # p 2863 ..... NO REPORT NUMBER
N92-27139* # p 2863 ..... NO REPORT NUMBER
N92-27140* # p 2863 ..... NO REPORT NUMBER
N92-27141* # p 2863 ..... NO REPORT NUMBER
N92-27142* # p 2863 ..... NO REPORT NUMBER
N92-27143* # p 2863 ..... NO REPORT NUMBER
N92-27144* # p 2863 ..... NO REPORT NUMBER
N92-27145* # p 2864 ..... NO REPORT NUMBER
N92-27146* # p 2864 ..... NO REPORT NUMBER
N92-27147* # p 2864 ..... NO REPORT NUMBER
N92-27148* # p 2864 ..... NO REPORT NUMBER
N92-27149* # p 2864 ..... NO REPORT NUMBER
N92-27150* # p 2864 ..... NO REPORT NUMBER
N92-27151* # p 2865 ..... NO REPORT NUMBER
N92-27152* # p 2865 ..... NO REPORT NUMBER
N92-27153* # p 2865 ..... NO REPORT NUMBER
N92-27154* # p 2865 ..... NO REPORT NUMBER
N92-27155* # p 2865 ..... NO REPORT NUMBER
N92-27156* # p 2865 ..... NO REPORT NUMBER
N92-27157* # p 2865 ..... NO REPORT NUMBER
N92-27158* # p 2865 ..... NO REPORT NUMBER
N92-27159* # p 2866 ..... NO REPORT NUMBER
N92-27160* # p 2866 ..... NO REPORT NUMBER
N92-27161* # p 2866 ..... NO REPORT NUMBER
N92-27162* # p 2866 ..... NO REPORT NUMBER
N92-27163* # p 2866 ..... NO REPORT NUMBER
N92-27164* # p 2866 ..... NO REPORT NUMBER
N92-27165* # p 2866 ..... NO REPORT NUMBER
N92-27166* # p 2866 ..... NO REPORT NUMBER
N92-27167* # p 2867 ..... NO REPORT NUMBER
N92-27168* # p 2867 ..... NO REPORT NUMBER
N92-27169 # p 2985 ..... AD-A247204
AFOSR-92-0118TR
N92-27170* # p 3014 ..... NAS 1.15:104173
NASA-TM-104173
REPT-12
N92-27171 # p 3008 ..... AD-A246919
N92-27172 # p 2850 ..... AD-A247207
AFOSR-92-0086TR
N92-27173 # p 2913 ..... AD-A247208
AFOSR-92-0093TR
N92-27174 # p 2989 ..... AD-A246929
TR-227
N92-27175 # p 2989 ..... AD-A247105
CMS-TSR-92-09
N92-27176 # p 2895 ..... AD-A247254
N92-27177 # p 2978 ..... AD-A247268
GR-7670-1317(NP)
STARS-TC-04041/001/00
N92-27178 # p 2913 ..... AD-A247282
N92-27179 # p 2970 ..... AC/243(PANEL 8)TR/1
AD-A247346
N92-27180 # p 2989 ..... AD-A247146
N92-27181 # p 2910 ..... AD-A247147
N92-27182 # p 2991 ..... AD-A247148
N92-27183* # p 2981 ..... NAS 1.26:190428
NASA-CR-190428
PCS-TR91-154
N92-27184 p 2993 ..... AD-D015214
US-PATENT-APPL-SN-481421
US-PATENT-CLASS-G015-15.00
US-PATENT-5,068,832
N92-27185 # p 2853 ..... AD-D015215
US-PATENT-APPL-SN-453658
US-PATENT-CLASS-244-12.1
US-PATENT-5,071,088
N92-27186 p 2998 ..... AD-D015218
US-PATENT-APPL-SN-465677
US-PATENT-CLASS-356-345
US-PATENT-5,054,922
N92-27187 p 2883 ..... AD-D015219
US-PATENT-APPL-SN-500979
US-PATENT-CLASS-204-192-19
US-PATENT-5,062,939
N92-27188 p 2853 ..... AD-D015237
US-PATENT-APPL-SN-605902
US-PATENT-CLASS-89-1.51
US-PATENT-5,070,760
N92-27189* # p 2891 ..... NAS 1.15:107598
NASA-TM-107598
N92-27190 # p 3010 ..... AD-A234900
N92-27191* # p 2850 ..... NAS 1.26:190452
NASA-CR-190452
N92-27192* # p 2880 ..... DOE/NASA/33408-6
E-6978
NAS 1.15:105635
NASA-TM-105635
N92-27193* # p 2905 ..... L-17013
NAS 1.15:4374
NASA-TM-4374
N92-27194* # p 2883 ..... L-17023
NAS 1.60:3226
NASA-TP-3226
N92-27195* # p 2926 ..... JPL-PUBL-90-33
NAS 1.26:190458
NASA-CR-190458
N92-27196* # p 2989 ..... E-6950
ICOMP-92-01
NAS 1.15:105612
NASA-TM-105612
N92-27197* # p 2886 ..... E-6816
NAS 1.15:105410
NASA-TM-105410

Appendix

NASA SCIENTIFIC AND TECHNICAL INFORMATION PROGRAM PRODUCTS AND SERVICES

The NASA Scientific and Technical Information (STI) Program provides for the collection and announcement of aerospace-related reports and literature obtained worldwide through agreements and exchanges. The result of the collection is the comprehensive NASA STI Database that covers aeronautics, space, and supporting disciplines.

The STI Database, documents generated or obtained by NASA, and products and services derived from or supporting the database are made available to the NASA research community and to the public. Descriptions and sources of these items are presented in the following pages.

Scientific and Technical Aerospace Reports (*STAR*) is an abstract journal, listing citations with abstracts for aerospace-related reports obtained from worldwide sources. *STAR* is issued on the 8th and 23rd of each month and announces current documents that have been entered into the NASA STI Database during the previous two weeks. The reports are of the following types:

- NASA, NASA contractor, and NASA grantee reports;
- Reports issued by other U.S. Government agencies, domestic and foreign institutions, universities, and private firms;
- Translations in report form;
- NASA-owned patents and patent applications;
- Other U.S. Government agency and foreign patents and patent applications;
- Domestic and foreign dissertations and theses.

Journal, book, and conference literature, journal translations, and certain foreign dissertations having the same subject scope as *STAR* are announced in a companion journal, *International Aerospace Abstracts* (*IAA*). *IAA* is issued on the 1st and 15th of each month and is available from the American Institute of Aeronautics and Astronautics, Technical Information Service, 555 West 57th Street, 12th Floor, New York, NY 10019.

ELIGIBILITY AND REGISTRATION FOR NASA STI PRODUCTS AND SERVICES

Organizations of the type listed below that have registered with NASA can receive products and services.

- NASA offices and installations, contractors, subcontractors, grantees, and consultants;
- Other U.S. Government agencies and their contractors;
- Libraries in the United States that have arrangements with NASA to maintain collections of NASA documents for public reference;
- Other organizations in the United States having a need for NASA documents in work related to aeronautics and space research;
- Organizations abroad that have established reciprocal documents exchange arrangements with NASA.

Only the central service points or central points of document acquisition and control within qualified organizations are eligible to register for NASA STI products and services. Domestic organizations that may be eligible to receive various classes of NASA publications and services should address their requests for registration or further information to:

NASA Center for AeroSpace Information
ATTN: Registration Services
P.O. Box 8757
Baltimore, MD 21240-0757
301-621-0153

Organizations abroad should direct requests to:

National Aeronautics and Space Administration
Director, Scientific and Technical Information Program
Code JTT
Washington, DC 20546
USA
703-271-5640

SUBJECT SCOPE

The subject scope of *STAR* and *IAA* includes all aspects of aeronautics and space research and development, supporting basic and applied research, and applications. Aerospace aspects of Earth resources, energy development, conservation, oceanography, environmental protection, urban transportation, and other topics of high national priority are also covered.

HOW TO USE *STAR* SUBJECT CATEGORIES

Abstracts in *STAR* are categorized by 10 major subject divisions that are divided further into 76 specific subject categories. The subject divisions and categories are listed in the Table of Contents together with a note for each that defines its scope and provides any cross-references. For example:

16 SPACE TRANSPORTATION
Includes passenger and cargo space transportation, e.g., shuttle operations; and space rescue techniques. For related information see also *03 Air Transportation and Safety* and *18 Spacecraft Design, Testing and Performance.* For space suits see *54 Man/System Technology and Life Support.*

CROSS-REFERENCES

Individual *STAR* abstracts are not ordinarily cross-referenced, except for certain conference reports or book translations that have had separate abstracts written for their component papers or chapters. Citations and abstracts of the components follow immediately after those of the parent document. When the subject content of a component differs sufficiently from the general content of the parent, a cross-reference citation also is printed at the end of the category to which it normally would have been assigned if it were independent.

DOCUMENTS ON MICROFICHE

Documents available on microfiche are designated by a pound sign (#) following the accession number.

LIMITED REPRODUCIBILITY

A note of limited reproducibility appears in the citation, if there are factors affecting the reproducibility of more than 20% of the document. These factors include faint or broken type, color photographs, black and white photographs, foldouts, dot matrix print, or some other factor that limits the reproducibility of the document. This notation also appears on the microfiche header with the specific factor checked off on a list visible in the second frame.

COLOR COPIES

An increasing number of NASA scientific and technical reports are being produced with color graphs, charts, illustrations, and photographs. An indication that a document has color pages follows the source and pricing (SAP) information in the *STAR* citation.

Registered users of the NASA Scientific and Technical Information Program will receive ordered documents with color at no additional cost, as long as stock copies of the document are available. Otherwise, an additional fee of $2.00 per color page will be charged. The NASA Center for AeroSpace Information staff will contact registered users to determine individual user's needs.

NASA PATENTS AND PATENT APPLICATIONS

Patents and patent applications owned by NASA are announced in *STAR* under appropriate subject categories and are referenced in the *STAR* indexes. In the Report/Accession Number Index, patents are indexed by the NASA Case Number, and the U.S. Patent Class. Patent applications are indexed by the NASA Case Number and the U.S. Patent Application Serial Number.

Printed copies of patents (which are not microfiched) are available for purchase from the U.S. Patent and Trademark Office.

NASA patent application specifications are sold in both paper copy and microfiche by the National Technical Information Service (NTIS). The US-Patent-Appl-SN-number should be used in ordering either paper copy or microfiche from NTIS.

When ordering patents, the U.S. Patent Number should be used, and payment must be remitted in advance, by money order or check payable to the Commissioner of Patents and Trademarks. Prepaid purchase coupons for ordering are also available from the U.S. Patent and Trademark Office.

The patents and patent applications announced in *STAR* are owned by NASA and are available for royalty-free licensing. Requests for licensing terms and further information should be addressed to:

National Aeronautics and Space Administration
Associate General Counsel for Intellectual Property
Code GP
Washington, DC 20546

SOURCES FOR DOCUMENTS

One or more sources from which a document announced in *STAR* is available to the public is given in each citation. The most commonly indicated sources and their acronyms or abbreviations are listed on page A-6. If the publication is available from a source other than those listed, the publisher and address will be displayed on the availability line or in combination with the corporate source line.

Avail: NTIS. Sold by the National Technical Information Service. Prices for hard copy (HC) and microfiche (MF) are indicated by a price code following the letters HC or MF in the *STAR* citation. Current values for the price codes are given in the tables on page A-7.

Initially distributed microfiche under the NTIS SRIM (Selected Research in Microfiche) is available at greatly reduced unit prices. For this service and for information concerning subscription to NASA printed reports, consult the NTIS Subscription Section, Springfield, VA 22161.

NOTE ON ORDERING DOCUMENTS: When ordering NASA publications (those followed by the * symbol), use the N accession number. NASA patent applications (only the specifications are offered) should be ordered by the US-Patent-Appl-SN number. Non-NASA publications (no asterisk) should be ordered by the AD, PB, or other *report number* shown on the last line of the citation, not by the N accession number. It is also advisable to cite the title and other bibliographic identification.

Avail: SOD (or GPO). Sold by the Superintendent of Documents, U.S. Government Printing Office, in hard copy. The current price and order number are given following the availability line. (NTIS will fill microfiche requests, as indicated above, for those documents identified by a # symbol.)

Avail: BLL (formerly NLL): British Library Lending Division, Boston Spa, Wetherby, Yorkshire, England. Photocopies available from this organization at the price shown. (If none is given, address inquiry to the BLL.)

Avail: DOE Depository Libraries. Organizations in U.S. cities and abroad that maintain collections of Department of Energy reports, usually in microfiche form, are listed in *Energy Research Abstracts.* Services available from the DOE and its depositories are described in a booklet, *DOE Technical Information Center - Its Functions and Services* (TID-4660), which may be obtained without charge from the DOE Technical Information Center.

Avail: ESDU. Pricing information on specific data, computer programs, and details on Engineering Sciences Data Unit (ESDU) topic categories can be obtained from ESDU International Ltd. Requesters in North America should use the Virginia address while all other requesters should use the London address, both of which are on page A-6.

Avail: Fachinformationszentrum, Karlsruhe. Sold by the Fachinformationszentrum Energie, Physik, Mathematik GMBH, Eggenstein Leopoldshafen, Federal Republic of Germany, at the price shown in deutschmarks (DM).

Avail: HMSO. Publications of Her Majesty's Stationery Office are sold in the U.S. by Pendragon House, Inc. (PHI), Redwood City, CA. The U.S. price (including a service and mailing charge) is given, or a conversion table may be obtained from PHI.

Avail: NASA Public Document Rooms. Documents so indicated may be examined at or purchased from the National Aeronautics and Space Administration, Public Documents Room (Room 126), 600 Independence Ave., S.W., Washington, DC 20546, or public document rooms located at NASA installations, and the NASA Pasadena Office at the Jet Propulsion Laboratory.

Avail: Univ. Microfilms. Documents so indicated are dissertations selected from *Dissertation Abstracts* and are sold by University Microfilms as xerographic copy (HC) and microfilm. All requests should cite the author and the Order Number as they appear in the citation.

Avail: US Patent and Trademark Office. Sold by Commissioner of Patents and Trademarks, U.S. Patent and Trademark Office, at the standard price of $1.50 each, postage free. (See discussion of NASA patents and patent applications below.)

Avail: (US Sales Only). These foreign documents are available to users within the United States from the National Technical Information Service (NTIS). They are available to users outside the United States through the International Nuclear Information Service (INIS) representative in their country, or by applying directly to the issuing organization.

Avail: USGS. Originals of many reports from the U.S. Geological Survey, which may contain color illustrations, or otherwise may not have the quality of illustrations preserved in the microfiche or facsimile reproduction, may be examined by the public at the libraries of the USGS field offices whose addresses are listed on page A-6. The libraries may be queried concerning the availability of specific documents and the possible utilization of local copying services, such as color reproduction.

Avail: Issuing Activity, or Corporate Author, or no indication of availability. Inquiries as to the availability of these documents should be addressed to the organization shown in the citation as the corporate author of the document.

FEDERAL DEPOSITORY LIBRARIES: To provide the general public with greater access to U.S. Government publications, Congress established the Federal Depository Library Program under the Government Printing Office (GPO), with 53 regional depositories responsible for permanent retention of material, inter-library loan, and reference services. (These libraries are not sales outlets.) At least one copy of nearly every NASA and NASA-sponsored publication, either in printed or microfiche format, is received and retained by the 53 regional depositories. A list of the regional GPO libraries, appears on page A-8. A local library can contact a regional depository library to help locate specific reports, or direct contact may be made by an individual.

PUBLIC COLLECTION OF NASA DOCUMENTS

An extensive collection of NASA and NASA-sponsored publications is maintianed by the British Library Lending Divison, Boston Spa, Wetherby, Yorkshire, England, for public access. The British Library Lending Division also has available many of the non-NASA publications cited in *STAR*.

European requesters may purchase facsimile copy or microfiche or NASA and NASA-sponsored documents, those identified by both the symbols # and * from ESA—Information Retrieval Service, European Space Agency, 8-10 rue Mario-Nikis, 75738 Paris CEDEX 15, France.

SUBMITTING DOCUMENTS

All users of this abstract service are urged to forward reports to be considered for announcement in *STAR*. This will aid NASA in its efforts to provide the fullest possible coverage of all scientific and technical publications that might support aeronautics and space research and development. If you have prepared relevant reports (other than those you will transmit to NASA, DOD, or DOE through the usual contract- or grant-reporting channels), please send them for consideration to the NASA Center for AeroSpace Information, P.O. Box 8757, Baltimore, MD 21240-0757.

Reprints of journal articles, book chapters, and conference papers are also welcome. These will be considered for announcement in *STAR*'s companion journal, *IAA*.

You may specify a particular source to be included in a report announcement if you wish; otherwise the report will be placed on a public sale at the National Technical Information Service. Copyrighted publications will be announced but not distributed or sold.

PURCHASE OF *STAR*

STAR is publicly available on annual subscription from the Superintendent of Documents, U.S. Government Printing Office, Washington, DC 20402.

STAR is available to registered users on annual subscription from the NASA Center for AeroSpace Information, ATTN: Registration Services, P.O. Box 8757, Baltimore, MD 21240-0757.

Microfiche of the abstract sections of *STAR* are available, on annual subscription only, from NTIS as PB92-911300, Attn: Subscriptions, 5285 Port Royal Road, Springfield, VA 22161. Annual subscription rates are $100.00 North America; $200.00 foreign. Abstract sections for previous years retroactive to 1964 are available at the current rates.

ADDRESSES OF ORGANIZATIONS

American Institute of Aeronautics and Astronautics
Technical Information Service
555 West 57th Street, 12th Floor
New York, New York 10019

British Library Lending Division,
Boston Spa, Wetherby, Yorkshire,
England

Commissioner of Patents and Trademarks
U.S. Patent and Trademark Office
Washington, DC 20231

Department of Energy
Technical Information Center
P.O. Box 62
Oak Ridge, Tennessee 37830

European Space Agency-Information Retrieval Service
ESRIN
Via Galileo Galilei
00044 Frascati (Rome) Italy

Engineering Sciences Data Unit International
P.O. Box 1633
Manassas, Virginia 22110

Engineering Sciences Data Unit International, Ltd.
251-259 Regent Street
London, W1R 7AD, England

Fachinformationszentrum Energie, Physik, Mathematik
GMBH
7514 Eggenstein Leopoldshafen
Federal Republic of Germany

Her Majesty's Stationery Office
P.O. Box 569, S.E. 1
London, England

NASA Center for AeroSpace Information
P.O. Box 8757
Baltimore, Maryland 21240-0757

National Aeronautics and Space Administration
Scientific and Technical Information Program (JTT)
Washington, DC 20546-0001

National Technical Information Service
5285 Port Royal Road
Springfield, Virginia 22161

Pendragon House, Inc.
899 Broadway Avenue
Redwood City, California 94063

Superintendent of Documents
U.S. Government Printing Office
Washington, DC 20402

University Microfilms
A Xerox Company
300 North Zeeb Road
Ann Arbor, Michigan 48106

University Microfilms, Ltd.
Tylers Green
London, England

U.S. Geological Survey Library National Center
MS 950
12201 Sunrise Valley Drive
Reston, Virginia 22092

U.S. Geological Survey Library
2255 North Gemini Drive
Flagstaff, Arizona 86001

U.S. Geological Survey
345 Middlefield Road
Menlo Park, California 94025

U.S. Geological Survey Library
Box 25046
Denver Federal Center, MS914
Denver, Colorado 80225

NTIS PRICE SCHEDULES

(Effective October 1, 1991)

Schedule A
STANDARD PRICE DOCUMENTS AND MICROFICHE**

PRICE CODE	NORTH AMERICAN PRICE	FOREIGN PRICE
A01	$ 9.00	$ 18.00
A02	12.50	25.00
A03	17.00	34.00
A04-A05	19.00	38.00
A06-A09	26.00	52.00
A10-A13	35.00	70.00
A14-A17	43.00	86.00
A18-A21	50.00	100.00
A22-A25	59.00	118.00
A99	*	*
N01	60.00	120.00
N02	59.00	118.00
N03	20.00	40.00

Schedule E
EXCEPTION PRICE DOCUMENTS AND MICROFICHE**

PRICE CODE	NORTH AMERICAN PRICE	FOREIGN PRICE
E01	$11.00	$ 22.00
E02	14.00	28.00
E03	16.00	32.00
E04	19.00	38.00
E05	21.00	42.00
E06	24.00	48.00
E07	27.00	54.00
E08	30.00	60.00
E09	33.00	66.00
E10	36.00	72.00
E11	39.00	78.00
E12	43.00	86.00
E13	46.00	92.00
E14	50.00	100.00
E15	54.00	108.00
E16	59.00	118.00
E17	64.00	128.00
E18	69.00	138.00
E19	76.00	152.00
E20	88.00	176.00
E99	*	*

* Contact NTIS for price quote.

** Effective January 1, 1991, the microfiche copy of any new document entering the NTIS collection will be priced the same as the paper copy of the document.

IMPORTANT NOTICE

NTIS Shipping and Handling Charges

U.S., Canada, Mexico — ADD $3.00 per TOTAL ORDER

All Other Countries — ADD $4.00 per TOTAL ORDER

Exceptions — Does NOT apply to:

ORDERS REQUESTING NTIS RUSH HANDLING

ORDERS FOR SUBSCRIPTION OR STANDING ORDER PRODUCTS *ONLY*

NOTE: Each additional delivery address on an order requires a separate shipping and handling charge.

FEDERAL REGIONAL DEPOSITORY LIBRARIES

ALABAMA

AUBURN UNIV. AT MONTGOMERY LIBRARY
Documents Dept.
7300 University Drive
Montgomery, AL 36117-3596
(205) 244-3650 FAX: (205) 244-0678

UNIV. OF ALABAMA
Amelia Gayle Gorgas Library
Govt. Documents
Box 870266
Tuscaloosa, AL 35487-0266
(205) 348-6046 FAX: (205) 348-8833

ARIZONA

DEPT. OF LIBRARY, ARCHIVES, AND PUBLIC RECORDS
Federal Documents
Third Floor State Capitol
1700 West Washington
Phoenix, AZ 85007
(602) 542-4121 FAX: (602) 542-4400; 542-4500

ARKANSAS

ARKANSAS STATE LIBRARY
State Library Services
One Capitol Mall
Little Rock, AR 72201
(501) 682-2869

CALIFORNIA

CALIFORNIA STATE LIBRARY
Govt. Publications Section
914 Capitol Mall - P.O. Box 942837
Sacramento, CA 94237-0001
(916) 322-4572 FAX: (916) 324-8120

COLORADO

UNIV. OF COLORADO - BOULDER
Norlin Library
Govt. Publications
Campus Box 184
Boulder, CO 80309-0184
(303) 492-8834 FAX: (303) 492-2185

DENVER PUBLIC LIBRARY
Govt. Publications Dept. BS/GPD
1357 Broadway
Denver, CO 80203
(303) 571-2135

CONNECTICUT

CONNECTICUT STATE LIBRARY
231 Capitol Avenue
Hartford, CT 06106
(203) 566-4971 FAX: (203) 566-3322

FLORIDA

UNIV. OF FLORIDA LIBRARIES
Documents Dept.
Library West
Gainesville, FL 32611-2048
(904) 392-0366 FAX: (904) 392-7251

GEORGIA

UNIV. OF GEORGIA LIBRARIES
Govt. Documents Dept.
Jackson Street
Athens, GA 30602
(404) 542-8949 FAX: (404) 542-6522

HAWAII

UNIV. OF HAWAII
Hamilton Library
Govt. Documents Collection
2550 The Mall
Honolulu, HI 96822
(808) 948-8230 FAX: (808) 956-5968

IDAHO

UNIV. OF IDAHO LIBRARY
Documents Section
Moscow, ID 83843
(208) 885-6344 FAX: (208) 885-6817

ILLINOIS

ILLINOIS STATE LIBRARY
Reference Dept.
300 South Second
Springfield, IL 62701-1796
(217) 782-7596 FAX: (217) 524-0041

INDIANA

INDIANA STATE LIBRARY
Serials/Documents Section
140 North Senate Avenue
Indianapolis, IN 46204
(317) 232-3678 FAX: (317) 232-3728

IOWA

UNIV. OF IOWA LIBRARIES
Govt. Publications Dept.
Washington & Madison Streets
Iowa City, IA 52242
(319) 335-5926 FAX: (319) 335-5830

KANSAS

UNIV. OF KANSAS
Govt. Documents & Map Library
6001 Malott Hall
Lawrence, KS 66045-2800
(913) 864-4660 FAX: (913) 864-5380

KENTUCKY

UNIV. OF KENTUCKY LIBRARIES
Govt. Publications/Maps Dept.
Lexington, KY 40506-0039
(606) 257-3139 FAX: (606) 257-1563; 257-8379

LOUISIANA

LOUISIANA STATE UNIV.
Middleton Library
Govt. Documents Dept.
Baton Rouge, LA 70803
(504) 388-2570 FAX: (504) 388-6992

LOUISIANA TECHNICAL UNIV.
Prescott Memorial Library
Govt. Documents Dept.
305 Wisteria Street
Ruston, LA 71270-9985
(318) 257-4962 FAX: (318) 257-2447

MAINE

TRI-STATE DOCUMENTS DEPOSITORY
Raymond H. Fogler Library
Govt. Documents & Microforms Dept.
Univ. of Maine
Orono, ME 04469
(207) 581-1680

MARYLAND

UNIV. OF MARYLAND
Hornbake Library
Govt. Documents/Maps Unit
College Park, MD 20742
(301) 454-3034 FAX: (301) 454-4985

MASSACHUSETTS

BOSTON PUBLIC LIBRARY
Govt. Documents Dept.
666 Boylston Street
Boston, MA 02117
(617) 536-5400 ext. 226
FAX: (617) 267-8273; 267-8248

MICHIGAN

DETROIT PUBLIC LIBRARY
5201 Woodward Avenue
Detroit, MI 48202-4093
(313) 833-1440; 833-1409
FAX: (313) 833-5039

LIBRARY OF MICHIGAN
Govt. Documents Unit
P.O. Box 30007
Lansing, MI 48909
(517) 373-0640 FAX: (517) 373-3381

MINNESOTA

UNIV. OF MINNESOTA
Wilson Library
Govt. Publications Library
309 19th Avenue South
Minneapolis, MN 55455
(612) 624-5073 FAX: (612) 626-9353

MISSISSIPPI

UNIV. OF MISSISSIPPI
J.D. Williams Library
Federal Documents Dept.
106 Old Gym Bldg.
University, MS 38677
(601) 232-5857 FAX: (601) 232-5453

MISSOURI

UNIV. OF MISSOURI - COLUMBIA
Ellis Library
Govt. Documents
Columbia, MO 65201
(314) 882-6733 FAX: (314) 882-8044

MONTANA

UNIV. OF MONTANA
Maureen & Mike Mansfield Library
Documents Div.
Missoula, MT 59812-1195
(406) 243-6700 FAX: (406) 243-2060

NEBRASKA

UNIV. OF NEBRASKA - LINCOLN
D.L. Love Memorial Library
Documents Dept.
Lincoln, NE 68588
(402) 472-2562

NEVADA

UNIV. OF NEVADA
Reno Library
Govt. Publications Dept.
Reno, NV 89557
(702) 784-6579 FAX: (702) 784-1751

NEW JERSEY

NEWARK PUBLIC LIBRARY
U.S. Documents Div.
5 Washington Street - P.O. Box 630
Newark, NJ 07101-0630
(201) 733-7812 FAX: (201) 733-5648

NEW MEXICO

UNIV. OF NEW MEXICO
General Library
Govt. Publications Dept.
Albuquerque, NM 87131-1466
(505) 277-5441 FAX: (505) 277-6019

NEW MEXICO STATE LIBRARY
325 Don Gaspar Avenue
Santa Fe, NM 87503
(505) 827-3826 FAX: (505) 827-3820

NEW YORK

NEW YORK STATE LIBRARY
Documents/Gift & Exchange Section
Federal Depository Program
Cultural Education Center
Albany, NY 12230
(518) 474-5563 FAX: (518) 474-5786

NORTH CAROLINA

UNIV. OF NORTH CAROLINA - CHAPEL HILL
CB#3912, Davis Library
BA/SS Dept.—Documents
Chapel Hill, NC 27599
(919) 962-1151 FAX: (919) 962-0484

NORTH DAKOTA

NORTH DAKOTA STATE UNIV. LIBRARY
Documents Office
Fargo, ND 58105
(701) 237-8886 FAX: (701) 237-7138
In cooperation with Univ. of North Dakota, Chester Fritz Library
Grand Forks

OHIO

STATE LIBRARY OF OHIO
Documents Dept.
65 South Front Street
Columbus, OH 43266
(614) 644-7051 FAX: (614) 752-9178

OKLAHOMA

OKLAHOMA DEPT. OF LIBRARIES
U.S. Govt. Information Div.
200 NE 18th Street
Oklahoma City, OK 73105-3298
(405) 521-2502, ext. 252, 253
FAX: (405) 525-7804

OKLAHOMA STATE UNIV.
Edmon Low Library
Documents Dept.
Stillwater, OK 74078
(405) 744-6546 FAX: (405) 744-5183

OREGON

PORTLAND STATE UNIV.
Millar Library
934 SW Harrison - P.O. Box 1151
Portland, OR 97207
(503) 725-3673 FAX: (503) 725-4527

PENNSYLVANIA

STATE LIBRARY OF PENN.
Govt. Publications Section
Walnut St. & Commonwealth Ave. - P.O. Box 1601
Harrisburg, PA 17105
(717) 787-3752

SOUTH CAROLINA

CLEMSON UNIV.
Cooper Library
Public Documents Unit
Clemson, SC 29634-3001
(803) 656-5174 FAX: (803) 656-3025
In cooperation with Univ. of South Carolina, Thomas Cooper Library, Columbia

TENNESSEE

MEMPHIS STATE UNIV. LIBRARIES
Govt. Documents
Memphis, TN 38152
(901) 678-2586 FAX: (901) 678-2511

TEXAS

TEXAS STATE LIBRARY
United States Documents
P.O. Box 12927 - 1201 Brazos
Austin, TX 78711
(512) 463-5455 FAX: (512) 463-5436

TEXAS TECH. UNIV. LIBRARY
Documents Dept.
Lubbock, TX 79409
(806) 742-2268 FAX: (806) 742-1920

UTAH

UTAH STATE UNIV.
Merrill Library & Learning Resources Center, UMC-3000
Documents Dept.
Logan, UT 84322-3000
(801) 750-2684 FAX: (801) 750-2677

VIRGINIA

UNIV. OF VIRGINIA
Alderman Library
Govt. Documents
Charlottesville, VA 22903-2498
(804) 924-3133 FAX: (804) 924-4337

WASHINGTON

WASHINGTON STATE LIBRARY
Document Section
MS AJ-11
Olympia, WA 98504-0111
(206) 753-4027 FAX: (206) 753-3546

WEST VIRGINIA

WEST VIRGINIA UNIV. LIBRARY
Govt. Documents Section
P.O. Box 6069
Morgantown, WV 26506
(304) 293-3640

WISCONSIN

ST. HIST. SOC. OF WISCONSIN LIBRARY
Govt. Publications Section
816 State Street
Madison, WI 53706
(608) 262-2781 FAX: (608) 262-4711
In cooperation with Univ. of Wisconsin-Madison, Memorial Library

MILWAUKEE PUBLIC LIBRARY
Documents Div.
814 West Wisconsin Avenue
Milwaukee, WI 53233
(414) 278-2167 FAX: (414) 278-2137

* U.S. G.P.O.:1992-313-125:60017

National Aeronautics and
Space Administration
Code JTT
Washington, D.C.
20546-0001

Official Business
Penalty for Private Use, $300

SPECIAL FOURTH-CLASS RATE
POSTAGE & FEES PAID
NASA
PERMIT No. G27

POSTMASTER: If Undeliverable (Section 158
Postal Manual) Do Not Return